

# FUNDAMENTALS OF GAS LIFT ENGINEERING

**Well Design and Troubleshooting**

Ali Hernández



G/P  
P/U

# Fundamentals of Gas Lift Engineering

## Well Design and Troubleshooting

**Ali Hernández**



**ELSEVIER**

AMSTERDAM • BOSTON • HEIDELBERG • LONDON  
NEW YORK • OXFORD • PARIS • SAN DIEGO  
SAN FRANCISCO • SINGAPORE • SYDNEY • TOKYO

Gulf Professional Publishing is an imprint of Elsevier



Gulf Professional Publishing is an imprint of Elsevier  
50 Hampshire Street, 5th Floor, Cambridge, MA 02139, USA  
The Boulevard, Langford Lane, Kidlington, Oxford, OX5 1GB, UK

Copyright © 2016 Elsevier Inc. All rights reserved.

No part of this publication may be reproduced or transmitted in any form or by any means, electronic or mechanical, including photocopying, recording, or any information storage and retrieval system, without permission in writing from the publisher. Details on how to seek permission, further information about the Publisher's permissions policies and our arrangements with organizations such as the Copyright Clearance Center and the Copyright Licensing Agency, can be found at our website: [www.elsevier.com/permissions](http://www.elsevier.com/permissions).

This book and the individual contributions contained in it are protected under copyright by the Publisher (other than as may be noted herein).

#### **Notices**

Knowledge and best practice in this field are constantly changing. As new research and experience broaden our understanding, changes in research methods, professional practices, or medical treatment may become necessary.

Practitioners and researchers must always rely on their own experience and knowledge in evaluating and using any information, methods, compounds, or experiments described herein. In using such information or methods they should be mindful of their own safety and the safety of others, including parties for whom they have a professional responsibility.

To the fullest extent of the law, neither the Publisher nor the authors, contributors, or editors, assume any liability for any injury and/or damage to persons or property as a matter of products liability, negligence or otherwise, or from any use or operation of any methods, products, instructions, or ideas contained in the material herein.

#### **British Library Cataloguing-in-Publication Data**

A catalogue record for this book is available from the British Library

#### **Library of Congress Cataloging-in-Publication Data**

A catalog record for this book is available from the Library of Congress

ISBN: 978-0-12-804133-8

For information on all Gulf Professional Publishing  
visit our website at <http://store.elsevier.com/>



Working together  
to grow libraries in  
developing countries

[www.elsevier.com](http://www.elsevier.com) • [www.bookaid.org](http://www.bookaid.org)

*Dedicated with love and gratitude to Carmen and Mauricio for their continuous support and understanding*

*And*

*In memory of my friend and mentor Walter George Zimmerman, a very practical engineer who always based his technical decisions on sound engineering judgment.*

# Contents

Acknowledgments.....	xiii
<b>CHAPTER 1 Gas Properties .....</b>	<b>1</b>
1.1 Equation of State.....	2
1.2 Gas Viscosity .....	13
1.3 Solubility of Natural Gas in Water.....	14
1.4 Solubility of Water Vapor in Natural Gas .....	16
1.5 Hydrates.....	18
1.6 Specific Heat Ratio .....	22
References .....	23
<b>CHAPTER 2 Single-Phase Flow .....</b>	<b>25</b>
2.1 Single-Phase Gas Flow .....	25
2.1.1 Static Gas Gradients in Vertical Pipes and Annuli.....	26
2.1.2 Gas Pressure Gradients in Vertical Pipes Considering Frictional Pressure Drop.....	33
2.1.3 Gas Flow in Horizontal Pipes .....	42
2.2 Single-Phase Liquid Flow.....	62
2.2.1 Static Pressure Gradient.....	62
2.2.2 Dynamic Gradient.....	69
References .....	79
<b>CHAPTER 3 Multiphase Flow .....</b>	<b>81</b>
3.1 Qualitative Aspects .....	81
3.2 General Quantitative Aspects in Multiphase Flow .....	88
3.2.1 General Definitions.....	89
3.2.2 Equations for Multiphase Flow Pressure and Temperature Gradients.....	93
3.3 Examples of Correlations and Mechanistic Models Developed for Vertical Upward Multiphase Flow .....	108
3.4 Horizontal Multiphase Flow .....	113
3.5 Unified Models .....	117
3.5.1 Horizontal Flow .....	117
3.5.2 Vertical Flow .....	118
3.5.3 Unified Models .....	118
3.6 Fluid Flow Through Annular Cross-Sections .....	118
3.6.1 Flow Pattern Prediction .....	119
3.6.2 Models Developed for Liquid Holdup and Pressure Drop Calculations.....	121
References .....	122

<b>CHAPTER 4 Single and Multiphase Flow Through Restrictions .....</b>	<b>127</b>
4.1 Gas Flow Through Restrictions .....	131
4.2 Liquid Flow Through Restrictions.....	139
4.3 Multiphase Flow Through Restrictions .....	140
References .....	148
<b>CHAPTER 5 Total System Analysis Applied to Gas Lift Design .....</b>	<b>151</b>
5.1 Determination of the Depth of the Operating Point of Injection.....	152
5.1.1 Determination of the Injection Point Depth Assuming Constant Wellhead Production Pressure .....	154
5.1.2 Finding the Injection Point Depth with Variable Wellhead Pressure.....	161
5.1.3 Use of Computer Programs to Find the Point of Injection and Perform Additional Useful Operations .....	163
5.2 Examples of the Effect that Different Gas Lift System's Components or Fluid Properties Might have on the Liquid Production of a Well on Gas Lift .....	182
5.3 Calculation Examples .....	187
5.3.1 Example of Preliminary Calculations Needed to Implement the Gas Lift Method to Boost the Liquid Production of a Well that can Produce on Natural Flow .....	187
5.3.2 Example of Preliminary Calculations to Design a Gas Lift Well that Cannot Produce on Natural Flow .....	203
<b>CHAPTER 6 Gas Lift Equipment .....</b>	<b>211</b>
6.1 Gas Lift Valves and Latches .....	211
6.2 Gas Lift Mandrels.....	226
6.3 Wireline Equipment .....	237
6.4 Types of Completions for Gas Lift Installations.....	250
6.4.1 Single Completions.....	250
6.4.2 Gas Lift as a Backup Method for Electric Submersible Pumps.....	255
6.4.3 Accumulation Chambers.....	260
6.4.4 Dual Wells.....	276
6.4.5 Use of Coiled Tubing.....	282
6.4.6 Intermittent Gas Lift with Metallic Plungers.....	287
<b>CHAPTER 7 Gas Lift Valve Mechanics .....</b>	<b>295</b>
7.1 Force-Balance Equations for the Different Types of Gas Lift Valves.....	295
7.1.1 Injection-Pressure-Operated Valves.....	296
7.1.2 Production-Pressure-Operated Valves.....	301

7.2	Calculation of the Nitrogen Pressure at Different Conditions.....	304
7.3	Determination of the Port and Bellows Areas .....	308
7.4	Examples of Problems Using the Force-Balance Equations for Designing and Troubleshooting Gas Lift Installations .....	309
	Reference.....	313
<b>CHAPTER 8</b>	<b>Gas Flow Through Gas Lift Valves .....</b>	<b>315</b>
8.1	Use of the Thornhill–Craver Equation for Gas Lift Valves .....	320
8.2	Mathematical Models for the Dynamic Behavior of Gas Lift Valves .....	331
8.2.1	Simple Mechanistic Model for Single Element, IPO, Gas Lift Valves (without Dynamic Effect) .....	336
8.2.2	Mechanistic Model for Single Element, IPO, Gas Lift Valves (with Dynamic Effect) .....	340
8.2.3	Dynamic Model for Pilot Valves.....	353
8.3	Use of Chokes Installed Downstream of the Seat.....	357
8.4	Use of Chokes Installed Upstream of the Seat .....	359
8.5	Orifice Valves with Special Geometry Seats .....	361
	References .....	363
<b>CHAPTER 9</b>	<b>Design of Continuous Gas Lift Installations.....</b>	<b>365</b>
9.1	Determination of the Operating Injection Point Depth, Target Injection Gas Flow Rate, and the Liquid Flow Rate the Well can Produce .....	377
9.1.1	Iterative Procedure.....	377
9.1.2	Fixed Drawdown or Fixed Liquid Production.....	383
9.1.3	Constant Liquid Production.....	384
9.2	Gas Lift Mandrel Spacing Procedures and Valve Design Calculations....	385
9.2.1	Mandrel Spacing for IPO Valves .....	387
9.2.2	Mandrel Spacing for PPO Valves .....	420
9.2.3	Unloading Liquid Flow Rate and Required Injection Gas Flow Rate at Each Unloading Valve .....	424
9.2.4	Injection Gas Temperature at Depth and Valve Operating Temperature Calculation .....	433
9.2.5	Determination of the Seat Diameters of the Operating and Unloading Valves .....	444
9.2.6	Dual Wells (with a Common Injection Gas Source).....	446
9.2.7	Redesign .....	455
9.2.8	Mandrel Spacing from the Reservoir Static Liquid Level .....	461
9.3	Stability Check of the Gas Lift Design.....	463
9.4	Examples of Gas Lift Designs .....	471
	References .....	477

<b>CHAPTER 10 Design of Intermittent Gas Lift Installations .....</b>	<b>479</b>
10.1 Description of the Production Cycle .....	479
10.2 General Fundamentals and Implementation Guidance for Intermittent Gas Lift .....	481
10.3 Types of Completions for Intermittent Gas Lift.....	494
10.4 Description of Pilot Valves.....	500
10.5 Types of Control of the Surface Gas Injection.....	507
10.6 Intermittent Gas Lift Design for Simple Type Completions .....	518
10.6.1 Design of the Operating Valve for Choke-Control Intermittent Gas Lift.....	521
10.6.2 Design Procedure with the Use of Surface Controllers (Intermitters) .....	570
10.6.3 Mechanistic Models for the Design of Simple Type Completions on Choke-Control Intermittent Gas Lift .....	572
10.7 Design of Accumulation Chambers .....	582
10.8 Simple Type Accumulator .....	592
10.9 Inserted Chambers and Inserted Accumulators.....	594
10.10 Intermittent Gas Lift In Dual Wells.....	597
10.10.1 One Zone on Continuous Gas Lift and the other on Intermittent Gas Lift.....	598
10.10.2 Both Zones on Intermittent Gas Lift.....	600
10.11 Plunger-Assisted Intermittent Gas Lift .....	601
10.12 General Considerations for Gas Lift Systems with Wells on Intermittent Gas Lift.....	604
References .....	609
 <b>CHAPTER 11 Continuous Gas Lift Troubleshooting .....</b>	 <b>611</b>
11.1 Introduction.....	611
11.2 General Difficulties Encountered when Trying to Perform Troubleshooting Analyses of Gas Lift Wells .....	612
11.3 Causes and Corrective Actions for Possible Failures and/or Loss of Lifting Efficiency.....	619
11.3.1 Most Common Failures and/or Loss of Lifting Efficiency...619	
11.3.2 Multiple Points of Injection .....	635
11.3.3 Handling Problems Associated with Emulsion Generation..639	
11.4 Methodology for Troubleshooting Analyses .....	642
11.4.1 High Wellhead Injection Pressure and the Well Does not Receive Injection Gas .....	646
11.4.2 Methodology for One or Several Stable Points of Injection below the Reservoir Static Liquid Level .....	651
11.4.3 Continuous Gas Injection but the Well Does not Produce Liquids.....	667



<b>11.5</b>	<b>Field Techniques for Troubleshooting a Gas Lift Well</b> .....	674
11.5.1	Communication Tests .....	674
11.5.2	Downhole Pressure and Temperature Surveys.....	681
11.5.3	Use of Sonic Devices .....	689
11.5.4	Use of CO <sub>2</sub> Injection to Determine the Point of Injection.....	695
11.5.5	Downhole Pressure and Temperature Measurements Using Permanent Downhole Sensors.....	706
11.5.6	Total Well Depth and Liquid Level Measurements Using Wireline Tools .....	711
11.5.7	Downhole Temperature Measurement Using Fiber-Optic Surveys (Distributed Temperature Sensors or DTS).....	712
11.5.8	Measurement of the Liquid Level (or Instantaneous Liquid Flow Rate) Inside the Test Separator .....	718
11.5.9	Use of Injection Gas Flow Rate Measurement Charts.....	720
11.5.10	Use of Wellhead Pressure Charts.....	724
<b>11.6</b>	<b>Automated Systems to Detect and Analyze Wells with Operational Problems in Gas Lift Fields with a Large Number of Wells (i-Field Solution)</b> .....	738
<b>11.7</b>	<b>Troubleshooting Examples</b> .....	743
11.7.1	Example #1: Continuous Liquid Production and Gas Injection: Injection Point Might be Plugged.....	743
11.7.2	Example #2: Fluctuating Injection Pressure and Continuous Liquid Production.....	746
11.7.3	Example #3: Time Intervals of Continuous Gas Injection and Liquid Production Followed by Time Intervals in which the Liquid Production and the Gas Injection Flow Rate Drop to Zero.....	749
11.7.4	Example #4: Well's Responses to Different Choke Diameters After a Workover Job.....	752
11.7.5	Example #5: Continuous Gas Injection but the Well Does not Produce Liquids.....	755
<b>11.8</b>	<b>Gas Lift Troubleshooting Guide</b> .....	756
11.8.1	Well is Flowing and Takes Gas (Stable Gas Injection and Liquid Production) .....	756
11.8.2	Well is Flowing and Takes Gas (Unstable Gas Injection and Liquid Production) .....	759
11.8.3	Well is only Circulating the Injection Gas (Well Takes Gas but Does not Produce Liquids) .....	761
11.8.4	Well is not Flowing and Does not Take Gas .....	763
	References .....	763

<b>CHAPTER 12 Intermittent Gas Lift Troubleshooting</b> .....	<b>765</b>
12.1 Introduction.....	765
12.2 Analysis of the Operation of Wells with Intermittent Gas Injection.....	769
12.2.1 Wells that should not be Analyzed as Intermittent Gas Lift Wells .....	770
12.2.2 Calculation Techniques for Wells that should be Analyzed as Intermittent Gas Lift Wells.....	783
12.3 Pressure and Temperature Surveys for Wells on Intermittent Gas Lift .....	833
12.3.1 Survey Procedure.....	833
12.3.2 Survey Analysis .....	837
12.3.3 Examples of Downhole Pressure and Temperature Surveys in Intermittent Gas Lift Wells .....	845
12.4 Use of Sonic Devices and Distributed Temperature Sensor (DTS) Using Fiber Optics .....	874
12.5 Wellhead Pressure Chart Interpretation .....	877
12.5.1 General Examples.....	877
12.5.2 Examples of Specific Field Cases.....	899
12.6 Intermittent Gas Lift Troubleshooting Examples .....	912
12.6.1 Example #1 (Well Might be Loaded with Liquids).....	913
12.6.2 Example #2 (Tubing-Annulus Communication) .....	918
12.6.3 Example #3 (Formation Damage).....	920
12.6.4 Example #4 (Optimized Well) .....	924
12.6.5 Example #5 (Large Fallback Losses).....	926
12.6.6 Example #6 (Tubing-Annulus Communication) .....	929
12.6.7 Example #7 (Pilot Valve Failure/Inadequate Spread) .....	930
12.6.8 Example #8 (Inadequate Continuous Gas Lift Design).....	935
12.6.9 Example #9 (Production Tubing Diameter too Large) .....	942
12.6.10 Example #10 (Formation Damage when the Well was Shifted to Produce on Intermittent Gas Lift).....	945
12.6.11 Example #11 (Intermittent Gas Lift with Surface Interrmitter).....	952
Subject Index .....	955

# Acknowledgments

The author wishes to recognize the collaboration given by the following persons:

*Herald W. Winkler, John Martinez, Gary Milam, Cleon Dunham, and the late Jack Blann* for their valuable advice on so many gas lift theoretical subjects and practical field applications; *Ken Decker and Juan Faustinelli Jr* for their guidance on the dynamic modeling of gas lift valves; *Wim der Kinderen* for his important contribution on gas lift design stability; *Dr Jesus Enrique Chacin* for his development of mechanistic models for intermittent gas lift; Wireline Expert *Hector Rivas* and Team Leader *Francisco Corrales* for their outstanding work in many of the gas lift field-scale research projects performed by the author; *Juan Carlos Iglesias* for his contribution during the research on the dynamic behavior of gas lift valves carried out by the author; *Balmiro Villalobos* for his collaboration in the implementation of wellhead intermitters and many other field applications; and *Crisanto Acevedo Caceres* and *Cesar A. Perez Montaner* for their contributions in the development of Accumulation Chambers and Insert Accumulators.

# Gas properties

The working fluid of a gas lift installation is, in most cases, the natural gas associated with the oil that is produced from the same field or from a nearby gas source. The calculation of the injection gas properties is a necessary first step to predict pressures, temperatures, flow rates, etc. at in-situ conditions in the different components of a gas lift installation. Without the knowledge of these properties, it is simply not possible to determine the important parameters that are frequently used in gas lift designs and troubleshooting analyses, such as the pressure and temperature gradients along the injection annulus that are used to locate the depths of the gas lift valves.

The correlations that can be used to calculate the properties of hydrocarbon gases are described in their general forms in the chapter. Many of the correlations given in the list of references in the chapter were developed a long time ago and have been successfully applied during the last decades; however, it is important to always use values of these properties that have been measured in field laboratories in order to: (1) corroborate the accuracy of these correlations for different operational conditions, and (2) calibrate the correlations that are used by commercially available gas lift design and troubleshooting software to calculate these properties.

The natural gas used as the injection gas in most gas lift installations is a mixture of different hydrocarbon substances of low molecular weight in gaseous state, such as methane, and some nonhydrocarbon impurities like nitrogen, hydrogen sulfide ( $H_2S$ ), and carbon dioxide ( $CO_2$ ). If the mixture has significant quantities of  $H_2S$  and/or  $CO_2$ , the gas is an “acid gas” because it forms an acidic solution in presence of water. An acid gas mixture is not recommended for use in a gas lift field because of the problems it creates for the safety of the personnel and the corrosion of tubular goods and equipment.

If the  $H_2S$  concentration is greater than 4 parts per million (ppm), the gas is also called a “sour gas,” otherwise the gas is called a sweet gas. It is important

to maintain the H<sub>2</sub>S concentration at values less than 4 ppm because higher concentrations could cause the following problems or inconveniences:

- Because these high concentrations are highly toxic, special safety measurements must be taken to avoid health related problems or even deadly accidents when dealing with sour gases.
- Sour gases can cause sulfur precipitation that can accumulate in the production tubing, flowline, injection gas lines, etc.
- Sour gases are also highly corrosive, especially in presence of salt water.

H<sub>2</sub>S reacts with water and iron to form iron sulfide and hydrogen. CO<sub>2</sub>, on the other hand, reacts with water to form carbonic acid, which then reacts with iron to form iron carbonate and hydrogen. A gas mixture could be corrosive if its CO<sub>2</sub> partial pressure (defined in [Section 1.1](#)) is greater than 3 psi. Actions that need to be taken to overcome the negative effects of CO<sub>2</sub>, H<sub>2</sub>S, and water are presented in different sections in this book. The necessary corrections in the calculation of the properties of natural gases and water vapor are addressed in the chapter if impurities such as CO<sub>2</sub> and H<sub>2</sub>S are present in small quantities, but the equations to calculate the properties of these impurities alone are not presented.

## 1.1 EQUATION OF STATE

It is very important in many gas lift calculation procedures to be able to express the volume that a given gas, or a mixture of several gases, occupies in terms of its pressure and temperature. The general gas law given in the form of [Eq. 1.1](#) is one of the many so-called “equations of state” that are used to correlate volume, pressure, and temperature of a gas:

$$PV = nR_u T \quad (1.1)$$

Where  $V$  is the volume the gas occupies,  $P$  is the gas absolute pressure,  $R_u$  is the universal gas constant,  $T$  is the absolute temperature of the gas, and  $n$  is the number of moles inside volume  $V$ .

A mole is a given number of molecules of a particular gas with a mass numerically equal to the molecular weight of the gas in the system of units being used. The number of molecules depends on the mole definition being used. For example: (1) in 1 pound-mole (lb-mol) there are  $2.73 \times 10^{26}$  molecules of the gas, (2) in 1 gram-mole (g-mol) there

**Table 1.1** Values of  $R_u$  for Different Units Used in Eq. 1.1

Units	$R_u$
atm-cc/(g-mole)-K	82.06
Btu/(lb-mole)-°R	1.987
psia-ft. <sup>3</sup> /(lb-mole)-°R	10.73
abs lb/ft. <sup>2</sup> -ft. <sup>3</sup> /(lb-mole)-°R	1545
atm-ft. <sup>2</sup> /(lb-mole)-°R	0.730
mm Hg-liters/(g-mole)-k	62.37
in.Hg-ft. <sup>3</sup> /(lb-mole)-°R	21.85
calorie/(g-mole)-K	1.987
KPa-m <sup>3</sup> /(kg-mole)-K	8.314
J/(kg-mole)-K	8314

are  $6.02 \times 10^{23}$  molecules and, (3) in 1 kilogram-mole (kg-mol) there are  $6.02 \times 10^{26}$  molecules.

It can be seen from Eq. 1.1 that, for a given pressure, temperature, and volume, the number of moles is the same for all gases. This is known as Avogadro's law, which only applies for low pressures or so-called ideal conditions. For this reason, Eq. 1.1 is called the "ideal gas law."

The mass of a mole of a given gas is known as the molecular weight of that gas in particular and is usually denoted as  $M$ . Examples of units of the molecular weight are: lbm/(lb-mol), g/(g-mol) or kg/(kg-mol). The number of moles,  $n$ , of a given mass,  $m$ , can be calculated from the following equation:

$$n = \frac{m}{M} \quad (1.2)$$

Combining Eqs. 1.1 and 1.2, the general gas law can be rewritten in the following ways:

$$P = \rho \frac{R_u}{M} T \quad (1.3)$$

$$Pv = \frac{R_u}{M} T \quad (1.4)$$

Where  $v$  is the gas specific volume and  $\rho$  its density. Some authors call  $R_u/M$  the "gas constant" of a particular gas, which is then denoted as  $R_g$ . The value of the universal gas constant,  $R_u$ , depends on the system of units being used. These values are given in Table 1.1.

**Problem 1.1**

Calculate the volume that 1 lb-mole of a gas occupies under standard conditions of temperature and pressure.

**Solution**

Standard conditions are defined as 14.7 psia and 520°R. Solving for  $V$  in Eq. 1.1:

$$V = \frac{nR_u T}{P} = \frac{(1 \text{ lb-mole}) \left( \frac{10.73 \text{ psia-ft.}^3}{(\text{lb-mole})-\text{°R}} \right) (520 \text{ °R})}{14.7 \text{ psia}} = 379.5 \text{ ft.}^3$$

**Problem 1.2**

Calculate the density of methane under standard conditions.

**Solution**

Knowing that the molecular weight of methane is 16 lbm/(lb-mole), the equation of state is used to find the density of methane as follows:

$$\rho = \frac{PM}{R_u T} = \frac{(14.7 \text{ psia}) \frac{16 \text{ lbm}}{(\text{lb-mole})}}{\left( \frac{10.73 \text{ psia-ft.}^3}{(\text{lb-mole})-\text{°R}} \right) 520 \text{ °R}} = 0.0421 \frac{\text{lbm}}{\text{ft.}^3}$$

Usually, the natural gas used as injection gas for gas lifting purposes is a mixture of different gases, where the most important components are methane and, to a lesser degree, ethane. The properties of gaseous mixtures are calculated using two fundamental laws known as Dalton's and Amagat's laws. Dalton's law states that each gas in a mixture of gases exerts a pressure equal to that which it would exert if it occupied the same volume as the total mixture. This pressure is called the "partial pressure" of the particular component of the mixture. The total pressure of the mixture is then the sum of the partial pressures of all its components. This law is valid only when the mixture, and each component of the mixture, obeys the ideal gas law. For example, if a mixture has three components  $a$ ,  $b$ , and  $c$ , then the total pressure of the mixture is the sum of the partial pressure of each component:

$P_a$ ,  $P_b$ , and  $P_c$ . Each of these components has a given number of moles:  $n_a$ ,  $n_b$ , and  $n_c$ . The total pressure of the mixture can be expressed in the following way:

$$P = P_a + P_b + P_c = n_a \frac{R_u T}{V} + n_b \frac{R_u T}{V} + n_c \frac{R_u T}{V} = N \frac{R_u T}{V} \quad (1.5)$$

Where  $N$  is the sum of  $n_a$ ,  $n_b$ , and  $n_c$ . Then, for component  $j$ :

$$\frac{P_j}{P} = \frac{n_j \frac{R_u T}{V}}{N \frac{R_u T}{V}} = \frac{n_j}{N} = y_j \quad (1.6)$$

Where  $y_j$  is known as the mole fraction of the  $j$ th component. Therefore, the partial pressure of component  $j$ , known as  $P_j$ , is equal to the total pressure of the mixture times its mole fraction,  $[(P)(y_j)]$ .

Another important law is Amagat's law. It states that the total volume of a gaseous mixture is the sum of the volumes that each component would occupy at the given mixture pressure and temperature. The volumes occupied by the individual components are known as partial volumes. This law only applies to ideal gases and it can be expressed as:

$$V = V_a + V_b + V_c = n_a \frac{R_u T}{P} + n_b \frac{R_u T}{P} + n_c \frac{R_u T}{P} = N \frac{R_u T}{P} \quad (1.7)$$

Therefore, for the  $j$ th component of the mixture:

$$\frac{V_j}{V} = \frac{n_j \frac{RT}{P}}{N \frac{RT}{P}} = \frac{n_j}{N} = y_j \quad (1.8)$$

The partial volume of the  $j$ th component, known as  $V_j$ , is equal to the total volume times its mole fraction, or  $[(V)(y_j)]$ .

One very important gas property for gas lift calculations is the apparent molecular weight of a gas mixture, known here as  $M_{ap}$ , which is defined as the summation of the molecular weight of each component multiplied by its respective mole fraction:

$$M_{ap} = \sum_j y_j M_j \quad (1.9)$$



**Table 1.2** Properties of Dry Air

Component	Mole fraction	Molecular weight
Nitrogen	0.78	28.01
Oxygen	0.21	32.00
Argon	0.01	39.94

**Problem 1.3**

Calculate the apparent molecular weight of dry air,  $M_{\text{air}}$ .

**Solution**

Table 1.2 shows the mole fraction and molecular weight of the three most important components of dry air.

$$M_{\text{air}} = (0.78)(28.01) + (0.21)(32.00) + (0.01)(39.94) = 28.97$$

From the apparent molecular weight of a given mixture, the specific gravity of that mixture,  $\gamma$ , can be calculated as:

$$\gamma = \frac{M_{\text{ap}}}{M_{\text{air}}} = \frac{M_{\text{ap}}}{29} \quad (1.10)$$

Where the molecular weight of air is approximated as being equal to 29 lbm/lb-mole. This is the apparent molecular weight of air, which is itself a mixture of several gases as indicated in the previous problem. The specific gravity of a pure gas (not a mixture) is defined in the same way: its molecular weight divided by the molecular weight of air.

The specific gravity of a gas is also defined as its density ( $\rho$ ), divided by the air density ( $\rho_{\text{air}}$ ), both at standard conditions, that is 14.7 psia and 60°F or 520°R. Using the general gas law, the following expression for the specific gravity of a gas is then:

$$\gamma = \frac{\rho}{\rho_{\text{air}}} = \frac{\frac{M_{\text{ap}} P}{(R_u)(T)}}{\frac{M_{\text{air}} P}{(R_u)(T)}} = \frac{M_{\text{ap}}}{M_{\text{air}}} \quad (1.11)$$

Eq. 1.1 at the beginning of this section is the general gas law that applies only to ideal conditions, but it is not very accurate for higher pressures. One

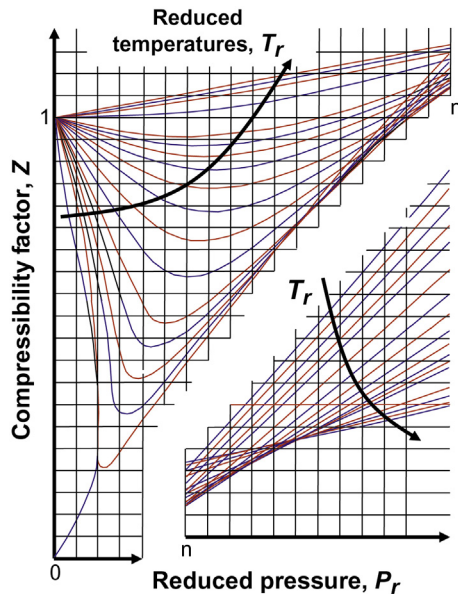
of the ways of applying the general gas law under any pressure and temperature is by introducing the compressibility factor,  $Z$ , of a particular “pure” gas in the following manner:

$$PV = nZR_uT \quad (1.12)$$

The compressibility factor of a pure gas is a function of its reduced pressure and temperature,  $P_r$  and  $T_r$ , which are defined as:

$$P_r = \frac{P}{P_c} \text{ and } T_r = \frac{T}{T_c} \quad (1.13)$$

where  $T_c$  and  $P_c$  are the critical temperature and pressure of the gas, respectively. The relationship between the compressibility factor of a pure gas and its reduced pressure and temperature is given in many reports from professional associations in the form that is presented in Fig. 1.1, where the law of corresponding states is applied to a “pure” hydrocarbon gas; see for example the work from Brown et al. (1948). The law of corresponding states establishes that all pure gases with the same values of the reduced pressure and temperature have the same compressibility  $Z$ . However, this law is not very accurate, and when a high degree of accuracy is desired, graphs as the one shown in Fig. 1.1, but developed for a particular gas, must be used.



■ FIGURE 1.1 Compressibility factor for pure hydrocarbon gases.

For a gas mixture, the compressibility factor is a function of the pseudo-reduced temperature and pressure, which are calculated as:

$$T_{pr} = \frac{T}{T_{pc}} \text{ and } P_{pr} = \frac{P}{P_{pc}} \quad (1.14)$$

where  $T_{pc}$  and  $P_{pc}$  are the pseudocritical temperature and pressure, which are calculated from the following equations:

$$T_{pc} = \sum y_j T_{cj} \quad (1.15)$$

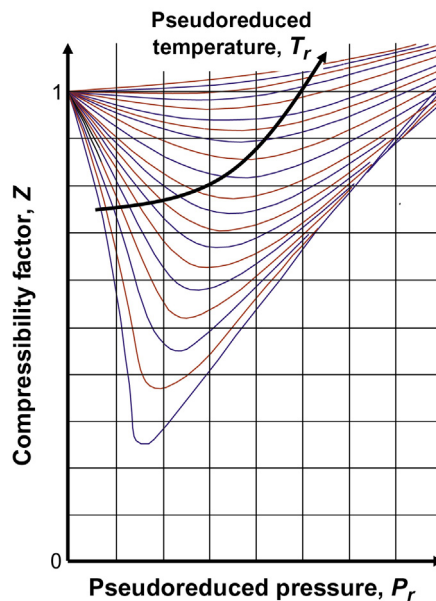
$$P_{pc} = \sum y_j P_{cj} \quad (1.16)$$

If the specific gravity of a gaseous mixture is known but not its composition, the following equations can be used to calculate the pseudoreduced temperature and pressure as functions of the mixture specific gravity,  $\gamma$ :

$$T_{pc} = 170.491 + 307.344 (\gamma) \quad (1.17)$$

$$P_{pc} = 709.604 - 58.718 (\gamma) \quad (1.18)$$

The relationship between the compressibility factor of a mixture of gases and its pseudoreduced pressure and temperature is given in many reports from professional associations in the form presented in Fig. 1.2; see for example the work from [Standing and Katz \(1942\)](#).



■ FIGURE 1.2 Compressibility factor of natural gas mixtures.

Sometimes the mole fraction of each component in a mixture is not given but the composition of the mixture is expressed in terms of the mass or volume percentage of each component. In these cases, the mole fraction of each component must be computed to calculate the mixture properties, as shown in the following problems.

#### Problem 1.4

A natural gas mixture consists of 60% methane ( $C_1$ ), 20% ethane ( $C_2$ ), and 20% propane ( $C_3$ ) by weight. Calculate the apparent molecular weight and the specific gravity of the mixture.

#### Solution

The total mass of the mixture is assumed to be equal to 100 lbm. The mixture then has 60 lbm of methane, 20 lbm of ethane, and 20 lbm of propane. The number of moles of each component is obtained by dividing its mass by its corresponding molecular weight:

$$n_{C_1} = 60/16 = 3.75$$

$$n_{C_2} = 20/30 = 0.67$$

$$n_{C_3} = 20/44 = 0.45$$

$$\text{Total } N = 3.75 + 0.67 + 0.45 = 4.87$$

The mole fraction of each component is:

$$y_{C_1} = 3.75/4.87 = 0.77$$

$$y_{C_2} = 0.67/4.87 = 0.1375$$

$$y_{C_3} = 0.45/4.87 = 0.0924$$

The apparent molecular weight is then:

$$M_{\text{ap}} = 0.77(16) + 0.1375(30) + 0.0924(44) = 20.51 \text{ lbm / lbm - mole}$$

And the specific gravity is:

$$\gamma = 20.51 / 29 = 0.707$$

These calculations could have been done assuming 100 kg as the mass of the mixture, using the molecular weight of each component expressed in kg/kg-mole, which are numerically equal to the ones expressed in lbm/lbm-mol.

**Table 1.3** Compressibility Factors for Components C<sub>1</sub>, C<sub>2</sub> and C<sub>3</sub> in Problem 1.5

Component	$T_r$	$P_r$	$Z$
C <sub>1</sub>	2.2	3.72	0.963
C <sub>2</sub>	1.4	3.53	0.708
C <sub>3</sub>	1.14	4.06	0.585

**Problem 1.5**

A mixture consists of 60% methane, 20% ethane, and 20% propane by volume. Calculate the composition of the mixture in terms of the mole fraction if the mixture pressure is 2500 psia and its temperature 300°F. The critical properties are:

$$T_{cC_1} = 343.1 \text{ }^\circ\text{R}; P_{cC_1} = 667.8 \text{ psia}$$

$$T_{cC_2} = 549.8 \text{ }^\circ\text{R}; P_{cC_2} = 707.8 \text{ psia}$$

$$T_{cC_3} = 665.7 \text{ }^\circ\text{R}; P_{cC_3} = 616.3 \text{ psia}$$

**Solution**

The total volume of the mixture is assumed equal to 100 ft.<sup>3</sup> The number of moles of each component is calculated by:

$$n = \frac{PV}{ZR_u T}$$

The value of  $Z$  for each component can be obtained from graphs such as the one shown in Fig. 1.1, using the reduced pressure and temperature of each component (Table 1.3):

$$n_{C_1} = \frac{(2500 \text{ psia})(60 \text{ ft.}^3)}{(0.963) \left( 10.73 \frac{\text{psia} \cdot \text{ft.}^3}{(\text{lbm} \cdot \text{mole}) \cdot ^\circ\text{R}} \right) (760 \text{ }^\circ\text{R})} = 19.1 \text{ lbm} \cdot \text{mole}$$

$$n_{C_2} = \frac{(2500 \text{ psia})(20 \text{ ft.}^3)}{(0.708) \left( 10.73 \frac{\text{psia} \cdot \text{ft.}^3}{(\text{lbm} \cdot \text{mole}) \cdot ^\circ\text{R}} \right) (760 \text{ }^\circ\text{R})} = 8.66 \text{ lbm} \cdot \text{mole}$$

$$n_{C_3} = \frac{(2500 \text{ psia})(20 \text{ ft.}^3)}{(0.585) \left( 10.73 \frac{\text{psia} \cdot \text{ft.}^3}{(\text{lbm} \cdot \text{mole}) \cdot ^\circ\text{R}} \right) (760 \text{ }^\circ\text{R})} = 10.48 \text{ lbm} \cdot \text{mole}$$

The total number of moles is then:  $19.1 + 8.66 + 10.48 = 38.24$  moles, and the mole fractions are:

$$y_{C_1} = 19.1/38.24 = 0.499$$

$$y_{C_2} = 8.66/38.24 = 0.226$$

$$y_{C_3} = 10.48/38.24 = 0.274$$

### Problem 1.6

A diver fills his 80-L tank with air at 3000 psig and 15°C, and quickly submerges to a depth of 33.9 ft. in a lake where the water density is 62.4 lbm/ft.<sup>3</sup>. After 35 min, the pressure inside the air tank has decreased to 500 psig and the diver must go back to the surface. If the air temperature is assumed to be constant throughout the process, calculate the average air consumption flow rate in Mcf/D: (1) at standard conditions, and (2) at the diver's surrounding pressure. The air compressibility factor,  $Z$ , at 3000 psig is 0.995, at 500 psig  $Z$  is 0.98, and at the diver's depth  $Z$  is 1.

### Solution

The volume of the tank is  $(80 \text{ L})(0.0353 \text{ ft.}^3/\text{L}) = 2.82 \text{ ft.}^3$  and the absolute temperature is 15°C or 518.67°R. The water pressure gradient is 0.433 psi/ft. ( $= 62.4/144$ ), so that the absolute pressure surrounding the diver is: 1 atm (or 14.7 psia) at the surface plus the pressure due to the water column above the diver of  $[(33.9 \text{ ft.})(0.433 \text{ psi/ft.})]$ , which gives a surrounding pressure of 29.37477 psia.

At 3000 psig (condition "1") the air in the tank must follow  $P_1 V_1 = Z_1 n_1 R_u T_1$  and, for the same number of moles but at standard conditions,  $P_{st} V_{st_1} = n_1 R_u T_{st}$ . Dividing both expressions and solving for  $V_{st_1}$  (which is the volume the initial gas in the tank would occupy at standard conditions):

$$V_{st1} = \frac{P_1 T_{st}}{P_{st} T_1} \frac{1}{Z_1} V_1 = \frac{3014.7}{14.7} \frac{520}{518.67} \frac{1}{0.995} 2.82 = 582.7268 \text{ scf}$$

At 500 psig (final condition or condition "2") the air inside the tank would occupy a volume at standard condition equal to:

$$V_{st2} = \frac{P_2 T_{st}}{P_{st} T_2} \frac{1}{Z_2} V_2 = \frac{514.7}{14.7} \frac{520}{518.67} \frac{1}{0.98} 2.82 = 101.01 \text{ scf}$$

The gas consumed at standard conditions is then equal to  $582.7268 - 101.01 = 481.7150$  scf. And the consumption rate is then  $(481.7150 \text{ scf}/35 \text{ min})(1440 \text{ min/D})(\text{Mscf}/1000 \text{ scf}) = 19.81 \text{ Mscf/D}$ .

To know the consumption rate at diver's conditions, the volume that 481.7150 scf would occupy at 29.37477 psia and 518.67°R must be calculated:

$$V_{\text{at depth}} = \frac{P_{\text{st}}}{P_{\text{at depth}}} \frac{T_{\text{at depth}}}{T_{\text{st}}} \frac{1}{1} V_{\text{st}} = \frac{14.7}{29.37477} \frac{518.67}{520} 481.7150 = 240.4478 \text{ cf}$$

The air consumption rate at diver's conditions is then:

$$(240.4478 \text{ cf} / 35 \text{ min})(1440 \text{ min} / D)(\text{Mcf} / 1000 \text{ cf}) = 9.89 \text{ Mcf} / D$$

As it was indicated at the beginning of the chapter, natural gases can have components, like CO<sub>2</sub> or H<sub>2</sub>S, which are nonhydrocarbon substances that are usually known as “impurities.” The graph shown in Fig. 1.2 is not applicable to hydrocarbon gaseous mixtures with impurities in concentrations greater than 2%. In this case, the reduced pressure and temperature must be corrected by any of the procedures that can be found in the literature; see for example the work from [Wichert and Aziz \(1972\)](#).

Once the reduced pressure and temperature have been determined from Eq. 1.14, using for that purpose the pseudocritical temperature and pressure obtained from the composition of the gas (Eqs. 1.15 and 1.16 without the impurities) or from the correlations given in terms of the specific gravity of the mixture (Eqs. 1.17 and 1.18 also without the impurities), their values are adjusted with the use of expressions of the following form:

$$T'_{pc} = T_{pc} + E \quad (1.19)$$

$$P'_{pc} = f(T_{pc}, T'_{pc}, P_{pc}, E, B) \quad (1.20)$$

Where:

$$E = g(A, B) \quad (1.21)$$

Functions  $f$  and  $g$  are simple polynomial equations, while  $B$  is the H<sub>2</sub>S mole fraction and  $A$  is the sum of the CO<sub>2</sub> and H<sub>2</sub>S mole fractions. These mole fractions are expressed from 0–1 and not as percentages. With these corrected pseudocritical values, the pseudoreduced pressure and temperature are calculated using Eq. 1.14 and then used in graphs, such as the one shown in Fig. 1.2, to find the compressibility factor of the mixture.

As a final point in this section, an expression for the gas formation volume factor,  $B_g$ , is developed. The gas formation volume factor is defined as the volume the gas occupies at in-situ conditions ( $V$ ), divided by the volume the same mass of gas occupies at standard conditions ( $V_{st}$ ). Because the number of moles multiplied by the universal gas constant must be a constant for any condition, the following expression is true for in situ and standard conditions:

$$nR_u = \frac{PV}{ZT} = \left( \frac{PV}{ZT} \right)_{st} \quad (1.22)$$

From which the formation volume factor can be solved:

$$B_g = \frac{V}{V_{st}} = \frac{P_{st}ZT}{T_{st}PZ_{st}} = \frac{(14.7 \text{ psi})ZT}{(520^\circ\text{R})P(1)} = 0.0283 \frac{ZT}{P} \quad (1.23)$$

Where  $T$  and  $P$  are the in situ conditions in  $^\circ\text{R}$  and psia, respectively, and  $Z$  is the gas compressibility factor at conditions  $P$  and  $T$ , calculated using the procedures described previously for pure substances or gaseous mixtures.

## 1.2 GAS VISCOSITY

There are several correlations that can be found in the literature to calculate the viscosity of a natural gas ( $\mu_g$  in centipoises) as a function of its temperature,  $T$ , in  $^\circ\text{R}$ , its molecular weight  $M$ , and its density  $\rho_g$ , in  $\text{gm}/\text{cm}^3$  at in-situ conditions (to convert  $\text{lbm}/\text{ft}^3$  to  $\text{gm}/\text{cm}^3$  divide by 62.4). The general form of these correlations is as follows:

$$\mu_g = F \exp(G\rho_g^H) \quad (1.24)$$

Where  $F$ ,  $G$ , and  $H$  are functions of several variables, for example:

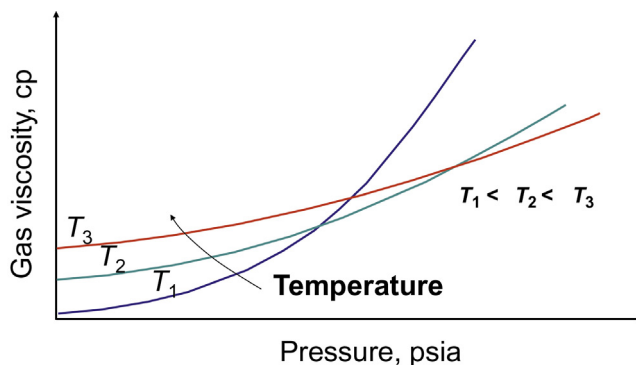
$$F = f(M, T) \quad (1.25)$$

$$G = g(M, T) \quad (1.26)$$

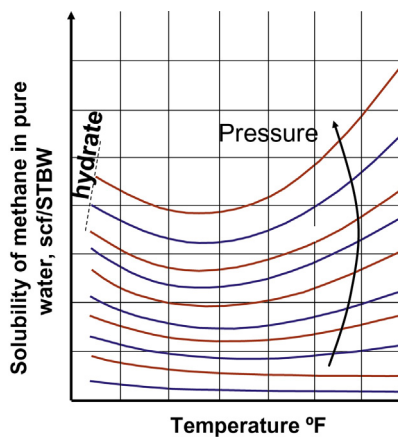
$$H = h(M, T) \quad (1.27)$$

One of the correlations most frequently used to find the viscosity of natural gases was developed by Lee et al. (1966). If the natural gas has  $\text{H}_2\text{S}$  and/or  $\text{CO}_2$ , the natural gas density is calculated using its compressibility factor found from the corrected pseudocritical properties.





■ FIGURE 1.3 Gas viscosity as a function of its pressure and temperature.



■ FIGURE 1.4 Solubility of methane in pure water, scf/STBW.

Fig. 1.3 shows a typical behavior of the gas viscosity as a function of its pressure and temperature.

### 1.3 SOLUBILITY OF NATURAL GAS IN WATER

Natural gas dissolves in water depending on the pressure and temperature of the phases. The relationship between pressure, temperature, and the solubility of methane in pure water is given in charts such as the one presented in Fig. 1.4; see for example the work of Culberson and McKetta (1951). The solubility of a natural gas is inversely proportional to its molecular weight. Methane is more soluble than ethane, ethane than propane, and so on. The solubility of methane in water can be used to estimate the solubility of a natural gas mixture in pure water with an accuracy of approximately 5%.

To account for the effect of water salinity, the result obtained from Fig. 1.4 must be adjusted by equations of the following form:

$$R_{sw} = R_{swp} (1 - aX_{sol}Y_{sol}) \quad (1.28)$$

Where  $R_{sw}$  is the gas solubility in brine in scf/(STBW),  $R_{swp}$  is the gas solubility in pure water found from charts such as the one shown in Fig. 1.4,  $Y_{sol}$  is the salinity of water in ppm, and  $X_{sol}$  is calculated by:

$$X_{sol} = b / T^c \quad (1.29)$$

Where  $T$  is the temperature in °F, and  $a$ ,  $b$ , and  $c$  are correlation parameters that must be found from experiments.

Fig. 1.4 can be used to find  $R_{swp}$  or, as a second alternative, the following equation can also be used:  $R_{swp} = A + B(P) + C(P^2)$ .  $P$  is the pressure in psia and:

$$A = a_1 + a_2(T) - a_3(T^2) \quad (1.30)$$

$$B = b_1 - b_2(T) + b_3(T^2) \quad (1.31)$$

$$C = c_1 + c_2(T) - c_3(T^2) \quad (1.32)$$

Again  $T$  is the temperature in °F and  $a_n$ ,  $b_n$ , and  $c_n$  are constants.

### Problem 1.7

Calculate how many scf of gas can be dissolved in brine containing 40,000 ppm at a pressure of 1,000 psia and a temperature of 300°F.

### Solution

From charts such as the one presented in Fig. 1.4, the solubility of gas in pure water at 1000 psia and 300°F is approximately 8 scf/STBW.

Using Eq. 1.29:

$X_{sol} = b/T^c = b/300^c$ , the numerical value is found for the appropriate values of  $b$  and  $c$ .

Then, using Eq. 1.28, the gas dissolved in brine is found as:

$$R_{sw} = R_{swp}(1 - aX_{sol}Y_{sol}) = 8[1 - aX_{sol}(40,000)]$$

and the numerical value is found from the appropriate value of  $a$ .

The solid content of water reduces the solubility of natural gas in brine (the value of  $1 - aX_{sol}40,000$  is less than unity). It is common to ignore

the gas dissolved in water while doing multiphase flow calculation in wells producing gas lift because its value is usually very small. ■

#### 1.4 SOLUBILITY OF WATER VAPOR IN NATURAL GAS

The amount of water vapor that can be present in a natural gas mixture depends on the temperature and pressure of the mixture, as well as on the salinity of water. It is very important to keep the water vapor content of natural gas at a value less than or equal to 7 lbm of water per each MMscf of the total gas mixture (natural gas plus water vapor) to avoid:

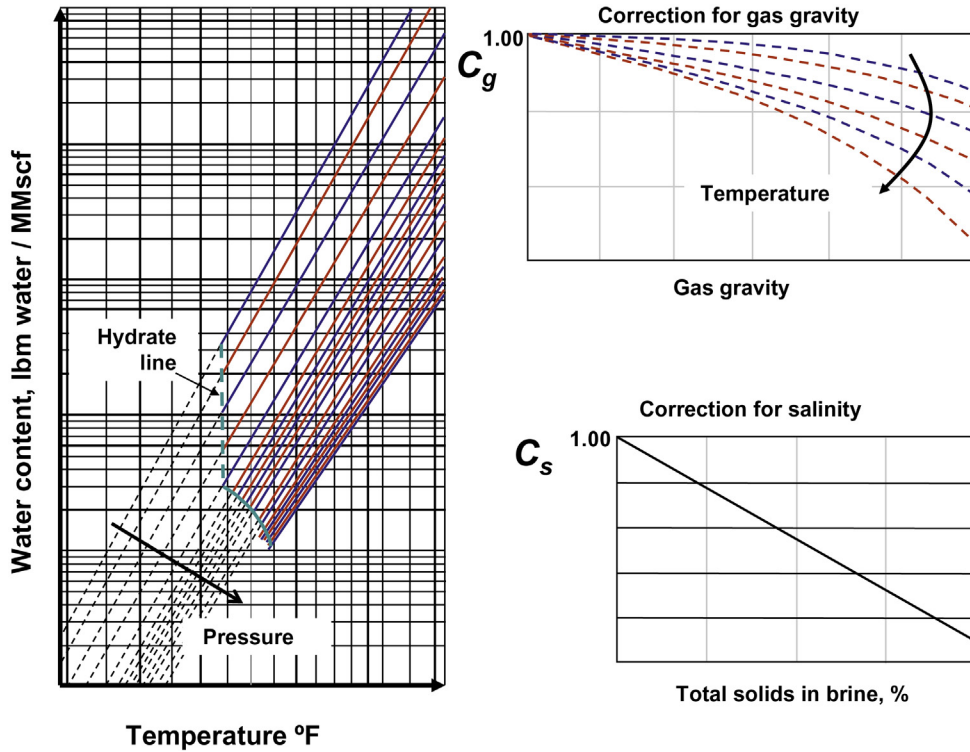
- hydrate formation
- problems measuring the injection gas flow rates
- corrosion
- high pressure drops in gas injection lines
- problems controlling the gas flow rate.

Charts like the one shown in Fig. 1.5 can be used to find the water content in pounds of water vapor per MMscf of total (water vapor plus hydrocarbon gas) “saturated” gas mixtures at any pressure or temperature; see for example the work of McKetta and Wehe (1958). The hydrate line shows the temperature at which hydrates will probably form at any given pressure for a gas with a specific gravity equal to the one for which the chart was constructed. Points to the left of this line represent the conditions at which hydrate will form. The chart cannot be completely accurate for all gases because the water content depends on the composition of the gas. The gas in the figure is saturated with water, thus any decrease in temperature at constant pressure will cause water condensation. For a given pressure and water content, the temperature corresponds to the dewpoint temperature. Because these charts usually correspond to a given specific gravity gas, the water content must be adjusted using the correction factor shown in the figure for other specific gravities. The same is true for the salinity.

Equations of the following form can be used to correct for water salinity:

$$W_s = W_{sp} [1 - a(Y_{wv}^b)] \quad (1.33)$$

Where  $W_s$  is the brine content in lbm/MMscf;  $W_{sp}$  is the water content from charts like the one shown in Fig. 1.5;  $Y_{wv}$  is the salinity of the water in ppm; and  $a$  and  $b$  are correlating parameters that must be obtained from experiments. As stated earlier, pipeline specifications usually require that the water vapor content of natural gas be 7 lbm/MMscf or less to minimize the problem of hydrate formation in pipelines.



■ FIGURE 1.5 Water vapor content of natural gas at saturation.

### Problem 1.8

A natural gas at 200 psia and 130°F has a water content of 10 lbm/MMscf of the total gas. If the pressure is kept constant, determine the temperature at which water will begin to condensate.

### Solution

It can be found in charts like the one shown in Fig. 1.5 that a gas at 200 psia and 130°F can hold up to almost 600 lbm of water vapor, so the gas is undersaturated. The 200 psia line intersects the horizontal water content line of 10 lbm/MMscf at a point in which the temperature is about 10°F, which represents the minimum temperature (for temperatures less than 10°F, water will begin to condensate). For a "saturated" gas at 200 psia and 130°F, lowering the temperature at constant pressure to 10°F will cause a condensation of a little less than  $(600 - 10) = 590$  lbm/MMscf. The volume of 590 lbm of liquid water is equal to 1.68 STB of water because the density of water at standard conditions is 350 lbm/STBW.

**Problem 1.9**

Show a way of finding the dewpoint curve for three different water contents using charts like the one shown in Fig. 1.5.

**Solution**

The dewpoint curve can be obtained as follows:

- On the chart, draw a horizontal line corresponding to a particular value of the water content  $W_s$ .
- Read the dewpoint temperatures for various pressures at the intersections of the horizontal line with each pressure line.
- Plot each pair of temperature and pressure on a semilog graph where the  $x$ -axis corresponds to the temperature and the  $y$ -axis corresponds to the pressure. This curve represents the dewpoint curve. If the condition of the gas falls to the left of this curve, water condensation will occur.

Thus, for water contents of 300, 200, and 100 lbm/MMscf, the results shown in Table 1.4 can be found from charts like the one shown in Fig. 1.5.

These pressures and temperatures are plotted as shown in Fig. 1.6. ■

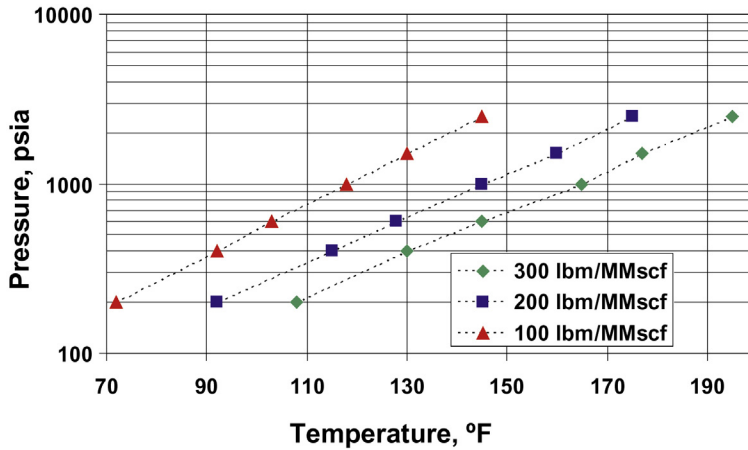
## 1.5 HYDRATES

Hydrates are solid crystals created by a reaction of natural gas with water at conditions that can be much greater than the freezing point of pure water. Hydrates are composed of approximately 10% hydrocarbons and 90% water.

If free water is present, hydrates will form when the gas temperature is less than the so-called “hydrate-formation temperature,” which depends on the

**Table 1.4** Presures and Temperatures for Each Water Content

300 lbm/MMscf		200 lbm/MMscf		100 lbm/MMscf	
T (°F)	P (psia)	T (°F)	P (psia)	T (°F)	P (psia)
195	2500	175	2500	145	2500
177	1500	160	1500	130	1500
165	1000	145	1000	118	1000
145	600	128	600	103	600
130	400	115	400	92	400
108	200	92	200	72	200



■ FIGURE 1.6 Dewpoint lines for each water vapor content of a natural gas.

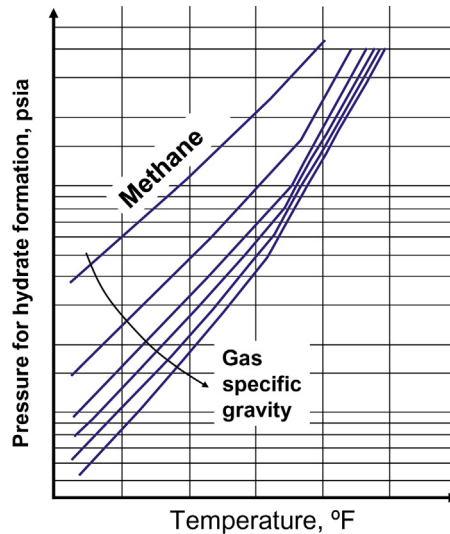
gas composition and its pressure. The hydrate-formation temperature should not be confused with the dewpoint temperature. The dewpoint temperature is the temperature at which water begins to condensate. In order for hydrates to form, it is necessary that free water be present. Therefore, the hydrate-formation temperature must be less than or equal to the dewpoint temperature. The dewpoint curve can be found from Fig. 1.5 as shown in problem 1.9.

Conditions that promote hydrate formation are:

- gas at a temperature less than or equal to its water dewpoint temperature (with free water present)
- low temperatures
- high pressures
- presence of  $H_2S$  and  $CO_2$ .

If the natural gas is saturated with water, part of the water vapor will condense if the temperature is reduced. As mentioned earlier, it is recommended not to exceed water content of 7.0 lbm/MMscf to avoid hydrate formation. Hydrates can form from two types of cooling effects: (1) due to heat transfer to the surroundings with no sudden pressure drop, such as in surface pipelines, and (2) due to a sudden expansion that takes place in orifices, back-pressure regulators, or chokes.

Graphs of the type shown in Fig. 1.7 can give approximate values of the hydrate-formation temperature as a function of pressure and specific gravity; see for example the work of Katz (1945). Hydrates will form whenever



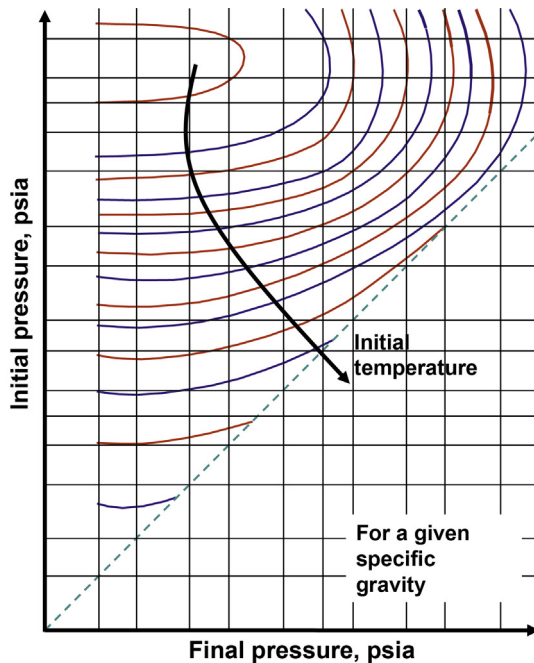
■ FIGURE 1.7 Pressure and temperature conditions for hydrate formation of sweet natural gases of different specific gravities.

temperature and pressure plot to the left of the hydrate-formation and water dewpoint curves for the specific gas being considered. This figure can be used in cases in which a gas is cooled along a pipeline. If the gas is saturated with water, the dewpoint temperature curve can be plotted on this graph.

Graphs of the type shown in Fig. 1.7 usually apply only to sweet natural gases, but it may be used as a guide for sour gases, keeping in mind that the presence of  $H_2S$  and  $CO_2$  will increase the hydrate temperature and reduce the pressure above which hydrates will form.

Sudden expansion in orifices, back pressure regulators, flow provers, or any other restriction along the gas injection lines, is accompanied by a temperature drop, which may cause hydrate formation. Charts like the one shown in Fig. 1.8 can be used to approximate the conditions for hydrate formation; see for example the work of Katz (1945). They were developed for sweet gases, but can be used as a guide for sour gases knowing that the presence of  $CO_2$  and  $H_2S$  will increase the minimum exit (or downstream) pressure and will increase the minimum initial (or upstream) temperature. These charts can be used in two ways:

- If the initial pressure and temperature are known, the charts can be used to predict the minimum downstream pressure of the gas at the exit of the restriction. A horizontal line is drawn from the initial pressure until it intersects the corresponding entrance (or initial) temperature.



■ FIGURE 1.8 Permissible expansion of a given specific gravity natural gas without hydrate formation.

From that intersection point, a vertical line is drawn downwards to the horizontal axis. The pressure that is read at the horizontal axis corresponds to the minimum final or exit pressure.

- If the upstream and downstream pressures are known, the minimum initial temperature can be found using these charts. The point with coordinates equal to the final and initial pressures is plotted on the graph. If the point lies on one of the minimum temperature curves, then that is the minimum temperature the gas must have at initial conditions. If the point lies between two minimum initial temperature curves, then the minimum temperature at the entrance must be interpolated between these two values.

### Problem 1.10

A 0.6-gravity gas is to be expanded from a pressure of 1000 psia at 80°F. Determine the minimum final pressure for no hydrate formation.

### Solution

From charts like the one shown in Fig. 1.8 for a 0.6-gravity gas, the intersection of the 1000 psi initial pressure (horizontal) line with the 80°F initial



temperature curve gives a final pressure of 340 psia. Therefore, lowering the pressure below 340 psia will probably result in hydrate formation if free water is present.

### Problem 1.11

A 0.6-gravity gas is to be expanded from 800 psia to 400 psia. Determine the minimum initial gas temperature to avoid hydrate formation.

### Solution

From charts like the one shown in Fig. 1.8 for a 0.6-gas gravity gas, the 800 psia initial pressure (horizontal) line intersects the 400 psia final pressure (vertical) line at an initial temperature of approximately 69°F. Therefore, if the gas at the entrance is cooler than 69°F, at 800 psia, hydrates may form if the gas is expanded to 400 psia and free water is present.

### Problem 1.12

A 0.6-gravity gas is to be expanded from a pressure of 800 psia at 110°F. Determine the minimum final pressure for no hydrate formation.

### Solution

From charts like the one shown in Fig. 1.8 for a 0.6-gravity gas, the 800 psi initial pressure (horizontal) line does not intersect the 110°F initial temperature curve. Hence, this gas may be expanded to atmospheric pressure without hydrate formation.

## 1.6 SPECIFIC HEAT RATIO

The partial derivative of the internal energy per unit mass,  $u_g$ , in Btu/lbm, with respect to the temperature,  $T$ , at a constant specific volume, is called specific heat at constant volume,  $C_v$ :

$$C_v = \left( \frac{\partial u_g}{\partial T} \right)_v \quad (1.34)$$

The partial derivative of the enthalpy per unit mass,  $h_g$ , in Btu/lbm, with respect to the temperature,  $T$ , at a constant pressure, is called specific heat at constant pressure,  $C_p$ :

$$C_p = \left( \frac{\partial h_g}{\partial T} \right)_p \quad (1.35)$$

The specific heat ratio,  $C_p/C_v$ , denoted here as  $k'$ , is an important variable used in the design of compressors and in calculations of the gas flow rate through orifices and flow control valves. Simple correlations that can be used to calculate the specific heat ratio are usually presented in the following form:

$$k' = \frac{a}{T^b} \quad (1.36)$$

Where  $T$  is the gas temperature in °R, and  $a$  and  $b$  are functions of the gas specific gravity. One example of this type of correlations was presented by Faires (1948).

## REFERENCES

- Brown, G.G., Katz, D.L., Oberfell, G.B., 1948. Natural Gasoline and Volatile Hydrocarbons. Natural Gasoline Association of America (N.G.A.A.), Tulsa, Okla.
- Culberson, O.L., McKetta, J.J., 1951. Solubility of methane in water at pressures to 10,000 psia. *J. Petrol. Tech.* 3, 223.
- Faires, V.M., 1948. *Applied Thermodynamics*. McMillan, New York.
- Katz, D.L., 1945. Prediction of conditions for hydrate formation in natural gases. *Trans. AIME* 160, 141–149.
- Lee, A.L., González, M.H., Eakin, B.E., 1966. The viscosity of natural gases. *J. Pet. Tech.*, 997–1000.
- McKetta, J.J., Wehe, A.H., 1958. Use this chart for water content of natural gases. *Pet. Refiner.* 37, 153.
- Standing, M.B., Katz, D.L., 1942. Density of natural gases. *Trans. AIME* 146, 140–149.
- Wichert, E., Aziz, K., 1972. Calculate  $Z$ 's for sour gases. *Hydrocarb. Process.* 51 (5), 119–122.

# Single-phase flow

Liquids and gas from the formation reach the flow station through a series of pipes, which are traditionally called the “production tubing” for the pipe that goes from the formation to the wellhead and the “flowline” for the pipe from the wellhead to the separator. Even though the production tubing is mostly vertical and the flowline is horizontal, it is possible to have production tubing strings with inclination angles from 0 to 90 degrees with respect to the vertical and flowlines with inclination angles from  $-90$  degrees (downward flow) to  $+90$  degrees (upward flow) with respect to the horizontal. From the separator, gases and liquids flow separately through gas and liquid gathering systems of different levels of complexity. On the other hand, the injection gas out of the compressor is transported to each well through a gas distribution system, which consists of the main gas lines, manifolds, and individual gas lines to each well. The injection gas can be injected down the annulus of the well and liquids produced up the production tubing or vice versa. There might be flow restrictions (intentionally or not), such as chokes or flow control valves, along any of the mentioned conduits. The design of a gas lift system requires then calculations of pressure drops in single-phase gas or liquid flows and in multiphase flow in pipes, annuli, and restrictions. The different equations and mathematical procedures for single-phase flows are presented in the chapter while multiphase flows are described in chapters: Multiphase Flow; Single and Multiphase Flow Through Restrictions.

## 2.1 SINGLE-PHASE GAS FLOW

In addition to the cases mentioned previously, single-phase gas flow is found in wells in which gas is injected down a pipe parallel to the production tubing or down the production tubing itself, or when gas flows alone up the production tubing when, for any unexpected reason, the injection gas is only being circulated (with no liquid production) through a gas lift valve, or a tubing hole, located above the reservoir static liquid level.

### 2.1.1 Static gas gradients in vertical pipes and annuli

In the great majority of cases in gas lift wells, gas is injected down the annulus between the casing and the production tubing. Typical production tubing nominal sizes are 2<sup>3</sup>/<sub>8</sub>, 2<sup>7</sup>/<sub>8</sub>, 3<sup>1</sup>/<sub>2</sub>, and 4 in. in diameter and the smallest casing size is usually 5<sup>1</sup>/<sub>2</sub> in. in diameter. Under these geometry configurations, frictional pressure drops are negligible even for very large gas flow rates and the bottomhole injection pressure is approximately equal to the surface gas pressure plus the hydrostatic pressure due to the weight of the gas column. The objective of the calculation procedures that are described next is to find a parameter, called the “gas pressure factor”, that gives the bottomhole pressure when it is multiplied times the surface gas pressure assuming that the frictional pressure drop is negligible. The expression being sought must then have the following form:

$$P_f = f_g P_s \quad (2.1)$$

$P_f$  is the bottomhole gas injection pressure,  $P_s$  is the surface gas injection pressure, and  $f_g$  is the gas pressure factor, which is a function of the surface injection pressure itself and the true vertical depth of the point where  $P_f$  is calculated. As it is explained in chapter: Gas Properties, the gas density can be calculated from:

$$\rho = \frac{P}{ZR_g T} \quad (2.2)$$

Where  $\rho$  is the gas density,  $P$  and  $T$  are, respectively, the absolute pressure and temperature of the gas,  $Z$  is the gas compressibility factor, and  $R_g$  is the universal gas constant,  $R_u$ , divided by the gas apparent molecular weight,  $M_{ap}$ . A differential change in pressure due to a differential change in depth can be expressed as:

$$dP = \rho \left( \frac{g}{g_0} \right) dX \quad (2.3)$$

Where  $X$  is the true vertical depth from the surface,  $g$  is the acceleration due to gravity equal to 32.174 ft./s<sup>2</sup>, and  $g_0$  is the proportionality constant equal to 32.174 (lbm-ft)/(lbf-s<sup>2</sup>). Introducing Eq. 2.2 in 2.3 yields:

$$dP = \left( \frac{P}{ZR_g T} \right) \left( \frac{g}{g_0} \right) dX \quad (2.4)$$

If oil field units are used and depth  $X$  is expressed in Mft., then:

$$dP(\text{psia}) = \left[ \frac{P(\text{psia})}{ZR_g \left( \frac{\text{lb-f-Mft.}}{^\circ\text{R-lbm}} \right) T(^\circ\text{R})} \right] \left[ \frac{g \left( \frac{\text{ft.}}{\text{s}^2} \right)}{g_0 \left( \frac{\text{lbm-ft.}}{\text{lb-f-s}^2} \right)} \right] dX(\text{Mft.}) \quad (2.5)$$

As mentioned earlier,  $R_g$  is equal to the universal gas constant,  $R_u$ , divided by the apparent molecular weight,  $M_{ap}$ , both given as:

$$R_u = 1544 \frac{\text{lb-f-ft.}^3}{\text{ft.}^2 \text{-(lb-mol)-}^\circ\text{R}} \cdot \frac{\text{Mft.}}{1000 \text{ ft.}} = 1.544 \frac{\text{lb-f-Mft.}}{(\text{lb-mol)-}^\circ\text{R}} \quad (2.6)$$

$$M_{ap} = \gamma_g M_a \left( \frac{\text{lbm}}{\text{lb-mol}} \right) \quad (2.7)$$

Where  $\gamma_g$  is the gas specific gravity and  $M_a$  is the molecular weight of air, which is approximately equal to 29 lbm/lb mol. Three different ways of integrating Eq. 2.3 are presented next.

*Variable gas temperature and fixed compressibility factor* The gas temperature can be approximated as a linear function of the true vertical depth with the following equation:

$$T = a + bX \quad (2.8)$$

Where  $a$  is a constant expressed in  $^\circ\text{R}$ ,  $b$  is another constant very similar, if not equal, to the geothermal temperature gradient in  $^\circ\text{R/Mft.}$ , and  $X$  is the true vertical depth in Mft.

If  $R'$  is defined as  $R_g g_0/g$ , and  $Z$  is considered a constant equal to the average compressibility factor along the depth of the well, Eq. 2.4 can then be integrated in the following way:

$$\int_{P_s}^{P_f} \frac{dP}{P} = \frac{1}{ZR'} \int_0^X \frac{dX}{(a + bX)} \quad (2.9)$$

Integrating Eq. 2.9 yields:

$$\ln(P_f) = \ln(P_s) + \frac{1}{ZR'b} \ln \left( \frac{a + bX}{a} \right) \quad (2.10)$$

This equation can be expressed as:

$$P_f = P_s \left( 1 + \frac{bX}{a} \right)^{\frac{1}{ZR'b}} \quad (2.11)$$

Factor  $f_g$  (for an average value of  $Z$ ) is then equal to:

$$f_g = \left(1 + \frac{bX}{a}\right)^{\frac{1}{2Rb}} \quad (2.12)$$

If  $Z = 0.895$ ,  $a = 540^\circ\text{R}$ ,  $b = 10^\circ\text{R/Mft.}$ , and  $\gamma_g = 0.727$ , the following expression is obtained for the gas factor  $f_g$ :

$$f_g = \left(1 + \frac{X}{54}\right)^{1.524} \quad (2.13)$$

This equation was developed for the conditions found in Lake Maracaibo gas lift field for cases in which the specific gas gravity was difficult to determine (the gas above the liquid during the liquid column generation period in intermittent gas lift, for example, is an unknown mixture of gas being produced from the formation and injection gas left from the previous injection cycle). It is important to indicate that factor  $b$  (corresponding to the geothermal gradient) is usually around  $15.6^\circ\text{R/Mft.}$  in Lake Maracaibo, but  $10^\circ\text{R/Mft.}$  gave more accurate results because the injection gas along the well's annulus is usually cooler due to its downward velocity.

### Problem 2.1

Calculate the injection pressures at 5000 ft. of depth for the following surface injection pressures: 500, 1000, 1500, and 2000 psig.

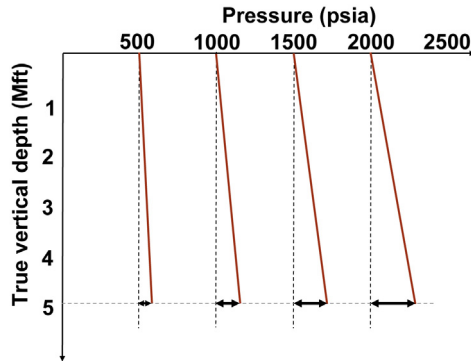
### Solution

With the value of  $X$  equal to 5 Mft., using Eq. 2.13 the gas factor  $f_g$  is found to be:

$$f_g = \left(1 + \frac{5}{54}\right)^{1.524} = 1.1444$$

The bottomhole pressure for 514.7 psia is  $1.1444 \times 514.7 = 589.02$  psia or 574.32 psig. In the same way, the bottomhole pressures for surface injection pressures of 1000, 1500, and 2000 psig are 1146.52, 1718.72, and 2290.92 psig, respectively.

These results are presented in Fig. 2.1, in which the pressure is plotted on the horizontal axis and the true vertical depth is plotted on the vertical axis (positive in the downward direction). It can be seen in the figure that as the surface injection pressure increases, the deviation angle of the gas pressure "line" with respect to the vertical also increases.



■ FIGURE 2.1 Bottomhole pressures calculated from the surface injection pressures.

Although Eq. 2.11 is not linear, the error made if the pressure distribution was treated as such is negligible. For example, if the surface injection pressure is equal to 1000 psia, the calculated pressures using this equation for 5,000 and 10,000 ft. of depth are 1144.4 and 1295.5 psia, respectively. But if the equation is assumed to be linear and the pressure at 5000 ft. is calculated from a linear interpolation between the calculated pressure at 10,000 ft. and the surface pressure, it would be the value of  $x$  in the following equation:

$$\frac{1295.5 - 1000}{10000} = \frac{x - 1000}{5000}$$

The value of  $x$  (the pressure at 5000 ft.) calculated from this interpolation is 1147.5 psia. The difference is 3.1 psia, which is an error of only 0.27%.

An increment in the accuracy of the calculated injection pressure at depth found from Eq. 2.11 can be obtained by using in Eq. 2.12 a new value of the gas compressibility  $Z$  (found from the average of the first calculated injection pressure at depth and the surface injection pressure) to modify the exponent in Eq. 2.13. For this operation, it is necessary to know the composition of the injection gas or, at least, its specific gravity.

*Variable temperature and compressibility factor* If the gas compressibility is not considered a constant, Eq. 2.4 can be integrated as:

$$\int_{P_s}^{P_f} \frac{dP}{P} = \frac{1}{R'} \int_0^X \frac{dX}{Z(a + bX)} \quad (2.14)$$

Again,  $R'$  is defined as  $R_g g_0 / g$ . The compressibility factor can be approximated as a linear function of depth by:

$$Z = A_z + B_z X \quad (2.15)$$

The following equations were derived by Zimmerman, 1982.  $A_z$  and  $B_z$  depend on the surface injection pressure  $P_s$  and the gas specific gravity  $\gamma_g$  in the following way:

$$A_z = 1.0009 + (3.6059 - 8.3492\gamma_g)10^{-4}(P_s) + (2.0677 - 6.5555\gamma_g + 6.0806\gamma_g^2)10^{-7}(P_s)^2$$

$$B_z = (3.4157\gamma_g - 1.3882)10^{-5}(P_s) + (2.5713\gamma_g - 2.3486\gamma_g^2 - 0.79398)10^{-8}(P_s)^2$$

The effect of temperature on  $Z$  is considered in Eq. 2.15 in the following way: the value of  $Z$  depends on  $X$  only because the gas temperature depends on depth. For a given gas specific gravity and surface injection pressure,  $A_z$  and  $B_z$  are constants that do not depend on depth, thus Eq. 2.14 can be integrated as explained next. If the following parameters are defined as  $A = a(A_z)$ ,  $B = a(B_z) + b(A_z)$ ,  $C = b(B_z)$ , and  $S_r = (B^2 - 4A \times C)^{1/2}$ , then Eq. 2.14 can be written as:

$$\int_{P_s}^{P_f} \frac{dP}{P} = \frac{1}{R'} \int_0^X \frac{dX}{(A + BX + CX^2)} \quad (2.16)$$

Integrating Eq. 2.16, the following result is obtained:

$$\ln(P_f) = \ln(P_s) + \frac{1}{R'S_r} \ln \left[ \frac{2CX(B + S_r) + B^2 - S_r^2}{2CX(B - S_r) + B^2 - S_r^2} \right] \quad (2.17)$$

Defining  $K_5 = 2C(B + S_r)$ ,  $K_6 = 2C(B - S_r)$ ,  $K_7 = 4AC$ , and  $m_g = 1/(R'S_r)$ ,  $f_g$  can be expressed as:

$$f_g = \left( \frac{K_5X + K_7}{K_6X + K_7} \right)^{m_g} \quad (2.18)$$

Again, the gas injection pressure at depth is found by multiplying the surface injection pressure by  $f_g$ . This equation has proved to be very accurate in wells with geothermal conditions similar to the ones existing in Lake Maracaibo and it can be easily adapted to other conditions.

### Problem 2.2

The injection opening pressure (at downhole operational conditions) of an injection-pressure-operated gas lift valve (described in chapters: Gas Lift Equipment; Gas Lift Valve Mechanics) at 10,000 ft. of depth is 1530 psig. The surface gas injection pressure is 1200 psia. Calculate the gas injection pressure at valve's depth and determine if the valve is opened or closed.



**Table 2.1** Parameters Needed in Eq. 2.18

Specific Gravity	0.65	0.82
$A_z$	0.8364	0.7244
$B_z$	0.008329	0.01314
$A$	459.05	397.59
$B$	17.61	18.51
$C$	0.1299	0.2049
$S_r$	8.47	4.09
$K_5$	6.78	9.27
$K_6$	2.37	5.91
$K_7$	238.59	326.01
$m_g$	1.44	3.79
$f_g$	1.25	1.37

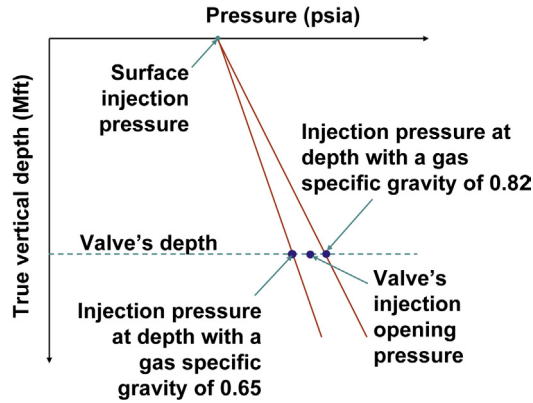
The gas specific gravity is not well known and its extreme possible values are asked to be investigated. These values are 0.65 and 0.82, for which the values of  $R'$  are 0.082 and 0.06446 (Mft.)/(°R), respectively. Assume a temperature distribution in Eq. 2.8 with  $a = 548.8$  °R and  $b = 15.6$  °R/Mft.

### Solution

Using the equations presented in this section, the following parameters are calculated for each gas specific gravity (Table 2.1).

For a gas specific gravity of 0.65, the gas injection pressure at depth is  $(1.25)(1200) - 14.7 = 1485.3$  psig, which is less than the valve's injection opening pressure, thus the valve should be closed. For a gas specific gravity of 0.82, the gas injection pressure at depth would be  $(1.37)(1,200) - 14.7 = 1629.3$  psig, which is greater than the valve's opening pressure, thus the valve should be opened for this specific gravity. Fig. 2.2 shows the effect of the gas specific gravity on the injection pressure at depth. Clearly, totally erroneous conclusions could be reached if the value of the gas specific gravity is not known.

*Iterative method with average temperature and pressure* An iterative method that is widely used consists in calculating first the average temperature between the surface temperature and the geothermal temperature at depth and assuming an initial average pressure throughout the depth of the well. Then, with these average temperature and pressure values, Eq. 2.4 is integrated with the depth in this case expressed in ft. (not in Mft.) and a gas compressibility  $Z_{\text{avg}}$  calculated at these initial average conditions of pressure and temperature:



■ FIGURE 2.2 Effect of the gas specific gravity.

$$\int_{P_s}^{P_f} \frac{dP(\text{psia})}{P(\text{psia})} = \frac{1}{Z_{\text{avg}} \left( 1544 \frac{\text{lb} \cdot \text{ft}}{(\text{lb} \cdot \text{mol})^\circ \text{R}} \right) \left( \frac{T_{\text{avg}} (\text{°R})}{\gamma_g 29 \frac{\text{lbm}}{\text{lb} \cdot \text{mol}}} \right)} \left( \frac{32.174 \frac{\text{ft}}{\text{s}^2}}{32.174 \frac{\text{lbm} \cdot \text{ft}}{\text{lb} \cdot \text{s}^2}} \right) \int_0^\ell dX(\text{ft}.)$$

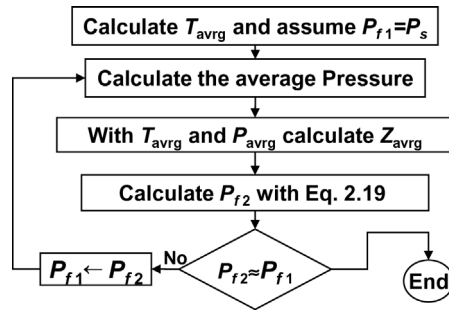
Where  $\ell$  is the true vertical depth in ft. After integrating the equation aforementioned, the following expression is obtained:

$$P_f = P_s \exp \left( \frac{0.01875 \gamma_g \ell}{Z_{\text{avg}} T_{\text{avg}}} \right) \quad (2.19)$$

Once the pressure at depth,  $P_f$ , is found in this way, a new average pressure, equal to  $(P_f + P_s)/2$ , is calculated and it can be used to determine a new value of  $Z_{\text{avg}}$  so that Eq. 2.19 can be used again to find a new value of  $P_f$ . This iteration process is repeated until  $P_f$  converges to a reasonably accurate value. This calculation procedure is easily understood with the help of the flow chart in Fig. 2.3.

### Problem 2.3

If the surface injection pressure is 1200 psia, determine the pressure at 10,000 ft. of depth using Eq. 2.19 with the same temperature distribution from Problem 2.2 and a gas specific gravity of 0.82. Compare the outcome of the iterations with the result obtained in Problem 2.2 for this gas specific gravity.



■ FIGURE 2.3 Calculation flow chart for the average pressure and temperature method.

### Solution

The temperature distribution is  $[88.8^\circ\text{F} + 15.6(\text{°R/Mft.})X(\text{Mft.})]$ . The temperature at depth is then  $244.8^\circ\text{F}$  or  $704.8^\circ\text{R}$  and the average temperature from the surface to 10,000 ft. of depth is  $626.8^\circ\text{R}$ . Using Eq. 2.19, the results shown in Table 2.2 are obtained.

The pressure at depth is then equal to  $1633.06 - 14.7 = 1618.36$  psig, which is 11 psig less than the result from Problem 2.2. This error is much smaller for shallower depths. As can be appreciated in the Table 2.2, the results that follow the second iteration do not change in a significant way.

## 2.1.2 Gas pressure gradients in vertical pipes considering frictional pressure drop

When gas is injected down a small diameter string, parallel to the production tubing, or down the production tubing to produce the liquids up the annulus, it is important to account for frictional pressure drop while doing troubleshooting analyses or mandrel-spacing calculations for the unloading valves. Frictional pressure drop also plays a major role along horizontal injection

**Table 2.2** Results of the Iterations

Iteration Number	Initial Average Pressure (psia)	Z Average	Calculated Pressure at Depth (psia)	Final Average Pressure (psia)
1	1200.00	0.820	1616.42	1409.21
2	1409.21	0.796	1632.59	1416.29
3	1416.29	0.796	1633.05	1416.52
4	1416.52	0.796	1633.06	1416.53

gas lines from the compressor's discharge to the wellhead and along gas gathering lines from the separator to the compressor's inlet, as explained in the next section. Additionally, if the well is circulating gas without liquid production, it is sometimes necessary to calculate the frictional pressure drop of the gas that is flowing up the production tubing.

When gas is in motion inside a pipe or an annulus, frictional pressure drops could become very large. The equation that can be used to calculate the total pressure drop in gas flow is derived from the first and second laws of thermodynamics. The first law of thermodynamics applied to a differential mass that moves in a small section  $dL$  of a pipe, under steady state condition, is given by:

$$dq_{\text{heat}} = dh_g + d(e_c) + d(e_p) \quad (2.20)$$

Where  $dq_{\text{heat}}$  is the heat per unit mass supplied to the gas,  $dh_g$  is the differential increment of the gas enthalpy per unit mass,  $d(e_c)$  is the differential increment of the gas kinetic energy per unit mass, and  $d(e_p)$  is the differential increment of the gas potential energy per unit mass. If  $g$  is the acceleration of gravity,  $V_g$  is the gas velocity,  $h_g$  is the gas enthalpy per unit mass,  $z$  is the elevation with respect to a reference point,  $\rho$  is the gas density, and  $u_g$  is the gas internal energy per unit mass, then the energy-balance equation in its differential form can be written in the following way (using the definition of  $h_g$  as  $u_g + P/\rho$ ):

$$d\left(\frac{P}{\rho}\right) + g dz + V_g dV_g + du_g - dq_{\text{heat}} = 0 \quad (2.21)$$

Expanding  $d(P/\rho)$  and rearranging terms:

$$\frac{dP}{\rho} + g dz + V_g dV_g + du_g + Pd\left(\frac{1}{\rho}\right) - dq_{\text{heat}} = 0 \quad (2.22)$$

It is known from the second law of thermodynamics that, for reversible or irreversible processes,  $du_g + Pd(1/\rho)$  is equal to the absolute temperature times the differential change of the entropy of the gas,  $Tds$ . That is:

$$\frac{dP}{\rho} + g dz + V_g dV_g + Tds - dq_{\text{heat}} = 0 \quad (2.23)$$

$Tds - dq_{\text{heat}}$  is equal to zero if the flow is reversible or greater than zero if it is irreversible.  $Tds - dq_{\text{heat}}$  represents then irreversible losses that are always greater than or equal to zero. The energy-balance equation can be written as:

$$\frac{dP}{\rho} + g dz + V_g dV_g + d(\text{losses}) = 0 \quad (2.24)$$

From elementary fluid mechanics, losses for a differential pipe length  $dL$  are defined as:

$$d(\text{losses}) = \frac{4f_F V_g^2}{2D} dL \quad (2.25)$$

Where  $f_F$  is the Fanning friction factor, which is the friction factor,  $f$ , found from the [Moody \(1944\)](#) diagram divided by 4, and  $D$  is the pipe inside diameter. The derivation of [Eq. 2.25](#) is presented in [Section 2.2.2](#) for single-phase, liquid flows, see [Eq. 2.107](#).

If [Eq. 2.24](#) is divided by the acceleration of gravity  $g$  and field units are used, then:

$$\frac{dP}{\rho(g/g_0)} + dz + \frac{V_g}{g} dV_g + \frac{4f_F V_g^2}{2gD} dL = 0 \quad (2.26)$$

Where  $g_0$  is 32.174 (lbm-ft.)/(lbf-s<sup>2</sup>). To integrate [Eq. 2.26](#), the following

substitutions should be made:  $V_g = \frac{\dot{m}}{A_t} v$ ,  $Q = \dot{m} v$ ,  $dV_g = \frac{\dot{m}}{A_t} dv$ ,  $\frac{dz}{dL} = \cos(\theta)$ ,  $v = \frac{R_u}{(M_a)\gamma_g} \frac{TZ}{P}$ , and  $dv = -\frac{R_u}{(M_a)\gamma_g} \frac{TZ}{P^2} dP$ .

Where  $\dot{m}$  is the mass flow rate, which is constant because the flow is under steady state condition,  $A_t$  is the cross-sectional area of the pipe,  $v$  is the gas specific volume,  $Q$  is the gas volumetric flow rate,  $\theta$  is the pipe angle with respect to the vertical,  $R_u$  is the universal gas constant,  $M_a$  is the air molecular weight,  $\gamma_g$  is the gas specific gravity,  $T$  is the absolute temperature,  $Z$  is the gas compressibility factor, and  $P$  is the absolute pressure.

Of all the previous substitutions, the last one is the key for the integration of the energy balance equation that is presented later, in which it is assumed that, for a differential pipe length  $dL$ , there is a differential change in the specific volume due to a differential change in pressure, while  $T$  and  $Z$  are treated as constants equal to their average values inside  $dL$ . The treatment given to variables  $v$ ,  $z$ ,  $T$ , and  $P$  is consistent with the numerical method of integration that is shown in this section to integrate the energy balance equation.

Introducing these substitutions into [Eq. 2.26](#) and with the appropriate unit conversions, it is found that the energy-balance equation can be integrated in the following way if field units are used:

$$\int_{P_1}^{P_2} \left[ \frac{\frac{P}{ZT} - 2.082 \frac{\gamma_g Q_{MM}^2}{d^4 P}}{2.6665 \frac{f_F Q_{MM}^2}{d^5} \pm \cos(\theta) \frac{(P/(TZ))^2}{1000}} \right] dp = -18.74203 \gamma_g L_{\text{pipe}} \quad (2.27)$$

Where  $Q_{MM}$  is expressed in MMscf/D,  $P$  in psia,  $T$  in °R, and  $d$  is the pipe inside diameter in inches. The term  $2.082\gamma_g Q_{MM}^2/(d^4 P)$  represents the acceleration pressure drop, which is usually very small and many times dropped in gas lift design calculations.

In Eq. 2.27,  $P_1$  is the inlet pressure in the flow direction and  $P_2$  is the outlet pressure.  $L_{\text{pipe}}$  is the total length of the pipe in feet. The term associated with  $\cos(\theta)$  is positive if the flow is in the upward direction and negative otherwise. Note that when the sign is negative, it is possible that the denominator becomes equal to zero (the gas pressure neither increases nor decreases with depth).

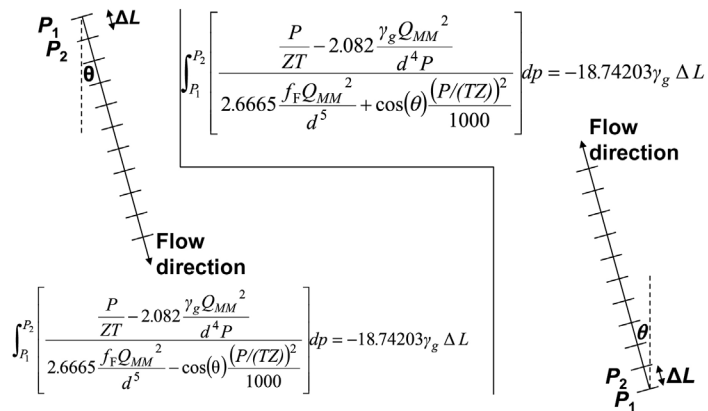
For the numerical integration of Eq. 2.27, the pipe is divided into small segments of length  $\Delta L$ , as shown in Fig. 2.4, and the integral can be solved using the trapezoidal rule with only two values, at the inlet and the outlet of the pipe segment. If  $I_n$  is the value of all terms inside the integral, the trapezoidal rule for one pipe segment establishes:

$$\frac{1}{2}(I_1 + I_2)(P_2 - P_1) = -18.74203\gamma_g \Delta L \tag{2.28}$$

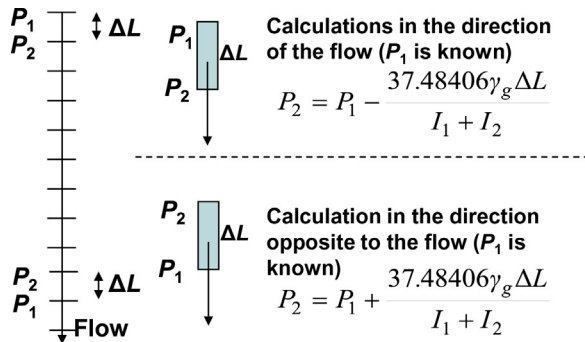
If the value of the inlet pressure  $P_1$  is known, the pressure at the exit  $P_2$  must be calculated so that  $I_2$  satisfies Eq. 2.28:

$$P_2 = P_1 - \frac{37.48406\gamma_g \Delta L}{I_1 + I_2} \tag{2.29}$$

If calculations are made in the opposite direction of the flow (because the outlet pressure is known but not the inlet pressure), and if the known pressure is now called  $P_1$ , Eq. 2.29 changes to Eq. 2.30, see Fig. 2.5.



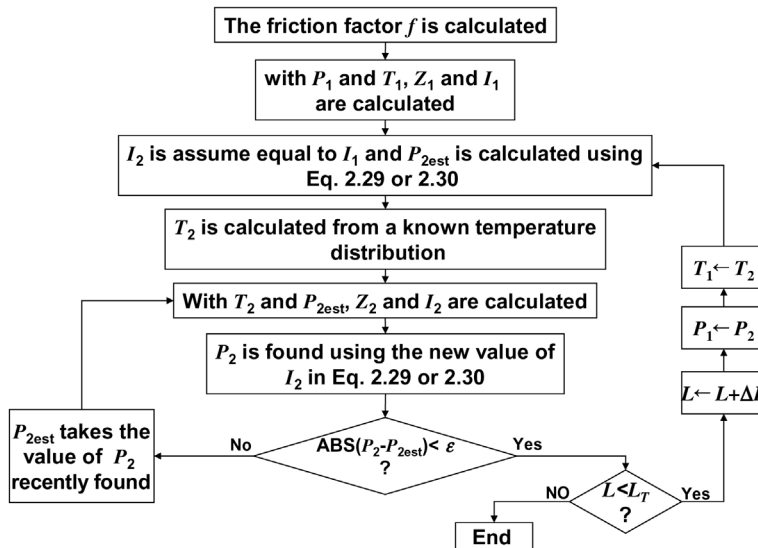
■ FIGURE 2.4 Sign of the  $\cos(\theta)$  term.



■ FIGURE 2.5 Direction of the calculation process.

$$P_2 = P_1 + \frac{37.48406\gamma_g \Delta L}{I_1 + I_2} \quad (2.30)$$

The iterative procedure that is used to find the pressure distribution along the entire pipe length is given in the flow chart presented in Fig. 2.6, in which  $P_{2\text{est}}$  is the estimated value of the unknown pressure for a particular segment,  $L_T$  is the total length of the pipe and  $\epsilon$  is a tolerance number given by the designer for the iteration on  $P_2$ .



■ FIGURE 2.6 Iterative method for calculating the pressure distribution along the pipe.

The friction factor,  $f_F$ , must be calculated for turbulent flow taking into consideration the value of the Reynolds number. The equations given earlier were developed for turbulent flow using the Fanning friction factor. For turbulent flow with small Reynolds number, the laminar layer is greater than the absolute roughness of the pipe and the friction factor depends on the Reynolds number but not on the pipe roughness. For this case, the friction factor can be found from the following equation:

$$\frac{1}{\sqrt{f_F}} = a \log_{10} (R_c \sqrt{f_F}) - b \quad (2.31)$$

Where  $R_c$  is the Reynolds number. Constants  $a$  and  $b$  must be found from experiments. When the Reynolds number is greater than a certain value, the friction factor does not depend on the Reynolds number but on the pipe roughness. For this case, the friction factor is found from the following equation:

$$\frac{1}{\sqrt{f_F}} = a \log_{10} (r_{\text{pipe}} / \varepsilon) + b \quad (2.32)$$

Where  $r_{\text{pipe}}$  is the pipe radius in inches and  $\varepsilon$  is the pipe absolute roughness also in inches. Constants  $a$  and  $b$  must be found from experiments. In most cases the absolute roughness can be approximated as being equal 0.0006 in.

The following equation, proposed by [Jain \(1976\)](#), is an explicit expression for  $f_F$  (for turbulent flow in general) that shows an acceptable level of accuracy and that can be used instead of the equations given earlier ([Eqs. 2.31 and 2.32](#)):

$$\frac{1}{\sqrt{f_F}} = 2.28 - 4 \log_{10} \left( \frac{\varepsilon}{2r_{\text{pipe}}} + \frac{21.25}{R_c^{0.9}} \right) \quad (2.33)$$

If the friction factor from the [Moody \(1944\)](#) diagram ( $f = 4f_F$ ) is used, the previous equation changes to:

$$\frac{1}{\sqrt{f}} = 1.14 - 2 \log_{10} \left( \frac{\varepsilon}{2r_{\text{pipe}}} + \frac{21.25}{R_c^{0.9}} \right) \quad (2.34)$$

The Reynolds number can be calculated from the following equation:

$$R_c = \frac{D(\text{ft.})V_g \left( \frac{\text{ft.}}{\text{s}} \right) \rho \left( \frac{\text{lbm}}{\text{ft.}^3} \right)}{\mu \left( \frac{\text{lbm}}{\text{ft.-s}} \right)} \quad (2.35)$$



$R_c$  is then dimensionless. Usually, the diameter of the pipe is expressed in inches and denoted as  $d$ , the velocity  $V_g$  is found in terms of the gas flow rate, the density  $\rho$  is determined from the equation of state, and the viscosity  $\mu$  is given in centipoise (cP). Therefore, the following steps must be taken to find the Reynolds number based on these variables. As described in chapter: Gas Properties, the density is found from:

$$\rho \left( \frac{\text{lbm}}{\text{ft}^3} \right) = \frac{29 \left( \frac{\text{lbm}}{\text{lbmol}} \right) \gamma_g P (\text{psia})}{Z \left( 10.73 \frac{\text{psia} \cdot \text{ft}^3}{\text{lbmol} \cdot ^\circ\text{R}} \right) T (^{\circ}\text{R})} = 2.7027 \frac{\gamma_g P}{ZT} \left( \frac{\text{lbm}}{\text{ft}^3} \right) \quad (2.36)$$

The gas velocity is equal to the in situ flow rate divided by the flow area,  $q_{\text{insitu}}/A_f$ . The in situ gas flow rate,  $q_{\text{insitu}}$ , is related to the gas flow rate at standard conditions,  $q_{\text{gsc}}$  in MMscf/D, in the following way:

$$\begin{aligned} q_{\text{insitu}} \left( \frac{\text{ft}^3}{\text{s}} \right) &= q_{\text{gsc}} \left( \text{MMscf/D} \frac{10^6 \text{ft}^3}{\text{MMscf}} \frac{1\text{D}}{24 \cdot 60 \cdot 60 \text{s}} \right) \frac{14.7 (\text{psia})}{P (\text{psia})} \frac{ZT (^{\circ}\text{R})}{520^{\circ}\text{R}} \\ &= 0.32719 \frac{q_{\text{gsc}} ZT}{P} \left( \frac{\text{ft}^3}{\text{s}} \right) \end{aligned} \quad (2.37)$$

The flow area  $A_f$  can be expressed as:

$$A_f (\text{ft}^2) = \frac{\pi}{4} \frac{d^2 (\text{in}^2)}{(144 \text{in}^2/\text{ft}^2)} = 0.005454 d^2 (\text{ft}^2) \quad (2.38)$$

The velocity is then equal to:

$$\begin{aligned} V_g \left( \frac{\text{ft}}{\text{s}} \right) &= \frac{q_{\text{gsc}} \left( \text{MMscfD} \frac{10^6 \text{ft}^3}{\text{MMscf}} \frac{1\text{D}}{24 \cdot 60 \cdot 60 \text{s}} \right) \frac{14.7 \text{psia}}{P (\text{psia})} \frac{ZT (^{\circ}\text{R})}{520^{\circ}\text{R}}}{\frac{\pi}{4} d^2 (\text{in}^2) / \left( 144 \frac{\text{in}^2}{\text{ft}^2} \right)} \\ &= 59.9891 \frac{q_{\text{gsc}} ZT}{d^2 P} \left( \frac{\text{ft}}{\text{s}} \right) \end{aligned} \quad (2.39)$$

Thus Eq. 2.35 can be written as:

$$\begin{aligned} R_c &= \frac{D (\text{ft}) V_g \left( \frac{\text{ft}}{\text{s}} \right) \rho \left( \frac{\text{lbm}}{\text{ft}^3} \right)}{\mu \left( \frac{\text{lbm}}{\text{ft} \cdot \text{s}} \right)} \\ &= \frac{d (\text{in}) \left( \frac{\text{ft}}{12 \text{in}} \right) 59.9891 \frac{q_{\text{gsc}} ZT}{d^2 P} \left( \frac{\text{ft}}{\text{s}} \right) 2.7027 \frac{\gamma_g P}{ZT} \left( \frac{\text{lbm}}{\text{ft}^3} \right)}{\mu (\text{cP}) 6.7197 \times 10^{-4} \left( \frac{\text{lbm}/(\text{ft} \cdot \text{s})}{\text{cP}} \right)} \end{aligned} \quad (2.40)$$

And after simplifying:

$$R_e = \frac{2.01 \times 10^4 q_{\text{gsc}} \gamma_g}{\mu d} \quad (2.41)$$

Where  $q_{\text{gsc}}$  is the gas flow rate in MMscf/D,  $d$  is the pipe inside diameter in inches, and  $\mu$  is the gas viscosity in cP.

Eq. 2.27 can be used for cases in which the gas flow rate is equal to zero and the pressure increment is due only to the weight of the gas column, as shown in the following equation:

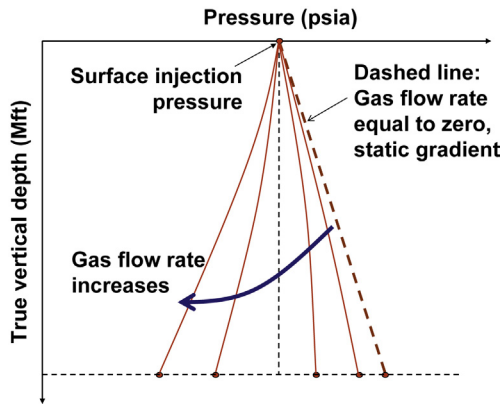
$$\int_{P_1}^{P_2} \left[ \frac{\frac{P}{ZT}}{\pm \cos(\theta) \frac{(P/(TZ))^2}{1000}} \right] dp = -18.7420 \gamma_g L_{\text{pipe}} \quad (2.42)$$

This equation is solved in exactly the same way it was shown previously for gas flow rates greater than zero.

In gas lift wells, gas is usually injected down the annulus between the production tubing and the casing. The gas flow rate injected in the great majority of cases is not large enough to cause significant frictional pressure drops, thus the injection pressure at depth is calculated as if the gas column was under static conditions. However, in some cases, frictional pressure drops in the annulus are not negligible and they must be calculated. The pressure at depth in annular flow can be calculated using Eq. 2.27 modifying the frictional pressure drop term to  $2.6665 \frac{f_F (d_2 + d_1) Q_{MM}^2}{(d_2^2 - d_1^2)^3}$ , where  $d_2$  is the casing inside diameter and  $d_1$  is the outside diameter of the production tubing. The effective diameter for annular spaces is assumed equal to  $d_2 - d_1$ . If the effective diameter is used, Eq. 2.32 for the friction factor changes to:

$$\frac{1}{\sqrt{f_F}} = a \log_{10} [(d_2 - d_1)/(2\varepsilon)] + b \quad (2.43)$$

The absolute roughness for annular flow should be greater than 0.0006 in., which is the assumed roughness for gas flow in circular pipes. In fact, it is difficult to determine the value of the absolute roughness to be used in annular flow because the production tubing outer surface is very irregular, with tubing couplings and mandrels, for which there is no experimental data to estimate the roughness to be used in Eq. 2.43. Some authors recommend using up to 0.001 in. for annular flow in oil wells.

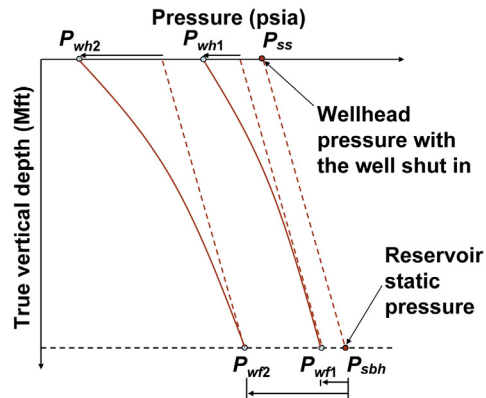


■ FIGURE 2.7 Effect of friction on the bottomhole injection pressure.

Frictional pressure losses should always be taken into consideration to determine if they are significant, especially when doing gas lift designs in wells in which, for some reason, the gas is injected down the production tubing or through a small diameter pipe that is parallel to the production tubing. Small-diameter parallel injection pipes are used in wells where the casing cannot withstand the high gas injection pressures or the injection gas might cause corrosion problems to the completion.

Fig. 2.7 shows the effect that friction losses have on the injection pressure at depth. Gas is injected at a constant surface injection pressure and, as can be appreciated in the figure, the greater the injection gas flow rate is, the lower the downhole gas injection pressure becomes. When the gas flow rate increases to very high values, the frictional pressure drop can even be greater than the increase in pressure due to the weight of the gas column. This effect makes it necessary for gas lift mandrels to be placed at shallower depths. Gas lift mandrel spacing is covered in chapter: Design of Continuous Gas Lift Installations.

Fig. 2.8 shows what happens in a gas well. If the well is shut in, the production wellhead pressure,  $P_{ss}$ , plus the weight of the gas column must be equal to the static reservoir pressure,  $P_{sbh}$  (unless a liquid column exists at the bottom of the well, in which case the surface pressure would be lower). In order for the well to produce gas, the bottomhole pressure should be lower than the static reservoir pressure,  $P_{sbh}$ . With a bottomhole flowing pressure equal to  $P_{wfl}$  in the figure, the corresponding wellhead pressure is  $P_{wh1}$  and the pressure distribution, represented by the solid curve, is clearly different from the pressure distribution for the well under static conditions shown by the dashed line next to the solid curve from  $P_{wfl}$ . This difference



■ FIGURE 2.8 Effect of friction in gas wells.

increases as the gas flow rate increases. To increase the gas flow rate, the bottomhole flowing pressure should be further reduced, as shown for  $P_{wf2}$ ; because the gas flow rate in this case is greater, the frictional pressure drop is larger, increasing the difference between the pressure distributions under flowing and static conditions. If the wellhead flowing pressure is as low as it can be for current surface-facility operational pressure, the only way to increase the gas flow rate is by installing a booster compressor at the wellhead or by using a larger production tubing diameter to reduce the frictional pressure drop. It might not be possible to increase the tubing diameter if the well produces some amount of liquids because the lower gas velocities might make the well load up with liquids; in this case, the liquid is usually removed with the use of metallic plungers as explained in chapter: Gas Lift Equipment.

Even though this book is not concerned with gas wells, it is necessary to explain the available tools to calculate the pressure distribution in upward gas flow because in many cases gas lift wells stop producing liquids and the injection gas is constantly being circulated up the production tubing. This could be due to a poor gas lift design, a cool or damaged unloading valve above the static liquid level that would not close, or a hole in the tubing, etc. These causes are analyzed in chapters: Continuous Gas Lift Troubleshooting; Intermittent Gas Lift Troubleshooting.

### 2.1.3 Gas flow in horizontal pipes

The hydrostatic and acceleration pressure drops are usually neglected in gas flow in horizontal pipes. Taking only frictional pressure drop into consideration, Eq. 2.26 can then be written in the following way:

$$\frac{dP}{dL} = -\frac{\rho f V_g^2}{2g_0 D} \quad (2.44)$$

Where  $f$  is the Moody friction factor, [Moody \(1944\)](#). Usually, the negative sign in [Eq. 2.44](#) is dropped because the pressure drop is considered to be positive in flow direction. If the density  $\rho$  is expressed in  $\text{lbm}/\text{ft}^3$ , the velocity  $V_g$  in  $\text{ft}/\text{s}$ , the diameter  $D$  in  $\text{ft}$ ., the length of the pipe  $L$  in  $\text{ft}$ ., and  $g_0$  is equal to  $32.2 \text{ (lbm ft.)}/(\text{lb f s}^2)$ , then the pressure  $P$  is expressed in  $\text{lb f}/\text{ft}^2$ . The following steps are taken to express the previous equation in the way it is usually presented for horizontal pipe flow.

First of all, the density can be expressed as:

$$\begin{aligned} \rho \left( \frac{\text{lbm}}{\text{ft}^3} \right) &= \frac{PM}{ZR_u T} = \frac{P(\text{psia})M \left( \frac{\text{lbm}}{\text{lb-mol}} \right)}{Z \left( 10.73 \frac{\text{psia-ft}^3}{(\text{lb-mol}) \cdot ^\circ \text{R}} \right) T(^{\circ} \text{R})} \\ &= \frac{P(\text{psia})29\gamma_g \left( \frac{\text{lbm}}{\text{lb-mol}} \right)}{Z \left( 10.73 \frac{\text{psia-ft}^3}{(\text{lb-mol}) \cdot ^\circ \text{R}} \right) T(^{\circ} \text{R})} \end{aligned} \quad (2.45)$$

Where  $P$  and  $T$  are the average absolute pressure and temperature in the pipe segment  $dL$ ,  $Z$  is the gas compressibility factor at the average temperature and pressure,  $M$  is the gas molecular weight, and  $\gamma_g$  is the gas specific gravity, equal to  $M/29$ , in which the air molecular weight is approximated as  $29 \text{ lbm}/(\text{lb mol})$ .

On the other hand, the in situ velocity can be expressed in terms of the in situ gas flow rate  $q_{MM\text{insitu}}$  and the flow area, using the following equation:

$$V_{\text{insitu}} \left( \frac{\text{ft.}}{\text{s}} \right) = \frac{q_{MM\text{insitu}} \left( \frac{\text{MMft}^3}{\text{D}} \right)}{\frac{\pi}{4} d^2 (\text{in.}^2) \left( \frac{1 \text{ft.}^2}{144 \text{in.}^2} \right)} \left( \frac{10^6 \text{ft.}^3}{1 \text{MMft}^3} \right) \left( \frac{1 \text{D}}{(24)(60)(60) \text{s}} \right) \quad (2.46)$$

The in situ gas flow rate can be expressed in terms of the gas flow rate at standard conditions,  $q_{\text{gsc}}$ , using the following equation:

$$q_{MM\text{insitu}} = q_{\text{gsc}} \left( \frac{\text{MMscf}^3}{\text{Day}} \right) \frac{14.7(\text{psia}) Z T(^{\circ} \text{R})}{P(\text{psia}) 520^{\circ} \text{R}} \quad (2.47)$$

Combining the two previous equations, the in situ velocity can be calculated from the following equation:

$$\begin{aligned}
 V_{\text{insitu}} \left( \frac{\text{ft.}}{\text{s}} \right) &= \frac{q_{\text{gsc}} \left( \frac{\text{MMscf}^3}{\text{D}} \right)}{\frac{\pi}{4} d^2 (\text{in.}^2) \left( \frac{1 \text{ft.}^2}{144 \text{in.}^2} \right)} \left( \frac{10^6 \text{ft.}^3}{1 \text{MMscf}^3} \right) \left( \frac{1 \text{D}}{(24)(60)(60) \text{s}} \right) \frac{14.7 (\text{psia}) Z T (^{\circ} \text{R})}{P (\text{psia}) 520^{\circ} \text{R}} \\
 &= 59.98917 \frac{q_{\text{gsc}} Z T \left( \frac{\text{ft.}}{\text{s}} \right)}{d^2 P} \quad (2.48)
 \end{aligned}$$

Introducing Eqs. 2.48 and 2.45, Eq. 2.44 can be written as:

$$\begin{aligned}
 \frac{dP}{dL} &= - \frac{f}{2d (\text{in.}) \left( \frac{1 \text{ft.}}{12 \text{in.}} \right) 32.2 \left( \frac{\text{lbm ft.}}{\text{lb f s}^2} \right)} \left[ \frac{P 29 \gamma_{\text{g}} \left( \frac{\text{lbm}}{\text{ft.}^3} \right)}{Z (10.73) T} \right] \left[ 59.98917 \frac{q_{\text{gsc}} Z T \left( \frac{\text{ft.}}{\text{s}} \right)}{d^2 P} \right]^2 \\
 &= -1812.34 \frac{(q_{\text{gsc}}^2) f \gamma_{\text{g}} Z T \left( \frac{\text{lb f / ft.}^2}{\text{ft.}} \right)}{d^5 P} \quad (2.49) \\
 &= -12.58 \frac{(q_{\text{gsc}}^2) f \gamma_{\text{g}} Z T}{d^5 P} (\text{psia / ft.})
 \end{aligned}$$

Assuming an average temperature, this equation can be integrated in the following way:

$$\int_{P_1}^{P_2} P dp = -12.58 \frac{(q_{\text{gsc}}^2) f \gamma_{\text{g}} Z T}{d^5} \int_0^L dL \quad (2.50)$$

Which gives the following result:

$$\frac{P_1^2 - P_2^2}{2} = 12.58 \frac{(q_{\text{gsc}}^2) f \gamma_{\text{g}} Z T L}{d^5} \quad (2.51)$$

This equation can be expressed in the following approximate way:

$$P_1^2 - P_2^2 = 25 \frac{(q_{\text{gsc}}^2) f \gamma_{\text{g}} Z T L}{d^5} \quad (2.52)$$

This equation was derived taking the base temperature and pressure equal to 520°R and 14.7 psia, respectively. But this equation can be solved for any base temperature and pressure,  $T_{\text{base}}$  and  $P_{\text{base}}$ , as:

$$q = \frac{C T_{\text{base}}}{P_{\text{base}}} \left[ \frac{P_1^2 - P_2^2}{\gamma f T Z L} \right]^{0.5} d^{2.5} \quad (2.53)$$

The value of  $C$  depends on the units used in the equation. Table 2.3 shows the values of  $C$  for different combinations of units that are frequently used. The units of the gas flow rate,  $q$ , will depend on the units used according to Table 2.3.

**Table 2.3** Values of  $C$  in Eq. 2.53 for Several Combinations of Units Used in the Equation

$P$	$T$	$d$	$L$	$q$	$C$
psia	R	in.	mi	scf/D	77.54
psia	R	in.	ft.	scf/D	5634
psia	R	in.	ft.	MMscf/D	$5.634 \times 10^{-3}$
KPa	K	m	m	$m^3/D$	$1.149 \times 10^6$

As can be seen in the following problem, if the pressure drop for a given gas flow rate is unknown, Eq. 2.52 or 2.53 are solved by an iteration procedure because the gas compressibility factor must be calculated for the average pressure (not known a priori) and temperature in the pipe. On the other hand, if the gas flow rate for a given pressure drop is unknown, the solution is also found by iteration because the friction factor,  $f$ , depends on the Reynolds number, which in turn depends on the gas flow rate which is unknown. This is shown in Problem 2.5.

### Problem 2.4

If the gas flow rate in a horizontal pipe is equal to 300 MMscf/D and the outlet pressure is 500 psia, find the required inlet pressure for the following data: Average temperature = 540°R; Gas specific gravity = 0.7; pipe diameter = 26 in.; pipe length = 80 miles = 422,400 ft.; pipe roughness = 0.0006 in.; gas viscosity = 0.0115 cP.

### Solution

To initiate the iterations, the inlet pressure can be estimated from the pressure drops that are usually found in horizontal pipe flow, which go from 0.0003 to 0.0006 psi/ft. The value of 0.0004 psi/ft. is taken as the pressure drop to begin calculations, so the inlet pressure,  $P_1$ , is equal to:

$$P_1 = P_2 + (0.0004 \text{ psi/ft.})(422,400 \text{ ft.}) = 670 \text{ psia approximately.}$$

The average pressure is then  $(670 + 500)/2 = 585$  psia.

To determine the gas compressibility factor,  $Z$ , the pseudocritical pressure and temperature are found first from Eqs. 1.17 and 1.18:

$$T_{pc} = 170.5 + 307.3 (\gamma_g) = 170.5 + 307.3 (0.7) = 385.61^\circ\text{R}$$

$$P_{pc} = 709.6 - 58.7 (\gamma_g) = 709.6 - 58.7 (0.7) = 668.51 \text{ psia}$$

The average pseudoreduced pressure and temperature,  $P_{pr}$  and  $T_{pr}$ , are calculated as:

$$P_{pr} = 585/668.51 = 0.875$$

$$T_{pr} = 540/385.61 = 1.4$$

From charts like the one shown in Fig. 1.2, the value of  $Z$  is found to be approximately equal to 0.89.

The Reynolds number can be calculated from the following equation:

$$R_e = \frac{20011\gamma_g q_{gsc}}{\mu d} = \frac{20011(0.7)(300)}{(0.0115)(26)} = 14.05 \times 10^6$$

The friction factor can be calculated with Eq. 2.34:

$$\frac{1}{\sqrt{f}} = 1.14 - 2 \log \left( \frac{\varepsilon}{d} + \frac{21.25}{(R_e)^{0.9}} \right) = 1.14 - 2 \log \left( \frac{0.0006}{26} + \frac{21.25}{(14.05 \times 10^6)^{0.9}} \right)$$

With this equation, the friction factor is found to be equal to 0.009688. With this last calculation, all the required parameters needed to calculate the inlet pressure with Eq. 2.52 have been found:

$$P_1^2 = P_2^2 + 25 \frac{(q_{gsc}^2) f \gamma_g Z T L}{d^5} = 500^2 + \frac{25(300)^2 (0.009688)(0.7)(0.89)(540)(422400)}{(26)^5}$$

Thus the initial value of  $P_1$  is equal to 714.64 psia.

With this new value of  $P_1$ , the average pressure in the pipe is  $(714.64 + 500)/2 = 607.32$  psia. The pseudoreduced temperature remains the same, but the new pseudoreduced pressure is  $607.32/668.51 = 0.908$ . Using charts like the one shown in Fig. 1.2, the new value of  $Z$  is 0.885 and, because the friction factor does not change, the new value of  $P_1$  is found from:

$$P_1^2 = P_2^2 + 25 \frac{(q_{gsc}^2) f \gamma_g Z T L}{d^5} = 500^2 + \frac{25(300)^2 (0.009688)(0.7)(0.885)(540)(422400)}{(26)^5}$$

This gives a new value of  $P_1$  equal to 713.61 psia, which is very similar to the pressure from the previous iteration and calculations can be stopped at this point. ■

### Problem 2.5

Calculate the gas flow rate in an 80-mile long pipe under the following conditions: average temperature = 540°R; inlet pressure = 713.61 psia; outlet pressure = 500 psia; gas specific gravity = 0.7; pipe diameter = 26 in.; Pipe roughness = 0.0006 in.; viscosity = 0.0115 cP; gas pseudocritical temperature = 385.61°R; gas pseudocritical pressure = 668.51 psia; gas compressibility factor = 0.885.



**Solution**

With the units in the third row of Table 2.3, Eq. 2.53 can be used in the following way:

$$q_{\text{gsc}} = \frac{5.634 \times 10^{-3} (520^\circ\text{R})}{(14.7 \text{ psia})} \left[ \frac{P_1^2 - P_2^2}{\gamma_g f T Z L} \right]^{0.5} d^{2.5}$$

The Reynolds number cannot be calculated because the gas flow rate is not known; therefore, the friction factor cannot be determined. For this reason, the gas flow rate must be found by iteration.

A first value of the friction factor of 0.01 is used to begin the iterations. The gas flow rate is then:

$$\begin{aligned} q_{\text{gsc}} &= 5.634 \times 10^{-3} \frac{520}{14.7} \left[ \frac{713.61^2 - 500^2}{(0.7)(0.01)(540)(0.885)(422400)} \right]^{0.5} 26^{2.5} \text{ MMscf/D} \\ &= 294.24 \text{ MMscf/D} \end{aligned}$$

With this flow rate, the Reynolds number can be calculated:

$$R_e = \frac{20110 \gamma_g q_{\text{gsc}}}{\mu d} = \frac{20011(0.7)(294.24)}{(0.0115)(26)} = 13.78 \times 10^6$$

With this Reynolds number the friction factor  $f$  is calculated using the following equation:

$$\frac{1}{\sqrt{f}} = 1.14 - 2 \log \left( \frac{\epsilon}{d} + \frac{21.25}{(R_e)^{0.9}} \right) = 1.14 - 2 \log \left( \frac{0.0006}{26} + \frac{21.25}{(13.78 \times 10^6)^{0.9}} \right)$$

From this equation  $f = 0.00969$ .

This value of  $f$  is used to calculate a new gas flow rate with:

$$\begin{aligned} q_{\text{gsc}} &= 5.634 \times 10^{-3} \frac{520}{14.7} \left[ \frac{713.61^2 - 500^2}{(0.7)(0.00969)(540)(0.885)(422400)} \right]^{0.5} 26^{2.5} \text{ MMscf/D} \\ &= 298.91 \text{ MMscf/D} \end{aligned}$$

With this gas flow rate, new values of the Reynolds number and the friction factor are calculated:

$$R_e = \frac{20110 \gamma_g q_{\text{gsc}}}{\mu d} = \frac{20011(0.7)(298.91)}{(0.0115)(26)} = 14 \times 10^6$$

$$\frac{1}{\sqrt{f}} = 1.14 - 2 \log \left( \frac{\varepsilon}{d} + \frac{21.25}{(R_e)^{0.9}} \right) = 1.14 - 2 \log \left( \frac{0.0006}{26} + \frac{21.25}{(14 \times 10^6)^{0.9}} \right)$$

$f$  is then equal to 0.009689 and the new gas flow rate is 298.92 MMscf/D, which is very similar to the gas flow rate from the previous iteration. ■

The previous problems illustrate the fact that iterations are needed to find the pressure drop or the gas flow rate. If the gas flow rate and pressure drop are known (which is usually the case in gas line designs) and it is desired to find the pipe diameter, it will still be necessary to iterate because the diameter should be known to calculate the Reynolds number and the friction factor. This has promoted the development of equations that can be used to find the friction factor,  $f$ , so that iterations are not necessary when calculating the pipe diameter or the gas flow rate. These equations can depend on the Reynolds number or the tubing diameter only. None of them depends on the pipe roughness.

The well-known [Weymouth \(1912\)](#) equation, for example, introduced the following equation to calculate the friction factor used in the [Moody \(1944\)](#) diagram:

$$f = \frac{0.032}{d^{1/3}} \quad (2.54)$$

Where  $d$  is the pipe inside diameter in inches.

With this simplification, [Eq. 2.53](#) changes to:

$$q_h = 18.062 \frac{T_{\text{base}}}{P_{\text{base}}} \left[ \frac{(P_1^2 - P_2^2) d^{16/3}}{\gamma_g TLZ} \right]^{0.5} \quad (2.55)$$

Where  $q_h$  is the gas flow rate in cubic feet per hour at the base pressure and temperature,  $P_{\text{base}}$  and  $T_{\text{base}}$ , respectively, while  $d$  is expressed in inches, the temperature in  $^{\circ}\text{R}$ , the pressure in psia, and  $L$  in miles. If the gas flow rate is expressed in  $\text{ft}^3/\text{D}$ , then the number “18.062” in the equation changes to “433.5.”

Another way of eliminating the iterative process for calculating the gas flow rate or the pipe diameter is achieved by using the so-called Panhandle A or B equations.

For Panhandle A equation, the friction factor is calculated from:

$$f = \frac{0.085}{R_e^{0.147}} \quad (2.56)$$

The equation for gas flow in pipes is then:

$$q = 435.87 \left( \frac{T_{\text{base}}}{P_{\text{base}}} \right)^{1.07881} \left( \frac{P_1^2 - P_2^2}{TLZ} \right)^{0.5394} \left( \frac{1}{\gamma} \right)^{0.4604} d^{2.6182} \quad (2.57)$$

$q$  is given in  $\text{ft}^3/\text{D}$  at  $T_{\text{base}}$  and  $P_{\text{base}}$  and all the other terms have the same units used in the Weymouth equation.

For Panhandle B, the friction factor is:

$$f = \frac{0.015}{R_e^{0.0392}} \quad (2.58)$$

The equation for gas flow in pipes is then:

$$q = 737 \left( \frac{T_{\text{base}}}{P_{\text{base}}} \right)^{1.02} \left( \frac{P_1^2 - P_2^2}{TLZ \gamma^{0.961}} \right)^{0.510} d^{2.530} \quad (2.59)$$

The units in this equation are the same ones used in [Eq. 2.57](#).

### Problem 2.6

Using the data for Problems 2.4 and 2.5, calculate the gas flow rate with the Weymouth, Panhandle B, and Panhandle A equations and compare the results with the one obtained from the general pipe flow equation. Data: inlet pressure = 713 psia; outlet pressure = 500 psia; pipe diameter = 26 in.; pipe length = 80 miles or 422,400 ft.; gas specific gravity = 0.7; average temperature = 540°R; gas compressibility factor = 0.885.

### Solution

Terms common to all equations are calculated first:

$$\frac{P_1^2 - P_2^2}{TZL} = \frac{713^2 - 500^2}{(540)(0.885)(80)} = 6.7579$$

$$\frac{T_{\text{base}}}{P_{\text{base}}} = \frac{520}{14.7} = 35.3740$$

Weymouth:

$$q = 433.5(35.374)(6.7579)^{0.5} \left( \frac{1}{0.7} \right)^{0.5} (26)^{2.667} = 282985415 \frac{\text{ft}^3}{\text{D}} = 282.99 \text{ MMscf/D}$$

Panhandle B:

$$q = 737(35.374)^{1.02}(6.7579)^{0.51} \left( \frac{1}{0.7} \right)^{0.49} (26)^{2.53} = 335825656 \frac{\text{ft}^3}{\text{D}} = 335.83 \text{ MMscf/D}$$

Panhandle A:

$$q = 435.87(35.374)^{1.0788} (6.7579)^{0.5394} \left(\frac{1}{0.7}\right)^{0.4604} (26)^{2.618} = 341503386.1 \frac{\text{ft.}^3}{\text{D}}$$

$$= 341.5 \text{ MMscf/D}$$

As can be seen, the results do not coincide for any of the equations used and they are different from the 300 MMscf/D obtained from the more rigorous equation used in Problems 2.4 and 2.5. If 300 MMscf/D is assumed to be the correct value, then the Weymouth equation must be multiplied by an efficiency factor equal to 1.06, while the Panhandle B and A should be multiplied by 0.893 and 0.878, respectively. It is difficult to know which of these equations should be used. Panhandle A equation is usually recommended for Reynolds number in the transition region and Panhandle B for totally turbulent flows. ■

In general, if the pipe roughness is known, Eq. 2.53 is recommended for finding the gas flow rate. But even for the most rigorous procedures, it is possible that some restrictions caused by liquids or solid depositions make it necessary for Eq. 2.53 to be multiplied by an efficiency factor  $E'$  that would take care of these flow restrictions. Table 2.4 can be used to estimate the efficiency factors for three different liquid contents.

As can be seen in Table 2.4, the presence of liquids in the gas can significantly reduce the gas flow rate for a given pressure drop in a gas pipe. This is very important in gas lift fields because the available injection pressure at the wellhead should be close to the one considered in the design of the gas lift completion. It is not unusual to find gas lift fields with large pressure drops along the gas injection lines caused by liquid accumulation or solid depositions (such as hydrates or debris).

When the pipe's inlet and outlet are at different elevations, the equations for "horizontal" gas flow in pipes (with some modifications) can be used with a reasonable level of accuracy. For this purpose, Eq. 2.19 can be used as one of the different available alternatives to add or subtract the gas column weight

**Table 2.4** Efficiency Factors for Different Liquid Contents

Type of Gas	Liquid Contents, gal/MMcf	$E'$
Dry gas	0.1	0.925
Associate gas	7.5	0.775
Condensate	800	0.65

caused by the difference in elevation. This pressure correction can be made for the entrance or the exit pressure. The approximation consists in treating the problem as if the flow was totally horizontal, calculating the pressure drop for the entire length of the pipe but modifying the exit or entrance pressure by adding or subtracting the hydrostatic pressure, depending on the elevation difference. To illustrate this approximate method, Eq. 2.53 can be written as:

$$q = \frac{CT_{\text{base}}}{P_{\text{base}}} \left[ \frac{P_1^2 - P_2'^2}{\gamma_g fTZL} \right]^{0.5} d^{2.5} \quad (2.60)$$

$P_2'$  is the outlet pressure if the pipe was horizontal and  $L$  is the total length of the pipe, not the horizontal length. Because there is an elevation difference, pressure  $P_2'$  can be calculated using Eq. 2.19:

$$P_2' = P_2 \exp\left(\frac{0.01875\gamma_g \ell}{ZT}\right) \quad (2.61)$$

Where  $\ell$  is the outlet minus the inlet elevation (referred to some arbitrary point). If the outlet of the pipe is below the inlet,  $\ell$  is negative. In this way the hydrostatic pressure is subtracted from the real pressure  $P_2$  to change it to the pressure that would exist at the exit of the pipe if it was horizontal. Eq. 2.53 is then equal to:

$$q = \frac{CT_{\text{base}}}{P_{\text{base}}} \left[ \frac{P_1^2 - P_2^2 \exp\left(\frac{0.0375\gamma_g \ell}{ZT}\right)}{\gamma_g fTZL} \right]^{0.5} d^{2.5} \quad (2.62)$$

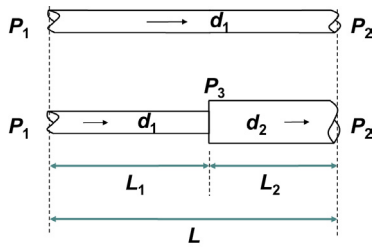
If the correction is made for the entrance pressure, it is then calculated as:

$$P_1' = P_1 \cdot \exp\left(-\frac{0.01875\gamma_g \ell}{ZT}\right) \quad (2.63)$$

A more rigorous equation to calculate the gas flow rate when there is an elevation difference is given as:

$$q = \frac{CT_{\text{base}}}{P_{\text{base}}} \left\{ \frac{P_1^2 - P_2^2 \cdot \left[ \exp\left(\frac{0.0375\gamma_g \ell}{ZT}\right) \right]}{\gamma_g fTZ \left[ \exp\left(\frac{0.0375\gamma_g \ell}{ZT}\right) - 1 \right] L} \left( \frac{0.0375\gamma_g \ell}{ZT} \right) \right\}^{0.5} d^{2.5} \quad (2.64)$$

In a gas lift field, it might be necessary to modify the gas flow rate through gas injection lines while keeping the pressure drop at constant levels.



■ FIGURE 2.9 Pipes in series.

For example, the number of wells that are connected to the main gas lines of the gathering system could increase with time. It is also possible that, due to a decrease in the reservoir pressure, the separator pressure should be reduced to lower the production wellhead pressure. This pressure reduction increases the gas velocity and, in consequence, the frictional pressure drop is also increased. To solve these problems, it is necessary to modify the capacity of the gas gathering lines to handle larger gas flow rates at fixed pressure conditions or the same gas flow rate at different pressures. On the other hand, if new compressors are installed in the field, the main gas distribution lines should also be somehow modified to handle the increase in the injection gas flow rate, keeping the injection pressure at the wellhead unchanged.

Increasing the gas handling capacity of a gas line does not necessarily mean replacing the entire line. There are three more economical ways of achieving this goal: (1) Replace only one section of the gas line by another of a larger diameter, (2) Connect an additional line in parallel along the entire length of the old line or only along part of it (this is called “looping”), or (3) a combination of the two previous solutions. The first solution implies the use of different lines in series. Fig. 2.9 shows a pipe with inside diameter  $d_1$  and length  $L$ . A portion of this line is replaced with a pipe with inside diameter  $d_2$  and length  $L_2$ , which leaves essentially two different lines in series. Usually, the larger diameter pipe is installed at the exit end of the line because that is where gas velocities are larger due to the lower pressure of the gas flow.

An approximate way of calculating the increase in the gas flow rate when part of the line is replaced by a larger diameter pipe is presented next.

If the pressure drop,  $P_1 - P_2$ , is kept constant, the task is then to find the increase in the gas flow rate that can be handled by the use of a larger diameter pipe segment. Eq. 2.55 can be written as:

$$q = k' \left( \frac{d^{16/3}}{L} \right)^{0.5} \quad (2.65)$$

The length  $L$  is then found from:

$$L = k \frac{d^{16/3}}{q^2} \quad (2.66)$$

This equation states the fact that, to sustain a given gas flow rate for a fixed pressure drop, the length of the line is proportional to its diameter raised to 16/3. In other words, if the pipe diameter is increased, the distance the gas

can travel for the same pressure drop and gas flow rate is also increased. Therefore, the equivalent length  $L'_1$  of a pipe with diameter  $d_1$  that would have the same pressure drop found in a pipe with diameter  $d_2$  and length  $L_2$  is given by:

$$\frac{L'_1}{L_2} = \left(\frac{d_1}{d_2}\right)^{16/3} \quad \text{or} \quad L'_1 = L_2 \left(\frac{d_1}{d_2}\right)^{16/3} \quad (2.67)$$

And the pipes in series shown in the figure would have an equivalent length,  $L_{\text{1eq}}$ , equal to:

$$L_{\text{1eq}} = L_1 + L'_1 = L_1 + L_2(d_1/d_2)^{16/3} \quad (2.68)$$

The gas flow rate through these pipes in series for a pressure drop  $P_1 - P_2$  and a given average temperature is calculated with this equivalent length using Eq. 2.55:

$$q_{\text{new}} = 18.062 \frac{T_{\text{base}}}{P_{\text{base}}} \left[ \frac{(P_1^2 - P_2^2) d_1^{16/3}}{\gamma_g T (L_{\text{1eq}}) Z} \right]^{0.5} \quad (2.69)$$

This is only an approximation because the pressure and temperature distributions are affected by the pipe configuration (in Fig. 2.9, for example, it is not the same to install the pipe with diameter  $d_2$  at the entrance or at the exit, but the difference in the net effect is very small).

The gas flow rate before installing the larger diameter pipe segment is:

$$q_{\text{old}} = 18.062 \frac{T_{\text{base}}}{P_{\text{base}}} \left[ \frac{(P_1^2 - P_2^2) d_1^{16/3}}{\gamma_g T (L) Z} \right]^{0.5} \quad (2.70)$$

For the same pressure drop, average temperature, and gas specific gravity, the following equation gives an approximate value of the gas flow rate increase that can be expected by replacing part of the pipe as shown in the figure:

$$\Delta q\% = \frac{q_{\text{new}} - q_{\text{old}}}{q_{\text{old}}} \times 100 = \frac{(1/L_{\text{1eq}})^{0.5} - (1/L)^{0.5}}{(1/L)^{0.5}} \times 100 \quad (2.71)$$

### Problem 2.7

Five miles of a 15-mile long gas pipe with a constant inside diameter of 5 in. is replaced with a 7-in. diameter pipe. Calculate the approximate increase in the gas flow rate that can be achieved for the same pressure drop.

**Solution**

The equivalent length of the new 7-in. diameter section is:

$$L'_1 = 5 (5/7)^{16/3} = 0.831 \text{ miles}$$

And the equivalent length,  $L_{1\text{eq}}$  of the pipes in series is  $10 + 0.831 = 10.831$  miles. The increment in the gas flow rate is approximately calculated as:

$$\Delta q\% = \frac{(1/L_{1\text{eq}})^{0.5} - (1/L)^{0.5}}{(1/L)^{0.5}} \times 100 = \frac{(1/10.831)^{0.5} - (1/15)^{0.5}}{(1/15)^{0.5}} \times 100 = 17.68\%$$

Eq. 2.67 was derived using the Weymouth equation. If the pipes in series have different friction factors, the following equation can be obtained from Eq. 2.53 following the same steps used in the derivation of Eq. 2.67:

$$L'_1 = L_2 \left( \frac{f_2}{f_1} \right) \left( \frac{d_1}{d_2} \right)^5 \quad (2.72)$$

Where  $L'_1$  is the length of a pipe with diameter  $d_2$  and friction factor  $f_2$  equivalent to a pipe of diameter  $d_1$  with friction factor  $f_1$  and length  $L_1$ .

Calculation of  $P_3$  at the junction of two pipes with diameters  $d_1$  and  $d_2$  can be done with the simultaneous application of Eq. 2.55 and using the fact that the gas flow rate is the same for both pipes. For pipe  $L_2$  in Fig. 2.9:

$$q = 18.062 \frac{T_{\text{base}}}{P_{\text{base}}} \left[ \frac{(P_3^2 - P_2^2) d_1^{16/3}}{\gamma_g T (L_1') Z_{3-2}} \right]^{0.5} \quad (2.73)$$

For pipe  $L_1$  in the figure, the gas flow rate is:

$$q = 18.062 \frac{T_{\text{base}}}{P_{\text{base}}} \left[ \frac{(P_1^2 - P_3^2) d_1^{16/3}}{\gamma_g T (L_1) Z_{1-3}} \right]^{0.5} \quad (2.74)$$

Combining the two previous equations:

$$\frac{P_3^2 - P_2^2}{(L_1') Z_{3-2}} = \frac{P_1^2 - P_3^2}{(L_1) Z_{1-3}} \quad (2.75)$$

This equation can be solved by trial and error, changing the value of  $P_3$  until the equation is satisfied. Eq. 2.67 can be extended to three or more pipes in series, considering the fact that the gas flow rate through them is the same



and the total pressure drop is the sum of the pressure drop at each of the pipes in series. Applying Eq. 2.55 to three pipes in series for which the inlet pressure is  $P_1$  and the outlet pressure is  $P_4$ :

$$\begin{aligned} (P_1^2 - P_4^2) &= \frac{\gamma_g Z T q_1^2 P_{\text{base}}^2 L_{\text{eq}}}{(18.062)^2 T_{\text{base}}^2 d^{16/3}} \\ &= \frac{\gamma_g Z T P_{\text{base}}^2}{(18.062)^2 T_{\text{base}}^2} \left[ \frac{q_1^2 L_1}{d_1^{16/3}} + \frac{q_2^2 L_2}{d_2^{16/3}} + \frac{q_3^2 L_3}{d_3^{16/3}} \right] \end{aligned} \quad (2.76)$$

Where  $q_1$  is the total gas flow rate. Because  $q_1$ ,  $q_2$ , and  $q_3$  are each equal to  $q$ , the following equation is valid:

$$\frac{L_{\text{eq}}}{d^{16/3}} = \left[ \frac{L_1}{d_1^{16/3}} + \frac{L_2}{d_2^{16/3}} + \frac{L_3}{d_3^{16/3}} \right] \quad (2.77)$$

Where  $L_{\text{eq}}$  is the length of the pipe with a uniform diameter  $d$  equivalent to the length of the three pipes.

If Eq. 2.53 is used, following the steps explained earlier, it can be demonstrated that:

$$\frac{f L_{\text{eq}}}{d^5} = \left[ \frac{f_1 L_1}{d_1^5} + \frac{f_2 L_2}{d_2^5} + \frac{f_3 L_3}{d_3^5} \right] \quad (2.78)$$

Parallel lines also increase the gas flow rate capacity. In this case, for a constant pressure difference, the gas flow rate of two pipes in parallel is equal to  $q_1 + q_2$ , where  $q_1$  is the gas flow rate in the pipe with diameter  $d_1$  and  $q_2$  is the gas flow rate through the additional pipe with diameter  $d_2$ .  $q_2$  is then the net gas flow rate increment. The lengths of both lines are in this case equal to  $L$ . If Eq. 2.55 is used for a given differential pressure, then:

$$q = \text{Constant} (d^{16/3})^{0.5} = \text{Constant} (d^{8/3}) \quad (2.79)$$

The percent increment in the gas flow rate is then:

$$\Delta q\% = \frac{q_2}{q_1} \times 100 = 100 \left( \frac{d_2}{d_1} \right)^{8/3} \quad (2.80)$$

### Problem 2.8

A 15-mile long, 7-in. diameter pipe is connected in parallel to an existing 5-in. pipe of the same length. Calculate the percent increment in the gas flow rate that is achieved by using both lines in parallel.

**Solution**

$$\Delta q\% = \frac{q_2}{q_1} \times 100 = 100 \left( \frac{7}{5} \right)^{8/3} = 245.29\%$$

If the parallel lines are of different lengths but still connected at both ends, Eq. 2.79 changes to:

$$q = (\text{Constant})(d^{16/3}/L)^{0.5} = (\text{Constant})(d^{8/3}/L^{0.5}) \quad (2.81)$$

The percent increment in the gas flow rate is then:

$$\Delta q\% = \frac{q_2}{q_1} \times 100 = 100 \left( \frac{d_2}{d_1} \right)^{8/3} \left( \frac{L_1}{L_2} \right)^{0.5} \quad (2.82)$$

Where  $L_1$  is the length of the existing line and  $L_2$  is the length of the parallel line connected to both extremes of the initial line. For three or more lines connected in parallel, the total gas flow rate is the sum of the gas flow rate through each pipe and the pressure drop is the same for all pipes. Using the Weymouth equation, the following expression for the equivalent length is derived:

$$\begin{aligned} q &= \frac{18.062 T_{\text{base}}}{\sqrt{\gamma_g TZ} P_{\text{base}}} \left[ \frac{(P_1^2 - P_2^2) d^{16/3}}{L_{\text{eq}}} \right]^{0.5} \\ &= \frac{18.062 T_{\text{base}}}{\sqrt{\gamma_g TZ} P_{\text{base}}} (P_1^2 - P_2^2)^{0.5} \left[ \left( \frac{d_1^{16/3}}{L_1} \right)^{0.5} + \left( \frac{d_2^{16/3}}{L_2} \right)^{0.5} + \left( \frac{d_3^{16/3}}{L_3} \right)^{0.5} \right] \end{aligned} \quad (2.83)$$

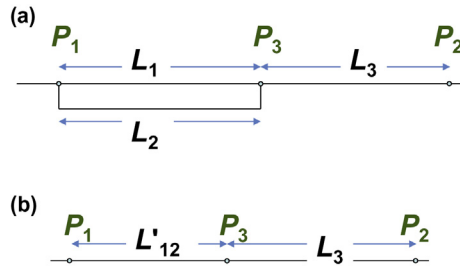
Where  $L_{\text{eq}}$  is the equivalent length a pipe with a diameter  $d$  would have for the same gas flow rate and pressure drop of the three pipes in parallel:

$$\left( \frac{d^{16/3}}{L_{\text{eq}}} \right)^{0.5} = \left( \frac{d_1^{16/3}}{L_1} \right)^{0.5} + \left( \frac{d_2^{16/3}}{L_2} \right)^{0.5} + \left( \frac{d_3^{16/3}}{L_3} \right)^{0.5} \quad (2.84)$$

If Eq. 2.53 is used instead of the Weymouth equation, a more general equation that takes into account the different friction factors each parallel pipe might have is given as follows:

$$\left( \frac{d^5}{fL_{\text{eq}}} \right)^{0.5} = \left( \frac{d_1^5}{f_1 L_1} \right)^{0.5} + \left( \frac{d_2^5}{f_2 L_2} \right)^{0.5} + \left( \frac{d_3^5}{f_3 L_3} \right)^{0.5} \quad (2.85)$$

Only part of the pipe might be connected in parallel to another pipe, as shown in Fig. 2.10. This arrangement is frequently found in gas lift fields



■ **FIGURE 2.10** Lines partially connected in parallel. (a) Line  $L_2$  partially connected in parallel to line  $L_1+L_3$  and (b) Line  $L'_{12}$  (equivalent to the parallel lines), connected in series to line  $L_3$ .

because of the increase in gas flow rate handling capacity it can provide at a very low cost.

As can be seen in Fig. 2.10, the lines partially connected in parallel can be shown as a system of lines in series, see Fig. 2.10b. The Weymouth equation for the lines in parallel establishes:

$$q = \text{Constant} \left( \frac{d^{16/3}}{L} \right)^{0.5} \quad (2.86)$$

From Eq. 2.84, lines  $L_1$  and  $L_2$  can be replaced with a single line of diameter  $d'_{12}$  and of equivalent length  $L'_{12}$ :

$$\left( \frac{d'^{16/3}_{12}}{L'_{12}} \right)^{0.5} = \left( \frac{d_1^{16/3}}{L_1} \right)^{0.5} + \left( \frac{d_2^{16/3}}{L_2} \right)^{0.5} \quad (2.87)$$

From which the equivalent length of the lines in parallel is:

$$L'_{12} = \frac{1}{\left[ \left( \frac{d_1}{d'_{12}} \right)^{8/3} \left( \frac{1}{L_1} \right)^{1/2} + \left( \frac{d_2}{d'_{12}} \right)^{8/3} \left( \frac{1}{L_2} \right)^{1/2} \right]^2} \quad (2.88)$$

The initial lines, section  $L_1$  and  $L_3$ , have the same diameter. If the equivalent diameter of the lines in parallel,  $d'_{12}$ , is chosen to be equal to the initial line diameter ( $= d_1 = d_3$ ) and if the length  $L_1$  is equal to  $L_2$ , Eq. 2.88 can be written as:

$$L'_{12} = \frac{1}{\left\{ \left( \frac{1}{L_1} \right)^{1/2} \left[ 1 + \left( \frac{d_2}{d_3} \right)^{8/3} \right] \right\}^2} \quad (2.89)$$

The ratio of the gas flow rate  $q$  that can be attained by the addition of the parallel section over the gas flow rate that could pass through the initial line  $q_0$  for the same pressure drop is given as:

$$\frac{q}{q_0} = \left( \frac{L_0}{L'} \right)^{0.5} \quad (2.90)$$

Where  $L_0$  is the initial pipe length, or  $L_1 + L_3$ , and  $L'$  is the equivalent length of the entire arrangement (once pipe  $L_2$  is connected), which is equal to  $L'_1 + L_3$ .

The percent increment in the gas flow rate obtained by installing  $L_2$  partially parallel to line  $L_1 + L_3$  is then:

$$\Delta q\% = 100 \left( \frac{q - q_0}{q_0} \right) = 100 \left[ \left( \frac{L_0}{L'} \right)^{0.5} - 1 \right] \quad (2.91)$$

### Problem 2.9

A 5-mile long, 7-in. diameter pipe is connected in parallel to the first 5 miles of a 15-mile long, 5-in. diameter gas line. Calculate the percent increment in the gas flow rate obtained by installing the additional pipe in parallel.

#### Solution

The equivalent length of the two pipes in parallel is:

$$L'_{12} = \frac{1}{\left\{ \left( \frac{1}{L_1} \right)^{1/2} \left[ 1 + \left( \frac{d_2}{d_3} \right)^{8/3} \right] \right\}^2} = \frac{1}{\left\{ \left( \frac{1}{5} \right)^{1/2} \left[ 1 + \left( \frac{7}{5} \right)^{8/3} \right] \right\}^2} = 0.419 \text{ miles}$$

The equivalent length of the parallel section in series with the rest of the pipe (section  $L_3 = 10$  miles) is then:

$$L' = 0.419 + 10 = 10.419 \text{ miles}$$

The gas flow rate ratio is then equal to:

$$\frac{q}{q_0} = \left( \frac{L_0}{L'} \right)^{0.5} = \left( \frac{15}{10.419} \right)^{0.5} = 1.19986$$

The percent increment in the gas flow rate is:

$$\Delta q\% = 100 \left( \frac{q - q_0}{q_0} \right) = 100 \left[ \left( \frac{15}{10.419} \right)^{0.5} - 1 \right] = 19.98\%$$

With 33% of the original pipe length connected in parallel to a second pipe, an almost 20% increase in the gas flow rate is achieved for the same pressure drop.

The following steps should be taken to find a relationship that can serve as the basis for generating graphs that would allow a practical determination of the increment in the gas flow rate obtained by the installation of lines partially connected in parallel:

Eq. 2.90 can be written as:

$$\frac{q}{q_0} = \left( \frac{L_0}{L'_{12} + L_3} \right)^{0.5} \quad (2.92)$$

This in turn can be rearranged to:

$$L'_{12} + L_3 = L_0 \left( \frac{q_0}{q} \right)^2 \quad (2.93)$$

Using Eq. 2.89 for  $L'_{12}$  gives:

$$\frac{1}{\left\{ \left( \frac{1}{L_1} \right)^{1/2} \left[ 1 + \left( \frac{d_2}{d_3} \right)^{8/3} \right] \right\}^2} + L_3 = L_0 \left( \frac{q_0}{q} \right)^2 \quad (2.94)$$

Defining  $W = (d_2/d_3)^{8/3}$  and because  $L_3 = L_0 - L_1$ , then:

$$\frac{L_1}{(1+W)^2} + L_0 - L_1 = L_0 \left( \frac{q_0}{q} \right)^2 \quad (2.95)$$

If the percentage of the existing line to which a parallel line is connected is  $Y_p = L_1/L_0$ , then:

$$\frac{Y_p}{(1+W)^2} + 1 - Y_p = \left( \frac{q_0}{q} \right)^2 \quad (2.96)$$

This can be expressed as:

$$Y_p = \frac{1 - \left( \frac{q_0}{q} \right)^2}{1 - 1/(1+W)^2} \quad (2.97)$$

The existing line diameter  $d_3$  is equal to  $d_0$ . If Eq. 2.53 is used instead of the Weymouth equation,  $W$  becomes  $(d_2/d_0)^{2.5}(f_0/f_2)^{0.5}$ , where  $f_0$  is the friction factor of the original line and  $f_2$  is the friction factor of the new line connected in parallel to the existing line.

Gas velocities in gas lines can sometimes be very large. It is important then to be aware of the maximum allowed gas velocity to avoid erosion of the pipe, especially in old installations with pipes that might fail and where, additionally, solid particles (which are the products of corrosion) can travel at high speeds. The problem could be serious for in situ velocities above 60 ft./s; however, it is very difficult to estimate the gas velocity at which erosion problems begin to occur. Despite the complexity of the problem, attempts have been made to calculate the erosion velocity, relating it to the density of the gas being transported, as given in the next equation:

$$V_e = C/\sqrt{\rho} \quad (2.98)$$

Where  $V_e$  is the erosion velocity (or maximum allowed velocity) in ft./s,  $\rho$  is the gas density in lbm/ft.<sup>3</sup> and  $C$  is a constant that could go from 70 to 160. Some experts have found  $C = 100$  to be appropriate for most practical cases. Knowing that the gas density (as indicated in chapter: Gas Properties) can be written as  $29P\gamma_g/(ZR_uT)$  and taking  $C$  equal to 100:

$$V_e = \frac{100}{\sqrt{29P\gamma_g/(ZR_uT)}} \quad (2.99)$$

Where  $Z$ ,  $P$ , and  $T$  correspond to the in situ conditions,  $R_u$  is the universal gas constant, and  $\gamma_g$  is the gas specific gravity. If  $q_{sc}$  is the gas flow rate at standard conditions, the previous equation can be written as:

$$q_{sc} = 1.86 \times 10^5 (A_t) \sqrt{\frac{P}{ZT\gamma_g}} \quad (2.100)$$

Where  $q_{sc}$  is expressed in Mscf/D,  $A_t$  is the flow area in ft.<sup>2</sup>,  $P$  is the lowest pressure found in the pipe in psia,  $T$  is the temperature in °R at the lowest pressure point in the pipe, and  $Z$  is the gas compressibility factor at  $P$  and  $T$ .

As much as it is true that the gas velocity cannot exceed the erosion velocity, it is equally important not to have very low velocities because they promote liquid accumulation at low points along the pipe. These liquids could cause pressure drops and corrosion of the pipe. When the gas flow rate is very low, or the pipe will remain close for a long period of time, it is recommended to periodically vent the gas line at reasonably high velocities to get rid of the liquids. In many gas lift fields, old gas lines are also periodically vented to

get rid of solid particles that might erode the pipe, cut gas lift valve seats, or not allow these valves to close.

### Problem 2.10

Determine the maximum gas flow rate that should be allowed through a production tubing string in a gas well of 2.875 in. in diameter to avoid erosion of the pipe under the following conditions: 700 psia of minimum pressure at a temperature of 150°F. The gas specific gravity is 0.65 and the gas compressibility factor is 0.9.

### Solution

$$q_{sc} = 1.86 \times 10^5 (A_t) \sqrt{\frac{P}{ZT\gamma_g}} = 1.86 \times 10^5 \left[ \frac{\pi \left( \frac{2.875}{12} \right)^2}{4} \right] \sqrt{\frac{700}{(0.9)(610)(0.65)}}$$

$$= 11744 \text{ Mscf/D}$$

Deciding the size of gas lines to be used in gas lift fields is a complex task. It is possible that the number of wells that would need gas injection during the first years of operation might be very small and it would not be a good decision, from an economic point of view, to install a large diameter pipe that will not be used to its full capacity for a long time. It is important then to know that the determination of the size of a gas line to be installed is not based solely on technical facts but also on economic considerations. But the economic concepts that are applied in the design of pipelines for transportation of natural gas to be used for domestic or industrial purposes are different from the ones handled by the design of gas lift fields, where the most important points are:

- The pressure drop from the compressor to the wellhead should be minimized to be able to place the point of injection as deep as possible in the well and to guarantee a stable operation. This is achieved by the correct selection of the injection gas line diameters and the adequate determination of the number and locations of main (or high pressure) manifolds and local manifolds from which gas lines are directed to individual wells.
- Gas lines also serve as storage volumes for high and low pressure injection gas. If these storage volumes are properly designed, injection, and gathering pressure fluctuations are minimized. These pressure fluctuations are caused by many factors: intermittent gas lift wells, wells that are suddenly shut in or put back in production, compressor shut downs or start ups, etc.

- Provide redundant connections of injection gas distribution to the wells and gas gathering lines from the well so that injection gas can be transported or gathered in different ways to and from the wells. In this manner, if a gas line fails or one compressor trips, the number of wells that cannot be kept in production is reduced.

## 2.2 SINGLE-PHASE LIQUID FLOW

Single-phase liquid flow is present in the production tubing below the gas injection point if the pressure is greater than the bubble point pressure. It is also found during the first stages of the unloading operation of a well that is filled with liquids that need to be taken out of the well. It is important then to be able to calculate static and dynamic liquid gradients for mandrel spacing and gas lift design in general.

Equations to calculate the pressure drop in single-phase liquid flow and pressure gradients in static liquid columns are presented in this section.

### 2.2.1 Static pressure gradient

There are situations in gas lift design and troubleshooting analyses in which it is important to know the pressure profile along a liquid column that is moving very slowly or not moving at all. This is what happens, for example, during the liquid column generation stage in intermittent gas lift. For this case, the bottomhole pressure at the operating valve's depth is equal to the wellhead pressure plus the hydrostatic pressures of the gas and liquid columns above the operating valve.

The bottomhole pressure of a static liquid column in a truly "vertical" pipe can be calculated from an equation identical to the one used for static gas columns given in [Section 2.1.1](#):

$$dP = \rho_L \left( \frac{g}{g_0} \right) dX \quad (2.3)$$

Where  $\rho_L$  is the liquid density in this case,  $X$  is the true vertical depth from the surface,  $g$  is the acceleration due to gravity equal to 32.174 ft./s<sup>2</sup>, and  $g_0$  is the proportionality constant equal to 32.174 (lbm ft.)/(lbf-s<sup>2</sup>). For a pipe with an inclination angle  $\theta$  with respect to the vertical, [Eq. 2.3](#) changes to:

$$dP = \rho_L \left( \frac{g}{g_0} \right) \cos(\theta) dX \quad (2.101)$$

Where  $X$  is the measured depth as opposed to the true vertical depth in [Eq. 2.3](#). In contrast to what happens in a gas column, [Eq. 2.101](#) is easily



integrated for a liquid column because the liquid density,  $\rho_L$ , is basically a constant. For an oil–water mixture, the mixture density is defined as:

$$\rho_L = w\rho_w + (1-w)\rho_o \quad (2.102)$$

Where  $w$  is the water cut, defined as the volume occupied by the water over the total volume occupied by the mixture,  $\rho_w$  is the water density, and  $\rho_o$  is the oil density. If this equation is divided by the water density, then the following equation is obtained:

$$\gamma_f = w\gamma_w + (1-w)\gamma_o \quad (2.103)$$

Where  $\gamma_o$  is the oil specific gravity,  $\gamma_w$  is the water specific gravity, which is a number very close to unity and can be approximated as such. Using the definition of the API gravity  $G_{API}$ , for which the oil specific gravity is equal to  $141.5/(131.5 + G_{API})$ , and assuming the specific gravity of water equal to unity, the density of the mixture of oil and water can be expressed as:

$$\rho_L = \rho_w \left[ w + (1-w) \left( \frac{141.5}{131.5 + G_{API}} \right) \right] \quad (2.104)$$

Introducing Eq. 2.104 in Eq. 2.101, and expressing the result in integral form:

$$\int_{P_s}^{P_f} dP = \rho_w \left[ w + (1-w) \left( \frac{141.5}{131.5 + G_{API}} \right) \right] \left( \frac{g}{g_0} \right) \int_0^L \cos(\theta) dX \quad (2.105)$$

Where  $P_s$  is the surface pressure,  $P_f$  is the bottomhole pressure, and  $L$  is the measured depth of the pipe (assuming it is completely filled with liquids). The integral on the right-hand side of the equation is then the true vertical depth,  $L_{tv}$ . The pressure at depth is then:

$$P_f = P_s + \rho_w \left[ w + (1-w) \left( \frac{141.5}{131.5 + G_{API}} \right) \right] \left( \frac{g}{g_0} \right) L_{tv} \quad (2.106)$$

If the water-oil mixture is homogeneous, the pressure distribution along the pipe is a linear function of the true vertical depth at each point. If, additionally, the pipe is straight (inclined or not), the pressure distribution along the pipe is also a linear function of the measured depth.

### Problem 2.11

A well has been shut in for a period of time long enough for the bottomhole pressure to be equal to the static reservoir pressure. The well is vertical and the liquid pressure gradient is 0.433 psi/ft. The depth of the perforations is

2000 ft. and the static reservoir pressure is 1100 psi. What is the depth of the liquid level if the wellhead pressure is equal to 600 psi? Use Eq. 2.13 to calculate the gas factor  $f_g$  in the gas column above the liquid.

### Solution

The bottomhole pressure (equal to 1100 psi) must be equal to the wellhead pressure plus the hydrostatic pressure exerted by the gas and the liquid columns. If  $X$  is the depth of the liquid level in Mft., then the pressure  $P_g$  just above the liquid level is:

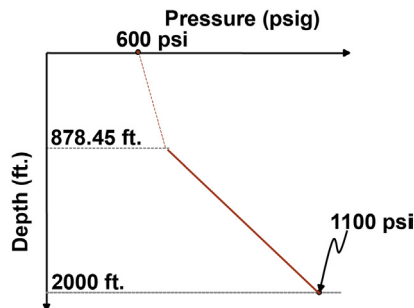
$$P_g = 600 \left( 1 + \frac{X}{54} \right)^{1.5240}$$

On the other hand, the contribution of the liquid column is  $[(2-X) \text{ Mft.} \times (433) \text{ psi/Mft.}]$ , because  $(2-X)$  is the length of the liquid column in Mft. The equation to be solved is then:

$$600 \left( 1 + \frac{X}{54} \right)^{1.5240} + (2-X) 433 = 1100$$

The value of  $X$  that satisfies this equation can be found by trial and error. To begin the iterations, the gas factor,  $f_g = \left( 1 + \frac{X}{54} \right)^{1.5240}$ , is assumed to be equal to one, which gives a value of  $X = 0.845$  Mft. If this value is used in the equation to be solved, the left-hand side of this equation would be equal to 1114.48 psi. This value is 14.48 psi greater than 1100 psi. This represents  $11.48/0.433 = 33.45$  ft. in excess of the liquid column, so a new value of the liquid level depth equal to  $0.845 + 0.03345 = 0.87845$  Mft. is used. With this liquid level depth, the terms on the right-hand side become equal to 1,100.56 psi, which is 0.56 psi still greater than 1100 psi but very close to it. The iterations can continue until a desired level of accuracy is reached.

Fig. 2.11 shows the pressure distribution (not to scale). If more precision is



■ FIGURE 2.11 Pressure distribution along the well for problem 2.11.

required, Eq. 2.13 used in the calculation of the gas pressure at depth can be replaced with a more sophisticated equation, like the ones given at the beginning of the chapter, as long as the gas specific gravity is known.

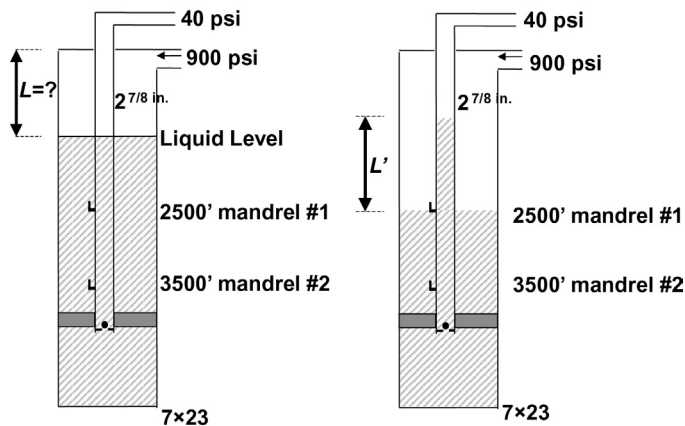
### Problem 2.12

For the well in Fig. 2.12, find the minimum value of the liquid level depth  $L$  for which it will be possible to initiate the unloading of the well from the first mandrel with a surface injection pressure of 900 psi without having to pull the standing valve out of the well. It is assumed that, at the beginning of the unloading process, the depths of the liquid levels in the annulus and in the tubing are equal and that the gas factor,  $f_g$ , in the tubing is equal to unity. The liquid gradient is equal to 433 psi/Mft. The volumetric capacities of the tubing and annulus are 5.788 Br/Mft. and 31.3377 Br/Mft., respectively. Use Eq. 2.13 to find the gas pressure at depth in the annulus.

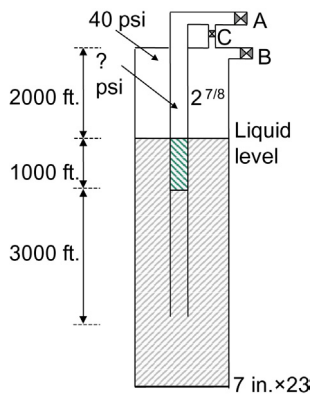
### Solution

When gas is injected down the annulus, the liquids in the annulus are displaced toward the production tubing. A liquid column of length  $L'$  is generated inside the tubing just when the liquid level in the annulus reaches the first mandrel. At that moment, the 900 psi surface pressure plus the hydrostatic pressure due to the gas column in the annulus must be equal to the hydrostatic pressure of the liquid column of length  $L'$  plus the well-head production pressure of 40 psi:

$$900 \left( 1 + \frac{2.5}{54} \right)^{1.524} = 433L' + 40$$



■ FIGURE 2.12 Well to be unloaded.



■ FIGURE 2.13 Closed well with tubing-annulus communication at the bottom.

This gives a value of  $L'$  equal to 2.13456 Mft. Because the volumetric capacity of the tubing is 5.788 Br/Mft., then a maximum of 12.3548 barrels of liquids can be contained in a liquid column of length  $L'$ . This volume was originally distributed in the tubing and in the annulus, forming a column of length  $(2.5 - L)$  Mft. The liquid volume balance can be expressed as:  $12.3548 \text{ Br} = (2.5 - L) \text{ Mft.}(31.3377 + 5.788) \text{ Br/Mft.}$ , from which the value of  $L$  is equal to 2.1672 Mft. This means that, with the current well completion, a liquid column of only 332 ft. above the first mandrel would allow the well to be unloaded without problems.

A liquid column of 332 ft. represents a hydrostatic pressure of only 143.75 psi, which should be easy to unload. The problem is that 332 ft. of liquids in the annulus generates a liquid column of 2134.56 ft. in the tubing (because of the difference in the volumetric capacities of the tubing and the casing). If the standing valve is installed in the well and  $L$  is less than 2.1672 Mft., it would not be possible to unload the well unless the standing valve is pulled out of the well, gas is injected down the annulus until line pressure is achieved in the annulus at the wellhead, and the well is given sufficient time for the liquids in the tubing to be absorbed by the reservoir (if it would not cause any damage to the formation). In this way, the liquid level in the tubing might drop to a point in which the production tubing pressure at the first valve could be overcome by the gas injection pressure in the annulus. Injecting gas into the top of the tubing can also be tried to force the liquids back into the formation in less time (again, if no damage is caused to the formation).

### Problem 2.13

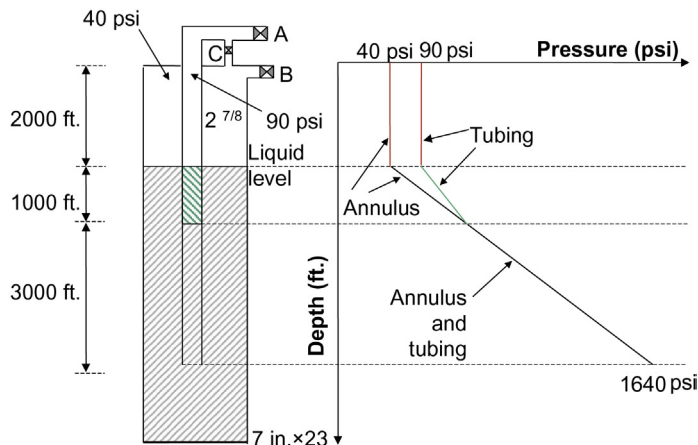
The well in Fig. 2.13 has a 1000-ft. liquid column in the tubing with a pressure gradient of 0.35 psi/ft. Below this column and in the annulus, the liquid pressure gradient is 0.4 psi/ft. On top of the liquid in the annulus and in the tubing there is a 2000-ft. gas column. It is assumed that the gas factor is equal to unity. It is also assumed that the gas temperature is equal to the average geothermal temperature from the surface to 2000 ft. of depth. The tubing volumetric capacity is 5.788 Br/Mft. (32.47 ft.<sup>3</sup>/Mft.) and the annular volumetric capacity is 31.3377 Br/Mft. (175.8 ft.<sup>3</sup>/Mft.).

1. If valves A, B, and C are closed, what should the surface tubing pressure be if the surface annular pressure is 40 psi and the liquid level in the annulus and in the tubing are equal?
2. Keeping valves A and B closed, valve C is opened allowing the surface pressure in the annulus and tubing to be equalized. What will be the

new liquid level in the annulus and in the tubing? What will be the new gas pressure if it is assumed to be an ideal gas and the temperature is constant? Assume the well has not been perforated, so the reservoir can neither provide nor absorb liquids.

### Solution

- At the bottom of the production tubing, the pressures in the annulus and in the tubing are equal. If the hydrostatic pressure components for each side are added and set equal to each other, an equation is found that can be solved for the gas pressure in the tubing: In the annulus, the bottomhole pressure is:  $40 \text{ psi} + (4000 \text{ ft.})(0.4 \text{ psi/ft.}) = 1640 \text{ psi}$ , which must be equal to the pressure at the bottom of the tubing.  $P$  is the gas pressure at the top of the tubing that must be calculated. In the tubing:  $P + (1000 \text{ ft.})(0.35 \text{ psi/ft.}) + (3000 \text{ ft.})(0.4 \text{ psi/ft.})$  must be equal to the pressure at the bottom of the tubing, which was found to be 1640 psi. Therefore:  $P + 350 + 1200 = 1640$ . The gas pressure  $P$  at the top of the tubing must then be equal to 90 psi for the liquid levels in the tubing and in the annulus to be at the same depth. Fig. 2.14 shows the pressure distribution diagram (not to scale for didactical purposes) along the well's depth.
- If valve "C" is opened, the gas pressure in the tubing and in the annulus are the same and due to the fact that the pressure at the bottom of the tubing must be the same for the tubing and the annulus, the liquid level in the annulus must descend a distance  $X$  and the level in the tubing must rise a distance  $Y$  (because the liquids in the annulus are



■ FIGURE 2.14 "Pressure-depth" diagram along the well's depth.

heavier than in the tubing). From the volumetric capacities, the following expression for  $Y$  in terms of  $X$  is found:

$$Y = (31.3377/5.788)(X) = 5.414 X$$

A pressure balance at the bottom of the production tubing gives:

$$P_{\text{final}} + (4000 - X)0.4 = P_{\text{final}} + (3000 + 5.414X)0.4 + (1000)0.35$$

$P_{\text{final}}$  is the final pressure of the gas in the tubing and in the annulus and cancels out.  $X$  is then found to be 19.48 ft.  $Y$  is then 5.414 times greater, or 105.5 ft., which is the distance the liquid level in the tubing must rise.

To find the final gas pressure, it is necessary to use the equation of state for an ideal gas. Once the pressure and temperature have stabilized, the following equation must be satisfied:

$$(P_{\text{final}})(V_{\text{total}}) = (N_{\text{total}})(R_u)(T)$$

$R_u$  is the universal gas constant and  $T$  is the final average temperature.  $V_{\text{total}}$  is the total volume occupied by the gas in the tubing and in the annulus. The liquid is incompressible so the total gas volume must be equal to the initial volume occupied by the gas in the annulus and in the tubing. The initial volume in the annulus is  $(2 \text{ Mft.})(175.8 \text{ ft.}^3/\text{Mft.}) = 351.6 \text{ ft.}^3$ . The initial volume of the gas in the tubing is  $(2 \text{ Mft.})(32.47 \text{ ft.}^3/\text{Mft.}) = 64.94 \text{ ft.}^3$ . So the total volume is then  $416.54 \text{ ft.}^3$ .  $N_{\text{total}}$  is the total number of moles of the gas, which is the same number of moles initially in the tubing plus the number of moles initially in the annulus, so that the total number of moles can be calculated as:

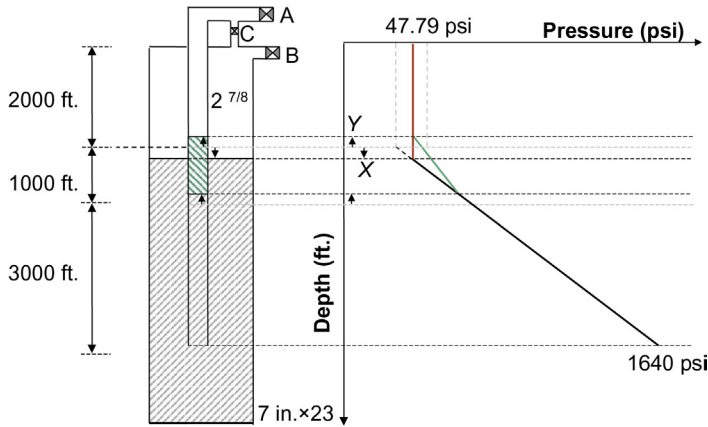
$$N_{\text{total}} = N_{\text{annular}} + N_{\text{tubing}} = \left( \frac{(P_{\text{annular}})(V_{\text{annular}})}{R_u T} + \frac{(P_{\text{tubing}})(V_{\text{tubing}})}{R_u T} \right)$$

$P_{\text{annular}}$  and  $P_{\text{tubing}}$  are the initial pressures in the annulus and in the tubing, respectively. Introducing  $N_{\text{total}}$  in the equation of state for the final conditions gives:

$$(P_{\text{final}})(V_{\text{total}}) = \left( \frac{(P_{\text{annular}})(V_{\text{annular}})}{R_u T} + \frac{(P_{\text{tubing}})(V_{\text{tubing}})}{R_u T} \right) R_u T$$

$R_u T$  cancels out and  $P_{\text{final}}$  can be solved as:

$$P_{\text{final}} = \frac{V_{\text{annular}}}{V_{\text{total}}} P_{\text{annular}} + \frac{V_{\text{tubing}}}{V_{\text{total}}} P_{\text{tubing}} = \frac{351.6}{416.54} 40 + \frac{64.94}{416.54} 90 = 47.79 \text{ psi}$$



■ FIGURE 2.15 Final pressure distribution along the well's depth.

The final pressure, 47.79 psi, is very close to the initial annular pressure due to the fact that the initial annular gas volume is much larger than the initial gas volume in the tubing. The final pressure distribution in the well is shown in Fig. 2.15 (again, not to scale for didactical purposes).

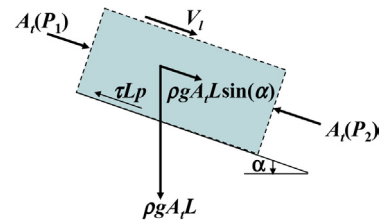
### 2.2.2 Dynamic gradient

Frictional pressure drop should be taken into consideration when the liquid is in motion. For steady state, turbulent, incompressible flow in a pipe of constant diameter, it has been experimentally found that the shear stress on the liquid at the pipe wall is directly proportional to the square of the velocity of the liquid. This shear stress can be found from the following equation:

$$\tau = f_F \frac{\rho}{2} V_1^2 \quad (2.107)$$

Where  $\tau$  is the shear stress,  $f_F$  is the Fanning friction factor,  $\rho$  is the liquid density, and  $V_1$  is the liquid velocity.

Fig. 2.16 shows a control volume equal to a segment of the pipe of length  $L$  and the forces that act on the liquid inside the control volume.  $A_t$  is the cross-sectional area of the pipe,  $P_1$  and  $P_2$  are the pressures at the entrance and exit of the control volume,  $g$  is the acceleration due to gravity, and  $p$  is the wetted perimeter which, for circular pipes, is equal to  $\pi D$ , with  $D$  being the pipe inside diameter.



■ FIGURE 2.16 Section of the pipe of length  $L$  taken as a control volume.

Because it is a steady state flow, the summation of the forces on the liquid in the control volume must be equal to zero:

$$(A_1)(P_1) + \rho g(A_1)[L\sin(\alpha)] = (A_1)(P_2) + \tau(L)(p) \quad (2.108)$$

$L\sin(\alpha)$  is the difference in elevation between the entrance and the exit of the pipe segment. If  $z_1$  is the elevation at the entrance and  $z_2$  is the elevation at the exit, both referred to an arbitrary point,  $\Delta z$  is equal to  $z_1 - z_2$ , which is the same as  $L\sin(\alpha)$  and if, additionally,  $\Delta P$  is defined as  $P_1 - P_2$  and the hydraulic radius  $\mathcal{R}$  is  $A_1/p$ , then Eq. 2.108 can be expressed as:

$$\frac{\Delta P + \rho g \Delta z}{L} = \frac{f_F \rho V_1^2}{2\mathcal{R}} \quad (2.109)$$

For circular pipes the hydraulic radius  $\mathcal{R}$  is equal to the pipe inside diameter divided by 4, or  $D/4$ . If the Moody friction factor  $f$  is used (equal to four times the Fanning friction factor), then Eq. 2.109 changes to:

$$\frac{\Delta P + \rho g \Delta z}{L} = \frac{f \rho V_1^2}{2D} \quad (2.110)$$

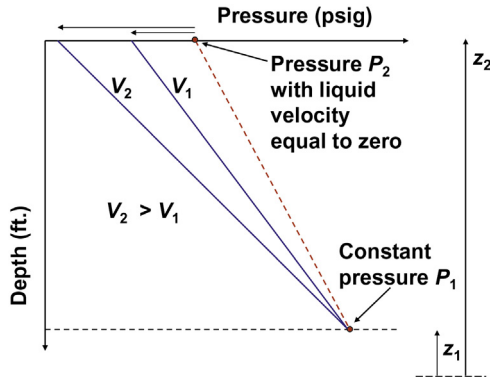
The pressure drop is then equal to:

$$P_1 - P_2 = \rho g(z_2 - z_1) + \frac{f \rho L V_1^2}{2D} \quad (2.111)$$

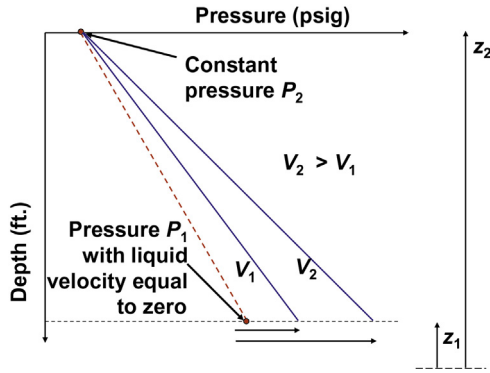
The first and second terms on the right-hand side of Eq. 2.111 represent the hydrostatic and frictional pressure drop, respectively. The pressure drop of a liquid flowing in a pipe of constant diameter is then equal to the sum of the hydrostatic pressure drop plus the frictional pressure drop. The two terms on the right-hand side of Eq. 2.111 must be divided by  $g_0$ , equal to 32.174 (lbm ft.)/(lbf s<sup>2</sup>), when British units are used and the pressure is expressed in lbf/ft.<sup>2</sup> Because the liquid density is constant, the pressure distribution along the pipe must be a linear function of the measured depth if the pipe (inclined or not) is straight.

Fig. 2.17 shows what happens in a straight, vertical pipe when there is a constant bottomhole pressure  $P_1$ , and the liquid flows up the pipe at different velocities. As the velocity increases, the surface pressure  $P_2$  decreases (due to frictional losses) if the bottomhole pressure is kept constant. Fig. 2.18 shows what happens in a straight, vertical pipe when there is a constant surface pressure  $P_2$ , and the liquid flows up the pipe at different velocities. As the liquid velocity increases, the bottomhole flowing pressure must also increase (due to frictional losses) if the surface pressure  $P_2$  is kept constant. Fig. 2.19 shows the pressure distribution for a vertical, downward,

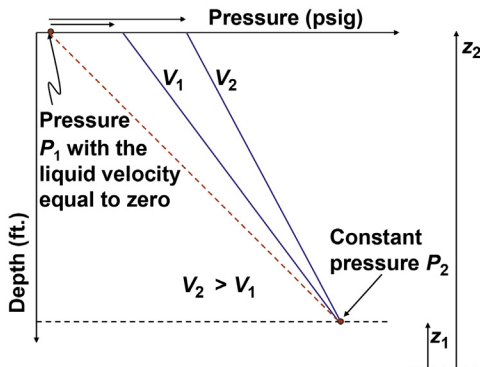




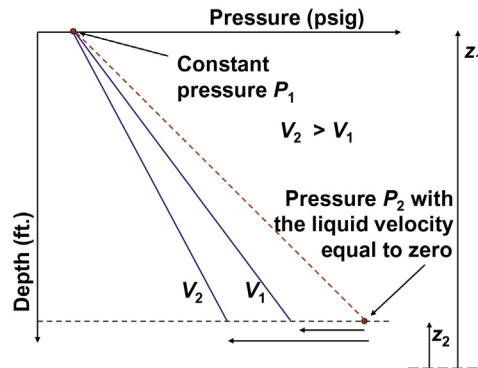
■ FIGURE 2.17 Vertical, upward, single-phase liquid flow in a straight pipe with constant bottomhole pressure.



■ FIGURE 2.18 Vertical, upward, single-phase liquid flow in a straight pipe with constant surface pressure.



■ FIGURE 2.19 Vertical, downward, single-phase liquid flow in a straight pipe with constant bottomhole pressure.



■ FIGURE 2.20 Vertical, downward, single-phase liquid flow in a straight pipe with constant surface pressure.

single-phase flow, when the bottomhole pressure is kept at a constant value  $P_2$ . If the liquid flow rate is increased, the surface pressure must also increase due to the increase in the frictional pressure losses. In this case, as the liquid travels downwards, its pressure increases because of the increase in the hydrostatic component, but this increment is reduced by frictional losses. In other words, the signs of the two pressure components (hydrostatic and friction) in Eq. 2.111 are opposite. Fig. 2.20 shows vertical, downward, liquid flow with a constant surface pressure  $P_1$ . In this case, if the liquid flow rate is increased and the surface pressure is kept constant, the bottomhole pressure is reduced because of the increment in frictional losses. In all of these figures,  $V_2$  is greater than  $V_1$ .

Returning to Eq. 2.111, the friction factor  $f$  used in this case is four times the Fanning friction factor because it is the friction factor found from the Moody diagram. This factor, far from being a constant, depends on the liquid density, velocity, and viscosity, as well as on the pipe diameter and roughness. For laminar flow, it has been demonstrated that the friction factor to be used in Eq. 2.111 is equal to  $64/R_e$ , where  $R_e$  is the Reynolds number. If the Reynolds number is less than 2100, then the flow is considered laminar. For turbulent flow, as it was pointed out in Section 2.1.2, the relationship proposed by Jain (1976) can be used to get the friction factor in an approximate, but explicit, manner:

$$f = \frac{1}{\left[ 1.14 - 2 \log_{10} \left( \frac{\epsilon}{D} + \frac{21.25}{R_e^{0.9}} \right) \right]^2} \quad (2.112)$$

Depending on the variable to be calculated, there are three types of problems for which different calculation procedures are used:

1. The flow rate, tubing diameter, and length are known and the pressure drop needs to be calculated. This is the easiest type of problem. The Reynolds number is calculated first. Then, depending on the value of the Reynolds number and the pipe roughness, the friction factor is calculated from the appropriate equation and then the pressure drop is found from Eq. 2.111.
2. For a given pipe length and diameter, the liquid flow rate for a known differential pressure needs to be calculated. This case is more complicated because the liquid velocity is unknown and therefore the Reynolds number cannot be calculated. Calculations are done following an iteration procedure:
  - a. An initial friction factor,  $f$ , is estimated.
  - b. Using this value of  $f$  and the expected pressure drop, Eq. 2.111 is used to find the liquid velocity (from which the flow rate can be calculated as  $Q = V_1 A_1$ ).
  - c. With this velocity, the Reynolds number can be found and used in the Moody diagram (or the appropriate equation) to determine a new value of the friction factor.
  - d. With this new friction factor, the previous steps are repeated until convergence is achieved at a reasonably accurate value of  $f$ .
  - e. To determine the flow rate, the velocity is multiplied by the pipe cross-sectional area.
3. The liquid flow rate and the pressure drop are known and the pipe diameter needs to be found. There are three unknowns in this case: the friction factor, the liquid velocity, and the tubing diameter. Because the velocity is equal to the flow rate divided by flow area, then:

$$V_1 = Q / \left( \frac{\pi}{4} D^2 \right) \quad (2.113)$$

Where  $V_1$  is the liquid velocity,  $Q$  is the liquid flow rate, and  $D$  is the diameter of the pipe. If the expression for  $V_1$  in Eq. 2.113 is introduced in Eq. 2.111 (considering the fact that the flow rate and the pressure drop are constant) the following equation for the pipe diameter is derived:

$$D^5 = k_1 f \quad (2.114)$$

Where  $f$  is the friction factor and  $k_1$  is a constant equal to:

$$k_1 = \frac{\rho L Q^2}{2 \left( \frac{\pi}{4} \right)^2 [(P_1 - P_2) + \rho g (z_1 - z_2)]}$$

On the other hand, if the expression for the velocity (Eq. 2.113) is used in the definition of the Reynolds number, the following equation is obtained:

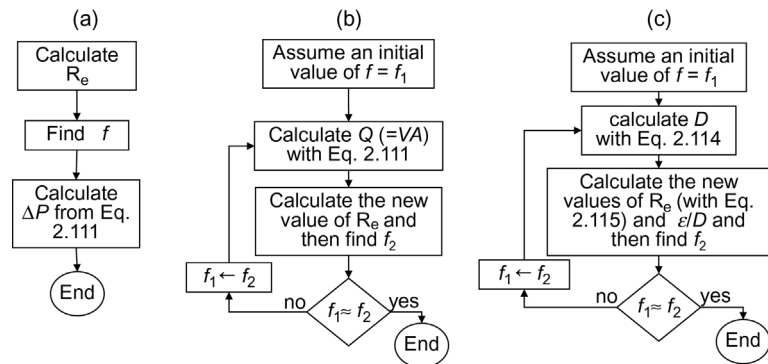
$$R_e = \frac{k_2}{D} \quad (2.115)$$

Where  $R_e$  is the Reynolds number and  $k_2$  is given by  $k_2 = \frac{4\rho Q}{\pi\mu}$ .

All variables that define  $k_1$  and  $k_2$  are known so these constants can be calculated at the beginning of the iterations. The iteration procedure consists of:

- An initial value of the friction factor  $f$  is assumed.
- Using Eq. 2.114, the value of  $D$  is calculated.
- The Reynolds number is found using Eq. 2.115.
- Knowing the absolute roughness,  $\varepsilon$ , the relative pipe roughness,  $\varepsilon/D$ , can then be determined.
- With the Reynolds number and pipe roughness, a new value of  $f$  is found from the Moody diagram or using the appropriate equation.
- With this value of  $f$  all previous calculation are repeated to get a new value of  $f$ . These iterations are repeated until  $f$  does not change by more than a given tolerance number.

Calculation procedures for each type of problem are presented in the following flow charts (Fig. 2.21).



■ FIGURE 2.21 Flow charts for the three types of problems. (a) Given  $Q$  and  $D$ , find  $\Delta P$ ; (b) Given  $D$  and  $\Delta P$ , find  $Q$ ; and (c) Given  $Q$  and  $\Delta P$ , find  $D$ .

**Problem 2.14**

Find the pressure drop in a 600-ft. long flowline of 4 in. in diameter for each of the following liquid flow rates: (1) 2,000 Br/D and (2) 14,000 Br/D. The liquid viscosity is 48 cP and its density is 57 lbm/ft.<sup>3</sup>.

**Solution**

The viscosity of 48 cP must be multiplied by  $2.0890(10)^{-5}$  lbf·s/(cP·ft.<sup>2</sup>) to give  $100.2720(10)^{-5}$  lbf·s/(ft.<sup>2</sup>). The diameter is equal to 4 in. or 0.3333 ft. The flow area is  $(\pi/4)(0.3333)^2 = 0.087266$  ft.<sup>2</sup>

1. For a liquid flow rate of 2000 Br/D:

2000 Br/D corresponds to  $(2000 \text{ Br/D})(5.61 \text{ ft.}^3/\text{Br})/(86,400 \text{ s/D}) = 0.12986 \text{ ft.}^3/\text{s}$ . The velocity is equal to the flow rate divided by the flow area, that is,  $(0.12986/0.087266) = 1.4880 \text{ ft./s}$ . The Reynolds number is given by:

$$R_e = \frac{\rho DV}{\mu g_0} = \frac{57(\text{lbm/ft.}^3)(0.333 \text{ ft.})(1.4880 \text{ ft./s})}{100.2720(10^{-5})(\text{lbf}\cdot\text{s/ft.}^2)32.2(\text{lbm}\cdot\text{ft./}(\text{lbf}\cdot\text{s}^2))} = 874.76$$

Because the Reynolds number is less than 2100, the flow is laminar and the friction factor is  $64/R_e = 0.07316$ . The pressure drop is found from Eq. 2.111 for a horizontal pipe:

$$\Delta P = \frac{\rho f V^2 L}{2g_0 D} = \frac{0.07316 \left( 57 \frac{\text{lbm}}{\text{ft.}^3} \right) \left( 1.4880 \frac{\text{ft.}}{\text{s}} \right)^2 600 \text{ ft}}{2(0.333 \text{ ft.}) \left( 32.2 \frac{\text{lbm}\cdot\text{ft.}}{\text{lbf}\cdot\text{s}^2} \right)} = 258.33 \frac{\text{lbf}}{\text{ft.}^2} = 1.79 \text{ psi}$$

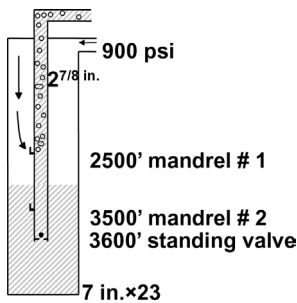
2. For a liquid flow rate of 14,000 Br/D:

14,000 Br/D is equal to  $(14,000 \text{ Br/D})(5.61 \text{ ft.}^3/\text{Br})/(86,400 \text{ s/D}) = 0.909 \text{ ft.}^3/\text{s}$ . The velocity is equal to the flow rate divided by the flow area, that is,  $(0.909/0.087266) = 10.4164 \text{ ft./s}$ . The Reynolds number is given by:

$$R_e = \frac{\rho DV}{\mu g_0} = \frac{57(\text{lbm/ft.}^3)(0.333 \text{ ft.})(10.4164 \text{ ft./s})}{100.2720(10^{-5})(\text{lbf}\cdot\text{s/ft.}^2)32.2(\text{lbm}\cdot\text{ft./}(\text{lbf}\cdot\text{s}^2))} = 6123.52$$

Because the Reynolds number is greater than 2100, the flow is turbulent and the friction factor can be found from Eq. 2.112 with an absolute roughness of 0.0006 ft.:

$$f = \frac{1}{\left[ 1.14 - 2 \log_{10} \left( \frac{\epsilon}{D} + \frac{21.25}{R_e^{0.9}} \right) \right]^2} = \frac{1}{\left[ 1.14 - 2 \log_{10} \left( \frac{0.0006}{0.333} + \frac{21.25}{6123.52^{0.9}} \right) \right]^2} = 0.03798$$



■ FIGURE 2.22 Gas lift well without production packer. Injection through the first valve under stable conditions.

The pressure drop is calculated from Eq. 2.111 for a horizontal pipe:

$$\Delta P = \frac{\rho f V^2 L}{2g_0 D} = \frac{0.03798 \left( 57 \frac{\text{lbm}}{\text{ft}^3} \right) \left( 10.4164 \frac{\text{ft.}}{\text{s}} \right)^2 600 \text{ ft.}}{2(0.333 \text{ ft.}) \left( 32.2 \frac{\text{lbm} \cdot \text{ft.}}{\text{lb} \cdot \text{s}^2} \right)}$$

$$= 6571.83 \frac{\text{lb} \cdot \text{ft.}}{\text{ft.}^2} = 45.64 \text{ psi}$$

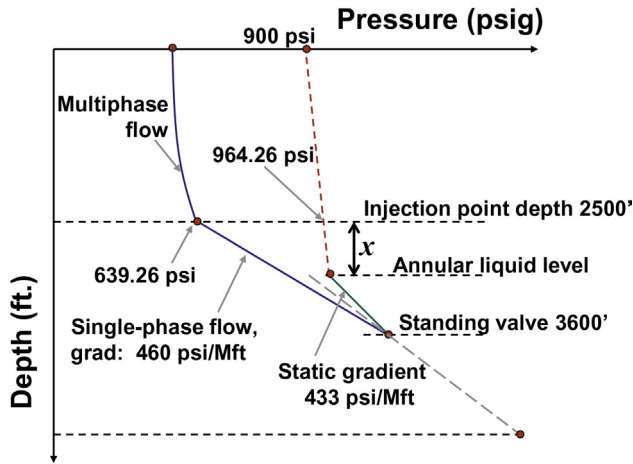
### Problem 2.15

Fig. 2.22 shows a vertical well that, for some reason, does not have a packer but produces in a stable manner while the gas is supposedly being injected through the first (shallower) gas lift valve at 2500 ft. The flow in the tubing below the injection point is single-phase liquid. The liquid level in the annulus is constant. The static liquid pressure gradient in the annulus is 433 psi/Mft. and, due to friction, the single-phase pressure gradient inside the tubing is equal to 460 psi/Mft. Find the depth of the liquid level in the annulus if the pressure drop across the first gas lift valve is equal to 325 psi. The bottom of the tubing is at 3.6 Mft. Use Eq. 2.13 to find the gas pressure at depth in the annulus. The assumption is that the first valve has failed open and the annular pressure is less than the opening pressure of the second valve (so it remains closed). If the second valve is indeed opened (but below the annular liquid level), it can be assumed (as a first approximation) that the liquid flow rate through the second gas lift valve (into the tubing) at 3500 ft. is so small that it does not significantly change the pressure gradients along the tubing and the annulus. To confirm the state of the second valve, the valve's mechanic equations must be used as part of a broader troubleshooting analysis using the calculation procedures explained in chapter: Continuous Gas Lift Troubleshooting.

### Solution

The key to solving this problem is to know that the pressure in the annulus and in the tubing is the same at the bottom of the tubing (right below the standing valve). The problem is better understood with the help of a pressure–depth diagram like the one shown (not to scale) in Fig. 2.23:

Using Eq. 2.13, the gas injection pressure at 2.5 Mft. is found to be 964.26 psi. If the pressure drop across the first gas lift valve is subtracted from 964.26 psi, then the tubing pressure at the point of injection is  $964.26 - 325 = 639.26$  psi. It is seen in the figure that the pressure distribution in the tubing is linear below the point of injection and, due to



■ FIGURE 2.23 Pressure distribution along the well's depth under steady state conditions.

frictional losses, the slope is not as steep as the slope of the pressure line in the annulus. This effect is explained in Fig. 2.17. The pressure-line slope below the bottom of tubing (dashed line) is slightly less than the one in the annulus above the bottom of the tubing, but greater than the slope of the flow inside the production tubing: this is due to the lower frictional pressure drop in the casing (below the bottom of the tubing) than in the tubing because the tubing has a much smaller diameter.

The gas pressure right above the liquid level in the annulus plus the hydrostatic pressure of the liquids in the annulus (from the liquid level to the bottom of the tubing) must be equal to the tubing pressure at the point of injection plus the dynamic pressure drop in the tubing between the injection point and the bottom of the tubing. If  $x$  is the vertical distance from the liquid level in the annulus to the point of injection, this pressure balance is expressed as:

$$900 \left( 1 + \frac{2.5 + x}{54} \right)^{1.524} + 433 [3.6 - (2.5 + x)] = 639.26 + 460(3.6 - 2.5)$$

Following the iterative procedure described in Problem 2.11, the value of  $x$  is found to be equal to 0.72799 Mft.; therefore, the liquid level depth is  $2.5 + 0.72799 = 3.22799$  Mft. The liquid level is then confirmed to be between the first and the second gas lift valve. If it turns out that the calculated liquid level depth is below the second valve, all calculations would have to be repeated assuming that the point of injection is the second

valve and not the first one and, additionally, valve mechanic equations (explained in chapter: Gas Lift Valve Mechanics) need to be used to determine if only one or both gas lift valves are opened. This type of analysis, together with the use of the inflow performance relationship (IPR) curve of the reservoir, is the basis of the troubleshooting analyses that need to be carried out to determine the most probable point of injection depth. Trouble shooting of gas lift wells is explained in chapters: Continuous Gas Lift Troubleshooting; Intermittent Gas Lift Troubleshooting.

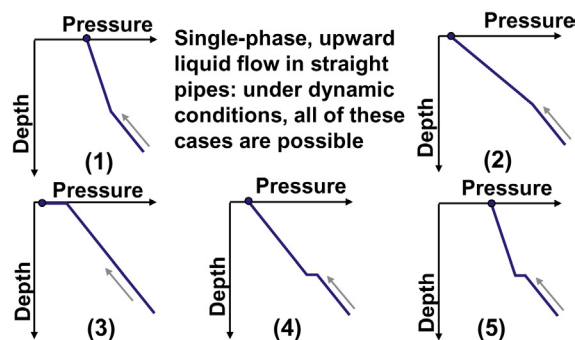
It is many times convenient to express the Reynolds number in terms of field units commonly used in the oil industry. The Reynolds number,  $R_e$ , in terms of the liquid flow rate  $q$  in Br/D, can be found knowing that the liquid velocity  $V_l$  is given by  $V_l = q/A_p$ , where  $A_p$  is the flow area expressed as  $(\pi/4)(d)^2$  with  $d$  being the tubing diameter in inches. Using field units, the Reynolds number is then:

$$R_e = \frac{\rho V_l d}{\mu} = \frac{4q\rho}{\pi d\mu}$$

$$= \frac{4q \left( \frac{\text{Br}}{1 \text{ day}} \right) \left( \frac{5.615 \text{ ft.}^3}{\text{Br}} \right) \left( \frac{1 \text{ day}}{86400 \text{ s}} \right) \rho \left( \frac{\text{lbm}}{\text{ft.}^3} \right)}{\pi d (\text{in.}) \left( \frac{\text{ft.}}{12 \text{ in.}} \right) \mu (\text{cP}) \left( \frac{6.72 \times 10^{-4} \text{ lbm}}{(\text{ft.})(\text{s}) \text{ cP}} \right)} = \frac{1.48q\rho}{d\mu} \quad (2.116)$$

Where  $q$  is in Br/D,  $\rho$  is the density in lbm/ft.<sup>3</sup>,  $d$  is the pipe diameter in inches, and  $\mu$  is the viscosity in cP.

As a final point in this section, Fig. 2.24 shows different pressure distributions that can be found in wells with straight tubing strings in which the flow is single-phase liquid: (1) The flow goes from a tubing string into another



■ FIGURE 2.24 Pressure distributions for single-phase liquid flows in straight pipes.



one that has a larger inside diameter. (2) The flow goes from a tubing string into another one that has a smaller inside diameter. (3) The tubing diameter is constant throughout the well and there is a restriction at the wellhead. (4) The tubing diameter is constant throughout the well and there is a restriction (a subsurface safety valve, for example) at a given depth between the wellhead and the bottom of the well. (5) The flow travels from a smaller diameter tubing string, passes through a restriction and then enters a larger diameter tubing string. Under static conditions case “b” would not be physically possible because there would be two liquids with different gradients and the heavier one could not be on top: if there are two liquids with different densities under static conditions, only case “a” is possible unless it has not been given sufficient time for the liquid mixture to settle in the well.

## REFERENCES

- Jain, A.K., 1976. An accurate explicit equation for friction factor. *J. Hydr. Div. ASCE* 102, No. HY5.
- Moody, L.F., 1944. Friction factor for pipe flow. *Trans. ASME* 66, 671–684.
- Weymouth, T.R., 1912. Problems in natural gas engineering. *Trans. ASME* 34, 185–231.
- Zimmerman, W.G., 1982. *Manual Básico de Gas Lift*. Informe interno de Lagoven, S.A. Tía Juana, Venezuela.

# Multiphase flow

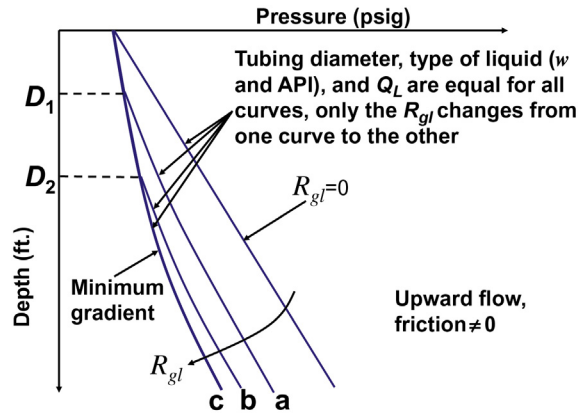
Multiphase flow plays a major role in the designs and troubleshooting analyses of gas lift wells. By definition, the flow above the point of injection must be multiphase flow unless the well is only circulating the injection gas above the static liquid level through: (1) a tubing hole or unwanted communication, (2) a damaged gas lift valve, (3) a gas lift valve not properly set inside the pocket of the gas lift mandrel, or (4) a nitrogen-charged gas lift valve, in good working conditions, at a temperature (below its design value) that keeps the valve open.

The introduction of a gas phase in a liquid flow considerably increases the level of complexity of the calculations required to find the pressure distribution in the well. Today, gas lift designers have at their disposal a great number of mathematical procedures (from the traditional empirical correlations to the new and advanced mechanistic models) to calculate the pressure traverse along the production tubing. However, due to the difficult nature of the subject, to this date no single model or correlation can be accurately applied to all operational conditions. It is always necessary to check which correlation fits best the actual pressure distribution. That is the reason why it is very important to run downhole pressure and temperature surveys in a certain number of wells that can represent the universe of wells producing from a given reservoir and, in this way, find out which correlations are better suited for current operational conditions.

Multiphase flow is a broad subject that is treated in many specialized textbooks. The intention of presenting multiphase flow in this chapter is to give a general view that will allow the reader to understand the calculation procedures described for gas lift design and troubleshooting analyses, as well as to describe a list of the most important publications available in the literature.

## 3.1 QUALITATIVE ASPECTS

Fig. 3.1 shows the pressure distribution along the production tubing for the case in which the following parameters are kept constant: type of liquid, tubing diameter, wellhead pressure, and liquid flow rate. Only the gas/liquid ratio

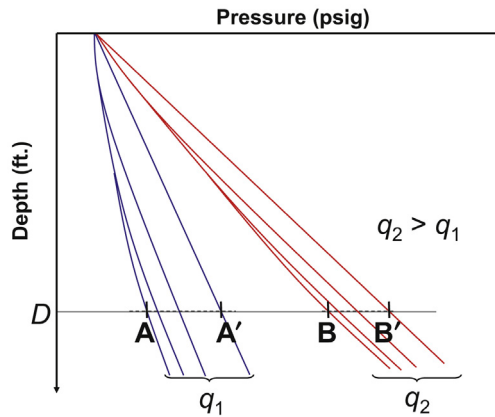


■ FIGURE 3.1 Pressure distribution along the well's depth for different gas/liquid ratios while keeping constant the liquid flow rate, type of liquid, tubing diameter, and wellhead pressure.

( $R_{gl}$ ) is allowed to vary from zero to a point at which the pressure gradient reaches a minimum value. If gas is injected at a gas/liquid ratio greater than the ratio required to achieve the minimum pressure gradient, the frictional pressure drop will increase and the pressure traverse curves will move to the right, even if the wellhead pressure is somehow kept constant. In a real well, it is common that as the injection gas/liquid ratio is increased, the wellhead pressure increases also. This is due to the higher frictional pressure drop attained in the surface flowline (from the wellhead to the separator) caused by the increase in the gas flow rate. For the purpose of this introduction, the flowline is assumed to be very short or its diameter is such that frictional pressure drops at the surface are negligible. This topic is analyzed in detail in chapter: Total System Analysis Applied to Gas Lift Design, see Fig. 5.2.

The following points can be appreciated in Fig. 3.1:

- The pressure distribution is linear if the gas/liquid ratio is equal to zero (and the pipe is a straight pipe).
- If the gas/liquid ratio is larger than zero, the linear pressure distribution is seen at depths below a certain point where the pressure is high and all gas is in solution.
- At depth  $D_1$ , the minimum gradient is reached with a gas/liquid ratio equal to "a", but at depth  $D_2$  the minimum gradient is reached at a gas/liquid ratio "b" greater than "a" for the same liquid flow rate. In other words, at greater depths the gas/liquid ratio that is required to reach the minimum gradient is larger. This is the reason the gas lift efficiency decreases for deeper wells producing at the same liquid flow rate. The objective of the gas lift method is to decrease, as much as possible, the

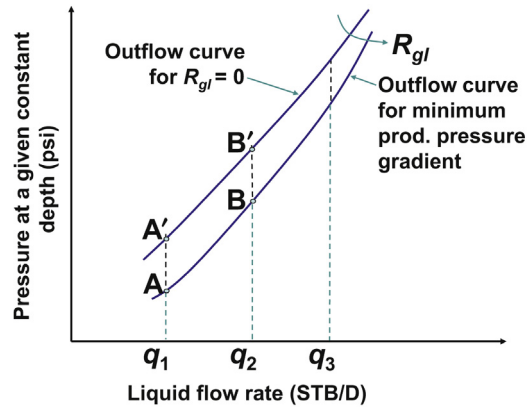


■ FIGURE 3.2 Pressure distribution along the production tubing for two different liquid flow rates.

production pressure at the bottom of the well to increase the liquid flow rate from the reservoir.

As previously indicated, the liquid flow rate in Fig. 3.1 is constant. Fig. 3.2 shows what happens when two considerably different liquid flow rates (but with the same gas/liquid ratios) are plotted on the same graph (while keeping constant all the other parameters). The liquid flow rate  $q_2$  is greater than  $q_1$ . The increase of the liquid flow rate causes an increase in the frictional pressure drop, thus the total pressure gradient is also increased. With liquid flow rate  $q_2$ , the liquid phase appears to have a greater specific gravity; in fact, this same graph could have been found for two fluids with very different densities, both flowing at the same liquid flow rate.

It can be seen in Fig. 3.2 that, at depth  $D$ , as the gas/liquid ratio is increased from zero to a point in which the minimum gradient curve is achieved, the production pressure goes from  $A'$  to  $A$  for liquid flow rate  $q_1$ , and from  $B'$  to  $B$  for  $q_2$ . If these bottomhole pressures ( $A$ – $A'$  and  $B$ – $B'$ ) are plotted in the same way in which the reservoir inflow performance relationship (IPR) curves are plotted (with the bottomhole flowing pressure on the vertical axis and the liquid flow rate on the horizontal axis), the so-called “outflow” curves for depth  $D$  are obtained. These curves are shown in Fig. 3.3, on which points  $A$ ,  $A'$ ,  $B$ , and  $B'$  are plotted. One way of obtaining the outflow curve is by joining together, in one curve, all the points that, for different liquid flow rates, have the same gas/liquid ratio. Outflow curves can also be obtained by joining all the points that, for different liquid flow rates, have gas/liquid ratios that gives the minimum pressure gradient; this is precisely the lower curve shown in Fig. 3.3. Furthermore, outflow curves can also be



■ FIGURE 3.3 Outflow curves.

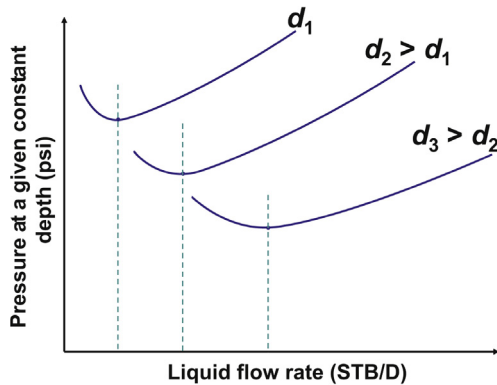
constructed by joining all the points that, for different liquid flow rates, have the same injection gas flow rate.

If the IPR curve is also plotted on the graph shown in Fig. 3.3, the intersection point of the IPR curve with an outflow curve for a given gas/liquid ratio (or gas flow rate, if that was the way the outflow curve was obtained) will give the bottomhole pressure and the liquid flow rate the well is able to produce for the selected gas/liquid ratio or gas flow rate. This type of analysis is explained in great detail in chapter: Total System Analysis Applied to Gas Lift Design and constitutes the basis for many different operations that are required to optimize gas lift wells.

For the curves shown in Fig. 3.3, if the gas/liquid ratio is equal to zero then the minimum pressure is found when the liquid flow rate is equal to zero. If the gas/liquid ratio is greater than zero, the minimum pressure is reached at a point where the liquid flow rate is greater than zero. The value of the liquid flow rate at the minimum pressure point depends on the tubing diameter, the wellhead pressure, and the total gas/liquid ratio. Keeping all these parameters constant, Fig. 3.4 shows how the point of minimum pressure changes as the tubing diameter  $d$  is changed.

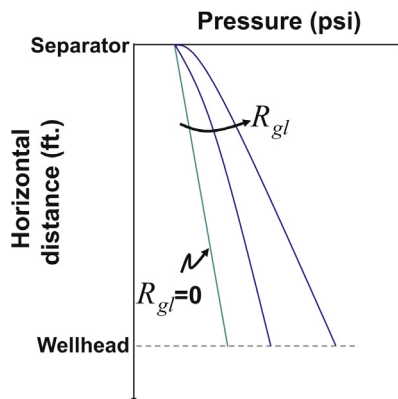
As illustrated in chapter: Total System Analysis Applied to Gas Lift Design, the outflow curves shown in Fig. 3.4 can be used to explain instability problems in gas lift wells. These curves can also be used in the selection of the most appropriate tubing diameter for a particular gas lift well.

Opposite to what takes place in most of the other artificial lift methods, horizontal multiphase flow plays an important role in gas lift design because what happens in the flowline (from the wellhead to the separator) directly affects



■ FIGURE 3.4 Effect of the tubing diameter on the minimum pressure point of outflow curves.

the flowing pressure at the top of the perforations. Fig. 3.5 shows the pressure distribution along the flowline from the wellhead to the gas-liquid separator (or the production manifold) at the flow station. In the figure, the separator pressure, the type of liquid, the tubing diameter, and the liquid flow rate are kept constant and only the gas/liquid ratio ( $R_{gl}$ ) is changed. It is seen that the effect of increasing the gas flow rate is to always increase the required wellhead pressure to sustain the same liquid flow rate. This fact acts against the gas lift method because as gas is injected to lower the pressure in the production tubing, the wellhead pressure increases, shifting the vertical pressure curve along the production tubing to the right. However, in most cases, the effect of lowering the tubing pressure is much greater than the increase in the wellhead pressure caused by the increase in the injection gas flow rate.

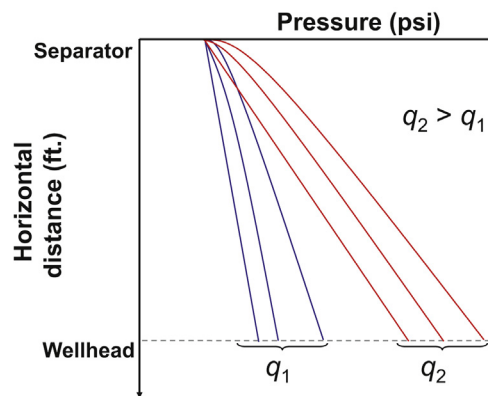


■ FIGURE 3.5 Behavior of the horizontal multiphase flow in the flowline.

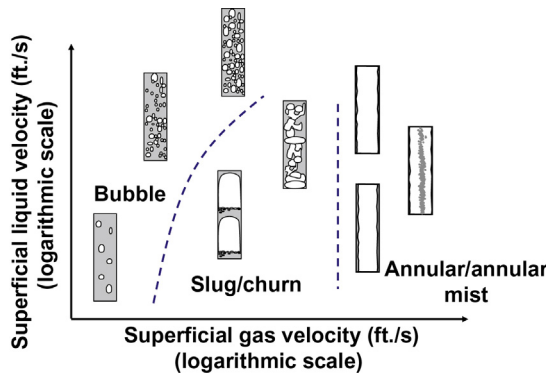
In horizontal multiphase flow, friction plays a relatively more important role than in vertical flow. As the gas flow rate is increased, the space the liquid occupies is reduced, causing a greater liquid velocity, which induces a greater frictional pressure drop. This effect is also present in vertical flow; however, in this case, the total density is reduced at the same time, reducing in this way the hydrostatic pressure gradient that, at first, overcomes the increase in the frictional pressure gradient. But, as mentioned earlier, if the gas flow rate is increased beyond a certain value, the increase in frictional pressure drop becomes greater than the reduction of the hydrostatic pressure drop. Hydrostatic and frictional pressure drops are defined in Eq. 2.111.

Fig. 3.6 shows the effect that increasing the liquid flow rate  $q$  has on the wellhead pressure (keeping everything else constant).

Another important feature of multiphase, horizontal, or vertical flow is the distribution of the phases in the so-called “flow patterns.” Each flow pattern corresponds to a particular spatial distribution of the phases. As flow conditions are changed (like gas or liquid flow rates), flow patterns change from one configuration to another. The distribution of the flow patterns for different flow conditions is known as a flow pattern map. There are numerous ways of classifying flow patterns and constructing flow pattern maps. In this section, and for the purpose of a purely qualitative introduction, flow pattern maps are constructed by plotting the superficial liquid and gas velocities on the vertical and horizontal axes, respectively (using logarithm scales for both axes). As defined later in this section, the superficial velocity of a given phase is the in situ flow rate of that particular phase divided by the pipe’s total cross-sectional area. The superficial velocity of a particular phase is then the velocity that this phase would have if it flowed alone in the pipe at the same flow rate.



■ FIGURE 3.6 Effect of the liquid flow rate on the wellhead pressure.

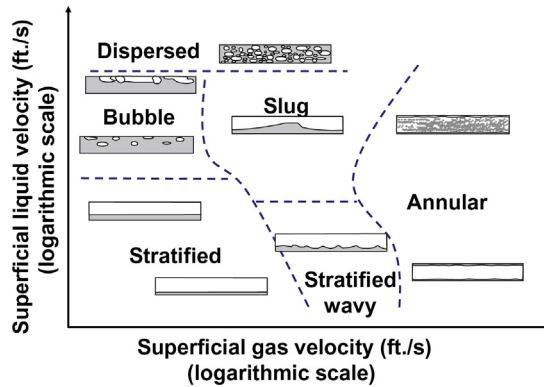


■ FIGURE 3.7 Flow pattern map for vertical upward flows.

Fig. 3.7 shows the flow patterns in a vertical pipe with the flow in the upward direction. At low superficial liquid and gas velocities, the flow pattern is called “bubble flow” because the liquid is the continuous phase and the gas travels in small bubbles. As the superficial gas velocity is increased, the flow pattern turns into the so-called “slug” flow, in which the gas travels in long bullet-shaped bubbles that almost entirely occupy the pipe cross-sectional area and in small bubbles in the liquid phase that travels between these long bubbles. If the superficial gas velocity is further increased, the flow pattern changes to annular flow, where the liquids form a film on the wall of the pipe and the gas phase travels at the center of the pipe. Finally, for even greater superficial gas velocities, the flow pattern is still annular flow but now a large amount of liquid droplets travels with the gas in the center of the pipe forming what is called the “annular mist” flow pattern. Between annular and slug flow, a highly irregular and turbulent flow pattern can be identified. This pattern is called “churn” flow, for which both phases can be considered dispersed.

In a gas lift well, bubble flow can take place at the bottom of the tubing and, as the gas expands as it travels toward the surface, the flow pattern changes to slug flow and then into churn flow. Slug and churn flows are the most common types of flow patterns found in a gas lift well. It is highly possible that a gas lift well producing in annular flow is being over injected with an injection gas/liquid ratio beyond the maximum economic gas/liquid ratio limit. Usually, when the production tubing diameter is too large for the liquid production of the well, the only way to have a stable production is by injecting gas at a very high flow rate and, in consequence, the flow pattern is annular or annular-mist. It might be possible that, by reducing the tubing diameter, a stable production can be achieved without having to inject gas at a large flow rate. However, it is important to know that this is not always a feasible solution





■ FIGURE 3.8 Flow pattern map for horizontal flow.

because, as the tubing diameter is reduced, the frictional pressure drop is increased and, in consequence, the reservoir pressure must be high enough for the well to be able to produce with a higher bottomhole flowing pressure.

Horizontal flow patterns are shown in Fig. 3.8. Stratified flow takes place at conditions in which the superficial gas and liquid velocities are low. In offshore wells, it is common to find wells with flowlines on the seafloor followed by risers that connect the flowlines to the flow station at the surface. It is important to indicate that if a vertical pipe is preceded by a horizontal pipe where the flow is stratified, large slugs can be generated from time to time and create problems at the flow station. Stratified flow can also promote corrosion problems if the water stays at the bottom of the pipe for a long time. At the other extreme, if the pipe diameter is very small, erosion might become a problem, especially if the well produces sand. Small diameter pipes are also not recommended for gas lift wells because frictional pressure drop will increase the wellhead pressure, reducing in this way the drawdown and, in consequence, reducing also the liquid production.

The flow patterns that are shown in Fig. 3.8 are exclusively for perfectly horizontal pipes. These flow patterns could be very different if the pipe is slightly inclined with positive or negative inclination angles with respect to the horizontal.

### 3.2 GENERAL QUANTITATIVE ASPECTS IN MULTIPHASE FLOW

Only general aspects are covered in this book because the multiphase flow theory is very broad and the reader is advised to consult textbooks that deal exclusively with multiphase flow.

### 3.2.1 General definitions

The most important variables that are common to many multiphase flow correlations and models are defined first in this section. The physical meaning of each definition should be understood before complex multiphase flow correlations for pressure-drop calculations are analyzed.

One of the most important variables is the liquid holdup,  $H_L$ , which is defined as the fraction of the volume of a section of the pipe that is occupied by the liquid phase at a given instant:

$$H_L = \frac{\text{Liquid volume in a section of the pipe}}{\text{Total volume of the pipe section}} \quad (3.1)$$

Knowing the liquid holdup, other important variables, such as the density of the gas–liquid mixture or the in situ velocity of each phase, can be calculated. Due to the fact that the multiphase mixture is constantly changing, with the phases exchanging location in usually highly turbulent flows, the liquid holdup is calculated as the time-average fraction of the volume that the liquid occupies in a given section of the pipe. If only the gas phase is present, the liquid holdup is equal to zero. If the flow is 100% liquid, the liquid holdup is equal to one. The gas holdup or void fraction,  $H_g$ , is defined as the fraction of the volume of a section of the pipe that is occupied by the gas phase, so that  $H_g = 1 - H_L$ . Because the velocities of the phases are different (the gas traveling faster than the liquid in upward flow), the analytical calculation of the liquid holdup is extremely complex and that is the reason why empirical correlations are used to find the liquid holdup.

If both phases travel at the same velocity, the liquid holdup can be directly calculated from the flow rates of each phase. This only takes place under extreme situations where one of the phases can be recognized as the continuous phase and the other as the dispersed phase. These flow patterns are called “homogeneous” patterns. Dispersed bubble flow and mist flow can be approximately considered homogeneous flows but, as stated earlier, they are not very common in gas lift wells. In any case, the homogeneous liquid holdup is calculated from the following equation:

$$\lambda_L = \frac{q_l}{q_l + q_g} \quad (3.2)$$

Where  $q_l$  and  $q_g$  are the liquid and gas flow rates, respectively, at in situ conditions.

The homogeneous void fraction is then equal to  $\lambda_g = 1 - \lambda_L$ . From Eq. 3.2, the homogeneous void fraction is then given by:

$$\lambda_g = \frac{q_g}{q_l + q_g} \quad (3.3)$$

Once the liquid holdup is known, the density of the gas–liquid mixture can be calculated. This density plays a very important role in the calculation of the hydrostatic pressure drop. The mixture density is found from the following equation:

$$\rho_s = \rho_L H_L + \rho_g H_g \quad (3.4)$$

Subscript s in Eq. 3.4 stands for “slippage” and it is used to identify the density that is calculated assuming that the liquid and gas velocities are different.  $\rho_L$  and  $\rho_g$  are the densities of the liquid and gas phases, respectively.

If the phases travel at the same velocity, the gas–liquid mixture density can be easily calculated from the following equation:

$$\rho_n = \rho_L \lambda_L + \rho_g \lambda_g \quad (3.5)$$

Where the n stands for “no-slip” (to identify the density that is calculated assuming that the liquid and gas phases travel at the same velocity). Some multiphase pressure drop correlations use more complex equations to calculate the density of the mixture and these densities are then used to calculate parameters such as the Reynolds number. One example is given by the following definition of the no-slip density:

$$\rho_n = \frac{\rho_L \lambda_L^2}{H_L} + \frac{\rho_g \lambda_g^2}{H_g} \quad (3.6)$$

Many multiphase pressure drop correlations use the correlating parameter known as the superficial velocity of a given phase, which is the velocity that a particular phase would have if it flowed alone in the pipe. The superficial liquid velocity is calculated as:

$$V_{sl} = \frac{q_l}{A_t} \quad (3.7)$$

Where  $A_t$  is the cross-sectional area of the pipe and  $q_l$  is the in situ liquid flow rate. The actual velocity  $V_l$  is given by a similar equation but the area is, in this case, equal to the actual area that is occupied by the liquid, which can only be calculated if the liquid holdup is known:

$$V_l = \frac{q_l}{A_t H_L} \quad (3.8)$$

The actual liquid velocity at in situ conditions is very hard to determine because the liquid holdup needs to be calculated.

For the gas phase, the superficial and actual velocities,  $V_{sg}$  and  $V_g$ , are given by:

$$V_{sg} = \frac{q_g}{A_t} \quad (3.9)$$

$$V_g = \frac{q_g}{A_t H_g} \quad (3.10)$$

If the in situ gas and liquid velocities are equal, using Eqs. 3.10 and 3.8 and the fact that  $H_g = 1 - H_L$ , it is found that  $q_l/(A_t H_L) = q_g/[A_t(1 - H_L)]$  and, therefore,  $H_L = q_l/(q_l + q_g)$ , or  $H_L = \lambda_L$ .

Some authors define a mixture velocity as:

$$V_m = \frac{q_l + q_g}{A_t} \quad (3.11)$$

Another very important variable that is frequently found in dimensionless numbers commonly used in pressure drop correlations is the “mixture viscosity,” which is calculated in different ways and in terms that are not very well defined in terms of their physical meanings; therefore, this mixture viscosity is just a correlating parameter. The following equations are three examples of how the mixture viscosity is calculated by several authors:

$$\mu_n = \mu_L \lambda_L + \mu_g \lambda_g \quad (3.12)$$

$$\mu_s = \mu_L^{H_L} + \mu_g^{H_g} \quad (3.13)$$

$$\mu_s = \mu_L H_L + \mu_g H_g \quad (3.14)$$

### Problem 3.1

In a multiphase flow, the superficial gas and liquid velocities are 3 and 1 ft./s, respectively. If the difference between the actual gas and liquid velocities is equal to 1 ft./s, what would be the value of the liquid holdup  $H_L$ ? Find also the liquid holdup for actual velocity differences of 0 and 2 ft./s.

#### Solution

From Eqs. 3.7 to 3.10:

$$\begin{aligned} V_g - V_l &= V_{sg}/(1 - H_L) - V_{sl}/(H_L) \\ 1 \text{ ft./s} &= (3 \text{ ft./s})/(1 - H_L) - (1 \text{ ft./s})/(H_L) \\ H_L^2 + 3H_L - 1 &= 0 \end{aligned}$$

Solving for  $H_L$ :

$$H_L = \left[ \frac{-3 + (13)^{0.5}}{2} \right] = 0.30278$$

Repeating these calculations for actual in situ velocity differences of 0 and 2 ft./s, the values of the liquid holdup  $H_L$  are 0.25 and 0.366025, respectively. In other words, the greater the gas velocity with respect to the liquid velocity is, the greater the liquid holdup becomes if the flow rates of the phases are kept constant (the superficial velocities are held constant in this problem). The minimum holdup value is the one obtained when the phases travel at the same velocity. In multiphase vertical upward flow, it is not physically possible to have liquid holdups less than this minimum value because the gas always tends to travel at a higher velocity than the liquid. The minimum value of the liquid holdup in vertical flow corresponds then to the homogeneous liquid holdup,  $\lambda_L$ .

The liquid phase in a well is usually a mixture of water and oil. To determine the effect that each of these components has on physical properties (such as the liquid density or viscosity), the oil fraction  $f_o$  and the water fraction  $f_w$  are used. These fractions are defined by the following equations:

$$f_o = q_o / (q_o + q_w) \quad (3.15)$$

$$f_w = q_w / (q_o + q_w) \quad (3.16)$$

Where  $q_o$  and  $q_w$  are the oil and water in situ flow rates, respectively. It is easy to show that  $f_o = 1 - f_w$ . To calculate  $f_o$  and  $f_w$  at in situ conditions from the oil and water flow rates measured at the surface, it is necessary to use the oil and water formation volume factors,  $B_o$  and  $B_w$ , respectively. The liquid volume at reservoir conditions decreases as the liquid travels up the production tubing and the pressure is reduced. The reduction of the liquid volume is mainly due to the fact that gas, initially in solution in the liquid, evolves from the liquid as free gas as the pressure decreases. This reduction in volume can be of significant value if the initial gas in solution is large. The oil formation volume factor  $B_o$  is defined as the volume of liquid at reservoir conditions that is reduced to one barrel of oil at stock-tank conditions. Stock-tank conditions are 60°F and atmospheric pressure. The water formation volume factor is defined in the same way. If  $q'_w$  and  $q'_o$  are the water and oil flow rates at stock-tank conditions, then the flow rates at in situ conditions can be expressed as:

$$q_w = q'_w B_w \quad (3.17)$$

$$q_o = q'_o B_o \quad (3.18)$$

The oil fraction is given then by:

$$f_o = q'_o B_o / (q'_o B_o + q'_w B_w) = 1 / (1 + R_{wo} (B_w / B_o)) \quad (3.19)$$

Where  $R_{wo}$  is the water/oil ratio,  $q'_w/q'_o$ , measured at stock-tank conditions. The liquid phase density  $\rho_L$ , its viscosity  $\mu_L$ , and its surface tension  $\sigma_L$ , can be found from the following equations:

$$\rho_L = f_o(\rho_o) + f_w(\rho_w) \quad (3.20)$$

$$\mu_L = f_o(\mu_o) + f_w(\mu_w) \quad (3.21)$$

$$\sigma_L = f_o(\sigma_o) + f_w(\sigma_w) \quad (3.22)$$

In case of emulsions, Eq. 3.21 should not be used; instead, specially formulated equations to calculate the viscosity of an emulsion should be used. Unfortunately, these special equations do not apply to all operational conditions and types of fluids.

### 3.2.2 Equations for multiphase flow pressure and temperature gradients

The development of the equation used to calculate the pressure gradient in multiphase flow is based on Eq. 2.26, derived in chapter: Single-Phase Flow for gas flow and based on the first and second law of thermodynamics:

$$\frac{dP}{\rho(g/g_o)} + dz + \frac{V_g}{g} dV_g + \frac{4f_F V_g^2}{2gD} dL = 0 \quad (2.26)$$

If the pressure drop is considered positive in the flow direction, the Moody friction factor  $f$  is used, and terms are rearranged, then the previous equation can be written (for any type of fluid and using field units) as:

$$\frac{dP}{dL} = \rho \frac{g}{g_o} \frac{dz}{dL} + \rho \frac{V_{in\ situ}}{g_o} \frac{dV_{in\ situ}}{dL} + \rho \frac{f V_{in\ situ}^2}{2g_o D} \quad (3.23)$$

Where  $g$  is the acceleration due to gravity,  $g_o$  is 32.174 lbf ft./lbf s<sup>2</sup>,  $D$  is the inside diameter of the pipe,  $z$  is the elevation with respect to a reference point,  $\rho$  is the density,  $L$  is the measured length along the pipe, and  $P$  is the pressure inside the pipe. The velocity  $V_{in\ situ}$  is no longer the gas velocity considered in Eq. 2.26; instead, the velocity is defined in different ways, depending on the flow pattern and the particular correlation being used. The three terms on the right-hand side of Eq. 3.23 are called (from left to right):

(1) hydrostatic pressure gradient, (2) acceleration pressure gradient, and (3) frictional pressure gradient. For a differential section of the pipe  $dL$ , the ratio  $dz/dL$  can be approximated as the sine of the angle  $\alpha$  that the pipe makes with respect to the horizontal. The mixture density used in Eq. 3.23 is defined by Eq. 3.4 if the phases travel at different velocities or by Eq. 3.5 if the phases travel at the same velocity. The hydrostatic pressure gradient for nonhomogeneous flow is determined then by:

$$\left(\frac{dP}{dL}\right)_h = \rho_s \frac{g}{g_0} \sin \alpha \quad (3.24)$$

If the phases travel at different velocities, it is necessary then to find the liquid holdup  $H_L$ , which requires the use of empirical correlations that are found from laboratory or field experiments. The hydrostatic pressure gradient plays an important role in gas lift because it usually represents around 70% of the total pressure gradient in vertical pipes. To reduce the hydrostatic pressure gradient, it is necessary to reduce the density of the multiphase mixture, which is achieved by reducing the liquid holdup  $H_L$  injecting gas as deep as possible in the well. But, as it has been indicated earlier, if the gas flow rate is very large, the frictional pressure gradient increase becomes larger than the reduction of the hydrostatic pressure gradient so that the total pressure gradient actually increases.

The frictional pressure gradient is usually the second most important gradient in a vertical pipe. The friction factor, velocity, and density ( $f$ ,  $V_{in\ situ}$ , and  $\rho$ ) are defined in different ways (depending on the multiphase correlation being used). The following three equations are just a few examples of the different ways in which the frictional pressure gradient can be defined:

$$\left(\frac{dP}{dL}\right)_f = \rho_L \frac{f_{Lp} V_{sL}^2}{2g_0 D} \quad (3.25)$$

$$\left(\frac{dP}{dL}\right)_f = \rho_g \frac{f_{gp} V_{sg}^2}{2g_0 D} \quad (3.26)$$

$$\left(\frac{dP}{dL}\right)_f = \rho_f \frac{f_{fp} V_m^2}{2g_0 D} \quad (3.27)$$

Where  $f_{Lp}$  and  $f_{gp}$  are the Moody friction factors considering, respectively, the liquid or the gas phase as the only one in contact with the pipe. Eq. 3.25 is used for bubble flow, while Eq. 3.26 is used for mist flow. For other flow patterns, Eq. 3.27 is frequently used with different definitions of the friction

factor  $f_p$  and the density  $\rho_f$ , which could both be considerably different for different authors. The friction factor is usually correlated with some particular way of defining the Reynolds number.

The acceleration pressure gradient is most of the time totally ignored. This is due to the fact that it only represents a small fraction, usually less than 10%, of the total pressure gradient. Some authors do consider it, but not for all flow patterns.

The development of correlations to predict the total multiphase flow pressure gradient concentrates on finding methods to calculate the liquid holdup and the friction factor.

To find the pressure distribution along the production tubing or flowline, the pipe is divided into small segments. Fluid properties and pressure gradients are calculated at average conditions of pressure, temperature, and pipe inclination angle within each of these pipe segments. The following iterative calculation procedure can be used to find the pressure distribution along the tubing or flowline when the temperature distribution is known:

1. The pipe is divided into small segments  $\Delta L$ .
2. Calculations begin at the point where the pressure is known, which can be the entrance or the exit of the tubing string or flowline. The known pressure at that point is called  $P_1$ . At the opposite end of the first differential segment, a pressure differential  $\Delta P_a$  is added to or subtracted from pressure  $P_1$  (see explanation given later in the chapter regarding the sign to be used). The initial value of the pressure differential  $\Delta P_a$  is arbitrary and should not be greater than 10% of pressure  $P_1$ .
3. The average pressure and temperature within the differential segment of the pipe are calculated. Under these average conditions, gas and liquid properties are then calculated.
4. Using one of the many available correlations for multiphase flow, the pressure gradient  $dP/dL$  for the pipe segment is calculated. With this pressure gradient, a new pressure differential between the exit and the entrance of the pipe segment is calculated as:  $\Delta P_c = |\Delta L|(dP/dL)$ .
5. If  $\Delta P_a$  and  $\Delta P_c$  are not approximately equal, the new calculated value  $\Delta P_c$  is assigned to  $\Delta P_a$  and calculations are repeated from step 3 to find a new value of  $\Delta P_c$ . This iteration continues until the pressure differentials  $\Delta P_a$  and  $\Delta P_c$  become approximately equal.
6. Once  $\Delta P_c$  is approximately equal to  $\Delta P_a$ , the exit (or entrance) pressure of the pipe segment is determined as equal to  $P_1 \pm \Delta P_a$  (again, see the explanation given later in the chapter, for the sign to be used) and calculations are initiated for the next pipe segment from step 2.



7. The calculation of the pressure distribution along the pipe ends when the sum of all pipe segments becomes equal to the total pipe length and calculations are completed for the last pipe segment.

If the flow is in the upward direction and the bottomhole pressure is known, the hydrostatic and frictional pressure drops are sequentially subtracted from the bottomhole pressure to find the wellhead pressure. On the other hand, if the flow is also in the upward direction and the wellhead pressure is known, the hydrostatic and frictional pressure drops are sequentially added to the wellhead pressure to find the bottomhole pressure.

If the flow is in the downward direction and the wellhead pressure is known, the hydrostatic pressure drop is added to the wellhead pressure while the frictional pressure drop is subtracted from the wellhead pressure to find the bottomhole pressure. If the flow is in the downward direction and the bottomhole pressure is known, the hydrostatic pressure drop is subtracted and the frictional pressure drop is added to the bottomhole pressure to find the wellhead pressure.

A more rigorous, but much more difficult, way of finding the pressure distribution along the pipe is obtained by the simultaneous calculation of the pressure and temperature distribution. For this task, the energy balance equation should be used, taking into account the heat transfer to and from the surroundings. The energy balance given by Eq. 2.22 in chapter: Single-Phase Flow and the definition of the fluid's enthalpy are used in the iterations:

The enthalpy per unit mass  $h_m$  is defined as  $u_m + P/\rho_m$ , where  $u_m$  is the internal energy per unit mass of the multiphase mixture. Introducing this definition into Eq. 2.22, using the second law of thermodynamic, dividing by  $dL$ , and rearranging terms, the following expression is obtained:

$$\frac{dh_m}{dL} = -\frac{g \sin \alpha}{g_0} - \frac{V_{\text{in situ}} dV_{\text{in situ}}}{g_0 dL} + \frac{dq_{\text{heat}}}{dL} \quad (3.28)$$

Where  $dq_{\text{heat}}/dL$  is given by the global heat transfer equation:

$$\frac{dq_{\text{heat}}}{dL} = \frac{U(\pi D)}{w_t} (T_{\text{ground}} - T) \quad (3.29)$$

Where  $T$  is the average temperature in the pipe segment  $dL$ ,  $T_{\text{ground}}$  is the ambient temperature that surrounds the pipe segment,  $U$  is the global heat transfer coefficient,  $D$  is the pipe diameter, and  $w_t$  is the total mass flow rate.

The global heat transfer coefficient can be extremely difficult to calculate due to the complexity of the different components that surround the pipe

segment: (1) First, the convective heat transfer from the multiphase mixture toward the pipe is found (this step is by itself very difficult to calculate for multiphase flow). (2) Then, the conduction heat transfer through the pipe must be calculated. (3) Finally, the convective heat transfer toward the well's annulus and the conductive heat transfer to the ground need to be found. The equations that can be used to find the global heat transfer coefficient depend on the configuration of the completion.

The temperature  $T$  within the pipe segment is adjusted in an iterative procedure so that the enthalpy found from Eq. 3.28 becomes equal to the enthalpy of the fluids found from enthalpy flash calculation of each component of the multiphase mixture, which adds an additional difficulty to the calculation process. The enthalpy of the mixture is given by:

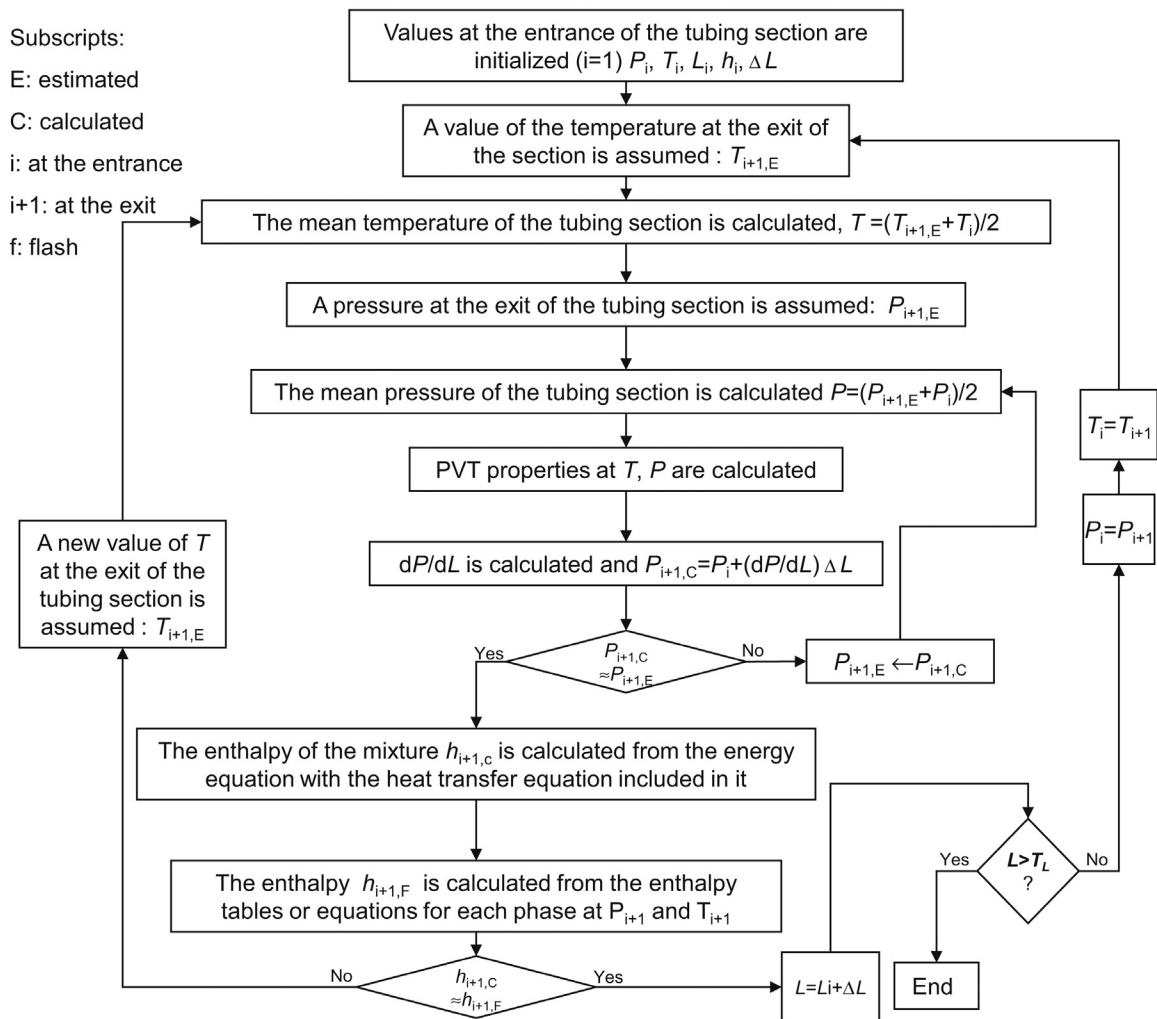
$$h_m = h_L(1-x) + h_g x \quad (3.30)$$

Where  $h_m$  is the enthalpy per unit mass of the total mixture,  $h_L$  is the enthalpy per unit mass of the liquids,  $h_g$  is the enthalpy per unit mass of the gas, and  $x$  is the gas mass flow rate divided by the total mass flow rate and its value can be determined from the following equation:

$$x = \frac{\rho_g \lambda_g}{\rho_L \lambda_L + \rho_g \lambda_g} \quad (3.31)$$

Simultaneous solution of the pressure and temperature distribution along the well requires the double iteration that is shown in the flow chart presented in Fig. 3.9. Because the enthalpy is more sensitive to changes in temperature than to changes in pressure, the pressure iteration is performed within the temperature iteration, minimizing in this way the number of required calculations to reach a final convergence on both, pressure and temperature. This type of double iteration is very difficult to perform for oil wells because of the difficulties found in calculating the enthalpy of the mixture and the global heat transfer coefficient.

Fortunately, the pressure distribution along the pipe is not very sensitive to temperature: large errors in temperature estimation cause only minor deviations to the pressure distribution along the pipe. Calculations shown by [Shiu and Beggs \(1980\)](#) indicated that for a  $-20\%$  error in the estimation of the surface temperature, the deviations induced on the calculation of the bottomhole flowing pressure were approximately  $5\%$  for the Orkiszewski multiphase pressure gradient correlation, a little less than  $3\%$  for the Hagedorn and Brown correlation, approximately  $2\%$  for the Beggs and Brill correlation, and almost  $0\%$  for the Duns and Ros correlation. If the error in estimating the wellhead temperature was  $+20\%$ , the deviations in the calculated



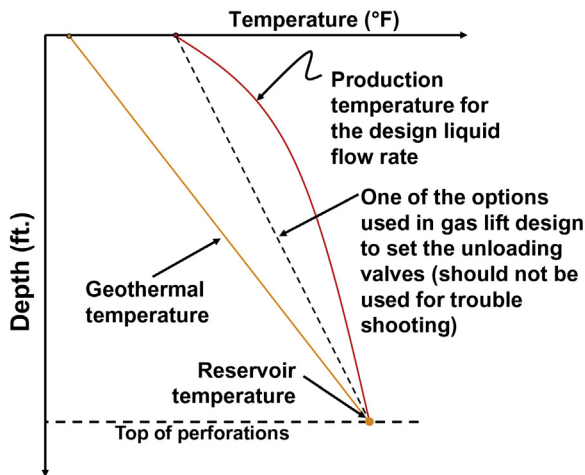
■ FIGURE 3.9 Flow chart for the simultaneous calculation of the pressure and temperature distribution ( $T_L$  is the total length of the tubing).

bottomhole flowing pressure were between 0% and -2.5%. An uncertainty in the estimation of the wellhead temperature of 40% induced a total deviation in the calculation of the bottomhole flowing pressure of 7.5% at the most. This error is insignificant for injection-pressure-operated (IPO) gas lift valve designs because an error of 7.5% in the production pressure represents an error of only 1.5% in the estimation of the gas lift valve opening pressure for the worst cases (large ported valves) and no greater than 1% for the port sizes usually found in unloading gas lift valves. IPO valves are described in great detail in chapters: Gas Lift Equipment; Gas Lift Valve Mechanics.

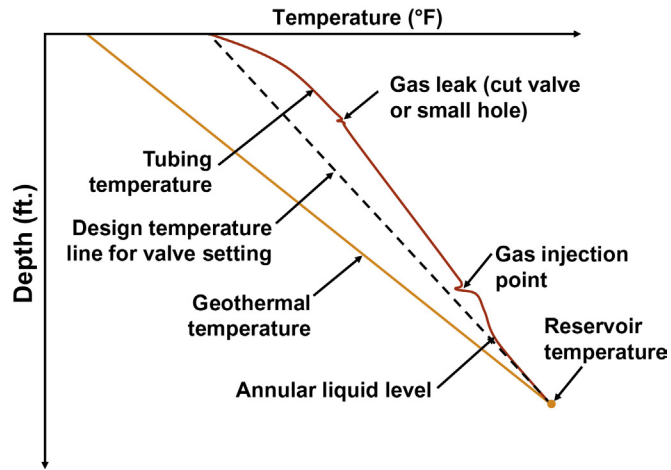
As can be seen in the flow chart presented earlier, the simultaneous calculation of the pressure and temperature distribution is a complex task. For this reason, several correlations that can be used to calculate the temperature along the production tubing and flowline have been developed. These correlations are explained in this section.

Fig. 3.10 shows a typical temperature distribution along the tubing string. Usually, for pressure traverse calculation purposes and for unloading gas lift valve design, a linear temperature distribution along the pipe (as the one shown in the figure as a dashed line from the reservoir temperature to the wellhead flowing temperature) is assumed.

To estimate the temperature of an unloading gas lift valve during the unloading process, the temperature at each depth along the well is usually found from the dashed line that connects the surface temperature to the reservoir temperature. This makes the design valve temperature somewhat cooler than the actual temperature the valve will have when the well is in operation after being unloaded. In this way, nitrogen-charged valves are lock closed during normal operation of the well. The geothermal temperature should not be used as the design valve temperature because it is cooler than the tubing temperature of the well during the unloading process: the desired point of injection might not be reached because the unloading valves might close prematurely due to high temperature. The final production temperature of the well (once it has been unloaded) should not be used either as the design valve temperature because this temperature is higher than the expected temperature during the unloading process and one valve might stay open, or



■ FIGURE 3.10 Typical temperature distribution for a well producing on natural flow.



■ FIGURE 3.11 Temperature distribution in a gas lift well.

serious valve interference problems could arise, before reaching the design point of injection.

Fig. 3.11 shows a typical temperature distribution for a gas lift well. The gas expansion through the gas lift valve makes the temperature drop just above the point of injection. This is easily detected by a downhole temperature survey. Downhole pressure and temperature sensors should always be run simultaneously in gas lift wells so that they can be used for troubleshooting purposes. For wells with low liquid flow rates and high formation gas/liquid ratios, it might be possible for the production pressure gradient to be approximately equal above and below the point of injection depth; therefore, pressure surveys alone sometimes do not detect the point of injection. On the other hand, if the liquid flow rate is very large, it might not be possible to detect the local cooling effect created by the gas expansion if highly sensible temperature sensors are not used and/or the temperature is measured at a distance too far apart from the injection point. In these cases, it is recommended to use the new available techniques for continuous temperature and pressure surveys explained in chapter: Continuous Gas Lift Troubleshooting.

Fig. 3.11 shows a variation in the temperature gradient a certain distance below the current point of injection (it has been exaggerated for didactical purposes). This variation is due to the change in the global heat transfer coefficient caused by the liquid in the annulus. In this case, the liquid level is below the current point of injection because the well was previously unloaded to a gas lift valve below the current operating valve. The gas in the

annulus above the liquid level isolates the production temperature inside the tubing keeping it warm. This change in temperature gradient is usually smaller than shown in the figure and in the majority of cases the effect of liquids in the annulus of gas lift wells is irrelevant because the operating gas lift valves are usually located close to the bottom of the well and also because the change in the temperature gradient is not very large.

Fig. 3.11 also shows a smaller cooling effect taking place at a shallower depth above the point of injection. This could be due to an unloading gas lift valve that is leaking gas because its seat is cut or the valve is partially opened due to dirt between the ball and the seat of the valve. Gas leaks of this type are very frequent in gas lift wells and the gas flow rates through these leaks are usually insignificant. If the gas leak does not coincide with a gas lift mandrel, the leak might be caused by a hole in the tubing or a leaking tubing coupling. Leaks that are not associated with a gas lift mandrel are not detected when the temperature survey is performed in the traditional way, with well-defined stops that usually last from 5 to 10 min at specific locations along the tubing. This is another reason why new techniques for measuring pressure and temperature along the well in a continuous fashion (running in the well the sensors at a constant speed) are preferred when the production of the well is “stable.” If the production pressure is fluctuating, stops should be made only at points of interest for a period of time at least 20% longer than the duration of pressure fluctuation cycles measured at the wellhead. Another, more expensive at the moment, way of performing temperature surveys when the pressure is fluctuating consists in measuring the temperature along the well in real time by means of fiber optic technology, which will identify cool spots at any point in the tubing. All these troubleshooting techniques are explained in detail in chapter: Continuous Gas Lift Troubleshooting.

In the past, manuals and books on gas lift design limited the explanation of “how to find the production tubing temperature gradient” to the presentation of the Kirkpatrick’s chart (Kirkpatrick, 1962). This chart was used to calculate the production tubing temperature gradient from the liquid production flow rate, the tubing diameter, and the geothermal gradient. For gas lift design, the problem of using the Kirkpatrick’s chart is not that it gives a linear temperature distribution (instead of the real temperature curve) because, as it was pointed out earlier, linear temperature distributions are acceptable for gas lift design. The problem might be found (in some situations) in the accuracy of the wellhead temperature prediction. The straight temperature line used for design purposes, shown in Fig. 3.11, is acceptable (for the calculation of the dome pressure of the unloading gas lift valves) only if the wellhead production temperature is found in a precise manner.

The Kirkpatrick's chart has been successfully used for many years because the design temperature line has nothing to do with the actual tubing temperature once the well has been unloading and it is operating at its design point of injection. The most serious mistake that can be made in the design of a gas lift installation with nitrogen-charged gas lift valves is to calculate the design temperature of the unloading valves at values greater than the temperature they will have after the well is unloaded because this causes valve interference and one or several unloading valves could remain open, see the explanation given in chapter: Design of Continuous Gas Lift Installations for Fig. 9.38. Even with the use of the "rudimentary" Kirkpatrick's chart, this mistake is rarely made. For precise troubleshooting calculations of gas lift wells, on the other hand, the Kirkpatrick's chart might cause serious problems because the temperatures predicted from this chart are very different from the actual temperatures found in wells during normal and, especially, abnormal operational conditions.

One equation that is frequently used to calculate the fluid temperature at a distance  $L_d$  from the bottom of the well, where the fluid temperature is known, has the following form:

$$T_L = T_1 - g_T \{L_d - A_R[1 - \exp(-L_d / A_R)]\} \quad (3.32)$$

Where  $T_1$  is the temperature in °F of the fluids at  $L_d = 0$ ,  $T_L$  is the temperature in °F at a distance  $L_d$  measured in feet above the initial point where  $T = T_1$ ,  $g_T$  is the geothermal gradient in °F/ft., and  $A_R$  is a function  $f$  of several parameters, given in different forms from different authors:

$$A_R = f(\rho_L, d, G_{API}, G_g, w_t) \quad (3.33)$$

Where  $A_R$  is usually expressed in feet,  $w_t$  is the total mass flow rate in lbm/s,  $\rho_L$  is the liquid density at standard conditions in lbm/ft<sup>3</sup>,  $d$  is the tubing inside diameter in inches,  $G_{API}$  is the API gravity of the oil, and  $G_g$  is the gas specific gravity.  $A_R$  was originally considered by Ramey (1962) equal to a function of  $w_t$ ,  $C_p$ ,  $U$ , and,  $d$ , where  $C_p$  is the specific heat of the fluids and  $U$  is the global heat transfer coefficient.

The form of the function for  $A_R$  used by Shiu and Beggs (1980), for example, is given as:

$$A_R = C_1 (w_t)^{C_2} (\rho_L)^{C_3} (d)^{C_4} (G_{API})^{C_5} (G_g)^{C_6} \quad (3.34)$$

This model is applicable only if the well has been producing for a long period of time because it does not consider transient effects. The coefficients in Eq. 3.34 (published in Shiu and Beggs work) were found from a linear

multiple regression analysis. The data used by Shiu and Beggs came from a total of 270 wells under very different operational conditions.

For horizontal flow, the following equation is used to find the temperature  $T_{L_H}$  at a distance  $L_H$  from the entrance of a horizontal flowline, as long as the ambient temperature  $T_s$  is constant:

$$T_{L_H} = T_s + (T_1 - T_s) \exp(-L_H / A_R) \quad (3.35)$$

Where  $T_1$  is the temperature in °F at the entrance of the horizontal flowline and all other terms in this equation are the same as the ones in Eq. 3.32.

For vertical or horizontal flow, it is very difficult to find  $A_R$  but, by means of a very simple procedure, its value can be approximated. This procedure, as presented by Beggs (1991), is as follows:

- There must be at least one measurement of the total mass flow rate and the corresponding entrance and exit temperatures of the production tubing or flowline. With these parameters, Eq. 3.35 or Eq. 3.32 can be solved for the value of  $A_R$  in a flowline or a production tubing string, respectively.
- If all terms in  $A_R$  are considered to be of constant values except the total mass flow rate, a constant  $C$  equal to  $A_R/w_t$  is calculated. For a different mass flow rate, the new value of  $A_R$  is simply equal to  $C$  times the new mass flow rate. This new value of  $A_R$  is then used to find the new temperature from Eqs. 3.35 or 3.32.

This method can be used for oil or gas wells.

Correlations that are more sophisticated than the Shiu and Beggs' correlation have the problem of requiring data, such as the specific heat of the production fluids or the global heat transfer coefficient, that are very difficult to find and for which it is necessary to know (among other factors): (1) the thermal conductivity of cement and liquid (or gas) inside the annulus, (2) the liquid level in the annulus, and (3) the condition of the cement and if the well was totally or partially cemented. For this reason, if Eq. 3.34, combined with Eq. 3.32, does not accurately predict the temperature distribution in a given gas lift field, it is usually better for design calculation purposes to adjust Eq. 3.34 to local conditions rather than trying to use more sophisticated models that are impossible to implement in an accurate manner. However, if most of the data are available, the use of these advanced correlations might be justified for troubleshooting analyses.

Coefficients  $C_1$  through  $C_6$  in Eq. 3.34 can be found in the following way: for each well in a selected number of wells  $N$ , all variables in Eq. 3.32,



except  $A_R$ , are measured. Eq. 3.32 is used for the wellhead temperature only. Eq. 3.32 is then solved for  $A_R$ . Additionally, for each value of  $A_R$ , the associated values of the variables found in Eq. 3.34 (that is  $w_t$ ,  $\rho_L$ ,  $d$ ,  $G_{API}$ , and  $G_g$ ), are also measured. Then, for each well or operational condition  $n$ , the following equations must be true:

$$A_{R_1} = C_1 (w_{t_1})^{C_2} (\rho_{L_1})^{C_3} (d_1)^{C_4} (G_{API_1})^{C_5} (G_{g_1})^{C_6}$$

$$A_{R_2} = C_1 (w_{t_2})^{C_2} (\rho_{L_2})^{C_3} (d_2)^{C_4} (G_{API_2})^{C_5} (G_{g_2})^{C_6}$$

.....  

$$A_{R_n} = C_1 (w_{t_n})^{C_2} (\rho_{L_n})^{C_3} (d_n)^{C_4} (G_{API_n})^{C_5} (G_{g_n})^{C_6}$$
  
 .....

$$A_{R_N} = C_1 (w_{t_N})^{C_2} (\rho_{L_N})^{C_3} (d_N)^{C_4} (G_{API_N})^{C_5} (G_{g_N})^{C_6}$$

All values in these equalities have been determined and only constants  $C_1$  through  $C_6$  that best fit the measured data need to be determined. These equations can be expressed as linear functions in the following way ( $n$  going from 1 to  $N$ ):

$$\begin{aligned} \text{Ln}(A_{R_n}) = & \text{Ln}(C_1) + C_2 \text{Ln}(w_{t_n}) + C_3 \text{Ln}(\rho_{L,n}) \\ & + C_4 \text{Ln}(d_n) + C_5 \text{Ln}(G_{API_n}) + C_6 \text{Ln}(G_{g,n}) \end{aligned}$$

With  $y_n = \text{Ln}(A_{Rn})$ ,  $C_1' = \text{Ln}(C_1)$ ,  $x_{1n} = \text{Ln}(w_{tn})$ ,  $x_{2n} = \text{Ln}(\rho_{Ln})$ ,  $x_{3n} = \text{Ln}(d_n)$ ,  $x_{4n} = \text{Ln}(G_{API_n})$ ,  $x_{5n} = \text{Ln}(G_{gn})$ , and if additionally  $a_0 = C_1'$ ,  $a_1 = C_2$ ,  $a_2 = C_3$ ,  $a_3 = C_4$ ,  $a_4 = C_5$ ,  $a_5 = C_6$ , a more familiar notation to handle linear, multiple-regression analysis is obtained:

$$y_n = a_0 + a_1 x_{1,n} + a_2 x_{2,n} + a_3 x_{3,n} + a_4 x_{4,n} + a_5 x_{5,n}$$

And the algebraic equation in matrix form (found from the minimum squares of the deviations) that needs to be solved for the  $a_0$  to  $a_5$  terms is (each summation with  $n$  going from 1 to  $N$ ):

$$\begin{bmatrix} N & \sum x_{1,n} & \sum x_{2,n} & \sum x_{3,n} & \sum x_{4,n} & \sum x_{5,n} \\ \sum x_{1,n} & \sum x_{1,n}^2 & \sum x_{1,n} x_{2,n} & \sum x_{1,n} x_{3,n} & \sum x_{1,n} x_{4,n} & \sum x_{1,n} x_{5,n} \\ \sum x_{2,n} & \sum x_{2,n} x_{1,n} & \sum x_{2,n}^2 & \sum x_{2,n} x_{3,n} & \sum x_{2,n} x_{4,n} & \sum x_{2,n} x_{5,n} \\ \sum x_{3,n} & \sum x_{3,n} x_{1,n} & \sum x_{3,n} x_{2,n} & \sum x_{3,n}^2 & \sum x_{3,n} x_{4,n} & \sum x_{3,n} x_{5,n} \\ \sum x_{4,n} & \sum x_{4,n} x_{1,n} & \sum x_{4,n} x_{2,n} & \sum x_{4,n} x_{3,n} & \sum x_{4,n}^2 & \sum x_{4,n} x_{5,n} \\ \sum x_{5,n} & \sum x_{5,n} x_{1,n} & \sum x_{5,n} x_{2,n} & \sum x_{5,n} x_{3,n} & \sum x_{5,n} x_{4,n} & \sum x_{5,n}^2 \end{bmatrix} \begin{Bmatrix} a_0 \\ a_1 \\ a_2 \\ a_3 \\ a_4 \\ a_5 \end{Bmatrix} = \begin{Bmatrix} \sum y_n \\ \sum x_{1,n} y_n \\ \sum x_{2,n} y_n \\ \sum x_{3,n} y_n \\ \sum x_{4,n} y_n \\ \sum x_{5,n} y_n \end{Bmatrix}$$

From which the values of the  $a_m$  (for  $m$  from 0 to 5) coefficients, and therefore of the  $C$  coefficients also, are found. The person interested in tuning

Eq. 3.34 to a particular gas lift field can add new variables, like the water cut or the gas/liquid ratio, or even change the form of the equation.

### Problem 3.2

Find the surface production temperature for a well producing under the following operational conditions: oil flow rate: 800 STBO/D; water flow rate: 50 STBW/D; total gas flow rate: 200 Mscf/D; tubing inside diameter: 2.992 in.; oil API gravity: 26°API; gas specific gravity: 0.75; water specific gravity: 1.01; geothermal gradient: 0.015°F/ft.; top of perforations' depth: 6000 ft.; and temperature at the top of the perforations: 178.8°F.

### Solution

The water mass flow rate is:

$$\begin{aligned} w_w &= 62.4 \left[ \frac{\text{lbm}}{\text{ft.}^3} \right] \gamma_w q'_w \left[ \frac{\text{STB}}{\text{Day}} \right] 5.615 \left[ \frac{\text{ft.}^3}{\text{STB}} \right] \frac{1 \text{Day}}{86,400 \text{ s}} \\ &= 62.4(1.01)(50)5.615 \frac{1}{86,400} = 0.2048 \left[ \frac{\text{lbm}}{\text{s}} \right] \end{aligned}$$

The oil mass flow rate is:

$$\begin{aligned} w_o &= 62.4 \left[ \frac{\text{lbm}}{\text{ft.}^3} \right] \left[ \frac{141.5}{131.5+26} \right] q'_o \left[ \frac{\text{STB}}{\text{Day}} \right] 5.615 \left[ \frac{\text{ft.}^3}{\text{STB}} \right] \frac{1 \text{Day}}{86,400 \text{ s}} \\ &= 62.4 \frac{141.5}{131.5+26} (800)5.615 \frac{1}{86,400} = 2.91 \left[ \frac{\text{lbm}}{\text{s}} \right] \end{aligned}$$

The gas mass flow rate is:

$$\begin{aligned} w_g &= \rho_{\text{air}} \left[ \frac{\text{lbm}}{\text{scf}} \right] q'_{\text{sc}} \left[ \frac{\text{scf}}{\text{Day}} \right] \gamma_g \frac{1 \text{Day}}{86,400 \text{ s}} = 0.0764(200000)(0.75) \frac{1}{86,400} \\ &= 0.132 \left[ \frac{\text{lbm}}{\text{s}} \right] \end{aligned}$$

The total mass flow rate is then  $0.2048 + 2.91 + 0.132 = 3.2468 \text{ lbm/s}$

The liquid density is given by:

$$\rho_L = \rho_w \frac{q'_w}{q'_o + q'_w} + \rho_o \frac{q'_o}{q'_o + q'_w}$$

With  $\rho_w = \gamma_w 62.4$ ,  $\rho_o = \gamma_o 62.4$ , and  $\gamma_o = \frac{141.5}{131.5+26}$ , the liquid density is:

$$\rho_L = \left[ (1.01) \frac{200}{1000} + \frac{141.5}{131.5+26} \frac{800}{1000} \right] 62.4 = 57.45 \frac{\text{lbm}}{\text{ft.}^3}$$

Using Eq. 3.34, factor  $A_R$  would be:

$$A_R = C_1 (3.2468)^{C_2} (57.45)^{C_3} (2.992)^{C_4} (26)^{C_5} (0.75)^{C_6}$$

And the surface temperature is found from Eq. 3.32:

$$\begin{aligned} T_L &= T_1 - g_T \{L_d - A_R [1 - \exp(-L_d / A_R)]\} \\ &= 178.8 - 0.015 \{6000 - A_R [1 - \exp(-6000 / A_R)]\} \end{aligned}$$

### Problem 3.3

A 30 degree API oil flows in a flowline at a constant flow rate of 100 STB/D. The flowline entrance temperature is 80°F and the ambient temperature is 45°F. If, at this flow rate, the temperature 3000 ft. downstream from the entrance is 50°F, find the exit temperature for a liquid flow rate of 200 B/D.

### Solution

The oil specific gravity is equal to  $141.5 / (131.5 + 30) = 0.8762$ . The oil density at standard conditions is then equal to  $62.4(0.8762) = 54.67$  lbm/ft.<sup>3</sup> The mass flow rate is then:

$$w_t = \frac{5.615 \text{ ft.}^3 / \text{Br}}{86400 \text{ s/D}} 54.67 \text{ lbm/ft.}^3 (100 \text{ Br/D}) = 0.355 \text{ lbm/s}$$

Using Eq. 3.35:

$$50 = 45 + (80 - 45) \exp(-3000 / A_R)$$

So that  $A_R$  is:

$$A_R = -3000 / \{\ln[(50 - 45) / (80 - 45)]\} = 1541.69 \text{ ft.}$$

Constant  $C$  is then equal to  $1541.69 / 0.355 = 4342.8$ .

At a mass flow rate twice the one calculated earlier, the new value of  $A_R$  is  $(4342.8)(2)(0.355) = 3083.38$  and the exit temperature is then:

$$T_{L1} = 45 + (80 - 45) \exp(-3000 / 3083.38) = 58.23^\circ\text{F}$$

The equation developed by Zimmerman (1982), to calculate the temperature gradient along the production tubing, represents a practical and reliable way of finding the temperature of the production fluids:

$$G_t = 1.35 - \frac{11.02}{d^2} \ln\left(\frac{q'}{1000}\right) + 1.5 \ln\left(\frac{R_{gl}(0.0125T_{res} + 12.75)}{P_{pd} + 14.7}\right) \quad (3.36)$$

Where  $G_t$  is the temperature gradient in °F/Mft,  $d$  is the inside diameter of the production tubing in inches,  $q'$  is the liquid production in STBL/D,  $P_{pd}$  is the production pressure in psig at the point where the temperature is being calculated,  $T_{res}$  is the temperature at the top of the perforations in °F,  $R_{gl}$  is the formation gas/liquid ratio for depths below the point of injection or the total gas/liquid ratio for points above the point of injection, both in scf/STB.

The following equation is used to calculate the temperature  $T_D$  in °F at a depth  $D_x$ :

$$T_D = T_{res} - G_t (D_{res} - D_x) / 1000 \quad (3.37)$$

Where  $T_D$  is the fluid temperature at depth  $D_x$  and  $D_{res}$  is the top of the perforations' depth.  $D_{res}$  and  $D_x$  are expressed in feet.

The equation published by Zimmerman was developed from measurements mostly taken in gas lift wells (only a small percentage of the wells considered in this study were producing on natural flow) in Lake Maracaibo gas lift field in Venezuela.

The following models have been developed during the last decades to find the temperature distribution in oil wells and pipelines. The reader that is interested in studying this subject at greater depths is referred to these publications.

[Coulter and Bordon \(1979\)](#) published a model that can be used to find the temperature distribution in horizontal pipelines. This model was based on a rigorous analysis of the thermodynamic behavior of the fluids. It is limited to horizontal flow in pipelines under steady state conditions with a constant surrounding temperature.

[Sagar et al. \(1991\)](#) developed a sophisticated model to find the temperature distribution along the production tubing of oil wells. This rather complicated model was later used as the basis for the development of a simplified model that can be applied in a practical way. The simplified model was also based on 392 measured temperature profiles from real wells. These measurements were gathered from the original Shiu and Beggs' data base and from the data provided by the Amerada Hess Corporation from 55 wells, of which 10 wells from the Louisiana Gulf Coast and the Williston Basin were on gas lift, and 45 wells from the Permian Basin in west Texas were on natural flow.

[Alves et al. \(1992\)](#) presented a model applicable to both wellbores and pipelines. The model is applicable in the entire range of inclination angles and was derived from mass, momentum, and energy balances. The model can be used for single or multiphase flows.

Hasan and Kabir (1993;1994) presented temperature prediction equations for multiphase flow in gas lift or natural flowing wells. The model incorporated the hydrodynamics of the different flow patterns, the influence of the well deviation and geometry, and the heat transfer mechanisms in the annulus.

Farshad et al. (1999) presented two models that use artificial neural networks to predict temperature distribution in oil wells. These networks were tested with the data obtained from 17 wells in the Gulf of Mexico and showed a mean absolute error of 6%. The authors indicated that the neural networks presented the lowest mean absolute errors when they were compared with the Shiu–Beggs' correlation or the Kirkpatrick's chart; the Shiu–Beggs' correlation showed an error of 7.3% while the Kirkpatrick's chart gave a 9.1% error. They also found (from regression analysis) an equation that fits the Kirkpatrick's chart with a coefficient of determination  $R^2 = 0.9997$ .

### 3.3 EXAMPLES OF CORRELATIONS AND MECHANISTIC MODELS DEVELOPED FOR VERTICAL UPWARD MULTIPHASE FLOW

There are many calculation procedures that can be used to find the pressure distribution along the production tubing. These procedures can be categorized as follows:

- Empirical correlations that assume homogeneous flow and do not take into consideration the flow pattern. These were the first correlations used in the oil industry and they are seldom used today because they do not give precise results. An example of this type of correlation is the [Poettmann and Carpenter \(1952\)](#).
- Empirical correlations that do not consider the flow pattern in their calculation procedures but do take into account the fact that the phases can travel at different velocities and therefore the estimation of the liquid holdup plays an important role. This is the case of the [Hagedorn and Brown correlation \(1965\)](#).
- Empirical correlations that have different calculation procedures for each flow pattern. They take into consideration the fact that for most flow patterns, but not for all, the phases can travel at different velocities. Examples of this type of correlation, among many others, are the [Orkiszewski correlation \(1967\)](#) for vertical flow, and the [Beggs and Brill correlation \(1973\)](#) for any pipe inclination angle.
- Mechanistic models that use the hydrodynamic behavior of each flow pattern to develop calculation procedures based on mass- and momentum-balance equations, as well as on many closure

relationships. The models proposed by [Ansari et al. \(1994\)](#) and by [Kaya et al. \(1999\)](#) are examples of these mechanistic models.

Despite the effort made to understand and predict multiphase flow, to this date there is no single correlation or model that can be accurately applied to find the pressure gradient for all operational conditions. This is the reason why downhole pressure and temperature surveys must be run to determine which correlations will give better results for a given group of wells in a gas lift field. The parameters involved in the calculations are just too many and the best that can be done is to select the correlation or model that can give better predictions for specific operational conditions. It could be possible that, even for a given well, one correlation might be better for a given section of the production tubing but not for its entire length. This introduces a serious challenge when trying to design a gas lift well in the following cases: (1) exploratory wells for which little information that can be used to predict the liquid flow rate is available; (2) old or new wells for which a reasonable amount of information is not available; (3) wells with operational conditions that are experiencing changes, like a sudden increase in the water cut or in the gas/liquid ratio.

For the cases mentioned in the last paragraph, there are gas lift design methods described in chapter: Design of Continuous Gas Lift Installations that minimize the impact of not accurately knowing what the production pressure will be. These procedures generally increase the possibility of being able to produce the well in a stable manner while injecting gas through a point equal to the optimum point of injection or very close to it. But their results usually include more gas lift mandrels to be installed in the well and, possibly, the first gas lift valve design would need to be replaced by a new one once the real production potential of the well is known. For these special situations, it is better to install injection-pressure-operated (IPO) valves because they are less sensitive to the production pressure than production-pressure-operated valves are (it is much easier to calculate the injection gas pressure at depth than to know the production pressure along the tubing). It is also advisable in these cases to install gas lift valves with seats as small as possible that are capable of passing the required gas injection flow rate at the same time. These steps minimize the effect the production pressure has on the opening and closing pressures of an IPO gas lift valve. Injection- and production-pressure-operated valves are explained in detail in chapter: Gas Lift Valve Mechanics.

The development of empirical correlations concentrates on finding the liquid holdup and the friction factor in multiphase flow. The procedures to achieve these two goals have progressively been developed and improved during the last decades.

The first widely used multiphase flow correlation was developed by [Poettmann and Carpenter \(1952\)](#). This correlation was used for many years even though it gives very inaccurate results if it is applied under operational conditions different from those found during its development. It is based on data gathered from 334 naturally flowing wells and 15 wells on gas lift. The production-tubing strings were  $2\frac{3}{8}$ ,  $2\frac{7}{8}$ , and  $3\frac{1}{2}$  in. in diameter. The production rates of these wells were less than 500 STB/D, with gas/liquid ratios less than 1500 scf/STB. The authors of this correlation measured the wellhead and bottomhole pressures but not the liquid holdup. They only developed a correlation for the friction factor for multiphase flow. The mixture density was calculated using the homogeneous liquid holdup. Flow patterns and acceleration pressure drops were ignored. The Poettman and Carpenter correlation was first modified by [Baxendell and Thomas \(1961\)](#) and later by [Fancher and Brown \(1963\)](#).

[Hagedorn and Brown \(1965\)](#) developed a correlation that is still widely used in the oil industry because, as recent comparative studies indicate, it gives reasonably accurate results even when compared to the more recent mechanistic models. This correlation was obtained from measurements of the pressure drop and flow rates in a 1500-ft. deep, experimental, vertical well. Tubing strings of  $1\frac{1}{4}$  and  $2\frac{7}{8}$  in. in diameter were used with a considerable number of different gas and liquid flow rates. The effect of the liquid viscosity was studied and, for that purpose, different liquids, like water and several types of oils, with viscosities of 10, 35, and 110 cP, were used. The liquid holdup was not measured and the flow pattern was not taken into consideration; however, an empirical correlation for the nonhomogeneous liquid holdup was developed. The friction factor is obtained from the [Moody \(1944\)](#) diagram but using a special Reynolds number that requires knowing the liquid holdup for its calculation. Two important modifications have been made to the Hagedorn and Brown correlation: it was found that in some cases the calculated liquid holdup was smaller than the homogeneous liquid holdup, which is not possible for vertical-upward flow because the gas phase always travels at a velocity greater than or equal to the liquid velocity. Thus, a lower liquid holdup limit equal to the homogeneous holdup was imposed on the calculated liquid holdup. On the other hand, if it is found (by calculation procedures not developed by Hagedorn and Brown) that the flow pattern was bubble flow, then the [Griffith \(1962\)](#) correlation is used to calculate the pressure gradient.

[Duns and Ros \(1963\)](#) developed a correlation that is also widely used today. It is based on laboratory-scale tests performed at low pressures with air, oil, and water as the working fluids. The length of the test-pipe section was 32.8-ft. long with diameters from  $1\frac{1}{4}$  to 3.15748 in. The liquid holdup

was measured using radioactive traces and the flow pattern was observed at the transparent section of the pipe. A flow pattern map was developed in which the flow pattern was identified based on the superficial velocity of each phase. The three flow patterns defined by this correlation were: bubble, slug, and mist flow. The boundaries of each of these flow patterns are determined from equations based on dimensionless numbers. The developed correlation for the pressure drop in mist flow is also used in the [Orkiszewski \(1967\)](#) and the [Aziz et al. \(1972\)](#) correlations. Duns and Ros were the first researchers to consider the flow pattern to calculate the pressure gradient.

In 1967 Orkiszewski developed a correlation based on the data gathered by Hagedorn and Brown and on the measurements taken in 148 wells. The equations for slug flow were entirely developed by them while the Duns and Ros correlation was used for mist flow and the [Griffith and Wallis \(1961\)](#) correlation was used for bubble flow. The acceleration pressure drop is ignored for all flow patterns except for the mist flow. The Orkiszewski correlation is also used today in the oil industry because it gives good results under many operational conditions.

[Aziz et al. \(1972\)](#) presented a correlation with new equations to determine the flow pattern and pressure drop in bubble and slug flows. For mist flow, they recommended the use of the Duns and Ros' correlation.

[Chierici et al. \(1973; 1974\)](#) published a correlation that in reality is a modified version of the Orkiszewski's correlation. They found that the calculations of the fluid properties deeply affected the determination of the pressure gradient and they gave recommendations as to which type of fluid property correlation to use in conjunction with their pressure–gradient correlation.

[Beggs and Brill \(1973\)](#) proposed a correlation for the pressure gradient obtained from the data gathered at laboratory-scale tests performed in pipes with a variety of upward and downward inclination angles. Even though this correlation can be applied at any pipe inclination angle, it is more frequently used in horizontal flow. A recent comparison study performed in the Middle East by [Usman and Al Gahtani \(2010\)](#) indicated that this correlation is suitable for vertical flow with large liquid flow rates. Beggs and Brill used 1- and 1.5-in. diameter pipes of 90 ft. in length. Only water and air were used as the working fluids. The gas and liquid flow rates were adjusted so that all horizontal flow patterns could be observed. Once a given set of values for the gas and liquid flow rates was established, the pipe inclination angle was changed to investigate the effect of the pipe inclination on the liquid holdup and the pressure gradient. The inclination angle was allowed to change in positive and negative angles of 5, 10, 15, 20, 35, 55, 75, and 90 degrees. Flow patterns were classified in three large groups:



(1) segregated, which includes stratified, stratified wavy, and annular flows; (2) intermittent, for plug and slug flows; (3) distributed, for bubble and mist flows. Specific correlations for the liquid holdup were developed for each of these three groups of flow patterns. The liquid holdup the flow would have if it was horizontal is calculated first and then it is corrected depending on the pipe inclination angle. They found that the maximum value of the liquid holdup takes place at an inclination angle of +50 degrees (upward) and the minimum at -50 degrees (downward). The friction factor is found by a calculation procedure common to all flow patterns, but this factor depends on, among many other parameters, the liquid holdup, which in turn depends on the flow pattern.

Asheim (1986) described a correlation included in a program called MONA, which is used for multiphase flow calculations. This program was developed by the Norwegian Institute of Technology and it can be applied in horizontal or vertical pipes. No experimental data was used for the development of the program and it did not consider the flow pattern. The liquid holdup is not directly calculated; instead, a linear function between the gas and liquid velocity is used to find the density of the mixture. An extension of the equation introduced by Dukler et al. (1969) is used to find the friction factor. Field tests have demonstrated that this correlation is slightly more accurate than: (1) the Beggs and Brill (1973) method, and (2) the combination of the Dukler (1969) and Eaton et al. (1967) correlations that are used many times in the field.

Hasan and Kabir (1986) presented a model that was specially developed for inclined wells. This model predicts the flow pattern and the pressure gradient. It is based on the data obtained from a 5-in. diameter pipe with an inclination angle of up to 32 degrees with respect to the vertical.

The development of mechanistic models began during the 1980s and 1990s. These models take into account the hydrodynamic behavior of the flow in the development of the equations for each flow pattern. In this way, specific models were developed for each flow pattern. Hasan and Kabir (1988), Ansari and Sylvester (1988), and Caetano et al. (1992b), developed models for bubble flow. Fernandes et al. (1983), Sylvester (1987), and Vo and Shoham (1989), developed models for slug flow. Oliemans et al. (1986) and Alves (1991) developed models for annular flow. Global mechanistic models for vertical flows were presented by Ozon et al. (1987), Hasan and Kabir (1988), Ansari et al. (1990), Chokshi et al. (1996), and Kaya et al. (1999). The reader interested in this subject should consult specialized books on multiphase flow. One of the best references is the book published by Shoham (2006), which gives a precise and detailed explanation of the most important mechanistic models for vertical and horizontal flows. It also presents the

so-called unified models, which are mechanistic models that can be applied to any pipe inclination angle.

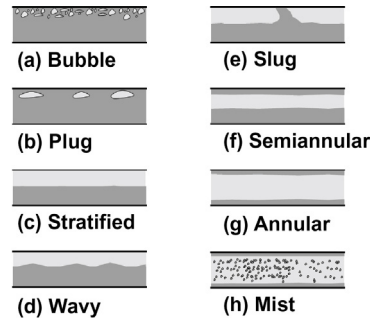
### 3.4 HORIZONTAL MULTIPHASE FLOW

Horizontal multiphase flow plays an important role in gas lift because anything that happens in the flowline, from the wellhead to the flow station, has a direct impact on the pressure at the perforations. Horizontal multiphase flow calculations are made to adequately size flowlines, gas, and liquid gathering systems, and gas lines that might carry some liquids. As far as the well is concerned, pressure drops in the flowline could have a decisive impact if the flowline is too long or its diameter is too small. In some cases, the pressure drop in the flowline could be above 30% of the difference between the reservoir's pressure minus the separator pressure, possibly making other artificial lift methods more attractive than gas lift. In the newly drilled horizontal wells, called "extended reach wells," in which the horizontal section can have tens of thousands of feet, understanding horizontal multiphase flow is very important to prevent instability problems or to be able to handle severe slugging.

The general multiphase flow pressure gradient equation derived for vertical pipes also applies to horizontal pipes and the three pressure gradient components (hydrostatic, friction, and acceleration) are also present in flowline calculations. If the flowline is horizontal, the hydrostatic pressure gradient is zero. But, in many occasions, flowlines are installed in hilly terrains. In these cases, the pressure decreases in the upward direction but then it does not go back to its initial value when the downward flow reaches the initial elevation again. Pipe inclinations with respect to the horizontal also have an impact on the flow pattern, making calculations of the liquid holdup and the pressure drop much more complex.

It is not only important to calculate the pressure drop along the flowline, it is also necessary to know the flow pattern and liquid holdup under certain operational conditions, even if the flow is truly horizontal. This is because the separator should be properly designed to handle large liquid slugs or any other liquid holdup fluctuations that might cause liquids to enter the gas gathering system. Separators are designed to handle stable flows of gas and liquids. If large liquid slugs periodically reach the separator, provisions must be made to handle these occasionally high volumes of liquids.

To design surface facilities in general, it is then necessary to know the flow pattern as precisely as possible. At least eight flow patterns have been described for horizontal flow, as shown in [Fig. 3.12](#).



■ FIGURE 3.12 Horizontal flow patterns.

DeGance and Atherton (1971) classified the flow patterns in only three categories, which were later used by Beggs and Brill (1973) in their correlation (as explained in Section 3.3). However, before Degance and Atherton published their work, one of the first attempts to predict the flow pattern using flow pattern maps was carried out by Baker (1954), for which the horizontal axis corresponds to the values of the group defined as  $G_{Lmf} \lambda \phi / G_{gmf}$  while  $G_{gmf} / \lambda$  is plotted on the vertical axis.  $G_{Lmf}$  and  $G_{gmf}$  are the liquid and gas mass fluxes, respectively, both in  $\text{lbm/hr ft.}^2$ , and:

$$\phi = \frac{73}{\sigma_L} \left[ \mu_L \left( \frac{62.4}{\rho_L} \right)^2 \right]^{1/3}, \text{ where } \mu_L \text{ is the liquid viscosity and } \sigma_L \text{ is the surface tension.}$$

$$\lambda = \left[ \left( \frac{\rho_g}{0.075} \right) \left( \frac{\rho_L}{62.4} \right) \right]^{1/2} \text{ where } \rho_g \text{ and } \rho_L \text{ are the gas and liquid densities, respectively.}$$

Mandhane et al. (1974) published a flow pattern map that is still in use in the oil industry. It was based on an extensive experimental database. The coordinates for this map are the superficial gas and liquid velocities, which are the coordinates more frequently used today in most flow pattern maps.

All of the flow pattern maps indicated earlier only apply to a perfectly horizontal flow. If the pipe is inclined in the upward direction, stratified flow cannot exist; instead, slug flow will be found at the same superficial velocities of the phases. If, on the other hand, the pipe is inclined in the downward direction, the predominant flow pattern is stratified while slug flow cannot take place where horizontal maps indicate. Recently developed unified models, for which the pipe inclination is considered in the flow pattern determination, are being recognized for their accuracy in their predictions.

Regarding liquid holdup and pressure drop calculations for horizontal flow, correlations and models were developed more than half a century ago and have evolved in the same way as models and correlations for vertical flow have.

[Lockhart and Martinelli \(1949\)](#) published a procedure to calculate the pressure gradient in horizontal pipes in terms of single-phase pressure gradients multiplied by a correction factor. The single-phase pressure gradients are calculated as if each phase traveled alone in the pipe. They also presented a correlation for the liquid holdup even though it is not used in the calculation of the pressure gradient.

[Hughmark and Pressburg \(1961\)](#) presented a correlation to calculate the liquid holdup in vertical pipes that has been used in horizontal pipes with some degree of success.

[Eaton et al. \(1967\)](#) published a correlation to predict the friction pressure drop and the liquid holdup. This correlation was obtained from an extensive work carried out at an experimental facility that had horizontal pipes of 1700 ft. in length. Tubing diameters of 2 and 4 in. were used. Three types of liquids were used as the working fluids. The gas flow rates ranged from 0 to 10 MMscf/D, the liquid flow rate varied from 50 to 5500 STB/D, with viscosities from 1 to 13.5 cP. The pressure was allowed to change from 70 to 950 psig. The friction factor and the liquid holdup were correlated with dimensionless numbers using regression analysis. The liquid holdup was measured by trapping the flow between two quick closing valves. Neither the flow pattern nor the pipe inclinations were considered in the correlation. The liquid holdup correlation is considered to be one of the best correlations for horizontal flow but the friction factor correlation does not converge to single-phase flow when it approaches single-phase liquid or single-phase gas flows. For small gas/liquid ratios, the friction factor becomes very large.

In 1969, Dukler et al. published the results of an experimental study sponsored by the American Gas Association that gathered more than 20,000 experimental points obtained at laboratory- and field-scale tests. These tests were then reduced to 2600 tests after eliminating unreliable or suspiciously wrong data. A correlation was developed for the frictional pressure gradient from these tests. A method to find the void fraction was also obtained. The void fraction is used to calculate the mixture density, which is used in turn as one of the parameters to calculate frictional pressure gradient. Dukler's method has been extensively used in the oil industry and it has demonstrated to give good results for small and large pipe diameters. Even though this correlation does not include the effect of pipe inclination, it has been combined with the method proposed by [Flanigan \(1958\)](#) for inclined pipes. Flanigan carried out an extensive research work mostly in a 16-in. diameter

pipe (among other pipe diameters) and developed a method to calculate the frictional and hydrostatic pressure gradient.

Beggs and Brill (1973) published a correlation to determine all the components of the pressure drop in multiphase flow, taking into consideration the flow pattern and the pipe's inclination angle. Even though it can be used for any inclination angle, its major application has been for horizontal flowlines rather than for production tubing designs.

Gregory et al. (1974) published a model that combines several correlations available at the time for multiphase, horizontal flow. They used a data bank that had 2,685 liquid-holdup measurements and more than 10,000 pressure-drop measurements. This data bank was used to select the best correlation to be applied for each flow pattern. The flow pattern for each experimental point was obtained using the map developed by Mandhane. Then, the most precise correlations for the liquid holdup and the frictional pressure drop were selected for each flow pattern. These correlations are as follows:

- For liquid holdup: (1) bubble flow: Hughmark (1962); (2) stratified flow: Agrawal et al. (1973); (3) wavy flow: Chawla (1969); (4) slug flow: Hughmark (1962); (5) annular flow: Lockhart and Martinelli (1949); dispersed flow: Beggs and Brill (1973).
- For friction loss: (1) bubble flow: Chenoweth and Martin (1955); (2) stratified flow: Agrawal et al. (1973); (3) wavy flow: Dukler et al. (1964); (4) slug flow: Dukler et al. (1964); (5) annular flow: Chenoweth and Martin (1955); dispersed flow: Lockhart (modified) (1949).

Oliemans (1976) published a work that introduced a new concept to multiphase, horizontal-flow calculations. Even though he did not develop a correlation for the liquid holdup, his equations use the liquid holdup (calculated from other correlations) to find the frictional pressure gradient.

Asheim (1986) described a correlation found in a computer program named MONA, which was developed for multiphase flow calculations. This program was developed by the Norwegian Institute of Technology and it was used for horizontal and vertical flows. The program was not based on any experimental data and it did not consider the flow pattern in its calculations. The liquid holdup is not directly calculated; instead, a linear function of the gas and liquid velocities is used to find the mixture density. An extension of the Dukler's correlation is used to find the friction factor. Field tests have indicated that this correlation gives results which are slightly more precise than the Beggs and Brill correlation or the combined Dukler–Eaton correlation.

Xiao et al. (1990) published a mechanistic model developed for horizontal or nearly horizontal flows. The model can predict the flow pattern, the liquid

holdup, and the pressure gradient. The flow patterns considered by this model were: stratified, intermittent, annular, and dispersed bubble flow.

### 3.5 UNIFIED MODELS

The so-called “unified models” have been under development during recent years. These models can be used for any pipe inclination angle and that is why they are called “unified.” The unified model presented by [Gomez et al. \(1999\)](#) can predict the flow pattern, liquid holdup, and pressure drop in pipes with inclination angles from horizontal (0 degrees) to upward vertical flow (+90 degrees). It consists of: (1) a unified model to predict the flow pattern, and (2) unified individual mechanistic models to predict the pressure drop and liquid holdup in stratified, slug, bubble, annular, and dispersed bubble flow.

The first models were in reality empirical correlations specifically, and separately, developed for horizontal or vertical flow. This is the case of the correlations developed by Dukler or by Oliemans for horizontal flow, or by Hagedorn and Brown and by Duns and Ros for vertical flow, among many others. According to Gomez et al., for more than 40 years these correlations were used with deviations of up to  $\pm 30\%$  and no better overall accuracy seemed to be possible through this approach.

Since the early 1980s, the new mechanistic models began to be developed and, in consequence, the accuracy in the prediction of the liquid holdup and pressure gradient has improved during recent years. These models concentrate on the development of equations, such as the momentum- and mass-balance equations, in conjunction with the so-called constitutive equations, to describe a specific flow pattern. These equations depend on the geometry and hydrodynamic characteristics of each flow pattern. The first goal of this type of models is then to be able to predict the flow pattern for a given operational condition.

At the beginning, mechanistic models were developed for horizontal and vertical flows separately.

#### 3.5.1 Horizontal flow

One of the first models that were developed to predict the flow pattern was the [Taitel and Dukler model in 1976a](#). For the pressure drop and liquid holdup, separate hydrodynamic models for each flow pattern were developed during the 1970s and 1980s.

- For stratified flow: [Taitel and Dukler \(1976b\)](#), [Cheremisinoff and Davis \(1979\)](#), [Shoham and Taitel \(1984\)](#), and [Issa \(1988\)](#).

- For slug flow: Dukler and Hubbard (1975), Nicholson et al. (1978), and Kokal and Stanislav (1989).
- For annular flow: Laurinat et al. (1985) and James et al. (1987).
- For dispersed bubble flow: Wallis (1969).
- A comprehensive mechanistic model, incorporating a flow pattern prediction model and separate models for the different flow patterns, was developed by Xiao et al. (1990) for pipe line design.

### 3.5.2 Vertical flow

Taitel et al. (1980) proposed a model to predict the flow pattern. This model was enhanced by Barnea et al. (1985) to include vertical pipes with large inclination angles. The following hydrodynamic mechanistic models were developed for each flow pattern in vertical flow.

- For bubble vertical flow: Hasan and Kabir (1988) and Caetano et al. (1992b).
- For slug vertical flow: Fernandes et al. (1983), Sylvester (1987), and Vo and Shoham (1989).
- For annular vertical flow: Oliemans et al. (1986) and Alves (1991).
- Comprehensive mechanistic models for vertical flow have been developed by Ozon et al. (1987), Hasan and Kabir (1988), Ansari et al. (1994), and Chokshi et al. (1994; 1996).

### 3.5.3 Unified models

Recent developments concentrate on unified models that are applicable for the entire range of inclination angles. Barnea (1987) published a model that can be used to predict the flow pattern in pipes with inclination angles from +90 to -90 degrees with respect to the horizontal. Felizola and Shoham (1995) presented a unified model for slug flow. Petalas and Aziz (1996) presented a unified mechanistic model that can be applied to horizontal flow and downward or upward vertical flows. Gomez et al. (1999) presented a unified model that can predict the liquid holdup in the liquid slug body of the slug flow model.

Parallel to the development of the comprehensive unified mechanistic model presented by Gomez et al. (1999), Kaya et al. (1999) presented a mechanistic model for vertical flow in inclined pipes.

## 3.6 FLUID FLOW THROUGH ANNULAR CROSS-SECTIONS

Multiphase flow in annular conduits might take place in a variety of operational conditions in the production of an oil or gas well. The following is a list of examples in which it is necessary to have fluid flow through annular cross-sections:

- In wells where it would be highly restrictive, due to frictional losses, to produce them through the production tubing. In these cases, it is preferable to produce the wells up the annulus between the casing and the tubing. This type of operation usually takes place in wells with high reservoir pressures.
- Contrary to the previous point, in oil or gas wells for which a reduction in the reservoir pressure makes it necessary to install a blind tubing, or velocity string, inside the production tubing to reduce the flow area and increase the fluid velocity, thereby avoiding liquid accumulation at the bottom of the well that might lead to a reduction or complete stop of liquid and/or gas production. The well is produced up the annulus between the existing production tubing and the newly installed, small-diameter tubing.
- In dual wells with concentric completions, where it is desired to produce the upper zone up the external annulus and the lower zone up the production tubing.
- In wells produced by sucker rod pumps, in which the liquids and gas travel up the annulus between the production tubing and the rods.
- In gas lift wells with different accumulation chamber configurations.
- During the drilling operations of a well.

Many situations are presented in the chapter: Gas Lift Equipment for which annular flow is unavoidable. For example, Fig. 6.48 shows several alternatives that can be used to produce a gas lift well up the annulus. On the other hand, Fig. 6.73 shows completions with two concentric production strings to produce from two different zones. Advantages, disadvantages, and important limitations regarding the use of annular conduits to produce oil wells are also given in the chapter: Gas Lift Equipment.

The most important models that have been developed to calculate the pressure drop in single and multiphase flow through annuli are enumerated in this section.

Despite the recent achievements made in the development of mathematical models to predict the pressure drop in annular conduits, no correlation or mechanistic model has been extensively tested against field data. It is very difficult to find field data, especially along the production annulus, because it is not possible to run pressure and temperature surveys down the casing-tubing annulus.

### 3.6.1 Flow pattern prediction

[Kelessidis and Dukler \(1989\)](#) and [Caetano et al. \(1992a\)](#) presented important research studies to predict the flow pattern in annuli. Just as it was the



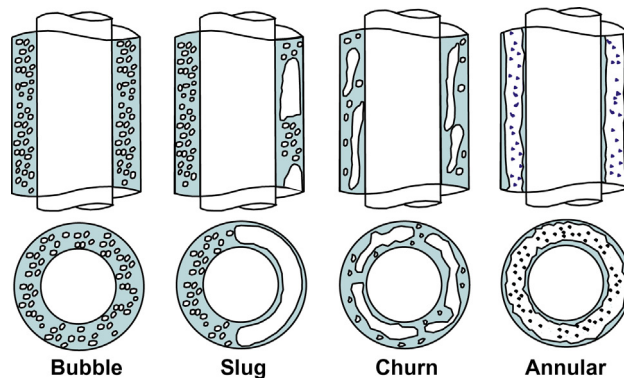
case for circular pipes, the prediction of the flow patterns in annular spaces is very important because the models that are used to calculate the liquid holdup and pressure drop in annuli are developed for each flow pattern in particular.

Kelessidis and Dukler (1989) carried out laboratory-scale experiments in multiphase flow in concentric and 50% eccentric annuli. They developed a method to identify flow patterns in a more objective way than just by simple visual observation. The flow patterns that were identified were very similar to the ones found in circular pipes: bubbly, slug, churn, and annular flow. Fig. 3.13 shows the flow patterns that are commonly encountered in multiphase flows in annuli.

In slug flow, the Taylor bubbles do not travel in the annulus in a concentric way as they do in circular pipes; instead, they travel in only one side of the annulus with the other side mostly filled with liquids.

Based on experimental observations, flow pattern maps for concentric and eccentric annuli have been constructed. These maps constitute the basis for the development of the mathematical models that describe the flow pattern boundaries. The criteria used in the equations that determine the flow pattern transitions presented by Kelessidis and Dukler, are mostly based on the work of Taitel et al. (1980).

As in the work of Kelessidis and Dukler, Caetano et al. (1992a) modified the model developed by Taitel et al. (1980) for circular pipes to predict the flow pattern in annuli. The experimental observations made by Caetano et al. (1992a) identified the same flow patterns described by Kelessidis and Dukler: bubble, dispersed bubble, slug, churn, and annular flow. In the experimental work performed by Caetano et al. (1992a), the outer pipe had



■ FIGURE 3.13 Flow patterns in upward, vertical, concentric annuli.

an inside diameter of 3 in. and the inner pipe outside diameter was equal to 1.66 in.. The total length of the test section was equal to 44.95 ft. Quick-closing ball valves were installed at both ends of the test section. Water and kerosene were used as the working liquids while compressed air was used for the gas phase. Water and kerosene were used in concentric annuli while only water was used in totally eccentric annuli.

### 3.6.2 Models developed for liquid holdup and pressure drop calculations

The most important models developed during the last decades for the prediction of the liquid holdup and the friction drop in annular cross-sections are enumerated in this section. This model-development process has followed three different paths.

The first approach was the use of the hydraulic diameter to apply the known correlations developed for multiphase flow in circular pipes. The work done by [Sanchez \(1972\)](#) is an example of this type of approach.

The second approach consists in using correlations specifically developed from experimental data obtained in annuli. Examples of this type of correlations are: [Baxendell \(1958\)](#), [Gaither et al. \(1963\)](#), [Angel and Welchon \(1964\)](#), [Winkler \(1968\)](#), and [Cornish \(1976\)](#). The first three examples do not take into consideration the existence of different flow patterns, while the work presented by Winkler is only for slug flow and the model developed by Cornish applies only to homogeneous flow.

The third type of approach is the development of mechanistic models to predict the flow pattern and, for each flow pattern, to find the liquid holdup and the pressure drop. [Sadatomi et al. \(1982\)](#) presented a theoretical and experimental work, which does not include mechanistic models for the pressure drop but only for the prediction of the liquid holdup. Even though the Sadatomi et al. liquid-holdup model follows the approach of a mechanistic model, the flow pattern for which this model was developed was not specified. Regardless of these facts, the work presented by Sadatomi et al. is important because it showed the measurements made of the bubble velocity under different operational conditions. [Caetano et al. \(1992b\)](#) presented the first mechanistic model exclusively developed for multiphase flow in annular cross-sections.

[Lage and Time \(2002\)](#) presented a mechanistic model to predict the behavior of multiphase flow in concentric annuli which consisted in a procedure that can be used to predict the flow pattern and a series of independent models for the determination of the void fraction and the pressure drop for each of the

following flow patterns: bubble, dispersed-bubble, slug, and annular flow. Some aspects that have to do with churn flow (which were totally ignored by Caetano (1992b)) were also presented by Lage and Time. A very important point regarding the work of Lage and Time is the fact that they conducted an experimental study in a 1278-m deep well with a field-scale annulus.

Only a few publications were presented between the study conducted by Caetano et al. and the one by Lage and Time. Papadimitriou and Shoham (1991) presented some improvements made on the Caetano's model (1992b) but only for bubble and slug flows; Hasan and Kabir (1992) focused their attention on the prediction of the flow pattern and the liquid holdup but they did not present a model for the pressure drop and did not consider the annular-flow pattern.

Yu et al. (2009) presented a mechanistic model to predict the flow pattern, the liquid holdup, and the pressure gradient for multiphase flow in annular ducts. The models used for flow pattern transitions were the unified model developed by Zhang et al. (2003a) for dispersed bubble and annular flow, Caetano (1985) for the bubble-flow transition, and the modified model of Kaya et al. (2001) for the transition from slug to churn flow. The churn-flow model was based on the modified model developed by Zhang et al. (2003b) for circular pipes.

## REFERENCES

- Agrawal, S.S., Gregory, G.A., Govier, G.W., 1973. An analysis of horizontal stratified two-phase flow in pipes. *Can. J. Chem. Eng.* 51 (3), 280–286.
- Alves, I.N., 1991. Slug flow phenomena in inclined pipes. PhD dissertation. The University of Tulsa, Tulsa, OK.
- Alves, I.N., Alhanati, F.J.S., Shoham, O., 1992. A unified model for predicting flowing temperature distribution in wellbores and pipelines. SPEPF 363.
- Angel, R.R., Welchon, J.K., 1964. Low-ratio gas-lift correlation for casing-tubing annuli and large-diameter tubing. *API Drill. Prod. Pract.* 100.
- Ansari, A.M., Sylvester, N.D., 1988. A mechanistic model for two-phase bubble flow in vertical pipes. *AIChE J.* 34 (8), 1392–1394.
- Ansari, A.M., Sylvester, N.D., Shoham, O., Brill, J.P., 1990. A comprehensive mechanistic model for upward two-phase flow in wellbores. Paper SPE 20630 presented at the Annual Technical Conference and Exhibition of the Society of Petroleum Engineers, New Orleans, Louisiana, September 23–26.
- Ansari, A.M., Sylvester, N.D., Sarica, C., Shoham, O., Brill, J.P., 1994. A comprehensive mechanistic model for upward two-phase flow in wellbores. *SPEPF J.*, pp. 143–152.
- Asheim, H., 1986. MONA, an accurate two-phase well flow model based on phase slippage. *SPE Prod. Eng. J.*, 221–230.
- Aziz, k., Govier, G.W., Fogarasi, M., 1972. Pressure drop in wells producing oil and gas. *J. Can. Pet. Technol.* 11 (3), 38–48.

- Baker, O., 1954. Design of pipelines for simultaneous flow of oil and gas. *Oil Gas J.* 53, 185–195.
- Barnea, D., Shoham, O., Taitel, Y., Dukler, A.E., 1985. Gas–liquid flow in inclined tubes: flow pattern transitions for upward flow. *Chem. Eng. Sci.* 40, 131–136.
- Barnea, D., 1987. A unified model for predicting flow pattern transition for the whole range of pipe inclinations. *Int. J. Multiphase Flow* 13 (1), 1–12.
- Baxendell, P.B., 1958. Calculation of Vertical Flow Gradients for 7"x2-7/8" Annuli. Shell de Venezuela, internal report.
- Baxendell, P.B., Thomas, R., 1961. The calculation of pressure gradients in high-rate flowing wells. *J. Pet. Technol.* 13, 1023–1028.
- Beggs, H.D., 1991. *Production Optimization Using Nodal Analysis*. OGCI Publications, Oil and Gas Consultants International Inc, Tulsa, OK.
- Beggs, H.D., Brill, J.P., 1973. A study of two-phase flow in inclined pipes. *J. Pet. Technol.* 25 (5), 607–617.
- Caetano, E.F., 1985. Upward vertical two-phase flow through an annulus. PhD dissertation. The University of Tulsa, OK.
- Caetano, E.F., Shoham, O., Brill, J.P., 1992a. Upward vertical two-phase flow through an annulus—part I: single-phase friction factor, Taylor bubble rise velocity, and flow pattern prediction. *J. Energy Resour. Technol.* 114, 1–13.
- Caetano, E.F., Shoham, O., Brill, J.P., 1992b. Upward vertical two phase flow through an annulus part II: modeling bubble, slug, and annular flow. *ASME J. Energy Resour. Technol.* 114, 13–30.
- Chawla, J.M., 1969. Liquid content in pipes in two-phase flow of gas–liquid mixtures. *Chimi. Ingenieur. Technic.* 41 (5–6), 328–330.
- Chenoweth, J.M., Martin, M.W., 1955. Turbulent two-phase flow. *Pet. Ref.* 34 (10), 151–155.
- Cheremisinoff, N.P., Davis, E.J., 1979. Stratified turbulent–turbulent gas–liquid flow. *AIChE J.* 25 (1), 48–56.
- Chierici, G.L., Cuicci, G.M., Sclocchi, G., 1974. Two-phase vertical flow in oil wells—prediction of pressure drop. *J. Pet. Technol.* 26 (8), 927–939.
- Chokshi, R.N., 1994. Prediction of pressure drop and liquid holdup in vertical two-phase flow through large diameter tubing. PhD dissertation, The University of Tulsa.
- Chokshi, R.N., Schmidt, Z., Doty, D.R., 1996. Experimental study and the development of a mechanistic model for two-phase through vertical tubing. Paper SPE 35676.
- Cornish, R.E., 1976. The vertical multiphase flow of oil and gas at high rates. *J. Pet. Technol.* 28 (7), 825–831.
- Coulter, D.M., Bordon, M.F., 1979. Revised equation improves flowing gas temperature prediction. *Oil Gas J.* 26, 107–108.
- DeGance, A.E., Atherton, R.W., 1971. Chemical engineering aspects of two-phase flow. *Chem. Engr. Mar.* 23, Apr. 20, May 4, Jul. 13, Aug. 10, Oct. , Nov. 2, 1970, Feb. 22, 1971.
- Dukler, A.E., et al., 1969. Gas–Liquid Flow in Pipelines, I. Research Results. AGA-API Project NX-28.
- Dukler, A.E., Hubbard, M.G., 1975. A model for gas–liquid slug flow in horizontal and near horizontal tubes. *Ind. Eng. Chem. Fundam.* 14, 337–347.
- Dukler, A.E., Wickes, M., Cleveland, R.G., 1964. Frictional pressure drop in two-phase flow, an approach through similarity analysis. *AIChE J.* 10 (1), 44–51.

- Dukler, A.E., et al., 1969. Gas-liquid flow in pipelines, I. research results. AGA-API Project NX-28.
- Duns, H., Ros N.C., 1963. Vertical flow of gas and liquid mixtures in wells. Proceedings of the Sixth World Petroleum Congress, 451.
- Eaton, B.A., Knowles, C.R., Silberberg, I.H., 1967. The prediction of flow patterns, liquid holdup and pressure losses occurring during continuous two-phase flow in horizontal pipelines. *J. Pet. Technol.* 19 (6).
- Fancher, G.H., Brown, K.E., 1963. Prediction of pressure gradients for multiphase flow in tubing. *Soc. Pet. Eng. J.* 3 (1), 59-69.
- Farshad, F., Garber, J.D., Lorde, J.N., 1999. Predicting temperature profiles in producing oil wells using artificial neural networks. SPE 53738.
- Felizola, H., Shoham, O., 1995. A unified model for slug flow in upward inclined pipes. *ASME J. Energy Resour. Technol.* 117, 1-6.
- Fernandes, R.C., Semiat, R., Dukler, A.E., 1983. Hydrodynamic model for gas-liquid slug flow in vertical tubes. *AIChE J.* 29, 981-989.
- Flanigan, O., 1958. Effect of uphill flow on pressure drop in design of two-phase gathering systems. *Oil Gas J.* 10, 132-141.
- Gaither, O.D., Winkler, H.W., Kirkpatrick, C.V., 1963. Single and two-phase fluid flow in small diameter vertical conduits including annular configurations. *J. Pet. Technol.*, 309-320.
- Gomez, L. E., Shoham, O., Schmidt, Z., Chokshi, R. N., Brown, A., Northug, T. 1999. A unified mechanistic model for steady-state two-phase flow in wellbores and pipelines. Paper SPE 56520 presented at the 1999 SPE Annual Technical Conference and Exhibition, Houston, Texas, October 3-6 .
- Gregory, G.A., Mandhane, J.M., Aziz, K., 1974. Some design considerations for two-phase flow in pipes. C.I.M. Paper No. 374020.
- Griffith, P., 1962. Two-Phase Flow in Pipes. Special Summer Program. Massachusetts Institute of Technology, Cambridge, MA.
- Griffith, P., Wallis, G.B., 1961. Two-Phase Slug Flow. *J. Heat Transfer Trans. ASME* 83, 307-320.
- Hagedorn, A.R., Brown, K.E., 1965. Experimental study of pressure gradients occurring during continuous two-phase flow in small-diameter vertical conduits. *J. Pet. Technol.* 17 (4), 475-484.
- Hasan, A.R., Kabir, C.S., 1986. Predicting multiphase flow behavior in a deviated well. Paper SPE 15449.
- Hasan, A.R., Kabir, C.S., 1988. A study of multiphase flow behavior in vertical wells. *SPE Production Engineering. AIME* 285, 263-272.
- Hasan, A.R., Kabir, C.S., 1992. Two-phase flow in vertical and inclined annuli. *Int. J. Multiphase Flow* 18 (2), 279.
- Hasan, A.R., Kabir, C.S., 1993. Predicting fluid temperature profiles in gas-lift wells. SPE 26098.
- Hasan, A.R., Kabir, C.S., 1994. Aspects of wellbore heat transfer during two-phase flow. SPEPF 211.
- Hughmark, G.A., 1962. Holdup in gas-liquid flow. *Chem. Eng. Prog.* 58 (4), 62-65.
- Hughmark, G.A., Pressburg, B.S., 1961. Holdup and pressure drop with gas-liquid flow in a vertical pipe. *AIChE J.* 7, 677.
- Issa, R.I., 1988. Prediction of turbulent stratified two-phase flow in inclined pipes and channels. *Int. J. Multiphase Flow* 14 (21), 141-154.

- James, P.W., Wilkes, N.S., Conkie, W., Burnes, A., 1987. Developments in the modeling of horizontal annular two-phase flow. *Int. J. Multiphase Flow* 13 (2), 173–198.
- Kaya, A.S., Sarica, C., Brill, J. P., 1999. Comprehensive mechanistic modeling of two-phase flow in deviated wells. Paper SPE 56522 presented at the 1999 SPE Annual Technical Conference and Exhibition, Houston, Texas, October 3–6 .
- Kaya, A.S., Sarica, C., Brill, J.P., 2001. Mechanistic modeling of two-phase flow in deviated wells. *SPE J.* 16 (3), 156–165.
- Kelessidis, V.C., Dukler, A.E., 1989. Modeling flow pattern transitions for upward gas–liquid flow in vertical concentric and eccentric annuli. *Int. J. Multiphase Flow* 15 (2), 173–191.
- Kirkpatrick, C.V., 1962. Advances in gas lift technology. *J. Pet. Technol.* 14, 427.
- Kokal, S.L., Stanislav, J.F., 1989. An experimental study of two-phase flow in slightly inclined pipes ii: liquid holdup and pressure drop. *Chem. Eng. Sci.* 44 (3), 681–693.
- Lage, A., Time, R., 2002. An experimental and theoretical investigation of upward two-phase flow in annuli. *SPE J.* 7 (3), 325–336.
- Laurinat, J.E., Hanratty, T.J., Jepson, W.P., 1985. Film thickness distribution for gas–liquid annular flow in a horizontal pipe. *Int. J. Multiphase Flow* 6, 179–195.
- Lockhart, R.W., Martinelli, R.C., 1949. Proposed correlation of data for isothermal two-phase, two-component flow in pipes. *Chem. Eng. Prog.* 45, 39.
- Mandhane, J.M., Gregory, G.A., Aziz, K., 1974. A flow pattern map for gas–liquid flow in horizontal pipes. *Int. J. Multiphase Flow* 1, 537–553.
- Moody, L.F., 1944. Friction Factor for Pipe Flow. *ASME Transactions* 66, 671–684.
- Nicholson, K., Aziz, K., Gregory, G.A., 1978. Intermittent two phase flow in horizontal pipes, predictive models. *Can. J. Chem. Eng.* 56, 653–663.
- Oliemans, R.V.A., 1976. Two-phase flow in gas-transmission pipelines. *ASME paper* 76-Pet-September 25 1976.
- Oliemans, R.V.A., Pots, B.F.M., Trope, N., 1986. Modeling of annular dispersed two-phase flow in vertical pipes. *Int. J. Multiphase Flow* 12 (5), 711–732.
- Orkiszewski, J., 1967. Predicting two-phase pressure drops in vertical pipes. *J. Pet. Technol.* 19, 829–838.
- Ozon, P.M., Ferschneider, G., Chwetzof, A., 1987. A new multiphase flow model predicts pressure and temperature profiles. Paper SPE 16535. September, 1987.
- Papadimitriou, D.A., Shoham O., 1991. A mechanistic model for predicting annulus bottomhole pressures in pumping wells. Paper SPE 21669.
- Petalas, N., Aziz, K., 1996. Development and testing of a new mechanistic model for multiphase flow in pipes. *Proc. ASME Fluids Eng. Division* 236 (1), 153–159.
- Poettmann, F.H., Carpenter, P.G., 1952. The multiphase flow of gas, oil and water through vertical flow strings with application to the design of gas-lift installations. *API Drill. Prod. Pract.*, 257–317.
- Ramey, H.J., 1962. Wellbore heat transmission. *J. Pet. Technol.* 14 (4), 427.
- Sadatom, M., Sato, Y., Saruwatari, S., 1982. Two-phase flow in vertical noncircular channels. *Int. J. Multiphase Flow* 8 (6), 641–655.
- Sagar, R., Doty, D., Schmidt, Z., 1991. Predicting temperature profiles in a flowing well. SPEPF 441.
- Sanchez, M.J., 1972. Comparison of correlations for predicting pressure losses in vertical multiphase flow. Masters Thesis. The University of Tulsa, Tulsa, OK.

- Shiu, K.C., Beggs, H.D., 1980. Predicting temperatures in flowing oil wells. *Trans AIME 2 J. Energy Res. Technol.* 102 (1), 2–11.
- Shoham, O., 2006. *Mechanistic Modeling of Gas–Liquid Two-Phase Flow in Pipes*. Society of Petroleum Engineers, Richardson, TX.
- Shoham, O., Taitel, Y., 1984. Stratified turbulent–turbulent gas liquid flow in horizontal and inclined pipes. *AIChE J.* 30, 377–385.
- Sylvester, N.D., 1987. A mechanistic model for two-phase vertical slug flow in pipes. *ASME J. Energy Resour. Technol.* 109, 206–213.
- Taitel, Y., Barnea, D., Dukler, A.E., 1980. Modeling flow pattern transitions for steady upward gas–liquid in vertical tubes. *AIChE J.* 26, 345–354.
- Taitel, Y., Dukler, A.E., 1976a. A model for predicting flow regime transitions in horizontal and near horizontal gas–liquid flow. *AIChE J.* 22 (1), 47–55.
- Taitel, Y., Dukler, A.E., 1976b. A theoretical approach to the Lockhart–Martinelli correlation for stratified flow. *Int. J. Multiphase Flow* 2, 591–595.
- Usman, A., Al Gahtani, A., 2010. A comparative study between empirical correlations and mechanistic models of vertical multiphase flow. Paper SPE 136931 presented at the 2010 SPE/DGS Annual Technical Symposium and Exhibition held in Al-Khobar, Saudi Arabia, April 4–7.
- Vo, D.T., Shoham, O., 1989. A note on the existence of a solution for upward vertical two-phase slug flow in pipes. *ASME J. Energy Resour. Technol.* 111, 64–65.
- Wallis, G.B., 1969. *One-Dimensional Two-Phase Flow*. McGraw-Hill Book Co, Inc, New York.
- Winkler, H.W., 1968. Single and two-phase vertical flow through  $0.996 \times 0.623$  inch fully eccentric plain annulus configuration. PhD dissertation, University of Texas, Austin, TX.
- Xiao, J.J., Shoham, O., Brill, J. P., 1990. A comprehensive mechanistic model for two-phase flow in pipelines. Paper SPE 20631 presented at the Sixty-Sixth SPE Annual Technical Conference and Exhibition, New Orleans, Louisiana, September 23–26.
- Yu, T.T., Zhang, H.Q., Li M.X., Sarica, C., 2009. A mechanistic model for gas/liquid flow in upward vertical annuli. Paper SPE 124181 presented at the 2009 SPE Technical Conference and Exhibition, New Orleans, Louisiana, October 4–7.
- Zhang, H.Q., Wang, Q., Sarica, C., Brill, J.P., 2003a. Unified model for gas–liquid pipe flow model via slug dynamics – part I: model development. *J. Energy Resour. Technol.* 125, 274–283.
- Zhang, H.Q., Wang, Q., Sarica, C., Brill, J.P., 2003b. A unified mechanistic model for slug liquid holdup and transition between slug and dispersed bubble flows. *Int. J. Multiphase Flow* 29, 97–107.
- Zimmerman, W.G., 1982. *Manual Básico de Gas Lift*. Informe interno de Lagoven, S. A. Tía Juana, Venezuela.

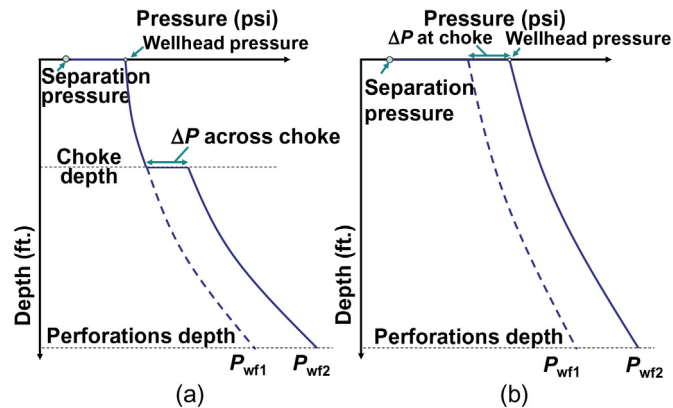
# Single and multiphase flow through restrictions

The use of gas lift system components that cause “intentional” restrictions in the injection gas line, production tubing, and flowline, is extremely important because it provides the means for an effective control of the operation of oil producing wells. These components are available in a variety of types and purposes. For example, the injection gas into the well and the total gas out of the separator may pass through a restriction called “orifice plate” that is usually used in gas lift fields to measure the gas flow rate. Orifice plates generate local pressure drops that are large enough to be accurately measured and correlated with the gas flow rate. An orifice plate is designed in such a way that the downstream pressure (away from the orifice plate) is restored back to almost the same value of the upstream pressure, minimizing permanent pressure drops. But there are other applications specifically designed to control the gas or liquid flow rate, for which permanent pressure drops are necessarily large. This is the case of surface chokes. A choke is usually nothing more than a small diameter conduit of around 6 in. in length. In a gas lift well, the injection gas flow rate is normally controlled by means of a needle valve that acts as a choke of variable inside diameter, although in some cases regular chokes are also used for that purpose. For example, to avoid gas over injection in a “choke-control intermittent gas lift well” (see Section 10.5 for the different types of gas injection control systems in intermittent gas lift), it might be necessary to limit the effect of a very long surface injection gas line (or any gas line with a large diameter) by installing a choke as close as possible to the wellhead. In this way, the volume of gas stored in the injection gas line is choked and kept from being injected into the well’s annulus every time the downhole pilot valve opens. In this case, the choke only allows a very small gas flow rate to pressurize the well’s annulus while the downhole gas lift valve is closed. Once the gas lift valve opens, the choke will not allow the very large surface gas flow rate that would otherwise take place.

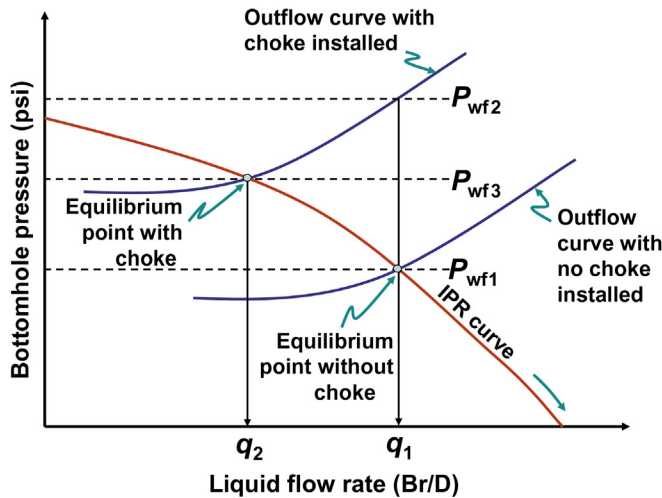


The seat of a gas lift valve is in reality a choke that controls the maximum gas flow rate from the annulus into the production tubing (or from the tubing into the annulus if the lift gas is injected down the tubing). As it is explained in chapter: Gas Lift Equipment, a gas lift valve can be a simple orifice valve or a calibrated valve. In the former case, the valve acts as a fixed-diameter choke and in the latter case the valve acts as a choke of variable inside diameter. The equations that are used to predict the gas flow rate through orifice valves are derived in this chapter, while the equations (or dynamic models) that need to be applied in case of calibrated valves are explained in detail in chapter: Gas Flow Through Gas Lift Valves.

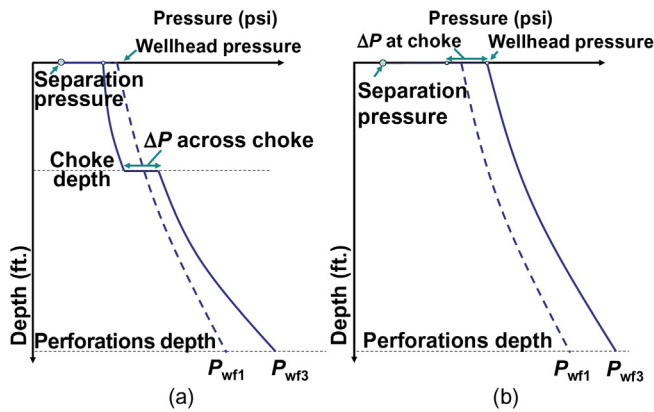
The use of chokes in the production tubing, or in the flowline, is not recommended for gas lift wells. Opposite to other artificial lift methods, any restriction found from the separator to the bottom of the well will have a direct impact on the bottomhole flowing pressure of wells producing on natural flow or on gas lift; therefore, the liquid production will also be affected. This is shown in Fig. 4.1, in which the effect of a restriction at a given point along the production tubing (Fig. 4.1a) or at the wellhead (Fig. 4.1b) on the bottomhole flowing pressure (for a fixed production flow rate) can be appreciated. For a given production flow rate, the bottomhole flowing pressure is equal to  $P_{wf1}$  if the well has no restriction and equal to  $P_{wf2}$  if there is a restriction in the production tubing or in the flowline. In reality, at this new bottomhole pressure  $P_{wf2}$ , the reservoir cannot provide the same liquid flow rate  $q_1$ , as shown in Fig. 4.2, where it can be seen that the outflow curve is displaced upwards due to the effect of the choke, making the new equilibrium bottomhole pressure (where the outflow curve intersects the IPR



■ FIGURE 4.1 Effect of a restriction in the production tubing or in the flowline: pressure profiles for a fixed production flow rate. (a) Subsurface restriction, (b) surface restriction.



■ FIGURE 4.2 Outflow curves and equilibrium points with and without choke.



■ FIGURE 4.3 Effect of a restriction in the production tubing or flowline: pressure profile at the equilibrium liquid flow rate. (a) Subsurface restriction, (b) surface restriction.

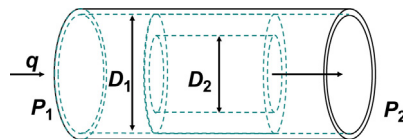
curve) equal to  $P_{wf3}$ , for which the equilibrium liquid flow rate is  $q_2$ . The production pressure profiles that are obtained with a liquid flow rate  $q_2$  are shown in Fig. 4.3a, b.

Despite its negative effects, there are situations in which it is required to install components that become important restrictions to the flow of fluids in the production tubing or in the flowline. For example, it is usually necessary to install subsurface safety valves (storm valves) in offshore wells that can cause some restriction to the production flow. These valves will close in case a

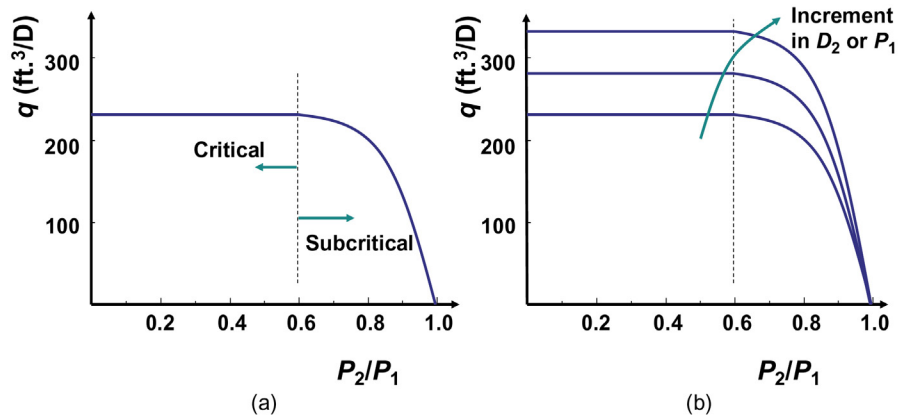
rupture at the wellhead or the flowline occurs due to a collision with a ship or a powerful storm. In other cases, it is important to start the well after a work-over job with a choke temporarily installed at the wellhead; in this way, the production of the well can be controlled during the first stages of production, avoiding possible formation damages caused by sand accumulation or water coning. This will undoubtedly cause inefficiencies in the use of the injection gas, but it will prevent instability problems that are usually encountered when trying to lower the liquid flow rate by reducing the injection gas flow rate or, if the well could indeed be operated in a stable manner at low injection gas flow rates, it will prevent formation damage caused by an unaware operator increasing the gas flow rate while the well is still under evaluation.

In intermittent gas lift operations, it is extremely important not to have any restriction at the wellhead or in the flowline near the wellhead that could cause an increase in the liquid fallback losses. The wellhead choke and its housing, as well as any unnecessary elbows, valves, or Ts, should be removed. If the separator is not capable of handling the liquid slugs when the well is switched to intermittent gas lift, then a choke can be temporarily installed at a distance from the wellhead that would guarantee that the entire liquid slug has surfaced when it plunges against the choke. This should be a temporary solution while the right size separator is installed because even though the liquid fallback is reduced by installing the choke away from the wellhead, it is also true that the time required for the wellhead pressure to go back down to the separation pressure is increased if a surface choke is installed.

Fig. 4.4 shows the typical geometry of a choke.  $D_1$  and  $D_2$  are the pipe and choke diameters, respectively. When the fluid approaches the choke, the flow accelerates and its pressure begins to decrease.  $P_1$  is the pressure upstream of the choke. At the exit of the choke, the fluid velocity decreases until pressure  $P_2$  is reached at a certain distance downstream of the choke. If pressure  $P_1$  is held constant and pressure  $P_2$  is reduced, the flow rate increases. If pressure  $P_2$  continues to decrease, a point is reached at which sonic velocity is achieved at the choke and lowering pressure  $P_2$  any further would not cause any increase in the flow rate. When this condition is found, the flow is called “critical flow.” Usually, critical flow occurs when the ratio of  $P_2/P_1$  is equal to a value in the neighborhood of 0.5–0.6. If  $P_2$  is not small



■ FIGURE 4.4 Choke geometry.



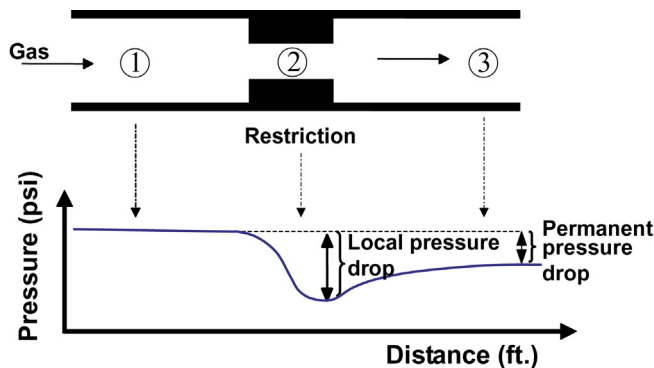
■ FIGURE 4.5 Fluid flow rate as a function of the pressure ratio: (a) For a constant pressure  $P_1$  and a given choke diameter  $D_2$ ; (b) for variable  $P_1$  or  $D_2$ .

enough to reach critical flow, the flow is called “subcritical.” There are correlations that can be used exclusively for critical flow while others can be applied to both, critical and subcritical flows. Fig. 4.5a shows a typical curve of fluid flow rate versus the pressure ratio  $P_2/P_1$  for a constant injection pressure  $P_1$  and a given choke size.

It can be seen in Fig. 4.5a that for fixed values of  $P_1$  and  $D_2$ , there is one maximum flow rate that can be achieved. If it is desired to increase the fluid flow rate,  $P_1$  or  $D_2$ , or both, must be increased. Fig. 4.5b shows the effect of increasing  $P_1$  or  $D_2$  on the maximum fluid flow rate.

#### 4.1 GAS FLOW THROUGH RESTRICTIONS

The development of the equations that are used to predict the gas flow rate through chokes and restrictions is presented in this section. First, the gas flow rate across restrictions as the one shown in Fig. 4.6 is explained.



■ FIGURE 4.6 Gas pressure profile through a restriction.

From an energy balance for compressible, adiabatic flow, the following equation is obtained:

$$\frac{P_1}{\rho_1} + \frac{V_{g1}^2}{2g_0} + u_{g1} = \frac{P_2}{\rho_2} + \frac{V_{g2}^2}{2g_0} + u_{g2} \quad (4.1)$$

Where  $P$  is the gas pressure,  $V_g$  its velocity,  $\rho$  its density,  $u_g$  the gas internal energy per unit mass, and  $g_0$  is the proportionality factor equal to 32.2 lbf ft./lbf s<sup>2</sup>. Subscripts “1” and “2” correspond to the positions “1” and “2” shown in Fig. 4.6.

Eq. 4.1 can be expressed as:

$$\frac{1}{2g_0}(V_{g2}^2 - V_{g1}^2) = \left(u_{g1} + \frac{P_1}{\rho_1}\right) - \left(u_{g2} + \frac{P_2}{\rho_2}\right) \quad (4.2)$$

Where the two terms on the right hand side correspond to the gas enthalpy  $h_g$ :

$$\frac{1}{2g_0}(V_{g2}^2 - V_{g1}^2) = h_{g1} - h_{g2} \quad (4.3)$$

The following equation applies to isentropic flow:

$$h_{g1} - h_{g2} = \int_{P_2}^{P_1} \frac{dP}{\rho} \quad (4.4)$$

or

$$h_{g1} - h_{g2} = \int_{P_2}^{P_1} v dP \quad (4.5)$$

Where  $v$  is the gas specific volume. For isentropic flow, the following equation is also valid:

$$P(v^{k'}) = c \quad (4.6)$$

Where  $k'$  is the specific heat ratio  $C_p/C_v$  and  $c$  is a constant. Therefore:

$$h_{g1} - h_{g2} = P_1 v_1 (1 - r^{(k'-1)/k'}) [k' / (k' - 1)] \quad (4.7)$$

Where  $r = P_2/P_1$ .

Combining Eqs. 4.3 and 4.7 yields:

$$\frac{1}{2g_0}[V_{g2}^2 - V_{g1}^2] = \frac{P_1}{\rho_1}(1 - r^{(k'-1)/k'})(k' / (k' - 1)) \quad (4.8)$$

A mass balance gives:

$$A_{11} V_{g1} \rho_1 = A_{12} V_{g2} \rho_2 = \dot{m} \quad (4.9)$$

Where  $A_{11}$  and  $A_{12}$  are the cross-sectional areas at points “1” and “2” in Fig. 4.6,  $\dot{m}$  is the mass flow rate, which must be the same for points “1” and “2” if the flow is in steady state. Solving for  $V_{g1}$ :

$$V_{g1} = \left( \frac{A_{12}\rho_2}{A_{11}\rho_1} \right) V_{g2} \quad (4.10)$$

Knowing that for isentropic flow the following equation applies:

$$\frac{\rho_2}{\rho_1} = r^{1/k'} \quad (4.11)$$

Eq. 4.10 can be expressed as:

$$V_{g1} = \left( \frac{A_{12}}{A_{11}} \right) r^{1/k'} V_{g2} \quad (4.12)$$

Introducing Eq. 4.12 in 4.8 yields:

$$\frac{V_{g2}^2}{2g_0} \left[ 1 - \left( \frac{A_{12}}{A_{11}} \right)^2 r^{2/k'} \right] = \frac{P_1}{\rho_1} (1 - r^{(k'-1)/k'}) [k' / (k' - 1)] \quad (4.13)$$

or

$$\frac{V_{g2}^2}{2g_0} \left[ 1 - \left( \frac{A_{12}}{A_{11}} \right)^2 r^{2/k'} \right] = P_1 v_1 (1 - r^{(k'-1)/k'}) [k' / (k' - 1)] \quad (4.14)$$

Solving for  $V_{g2}$  gives:

$$V_{g2} = \left[ \frac{2g_0 P_1 v_1 k' (1 - r^{(k'-1)/k'})}{\left( 1 - \left( \frac{A_{12}}{A_{11}} \right)^2 r^{2/k'} \right) (k' - 1)} \right]^{1/2} \quad (4.15)$$

Introducing Eq. 4.9 in 4.15:

$$\dot{m} = A_{12}\rho_2 \left[ \frac{2g_0 P_1 v_1 k' (1 - r^{(k'-1)/k'})}{\left( 1 - \left( \frac{A_{12}}{A_{11}} \right)^2 r^{2/k'} \right) (k' - 1)} \right]^{1/2} \quad (4.16)$$

Using the next two equations and knowing that  $\rho_2 = \rho_1 r^{1/k'}$ :

$$P_1 = \frac{P_1 - P_2}{1 - r} \quad (4.17)$$

$$\beta = \left( \frac{A_{12}}{A_{11}} \right)^{1/2} \quad (4.18)$$

Eq. 4.16 can be changed to:

$$\dot{m} = A_{12} \left[ \frac{2g_0 \rho_1 (P_1 - P_2) r^{2/k'} k' (1 - r^{(k'-1)/k'})}{(1 - \beta^4 r^{2/k'}) (k' - 1) (1 - r)} \right]^{1/2} \quad (4.19)$$

The gas expansion factor is defined as:

$$Y = \left[ \frac{r^{2/k'} k' (1 - r^{(k'-1)/k'}) (1 - \beta^4)}{(1 - \beta^4 r^{2/k'}) (k' - 1) (1 - r)} \right]^{1/2} \quad (4.20)$$

Thus Eq. 4.19 can be written as:

$$m = A_{12} Y \left[ \frac{2g_0 \rho_1 (P_1 - P_2)}{1 - \beta^4} \right]^{1/2} \quad (4.21)$$

The equation of state for real gases, see Eq. 1.12 in chapter: Gas Properties, indicates:

$$\rho_1 = \frac{P_1 M}{Z_1 R_u T_1} = \frac{P_1 \gamma_g (28.964)}{Z_1 R_u T_1} \quad (4.22)$$

Where  $M$  is the gas molecular weight,  $\gamma_g$  is the gas specific gravity, the molecular weight of air is approximated as 28.964 lbm/lbmol;  $Z_1$  is the gas compressibility at the entrance of the restriction; and  $R_u$  is the universal gas constant. With Eq. 4.22, Eq. 4.21 changes to:

$$\dot{m} = A_{12} Y \left[ \frac{2g_0 (P_1 - P_2)}{1 - \beta^4} \frac{P_1 M}{Z_1 R_u T_1} \right]^{1/2} \quad (4.23)$$

The volumetric gas flow rate,  $Q_{gi}$ , at standard conditions (14.73 psia and 60°F) is given by:  $Q_{gi} = \frac{\dot{m}}{\rho_{sc}}$

Where the density at standard conditions is

$$\rho_{sc} = \frac{P_{sc} M}{Z_{sc} R_u T_{sc}} = \frac{14.73 (\text{psia}) \left( 28.964 \gamma_g \frac{\text{lbm}}{\text{lbmol}} \right)}{(1) \left( 10.73 \frac{\text{psia} \cdot \text{ft}^3}{\text{lbmol} \cdot ^\circ\text{R}} \right) (519.69^\circ\text{R})} = 0.076509 \gamma_g \frac{\text{lbm}}{\text{ft}^3}$$

If field units are used, with the flow rate in Mscf/D, Eq. 4.23 divided by the gas density at standard conditions gives the gas flow rate through the restriction:

$$Q_{gi} = \frac{A_p (\text{in}^2) \frac{1 \text{ft}^2}{144 \text{in}^2} Y}{0.076509 \gamma_g \frac{\text{lbm}}{\text{ft}^3}} \left[ \frac{2(32.174) \frac{\text{lbm} \cdot \text{ft}}{\text{lbf} \cdot \text{s}^2} (P_1 - P_2) (\text{psi}) P_1 (\text{psia}) 28.964 \gamma_g \left( \frac{\text{lbm}}{\text{lbmol}} \right) \frac{144 \text{in}^2}{\text{ft}^2}}{(1 - \beta^4) Z_1 10.73 \left( \frac{\text{psia} \cdot \text{ft}^3}{\text{lbmol} \cdot ^\circ\text{R}} \right) T_1 (^\circ\text{R})} \right]^{1/2} \frac{60 \times 60 \times 24 \text{s}}{1 \text{day}} \frac{1 \text{Mscf}}{1000 \text{ft}^3}$$

Which is equal to:

$$Q_{gi} = 1240.3 A_p Y \left[ \frac{P_1 (P_1 - P_2)}{(1 - \beta^4) Z_1 \gamma_g T_1} \right]^{1/2} \text{ Mscf/D} \quad (4.24)$$

Where  $\gamma_g$  is the gas specific gravity,  $A_p$  is the choke cross-sectional area in square inches, pressures  $P_1$  and  $P_2$ , are expressed in psia, and the temperature  $T_1$  in °R. Eq. 4.24 identifies the important parameters that should be considered when trying to model the gas flow rate through a restriction. A discharge coefficient that can be experimentally found should be used in Eq. 4.24 to account for irreversible losses. Another point is that Eq. 4.24 considers the downstream pressure to be at point “2” in Fig. 4.6, instead of the restored pressure at point “3” which is the one that is normally used in equations that predict the pressure drop through chokes or gas lift valves. Some authors, like Nieberding (1988) in his model for the dynamic behavior of gas lift valves, have used Eq. 4.24 with  $P_3$  instead of  $P_2$ , which can be easily achieved by calibrating the discharge coefficient for pressures  $P_1$  and  $P_3$  as the upstream and downstream pressures, respectively.

Traditionally, the gas flow rate through a gas lift valve is correlated with the permanent pressure drop ( $P_1 - P_3$ ) using the Thornhill–Craver equation. This equation was empirically developed by Cook and Dotterweich (1946) to model the gas flow through wellhead choke beams (used to control gas wells) manufactured by the Thornhill–Craver Company:

$$Q_{gi} = \frac{155.5 C_d (A_p) P_1 \sqrt{2g \left( \frac{k'}{k' - 1} \right) (r^{2/k'} - r^{(k'+1)/k'})}}{\sqrt{\gamma_g T}} \quad (4.25)$$

Where  $Q_{gi}$  is the gas flow rate in Mscf/D;  $C_d$  is the discharge coefficient for a particular choke diameter;  $A_p$  is the area of the choke in square inches;  $r$  is the pressure ratio  $P_2/P_1$ ;  $P_1$  is the upstream pressure in psia;  $P_2$  is in this case the recovered downstream pressure also in psia (equivalent to  $P_3$  in Fig. 4.6);  $g$  is the acceleration due to gravity equal to 32.16 ft./s<sup>2</sup>;  $k'$  is the gas specific heat ratio;  $\gamma_g$  is the gas specific gravity; and  $T$  is the absolute gas temperature in °R upstream of the choke.

If the value of  $r$  is smaller than  $r_{crit}$ , where  $r_{crit} = \left( \frac{2}{k' + 1} \right)^{k'}$ , then  $r_{crit}$  is used instead of  $r$  in Eq. 4.25.

The accuracy of Eq. 4.25, when used for gas lift valves, is discussed in detail in chapter: Gas Flow Through Gas Lift Valves. Eq. 4.25 can be used to solve four different types of problems, which (in order of increasing complexity) are explained in the next paragraphs.



In the first place, if the gas flow rate and the upstream and downstream pressures are known, the equation can be easily applied to directly find the required choke diameter.

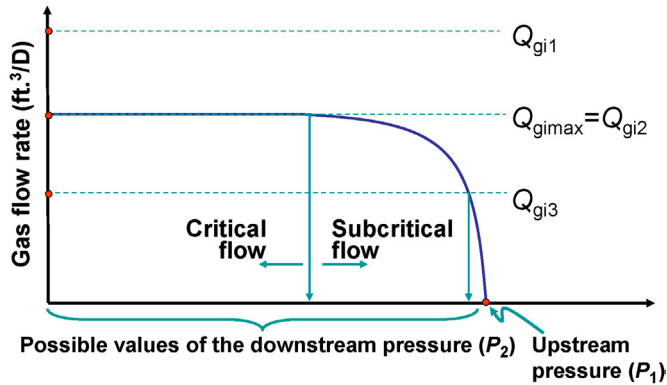
If, on the other hand, the choke diameter is known, there exist three possible types of problems:

- The upstream and downstream pressures are known and the gas flow rate needs to be calculated. In this case, Eq. 4.25 is directly applied to find the gas flow rate.
- The gas flow rate and the upstream pressure are known, but the downstream pressure needs to be calculated. This introduces an additional level of complexity because the equation cannot be directly solved for the downstream pressure and, in consequence, it needs to be determined by iteration.
- The gas flow rate and the downstream pressure are given and it is desired to find the upstream pressure. This is the most complex type of problem for the reasons explained below and iterations are also required.

The required steps to find the downstream pressure when the choke diameter, the gas flow rate, and the upstream pressure are known are presented first. In gas lift, for example, it is relatively easy to calculate the gas injection pressure at depth from the measured surface injection pressure. If, additionally, the gas flow rate and the gas lift valve seat diameter are known, the production pressure just downstream of the valve can be calculated. This allows the production engineer determine if the production pressure obtained in this way matches the production pressure calculated from multiphase flow correlations in order to check if the gas lift valve under investigation is indeed the current point of injection. As explained in chapter: Gas Flow Through Gas Lift Valves, Eq. 4.25 can be used if and only if the valve is an orifice valve or it is a fully opened calibrated valve (using the appropriate corrections in this case). In most cases, calibrated valves will throttle the lift gas, thus Eq. 4.25 is not applicable.

Fig. 4.7 helps explain the logical steps that must be taken to find the pressure downstream of the gas lift valve, knowing the upstream pressure, the gas flow rate, and the valve's seat diameter.

If pressure  $P_1$  is known, then the gas flow rate curve as a function of the downstream pressure can be constructed for a given choke diameter. If critical flow is assumed, the maximum gas flow rate the choke is capable of passing,  $Q_{gi \max}$ , can be readily calculated using Eq. 4.25 with  $r = r_{crit}$ . If the known gas flow rate  $Q_{gi}$  is greater than  $Q_{gi \max}$ , the choke cannot handle the proposed gas flow rate for any value of the downstream pressure  $P_2$ . This

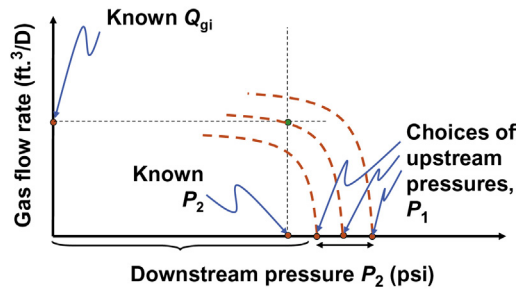


■ FIGURE 4.7 Calculation of  $P_2$  from the know values of pressure  $P_1$  and the gas flow rate  $Q_{gi}$ .

is the case of  $Q_{gi1}$  in Fig. 4.7. If  $Q_{gimax}$  is equal to the proposed gas flow rate  $Q_{gi}$ , there are infinite solutions of  $P_2$  from zero to the value of  $P_2$  at the boundary between critical and subcritical flow. This corresponds to the gas flow rate  $Q_{gi2}$  in Fig. 4.7 and it introduces a serious problem when trying to calculate the downstream production pressure. If the value of the known gas flow rate  $Q_{gi}$  is smaller than  $Q_{gimax}$ , the value of  $P_2$  can be graphically obtained as indicated in the figure, or, if a numeric solution is desired, iterations must be performed to find  $P_2$ . This is the case for  $Q_{gi3}$  in the figure. For the numeric solution, an initial value of  $P_2$  is assumed and the corresponding gas flow rate is then calculated. If the calculated gas flow rate is greater than the desired, or known, gas flow rate, the new assumed value of  $P_2$  must be increased and vice versa (the difference between the calculated and desired gas flow rates is used in the iterations to find  $P_2$ ).

The problem is much more complex if the gas flow rate and the downstream pressure are known and it is asked to find the upstream pressure. This is due to the fact that if the upstream pressure  $P_1$  is not known, then it is not possible to construct the gas flow rate curve. Fig. 4.8 illustrates this type of problem.

As can be appreciated in Fig. 4.8, it is necessary to iterate with several gas flow rate curves to find the one that intersects the known point  $(P_2, Q_{gi})$ . For these iterations, an initial value of  $P_1$  is assumed and the gas flow rate that corresponds to  $P_2$  is calculated. If the calculated gas flow rate is less than the known gas flow rate, the assumed value of  $P_1$  must be increased for the next iteration and vice versa. In both cases, the difference between the calculated and desired gas flow rates is used in the iterations to find  $P_1$ . It is not always necessary to iterate to find  $P_1$ . It can be appreciated in Fig. 4.9 that, for a

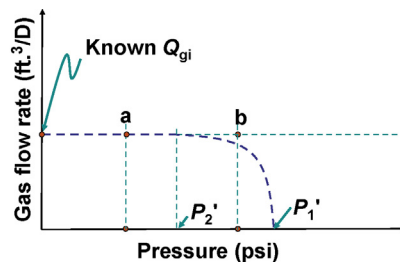


■ FIGURE 4.8 Calculation of upstream pressure  $P_1$  from the given downstream pressure  $P_2$  and the known gas flow rate  $Q_{gi}$ .

given value of the known gas flow rate  $Q_{gi}$ , there is one and only one value of  $P_1$  for which the flow is critical. This unique value of  $P_1$  (known here as  $P_1'$ ) can be directly found from Eq. 4.25 using  $r = \left(\frac{2}{k'+1}\right)^{\frac{k'}{k'+1}}$  and the known gas flow rate  $Q_{gi}$ . Then the value of  $P_2'$ , or boundary between critical and subcritical flow, can be calculated as  $r(P_1')$ . If the known value of  $P_2$  is smaller than or equal to  $P_2'$ , the solution for  $P_1$  is precisely  $P_1'$ . This would correspond to case “a” in Fig. 4.9. Otherwise, it is necessary to iterate to get the solution for  $P_1$ , case “b” in the figure.

An important example where it is necessary to know the pressure upstream of a restriction takes place when the injection pressure at valve’s depth needs to be determined from the gas flow rate and the production tubing pressure. This gives the optimization engineer an idea of the injection pressure that is required to pass a certain gas flow rate for a particular liquid production.

The steps that have just been described to solve the different types of problems for gas flow through chokes can also be applied to liquid and multiphase flows.



■ FIGURE 4.9 Determining the need to iterate.

**Problem 4.1**

Find the gas flow rate through a 0.1875 in. diameter choke, with an upstream pressure of 500 psia and downstream pressures of: (1) 400 psia and (2) 100 psia. The gas specific heat ratio is equal to 1.25, its specific gravity is 0.69, and the upstream temperature is 120°F.

**Solution**

The pressure ratio needed to achieve critical flow is

$$r = \left( \frac{2}{k' + 1} \right)^{k'/(k-1)} = \left( \frac{2}{1.25 + 1} \right)^{1.25/(1.25-1)} = 0.5549 \quad \text{and the discharge coefficient, for the given choke size, is 0.8049.}$$

1. For  $P_2 = 400$  psia, the value of  $r$  is  $400/500 = 0.8$ , which is greater than 0.5549 and therefore the flow is subcritical. Using Eq. 4.25:

$$\begin{aligned} Q_{gi} &= \frac{155.5 C_d (A_p) P_1 \sqrt{2g \left( \frac{k'}{k'-1} \right) \left( r^{2/k'} - r^{(k'+1)/k'} \right)}}{\sqrt{\gamma_g T}} \\ &= \frac{155.5(0.8049) \frac{\pi}{4} (0.1875^2) 500 \sqrt{2(32.16) \left( \frac{1.25}{0.25} \right) \left( 0.8^{2/1.25} - 0.8^{2.25/1.25} \right)}}{\sqrt{0.69(120 + 460)}} \\ &= 270.71 \text{ Mscf/D} \end{aligned}$$

2. For  $P_2 = 100$  psia, the value of  $r$  is  $100/500 = 0.2$ , which is smaller than 0.5549 and therefore the flow is critical and the value of  $r$  to be used is 0.5549. Using Eq. 4.25:

$$\begin{aligned} Q_{gi} &= \frac{155.5 C_d (A_p) P_1 \sqrt{2g \left( \frac{k'}{k'-1} \right) \left( r^{2/k'} - r^{(k'+1)/k'} \right)}}{\sqrt{\gamma_g T}} \\ &= \frac{155.5(0.8049) \frac{\pi}{4} (0.1875^2) 500 \sqrt{2(32.16) \left( \frac{1.25}{0.25} \right) \left( 0.5549^{2/1.25} - 0.5549^{\frac{2.25}{1.25}} \right)}}{\sqrt{0.69(580)}} \\ &= 322.3 \text{ Mscf/D} \end{aligned}$$

**4.2 LIQUID FLOW THROUGH RESTRICTIONS**

The flow through wellhead chokes is usually multiphase flow in gas lift wells; however, if the choke is installed at a depth in the production tubing below the point of injection and with a production pressure greater than the

bubble point pressure, then the flow through the choke is single-phase liquid. Under these conditions, the flow is usually subcritical because the speed of sound is very large for liquid flow and the following equation, suggested by Beggs (1991), can be used to calculate the liquid flow rate,  $q'$ , as a function of the liquid specific gravity  $\gamma_L$ , the choke diameter  $d_2$ , and the pressure drop ( $P_1 - P_2$ ) through the choke:

$$q' = 1022.7 C_d (d_2)^2 \sqrt{\frac{P_1 - P_2}{\gamma_L}} \quad (4.26)$$

Where  $q'$  is expressed in STBL/D,  $d_2$  in inches and the pressure drop in psi.  $C_d$  is the discharge coefficient, which can be approximated as 0.85 if its exact value for the choke's specific geometry is unknown.

#### Problem 4.2

A 0.86 specific gravity oil flows through a 20/64 in. diameter choke with a pressure drop of 22 psi. Find the liquid flow rate if the discharge coefficient is assumed to be 0.85.

#### Solution

$$q' = 1022.7(0.85)(20/64)^2 \sqrt{\frac{22}{0.86}} = 429.37 \text{ STB/D}$$

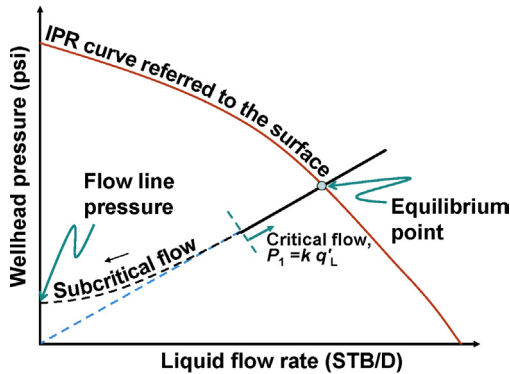
### 4.3 MULTIPHASE FLOW THROUGH RESTRICTIONS

Only a brief history of the development of the most important correlations developed for multiphase flow through chokes is presented in the remaining of this chapter. Multiphase flow is a broad subject that is covered in specialized textbooks.

Multiphase flow through chokes is considerably more complex than single-phase flow. The first correlations that were developed to model multiphase flow through chokes applied only to critical flow. The most important examples of these critical flow correlations are: Gilbert (1954), Baxendell (1958), Ros (1960), Achong (1961), and Omana et al. (1969).

In 1954, Gilbert published a correlation for multiphase critical flow that has the following form:

$$P_1 = \frac{aq'_L R_{gl}^b}{d^c} \quad (4.27)$$



■ FIGURE 4.10 Equilibrium point of a well producing with a wellhead choke in critical flow.

Where constants  $a$ ,  $b$ , and  $c$  must be found from experiments.  $P_1$  is the pressure upstream of the choke in psig,  $q'_L$  is the liquid flow rate in STB/D,  $R_{gl}$  is the gas/liquid ratio in scf/STB, and  $d$  is the choke diameter in inches. This equation was derived from approximately 2,000 tests in wells producing from 30 to 3,000 STB/D, with gas/liquid ratios from 100 to 50,000 scf/STB and wellhead pressures from 70 to 20,000 psig. For a given choke size and a constant gas/liquid ratio, Eq. 4.27 can be written as  $P_1 = k(q'_L)$ , where  $k$  is a constant. This is a straight line equation in a wellhead pressure versus liquid flow rate graph, like the one shown in Fig. 4.10. As long as the flow is critical, the pressure upstream of the choke is a linear function of the liquid flow rate. The point where this line intersects the IPR curve (referred to the surface) corresponds to the equilibrium point that defines the liquid production of the well.

Baxendell (1958) published a correlation which, in reality, is a slight modification of the Gilbert's equation (the only difference is that parameters  $a$ ,  $b$ , and  $c$  in Eq. 4.27 have different values).

Ros (1960) published another equation that is very similar to Gilbert's equation, but it is based on experimental data with greater gas/liquid ratios. In this case  $P_1$  is in psia. Again, parameters  $a$ ,  $b$ , and  $c$  in Eq. 4.27 have different values.

Achong (1961) evaluated Ros' equation with more than 100 experimental points obtained from wells in Lake Maracaibo. The equation proposed by Achong is also a modification of Gilbert's equation.

An example of a more complex model for critical multiphase flow is the equation developed by Omana et al. (1969). This equation is based on a dimensional analysis from tests performed with natural gas and water and it is

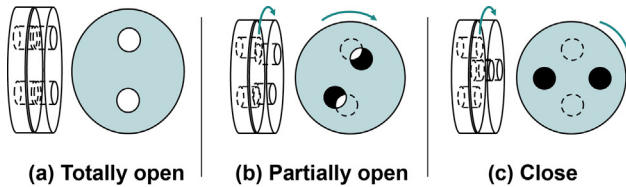
recommended for liquids with viscosities similar to the viscosity of water and for choke diameters smaller than or equal to a 14/64 in.

One of the first correlations for subcritical multiphase flow through chokes was the one published by [Ashford and Pierce \(1974\)](#). The theoretical development was in part based on measurements taken in a single oil well, in which an Otis 22J037 safety valve was installed at 3500 ft. of depth. Tests were performed with inside diameters of the safety valve equal to 14/64, 16/64, and 20/64 in. The equation developed by Ashford and Pierce is an extension of the theory initially presented by Ros, but with the following improvements:

- The new model considers the adiabatic expansion of the gas simultaneously flowing with oil and water, using a polytropic expansion ratio.
- It takes into account the free and dissolved gas.
- For each operational condition, the model predicts if the flow is critical or subcritical.
- It provides a relationship that considers the fluid properties and relates the pressure drop across the choke to the oil, water, and gas flow rates.

Another important model that has been developed to predict subcritical multiphase flow through chokes is the one published by [Sachdeva et al. \(1986\)](#). The model was based on an experimental study carried out in a test loop with a 2.067-in. diameter pipe using 6-in. long chokes of 16/64, 20/64, 24/64, 28/64, and 32/64 in. in diameter. The working fluid mixtures were air and kerosene or air and water. A total of 223 tests were made in critical flow, 220 in subcritical flow, and 110 at the boundary between critical and subcritical flows. The maximum upstream pressure was 99.5 psig. The point where air was mixed with the liquids was located 200 ft. away from the choke to guarantee a fully developed flow pattern just upstream of the choke. The superficial velocities of the phases were capable of sustaining all known horizontal flow patterns except annular flow. The choke was installed horizontally so that the effect of an elbow close to the entrance of the choke was eliminated. The maximum liquid flow rate was 1340 STB/D and the maximum gas flow rate was 136 Mscf/D.

An additional contribution given by Sachdeva is his comparative study of the most widely used correlations to predict multiphase flow through chokes by 1984, which was the year he published his Master's thesis. The basis of comparison for the critical flow data was the upstream pressure, with the exception of the Ashford correlation, for which the liquid flow rate was the evaluated parameter. The pressure differential across the choke was the basis of evaluation for the Pilehvari subcritical flow correlation. The majority



■ FIGURE 4.11 Multiple-orifice chokes. (a) Totally open. (b) Partially open. (c) Close.

of the correlations do not perform very well for the experimental conditions present during Sachdeva's tests. Gilbert's correlation shows a good performance for air–kerosene mixtures but not for air–water mixtures. The Achong correlation does show a good performance for air–water mixtures. The standard deviation for Omana's correlation is very small, indicating a good opportunity to improve it. Sachdeva's study also indicates that, for his experimental conditions, the correlation proposed by Ashford tends to over predict the transition from critical to subcritical flow.

Surbey et al. (1988) published a correlation specifically developed for multiple-orifice chokes as the one shown in Fig. 4.11. These chokes consist of two ceramic discs, in which only one of them is able to rotate with respect to the other. For the choke shown in the figure, each disc has two orifices. When these orifices are aligned, the effective maximum choke area is achieved.

Perkins (1990) published a correlation to calculate the mass flow rate in critical and subcritical flow through chokes. This equation was developed from the energy conservation equation, assuming isentropic flow and it was corrected to account for irreversible losses by an average discharge coefficient obtained from 1432 data points published by other authors. The following assumptions were made by Perkins in the development of his correlation:

- Neither phase condensation nor evaporation takes place across the choke.
- The temperature and velocity change with position but, at each point, the phases are at the same temperature and velocity.
- The gas compressibility factor is constant.
- The liquid compressibility is negligible compared to the gas compressibility.
- Elevation changes are ignored.
- The flow is frictionless and adiabatic.

Ghassan and Maha (1991) published a comparative study of 10 critical flow correlations combined with 4 correlations to calculate PVT fluid properties. Different combinations of these two sets of correlations were evaluated with the data taken from 210 wells, which had a great variety of liquid flow rates, choke diameters, upstream pressures, gas/liquid ratios, and oil API



gravities. The original field data (before an elimination process) came from 56 tests performed in Irak, 108 tests obtained from Poettmann's study, 27 tests from Ashford's work, and 37 tests from Omana's experimental work. The great diversity of the values (considered by Ghassan and Maha) of the variables that play an important role in multiphase flow through chokes, makes this comparative work a very important one that should be taken into consideration when selecting a correlation to use. The correlations considered by the authors were:

- Multiphase flow correlations through chokes: Gilbert (1954), Ros (1960), Baxendell (1958), Achong (1961), Poettmann and Beck (1963), Omana et al. (1969), Ashford and Pierce (1974), Pilehvari (1981), Sachdeva et al. (1986), and Al-Attar and Ghassan (1988).
- PVT property correlations: (1) For the formation volume factor: Standing (1977), Vazquez and Beggs (1980), and Ghassan and Naeema (1988); (2) For the solution gas/liquid ratio: Standing (1977), Lasater (1958), and Vazquez and Beggs (1980).

Ghassan and Maha used the criterion developed by Sachdeva et al. to determine if the flow was critical or subcritical. The tests that were in subcritical flow were discarded. Those tests in which all correlations gave average percent errors greater than 20% were also eliminated. From the performance of the correlations, the authors reached three important conclusions: (1) PVT correlations had a minor impact on the overall performance; (2) all correlations were highly sensible to the choke diameter; and (3) the majority of the correlations showed poor performances, but some correlations performed better than others. Gilbert's correlation gave good results for choke diameters greater than 30/64 in.. For diameters smaller than 30/64 in. and greater than or equal to 10/64 in., the correlation proposed by Sachdeva et al. gave the best results. For choke sizes smaller than 10/64 in., Poettmann–Beck and Ros correlations were the most accurate ones. Correlations developed by Achong, Omana, Pilehvari, and Al-Attar-Ghassan gave totally unsatisfactory results. Omana's correlation showed the worst overall performance.

Rastoin et al. (1992) published another comparative study that concentrated on the mechanistic models developed to predict the behavior of multiphase flows through chokes in critical and subcritical flow. In this study, the models that were considered were: Ashford and Pierce (1974), Sachdeva et al. (1986), and Perkins (1990). Regarding these models, Rastoin et al. made the following observations:

- Compared with other models, the Ashford–Pierce model was derived in a simpler way. The use of the specific heat ratio  $k'$  implies that the flow is isentropic when in reality it is polytropic.

- The isentropic specific heat ratio  $k'$  and the polytropic exponent  $n$  are both used in Sachdeva equation. Rastoin et al. decided to use only coefficient  $n$  in this equation and called it “Sachdeva N.”
- Perkins consistently used the polytropic coefficient  $n$  in his derivation. Perkins did not disregard the use of the mixture velocity upstream of the choke and this, according to Rastoin et al., minimized the error in the application of Perkins’ equation in chokes with large diameter ratios.

A total of 1239 experimental points were used as the basics for the comparative study published by Rastoin et al. These points were selected from the data obtained by [Sachdeva \(1984\)](#), [Pilehvari \(1980, 1981\)](#), and [Omana et al. \(1969\)](#). The type of flow was individually established by each researcher. The liquid flow rates were from 1 to 1,550 STBL/D, while the gas flow rates were from 400 to 295,000 scf/D. The Choke configuration was different for each author: Omana used chokes in a straight vertical pipe, while Pilehvari used a typical wellhead configuration with an elbow just upstream of the choke, and Sachdeva installed the chokes in straight horizontal pipes. Rastoin et al. took these configurations into consideration in their study. The database was used to find the predictive accuracy of each correlation. The observations made by Rastoin et al. are presented in following paragraphs.

Perkins and Sachdeva-N models showed approximately the same results. With the exception of the air-water data in Sachdeva database for critical flow, Sachdeva-N and Perkins models gave more accurate results than the model developed by Ashford, which over predicts the flow rate. All models showed more accurate results for the critical flow data than for subcritical flow. Omana’s data points appear to be suspicious because all models presented larger errors and standard deviations in comparison to the ones obtained with the other databases. Rastoin et al. indicated that this could be due to the fact that Omana used very small choke sizes. On the other hand, Ashford’s model predicted more points as being in subcritical flow when in reality they were observed in critical flow. The accuracy of Ashford’s model was improved by introducing the discharge coefficient in the model; but, for all methods and all categories of the available data, the standard deviation remained almost unchanged.

Rastoin et al. recommended using an average discharge coefficient of 0.856 for chokes with a wellhead configuration, 0.987 for chokes installed in straight horizontal pipes, and 0.71 for chokes installed in straight vertical pipes.

[Towailib and Marhoun \(1994\)](#) published a correlation that must be seriously considered (even though it applies to critical flow only) because it is based

on 3554 data points from a group of wells in the Middle East in which large liquid production wells were included. Towailib and Marhoun used Fortunati's correlation (Fortunati, 1972) to determine if the flow was critical or subcritical. They only took into account points that were predicted as being in critical flow. Towailib and Marhoun also carried out a comparative study (with the data used for the development of their correlation) and found that their correlation gave excellent results. Ros' correlation also exhibited a very good performance even though its development was not based on the data used for this comparison study. Gilbert and Surbey correlations also gave good results but with higher absolute errors. Omana correlation showed the worst results for this experimental data.

To study the performance of the new correlation proposed by Towailib and Marhoun and compare its accuracy with previous critical flow correlations, all correlations were additionally evaluated using the experimental data gathered by Ghassan and Maha (1991), which was not used in the development of the correlation proposed by Towailib and Marhoun. The results indicate that the Towailib–Marhoun and the Fortunati correlations showed excellent performances for this set of data points. The correlations proposed by Gilbert, Ros, and Surbey, showed good results, while the correlations proposed by Omana and by Osman and Dokla (1990) kept giving poor results.

Elgibaly and Nashawi (1998) presented two new empirical correlations for critical and subcritical flows, developed for wells in the Middle East. These correlations are extremely simple. The study is based on 154 tests in critical flow and 106 tests in subcritical flow. The data for critical flow included experimental points from Egypt, Iraq, United Arab Emirates, and Kuwait. The data for subcritical flow came from measurements taken in Iraq, Kuwait, and the data provided by Ashford and Pierce. The Ashford and Pierce correlation was used to determine if the flow was critical or subcritical.

Besides doing a comparative study of their new correlations, Elgibaly and Nashawi also determined the effect that PVT correlations have on the Ashford and Pierce (1974) correlation. It must be indicated that the Ashford and Pierce correlation was modified by Ghassan and Aswad (1990) in a study where the Standing (1947; 1977) correlations were used to predict the gas/oil ratio, the formation volume factors, and the gas compressibility. The modification consisted in adjusting the discharge coefficient to minimize the error for the field data that was used. Elgibaly and Nashawi also modified the Ashford and Pierce correlation in a similar study where the correlation developed by Al-Marhoun (1988) to calculate the solution gas/oil ratio and the formation volume factor for oils from the Middle East was used.

Elgibaly and Nashawi used the [Dranchuk et al. \(1974\)](#) correlation to calculate the gas compressibility. Because the comparative study presented was conducted with the data that was used by Elgibaly and Nashawi to develop their own correlation, it is not surprising that it was precisely this correlation that exhibited the best performance. But this comparative study can be used to visualize how other correlations performed for this experimental data. For example, it can be appreciated that Pilehvari's correlation is not very accurate for these operational conditions. On the other hand, the modification made by Ghassan and Aswad to the Ashford and Pierce correlation did not make it more accurate than the rest of the correlations considered in the study. Additionally, the modification made by Elgibaly and Nashawi to the Ashford and Pierce correlation only slightly improved its accuracy.

Experimental points published by [Ghassan and Maha \(1991\)](#) were used to validate the correlation developed by Elgibaly and Nashawi. This data were not used in the development of the correlation proposed by Elgibaly and Nashawi. The best performance was shown by the correlation developed by Elgibaly and Nashawi. The correlations developed by Gilbert, Ros, Baxendell, and Achong gave better results than the Ashford and Pierce correlation.

The correlation developed by Elgibaly and Nashawi for subcritical flow was compared with the Ashford and Pierce correlation with the same data that was used to develop the Elgibaly and Nashawi correlation. The absolute error is practically the same for all correlations. The Ashford and Pierce correlation, modified by Elgibaly and Nashawi using the Al-Marhoun PVT correlation, proved to be slightly more accurate.

The evaluation of the subcritical correlations was based on the data provided by Ashford and Pierce, which is probably the reason why this correlation showed the best performance; however, the Elgibaly and Nashawi correlation showed a good performance even though the data used in the evaluation was totally different from the one used in the development of this correlation and considering also the fact that this correlation is much simpler than the one developed by Ashford and Pierce.

Additional critical and subcritical flow correlations were introduced by [Al-Attar \(2009\)](#) for wells in the Middle East. One of the highlights of this study is having taken into consideration the type of chokes used in the tests. Cameron LD, Cameron F, and simple tubular chokes (bean settings) were used. The PVT correlations used by Al-Attar were also reported. A weak aspect of the correlation proposed by Al-Attar is the fact that it was based on tests in which only one API gravity was used and the water cut was equal to zero for all experimental points. Additionally, in comparison to other experimental studies, the number of data points considered by Al-Attar was

very small. An important comparative study presented in this work shows the behavior of other correlations for the experimental conditions considered by Al-Attar.

One of the contributions made by Al-Attar was the determination of the discharge coefficients for the Ashford–Pierce and Fortunati subcritical correlations using the operational conditions found in his study.

Al-Attar carried out a comparative study for subcritical flow. The selected existing correlations were the Ashford–Pierce and the Fortunati correlations, both modified with the discharge coefficients adapted for the conditions found in the experimental data used by Al-Attar. The field data used in this comparative study for subcritical flow is the same data used to develop the subcritical correlation proposed by Al-Attar and that is probably the reason why this correlation gave good results. But it should be mentioned that the Fortunati and the Ashford–Pierce correlations were also adapted for the field data used in this comparative study and that might also be the reason why all correlations show the same degree of accuracy.

## REFERENCES

- Achong, I., 1961. Revised bean performance formula for Lake Maracaibo wells. Internal report, Shell Oil Company, Houston, TX (October 1961).
- Al-Attar, H.H., 2009. New correlations for critical and subcritical two-phase flow through surface chokes in high-rate oil wells. SPE Paper 120788 presented at the 2009 SPE Latin American and Caribbean Petroleum Engineering Conference. Cartagena, Colombia, 31 May, 3 June, 2009.
- Al-Attar, H.H., Ghassan, A.M., 1988. Revised bean performance equation for east Baghdad oil wells. *SPE Prod. Eng.* 3 (1), 127–131.
- Ashford, F.E., Pierce, P.E., 1974. The determination of multiphase pressure drops and flow capacities in downhole safety valves (Strom Chokes). SPE Paper 5161 presented at the SPE Forty-Ninth Annual Fall Meeting, Houston, October 6–9, 1974.
- Baxendell, P.B., 1958. Producing wells on casing flow- an analysis of flowing pressure gradients. *Pet. Trans. AIME* 213 (8027), 202–206.
- Beggs, H.D., 1991. *Production Optimization Using Nodal Analysis*. OGCI Publications, Oil and Gas Consultants International Inc, Tulsa, OK.
- Cook, H.L., Dotterweich, F.H., 1946. Report on Calibration of Positive Flow Beans Manufactured by Thornhill-Craver Company, Inc. Department of Engineering, Texas College of Arts and Industries. Third Printing, Kingsville, Texas.
- Dranchuk, P.M., Purvis, R.A., Robinson, D.B., 1974. Computer calculation of natural gas compressibility factors using the Standing and Katz correlations. Institute of Petroleum Technical Series, No. IP74-008, pp. 1–13.
- Elgibaly, I.S., Nashawi, I.S., 1998. New correlations for critical and subcritical two-phase flow through wellhead chokes. *J. Can. Pet. Technol.* 37 (6), 36–43.
- Fortunati, F., 1972. Two-phase flow through wellhead chokes. SPE 3472, SPE European Meeting, Amsterdam.

- Ghassan, A.M., Aswad, Z.A., 1990. A new approach for estimating the orifice discharge coefficient required in Ashford and Pierce correlation. *J. Pet. Sci. Eng.* 5, 25–33.
- Ghassan, A.M., Maha, A.A., 1991. Correlations developed to predict two-phase flow through wellhead chokes. *J. Can. Pet. Technol.* 30 (6), 47–55.
- Ghassan, A.M., Naeema, H.S., 1988. An empirical correlation for oil FVF prediction. *J. Can. Pet. Technol.* 27 (6), 118–122.
- Gilbert, W.E., 1954. Flowing and gas-lift well performance. *API Drill. Prod. Pract.* 143, 127–157.
- Lasater, J.A., 1958. Bubble point pressure correlation. *Trans. AIME* 213, 379–381.
- Marhoun, M.A., 1988. PVT correlations for Middle East crude oils. *J. Pet. Technol.* 40 (5), 650–666, *Trans. AIME* 285.
- Nieberding, M.A., 1988. Normalization of nitrogen loaded gas-lift valve performance data. MS thesis. The University of Tulsa, Tulsa, OK.
- Omana, R., Houssiere, C., Brown, K.E., Brill, J.P., Thompson, R.E., 1969. Multiphase flow through chokes. *SPE Paper* 2682.
- Osman, M.E., Dokla, M.E., 1990. Gas condensate flow through chokes. Unsolicited paper *SPE* 20988.
- Perkins, T.K., 1990. Critical and subcritical flow of multiphase mixtures through chokes.
- Pilehvari, A.A., 1980. Experimental study of subcritical two-phase flow through wellhead chokes. University of Tulsa, Fluid Flow Projects Report.
- Pilehvari, A.A., 1981. Experimental study of critical two-phase flow through wellhead chokes. University of Tulsa, Fluid Flow Projects Report.
- Poettmann, F.H., Beck, R.L., 1963. New charts developed to predict gas-liquid flow through chokes. *World Oil*, March 1963, 95–101.
- Rastoin, S., Schmidt, Z., Doty, D.R., 1992. A review of multiphase flow through chokes. Annual ASME Winter Meeting Multiphase Flow in Wells and Pipelines, FED-vol. 144, pp. 51–62.
- Ros, N.C.J., 1960. An analysis of critical simultaneous gas/liquid flow through a restriction and its application to flow metering. *Appl. Sci. Res.* 9 (Sec. A), 9 (1), 374–388.
- Sachdeva, R., 1984. Two-phase flow through chokes. MS thesis, University of Tulsa, OK.
- Sachdeva, R., Schmidt, Z., Brill, J.P., Blais, R.M., 1986. Two-phase flow through chokes. *SPE Paper* 15657.
- Standing, M.B., 1947. A pressure-volume-temperature correlation for mixtures of California oils and gases. *API Drill. Prod. Pract.* API-47-275, 275–287.
- Standing, M.B., 1977. Volumetric and phase behavior of oil field hydrocarbon system. *SPE AIME*, 122.
- Surbey, D.W., Kelkar, B.G., Brill, J.P., 1988. Study of subcritical flow through multiple-orifice valves. *SPE Prod. Eng.* 3 (1), *SPE Paper* 14285-PA.
- Towailib, A.I., Marhoun, M.A., 1994. A new correlation for two-phase flow through chokes. *J. Can. Pet. Technol.* 33 (5), 40–43.
- Vazquez, M., Beggs, H.D., 1980. Correlations for fluid physical property prediction. *J. Pet. Technol.* 32, 968–970.

# Total system analysis applied to gas lift design

The main goals in the design of a gas lift well are to find the depths, area ratios, and calibration pressures of the operating and unloading valves. The gas lift valve through which gas is injected during the normal operation of the well is called the “operating” valve and its depth is referred to as the “point of injection depth.” All valves above the operating valve are called “unloading” valves because they are only used to unload the well. The unloading operation consists in displacing the liquids in the casing–tubing annulus with injection gas until the annular liquid level reaches the point of injection depth. The unloading operation is explained in chapter: Design of Continuous Gas Lift Installations, while design methods for continuous and intermittent gas lift are explained in detail in chapters Design of Continuous Gas Lift Installations and Design of Intermittent Gas Lift Installations, respectively. Before design calculations can be performed, it is necessary to know the well’s target liquid production, the operating injection point depth, and the required injection gas flow rate. All of these parameters can be found following the calculation procedures presented in the chapter. These procedures take into consideration all the gas lift system’s components that play a role in the production of the well: the reservoir, the production tubing, the flowline, and the conditions at the separator or flow station. The explanations given in the chapter focus mainly on the determination of the point of injection depth, the well’s liquid production, and the corresponding injection gas flow rate, which are all explained in Section 5.1. Other types of analyses, with different objectives, that take into account all system’s components are also presented in the first part of the chapter. These additional analyses are usually very helpful in designing and troubleshooting activities. At the end of the chapter, in Sections 5.2 and 5.3, different examples of the effect that each system’s component has on the operation of the well, as well as an example problem, are presented. The reader should be familiar with IPR and outflow curves. The explanation given for Fig. 3.3 describes how outflow curves are constructed. In the chapter, the produced gas–liquid

mixture is assumed to flow up the tubing while the gas is injected down the casing–tubing annulus; but the theory presented here works for annular or tubing production and, to avoid confusion, the pressure of the produced gas–liquid mixture is called the “production” pressure and the pressure of the injection gas is simply called the “injection” pressure.

### 5.1 DETERMINATION OF THE DEPTH OF THE OPERATING POINT OF INJECTION

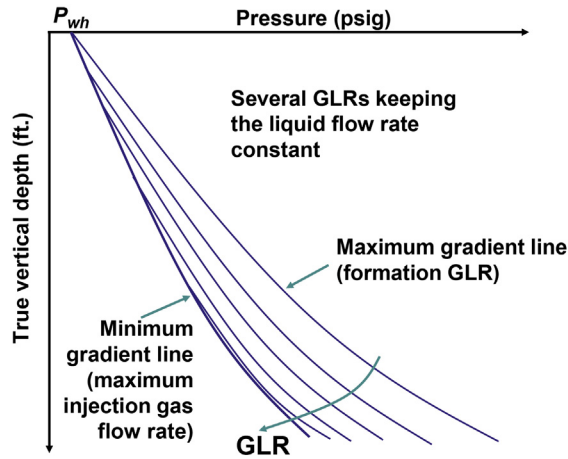
The first step in the design of a gas lift well is finding out the optimum depth of the “operating” valve which, as explained earlier, is the final point of injection once the well has been unloaded. This can be done by following procedures that (with a few minor variations) can be applied to all types of gas lift valves. Together with the determination of the injection point depth, the production liquid flow rate and the required injection gas flow rate are simultaneously calculated.

The main objective at this stage is to locate the operating point of injection as deep as the available surface injection pressure allows it to be. The deeper the point of injection is, the more efficient the gas lift method becomes because a greater drawdown can be achieved; however, it is not always possible to inject gas at the deepest point available in the well because of one, or several, of the following reasons:

- The available injection pressure might not be large enough.
- The maximum gas flow rate might be limited.
- Mandrels and/or gas lift valves might not be able to withstand downhole conditions at great depths.
- The inclination angle of the tubing might be greater than 60–70 degrees (with respect to the vertical), making it very hard for wireline operators to install or retrieve gas lift valves with conventional wireline tools. Although new wireline equipment are making it possible to install and retrieve gas lift valves in horizontal tubing strings, injecting gas at very large inclination angles might actually increase the bottomhole flowing pressure because: (1) the friction component of the pressure drop is increased, and (2) the multiphase flow tends to stratify, increasing the liquid holdup (therefore increasing also the hydrostatic component of the pressure drop along the production tubing).

The procedures described here assume unlimited gas flow rate availability. If that is not the case, these procedures would basically be the same, but it would simply be necessary to check, at each step, if the maximum injection gas flow rate has been reached so that it will not be exceeded.



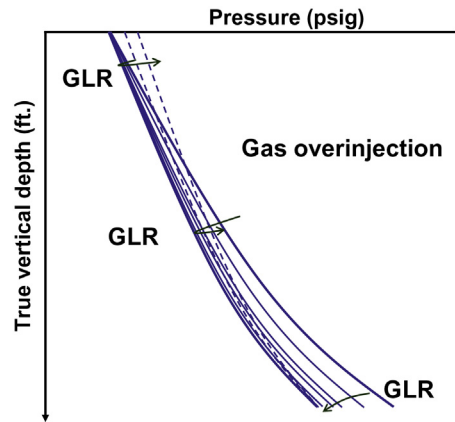


■ FIGURE 5.1 Production pressure curves for different gas/liquid ratios GLR (all curves have the same liquid flow rate and wellhead pressure).

Before getting into the details of the calculation procedures, a few explanations regarding pressure traverse curves along the production tubing are presented. The effect of increasing the total gas/liquid ratio (keeping the wellhead pressure and the liquid flow rate constant) is shown in Fig. 5.1. As the gas/liquid ratio is increased, the tubing pressure decreases until a limit is reached in which the tubing pressure starts to increase. The curve with the minimum production pressure possible is called the “minimum gradient curve.” As shown in Fig. 5.1, the gas/liquid ratio needed to reach the minimum gradient curve increases for deeper depths along the tubing.

But if the wellhead pressure is not constant (because the pressure losses in the flowline are not negligible and should be considered), there might be an increase in the wellhead pressure that has the opposite effect the gas/liquid ratio has on the production tubing pressure, as the injection gas flow rate is increased from very low values. In this case, as the gas/liquid ratio is increased, the pressure drop along the surface flowline increases, therefore increasing the wellhead pressure and causing a displacement of the vertical pressure curves to the right of the graph, as can be seen in Fig. 5.2. It is possible then that, thanks to the increase of the pressure drop in the flowline, the bottomhole flowing pressure stops decreasing before reaching the minimum gradient curve as the gas/liquid ratio is increased from very low values.

The liquid flow rate is kept constant in Figs. 5.1 and 5.2 for didactical purposes. In reality, any change in the injection gas flow rate will cause a change in the liquid production due to the change in the bottomhole flowing



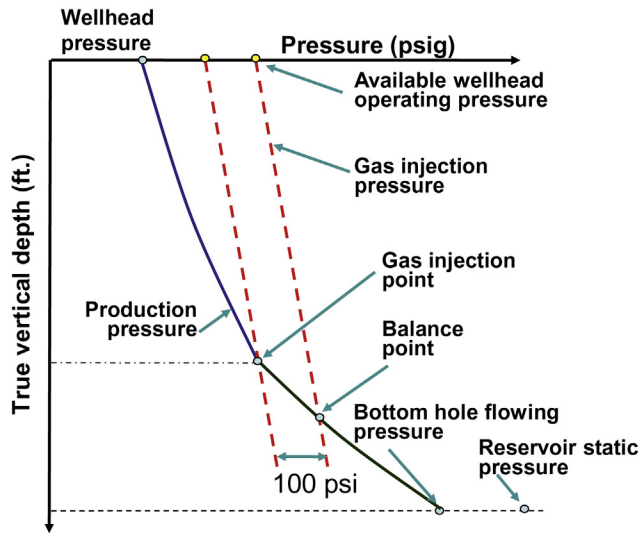
■ FIGURE 5.2 Production pressure curves for different gas/liquid ratios (the liquid flow rate is kept constant but the wellhead pressure is allowed to change with increasing gas flow rate).

pressure and the way the flow from the reservoir adapts to this new pressure. Understanding how these interactions between the different components of a gas lift well take place is precisely the main objective of the chapter. In [Sections 5.1.1 and 5.1.2](#), several procedures, with increasing level of complexity, that can be used to find the depth of the point of injection, are presented. The intention in these sections is to familiarize the reader with the role of each system's component. The actual procedures currently being used by commercially available software to find the depth of the point of injection are explained at the end of [Section 5.1.3](#), after some useful additional operations are explained.

### 5.1.1 Determination of the injection point depth assuming constant wellhead production pressure

When the wellhead is near the separator or the flowline length and diameter are such that the pressure drop along the flowline is negligible, the wellhead production pressure can be assumed constant. This is the simplest case possible and an ideal condition to illustrate the required calculations to find the injection point depth. The pressure–depth diagram that describes the location of the point of injection is shown in [Fig. 5.3](#). All procedures presented in the chapter can be easily understood by referring to this type of diagram.

*Procedure using several gas/liquid ratios to connect the wellhead production pressure to the production pressure at the injection point depth. The*



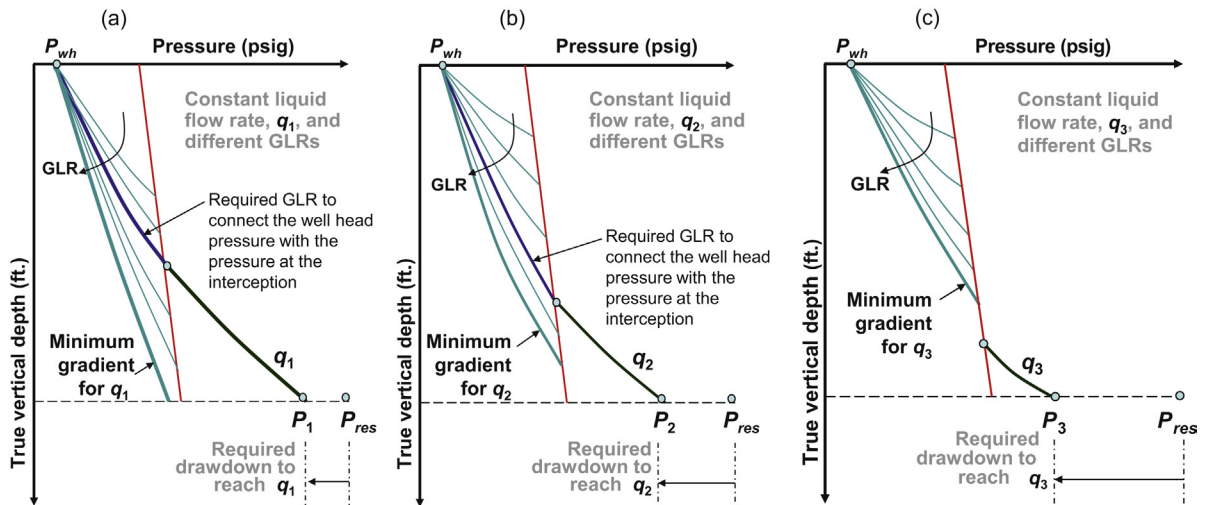
■ FIGURE 5.3 Location of the operating gas injection point.

procedure that illustrates how the depth of the operating point of injection is found using this approach is as follows:

- In a pressure–depth diagram, like the one shown in Fig. 5.3, the available surface injection pressure and the static reservoir pressure are plotted. The available surface injection pressure is the minimum pressure at the injection manifold (taking pressure fluctuations at the manifold into consideration) minus the following factors: (1) from 50–100 psi (so that a sufficiently large differential pressure between the manifold and the well is available to provide an adequate injection gas flow rate when the first valve is uncovered). A differential pressure larger than 100 psi might be recommended in cases where the gas lift system’s pressure is not very stable; and (2) The number of unloading valves times the required surface injection pressure drop per unloading valve (in case of injection-pressure-operated valves). Because the total number of unloading valves is not known a priori, a reasonable first guess is used to start the iterations. The number of unloading valves is determined during the mandrel spacing procedure (explained in chapter: Design of Continuous Gas Lift Installations) performed after the present calculations are finished. If during the mandrel spacing procedure the point of injection depth calculated here is not reached, all the calculations that are described next should be repeated with a lower (more realistic)

surface injection pressure. This is why the global design (which consists of the total system analyses explained in this chapter plus the mandrel spacing procedures explained in chapter: Design of Continuous Gas Lift Installations) is an iterative process.

- From the available surface injection pressure, several injection pressures are calculated at different depths. This gives the gas injection line along the casing–tubing annulus (assuming that the gas is injected down the annulus). The injection pressure at depth is usually determined as a static gas column, but there are cases in which frictional losses are not negligible, for example: (1) very large injection gas flow rates, (2) gas is injected down the tubing and the liquid is produced up the annulus, or (3) gas is injected down a parallel string, see Fig. 6.46c.
- An additional 100 psi is subtracted from the injection pressure line found in the previous step to determine the gas injection line that is actually used in finding the point of injection. This pressure drop corresponds to the minimum pressure drop that should take place through the gas lift valve so that the injection gas is capable of entering the production tubing. To avoid instability problems (like the one shown in Fig. 8.4), a safer pressure drop across the gas lift valve will be one not smaller than 20% of the value of the injection pressure at the maximum depth where a gas lift valve can be installed (the use of the instability criteria, as explained at the end of chapter: Design Of Continuous Gas Lift Installations, might be required to determine the exact value of the pressure drop across the gas lift valve to use in the determination of the depth of the point of injection). For the purpose of this introduction, 100 psi will be taken as the minimum pressure drop across the operating gas lift valve.
- From the IPR curve, the bottomhole flowing pressure is calculated for different liquid flow rates ( $q_1$ ,  $q_2$ , and  $q_3$ , for example). These pressures are plotted at mid perforations' depth. Then, using the formation gas/liquid ratio, production pressure curves are calculated from the bottomhole flowing pressures (for each liquid flow rate being considered) to the point where they intersect the gas injection line; see Fig. 5.4 ( $q_1$ ,  $q_2$ , and  $q_3$  are shown in Fig. 5.4a, b, c, respectively).
- Using a multiphase flow correlation for each liquid flow rate, the production pressure is calculated from the wellhead to the gas injection line for different total gas/liquid ratios. This is done separately for each liquid flow rate. At each liquid flow rate, there is one and only one total gas/liquid ratio for which the pressure curve

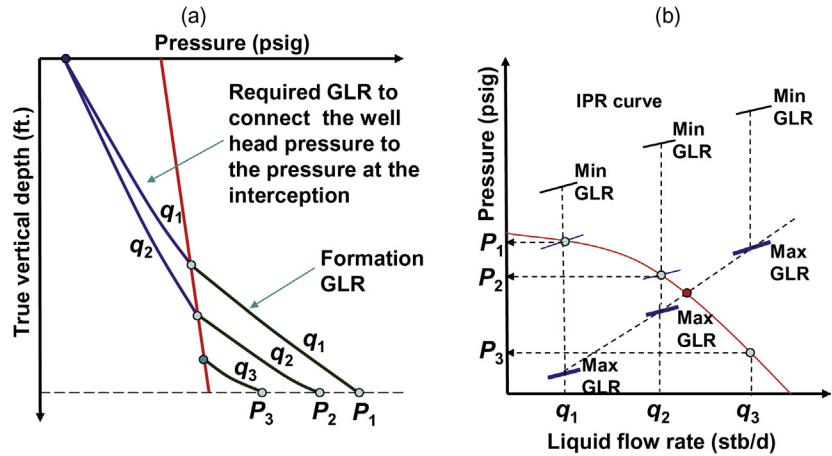


■ FIGURE 5.4 Procedure to find the liquid production with the minimum gradient curve. (a) Liquid flow rate  $q_1$ , (b) Liquid flow rate  $q_2$ , (c) Liquid flow rate  $q_3$ .

coming from the perforation (with the formation gas/liquid ratio) is connected to the production pressure curve from the wellhead (with the total gas/liquid ratio), so that the injection gas flow rate and the depth of the point of injection are simultaneously determined for each liquid flow rate.

- The procedure described in the previous step is repeated for each liquid flow rate, in increasing order ( $q_1$ ,  $q_2$ , and  $q_3$  are respectively shown in Fig. 5.4a, b, c), until a liquid flow rate is found for which the wellhead production pressure is connected to the bottomhole flowing pressure with the minimum gradient curve. For larger liquid flow rates, there is no way of connecting the wellhead pressure to the bottomhole flowing pressure because the pressure at the intersection of the “minimum gradient curve” (from the wellhead) with the gas injection line is greater than the pressure at the intersection of the “production–pressure curve” (from the perforations) with the “gas injection line,” (Fig. 5.4c). Notice that as the liquid flow rate increases ( $q_1 < q_2 < q_3$ ), the production pressure curves become “heavier” (more horizontally inclined).

The bottomhole flowing pressures for different gas/liquid ratios and different liquid flow rates are superimposed on the IPR curve in Fig. 5.5b.  $GLR_{MIN}$  corresponds to the formation gas/liquid ratio while  $GLR_{MAX}$  is the gas/liquid ratio at which the pressure traverse curve with the minimum pressure gradient is found.  $GLR_{MIN}$  and  $GLR_{MAX}$  curves seem to be independent, parallel curves and not a continuous curve like the ones shown in Fig. 3.3. This is due



■ FIGURE 5.5 Determination of the injection point depth with variable gas/liquid ratio. (a) Pressure traverse curves, (b) Inflow-outflow curves.

to the fact that points in Fig. 5.5 correspond to different injection point depths while the ones in chapter: Multiphase Flow are for a constant gas injection point depth. The point at which the maximum liquid flow rate is obtained corresponds to the point where the  $GLR_{MAX}$  curve intersects the IPR curve. This takes place between liquid flow rates  $q_2$  and  $q_3$  as can be appreciated in Fig. 5.5b. The liquid flow rate so obtained is the maximum rate the well can produce for the available injection pressure. This procedure also gives the injection gas flow rate because it is equal to the liquid flow rate found in this procedure times the difference of the total gas/liquid ratio to reach the minimum pressure gradient minus the formation gas/liquid ratio.

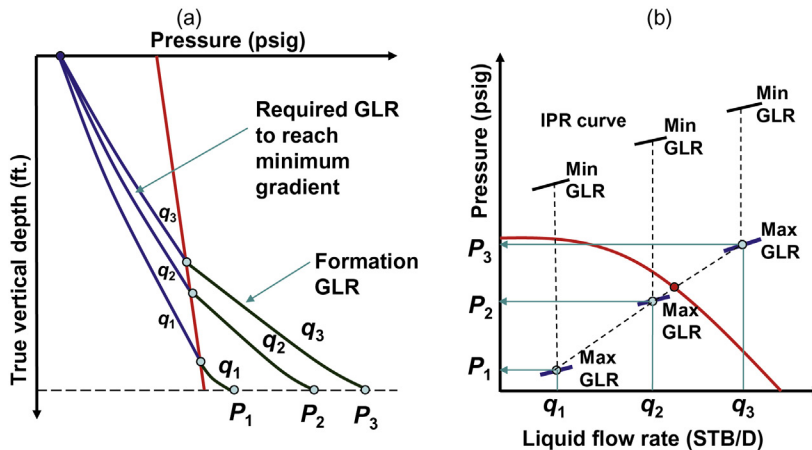
*Procedure using the minimum pressure gradient at each step.* The determination of the injection point depth (with constant wellhead pressure) can also be illustrated using the following approach:

- In a pressure–depth diagram like the one shown in Fig. 5.3, the static reservoir pressure and the surface available injection pressure are plotted. The available surface injection pressure is the same pressure defined in the previous procedure.
- From the surface available pressure, injection pressures are calculated at different depths to find the gas injection line along the annulus. The injection pressure at depth is usually determined as a static gas column; but, as explained in the previous procedure, there are cases in which frictional losses are not negligible.
- 100 psi (or 20% of the gas injection pressure at the maximum depth where a gas lift valve can be installed) is subtracted from the line found

in the previous step to give the gas injection line that is actually used in finding the point of injection. As in the previous procedure, this pressure drop is the minimum pressure drop that should take place through the gas lift valve.

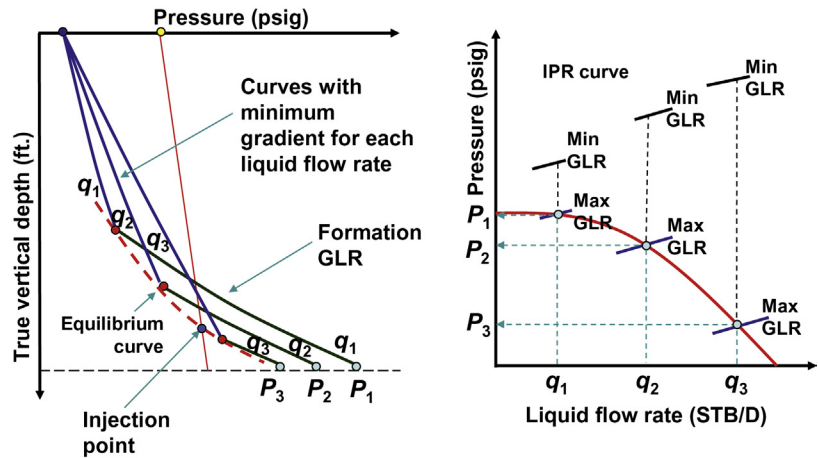
- From the wellhead production pressure, pressure traverse curves are calculated for several probable liquid flow rates ( $q_1 < q_2 < q_3$ ), all of them with the injection gas/liquid ratio that gives the minimum gradient curve. These curves are plotted from the wellhead to the point where they intersect the annulus gas injection pressure line minus 100 psi (or minus 20% of the gas injection pressure at the maximum depth where a gas lift valve can be installed). From that point to the perforations, production pressure curves are plotted with their respective liquid flow rates (but with the formation gas/liquid ratio) to obtain the flowing bottomhole pressures for the different liquid flow rates that were considered.
- The bottomhole flowing pressure for each liquid flow rate is plotted together with the IPR curve of the well, see Fig. 5.6b. The intersection of the IPR curve with the curve that joints all of the bottomhole flowing pressures (at  $GLR_{MAX}$ ) determines the liquid production, the required injection gas flow rate, and the depth of the point of injection.

*Procedure using equilibrium curves.* The minimum-gradient production pressure curves, for different liquid flow rates, are plotted from the wellhead production pressure to the bottom of the well. Each of these curves should intersect its corresponding curve (the one with the same liquid flow rate)



■ FIGURE 5.6 Determination of the injection point depth with the minimum gradient curve.

(a) Pressure traverse curves, (b) Inflow-outflow curves.



■ FIGURE 5.7 Determination of the injection point depth using the minimum-production-pressure-gradient equilibrium curve. (a) Pressure traverse curves, (b) Inflow-outflow curves.

plotted from midperforations' depth using the formation gas/liquid ratio and starting at the flowing bottomhole pressure predicted from the IPR curve for each liquid flow rate. The curve obtained by joining all the intersection points corresponding to each liquid flow rate is called "the equilibrium curve with variable injection gas flow rate." The intersection of this equilibrium curve with the injection pressure line (which is the pressure in the annulus minus 100 psi or minus 20% of the gas injection pressure at the maximum depth where a gas lift valve can be installed) corresponds to the injection point depth, see Fig. 5.7.

The equilibrium curve presented in Fig. 5.7 is the curve that guarantees the maximum possible liquid production for a given injection pressure. Each point on this curve corresponds to a different liquid production and injection gas flow rate. There is another type of equilibrium curve that is obtained with a constant injection gas flow rate for all points. This constant-injection-gas-flow-rate equilibrium curve makes calculations easier, but it does not guarantee that the calculated point of injection will correspond to the maximum liquid production (unless several of them are built, each for a particularly fixed injection gas flow rate, so that a maximum liquid production is found from the curve that intersects the injection pressure line at the deepest point). Constant-injection-gas-flow-rate equilibrium curves are very useful when trying to understand complex troubleshooting and design calculations and they are explained in detail in Section 5.1.3. The principal reason constant-injection-gas-flow-rate equilibrium curves are used is because it is very difficult to write a computer program to performed the calculations that



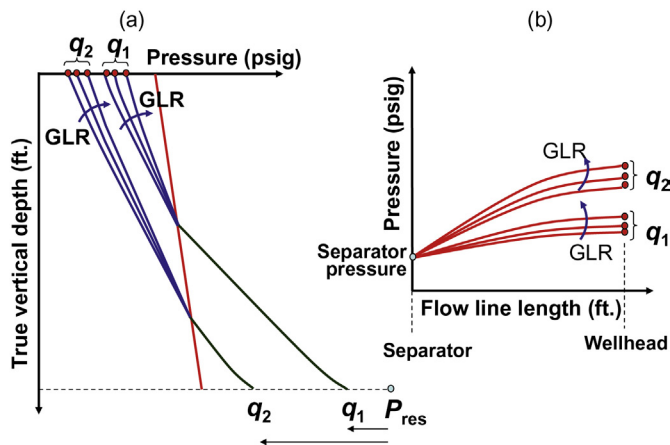
are described in Fig. 5.7. Years ago, before computer programs were used to design gas lift installations, calculations were performed manually using the equilibrium curve shown in Fig. 5.7. Even though it was a time-consuming and not an accurate procedure, doing these calculations by hand is not as complicated as writing a computer program to generate equilibrium curves with variable injection gas flow rates.

As can be seen in Fig. 5.7, it is not possible to obtain liquid flow rate  $q_3$  because the available injection pressure is not high enough to inject gas at the intersection point depth for that liquid flow rate.

### 5.1.2 Finding the injection point depth with variable wellhead pressure

Taking into consideration the possible changes in the wellhead pressure is a more realistic approach which is many times unavoidable. The wellhead production pressure changes because the pressure drop along the flowline depends on the liquid flow rate and the total gas/liquid ratio. The following steps describe the calculation procedure with variable wellhead pressure, see Fig. 5.8:

- The first step is to calculate and plot the flowing bottomhole production pressure for each liquid flow rate being considered ( $q_1, q_2, \dots$ ). This is done using the IPR curve of the well.
- Production pressure curves are then plotted from the bottomhole flowing pressure for each liquid flow rate until they intersect the gas



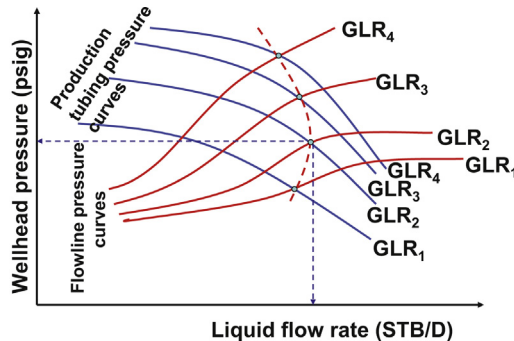
■ FIGURE 5.8 Wellhead pressures found from (a) the perforations, and (b) the separator.

injection pressure line in the annulus of the well minus 100 psi (or minus 20% of the gas injection pressure at the maximum depth where a gas lift valve can be installed), see Fig. 5.8a.

- From the intersection points found in the previous step, production pressure curves are plotted to the surface with different total gas/liquid ratios for each liquid flow rate that was considered in the first step. In this way, for each liquid flow rate, several wellhead pressures are found as a function of the total gas/liquid ratio, see Fig. 5.8a.
- With the same liquid flow rates and gas/liquid ratios used in the previous steps, the wellhead pressure is calculated but this time starting at the separator (or production manifold), see Fig. 5.8b.
- In a “wellhead pressure” versus “liquid flow rate” diagram, two sets of wellhead pressure curves are plotted. Each of these curves corresponds to a single total gas/liquid ratio. One set of wellhead pressure curves is found from the bottomhole flowing pressure and the other set is found from the separator’s pressure, following the procedure explained earlier. The intersections of each set of curves with the same total gas/liquid ratio generate the dashed line shown in Fig. 5.9, from which the maximum liquid flow rate and its corresponding wellhead pressure are found.

It is worthwhile noting that, contrary to the case in which the wellhead pressure is constant, the gas/liquid ratio found for the maximum liquid production might not be the gas/liquid ratio that gives the minimum gradient curve in the production tubing. This is due to the following factors:

- In multiphase vertical flow, the hydrostatic pressure drop is the principal component of the total pressure drop and friction plays a secondary role. This means that, if the wellhead pressure is constant, the important point to consider while trying to reach the deepest point



■ FIGURE 5.9 Finding the injection point depth for variable wellhead pressure.

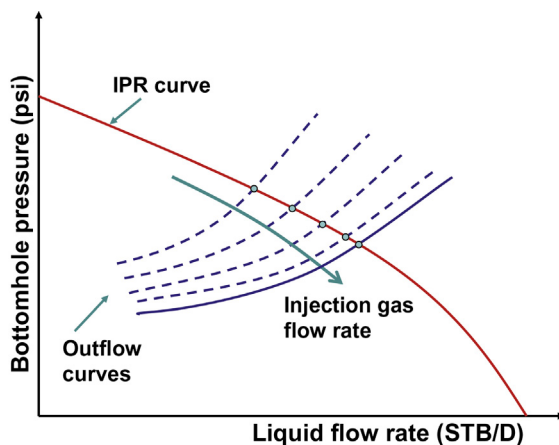
of injection is to make the liquid column in the tubing as light as possible.

- The friction component of the total pressure drop is the most important one in horizontal multiphase flow. In this case, the wellhead pressure could increase while trying to reduce the gas-liquid mixture density in the tubing; therefore, the increase in the wellhead pressure could overcome the effect of reducing the density of the production fluids in the tubing before reaching the minimum pressure–gradient curve.

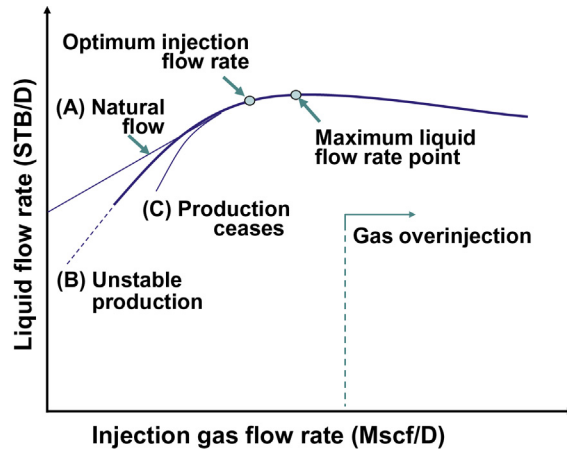
### 5.1.3 Use of computer programs to find the point of injection and perform additional useful operations

The procedures presented in the previous sections illustrate how each component of the system plays a particular role in the production of the well. However, following these procedures is not practical and, in many cases, not even necessary to design a gas lift well. If the available injection pressure is high enough to reach the desired point of injection, the maximum liquid flow rate and the required injection gas flow rate are easily determined because the calculations involve a single point of injection depth. The maximum liquid production is found by performing a total system analysis for different total gas/liquid ratios as shown in Fig. 5.10, where the outflow curves intersect the IPR curve at different points.

The results obtained from the simulations shown in Fig. 5.10 are better appreciated if the liquid and injection gas flow rates, from each intersection



■ FIGURE 5.10 Total system analysis for different injection gas flow rates keeping the point of injection at a constant depth.



■ FIGURE 5.11 Liquid production versus injection gas flow rate.

point of the outflow and inflow curves, are plotted in a diagram like the one shown in Fig. 5.11.

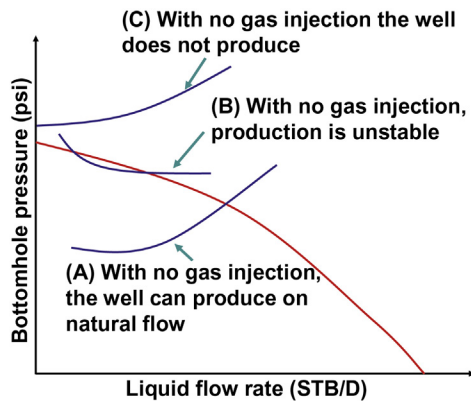
It can be seen in Fig. 5.11 that there is one injection gas flow rate for which the liquid production is maximized. But this point does not necessarily represent the condition at which profitability is maximized. It might be possible to reduce the injection gas flow rate without drastically affecting the liquid production so that savings on gas compression and produced-water treatment and handling can be realized, maximizing in this way the profitability of the well (this reduced injection gas flow rate is called the “optimum injection flow rate” as shown in Fig. 5.11). Fig. 5.11 also shows the different events that could take place as the injection gas flow rate is reduced to zero (cases A, B, and C). As the gas flow rate is reduced, one of the following responses can occur in the well (depending on the reservoir pressure and operational conditions).

- If the reservoir pressure is high enough, the well can be produced on natural flow without gas injection. In this case, without gas injection, the liquid production could be stable, case “A” in Fig. 5.11, or unstable (heading), case “B.”
- If the outflow curve with no gas injection does not intersect the inflow curve, the well simply cannot produce without gas injection, case “C.” In this case, even at very low injection gas flow rates the production can be greater than zero but it will be unstable until the gas flow rate is increased to a certain level above which the production stabilizes. The instability that takes place when the injection gas flow rate is

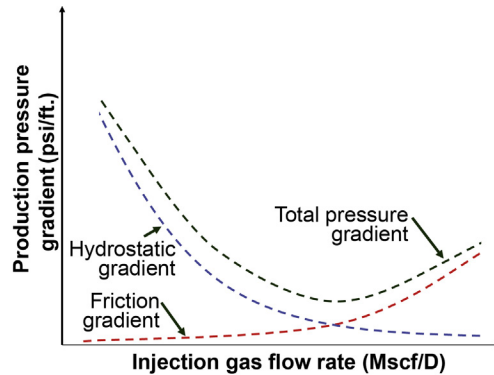
less than a certain level could occur for different reasons: (1) If at the point of injection there is an injection-pressure-operated gas lift valve (which are explained in chapter: Gas Lift Valve Mechanics), then it is possible that at low injection gas flow rates the injection pressure decreases to the valve's closing pressure and the valve closes but because the gas injection into the well's annulus is continuous, the injection pressure will increase, eventually opening again the operating valve to start a new injection cycle; and (2) If there is an orifice valve installed at the point of injection, the production pressure increases (due to lack of sufficient lift gas) until it becomes greater than the injection pressure at depth so that the gas injection into the tubing ceases; however because the gas injection at the surface is continuous, eventually the injection pressure will increase and overcome the tubing pressure and a new injection cycle is repeated. These sources of instabilities explain here for case "C" could happen for all cases (A, B, or C) if gas injection is kept at a very low rate; therefore, it is always necessary (even for wells that can produce on natural flow) to check the minimum injection gas flow rate that will provide stable liquid production.

The alternatives just described can be explained by the behavior of the outflow curves (without gas injection) with respect to the IPR curve as shown in Fig. 5.12.

It can also be appreciated in Fig. 5.11 that if too much gas is injected into the well, the liquid flow rate is actually reduced. This is due to the increase in the frictional pressure drop that takes place in the flowline and in the



■ FIGURE 5.12 Alternatives that can take place when the gas flow rate is reduced to zero. (inflow and outflow curves).



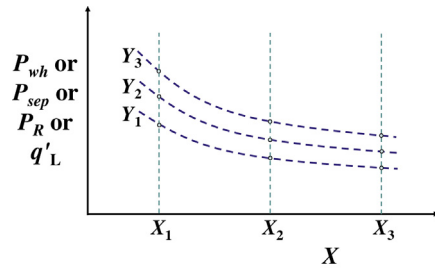
■ FIGURE 5.13 Effect of the injection gas flow rate on the total pressure gradient.

production tubing. The hydrostatic pressure component in the tubing becomes very small (because the injection gas occupies more space) but the friction component (in the tubing and flowline) increases, making the total pressure gradient larger than its minimum possible value. This is shown in Fig. 5.13. The decline in liquid production due to gas overinjection (Fig. 5.11) usually has a small downward slope with no drastic drop in the liquid production and this is the reason why many wells can be over injected for a long time without being noticed.

If the injection pressure is not high enough to reach the maximum possible depth of the point of injection (usually located right above the production packer), total system analysis should be performed to find the point of injection for which the liquid production (or the net profit) of the well is maximized. The different calculation procedures that can be performed today, thanks to the calculation power offered by personal computers, are explained in the following sections. One of these procedures is the “practical” determination of the depth of the point of injection, which is explained towards the end of this section after the following useful operations are described first.

*Total system analysis.* Current computational programs can perform simultaneous operations that give results like the ones shown in Fig. 5.14. The variable that needs to be found appears on the vertical axis and the user usually has the following options for this variable:

- Liquid flow rate: the program calculates the liquid flow rate,  $q'_L$ , the well can produce. The inlet and outlet pressure of the system should be entered by the user to perform the operation.



■ FIGURE 5.14 Typical results from a total system analysis.

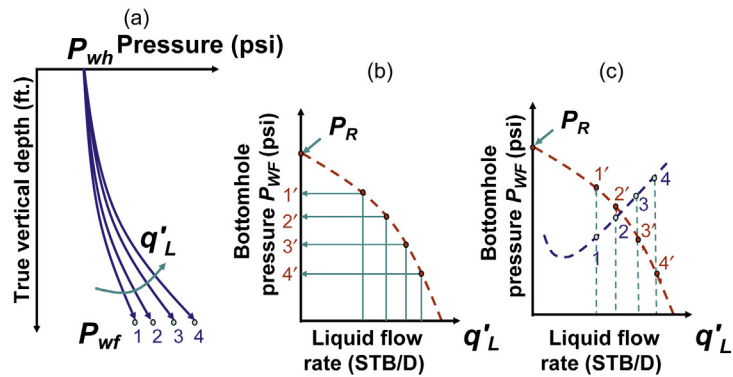
- Outlet pressure: the program calculates the outlet pressure, which could be the wellhead pressure,  $P_{wh}$ , or the separator pressure (or production manifold pressure),  $P_{sep}$ , if the effect of the flowline is considered. The inlet pressure and the liquid production should be entered by the user.
- Inlet pressure: the program calculates the inlet pressure, which is usually taken as the reservoir pressure,  $P_R$ . The liquid flow rate and the outlet pressure should be entered.

On the other hand, any variable  $X$  (defined later) is plotted on the horizontal axis of Fig. 5.14. The influence of variable  $X$  on the operation of the system is easily investigated in this way. For each value of  $X$ , a sensitivity analysis can be performed with another variable  $Y$  so that its influence can also be studied. The options for  $X$  and  $Y$  are the same for both variables and they can be classified as:

- Fluid properties: water cut, gas or water specific gravity, oil API gravity, formation gas/oil ratio, etc.
- System data: separator or wellhead pressure, injection gas flow rate, etc.
- Reservoir data: productivity index, reservoir pressure, or temperature, etc.
- Tubing or flowline data: inside diameter, pipe roughness, etc.

For each possible combination of  $X$  and  $Y$ , the computer program determines the value of one of the following variables (depending on the selected option for the variable on the vertical axis): liquid flow rate, outlet pressure, or inlet pressure.

For the first option (liquid flow rate calculation), given the fact that the reservoir pressure is known, the program determines the maximum liquid production the reservoir can provide with a bottomhole flowing pressure equal to zero. This flow rate is known as the absolute open flow (AOF) potential. Then, for a number of liquid flow rates less than the AOF, the bottomhole



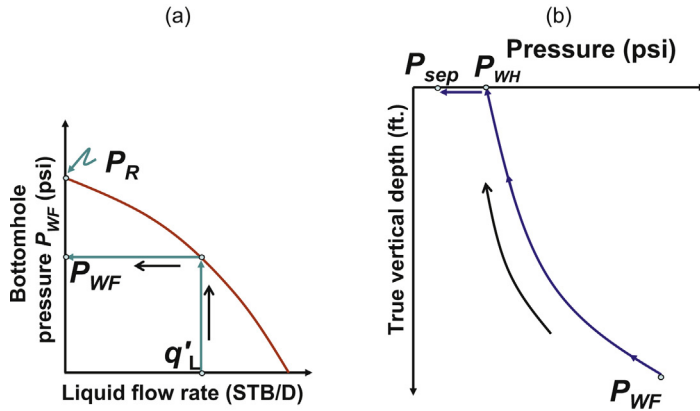
■ FIGURE 5.15 Liquid flow rate determination.

flowing pressures are calculated from the outlet pressure (from top to bottom) as shown in Fig. 5.15a. Due to the fact that the reservoir pressure is known, the program can calculate the required drawdown for each liquid flow rate being considered (from the reservoir to the sand face) as shown in Fig. 5.15b. Both sets of pressures, the bottomhole flowing pressures calculated from the outlet pressures (out flow curve) and the bottomhole flowing pressures calculated from the reservoir drawdown (inflow curve), are plotted as shown in Fig. 5.15c. The point where the inflow curve intersects the outflow curve determines the liquid flow rate the well can produce and the corresponding bottomhole flowing pressure, for the particular values of  $X$  and  $Y$  being considered. This calculation process is repeated for each  $X$ – $Y$  combination.

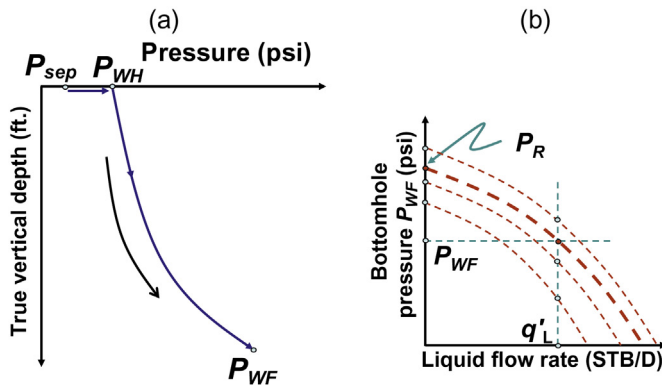
For the second option (outlet pressure calculation), given the fact that the reservoir pressure and the liquid flow rate are known, the program determines the bottomhole flowing pressure first, as shown in Fig. 5.16a (from the IPR curve). From this calculated bottomhole flowing pressure and the known liquid flow rate, the program calculates the outlet pressure as shown in Fig. 5.16b (from the bottom of the well to its outlet) for the particular values of sensitivity variables  $X$  and  $Y$  being considered. This calculation procedure is repeated for all combinations of variables  $X$  and  $Y$ .

For the third option (inlet pressure calculation), given the fact that the liquid flow rate and the outlet pressure are known, the program calculates the bottomhole flowing pressure first, in the direction shown in Fig. 5.17a (from top to bottom). This determines the point ( $q'_L$ ,  $P_{wf}$ ) shown in Fig. 5.17b. By means of an iterative procedure, a reservoir pressure,  $P_R$ , is found so that





■ FIGURE 5.16 Outlet pressure determination.

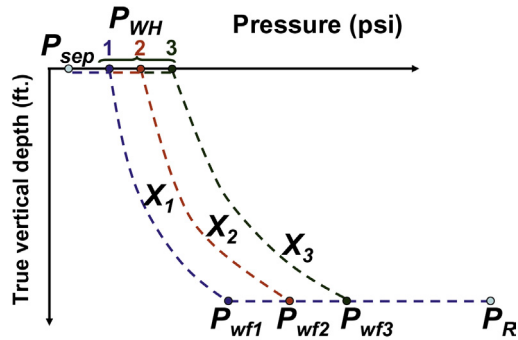


■ FIGURE 5.17 Inlet pressure calculation.

the point defined by the calculated bottomhole flowing pressure,  $P_{wf}$ , and the liquid flow rate,  $q'_L$ , lies on the IPR curve for the particular values of sensitivity variables  $X$  and  $Y$  being considered.

Besides variable  $Y$ , there are programs that allow simultaneous calculations for several sensitivity variables (and not just one):  $Y, Z, W$ , etc. For example, the user might want to calculate the liquid production for different injection gas flow rates, taken as  $X$ , with the oil API gravity and the formation gas/oil ratio as sensitivity variables  $Y$  and  $Z$ , respectively.

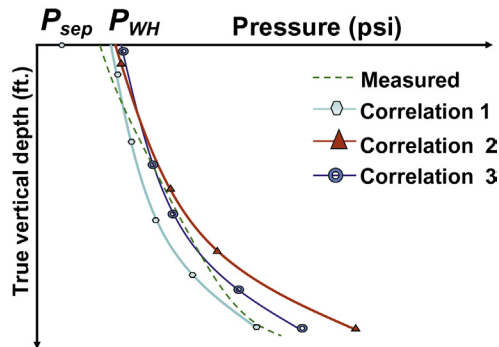
*Pressure and temperature profile determination.* This operation gives the pressure and temperature distribution along the tubing and flowline for



■ FIGURE 5.18 Pressure and temperature profile.

different sensitivity variables,  $X$ , as shown in Fig. 5.18, where three values of the sensitivity variable are shown. The options for sensitivity variables to use are the same as the ones given for the “total system analysis” operation described earlier. Here too, the user must enter two of the following three variables: inlet pressure, outlet pressure, or liquid flow rate. The program calculates the unknown variable following the same steps described for “total system analysis,” but in this case the program shows the pressure and temperature profile for each solution.

*Multiphase flow correlation comparison.* This operation is identical to the previous one only that instead of having different sensitivity variables, the program shows the results obtained from the different vertical and/or horizontal correlations selected by the user. As with the other operations, two of the following variables must be entered and the program calculates the unknown one using the same calculation procedures presented previously for total system analysis: inlet pressure, outlet pressure, or liquid flow rate. Fig. 5.19

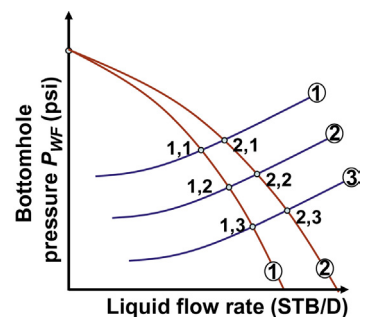


■ FIGURE 5.19 Multiphase flow correlation comparison.

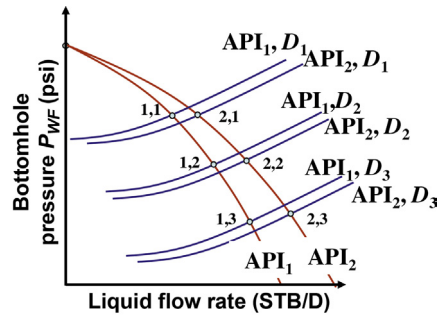
shows a typical result of this type of operation. Usually, the user can introduce the results from a downhole pressure and temperature survey to compare them with the calculated values obtained from the different selected correlations. In this way, the correlation that fits the measured values more accurately can be used for other types of analysis. Some computer programs allow the use of one correlation above a certain depth and a different one below this point. This is particularly advantageous in long tubing strings in which the bottomhole pressure is above the bubble point pressure but the gas/oil ratio is large enough to have slug flow at shallow depths. Some computer programs also provide the means to automatically select the best correlation and, at the same time, adjust coefficients like the friction factor, the holdup factor and/or the heat transfer coefficient. In this case, the user is allowed to define the range of values that will be allowed for these factors. The deviations of these factors should not be too large (important deviations are usually the result of poorly calibrated PVT models used in the calculations or poor quality of the field measurements).

*Nodal analysis.* This operation is identical to the “total system analysis” operation presented earlier but with only the liquid flow rate as the variable to be determined. Another difference is that the user has the option of selecting the point of the system for which the inflow and outflow pressures are shown. This point is known as the “nodal point” or just the “node.” Additionally, the user can select one sensitivity variable upstream of the node and/or one sensitivity variable downstream of the node. For example, if the user sets the node at the bottom of the well, the tubing diameter could be a downstream sensitivity variable and the reservoir pressure could be an upstream sensitivity variable. In Fig. 5.20, there are two values for the inflow (upstream) sensitivity variable and three values for the outflow (downstream) sensitivity variable. Inflow pressures are calculated (for each liquid flow rate) from the reservoir to the nodal point, while the outflow pressures are calculated (for the same liquid flow rates) from the wellhead (or the separator, if the flow line is considered in the calculations) to the nodal point.

The six intersections correspond to the six possible solutions for each of the two upstream sensitivity variables and the three downstream sensitivity variables. When an upstream variable affects both, the upstream and the downstream calculations (like the oil API gravity, which affects the upstream calculation for some of the available IPR models, and also affects the multiphase flow calculations in the tubing and flowline) complex graphs are generated that look like Fig. 5.21. In the figure, two oil API gravities are given as the inflow sensitivity variable and three values of the tubing diameter  $D$  as the outflow sensitivity variable. This generates 12 intersections



■ FIGURE 5.20 Nodal analysis.



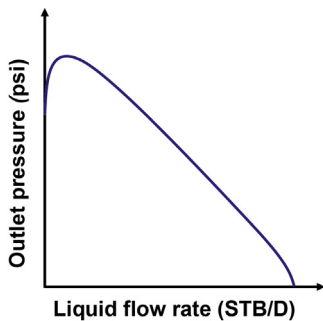
■ FIGURE 5.21 Nodal analysis with an inflow sensitivity variable that affects the outflow curves.

of which only 6 are solutions (the intersections must correspond to curves having the same oil API gravity for consistency).

*Outlet pressure as a function of the liquid flow rate.* Some programs generate outlet pressure curves as function of the liquid flow rate, like the one shown in Fig. 5.22. These curves can then be exported to be used by other operations that, for example, determine the total liquid flow rate a group of wells belonging to the same gathering system can provide for a given operational condition at the flow station where the wells are directed to.

As explained in Fig. 5.16, the program generates the curve shown in Fig. 5.22 in the following way: (1) for liquid flow rates less than the AOF, the bottomhole flowing pressures  $P_{wf}$  are determined from the IPR curve; (2) then, by means of multiphase-flow correlations, the outlet pressure  $P_{wh}$  is calculated from the flowing bottomhole pressure for each liquid flow rate.

*Liquid production and injection gas flow rate for a given surface gas injection pressure.* For a given size of the downhole gas injection orifice and a given set of reservoir, outlet, and surface injection pressures, there is one and only one possible combination of liquid production and injection gas flow rates. It is explained in this section how, with the mentioned input variables (orifice size, as well as reservoir, outlet, and injection pressures), a computer program can determine this unique liquid production rate and its (equally unique) corresponding injection gas flow rate. This is a very important operation because it allows the user to explore the real possibility of producing the well on gas lift, giving the fact that it might be possible to meet the gas flow rate requirements but not the required injection pressure, or vice versa. The following data must be entered to run this operation: PVT fluid properties; IPR curve; vertical and horizontal correlation to be used; completion and flowline details including the point of injection depth; and

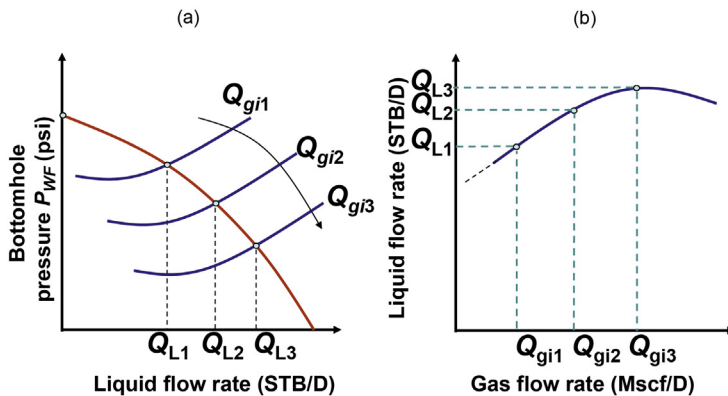


■ FIGURE 5.22 Outlet pressure versus liquid production.

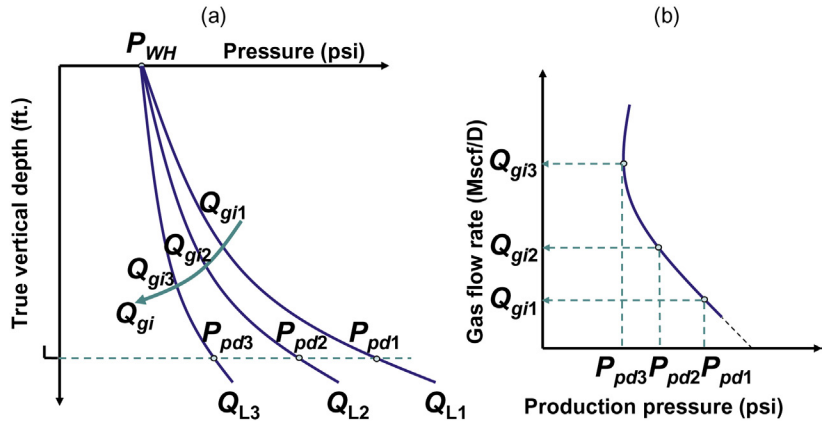
exit pressure (wellhead pressure if the flowline is not considered or separation pressure if calculations include flowline losses).

The following additional gas lift data must also be entered: maximum injection gas flow rate available; injection gas surface temperature and specific gravity (which are used to calculate the injection pressure at depth); injection orifice diameter and its discharge coefficient; and the minimum and maximum injection pressures to be explored. When the operation is executed, the program finds out how the well reacts to different surface injection pressures, from the minimum to the maximum value entered by the user. In this way, the liquid production from the well and the required injection gas flow rate are determined for each injection pressure being considered. The calculation procedure is explained in the following steps, see Figs. 5.23–5.25:

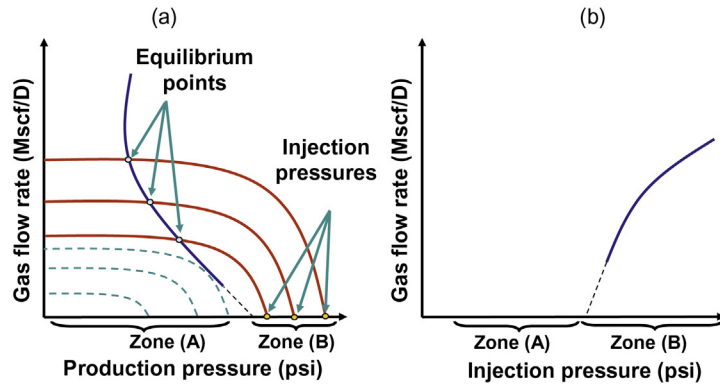
1. The outflow curves for  $n$  different injection gas flow rates ( $Q_{gin}$ ) intersect the IPR curve at points that define the liquid flow rates ( $Q_{L,n}$ ) and the bottomhole flowing pressures ( $P_{wfn}$ ) for each of these injection gas flow rates. This is shown in Fig. 5.23a.
2. The liquid flow rate,  $Q_L$ , as a function of the injection gas flow rate,  $Q_{gi}$ , is plotted for each intersection of the IPR curve as shown in Fig. 5.23b.
3. For each liquid flow rate at the intersection of the IPR curve (corresponding to a given injection gas flow rate) the tubing pressure profile is plotted. The production pressure specifically at the point of injection depth,  $P_{pd}$ , is in this way found as a function of the injection gas flow rate, see Fig. 5.24a.



■ FIGURE 5.23 Nodal analysis having the injection gas flow rate,  $Q_{gi}$ , as the sensitivity variable.



■ FIGURE 5.24 Production pressure for each liquid flow rate found by nodal analysis.



■ FIGURE 5.25 Equilibrium point for each gas injection pressure.

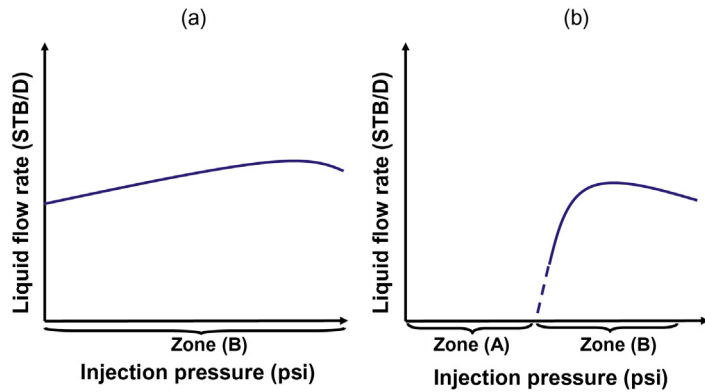
4. The injection gas flow rate and its corresponding production pressure at the injection point depth are plotted as shown in Fig. 5.24b. Notice that when the injection gas flow rate is very low, the production pressure is high and, as the injection gas flow rate is increased, the production pressure decreases, reaching a minimum value which correspond to the point of maximum liquid production.
5. It is recommended that the reader review the explanation given for Fig. 8.1, on gas flow rate through orifices, to understand this step (the gas injection through orifices is also explained in Section 4.1). On the same graph obtained in the previous step, Fig. 5.24b, different curves corresponding to the gas flow rate that the installed orifice can

pass for different injection pressures (at depth) are superimposed, Fig. 5.25a. Notice that for each injection pressure (as shown in the figure) there is one and only one possible gas flow rate, which is determined by the intersection of the “orifice gas flow rate curve” and the curve previously obtained in step (4). These intersections are called “equilibrium points.” Gas injection pressures (used to generate gas flow rate curves) in zone “A” correspond to gas injection pressures that are less than the production pressure at valve’s depth and therefore the injection gas flow rate is not possible in this zone (there are no possible intersection points). In zone “B” the injection pressures generate curves of the gas flow rate through the orifice that do intersect the curve found in step (4) at their respective equilibrium points. As the injection pressure is increased, the injection gas flow rate also increases. On the other hand, for each injection pressure at the point of injection depth, there is one and only one surface injection pressure, which can be calculated from the different “gas factors” that are explained in Section 2.1. At low injection gas flow rates, one orifice gas flow rate curve can actually intersect the curve generated in step (4) at two different points. This double intersection constitutes the basis for the stability criterion explained in chapter: Design of Continuous Gas Lift Installations (not shown here to avoid confusion) and it happens in a zone “C” between zones “A” and “B”. The gas lift design is unstable for injection pressures in zone “C.”

6. The gas flow rates corresponding to the equilibrium points found in the previous step are plotted as a function of the surface injection pressure in the way that is shown in Fig. 5.25b.

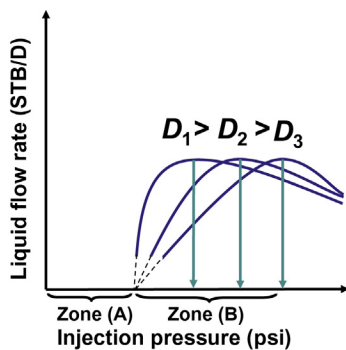
For each injection pressure shown in Fig. 5.25a (in stable zone “B”), there is one injection gas flow rate and, therefore, one liquid flow rate as determined in Fig. 5.23b. The liquid flow rate can then be plotted as a function of the injection pressure as shown in Fig. 5.26a “if the well can produce on natural flow,” or as shown in Fig. 5.26b “if the well needs a minimum injection gas flow rate in order for it to produce liquids.”

As can be seen, this operation gives a good idea of what the well can produce for each value of the injection gas flow rate and, at the same time, it gives the required gas injection pressure to be able to inject gas at that particular flow rate. The nodal analysis operation by itself cannot indicate the required injection pressure for a given liquid production. It is possible that the required injection pressure is greater than the maximum available pressure or greater than the opening pressure of the upper unloading valve and it will simply be impossible to produce the liquid flow rate obtained from nodal analyses alone.



■ FIGURE 5.26 Liquid production as a function of the gas injection pressure. (a) the well can produce on natural flow, (b) the well cannot produce on natural flow.

To determine the adequate orifice size for the operational conditions of the well, the analysis just described should be performed for different orifice diameters. Fig. 5.27 shows three curves corresponding to three different orifice diameters. If the orifice diameter  $D$  is too small, the required gas injection pressure could be too large. But, on the other hand, if the orifice diameter is too large, it is possible that the injection pressure at depth might be too close to the production pressure, promoting instability problems (see the explanation given in Fig. 8.4, to learn more about this type of instability problem). It is usually recommended that the injection pressure minus the production pressure across the gas lift valve be at least greater than or equal to 10–20% of the injection pressure, although this is not a rule that guarantees well stability in all situations. Notice that the maximum liquid production is the same for all diameters and only the injection pressure changes to achieve a given gas or liquid flow rate.



■ FIGURE 5.27 Sensitivity analysis for different orifice diameters,  $D$ .

It should be said that these calculation steps predict the operation of the well within an acceptable level of accuracy only if there is an orifice installed at the point of injection. If a spring-loaded or nitrogen-charged valve is installed, the dynamic behavior of this valve could give totally inaccurate results unless the valve is fully open. The dynamic behavior of gas lift valves is explained in chapter: Gas Flow Through Gas Lift Valves.

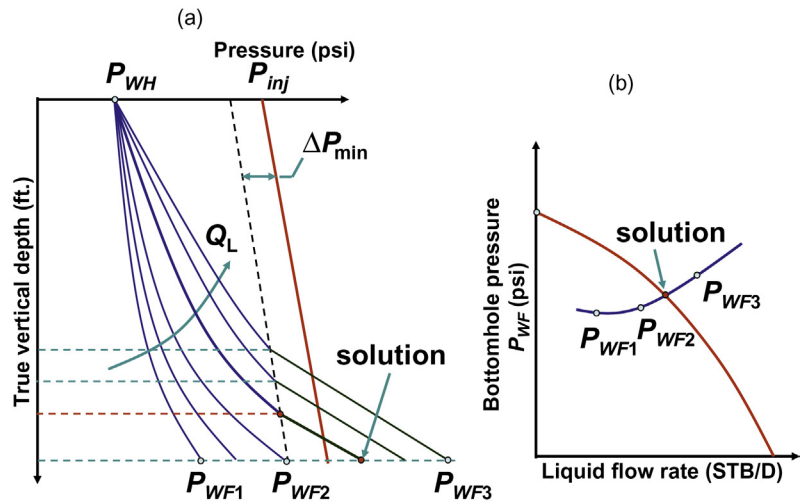
*Calculation of the point of injection depth.* Another important operation that can be easily performed by commercially available computer programs is the determination of the point of injection depth. The following data should be entered to perform this operation: PVT properties, reservoir pressure ( $P_R$ ), IPR curve, multiphase flow correlations to be used, completion details (production tubing and flowline), and outlet pressure. The flowline is



optional but if it is introduced, the outlet pressure is the pressure at the separator,  $P_{\text{sep}}$ . If the flowline is not considered, the outlet pressure is the wellhead production pressure,  $P_{\text{wh}}$ . Regarding the gas lift variables, the computer program requires the following data: injection gas flow rate, surface injection temperature and pressure, specific gravity of the injection gas, the minimum pressure drop across the gas lift valve, and the maximum possible injection point depth. Notice that for this operation the orifice diameter (or valve seat size) is not entered because it does not play any role in the calculations. This is due to the fact that this operation constitutes the basis for the mandrel spacing and valve design operations and only the minimum allowable pressure drop across the gas lift valve at the point of injection is needed at this stage. This minimum pressure drop is usually equal to 100 or 150 psi (or 10–20% of the gas injection pressure at the maximum depth where a gas lift valve can be installed).

Two possible calculation procedures to find the point of injection depth and the well's liquid production are explained next. In both procedures, the injection gas flow rate is "constant" and should be provided by the user; therefore, the maximum liquid production is found by repeating the procedures with different injection gas flow rates.

*First calculation procedure.* The first step is to select several liquid flow rates that are less than the maximum possible liquid production the reservoir can provide, defined as AOF. For each liquid flow rate being considered, the program calculates the bottomhole flowing pressure starting from the outlet or exit pressure (which is the wellhead or separation pressure, depending on the choice of the designer). As the program calculates the production pressure from the wellhead to the bottom of the well, it checks if the production pressure is equal to the injection pressure at depth minus the minimum pressure drop across the gas lift valve. If this is the case (before reaching the bottom of the well) the program continues performing the production pressure calculation but with the formation gas/liquid ratio and not with the total gas/liquid ratio, as shown in Fig. 5.28a. Of all liquid flow rates lower than AOF, only one should coincide with the liquid flow rate the reservoir can produce (unless there is no solution possible because the injection gas flow rate is not large enough for the outflow curve to intersect the inflow curve). This unique liquid flow rate is easily found if the calculated bottomhole pressures are plotted together with the IPR curve, as shown in Fig. 5.28b (keep in mind that each point of the outflow curve in this case might correspond to a different point of injection). The intersection of the outflow curve with the IPR curve gives the only possible liquid flow rate and the injection point depth for the injection gas flow rate considered. This procedure is illustrated in Fig. 5.28.

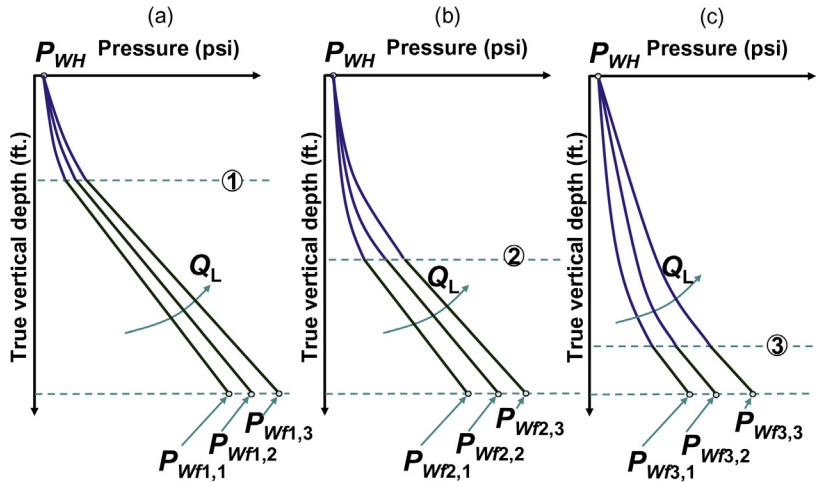


■ FIGURE 5.28 Calculation of the injection point depth (the injection gas flow rate is kept constant).

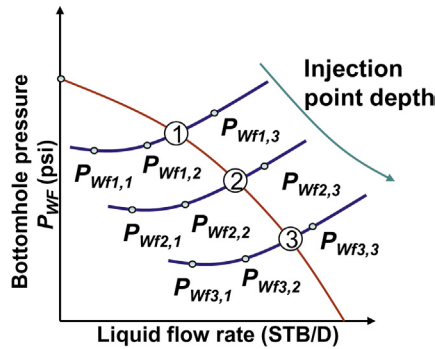
The operation just described can be repeated for different injection gas flow rates. For each gas flow rate there will be a solution that can be plotted in a graph identical to Fig. 5.11, from which the injection gas flow rate that maximizes production or profitability can be selected.

*Second calculation procedure.* Another way of finding the liquid flow rate and the depth of the point of injection using a computer program is by applying the “constant-injection-gas-flow-rate equilibrium curves.” The program determines a set of possible injection point depths (from the wellhead to the maximum allowed depth) by simply dividing the length of the production tubing into an arbitrary number of equal-length sections. For each point of injection, the program calculates the flowing bottomhole pressures for different liquid flow rates (from very small values to AOF), keeping the injection gas flow rate constant, see Fig. 5.29 (in which, for simplicity, only three points of injection and three liquid flow rates have been plotted). On the IPR diagram, all the points corresponding to the bottomhole flowing pressures for a given injection point depth form an outflow curve that intersects the IPR curve at only one point, which determines the only liquid flow rate possible for that injection point depth, see Fig. 5.30.

For each possible liquid flow rate corresponding to the solution at each point of injection depth, the respective production pressure at the point of injection can be plotted on a pressure-depth diagram. All the production pressure solutions (unique to each injection point depth) form the curve presented in



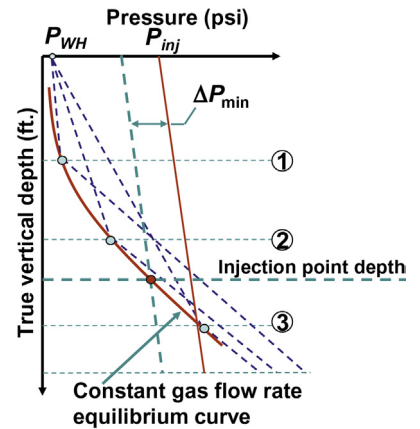
■ FIGURE 5.29 Bottomhole flowing pressures for point of injection depths 1, 2, and 3.



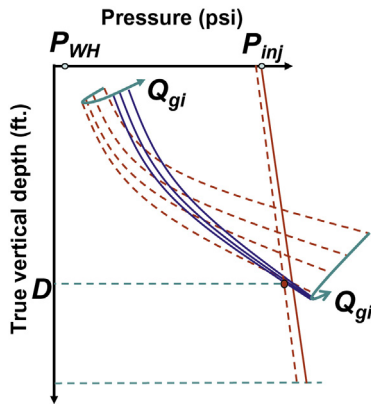
■ FIGURE 5.30 Liquid flow rate calculation for each injection point depth.

Fig. 5.31, which is known as the “constant-injection-gas-flow-rate equilibrium curve.” The point where this equilibrium curve intersects the gas injection pressure minus the minimum pressure drop across the gas lift valve determines the depth of the point of injection for the given available surface injection pressure and the injection gas flow rate being considered.

The equilibrium curve presented in Fig. 5.31 is different from the one in Fig. 5.7 because the latter is built from different injection gas flow rates that correspond to the maximum liquid production the well can produce for each injection point depth. On the other hand, the constant-gas-injection equilibrium curves (as the one in Fig. 5.31) simply give the liquid production



■ FIGURE 5.31 Equilibrium curve for a given injection gas flow rate.



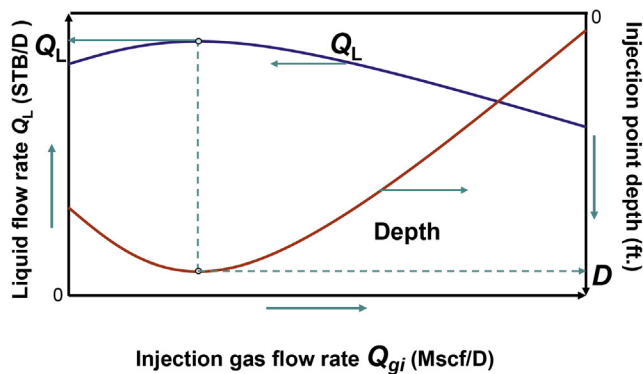
■ FIGURE 5.32 Behavior of "constant-injection-gas-flow-rate equilibrium curves" for different injection gas flow rates,  $Q_{gi}$ .

the well can produce for each point of injection depth and the fixed value of the injection gas flow rate considered in the calculations.

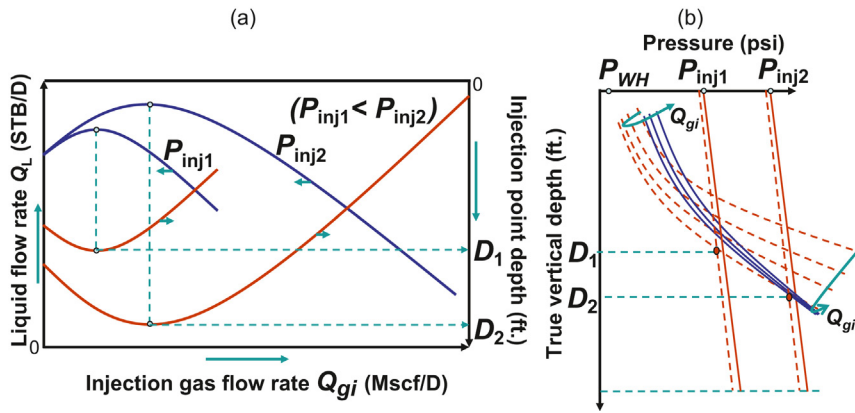
Several constant-gas-flow-rate equilibrium curves can be generated for different injection gas flow rates. As the gas flow rate is increased, these equilibrium curves are displaced downward, until reaching a point in which they start to move upwards, indicating that gas is being over injected. The way they appear on a pressure-depth diagram depends on the production characteristics of the well; see Fig. 5.32 (in which the behavior of the equilibrium curves has been exaggerated to show how these curves are influenced by the injection gas flow rate  $Q_{gi}$ ). The actual constant-gas-flow-rate equilibrium curve looks as shown in Fig. 5.51a (for a well that can produce on natural flow) and in Fig. 5.56 (for a well that cannot produce on natural flow).

All calculations explained previously to find the point of injection can be repeated for each of the different injection gas flow rates that are selected to be studied. The points of injection are simply the intersections of the injection pressure at depth (minus the minimum pressure drop across the gas lift valve) with the different equilibrium curves. In this way, a graph of the liquid flow rate  $Q_L$  versus the injection gas flow rate  $Q_{gi}$  can be generated to find the gas flow rate that maximizes the liquid production, which will simultaneously give the corresponding point of injection depth. The results from these calculations are usually given in graphs such as the one shown in Fig. 5.33 for a given injection pressure. In the particular case presented in the figure, the well that can produce on natural flow (the liquid production does not go down to zero when the gas flow rate is reduced to zero).

As can be seen in Fig. 5.33, this operation is very important because it determines the injection point depth and the injection gas flow rate required



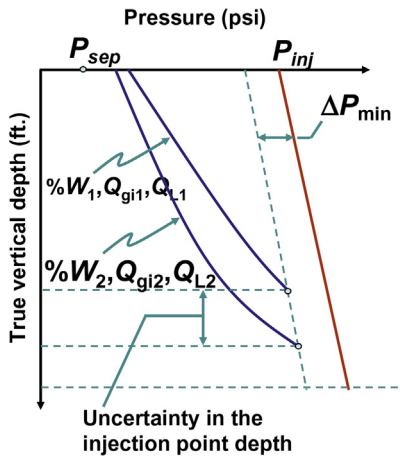
■ FIGURE 5.33 Injection gas flow rates for which the liquid production is maximized.



■ FIGURE 5.34 Effect of the injection pressure on the liquid production, the required injection gas flow rate and the point of injection depth.

to maximize the liquid production. This operation can be repeated for several surface injection pressures, which will give the basic information to start the mandrel spacing and valve design procedures explained in chapter: Design of Continuous Gas Lift Installations. Fig. 5.34a shows how these curves will look like for two different injection pressures  $P_{inj1}$  and  $P_{inj2}$ . In Fig. 5.34b the equilibrium curves are presented together with two injection pressures which determine depths  $D_1$  and  $D_2$  that give the maximum liquid production for each injection pressure.

*Bracketing.* It frequently happens that the information needed to determine the point of injection depth is either not too accurate or part of it is just missing. This uncertainty makes the designer look for different point of injection depths if some of the not well known variables are allowed to change within a range of possible values. One function that helps the designer determine the level of uncertainty regarding the depth of the point of injection is called “bracketing.” This operation consists in finding the maximum and minimum point of injection depth if the value of one (or several) of the following variables is changed: (1) liquid flow rate the well can produce, (2) injection gas flow rate, and (3) water cut of the produced fluids. The computer program performs the calculation in a practical way, without taking into consideration the IPR curve of the well because it is the user who indicates the liquid production, based on nearby wells producing from the same reservoir or from the production history of the well itself. Pressure calculations are performed from the outlet pressure (wellhead or separation pressure) to the point where the production pressure is equal to the injection pressure at depth minus the minimum pressure drop across the gas lift valve.



■ FIGURE 5.35 Uncertainty in the determination of the depth of the point of injection.

The input data needed to perform this operation are: “PVT” properties; multiphase flow correlations to be used; outlet pressure (wellhead or separation pressure); wellhead pressure and temperature, and specific gravity of the injection gas; the minimum pressure drop across the gas lift valve; and the maximum allowable depth of the point of injection. Additionally, the user must introduce two sets of different values of the liquid flow rate ( $Q_L$ ), the water cut ( $W$ ), and the injection gas flow rate ( $Q_{gi}$ ). These variables are used by the computer program to calculate the pressure profile along the production tubing. These are the variables that, for a given tubing diameter, have the greatest impact on the production pressure profile along the tubing and, therefore, the depth of the point of injection. With the input data, the program calculates the pressure profile along the flowline and the production tubing for each of the two sets of variables mentioned previously. As the computer program calculates the pressure down the tubing, it checks if the production pressure becomes equal to the injection pressure at depth minus the minimum pressure drop across the gas lift valve. The injection point depth is established when the production pressure for each set is equal to the injection pressure at depth minus the minimum pressure drop across the gas lift valve, see Fig. 5.35.

Some designers place several gas lift mandrels between the two depths found in this operation. This number of mandrels is equal to the integer part of the ratio of the measured length interval bounded by these two depths over the minimum mandrel spacing between two consecutive mandrels allowed by the operating company. The minimum mandrel spacing depends on the productivity index of the well, as explained in chapter: Design of Continuous Gas Lift Installations. This allows for the precise location of the optimum point of injection once the first attempt is in operation and the production capability of the well is understood.

## 5.2 EXAMPLES OF THE EFFECT THAT DIFFERENT GAS LIFT SYSTEM’S COMPONENTS OR FLUID PROPERTIES MIGHT HAVE ON THE LIQUID PRODUCTION OF A WELL ON GAS LIFT

The total system analysis is an important design tool for current and future operational conditions of a well producing on gas lift. The following results were obtained from total system analyses to illustrate the effect of the different system’s components and fluid properties on the liquid production of a well producing on gas lift. The input data are as follows:

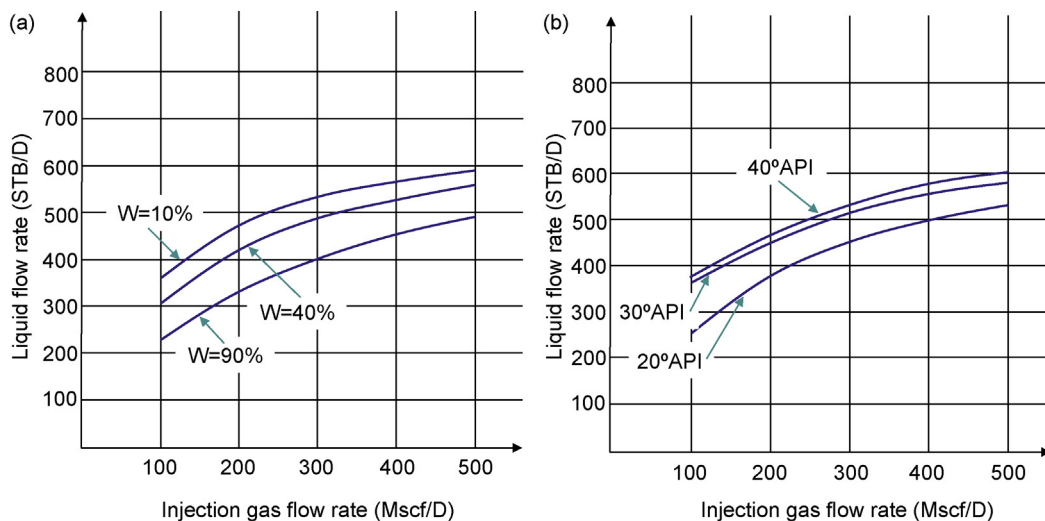
- Fluid properties: 22 degrees API oil; water cut = 50%; formation water specific gravity = 1.02; formation gas specific gravity = 0.7; gas/oil

ratio = 400 scf/STBO; injection gas specific gravity = 0.65; and bubble point pressure = 2937.74 psi.

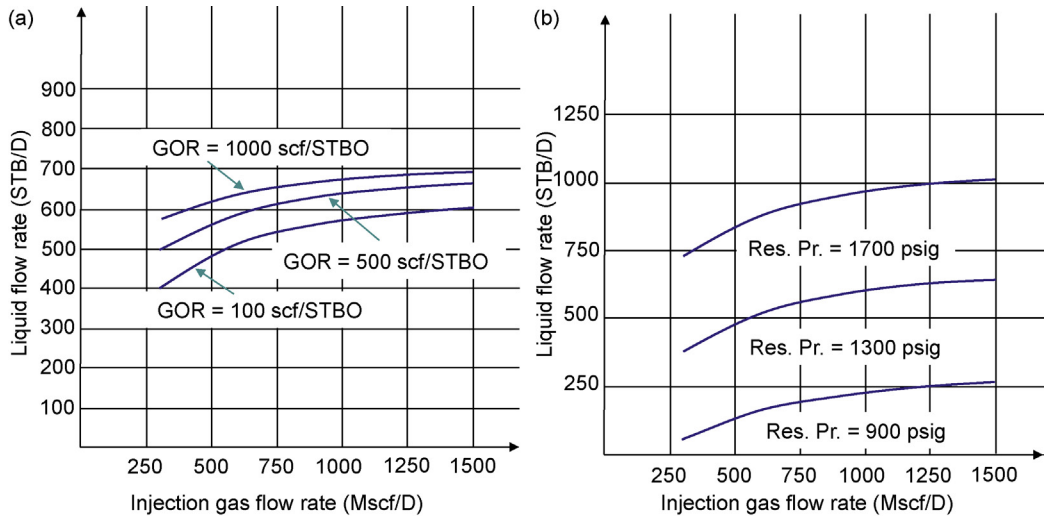
- Completion data: tubing diameter = 2.992 in. ID down to 4000 ft. (vertical well); casing diameter = 6.366 in. ID; top of perforations depth = 4500 ft.; injection point depth = 3500 ft.
- Flowline: from wellhead = 2000 ft. of 4 in. ID pipe and 1500 ft. of 5 in. I.D. pipe.
- Reservoir: static pressure = 1500 psig; temperature = 150°F; and PI = 1 Br/(psi-D).
- Surface conditions: separator pressure = 80 psig; separator temperature = 100°F; wellhead temperature = 110°F.

Use Vogel to find the IPR curve, Dons and Ross correlation for vertical multiphase flow calculations, and Dukler–Flanigan correlation for horizontal multiphase flow calculations.

Fig. 5.36a shows the effect of the water cut on the production of the well. As the water cut increases, the bottomhole flowing pressure also increases and the liquid flow rate coming from the reservoir decreases. It might not be possible to perform this type of analysis for water cuts between 40 and 70% because of emulsion formation. With emulsions, it is very difficult to calculate the viscosity of the fluids. The viscosity of an emulsion could be considerably larger than the viscosity of the water



■ FIGURE 5.36 (a) Effect of the water cut ( $W$ ); (b) effect of the oil API gravity.



■ FIGURE 5.37 (a) Effect of the gas/oil ratio (scf/STB); (b) effect of the reservoir pressure (psi).

or the oil, separately. The viscosity affects the pressure drop along the flowline and the production tubing.

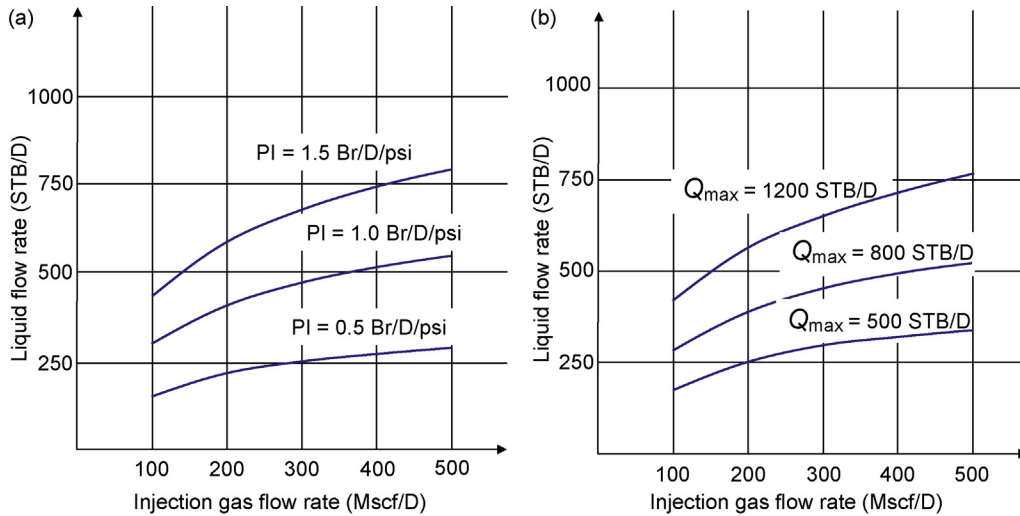
Fig. 5.36b indicates that as the API gravity of the oil increases, the liquid production also increases. This is due to the fact that oils with greater API gravities offer less friction resistance in the flowline and in the production tubing. Additionally, the higher the API gravity is, the lighter the oil becomes, so that the hydrostatic pressure in the production tubing is reduced.

Fig. 5.37a shows that an increase in the gas/oil ratio might cause an increase in the liquid production. One important reason for this to happen is that the gas reduces the hydrostatic pressure of the fluids from the perforations, at 4500 ft. of depth, to the point of injection, at 3500 ft. Fig. 5.37b shows that as the reservoir pressure decreases, so does the liquid production for a given injection gas flow rate.

Fig. 5.38a shows a drastic increase in the liquid production when the productivity index goes from 0.5–1.5 STB/(psi-D). The increase in the maximum liquid flow rate used in the Vogel equation from 500–1200 STB/D, causes an increase in liquid production of the well that is very similar to the one shown for the increase in the productivity index, see Fig. 5.38b.

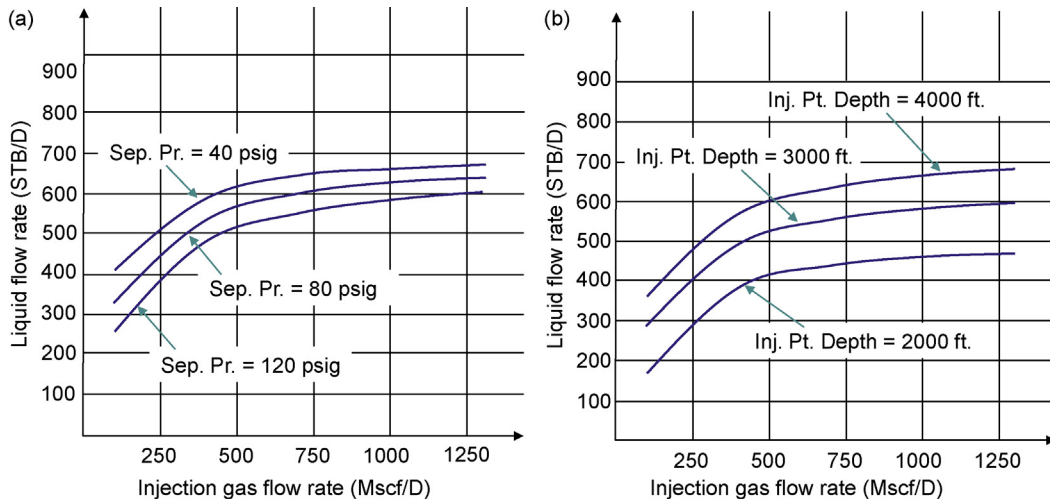
Fig. 5.39a shows that an increase in the separation pressure causes a decrease in the liquid production. Trying to lower the separation pressure is a good recommendation when the reservoir pressure has declined; however,



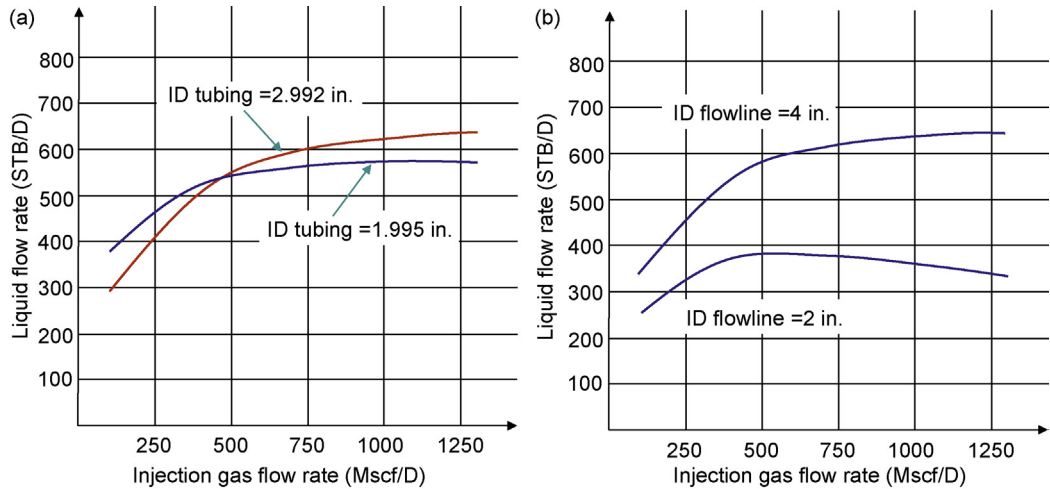


■ FIGURE 5.38 (a) Effect of the productivity index STB/(psi-D); (b) effect of  $Q_{\max}$  Vogel (STB/D).

the gas velocity at the separator increases as the pressure is reduced and the ability of the separator to handle this new velocity should be checked. Additionally, the suction pressure of the compressor is usually a fixed value and it is possible that some type of modification to the compression equipment might need to be introduced (like the installation of a booster compressor



■ FIGURE 5.39 (a) Effect of the separation pressure (or production manifold pressure) (psi); (b) effect of the injection point depth (ft.).



■ FIGURE 5.40 (a) Effect of the tubing inside diameter (in.); (b) effect of the flowline inside diameter (in.).

to bring back up the pressure to the main compression suction pressure). The effect of the point of injection depth is shown in Fig. 5.39b. The deeper the point of injection is located, the lower the bottomhole flowing pressure would be because a greater length of the production tubing is occupied by the injection gas so that the total hydrostatic pressure component is reduced more effectively. In very deep wells, it might be possible that the maximum injection point depth is not as deep as it should be due to an insufficiently high injection pressure or the gas lift equipment might not withstand the operational conditions.

Fig. 5.40a shows the effect of two different production tubing diameters. It can be observed that at low injection gas flow rates the largest liquid production is obtained with the 1.995-in. diameter tubing while at higher injection gas flow rates the 2.992-in. diameter tubing has the largest liquid production. But the increase in the liquid production at high injection gas flow rate is only around 10% and further analysis should be performed to select the 2.992-in. diameter tubing (which is more expensive) taking into account how the well will perform under changes in future operation conditions, like a reduction of the reservoir pressure or an increase of the water cut, among other variables. In Fig. 5.40b the impact of the flowline diameter can be appreciated. A very small flowline diameter causes an increase in the wellhead production pressure due to the greater frictional pressure drops along the flowline. This increase in the wellhead pressure has a large influence on the liquid production of the well as shown in Fig. 5.39a.

### 5.3 CALCULATION EXAMPLES

#### 5.3.1 Example of preliminary calculations needed to implement the gas lift method to boost the liquid production of a well that can produce on natural flow

A well capable of producing on natural flow will have a decline in oil production as the water cut increases in time. It is desired to maintain the oil production according to the production plan, shown in [Table 5.1](#), obtained from strategic reservoir simulations.

If possible, the injection gas/oil ratio should be maintained at, or below, 500 scf/STBO. It is necessary to determine the injection gas flow rates and the point of injection depths that will be necessary to meet the planned oil production rates and confirm if the restriction imposed on the injection gas/oil ratio can be met in all cases. The available pressure at the injection manifold is equal to 1800 psig. The specific gravity of the injection gas is 0.8 and its temperature at the wellhead is equal to 80°F.

The well's deviation survey is given in [Table 5.2](#). The point of injection is not to exceed 7000 ft. of true vertical depth (TVD) to avoid complications related to the installations of gas lift valves at large tubing inclination angles. The table shows the measured depths (MD) with respect to the wellhead, along with the corresponding true vertical depths and inclination angles.

**Table 5.1** Production Plan for the Next 5 Years

Year	Water Cut (%)	Oil Production (STBO/D)
1	30	7000
3	40	6000
5	50	5000

**Table 5.2** Well's Deviation Survey

MD	TVD	Angle	MD	TVD	Angle	MD	TVD	Angle
0	0	0.00	5661.9	5117.8	39.38497	10262	7444.1	80.29938
1161.9	1161.7	5.315298	6161.9	5490.1	47.42926	10362	7461	82.0563
1461.9	1459.2	12.09542	6561.9	5747.7	55.03332	10562	7485.6	85.61259
1561.9	1557	15.58136	8961.9	6998.5	63.08938	10798	7498.6	89.07453
2161.9	2131.1	20.85248	9161.9	7089	65.67575	10862	7499.7	89.78779
2461.9	2407.3	26.7091	9715	7304.4	71.89844	10924	7499.9	
2561.9	2496.6	29.01414	9813.4	7334.9	73.75015			
5361.9	4876	35.10495	9961.9	7375.8	75.10787			

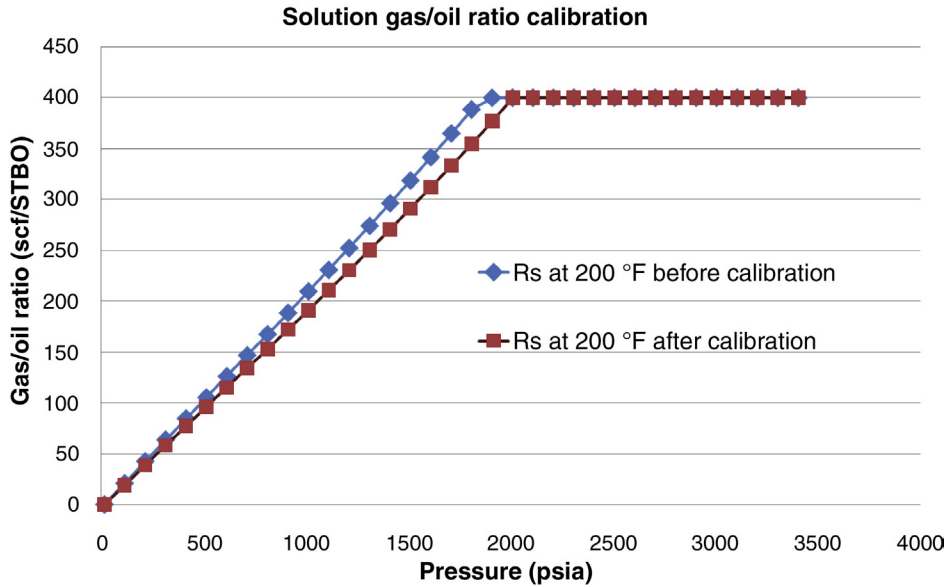
- Fluid data: current water cut = 10% (but it will increase very rapidly); gas/oil ratio = 400 scf/STBO (equal to the solution gas oil ratio at bubble point of 2010 psia and 200°F; formation gas specific gravity = 0.8; water specific gravity = 1.05; API gravity = 33; dead oil viscosity at 200 and 60°F = 1.6 and 10.5cP, respectively; live oil viscosity = 1.2 cP at 200°F and 2010 psia; formation volume factor of 1.23 at 1510 psi and 200°F; formation volume factor of 1.25 at 3305 psia and 200°F; gas viscosity = 0.012 cP at 613 psia and 60°F; gas compressibility factor = 0.68 at 1610 psia and 60°F.
- Reservoir data: static pressure = 3850 psi (the reservoir pressure will be maintained at this value throughout the life of the project); reservoir temperature = 200°F; productivity index = 9 STBO/D/psi. Assume that the productivity index will not be affected in a significant way by changes in the water cut in this reservoir. Because the reservoir pressure is much higher than the bubble point pressure, it is possible that the IPR curve will be a straight line in most cases. Use Vogel equation if the bottomhole flowing pressure drops below the bubble point pressure.
- Geothermal temperature = 110°F at the surface and 210°F at 10,924 ft. MD; overall heat transfer coefficient = 3 Btu/hr per ft<sup>2</sup> per °F.
- Production tubing I.D.: 3.958 in. from the wellhead to 9,701 ft. MD; Linner I.D.: 5.921 in. from 9,701–10,924 ft. MD.

The wellhead pressure will be kept constant at 350 psig. A pressure survey with the well producing 9800 STB/D against a wellhead pressure of 350 psig was run and the results are given in [Table 5.3](#).

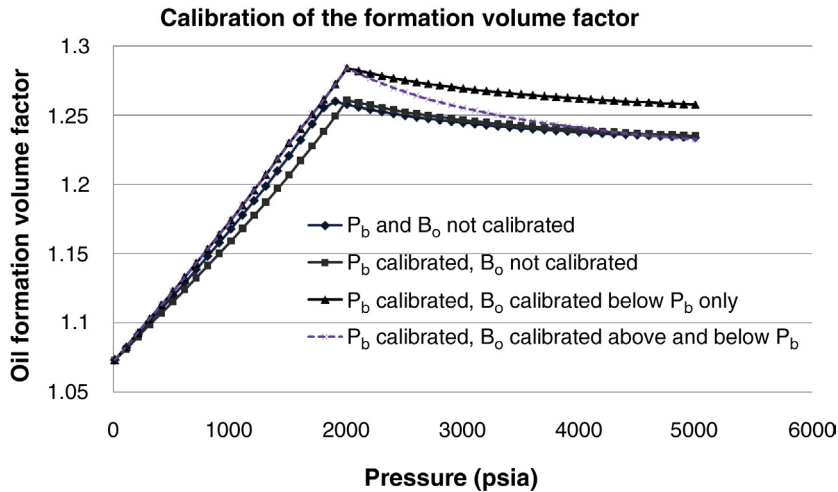
*Answer.* After building the well model using the software available for this purpose, the first task to do is to calibrate the PVT data. This is easily done in most commercially available software by just inputting the measured gas and liquid properties at their respective measured pressures and temperatures in the entry fields used by the software to calibrate the selected

**Table 5.3** Results from Flowing Pressure Survey

Stop	Measured Depth (ft.)	Pressure (psig)
1	0	350
2	1606.5	697
3	2453.0	907
4	4340.0	1393
5	6324.0	1948
6	7798.0	2245
7	9431.0	2553



■ FIGURE 5.41 Calibration of the solution gas/oil ratio.

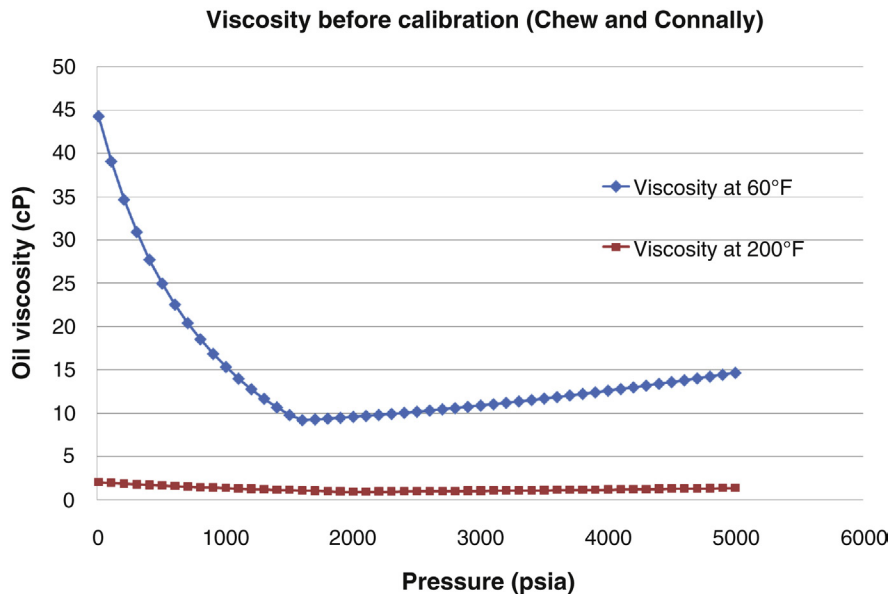


■ FIGURE 5.42 Calibration of the oil formation volume factor.

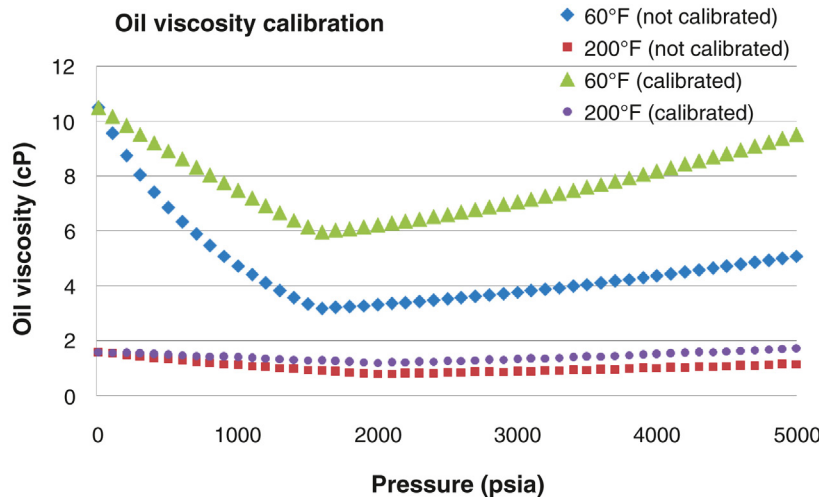
PVT correlations. Fig. 5.41 shows the solution gas/oil ratio predicted by the Lasater correlation with and without calibration. The original correlation (without calibration) predicts a lower value of the bubble point pressure; therefore, at any other pressure below the actual bubble point pressure, the actual solution gas/oil ratio is lower than its predicted value. The impact of

the actual solution gas/oil ratio on the calculation of the hydrostatic pressure drop along the production tubing can, in most gas lift wells, be very significant; but this is not the case for this particular well because: (1) the gas/oil ratio is not very large, and (2) the reservoir pressure is much higher than the bubble point pressure (the first bubbles will appear at relatively shallow depths).

The calibration of the oil formation volume factor ( $B_o$ ) is presented in Fig. 5.42, where four curves of the oil formation volume factor as functions of the absolute pressure (for a constant temperature of 200°F) are shown: (1)  $B_o$  before the calibration of the bubble point pressure ( $P_b$ ), (2)  $B_o$  after the calibration of  $P_b$ , (3)  $B_o$  after the calibration of both,  $P_b$  and  $B_o$  (but  $B_o$  is calibrated using only the calibration measurement made below  $P_b$ ), and (4)  $B_o$  after  $P_b$  and  $B_o$  (above and below the bubble point pressure) have been calibrated. The formation volume factor plays an important role in the calculation of the in situ velocity of the liquid phase. This velocity, in turn, affects the calculation of the frictional pressure drop along the production tubing. Before calibrating the correlations for  $P_b$  and  $B_o$ , the value of  $B_o$  was 1.2206 at 1510 psia and 200°F, and 1.2421 at 3305 psia and 200°F. After calibrating the correlations for  $P_b$  and  $B_o$ , the value of  $B_o$  became 1.23 at 1510 psia and 200°F, and



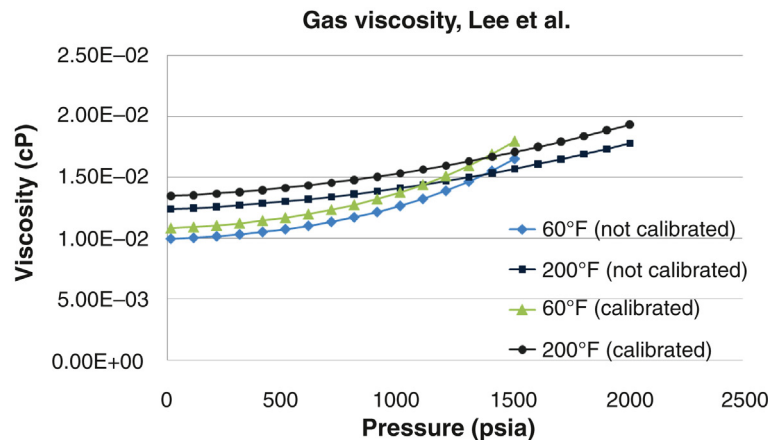
■ FIGURE 5.43 Oil viscosity as a function of pressure (before calibration).



■ FIGURE 5.44 Before and after live-oil calibration (dead-oil viscosity already calibrated).

1.25 at 3305 psia and 200°F. The correlations used to calculate  $B_o$  above and below the bubble point pressure were Vasquez–Beggs and Standing, respectively.

The other PVT property that plays an important role in the frictional pressure drop is the viscosity of the oil. Fig. 5.43 shows the oil viscosity before calibration. The Beggs–Robinson correlation predicts a dead-oil viscosity



■ FIGURE 5.45 Gas viscosity calibration, Lee et al.

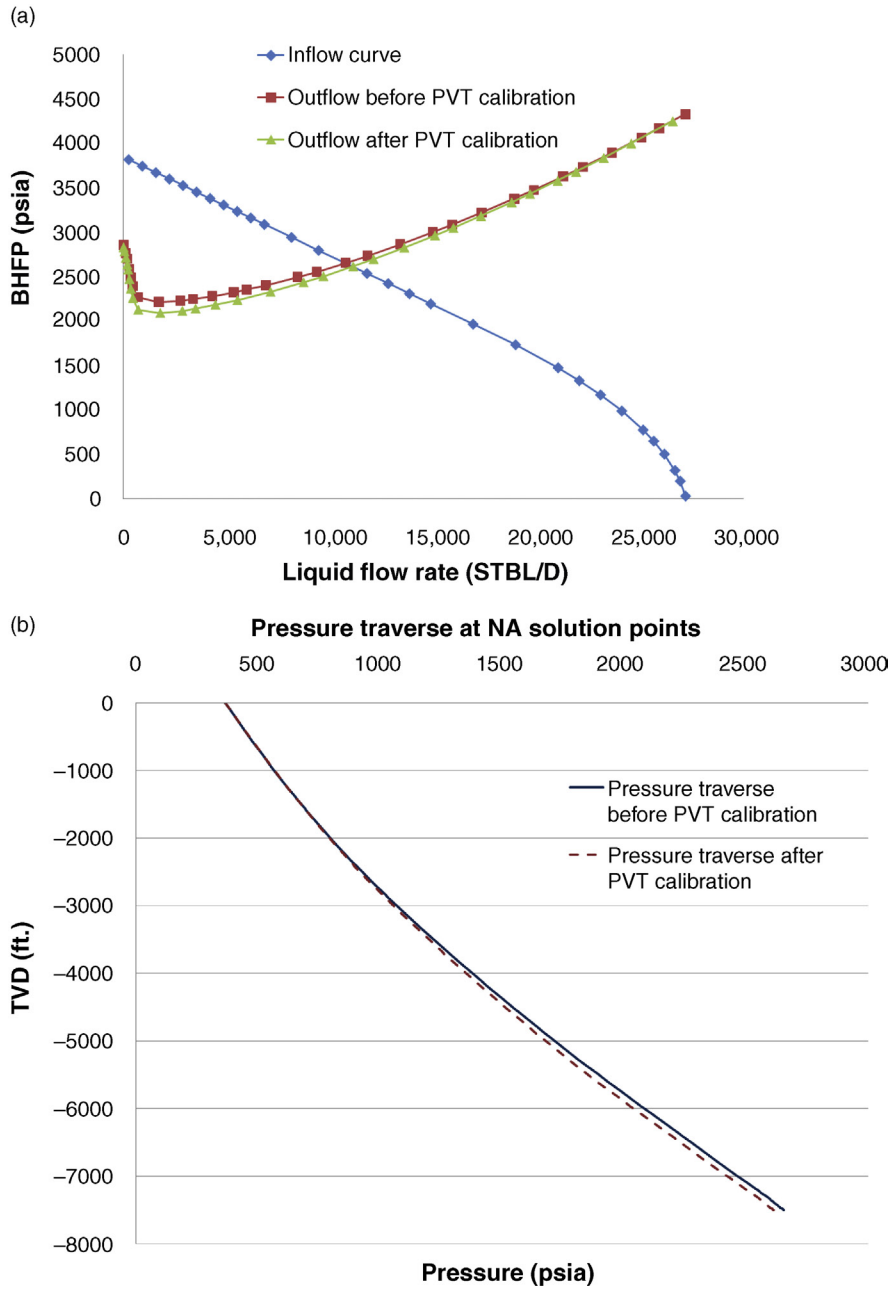
of 2.07 cP at 200°F and 44.25 cP at 60°F. The measured viscosities were significantly lower (1.6 cP at 200°F and 10.5 cP at 60°F). The live-oil viscosity was measured at 1.2 cP for 2010 psia and 200°F. Before calibrating the live-oil viscosity, the Chew and Connally correlation predicted a viscosity of 0.7985 cP at 2010 psia and 200°F (after the dead-oil viscosity was calibrated). Fig. 5.44 shows the impact of introducing this live-oil calibration point, as well as the dead-oil calibration points, on the viscosities of the oil at 60 and 200°F.

Gas viscosity plays a minor role in the calculation of the pressure along the production tubing string and it is usually not measured. Fig. 5.45 shows the viscosities before and after calibration for temperatures of 60 and 200°F. Before calibration, the correlation developed by Lee et al. predicted a gas viscosity of 0.011 cP at 613 psia and 60°F and 0.0132 cP at 613 psia and 200°F. The measured viscosity was equal to 0.012 at 613 psia and 60°F. Introducing this calibration point gives the results shown in Fig. 5.45.

A nodal analysis (performed before calibrating the PVT properties) gave, for a wellhead pressure of 350 psig, a liquid flow rate of 10,762.52 STB/D and a bottomhole flowing pressure of 2,654 psia. Bubbles began to appear at a depth of 5490 ft. TVD and the calculated wellhead temperature was 191°F. After PVT calibration, the calculated liquid flow rate was equal to 11,139.62 STB/D, which represents an increment in production of only 3.5%. The bottomhole flowing pressure was 2612.26 psia and gas began to appear at 5969 ft. TVD. This relatively low impact on the production of the well is due to the low production gas/oil ratio and the large value of the bottomhole flowing pressure in comparison to the bubble point pressure (both factors make bubbles appear at shallower depths), but this is not always the case and PVT calibration should always be done before any serious gas lift analysis is attempted. The low impact of the PVT calibration is appreciated in Fig. 5.46. The multiphase flow correlations used were the Hagedorn–Brown correlation for vertical flow and the Beggs–Brill correlation for horizontal flow.

Once the PVT properties have been calibrated, the data from the flowing pressure survey (Table 5.3) can be used to select the multiphase flow correlation that gives pressures closer to the ones measured during the survey. Additionally, most of the commercially available software are able to provide the means to tune the selected correlation to match the measured data. Optimization routines calculate the optimal values of parameters that are used to match the measured temperature and pressure data more accurately. These parameters are multipliers that can be used





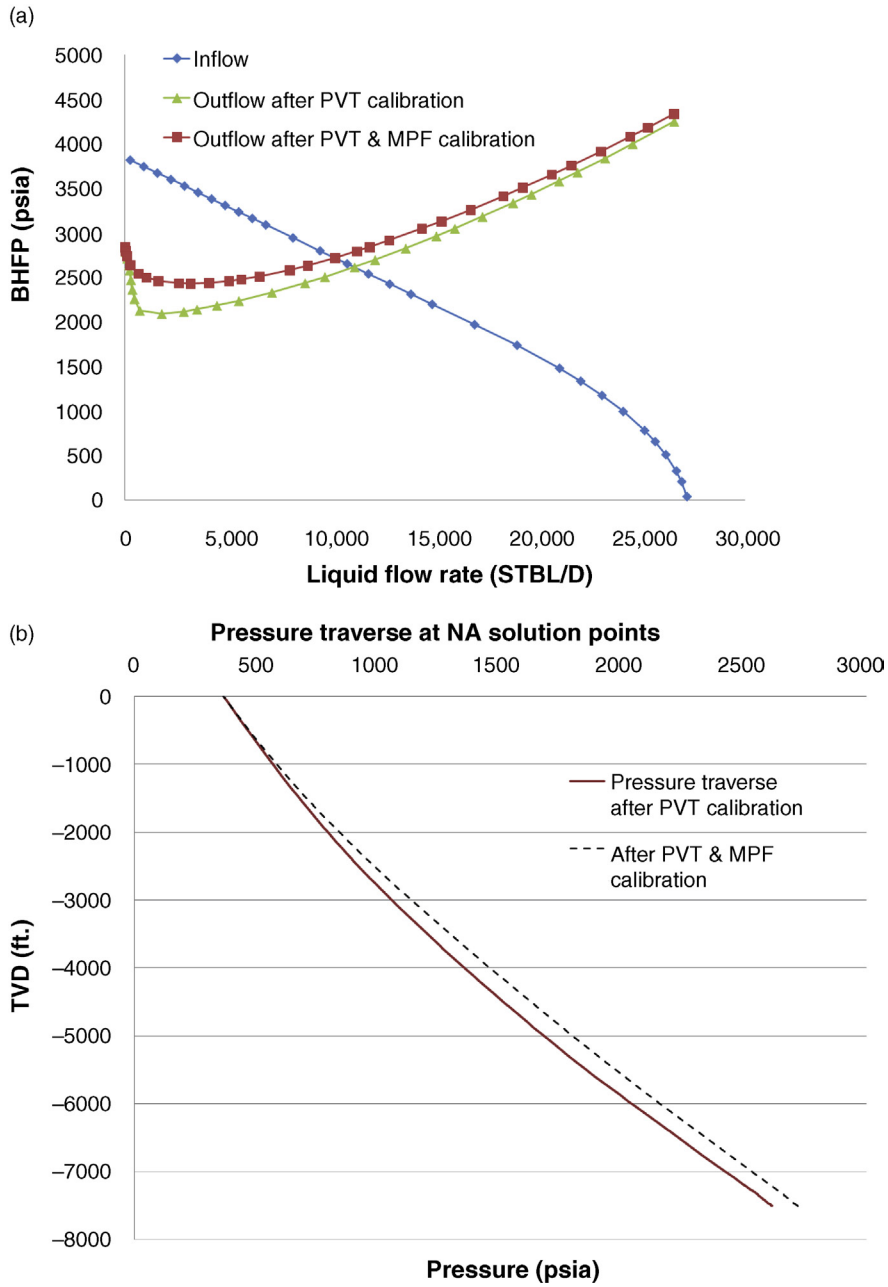
■ FIGURE 5.46 Impact of PVT calibration on the performance of the well.

to adjust the friction and holdup pressure gradient for the multiphase flow correlation and to adjust the overall heat transfer coefficient used in the model. In this case, the best correlation was found to be the Duns and Ros correlation and the software that was used to select this correlation tuned it with a friction factor multiplier equal to 0.95 and a holdup factor multiplier of 1.19 (factors below 0.8 or above 1.2 are indications of either inaccurate flowing gradient and/or well test data, or the PVT calibration has not been done correctly). A new nodal analysis was performed using the tuned Duns–Ros correlation for the vertical multiphase flow calculations. The calculated liquid flow rate was 10,181 STBL/D with a flowing bottomhole pressure of 2,718.76 psia. Gas bubbles began to appear at a depth of 5625 ft. TVD. Fig. 5.47 shows the output of the nodal analysis with two outflow curves: (1) outflow curve with only the PVT properties calibrated, and (2) outflow curve with both, the PVT and multiphase flow correlations, already calibrated.

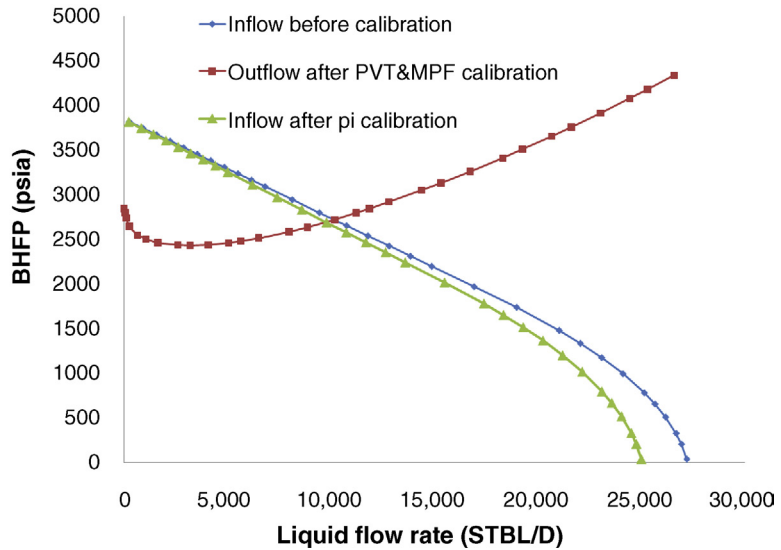
After the PVT and multiphase flow correlations have been calibrated, it is time to adjust the IPR curve. Either the static reservoir pressure or the productivity index can be adjusted to match the measured liquid flow rate and the bottomhole flowing pressure during the survey. In this particular example, the reservoir pressure is more accurate than the estimated productivity index, which is supposed to have a value between 8 and 10 (STB/D)/psi. The productivity index is then the parameter that needs to be adjusted. The adjusted value of the productivity index can be obtained manually by performing the nodal analysis operation for several values of the productivity index until the calculated liquid flow rate is equal to the liquid flow rate measured during the survey (the outlet pressure in the model should be equal to the one measured during the survey). The productivity index for which the calculated liquid flow rate matches the one measured during the well test corresponds to the “tuned” productivity index. Most of the commercially available software are able to perform this operation automatically.

Following the procedure described in the previous paragraph, the productivity index was found to be equal to 8.47 (STB/D)/psi, which is slightly lower than the first estimate given by reservoir simulations of 9 (STB/D)/psi. Fig. 5.48 shows the results of the nodal analysis performed with the old and new value of the productivity index. The liquid production and bottomhole flowing pressure went from 10,181 STB/D and 2,718 psia to 9,805 STB/D and 2,692 psia, respectively.

Once the well model is calibrated, the next thing to do is to study the impact of the water cut increase on the production of the well without gas injection. This can be done using two of the operations described in Section 5.1.3:



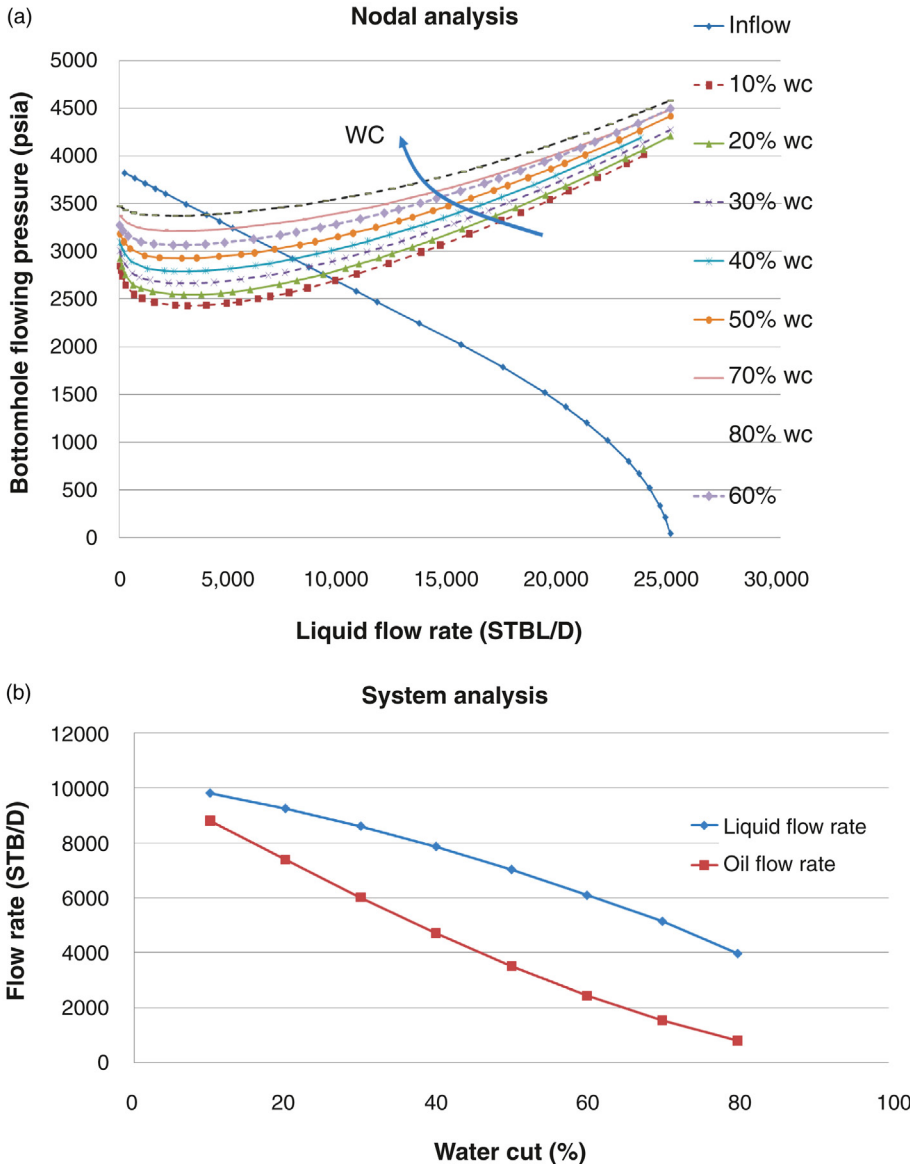
■ FIGURE 5.47 Impact of the calibration of the multiphase flow correlation on the performance of the well.



■ FIGURE 5.48 Impact of the calibration of the productivity index (PI) on the performance of the well.

nodal analysis and system analysis. Fig. 5.49 shows the results from these operations.

It can be seen in Fig. 5.49 that the planned oil production cannot be met if gas lift, or any other artificial lift method, is not implemented to boost the liquid production. The estimation of the injection gas flow rates and the point of injection depths that will be required to meet the production plan are carried out with the help of the calculation procedure that was presented in Section 5.1.3 with the results shown in Fig. 5.33. Some of the commercially available software for gas lift design can automatically calculate the results shown in Figs. 5.33 and 5.34 for as many injection gas flow rates and injection pressures as desired by the user. However, if such operation is not available, the designer would have to individually find the depths of the point of injection and liquid flow rates using the “constant-injection-gas-flow-rate-equilibrium-curve procedure” for several injection gas flow rates (as shown in Fig. 5.31). In any case, the liquid production and point of injection depth must be calculated for a range of injection gas flow rates and probable surface operating injection pressures. The injection gas flow rate is usually an unknown parameter and the user has to iterate with several values until the desired liquid flow rate is achieved. A range of injection gas flow rates from 0 to 10 MMscf/D was used for this particular case. The operating injection pressure (which is the wellhead injection pressure the well will have under normal operation), on the other hand, is roughly estimated from the available



■ FIGURE 5.49 Impact of the water cut on the performance of the well.

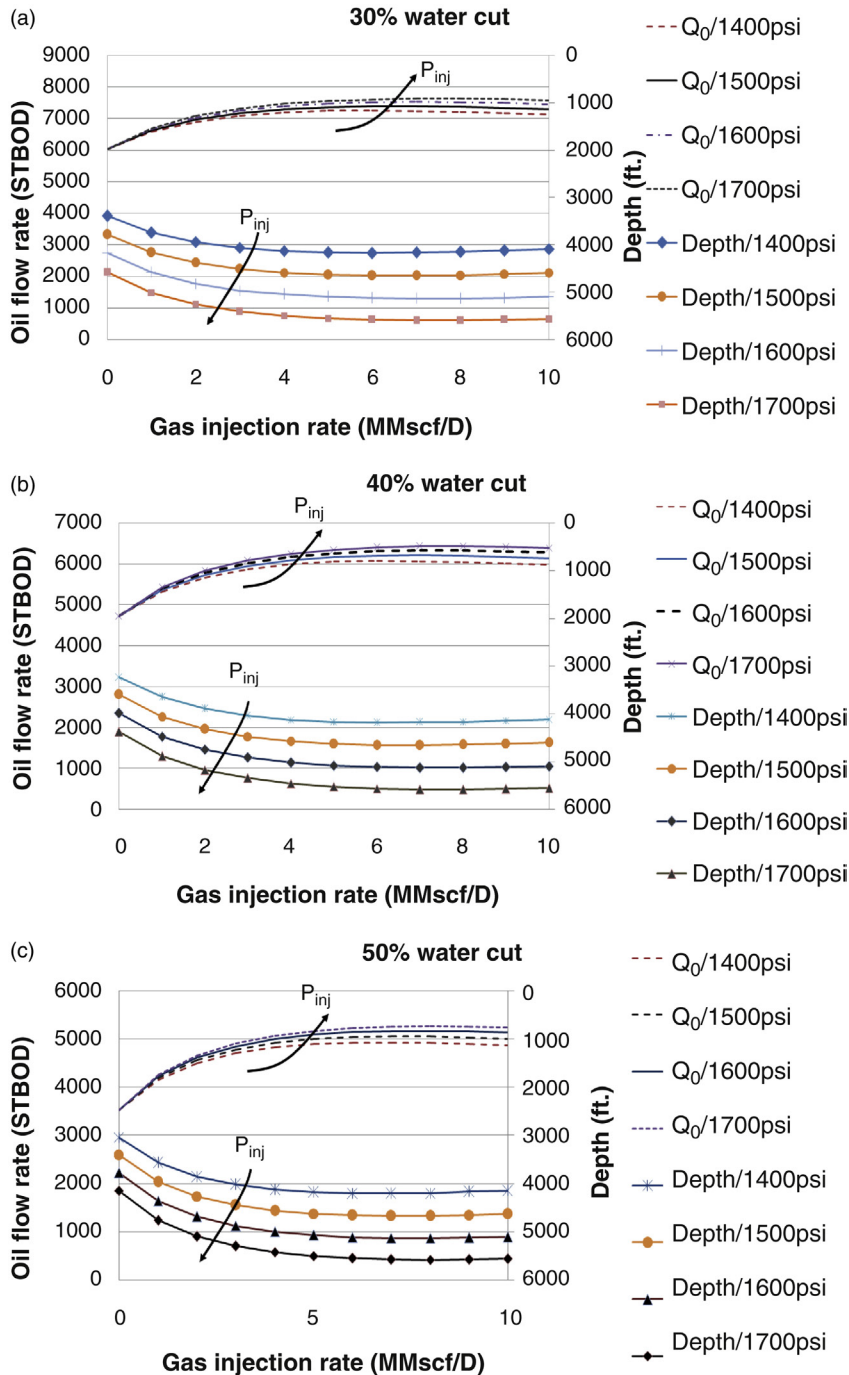
pressure at the injection manifold and the number of unloading valves that is required for similar wells in the field. In this case, the manifold pressure is equal to 1800 psig and the number of unloading valves might be equal to 3 or 4 valves, for which the sequential pressure drop per valve (explained in chapter: Design of Continuous Gas Lift Installations for several mandrel spacing

techniques) may have a value that could go from 30 to 80 psi if it is desired to use injection-pressure-operated gas lift valves. The usual nodal-analysis approach (for several injection gas flow rates) assuming that the point of injection is located at the maximum available depth (usually 60 ft. above the production packer) is not advisable in this case because the injection pressure might not be high enough to reach this depth for all cases.

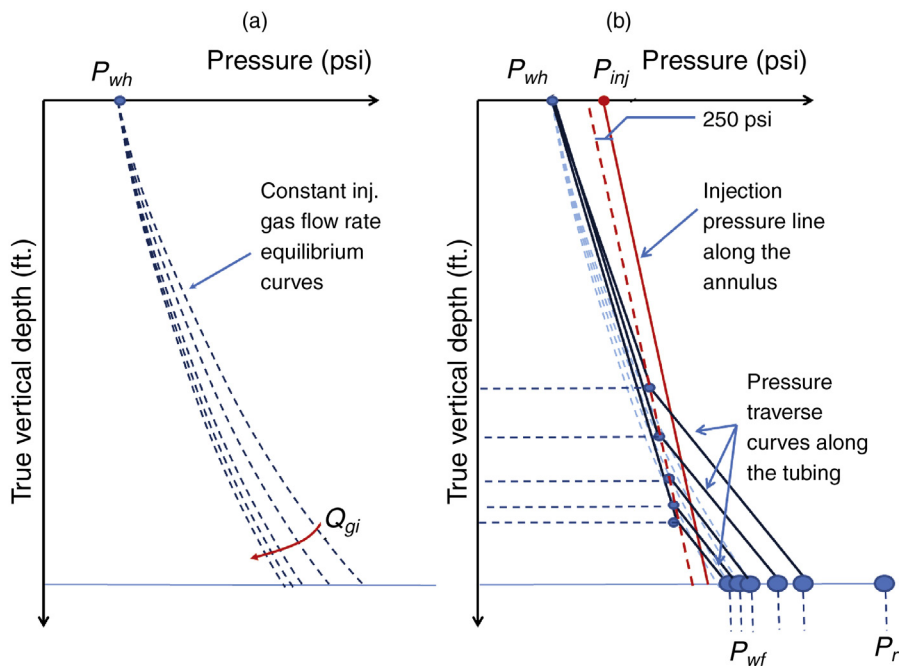
Calculations were carried out considering a constant wellhead production pressure of 350 psig and a pressure drop across the orifice valve (at the point of injection) equal to 250 psi, which is larger than the usual 100 psi that is normally considered for lower injection pressures (this is because the pressure drop across the orifice valve should not be smaller than 10% of the injection pressure at valve's depth to avoid instability problems). In this case, the injection pressure at 7000 ft. TVD, with a surface injection pressure of 1700 psig, will be equal to 2200 psig; thus, a 250 psi pressure drop across the orifice valve at the point of injection is a reasonable value to use. Fig. 5.50 shows the results for water cuts of the production liquids of 30, 40, and 50%, and surface injection pressures of 1400, 1500, 1600, and 1700 psig. The exact value of the final surface operating injection pressure will be determined from the gas lift design calculations. At this stage, only the possible depths of the points of injection and the required gas flow rates to meet the production plan are calculated.

Fig. 5.50 clearly shows that the effect of the injection pressure on the point of injection true vertical depth is very strong but, on the other hand, the point of injection depth has a rather small influence on the oil production. The explanation for this behavior is easily understood by analyzing the geometry of the constant-injection-gas-flow-rate equilibrium curves. For this example, these curves are almost vertical and closely packed, see Fig. 5.51a. As the gas flow rate  $Q_{gi}$  is increased, they become more closely spaced. This is the reason why, for a given injection pressure, the effect of the gas flow rate on the liquid production and the point of injection depth diminishes as the gas flow rate is increased, as shown in Fig. 5.51b. The geometry of the constant-injection-gas-flow-rate equilibrium curves also explains the reason why the injection pressure has a strong effect on the point of injection depth, but not on the liquid production. As can be appreciated in Fig. 5.52, for a given gas flow rate, as the injection pressure increases, the point of injection reaches greater depths but the downhole flowing pressure changes very little and, in consequence, the increase in the liquid flow rate is very small.

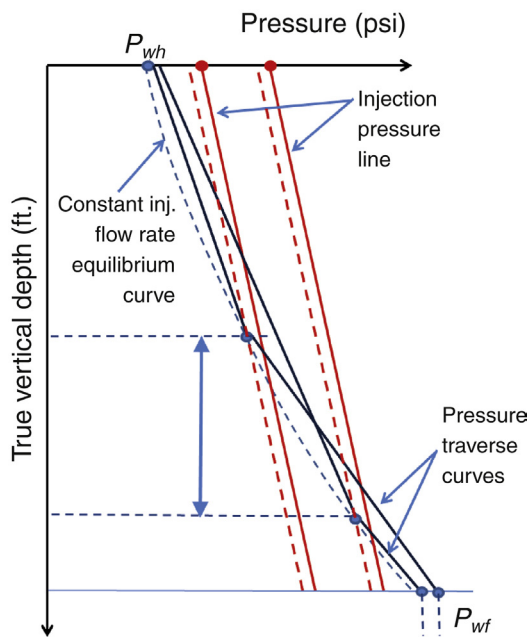
The opportunity in this example is then to use the available injection pressure to increase the sequential pressure drop per valve during the mandrel spacing calculations explained in chapter: Design of Continuous Gas Lift Installations (to come up with very stable gas lift designs that are at the same



■ FIGURE 5.50 Oil flow rates and point of injection depths for several wellhead injection pressures and water cut values.



■ FIGURE 5.51 (a) Equilibrium curves for different injection gas flow rates. (b) Pressure traverse curves for different injection gas flow rates and constant surface injection pressure  $P_{inj}$ .



■ FIGURE 5.52 Pressure traverse curves for two different surface injection pressures  $P_{inj}$  and the same injection gas flow rate.



**Table 5.4** Injection Gas Flow Rates and Depths of Points of Injection for the Targeted Oil Production at Each Water-Cut Value

30% Water Cut					
Injection Pressure (psig)	Injection $Q_{gi}$ (MMscf/D)	$Q_L$ (STBLD)	$Q_o$ (STBOD)	Depth (TVD ft.)	Injection $R_{go}$ (scf/STBO)
1,400	2.6	10,025.06	7,017.541	4,018.93	370.50
1,500	2.2	10,011.86	7,008.301	4,411.77	313.91
1,600	2	10,030.48	7,021.339	4,817.39	284.84
1,700	1.8	10,017.62	7,012.335	5,218.02	256.69
40% Water Cut					
Injection Pressure (psig)	Injection $Q_{gi}$ (MMscf/D)	$Q_L$ (STBLD)	$Q_o$ (STBOD)	Depth (TVD ft.)	Injection $R_{go}$ (scf/STBO)
1,400	4.2	10,002.01	6,001.203	4,137.96	699.85
1,500	3.4	10,014.71	6,008.825	4,522.52	565.83
1,600	2.9	10,000.12	6,000.072	4,900.83	483.32
1,700	2.6	10,000.31	6,000.186	5,294.25	433.31
50% Water Cut					
Injection Pressure (psig)	Injection $Q_{gi}$ (MMscf/D)	$Q_L$ (STBLD)	$Q_o$ (STBOD)	Depth (TVD ft.)	Injection $R_{go}$ (scf/STBO)
1,400	—	—	—	—	—
1,500	5.00	10,004.79	5,002.393	4,626.40	999.52
1,600	4.1	10,017.32	5,008.66	5,006.09	818.58
1,700	3.60	10,015.22	5,007.609	5,380.58	718.90

time very easy to trouble shoot with shallower and fewer gas lift mandrels) instead of using the available injection pressure to reach deeper points of injection (which will not provide a significant increase in the liquid production). Shallower points of injection do have the disadvantage of increasing the required injection gas/liquid ratio to obtain a given liquid flow rate, so a compromise must be established between more stable and easy to trouble shoot designs on one hand, and lower injection gas/liquid ratios on the other.

Table 5.4 shows the required injection gas flow rates ( $Q_{gi}$ ), the depths of the points of injection and the injection gas/oil ratios ( $R_{go}$ ) to meet the planned oil production ( $Q_o$ ) for each value of the water cut under this study. The planned oil production can be met for water cuts of up to 30% with an appropriate gas/oil ratio for all surface injection pressures considered in this study. For 40% water cut, the production plan can be met at injection gas/oil ratios less than 500 scf/STBO only if the operating injection pressure

is between 1500 and 1600 psig, which is something that might not be possible to accomplish if the required number of unloading gas lift valves to reach a point of injection depth of approximately 4900 ft. is such that the available manifold injection pressure minus all the sequential pressure drop per valve is less than this range of injection pressure. For 50% water cut, it will not be possible to produce 5000 STBO/D with a gas/oil ratio less than or equal to 500 scf/STBO for the range of injection pressures being considered (lower injection gas/oil ratios could be obtained for higher gas injection pressures, but the increase in gas compression and transportation costs might reduce the economic limit of the injection gas/oil ratio to values less than 500 scf/STBO). As stated in the previous paragraph, the required gas/oil ratio decreases for deeper points of injection depth. This increase in the lifting efficiency is due to the fact that if gas can be injected deeper, a greater length of the production string can be aerated and, in consequence, less gas is required to obtain the same bottomhole flowing pressure that would create the same drawdown to keep the liquid production at a constant value.

A final computational operation could be run to gain more information on the capability of the gas lift system to meet the required injection gas flow rates within the range of available surface injection pressures. The calculation procedure that gives the results shown in Fig. 5.25 is offered by some of the commercially available software. This is the “Gas Lift Rate versus Casing Head Pressure” operation that can be run for several injection orifice diameters, located at the approximate depth of the point of injection, to learn more about the expected surface injection pressures that will be required to inject the gas flow rates already found for each water cut. In this particular case, the available manifold pressure of 1800 psig can be used as the kickoff pressure because the injection manifold is very close to the well. The kickoff pressure is the required injection pressure to uncover the first (shallowest) valve during the unloading operation of the well. The operating injection pressure for the first valve, on the other hand, should be lower than the kickoff pressure to account for any fluctuation in the gas lift system’s pressure and to be able to provide a pressure differential that will make it possible to inject the required gas flow rate through the first valve to uncover the second valve. An operating pressure of 1750 psig is a reasonable value that will provide a 50 psi pressure differential to take care of any pressure fluctuation at the injection manifold (the operating surface injection pressure of a particular valve is the required surface injection pressure to uncover the next deeper valve while unloading the well from this particular valve). A sequential operating pressure drop per unloading valve of 30–50 psi will be required to make sure the unloading valves would be closed when gas is injected through the final point of injection (if injection-pressure-operated

unloading valves are used). Depending on the number of gas lift valves required to unload the well, the final operating injection pressure could be as high as 1730 psig (if only one unloading valve is needed) or as low as 1600 psig (if three unloading gas lift valves are needed).

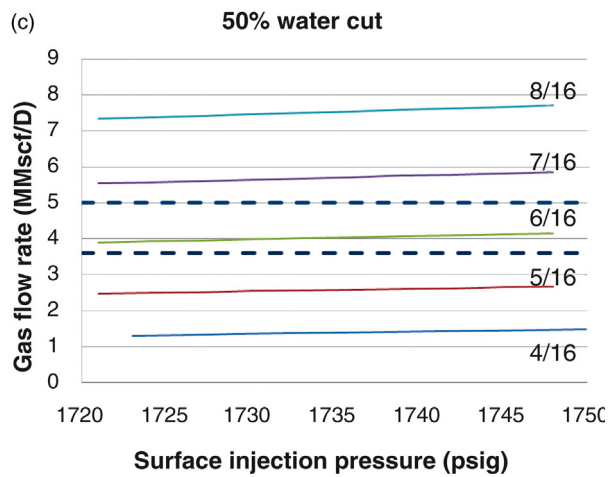
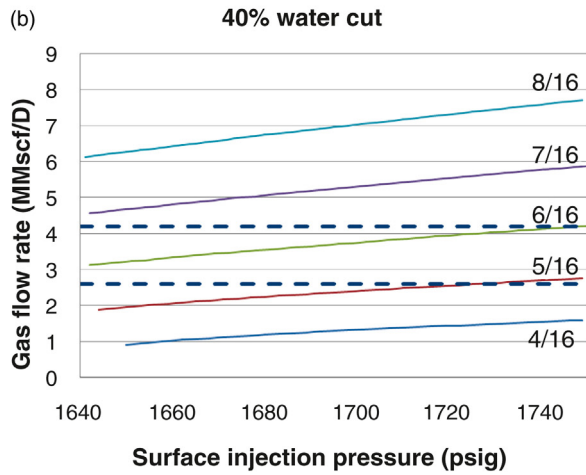
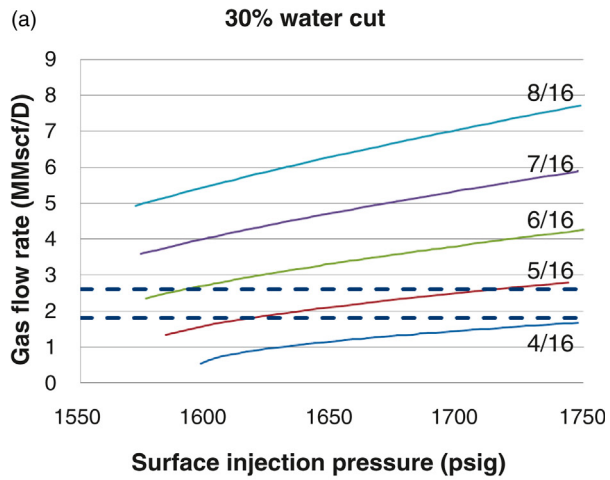
Fig. 5.53 shows the results obtained from running the “Gas Lift Rate versus Casing Head Pressure” operation for the approximate range of available surface injection pressures. The point of injection depth was assumed to be equal to 5200 ft. TVD and the wellhead production pressure was fixed at 350 psig. The results of this operation are based on nodal analysis: for a given reservoir static pressure, wellhead production pressure, injection orifice diameter, and surface gas injection pressure, there is one and only one possible liquid production flow rate and one gas injection flow rate. The required diameters of the injection orifices are as follows:

- A 5/16-in. orifice will be required to inject the gas flow rates found for a water cut of 30% (from 1.8 to 2.6 MMscf/D). A 6/16-in. orifice might be required if the injection pressure turns out (in the design) to be below 1620 psig.
- A 6/16-in. orifice will be required to inject the gas flow rates found for a water cut of 40% (from 2.6 to 4.2 MMscf/D). A 7/16-in. diameter might be required if the injection pressure turns out (in the design) to be below the range of injection pressures shown in the figure.
- A 6/16-in. orifice will be required to inject the gas flow rates found for a water cut of 50% (from 3.6 to 5 MMscf/D). A 7/16-in. orifice might be required if the injection pressure turns out (in the design) to be below the range of injection pressures shown in the figure.

Because this well can produce on natural flow, the unloading operation needs to be carried out even more carefully than it is required for usual gas lift wells, which are not capable of producing on natural flow. If a well can produce on natural flow, when it is opened to production for the first time after a gas lift valve change out, liquids from the annulus will flow into the tubing even before injecting gas into the casing. Very large liquid flow rates through the gas lift valves can be attained at this stage. Clearly, current API recommended practices for unloading this type of wells might not be applicable.

### 5.3.2 Example of preliminary calculations to design a gas lift well that cannot produce on natural flow

A well with the exact input data as the one presented in Section 5.3.1, but with a reservoir pressure of only 2000 psig, is to be designed on gas lift. A simple nodal analysis has shown that, with this reservoir pressure, the well

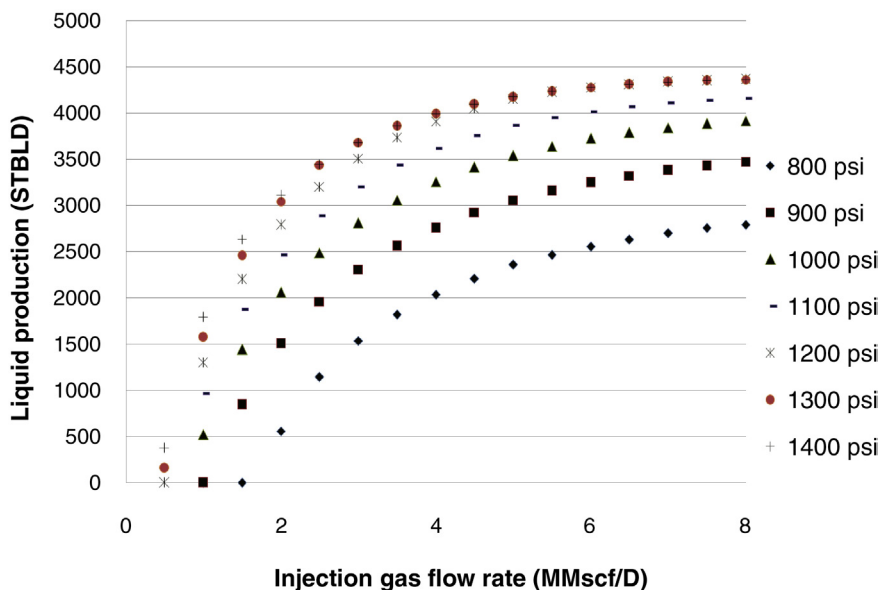


■ FIGURE 5.53 Gas lift rate versus casing head pressure.

cannot produce on natural flow. It is asked to find the possible depth of the point of injection and estimate the liquid production and the required injection gas flow rate if the water cut will remain constant at 10%.

As for the well in [Section 5.3.1](#), the estimation of the injection gas flow rate and the point of injection depth that will be required are carried out with the help of the calculation procedure that was presented in [Section 5.1.3](#) with the results shown in [Fig. 5.33](#). Some of the commercially available software for gas lift design can automatically calculate the results shown in [Figs. 5.33 and 5.34](#) for as many injection gas flow rates and injection pressures as desired by the user. However, if such operation is not available, the designer would have to individually find the depths of the point of injection and liquid flow rates using the “constant-injection-gas-flow-rate-equilibrium-curve procedure” for several injection gas flow rates (as shown in [Fig. 5.31](#)). In any case, the liquid production and point of injection depth must be calculated for a range of injection gas flow rates and probable surface operating injection pressures. The injection gas flow rate is usually an unknown parameter and the user has to iterate with several values until the desired liquid flow rate is achieved. A range of injection gas flow rates from 0 to 8 MMscf/D was used for this particular case. The operating injection pressure (which is the wellhead injection pressure the well will have under normal operation), on the other hand, is roughly estimated from the available pressure at the injection manifold and the number of unloading valves that is required for similar wells in the field. In this case, the manifold pressure is equal to 1800 psig and the number of unloading valves might be equal to 3 or 4 valves, for which the sequential pressure drop per valve (explained in chapter: Design of Continuous Gas Lift Installations for several mandrel spacing techniques) may have a value that could go from 30 to 80 psi if it is desired to use injection-pressure-operated gas lift valves. The usual nodal-analysis approach (for several injection gas flow rates as the outflow sensitivity variable) assuming that the point of injection is located at the maximum available depth (usually 60 ft. above the production packer) might not be advisable in this case because the injection pressure might not be high enough to reach this depth for all cases; but, as shown later for this well, the required injection pressures do not have to be as high as in the example in [Section 5.3.1](#) because the production pressures are not very large (due to the lower liquid flow rates) and a simple nodal-analysis approach could be taken if the operating pressure is greater than 1200 psi.

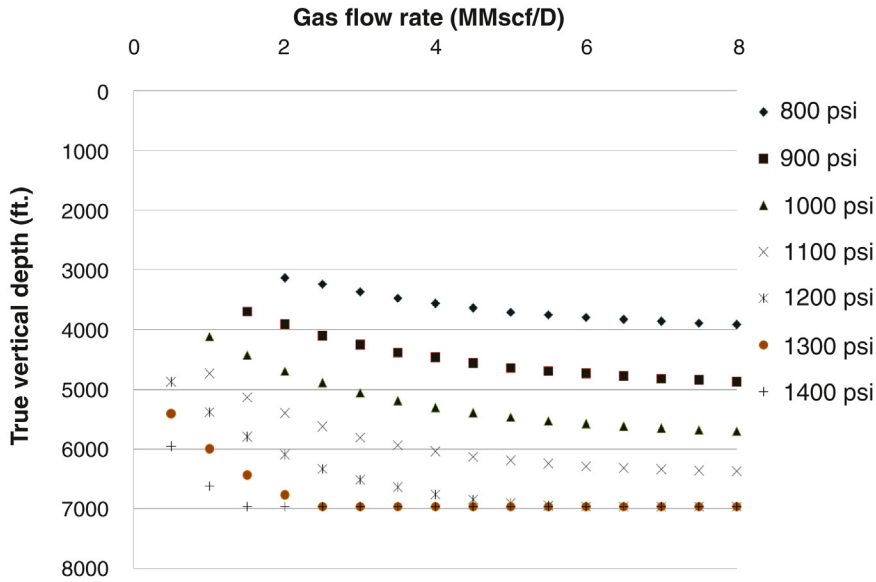
Calculations were carried out considering a constant wellhead production pressure of 350 psig and a pressure drop across the orifice valve (at the point of injection) equal to 250 psi, which is larger than the usual 100 psi that is normally considered for lower injection pressures (this is because the pressure drop across the orifice valve should not be smaller than 10%



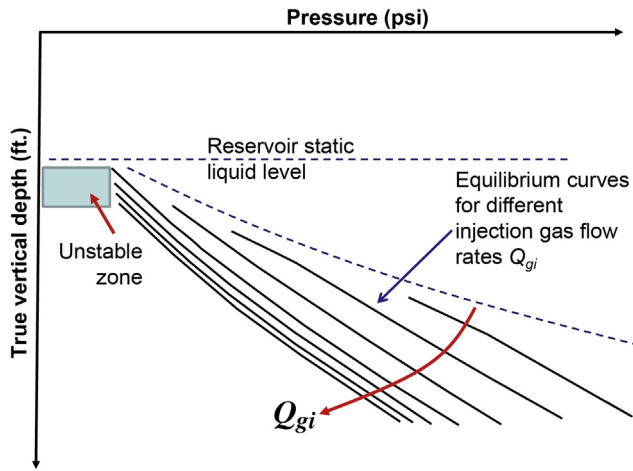
■ FIGURE 5.54 Liquid flow rates for several wellhead injection pressures.

of the injection pressure at valve's depth to avoid instability problems). Figs. 5.54 and 5.55 show the results for surface injection pressures from 800 to 1400 psi. The exact value of the final surface operating injection pressure will be determined from the gas lift design calculations. At this stage, only the possible depths of the points of injection and the required gas flow rates are calculated.

Figs. 5.54 and 5.55 clearly show that the effect of the injection pressure on the liquid production and point of injection true vertical depth is very strong. This was not the case for the example shown in Section 5.3.1. The explanation for this behavior is easily understood by analyzing the geometry of the constant-injection-gas-flow-rate equilibrium curves. For this example, these curves are not as vertical and closely packed as for the previous example. In this case, the equilibrium curves can only reach the depth of the reservoir static liquid level, see Fig. 5.56. As was the case for the previous example in Section 5.3.1, as the gas flow rate  $Q_{gi}$  is increased, the equilibrium curves become more closely spaced. This is the reason why, for a given injection pressure, the effect of the gas flow rate on the liquid production and the point of injection depth diminishes as the gas flow rate is increased, as shown in Fig. 5.57. The geometry of the constant-injection-gas-flow-rate equilibrium curves also explains the reason why the injection pressure has a strong effect on the point of injection depth

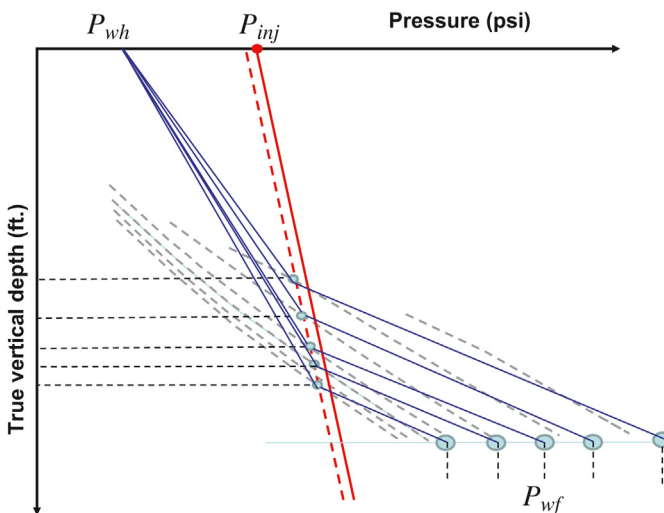


■ FIGURE 5.55 Injection point depths for several wellhead injection pressures.

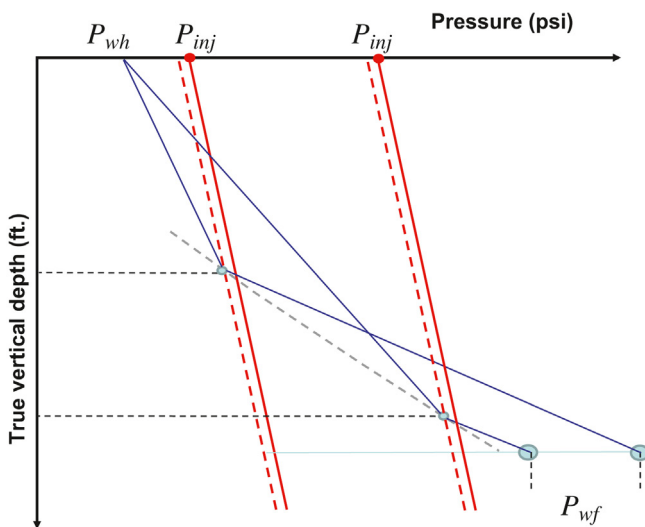


■ FIGURE 5.56 Equilibrium curves for different injection gas flow rates for a well that cannot produce on natural flow.

and the liquid production. As can be appreciated in Fig. 5.58, as the injection pressure increases (keeping the injection gas flow rate constant), the point of injection reaches greater depths and the downhole flowing pressure is reduced in a significant way, thus increasing the liquid production in an appreciable manner.



■ FIGURE 5.57 Pressure traverse curves for different injection gas flow rates and constant surface injection pressure  $P_{inj}$ .



■ FIGURE 5.58 Pressure traverse curves for two different surface injection pressures  $P_{inj}$  and the same injection gas flow rate.



Fig. 5.54 shows that, if the injection pressure is 800 psi, the maximum liquid flow rate is approximately equal to 2800 STBL/D for an injection gas flow rate of 8 MMscf/D. The injection gas/oil ratio will be (for a 10% water cut) equal to approximately 3200 scf/STBO, which is very high. This is a consequence of having the point of injection depth equal to only 4000 ft. TVD. Contrary to the case shown in Section 5.3.1 for a natural flowing well, in this case reaching a deeper point of injection can significantly improve the efficiency of the lifting method. This is achieved by increasing the injection pressure. For an injection pressure of 1400 psi, with an injection gas flow rate of 6 MMscf/D, the liquid production is equal to 4300 STBL/D and the injection gas/oil ratio is only 1550 scf/STBO. This injection gas/oil ratio is just below half the injection gas/oil ratio for an injection pressure of 800 psi. This is because the point of injection depth is equal to 7000 ft. TVD, for which greater drawdown can be achieved. The same depth, liquid production, and injection gas/oil ratio can also be achieved with 1200 psi of surface injection pressure. An economic analysis is needed to determine if it is feasible to increase the compressor's outlet pressure in order to be able to inject at 1200 psi instead of 800 psi because this decision depends on the number of wells that will benefit from higher injection pressures in a particular field and the additional cost of gas compression and transportation.

# Gas lift equipment

The required subsurface equipment and completions used in gas lift wells are presented in this chapter. A detailed explanation of important topics related to gas lift valves is given in the first part of the chapter: types of valves, their internal components, and working mechanisms. The different types of latches that are used to secure gas lift valves inside the gas lift mandrels where they are installed are also presented, followed by a description of the gas lift mandrels currently used in gas lift installations. The most common wireline tools that are used to perform the different wireline jobs in gas lift wells are presented and illustrated with the help of many figures. Finally, a detailed explanation is presented of the many types of well completions that can be used to produce a well on gas lift, such as: single completions, accumulation chambers, accumulators, dual completions, use of coiled tubing, and plunger-assisted gas lift installations. The advantages and disadvantages of these completions, as well as many practical recommendations regarding their installation and operation, are covered in detail.

## 6.1 GAS LIFT VALVES AND LATCHES

Several gas lift valves are commonly installed in a single well because it is necessary to locate the point of injection as deep as possible in the well and the use of just one valve is, most of the time, insufficient. The deeper the point of injection is, the lower the bottomhole flowing pressure becomes and a greater liquid production can be achieved. The available injection pressure is usually not high enough to unload the well to the deepest point of injection possible. This is the reason why the unloading process is performed at different stages, with several unloading valves located along the production tubing. At the beginning of the unloading operation, most of the unloading valves, if not all, are open and every time a deeper valve is uncovered (that is, the liquid level descends to the depth of the deeper valve due to the action of the injection gas), the upper valve closes and this process continues until the final point of injection is uncovered. In this way, the available surface injection pressure does not need to be very high to reach

the deepest possible point of injection and gas compression and distribution costs are reduced. The unloading process of gas lift wells is described at the beginning of chapter: Design of Continuous Gas Lift Installations.

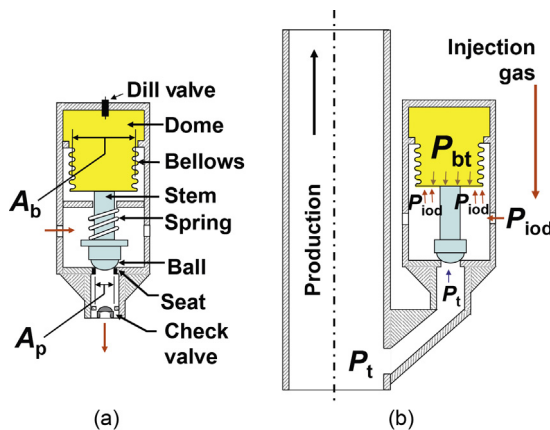
The valve with the simplest design will most of the time be the best selection for lifting gas lift wells. According to the type of gas lift mandrel used, gas lift valves can be categorized as follows:

- Wireline-retrievable valves. These valves are located inside the production tubing in the side pocket of gas lift mandrels and they can be installed or retrieved by wireline operations performed inside the tubing. They are usually 1 or 1.5 in. in outside diameter, although new 1.75-in., high-pressure valves, for high injection pressure applications, are entering the market. High-pressure valves are also available in 1.5-in. OD valves. In normal operation, wireline-retrievable valves acquire a temperature that lies between the injection gas temperature and the production temperature (the temperature of the gas–liquid mixture along the production tubing is known as the “production temperature”). For some types of valves, their temperatures in normal operation are closer to the production temperature while for others their temperatures are closer to the injection gas temperature, see Section 9.2.4.
- Tubing-retrievable valves, also called conventional valves. It is necessary to pull the tubing string out of the well to retrieve these valves. They usually come in sizes of  $\frac{5}{8}$ , 1, or 1.5 in. in diameter. The 1.5-in. diameter valves are installed in conventional mandrels in which the valves are outside the tubing and their temperatures are equal to the injection gas temperature. The 1-in. valves can also be installed in mandrels like the ones used for 1.5-in. valves, but they can also be installed inside the tubing in mandrels specially designed for macaroni-type tubing or in mandrels for packoff completions. Macaroni tubing and packoff completions are explained in [Section 6.4](#). The  $\frac{5}{8}$ -in. diameter valves are only installed in macaroni or packoff mandrels. In packoff installations, there might be either an unwanted hole in the tubing or the tubing was punched on purpose at a given depth and then a smaller diameter tubing section (of length usually not greater than 30 ft.), with a special type of gas lift mandrel and packers at each end, is installed in such a way that the punched (or unwanted) tubing-annulus communication is isolated and the injection gas from the annulus is forced to pass through the gas lift valve installed in the special mandrel.
- Special valves for coiled tubing completion. These valves are most of the time installed in concentric mandrels inside the coiled tubing and are usually small in size. There are special mandrels used with coiled

tubing in which wireline-retrievable valves can be installed, but they are usually available for coiled tubing nominal diameters of 2 in. or greater.

The valves that are used in continuous gas lift are called “single-element valves” because they have only one moving component. A different type of valve, called “pilot valve” has been developed for intermittent gas lift. Only single-element valves are explained in this chapter. With a few exceptions, single-element valves are not recommended for intermittent gas lift. Pilot valves are more complex and the way they operate (and fail) is explained in chapter: Design of Intermittent Gas Lift Installations.

According to the forces that try to open the valve, gas lift valves (single element or pilot valves) are classified as injection-pressure-operated (IPO) valves or production-pressure-operated (PPO) valves. The injection pressure is the pressure of the injection gas at valve’s depth, while the production pressure is the pressure downstream of the valve, also at valve’s depth. For both types of valves, the production and injection pressure try to open the valve, but for PPO valves the effect of the production pressure is greater because the production pressure acts on a greater area, while the opposite is true for IPO valves. Figs. 6.1 and 6.3 show, respectively, schematic views of single-element IPO and PPO valves and even though they are represented here as tubing-retrievable valves, their internal components are basically the same as the wireline-retrievable ones. Fig. 6.1a shows a schematic view of an IPO valve. The dome is usually charged with nitrogen at a pressure that is determined during the design of the gas lift installation. Nitrogen is injected into the dome through a dill valve, which is protected by a tail plug that is



■ FIGURE 6.1 IPO valve.

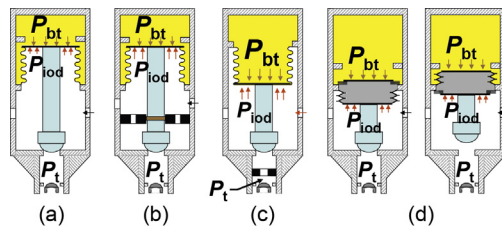
shown in a more realistic way in Fig. 6.4 later in the chapter. The bellows is a metallic component that can expand or contract in response to changes in its internal and external pressures. It is usually filled with a viscous damping fluid that protects the bellows from sudden changes in pressure. A very small-diameter wire is usually wrapped around two or three convolutions of the bellows located at each end to protect the integrity of the bellows. Inside the bellows, there are internal components with passageways through which the damping fluid must flow every time the bellows expands or contracts (not shown in the figure). For protection, these internal components also provide a guide for the bellows movement (so that it would only move up and down and not sideways) and a stop (that would prevent the bellows from moving once it has contracted to a minimum allowed length).

The upper part of the stem is connected to the lower end of the bellows assembly and the lower part of the stem is connected to the ball of the valve. When the valve is closed, the ball sits on the seat of the valve and does not allow gas injection into the well. The ball and the seat of the valve are manufactured from different types of materials, depending on the erosion resistance that is required of them. The commercially available flow area of the seat might slightly change depending on the type of material used for its construction. The spring provides an additional force that, together with the nitrogen pressure, tries to close the valve. The spring is used only to add this additional force (smaller than the one provided by the nitrogen) to protect the bellows. Valve manufacturing companies establish the equivalent calibration pressure of the spring, which is usually a constant for a given valve model. The great majority of nitrogen-charged IPO valves in use today do not have this type of spring installed. On the other hand, there are IPO valves for which the only closing force comes from the spring and the dome is sealed at atmospheric pressure; however, valves of this type are rarely used for the reasons that are explained later in this chapter.

Finally, an integral check valve is installed inside the gas lift valve to prevent the fluids from flowing from the tubing to the annulus if the valve is opened and the production pressure is greater than the injection pressure. Due to the small volume of the space between the check valve and the main seat of the gas lift valve right above (besides the fact that most check valves do not provide a totally hermetic seal) the following can be established. As much as it is true that the integral check valve prevents the fluids from entering the annulus, this check valve does allow the production pressure to be transmitted to the space just above it so that the ball is subjected to the production pressure (which is the tubing pressure in case of Fig. 6.1) if the valve is closed. An IPO gas lift valve then responds to both, the production and the injection pressure, but the injection pressure ( $P_{\text{iod}}$  in Fig. 6.1) is

exerted over a larger area (bellows area minus the seat area) while the production pressure ( $P_t$ ) only acts on the seat area. This is why they are called “IPO valves.” Recently developed integral check valves can withstand pressure differentials of up to 10,000 psi, making it an effective barrier when it is absolutely necessary to keep the production fluids from entering the casing annulus. Even if the check valve provides a tight hermetic seal that would not allow any communication from the tubing to the interior of the gas lift valve, the value of  $P_t$  is still acting on the ball of the valve. This is because the ball-seat contact always allows a small leak of gas from the casing–tubing annulus into the tubing and, as soon as the pressure of the volume located between the ball and the check valve gets to be higher than  $P_t$ , gas will pass through the check valve toward the tubing, keeping in this way the pressure on the ball constant at  $P_t$  for as long as the valve remains closed and the pressure in the annulus is greater than the pressure in the tubing at valve’s depth. Check valves that offer a tight hermetic seal are relatively new and most check valves used today in the industry do allow pressure transmission from the tubing into the volume located between the ball and the seat.

Fig. 6.1b shows a nitrogen-charged IPO valve without a spring, together with the pressures that try to open or close the valve. The annular gas injection pressure,  $P_{iod}$ , acts on an area equal to the bellows area,  $A_b$ , minus the port area,  $A_p$ , and it tries to open the valve. On the other hand, the production or tubing pressure,  $P_t$ , acts on the seat or port area  $A_p$  and also tries to open the valve, but it has a reduced effect because the area of the seat is smaller and usually the production pressure is also smaller than the injection pressure. The nitrogen pressure inside the dome,  $P_{bt}$ , acts on the entire bellows area and tries to close the valve. When the forces trying to open the valve are greater than those that try to close it, the valve opens and gas can be injected into the tubing if the injection pressure is greater than the production pressure. Some IPO valves have their bellows installed as shown in Fig. 6.2a, b, with the purpose of being able to withstand greater calibration pressures because the dome pressure acts on the outside surface of the bellows (not



■ FIGURE 6.2 Different available configurations of IPO valves.

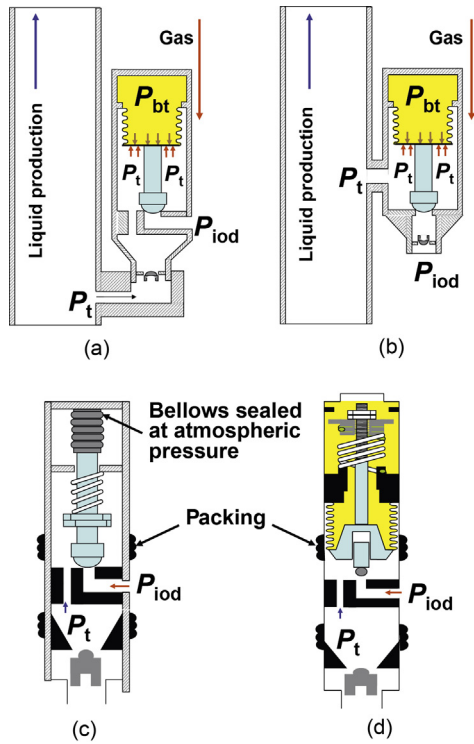
on the inside) and the bellows is expanded, and not compressed, when the valve opens. This bellows configuration also allows the valve to be fully open with a lower pressure increase above the valve's opening pressure, which is important during the unloading process because the required injection gas flow rate can be easily attained.

Chokes can be installed upstream or downstream of the seat of the valve as shown in Fig. 6.2b, c, respectively. Chokes upstream of the seat reduce the valve spread (defined as the difference between the valve's opening and closing pressures) to a minimum value. This effect and the advantages it brings are explained in chapter: Design of Continuous Gas Lift Installations. Chokes downstream of the seat are installed so that the main pressure drop across the valve takes place through the choke and not through the seat. This has two advantages: it protects the seat from being eroded and helps stabilize the operation of the valve as explained in Section 8.3.

The bellows of most commercially available gas lift valves can withstand test-rack calibration pressures from 1800 to 2200 psi; but there are gas lift valves manufactured for high-pressure applications (with traditional bellows technology) that can withstand greater calibration pressures. Additionally, there are new gas lift valves in the market that do not use the traditional metallic bellows but a special arrangement of metallic rings (welded together at their inner and outer edges) that encapsulates a liquid inside a fixed total volume that can change in shape (as shown in Fig. 6.2d for a closed and opened valve). These valves can be used for very high test-rack calibration pressures. Nitrogen, at a pressure equal to  $P_{bt}$ , is applied inside the dome and not inside of the encapsulated liquid volume (which is sealed).

Fig. 6.3 shows different possible configurations of PPO valves.

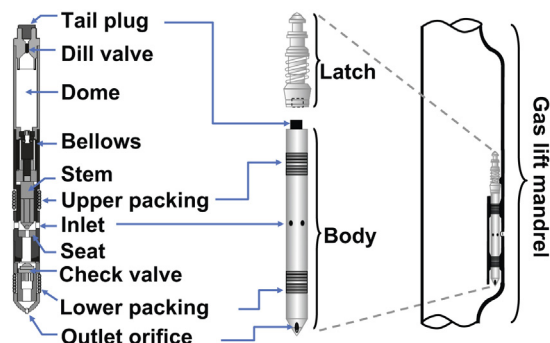
The internal configuration shown in Fig. 6.3a is used for conventional and wireline-retrievable valves. The configuration shown in Fig. 6.3b is only used for conventional valves. In both cases (a and b), the production pressure,  $P_t$ , is applied over the bellows area minus the port area,  $A_b - A_p$ , while the gas injection pressure,  $P_{iod}$ , is applied over the port area  $A_p$ . Both of these pressures try to open the valve while the nitrogen pressure in the dome,  $P_{bt}$ , tries to close it. When the forces that try to open the valve are greater than the ones trying to close it, the valve opens and gas is injected from the annulus into the tubing if the injection pressure is greater than the production pressure. Usually, PPO valves are spring loaded and the bellows is sealed at atmospheric pressure as shown in Fig. 6.3c, d, which are wireline-retrievable valves. The configuration shown in Fig. 6.3c is the most frequently one used. Gas lift wells with PPO valves are very difficult to troubleshoot because it is difficult to accurately calculate the production pressure, which



■ FIGURE 6.3 PPO valves.

is not the case for the much easier calculation of the gas injection pressure at depth. An additional disadvantage PPO valves with the configurations in Fig. 6.3a, c, d have is that the seats for these valves are very restrictive (they have smaller discharge coefficients). These seats are called crossover seats: the gas enters the stem-tip area through a lateral orifice and then it is directed downward through five or six parallel holes that direct the gas flow toward the nose of the valve (these holes have a combined flow area that is larger than the flow area of the lateral orifice). Recently developed crossover seats offer a flow area larger than the one provided by the five or six parallel holes. Despite their disadvantages, PPO valves are recommended in places where the injection pressure is very low or it is constantly fluctuating. PPO valves are also recommended for dual wells to minimize the role the gas injection pressure plays on the opening and closing of the valves. Some experts do not recommend the use of PPO gas lift valves in wells that produce sand because the valve can get completely sand packed around the bellows and bellows adapter.

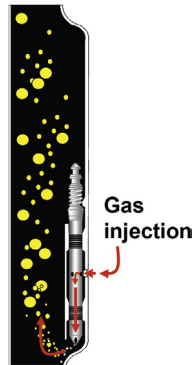




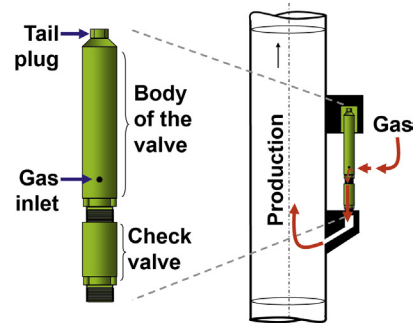
■ FIGURE 6.4 Internal components of a wireline retrievable, IPO, gas lift valve.

Fig. 6.4 shows a more realistic view of the internal components of a wireline retrievable, IPO, gas lift valve. It also shows how the gas lift valve is installed and secured inside the pocket of a gas lift mandrel. Different geometries of gas lift mandrels are given in the next section.

The tail plug shown in Fig. 6.4 is very important. If this plug fails and the outside pressure surrounding the valve is greater than the dome pressure, the dome will be pressurized because the dill valve opens whenever the outside pressure is greater than the dome's inside pressure. A copper washer below the plug and an O-ring (or two) surrounding the plug are used to seal the tail plug. The latch that secures the gas lift valve to the mandrel is installed above the tail plug. The injection pressure inside the valve could unseat the valve off the mandrel's pocket if a latch is not used. There are several types of latches that correspond to the type of gas lift mandrel being used. The different ways latches secure gas lift valves inside the pocket are explained at the end of this section. The gas lift valve upper and lower packing shown in Fig. 6.4 force the injection gas to pass from the mandrel's ports to the inside of the gas lift valve only. The packing's outside diameter is such that it offers a perfect seal against the pocket's polished bore. The packings are made out of nonmetallic materials of different compositions depending on the type of application: "common elastomeric materials" for normal operations or "special materials" for acid job environments or hot applications for wells that have been subjected to steam injection. Fig. 6.5 shows the way the gas is injected from the annulus, through the gas lift valve, and into the tubing. The injection gas usually enters the tubing through the nose of the valve in a direction opposite to the direction of the liquid flow. This fact does not affect the production of the well because the usual in situ gas flow rates and the density of the injection gas are not sufficiently high to slowdown the liquids from the formation.



■ FIGURE 6.5 Gas flow from the injection annulus, through the gas lift valve, and into the production tubing.



■ FIGURE 6.6 Conventional valve installed in a conventional mandrel.

Tubing-retrievable valves are called “conventional valves” because they were the only ones used before the development of wireline-retrievable valves. The components of a conventional valve (as they actually look like) and the way they are installed in conventional mandrels are shown in Fig. 6.6. Most conventional mandrels are a lot cheaper than side-pocket mandrels. Different types of mandrels for tubing-retrievable valves are shown in the next section. As explained in Section 6.2, conventional valves are still in used around the world.

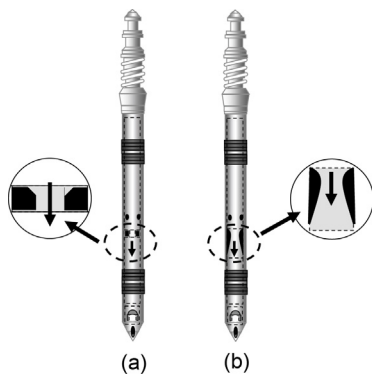
The size of a gas lift valve is an important issue. The 1.5-in. diameter valves are highly recommended because they offer the following advantages:

- They allow higher gas injection flow rates.
- They last longer without failures.
- They have a wider range of area ratios. The area ratio is defined as the area of the seat divided by the area of the bellows. The role the area ratio of the valve plays on the opening and closing pressures of gas lift valves and the benefits of having area ratios from very small to very large values are explained in chapter: Gas Lift Valve Mechanics.
- For continuous gas lift operations, it is better to have smaller values of the spread of the valve (the spread is defined earlier as the difference of the opening pressure minus the closing pressure of the valve). This avoids an operational instability known as “valve interference” in which more than one valve are opened at the same time. The smaller the area ratio of the valve is, the smaller its spread becomes. The 1.5-in. diameter valves have area ratios that are smaller than the ones for 1-in. valves of the same seat diameter. This is why 1.5-in. diameter valves

tend to have less valve interference problems than 1-in. valves do. Valve interference is explained in chapters: Design of Continuous Gas Lift Installations; Continuous Gas Lift Troubleshooting. Additionally, if the area ratio is very small, the effect of the production pressure on the opening of the valve is reduced: this makes troubleshooting analysis simpler because the errors made in the calculation of the production pressure (which is difficult to accurately calculate) do not have a great impact on the prediction of the opening pressure of the valve.

- Once a 1.5-in. diameter valve is opened, the increment in the injection pressure needed to completely open the valve is smaller than the one required for 1-in. diameter valves. It is very important to be able to open the valve as wide as possible so that the ball would not interfere with the injection gas flow. The increase in injection pressure needed to move the ball a given length is proportional to what is called the “bellows load rate,” which is the ratio of the injection pressure increase to the stem traveled distance this pressure increment causes under quasistatic conditions (very small gas flow rates). If the bellows load rate is small, the increase in pressure needed to completely open the valve is reduced (nitrogen-charged, 1.5-in. diameter valves have smaller bellows load rates because the volume the nitrogen occupies in the dome is larger).

One minor disadvantage that 1.5-in. OD valves have is that they are slightly more difficult to pull out of side-pocket mandrels using wireline tools because higher loads need to be imposed on these tools. Wireline service companies need to maintain kickover, running and pulling tools in excellent conditions to avoid operational problems while retrieving or installing 1.5-in. valves. Installing 1.5-in. OD valves can also be more difficult in deviated production tubing strings because the weight of the valve might not allow it to align with the side-pocket entrance.



■ FIGURE 6.7 Orifice valves.

The great majority of wells on gas lift have what is called “orifice valves” installed at the operating point of injection (the deepest possible point of injection in the well) while “calibrated valves” (as the ones shown so far) are used as the unloading valves. Orifice valves are shown in Fig. 6.7. An orifice valve looks identical to a calibrated gas lift valve on the outside; but, only the port and the integral check valve are installed in the inside of orifice valves and, in consequence, they are always “open.” The seats are usually the same as those found in calibrated valves, but there are orifice valves that have a more streamlined seat design, like the one shown in Fig. 6.7b. As explained in chapter: Gas Flow Through Gas Lift Valves, this special type of seat design helps stabilize the production of the well.

The advantages of having an orifice valve installed at the operating point of injection are:

- The injection pressure can drop to low values without causing the valve to close (simply because they are always opened).
- They offer less resistance to the injection gas flow because they do not have the stem and the ball of a calibrated valve interfering with the flow.
- The gas flow rate is calculated with very simple equations instead of the complex models that are needed for calibrated gas lift valves.
- They are less expensive.

However, there are situations in which it is better to have calibrated valves installed at the operating point of injection. For example, if the compressor plant trips and the reservoir pressure is low, the injection gas pressure in the annulus will drop to very low values if an orifice is installed at the operating point of injection. The operating injection pressure will have to be restored once the compressor is started again. If the well is not immediately shut in, the gas lost from the annulus goes into the separator and to the gas gathering lines that go to the inlet of the compressor. The compressor suction pressure is usually a fixed value that cannot be surpassed, so it might be necessary to vent part of the gas coming from the wells after the compressor has tripped, unless the gas can be directed to a low-pressure sales line. If a calibrated valve is installed at the operating point of injection, once the compressor is down the injection pressure in the annulus of the well only drops to the valve's closing pressure and it stays at that value until the compressor is restarted.

Calibrated valves installed at the point of injection also make it easier to troubleshoot the well. If an IPO valve at the operating point of injection, or any IPO unloading valve, is damaged, it is easily detected by shutting off the gas injection to the well. If the injection pressure decreases below the injection closing pressure of the operating valve, one of the valves installed in the well must have failed and it is open.

An additional advantage calibrated valves have is that they tend to stabilize the operation of the well if the instability problem is not too severe.

Usually, the surface injection pressure downstream of the surface gas flow rate control valve (or choke) is an indication of the production pressure at the depth of the gas lift orifice valve (as indicated earlier, the production pressure is the pressure downstream of the valve). If this production pressure is much lower than its expected design value, the surface injection pressure might also be very low and, due to the high pressure drop, hydrate

formation across the surface injection control valve (or choke) could interrupt the injection gas flow into the casing–tubing annulus. This problem is easily solved by installing a calibrated valve at the point of injection to keep a high surface injection pressure, regardless of the value of the production pressure at depth.

Orifices and seats should be built to resist abrasion. Cut seats are very common in gas lift wells. Solid particles carried with the injection gas, or with the liquids during the unloading of the well, can cut the seat of the valve. Some quantity of gas, usually very small, leaks through a gas lift valve with an eroded or cut seat. This is easily verified by a downhole temperature survey; a slight decrease in temperature is usually observed at unloading valves. These gas leaks are usually not very important, but sometimes they considerably reduce the lifting efficiency. For normal operations, seats are made out of standard monel and for high abrasion resistance they are made out of solid carbide. For some valve models, the flow area of the seat slightly changes with the type of material used in its construction.

Up to this point, it has been assumed that the gas is injected down the annulus and the liquids are produced up the tubing. In some cases, it is beneficial to inject the gas down the production tubing and produce the liquids up the annulus. This is recommended in wells with a very high liquid production flow rate for which the pressure drop in the tubing would be too large. When the liquids are produced up the annulus, it should be checked if corrosive elements such as  $\text{CO}_2$  or  $\text{H}_2\text{S}$  in presence of water, or any other corrosive agent that can damage the casing, are not present. There are special mandrels (for wireline-retrievable valves) that are specifically designed for annular liquid production, although normal mandrels can also be used for that purpose. All these possibilities explain why there are many available internal configurations of gas lift valves: to adapt their operations to the type of mandrel and flow (annular or tubing production) in which the well is producing. These valve configurations are shown in the next section after the different types of mandrels are described, see [Figs. 6.23 and 6.24](#).

Sometimes it is necessary to isolate the tubing–annulus communication provided by a gas lift mandrel. This happens when an unloading valve is no longer needed because the production pressure has declined and the mandrel can be skipped (during the unloading operation) to reach deeper in the well. In those situations, a solid metallic bar, shaped like a gas lift valve (with upper and lower packings and latch) is simply installed in the side pocket of the unloading mandrel that is no longer needed. They are called “dummy valves.” If a dummy valve needs to be installed in a mandrel, between two production packers, that is used to communicate an oil, gas, or water

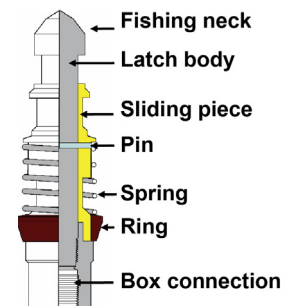
producing zone with the tubing, a special dummy valve, called an “equalizing dummy” should be installed in the mandrel. If an ordinary dummy valve is installed, the pressure in the annulus might be higher than the pressure in the tubing and the wireline tools might be blown up the tubing once the latch of the dummy valve has been released. With equalizing dummies, both pressures are equalized first by pulling out a prong installed inside the dummy valve and establish in this way a tubing-annulus communication before the latch is released. Most equalizing dummies require two wireline trips, one to equalize the pressures and the other to pull the valve out of the well; however, some models allow both operations in just one wireline trip.

There are situations in which gas lift mandrels with dummy valves are installed in new wells that can produce on natural flow. When the water cut increases or the reservoir pressure decreases and the well can no longer produce on natural flow, these dummy valves can then be replaced by calibrated valves to be able to produce the well on gas lift. There are new products that eliminate the need of using dummy valves in new wells: instead of using dummy valves, calibrated valves can be run in the new well at the beginning of its operation, but these valves are intentionally plugged with a special sealing material that can be dissolved by injecting the appropriate chemicals once the well needs to be operated on gas lift. There is also a type of dummy valve that can be transformed into an orifice valve by pulling out a prong installed inside the dummy valve (without unlatching it), leaving a hollow valve with a seat of a given diameter that can then be used as an orifice valve at the operating point of injection.

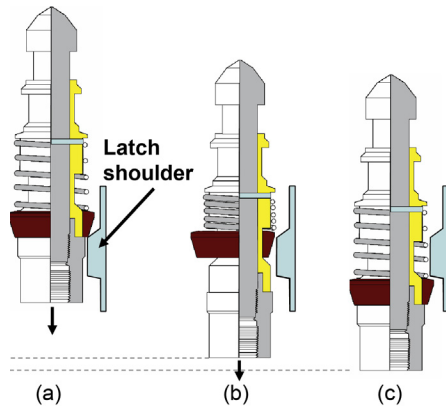
In places where organic or inorganic depositions can accumulate inside the production tubing, mandrels and gas lift valves can be ordered with special coating materials that prevent the accumulation of such depositions in critical places like the latch.

As shown in Fig. 6.4, the latch is installed in the upper part of a wireline-retrievable valve to secure it to the gas lift mandrel where the gas lift valve is installed. Fig. 6.8 shows a latch in which the locking element is a ring.

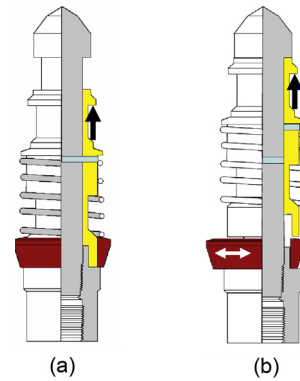
The pin keeps the sliding piece fixed to the latch body. Fig. 6.9 shows how the latch is inserted into the space where the latch shoulder is located, right above the pocket of the gas lift mandrel. As the valve enters the pocket, the latch ring makes contact with the latch shoulder in the mandrel. In Fig. 6.9a, the ring (as it moves downward) contacts the latch shoulder. Then, as the latch continues to move, the ring moves sideways thanks to the shape of the sliding piece, allowing the latch to pass through the latch shoulder, Fig. 6.9b. Once the ring has passed the latch shoulder, the spring pushes the ring back down to its initial position and the gas lift valve is secured in the mandrel:



■ FIGURE 6.8 Ring-type latch.



■ FIGURE 6.9 Gas lift valve latching mechanism.

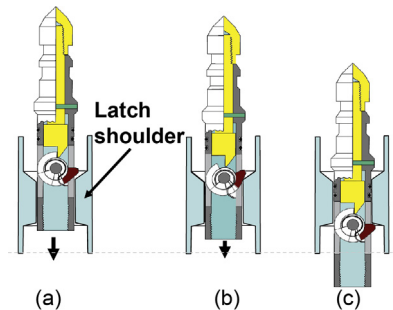


■ FIGURE 6.10 Unlatching mechanism.

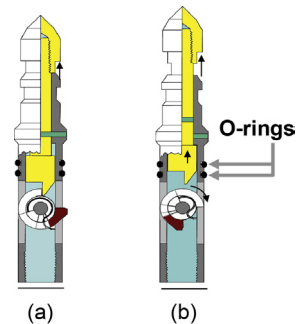
the only way to unlatch the valve is to shear the pin so that the sliding piece moves upward and the ring can move sideways to retrieve the gas lift valve.

To unlatch the valve, the sliding piece should be stroked in the direction of the arrow shown in Fig. 6.10a, until the pin is sheared and the sliding piece can move upward, allowing the latch ring to move sideways, Fig. 6.10b.

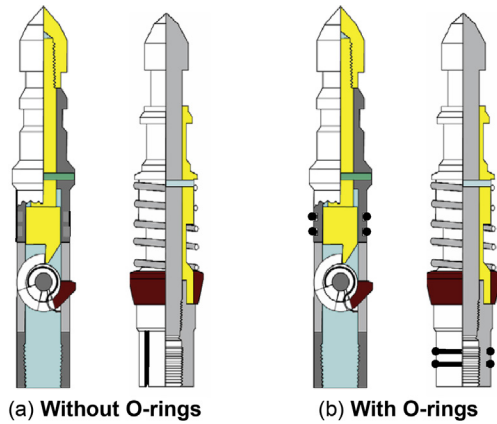
The latch shoulder for ring-type latches is a semicircle (not a 360-degree shoulder). It is important to know that for 1.5-in. diameter valves, there are also 360-degree latch shoulders, where it is not possible to install ring-type latches. Fig. 6.11 shows the latching process in a mandrel with a 360-degree latch shoulder. The way this type of latch can be pulled out of the mandrel is shown in Fig. 6.12. Latches for 1-in. OD gas lift valves are



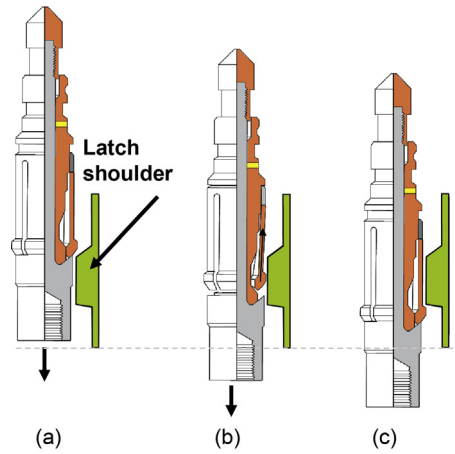
■ FIGURE 6.11 Gas lift valve latching mechanism in mandrels with 360-degree latch shoulders.



■ FIGURE 6.12 Unlatching mechanism (360-degree latch shoulder).



■ FIGURE 6.13 Latches with and without O-rings.



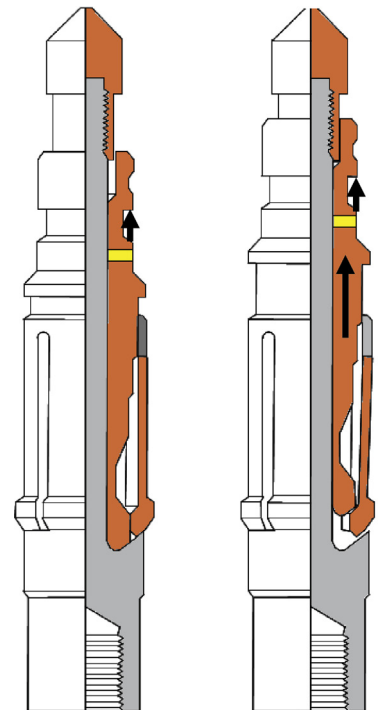
■ FIGURE 6.14 Installation of a collect-type latch.

all for 180-degree latch shoulders, while for 1.5-in. OD gas lift valves there are latches for 180- and 360-degree latch shoulders.

The O-rings in the latch shown in Fig. 6.12 are used in case it is desired to isolate the lower part of the latch to avoid dirt accumulation that might make it hard to pull the valve out of the pocket. But there are situations in which it is desired to allow liquid or gas flow around the latch. Some gas lift valves used in the past had their gas outlet ports in the upper part of the valve and not in the nose. This type of valve is shown in an example in the next section; see Figs. 6.21 and 6.22. These valves need to be installed with latches without O-rings. Some circulating valves are also installed using latches without O-rings (circulating valves are installed in gas lift mandrels to protect the polished bore of the side pocket when the well is circulated with clean fluids after a workover job). Fig. 6.13 shows the two types of latches presented so far, with and without O-rings. The ones without O-rings usually have a groove along the lower box connection.

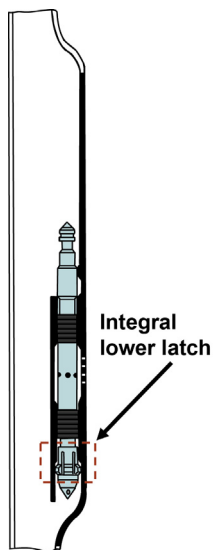
A third type of latch is described in Figs. 6.14 and 6.15. This type of latch is called a “collect latch” and its main advantage is that it can slide into the mandrel very easily, making it ideal for places where it is difficult to jar downward to install the gas lift valve.

Some 1-in. diameter gas lift valve models have latches very similar to the one described in Figs. 6.14 and 6.15, that are integral part of the valve but located just above the nose of the valve, as shown in Fig. 6.16. It is



■ FIGURE 6.15 Unlatching mechanism (collect latch).





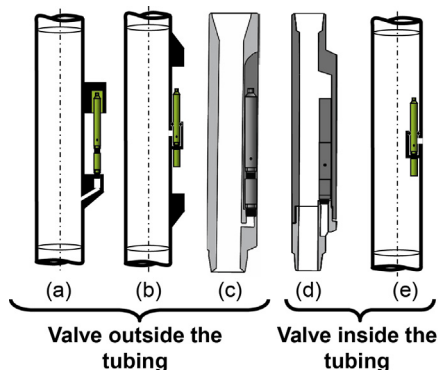
■ FIGURE 6.16 1-in. valve with integral lower latch.

important to keep in mind that these type of valves cannot be installed in most gas lift mandrels designed for annular flow or for accumulation chambers; both of these mandrels are explained in the next section.

## 6.2 GAS LIFT MANDRELS

As indicated in the previous section, gas lift mandrels can be classified as: (1) mandrels for conventional or tubing-retrievable valves, and (2) mandrels for wireline-retrievable valves. Different types of conventional mandrels are shown in Fig. 6.17. Conventional mandrels were developed before mandrels for wireline-retrievable valves were introduced. Today, the great majority of mandrels used in the industry are for wireline-retrievable valves, but conventional mandrels are still manufactured and installed in some wells. The main advantage of conventional mandrels is their low cost. Conventional mandrels are also used in wells that are not very deep because they are easily pulled out of the well. On the other hand, in wells of moderate depths some operators install conventional mandrels above the static liquid level and mandrels for wireline-retrievable valves below the static liquid level because the probability of failure increases at greater depths. In some wells on plunger-assisted intermittent gas lift (see Fig. 6.88a), conventional mandrels could be used for the unloading valves so that the plunger can pass through the unloading mandrel without problem.

Configurations in Fig. 6.17a–c, correspond to mandrels where the gas lift valve is installed outside the tubing, while configurations in Fig. 6.17d, e are for valves installed inside the tubing. The designer should have a good idea of the temperature of nitrogen-charged gas lift valves; therefore, the

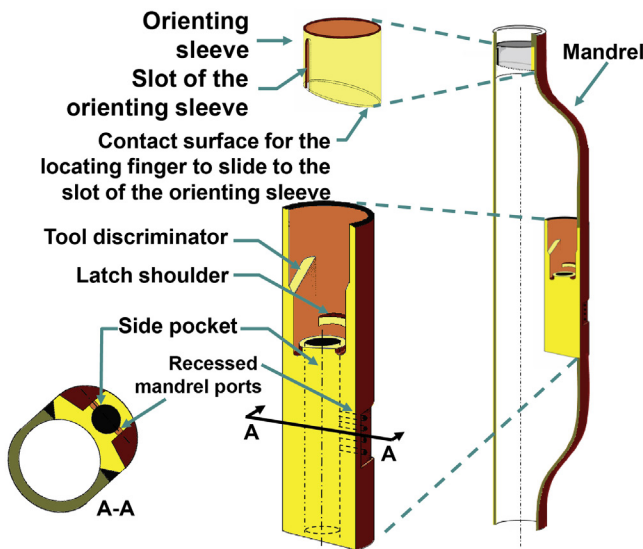


■ FIGURE 6.17 Mandrels for conventional valves (tubing-retrievable valves).

position of the valve with respect to the production fluids is important as it affects the temperature of the valve. When the liquids are produced up the tubing string, conventional valves installed inside the tubing have a temperature closer (if not equal) to the production temperature than to the injection gas temperature. Valves completely outside the tubing have temperatures equal to the gas injection temperature at valve's depth. The opposite is true when the well is produced up the annulus: valves outside the tubing would have temperatures equal to the production temperature, while valves installed inside the tubing would have temperatures equal to the injection gas temperature (which in most situations is only slightly lower than the liquid production temperature). Configuration shown in Fig. 6.17c is ideal for small-diameter casing, while the configuration shown in Fig. 6.17e is used in coiled tubing completions.

Fig. 6.18 shows a mandrel for wireline-retrievable valves that has several features that are now standard but not present in early designs of this type of mandrel. Some of these features are:

- The orienting sleeve is a tool guide that allows the installation of gas lift valves in wells with inclination angles of up to 70 degrees with respect to the vertical. The way the orienting sleeve is used in the valve installation process is explained in this chapter in the section



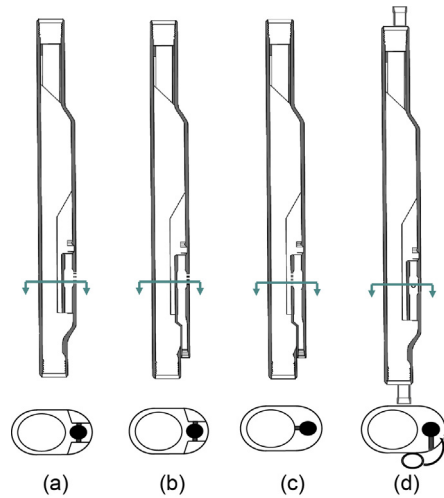
■ FIGURE 6.18 Side pocket mandrel for wireline-retrievable valves.

devoted to wireline equipment. With orienting sleeves, valves can be installed in wells with inclinations of up to 50 degrees with respect to the vertical without the use of special wireline tools. For inclinations between 50 and 70 degrees, it might be necessary to use special wireline tools to install the valve (especially 1.5-in. OD gas lift valves because they are heavier and, in consequence, harder to maintain at the right approaching angle to enter the pocket of the gas lift mandrel). Even though new wireline tools can be used to install gas lift valves at larger inclination angles (even at 90 degrees with respect to the vertical), it might not be beneficial to install valves at inclination angles greater than 70 degrees with respect to the vertical. Injecting gas at very large inclination angles might actually increase the bottomhole flowing pressure because: (1) the friction component of the pressure drop is increased, while (2) the multiphase flow tends to stratify, increasing the liquid holdup (therefore increasing also the hydrostatic component of the pressure drop along the production tubing).

- The tool discriminator guides side-pocket devices (with the proper diameter) into the mandrel's side pocket and deflects larger tools toward the tubing bore.
- Recessed mandrel ports allow full gas flow even if the mandrel leans against the casing, contacting it right where the ports are located. However, even mandrels with recessed ports can present problems if the tubing inclination angle with respect to the vertical is approaching 90 degrees because dirt can accumulate at these ports if the mandrels lean against the casing precisely where the ports are located. This is yet another reason for not installing gas lift mandrels at such high inclination angles. Most of the time, it is not necessary to install mandrels at very steep inclination angles with respect to the vertical because the net gain in true vertical depth might not be worth the effort of trying to reduce the hydraulic pressure component. Also, as indicated earlier, injecting gas in nearly horizontal pipes might just increase the segregation of the phases, increasing the slip velocity (difference between the gas and liquid in situ velocities), therefore achieving a very small decrease of the liquid holdup.
- Integrally forged side pockets allow higher test pressures in new mandrels.

There are several types of side-pocket mandrels for wireline-retrievable valves, such as the ones shown in [Fig. 6.19](#).

Referring to [Fig. 6.19](#), configuration (a) is identical to the one in [Fig. 6.18](#). This type of mandrel is regularly used to inject gas from the casing–tubing



■ FIGURE 6.19 Side pocket mandrel configurations for wireline-retrievable gas lift valves.

annulus into the tubing, although it can also be used to inject gas from the tubing into the annulus by reversing the orientation of the check valve inside the gas lift valve, but in this case PPO valves will behave as IPO valves do and vice versa.

With configuration (b), when the gas lift valve opens the gas flows from the annulus into a snorkel instead of flowing toward the tubing. The snorkel is usually connected to a special production packer that directs the gas flow into an accumulation chamber located below the upper packer. Accumulation chambers are described in the next section. The 1-in. diameter valves with integral lower latch might not be installed in this type of mandrel (the designer should check with the manufacturer of the mandrel).

Configuration (c) corresponds to a mandrel specially designed for annular liquid production. The ports of the mandrel communicate the inside of the production tubing to the side pocket. The side-pocket outlet is directed toward the annulus by means of a snorkel located below the side pocket. In this way, the gas is injected toward the annulus with less pressure drop across the gas lift valve than when configuration (a) is used for annular flow. Additionally, with configuration (c) IPO valves still behave as IPO valves when gas is injected down the tubing. It should be kept in mind (while performing design or troubleshooting calculations) that the temperature of the valve is equal to the temperature of the injection gas when the gas is

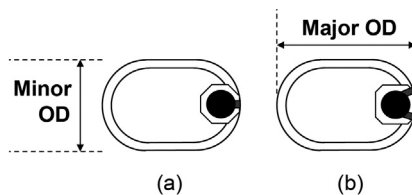
injected down the tubing but the temperature of the gas in this case is almost identical to that of the fluids being produced up the annulus. It might not be possible to install 1-in. valves with integral lower latch in mandrels with configuration (c).

Configuration (d) has a side pipe (parallel to the mandrel) through which the lift gas is injected. The ports of the mandrel communicate the side pipe with the pocket of the mandrel. This type of mandrel is ideal for wells in which the casing cannot withstand the high injection pressures or for inserted accumulation chambers for which the point of injection is too far below the production packer (examples of inserted accumulation chambers are given in the next section). The designer should take into consideration the friction pressure drop along the side pipe. This type of mandrel is also recommended in cases in which the injection gas is highly corrosive and might damage the casing.

Side pocket mandrels can be ordered with integral guard devices and longitudinal grooves to protect chemical injection conduits, electric cables, or fiber optic cables being run in the well simultaneously with the mandrel.

There are new side-pocket mandrels with the configuration presented in Fig. 6.19a, in which their ports communicate with the annulus by means of an integral check valve (injection gas from the casing–tubing annulus has to pass through this check valve before entering the side pocket). In this way, when the gas lift valve (installed in the side pocket) is retrieved, the fluids inside the tubing do not enter the annulus. This avoids having to unload the well every time a gas lift valve needs to be replaced. The two disadvantages of this type of mandrel are: (1) if the check valve stops working properly, the tubing needs to be pulled out of the well to replace the mandrel, and (2) the pressure drop through the integral check valve might be too large for high-injection-gas-flow-rate applications.

With the exception of mandrels designed for annular liquid production, all mandrels shown in Fig. 6.19 have recessed ports, but that is not the case for old side-pocket mandrels, such as the ones shown in Fig. 6.20 which are



■ FIGURE 6.20 Cross-sectional view of old mandrel geometries.

still in use in many wells around the world. These mandrels might not allow full gas flow if they are up against the casing. The configuration shown in Fig. 6.20b is an improved geometry present in more recent, but still old, models.

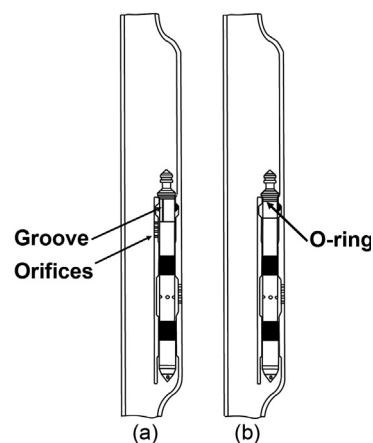
Some mandrels are designed with a completely circular cross-section instead of the oval shape shown so far. These mandrels have higher test pressures than the ones with oval cross-sectional geometries. It is important to know the maximum internal and external pressures that a mandrel can withstand, especially for the deeper ones installed in a well (or all of them if the well will be subjected to hydraulic fracturing jobs). It is also important to keep in mind that some mandrels have their major diameters reduced so that they can fit inside the casing (major and minor diameters are shown in Fig. 6.20); therefore, these mandrels have lower test pressures. Some mandrels are heat treated for corrosive environments and they usually have lower test pressures.

Besides limitations imposed by maximum internal and external pressures, there are geometry constraints that might not allow the installation of a given gas lift mandrel:

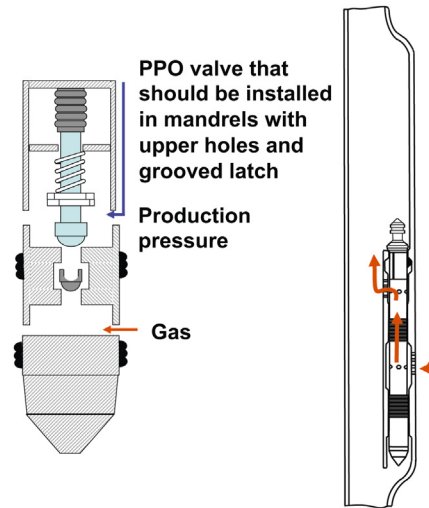
- The major diameter should be small enough so that the mandrel can be installed inside the casing without blocking gas injection.
- The mandrel's internal drift diameter should be compatible with the rest of the completion. For example, a landing nipple with a drift diameter greater than the drift diameter of a gas lift mandrel (located above this landing nipple) will be useless.
- A mandrel without an orienting sleeve should not be installed in an inclined well. But even mandrels with orienting sleeves should not be installed in wells with inclination angles with respect to the vertical greater than 70 degrees for the reasons given earlier.

Fig. 6.21 shows two old mandrel models; they do not have either orienting sleeve or tool discriminator. The latch shoulder is a complete circle (360-degree type), which are unusual nowadays. The pocket in Fig. 6.21a has upper orifices and the latch is grooved to allow gas or liquid flow, depending on the type of application for which the mandrel was installed. The pocket of the mandrel shown in Fig. 6.21b has O-rings to prevent dirt accumulation on top of the latching mechanism.

The valve shown in Fig. 6.22 should be installed in mandrels like the one shown in Fig. 6.21a. The tubing pressure is transmitted into the inside of the gas lift valve through the upper orifices of the mandrel pocket (and through the grooved latch) to open the gas lift valve, which is therefore a PPO valve.



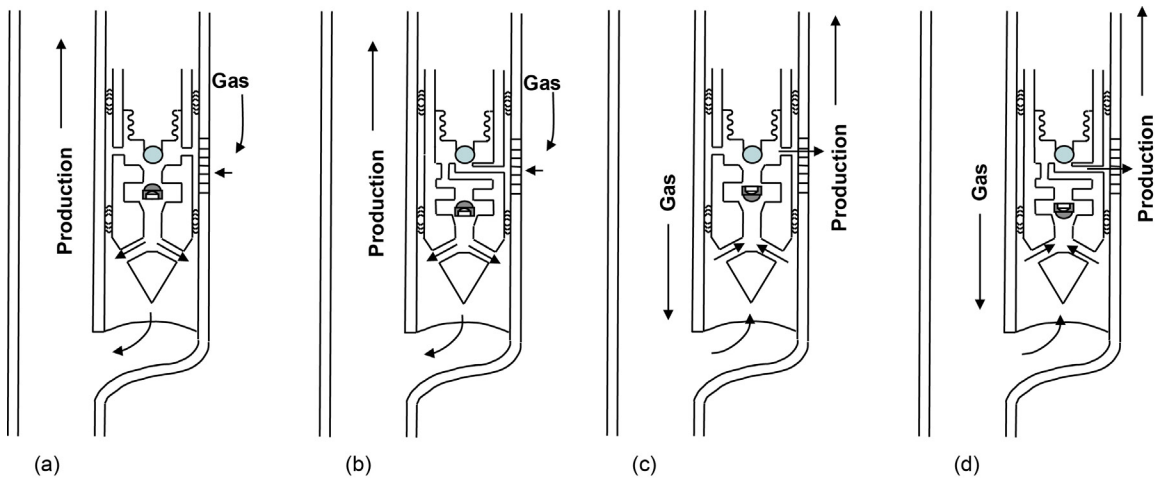
■ FIGURE 6.21 Old mandrel models.



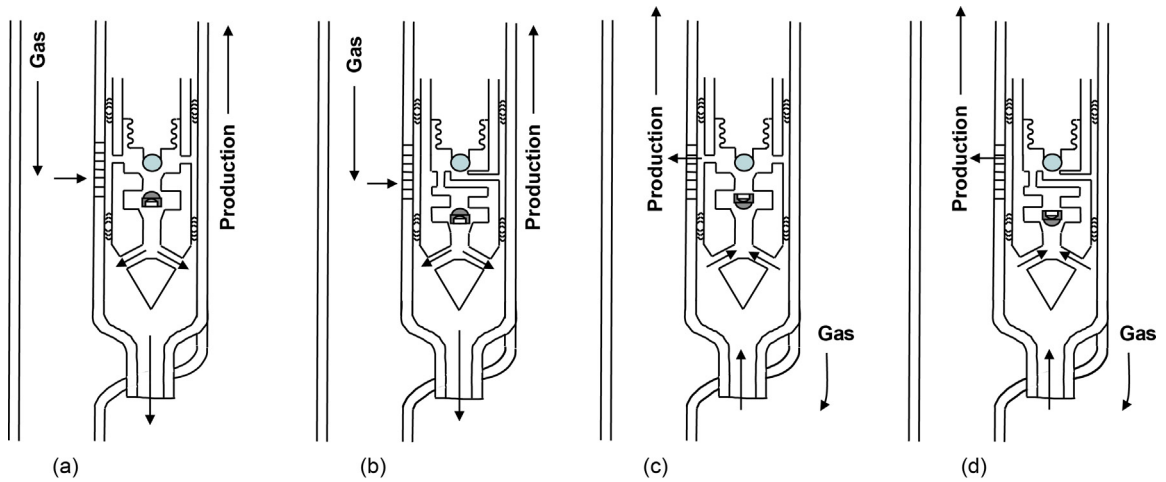
■ FIGURE 6.22 PPO valve with upper gas outlet.

The gas from the annulus then enters the tubing directly through the upper pocket orifices.

The different types of gas lift mandrels and the possibility of having tubing or annular flow, make it necessary for gas lift valves to have different internal configurations to adapt to each combination of operational condition, as shown in Figs. 6.23 and 6.24.



■ FIGURE 6.23 Different valve configurations for standard-type mandrels.



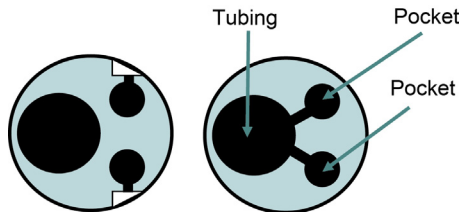
In Fig. 6.23a, b, the gas lift valves are exposed to the production temperature and they behave in the way they were designed for: PPO or IPO valves. The following aspects should be considered in Fig. 6.23c, d:

■ FIGURE 6.24 Different valve configurations for mandrels specially built for annular flow.

- The valves are exposed to the injection gas temperature.
- The frictional pressure drop along the tubing could be significant for large gas flow rates.
- IPO valves behave as PPO valves and vice versa.

In Fig. 6.24a, b, the valves are exposed to the injection gas temperature and the frictional pressure drop along the production tubing should be taken into account. The valves installed in this manner behave in the way for which they were designed: as IPO or PPO valves. In Fig. 6.24c, d, valves are exposed to the production temperature. In this case, PPO valves behave as IPO valves and vice versa.

Sometimes it is necessary to inject gas at an extremely high flow rate. For these cases, there are mandrels with more than one side pocket. In Fig. 6.25 two possible configurations of multipocket mandrels are shown. In the



■ FIGURE 6.25 Mandrels with more than one pocket.

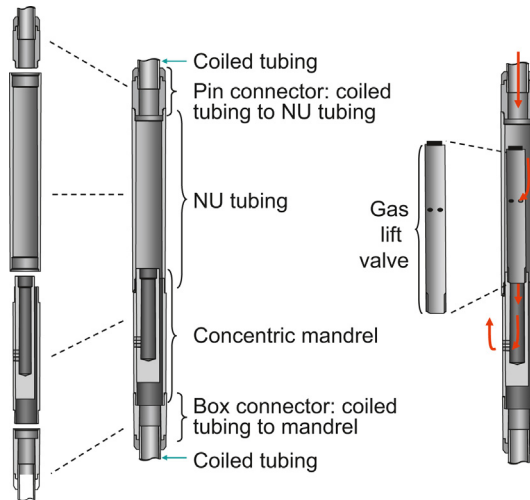


configuration to the left, the external mandrel's ports are connected to the pockets, which is the usual case for annular gas injection. In the configuration to the right, the mandrel's ports are internally connected to the pockets, which is the design for annular liquid production. There are mandrels with up to five pockets but they can only be installed in wells with very large casings. In all cases, special wireline kickover tools must be used to install or retrieve the gas lift valves.

There are new mandrels with two pockets that are used to increase the protection of the casing–tubing annulus by providing a constant and stronger barrier to keep production fluids from entering the annulus in normal operation or, especially, while replacing the current gas lift valve. An orifice valve (with a very large seat and a high differential pressure check valve) is installed in one pocket and in the other pocket the actual (according to the gas lift design) gas lift valve is installed. The external ports of the mandrel connect the well's annulus to the first pocket (where the orifice valve is installed) only. Gas from the annulus is injected into the orifice valve following the same path the gas flows into any orifice valve (through the ports of the valve first, then through its seat, and finally through the check valve at the nose of the valve). The first pocket is connected to the second pocket so that the gas out of the nose of the orifice valve is injected into the gas lift valve in the second pocket. Gas enters the gas lift valve in the second pocket in the same way it does in any gas lift valve (through the ports of the valve first, then through its ball-seat flow area, and finally through the check valve at the nose of the gas lift valve). The gas coming out of the gas lift valve installed in the second pocket then finally flows into the production tubing. This arrangement allows the gas lift valve (in the second pocket) to be pulled out of the well without liquids from the production tubing entering the annulus. At the same time, this type of mandrel offers two check valves (one in the gas lift valve and the other in the orifice valve) that serve as a high-pressure barrier to keep the production liquid from entering the annulus.

The advantage of the mandrel described in the previous paragraph (over the mandrels that have their own check valve as an integral part of the mandrel to prevent liquids from entering the annulus) is that the orifice valve can be pulled out of the well for repair. Its main disadvantage is that they are only offered in large diameters that do not fit inside commonly used production casings.

With the introduction of coiled tubing applications, different types of mandrels have been developed that can be welded to the coiled tubing or

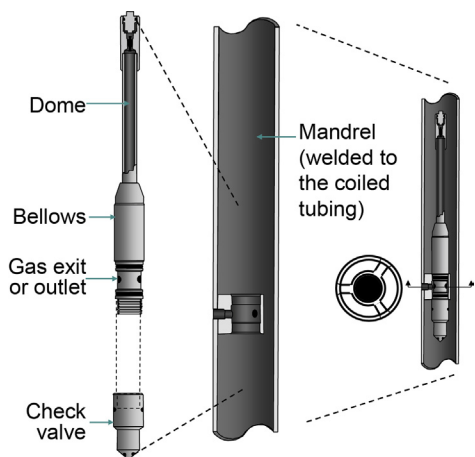


■ **FIGURE 6.26** Concentric mandrel connected to a coiled tubing string by special connectors.

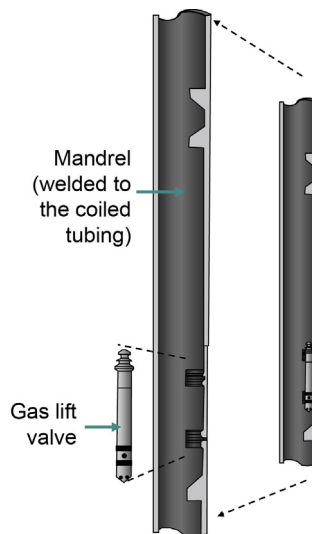
connected to it by means of special connections so that these mandrels can pass through the wellhead while running the coiled tubing in an underbalance operation (which is an operation that reduces the risk of formation damage). The great advantages of coiled tubing completions are that their installation is fast, does not need big workover or completion rigs and formation damage can be avoided. A concentric gas lift mandrel connected to a coiled tubing string is shown in Fig. 6.26. The coiled tubing above the mandrel has a pin connector that is coupled to a NU tubing joint. The lower end of the NU joint is connected to the mandrel. Below the mandrel, the coiled tubing has a special box connector that is coupled to the lower end of the mandrel. Valves installed in this way cannot be retrieved by wireline operations.

Fig. 6.27 shows a gas lift mandrel in which a gas lift valve is permanently installed. The mandrel and the valve can be spooled together with the coiled tubing and sent to the well site for its installation, so there is no need to stop running the coiled tubing in the well to install the gas lift mandrel. Gas can be injected down the annulus between the production tubing and the coiled tubing (liquid production would be up the coiled tubing) or down the coiled tubing (for annular liquid production). These valves cannot be retrieved by wireline.

Coiled tubing mandrels described so far are for tubing-retrievable valves. But there are mandrels (that can be welded to the coiled tubing) that are



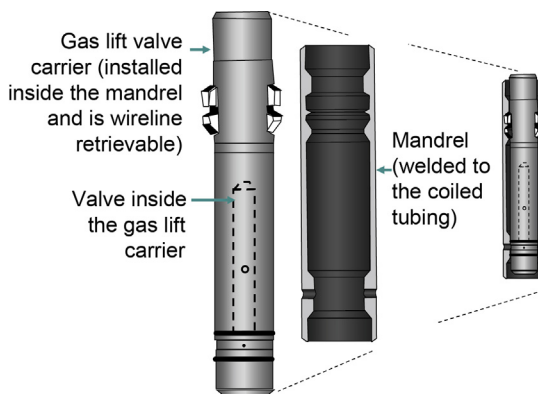
■ FIGURE 6.27 Special gas lift mandrel for coiled tubing.



■ FIGURE 6.28 Coiled tubing mandrel for wireline-retrievable valves.

used for wireline-retrievable valves, like the one shown in Fig. 6.28. These mandrels are available for coiled tubing diameters of up to 3½ in.

Another type of coiled tubing mandrel that is used for wireline-retrievable valves is shown in Fig. 6.29. In this case, the gas lift valve is installed inside a valve carrier capsule, which is actually the one that is installed in the mandrel. The mandrel is welded to the coiled tubing. The capsule can be retrieved by wireline.



■ FIGURE 6.29 Coiled tubing mandrel for wireline-retrievable gas lift valves.

### 6.3 WIRELINE EQUIPMENT

The great majority of gas lift valves used today are installed and retrieved by wireline operations inside the production tubing. Besides gas lift valves, many other downhole production tools and equipment, like tubing stops, plugs, standing valves, subsurface safety valves, etc., are also installed by wireline. A brief explanation of surface and subsurface equipments needed to perform most wireline jobs directly or indirectly related to gas lift operations is given next.

The most important wireline tools and equipment are: power unit; wireline reel; lubricators with safety valves; weight indicator; odometer (to measure the length of the wireline run in the well); subsurface tool string for gas lift valve installation and other operations; tools for related operations, such as: tubing end locator, tubing gauge/paraffin cutter, sand bailers, and sample bailers, among others.

The power unit could be an internal combustion engine or an electrical motor and its function is to transmit the energy to the fluid used by the hydraulic unit to drive the wireline reel. Motors are usually from 40 to 60 Hp, which operate at 2000 RPM. The motor is connected to a pump of around 20 GPM in capacity. The hydraulic fluid is usually stored in an 80 gal tank. To carry the power fluid to the hydraulic unit, two high-pressure hoses of about 50 ft. in length are used. The wireline reel is driven by the hydraulic unit coupled to a transmission that allows the operator to raise or lower the wireline tools in or out of the well. The reel has a braking system that is used by the operator to quickly reduce the velocity of the wireline as required by a normal installation procedure or in case of an emergency. The wireline unit has an odometer to measure the depth where the wireline tools are located in the well. This depth is known as “wireline measured depth” because it is not the real depth where the tools are located but the length of wireline required to reach a certain point in the well. The real depth of a particular point and its wireline measured depth are different because the weight of the tools and the wireline itself elongate the wireline inside the well. The wireline is usually a single solid wire, but stranded wirelines are occasionally used in jobs where large tension forces are expected. It is important to properly maintain the wireline so that it would not break. Records should be kept regarding the number of times the wireline has been used, as well as the duration and conditions of previous jobs. The service life of the wireline, as provided by the manufacturer, should never be exceeded.

The most commonly used solid wireline diameters in gas lift related operations are: 0.072 in. for tension forces of up to 961 lb, 0.082 in. for up to 1240 lb and 0.092 in. for up to 1550 lb. Wirelines are usually commercially

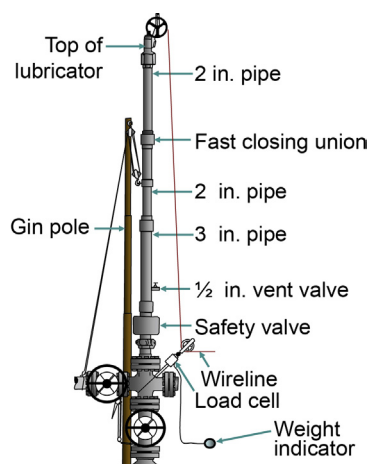
available in lengths from 18,000 to 25,000 ft. For safety reasons, it is advisable not to exceed a tension force of 750 lb; but, if much greater tension forces are required (for swabbing or certain fishing jobs), the following wireline diameters are recommended:

- 0.108 in.: for up to 2100 lb.
- 3/16 in.: for up to 4200 lb.
- 5/16 in.: for up to 8000 lb.

For these high-strength wireline diameters, the surface lubricator (which is used to insert the tool string into the well, see Fig. 6.30) should be able to contain the internal tubing pressure and they are usually somewhat different from the ones used for smaller wireline diameters. For CO<sub>2</sub> or H<sub>2</sub>S environments, the wireline should be manufactured with special materials that usually resist lower tension forces or jarring operations because they are not as flexible as the wirelines made out of standard materials with standard heat treatment. Wirelines that can be used in presence of H<sub>2</sub>S are: AISI-316, AISI-18-18-2, or URANUS 50. When both, H<sub>2</sub>S and CO<sub>2</sub>, are present, it is recommended to use: URANUS B-6 for temperatures less than 200°F, and MP-35N for temperatures between 200 and 400°F.

The following preventive steps are recommended:

- For each 4-h service time, cut 20 ft. off the wireline at the end of the job.
- Crystallization tests should be conducted by bending the wire as indicated by the manufacturer.
- 0.082- and 0.092-in. wirelines should not be used after 250–300 accumulated hours of service.
- 0.105-in. wireline should not be used after 300–350 accumulated hours of service.
- As the wireline is pulled out of the well, it should be constantly cleaned and oiled.



■ FIGURE 6.30 Wellhead wireline equipment.

To perform any wireline job, it is necessary to be able to insert the wireline tool string into the well. This is accomplished by the use of a lubricator that is installed on top of the Christmas tree as shown in Fig. 6.30. The wireline tools are placed first inside the lubricator at atmospheric pressure and then the lubricator is coupled to the wellhead. There is an orifice at the top of the lubricator through which the wireline is run in or pulled out of the well. At that orifice, there is a sealing mechanism (stuffing box) that keeps the lubricator at the wellhead production pressure when the crown valve is opened and the well is in communication with the lubricator. The type of lubricator to be used depends on the wireline tool diameters, wellhead pressure,

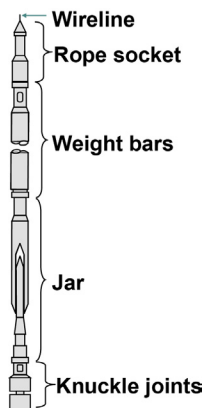
and the type of fluids the well produces. If the oil is too viscous, it might be necessary to use many weight bars, so that the lubricator would have to be very long and a rig, instead of a gin pole, might be needed to install the lubricator on top of the wellhead. A safety valve is installed on top of the Christmas tree and its function is to close the well as fast as possible even if the wireline is inside the well. The internal components of the safety valve are designed in a way that the valve will not cut the wire when it closes. A ½-in. valve is used to bleed the pressure off the lubricator before uncoupling it from the wellhead.

The weight indicator allows the operator to know the tension force on the wireline. The tension is transmitted from the load cell by a ¼-in. hose. Weight indicators are usually available from 0 to 2,000 lb or from 0 to 10,000 lb. The latter is used in operations with 0.108-in. wirelines and above.

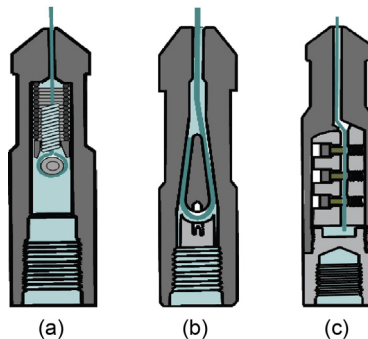
The following tools are the basic tools that should always be installed together with the rest of the tools needed for a particular job (in the order shown in Fig. 6.31): (a) rope socket, (b) weight bars, (c) jar, and (d) knuckle joint.

The rope socket is used to attach either solid or stranded wirelines to a wireline tool string. Three types of rope sockets are available: spool, wedge, and clamp, as shown in Fig. 6.32.

The weight bar shown in Fig. 6.33 is the second component in the tool string and it is used to add weight to the wireline tool string to counteract the force of wellbore pressure on the cross-sectional area of the wire and to increase the effectiveness of upward or downward jarring with link or tubular jars.



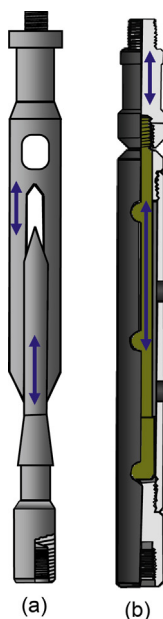
■ FIGURE 6.31 Basic wireline tool string.



■ FIGURE 6.32 Types of rope sockets.



■ FIGURE 6.33 Weight bar.



■ FIGURE 6.34 Jars. (a) Link jar;  
(b) tubular jar.

**Table 6.1** Weight Bars Used in Gas Lift Related Wireline Jobs

Weight Bar OD (in.)	Fishing Neck (in.)
1-1/4	1-3/16
1-1/2	1-3/8
1-3/4	1-3/4
1-7/8	1-3/4

(shown in Fig. 6.34). The most commonly used weight bars are given in Table 6.1.

Jars can be classified as mechanical or hydraulic jars. Mechanical jars are used more often because the force they transmit is large enough to perform most downhole wireline jobs in the well. The two types of mechanical jars are shown in Fig. 6.34. Link jars consist of interlocking steel links with a fishing neck and a pin-thread connection on the upper end and a box-thread connection on the lower end. These links can be extended or collapsed by manipulating the wireline at the surface to produce upward or downward jarring. The intensity of the impact depends on the weight bars installed above the jar, the depth at which the jar is located, the stroke length of the jar, and the density of the well's fluids.

The dimensions of most commonly used link jars are given in Table 6.2.

Tubular jars consist of a tube perforated for fluid bypass and a telescoping rod that moves vertically within the tube. The telescoping rod has a fishing neck and a pin-thread connection on the upper end, and the tube has a box-thread connection on the lower end. They are operated in the same way link

**Table 6.2** Dimensions of Most Commonly Used Link Jars in Gas Lift Related Wireline Jobs

Diameter (in.)	Completion Tubing OD (in.)	Stroke (in.)	Fishing Neck (in.)
1	1-1/4	20	1
1-1/4	1-1/2	20	1.187
1-1/4	1-1/2	30	1.187
1-1/2	2	20	1.375
1-1/2	2	30	1.375
1-7/8	2-1/2	20	1.750
1-7/8	2-1/2	30	1.750

jars are. These jars are especially effective in fishing a wireline that broke and was left in the production tubing.

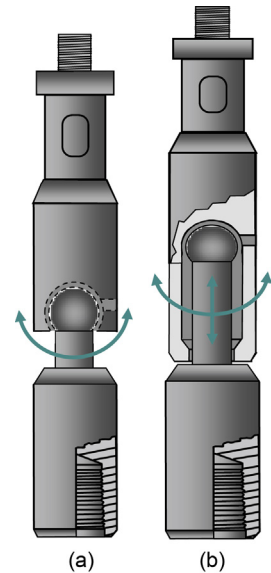
Hydraulic jars are used when large impacts are required, but this type of jar can only deliver upward jarring forces.

Knuckle joints are used to provide flexibility at specific points in the wireline tool string, see Fig. 6.35. They consist of a ball and socket assembly that has a fishing neck and a pin-thread connection on the upper end and a box-thread connection on the lower end. Knuckle jars, which also provide short jarring action, are used only in special applications, see Fig. 6.35b.

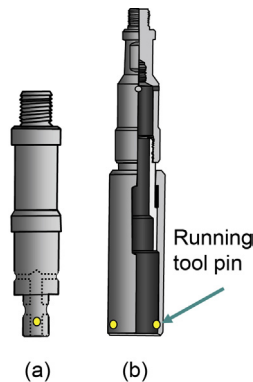
Weight bars, jars, and knuckles joints are connected to each other by the upper pin connections and the lower box connections common to all of them. All of these tools have a fishing neck so that they can be pulled out of the well by a conventional pulling tool in case the tool string breaks.

When a gas lift valve is run in the well, it is attached to a wireline tool called “running tool.” There should be a kickover tool (explained later in the chapter) above the running tool, which in turn should be connected to the basic tool string shown in Fig. 6.31. Running tools are shown in Fig. 6.36. Gas lift valves are usually attached to a running tool like the one shown in Fig. 6.36b, with the running tool pin attached to the latch of the gas lift valve. Once the valve is installed in the gas lift mandrel, upper jarring will shear the running tool pin so that the tool string can be pulled out of the well, leaving the gas lift valve inside the pocket of the gas lift mandrel.

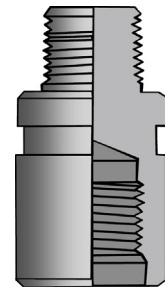
Sometimes it is necessary to install components of the wireline tool string that have different size thread connections. In those cases, crossovers like the one shown in Fig. 6.37 are used.



■ FIGURE 6.35 (a) Knuckle joint; (b) knuckle jar.

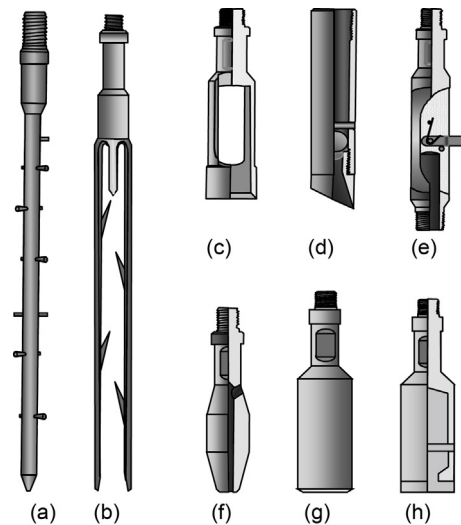


■ FIGURE 6.36 Running tools. (a) for female fishing neck; (b) for male fishing neck.



■ FIGURE 6.37 Crossover.





■ FIGURE 6.38 Commonly used wireline tools.

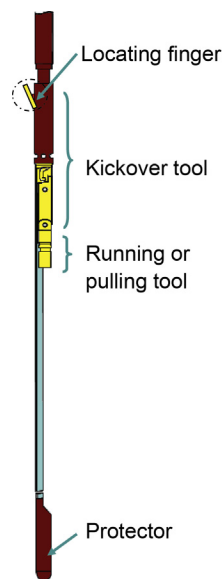
Several tools used for different purposes are shown in Fig. 6.38:

- a. Paraffin scratcher: used to loosen paraffin from the tubing-string inside walls.
- b. Wireline grab: used to retrieve broken wirelines from the tubing string.
- c. Tubing gauge or paraffin cutter: used to gauge the tubing string inside diameter or remove paraffin. It should always be used prior to any wireline job to make sure the drift diameter of the tubing is large enough for the wireline job to be performed.
- d. Sample bailer: used to retrieve samples of fluids and solids from the bottom of a well. Downward movement of the sample bailer forces well fluids and solids through the ball check valve into the bailer tube. The check valve retains the sample inside the bailer tube.
- e. Tubing end locator: used to determine the depth of either the bottom of the tubing or a break in the tubing. The spring-loaded finger is compressed within the body until the tool is lowered just past the bottom of the tubing. The finger then rotates outward against the shear pin. As the tool is retrieved, the finger catches on the end of the tubing and registers an increase on the surface weight indicator to indicate the depth. Continued upward pull shears the pin and compresses the finger to allow the tool to be retrieved. They are most of the time used in combination with sample bailers.
- f. Tubing swage: used to force out constricted areas in the tubing string.
- g. Blind box: used to deliver downward jarring blows on equipment or debris downhole.

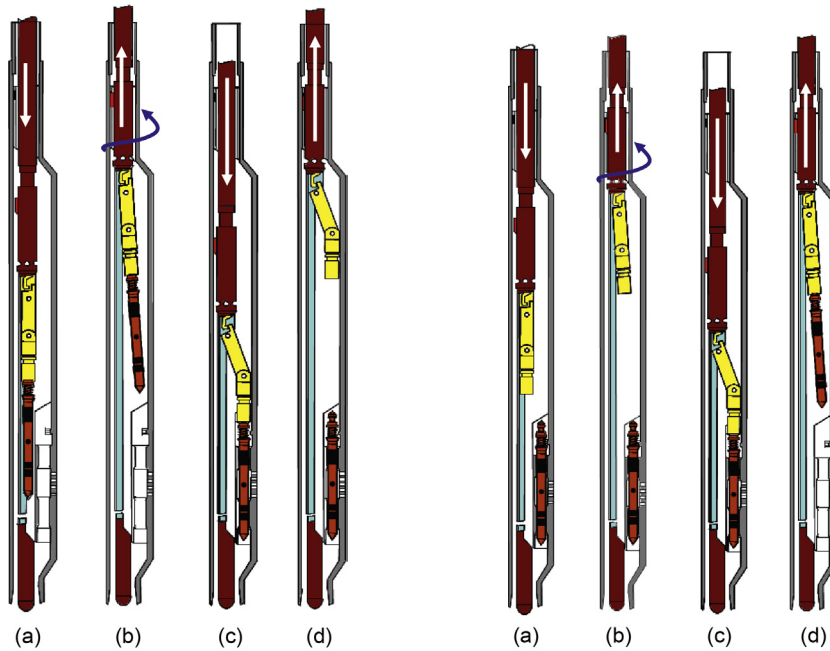
- h. Impression blocks: used to take impressions of objects in the tubing string. Impression blocks consist of a steel housing and a molded lead insert held in the lower end by steel pins. They are usually used during fishing operations to obtain the shape and position of the object being retrieved.

The steps and required wireline equipment to retrieve or install a gas lift valve are described next. The following activities should be performed before doing any wireline job in the well: (1) gauge the production tubing to verify that no restrictions are present; and (2) measure the total depth of the well. The total depth of the well should be checked to determine if sand has accumulated at the bottom, partially or totally blocking the perforations. This is carried out by running in the well the basic wireline tool string plus a tubing end locator and a sample bailer at the end of the tool string. The tubing end locator is necessary to get the wireline measured depth of the end of the tubing and compare it to its actual depth from the well's file. This allows the operator to correlate the measured total depth of the well to its actual value and verify that the well is clean; otherwise, it would not be possible to estimate the actual total depth of the well. An additional step that might be of interest before doing the requested wireline job is to try to measure the liquid level found in the well. This could be done by detecting sudden changes in wireline tension and/or velocity as the tool string is carefully run in the well.

Once these previous steps have been successfully completed, a tubing stop should be installed below the last gas lift mandrel where a gas lift valve is going to be installed. This is done to avoid dropping a gas lift valve, or any wireline tool, to the bottom of the well (below the tubing end) if the gas lift valve, or the wireline tool string, breaks free. The tubing stop should be installed in a collar recess or a landing nipple, always below the liquid level (to provide a damping force for free falling objects). If a complete valve change out is going to be performed, all the valves are first removed from the well, starting from the deepest one until the upper one is retrieved and then the new valves are installed in the reverse order (starting from the one closest to the surface). Before retrieving the first valve, the wellhead production and surface casing pressures must be equalized. If the pressures are not equal, it is possible to blow the tool string up the tubing when the first valve is removed from the mandrel, tangling the wireline and making it difficult to retrieve. The wellhead pressures can be equalized using a high-pressure hose to connect the casing to the tubing. To retrieve a gas lift valve, the basic tool string is run in the well with a kickover tool and an appropriate pulling tool attached to it. The kickover tool, as well as the running or pulling tools are shown in Figs. 6.39–6.41 for mandrels with orienting sleeve, or in Figs. 6.42 and 6.43 for mandrels without orienting sleeve. Just before reaching the mandrel, the tool string is suspended for a moment to verify the wireline tension without



■ FIGURE 6.39 Kickover tool required for mandrels with orienting sleeve.



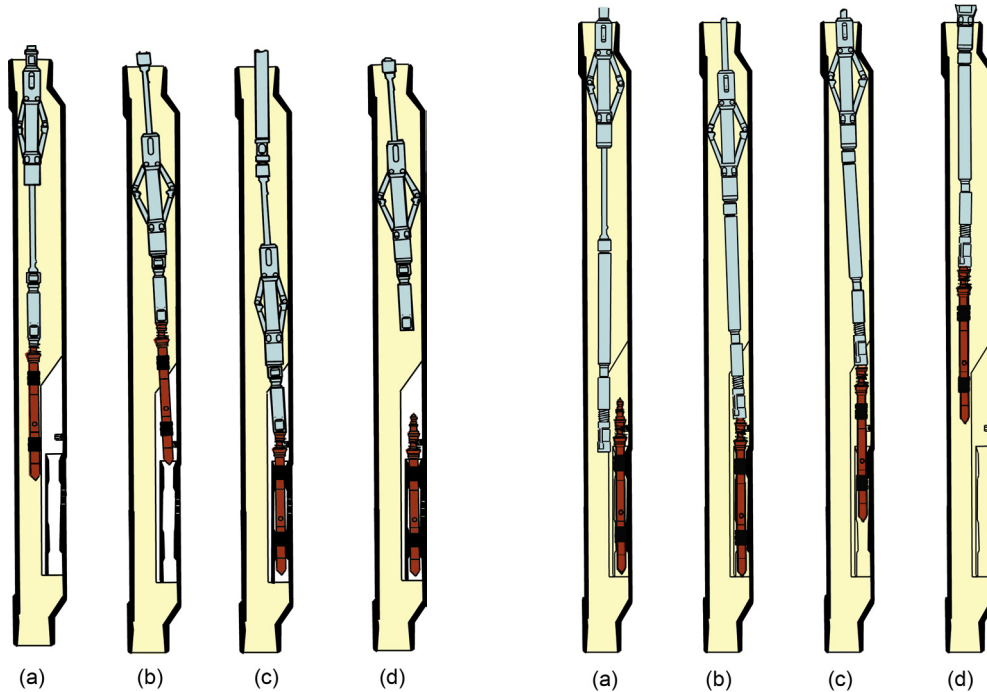
■ FIGURE 6.40 Running the valve in the well.

■ FIGURE 6.41 Pulling the valve out of the well.

the valve attached to the tool string. This tension will be compared to the final tension at the same depth after completing the operation to verify that the valve has been pulled out of the mandrel.

If a kickover tool for orienting sleeve is used, the following steps are taken to retrieve a gas lift valve, see [Fig. 6.41](#):

- Lower the tool string below the selected mandrel.
- Slowly raise the tools through the mandrel until they stop, indicating the locating finger in the kickover tool has contacted the top of the slot in the orienting sleeve of the mandrel.
- By pulling the wireline, increase the tension on the wireline to a certain value greater than the initial tension (before pulling it). The required increase in tension depends on the kickover tool being used. For an OM kickover tool model, for example, the recommended tension increase is a force of approximately 150 lb. The kickover tool will release and kick the pulling tool over into position above the side pocket in the mandrel.
- Slowly lower the tools until the tension decreases, indicating that the kickover tool has kicked over and located the side pocket of the mandrel (no weight loss means the kickover tool did not release to the



■ FIGURE 6.42 Running the valve in the well.

■ FIGURE 6.43 Pulling the valve out of the well.

kicked over position and the kickover tool must be raised again to try to release it).

- Jar downward to secure the pulling tool to the running head (latch) of the valve.
- Jar upward to pull the valve from the side pocket of the mandrel (if it is not possible to pull the valve, downward jarring will shear a pin in the pulling tool, releasing it from the valve so that the tool string can now be pulled out of the well).
- As the kickover tool is pulled upward through the mandrel, the locating finger will stop in the slot of the orienting sleeve. Sharp upward jarring will shear a pin in the locating finger to allow the kickover tool to pass through the mandrel.

If a kickover tool for mandrels without orienting sleeve is used, the following pulling procedure is executed, see Fig. 6.43:

- Lower the tool string through the tubing until the kickover tool is below the selected mandrel.
- Pull the kickover tool up rapidly until the tool passes through the selected mandrel. Stop when the tool is just above the selected mandrel.

- Lower the kickover tool through the mandrel until a loss of weight indicates that the kickover tool has kicked over and has located the side pocket of the mandrel.
- Jar downward to secure the pulling tool to the valve latch.
- Jar upward to pull the valve from the side pocket of the mandrel (if it is not possible to pull the valve out of the side pocket, heavy downward jarring will shear a pin in the pulling tool, releasing the pulling tool from the valve).
- Remove the wireline tool string from the well.

Sometimes it is not possible to pull the valve out of the side pocket of the mandrel and actions, like chemical injection right on top of the latch by means of dump bailing tools or removing debris from the latch area using sand bailing, are required. A valve might get stuck for several reasons: asphaltene or carbonate deposition, sand accumulation, etc.

Running (installing) procedure when kickover tools for orienting sleeves are used is as follows, see [Fig. 6.40](#):

- Lower the tool string until the kickover tool is below the selected mandrel.
- Slowly raise the tools through the tubing until they stop, indicating that the locating finger in the kickover tool has contacted the top of the slot in the orienting sleeve of the mandrel.
- By pulling the wireline, increase the tension on the wireline to a certain value greater than the initial tension (before pulling it). The required increase in tension depends on the kickover tool being used. For an OM kickover tool model, for example, the recommended tension increase is of approximately 150 lb. The kickover tool will release and kick the valve over into position above the side pocket in the mandrel.
- Slowly lower the tools until a weight loss registers on the weight indicator, meaning that the kickover tool has kicked over and located the side pocket of the mandrel. No weight loss indicates that the kickover tool did not release to the kicked over position and it should be raised again.
- Jar downward to drive the valve into the side pocket of the mandrel.
- Jar upward. This releases the running tool from the latch and gives a positive indication that the latch and valve are firmly locked in the side pocket of the mandrel.
- The tool string can now be removed from the well. As the kickover tool is pulled upward through the mandrel, the locating finger will stop in the slot of the orienting sleeve. Sharp upward jarring will shear a pin in the locating finger to allow the kickover tool to pass through the mandrel.

If the mandrel does not have an orienting sleeve, the following running procedure must be followed, see Fig. 6.42:

- Lower the tool string through the tubing until the kickover tool is below the selected mandrel.
- Pull the kickover tool up rapidly until the tool passes through the selected mandrel. Stop when the tool is just above the selected mandrel.
- Lower the kickover tool through the mandrel until a loss of weight indicates that the kickover tool has kicked over and has located the side pocket of the mandrel.
- Jar downward to drive the valve into the side pocket of the mandrel.
- Jar upward to release the running tool from the valve latch, giving the operator a positive indication that the latch and the valve are locked in the side pocket of the mandrel.
- Remove the wireline tool string from the well.

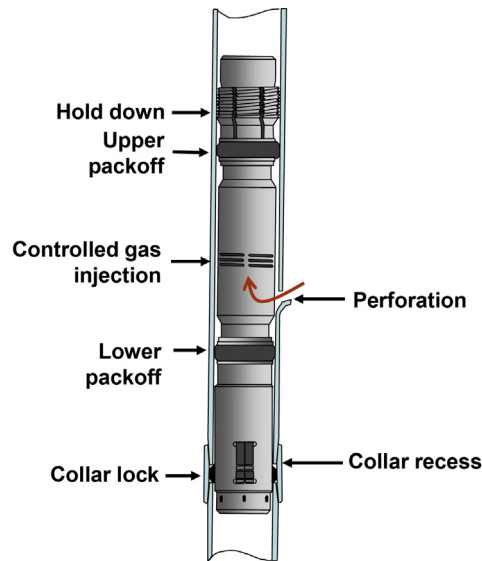
Once the deeper valve (which should be the last one to install) has been installed, the tubing stop should be pulled out of the well and the lubricator removed from the wellhead. The well should then be unloaded following the procedure described in chapter: Design of Continuous Gas Lift Installations, for which the valves at the injection manifold, wellhead, and flow station should be opened and properly aligned to start the unloading of the well.

There are new kickover tools that can be used to retrieve the old valve and install a new one in just one wireline trip. These tools can save precious time (especially in large-production-rate wells). Longer lubricators, installed on top of the wellhead, are required for these new kickover tools.

The following unwanted tubing-annulus communications can take place in wells producing on gas lift:

1. Injection gas leaks through holes or tubing couplings in the tubing string.
2. Damaged circulating sleeves which, for some unexpected reason like sand depositions, cannot close.
3. Gas lift mandrels with damaged gas lift valves that cannot be retrieved because they are stuck inside the side pocket or they are installed in conventional (tubing retrievable) mandrels.

For these problems, there might be a solution that does not require the production tubing string to be pulled out of the well to seal these unwanted tubing-annulus communications. For example, the so-called “packoff completions” can be used to isolate any unwanted tubing-annulus communication or to control the injection gas flow rate through an unintentional (or



■ FIGURE 6.44 Packoff gas lift assembly.

intentional) tubing–annulus communication. The reason why packoff completions are presented here is because they can be installed and retrieved by wireline procedures. Fig. 6.44 shows a packoff assembly that was specifically installed to allow a controlled gas injection flow into the tubing. The lower collar stop is set by wireline first. The tubing is then perforated (if the communication is done intentionally) using a special tool (tubing punch). Finally, the entire upper assembly (bottom packoff, gas lift mandrel and valve, upper packoff, and upper tubing stop) can be run in the well with just one wireline trip. This type of wireline job might require the installation of a rig at the wellhead because the lubricator might need to be very long to accommodate the packoff assembly. The packoff assembly shown in the figure has a collar-recess stop which can only be installed in API tubing. For other types of tubing strings, a slip type stop might be needed. The upper and lower packoff seals force the gas to enter the tubing only through the gas lift mandrel. The gas lift valve installed in this way could be used to help unload the well to a deeper point of injection or to be the actual point of injection when the well is in normal operation. In fact, more than one point of injection can be installed in a well following this technique (the deeper one for the operating point of injection and the others as unloading gas injection points). Fig. 6.44 shows a gas lift mandrel in which the valve is installed inside the tubing as shown in Fig. 6.17d, but the most popular type of gas lift mandrel installed in packoff completions is the one shown in Fig. 6.17c.

Gas lift valves of  $\frac{5}{8}$ -in. or 1-in. OD are usually installed in packoff gas lift mandrels. There are some packoff-mandrel models, like the ones shown in Fig. 6.17c or d, in which not just one but two gas lift valves can be installed (providing more gas flow rate capacity at the expense of restricting the liquid flow rate through them).

A tubing joint that completely isolates the hole in the production tubing could also be installed between the upper and lower packers if a gas injection point is not needed at that depth. This is usually done in offshore wells or in very deep wells in general, that are very expensive to repair when an unwanted tubing-annulus communication, possibly caused by corrosion of the tubing string, appears.

A well on natural flow that can no longer produce (or its production has seriously declined) because its reservoir pressure has declined or the water cut has increased, could temporarily increase its liquid production on gas lift by installing a packoff assembly as shown in the Fig. 6.44. In this case, due to the fact that the reservoir pressure might still be high enough to be able to increase the liquid production using a shallow point of injection, a single point of injection might be a solution (while waiting for a workover rig to pull out the tubing string and run a gas lift completion in the well). In this case, the location of the perforated hole in the production tubing must be carefully calculated because the available gas injection pressure should be able to overcome the hydrostatic pressure of the liquid column that is generated when the liquids in the annulus are displaced by the injection gas into the tubing during the unloading operation. There are three ways of approaching this calculation:

1. The most conservative (safe) way of calculating the depth of the point of injection is to assume that the reservoir will not be able to absorb the liquid column that is generated after the liquids from the annulus are displaced into the tubing. In this case, it should be kept in mind that the volumetric capacity of the annulus is much greater than the volumetric capacity of the tubing; therefore, the liquid column length that is generated in the tubing is much greater than the change in depth of the annular liquid level. For that reason, the point of injection is not going to be very far down below the static liquid level. This might not be very efficient because the injection point could be too high up in the well.
2. The point of injection is calculated assuming that the reservoir will absorb the entire liquid column that is generated after the fluids in the annulus are displaced by the injection gas into the tubing. In this case, the gas is injected into the annulus until line pressure is achieved at



the wellhead. Then, it might be necessary to wait for several hours or days until the liquid level in the tubing descends to the static reservoir liquid level. With this procedure, the single point of injection is located as far down as possible, but it might not be a good solution: the gas pressure might not be sufficiently high to overcome the tubing pressure (if the data used in the calculations are slightly inaccurate) or it might be necessary to wait for a very long time to uncover (reach) the tubing–annulus communication. If the well does not produce sand and the fluids in the annulus do not cause formation damage, the waiting time could be reduced by injecting high-pressure gas into the tubing (on top of the liquid column) to force the liquid into the formation and be able to start liquid production sooner.

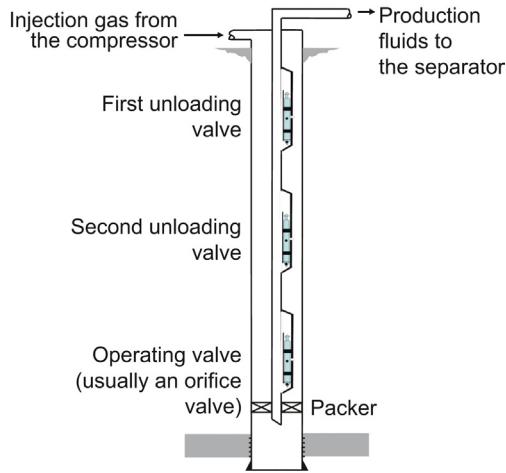
3. It might be a better solution to locate the tubing perforation somewhere in-between the two extremes just described. In this way, the point of injection might not be as deep as it could be, but the chances of being able to produce the well are increased.

## 6.4 TYPES OF COMPLETIONS FOR GAS LIFT INSTALLATIONS

Several types of completions that are currently used in gas lift installations are described in this section, together with their advantages and disadvantages and the operational conditions for which each of them is specifically suited.

### 6.4.1 Single completions

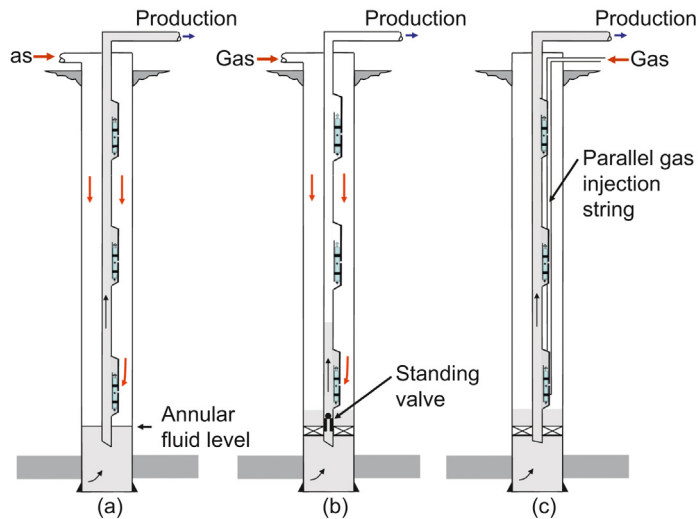
Fig. 6.45 shows the type of completion most frequently found in gas lift wells. This completion is called “semiclosed” because it has a packer that isolates the injection gas in the annulus but it does not have a standing valve installed at the bottom of the production tubing. Semiclosed installations can be used to produce the fluids up the tubing on continuous or intermittent gas lift. The gas lift valves could be wireline or tubing retrievable. The production tubing inside diameter should be adequate for the production flow rate. For continuous flow, a very small tubing diameter might restrict the liquid flow; however, if the diameter is too large, it might be necessary to have a very large injection flow rate to produce the well in a stable manner. For intermittent gas lift, very small-diameter tubing implies very small liquid volume lifted per cycle, for which a high cycle frequency is required, thereby increasing the injection gas/liquid ratio; however, if the tubing diameter is too large, the fallback losses might be very large because it would be necessary to inject the lift gas into the tubing at a very high flow rate to impart the liquid column an adequate velocity so that the gas will not bubble through the liquids.



■ FIGURE 6.45 Typical completion of a gas lifted well.

Fig. 6.46a shows an open completion (does not have a packer). This type of completion should not be used in gas lift installations because of the problems it creates:

- Formation fluids might damage the casing.
- The well could operate in an unstable manner because any change in the injection pressure induces a change in the annular liquid level.



■ FIGURE 6.46 Completions for gas lift wells with tubing liquid production.

- The annular liquid level should not reach the end of the tubing string because if it does, it could cause a considerable increase in the gas flow rate into the tubing that will make the injection pressure drop very fast and once the injection pressure is low, the reservoir pressure will be able to rapidly generate a new liquid column in the annulus until it is overcome again by the gas injection pressure (that has been increasing during this period because the surface gas injection flow rate has been maintained) to indefinitely repeat the injection cycle. Large liquid slugs produced in this way could increase the injection gas/liquid ratio, create serious problems at the flow station, and promote formation damage.
- Because the annular liquid level should be maintained between the point of injection and the end of the production tubing, it is not possible to decrease the bottomhole flowing pressure to its minimum possible value and, in consequence, the well cannot produce at its full potential.
- Every time gas injection into the well's annulus needs to be interrupted, it might be necessary to partially unload the well to start the well producing again. This could erode the deeper gas lift valves installed in the well.

Fig. 6.46b represents a closed completion because it has the production packer and a standing valve at the bottom of the tubing. This type of completion is used in intermittent gas lift operation, although the standing valve is not always necessary to produce the well on intermittent gas lift. If the point of injection is close to the formation, there is no sand production, and the injectivity of the well is small, standing valves are not necessary. But if the operating injection point is far from the formation and the liquid column below the injection point has a high gas content, then it is very important to install a standing valve just below the gas lift operating valve, otherwise a great percentage of the gas injection energy will be spent in compressing the gas–liquid column in the tubing below the point of injection.

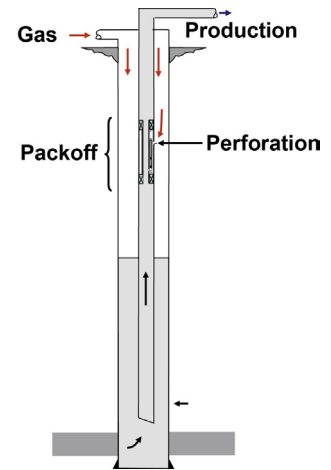
Fig. 6.46c shows a completions for wells in which the casing cannot withstand the high gas injection pressures or the injection gas is highly corrosive and should not contact the casing. In these situations, the gas is injected down a smaller diameter side pipe. The mandrel to be used in this type of completion is the one shown in Fig. 6.19d. When doing design calculations for this type of completion, it is very important to take into consideration the friction pressure drop along the parallel injection pipe. These pressure losses, and the fact that the high-pressure gas-storage volume is reduced, make this type of completion inadequate for choke-control intermittent gas lift, as explained in chapter: Design of Intermittent Gas Lift Installations (intermittent gas lift can only be implemented if surface intermitters are installed).

Fig. 6.47 represents a well that might have been producing on natural flow and it became necessary to inject gas to maintain the well producing at the desired liquid flow rate. Instead of pulling the completion out of the well and installing a gas lift completion, it might be temporarily convenient to simply punch a hole in the tubing and install a packoff assembly like the one shown in Fig. 6.44 in the previous section. Note that the annular liquid level is well below the point of injection (at the equilibrium point) and not just below it, as it would be if the well had a packer installed to isolate the annulus from the reservoir's fluids.

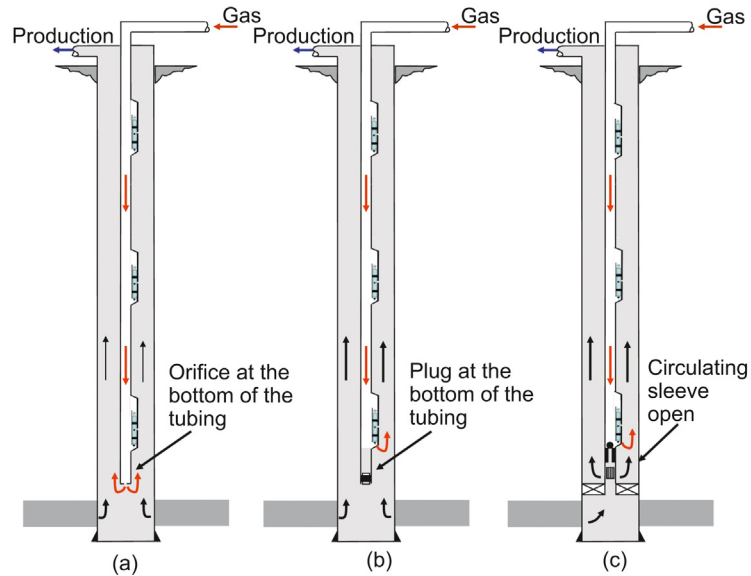
The depth of the point of injection must be calculated taking into account the available gas injection pressure at the surface. To increase the lifting efficiency, it is necessary to inject the gas as deep as possible. Several choices of calculating the point of injection for packoff installations are presented at the end of the previous section.

With the depth calculated by assuming that the reservoir will absorb the liquid column that is generated in the tubing when the fluids in the annulus are displaced into the tubing, it is not possible to quickly initiate liquid production because it is necessary to wait for the reservoir to absorb the liquids until the liquid level in the production tubing descends to the reservoir static liquid level. Even though it might take hours or days to start production, the injection point depth will be as deep as the injection pressure allows it to be. The waiting time can be reduced by following the recommendations indicated at the end of the previous section.

Fig. 6.48 shows several alternatives that can be used to inject the lift gas down the production tubing string and produce the liquids up the annulus. Mandrels for all of these completions could be the usual ones shown in Fig. 6.19a, or the ones specially designed for annular flow shown in Fig. 6.19c. Annular production is not recommended if the production fluids might damage the casing. It should also be pointed out that annular flow could be highly unstable if the well is not capable of producing at a liquid flow rate high enough to maintain a stable flow pattern (a very high injection gas/liquid ratio will then be necessary to stabilize the operation of the well). When the pressure losses in the tubing are very large, it might be advisable to produce the well in annular flow. Nodal analysis might be used to decide if the well is capable of sustaining annular flow but only as a rough approximation because multiphase flow correlations for annular flow are still in a developing stage. Fig. 6.48c shows a completion that can be used for both, annular or tubing flow. The well could initially produce on annular flow and then, when the reservoir pressure has declined, it can be produced on tubing flow (it is better not to use mandrels specially designed for annular flow for



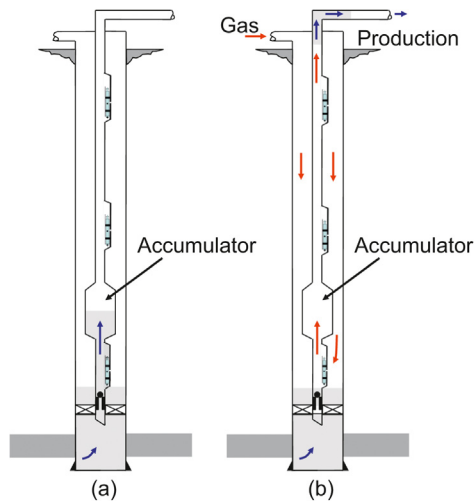
■ FIGURE 6.47 Packoff completion.



■ FIGURE 6.48 Completions for annular flow.

this type of completion). Completions shown in Fig. 6.48a, b have the advantage of being able to lower the point of injection below the perforations, which is a good option if the perforated interval (or the rat hole) is very long.

Fig. 6.49 shows a completion that is simply known as an “accumulator.” This completion is recommended for intermittent gas lift wells that would otherwise be good candidates for accumulation chambers if it were not for the high formation gas/oil ratio they produce. Accumulation chambers are described in Section 6.4.3. The size of the accumulator should be approximately 20% smaller than the length of the liquid column when the well is producing at the optimum injection frequency, so that it will be acceptable for future lower reservoir pressures (the optimum injection frequency gives the cycle time for which the daily liquid production is maximized). The inside diameter of the accumulator should not be very large to prevent large liquid fallback losses, as explained in chapter: Design of Intermittent Gas Lift Installations. Another reason for not having an accumulator with a very large inside diameter is to avoid very long liquid columns (generated when all the liquid has entered the smaller diameter production tubing located above the accumulator) that might be hard, or even impossible, to lift. Accumulators have the disadvantage of possessing smaller volumetric capacities, as compared to accumulation chambers, but they allow the formation gas to be vented to the surface more easily than in accumulation chambers. It is advisable to install

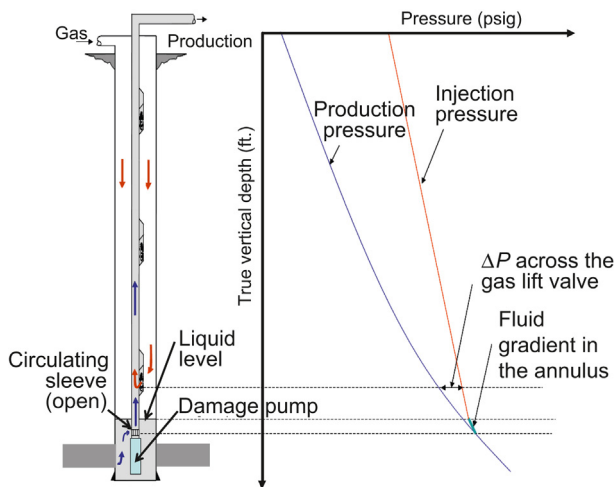


■ FIGURE 6.49 Simple-type accumulator.

two or three tubing joints (of a smaller diameter) between the deepest gas lift mandrel and the lower end of the accumulator, not only to have a gas lift mandrel of smaller diameter at the injection point, but also to allow the liquids to acquire a velocity greater than zero when the injection gas enters the accumulator, preventing in this way the large fallback losses that take place when trying to accelerate a liquid slug in a large-diameter tubing.

### 6.4.2 Gas lift as a backup method for electric submersible pumps

Electric submersible pumps are usually installed as the only artificial lift method in an oil well. There are oil fields in which gas lift and submersible pumps coexist but they are applied separately to each well. The wells with higher liquid production and lower formation gas/oil ratios are usually selected to be produced with electric submersible pumps; however, in some places, the completion is designed for both types of artificial lift methods because lift gas is readily available. The idea is to use gas lift as a backup method in case the pumping system fails. In this way, as soon as the well cannot produce on submersible pump, production is quickly started on gas lift while arrangements are made to fix the problem with the pumping system, which is a process that might take several weeks (or even months in remote places) to accomplish. It has been demonstrated that producing the well on electric submersible pump while injecting gas at the same time does not increase the efficiency of the lifting process. However, there are situations in which simultaneous application of both lifting methods represents a good



■ FIGURE 6.50 Open completion (well producing on gas lift).

engineering solution (eg, in a well where the required pump will not fit inside the casing, the same liquid flow rate can be obtained with a smaller pump and the help of aerating the tubing pressure using gas lift above the pump).

The completion shown in Fig. 6.50 is recommended only if the reservoir pressure is sufficiently large so that the distance between the operating point of injection and the circulating sleeve is long enough to keep the liquid level from reaching the circulating sleeve. If the circulating sleeve is too close to the gas lift mandrel, it is possible that the injection gas enters the circulating sleeve causing serious instability problems. This is the best completion for venting the formation gas to the surface when the pump is working, but the worst completion for gas lift. The injection point cannot be as deep as possible and, being an open completion, it tends to be more unstable. The liquid level in the annulus will be at the equilibrium point and it should be carefully calculated so that it would be located between the gas lift mandrel and the circulating sleeve.

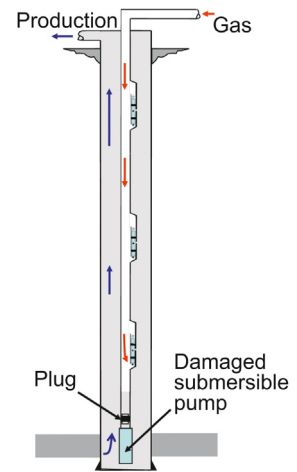
It can be seen in the pressure–depth diagram shown in Fig. 6.50 that the annular and tubing pressures are equal at the circulating sleeve. Above the circulating sleeve, the liquid gradient in the annulus (as shown in the figure for didactical purposes) is lighter (more vertically inclined) than in the tubing, but in reality they are usually very similar. The annular liquid level is the intersection point of the liquid and gas pressure curves in the annulus. A slight increment in the surface injection pressure could make the liquid level reach the circulating sleeve and the well might begin producing in an unstable manner. To avoid gas injection through the circulating sleeve, the production pressure should be accurately estimated using nodal analysis. With the tubing pressure and the injection pressure at depth, the pressure drop across

the gas lift valve ( $\Delta P$ ) can be calculated. The pressure drop across the valve is in turn used to precisely calculate the diameter of the injection orifice to be used so that the liquid level stays above the circulating sleeve.

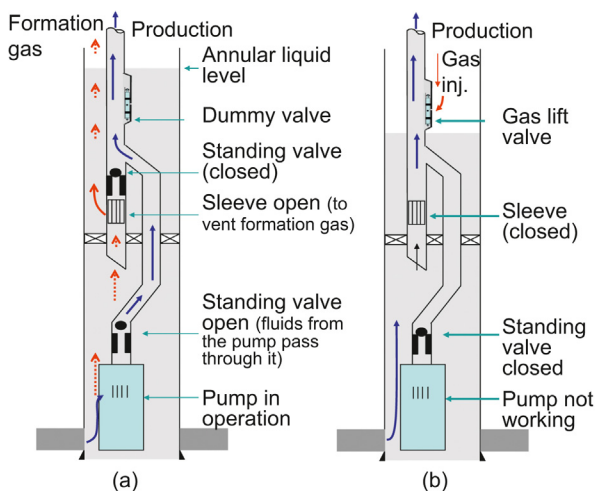
If the well is a good producer, capable of sustaining stable annular liquid production, a better choice is to use the completion shown in Fig. 6.50 but with the necessary modifications to inject the lift gas down the tubing and produce the liquids up the annulus as shown in Fig. 6.51, which is an alternative that has the advantage of not needing a packer to isolate the annulus (it is recommended to use mandrels specially designed for annular flow for this type of operation).

Fig. 6.52 shows a completion that allows the formation gas to be vented through the circulating sleeve installed above the special production packer. The standing valve above the circulating sleeve closes when the pump is turned on because the liquids coming from the pump are at a higher pressure. To produce the well on gas lift, the plug should be removed by wireline tools and the circulating sleeve needs to be closed. The point of injection can be located as deep as possible without having the typical instability problems present in open completions. Fig. 6.53 shows a completion that is basically the same as the one shown in Fig. 6.52, but with different equipment; a plug is installed instead of a standing valve when the well is on submersible pump. When the well is produced on gas lift, a packoff assembly could sometimes be used to isolate the pump but it is usually not required.

Fig. 6.54 shows an alternative in which a flapper valve is used. This valve is open only when the pump is in operation because it opens by the high

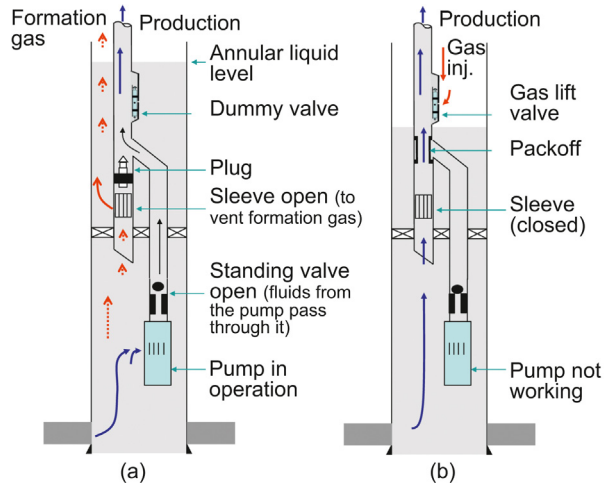


■ FIGURE 6.51 Open completion (well producing on gas lift with gas injection through the production tubing).



■ FIGURE 6.52 Completion with special packer and check valve.

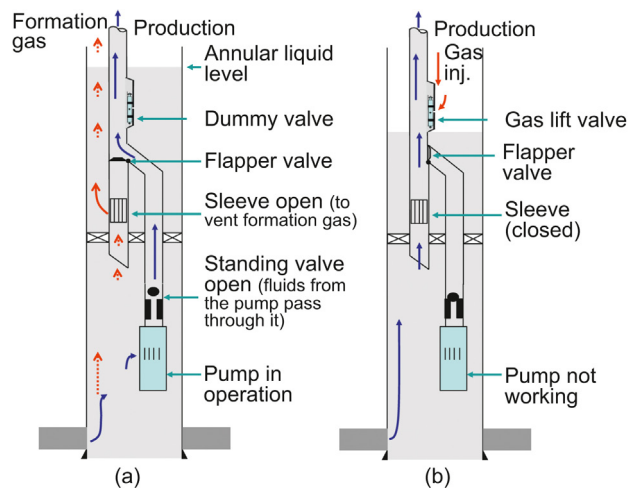




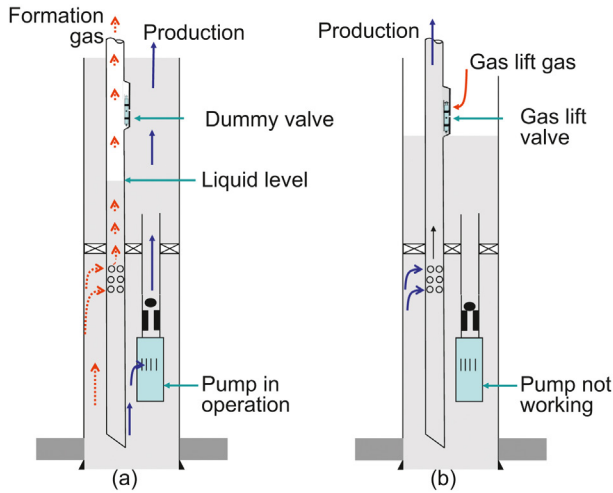
■ FIGURE 6.53 Completion with special packer and tubing plug.

pressure from the pump's discharge. The wireline jobs to be performed are fewer in this case; however, a wireline job is required to close the circulating sleeve and start the well producing on gas lift.

Fig. 6.55 shows a much simpler completion in which the pump produces directly to the annulus above the special production packer. When the well is produced on gas lift, the annulus is unloaded and gas is injected down the annulus as in a standard gas lift well. If the pump outside diameter is too



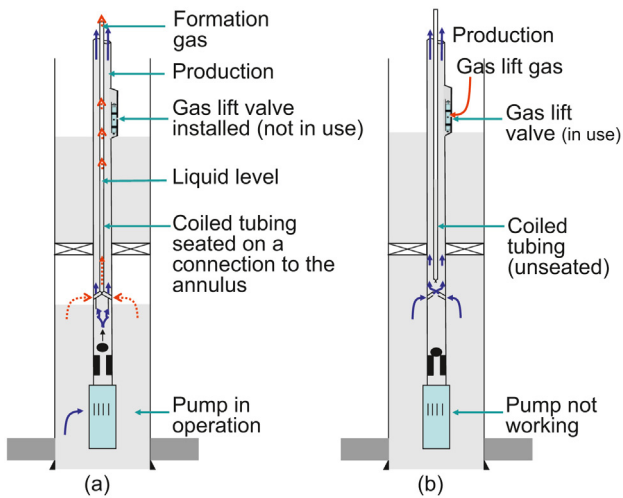
■ FIGURE 6.54 Completion with special packer and flapper valve.



■ FIGURE 6.55 Pump producing directly to the annulus.

large, the long, perforated tail pipe (tubing string below the packer) might not be installed (this pipe is only useful to promote gas–liquid separation when the pump is in operation).

Fig. 6.56 shows a completion that has the advantage of using a simple packer instead of a special one. When the pump is in operation, the formation gas is vented up a coiled tubing installed inside the production tubing with

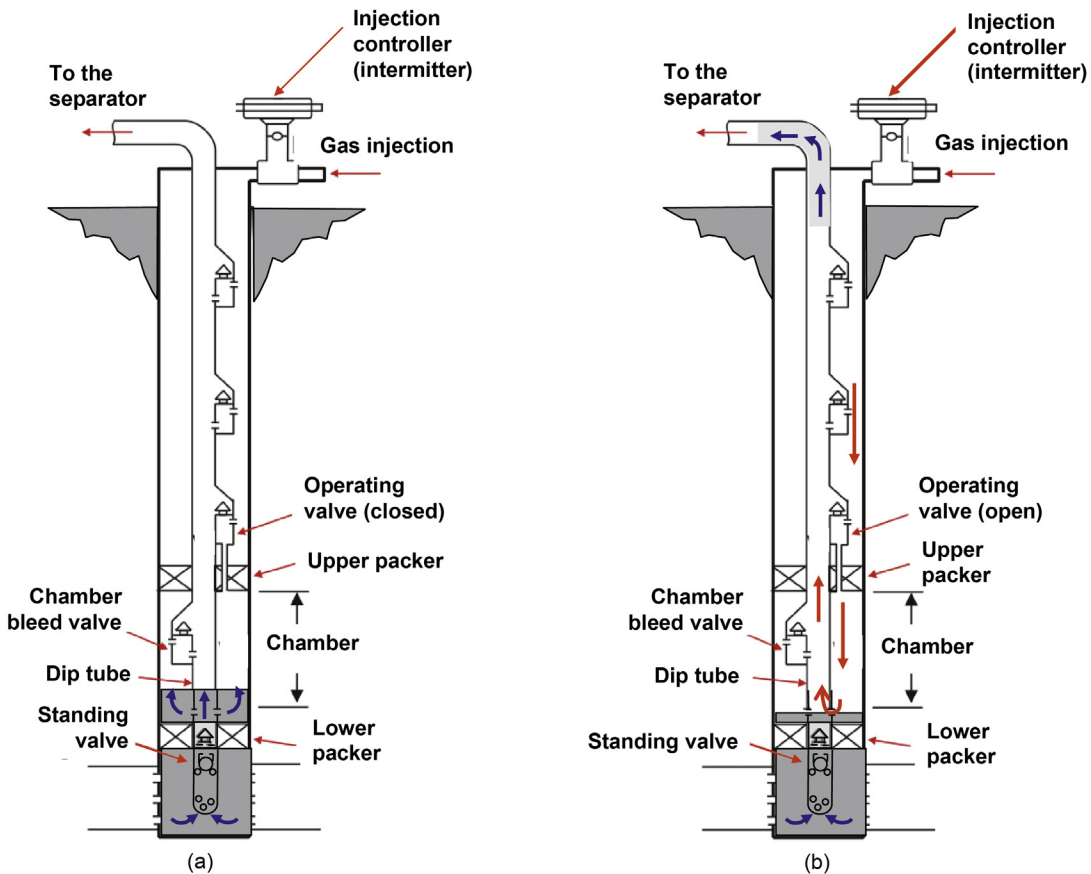


■ FIGURE 6.56 Formation gas vented through a central coiled tubing installation while the pump is in operation.

its lower end connected to a crossover seat. The fluids being pumped simply go around the coiled tubing connection on their way to the surface. When the well's lifting method is shifted to gas lift, the coiled tubing is unseated and neither gas nor liquids need to pass through it.

### 6.4.3 Accumulation chambers

Fig. 6.57 shows a double-packer accumulation chamber. Fluids from the formation enter the annular volume, enclosed between the two packers, through a perforated nipple located right above the lower packer. As the liquid level rises in the accumulation chamber's annulus, the gas trapped below the upper packer is vented to the production tubing through a bleed

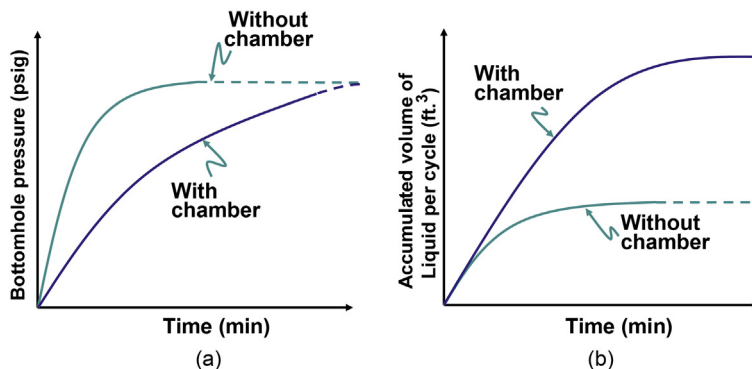


■ FIGURE 6.57 Double-packer accumulation chamber.

valve located right below the upper packer. The orifice diameter of the bleed valve should be large enough to allow all the gas trapped in the annulus to be vented as fast as possible, otherwise the liquid level in the dip tube will rise faster than the liquid level in the annulus. The bleed valve is usually a differential valve, although sometimes orifice valves of small diameters are used. In choke-control operations (without the use of surface intermitters, as explained in chapter: Design of Intermittent Gas Lift Installations) as the chamber is being filled with liquids, the lift gas at the surface is injected into the annulus above the upper packer, so that the injection annular pressure increases. The moment the liquid level in the chamber reaches the bleed valve should coincide with the injection pressure in the annulus reaching the opening pressure of the gas lift valve installed in the mandrel right above the upper packer. When the gas lift valve opens, high-pressure gas enters the upper part of the chamber, pushing the liquids downward and through the perforated nipple into the dip tube and from there to the surface. While gas is being injected, the standing valve located below the perforated nipple and the bleed valve are both closed. The distance between the standing valve and the perforated nipple should be long enough to accommodate the wireline tools needed to perform downhole pressure and temperature surveys as described in chapter: Intermittent Gas Lift Troubleshooting. This implies setting the lower packer as close as possible to the top of the perforations but the entrance of the production tubing could be located several feet below the lower packer. The standing valve should be located just above the entrance of the production tubing so that the pressure and temperature sensors can be placed between the standing valve and the lower packer. The perforated nipple should be located above the lower packer but as close as possible to it. Especial designs for the location of the standing valve and the entrance of the liquids into the annulus through the perforated nipple to handle sand and/or formation gas are shown in Figs. 10.5 and 10.31 in chapter: Design of Intermittent Gas Lift Installations.

In most cases, the injection gas/liquid ratio can be reduced in wells producing on intermittent gas lift by installing an accumulation chamber. This is due to the following factors:

1. For a given reservoir pressure, accumulation chambers allow the formation of larger liquid slugs at each cycle.
2. The increase in volume of gas injected per cycle needed to lift larger slugs is not as pronounced as the increase in the volume of liquid produced per cycle.
3. Since fewer cycles per day are needed when an accumulation chamber is installed, less time is spent injecting gas into the tubing to produce the liquid slugs.



■ FIGURE 6.58 Bottomhole flowing pressure and accumulated volume of liquid per cycle diagrams (with and without accumulation chambers).

Fig. 6.58 shows that with or without a chamber installed in the well the final bottomhole pressure is the same but the final accumulated liquid volume is much greater if a chamber is installed. The problem is that the time needed to fill the chamber with liquids is also greater than the time needed to generate a liquid column in a simple type completion. This is the reason why accumulation chambers usually do not increase the daily liquid production in a considerable manner, unless the productivity index is so large that it would take a very short time to fill the entire accumulation chamber with liquids.

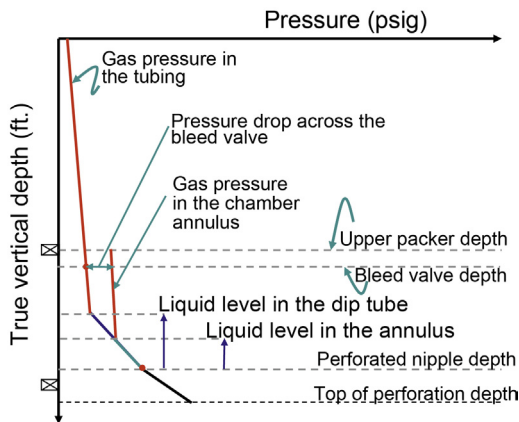
Double-packer accumulation chambers have the greatest volumetric capacity of all types of accumulation chambers. But these chambers are not recommended when the formation gas/liquid ratio is very large because the annulus could be filled with liquids with high gas content that might be difficult to vent. On the other hand, if the well produces sand it might be difficult to pull the completion out of the well if needed. In any case, accumulation chambers in general are more complex completions that increase the possibility of mechanical failures. The operating valve of the completion shown in Fig. 6.57 is installed in a specially designed mandrel for chamber completions. The gas exits the gas lift valve into a snorkel that directs the flow through the upper bypass packer and into the chamber annulus. The snorkel is usually a pipe of 0.5 in. in diameter. Valves installed in these mandrels cannot have lower integral latches in most cases. Fig. 6.19b shows the usual cross-section of the mandrels that are installed above the upper packer.

It is also important to know that the operating valve cannot be used to unload the well. For example, if the mandrel spacing calculation procedure indicates that an unloading valve should be located right above the upper packer, then the operating valve should be installed above the upper packer and the unloading valve should be installed 30–60 ft. above the operating valve. If the

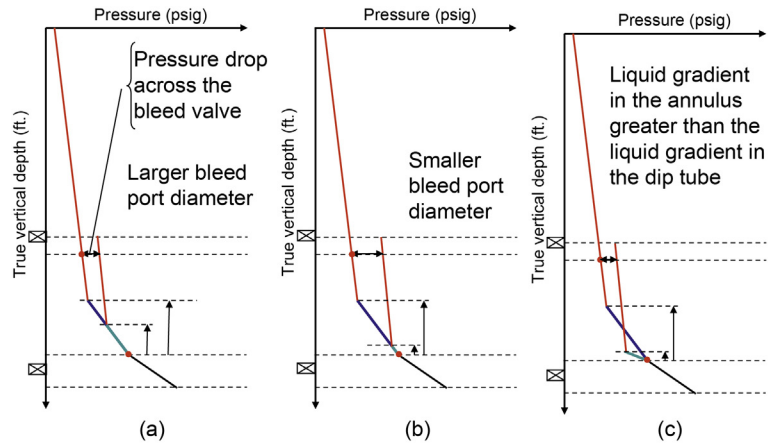
operating valve is also used as an unloading valve (as it is done for simple type completions), then the operating valve should be able to unload the fluids located above the chamber and inside of it at the same time, which would require an injection pressure that might be larger than the available injection pressure.

The optimum size of an accumulation chamber for a particular well (the size that maximizes the well's daily liquid production) might not be possible to be properly operated because the available injection pressure might not be large enough. Once the fluids enter the production tubing above the accumulation chamber, the liquid column that is generated might be so large that a very high hydrostatic pressure would need to be overcome to lift the fluids at an acceptable velocity (as explained in chapter: Design of Intermittent Gas Lift Installations, large liquid fallback losses are obtained when the slug velocity is very low). On the other hand, this high hydrostatic pressure might also open an unloading valve as the liquid slug travels to the surface making the lifting process less efficient. In these cases, it is better to have shorter accumulation chambers that will be fully filled with liquids (instead of having long accumulation chambers that can only be partially filled with liquids, which is something that will increase the injection gas/liquid ratio because the entire chamber needs to be filled with high-pressure gas to produce the liquid slug at each cycle). If the reservoir pressure is expected to decrease, it is also recommended to install accumulation chambers of sizes that are shorter than their current optimum lengths.

Fig. 6.59 shows a pressure–depth diagram with the conditions that take place as the accumulation chamber is being filled with liquids. As it can be appreciated in the diagram, the liquid levels in the annulus and in the



■ FIGURE 6.59 Gas and liquid pressure profiles along a chamber installation as it is being filled with liquids.

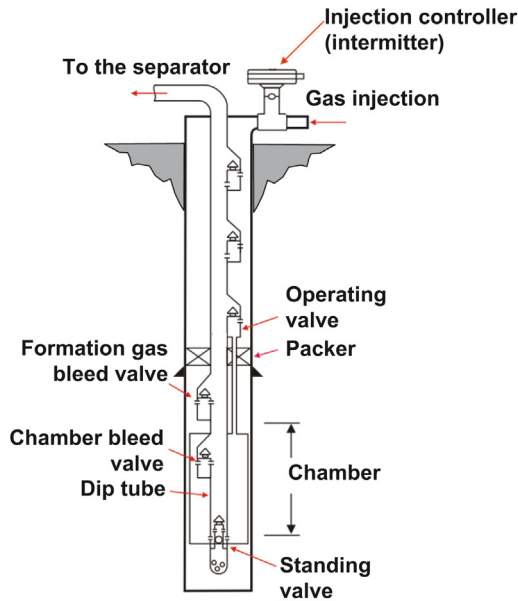


■ FIGURE 6.60 Effect that the bleed valve orifice size and the liquid pressure gradients have on the difference between the liquid levels in the annulus and in the dip tube.

dip tube are different because of the pressure drop across the bleed valve. Fig. 6.60b shows what could happen if the orifice diameter of the bleed valve is very small: a slight increment in the pressure drop across the bleed valve causes a considerable difference between the liquid levels in the annulus and in the dip tube. On the other hand, Fig. 6.60c shows what happens if the well produces too much gas. The gas separation that takes place as the liquids enter the annulus could make the pressure gradient in the dip tube be much smaller than the gradient in the annulus so that, even with a small pressure drop across the bleed valve, the difference between the liquid levels in the annulus and in the dip tube could be very large.

In the installation of double-packer accumulation chambers, once the setting depth has been reached and the lower packer is set, setting down several thousands pounds of tubing weight onto the upper packer (known as the bypass packer) will shear the bypass-packer shear pin and compress its rubber seals against the casing wall. Additional tubing weight is then placed on the bypass packer to complete its installation. To retrieve the chamber, it is usually only necessary to pull the tubing string upward to allow the seals of the bypass packer to return to their original position. If rotation of the tubing is necessary to release the lower packer, rotation may be achieved through most bypass packers. Once the lower packer is released, the entire installation can be pulled out of the well.

Fig. 6.61 shows an inserted accumulation chamber. This type of accumulation chamber is recommended if the perforated interval (or the rat hole) is very long. In this type of completion, the fluids inside the accumulation



■ FIGURE 6.61 Inserted accumulation chamber.

chamber do not exert any pressure on the formation. These accumulation chambers can achieve the lowest possible bottomhole flowing pressures. For these reasons, inserted accumulation chambers always increase the liquid production, independently of the value of the productivity index. Inserted accumulation chambers also reduce the injection gas/liquid ratio for the same reasons explained earlier for double-packer accumulation chambers.

As explained for double-packer accumulation chambers, for inserted accumulation chambers the operating valve cannot be used as an unloading valve. Also, care should be taken to avoid the formation of large liquid columns in the tubing (above the packer) that might be difficult to lift or that might open an unloading valve.

Two gas bleed valves are required, one for the internal annulus of the inserted accumulation chamber itself and another one for the gas–liquid mixture between the casing and the inserted accumulation chamber. The accumulation chamber gas bleed valve could be a differential valve or a small-diameter orifice valve. The calculation of the size of the bleed valve port is explained in chapter: Design of Intermittent Gas Lift Installations.

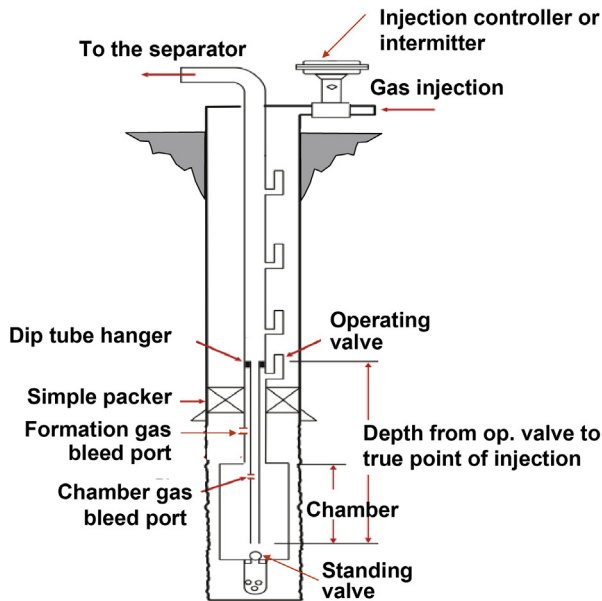
The formation gas bleed valve (right below the packer) requires a more profound explanation. Due to the fact that an inserted accumulation chamber



behaves like a gas–liquid separator, in which liquids enter the accumulation chamber through the lower chamber inlet and the gas tends to travel upward and enters the tubing string through the formation gas bleed valve, a complex multiphase flow pattern takes place in the annulus between the casing and the accumulation chamber. Due to the formation gas, the pressure gradient in the annulus (between the casing and the inserted accumulation chamber) is smaller than the pressure gradient of the fluids that accumulate at the bottom of the accumulation chamber. This difference in pressure gradient forces the lower standing valve to close at the early stages of the liquid accumulation period. From that moment on, all gas and liquids coming from the formation must be handled by the formation gas bleed valve located between the packer and the accumulation chamber. For this reason, the formation gas bleed valve should be designed to handle multiphase flow and not just single-phase gas flow. Instead of a typical bleed valve for the formation gas, it is better to install a large diameter check valve. This valve will allow the flow of gas and liquids from the formation when the lower standing valve closes, but it should close as soon as the operating gas lift valve opens and high-pressure gas enters the chamber to produce the accumulated liquids. At the early stages of the liquid accumulation period, the liquids enter the chamber through the lower standing valve until this valve closes. Then, the liquids that enter the tubing through the upper check valve (above the chamber) drop to the bottom of the chamber, filling the chamber with liquid from above while the formation gas is vented upwardly toward the wellhead. The pressure–depth diagram that explains this process is very similar to the one used for the “inserted accumulator” that is presented at the end of this section, see [Figs. 6.71 and 6.72](#).

As with double-packer accumulation chambers, inserted accumulation chambers do not operate efficiently if the formation gas/liquid ratio is very large, but due to the gas–liquid separation effect that inserted accumulation chambers introduce, these inserted completions can handle formation gas better (as long as the upper check valve has been correctly designed for multiphase flow). Inserted accumulation chambers should never be used if the well produces sand because it might be very difficult to pull them out of the well. Inserted accumulation chambers introduce an additional level of complexity to the completion, increasing the probability of mechanical failures.

Because of the way the dip tube is installed, the inserted accumulation chamber shown in [Fig. 6.62](#) does not need a special (usually expensive) packer. This dip tube should be carefully designed because it might create a high flow restriction as the liquid slug passes through it. Another disadvantage of this type of completion is that the dip tube should be pulled out of the well every time the gas lift valve needs to be replaced. Finally, a



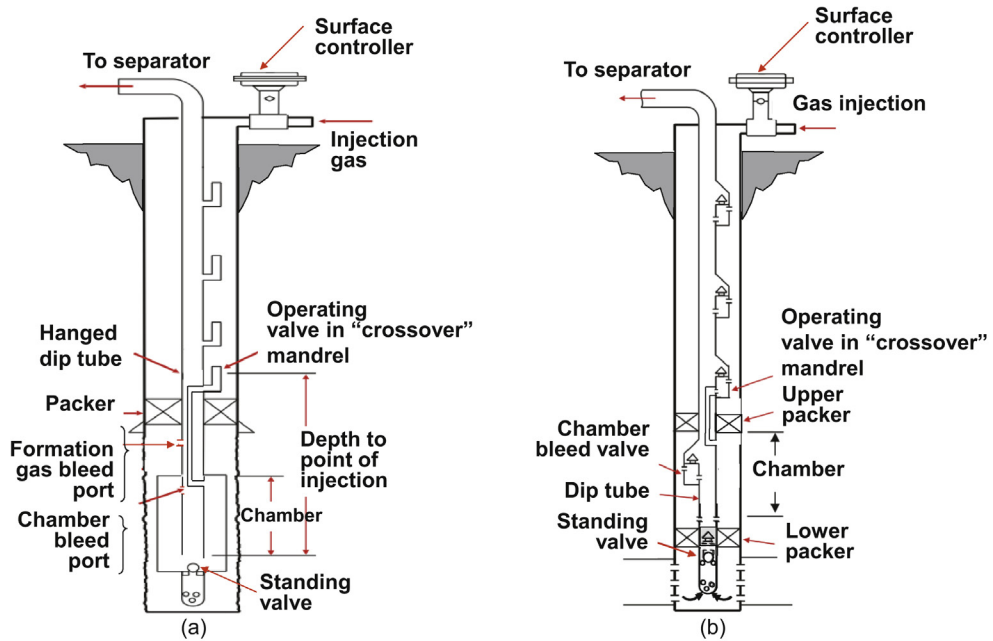
■ FIGURE 6.62 Inserted accumulation chamber with a simple-type packer.

large check valve (instead of a standard bleed valve) should be used to vent the formation gas (for the same reasons explained for the inserted chamber shown in Fig. 6.61).

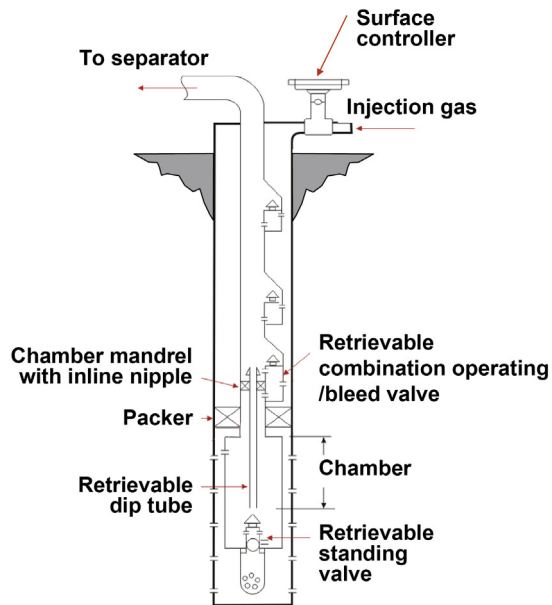
Fig. 6.63 shows an insert accumulation chamber and a double-packer accumulation chamber with crossover mandrels that allow the use of simple type packer with the additional advantage that gas lift valves can be replaced without having to pull the dip tube out of the well. But all the other disadvantages explained for the inserted accumulation chamber shown in Fig. 6.62 also apply to this type of completion.

Fig. 6.64 shows another type of arrangement for insert accumulation chamber in which the operating gas lift valve behaves as a bleed valve while the chamber is being filled with liquids. When the injection pressure in the annulus reaches the valve opening pressure, the gas lift valve stops functioning as a bleed valve and operates as an injection valve. The dip tube can, in most cases, be retrieved by a simple wireline operation. The limitations explained for the last two completions above also apply to this type of insert chamber.

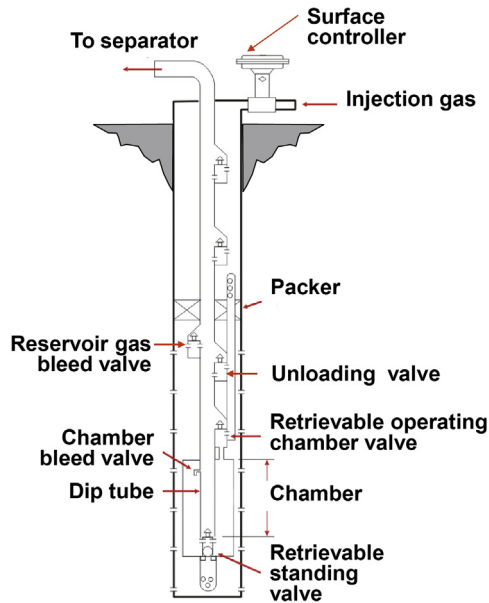
Fig. 6.65 shows an insert accumulation chamber located far below the packer. This type of completion might require unloading valves below the



■ FIGURE 6.63 Insert and double-packer accumulation chambers with crossover mandrel.



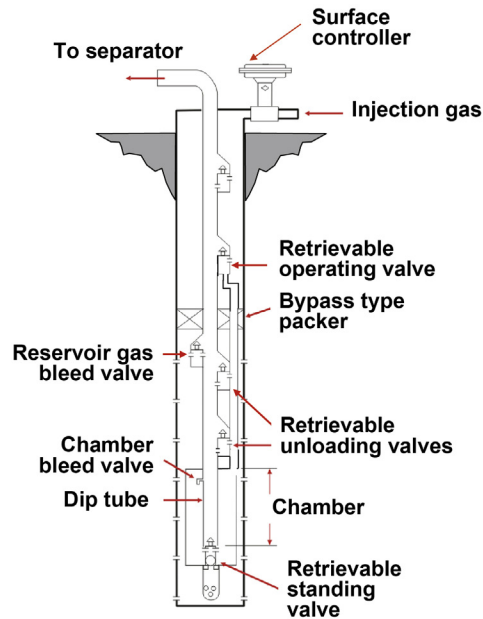
■ FIGURE 6.64 Insert chamber with dual-action gas lift valve.



■ FIGURE 6.65 Insert accumulation chamber located very far below the packer (unloading valves are required below the packer).

packer, as shown in the figure. This arrangement might have problems if it is produced on choke-control intermittent lift instead of using a surface intermitter. The intermitter needs to be used to force the operating gas lift valve (the chamber valve right above the chamber) to remain open while the surface intermitter is opened. This is due to the fact that the instantaneous gas flow rate that takes place when the gas lift valve opens is usually so high that the injection pressure drop due to friction in the parallel injection pipe is very large. On choke-control, the injection pressure at valve's depth might reach the operating valve's closing pressure before the pressure in the annulus (above the packer) can be reduced to its required value to inject all the volume of gas needed per cycle.

The problem described in the last paragraph can be overcome (so that choke-control intermittent gas lift can be implemented) by installing the completion shown in Fig. 6.66, where the operating valve is installed right above the packer and not on top of the chamber. This valve is calibrated with an opening pressure lower than the closing pressures of all the gas lift valves installed below the packer. In this way, the operating valve (just above the packer) is always open during the unloading of the well below the

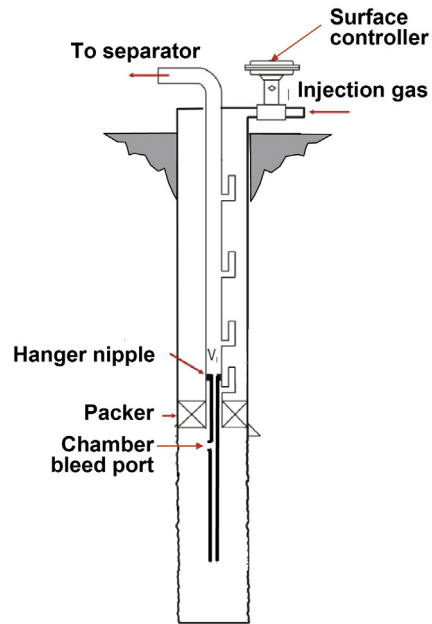


■ FIGURE 6.66 Insert accumulation chamber located very far below the packer, with the operating valve above the packer and the unloading valves below the packer.

packer; however, during the normal operation of the well (after it has been unloaded), the operating valve above the packer opens and closes while all the gas lift valves below the packer remain closed all the time.

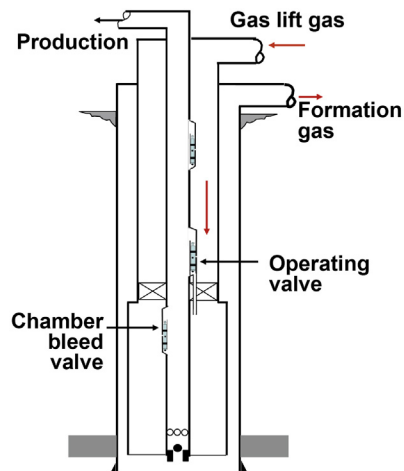
Fig. 6.67 shows an arrangement that can be used in openhole completions for consolidated sands. The volume between the production sand and the dip tube is used as an accumulation chamber. The dip tube is hanged just above a conventional gas lift valve or a wireline-retrievable valve in a crossover mandrel. It is important to have a bleed port in the dip tube to be able to vent the formation gas (in case a dual-action gas lift valve is not installed as shown in Fig. 6.64). The problem with this type of completion is that the dip tube might restrict the liquid flow when the liquid slug passes through it. If a crossover mandrel is not used, it might be necessary to pull the dip tube out of the well to change the operating gas lift valve.

Fig. 6.68 shows an accumulation chamber (totally isolated from the casing) that could be a good solution if the casing cannot be exposed to high gas injection pressures or the injection gas is highly corrosive. The advantages of this type of completion are: (1) it can be installed at, or below, the perforations, and (2) it is an excellent way of venting the formation gas before the



■ FIGURE 6.67 Insert accumulation chamber for openhole completions in consolidated formations.

liquids enter the accumulation chamber. The main disadvantage (besides the additional tubular goods that are needed) is its reduced volumetric capacity (for the injection gas above the packer as well as for liquid accumulation in the accumulation chamber) compared to a standard double-packer

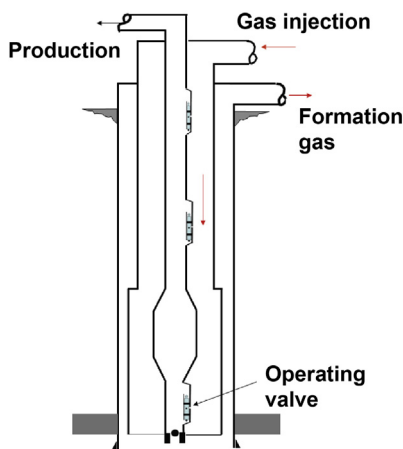


■ FIGURE 6.68 Accumulation chamber isolated from the casing.

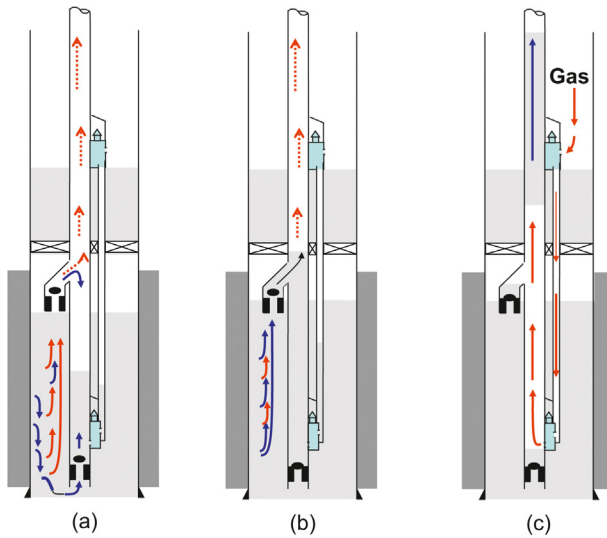
accumulation chamber. If the volume of the inner annulus above the packer that is used to store high-pressure injection gas (between the production tubing and the production casing) is very small, it might not be possible to implement choke-control intermittent gas lift because the required gas lift valve area ratio could be larger than the largest commercially available area ratio. As explained in chapter: Design of Intermittent Gas Lift Installations, the larger the operating gas lift valve's area ratio is, the larger the difference between the valve's opening and closing pressure (known as the spread of the valve) becomes and therefore a larger volume of gas (from the annulus into the chamber) can then be injected per cycle. If the largest available area ratio is still too small, an intermitter needs to be used to force the gas lift valve to remain open for as long as it is necessary to inject the required volume of gas per cycle.

The explanation given in the last paragraph for the accumulation chamber of Fig. 6.68 also applies to the accumulator shown in Fig. 6.69. The additional disadvantage of the accumulator shown in Fig. 6.69 is that its volumetric capacity is even smaller than the completion shown in Fig. 6.68. The inherent advantage that accumulators in general have (of being able to handle formation gas better) might not be important in the type of isolated completion shown in Fig. 6.69 because the outer annulus already acts as a formation gas/liquid separator.

Fig. 6.70 shows an insert accumulator. This type of completion is recommended for wells with long perforated intervals or long rat holes. As it is the case for accumulation chambers, insert accumulators also reduce the injection gas/liquid ratio but, at the same time, they can increase the liquid



■ FIGURE 6.69 Accumulator isolated from the casing.

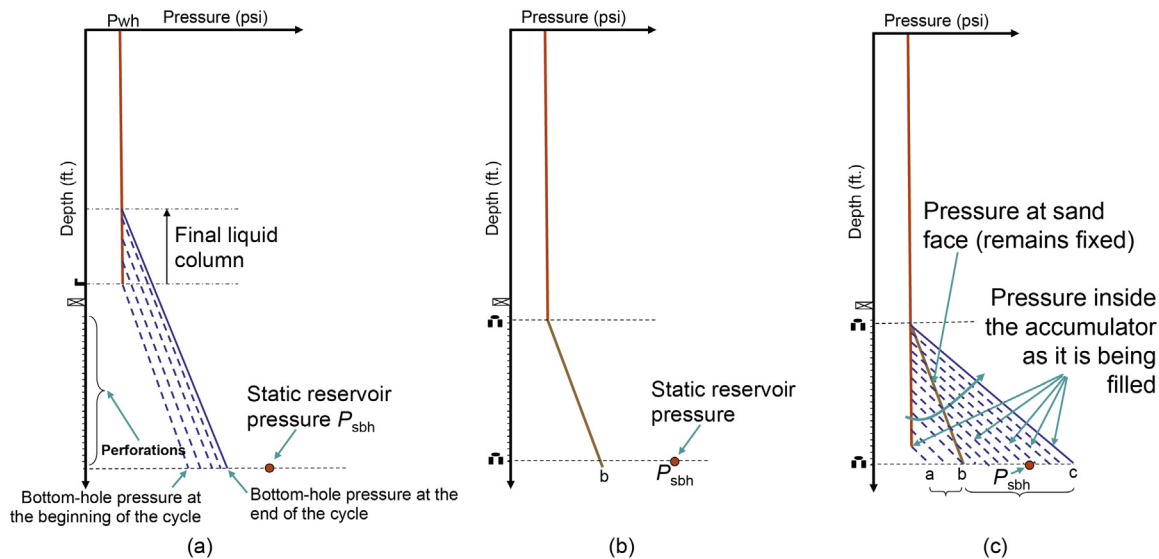


■ **FIGURE 6.70** Insert accumulator. (a) initial liquid accumulation stage; (b) final liquid accumulation stage; (c) gas injection.

production even if the productivity index is not very large because of the very low bottomhole flowing pressures they can achieve at, or below, the perforations. They also handle formation gas better than any type of accumulation chamber installation. Additionally, they are not very complex installations; therefore, the possibility of any mechanical failure is reduced. The operating valve should be installed in the upper mandrel right above the packer. If this valve is installed in the lower mandrel, it is possible that the valve closes prematurely. This is due to the fact that the instantaneous gas flow rate (when the gas lift valve opens) is usually very large, so the injection pressure drop in the parallel injection pipe is also very large. If the valve is installed at the lower mandrel, the injection pressure at valve's depth might reach the operating valve's closing pressure before the pressure in the annulus above the packer can be reduced to its required value to inject all the volume of gas needed per cycle. Another point to consider is that the diameter of the accumulator should not be very large because of the following reasons: (1) to avoid very large liquid slugs (when they travel in the production tubing above the packer), which might be difficult to produce or might open an unloading valve, and (2) to avoid large liquid fallback losses, common in large-diameter tubing.

Finally, just as explained for insert accumulation chambers, the formation gas bleed valve (upper standing valve in the Fig. 6.70) should be able to handle multiphase flow and not just single-phase gas flow. The accumulator





■ FIGURE 6.71 Pressure–depth diagrams for an insert accumulator.

(a) Conventional intermittent gas lift, (b) accumulator (pressure at sand face throughout the liquid accumulation period), (c) accumulator (pressure inside the accumulator during the liquid accumulation period).

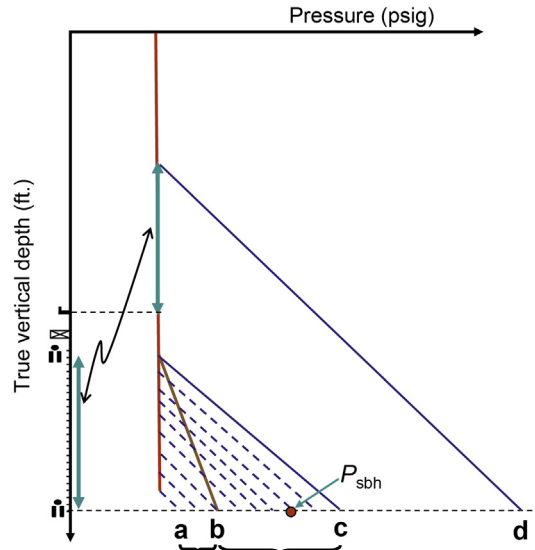
acts as a gas–liquid separator, in which a complex multiphase flow takes place in the annular volume located between the accumulator and the perforations, with the formation gas moving upward while part of the liquid falls to the bottom. At the beginning of the liquid accumulation period, liquids with very little gas enter the accumulator through the lower standing valve shown in the figure, generating a liquid column that, thanks to its low gas content, has a heavier pressure gradient than the pressure gradient in the annulus. This causes the lower standing valve to close very early in the cycle, forcing the gas and liquids from the formation to enter the accumulator through the upper standing valve only. The liquids through the upper standing valve then fall and accumulate at the bottom of the accumulator while the formation gas is produced to the surface. This latter way of accumulating the liquids inside the accumulator takes place during most of the liquid accumulation period. Once the accumulator has been filled with liquids, the gas lift valve opens and gas enters the accumulator through the lower mandrel (which should have a circulating valve to protect its side-pocket polished bore). While gas is being injected, its high pressure makes the upper and lower check valves close and the liquids are lifted to the surface. This process is illustrated in the pressure–depth diagrams shown in Fig. 6.71.

In Fig. 6.71a, the bottomhole flowing pressure as a function of time is illustrated for a well producing on intermittent gas lift with a conventional, simple type, closed, or semiclosed completion. The minimum bottomhole pressure possible is reached at the beginning of the cycle. Then, when the

bottomhole flowing pressure is approximately half the static reservoir pressure ( $= P_{sbh}/2$ ), the liquid column should be lifted because the time interval required to reach this bottomhole pressure usually coincides with the cycle time for which the daily liquid production is maximized. Waiting for the bottomhole pressure to increase any further would make the daily production decline because the rate at which the liquid level rises in the tubing declines to very low values as the bottomhole pressure increases. The time interval between two consecutive dashed lines in the figure is constant. Notice that the final dashed lines are drawn closer together. This is because it is more difficult to increase the liquid column length due to the greater pressure the liquid column itself exerts on the formation.

Fig. 6.71b shows the pressure at sand face (or annular volume below the packer) in a well with an insert accumulator while the inside of the accumulator is being filled with liquids. This annular pressure remains constant throughout the liquid accumulation period. In Fig. 6.71c both, the pressure at sand face and inside the accumulator, are shown. The pressure inside the accumulator increases as it is being filled with liquids. At the beginning, the pressure just above the lower standing valve (point “a”) is lower than the pressure at the same depth but outside the accumulator (sand face), which is at point “b.” While the pressure inside the accumulator goes from “a” to “b,” liquids are able to enter the accumulator through the lower and upper standing valves. But when the pressure at the bottom of the accumulator reaches point “b” the liquids enter into the accumulator only through the upper standing valve because the lower one is closed due to the weight of the low gas content liquid column that has been regenerated at the bottom of the accumulator. The accumulator continues to fill with liquids from above until the liquid level inside the accumulator reaches the upper standing valve. At that time, the pressure at the bottom of the accumulator is at point “c” which can very well be larger than the reservoir pressure. This is possible because the liquids inside the accumulator do not exert any pressure on the reservoir.

Two points should be noticed in Fig. 6.71c. First, the pressure gradient outside the accumulator is lighter (more vertically inclined) than the gradient inside of it because the liquids inside the accumulator have very little gas content, while at the outside the formation gas makes the pressure gradient lighter. Second, the dashed pressure lines inside the accumulator (after the bottom pressure inside the accumulator has reached point “b”) are shown at equal distance between each other to emphasize the fact that the accumulator fills at a constant rate (because the pressure at sand face is approximately constant). The time interval between two consecutive dashed lines is constant. This constant flow rate is approximately equal to the maximum liquid



■ FIGURE 6.72 Effect of a liquid column accumulated inside an insert accumulator if it could be placed right above the operating valve in a simple-type completion.

flow rate that can only be obtained in a well with a simple type completion on intermittent gas lift for a brief moment at the beginning of the liquid column generation period. As the liquid column increases in length, its own pressure will make this maximum rate to decline in a well with a simple type completion. This is why an insert accumulator always increases the liquid production if the perforated interval is long. In fact, if the liquid column an insert accumulator can generate is placed right above the operating valve, it will cause a bottomhole pressure much greater than the reservoir pressure, as illustrated in Fig. 6.72.

#### 6.4.4 Dual wells

When a well has two or more liquid- or gas-producing zones, there are many ways in which the completion can be installed to produce all zones simultaneously and separately from one another. In many cases, one zone is on natural flow and the other is produced on some type of artificial lift method. When both zones are produced on gas lift, the best thing to do is to have a different gas source for each zone. In this way, the gas flow rate that goes to each tubing string in the well can be separately controlled at the surface. If a single gas source is used to simultaneously lift both strings, it is advisable to follow the recommendations given in chapter: Design of Continuous

Gas Lift Installations regarding the design procedures for dual wells. In this latter case, it is extremely important to know the IPR curve of each zone to be able to design both strings.

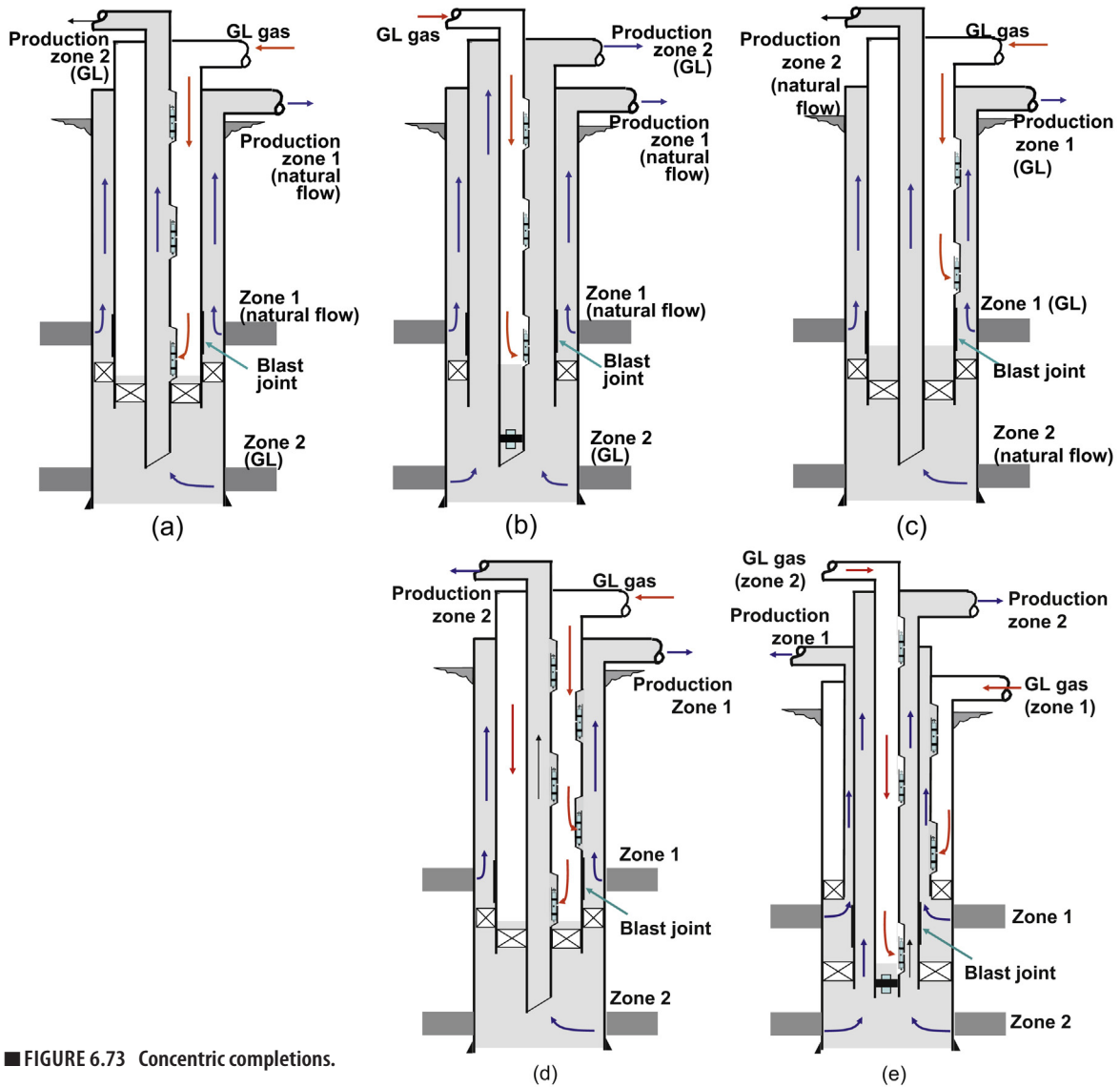
In all types of dual wells, it is necessary to use a blast joint at the point where one zone produces against the tubing string of the other zone. Fluids produced by one zone may contain sand that might hit the tubing string of the other zone at that depth and cause erosion. Blast joints are heavy-walled subs used for abrasion resistance opposite producing perforations.

Packers to be used in dual wells can be hydraulic or weight set packers. If one string has oval-shaped (or conventional) mandrels, then packers set or released by tubing rotation should not be used. Hydraulic packers are more expensive but they don't have the problems that are found in weight set packers. If the upper zone is on natural flow with a high reservoir pressure and the lower zone is produced on gas lift, a high pressure differential occurs across the top packer when the upper zone is shut in. This pressure differential might release the top packer. In these cases, an integral hydraulic hold-down for an upper retrievable type packer should be considered.

Wellheads for parallel-string completions must be large enough to allow the mandrels of one of the strings to move up or down without difficulty if both strings are not simultaneously run into or pulled out of the well. One tubing string should have beveled couplings or integral streamlined joints to prevent hanging up during running and pulling operations. External upset tubing couplings might be turned down for additional clearance.

For parallel-string dual completions, it is recommended to install landing nipples that can be used to: place plugs to set hydraulic packers, isolate one zone, test one string, install standing or safety valves, etc. The depths of the mandrels in parallel-string dual wells should be carefully evaluated. While running the second string, no two mandrels on this string should pass two mandrels on the other string at the same time. If the bottom mandrels for both strings are located near the same depth, the bottom mandrel for the second string should be located one joint above the bottom mandrel for the other string. A circulating device such as a sliding sleeve or a retrievable valve mandrel with equalizing dummy should be installed between the packers in a dual well for cleaning up, killing, or treating the upper zone.

Some examples of completions with concentric strings are described before presenting typical dual-well completions with parallel strings. [Fig. 6.73](#) shows several alternatives for concentric dual completions. They are less



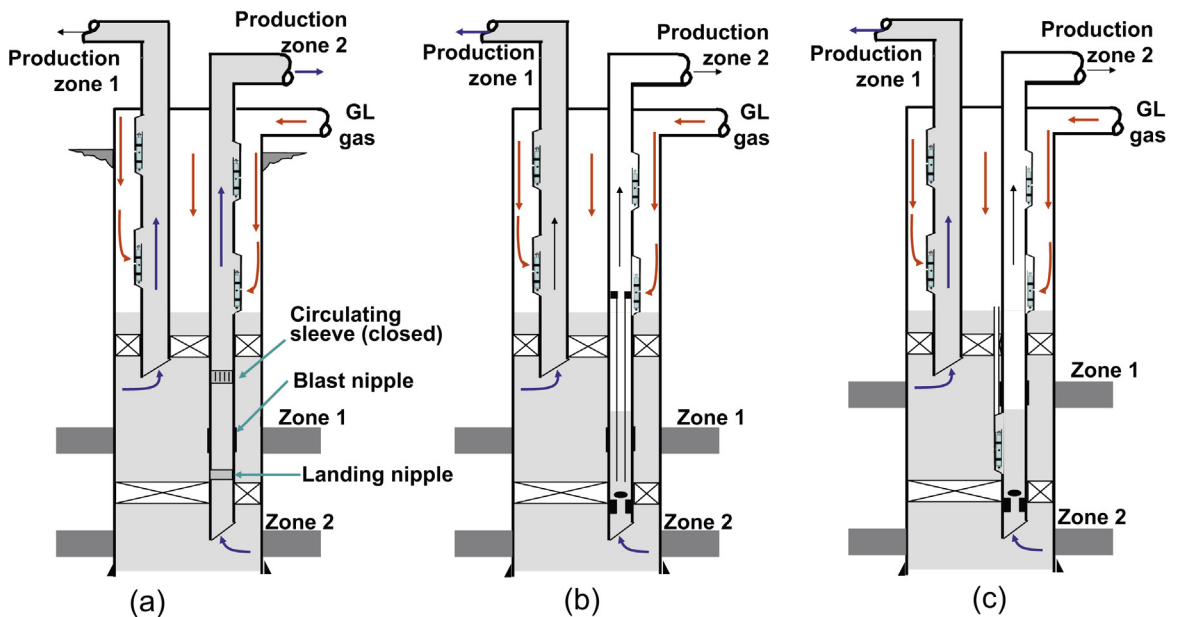
■ FIGURE 6.73 Concentric completions.

expensive because they do not require special wellheads or packers but, in general, these completions have the following serious problems:

- The following operations can only be performed in the central string: running bottomhole flowing pressure and temperature surveys, taking fluid and solid bottomhole samples, cleaning paraffin or any other deposition along the tubing.

- For completions shown in Fig. 6.73c–e, it is not possible to change the gas lift valves in the outer tubing without pulling the completion.
- For completions shown in Fig. 6.73b–e, intermittent gas lift cannot be implemented when the liquids are produced up the annulus because the fallback losses and the required volume of gas per cycle could be very large.
- The outer packers (installed below one of the producing zones) might be difficult to pull from the well if sand accumulates on top of them.
- Exposing the casing to the produced fluids might damage the well because of corrosion or abrasion of the casing.
- The production pressure must be high enough to produce the well up the annulus in a stable manner.
- There are no reliable multiphase flow correlations for flow in annular conduits.

Fig. 6.74 shows examples of parallel-string completions. In this type of completion, a special upper packer and a standard lower packer are required. The wellhead should be specially designed to hang two parallel strings. The main advantages of these completions are: (1) bottomhole fluids and solid samples can be taken from both zones; (2) downhole flowing temperature



■ FIGURE 6.74 Parallel completions for dual wells.

and pressure surveys can be run in both strings; (3) all gas lift valves can be installed and retrieved by wireline operations; (4) cleaning jobs to get rid of paraffin or other depositions can be performed in both strings; (5) intermittent gas lift can be implemented in one or both zones; and (6) the casing is not exposed to reservoir fluids.

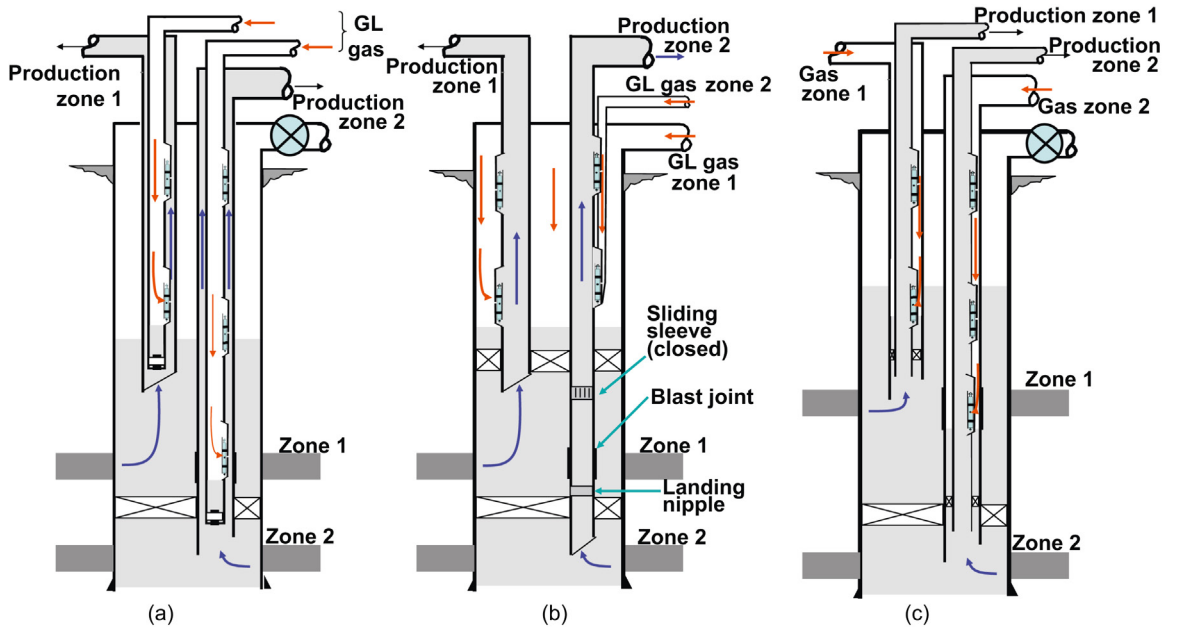
The most important disadvantages are: (1) the gas source is common to both strings, making it difficult to control the injection gas flow rate to each of them; (2) due to space limitations, only small-diameter tubing could be used (two strings of 2-in. nominal OD tubing can be installed in a 7-in. OD casing and two strings of 1.5-in. nominal OD tubing can be installed inside a 5½-in. OD casing); and (3) the point of injection of the long string could be located too far up above the perforations, with serious consequences if the reservoir pressure is very low.

Fig. 6.74b shows a completion in which the actual gas injection point of the long string is very close to zone 2 with an arrangement similar to an accumulation-chamber installation. This might be the only way to produce a lower zone if its reservoir pressure is too low or if it is located too deep below the upper packer. In these cases, the operating valve is a dual-operation valve (injection and venting action) but it could also be a standard valve if a formation gas bleed port is installed in the upper part of the dip tube.

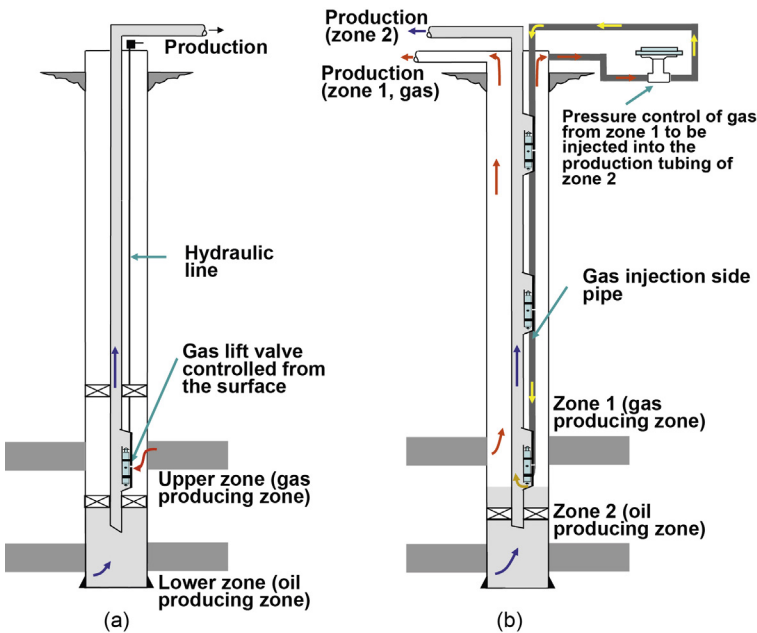
Fig. 6.74c represents an alternative to the completion shown in Fig. 6.74b. The injection gas is injected down the parallel pipe between the two packers. This pipe is directly communicated to the lower gas lift mandrel. For this type of arrangement, the lower mandrel should be equal to the one shown in Fig. 6.19d. As many mandrels as necessary to unload the long string below the upper packer can be installed in this type of completion. The problem with this completion is its complexity, which makes it more expensive and with a greater possibility of mechanical failures. They are also difficult to troubleshoot.

Fig. 6.75 shows several alternatives for dual wells with independent gas sources for each string. In this way, the injection gas flow rate to each string can be independently controlled at the surface. Because of lack of space inside the casing, these completions are usually limited to very small-diameter tubing.

Many wells are drilled through gas- and oil-producing zones. In these cases, it is possible to use the gas from the gas-producing zone to lift the oil-producing zone, as shown in Fig. 6.76. This is sometimes called: “in situ gas lift,” “natural gas lift,” or “internal gas lift.” In Fig. 6.76a, a hydraulic line is used to control the gas flow rate from the upper zone to lift the lower zone. As can be seen in the figure, with this type of completion two packers and one hydraulic line must be used (the upper packer is used only if the casing



■ FIGURE 6.75 Parallel completions with independent gas sources.



■ FIGURE 6.76 Two types of "in situ gas lift" installations.



above this packer cannot be in contact with the produced gas). One disadvantage of this completion is the inability to measure the injection gas flow rate. But the well's liquid production can still be optimized by testing the well at different settings of the gas injection valve. Another way of controlling the injection gas flow rate (and pressure) of the gas coming from the gas-producing zone is shown in Fig. 6.76b. In this case, it is necessary to use a side pipe (for gas injection) and special gas lift mandrels connected to this pipe. The gas flow rate can be measured and gas samples can be analyzed to know its specific gravity and be able to accurately calculate the injection gas pressure at depth from the measured surface injection pressure. It is important to take into account the friction pressure drop along the gas injection pipe to calculate the gas injection pressure at depth (this is usually not necessary in standard gas lift completions because the annular cross-sections are large and friction pressure drops are usually negligible). The other important point to remember is that the injection gas should not be corrosive; otherwise, the well might be lost because of a damaged casing. For both completions shown in Fig. 6.76, it might be necessary to install a standing valve at the deep end of the tubing to avoid cross flow (from the upper to the lower zone) in case the well needs to be shut in and the subsurface gas injection valve cannot be closed (this subsurface valve should also have a check valve to avoid liquids from the lower zone entering the annulus).

#### 6.4.5 Use of coiled tubing

The development of coiled tubing technology has introduced several new types of completions that are highly beneficial to the implementation of the gas lift method. The most important advantages of coiled tubing completions are:

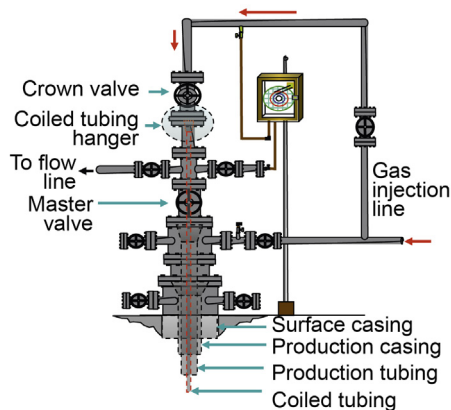
- It can be quickly installed in the well.
- The surface equipment, required to install or pull the coiled tubing, are few and do not occupy too much space.
- It can be installed in a well without having to kill it to control its reservoir pressure (killing a well is an operation that can cause formation damage and requires time, materials, and equipment to accomplish).
- It can be installed in wells without having to pull the existing completions.
- The required wellhead modifications and/or equipment are easy to implement and install.

One way in which coiled tubing strings have been installed in many existing gas lift wells is by simply inserting the coiled tubing string into the

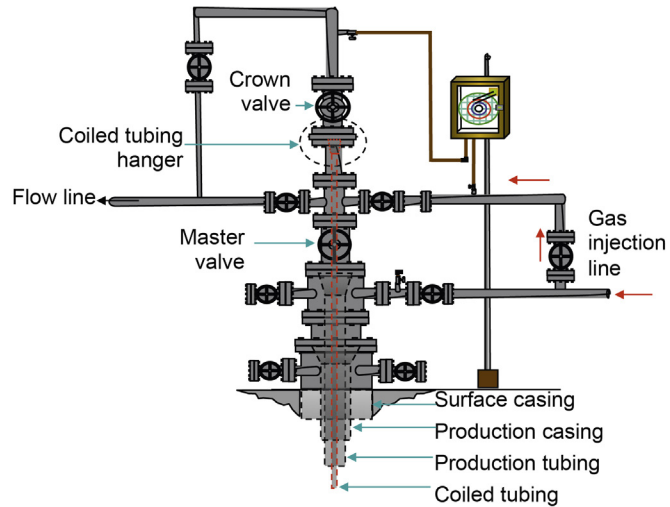
existing production tubing string without pulling the gas lift completion out of the well. Lift gas is then injected down the casing–tubing annulus and into the annulus between the production tubing and the coiled tubing through the existing gas lift valves. Liquids are produced up the annulus between the production tubing and the coiled tubing (the coiled tubing is used as a blind pipe in a gas lift well). This is done in gas lift wells in which the reservoir pressure has declined and it becomes necessary to reduce the flow area to lower the injection gas/liquid ratio and be able to produce the wells in a stable manner; otherwise, the injection gas flow rate would need to be increased to keep a stable production or produce the well on intermittent gas lift.

Coiled tubing, equipped with gas lift valves, can also be installed in naturally flowing wells that are beginning to need some kind of artificial lift method to increase the liquid production or in gas lifted wells in which the reservoir pressure has declined. Gas can be injected down the coiled tubing and produce the liquids up the annulus between the coiled tubing and the existing production tubing or vice versa. In both cases, the gas lift valves that were initially installed in the production tubing (if any) can be replaced with dummy valves to avoid leaks or they can be left in the well to unload the annulus between the production tubing and the coiled tubing. The latter option requires pulling the coiled tubing out of the well if a gas lift valve installed in the existing production tubing fails.

Fig. 6.77 shows a wellhead arrangement required to inject the lift gas down the coiled tubing or down the annulus between the existing production tubing and the casing.



■ FIGURE 6.77 Wellhead arrangement for concentric coiled tubing installations.



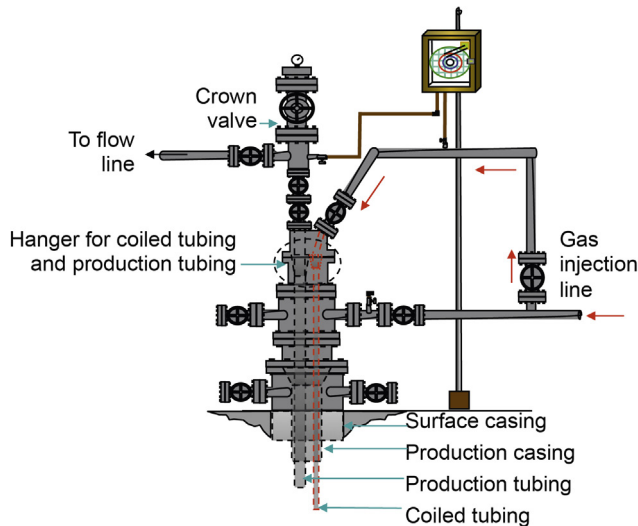
■ FIGURE 6.78 Wellhead arrangement for liquid production up the coiled tubing.

Fig. 6.78 shows a wellhead arrangement required for liquid production up the coiled tubing and gas injection down the annulus between the coiled tubing and the existing production tubing. With this arrangement, the lift gas can also be injected down the annulus between the production tubing and the casing.

Coiled tubing can also be used as parallel injection pipes, as explained in several examples in previous sections. For this purpose, it is necessary to have a wellhead arrangement as shown in Fig. 6.79. The tubing hanger is more expensive in this case, but not as expensive and bulky as the ones installed in dual wells.

As indicated earlier for gas lifted wells, coiled tubing can also be used in naturally flowing wells to simply reduce the flow area inside a production tubing with an inside diameter that is too large for current operational conditions. In this case, the coiled tubing is not used to inject gas or to produce liquids from the reservoir, but just as a “velocity string.” This type of application might also be recommended for gas wells that have a tendency to load up with liquids.

Coiled tubing diameters are available in different sizes and not just in small-diameter tubing. The existing production tubing can be replaced by large-diameter coiled tubing. There are gas lift mandrels that can be installed in 3-in. diameter coiled tubing. Several examples of gas lift mandrels for coiled tubing are presented at the end of Section 6.2. These mandrels can be

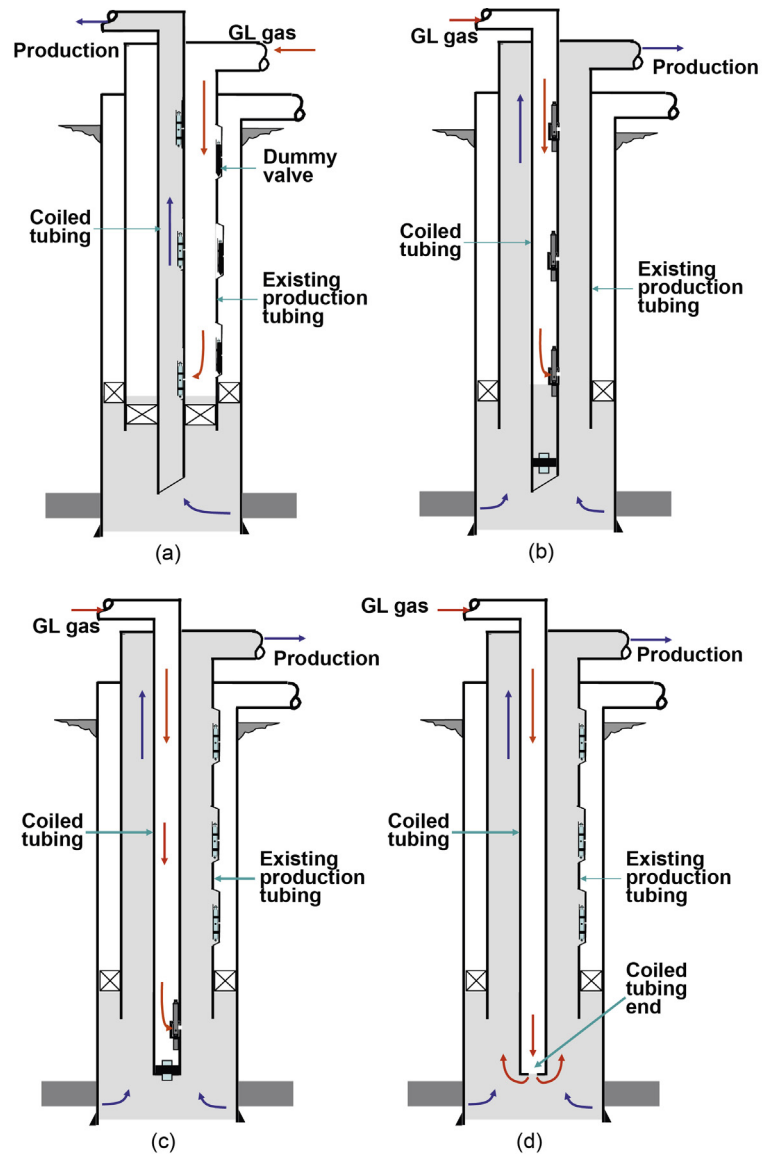


■ FIGURE 6.79 Wellhead arrangement to install the coiled tubing string parallel to the production tubing.

installed at the plant and spooled together with the coiled tubing (so that the operation of running in the well the coiled tubing does not have to be interrupted) or they can be installed at the well site.

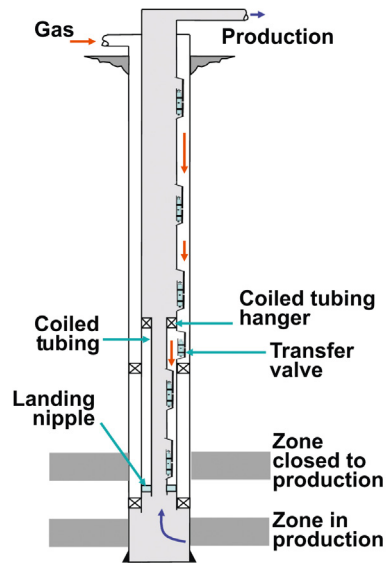
Several examples of how a coiled tubing can be used are presented in Fig. 6.80. In the completion shown in Fig. 6.80a, the lift gas is injected down the annulus between the existing production tubing and the coiled tubing. For this completion, it is necessary to set a packer inside the existing production tubing or the coiled tubing can be set at a landing nipple inside the production tubing. The existing gas lift valves in the production tubing have been replaced by dummy valves but, as indicated earlier, the gas lift valves can also be left in the well to use them to unload the annulus between the coiled tubing and the existing production tubing. Gas lift valves inside the coiled tubing can be wireline retrievable or not.

In the completion shown in Fig. 6.80b, the coiled tubing is used to inject gas into a well that was previously producing on natural flow. A plug is installed at the end of the coiled tubing to avoid a large and uncontrolled volume of injection gas blowing around the end of the coiled tubing. The point of injection can be located at the perforations (or below them) if the perforated interval is very long. In the completions shown in Fig. 6.80c, d, existing gas lift valves were left in the well to use them to unload the well. In this way, only one injection point needs to be located in the coiled tubing to inject



■ FIGURE 6.80 Examples of coiled tubing applications for gas lift completions.

the lift gas into the annulus between the coiled tubing and the production tubing. In the completion shown in Fig. 6.80c, the point of injection is a gas lift valve, while in Fig. 6.80d an orifice is installed at the end of the coiled tubing to control the gas injection through it. This orifice can be replaced with another one by a simple wireline job.



■ FIGURE 6.81 Use of coiled tubing to lower the point of injection.

An additional coiled tubing application, among many others, is presented in Fig. 6.81, where only the lower zone is desired to be in production but its reservoir pressure is very low and the operating valve would be located way above the top of the perforations if the coiled tubing was not installed as presented in the figure. The coiled tubing hangs just above the gas lift valve used as a transfer point. This transfer valve should not be used as an unloading valve but only as a valve that allows the injection gas from the upper annulus to be transferred into the lower annulus between the coiled tubing and the existing production tubing. It is recommended to install either an orifice or a circulating valve at this transfer point with an orifice diameter as large as possible to minimize the pressure drop across it. The orifice valve is used to protect the polished bore of the mandrel's pocket. The coiled tubing is set on a landing nipple installed in the production tubing to provide a seal for the injection gas so that it can only be injected through the gas lift valves installed in the coiled tubing.

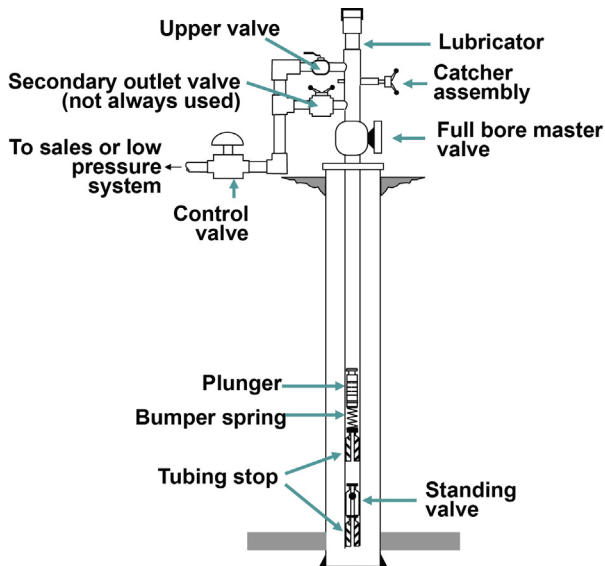
#### 6.4.6 Intermittent gas lift with metallic plungers

Conventional plunger lift is not considered as a gas lift sub method of production because the lift gas comes from the formation itself and not from a source outside the well. In some cases, conventional plunger lift does use some volume of gas per cycle from an outside source to speed up the annulus compression stage, but even in those cases it is still not considered a

truly gas lift method. The use of metallic plungers is only considered to be a part of the gas lift method of production when they are used to reduce the liquid fallback losses in conjunction with intermittent gas lift.

The conventional plunger lift is explained first in this section. This method is applied to wells with very high formation gas/liquid ratios and consists in closing the well to production at the wellhead for a given period of time to pressurize the annulus with formation gas while a liquid column is being generated at the bottom of the production tubing. When the annular pressure reaches a certain value (or after a predetermined period of time), the wellhead control valve opens (communicating the production tubing to the flow line) so that the gas in the annulus expands and pushes the liquid slug at the bottom of the tubing to the surface. Plungers are used to provide a solid and sealing interface between the liquid slug and the gas below it. If the well produces too much gas and the annular pressure reaches a very high value before the liquid slug has been accumulated, the excess gas can be produced directly from the annulus to a sales line through a control valve that opens after the annular pressure has reached a certain value and closes at the beginning of the liquid production stage. If, on the contrary, it takes a long time for the annular pressure to reach an acceptable value, liquid production can be maximized by injecting gas from an outside source into the annulus during the time it is being pressurized. The surface valve in the flow line can be opened by a control system based on the annular pressure or on time, or on a combination of both. Most installations have a way of detecting the plunger's arrival at the surface to close the valve in the flow line and start a new annulus pressurization period. The plunger can be detected by several means: mechanical or magnetic detection, or by a pressure differential signal. In wells with lower gas/liquid ratios, it is important to close the flow line valve as soon as the plunger arrives at the surface. Fig. 6.82 shows a typical conventional plunger lift installation

The metallic plunger sits on top of a bumper spring, which in turn is set with a tubing stop in the production tubing. The tubing stop can be installed in a landing nipple or in a collar recess (if API tubing is used) or along the tubing if a slip-type tubing stop is used. When the piston falls and strikes the bumper spring, usually a valve rod moves and closes an internal valve in the plunger. The internal valve in the close position does not allow the gas to pass through the inside of the plunger as it moves up while lifting the liquid slug. When the plunger reaches the surface and contacts the striker pad inside the lubricator, the valve rod is activated and the valve inside the plunger is opened. This allows the gas and/or liquids to pass through the plunger as it travels back down toward the bumper spring. The master valve at the wellhead must have a full bore equal to the tubing size to allow the plunger

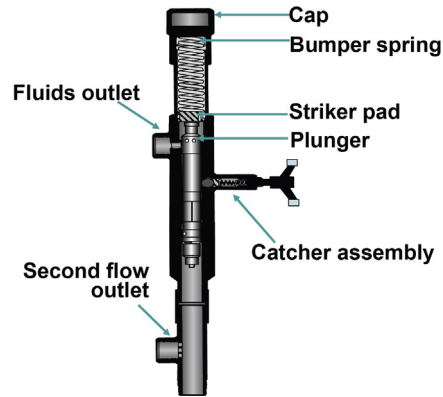


■ FIGURE 6.82 Typical conventional plunger lift installation.

to pass through it. The valve must not be oversized because this would allow excessive gas passage around the plunger and possibly prevent the plunger from reaching the lubricator. The plunger must reach the lubricator to: (1) allow removal for service, (2) activate a plunger arrival system (if used), and (3) activate the plunger valve rod (if the plunger has one).

The production tubing must be gauged. Plungers cannot be used if the tubing is bent or crushed, or there are paraffin depositions, scale, etc. Nipples with a smaller drift diameter might also prevent the usage of metallic plungers. Typical plunger installations do not have packers. If the tubing is set on a packer, either unseat the packer or perforate holes in the tubing to allow casing–tubing communication. If the annulus contains liquids that might cause formation damage, a tubing plug located at the end of the production string should be set before the holes are perforated above the plug; thus preventing potentially harmful fluids from contacting the formation. The liquids from the annulus can then be swabbed out before pulling the plug from the well. Fig. 6.83 shows the internal components of a typical lubricator in detail. The main functions of the lubricator are: (1) absorb the impact of the plunger using its bumper spring; (2) activate the valve rod to open the internal valve of the plunger (if the plunger has one); (3) If required, activate the catcher assembly to hold the plunger in the lubricator for easy removal; and (4) where the operating conditions of a plunger installation require rapid dissipation of tail gas or flow to a lower pressure system to lift the plunger

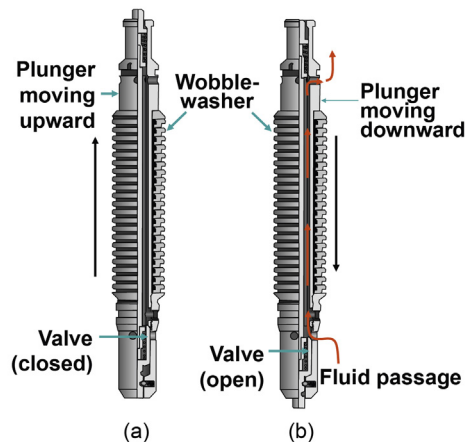




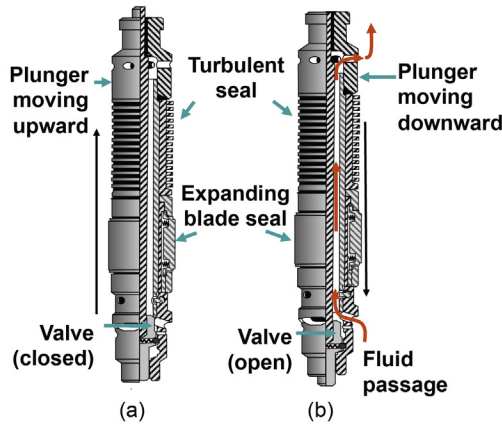
■ FIGURE 6.83 Wellhead lubricator with the plunger inside.

and accumulated liquids, a separate outlet is installed below the lubricator (this option might not be necessary in many wells).

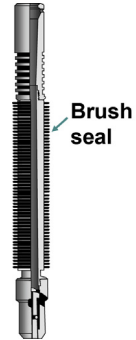
Different types of plungers are shown in the following figures. There are several seal types: (1) turbulent seal for fast plunger downward velocity, (2) expanding blade seal for closer fit to the tubing wall, thus minimizing gas bypass around the annulus as the plunger moves upward, or (3) brush-type seal. Different types of sealing elements can be present in a single plunger. Plungers may or may not have valve rods or they can be hollow or solid (Figs. 6.84–6.86).



■ FIGURE 6.84 Wobblewasher-type plunger with integral valve rod.



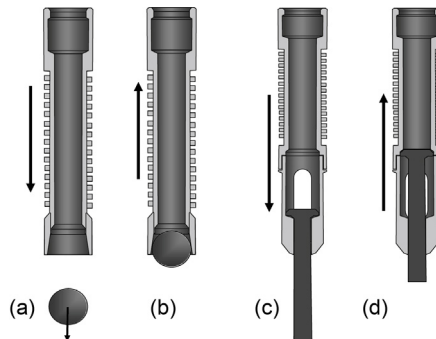
■ FIGURE 6.85 Plunger with integral valve rod showing both, turbulent seal and expanding blade seal.



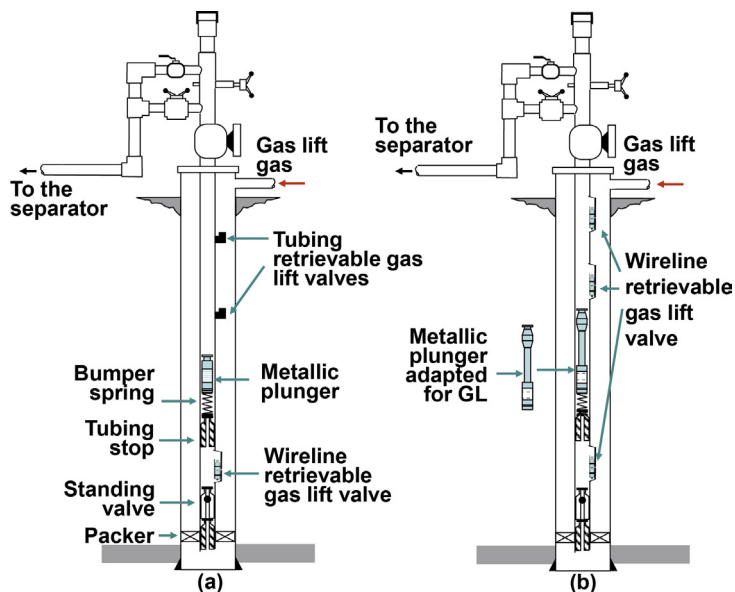
■ FIGURE 6.86 Brush-type plunger without integral valve rod (the striker pad contains a rod for activation of the plunger valve).

Recently developed plungers are designed to drop through the liquids at higher velocities. This is an advantage for wells that produce viscous fluids or that need very high cycle frequencies. Fig. 6.87a, b shows a two-piece plunger: a metallic ball and a hallow cylindrical plunger on top of the ball. When the plunger is being pushed upward, the ball is in contact with the cylinder, providing a sealing interface between the liquid slug and the gas below it. When the plunger is on its way down, the ball is designed to drop faster so that the two pieces travel separately, achieving higher velocities. Sometimes the surface lubricator allows the ball to fall first and, after a pre-determined period of time, the cylinder is allowed to fall.

Fig. 6.87c, d shows a hollow plunger with an internal rod that moves freely inside the plunger between the lower and upper stops. When the plunger



■ FIGURE 6.87 New plunger designs.



■ FIGURE 6.88 Intermittent gas lift with plunger.

is being pushed upward, the rod contacts the upper stop thus providing a sealing interface between the liquid slug and the gas below the plunger. When the plunger drops, the rod contacts the lower stop and liquids can pass through the large lateral ports in the walls of the lower part of the hollow plunger. This allows for higher falling velocities. Plungers shown in Fig. 6.87 are recently patented applications and the reader should contact the specific plunger manufacturing companies for more details

Besides being used in conventional plunger lift, metallic plungers have different applications in wells that might be producing on other types of artificial lift methods or on natural flow:

- Plungers can be used from time to time to clean paraffin deposition on the inside wall of the production tubing.
- Plungers can also be used to unload gas wells when liquids accumulate at the bottom.
- As mentioned earlier, plunger can also be used in conjunction with intermittent gas lift to reduce the liquid fallback losses.

A plunger-assisted intermittent gas lift installation is shown in Fig. 6.88. Fig. 6.88a shows a gas lift completion with conventional (tubing retrievable) gas lift valves in which the plunger can travel through the production tubing without problem. If side-pocket mandrels are installed in the well,

plungers need to be modified to be able to pass through the gas lift mandrels. The modification simply consists in adding an extension rod as shown in Fig. 6.88b. In any case, the idea of using plungers is only to reduce the liquid fallback losses in intermittent gas lift. The design procedures given for intermittent gas lift in chapter: Design of Intermittent Gas Lift Installations equally apply for intermittent gas lift with plungers only that the fallback factor used in the calculations should be very small. In wells that produce oil with gravities greater than or equal to 23 degrees API, plungers minimize the liquid fall back only if the liquid slug velocity is low. Experimental observation has shown that for slug velocities greater than or equal to 1000 ft./min, the liquid fallback losses are the same with or without the use of metallic plungers when lifting this type of crude.

The most important disadvantage of using metallic plunger is the increase in maintenance costs and the intensive field supervision that they need.

# Gas lift valve mechanics

Understanding gas lift valve mechanics is important because gas lift designs and troubleshooting analyses depend on the opening and closing pressures of the unloading and operating valves. Once gas lift mandrel-spacing calculations are done, the calibration of gas lift valves can be determined from the valve temperature at operating conditions and from the production and injection pressures at valve's depth. The mandrel-spacing and gas lift design procedures that are explained in chapter: Design of Continuous Gas Lift Installations determine the valve's port size and its operating temperature, as well as the production and injection pressures at valve's depth. Because these procedures depend on the type of the gas lift valve being used, it is advisable to understand first the ways in which the different types of gas lift valves operate and how they are calibrated.

The equations that are used to find the calibration pressure of a gas lift valve are derived from the balance of the forces that try to open and close the valve just before the valve opens or just before it closes. Calibration equations for different types of valves and for different calibration procedures (calibration by opening or by closing the valve) are presented in the chapter. The equations that are used to determine the nitrogen pressure at test-rack conditions from the known operating conditions and vice versa, are also presented. The equations presented in the chapter are only valid for static conditions in which the gas flow rate is very low or equal to zero. Under dynamic conditions, these equations should be replaced with the mathematical models explained in the next chapter. Several problems are solved at the end of the chapter to familiarize the reader with the required valve calibration calculations that are performed in gas lift designs and with the force balance needed for troubleshooting analyses.

## 7.1 FORCE-BALANCE EQUATIONS FOR THE DIFFERENT TYPES OF GAS LIFT VALVES

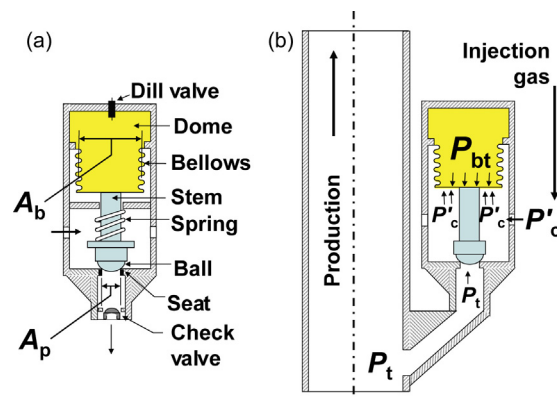
As it was explained in Section 6.1, some types of valves respond mainly to the injection pressure while others to the production pressure. Accordingly, gas lift valves are classified as either "injection-pressure-operated" (IPO) or

“production-pressure-operated” (PPO) valves. The force–balance equations explained in the chapter are based on the fact that a force is equal to the pressure times the area on which the pressure is applied. The area of the port of the valve is called  $A_p$  while the area of the bellows is  $A_b$ . The practical way in which these areas are determined is explained towards the end of the chapter. Usually, the values of  $A_p$  and  $A_b$  are provided by the valve’s manufacturer.

### 7.1.1 Injection-pressure-operated valves

Usually, IPO valves are nitrogen-charged valves. Very few models of nitrogen-charged IPO valves also have a spring that is used to provide an additional closing force (the spring in this case is used for bellows protection because the bellows’ inside pressure does not need to be very high). There are even fewer models available for IPO valves that are only spring-loaded, for which the dome is filled with a protecting liquid at atmospheric condition. These spring-loaded valves are used in wells with very high production temperature (probably caused by steam injection) or where the temperature is very hard to predict. The main reason why spring-loaded valves are seldom used is because they require a large pressure increase above the opening pressure to be fully open. Nitrogen-charged IPO valves are exclusively calibrated by opening the valve, therefore they only have calibration “opening pressures.” Spring-loaded IPO valves are most of the time calibrated by closing the valve, so they have calibration “closing pressures” although a few models are calibrated by determining the opening pressure.

*Nitrogen-Charged IPO Valves.* Fig. 7.1 shows the pressures that try to open and close a nitrogen-charged, IPO, gas lift valve.



■ FIGURE 7.1 Pressures that try to open and close a nitrogen-charged IPO valve. (a) main components, (b) pressures acting on the valve.

The forces that try to close the valve are:

- The dome pressure  $P_{bt}$ , which is the pressure of the nitrogen at operating conditions, multiplied by the area of the bellows,  $A_b$ . The temperature at operating conditions is much higher than the temperature at test-rack conditions, which is usually equal to 60°F.
- As indicated earlier, for a limited number of valve models, in addition to the force provided by the nitrogen pressure, a spring is used to help closing the valve. In most cases, the valve manufacturer assigns a fixed value to the equivalent pressure supplied by the spring, called  $P'_r$ , which is assumed to act on the bellows area  $A_b$  minus the seat or port area  $A_p$ .

The forces that try to open the valve are:

- The gas injection pressure at valve's depth,  $P'_c$ , multiplied by the bellows area minus the port area,  $(A_b - A_p)$ .
- The production pressure at valve's depth,  $P_t$ , multiplied by the seat or port area,  $A_p$ .

Even though the gas lift valve has an internal check valve, the value of  $P_t$  is still acting on the ball of the valve even if the check valve provides a tight hermetic seal that would not allow any communication from the tubing to the interior of the gas lift valve. This is because the ball-seat contact always allows a small leak of gas from the casing–tubing annulus into the tubing and, as soon as the pressure of the volume located between the ball and the check valve gets to be higher than  $P_t$ , gas will pass through the check valve towards the tubing, keeping in this way the pressure on the ball constant at  $P_t$  for as long as the valve remains closed and the pressure in the annulus is greater than the pressure in the tubing at valve's depth. Check valves that offer a tight hermetic seal are relatively new and most check valves used today in the industry do allow pressure transmission from the tubing into the volume between the ball and the seat.

If the force balance is performed just before the valve opens, the equation from which the injection opening pressure is determined is as follows:

$$(A_b - A_p)P'_c + (A_p)P_t = (A_b)P_{bt} + (A_b - A_p)P'_r \quad (7.1)$$

The left hand side of Eq. 7.1 corresponds to the forces that try to open the valve, while the forces that try to close it are given on the right hand side. These forces must be equal just before the valve opens. Dividing Eq. 7.1 by the bellows' area gives the following equation:

$$(1 - R)P'_c + (R)P_t = P_{bt} + (1 - R)P'_r \quad (7.2)$$

Where  $R$  is the area of the seat divided by the area of the bellows. Values of  $R$ ,  $P'_c$ , and  $P_t$  are determined right after the location of the valve has been found in the mandrel-spacing procedure used during the design calculation of a gas lift installation. On the other hand, the value of  $P'_r$  is supplied by the valve's manufactures. Thus, the value of the nitrogen pressure at operating conditions,  $P_{bt}$ , can be calculated from Eq. 7.2. Once the value of  $P_{bt}$  has been found, the pressure that the same number of nitrogen moles inside the dome will have at calibration conditions, usually equal to 60°F, can be determined from the equations given at the end of the chapter for that purpose (Eq. 7.16 or 7.17). If the valve does not have a spring to supply an additional force, the value of  $P'_r$  is simply equal to zero in Eq. 7.2.

Eq. 7.2 can be expressed at test-rack conditions, where the temperature is usually equal to 60°F, for which the corresponding dome pressure is now called  $P'_b$  instead of  $P_{bt}$ , and the production pressure  $P_t$  is equal to 0 psig because the valve in the test rack is only exposed to the calibration injection pressure (through the valve's entrance ports), leaving the exit ports at the nose of the valve open to the atmosphere. At test-rack conditions, Eq. 7.2 becomes:

$$(1 - R)P_{tr} = P'_b + (1 - R)P'_r \quad (7.3)$$

The value of  $R$  is known from the outcome of the design procedure being used,  $P'_r$  is a constant supplied by the valve's manufacturer, and  $P'_b$  is calculated from the value of  $P_{bt}$  with Eq. 7.16 or 7.17. In turn,  $P_{bt}$  is calculated from Eq. 7.2. Then, all the data needed to find  $P_{tr}$  (called the test-rack opening pressure) from Eq. 7.3 are known. It is advisable that  $P_{tr}$  is measured at the shop by a manometer calibrated according to recommendations given by the American Petroleum Institute. The dome pressure at 60°F,  $P'_b$ , is adjusted during the calibration process so that the valve opens at a pressure equal to  $P_{tr}$ . There is no need to measure  $P'_b$  directly. If the valve has a spring, the valve's opening pressure must be set first equal to  $P'_r$  (by adjusting the spring) with the bellow pressure equal to 0 psig (before injecting nitrogen into the dome).

In a well, at operating conditions and just before the valve opens, the injection pressure is only applied to the area ( $A_b - A_p$ ), while the production pressure is only applied to area  $A_p$ . Once the valve opens, the gas injection pressure is applied to the entire bellows area. Because the injection pressure is greater than the production pressure, once the valve has opened it would not close at the opening injection pressure but at a lower pressure, which is called the valve closing pressure. The difference between the valve opening and closing pressures is called the "spread of the valve" and it plays a major



role in intermittent gas lift. The larger the area ratio is, the larger the spread of the valve becomes because the production pressure plays a more important role in valves with larger seat diameters and, therefore, with larger area ratios.

From Eq. 7.3, the test-rack injection opening pressure,  $P_{tr}$ , is:

$$P_{tr} = \frac{P'_b}{(1-R)} + P'_r \quad (7.4)$$

Nitrogen-charged gas lift valves are never calibrated by closing the valve because the closing calibration pressure would have random values due to the behavior of the internal components of the valve (hysteresis) explained in the next chapter.

Theoretically, once the valve opens, the injection pressure could be reduced to close the valve at a constant closing pressure. In this case, the injection pressure just before the valve closes is assumed to act over the entire bellows area. The force balance equation at operating conditions just before the valve closes is in theory given by:

$$P_{cc} = P_{bt} + (1-R)P'_r \quad (7.5)$$

Where  $P_{cc}$  is the injection closing pressure. If the nitrogen-charged valve has no spring ( $P'_r = 0$ ), the injection closing pressure of the valve is equal to the dome pressure at operating conditions. If the gas lift design erroneously estimates the valve temperature at operating conditions to be lower than its actual value, the true opening pressure will be higher than the design injection opening pressure and it might not be possible to continue unloading the well for not having a sufficiently high injection pressure to open the valve. If, on the contrary, the estimated temperature is higher than the real temperature in the well while unloading it, the valve will be cooler under actual conditions and it is possible that the valve remains open and the unloading of the well cannot be continued unless the injection gas flow rate is considerably increased. These problems are analyzed in chapter: Design of Continuous Gas Lift Installations (eg, Figs. 9.37 and 9.38).

*Spring-Loaded, IPO Valves.* As indicated earlier, these valves are not frequently used and they are only installed in places where the production temperature is either too high or too difficult to predict. The force-balance equation is almost identical to the equation for nitrogen-charged valves, only that in this case  $P_{bt}$  is equal to zero and  $P'_r$  is now called  $P_{btr}$  and assumed to act over the entire bellows area and not just over the bellows

minus the port area as it is the case for  $P'_r$  in a nitrogen-charged IPO valve with a spring installed to provide an extra closing force for bellows protection. Thus, the equation at operating conditions just before the valve opens is given by:

$$(1 - R)P'_c + (R)P_t = P_{\text{btr}} \quad (7.6)$$

The values of  $R$ ,  $P'_c$  and  $P_t$  (defined previously for nitrogen-charged valves) are determined from the gas lift design procedure being used. Then, Eq. 7.6 is used to calculate  $P_{\text{btr}}$ , or the “equivalent spring pressure” as it is also called.

At test-rack conditions,  $P_t$  is equal to zero (for the same reasons given for nitrogen-charged valves),  $P'_c$  is the injection pressure measured at the shop, now called  $P_{\text{tr}}$ , and  $P_{\text{btr}}$  does not change because the spring force does not depend on temperature. Then, the test-rack opening pressure is:

$$P_{\text{tr}} = \frac{P_{\text{btr}}}{(1 - R)} \quad (7.7)$$

In this case,  $P_{\text{tr}}$  is the pressure supplied through the entrance ports of the valve and it is measured just before the valve opens with a precisely calibrated manometer.  $P_{\text{tr}}$  is usually called  $P_{\text{tro}}$  when the valve is calibrated by opening it. The spring is adjusted at the shop until the value of  $P_{\text{tr}}$  is equal to  $P_{\text{btr}}/(1 - R)$ .

Spring-loaded valves are usually calibrated by closing the valve and measuring the injection closing pressure. In this case because the valve is opened, the force balance that applies just before the valve closes is:

$$P_{\text{tr}} = P_{\text{btr}} \quad (7.8)$$

Where  $P_{\text{btr}}$  is calculated from Eq. 7.6. The instant the valve closes, the value of  $P_{\text{tr}}$  is measured and it is called  $P_{\text{trc}}$ . It is easier to calibrate spring-loaded valves than nitrogen-charged valves; however, spring-loaded IPO valves are seldom used. As stated earlier, the reason lies on the fact that spring-loaded valves require a large pressure increase above the opening pressure to fully open the valve. The bellows load rate is defined as the required injection pressure increase necessary to move the stem of the valve a given distance from the seat. The bellows load rate is usually given in psi/in. The bellows load rate is smaller for nitrogen-charged valves. The equivalent bellows load rate of a spring-loaded valve is much larger than the ones usually found in nitrogen-charged IPO valves. This is why it is necessary to increase the injection pressure to a value much higher than the injection opening pressure to be able to move the ball off the seat as

far as it can move. As it is shown in chapter Design of Continuous Gas Lift Installations, the design of gas lift installations with IPO valves requires a sequential drop in the valve's injection opening pressure per each unloading valve. This pressure drop per valve is usually smaller than the required pressure increment needed to fully open a spring-loaded IPO valve; thus, spring-loaded valves can only be used if the injection pressure is high enough to be able to reach the desired point of injection depth even with very large sequential pressure drops per valve. Regardless of their disadvantages, there are cases in which spring-loaded IPO valves should be used:

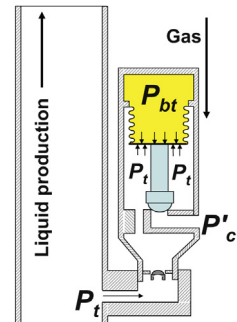
- In wells that have just been subjected to steam injection.
- In wells where it is difficult to predict the production temperature and the number of valves installed in the well is small.
- Pilot valves used in intermittent gas lift wells for which spring-loaded valves are highly recommended for the reasons explained in chapter: Design of Intermittent Gas Lift Installations.

PPO valves, on the other hand, are usually spring-loaded valves because: (1) the production pressure can decrease hundreds of psi during the unloading process, and (2) their calibration does not depend on temperature.

### 7.1.2 Production-pressure-operated valves

These valves are mainly opened by the production pressure that acts over the bellows area  $A_b$  minus the port area  $A_p$ . The gas injection pressure also tries to open the valve but because it is only applied over the port area, its effect is secondary. Fig. 7.2 shows a schematic view of a PPO valve. Other configurations of PPO valves are given in chapter: Gas Lift Equipment, Fig. 6.3.

Fig. 7.2 shows a PPO valve with the nitrogen pressure at operating conditions equal to  $P_{bt}$ . As it was the case for IPO valves, PPO valves can also be spring loaded with the bellows at atmospheric pressure, for which the only closing force comes from the spring. As was stated previously, spring-loaded valves are the most common type of PPO valves used in the industry. Nitrogen-charged PPO valves can also have a spring to provide an additional closing force and protect the bellows by not allowing its internal pressure be too high. The equivalent pressure provided by the spring in this case is assumed to act over the bellows area minus the port area and it is also called  $P'_c$ . For the injection gas to go from the casing-tubing annulus to the production tubing, it has to first travel upwards through the seat and then downwards through five or six parallel holes (only one of these holes is shown in Fig. 7.2) towards the check valve.



■ FIGURE 7.2 Pressures that try to open and close a PPO valve.

The combined area of the parallel holes is much greater than the flow area of the seat. The main gas restriction is then the seat of the valve and that is why the bellows area is always exposed to the production tubing pressure.

*Nitrogen-charged, PPO valves.* Forces that try to close the valve are:

- The nitrogen pressure  $P_{bt}$  at operating conditions multiplied by the bellows area  $A_b$ . At operating conditions the valve is much hotter than at test-rack conditions.
- If the valve has a spring, the additional closing force is equal to the equivalent spring pressure  $P'_r$  times the bellows area  $A_b$  minus the port area  $A_p$ .

The forces that try to open the valve are:

- The injection pressure at valve's depth  $P'_c$  multiplied by the port area  $A_p$ .
- The production pressure  $P_t$  multiplied by the bellows area minus the port area,  $A_b - A_p$ .

If the force balance is carried out just before the valve opens, the equation that can be used to calculate the production opening pressure is:

$$(A_p)P'_c + (A_b - A_p)P_t = (A_b)P_{bt} + (A_b - A_p)P'_r \quad (7.9)$$

The terms on the left hand side of Eq. 7.9 correspond to the forces that try to open the valve, while those on the right hand side correspond to the forces that try to close it. These opening and closing forces should be equal to each other just before the valve opens. Dividing Eq. 7.9 by the bellows area, Eq. 7.9 becomes:

$$(R)P'_c + (1 - R)P_t = P_{bt} + (1 - R)P'_r \quad (7.10)$$

Where  $R$  is the area of the port divided by the area of the bellows. The values of  $R$ ,  $P'_c$ , and  $P_t$  (defined earlier) are obtained from the design procedure being used (right after the valve's depth has been found). The value of  $P'_r$  is a constant usually given by the valve's manufacturer; therefore because all the other terms are known, the nitrogen pressure at operating conditions,  $P_{bt}$ , can be determined from Eq. 7.10. Once  $P_{bt}$  has been calculated, the dome pressure at test-rack conditions, known as  $P'_b$ , can be found from the equation given in Section 7.2. If the valve does not have a spring to provide an additional closing force, the value of  $P'_r$  is set equal to zero. At test-rack conditions, the injection pressure  $P'_c$  is equal to 0 psig because the lateral valve's inlet ports are exposed to atmospheric pressure

while the exit ports at the nose of the valve are exposed to the production calibration pressure. Then, at test-rack conditions Eq. 7.10 becomes:

$$(1 - R)P_{tr} = P'_b + (1 - R)P'_r \quad (7.11)$$

The value of  $R$  is known from the outcome of the design procedure being used,  $P'_r$  is a constant supplied by the valve's manufacturer, and  $P'_b$  is calculated with the equations given at the end of the chapter from the value of  $P_{bt}$ , which in turn is calculated from Eq. 7.10. Then, all the data needed to find  $P_{tr}$  (called test-rack production opening pressure) from Eq. 7.11 are known. It is advisable that  $P_{tr}$  is measured at the shop by a manometer calibrated according to the recommendations given by the American Petroleum Institute. The dome pressure at 60°F,  $P'_b$ , is adjusted during the calibration process so that the valve opens at a pressure equal to  $P_{tr}$ . There is no need to measure  $P'_b$  directly. If the valve has a spring to provide an additional closing force, the valve production opening pressure must be set first equal to  $P'_r$  (by adjusting the spring) with the bellows pressure equal to 0 psig (before injecting nitrogen into the dome). If the valve at operating conditions is opened, the production pressure is applied over the entire bellows area. If the production pressure decreases, a point is reached in which the valve closes; but, with the valve closed, the port area is now exposed to the injection pressure, which is usually much higher than the production pressure. In consequence, the valve opens and closes while the production pressure continues to decrease until the production pressure reaches a value below which the valve remains permanently closed. From Eq. 7.11 the test-rack production opening pressure  $P_{tr}$  is given by:

$$P_{tr} = \frac{P'_b}{(1 - R)} + P'_r \quad (7.12)$$

Eq. 7.12 is equal to Eq. 7.4 for IPO valves, but it should be remembered that for PPO valves  $P_{tr}$  is the pressure measured at the shop that is applied through the nose of the valve because it represent the production pressure.

*Spring-loaded PPO valves.* As stated earlier, spring-loaded PPO valves are the most widely used, compared with all of the other types of PPO valves, in the industry. The force–balance equation is almost identical to the equation for nitrogen-charged valves, only that in this case  $P_{bt}$  is equal to 0 and  $P'_r$  is now called  $P_{btr}$  and assumed to act over the entire bellows area and not just over the bellows minus the port area as it is the case for  $P'_r$  in nitrogen-charged valves. Therefore, the equation at operating conditions just before the valve opens is given by:

$$(R)P'_c + (1 - R)P_t = P_{btr} \quad (7.13)$$

The values of  $R$ ,  $P'_c$ , and  $P_t$  are determined from the gas lift design procedure being used. Then, Eq. 7.13 is used to calculate  $P_{\text{btr}}$ , or the “equivalent spring pressure” as it is also called. At test-rack conditions,  $P'_c$  is equal to 0 for the same reasons given for nitrogen-charged valves, while  $P_t$  is the production pressure measured at the shop (now called  $P_{\text{tr}}$ ) and  $P_{\text{btr}}$  does not change because the spring force does not depend on temperature. Then, the test-rack opening pressure is:

$$P_{\text{tr}} = \frac{P_{\text{btr}}}{(1 - R)} \quad (7.14)$$

In this case  $P_{\text{tr}}$  is the calibration pressure applied through the nose of the valve and it is measured just before the valve opens (for this reason, it is also known as  $P_{\text{tro}}$ , where “o” stands for “opening”). The spring should be adjusted until the value of  $P_{\text{tr}}$  is equal to  $P_{\text{btr}}/(1 - R)$ . Spring-loaded valves are usually calibrated by closing the valve and measuring the production closing pressure. In this case because the valve is opened, the force balance equation that applies just before the valve closes is:

$$P_{\text{tr}} = P_{\text{btr}} \quad (7.15)$$

Where  $P_{\text{btr}}$  is calculated from Eq. 7.13. The instant the valve closes, the value of  $P_{\text{tr}}$  is measured and it is called  $P_{\text{trc}}$  where the “c” stands for “closing”.

## 7.2 CALCULATION OF THE NITROGEN PRESSURE AT DIFFERENT CONDITIONS

For nitrogen-charged gas lift valves, the operating temperature  $T_v$  to be used in design and troubleshooting calculations depends on the type of installation:

- Wireline-retrievable valves, installed inside standard side pocket mandrels with gas injection down the annulus and liquid production up the tubing.
  - For design calculations, use a linear temperature distribution from the reservoir temperature to the production wellhead temperature. For troubleshooting analyses, use an intermediate temperature between the gas injection temperature and the production fluid temperature: (1) If the valve’s upper packings are above the bellows (usually the case for 1-in. OD valves) injection gas surrounds most of the valve and the dome temperature is estimated as the injection gas temperature at valve’s depth plus one-third the difference between the production temperature minus the gas injection temperature at valve’s depth; and (2) if the valve’s

upper packings are below the bellows (very common in 1.5-in. OD valves) production liquids surround most of the valve and the dome temperature is estimated as the injection gas temperature at valve's depth plus two-thirds the difference between the production temperature minus the gas injection temperature at valve's depth.

- Wireline-retrievable valves, installed inside standard side pocket or concentric mandrels (inside the production tubing) with gas injection down the tubing and liquid production up the annulus.
  - For design calculations, use a linear temperature distribution from the reservoir temperature to the production wellhead temperature (not the injection gas surface temperature). Temperature surveys in this case indicate that the injection gas rapidly acquires the temperature of the production fluids in the annulus when the well is in normal operation (after unloading) so it would be a mistake to estimate the valve design temperature equal to the linear temperature distribution from the reservoir temperature to the surface gas injection temperature. For troubleshooting analyses, a temperature virtually equal to the production temperature in the annulus at valve's depth can be used because, as previously indicated, the injection gas can be considered to be at that temperature.
- Tubing-retrievable valves located outside the production tubing with gas injection down the tubing and liquid production up the annulus.
  - For design calculations, use a linear temperature distribution from the reservoir temperature to the production wellhead temperature. For troubleshooting analyses, use the liquid production temperature at the valve's depth.
- Concentric mandrel with gas injection down the annulus and liquid production up the tubing.
  - For design calculations, use a linear temperature distribution from the reservoir temperature to the production wellhead temperature. For troubleshooting analyses use the liquid production temperature at valve's depth.
- Tubing-retrievable valves located outside the tubing with gas injection down the annulus.
  - For design calculations, use a linear temperature distribution from an average surface temperature (equal to the average of the gas surface injection temperature and the wellhead production temperature) to the gas temperature at the depth of the deepest valve. For troubleshooting analyses, use the gas injection temperature at valve's depth.

Beside the cases previously mentioned, there are situations where, for the reasons explained in chapter: Continuous Gas Lift Troubleshooting, the injection gas is injected only through an upper unloading valve that is located above the static liquid level and, in consequence, the well does not produce any liquids. In these cases, there are equations that can be used to determine the valve's temperature. The cooling effect caused by gas expansion through the gas lift valve and the lack of hot fluids coming from the reservoir, make the valve's closing pressure decrease to pressures below its design value and therefore the valve tends to remain open. This problem is explained in Section 11.4.3, where the equations to predict the valve's temperature are described in detail for troubleshooting analyses.

The nitrogen pressure at test-rack conditions ( $P'_b$  in psig at 60°F) is calculated from the nitrogen pressure at operating conditions ( $P_{bt}$  in psig), from the following equation:  $P'_b = C_1 P_{bt}$ ; where  $C_1$  is a factor that depends on the values of the nitrogen temperature,  $T_v$ , and the dome pressure,  $P_{bt}$ . Correlations for  $C_1$  can be found in the literature. In a general form, these correlations can be expressed as:

$$C_1 = G_1(A, B, C, P_{bt}) \quad (7.16)$$

Where  $G_1$  is a simple algebraic equation and  $A$ ,  $B$ , and  $C$  are linear functions of  $T_v$  and  $P_{bt}$ :

$$\begin{aligned} A &= f_1(T_v - 60) \\ B &= g_1(T_v - 60) \\ C &= h_1(T_v - 60, P_{bt}) \end{aligned}$$

If  $(520 P_{bt})/(460 + T_v)$  is greater than a certain pressure  $P_{\max 1}$ , a new function  $G_2$  is used, keeping the same form of  $G_1$  and changing only the values of  $A$ ,  $B$ , and  $C$  as:

$$\begin{aligned} A &= f_2(T_v - 60) \\ B &= g_2(T_v - 60) \\ C &= h_2(T_v - 60, P_{bt}) \end{aligned}$$

Linear functions  $f_n$ ,  $g_n$ , and  $h_n$ , as well as the value of  $P_{\max 1}$ , can be found in the literature; however, the reader must be aware of the fact that all these functions might give erroneous results for dome pressures above a certain limit. With the advent of gas lift valves that can be set at very high test-rack opening pressures, new linear functions  $f_3$ ,  $g_3$ , and  $h_3$ , as well as a new pressure limit  $P_{\max 2}$ , must be used.

When doing troubleshooting calculations, the value of  $P'_b$  can be calculated (using the equations explained in the previous section) from the value of  $P_{tr}$



found in the design of the well and then  $P_{bt}$  can be calculated for the current operating temperature  $T_v$ . This reverse calculation is more complex because it requires the iteration procedure given in Fig. 7.3.

A simpler alternative (for troubleshooting analysis or design calculations) to find  $P'_b$  in psig from  $P_{bt}$  (also in psig) or vice versa, is given by the following equation:

$$P'_b = \frac{P_{bt} + a}{b} \quad (7.17)$$

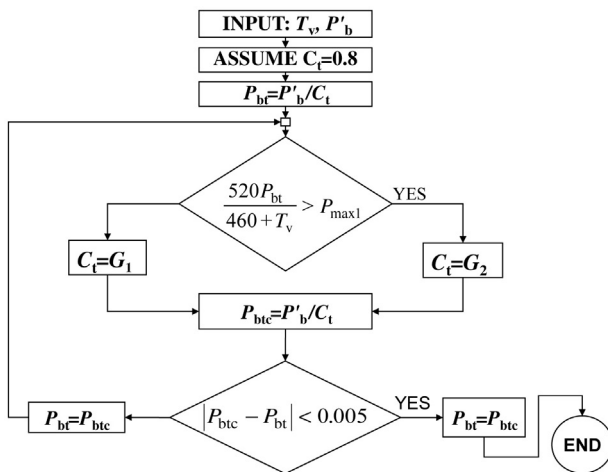
Where  $a$  and  $b$  are parameters given by:

$$a = 0.083(T_v - 60)$$

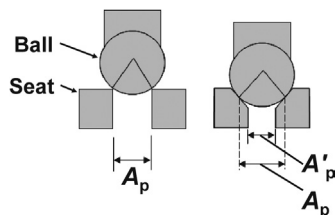
$$b = 1 + 0.002283(T_v - 60)$$

For troubleshooting analyses,  $P_{bt}$  is simply equal to  $(bP'_b - a)$ . Eq. 7.17 should not be used for values of  $P_{bt}$  larger than 2000 psig and operating temperatures above 220°F. This equation was developed by Zimmerman (1982).

It is important to indicate that tables to find the value of  $C_t$  are also presented in numerous books and manuals for gas lift design. These tables can be used with an acceptable level of accuracy for nitrogen pressures of values up to 1200 psig at 60°F. Higher than actually needed valve calibration pressures would be obtained if these tables are used for higher nitrogen pressures.



■ FIGURE 7.3 Calculation procedure to find  $P_{bt}$  from  $P'_b$  for troubleshooting analysis.



■ FIGURE 7.4 (a) Sharp-edged seats, (b) tapered seats.

### 7.3 DETERMINATION OF THE PORT AND BELLOWS AREAS

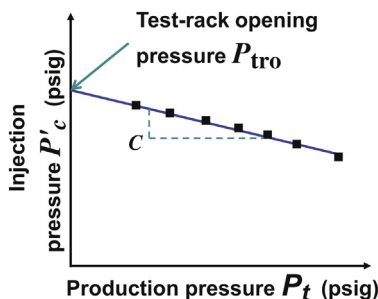
Fig. 7.4 shows two definitions of the port area to be used in the force balance equations presented in Section 7.1, corresponding to two types of seats: sharp-edged seats in Fig. 7.4a and tapered seats in Fig. 7.4b.

For sharp-edged seats, area  $A_p$  is used in the force balance equation and in the calculation of the gas flow rate (gas flow rate calculation is explained in chapter: Gas Flow Through Gas Lift Valves). For tapered seats, area  $A_p$  is used in the force balance equation and area  $A'_p$  is used in the calculation of the gas flow rate, knowing that the discharged coefficient is affected by the special geometry of the seat in this case. The value of  $A_p$  depends on the taper angle and the diameter of the ball.

Once the area of the seat is determined, the bellows area  $A_b$  is found from a very simple procedure carried out at the test rack, which is explained in the next paragraphs.

The valve is subjected to fixed upstream and downstream pressures. The valve is placed in such a way that the production pressure,  $P_t$ , and the injection pressure,  $P'_c$ , can be measured at the moment the valve opens. For each production pressure  $P_t$ , the injection pressure is slowly increased until the valve opens. The production and injection opening pressures are plotted as shown in Fig. 7.5 and the result should be a straight line.

The absolute value of the slope of the line in Fig. 7.5 is equal to the so called “tubing effect factor”, given by  $R/(1 - R)$  and denoted as  $P_{\text{Per}}$  (nowadays the tubing effect factor is called “production pressure effect factor”). Because  $R$  is equal to  $A_p/A_b$  and  $A_p$  is already known, the value of  $P_{\text{Per}}$  allows for the calculation of  $A_b$  from:



■ FIGURE 7.5 Results from a test to determine the bellows area to be used in the force balance equation.

$$A_b = A_p(1 + C)/C \quad (7.18)$$

Where  $C$  is the absolute value of the slope of the line in Fig. 7.5.

To demonstrate Eq. 7.18, a nitrogen-charged IPO valve, with no spring, is taken as an example. The force balance equation is given by Eq. 7.2:

$$(1 - R)P'_c + (R)P_t = P_{bt} \quad (7.2)$$

If the nitrogen pressure is kept constant and at a temperature of 60°F, then  $P_{bt}$  is equal to  $P'_b$ . Dividing Eq. 7.2 by  $(1 - R)$  and solving for  $P'_c$ :

$$P'_c = -[R/(1 - R)]P_t + P'_b/(1 - R) \quad (7.19)$$

Using Eq. 7.4 and the fact that Eq. 7.19 has a slope equal to  $-C$ :

$$P'_c = -C(P_t) + P_{tro} \quad (7.20)$$

$C$  is then equal to  $P_{per} = R/(1 - R)$ , from which  $R = C/(1 + C)$  and because  $R$  is equal to  $A_p/A_b$ , Eq. 7.18 is demonstrated.

## 7.4 EXAMPLES OF PROBLEMS USING THE FORCE-BALANCE EQUATIONS FOR DESIGNING AND TROUBLESHOOTING GAS LIFT INSTALLATIONS

Several examples of the use of the force–balance equations for designing and troubleshooting gas lift installations are given in this section.

### Problem 7.1

For the operating conditions given later, calculate the calibration pressure corresponding to the following cases:

1.  $P_{tro}$  for a nitrogen-charged IPO valve without a spring.
2.  $P_{tro}$  for a nitrogen-charged IPO valve with a spring ( $P'_r = 300$  psig).
3.  $P_{tro}$  for a spring-loaded IPO valve.
4.  $P_{trc}$  for a spring-loaded IPO valve.
5.  $P_{tro}$  for a nitrogen-charged PPO valve, without a spring.
6.  $P_{tro}$  for a nitrogen-charged PPO valve with a spring ( $P'_r = 300$  psig).
7.  $P_{tro}$  for a spring-loaded PPO valve.
8.  $P_{trc}$  for a spring-loaded PPO valve.

The gas injection pressure  $P'_c$  is equal to 1250 psig and the production pressure  $P_t$  is equal to 425 psig. The valve temperature is 180°F and its area ratio  $R$  is 0.028.

**Solution**

1. For this case  $P_{bt}$  is calculated using Eq. 7.2:

$$P_{bt} = (1 - 0.028)1250 + (0.028)425 = 1226.9 \text{ psig.}$$

Eq. 7.17 is used to calculate  $P'_b$  with  $a = 0.083(180 - 60) = 9.96$  and  $b = 1 + 0.002282(180 - 60) = 1.27396$ .

$$P'_b = \frac{P_{bt} + a}{b} = \frac{1226.9 + 9.96}{1.27396} = 970.8782$$

Finally, the test-rack opening pressure is calculated using Eq. 7.4:

$$P_{tr} = \frac{P'_b}{(1 - R)} + P'_r = \frac{970.8782}{(1 - 0.028)} = 998.84589 \text{ psig.}$$

2. The additional spring force is taken into consideration in Eq. 7.2:

$$P_{bt} = (1 - 0.028)1250 + (0.028)425 - (1 - 0.028)300 = 935.3 \text{ psig.}$$

As can be seen, the spring does protect the bellows because it can now be charged at a lower nitrogen pressure (compared with the bellows pressure in part "1" of this problem).

Eq. 7.17 is used to calculate  $P'_b$  with  $a = 0.083(180 - 60) = 9.96$  and  $b = 1 + 0.002282(180 - 60) = 1.27396$ .

$$P'_b = \frac{P_{bt} + a}{b} = \frac{935.3 + 9.96}{1.27396} = 741.9856$$

Finally, the test-rack opening pressure is calculated using Eq. 7.4:

$$P_{tr} = \frac{P'_b}{(1 - R)} + P'_r = \frac{741.9856}{(1 - 0.028)} + 300 = 1063.3596 \text{ psig.}$$

Even though the dome pressure is less than the one found in the previous case (part "1"), the calibration pressure is now 64.51 psig higher. It is important to remember that the calibration of the valve in this case is performed in two steps: First, with the bellows at 0 psig, the spring is adjusted until the valve's opening pressure becomes equal to 300 psig and then the dome is pressurized until the test-rack opening pressure is equal to 1063.3596 psig.

3. To calculate the calibration pressure of a spring-loaded IPO valve, the value of  $P_{btr}$  must be found first using Eq. 7.6:

$$(1 - R)P'_c + (R)P_t = P_{btr} = (1 - 0.028)1250 + (0.028)425 = 1226.9 \text{ psig}$$

The test-rack opening pressure is found from Eq. 7.7:  $P_{tr} = P_{btr}/(1 - R) = 1226.9/(1 - 0.028) = 1262.24$  psig. Note that for the same

operating conditions, spring-loaded valves require a greater test-rack opening pressure.

4. In this case, the calibration closing pressure is equal to the value of  $P_{bt}$  found in the previous case, which is 1226.9 psig.
5. For a nitrogen-charged PPO valve, Eq. 7.10 is used to find the dome pressure at operating conditions:

$$(0.028)1250 + (1 - 0.028)425 = P_{bt} = 448.1 \text{ psig.}$$

Eq. 7.17 is used to calculate  $P'_b$  with  $a = 0.083(180 - 60) = 9.96$  and  $b = 1 + 0.002282(180 - 60) = 1.27396$ .

$$P'_b = \frac{P_{bt} + a}{b} = \frac{448.1 + 9.96}{1.27396} = 359.5561$$

Finally, using Eq. 7.12, the test-rack opening pressure  $P_{tr}$  is found (this pressure should be applied through the nose or lower part of the valve because it is the production pressure):

$$P_{tr} = 359.5561 / (1 - 0.028) = 369.9136 \text{ psig}$$

6. In this case the additional spring force must be considered. Eq. 7.10 is used to find the dome pressure at operating conditions:

$$(0.028)1250 + (1 - 0.028)425 - (1 - 0.028)300 = P_{bt} = 156.5 \text{ psig}$$

Eq. 7.17 is used to calculate  $P'_b$  with  $a = 0.083(180 - 60) = 9.96$  and  $b = 1 + 0.002282(180 - 60) = 1.27396$ .

$$P'_b = \frac{P_{bt} + a}{b} = \frac{156.5 + 9.96}{1.27396} = 130.6634$$

Finally, using Eq. 7.12, the test-rack opening pressure,  $P_{tr}$ , (which must be applied through the nose of the valve) is found:

$$P_{tr} = 130.6634 / (1 - 0.028) + 300 = 434.4274 \text{ psig}$$

It is important to remember that the calibration of the valve in this case is performed in two steps: First, with the bellows at 0 psig, the spring is adjusted until the valve opening pressure becomes equal to 300 psig and then the dome is pressurized until the test-rack opening pressure is equal to 434.4274 psig.

7. For this case, pressure  $P_{btr}$  is calculated first using Eq. 7.13:

$$P_{btr} = (0.028)1250 + (1 - 0.028)425 = 448.1 \text{ psig}$$

The test-rack production opening pressure,  $P_{tr}$ , is found using Eq. 7.14:

$$P_{tr} = 448.1/(1 - 0.028) = 461 \text{ psig}$$

8. In this case, the test-rack closing pressure is equal to pressure  $P_{btr}$  found in the previous case, which is 448.10 psig.

### Problem 7.2

A well has a nitrogen-charged IPO valve without a spring. The production pressure at valve's depth is estimated to be 365 psig and the bellows temperature is 150°F. The valve's area ratio is 0.028 with  $P_{tro} = 700$  psig. Find the injection opening and closing pressures.

### Solution

This type of operation constitutes one of the different calculations that must be performed during a troubleshooting analysis with the purpose of finding the most probable point of injection. Using Eq. 7.4, the dome pressure at test-rack conditions,  $P'_b$ , is found:

$$P'_b = P_{tr} (1 - 0.028) = 700(1 - 0.028) = 680.4 \text{ psig}$$

To calculate the nitrogen pressure at operating conditions,  $P_{bt}$ , Eq. 7.17 is used. In this case:

$$a = 0.083(150 - 60) = 7.47$$

$$b = 1 + 0.002283 (150 - 60) = 1.20547$$

$$P_{bt} = P'_b b - a = 680.4(1.20547) - 7.47 = 812.73 \text{ psig.}$$

Eq. 7.2 is used to find the injection pressure at depth  $P'_c$ . For injection pressures greater than  $P'_c$ , the valve might be open:

$$\begin{aligned} P'_c &= P_{bt}/(1 - R) - (R)P_t/(1 - R) = 812.73/(1 - 0.028) - (0.028)365/(1 - 0.028) \\ &= 825.6276 \text{ psig} \end{aligned}$$

If the injection pressure at valve's depth is greater than or equal to 825.6276 psig, it is highly probable that the valve is open. In fact, the valve could be open if the injection pressure is greater than  $P_{bt}$ , which is the valve's closing pressure, as long as the following two conditions are true: (1) the valve was already opened and then the pressure decreased to a value between 825.6276 and 812.73 psi, and (2) the production pressure is high enough to help keep the valve open at this range of injection pressures (the dynamic models explained in chapter: Gas Flow Through Gas Lift Valves should be used to determine the state of the valve). To reach a final conclusion

that this is indeed the operating valve, the gas flow rate through the valve at operating conditions should be calculated and compared to the surface injection gas flow rate. Additionally, the bottomhole flowing pressure corresponding to this point of injection should also be calculated to establish if the liquid production calculated from the IPR curve corresponds to this bottomhole flowing pressure. The gas flow rate through an orifice valve is very easy to estimate using the equations given in chapter: Single and Multiphase Flow Through Restrictions. For calibrated valves, the gas flow rate calculation from current operational conditions is very difficult to do and the dynamic models explained in the following chapter must be used.

## REFERENCE

- Zimmerman, W.G., 1982. Manual Básico de Gas Lift. Publicación interna de la compañía Lagoven, S.A. Departamento de Producción, División Occidente, Tía Juana, Venezuela.

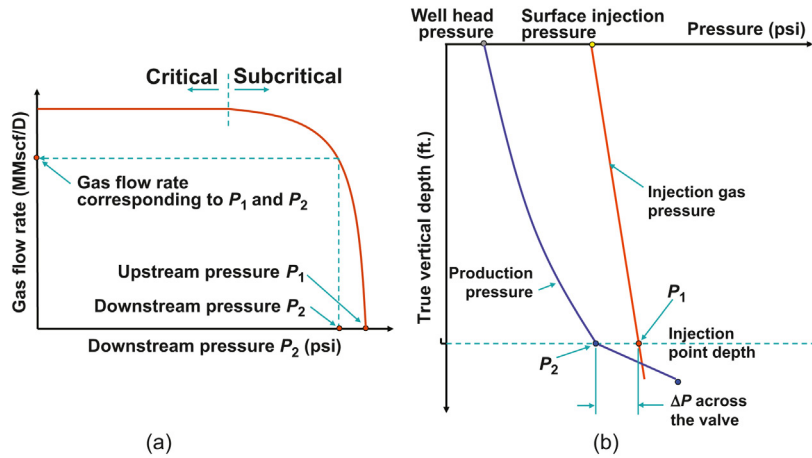
# Gas flow through gas lift valves

Predicting the gas flow rate through a gas lift valve for a given operational condition constitutes one of the most important steps in designing and troubleshooting gas lift wells. For a successful design or troubleshooting analysis of a well on gas lift, it is necessary to be able to predict how a gas lift valve, with a given calibration pressure and surrounding temperature, will react to a set of upstream and downstream pressures. It is important to determine if the valve is (partially or fully) opened or closed, and to predict the gas flow rate the valve will allow to pass for each of these cases.

The easiest valves to analyze are the so-called “orifice valves.” These valves are installed at the operating point of injection, which is the point of injection the well will have under normal operation (once it has been unloaded). The gas flow through an orifice valve is called “orifice flow” to distinguish it from the more complex flow found in calibrated valves, where the ball, or stem tip, strongly interferes with the flow if the valve is not fully open, inducing a different type of flow called “throttling flow.” Fig. 6.7, in chapter: Gas Lift Equipment, shows two types of orifice valves. Fig. 8.1a shows a typical curve of the gas flow rate through an orifice valve for a given constant injection (or upstream) pressure. In Fig. 8.1b, the injection (upstream) and production (downstream) pressures of a valve,  $P_1$  and  $P_2$ , respectively, are identified in a pressure–depth diagram.

As can be seen in Fig. 8.1, if the upstream pressure of the valve (at valve’s depth), namely  $P_1$ , is kept constant, for each downstream pressure  $P_2$  there is one and only one gas flow rate that the orifice valve allows to pass. If  $P_1$  and  $P_2$  are equal, the gas flow rate is equal to zero. This is the point in Fig. 8.1a where the curve intersects the horizontal axis. If pressure  $P_2$  is decreased (keeping  $P_1$  constant) the gas flow rate increases. If  $P_2$  is further decreased, a point is reached in which the gas flow rate attains a maximum value that remains constant for all other lower values of  $P_2$ . In this situation the flow is said to be choked and it is called “critical flow.” The gas velocity across the valve reaches the velocity of sound at the boundary between critical and subcritical flow. Any pressure fluctuation downstream of the valve



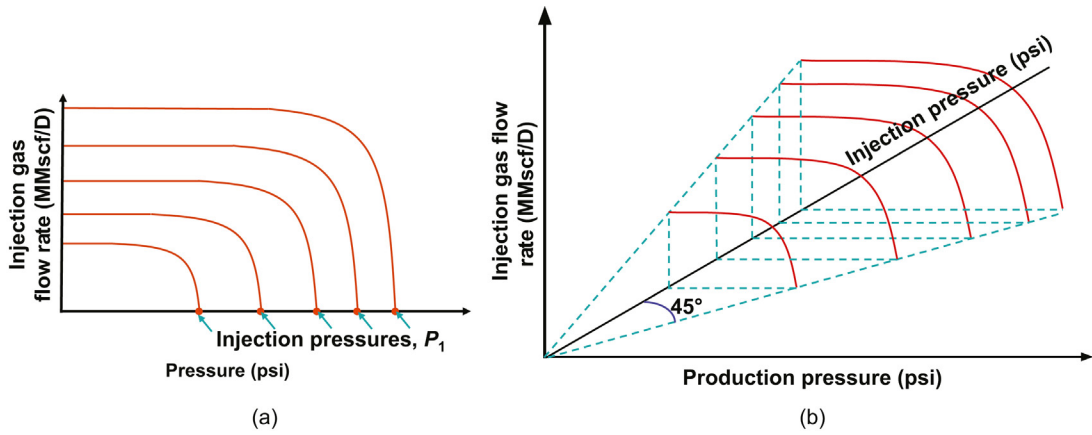


■ FIGURE 8.1 Orifice flow. (a) Gas flow rate diagram, (b) pressure–depth diagram.

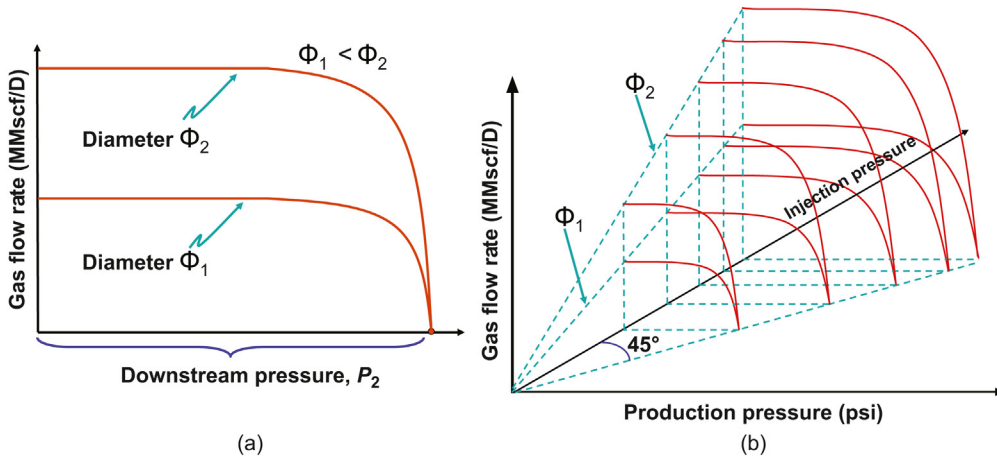
cannot propagate upstream of the orifice if the flow is critical. The equation to predict the transition from subcritical to critical flow and the equations that describe the gas flow through orifices are derived in chapter: Single and Multiphase Flow Through Restrictions.

Fig. 8.2a shows several gas flow rate curves corresponding to different injection pressures  $P_1$  at a location just upstream of the valve. As the injection pressure is increased, the maximum gas flow rate an orifice valve can pass also increases. Fig. 8.2b shows the same information presented in Fig. 8.2a but in a three-dimensional graph to familiarize the reader with this type of graphs, which are very important when dealing with gas flows through calibrated valves. The horizontal plane in this case is defined by the injection pressure ( $P_1$ ) axis and the production pressure ( $P_2$ ) axis. Along the 45-degree line on the horizontal plane, the gas flow rate is equal to zero because  $P_1$  and  $P_2$  are equal on this line. The set of all curves corresponding to all the injection pressures, for an orifice valve of constant orifice diameter, generates a surface that extends from the intersection of the three axes, where the gas flow rate is equal to zero, to a gas flow rate equal to infinity, provided the injection pressure could be indefinitely increased.

In reality, the available upstream injection pressure cannot be greater than a finite maximum value, either because that is the maximum pressure the compressor can deliver or because higher pressures would open an unloading valve located above the operating injection point. If the maximum upstream pressure has been reached and it is necessary to inject a higher injection gas flow rate, the orifice valve should be replaced with another one with a larger



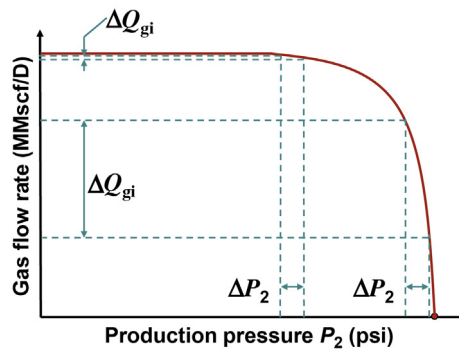
■ FIGURE 8.2 Gas flow through an orifice valve (constant orifice diameter) for different upstream injection pressures. (a) Two dimensional graph, (b) three dimensional graph with the same information.



■ FIGURE 8.3 Orifice flow for two different orifice diameters. (a) Two dimensional graph, (b) three dimensional graph of the same process.

orifice diameter. Fig. 8.3a shows two curves for two different orifice diameters and the same upstream injection pressure  $P_1$ . Clearly, the gas flow rate can be considerably increased by increasing the orifice diameter. Fig. 8.3b shows, in a three-dimensional graph, the gas flow rates for two orifice diameters,  $\Phi_1$  and  $\Phi_2$ , and different upstream injection pressures  $P_1$ .

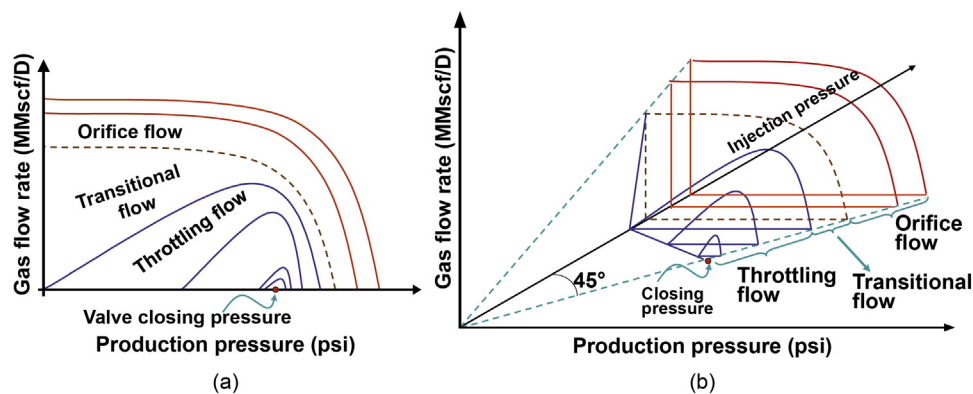
Critical flow requires a large pressure drop across the valve and it might be an indication that compression energy is being wasted; however, at the other extreme, having a subsurface orifice gas lift valve in subcritical flow with the injection pressure (in the annulus) very close to the production



■ FIGURE 8.4 Effect of the downstream (production) pressure fluctuation on the gas flow rate across an orifice valve.

pressure (in the tubing) could cause instability problems in the operation of the well. As shown in Fig. 8.4, any production pressure fluctuation ( $\Delta P_2$ ) in subcritical flow might induce a major change in the gas flow rate ( $\Delta Q_{gi}$ ) across the orifice valve that will not be present in critical flow. If, for example, there is a drop in the production pressure at valve's depth (caused by any surface disturbance in the flowline or at the flow station), the gas flow rate will increase and this increment in turn might reduce the production pressure even further if the original gas/liquid ratio was less than the ratio needed to obtain the minimum pressure gradient curve in the production tubing (minimum pressure gradient curves are explained in chapter: Total System Analysis Applied to Gas Lift Design, see Fig. 5.1). This could cause an additional increase in the gas flow rate, that might be followed by a reduction in the annular injection pressure (because the gas flow rate through the orifice valve might now be greater than the injection gas flow rate at the surface). Meanwhile, if the reduction of the production pressure in the tubing makes the reservoir react with a considerable increase in the liquid production, the production pressure will rapidly increase causing a decrease in the injection gas flow rate (which might even drop to zero) while the injection pressure is slowly trying to increase again. This process could manifest itself at the wellhead as small well headings or as very large pressure and liquid flow rate fluctuations that might affect the operation of the surface facilities and/or cause formation damage.

The gas flow rate through an orifice valve is much easier to describe than the dynamic behavior of a calibrated valve, in which the ball of the valve interferes with the gas flow, causing a restriction that depends on the position of the ball with respect to the seat of the valve. The position of the ball,



■ FIGURE 8.5 Gas flow through a calibrated valve. (a) Two dimensional graph, (b) three dimensional graph with the same information.

in turn, is a function of the calibration pressure of the valve and its upstream and downstream pressures. Fig. 8.5a shows what happens to the gas flow rate through a calibrated valve when the injection pressure is reduced while the valve's closing pressure is kept constant. For each set of injection and closing pressures, there is one curve that describes the gas flow through a calibrated valve. For high injection pressures, the gas flow appears to be identical to the gas flow through an orifice valve and this is why it is called "orifice flow," even though it takes place through a calibrated valve. This type of flow occurs when the valve is fully open. Although the type of flow seems to be orifice flow, the ball of the valve might still interfere with the gas flow, making it necessary for the equations derived for flows across orifice valves to be modified by introducing a smaller discharge coefficient. If the injection pressure is reduced, the curves begin to show a reduction in the gas flow rate at lower production pressures (for which the gas flow rate should remain constant in orifice flow). This type of flow is called "transitional flow." If the injection pressure is further reduced, eventually the curves intersect the production pressure axis at low values of the production pressure, indicating that the valve has closed even though the injection pressure is above the injection closing pressure. In this last case, the flow is called "throttling flow." If the injection pressure is further reduced, the valve's injection closing pressure is reached. Fig. 8.5b shows the dynamic behavior of a calibrated valve in a three-dimensional diagram.

The topics presented in this chapter begin with the description of the Thornhill–Craver equation (developed for gas flow through surface choke beans in gas producing wells) as applied to orifice gas lift valves and to calibrated gas lift valves under orifice flow conditions.

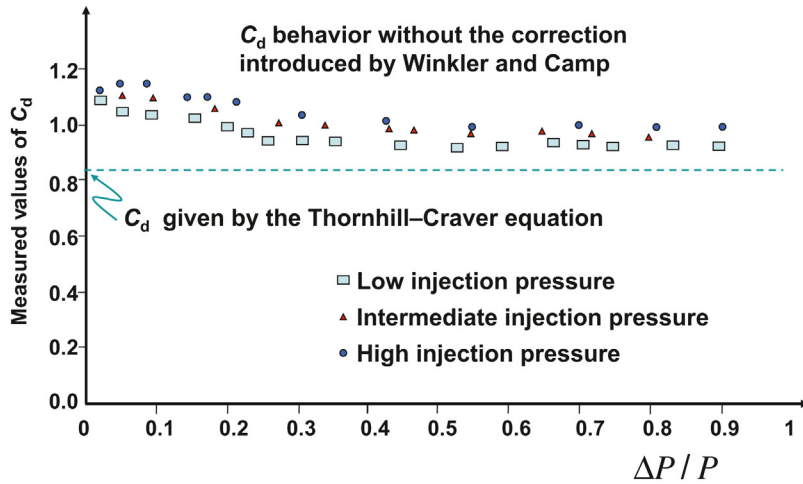
### 8.1 USE OF THE THORNHILL–CRAVER EQUATION FOR GAS LIFT VALVES

Finding the exact seat (or orifice) diameter of a gas lift valve to pass exactly the gas flow rate calculated in the gas lift design of a well is a very important task in the implementation of the gas lift method. For decades, the Thornhill–Craver equation (Cook and Dotterweich, 1981) has been used to predict the gas flow rate through orifice or calibrated gas lift valves. This equation is presented in chapter: Single and Multiphase Flow Through Restrictions, Eq. (4.25), and its behavior and recommendations for its use in gas lift designs are described in this chapter. The Thornhill–Craver equation was developed for gas well surface choke beans, which are cylindrical restriction of approximately 6 in. in length and available in different inside diameters. The diameters used in the derivation of the equation ranged from 1/8 to 3/4 in.

Until the mid 1980s, prior to the development of the models to predict the dynamic behavior of gas lift valves, the most commonly used equation for finding the seat diameter of a gas lift valve was the Thornhill–Craver equation. Even though important limitations of this equation were already identified by that time, they were not described in the literature in detail and only general and rather vague rules of thumb were used to take these limitations into account. But during the 1980s, several experimental studies that described, in a rather superficial way, the behavior of the Thornhill–Craver equation when applied to gas flows through gas lift valves, were published. Winkler and Camp (1985) published an interesting work that shows evidences of the limitations of the Thornhill–Craver equation. They found that in many cases the discharge coefficients, back-calculated from their own data, were much greater than those used in the Thornhill–Craver equation. They also modified the original equation by introducing the gas compressibility factor  $Z$  into the equation in the following manner:

$$Q_{gi} = \frac{155.5 C_d (A_p) P_1 \sqrt{2g \left( \frac{k'}{k' - 1} \right) \left( r^{2k'} - r^{\frac{k'+1}{k'}} \right)}}{\sqrt{\gamma_g Z T}} \quad (8.1)$$

Where  $Z$  is the gas compressibility factor that was not contemplated in the original equation,  $Q_{gi}$  is the gas flow rate in MMscf/D,  $C_d$  is the discharge coefficient for a given seat diameter,  $A_p$  is the seat flow area in square in.,  $r$  is the pressure ratio equal to  $P_2/P_1$ ,  $P_1$  is the pressure upstream of the valve in psia,  $P_2$  is the downstream pressure in psia,  $g$  is the acceleration due to gravity equal to 32.16 ft/s<sup>2</sup>,  $k'$  is the specific heat ratio of the injection gas

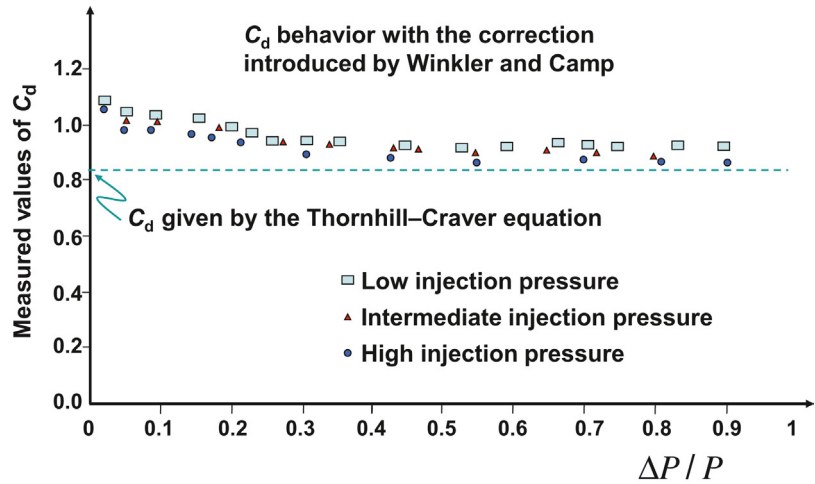


■ FIGURE 8.6 Behavior of the discharge coefficient back-calculated by Hernandez from the data found in small-diameter seats (without the correction introduced by Winkler and Camp).

equal to  $C_p/C_v$ ,  $\gamma_g$  is the gas specific gravity, and  $T$  is the absolute injection gas temperature upstream of the valve in °R. Experiments performed by the author of this book (at field conditions, with the gas lift valve held totally open by mechanical means, and with the internal check valve installed in the gas lift valve) demonstrated that the correction introduced by Winkler and Camp did not improve the behavior of the Thornhill–Craver equation in a significant way; therefore, further improvements of this equation are needed. Examples of the observations made on the behavior of the back-calculated discharge coefficient, as compared to the original discharge coefficients, are given in Figs. 8.6 and 8.7 (for small-diameter seats only). The discharge coefficients, calculated from the measured gas flow rates and the valve's upstream and downstream pressures, are plotted against the pressure drop across the valve divided by the upstream injection pressure. The flow area used in the calculation was the area of the seat for each case that was studied.

The following comments can be made from Figs. 8.6 and 8.7:

- With or without the correction introduced by Winkler and Camp, the original discharge coefficient is less than the values measured for small-diameter seats (the opposite is true for large-diameter seats, not shown here).
- With or without the correction introduced by Winkler and Camp, the actual discharge coefficient depends on the injection pressure and

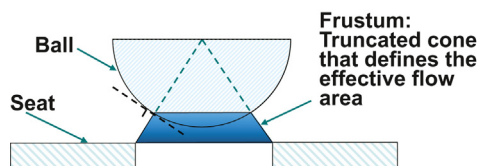


■ FIGURE 8.7 Behavior of the discharge coefficient back-calculated by Hernandez from the data found in small-diameter seats (with the correction introduced by Winkler and Camp).

the pressure drop across the valve. With the Winkler and Camp's correction, the discharge coefficient tends to decrease as the injection pressure is increased and the opposite is true without the correction. These observations also apply to large-diameter seats (not shown).

- For all cases, the actual discharge coefficient tends to increase as the pressure drop across the valve decreases, reaching values that are even greater than unity. This reveals the fact that the original and modified equations are not applicable in subcritical flows. This observation was also commented by Winkler and Camp in their work. A few years later, [Nieberding \(1988\)](#) also observed that the discharge coefficient changed as a function of the pressure drop across the valve, but he gave only general results without details regarding the effect of the injection pressure and the pressure drop across the valve on the discharge coefficient.
- The Winkler and Camp's correction causes the following effects: (1) the scatter of the discharge coefficient induced by the effect of the injection pressure is reduced; (2) the discharge coefficients, for small-diameter seats, are closer to the original value but still remain at greater values, especially in subcritical flow.

Winkler and Camp back-calculated the discharge coefficients of seats totally removed from the gas lift valve, in other words, without the typical upstream and downstream restrictions found in a gas lift valve (such as its entrance and exit ports, its internal passage way, and check valve). In



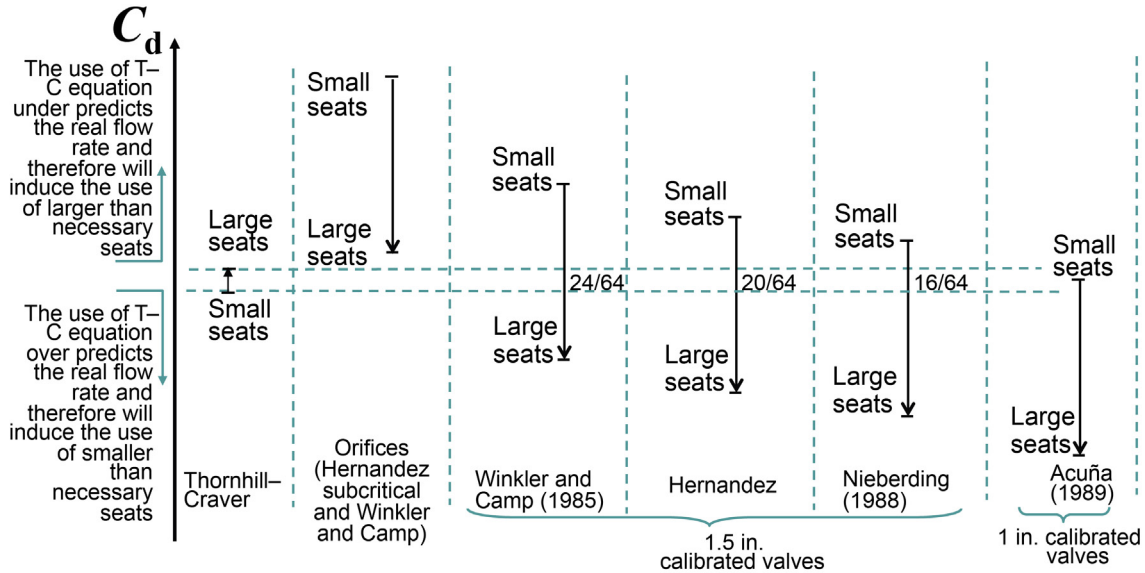
■ FIGURE 8.8 Effective flow area of a partially opened gas lift valve.

a different type of test, they used modified valves so that the position of the ball could remain at fixed positions by the use mechanical means. In this additional study, Winkler and Camp's tests were performed with the ball located in such a way that the frustum (the cone between the ball and the seat) would generate: (1) four flow areas smaller than the seat area, (2) one with the exact seat area, and (3) one with the valve totally open (with the ball located as far as possible from the seat). Discharge coefficients were back-calculated for each case using Eq. (8.1) with  $A_p$  equal to the area of the frustum and not the seat area (Fig. 8.8 shows the geometry that defines the area of the frustum). When the valve was totally open, the discharge coefficients were equal to those calculated with the ports removed from the valve. This indicates that the internal restrictions found in a gas lift valve do not have any effect on the gas flow rate for the experimental conditions used in Winkler and Camp's work. The average discharge coefficients, for diameters between 16/64 and 20/64 in. and different positions of the ball, were slightly smaller than the values found for seats removed from the valve and considerably smaller for 24/64-in. ports. For the seats studied by Winkler and Camp, the discharge coefficients were greater than or equal to those reported by the original Thornhill–Craver equation: 11% greater for 16/64-in. seats, 6% greater for 20/64-in. seats, and almost equal for 24/64-in. seats. These results were published without differentiating between critical and subcritical flow.

The observations made by Winkler and Camp and, to a certain degree, those made by Hernandez, indicate actual discharge coefficients for small-diameter seats being greater than those originally reported by the Thornhill–Craver equation. But Nieberding (1998) and Acuña (1989) published different results, almost always opposite to those reported by Winkler and Camp and by Hernandez. The reason for this discrepancy is explained further.

In the following paragraphs, valves with outside diameters equal to 1 in. are referred to as 1-in. valves while those with 1.5-in. outside diameters are referred to as 1.5-in. valves. This diameter should not be confused with the diameter of the seat (also referred as the “orifice” or “port”) of the valve (which usually goes from 1/8 to 32/64 in.).





■ FIGURE 8.9 Comparison of the results obtained by different authors for the discharge coefficient.

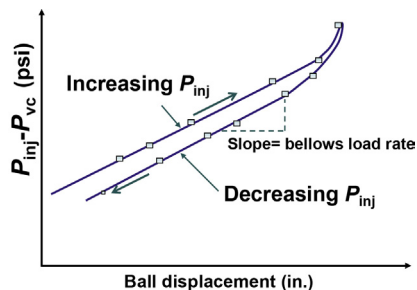
**Nieberding (1988)** carried out tests with 1.5-in., nitrogen-charged gas lift valves and his observations indicate that the original discharge coefficients are greater than those he back-calculated for seats greater than  $\frac{1}{4}$  in. in diameter, smaller for seats smaller than  $\frac{1}{4}$  in. in diameter and about the same for  $\frac{1}{4}$ -in. diameter seats. For critical flow only, the observations made by Hernandez are similar to those made by Nieberding regarding the fact that as the seat diameter is increased, the Thornhill–Craver equation goes from under predicting to over predicting the gas flow rate. But, while Nieberding found that the equation accurately predicts the gas flow rate for  $\frac{1}{4}$ -in. ports, Hernandez found that for those seats the equation still under predicts the gas flow rate. The results found by Hernandez indicate that the Thornhill–Craver equation under predicts the gas flow rates for all seats when the flow is subcritical and, in critical flow, the equation under predicts the gas flow rate for seats up to  $\frac{1}{4}$  in. in diameter. For 20/64-in. seats, Hernandez found that the equation accurately predicts the gas flow rate in critical flow. Acuña worked with 1-in., nitrogen-charged gas lift valves and found that, with few exceptions, even for ports smaller than  $\frac{1}{4}$  in. in diameter, the original discharge coefficients were greater than those he obtained and this deviation increases for larger seat diameters. Acuña also found that these deviations were greater for 1-in. diameter valves compared with those found in 1.5-in. diameter valves: 1-in. valves offer more resistance to the gas flow than the 1.5-in. valves. Fig. 8.9 shows, in a graphical way, the facts given in this paragraph.

The differences found between the experiments performed by Winkler and Camp and by Hernandez on one side, and those by Nieberding and by Acuña on the other, can be explained in the following way.

- First of all, the valves used by Hernandez were totally open by mechanical means, which maintained the ball far away from the seat, regardless of the upstream and downstream pressures of the valve.
- Even though Winkler and Camp located the ball at different positions, they always back-calculated the discharge coefficient using the area of the frustum and not the area of the seat.
- Nieberding and Acuña calculated the discharge coefficients using the seat area and assumed that the valves were totally open; but it is known that a valve might not be totally open and still exhibit orifice flow. The ball in Nieberding's and Acuña's experiments was free to settle at a distance from the seat established by the operational conditions.

It is possible then that the valves under the conditions present in Nieberding's and Acuña's tests were not totally open. For small ports, the ball only needs to move a short distance to consider the valve as totally open. For example, a valve with an 8/64-in. port only requires the ball to move 0.044 in. for the frustum area to be equal to the seat area, while for a 20/64-in. port, the ball must move 0.13 in. for the same purpose. Additionally, the force required to move the ball does not depend on the seat diameter but on the resistance offered by the bellows or the spring, which is identical for valves of a given model and calibration pressure.

All these facts explain why the tests carried out by Nieberding and Acuña indicate that the Thornhill–Craver equation under predicts the gas flow rate for “small-diameter” seats: the valves were indeed totally open in these cases and the discharge coefficient tends to agree with the larger values found by Winkler and Camp and by Hernandez. Valves with larger seats required higher injection pressures to be totally open and it was possible that the ball was interfering with the gas flow in the tests performed by Nieberding and Acuña. On the other hand, Acuña found that 1-in. valves offered more flow resistance than 1.5-in. valves did. This is explained not only by the fact that the internal flow passage of a 1-in. valve is more restrictive but, more importantly, because 1-in. valves require a greater differential pressure (above the opening pressure) to be totally open than 1.5-in. valves do. Pressures much higher than the injection opening pressure are required to open a 1-in. valve than to open a 1.5-in. valve to a given position of the ball. This is due to the fact that the bellows load rate (defined as a factor proportional to the spring constant of the bellows or the spring, see Fig. 8.10) for 1-in. valves is



■ FIGURE 8.10 Definition of the bellows' load rate.

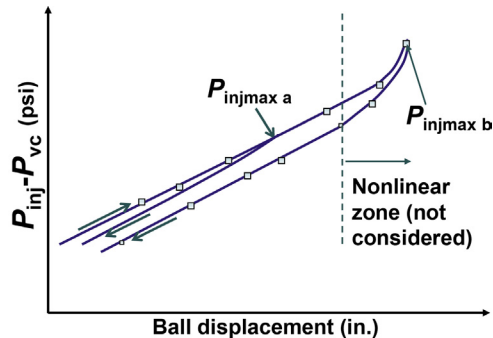
greater than for 1.5-in. valves. The definition of the bellows' load rate corresponds to the slope of the straight line obtained during especially designed tests in which the injection pressure under static conditions,  $P_{inj}$ , minus the valve's closing pressure at the operating temperature during the tests,  $P_{vc}$ , is plotted against the stem movement (equal to the distance traveled by the ball from the seat).

As can be seen in Fig. 8.10, the curve obtained by increasing the injection pressure is different from the one obtained while decreasing the injection pressure. This behavior is called “bellows hysteresis,” and it is one of the reasons why the models developed for throttling flow are not very accurate. But an even more disturbing observation is the fact that the magnitude of the hysteresis effect depends on the maximum injection pressure attained during the bellows' load-rate test. This can be observed in Fig. 8.11, where graphs for two maximum injection pressures,  $P_{injmax a}$  and  $P_{injmax b}$ , are shown.

The use of the Thornhill–Craver equation could lead to the selection of seat diameters not adequate for the conditions in the well.

- For orifice valves, the Thornhill–Craver equation could induce the use of orifices larger than required. This could cause a decrease in the annular injection pressure that, in extreme cases, might cause serious instability problems. Part of these problems has to do with the explanation given for Fig. 8.4 regarding subcritical flows.
- For calibrated valves (nitrogen-charged or spring-loaded) with large-diameter seats, the use of the Thornhill–Craver equation could result in the use of seats of smaller than required diameters. This problem is more severe for 1-in. valves.

These limitations on the use of the Thornhill–Craver equation were known before these experimental studies were published. Many authors gave



■ FIGURE 8.11 Effect of the maximum injection pressure on the bellows hysteresis.

general recommendations to correct the deviations obtained from the use of the Thornhill–Craver equation for gas lift valves. For example, some of the most popular alternatives were:

- For 1-in. valves up to 3/16-in. seats and for 1.5-in. valves up to 16/64-in. seats, use the original Thornhill–Craver equation (select the minimum port size that will pass at least the gas flow rate needed). (This is acceptable if the valve is not fully open, otherwise it will induce the use of seats larger than necessary.) For larger seats, it was recommended to increase the calculated seat diameter according to the designer's criteria.
- Use the original equation to find the port for the design injection gas flow rate and then use a port one size larger as a safety factor. (This is adequate for 1-in. valves in general and for 1.5-in. valves with ports greater than ¼ in. in diameter, but not for 1.5-in. valves with ports less than or equal to ¼ in. in diameter unless the valve is not fully open.)
- Size the port based on applying a 75 or 80% factor to the gas flow rate calculated with the original equation. (This is adequate for 1-in. valves in general and for 1.5-in. valves with ports greater than ¼ in. in diameter, but not for fully open 1.5-in. valves with ports smaller than or equal to ¼ in. in diameter).

No further details were given regarding critical or subcritical flow, spring-, or nitrogen-charged valves, etc.

Many commercially available computer programs use the original Thornhill–Craver equation but with the discharge coefficient modified in the following ways:

- For 1.5-in. injection-pressure-operated (IPO) valves, use the discharge coefficient equal to 0.76.

- For 1-in. IPO valves and for production-pressure-operated (PPO) valves of any size, use the discharge coefficient equal to 0.65.
- For 1.5-in. orifice valves, use the discharge coefficient equal to 0.86.
- For 1-in. orifice valves, use a discharge coefficient equal to 0.75 (this might be too small for an orifice valve).

It is important to check if the software used for the design of gas lift wells allows the user to input the discharge coefficient manually.

Regarding the dependency (found by Hernandez) of the discharge coefficient on the injection pressure, there are experimentally induced uncertainties in the field- and laboratory-scale work performed by the authors of the original Thornhill–Craver equation that might explain this dependency of the discharge coefficient. Even though they did not report the injection pressures used during the laboratory-scale tests, the difference between the minimum and maximum injection pressures used and reported for field-scale tests were very large for small diameter seats (from 330 to 1100 psi for 1/8-in. diameter seats) to very small values for large diameter seats (from 105 to only 128 psi for 3/4-in. diameter seats). This was probably due to problems regarding the maximum available gas flow rate that could be attained during the tests. For small-diameter seats, the difference between the maximum and minimum injection pressures was about 800 psi, while for large-diameter seats the injection pressure levels, as well as the differences between the maximum and minimum injection pressures, were smaller. These experimental limitations, together with the dependency of the discharge coefficient on the injection pressure found by Hernandez (see Figs. 8.6 and 8.7), explain why the scatter reported for the discharge coefficient in the original work was much greater for small diameter seats. The authors of the original work blamed these deviations on the variations of the diameters of the choke beans they used, which could explain part of the problem but not to the degree of the large values of the scatter found by Hernandez. Additionally, the experimental work used in the development of the original equation was carried out in critical flow and the derivation of the equation for subcritical flow was not reported.

---

### Problem 8.1

The design of a gas lift well indicates that 3.5 MMscf/D are required to flow through a 1-in. OD gas lift valve. The pressure and temperature at the entrance of the valve are 850 psia and 150°F, respectively. The gas specific gravity is 0.7 and its specific heat ratio is equal to 1.27. The gas compressibility factor at the entrance of the valve is 0.9 and the exit pressure is 420 psia. Find the required diameter of the seat of the gas lift valve if the

Thornhill–Craver equation is used with the correction made by Winkler and Camp and based on: (1) 100% of the calculated gas flow rate; and (2) 75% reduction of the calculated gas flow rate.

### Solution

As explained in chapter: Single and Multiphase Flow Through Restrictions, if the flow is critical,  $r$  ( $=P_2/P_1$ ) should be less than  $r_o$ , which is found by:

$$r_o = \left( \frac{2}{k'+1} \right)^{k'/(k'-1)} = \left( \frac{2}{1.27+1} \right)^{1.27/(1.27-1)} = 0.5512$$

Because  $P_2/P_1$  is  $420/850 = 0.49$ , which is smaller than 0.5512, the flow is critical and the gas flow rate is calculated using  $r_o$  as follows (the results are shown in Table 8.1):

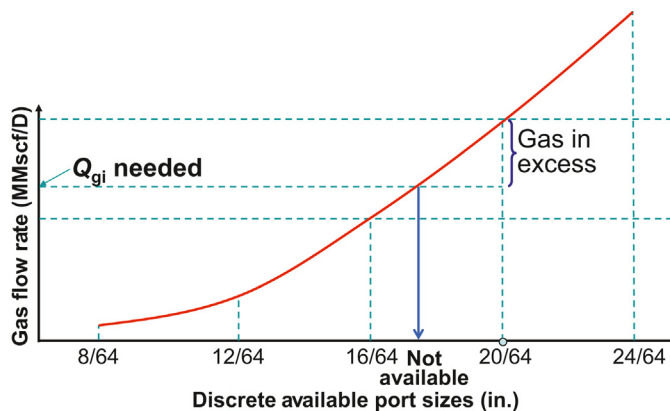
$$Q_{gi} = \frac{155.5C_d A_p 850 \sqrt{2(32.16) \left( \frac{1.27}{1.27-1} \right) \left( 0.5512^{2/1.27} - 0.5512 \frac{1.27+1}{1.27} \right)}}{\sqrt{(0.7)(0.9)(150+460)}} \\ = 25304 \left( \frac{\pi d^2}{4} \right) C_d$$

If the gas flow rate is assumed to be 100% of the calculated value, a 0.5-in. seat must be used because this is the smallest diameter capable of passing at least 3.5 MMscf/D. If the gas flow rate is assumed to be only 75% of the calculated value, a 5/8-in. diameter seat must be used. This is a step in the right direction because it is a 1-in. valve and the seat is not a small one. ■

Despite the limitations presented in this section regarding the use of the Thornhill–Craver equation, it continues to be a practical way of estimating the required diameter of the seat, within a reasonable margin of error,

**Table 8.1** Results of Gas Flow Rate Calculations for Several Seat Diameters  $d$

Seat Diameter $d$ (in.)	Calculated Gas Flow Rate (MMscf/D)	75% of the Calculated Gas Flow Rate (MMscf/D)
7/16	3.15	2.36
1/2	4.11	3.08
5/8	6.36	4.77
3/4	9.39	7.04



■ FIGURE 8.12 Required gas flow rate ( $Q_{gi}$  needed) in comparison to the flow rates the commercially available seats can provide.

for orifice valves and even for calibrated valves when they are fully open. In fact, it is almost always impossible in gas lift design to obtain a seat diameter that perfectly matches a commercially available size because seats are only available in a few number of discrete sizes, such as 8/64, 12/64, 16/64, or 20/64 in. The designer must select the smallest seat diameter that is capable of allowing at least the required injection gas flow rate. This usually implies the use of a seat that allows a larger than needed gas flow rate and the difference between this flow rate and the design gas flow rate is usually greater than the error introduced when applying the Thornhill–Craver equation, not to mention the general uncertainties in the design input data that the designer must usually face. This is presented in a graphical way in Fig. 8.12.

Then, the use of the Thornhill–Craver equation in design calculations might be adequate if some precautions (as explained previously) are taken; However, to carry out precise troubleshooting analyses, the Thornhill–Craver equation is of little use because, in the great majority of cases, calibrated valves are not fully open and, consequently, the gas flow rate calculated using the Thornhill–Craver equation for the given upstream and downstream pressures is usually much greater than the actual gas flow rate. Additionally, many times a calibrated valve closes at low production pressures even if the injection pressure is greater than the valve’s injection closing pressure. All these uncertainties have promoted the development of mathematical models capable of predicting the dynamic behavior of gas lift valves.

## 8.2 MATHEMATICAL MODELS FOR THE DYNAMIC BEHAVIOR OF GAS LIFT VALVES

Mathematical models for gas flow through orifices plates and chokes were developed long before the first models for gas lift valve behavior were published. No mathematical model able to predict the dynamic behavior of gas lift valves was published before the mid 1980s. Despite this fact, the way in which a calibrated gas lift valve would react to changes in the injection and production pressures was understood before the development of the first mathematical models. Independent studies performed by valve manufacturers showed the dynamic behavior of their own valves and some companies developed rudimentary models to predict the gas flow rate in throttling flow. This is the case of the Teledyne–Merla company, which manufactured spring-loaded, IPO valves, identified as “series L” which were used in throttling flow with a design procedure called “Proportional Response Method” in which graphs obtained by this company were used to determine the behavior of these valves. The valve manufacturer company McMurry also offered a set of tables that were used as a guide for the design of PPO, spring-loaded valves called S-FO and JR-FO. These tables would indicate the required increase in the production pressure (from the opening production pressure) to provide a given gas flow rate.

For many years, the simple force–balance equations (presented in chapter: Gas Lift Valve Mechanics) were used to calibrate gas lift valves and to predict if a valve was opened or closed. At the same time, the Thornhill–Craver equation was used to predict the gas flow rate through gas lift valves with the limitations given in Section 8.1. The work performed by [Neely et al. \(1973\)](#) was one of the first publications that recognized the fact that it was necessary to develop a model to predict the complex dynamic behavior of gas lift valves.

The mathematical models developed so far can then be categorized as follows: Mechanistic models: [Decker \(1986\)](#), [Hepguler \(1988\)](#), and [Sagar \(1991\)](#). Statistical models: [Nieberding \(1988\)](#), [Acuña \(1989\)](#), and [Rodriguez \(1992\)](#). Unified models: [Cordero \(1993\)](#), [Escalante \(1994\)](#), [Bertovic \(1995\)](#), and [Faustinelli \(1997\)](#).

With the exception of the work developed by [Decker \(1986\)](#) and the work explained in this book, all dynamic models known today were developed at the University of Tulsa under the research program known as the Tulsa University Artificial Lift Projects; therefore, special recognition should be given to the effort made by students and professors at the University of Tulsa on this difficult subject.



Biglarbigi (1985) presented a thesis on the gas passage performance of gas lift valves. He provided a procedure to estimate the gas passage through spring-loaded throttling valves. He also studied nitrogen-charged, IPO valves. His results showed that nitrogen-charged IPO valves can exhibit throttling and orifice flows and provided a criterion to predict the type of flow: If the injection pressure is greater than the test-rack opening pressure at the operating temperature (instead of the usual 60°F test-rack temperature), the valve will exhibit orifice flow, otherwise it will operate under throttling flow. The operating temperature is the temperature the valve has at a given downhole operating condition. Biglarbigi found the discharge coefficients that can be used in the Thornhill–Craver equation for orifice flow, but he did not provide a model for throttling flow in nitrogen-charged IPO valves.

In 1986, K. Decker published a paper describing the first complete model for spring-loaded IPO valves, which can be used for nitrogen-charged valves with the inclusion of additional routines. This model can be considered a truly mechanistic model from which later and more sophisticated models were developed. It considered a force–balance equation under dynamic conditions in which the pressure acting on the ball of the valve (which depends on the gas flow rate) is calculated using the ANSI/ISA-575.01 standard control valve sizing equation at numerous points on the surface of the ball. This force–balance equation determines the position of the ball, which in turn determines the flow coefficient to calculate the gas flow rate; because of the interdependency of the flow rate and the forces acting on the ball, the calculation process is an iterative procedure. To apply this model, not only the load rate of the valve and the flow coefficient as a function of the stem travel need to be experimentally found, but also the flow areas at different locations inside the valve (as functions of the stem travel) have to be determined from the valve’s internal geometry.

As pointed out by Decker, this model required several modifications: (1) the values of the flow coefficient  $C_v$  for different points along the inside of the valve need to be experimentally determined; (2) any minor change regarding the mapping of the pressure profile onto the ball surface has a profound influence on the gas flow rate, therefore a more sophisticated way of performing this task is needed; (3) the model does not handle critical flow because it did not account for normal shock waves that can take place between the ball and the seat. The fact that several values of the flow coefficient need to be experimentally found makes Decker’s model difficult to implement.

A similar approach taken by Decker was followed by Hepguler in 1988 to develop a new model. This model uses a dynamic force–balance equation to

calculate the stem position but, in this case, the effective pressure is found by an empirical equation obtained from measured effective pressures acting on the ball. To calculate the flow rate, the value of the expansion factor  $Y$  times the discharge coefficient  $C_d$  is needed. The product  $YC_d$  is found from extensive experiments in which the pressure in the interior of the valve needs to be measured. Hepguler used a definition of the load rate of the valve which is different from the one that is generally used. To obtain this load rate, especial tests are needed. The dome's internal pressure has to be measured during these especial tests. For gas flow rates greater than 1.4 MMscf/D, the model calculates the pressure drop across the check valve located just before the exit of the gas lift valve. Because of all the difficult measurements needed to calibrate this model, this approach is found to be highly impractical.

Nieberding (1988), Acuña (1989), and Rodriguez (1992) worked on the development of a different type of model, known here as “statistical models,” for orifice and throttling flows. These models treat the gas lift valve as a black box, so that only measurements taken outside the valve are considered. These models are not based on any physical characteristic of the valve and require extensive tests to correlate empirical factors that are used to determine the gas flow rate for a given operational condition. They are very easy to use and to incorporate in a computer program but they are not very accurate under operational conditions different from those used to calibrate the models.

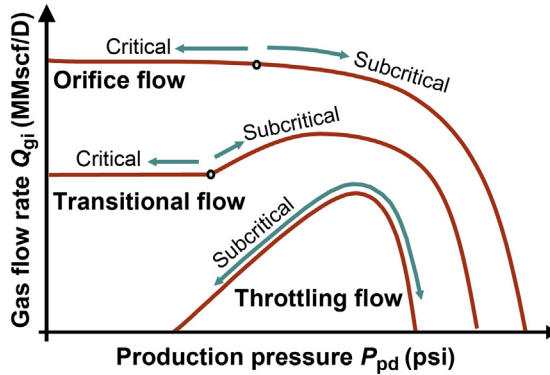
In 1991, Sagar presented a model that follows the same approach previously taken by Decker and Hepguler (known here as the “mechanistic approach”). In this case, the effective pressure on the ball is found by calculating the pressure along the ball using one-dimensional, compressible flow theory, including the calculation of the position of shock waves. This is done by assuming that the space between the ball and the seat can be treated as a converging-diverging nozzle, taking into consideration the flow area along the valve as a function of the stem travel but disregarding the actual shape of the flow passage. The flow area along the interior of the valve as a function of the stem travel is found from the internal geometry of the valve. The effective pressure on the ball is used in a force balance equation to determine the stem travel by means of an iterative procedure. The effective pressures calculated with Sagar's model agree with the measurements taken by Hepguler only for small values of the stem travel. Sagar attributed this discrepancy to the fact that his model does not consider the presence of boundary layers and the actual complexity of the flow passage around the ball and seat.

In 1993, Cordero introduced the first attempt to unify the throttling- and orifice-flow models into one single equation, but his work concentrated on PPO valves, which are not widely used.

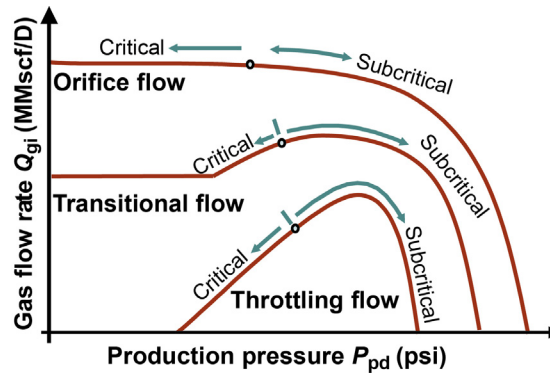
In 1994, Escalante developed a model that uses the orifice-flow equation for both orifice- and throttling-flow regimes. In this model, the orifice-flow equation is modified (with the purpose of also being used in the throttling-flow regime) simply by replacing the discharge coefficient times the expansion factor,  $C_d Y$ , with a correlating factor that is linearly proportional to the forces that try to open the valve. Unfortunately, this factor proved not to be linearly proportional to the opening forces in many cases and it is a weak correlating parameter, especially for large ported valves.

In 1995, Bertovic developed a unified model that was the first one to be able to predict the gas flow rate for orifice, throttling, and transitional flows with a single set of equations (that is the reason why this type of model is called “unified model”). The model uses: (1) the orifice-flow equation for the flow across the seat, and (2) a modified orifice-flow equation, that incorporates the correlating factor proposed by Escalante for the gas flow through the ball seat area (the correlating factor proposed by Escalante was used in a quadratic equation rather than in the linear function used by the Escalante’s model). The results of these two equations (orifice-flow and modified-orifice-flow) are set equal to each other to solve for an intermediate pressure between the minimum ball seat area and the seat itself. After this intermediate pressure is found, the gas flow rate is calculated using any of the two proposed equations. This model requires only six experimentally found coefficients, but they are difficult to find and they are not constants but functions of the valve’s closing pressure. These coefficients are relatively difficult to find because they must be determined from extensive dynamic tests.

Faustinelli indicated that Bertovic’s model was not physically correct because of the improper way of using the theoretical adiabatic equation from the minimum area to the area at the entrance of the check valve (located downstream of the seat). Faustinelli developed (and published in 1997) the second unified model that was capable of predicting the gas flow rate for all flow regimes. This model uses an empirical equation, based on the measurements made by Hepguler, to find the pressure at the seat from: the injection pressure, the production pressure, and an empirically found coefficient. The flow area between the ball and the seat is found using the same factor introduced by Escalante and used by Bertovic in his model. The flow is thermodynamically modeled at different points inside the valve and in different ways for each case: isentropic, constant pressure, or constant temperature



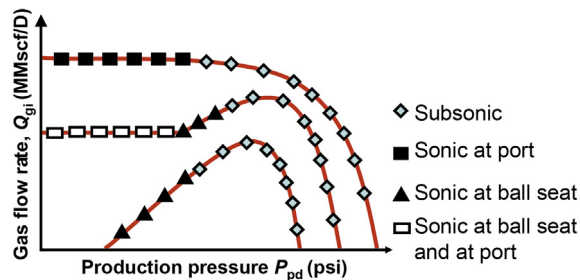
■ FIGURE 8.13 Transition between critical and subcritical flow at the seat.



■ FIGURE 8.14 Transition between critical and subcritical flow at the ball seat area.

flows. The model requires only four experimentally found coefficients. These coefficients are not constants but functions of the valve's closing pressure and extensive dynamic testing is required to determine their values.

One important contribution made by Bertovic and Faustinelli was to give an explanation for the internal process that determines the type of flow for a given operational condition. The boundaries between critical and subcritical flow, as determined by the model's output, are shown in the following figures for: (1) the seat (Fig. 8.13) and (2) the ball seat area (Fig. 8.14). The reason why the flow rate in transitional flow reaches a maximum value, then begins to drop to finally stay at a constant value as the production pressure is decreased to zero, has to do with the fact that critical flow is reached at the seat of the valve at low production pressures. With critical flow at the seat, the pressure upstream of the seat is constant, independently of the



■ FIGURE 8.15 Points where the boundary between sonic and subsonic flow takes place.

downstream production pressure below its critical value, so the movement of the ball stops and the gas flow rate becomes constant for lower production pressures. It can also be observed in the figures that, in the ball seat area, critical flow does not take place at the maximum gas flow rate as suggested by Sagar but, instead, it happens at a lower production pressure.

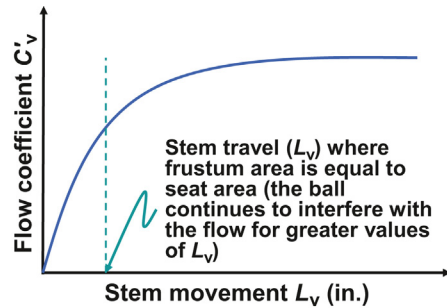
Figs. 8.13 and 8.14 can be simplified to just one, as shown in Fig. 8.15.

Because of the complexities of the aforementioned models and the difficulties encountered when trying to implement them, it is far more practical (and just as accurate) to use the simpler mechanistic models that are presented in Sections 8.2.1 and 8.2.2 for single element valves. A model for the more complex pilot valves is presented in Section 8.2.3.

### 8.2.1 Simple mechanistic model for single element, IPO, gas lift valves (without dynamic effect)

A very simple model that does not take into consideration any dynamic effect is explained in this section with the purpose of introducing the reader to this difficult subject. A more complex model that does take dynamic effect into consideration is explained in detail in Section 8.2.2. This latter model, as complex as it might seem, is still simpler than any of the mechanistic models developed in the past and it is also easier to calibrate for a given valve model and implement in a computer program.

The simplest model that can be derived and implemented is the one based only on two types of tests: the bellows-load-rate test and the flow-coefficient test, without taking into consideration the dynamic behavior of the gas lift valve. Decker (1986) was the first author to implement the basic concepts introduced in this simple model, which was followed afterwards by Hepguler and Sagar (each author, including Decker, incorporated some



■ FIGURE 8.16  $C'_v$  as a function of the stem movement for a given seat diameter.

additional factors to account for dynamic effects). In the bellows-load-rate test, the position of the ball under static conditions is measured for different injection pressures (greater than the closing pressure of the valve at the conditions of the test) and these values are plotted on a “Pressure” versus “Ball Position” diagram as shown in Fig. 8.10. The same injection pressure is applied to the ball and the bellows at the same time and it is first increased in discrete steps until the stem can no longer move and then the pressure is decreased, also in discrete steps, until the valve closes. This results in a curve that has a linear section with slightly different slopes for increasing and decreasing pressures. The average slope of the linear section of the curve is called the bellows’ load rate of the valve, usually given in psi/in. In the second test (flow-coefficient test), the position of the ball is held at a fixed value and the flow coefficient  $C'_v$  of the valve is calculated from tests performed at different injection and production pressures in which the gas flow rate is measured for each condition. The valve’s flow coefficient is calculated for several positions of the ball, giving a curve of the flow coefficient as a function of the position of the ball as shown in Fig. 8.16. Both of these tests are easy to perform.

The first step in the application of this simple type of model is to determine the distance the stem has moved from the seat. For this purpose, the static force–balance equation is used “above” the valve’s opening pressure (and not just before the valve opens as it is used in chapter: Gas Lift Valve Mechanics). According to this simple approach, the area of the ball over which the production pressure acts is kept constant at all time. This equation is given by:

$$P_{vcT} A_b + B_{lr} A_b L_v = P_{iod} (A_b - A_s) + P_{pd} A_s \quad (8.2)$$

Where  $P_{vcT}$  is the valve’s closing pressure at the operating temperature in psig (equal to the dome pressure  $P_{bt}$  at operating temperature,

see chapter: Gas Lift Valve Mechanics for the force–balance equation of IPO, nitrogen-charged or spring-loaded, gas lift valves);  $A_b$  is the bellows area in square in.;  $B_{lr}$  is the bellows load rate in psi/in.;  $L_v$  is the distance the stem has moved from the seat in in.;  $P_{iod}$  is the operating injection pressure at valve’s depth in psig;  $A_s$  is the area (in square in.) based on the diameter where the ball contacts the seat (see Fig. 7.4b in chapter: Gas Lift Valve Mechanics, in which  $A_p$  is equal to  $A_s$ ); and  $P_{pd}$  is the production pressure downstream of the valve in psig. According to this simple model, the area  $A_s$  (on which the production pressure acts) is kept constant, regardless of the position of the ball (which is a state that cannot exist under dynamic conditions). The heart of this simple model (and the reason for its simplicity) is then to assume that, independently of the position of the ball, the production pressure acts on the area of the ball exposed to the production pressure when the valve is closed. The implications of this oversimplification are described by means of three-dimensional graphs given in the more advanced mechanistic model presented in Section 8.2.2. As indicated previously, Eq. (8.2) was first used by Decker (1986), but it was also used (with the appropriate changes to introduce dynamic effects) by Hepguler (1988) and Sagar (1991).

The value of  $L_v$  can be found from Eq. (8.2) as:

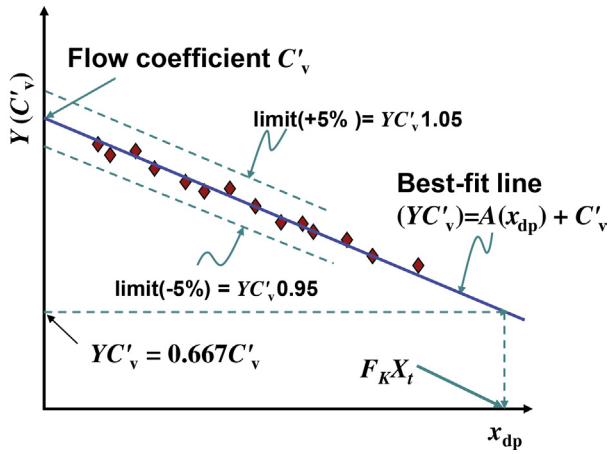
$$L_v = [P_{iod}(A_b - A_s) + P_{pd}A_s - P_{vCT}A_b] / (B_{lr}A_b) \quad (8.3)$$

The flow coefficient of the valve,  $C'_v$ , is a function of the stem displacement  $L_v$ . This function should be experimentally determined to obtain results as those shown in Fig. 8.16. Experimental tests have shown that the maximum value of  $C'_v$  is found at ball positions for which the area of the frustum is larger than the area of the seat of the valve. The frustum is the truncated cone between the ball and the seat shown Fig. 8.8.

Once the value of  $C'_v$  is found, a modified version of Eq. (4.24) from chapter: Single and Multiphase Flow Through Restrictions can be used to find the gas flow rate through the gas lift valve:

$$Q_{gi} = 32.64C'_v(P_{iod} + 14.7)Y \sqrt{\frac{x_{dp}}{\gamma(T_v + 460)Z_1}} \quad (8.4)$$

Where  $Q_{gi}$  is the gas flow rate in MMscf/D,  $C'_v$  is the flow coefficient of the valve,  $P_{iod}$  is the pressure upstream of the valve in psig,  $Y$  is the expansion factor,  $\gamma$  is the gas specific gravity,  $T_v$  is the gas temperature at the entrance



■ FIGURE 8.17 Determination of  $Y$  and  $C'_v$  for a given ball position.

of the valve in °F,  $Z_1$  is the gas compressibility factor at the entrance of the valve, and  $x_{dp}$  is given by:

$$x_{dp} = \frac{\Delta P}{P_{iod} + 14.7} \quad (8.5)$$

Where  $\Delta P$  is the pressure drop across the valve. This equation is regularly used to determine the appropriate size of control valves used in surface facilities.

To be able to use Eq. (8.4), it is necessary to find  $Y$  and  $C'_v$  as functions of the position of the ball. This requires a calibration process. For this purpose, the position of the ball is fixed at a certain value by mechanical means and the gas flow rate is measured for different injection pressures and pressure drops across the valve. Then, the gas flow rate measured at each point, divided by the gas flow rate calculated by Eq. (8.4) with  $Y$  and  $C'_v$  set equal to unity, is plotted as a function of  $x_{dp}$ . The best-fit line obtained for all the points corresponding to a given seat diameter and ball position gives a straight line that intersects the vertical axis at a point that defines the value of  $C'_v$  for that ball position, see Fig. 8.17. To find the value of  $Y$  as a function of  $x_{dp}$ , a horizontal line is traced from  $x_{dp} = 0$  and  $Y C'_v = 0.667 C'_v$  until it intersects the best-fit line previously found. The value of  $x_{dp}$  corresponding to this intersection point is equal to  $F_k X_t$ , where  $F_k$  is equal to  $k'/1.4$  and  $k'$  is the gas specific heat ratio. Knowing  $F_k$  and the product  $F_k X_t$ , the value of  $X_t$  is easily found. Unlike  $C'_v$ , the value of  $X_t$  is approximately constant for



a given seat diameter, regardless of the position of the ball. Then, knowing that  $Y = 1$  when  $x_{dp} = 0$ , factor  $Y$  as a function of  $x_{dp}$  is given by:

$$Y = 1 - x_{dp} / (3F_k X_t) \quad (8.6)$$

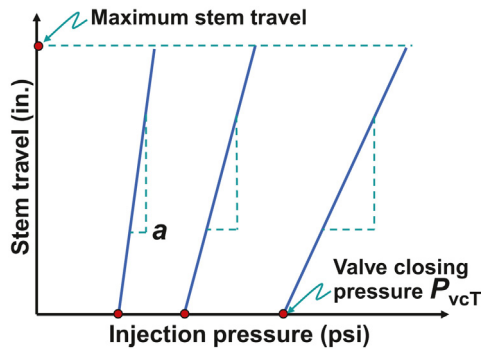
For subcritical flow,  $Y$  goes from 1 at  $x_{dp} = 0$  to 0.667 (which corresponds to the transition between critical and subcritical flow in which  $x_{dp}$  is equal to  $F_k X_t$ ). For values of  $x_{dp}$  greater than  $F_k X_t$ , the values of  $Y$  and  $x_{dp}$  in Eq. (8.4) are fixed at 0.667 and  $F_k X_t$ , respectively. This simple model requires then the experimental determination of the value of  $X_t$  for a given seat diameter and  $C'_v$  as a function of the position of the ball (or stem movement). These are valve's characteristics that can be easily found with an adequate test facility.

Then, for a given set of injection, production and valve's closing pressures, the gas flow rate is found by the following simple steps:

- Using Eq. (8.3), find the value of  $L_v$ ;
- With  $L_v$  already known, find the corresponding value of  $C'_v$  (using Fig. 8.16);
- Calculate  $Y$  with Eq. (8.6) and the value of  $X_t$  (which is a constant for a given seat diameter);
- Calculate the gas flow rate using Eq. (8.4), knowing that for values of  $x_{dp}$  greater than  $F_k X_t$ , the values of  $Y$  and  $x_{dp}$  in Eq. (8.4) are fixed at 0.667 and  $F_k X_t$ , respectively.

### 8.2.2 Mechanistic model for single element, IPO, gas lift valves (with dynamic effect)

Following the approach taken in the previous section, a simple mechanistic model that takes into consideration the dynamic effects can be developed. The model presented in this section is reasonably accurate and, not only much simpler to program in a computer, but it only requires seven experimentally found coefficients that are of constant value and very easy to find: two are found from the load rate tests, three from the flow coefficient tests, and only two from dynamic tests, with a very limited number of test points required in this last type of test. The model is based on finding the flow coefficient as a function of the injection, production, and closing pressures of the valve. For this purpose, the bellows-load-rate tests are combined with the flow-coefficient tests and with a small number of test points under dynamic conditions. These dynamic test points are used to find the dynamic production closing pressure in throttling flow. With the flow coefficient determined in this way, Eq. (8.4) is used to calculate the gas flow rate independently of



■ FIGURE 8.18 Results from the bellows' load-rate tests.

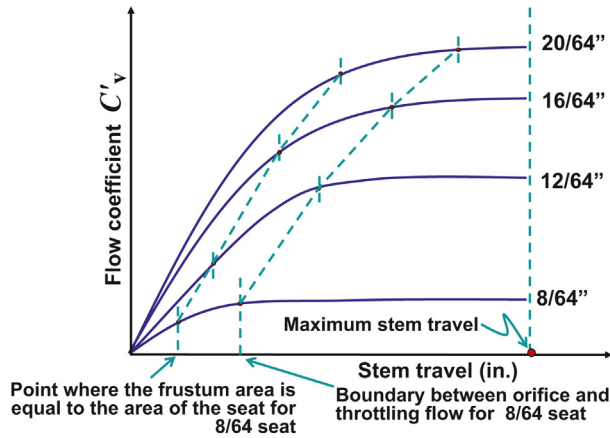
the type of flow (orifice, throttling, or transitional flow), thus the model can be defined as being mechanistic and unified at the same time. The model proposed here, for single element valves (not for pilot valves), can be regarded as a “unified model” because it uses only the orifice flow equation (as expressed in Eq. (8.4)) for all flow regimes, but with a flow coefficient  $C'_v$  that depends on the stem position.

In the load-rate tests, the valve is exposed to different injection pressures and, at each of these pressures, the position of the ball is measured. In this type of test, the gas flow rate is equal to zero at each value of the injection pressure; therefore, the test is performed under static conditions. Fig. 8.18 shows the results from bellows' load-rate tests in which, contrary to what is usually done, the horizontal axis is the injection pressure and the vertical axis is the distance traveled by the stem (up to the maximum effective stem travel). Averaging the hysteresis effect, the result is approximately a straight line with a slope  $a$  that decreases as the closing pressure increases. This dependency of the slope on the closing pressure is very small but it has been exaggerated in the figure so that it can be easily appreciated by the reader.

Each line in Fig. 8.18 corresponds to a given valve's closing pressure and can be expressed in the following way:

$$L_v = a(P_{inj} - P_{vcT}) \quad (8.7)$$

Where  $L_v$  is the stem travel expressed in inches,  $a$  is the slope of the line, and  $P_{inj}$  is the injection pressure above the valve's closing pressure at the operating temperature (known here as  $P_{vcT}$ ). Pressures  $P_{inj}$  and  $P_{vcT}$  can be expressed in psia, thus  $a$  is expressed in in./psi and it is the inverse of the bellows' load rate, which is usually expressed in psi/in. The load rate represents the required increase in the injection pressure in psi per in. of



■ FIGURE 8.19 Results from flow-coefficient tests (to find  $C'_v$  as a function of the stem travel).

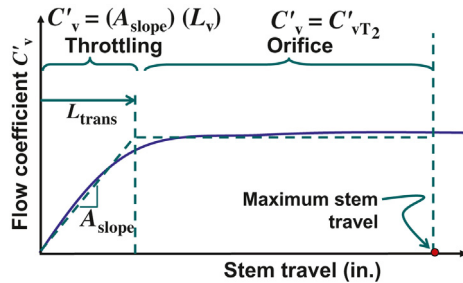
stem travel. Because of its dependency on the valve's closing pressure, the slope  $a$  can be expressed as a linear function of the valve's closing pressure at operating conditions:

$$a = a' P_{vcT} + b' \quad (8.8)$$

The coefficients that need to be determined from the load-rate tests are  $a'$  and  $b'$ . These coefficients are easily determined because the load-rate tests are performed under static conditions. These coefficients are constants that do not depend on the seat of the valve. They only depend on the valve model being used. The simple relationship expressed in Eq. (8.8) can be replaced with a more sophisticated one, but it will not increase the accuracy of the calculated value of the slope  $a$  in a considerable way because the dependency of  $a$  on  $P_{vcT}$  is very weak.

The flow-coefficient tests are performed with internally modified valves so that the position of the ball can remain at fixed values during the tests, independently of the upstream and downstream pressures. Tests in which the flow coefficient is back-calculated are performed for upstream pressures that are greater than their corresponding downstream pressures (thus the gas flow rate is greater than zero), maintaining the stem position fixed at a given value. Typical results from these tests are shown in Fig. 8.19, in which each curve corresponds to a different seat diameter.

The curves presented in Fig. 8.19 can be approximated as linear functions like those shown in Fig. 8.20, with  $L_{trans}$  being the stem travel that defines the



■ FIGURE 8.20 Linear approximation of the flow coefficient as a function of the stem travel.

transition between throttling and orifice flow. Any stem travel greater than  $L_{trans}$  will not cause a significant change in the flow coefficient  $C'_v$ . From experimental observations it was found that the value of  $L_{trans}$  is less than the maximum stem travel found in the bellows' load-rate tests, especially for small seats. On the other hand,  $L_{trans}$  is greater than the stem travel required for the ball seat area (frustum area) to be equal to the seat area.

For a stem travel between 0 and  $L_{trans}$ ,  $C'_v$  can be expressed by the following equation:

$$C'_v = A_{slope} L_v \quad (8.9)$$

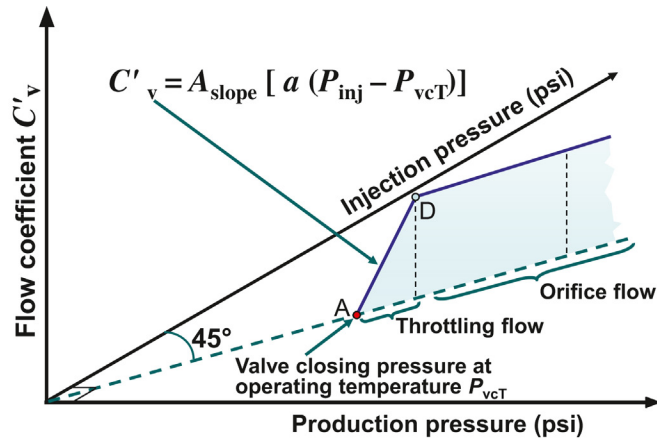
Where  $L_v$  is the stem travel and  $A_{slope}$  is the slope of the line. The coefficients that are used by the model and that can be easily obtained from the flow-coefficient tests are:  $L_{trans}$ ,  $A_{slope}$ , and  $X_t$ , where  $X_t$  is the pressure drop across the valve divided by the injection pressure and the factor  $[(C_p/C_v)/1.4]$  at the point where critical flow begins, see Fig. 8.17. These parameters are of constant values for a given valve and seat diameter.  $(C_p/C_v)$  is the specific heat ratio, known as  $k'$  in this book. Combining Eqs. (8.7) and (8.9), an expression is found for the flow coefficient in terms of the injection pressure and the valve's closing pressure at the operating temperature:

$$C'_v = A_{slope} [a(P_{inj} - P_{vcT})] \quad (8.10)$$

The injection pressure at the point where the flow goes from throttling to orifice flow is called  $P_{injT2}$  and it can be determined from Eq. (8.7) as:

$$P_{injT2} = P_{vcT} + (L_{trans}/a) \quad (8.11)$$

The value of  $C'_v$  found from Eq. (8.10), with  $P_{inj}$  equal to  $P_{injT2}$ , is called  $C'_{vT2}$  and it can be used in the gas flow rate equation for orifice flow only.

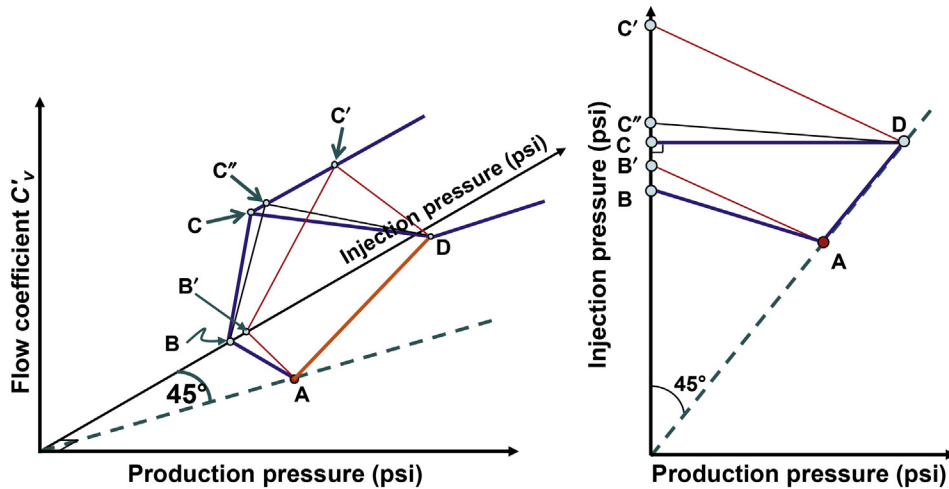


■ FIGURE 8.21  $C'_v$  line in the vertical plane at 45 degree angle with respect to the horizontal axes.

For throttling flow, the gas flow rate equation for orifice flow is also used but with a value of  $C'_v$  that is not a constant but that depends on the injection and production pressures. In throttling flow, Eq. (8.10) is only valid in the vertical plane that intersects the horizontal plane along the 45 degree line with respect to the horizontal axes in the three-dimensional graph shown in Fig. 8.21. In this graph, the horizontal axes are the production and injection pressures, while the vertical axis is the flow coefficient  $C'_v$ . The line that is defined by Eq. (8.10) on this vertical plane is line A–D shown in Fig. 8.21 and it is one of the most important lines on which this model is based. Due to dynamic effects, for any other point located outside this vertical plane, the value of  $C'_v$  also depends on the injection and the production pressures, but in a way that is much more complex than Eq. (8.10), as explained in next paragraphs.

One way of approximating the value of  $C'_v$  for transitional and throttling flow is by the use of surface A–B–C–D in Fig. 8.22, for which it is necessary to perform dynamic tests in which the stem is free to move according to the production and injection pressures. But the number of dynamic tests is small because they are only needed for finding the dynamic production closing pressure in throttling flow, which corresponds to line A–B in Fig. 8.22.

The model presented in this section approximates point C by simply projecting point D perpendicularly on the vertical plane where the production pressure is equal to zero. Line B–C corresponds then to an approximation of the transitional-flow regime that takes place for a very narrow range of the injection pressure between throttling and orifice flow. Point C' as shown

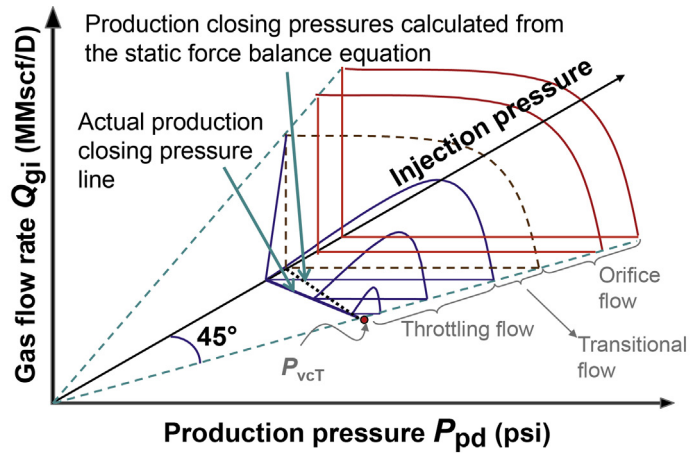


■ FIGURE 8.22 Flow coefficient  $C_v$  as a function of the injection and production pressures. (a) Three-dimensional graph; (b) horizontal projection.

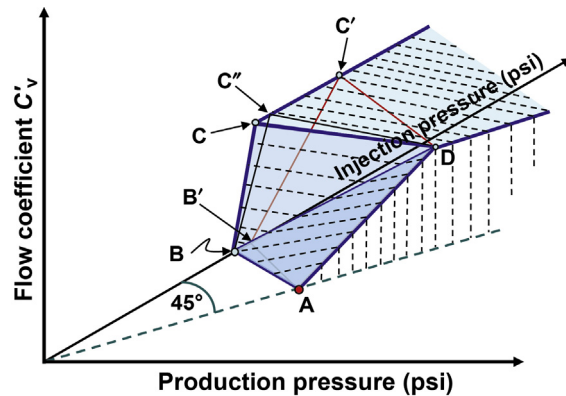
in Fig. 8.22 is in reality where point C should be located but the exact location of  $C''$  is extremely difficult to find experimentally and it is very close to point C anyway.

The model presented in this section is in reality a refinement of the model presented in Section 8.2.1, for which only the “static” force–balance equation is used to find the stem travel, independently of the dynamic effects that change the actual values of the pressure that acts on the ball. With this static stem travel, the value of  $C_v$  is found from the flow-coefficient-test results. Surface A–B'–C'–D would then be the one used by the simplified model presented in Section 8.2.1. The assumptions made in the simplified model dictate that line A–B' are parallel to line D–C'. The error made by using this simplified model can be appreciated in Fig. 8.22 by comparing surface A–B'–C'–D with A–B–C''–D. This error is a consequence of keeping the areas on which the upstream and downstream pressures are applied on the ball's surface at constant values, disregarding the dynamic effect of the gas flow. This dynamic effect makes line A–B' be in reality line A–B, which means that the valve tends to close at a lower production pressure, as demonstrated by Acuña (1989), see Fig. 8.23.

On the other hand, line D–C' considered by the simplified model, is in reality D–C''. So the simplified model presented in the previous section tends to under predict the gas flow rate in throttling flow. The top view of



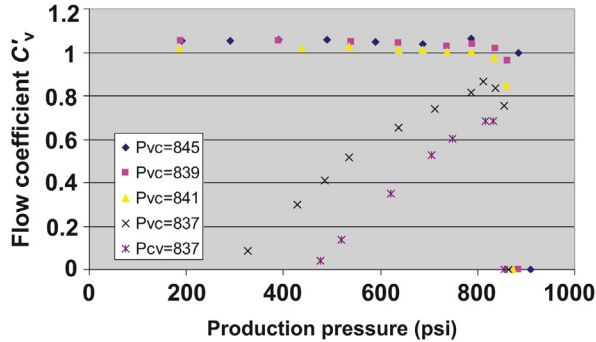
■ FIGURE 8.23 Effect of dynamic conditions on the production closing pressure.



■ FIGURE 8.24 Surface used by the dynamic model.

the surfaces shown in Fig. 8.22a can be appreciated in Fig. 8.22b. The major errors made by applying the simplified model will correspond to the areas D-C''-C' and A-B'-B. For the dynamic model presented in this section, the major errors will be made only in region D-C-C'' which is small and very difficult to investigate experimentally in a practical way. Knowing the complexity of other models, the approximated results that can be obtained from both, the simplified model and the dynamic one presented in this section, are reasonably accurate.

Fig. 8.24 shows the surface used by the dynamic model presented in this section. The simplest way to approximate surface A-B-C-D is by two plane



■ FIGURE 8.25 Flow coefficients calculated from the data obtained during actual dynamic tests (the stem of the valve was allowed to move freely).

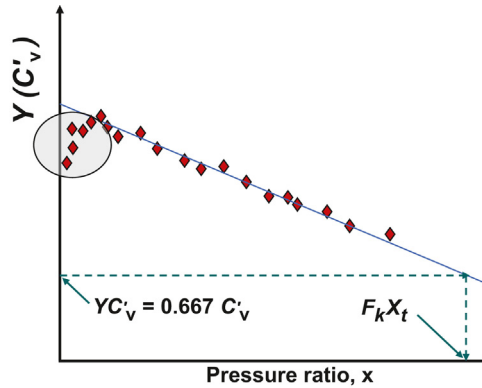
surfaces: A–B–D and B–C–D. The equations of these planes can be easily found using basic analytic geometry.

Each of the dashed lines in Fig. 8.24 corresponds to the values of  $C'_v$  for different production pressures with a common injection pressure. These lines do not necessarily need to be straight, but the data from dynamic tests showed that it is a good approximation to consider them as straight lines, as can be seen in Fig. 8.25 for curves with different injection pressures but with closing pressures that vary only within 1%.

As can be seen in Fig. 8.25,  $C'_v$  tends to decrease at the right hand side of these curves where the pressure drop across the valve is very small. This same behavior is found during flow-coefficient tests (which is a deviation from the predicted values according to the theory behind Eq. (8.4)).

In flow-coefficient tests, the stem is held at a fixed position by mechanical means; thus, the reduction of the flow coefficient at very small pressure drops across the valve cannot be attributed to dynamic effects on the position of the ball. This behavior is present if the data is analyzed with Eq. (8.4). On the other hand, if the Thornhill–Craver equation is used to analyze the data, the discharge coefficient tends to increase to values close to 1 for small pressure drops across the valve, as explained in Section 8.1. Fig. 8.26 shows a typical result from the flow-coefficient tests when the flow coefficient is the one used in Eq. (8.4). In this figure,  $x$  is the pressure drop across the valve divided by the injection pressure. It can be seen that, for small pressure drops across the valve, the values of  $YC'_v$  deviate from the straight line (the straight line is where the experimental points are supposed to be located according to the theory behind Eq. (8.4)). These deviations





■ FIGURE 8.26 Deviation of  $Y C'_v$  for small values of  $x$  in flow-coefficient tests (the stem of the valve is held at a fixed position).

simply indicate that the theories behind the different orifice flow equations do not accurately predict the gas flow rate for very small values of the pressure drop across the valve. This deviation poses no problem regarding the use of Eq. (8.4) in gas lift designs because the pressure drop across a gas lift valve should not reach very small values that might promote well instabilities.

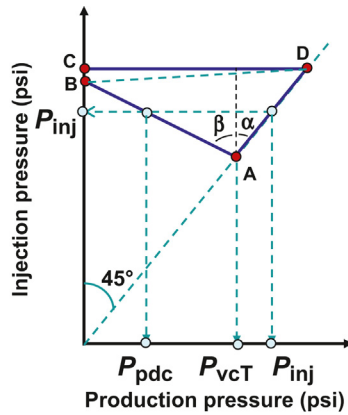
As was indicated previously, line A–B can be obtained from a small number of dynamic tests for different valve's closing pressures. Fig. 8.27 shows a horizontal projection of the surface presented in Fig. 8.24 with the notation used by Acuña (1989) in his derivation of line A–B. It can be seen in this figure that angles  $\alpha$  and  $\beta$  are constant in the throttling flow region.

From this geometry configuration, Acuña developed the following expression:

$$F_e = (P_{inj} - P_{vcT}) / (P_{inj} - P_{pdc}) \quad (8.12)$$

Where  $P_{pdc}$  is the dynamic closing pressure of the valve at operating conditions,  $P_{vcT}$  is the valve's closing pressure at operating conditions, and  $P_{inj}$  is the injection pressure at valve's depth.  $F_e$  was assumed by Acuña to be a constant that does not depend on  $P_{vcT}$ . According to the data reported by Acuña, the value of  $F_e$  presented a maximum deviation of around 30%. If  $F_e$  is considered a constant, the equation for line A–B is:

$$P_{pdc} = P_{inj} - (P_{inj} - P_{vcT}) / F_e \quad (8.13)$$



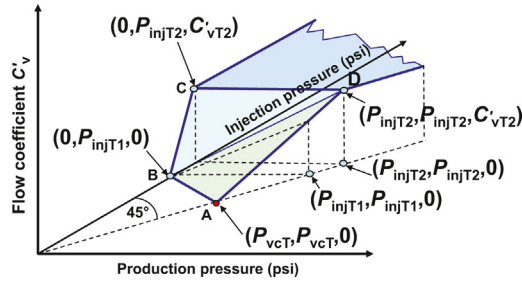
■ FIGURE 8.27 Horizontal projection of surface A–B–C–D.

This equation is the equation of line A–B where the dynamic effects have been taken into consideration. The simplified model presented in Section 8.2.1 gives an equation identical to Eq. (8.13), but with  $F_e$  replaced by the area ratio of the valve,  $R$  (the seat area divided by the bellows area). Acuña found that the value of  $F_e$  was slightly lower than  $R$  for almost all seat diameters he studied. If  $R$  is used instead of  $F_e$ , the production closing pressure for a given injection pressure would be greater than its actual value giving then line A–B' (as shown in Fig. 8.22) instead of line A–B shown in Fig. 8.27.

The scatter of the values of  $F_e$  found by Acuña could be due to the fact that  $F_e$  might not really be a constant but a function of the valve's injection closing pressure,  $P_{vct}$ . This could in turn be due to the dependency of the angle of line A–D with respect to the horizontal plane (in Fig. 8.22) on the injection closing pressure of the valve. This dependency is caused by the increase of the bellows' load-rate as the injection closing pressure is increased. Thus, the projection of line A–D on the horizontal plane changes for different values of  $P_{vct}$ . There is no reason to believe then that the value of  $F_e$  would not change for different values of  $P_{vct}$ . As it is the case for the bellows' load-rate, this dependency of  $F_e$  on  $P_{vct}$  should not be very strong. A simple equation for  $F_e$  in terms of  $P_{vct}$  could be:

$$F_e = cP_{vct} + d \quad (8.14)$$

The values of  $c$  and  $d$  are the only ones that are required by the model presented in this section that need to be found from dynamic tests. Dynamic tests are more difficult to perform than the bellows' load-rate tests and the flow-coefficient tests. Coefficients  $c$  and  $d$  are constant for each combination



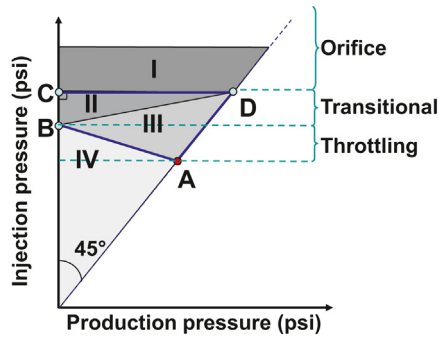
■ FIGURE 8.28 Notation used by the dynamic model.

of valve model and seat diameter. With  $F_e$  as a function of  $P_{vcT}$ , Eq. (8.13) can be used to find line A–B for a given value of  $P_{vcT}$ . Using the notation given in Fig. 8.28, the calculation procedure used by the dynamic model to find the gas flow rate is explained next.

$P_{injT1}$  (in psia) corresponds to the injection pressure where line A–B intersects the injection pressure axis.  $P_{injT2}$  (also in psia) is the minimum injection pressure for which the valve is considered to be fully open and where the flow coefficient is equal to  $C'_{vT2}$ . Referring to Fig. 8.29, region I corresponds to the orifice flow regime. Region II corresponds to the transitional flow regime where the flow coefficient is found by using the equation of plane B–C–D. Region III is divided into two parts: the upper part corresponds to the transitional flow, where the flow coefficient is found by the equation of the plane A–B–D, and the lower part corresponds to the throttling flow regime, where the flow coefficient is also found by the equation of the plane A–B–D. Region IV represents the area where the valve is closed: in the upper part of this region the valve is closed because of dynamic effects and in the lower part the valve is closed because the injection pressure is below the valve closing pressure  $P_{vcT}$ .

The data needed to calculate the gas flow rate is:

- The injection pressure,  $P_{inj}$ , in psia.
- The production pressure,  $P_{pd}$ , in psia.
- The valve closing pressure at operating temperature,  $P_{vcT}$ , in psia.
- The injection temperature,  $T_{inj}$ , in °R.
- The gas compressibility factor at  $T_{inj}$  and  $P_{inj}$ , which is  $Z_{inj}$ .
- The gas specific gravity,  $G_g$ , and the gas specific heat ratio,  $k'$ .
- The constants found from the bellows' load-rate tests:  $a'$  and  $b'$ .
- The constants found from the flow-coefficient tests:  $L_{trans}$ ,  $A_{slope}$ , and the critical pressure ratio  $X_t$ . Contrary to what is reported in the American Petroleum Institute (API) Recommended Practice 11V2,  $X_t$  is a



■ FIGURE 8.29 Horizontal view of the plane surfaces that are used to calculate  $C'_v$ .

constant that does not depend on the stem travel.  $X_r$  is found using the procedure given in Section 8.2.1, see Fig. 8.17.

- The constants found from the dynamic tests:  $c$  and  $d$ .

The calculations are done in the following order:

1. Using Eq. (8.8) find  $a$ .
2. Using Eq. (8.11) find  $P_{injT2}$ .
3. Using Eq. (8.9) with  $L_{trans}$  find  $C'_{vT2}$ .
4. Using Eq. (8.14) find  $F_e$ .
5. Calculate  $P_{injT1} = P_{vcT}/(1 - F_e)$ .
6. Next, the value of  $C'_v$  is found depending on the flow regime, using the equations from basic analytic geometry for the respective plane surface:

For region I in Fig. 8.29, the value of  $C'_v$  corresponds to the orifice flow regime:  $C'_{vt2}$ .

For region II the flow coefficient is calculated using the equation of the plane B–C–D, which is equal to:

$$C'_v = \frac{\beta''(P_{injT1} - P_{inj})}{\gamma'} \quad (8.15)$$

Where,  $\beta'' = C'_{vT2}P_{injT2}$  and  $\gamma' = P_{injT1}P_{injT2} - P_{injT2}^2$ .

For region III, the flow coefficient is calculated using the equation of the plane A–B–D, which is equal to:

$$C'_v = \frac{\alpha(P_{vcT} - P_{pd})\beta''(P_{vcT} - P_{inj})}{\gamma'} \quad (8.16)$$

$$\text{With now } \alpha = C'_{vT2} (P_{injT1} - P_{vcT}), \beta' = C'_{vT2} P_{vcT}, \text{ and} \\ \gamma' = P_{injT1} (P_{vcT} - P_{injT2}).$$

7. Calculate the pressure ratio  $x = (P_{inj} - P_{pd})/P_{inj}$ .
8. If  $x > X_f(k'/1.4)$  then fix the value of  $x$  at  $X_f(k'/1.4)$ .
9. Calculate  $Y = 1 - x/[3(k'/1.4)X_f]$ .
10. Finally, calculate the gas flow rate using:

$$Q_{gi} = 32.64 C'_v P_{inj} Y [x / (G_g T_{inj} Z_{inj})]^{1/2} \quad (8.17)$$

The following observations were made by the author of this book while doing load-rate and the flow-coefficient tests:

- The hysteresis effect found while doing the load-rate test cannot be attributed to the viscosity of the liquid inside the bellows because tests done with valves with no liquid inside the bellows showed the same behavior.
- When the pressure was raised to a point in which the valve was fully open, the hysteresis effect took its maximum value. However, if the maximum pressure of the test was less than the one that gives maximum stem travel, the hysteresis effect was not as pronounced and it can even be unnoticeable for small pressure increments above the closing pressure. This led to belief that the hysteresis effect was due to deformations of the shape of the bellows itself. Further tests were done with the dill valve removed so that the bellows pressure was constant and equal to the atmospheric pressure at all time. In this case, the bellows was compressed by a length equal to the maximum stem travel and then it was released. The length of the bellows did not return to its original one, showing a very small plastic deformation. This plastic deformation might be the reason why the pressure needs to be lowered by a certain amount below the pressure exerted on the way up to reach the same stem travel on the way down. This is a controversial issue that needs to be further investigated.

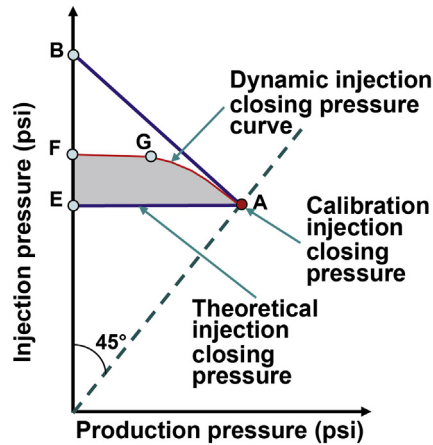
Another observation was that the critical pressure ratios  $X_f$  found while doing the flow coefficient tests did not depend on the stem travel but they behaved as a constant for a particular valve seat. Then, the graph of  $X_f$  as a function of the stem travel given in API Recommended Practice 11V2 is not accurate because it shows that  $X_f$  goes to zero as the stem travel goes to zero.

The values of  $C'_v$  found from the flow-coefficient tests tend to zero as the pressure drop across the valve tends to zero. The same is true for the  $C_d$  coefficient using the orifice flow equation developed at the University of Tulsa. The value of  $C_d$  for the Thornhill–Craver equation, on the other hand, tends to increase for small pressure drops.

Beside the fact, expressed previously, that line A–B in Fig. 8.22 could depend on the valve's closing pressure  $P_{vCT}$ , this line could also depend on the injection gas temperature. For a choke that has a fixed geometry, with given upstream and downstream pressures, the effect of the injection gas temperature is explicitly indicated in the orifice flow equation. In this case, as the temperature increases, the gas flow rate (expressed at standard conditions) decreases. For a gas lift valve, the gas flow rate can also change due to dynamic effects. Consider two cases in the throttling flow regime with the same dome, upstream, and downstream pressures, but with different injection temperature. The gas flow rate will be different for both cases, not only because of the temperature term present in the gas flow rate equation, but also because the dynamic effects could change the stem position and therefore affect the flow coefficient. This means that coefficients  $c$  and  $d$  in Eq. (8.14), considered constants for a particular seat diameter, could indeed depend on the injection temperature. The value of  $A_{slope}$  in Eq. (8.9) does not depend on temperature because no dynamic effects are considered to affect the valve along the 45 degree plane and therefore line A–D in Fig. 8.22 remains the same for all temperatures (as long as the valve's closing pressure is the same). Because line A–B, and probably line B–C'', in Fig. 8.22 are the only lines affected by temperature, it is expected that the effect of temperature plays only a minor role on the value of  $C'_v$ . Previous works have not elaborated on the effect of temperature, mainly because the tests were performed at ambient temperatures. Normal operating conditions at valve's depth can go from around 100°F to more than 200°F, thus it is recommended that the effect of temperature be studied experimentally in more detail.

### 8.2.3 Dynamic model for pilot valves

The behavior and proper use of pilot valves are presented in detail in chapter: Design of Intermittent Gas Lift Installations (the internal components of a pilot valve are presented in Fig. 10.6). Extensive experimental work conducted by the author of this book has shown that spring-loaded pilot valves close at pressures above the static injection closing pressure  $P_{ves}$ . In theory, the closing pressure of a spring-loaded pilot valve under normal operation in the well (that is, under dynamic conditions) should be identical to the static closing pressure, which is the test-rack closing pressure obtained at static conditions during the calibration of the valve. In Fig. 8.30, the closing pressure line for single element valves is line A–B, while the closing pressure of pilot valves should, in theory, be line A–E. The value of the injection pressure at point A is the static closing pressure  $P_{ves}$ . But the actual closing pressure takes place along curve A–G and line G–F.



■ FIGURE 8.30 Dynamic injection closing pressure curve.

The closing pressure of a spring-loaded pilot valve should, in theory, be line A–E because the ball and the bellows of the valve (located in the upper part of the pilot valve, see Fig. 10.6) should be equal to the injection pressure while the valve is opened (given the fact that the gas flow rate through the upper part of the valve is negligible). In reality, the pressure inside of the valve (in its upper section) does reach the pressure at line A–E while the pressure in the annulus, just upstream of the valve’s inlet ports, is still a little higher. In other words, the reduction of the pressure caused by the gas flow rate in the lower part of the valve (where the gas flow rate is very high), is felt at the upper section of the valve. The lower the production pressure downstream of the valve is, the higher the gas flow rate through the valve becomes and, in consequence, the valve tends to close at a higher injection pressure (curve A–G). When critical flow is reached at the lower section of the valve, the gas flow rate is constant for any production pressure below the pressure at point G and the valve closes at a constant injection pressure (line G–F). The larger the diameter of the ball is, the greater the effect of the lower section is felt at the upper section of the pilot valve and that is why the deviation of the actual closing pressure with respect to the static closing pressure is greater for larger balls.

The deviation of curve A–G and line G–F has been exaggerated in Fig. 8.30 for didactical purposes. In reality, the dynamic injection closing pressure is slightly higher (percentagewise) than the static closing pressure. Even though this difference (between the dynamic and the static closing pressures) is not very large, it has a profound impact on the volume of gas injected per cycle, as explained in chapter: Design of Intermittent Gas Lift Installations,

for choke-control intermittent gas lift. A deviation of only 5% in the closing pressure might represent a 70% reduction in the volume of gas injected per cycle. Nitrogen-charged pilot valves have a behavior opposite to the one shown in Fig. 8.30; nitrogen-charged valves tend to close at dynamic injection closing pressures lower than the static closing pressure. This is due to the drop in the temperature of the nitrogen (inside the dome of the valve) caused by the expansion of the injection gas as it exists the pilot valve at a very high flow rate. This drop in the nitrogen temperature lowers the valve's closing pressure. The volume of gas injected per cycle in this case could be considerably larger than expected. This temperature effect is more pronounced in 1-in. nitrogen-charged, pilot valves because the dome of the valve is surrounded by the injection gas. The calculation of the dynamic closing pressure for nitrogen-charged pilot valves is far more complex because it depends on the operational conditions surrounding the valve and complex heat-transfer calculations are required for each specific set of operational conditions.

Traditionally, the static closing pressure (usually equal to the valve's calibration pressure for spring-loaded valves) has been used as the dynamic closing pressure of spring-loaded pilot valves. The static closing pressure is easily calculated from the static force–balance equation:

$$P_{\text{ves}} = (1 - R)P'_c + (R)P_{\text{pd}} \quad (8.18)$$

Where  $P_{\text{ves}}$  is the closing pressure under static conditions (expressed in psig),  $R$  is the area of the seat at the pilot section of the valve divided by the bellows area,  $P'_c$  is the injection pressure in psig, and  $P_{\text{pd}}$  is the production pressure also in psig. Because this equation is based on static conditions (gas flow rate equal to zero at the upper and lower sections of the pilot valve), it is an excellent equation for predicting the opening pressure of the valve but not for estimating the valve's closing pressure under dynamic conditions. The high gas flow rate through the valve makes its internal pressure be lower than under static conditions and the valve closes at injection pressures higher than  $P_{\text{ves}}$ .

Milano (1999) found the following equation to calculate the dynamic closing pressure  $P_{\text{vc}}$ :

$$P_{\text{vc}} = P_{\text{ves}} + a(Y)^n \quad (8.19)$$

Where  $Y$  is equal to  $P_{\text{ves}} - P_{\text{pd}}$ . The pressure terms in Eq. (8.19) can be expressed in psig or psia, as long as all of them are consistent. If the production pressure is smaller than  $P_{\text{crit}}$ , defined as  $P_{\text{crit}} = P_{\text{ves}} \left( \frac{2}{k' + 1} \right)^{k'/(k'-1)}$ , then the

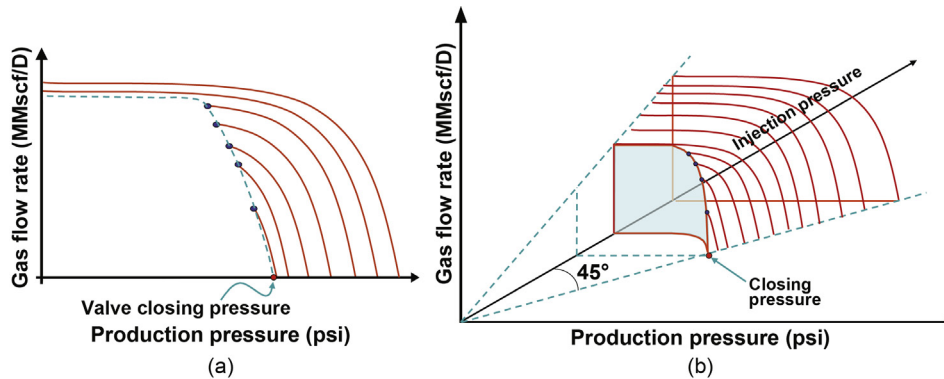


value of  $P_{\text{crit}}$  is used in Eq. (8.19) instead of  $P_{\text{pd}}$ . Coefficients  $a$  and  $n$  need to be found for each valve models and ball diameter.

Regarding the flow regime through the valve, pilot valves exhibit only orifice flow. Throttling flow cannot take place because the injection gas flows mainly through the lower section, which is either opened or closed. As soon as the upper section of the valve opens or closes, the lower section does likewise. The piston in the lower section of the valve cannot have an intermediate position (it is either fully opened or closed unless a malfunction of the valve is taking place). In single element valves, throttling flow takes place because of the regulating effect that the stem movement has on the flow rate. As can be seen in Fig. 8.15, if throttling flow takes place for a constant injection pressure, a decrease in the production pressure causes an initial increase in the gas flow rate but, if the production pressure is further decreased, the gas flow rate reaches a maximum value and then begins to decrease until the valve closes. Sonic flow can take place without freezing the ball position at one particular point because sonic flow takes place in the frustum area (between the ball and the seat) and not at the seat; therefore, the decrease in the production pressure is still felt in the lower part of the ball (which continues then to move towards the seat). As demonstrated by Bertovic and Faustinelli, in transition flow sonic velocity is reached at the seat (which is the minimum flow area for that flow regime) and, in consequence, any reduction in the production pressure is not felt at the ball so that the ball position freezes at a given position and the valve cannot close even if the production pressure is reduced to zero.

In pilot valves, orifice flow takes place regardless of position of the ball in its upper section (as long as the upper section of the valve is not closed). If the upper section closes because of a reduction of the injection or production pressure, the orifice flow through the lower section is simply, and abruptly, interrupted as soon as the upper section closes, as shown in Fig. 8.31.

The orifice flow equation derived in chapter: Single and Multiphase Flow Through Restrictions, Eq. 4.24, or Eq. (8.4) presented in Section 8.2.1, can be used for pilot valves, as long as the discharge or the flow coefficients to be used are specifically found for each pilot valve model and seat diameter available. The Thornhill–Craver equation should not be used because it tends to under predict the gas flow rate if the flow is subcritical and to over predict the flow rate if the flow is critical. This is the same result explained in Section 8.1 for single element valves. The use of the Thornhill–Craver equation might lead to the conclusion that the gas flow rate through the gas lift valve can be larger than the actual value that can be attained. The implication of this erroneous conclusion is explained in chapter: Design of Intermittent Gas Lift Installations.



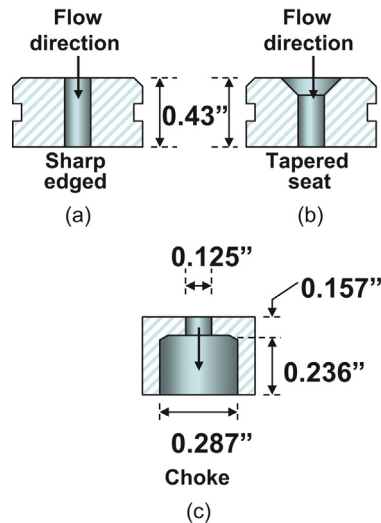
■ **FIGURE 8.31** Dynamic behavior of pilot valves. (a) Two dimensional diagram, (b) three dimensional diagram with the same information.

### 8.3 USE OF CHOKES INSTALLED DOWNSTREAM OF THE SEAT

Some operating companies install a choke inside IPO gas lift valves (downstream of the seat and close to the check valve, see Fig. 6.2c in chapter: Gas Lift Equipment) with the following objectives in mind:

- To protect the seats from erosion: the highest gas velocities are reached at the choke and not at the seat.
- To avoid throttling flow: the ball is exposed to higher pressures because the production pressure effect is not directly applied at the seat but below it. This could be used to help stabilize the operation of a well that would otherwise produce in an unstable fashion. The dynamic performance of an IPO valve with a choke downstream of the seat is qualitatively (not quantitatively) similar to the performance of a pilot valve, which is shown in Figs. 8.30 and 8.31. Referring to Fig. 8.30, a single element IPO valve without a choke will exhibit throttling flow for injection pressures from point B to F (on the y-axis) while the same single element valve with a choke downstream of the seat will operate in orifice flow.

Regardless of these advantages, these chokes can only be used in “unloading valves” in cases where the available injection pressure allows large sequential injection pressure drops per valve. The sequential injection opening pressure drop per valve is one of the techniques that are used in continuous gas lift design (different gas lift design procedures are explained in chapter: Design of Continuous Gas Lift Installations). The need for large sequential injection pressure drops per valve is due to the fact that, even though the gas flow rate is determined by the choke diameter, the spread of the valve (difference between its opening and closing pressures) continues to be determined by

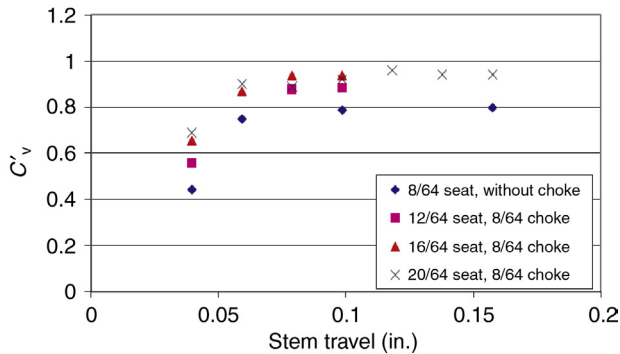


■ FIGURE 8.32 Typical seats' and chokes' dimensions.

the seat area (not the choke area) divided by the bellows area (this area ratio is simply known as the “area ratio of the valve”). The spread of the valve is directly proportional to its area ratio. Because the seat of the valve must necessarily be large when downstream chokes are used (otherwise the choke will be useless), the spread of the valve is also large. It is important to have large sequential injection opening pressure drop per valve (when the spreads of the valves are large) to avoid valve interference. Valve interference is an instability condition (explained in chapters: Design of Continuous Gas Lift Installations and Continuous Gas Lift Troubleshooting) in which two valves are opened at the same surface injection pressure because the deeper valve’s surface opening pressure is greater than the shallower valve’s surface closing pressure (because the spread of the shallower valve is too large).

Typical dimensions for sharp-edged and tapered seats, as well as for chokes, are shown in Fig. 8.32.

It is important to notice in Fig. 8.32 that the internal (longitudinal) length of the orifice, or wall thickness of a seat, is usually equal to approximately 0.43 in., while chokes usually have thickness of only 0.157 in. The longer the length of the conduit through an orifice or restriction is, the greater the permanent pressure drop across the orifice will be for a given gas flow rate. Seats of 8/64 in. in diameter exhibit larger pressure drops than chokes of the same diameter (8/64 in.) installed in valves with seat diameters larger than 8/64 in. Some results from flow-coefficient tests are shown in Fig. 8.33,



■ FIGURE 8.33 Measured discharge coefficients for different seat and choke combinations.

where the flow coefficient of a valve with “no choke” and a seat of 8/64 in. in diameter is compared with the flow coefficients of valves with a choke of 8/64 in. in diameter and seat diameters of 12/64, 16/64, and 20/64 in.

It can be seen in Fig. 8.33 that fully opened valves (stem travel greater than or equal to 0.1 in. in this case), with different seat diameters and the same 8/64-in. choke, have flow coefficients that are very similar among themselves but larger than the flow coefficient of the valve with no choke and a seat of 8/64 in. in diameter. Chokes offer less flow resistance and, in consequence, the use of any of the orifice flow equations will under predict the gas flow rate and would give choke diameters larger than necessary.

## 8.4 USE OF CHOKES INSTALLED UPSTREAM OF THE SEAT

There are gas lift valve models that have chokes downstream of the valve’s lateral-gas-entrance ports but upstream of the ball and the seat, see Fig. 6.2b in chapter: Gas Lift Equipment. With this arrangement, the ball is always exposed to the production pressure and the bellows to the injection pressure. The valve is still an unbalanced valve in the sense that both, the injection and production pressures, try to open the valve, but the spread of the valve is equal to zero. The injection opening pressure still depends on the value of the production pressure. If the production pressure is reduced, the injection opening pressure necessarily has to increase to open the valve (this production pressure effect increases for larger seat diameters). The size of the seat does not affect the valve’s discharge coefficient or the difference between the opening and closing pressure of the valve (known as the “spread of the valve,” which is equal to zero in this case). In this way, the unloading

valves can be designed for the same surface opening pressure but with a “design” production pressure larger than the “actual” production pressure, which is the one the well will have after the well has been unloaded and it is producing from the operating point of injection determined in the design (in other words, once the well is unloaded, the production pressure is less than the design production pressure). This reduction in the production pressure causes an increase in the opening pressures of the unloading valves, eliminating the need of having injection opening pressure drops per valve. In this way, the operating valve can be reached with the available maximum surface injection pressure. The reader is advised to review the design procedure for spacing and calibrating gas lift valves of this type, given in chapter: Design of Continuous Gas Lift Installations, Section 9.2.1, to gain more insight on the use of upstream chokes and on the concepts that are presented here.

The problem with valves with upstream chokes is that their discharge coefficients and dynamic behavior have not been reported yet. Usually, the choke is not a single orifice, but many small-diameter orifices.

If the valve is fully open, the discharge coefficient depends only on the geometry of the choke: number of orifices, their diameters, shape, axial length, etc. A good approximation to size the choke (if no information is available) is to use the Thornhill–Craver equation with the total area of the choke equal to the summation of all areas of the small orifices (the reduction of the discharge coefficient caused by having many orifices is compensated by the reduced thickness of the longitudinal length of the orifices).

The determination of the flow coefficient when the valve is not fully open is much more complex. The dynamic behavior of the valve restricts the gas flow rate in throttling flow in ways that have not been reported in the literature. The reader is advised to review [Sections 8.2.1 and 8.2.2](#) to have a better understanding of the explanations given in the next paragraphs.

Because the bellows is always exposed to the injection pressure and the ball to the production pressure, the simplified method described in [Section 8.2.1](#) can be used. With this method, the area of the horizontal plane that has to be used to determine the value of  $C'_v$  is A–B'–C'–D instead of the area A–B–C–D used by the dynamic model presented in [Section 8.2.2](#) for single element valves without chokes, see [Fig. 8.34](#).

For valves with upstream chokes, the determination of the flow coefficient is much more complex than just using the surface indicated by the simplified model presented in [Section 8.2.1](#) to find the value of  $C'_v$ . A valve without choke is fully open in the region above line C''–D, while a valve with upstream choke is fully open above C'–D; but, because the seat of the valve with upstream choke is usually large, a small stem movement will

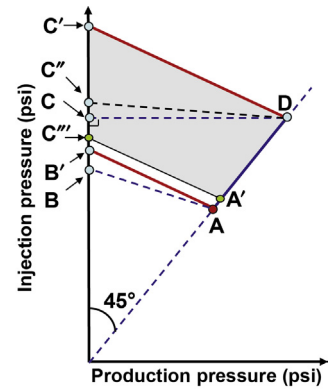
cause the ball seat area (frustum) to be larger than the area of the choke. The gray area in Fig. 8.34 ( $A'-C'''-C'-D$ ) represents the zone in which the valve is sufficiently open so that the area of the downstream ball seat frustum is larger than the area of the upstream choke. This is due to the fact that the area of the seat is greater than the area of the choke. A modified version of the simple model presented in Section 8.2.1 can then be used to find the flow coefficient: for practical purposes, the throttling flow region will only be  $A-B'-C'''-A'$ . For the region above line  $A'-C'''$  the ball is sufficiently away from the seat so that it is the area of the choke the one that is restricting the flow. The problem is limited then to only find (from dynamic tests) the position of the line  $A'-C'$  to be able to predict the gas flow rate in the gas lift design for a given combination of seat and choke diameters.

### 8.5 ORIFICE VALVES WITH SPECIAL GEOMETRY SEATS

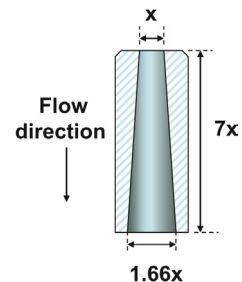
The flow coefficient of a seat or orifice depends not only on its diameter but also on its general geometry. As described in previous sections, the thickness of the seat (or longitudinal length of a choke) affects the flow coefficient. If the longitudinal length of a choke is short, its flow coefficient is greater than the one for a choke of the same diameter with a longer longitudinal length. Another aspect that affects the flow coefficient is the internal, longitudinal shape of the orifice. Winkler and Camp studied the effect of the entrance angle of tapered seats, see Fig. 8.32a, b. For 60 and 45 degree tapered seats, they found the discharge coefficients to be 10 and 6% greater than those for sharp-edged seats, respectively. A study performed by the author of this book, using orifices with the geometry shown in Fig. 8.35, demonstrated that this type of orifice presents important deviations with respect to the performance of standard seats that are worth mentioning.

Fig. 8.36 shows the comparison between the discharge coefficients for the Thornhill–Craver equation back-calculated from the data obtained with 16/64-in. diameter seats and those obtained with the special geometry seat shown in Fig. 8.35, which had an entrance diameter slightly greater than 16/64 in. The theoretical value of the discharge coefficient used in the Thornhill–Craver equation for 16/64-in. diameter seats is also shown in the figure (the constant value or horizontal line). The measured gas flow rates using the special geometry seat, together with the gas flow rates calculated with the Thornhill–Craver equation for a standard seat of diameter equal to the entrance diameter of the special geometry seat, are shown in Fig. 8.37.

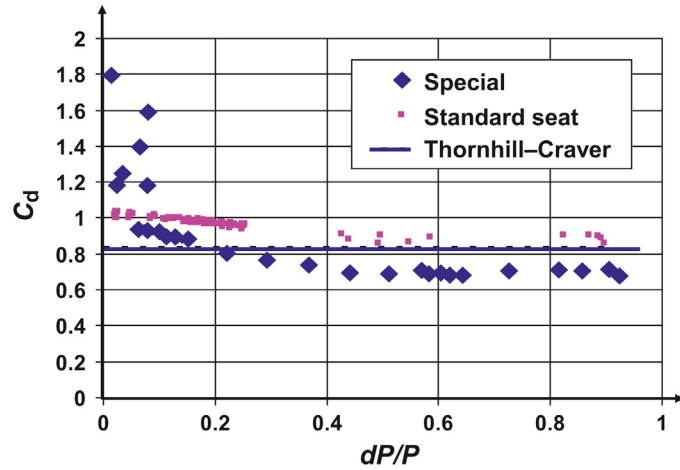
In critical flow, the gas flow rate for the special geometry seat is less than the flow rate for a sharp-edged seat. This is due to the length of the special geometry seat; however, in subcritical flow, the gas flow rate is greater for



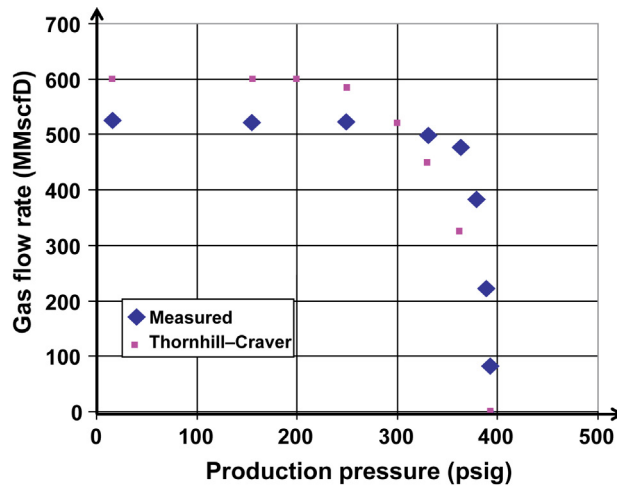
■ FIGURE 8.34 Dynamic behavior of valves with upstream chokes.



■ FIGURE 8.35 Dimensions of the special geometry seat studied by Hernandez.



■ FIGURE 8.36 Comparison of the discharge coefficients.

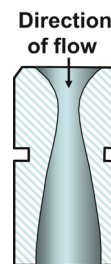


■ FIGURE 8.37 Measured and theoretical gas flow rates using special geometry valves.

the special geometry seat than the one for sharp-edged seats. It can also be noticed that the pressure ratio for critical flow is greater for the special geometry seat, which is an important feature to stabilize the flow of a well when the difference between the production and the injection pressures is very small. If the diameter of the special geometry seat (from which the results presented in Fig. 8.37 were obtained) was slightly increased, the gas

flow rate could be the same as the one obtained for a standard seat but with a better performance in subcritical flow.

There are orifices with the shape shown in Fig. 8.38 that offer a better performance than the one presented in Fig. 8.35 (regarding the increase in the gas flow rate capacity and the increase of the pressure ratio to achieve critical flow) but they are more expensive and, additionally, the problem with these special geometries (in Figs. 8.35 and 8.38) is that the gas flow rate cannot be varied with the flexibility that standard seats can provide (the gas flow rate is reduced to a very narrow range of values for a given injection pressure).



■ FIGURE 8.38 Special geometry seat used to increase the pressure ratio to achieve critical flow and to increase the gas flow rate capacity.

## REFERENCES

- Acuña, H.G., 1989. Normalization of one inch nitrogen charged pressure operated gas-lift valves. M.S. Thesis. The University of Tulsa, Tulsa, Oklahoma.
- Bertovic, D., 1995. Unified model for gas-lift valve performance incorporating temperature effects. M.S. Thesis. The University of Tulsa, Tulsa, Oklahoma.
- Biglarbigi, K., 1985. Gas passage performance of gas lift valves. M.S. Thesis. The University of Tulsa, Tulsa, Oklahoma.
- Cook, H.L., Dotterweich, F.H., 1981. Report on calibration of positive flow beans manufactured by Thornhill-Craver Company, Inc. Department of Engineering, Texas College of Arts and Industries. Kingsville, Texas. Third Printing.
- Cordero, O., 1993. Flow performance of one-inch fluid operated gas lift valves. M.S. Thesis. The University of Tulsa, Tulsa, Oklahoma.
- Decker, K.L., 1986. Computer modeling of gas-lift valve performance. Paper OTC 5246 Presented at the 18th Annual OTC, Houston, Texas.
- Escalante, S., 1994. Flow performance modeling of pressure operated gas-lift valves. M.S. Thesis. The University of Tulsa, Tulsa, Oklahoma.
- Faustinelli, J., 1997. Temperature and flow performance modeling of gas-lift valves. M.S. Thesis. The University of Tulsa, Tulsa, Oklahoma.
- Hepguler, G., 1988. Dynamic model of gas-lift valve performance. M. S. Thesis. The University of Tulsa, Tulsa, Oklahoma.
- Milano, P.E., 1999. Dynamic performance of the intermittent gas-lift valve. M.S. Thesis. The University of Tulsa, Tulsa, Oklahoma.
- Neely, A.B., Montgomery, J.W., Vogel, J.V., 1973. A field test and analytical study of intermittent gas lift. SPE paper 4538.
- Nieberding, M.A., 1988. Normalization of nitrogen loaded gas-lift valve performance data. M.S. Thesis. The University of Tulsa, Tulsa, Oklahoma.
- Rodriguez, M.A., 1992. Normalization of nitrogen charged gas-lift valves performance. M.S. Thesis. The University of Tulsa, Tulsa, Oklahoma.
- Sagar, R., 1991. Improved dynamic model of gas-lift valve performance. M.S. Thesis. The University of Tulsa, 1991.
- Winkler, H.W., Camp, G.F., 1985. Dynamic performance testing of single-element unbalanced gas-lift valves. SPE paper 14348.



# Design of continuous gas lift installations

As mentioned in several places in this book, gas can be injected into a gas lift well in a continuous or intermittent manner. Continuous gas injection is, by far, the most widely used way of injecting gas for lifting purposes. This chapter focuses on the different continuous gas lift design techniques that are more commonly used today in the oil industry.

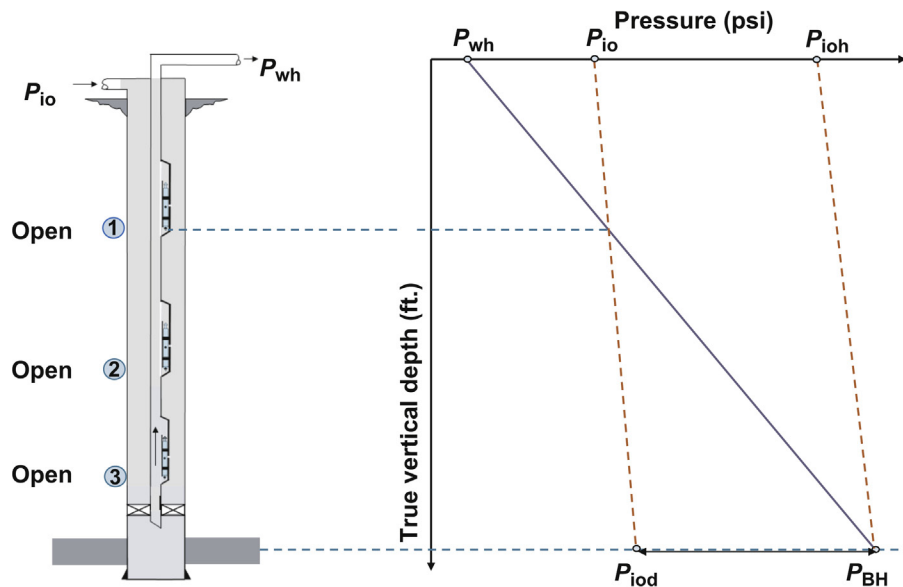
Continuous gas lift design consists in carrying out the following calculations:

- Finding the depths of the unloading valves and the operating point of injection by means of a calculation procedure known as “mandrel spacing.” Unloading valves are valves located above the operating valve and their function is limited to injecting gas during the unloading process only. They must be closed once the unloading of the well is completed (the unloading process is described further in this introduction). The operating valve is the one through which gas is injected during the normal operation of the well. The depth of the operating point of injection, the final injection gas flow rate, and the liquid production of the well should be known prior to performing mandrel spacing calculations and their determination is the initial part of the design process, which is covered in chapter: Total System Analysis Applied to Gas Lift Design.
- Calculating the unloading liquid production and the required injection gas flow rate for each of the unloading valves.
- Finding the seat diameters of the unloading and operating valves so that the right gas flow rate passes through each valve during the unloading process and during the normal operation of the well (after it has been unloaded). If the correct injection gas flow rate and valve’s seat diameter are determined, the operating pressure of a given unloading valve (which is the pressure needed to uncover the next valve below it) should be maintained at its design value while

unloading through that particular unloading valve. If the seat is too large, the gas flow rate through the valve will also be large and, in consequence, the injection pressure drops and it might not be possible to uncover the next valve below unless the surface gas flow rate is increased above its design value for that particular unloading valve. On the other hand, if the seat diameter is too small, the required injection pressure needed to pass the calculated gas flow rate could be too high and an upper valve might open.

- Determining the opening and closing pressures of the unloading and operating valves; from these pressures, the test-rack calibration pressures can be calculated. The calibration of the valves is done in such a way that each unloading valve sequentially closes, and remains closed, as the unloading process continues down the well until the operating valve is reached and all the gas is injected through this valve, at which time all unloading valves should be closed.

Unloading valves are necessary because the available injection pressure is usually not high enough to reach the deepest possible point of injection with only one valve. Fig. 9.1 shows the “pressure–depth” diagram that can be used to illustrate this fact. During the unloading process, the liquid accumulated in the casing-tubing annulus is displaced by the injection gas into the tubing until the operating valve is uncovered. Usually, the operating point is



■ FIGURE 9.1 Pressure profile before unloading.

located at the deepest depth that can be attained by the unloading procedures explained in this chapter. The deeper the point of injection is, the larger the liquid production can become because lower bottomhole flowing pressures can be achieved. Many times though, the deepest point of injection cannot be reached, not only for not having a sufficiently high injection pressure, but also because the subsurface gas lift equipment might not be able to withstand the high temperatures and pressures encountered at that depth or the tubing string has a very large inclination angle.

The production tubing string and the casing-tubing annulus of the well in [Fig. 9.1](#) are completely filled with liquids. The hydrostatic pressure of the liquid in the production tubing plus the wellhead pressure,  $P_{wh}$ , results in a very large bottomhole static pressure,  $P_{BH}$ , which is greater than the gas injection pressure at depth,  $P_{iod}$ . If a compressor capable of increasing the surface injection pressure to a value equal to  $P_{ioh}$  is available, it would not be necessary to use unloading valves because all that would be required is to install an orifice at the deepest point to unload the well and leave it operating at that point; however, the cost of compression could be considerably increased and, furthermore, this very high pressure would only be necessary during the unloading of the well (once the well is unloaded, the “operating” injection pressure will be much lower and very close to  $P_{io}$ ). Therefore, it is convenient to find ways of unloading the well using the maximum unloading injection pressure that will be as close as possible to the normal operating injection pressure of the well after unloading it, reducing in this way the costs of gas compression and transportation. In certain places, such as offshore oilfields, where it is extremely difficult to run in or pull out gas lift valves by wireline jobs or where gas lift valves are not able to withstand the high production pressures found in the well, some operating companies use a small-volume, high-pressure compressor for the unloading process only and a low-pressure, high-volume compressor for the normal operation of the wells. The wells then have only one orifice at the desired point of injection. But in the great majority of wells, where wireline operations are neither costly nor difficult to perform, it is far more practical to install unloading valves instead of having expensive, high-pressure compressors and special surface gas lines.

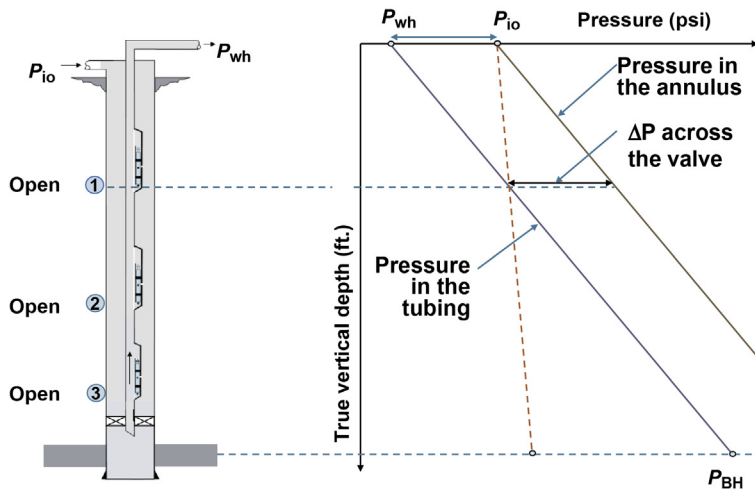
Even though the static reservoir liquid column level might be hundreds or thousands of feet below the wellhead, it is always advisable to perform design calculations assuming that the static liquid level is at the wellhead. This would guarantee the unloading of the well for the worst-case scenario. However, there are places where the available injection pressure is so low that it becomes necessary to start the design from the static liquid level and not from the surface. This point is addressed in [Section 9.2.8](#). If a new production tubing string is going to be installed in a well where the available

gas injection pressure is low, it is a good idea to space the mandrels as if the static liquid level is at the surface but installing dummy valves in the mandrels above the static liquid level and designing the unloading valves for the mandrels below. When designing the unloading valves from the static liquid level, it is important to install an unloading valve right at the static liquid level, or just above it (in this way, the well can be unloaded through this valve as the liquid in the annulus between this valve and the one right below it are being displaced into the tubing).

Mandrel spacing can be started at the static liquid level (without installing an unloading valve at that point) only in cases where the available injection pressure is extremely low and it is absolutely certain that the reservoir will absorb (reasonably fast) liquids accumulating in the tubing. When the liquids in the annulus between the static liquid level and the first valve below it are displaced into the tubing, a long liquid column in the tubing will form and its hydrostatic pressure could become equal to the injection pressure in the annulus so that the unloading process is momentarily stopped. But this liquid column can be absorbed by the reservoir, eventually reaching a point in which the unloading of the well can be reassumed. This procedure should not be attempted when the liquids in the well might cause formation damage or the waiting time is excessively long.

It is important to install a two-pen chart recorder at the wellhead or have the supervisory control and data acquisition (SCADA) system register the unloading process. The two-pen pressure chart (or the printed or electronically stored pressure trend from the SCADA system) should be kept in the well's file for future reference. If the well is filled with completion fluids that could damage the formation or the gas lift valves, the well should be circulated with clean fluids using circulating valves instead of gas lift valves. A standing valve should also be installed at the bottom of the production tubing string while the well is being circulated with clean fluids.

It is important to increase the surface injection pressure very slowly at the beginning of the unloading process (before reaching the first unloading valve). If it is not done with care, it is easy to increase the surface injection pressure (at the wellhead) to line pressure without allowing sufficient time for the fluids in the annulus to be displaced into the tubing having, as a result, a pressure drop across each unloading valve approximately equal to the line pressure  $P_{10}$ , minus the wellhead pressure  $P_{wh}$ , see Fig. 9.2. This is not recommended because gas lift valves are designed to pass gas and not liquids. Liquids can erode gas lift valves, especially if the liquids travel at very high velocities. On the other hand, even if the completion fluids had been circulated with clean fluids, there is no way of being certain that the

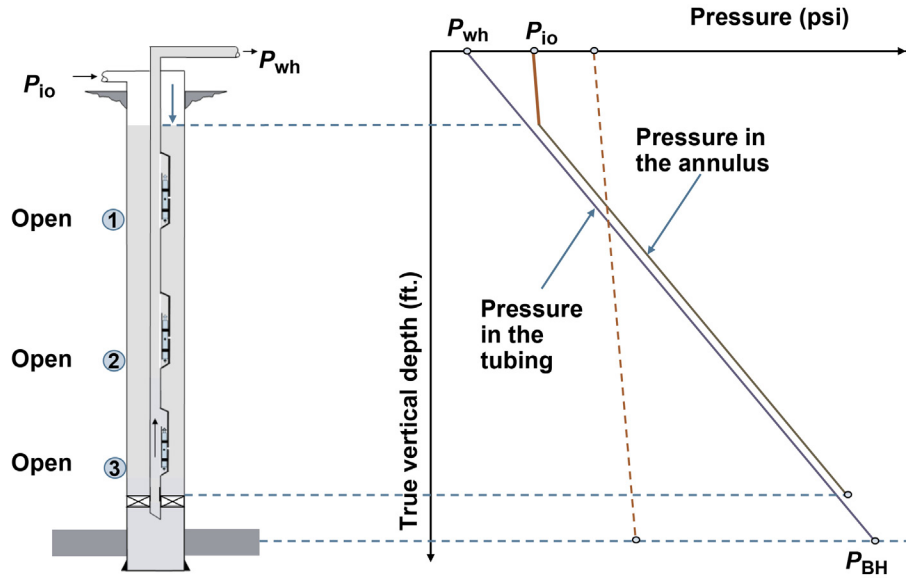


■ FIGURE 9.2 Excessive pressure drop across the unloading valves caused by unloading the well at a very high surface injection gas flow rate at the beginning of the unloading process.

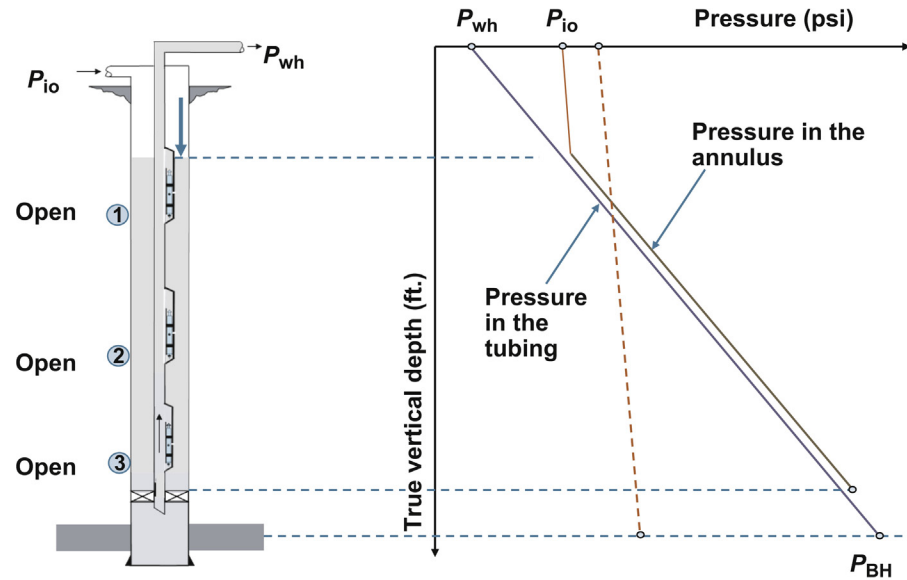
fluids in the well are free from abrasive particles. Unloading valves leaking gas through cut seats are very common. Even though these gas leaks are usually unimportant, sometimes they could cause serious problems, reducing the efficiency of the lifting process or not allowing the unloading of the well at all. Besides cut seats, the check valve inside the gas lift valve can also be eroded, compromising the integrity of the completion and allowing liquids to flow from the production tubing into the casing-tubing annulus. The liquid flow rate through a gas lift valve should not be greater than one barrel per minute to avoid damaging the valve.

Due to the hydrostatic pressure of the liquids in the annulus and in the tubing, at the beginning of the unloading process most gas lift valves (if not all) are open and it is very important to maintain a very low injection gas flow rate at the surface so that the pressure drops across the gas lift valves are very small, as can be appreciated in Figs. 9.3–9.5.

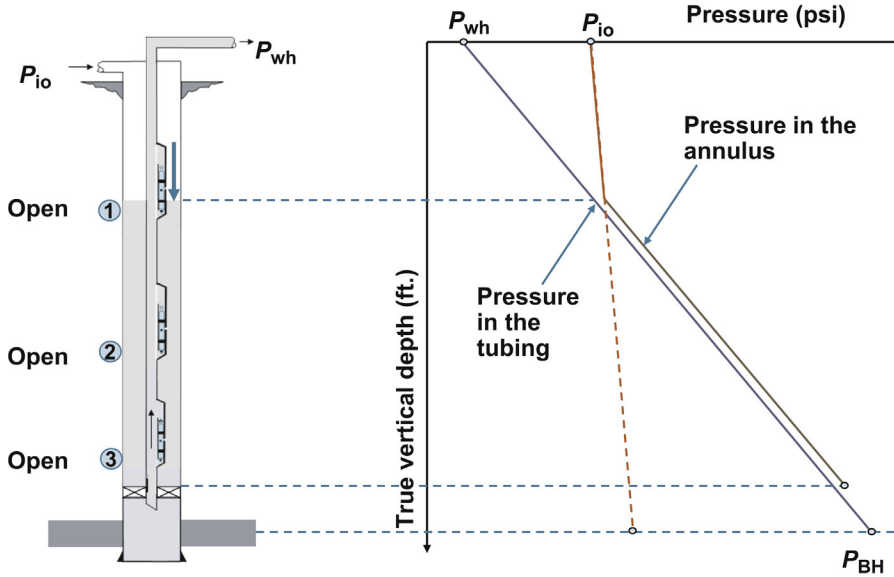
Fig. 9.6 shows what happens when the first valve is uncovered and injection gas enters the production tubing through this valve: the production pressure along the tubing decreases, causing an increase in the pressure drop across the unloading valves. But this increment in the pressure drop is not very important once the first valve has been uncovered because the liquid velocities through the valves below the first one are lower due to the fact that only



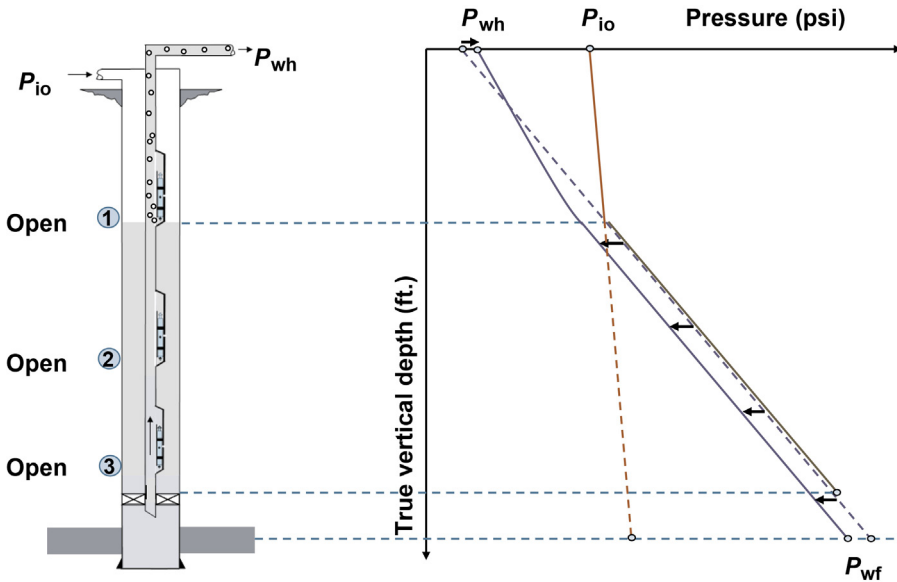
■ FIGURE 9.3 Liquid level in the annulus halfway between the wellhead and the first unloading valve.



■ FIGURE 9.4 The liquid level is approaching the first valve.



■ FIGURE 9.5 Just before uncovering the first valve: at this point the injection pressure reaches its maximum value during the unloading of the well.



■ FIGURE 9.6 Injection through the first gas lift valve is just beginning.

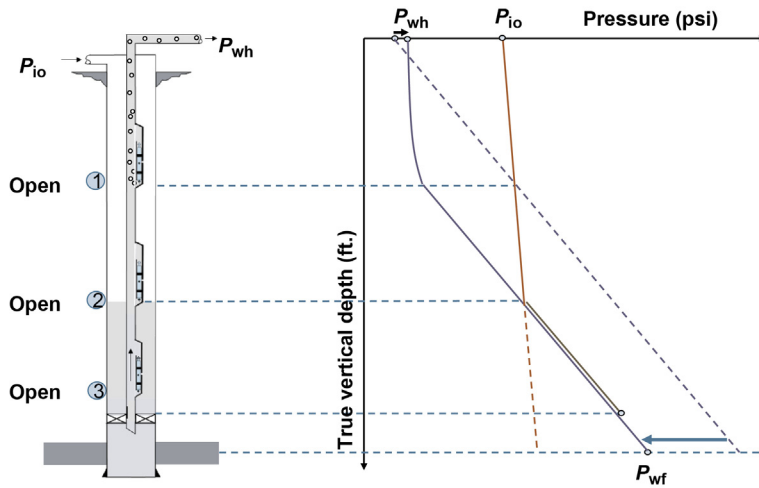
a small fraction of the gas that is injected into the annulus at the surface now goes to lower the liquid level in the annulus, while the rest of the gas is injected through the first valve to decrease the production tubing pressure. The wellhead production pressure increases because of the increase of the friction pressure drop along the flowline. The bottomhole flowing pressure,  $P_{wf}$ , decreases but not necessarily to the required level at which liquids from the reservoir begins to flow into the well. The injection pressure,  $P_{io}$ , is at its highest possible value, known as the “available injection pressure” or “operating pressure of the first valve,” which must be equal to the manifold injection pressure minus the usual pressure fluctuations at the manifold and minus a differential pressure that would allow the required gas flow rate while unloading through the first valve (this differential pressure is, most of the time, not smaller than 50 psi).

The concept of a “kickoff pressure” is used in mandrel spacing calculations. This is a pressure higher than the operating pressure for the first unloading valve (which is the shallowest unloading valve in the well). The kickoff pressure is used only to space the first valve deeper in the well and it is usually equal to the average manifold pressure; however, not all designers use this pressure in mandrel spacing calculations.

After gas injection is achieved through the first valve, the gas flow rate can be set at its final “target” value and the well should be able to unload without problems because this gas flow rate is larger than what it is usually required during the rest of the unloading process. However, under special circumstances, it may not be possible to reach the desired operating point of injection without momentarily increasing the gas flow rate at values greater than its final design value (due, for example, to an unloading valve with an oversized seat or because the well is capable of a higher-than-anticipated liquid production; these problems are usually, but not always, solved by temporarily injecting gas at the surface at a higher rate). For wells that can produce on natural flow and gas lift is only used to boost their liquid production, it is a good practice to keep a low injection gas flow rate throughout the unloading process. In these cases, the well should be opened to production (before initiating gas injection into the casing-tubing annulus) and let the well flow on its own until the liquid level in the annulus has stabilized at its equilibrium point.

Fig. 9.7 shows what happens at the moment just before uncovering the second valve. The pressure drop across the first valve is very large but only gas is flowing through it. The pressure differentials across the second and third valves continue to be small. The bottomhole pressure has further decreased and it might be possible that liquids from the reservoir are now flowing into the well.

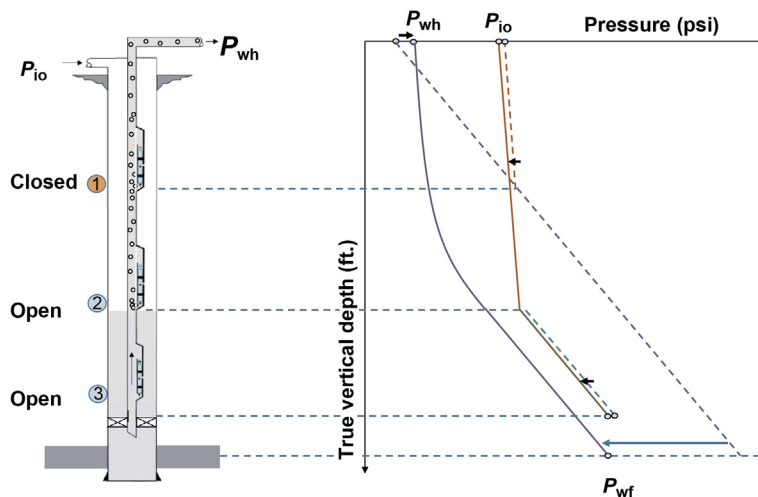




■ FIGURE 9.7 Just before uncovering the second valve (gas is not being injected through it yet).

Fig. 9.8 shows what happens when gas begins to flow through the second valve and the first valve closes. Momentarily, gas is injected through the first and second valves at the same time. This lowers the injection pressure because the gas flow rate at the surface is less than the one that enters the tubing through the two uncovered gas lift valves. If the first valve is an injection-pressure-operated (IPO) valve, then the reduction of the injection pressure makes the first valve close. If the first valve is a production-pressure-operated (PPO) valve, then it will close because of the reduction in the production tubing pressure that is achieved when gas injection is initiated through the second valve. If the first valve is a nitrogen-charged valve, its closing pressure will increase because its temperature is raised as warmer liquids from lower parts of the well are produced and this helps keeping this valve closed during the remaining part of the unloading of the well. Once the first valve closes, the injection pressure settles at a predetermined value below the operating pressure of the first valve if the valve is IPO (as shown in Fig. 9.8) or at the constant design injection pressure if the valve is PPO (not shown). In any case, the seat diameter of the second valve is sized in such a way that this new operating pressure is maintained until the third valve is uncovered.

The calibration of the valves at different opening pressures is what causes the valve to close in a sequential manner. For sequential pressure drops of

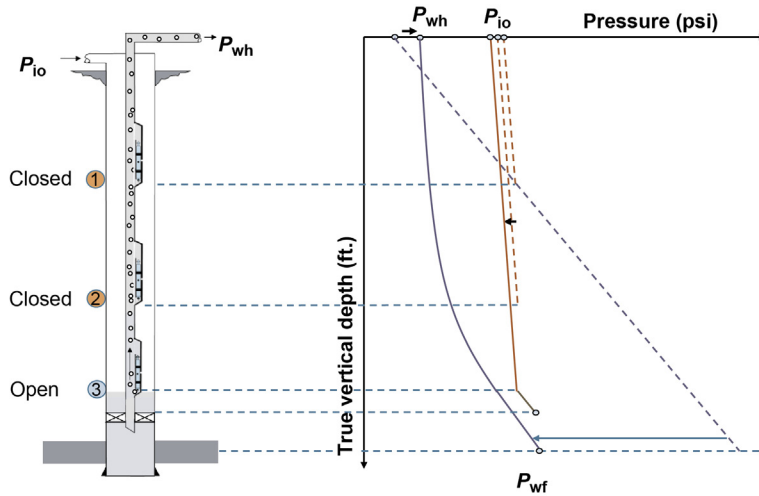


■ FIGURE 9.8 Gas is injected through the second valve.

the injection pressure, once the first valve is closed, the injection pressure is maintained at a value lower than the operating pressure of the first valve because the seat of the second valve has been designed to allow the required gas flow rate at this new operating pressure. If the second valve is mistakenly designed with a small seat, the injection pressure might increase when trying to pass the design gas flow rate through the second valve. This might cause the first valve to remain open. If, on the other hand, the second valve's seat is too large, the injection pressure might drop to a very low value that might cause the unloading process to stop for not having an injection pressure high enough to reach the third valve. This latter problem could be overcome by temporarily increasing the surface injection gas flow rate to increase the injection pressure and allow the unloading process to continue. The unloading of a well is then a dynamic process that can be accomplished by the correct calibration of each unloading valve and the precise selection of their seat diameters.

Finally, Fig. 9.9 shows the well fully unloaded, with the first and second valves closed and the injection gas passing through the third valve only.

As can be seen in Fig. 9.9, the final injection pressure is similar to the maximum required injection pressure for the unloading process. As mentioned previously, reaching the deepest possible injection point is necessary to achieve the lowest bottomhole flowing pressures so that large liquid productions from the reservoir can be obtained; however, the “desired” point of injection at a given time might not be the deepest point that



■ FIGURE 9.9 Unloading completed.

can be attained with the current available injection pressure and gas lift equipment because there might be many reasons for “voluntarily” having an upper final point of injection. It might be necessary to maintain a lower liquid production to avoid water coning or sand production, or to provide adequate reservoir pressure maintenance, or due to market and/or surface facilities restrictions, etc.

When it is desired to keep the liquid production at lower than feasible values, it is possible to do so by reducing the gas flow rate even if all the gas is injected through the deepest point of injection. But this could cause instability problems or simply the desired low liquid production might not be possible to achieve. For this reason, when designing a well to produce below its full potential, it is better to place the design point of injection above the deepest possible point but installing mandrels below this shallow injection point to lower the point of injection in the future, when a larger liquid flow rate might be desired or when the reservoir pressure has declined. The “design point of injection” has a series of considerations that are not necessary for the unloading valves. These considerations are described for each design procedure presented in this chapter and they are implemented to reduce the causes of instabilities and provide the means for positive identification when gas is indeed being injected through the design point of injection.

As it has been pointed out previously, the injection gas flow rate must be kept at low values before reaching the first unloading valve that would allow

gas injection into the production tubing, which does not necessarily has to be the shallowest valve because if, for example, the reservoir pressure is very low (and the liquid level in the annulus is very deep), the annular pressure does not have to increase to the opening pressure of the first valve and gas injection is usually initiated through the second or third unloading valve, which are valves that will open at lower injection pressures if they are IPO valves. Some operators follow these general recommendations: increase the wellhead injection pressure at 300 psi/h until reaching 400 psi, at which time the increase in pressure can be set at 400 psi/h until starting gas injection through the first valve that would allow gas flow into the tubing. Then, increase the gas flow rate to 50 or 60% of the final gas flow rate for 12–18 h and finally set the injection gas flow rate at its design value for the normal operation of the well (but many operator simply increase gas injection to the design injection gas flow rate as soon as the injection gas starts to flow into the tubing). Unloading valves above the static liquid level are usually designed based on an unloading liquid flow rate less than or equal to 200 Br/D to avoid damaging the gas lift valves.

If gas lift is being implemented in wells that are capable of producing on natural flow with the sole purpose of boosting their liquid production, it is important not to follow the recommendations given in the previous paragraph because they could lead to valve failures: as soon as the well is opened to production (even before injecting any gas into the casing-tubing annulus), the production tubing pressure will decrease because the well starts to flow, causing liquids from the annulus to flow into the tubing at rates that can be very large. If this is the case, it is recommended to open the well to production by opening the wellhead production choke very slowly and then allow the well to produce on natural flow for several hours before initiating gas injection into the well. These types of wells should be dynamically modeled (using currently available advanced software) to determine how to perform the unloading operation.

The unloading design calculations, as rigorous as they might be, never reveal what in reality takes place during the unloading operation of a gas lift well. This is due to many factors: (1) multiphase flow correlations are not very precise and they had been developed for steady state conditions, (2) fluid properties such as the water cut or the gas/oil ratio are usually not very well known, and (3) the data needed to calculate the inflow performance relationship (IPR) curve are many times inaccurate, etc. For all these reasons, it is a good practice to test the well at different injection gas flow rates right after the gas lift valves have been installed and the well has been unloaded and it is under normal operation. In this way, the well's true production potential and gas lift requirements are determined. It is also important to verify, by

means of troubleshooting analyses, if the design point of injection depth has indeed been reached.

The continuous gas lift design procedures most frequently used today in the oil industry are presented in this chapter. The best-suited type of design for a particular well depends on the kind of gas lift valve being used, the available injection pressure and injection gas flow rate, and the amount and accuracy of the available reservoir data.

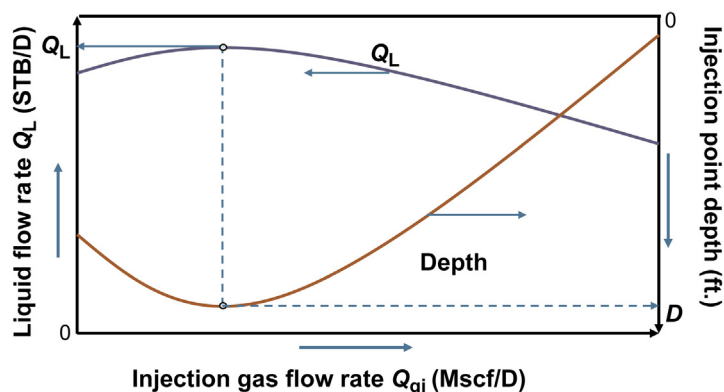
## 9.1 DETERMINATION OF THE OPERATING INJECTION POINT DEPTH, TARGET INJECTION GAS FLOW RATE, AND THE LIQUID FLOW RATE THE WELL CAN PRODUCE

The “operating” point of injection depth is defined as the depth of the operating valve, which is the only one that should be passing injection gas after unloading the well. Several methods that can be used to find the operating point of injection depth are described in this section. The right method to use depends on the sophistication level of the computer software being used for design calculations and on the amount and quality of the available data.

### 9.1.1 Iterative procedure

The determination of the operating injection point depth and liquid production for a given “operating” injection pressure is explained in detail in chapter: Total System Analysis Applied to Gas Lift Design. The reader is advised to review Section 5.1 (especially the points regarding the “constant-injection-gas-flow-rate equilibrium curves” that are presented in chapter: Total System Analysis Applied to Gas Lift Design, to explain Fig. 5.31) to understand the explanations given here. Fig. 9.10 shows the result obtained after doing the calculations explained in chapter: Total System Analysis Applied to Gas Lift Design, to find the injection point depth for a given “estimated” operating injection pressure. This estimated operating pressure is found in the following way:

- The usual system pressure fluctuations are subtracted from the manifold average available pressure. This gives the minimum pressure that can be found at the manifold.
- A differential pressure, usually not less than 50 psi, is subtracted from the minimum manifold pressure. This pressure differential is required because it will allow a range of injection gas flow rates available at the moment the first valve is uncovered.
- For IPO gas lift valves, the injection pressure drop per valve times the possible number of unloading valves to be installed should be further subtracted from the pressure obtained in the previous point. Because



■ FIGURE 9.10 Results of the calculation procedure to estimate the maximum liquid flow rate, optimum injection gas flow rate, and the deepest point of injection for a given operating injection pressure (from chapter: Total System Analysis Applied to Gas Lift Design).

the number of valves the well might require is not known a priori, the gas lift design is an iterative procedure.

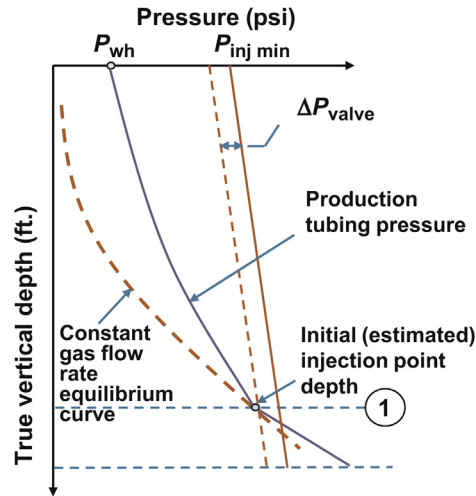
As it was indicated in chapter: Total System Analysis Applied to Gas Lift Design, to obtain the graph shown in Fig. 9.10, a pressure differential of 100 psi should be subtracted from the estimated operating injection pressure. This pressure drop represents the pressure drop across the gas lift valve. Some designers prefer to use 200 or 250 psi instead of 100 psi to avoid well instability problems. In any case, the pressure drop across the gas lift valve should not be smaller than 10% of the operating injection pressure at valve's depth to avoid the problems described in chapter: Gas Flow Through Gas Lift Valves, see Fig. 8.4.

The gas flow rate corresponding to the maximum liquid flow rate in Fig. 9.10 could be considered as the design injection gas flow rate, but a lower gas flow rate might be selected if gas compression and water handling costs are considered. In any case, the calculations described in chapter: Total System Analysis Applied to Gas Lift Design simultaneously determine the injection gas flow rate, the liquid production flow rate, and the depth of the point of injection, for a given operating injection pressure. The curves shown in Fig. 9.10 correspond to an "estimated" operating injection pressure. The selected injection gas flow rate is used to generate the "constant-injection-gas-flow-rate equilibrium curve" that is used in the iterations that are explained in the next paragraphs to find the definite (or realistic) point of injection depth and its corresponding operating injection pressure. Usually, commercially available

computer programs carry out the iterations for the injection gas flow rate selected by the user. However, it is up to the user to verify if the gas flow rate is still adequate for the final operating injection pressure, especially if this final operating pressure is too different from the one considered in the calculations to get the results presented in Fig. 9.10 (from which the estimated injection gas flow rate was found).

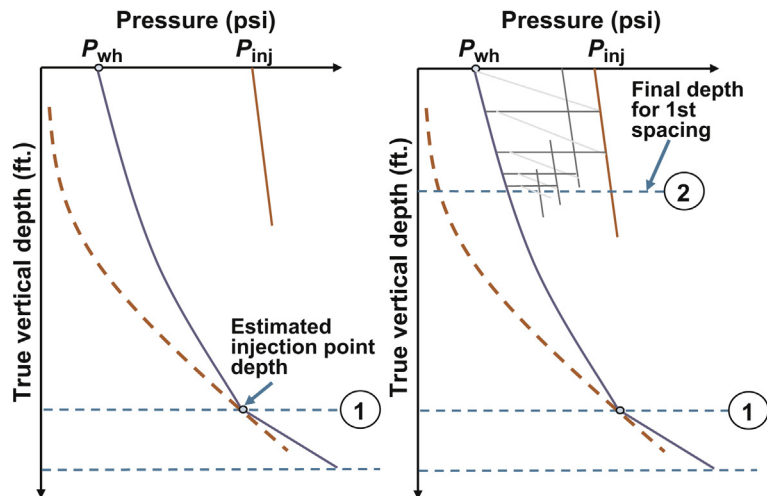
To perform the iterations, the program only requires the injection gas flow rate because the operating injection point depth, the final operating injection pressure, and the production liquid flow rate are found from the iteration process itself. At the beginning of the iterations, the program sets the operating point of injection depth at the deepest possible point and, by nodal analysis, the liquid production the well can provide (with this point of injection depth and selected gas flow rate) is calculated. This determines the production-pressure-traverse curve to perform the mandrel spacing procedure for the first iteration. As it is shown in chapter: Total System Analysis Applied to Gas Lift Design, the production pressure at the point of injection must be on the equilibrium curve determined for the selected injection gas flow rate. Fig. 9.11 shows the equilibrium curve for the selected injection gas flow rate, together with the production-pressure-traverse curve that is obtained with the initial point of injection, known as point “1.” As indicated previously, “constant-injection-gas-flow-rate equilibrium curves” are explained in chapter: Total System Analysis Applied to Gas Lift Design. In Fig. 9.11,  $P_{inj\ min}$  is the operating surface pressure that should be obtained at the end of the first mandrel spacing calculations. If this pressure obtained from the mandrel spacing calculation is equal to the “estimated” operating injection pressure (from which Fig. 9.10 was built), then iterations are not required because the estimated depth of the operating point of injection was correct. The pressure drop across the valve,  $\Delta P_{valve}$ , should be considered to provide a differential pressure to be able to pass the required gas flow rate through the gas lift valve. As previously indicated, this pressure drop should be at least 100 or 200 psi (depending on the preference of the designer and on general operational conditions to avoid well instabilities). If the operating point of injection depth at the end of the first mandrel spacing calculations turns out to be above the initially estimated depth, a new point of injection should be set above the initially estimated point of injection “1” and then continue with the iterations.

Fig. 9.12 shows the results of the first mandrel spacing procedure, using any of the mandrel spacing methods that are described later in this chapter. As can be seen, the initial point depth was too deep and the mandrel spacing calculations gave a point of injection depth “2” that is much higher up in the well; therefore, the initial operating pressure was unrealistically estimated. As it is explained in this chapter, a particular mandrel spacing procedure



■ FIGURE 9.11 Iterations to find the depth of the point of injection: initial injection point depth "1."

is stopped when the distance between two consecutive mandrels is shorter than a specified minimum distance (given by the designer) or when the difference between the injection pressure and the production pressure is smaller than a certain pressure drop specified also by the designer.  $P_{inj\ min}$  in Fig. 9.11 should not be confused with  $P_{inj}$  in Fig. 9.12;  $P_{inj\ min}$  is the estimated "operating" injection pressure (after a particular mandrel spacing calculation is finished), while  $P_{inj}$  in Fig. 9.12 is the "initial" injection



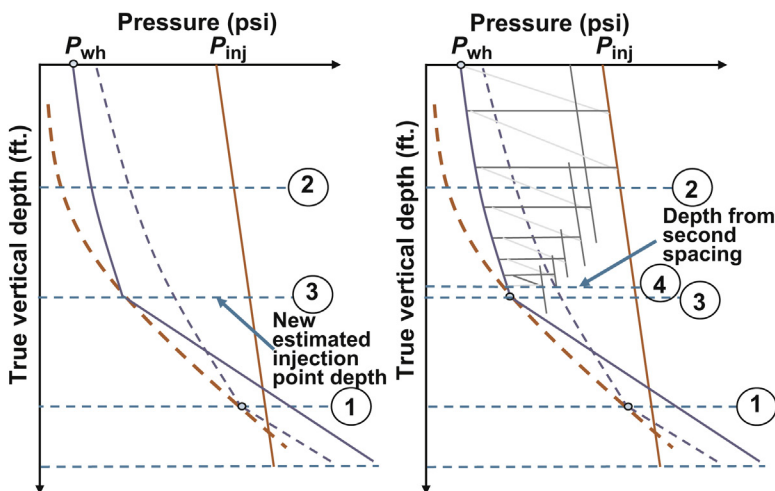
■ FIGURE 9.12 Result of the first mandrel spacing: depth no. 2.



pressure to start a particular mandrel spacing procedure, also known as the kickoff pressure in some cases.

If the estimated point of injection has been reached (none of the two situations given in the previous paragraph to stop mandrel spacing are met) and the injection pressure is still high enough to continue the mandrel spacing procedure, a deeper point of injection should be selected, unless the maximum possible point of injection has already been reached.

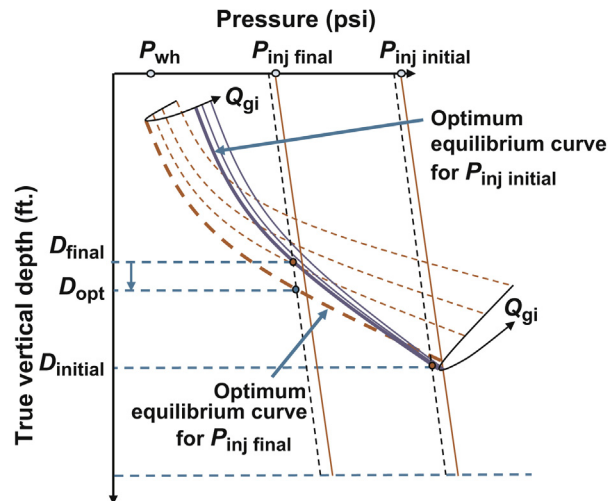
A new point of injection at depth “3” (between depths “1” and “2”) is then selected. A new pressure-traverse curve is calculated for this new injection point using nodal analysis with the same injection gas flow rate that was used at point of injection “1.” As can be seen in Fig. 9.13, because point of injection “3” is higher up than point “1,” by nodal analysis it is found that the liquid flow rate is now lower, so the production pressure is also lower in a large portion of the tubing compared to the production pressure for the first point of injection. This lower pressure in turn allows the mandrel spacing procedure to reach a point of injection deeper than achieved by the first mandrel spacing. The new depth of the second spacing, depth 4, is close to the second estimated depth “3.” The iterative process continues (with a constant injection gas flow rate) until the latest estimated depth and the one obtained from the mandrel spacing procedure coincide with each other within a given margin of error. Because this process is based on nodal analysis, once the injection point depth is found, the liquid flow rate is simultaneously calculated.



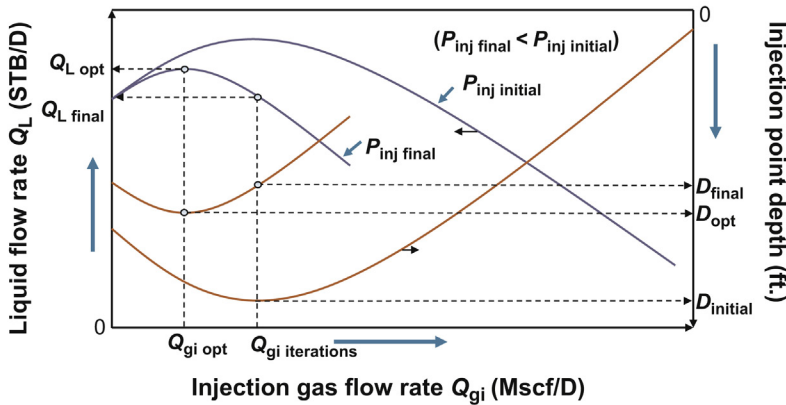
■ FIGURE 9.13 Result of the second mandrel spacing: depth no. 4.

Finally, if the iterations converge to a point of injection depth that is very different from the one found initially with an unrealistic operational injection pressure (estimated in Fig. 9.10 as explained in chapter: Total System Analysis Applied to Gas Lift Design), the designer must verify if the injection gas flow rate used during the iterations is adequate for this final injection point depth. Usually, if the initial operating injection pressure was realistically determined, the final point of injection depth at the end of the iterations should not be too different from the one estimated in Fig. 9.10. Fig. 9.14 shows the improvement that could be obtained if the injection gas flow rate is adjusted at the end of the iterations (this must be done by the designer).

Referring to Fig. 9.14, with the initially estimated operating injection pressure  $P_{inj\ initial}$ , an initial depth,  $D_{initial}$ , is reached but after the iterations, the operating injection pressure  $P_{inj\ final}$  turned out to be lower, for which the final injection point depth is  $D_{final}$ . Because depth  $D_{final}$  has been obtained using the optimum equilibrium curve for the initial injection gas flow rate, it is seen in Fig. 9.14 that it is possible to reduce the friction pressure drop and reach a deeper point of injection “ $D_{opt}$ ” (increasing the liquid production at the same time) by reducing the gas flow rate to the optimum gas flow rate corresponding to the more realistic injection pressure  $P_{inj\ final}$ . Fig. 9.15 shows, in a graphical way, what happens when estimating the new optimum gas flow rate corresponding to  $P_{inj\ final}$  in comparison to the optimum gas flow rate corresponding to  $P_{inj\ initial}$ . A new iteration (which should converge very fast) to find the injection point depth using the new gas flow rate must be performed.



■ FIGURE 9.14 Equilibrium curves for different injection gas flow rates.



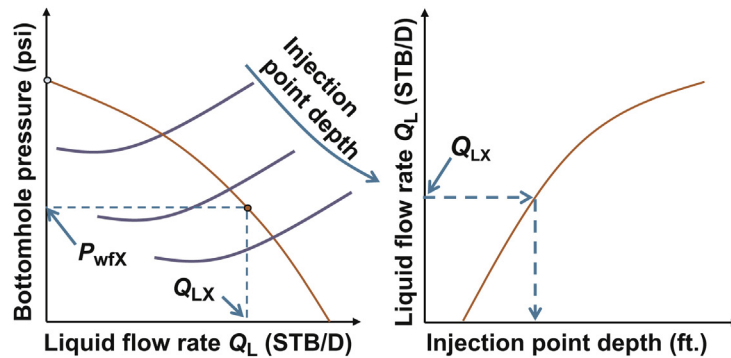
■ FIGURE 9.15 Liquid flow rates, injection gas flow rates, and point of injection depths for two operating injection pressures.

As can be seen in Fig. 9.15, the initial gas flow rate,  $Q_{gi \text{ iterations}}$ , is the best choice if it were possible to reach  $D_{\text{initial}}$  with pressure  $P_{\text{inj initial}}$ , but because a more realistic pressure is  $P_{\text{inj final}}$ , it is better to perform the iterations with the gas flow rate shown in the figure as  $Q_{gi \text{ opt}}$ , that would allow reaching a deeper injection depth  $D_{\text{opt}}$  (compared to the depth found in the iteration,  $D_{\text{final}}$ ) and a greater liquid flow rate,  $Q_{L \text{ opt}}$ . With  $Q_{gi \text{ iterations}}$  the well would be over injected and, in consequence, the bottomhole flowing pressure will be greater due to larger friction pressure drops along the tubing and flowline.

### 9.1.2 Fixed drawdown or fixed liquid production

There are less sophisticated computer programs that do take into consideration the IPR curve but do not calculate a different liquid flow rate if the injection pressure is not high enough to reach the desired point of injection. In other words, they do not perform the iterations described in the previous section.

With this type of computer program, the user introduces the injection gas flow rate and, additionally, either the well's liquid production,  $Q_{LX}$ , or the bottomhole flowing pressure,  $P_{wfx}$  (if the user enters the bottomhole flowing pressure, the program calculates the liquid production from the IPR curve and vice versa). The program calculates the injection point depth using the nodal analysis procedure shown in Fig. 9.16 by iteration: the program finds the point of injection depth that makes the outflow curve intersect the IPR curve precisely at point  $(Q_{LX}, P_{wfx})$ . This option is then very useful if it is desired to maintain the liquid flow rate at less than a certain maximum value, possibly because of: (1) low production requirements, (2) problems



■ FIGURE 9.16 Either the liquid flow rate or the bottomhole flowing pressure are known and the program calculates the injection point depth.

handling produced water, (3) the bottomhole pressure should be kept high to avoid sand production or water coning, etc.

For a given liquid flow rate (or drawdown) and an injection gas flow rate, there exists one and only one depth of the point of injection that can be calculated as shown in Fig. 9.16. If the mandrel spacing procedure cannot reach the point of injection calculated by nodal analysis in this way (mandrel spacing stops when the distance between two consecutive mandrels is shorter than a specified minimum distance, given by the designer, or when the difference between the injection pressure and the production pressure is smaller than a certain pressure drop specified also by the designer), the program simply indicates the maximum injection point depth found and the user should then make the necessary adjustment to reach the desired point of injection or select a smaller liquid production or drawdown. If the minimum pressure gradient in the production tubing has not been reached, it might be possible to space the mandrels down to the calculated point of injection by increasing the injection gas flow rate. Another possible adjustment is achieved by reducing the sequential injection pressure drop per valve if the unloading valves are IPO valves. If none of the adjustments are capable of spacing the mandrels down to the calculated point of injection, the liquid production flow rate must be decreased until the point of injection calculated by nodal analysis with the new liquid flow rate can be reached by the mandrel spacing procedure.

### 9.1.3 Constant liquid production

All of the design procedures described previously can only be accomplished if the IPR curve of the well is known. But commercially available computer programs offer the option of considering a constant liquid production (given

by the designer) in case the IPR curve is not known or it is not desired to use it. This is helpful in exploratory wells for which the IPR curve is unknown. But this option can also be used if the designer is certain of the liquid flow rate the well can produce. In this case, besides the liquid flow rate, the user must enter the injection gas flow rate, the point of injection depth, and the outlet pressure, which could be the wellhead pressure or, if the effect of the flowline is considered, the pressure at the separator. The gas flow rate is usually selected by the designer so that the minimum pressure gradient curve is attained along the production tubing. The program then performs the production pressure calculation along the production tubing string from the known outlet pressure to the bottom of the well, assuming that the injection point depth is the one indicated by the user. This production tubing pressure is then used to perform the mandrel spacing procedures that are explained in the next section. The injection point depth is simply the one where the mandrel spacing procedure stops due to the causes already mentioned: (1) that the minimum distance between two consecutive mandrels has been reached, (2) that a minimum pressure drop across the gas lift valve has been obtained or, in this case, (3) that the desired point depth supplied by the user has been reached.

## 9.2 GAS LIFT MANDREL SPACING PROCEDURES AND VALVE DESIGN CALCULATIONS

The heart of a gas lift design is the procedure known as “mandrel spacing” which is used to find the depths of the unloading valves and to determine, at each of these valves, the following parameters:

1. The unloading liquid flow rate.
2. The required unloading injection gas flow rate.
3. The valve seat diameter to be able to pass the required injection gas flow rate.
4. The test-rack calibration opening or closing pressure, as the case might be, that will allow the unloading valves to close in a sequential manner as the unloading of the well proceeds, leaving only the operating valve open when the unloading of the well is completed.

Mandrel spacing is presented in detail in this section. This operation depends on the type of gas lift valve that will be installed in the well and on the quantity and quality of the information available to perform the design. The starting point for mandrel spacing calculations is to find the production-pressure-traverse curve, the kickoff injection pressure and the operating injection pressure for the first valve. The production-pressure-traverse curve is determined from the liquid production, which is either given by the user

(constant-liquid-flow-rate option) or it is calculated by the program using the iterative procedure explained in the [Section 9.1](#) (in either case, this liquid production will be the final liquid production the well will have after the unloading operation is completed). The kickoff and operating injection pressures depend on the gas lift system as explained in the next paragraphs.

The final production-pressure-traverse curve is used only as a guide (during the mandrel spacing procedures) to find the production pressure (known as the transfer production pressure) from which the next deeper valve is located (for example, this transfer pressure would be point “1 pt” on the diagram shown in [Fig. 9.17](#), to locate the second mandrel starting at the depth of the first one). This final pressure-traverse curve is highly recommended for IPO valves. Using the final production-pressure-traverse curve as a guide will set the production pressures of the unloading valves (for their design calculations) as close as possible to their actual production pressures during the normal operation of the well (once it has been fully unloaded). If the production pressures used for the unloading valves in their design calculations are smaller than their corresponding final production pressures, then the injection opening pressure of each unloading valve will decrease when the well is fully unloaded because the actual higher production pressure will help open the valve, with the result of lowering its required injection opening pressure. This can create instability problems or prevent the well from unloading. Additionally, using the final pressure-traverse curve places the mandrels at shallower depths as a safety factor (in comparison to using lower production pressures to locate the next mandrel, which could result in mandrels that might be too deep to be reached). If, on the other hand, the design production pressure is too large compared with the final production pressure at a particular valve, then the injection opening pressure will increase as the unloading proceeds. This is not a problem and it is actually helpful in preventing valve instabilities; the setback in this case is that the next deeper valve will be placed at an unnecessarily shallower depth. Therefore, using the final production pressure as a guide during mandrel spacing and valve design procedures is recommended for IPO valves. For PPO valves, it has been found useful to use a design line, such as line “ $P_{d-g}$ ” in [Fig. 9.29](#) (instead of the final production-pressure-traverse curve). The pressures along this type of “design line” correspond to pressures that are larger than the actual production pressures once the well has been fully unloaded. In this way, each unloading PPO valve will close as the production pressure drops from its design value as the well is being unloaded. This type of production pressure design lines are sometimes used for IPO valves, probably giving a larger number of mandrels than necessary but the designs are also usually more flexible (which is specially helpful if the data needed for the design is missing or unreliable). Using a larger number

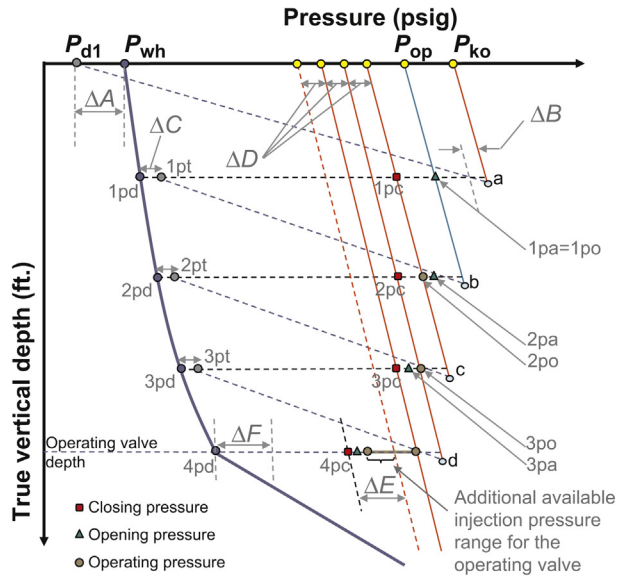
of mandrels increases the flexibility of the design but it also increases costs, number of potential failure points, and can make troubleshooting the operation of the well much more difficult. For redesign calculations, explained in Section 9.2.7, it is common to use a redesign production pressure line, see Fig. 9.49. The design procedure explained in Fig. 9.27 for gas lift valves with chokes upstream of the seat is an example of how the design production pressure line can be used for IPO valves. With some minor adjustments, his same design procedure (with a design production pressure line and constant unloading operating injection pressure) is used many a times for normal IPO valves (with no upstream chokes) but it has to be used with caution because it might promote valve interference, give more mandrels than needed, and make troubleshooting the operation of the well more difficult.

### 9.2.1 Mandrel spacing for IPO valves

Today, the IPO valve is by far the most widely used type of valve to unload gas lift wells. This is due to: (1) the fact that the operation of the well (with IPO valves) is mainly controlled by the injection pressure, which is easy to calculate at any depth from the injection pressure at the surface, making it easy to design and troubleshoot the well, and (2) the way in which these valves behave, most of the time allowing a smooth and stable unloading and general operation.

*Mandrel spacing by sequentially dropping the valve's closing pressure.* The mandrel spacing procedure by sequentially dropping the closing pressures of the unloading valves is explained in this section. This type of method guarantees that each unloading valve will close as the unloading proceeds. However, this method presents some problems in its implementation that are described further. Fig. 9.17 shows this mandrel spacing method. The production pressure along the depth of the well should be plotted from the wellhead pressure,  $P_{wh}$ , against the true vertical depth and not the measured depth.

The nomenclature used in Fig. 9.17 for the  $n$ th valve is as follows: “npd” is the production pressure equal to the pressure in the tubing (if the well is produced up the tubing) or in the annulus (if the well is produced up the annulus) at the  $n$ th valve's depth; “npt” is the transfer production pressure of the  $n$ th valve from which the unloading pressure gradient line is traced to find the depth of the next deeper valve; “npc” is the valve's closing injection pressure of the  $n$ th valve at the operating temperature; “npa” is the valve's opening injection pressure of the  $n$ th valve; and “npo” is the valve's operating injection pressure of the  $n$ th valve, which must remain constant until the next deeper valve is uncovered. Points “a,” “b,” “c,” and “d” are the intersection points of the unloading pressure gradient lines with the operating



■ FIGURE 9.17 Mandrel spacing procedure for IPO valves by sequentially dropping the injection closing pressure of each unloading valve.

injection pressures lines. These intersections are used to define the depths of the valves. The analytical way of calculating these intersections is explained at the end of this section (use Fig. 9.17 as a guide for the following paragraphs).

The following steps are performed by computational programs to space gas lift mandrels in the well and to design the unloading gas lift valves at each step.

- First of all, the kickoff pressure line is found from the kickoff pressure,  $P_{ko}$ , to determine the depth of the first valve. This kickoff pressure is greater than the operating pressure  $P_{op}$  of the first valve and could be equal to the average injection manifold pressure. The operating pressure,  $P_{op}$ , is, on the other hand, equal to the expected minimum manifold pressure minus a differential pressure that will allow sufficient gas flow rate to unload the well from the first to the second valve. The idea of using  $P_{ko}$  is to place the first valve as deep as possible and, in this way, reduce the number of mandrels to be run in the well; but the calibration of the first valve is determined from the value of the available operating pressure  $P_{op}$ . The designer must enter the values of  $P_{ko}$  and  $P_{op}$ . If these pressures are equal, then the depth and the calibration of the first valve are determined from the same pressure. It



is acceptable to have a high value of  $P_{ko}$  because the injection gas flow rate must be very small before reaching the first valve, which means that the wellhead injection pressure is very similar to the manifold pressure at that time (losses due to friction are very small and a great differential pressure at the manifold is not required for such a low gas flow rate either). Due to the importance of the kickoff pressure, some companies have a temporary external high-pressure source or a high-pressure portable compressor used only to kick off the well. However, there are operating companies that prefer having more mandrels installed in the well to increase the flexibility of their gas lift designs; thus, for these companies, the concept of the kickoff pressure as presented previously is not relevant because they prefer to use a lower initial injection pressure for spacing of the first valve.

- From the initial wellhead pressure,  $P_{d1}$ , a line with a slope equal to the unloading-liquid pressure gradient is traced. The unloading pressure gradient is usually equal to 0.45 psi/ft. As a safety factor, a large unloading pressure gradient is used, independently of the type of fluids that are currently in the well, so that in the future it can be unloaded with any type of completion fluids. In this way if, for example, the water cut increases during the life of the well, the mandrel spacing could still (up to a point) be adequate. If the unloading fluid pressure gradient (in psi/ft.) is not known, it can be calculated by multiplying the weight in pounds of 1 gallon of the unloading fluids by 0.52. Pressure  $P_{d1}$  is less than the wellhead pressure  $P_{wh}$  the well will have under normal operation because at the beginning of the unloading process the liquid flow rate is very small, so the wellhead pressure only needs to be slightly higher than the pressure at the separator. However, some designers prefer to trace the unloading pressure gradient line from  $P_{wh}$  as a safety factor: this gives a shallower depth of the first valve so that it can be reached with lower kickoff pressures (in fact, some designers use values of  $P_{d1}$  greater than  $P_{wh}$  to get an even shallower depth of the first mandrel). Sometimes, when the first valve cannot be uncovered, the unloading process can be initiated by unloading the well to a pit at atmospheric conditions. This allows the injection gas to uncover the first valve because the pressure  $P_{d1}$  is, in this case, lower than the pressure at the separator.
- The unloading pressure gradient line from  $P_{d1}$  intersects the injection pressure line from  $P_{ko}$  at point "a." The depth of the first valve is then determined by the horizontal line located above intersection "a" so that the differential pressure between the injection pressure and the production pressure is equal to  $\Delta B$  (given by the designer) when the valve is uncovered, allowing the injection gas from the annulus

to flow into the production tubing. The point where this horizontal line intersects the production-pressure-traverse curve determines the production pressure for the first valve,  $P_{1pd}$ . The point where the operating injection pressure line that starts at  $P_{op}$  intersects the horizontal line determines the valve's opening injection pressure  $P_{1pa}$ . In this case (as shown in the Fig. 9.17), the opening injection pressure is equal to the operating injection pressure. This is only true for the first valve. The operating injection pressure is the pressure that is used to find the depth of the second valve. Some designers set the opening pressure at a value slightly lower than the operating pressure at depth to make sure the first valve will operate in orifice flow and not in throttling flow (this point is explained further in this section).

- Then, following the steps that are presented in Section 9.2.3, the unloading liquid flow rate and its corresponding required injection gas flow rate are determined for the first valve. With the procedures that are described in Section 9.2.4, the valve's and injection gas' temperatures at depth are determined. The next step is to calculate the diameter of the seat of the first valve. This seat diameter must be the smallest of the available seat diameters capable of passing at least the unloading gas flow rate required for the first valve (seats larger than this are not recommended for the reasons explained in the following paragraphs). To calculate the seat diameter,  $P_{1pa}$  is taken as the valve's upstream pressure, while the transfer pressure  $P_{1pt}$  (defined in the following paragraphs) is taken as the valve's downstream pressure. The calculations required to determine the diameter of the seat are presented in Section 9.2.5 and in chapter: Gas Flow Through Gas Lift Valves. With the seat diameter already found, the valve's injection closing pressure is calculated with the valve mechanic equations presented in chapter: Gas Lift Valve Mechanics. The force–balance equation is used to find the valve's closing pressure  $P_{1pc}$  with: (1) the area ratio corresponding to the selected seat diameter, (2) pressure  $P_{1pa}$  as the opening pressure, and (3) the transfer production pressure  $P_{1pt}$  as the production pressure. The test-rack calibration pressure is then determined by finding the dome pressure at 60°F from the dome pressure at operating conditions (equal to  $P_{1pc}$ ) and following the steps that are presented in chapter: Gas Lift Valve Mechanics, for IPO valves. This is the last calculation required for the first valve. The next step is to find the depth of the second unloading valve.
- The unloading pressure gradient line is traced from point  $P_{1pt}$ , called “transfer pressure” until it intersects the “operating” pressure line of the first valve at point “b.” The transfer production pressure  $P_{1pt}$  is obtained by adding a differential pressure  $\Delta C$  (given by the designer) to

the production pressure  $P_{1pd}$ . This constitutes a safety factor that takes into account possible errors in the estimation of the production pressure of the first valve, placing the second valve (or mandrel) at a shallower depth. The depth of the second valve is established by a horizontal line located above intersection “b” so that the differential pressure between the injection pressure and the tubing pressure is equal to  $\Delta B$ , for the same reasons explained for the first valve.  $\Delta C$  can be a fixed pressure differential or a fixed percentage of the difference between the valve’s operating pressure and the production pressure at valve’s depth.

- The calculation sequence required to determine the calibration pressure of the second valve is different from the one explained for the first valve: now, the surface closing pressure of the second valve is equal to the surface closing pressure of the first valve minus a differential pressure  $\Delta D$ , defined by the designer. The surface operating pressure of the second valve (which is the pressure that is used to find the depth of the third valve), is now equal to the surface closing pressure of the first valve. This guarantees that the first valve is closed while gas is being injected through the second valve. Some designers use an additional safety factor making the surface operating pressure of the second valve equal to the surface closing pressure of the first valve minus a safety factor that is usually equal to 20 or 30 psi, which is not shown in Fig. 9.17. To maintain the operating pressure of the second valve constant as the injection gas flows through it, the determination of the second valve’s seat diameter is made with the operating pressure,  $P_{2po}$ , as the pressure upstream of the valve and the transfer production pressure,  $P_{2pt}$ , as the pressure downstream of the valve, using the equations given in chapters: Single and Multiphase Flow Through Restrictions and Gas Flow Through Gas Lift Valves. However, it is necessary to calculate the required gas flow rate through the second valve and its injection temperature before being able to calculate the valve seat diameter. The gas flow rate and its temperature just upstream of the valve are calculated following the steps that are explained in Sections 9.2.3 and 9.2.4, respectively. Once the seat diameter is found, the valve mechanic equations explained in chapter: Gas Lift Valve Mechanics are used to determine the valve’s opening pressure at operating conditions with: (1) the valve area ratio corresponding to the selected seat, (2) the valve closing pressure at valve’s depth (from the valve’s surface closing pressure determined previously), and (3) the transfer production pressure  $P_{2pt}$  as the production pressure to be used in the force–balance equation. Note that for the second valve, the opening pressure needs to be calculated while for the first valve, it is the closing pressure that has to be calculated.

- In the particular case shown in Fig. 9.17, the second valve opening pressure ended up being greater than its operating pressure. This is not always the case but it might happen and it is one of the problems that one might encounter with this type of mandrel spacing technique. This is purposely shown in the figure to point out the problem: It is not uncommon that the differences between the closing and opening pressures (called “spread”) of the first (shallower) valves are greater than the spread of the deeper valves. This is due to the fact that the production pressures of the upper valves are smaller. This problem is even worst for valves with large seats. The larger the seat (and therefore the valve’s area ratio), the larger the spread of the valve becomes. This is one of the reasons why it is necessary that the seats of the unloading valves be as small as possible. Additionally, 1-in. OD valves have larger area ratios than 1.5-in. OD valves for a given seat diameter. Then, the use of 1-in. OD valves could cause one or several upper valves to have opening pressures greater than the operating pressures. When the operating pressure is lower than the opening pressure, the valve operates in throttling flow and it might not be possible to pass the required unloading gas flow rate through the valve. In those cases, the problem could be avoided by increasing the closing pressure drop per valve,  $\Delta D$ . But increasing the sequential closing pressure drop could make it impossible to reach the desired point of injection. It can be seen in Fig. 9.17 that this problem is not present in the third valve because the spread of this valve is smaller. One effective way of dealing with this problem is by increasing  $\Delta D$  and, at the same time, installing valves above the reservoir static liquid level with small valve seats. This might make it longer for the well to unload, but the desired point of injection can be reached without having valves operating in throttling flow below the static reservoir liquid level (where it is really necessary to pass the design unloading gas flow rate). At the end of this section, the problem of valves operating in throttling flow (for having operating pressure lower than the opening pressure) is explained in more detail.
- Calculations for the third and fourth valves are identical to the ones for the second valve, with the exception that for the fourth valve (considered the “operating” valve in this example) an additional closing pressure drop equal to  $\Delta E$  (defined by the designer and usually equal to 30, 50, or 75 psi, depending on the available injection pressure) must be provided. A lower closing pressure has the following advantages:

  - Provides a positive identification of the operating point;
  - It helps closing the upper valves;

- It allows the operating valve to be completely open; and
- It enables a wider operating pressure range, in case the required injection gas flow rate needs to be greater than its estimated value.

Most designers prefer to install an orifice valve at the final operating point of injection instead of a calibrated valve. This has the following advantages:

- More flexibility in regard to the operating pressure because orifice valves are always open so they will not close at low injection pressures;
- They are cheaper and do not restrict the gas flow rate (wells that require injection gas flow rates above 1.4 MMscf/D should have an orifice valve at the point of injection because calibrated valves, in most cases, will restrict the gas flow rate); and
- They do not fail as easily as calibrated valves do.

On the other hand, the main disadvantages of having an orifice valve at the operating point of injection are:

- It does not allow positive identification of the operating valve because the operating pressure changes as it adapts itself to the production pressure, making it harder to troubleshoot the well;
  - If the compressor shuts down, the injection annular pressure (if gas is injected down the annulus) is bled off to a low value determined by the static liquid column in the tubing; and
  - Orifice valves do not have the regulating action that calibrated valves do. When the well has a tendency to head, it is better to install a calibrated valve to reduce the source of instability: if the production pressure increases, the operating valve opens wider and the gas flow rate is increased. This makes the production pressure reduce toward its original lower value. On the other hand, if the production pressure drops, the valve will tend to close and the injection gas flow rate will decrease. This makes the production pressure increase toward its original value. This controlling action is usually expected from operating valves because they normally operate in throttling flow. If the type of flow through the valve is “orifice flow” this self-regulating action would not be present, but it is important to point out that operating valves many times operate in throttling flow. The difference between throttling and orifice flows is presented at the beginning of chapter: Gas Flow Through Gas Lift Valves, see Fig. 8.5.
- Because the diameter of the seat of the operating valve was selected as the “commercially available” minimum size capable of passing at least the required gas flow rate, it is highly possible that the final operating pressure will be lower than the design operating pressure. This is due to

the fact that the seat installed in the well is greater than the calculated one because it is unlikely that the calculated seat diameter be exactly equal to a commercially available seat diameter. A larger than needed seat diameter is almost always installed in the well; therefore, for a given injection gas flow rate, the required injection pressure is lower. This low injection pressure could introduce instability problems (if a much larger than needed seat diameter is installed at the “operating” point of injection), or make it difficult to unload the well (for the case of unloading valves).

- For the reasons explained in the previous paragraph, it is always a good idea to back calculate the final operating pressure (using any of the equations or models presented in chapter: Gas Flow Through Gas Lift Valves) from: (1) the expected production pressure at valve’s depth, (2) the actual seat diameter of the operating valve, and (3) the required gas flow rate. If the operating injection pressure is too close to the production pressure (as determined by the procedure explained in [Section 9.3](#) regarding gas lift stability), calculations should be made to determine if a different valve model, with a smaller seat, could be installed without causing a large increase in the operating pressure that might open the next upper unloading valve.
- On the other hand, it is also possible that the maximum available orifice or seat size might still be too small for the required gas flow rate, causing the final operating pressure to be too high. In this case, the following alternatives should be tried (these recommendations apply to any mandrel spacing procedure):
  - Select a different valve model;
  - Install a mandrel with multiple pockets so that several valves can be installed;
  - Install two mandrels at an adequate distance between them to allow wireline operations.
- The designer should provide a minimum pressure differential  $\Delta F$  below which the difference between the operating pressure and the production pressure would not be acceptable and mandrel spacing calculations should be stopped. Mandrel spacing should also be stopped when (all depths are true vertical depths):
  - The minimum spacing  $\Delta D_{\min}$  between two consecutive mandrels has been reached; or
  - A depth  $D_{\max}$  has been found by the spacing procedure that is below the desired final injection point depth, known here as  $D_{\text{inj}}$ . In this case, if the distance between  $D_{\max}$  and  $D_{\text{inj}}$  is greater than  $\Delta D_{\min}$  (or any other differential depth given by the designer), some programs locate the operating valve at  $D_{\text{inj}}$  and set the new depths of the unloading valves equal to their respective initial depths

times the ratio  $D_{inj}/D_{max}$ . Other programs locate the operating valve at  $D_{inj}$  and adjust the mandrel depths of the unloading valves by subtracting from their initial depths a vertical distance equal to  $[n(D_{max} - D_{inj})/N]$ , where  $n$  is the number of the mandrel whose depth is adjusted and  $N$  is the total number of mandrels ( $n$  is equal to 1 for the shallowest mandrel). This latter adjustment procedure is better than the former because it guarantees that a particular mandrel would not be too high up in comparison to the next mandrel right below it. But if the distance between  $D_{max}$  and  $D_{inj}$  is shorter than  $\Delta D_{min}$  (or any other differential depth given by the designer), then it is a common practice to place the operating valve at  $D_{inj}$  and leave the unloading valves' depths unchanged.  $D_{inj}$  was usually 60 ft. (measured depth) above the packer to be able to operate old kickover tools but now, with the new types of mandrels,  $D_{inj}$  can be closer to the packer. If the final design point of injection  $D_{inj}$  (for current operational conditions) is above the maximum point where it is possible to install gas lift equipments,  $D_{max-possible}$ , it is recommended to install mandrels below  $D_{inj}$  for future lower reservoir pressures or higher injection pressures. The number of mandrels  $N_{below}$  below  $D_{inj}$  is the integer part of  $(D_{max-possible} - D_{inj})/(\Delta D_{min})$ . The spacing between these mandrels is then  $(D_{max-possible} - D_{inj})/N_{below}$ .  $\Delta D_{min}$  is assigned by the designer and it is usually 90 ft. for large productivity index (PI) wells or as long as 500 ft. for small PI wells. For wells from 4,000 to 10,000 ft. of total depth, it is usual to have  $\Delta D_{min}$  equal to 250 ft.

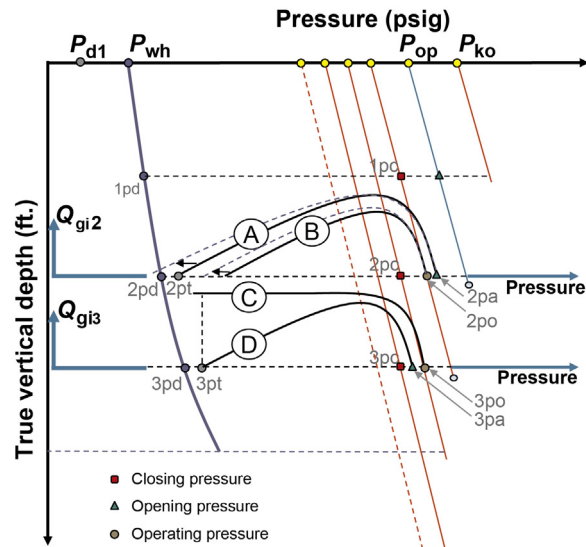
Mandrel spacing by sequentially dropping the valve's closing pressure is recommended in cases where the operating temperature is difficult to predict, like in wells with high and varying water cuts. It might be possible that the temperatures used in the calculations of the closing pressures are different from the actual temperatures in the well, but the error is made in a consistent manner for all valves, so the relative positions of the closing pressures are kept more or less constant. However, if temperature prediction is not a problem and it is desired to reach a point of injection as deep as possible in the well, the spacing technique explained in the next section is a better option. If the injection pressure is high enough to reach the maximum possible point of injection, then any of these two mandrel spacing techniques (the one explained in this section and in the next section) can be used.

If there are no problems related to hydrate formation and the injection pressure is high enough to reach points located even below the deepest possible point of injection, the sequential closing pressure drop per valve can be larger than its usual value. This allows for a smooth unloading operation and easier future troubleshooting activities. However, if hydrates can form in the

surface gas injection line (due to, for example, a large pressure drop across the injection gas flow rate control valve), it is better to keep the operating pressure at the surface at a high value and have a large pressure drop at the operating valve, where the gas is warmer than the hydrate formation temperature. This recommendation applies to all mandrel spacing techniques explained in this chapter.

Returning to the problem of having the opening pressure greater than the operating pressure (see second valve in Fig. 9.17), “Gas Flow Rate versus Production Pressure” graphs for valves “2” and “3” have been drawn on the valve spacing diagram presented in Fig. 9.18. Two flow-rate curves, one for the injection pressure equal to the opening pressure and the other for the injection pressure equal to the operating pressure, have been plotted for both valves as  $Q_{gi2A}$  and  $Q_{gi2B}$  for the second valve and as  $Q_{gi3D}$  and  $Q_{gi3C}$  for the third valve.

For valve number “2,” if the injection pressure is the valve opening pressure,  $P_{2pa}$ , then curve “A” represents the theoretical flow rate that can be injected through this valve,  $Q_{gi2}$ , as a function of the production pressure; the gas flow rate becomes equal to zero when the production pressure is  $P_{2pt}$ . In reality, due to dynamic effects, the valve can allow a slightly higher gas flow rate represented by the dashed curve just beside curve “A.” When the injection pressure is equal to  $P_{2po}$ , the theoretical and actual gas flow



■ FIGURE 9.18 Gas flow rates that can be injected through valves “2” and “3” for different injection pressures.

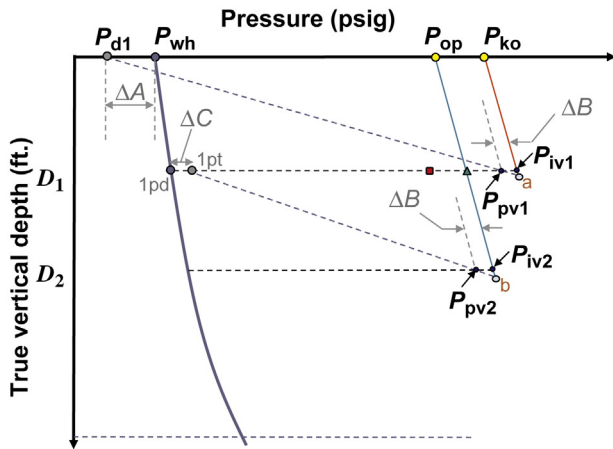


rates through valve “2” are represented by curve “B” and its corresponding dashed curve, respectively. As can be seen, for the latter case the valve closes at a production pressure higher than  $P_{2pt}$ . To unload the well, it would then be necessary to maintain the injection pressure at a value greater than  $P_{2pa}$ , for which the upper valve might remain open. If the first valve remains open, the third valve could be uncovered if the injection pressure is temporarily kept high by increasing the surface injection gas flow rate, which is many times (but not always) possible. It is seen that for valve number “3,” the gas flow rate is kept at an acceptable level when the injection pressure is the operating pressure  $P_{3po}$  and the production pressure is  $P_{3pt}$  (flow rate curve “C”), which allows uncovering the fourth valve without having to increase the stipulated gas flow rate while unloading from the third valve.

The analytical way of calculating the depth of the valve is presented next. This explanation applies to all mandrel spacing techniques given in this chapter. The determination of the depth of the valve is based on a pressure balance just before the valve is uncovered. Following the notation used in Fig. 9.19 below, the production pressure in the tubing at valve’s depth,  $P_{pv1}$ , plus the pressure differential  $\Delta B$ , must be equal to the injection pressure at valve’s depth,  $P_{iv1}$ :

$$P_{pv1} + \Delta B = P_{iv1} \tag{9.1}$$

Where  $P_{pv1} = P_{d1} + D_1 (g_s)$ ;  $P_{iv1} = P_{ko}/g_s$ ;  $D_1$  is the true vertical depth of the first valve that needs to be determined;  $g_s$  is the pressure gradient of the unloading fluids in the tubing, usually taken equal to 0.450 psi/ft.; and  $f_g$  is the



■ FIGURE 9.19 Analytical method that can be used to find the depths of the valves.

gas factor explained in chapter: Single-Phase Flow, and used to calculate the injection pressure at depth. Introducing the expressions for  $P_{pv1}$  and  $P_{iv1}$  in Eq. 9.1 and solving for  $D_1$ , the following equation is found for  $D_1$ :

$$D_1 = [P_{ko}(f_g) - P_{d1} - \Delta B]/g_s \quad (9.2)$$

Because the gas factor  $f_g$  depends on the depth of the valve, which is not known a priori, Eq. 9.2 must be solved by iterations.

The gas flow rate for the first valve is always very low and the pressure due to the gas column in the injection annulus can be calculated assuming a hydrostatic gas column (no friction losses) with any of the equations presented in chapter: Single-Phase Flow, for that purpose: Eqs. 2.13, 2.18, or 2.19. These equations for  $f_g$  can be applied to the rest of the unloading valves in the great majority of cases because the gas injection cross-sectional areas are usually large for the gas flow rates found most of the time in gas lift wells. The iterative method to find  $D_1$  for the first valve is as follows:

- Assume an initial depth  $D_1 = (P_{ko} - P_{d1})/g_s$ ;
- With this depth, calculate the first value of  $f_g$ ;
- With this new  $f_g$  factor,  $D_1$  is found from Eq. 9.2 given previously;
- With this new depth, a new value of  $f_g$  is calculated and then a new value of  $D_1$  is again found from Eq. 9.2. This process is repeated until convergence is achieved within a tolerance value given by the designer. This iteration should converge very fast.

The iterative process that can be used to find the depth of the second valve  $D_2$  (with no friction effect) is very similar to the one just explained for the first valve. In this case, the depth of the valve is determined from the pressure balance that establishes that the production tubing pressure at the depth of the second valve,  $P_{1pt} + (D_2 - D_1)g_s$  plus the differential pressure  $\Delta B$ , must be equal to the injection pressure at that depth,  $f_g P_{op}$ , so that:

$$D_2 = D_1 + [P_{op}(f_g) - P_{1pt} - \Delta B]/g_s \quad (9.3)$$

The gas factor  $f_g$  must be calculated at the depth of the second valve, which is not known a priori and therefore a similar iteration process is used, which (disregarding friction losses) is the following:

- An initial depth  $D_2$  is assumed to be equal to  $D_1 + (P_{op} - P_{1pt})/g_s$ .
- With this depth, the first value of the gas factor  $f_g$  is found using any of the equations given in chapter: Single-Phase Flow, for static gas columns.
- With the value of  $f_g$  calculated in the previous step, Eq. 9.3 is used to find the new depth  $D_2$ .

- With this new depth, a new value of  $f_g$  is found. Then, using the new value of  $f_g$ , Eq. 9.3 is used again to find a new value of  $D_2$ . This process is repeated until convergence is achieved within a tolerance value given by the designer. This iteration should also converge very fast.

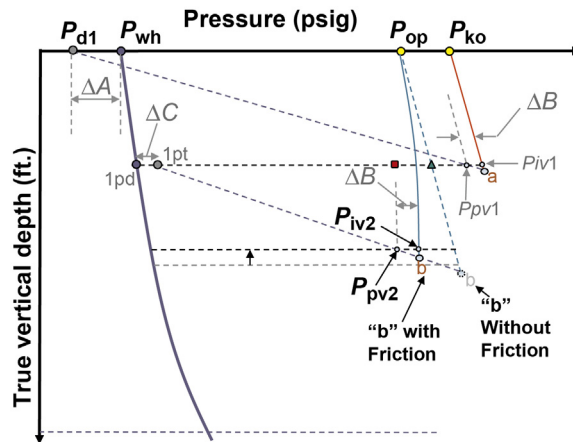
If friction is not considered, the analytical determination of the depths of the rest of the valves is done in the same way described for the second valve.

If the gas flow rate is very large and/or the injection cross-sectional flow area is very small, friction pressure losses should be considered for valves other than the first (frictional losses for the first valve should only be considered when it is placed below the reservoir static liquid level, which is usually not the case). The injection pressure  $P_{iv2}$  (calculated using the equations presented in chapter: Single-Phase Flow, Section 2.1.2, for gas flow with friction) must be equal to the production pressure  $P_{pv2}$  (when the second valve is uncovered) given by  $P_{1pt} + (D_2 - D_1)g_s$  plus the differential pressure  $\Delta B$ :

$$P_{iv2} = P_{1pt} + (D_2 - D_1)g_s + \Delta B \quad (9.4)$$

This equation should be solved by trial and error for different values of  $D_2$ , calculating at each step the value of  $P_{iv2}$  taking into consideration the friction pressure loss. For a given gas flow rate, there is one and only one value of  $D_2$  that satisfies Eq. 9.4. The additional problem in this case is the fact that the gas flow rate (for unloading purposes) depends on the depth of the valve. The iterations begin by assuming an initial value of  $D_2$ , for which the liquid flow rate that the well can produce and the corresponding injection gas flow rate (such that the production pressure is equal to the transfer production pressure at  $D_2$ ) must be calculated. These liquid and gas flow rates can be calculated following the steps explained in Section 9.2.3. If, for the selected value of  $D_2$ , the right hand side of Eq. 9.4 is greater than the left hand side, then calculations are repeated with a smaller value of  $D_2$  and vice versa. The depths of the rest of the valves are calculated in the same way as explained for the second valve. Fig. 9.20 shows that friction losses make the valve location be higher up in the well.

As soon as the valves are installed in the well, it is always a good practice to measure the liquid production for different injection gas flow rates to determine the well's real potential. But it is even more important to first make sure (by a complete troubleshooting analysis) that the point of injection is really the one stipulated in the design: the actual point of injection could be a different one located higher up in the well and this situation can go unnoticed for a long time, wasting the opportunity to produce the well at its full potential.



■ FIGURE 9.20 Effect of friction losses on the depth of the valves.

If, despite all the safety factors used in the spacing procedure, the well cannot be unloaded to the first (shallowest) gas lift valve, one of the following steps could be taken before deciding to pull the completion out of the well:

- Simultaneously inject gas down the tubing and the annulus until line pressure is reached. Leave the well alone for a few hours or days (depending on the injectivity index of the well) while the liquid is being absorbed by the formation. Then, suddenly open the well to production while injecting gas into the annulus. This is not recommended if the completion fluid can damage the formation or the well could produce sand.
- Circulate completion fluids with a lighter one. The deepest gas lift valve should be replaced with a circulating valve and dummy valves should be installed in the rest of the mandrels.
- Inject nitrogen down the tubing with a coiled tubing unit.
- Swabbing could be tried but this is a risky operation that might not be recommended in most cases.
- Direct the production fluids at the wellhead to a pit or a tank at atmospheric pressure. This reduces the value of  $P_{d1}$ .
- Temporarily shut off gas injection to nearby wells to increase the available injection pressure at the manifold.

Sometimes the well cannot be unloaded because the first valve is locked closed due to high temperature. In these cases, the well should be left alone for several hours until the valve cools down.

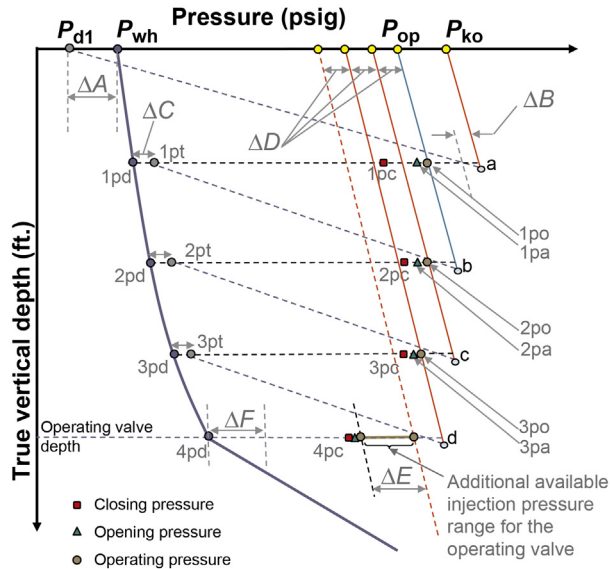
*Mandrel spacing by sequentially dropping the operating injection pressure.* This is the most widely used method in the industry today. Its main

advantage is that it allows to design each unloading valve in such a way that it is fully opened while injecting gas to uncover the valve right below. As explained previously, this is something that might not be possible using the previous spacing method. Another great advantage is that it requires smaller injection pressure drops per valve and, therefore, the operating valve can be located deeper in the well. But its major drawback is that it is sometimes not possible to close an unloading valve when the one right below it has just been uncovered, but this problem is most of the time overcome by temporarily increasing the unloading gas flow rate.

Some designers drop the valve opening pressure in a sequential manner (instead of the operating pressure) and use this opening pressure as the operating pressure. Even though doing it this way works most of the time, it induces the unloading valves to work in throttling flow because they will not be fully opened; however, this practice minimizes the risk of not being able to close the valve when the one below is uncovered. Other designers prefer a sequential drop in the “operating” pressure instead of the “opening” pressure. In this case, the opening pressure is a differential pressure (constant for all unloading valves) smaller than the operating injection pressure. This makes the unloading valves operate fully open (in orifice flow) if the operating injection pressure is at least equal to the injection pressure at the transition between throttling and orifice flow. This transition injection pressure is the one recommended here as the operating pressure because it allows smaller sequential pressure drops per valve and, in consequence, deeper depths for the final point of injection can be attained. If the available system pressure is high enough to reach the deepest point of injection, operating pressures larger than the transition pressure can be used as a safety factor to guarantee orifice flow across the valves.

The dynamic behavior of gas lift valves is explained in chapter: Gas Flow Through Gas Lift Valves. A criterion given in the aforementioned chapter that can be used to find the transition injection pressure (between throttling and orifice flow) is to have an operating injection pressure equal to the valve’s closing pressure at operating conditions divided by  $(1 - R)$ , where  $R$  is the valve’s area ratio. This criterion is not exact but it is a good guide. This is the pressure that is sequentially dropped per valve in Fig. 9.21. This would be the minimum injection pressure that would guarantee orifice flow across the valve.

The nomenclature used in Fig. 9.21 for the  $n$ th valve is as follows: “npd” is the production pressure equal to the fluid pressure in the tubing (if liquid production is up the tubing) at valve’s depth; “npt” is the transfer production pressure from which the unloading pressure gradient line is traced to find the depth of the next deeper valve; “npc” is the valve’s closing injection pressure at the operating temperature; “npa” is the valve’s opening injection



■ FIGURE 9.21 Mandrel spacing for IPO valves by sequentially dropping the operating injection pressure of each unloading valve.

pressure; and “npo” is the valve’s operating injection pressure, which must remain constant until the next deeper valve is uncovered. Points “a,” “b,” “c,” and “d” are the intersection points of the unloading pressure gradient lines with their corresponding operating injection pressures lines. These intersections are used to define the depths of the valves. The operating injection pressure “npo” is in this case the pressure that guarantees that the valve is totally open and, in consequence, operating under orifice flow. The following steps are performed by computer programs to space gas lift mandrels in the well and design the unloading gas lift valves (use Fig. 9.21 as a guide for the following paragraphs).

- First of all, the kickoff pressure line is found from the kickoff pressure  $P_{ko}$  to determine the depth of the first valve. This kickoff pressure is greater than the operating pressure  $P_{op}$  of the first valve and could be equal to the average manifold pressure. The operating pressure of the first valve  $P_{op}$  is, on the other hand, equal to the expected minimum manifold pressure minus a differential pressure that will allow sufficient gas flow rate to unload the well from the first to the second valve (usually equal to 50 or 100 psi). The idea of using  $P_{ko}$  is to place the first valve as deep as possible and, in this way, reduce the number of mandrels to be installed in the well. But the calibration of the first valve is determined from the value of the available operating pressure,

$P_{op}$ . The designer must enter the values of  $P_{ko}$  and  $P_{op}$ . If these pressures are equal, then the depth and the calibration of the first valve are determined from the same pressure. It is acceptable to have a high value of  $P_{ko}$  because before reaching the first valve the injection gas flow rate must be very small, which means that the wellhead injection pressure is very similar to the manifold pressure at that time (losses due to friction are very small and a great differential pressure is not required at the manifold for such a low gas flow rate either). Due to the importance of the kickoff pressure (to save on the number of mandrels to be purchased), some companies have a temporary external high-pressure source or a high-pressure portable compressor used only to kick off the well. But there are operating companies that prefer having more mandrels installed in the well to increase the flexibility of their gas lift designs; thus, for these companies, the concept of the kickoff pressure as presented previously is not relevant because they prefer to use a lower initial injection pressure for spacing of the first valve.

- From the initial wellhead production pressure,  $P_{d1}$ , a line with a slope equal to the unloading-liquid pressure gradient is traced. The unloading pressure gradient is usually equal to 0.45 psi/ft. As a safety factor, a large unloading pressure gradient is used, independently of the type of fluids that are currently in the well, so that in the future the well can be unloaded with any type of completion fluids. If the unloading-liquid pressure gradient is not known, it can be calculated (in psi/ft.) by multiplying the weight in pounds of 1 gallon of the unloading fluids by 0.52. Pressure  $P_{d1}$  is less than the wellhead production pressure the well will have under normal operation (after being unloaded), known here as  $P_{wh}$ , because at the beginning of the unloading process the liquid flow rate is very low, so the wellhead pressure only needs to be slightly higher than the pressure at the separator. But some designers prefer to trace the unloading pressure gradient line from  $P_{wh}$  as a safety factor: this gives a shallower depth for the first valve that can be reached with lower kickoff pressures (in fact, some designers use values of  $P_{d1}$  greater than  $P_{wh}$  to get an even shallower depth for the first mandrel). Sometimes, when the first valve cannot be uncovered, the unloading process can be initiated by unloading the well to a pit at atmospheric conditions. This allows the injection gas to uncover the first valve because pressure  $P_{d1}$  is, in this case, lower than the pressure at the separator. The unloading pressure gradient line from  $P_{d1}$  intersects the injection pressure line from  $P_{ko}$  at point "a." The depth of the first valve is then determined by the horizontal line located above intersection "a" such that the differential pressure between the injection pressure and the tubing pressure is equal to  $\Delta B$  (given by the designer)

when the valve is uncovered, allowing the injection gas to flow into the production tubing (if gas is injected down the annulus).

- The point where the horizontal line, found in the previous step, intersects the production-pressure-traverse curve determines the production pressure for the first valve,  $P_{1pd}$ . The point where the operating pressure line (which starts at the surface at  $P_{op}$ ) intersects the horizontal line, determines the operating pressure  $P_{1po}$  of the first valve. The operating pressure is the injection pressure that must be maintained in the injection annulus to find the depth of the second valve.
- Then, following the steps that are presented in [Section 9.2.3](#), the unloading liquid flow rate and its corresponding required injection gas flow rate are determined for the first valve. With the procedures that are described in [Section 9.2.4](#), the valve operating temperature and upstream injection gas temperature are determined. The next step is to calculate the diameter of the seat of the first valve. This seat diameter must be the smallest of the available seat diameters capable of passing the unloading gas flow rate required at the first valve (seats larger than this are not recommended for the reasons explained in the previous section). For the calculation of the diameter of the seat,  $P_{1po}$  is taken as the valve's upstream pressure, while the transfer pressure  $P_{1pt}$  (defined in the previous section) is taken as the valve's downstream pressure. The calculations required to determine the diameter of the seat are presented in [Section 9.2.5](#) and in chapter: Gas Flow Through Gas Lift Valves. With the seat diameter already found, the valve closing pressure is calculated. Because the operating pressure (already determined previously) must be at the transition between orifice and throttling flow, by definition (presented in chapter: Gas Flow Through Gas Lift Valves) its value should be equal to the valve's closing pressure at operating conditions (equal to the dome pressure at operating conditions if the valve is nitrogen charged with no spring for protection of the bellows) divided by  $(1 - R)$ , where  $R$  is the area ratio of the valve, which is determined once the valve's seat diameter is found. The injection closing pressure of the valve at operating conditions,  $P_{1pc}$ , is then equal to the operating pressure times  $(1 - R)$ . From the valve's force-balance equation presented in chapter: Gas Lift Valve Mechanics (Eq. 7.2 for IPO valves with  $P'_r$  set equal to zero because most nitrogen-charged valves commercially available today do not have springs), the opening pressure is calculated as  $P_{1pa} = (P_{1pc} - RP_{1pt})/(1 - R)$ . The test-rack calibration pressure is then determined by finding the dome pressure at 60°F from the dome pressure at operating conditions (equal to  $P_{1pc}$ ) and following the steps



that are presented in chapter: Gas Lift Valve Mechanics, for nitrogen-charged, IPO valves. This is the last calculation required for the first valve. The next step is to find the depth of the second unloading valve.

- The unloading pressure gradient line is traced from point  $P_{1pt}$  (called the “transfer pressure”) until it intersects the operating pressure line of the first valve at point “b.” As stated in the previous design method, the transfer production pressure  $P_{1pt}$  is obtained by adding a differential pressure  $\Delta C$  (given by the designer) to the production pressure  $P_{1pd}$ . This constitutes a safety factor that takes into account possible errors in the estimation of the production pressure of the first valve, placing the second valve (or mandrel) at a shallower depth. The depth of the second valve is established by a horizontal line located above intersection point “b” so that the differential pressure between the injection pressure and the tubing pressure is equal to  $\Delta B$ , for the same reasons explained for the first valve.  $\Delta C$  can be a fixed pressure differential or a fixed percentage of the difference between the valve’s operating pressure and the production pressure at valve’s depth. The calculations of the closing, opening, and calibration pressures for the second valve are identical to the ones for the first valve. The surface operating pressure of the second valve is equal to the surface operating pressure of the first valve minus a pressure differential  $\Delta D$  (given by the designer). This surface operating pressure times the gas factor  $f_g$  (calculated for the second valve), is equal to the operating pressure at the depth of the second valve. To maintain the operating injection pressure of the second valve constant as gas flows through it (to uncover the third valve), the determination of the second valve’s seat diameter is made with the operating pressure  $P_{2po}$  as the pressure upstream of the valve and the transfer production pressure,  $P_{2pt}$ , as the pressure downstream of the valve, using the equations given in chapters: Single and Multiphase Flow Through Restrictions and Gas Flow Through Gas Lift Valves. It is necessary to calculate the required gas flow rate through the second valve and its injection temperature before being able to calculate the valve seat diameter. The gas flow rate and its temperature just upstream of the valve are calculated following the steps that are explained in Sections 9.2.3 and 9.2.4, respectively.
- It can be seen in Fig. 9.21 that the surface operating injection pressure of the second valve is greater than the surface closing pressure of the first valve, so it might be difficult to close the first valve. Usually, in designs with this type of problem, the pressure drop that takes place when the second valve is uncovered is sufficiently large to close the first valve. As pointed out in the previous design method, this

pressure drop is caused by temporarily having two simultaneous points of injection when the second valve is uncovered. As also mentioned in the previous method, it is not uncommon that the differences between the closing and opening pressures (called “spread”) of the shallower valves are greater than the spread of the deeper valves. This is due to the fact that the production pressures of the upper valves are very small. This problem is even worst for valves with large seats. The larger the seat (and therefore the area ratio), the larger the spread of the valve becomes. This is one of the reasons why it is necessary that the seats of the unloading valves be as small as possible. The outside diameter of the valve is also important: 1-in outside diameter valves have larger area ratios than the ones for 1.5-in outside diameter valves for a given seat diameter. To avoid this problem (difficulty in closing the first valve in this example), it is necessary to increase the differential pressure drop per valve  $\Delta D$ . But this could make it impossible to reach the desired point of injection. Fig. 9.21 shows that the problem of not being able to close the upper valve is not present in the third valve because the spread of the second valve is not as large as the spread of the first valve. One effective way of dealing with this problem is to install valves with small seats above the reservoir static liquid level. This could make the unloading process take more time to complete but guarantees that the unloading valves will close at the right time.

- Calculations for the third and fourth valves are identical to the ones for the second valve, with the exception that for the fourth valve (considered the operating valve in this example) an additional operating pressure drop equal to  $\Delta E$  (defined by the designer) must be provided. A lower operating injection pressure has the following advantages: (1) positive identification of the operating point, (2) It helps closing the upper valves, (3) it allows the operating valve to be completely open, and (4) it is possible to have a wider injection pressure range, in case the required injection gas flow rate is different from its estimated value or it is desired to perform a multirate test.
- Most designers prefer to install an orifice valve at the injection point instead of a calibrated valve. This introduces some advantages and disadvantages that are explained toward the end of the previous section.
- The designer should provide a minimum pressure differential  $\Delta F$  below which the difference between the valve operating pressure and its production pressure would not be acceptable and mandrel spacing calculations should be stopped. Additionally, mandrel spacing should be stopped for the same reasons that are explained at the end of the previous method.

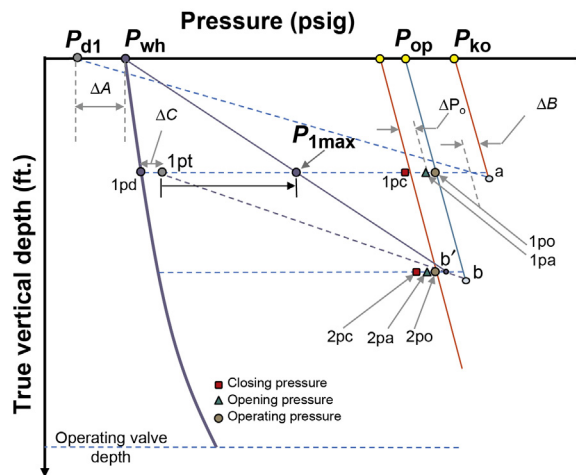
- The reader should also review what is said at the end of the previous method regarding the fact that the calculated seat diameter rarely coincides with one of the commercially available diameters (they might be too large or too small).

It has been recommended to have a value of the sequential pressure drop per valve  $\Delta D$  proportional to the so-called production pressure effect factor,  $P_{\text{Pef}}$ , which is equal to  $R/(1 - R)$ , where  $R$  is the area ratio of the valve. The greater this factor is, the more influence the production pressure has on the valve opening pressure and the greater the spread of the valve becomes, which could cause valve interference if the sequential operating pressure drop per valve is not large enough. Valve interference (explained in chapter: Continuous Gas Lift Troubleshooting) is an instability problem that takes place when two or more valves can be opening and closing at the same time. The minimum value that has been recommended by several authors for  $\Delta D$  is  $100(P_{\text{Pef}}) + F_s$ , where  $F_s$  is an optional safety factor given in Table 9.1. The maximum recommended value of  $\Delta D$  is equal to  $20 \text{ psi} + 200(P_{\text{Pef}})$ . If the available injection pressure is very large,  $\Delta D$  can be as large as possible, as long as the desired point of injection is reached and the injection gas flow rate control valve can operate with a large pressure drop and without causing hydrate formation.

*“Max–Min” Method.* This method is frequently used in wells with insufficient production data or in places where an efficient operating pressure drop per valve is required to reach the desired point of injection. This procedure is also based on sequentially dropping the operating injection pressure, but not by a fixed amount for all valves. Instead, the pressure drop per valve is exactly what is needed to close the valve at the moment the next unloading

**Table 9.1** Recommended Safety Factors

Valve OD (in.)	Valve Seat Diameter (in.)	Safety Factor, $F_s$ (psi)
5/8	1/8	10–15
	5/32	15–20
	3/16	20–25
1	1/8	5–10
	3/16	10–15
	1/4	15–20
	5/16	20–25
1½	3/16	5–10
	1/4	10–15
	5/16	15–20
	3/8	20
	7/16	25



■ FIGURE 9.22 Procedure used to find the operating pressure of the second valve using the “Max–Min” method.

valve below is uncovered. In this type of procedure, the sequential operating pressure drops of the shallower valves are greater than the ones for the deeper valves. This guarantees a smooth unloading operation while, at the same time, being able to reach the desired point of injection because the large pressure drops per valve only take place where they are really needed: at the shallower valves, which are the ones that usually exhibit large spreads (spread is defined as the difference between the opening and closing pressures of the valve at operating conditions). Fig. 9.22 shows the way in which the design is carried out with this type of mandrel spacing procedure. The depths of the first and second valves are determined first.

The depth of the first valve is found in the same way as it was explained for the two previous sections. The operating pressure of the first valve,  $P_{1po}$ , is fixed at the point where the operating pressure line intersects the horizontal line that determines the depth of the first valve.  $P_{1po}$  is taken as the operating pressure of the first valve that guarantees that it will remain totally open until the second valve is uncovered. As explained in the previous section,  $P_{1po}$  is equal to the dome pressure at operating conditions (which is the closing pressure of the first valve) divided by  $(1 - R)$ , where  $R$  is the area ratio of the valve. Thus, the operating pressure here is also the injection pressure that approximately defines the boundary between throttling and orifice flow through the gas lift valve (as was the case for the previous spacing method). An unloading pressure gradient line is then traced from the transfer production pressure of the first valve,  $P_{1pt}$ , until it intersects the operating pressure of the first valve at point “b.” The depth of the second valve is determined

by the horizontal line that is traced above point “b” so that the difference between the injection pressure and the production pressure is equal to  $\Delta B$  at the moment the second valve is uncovered. Then, a line is drawn from point b’ (see Fig. 9.22) to the wellhead production pressure  $P_{wh}$ . This is an approximation of what really takes place when the gas first enters the production tubing through the second valve: the pressure in the tubing at the depth of the first valve temporarily increases from the value it had just before the second valve was uncovered, equal to  $P_{1pt}$ , to the maximum pressure  $P_{1max}$ , which is assumed as the value of the production pressure when gas injection is beginning to take place from the second valve. This increment in the production pressure induces a reduction in the opening pressure of the first valve: a lower injection pressure is needed to open the first valve because of the extra help obtained from the production pressure increase, known here as  $\Delta P_t$ . The force–balance equation at the depth of the first valve establishes the following:

$$(P_{1pa} - \Delta P_o)(1 - R) + (P_{1pt} + \Delta P_t)R = P_{1pc} = P_{dome} \quad (9.5)$$

Where  $\Delta P_t$  is equal to  $(P_{1max} - P_{1pt})$  and  $\Delta P_o$  is the reduction in the first valve opening pressure caused by the increment in the production pressure.  $P_{dome}$  is the dome pressure at operating conditions, which is equal to the valve closing pressure,  $P_{1pc}$ , also at operating conditions. On the other hand, if the dome temperature of the first valve does not change in a significant way (which is a good approximation because the process takes place very fast), the dome pressure should remain approximately constant, and the following equation must be valid:

$$(P_{1pa})(1 - R) + (P_{1pt})R = P_{dome} \quad (9.6)$$

In reality, there is a slight increment in the dome temperature, but assuming a constant temperature introduces a safety factor in the calculation of the operating pressure of the second valve. Subtracting Eq. 9.6 from 9.5, the following expression is obtained for  $\Delta P_o$ :

$$\Delta P_o = [R/(1 - R)]\Delta P_t \quad (9.7)$$

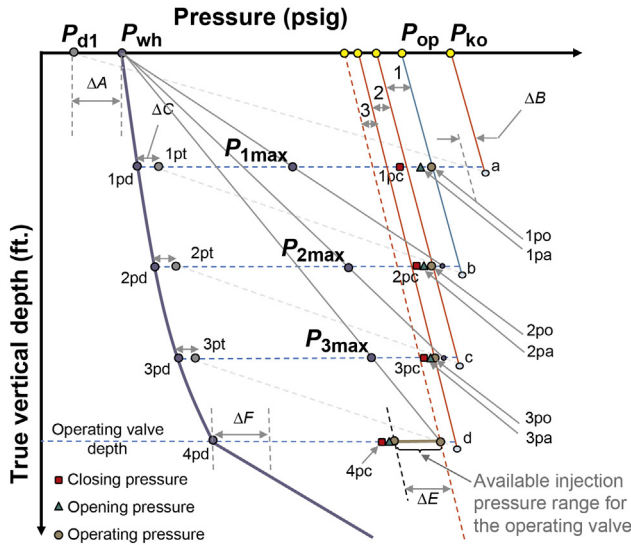
The surface operating pressure of the second valve is then fixed at  $(P_{1pa} - \Delta P_o - F_s)$  referred to the surface.  $P_{2po}$  is the operating pressure at the depth of the second valve that is used to uncover the third valve.  $F_s$  is an optional safety factor used mostly, but not exclusively, in cases where the system pressure is sufficiently high to reach the desired point of injection depth without problems. This safety factor is a precaution measure taken to avoid valve interference, making sure that single points of injection are achieved while unloading the well from each unloading valve.

Instead of using this safety factor, some designers prefer to verify that the surface closing pressure of a given valve is at least a differential pressure (given by the designer) lower than the surface closing pressure of the valve right above, which constitute a better safety factor because it is only applied if really needed. If the valve's surface closing pressure is too high (compared to the closing pressure of the valve above), then the valve's surface closing pressure is fixed at the surface closing pressure of the valve above minus a pressure differential given by the designer and, from this value, the valve's opening pressure is calculated using the force–balance equation. The valve's operating pressure in this case is this valve's closing pressure divided by  $(1 - R)$ .

Before calculating  $\Delta P_o$  for the first valve, it is necessary to know the seat diameter of the first valve so that the value of its area ratio  $R$  can be determined. To find the diameter of the first valve, it is first necessary to find the unloading liquid flow rate for the first valve and its corresponding required injection gas flow rate following the steps presented in Section 9.2.3. It is also necessary to find the operating temperature of the first valve and the injection gas temperature upstream of the valve, which are calculated with the procedures presented in Section 9.2.4.

The seat diameter of first valve is then found from: (1) the required gas flow rate, (2) the operating pressure  $P_{1po}$  as the seat's upstream pressure, and (3) the transfer production pressure  $P_{1pt}$  as the seat's downstream pressure. The calculations required to determine the diameter of the seat are presented in Section 9.2.5 and in chapter: Gas Flow Through Gas Lift Valves. Once the seat diameter is known, the first valve's closing pressure at operating conditions can be found because the operating injection pressure (determined previously) is equal to the boundary injection pressure (between throttling and orifice flow); thus, by definition, the closing pressure at operating conditions is equal to  $[P_{1po}(1 - R)]$  as it was mentioned previously for this method and for the previous one. With the first valve's closing pressure and its transfer production pressure, the first valve's opening pressure  $P_{1pa}$  and its calibration pressure can be found from the equation given in chapter: Gas Lift Valve Mechanics, for IPO valves, which indicates that the opening pressure is found from:  $P_{1pa} = (P_{1pc} - RP_{1pt})/(1 - R)$ .

The parameters for all other valves are calculated in the same way as for the first valve, taking into account the fact that the operating pressure drop must be calculated by Eq. 9.7. The operating valve (or final point of injection) has an additional operating pressure drop  $\Delta E$  which gives the advantages that are described in the previous two methods. Fig. 9.23 shows the spacing procedure for a well that needs three unloading valves to reach the operating point, which is the fourth valve. Mandrel spacing calculations stop for the

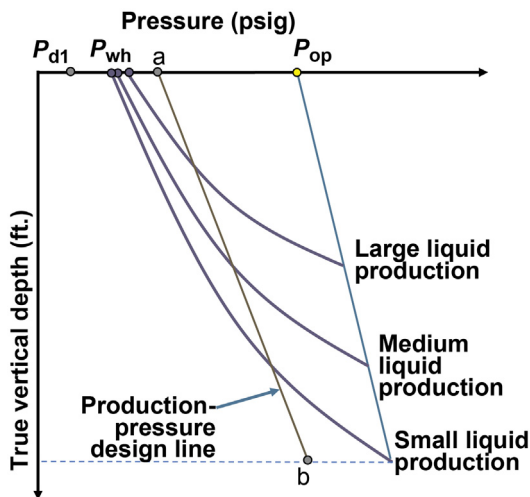


■ FIGURE 9.23 “Max–Min” mandrel spacing procedure.

same reasons that are specified in all previous procedures. Upper mandrel depths might need to be readjusted and additional mandrels might need to be placed below the operating point, all of which is done in the same way explained for the last two methods.

As can be seen in Fig. 9.23, the “Max–Min” method does not guarantee that the surface operating pressure of one valve be lower than the surface closing pressure of the next valve above it. This is the same problem that was presented when spacing the mandrels by dropping the operating pressure by a fixed pressure differential. The second valve in Fig. 9.23 has this problem. In this case, however, it might be easy to solve the problem by introducing a safety factor  $F_s$  (fixed for all valves) explained previously or by making sure that the surface closing pressure of the valve be a certain differential pressure lower than the surface closing pressure of the valve right above it.

*Use of the Max–Min method in cases where the liquid production is uncertain.* The “Max–Min” method can be used in wells for which the liquid production is totally unknown, which is the case of exploratory wells or wells that come from some workover jobs in which the “improved” productivity index value is uncertain. In these cases, instead of using the production pressure traverse curve (determined from the equilibrium curve with the techniques explained in chapter: Total System Analysis Applied to Gas Lift Design, and at the beginning of this chapter), a production–pressure design line, like the one shown in Fig. 9.24 (line a–b), should be used.



■ FIGURE 9.24 Production pressure design line “a–b.”

As can be seen in Fig. 9.24, the production pressure curves can go from very “light” curves, if the liquid production is very small, to very “heavy” curves, if the liquid production is large. For this reason, a design line a–b is taken as the design production pressure and the mandrel spacing procedure is performed as if this line was the production pressure along the entire depth of the well. It is always better to be prepared for large liquid flow rates when the actual liquid production of the well is unknown instead of considering only small liquid flow rates. It is also important to point out that any of the unloading valves could end up being the operating valve; in consequence, all valves should be able to pass the required injection gas flow rate.

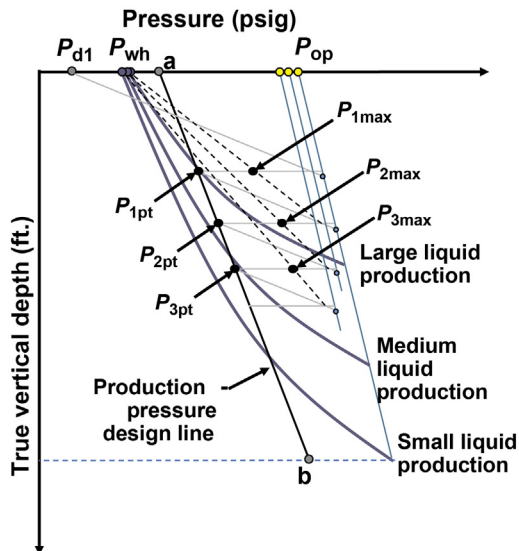
Line a–b is drawn in such a way that, at the upper part of the well, the design production pressure is just greater than the production pressure for a large liquid production and, in the lower part of the well, the design production pressure is closer to the production pressure for a small liquid production. In this way, the mandrel spacing procedure can cover all the length of the well for any value of liquid production that can be encountered as the well is being unloaded. The price that is paid for this flexibility is having more mandrels than it would otherwise be necessary and, additionally, once the well is opened to production, a valve redesign might be needed to optimize the operation of the well at its actual liquid production level. Point “a” in Fig. 9.24 is usually located at the expected maximum wellhead production pressure plus 20% of the difference of the available operating injection pressure for the first valve minus the maximum wellhead production pressure. Point “b” is located at the maximum depth where a mandrel can be installed and at a pressure 150 psi less than the available operating injection



pressure at depth. However, point “a” or “b” can be moved in any horizontal direction following the designer’s own criteria.

The procedure that is described next applies to wells with limited information about their actual liquid production potential. This procedure is also useful for wells with only one production tubing string but with several production zones (with good production information for each zone but with a wide range of production flow rates) separated by packers that can be selectively opened or closed to production by opening or closing circulating sleeves. Two or three possible liquid productions are selected and pressure traverse curves for each of these liquid productions (obtained with the minimum pressure gradient that can be attained with the available injection gas flow rate) are traced along the tubing string as shown in Fig. 9.25. Regarding the temperature distribution to be used in the design, the following recommendations can be used.

- Assume a production surface temperature based on what might be thought of as the most probable liquid flow rate the well can produce. If the liquid flow rate is less than expected, the gas lift valves are going to be at a lower temperature and might remain open causing valve interference (two or more valves opening and closing at the same time). If, on the other hand, the liquid flow rate is larger than anticipated, the valves might close prematurely due to high surrounding temperatures, probably not allowing the unloading process to continue to the desired point of injection.



■ FIGURE 9.25 Mandrel spacing for several possible liquid production rates.

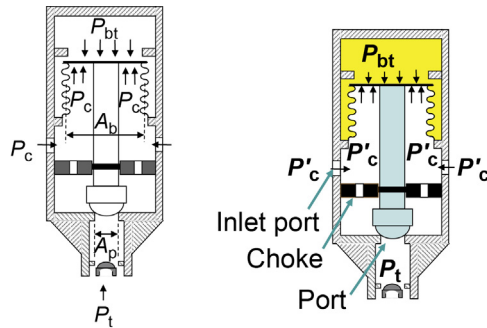
- If the difference between the maximum and minimum liquid flow rates is not very large, calculate the temperature distribution based on an average liquid production.
- If the difference between the possible liquid flow rates is very large, use a temperature distribution higher than the one expected for the average liquid production. For example, if the liquid production is expected to be between 200 and 1000 STB/D, then use the temperature distribution corresponding to a liquid production of 700 or 800 STB/D. In this way, it might be possible to keep the valves from closing prematurely.

Fig. 9.25 illustrates an example for three possible liquid flow rates where the first four mandrels have been located.

Calculations are carried out in the same way as shown in Fig. 9.23, with the following important modifications:

- The transfer production pressures (used to calculate the pressure drop per valve, the orifice diameter, and the valve opening pressure) are located along line “a–b.”
- The injection gas flow rate is calculated from the liquid flow rate of the particular pressure traverse curve that crosses line “a–b” at valve depth. For example, at the depth of the first valve, line a–b is intersected by the large-liquid-production pressure traverse curve. For this liquid-production traverse curve, the total gas/liquid ratio is the one that attains the minimum production pressure gradient, unless the available injection gas flow rate is limited, in which case the total gas flow rate is the maximum value that the gas lift system can provide to decrease the production pressure gradient as low as possible. The seat diameter is calculated to pass this injection gas flow rate. In general, large ports are required for this method because any of the unloading valves could be the operating valve. For the second valve in the figure, the liquid flow rate is half way between the large and the medium liquid production. In this case, the liquid flow rate and its required injection gas/liquid ratio are found by interpolation.

*IPO valves with choke upstream of the seat.* One way of using IPO valves without having to drop the operating injection pressure (in any of the ways described in the previous sections), is by using these valves with chokes installed upstream of their seats. These valves can be used in wells with two production strings or in places where the available injection pressure is either too low or it fluctuates too much (the design procedure, ie, explained here can also be used for IPO valves without upstream chokes, but it has to be used with caution because it might promote valve interference, use more mandrels than are really necessary, and could make troubleshooting



■ FIGURE 9.26 IPO valve with upstream choke.

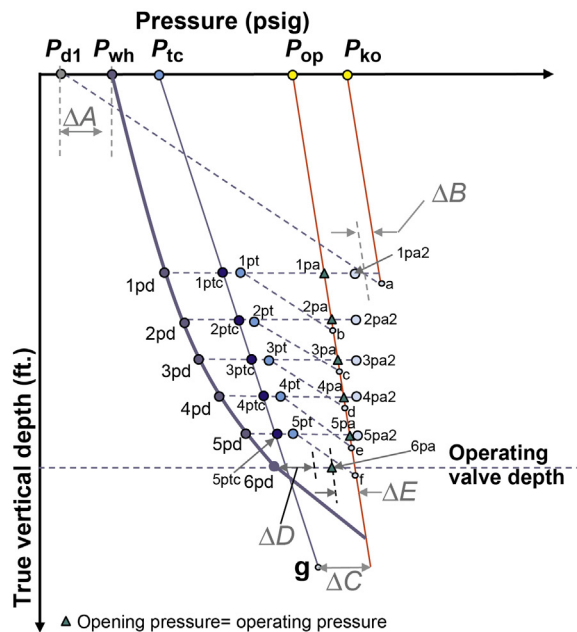
analyses more difficult). Fig. 9.26 shows, in a schematic way, the location of the choke in relation to the inlet ports of the valve and its port (or seat as it is also known). The idea is that the pressure drop will take place at the choke and not at the seat of the valve. In this way, the ball is always subjected to the production pressure. Because the seat for this type of valve is usually large, the valve is highly sensitive to the production pressure. The designer can use this large production pressure sensitivity to calibrate the valve without having to drop the surface operating injection pressure.

With the valve opened or closed, the ball is always exposed to the production pressure and the bellows to the injection pressure. For a given set of production and dome pressures, the injection opening pressure of the valve is equal to its closing pressure. In other words, the following force–balance equation applies to the valve opened (and just about to close) or closed (and just about to open):

$$P'_c(1 - R) + P_t(R) = P_{\text{dome}} \quad (9.8)$$

Where  $P'_c$  is the gas injection pressure,  $P_t$  is the production pressure,  $R$  is the area of the port  $A_p$  divided by the area of the bellows  $A_b$ , and  $P_{\text{dome}}$  is the dome pressure at operating conditions, also called  $P_{bt}$ . Without the choke installed in the valve, once the valve opens, the ball is exposed to a pressure that is greater than the production pressure (due to the effect of the injection pressure) which implies that the injection pressure must be decreased to a value that is lower than the injection opening pressure to be able to close the valve again. With the choke installed upstream of the seat, if the production and dome pressures remain constant, the injection opening and closing pressures are equal.

The design of the unloading valves with chokes upstream of their seats is done by keeping the operating injection pressure constant, see Fig. 9.27. This is possible because the production pressure at a given unloading valve



■ FIGURE 9.27 Mandrel spacing for IPO valves with chokes installed upstream of the seat.

decreases as the well is being unloaded, causing the valve's opening injection pressure to increase above its operating pressure so that the valve closes. It is the reduction of the production pressure (for which the valve is very sensitive due to its large port diameter) and not the reduction of the operating injection pressure that makes the valve close. Keeping the operating injection pressure constant for all unloading valves allows mandrel spacing to proceed to deeper points of injection and, therefore, to increase the liquid production. Because these valves close due to the reduction of the production pressure, they are suitable for wells with two or more production strings or in wells where the available injection pressure is too low or fluctuates too much.

The choke usually consists of many small orifices, whose combined flow area is smaller than the area of the seat of the valve, so that the following desired effect is achieved: to control the gas flow rate by the combined area of the orifices, keeping, at the same time, the opening injection pressure of the valve with a strong dependency on the production pressure. The gas flow rate through the valve is controlled by the combined area of the orifices as long as the valve is sufficiently open so that the flow area of the frustum (area of the cone between the ball and the seat, see Fig. 8.8) is larger than the area of the

choke. Because the seat is usually large in this type of valve, it is not necessary to move the ball away from the seat a great distance in order for the flow area between the ball and the seat to become larger than the area of the choke.

One disadvantage of using this type of valves is that they make it harder to troubleshoot the operation of the well because the operating injection pressures might be very similar for all valves (especially the deeper ones): it is not easy to know which one of them is the actual point of injection.

Fig. 9.27 shows the appropriate way of spacing mandrels when using valves with upstream chokes. As can be seen in the figure, the depth of the first valve is determined in the same way as it was explained for all previous procedures. To locate all other valves, the production pressure design line must be used. This design line goes from surface production pressure  $P_{tc}$  to point “g” at the bottom of the well. There are no general rules to determine the surface design production pressure  $P_{tc}$ . Some designers take  $P_{tc}$  to be equal to  $P_{wh}$  plus 30% of the difference between  $P_{op}$  and  $P_{wh}$ . On the other hand, point “g” is determined from the operating injection pressure at depth minus a differential pressure  $\Delta C$  given by the designer. The production pressure design line should not be too close to the injection pressure line because this will give a large number of mandrels to install in the well. But it cannot be too close to the real production-pressure-traverse curve either because this will make it difficult for the unloading valves to close as the well is unloaded. The objective of the design is to achieve a smooth unloading operation with the minimum number of mandrels possible.

The point where the operating injection pressure line intersects the horizontal line that corresponds to the depth of the first valve determines the opening injection pressure of the valve,  $P_{1pa}$ . The point where the production pressure design line intersects the horizontal line that corresponds to the depth of the first valve, determines the production pressure for which the valve closes,  $P_{1ptc}$ . When the well has been unloaded, the production pressure of the first valve is equal to  $P_{1pd}$  and the valve’s opening pressure is increased to a new value  $P_{1pa2}$ , as shown in the Fig. 9.27. If the surface operating pressure is kept constant, the unloading valves should close as the well is being unloaded because of the reduction in the production pressure at each valve. Once the depth of the first valve is found, the next step is to calculate the liquid flow rate and the required gas injection flow rate for the first valve. This is done following the procedures described in Section 9.2.3. Then, the valve’s temperature and the injection gas temperature upstream of the valve are calculated with the procedures given in Section 9.2.4.

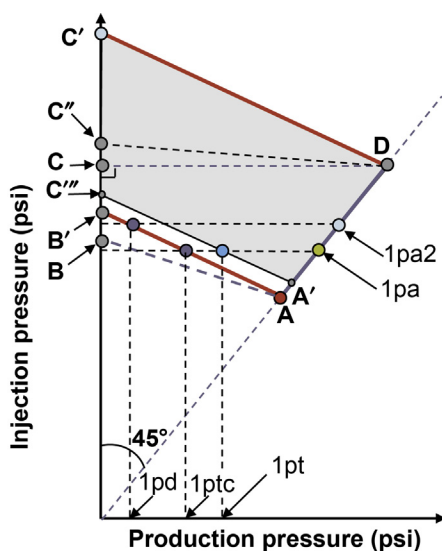
With the injection gas flow rate already determined, the choke area can be calculated using  $P_{1pa}$  as the upstream pressure and  $P_{1pt}$  (defined in the next

paragraphs) as the downstream pressure. With the production pressure  $P_{1ptc}$  and the injection pressure  $P_{1pa}$ , the dome pressure at operating conditions can be found from:

$$P_{1pa} (1 - R) + P_{1ptc} (R) = P_{dome} \quad (9.9)$$

Where  $R$  is the area ratio of the valve equal to the port area (not the choke area) divided by the bellows area. With the dome pressure at operating conditions already known, the test-rack opening pressure is found by dividing the dome pressure at test-rack conditions by  $(1 - R)$ .

The transfer production pressure,  $P_{1pt}$ , is a parameter used as a safety factor to avoid unnecessary gas restriction across the unloading valves while injecting gas to reach the next valve below. If this safety factor is not used, it might not be possible to reach the lower valve because of the reduced injection gas flow rate. In case of the first valve, the gas restriction problem can be solved by increasing the injection pressure without having to worry about opening an upper unloading valve, but that is not the case for the rest of the unloading valves. If an upper valve is opened while trying to pass the required gas flow rate, the unloading process might be inefficient and unstable. If the transfer production pressure is too large, the number of unloading valves could be unnecessarily large. Unfortunately, it is only possible to know exactly the value of  $P_{1pt}$  if the dynamic behavior of this type of valve, shown in Fig. 9.28, is known. The dynamic behavior of gas lift valves



■ FIGURE 9.28 Determination of the transfer production pressure  $P_{1pt}$ .

with chokes upstream of the seat has not been reported in the literature yet. The reader is advised to review Sections 8.2 and 8.4 in chapter: Gas Flow Through Gas Lift Valves, to have a better understanding of the explanations given in the next paragraphs.

Because the ball is always exposed to the production pressure and the bellows is always exposed to the injection pressure, the procedure given in Section 8.2.1 can be used to find the throttling flow region, which is given by the area A–B'–C'–D in Fig. 9.28. Below line A–B', the valve is closed and above line C'–D the valve is fully open. The flow restriction is mainly due to the choke if the flow area between the ball and the seat is larger than the choke area; therefore, it is not necessary to fully open the valve to reach the maximum flow rate. The gray area in Fig. 9.28 represents the area where the valve is sufficiently open for the flow to be determined by the choke flow area. Line A'–C''' corresponds to the line below which the valve restricts the flow due to the ball being too close to the seat. The horizontal line that passes through point  $P_{1pa}$  intersects the line A'–C''' where the production pressure should be equal to  $P_{1pt}$ . While the well is being unloaded through the first valve, the production pressure should not drop to values less than  $P_{1pt}$ , because the injection gas flow rate could be severely restricted. When the production pressure drops to values lower than  $P_{1ptc}$ , the valve closes. The production closing pressure for valves without upstream chokes is determined by line A–B and not by line A–B'. This is due to the dynamic effects that are introduced because the injection pressure affects the pressure that surrounds the ball when an upstream choke is not installed.

For valves with upstream chokes, when the production pressure drops to  $P_{1pd}$ , the new value of the injection opening pressure becomes  $P_{1pa2}$  as shown in Fig. 9.28.

The design of the rest of the valves is done in the same way as explained for the first one, with the exception of the operating valve, for which the actual production pressure should be used in the calculations instead of the design production pressure and, additionally, the operating injection pressure should be reduced by a differential pressure  $\Delta E$ , as shown in Fig. 9.27 for the same reasons explained in the previous methods. Most designers prefer to install an orifice at the operating point of injection, which introduces the advantages and disadvantages given previously for mandrel spacing by sequentially dropping the valve's closing pressure.

The designer must define a minimum pressure differential  $\Delta D$  between the operating pressure and the production pressure for which mandrel spacing should be stopped. The spacing procedure also ends when the minimum distance between two consecutive mandrels is obtained or when the desired

point of injection has been reached. Then, readjustments of all mandrel depths must be made and, if applicable, mandrel depths below the operating injection point should be defined following the steps presented in previous methods. The final operating injection pressure must be calculated because the available upstream choke diameter is usually larger than the calculated diameter. But, on the other hand, the required upstream choke diameter could be larger than the largest one commercially available (use two mandrels or a multi-pocket mandrel in this case). Once the valves are installed, the well should be tested for different injection gas flow rates to optimize its production.

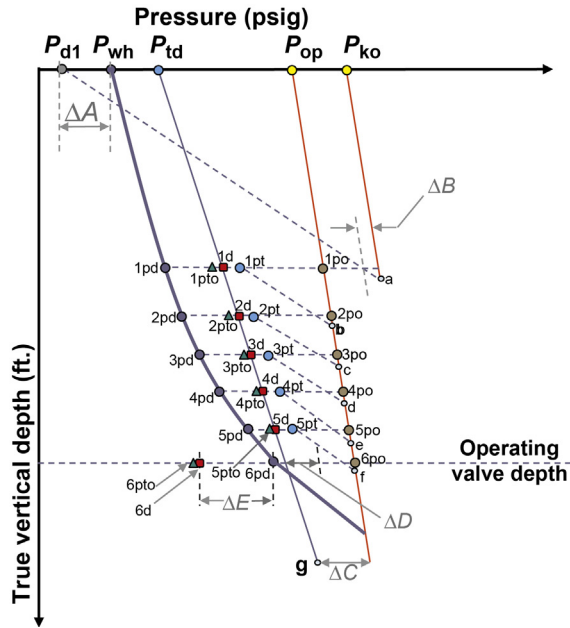
As much as this method could be used to reach deeper points of injection, care should be taken while trying to implement it because the design of the unloading valves could be very difficult and it might not be possible to reach the desired point of injection for not knowing the dynamic behavior of this type of valves. This method is only recommended if: (1) the increase in liquid production is worth the effort and there is no other way of reaching a deeper point of injection, (2) the IPR curve of the well and fluids properties are very well known, and (3) the designer knows the dynamic behavior of gas lift valves with upstream chokes.

### 9.2.2 Mandrel spacing for PPO valves

PPO valves are not widely used because: (1) Their operation tends to be unstable, (2) wells with PPO valves are difficult to troubleshoot, (3) a greater number of unloading valves are required, and (4) they offer more restrictions to the injection gas. However, these valves are used when the available injection pressure is too low or fluctuates too much and, in consequence, the unloading of the well is performed based on the reduction of the production pressure and not on the reduction of the injection pressure. This type of valve is also recommended for: (1) dual wells, (2) in wells where the temperature fluctuations are too large, or (3) where the difference between the temperature at no flow conditions and the one at normal liquid production operation of the well is too large. Fig. 9.29 shows the recommended procedure for mandrel spacing when using PPO valves.

The nomenclature in Fig. 9.29 for a particular  $n$ th valve is as follows: “npd” is the production pressure at the  $n$ th valve’s depth after the well has been unloaded; “nd” is the dome pressure at in situ, unloading conditions; “npto” is the production pressure at which the valve begins to open (if the production pressure is increasing) in an unstable process that ends once the production pressure reaches the dome pressure (known as “nd”); “npt” is the transfer production pressure from which the unloading pressure gradient line is





■ FIGURE 9.29 Mandrel spacing for PPO valves.

traced to locate the valve right below; and “npo” is the operating injection pressure, which is the same for all unloading valves.

For PPO valves, it is necessary to define the production pressure design line that goes from  $P_{td}$  at the surface to point “g” at the bottom of the well. There is no general rule to establish the exact values of these two points. Some designers define  $P_{td}$  as  $P_{wh}$  plus 20 to 30% of the difference between  $P_{op}$  and  $P_{wh}$ . The design production pressure line should not be too close to the operating injection pressure line because this will result in a large number of unloading valves to be used; but it cannot be too close to the production pressure curve (the one that the well will have after the unloading process is completed) either because this will make it difficult for the unloading valves to close as the unloading proceeds. The depth of the first valve is found in the same way explained for previous spacing procedures. The operating injection pressure of the first valve,  $P_{1po}$ , is fixed at the intersection of the operating injection pressure line and the horizontal line that determines the depth of the first valve. In the same manner, the dome pressure,  $P_{1d}$ , and the production pressure,  $P_{1pd}$ , are fixed once the depth of the valve is found. The transfer production pressure  $P_{1pt}$  (explained in the next paragraphs) is established once pressure  $P_{1d}$  has been found.

The second step is to determine the unloading liquid flow rate and its corresponding injection gas flow rate at the first valve. Then, the first valve temperature while the gas is flowing through it and the injection gas temperature upstream of the valve must be determined. These calculations (liquid flow rate, injection gas flow rate, valve's operating temperature, and injection gas temperature upstream of the valve) are explained in the next sections. Once the gas flow rate is known, the seat diameter is determined from: the gas flow rate, pressure  $P_{1po}$  as the pressure upstream of the seat and pressure  $P_{1pt}$  as the pressure downstream of the seat. Once the seat diameter is determined, the area ratio of the valve,  $R$ , is established from the smallest commercially available valve seat that is greater than or equal to the calculated diameter.

The production opening pressure,  $P_{1pto}$ , is found from the force–balance equation for PPO valves, given by:

$$P_{1pto} (1 - R) + P_{1po} (R) = P_{1d} \quad (9.10)$$

Where  $R$  is the valve's area ratio,  $P_{1po}$  is the gas injection pressure at valve's depth,  $P_{1pto}$  is the production opening pressure at the depth of the first valve, and  $P_{1d}$  is the dome pressure of the first valve at operating conditions. If the valve is spring-loaded,  $P_{1d}$  is the valve closing pressure at any temperature, which is equal to the valve's test-rack closing pressure,  $P_{trc}$ , if the valve's calibration is defined by its closing pressure. Because pressures  $P_{1po}$  and  $P_{1d}$  are fixed once the depth of the first valve is found, Eq. 9.10 is used only to find the value of  $P_{1pto}$ . Once the well is unloaded, production pressure  $P_{1pd}$  cannot be greater than or equal to  $P_{1pto}$  because the valve would not close. The reader is advised to review the equations given in chapter: Gas Lift Valve Mechanics, regarding the calibration of PPO valves.

The transfer production pressure of the first valve,  $P_{1pt}$ , is defined as the dome pressure  $P_{1d}$  plus a pressure increment defined by the designer. This increment is usually a percentage, constant for all valves, of the difference between the gas injection pressure at valve's depth and the dome pressure. While unloading the well to reach valve " $n + 1$ ," the production pressure at valve  $n$  should not fall below the dome pressure  $P_{nd}$  because the valve will begin to close. In fact, the production pressure should be high enough to avoid throttling the gas flow through the valve. These points explain why it is so important to accurately define the transfer production pressure (its definition is far more relevant for PPO valves than for IPO valves).

The designs of all other valves are done in the same way that is explained previously for the first valve, with the exception of the operating valve where the production pressure design line should not be used and, additionally, the dome pressure should be equal to the production pressure minus a

differential pressure  $\Delta E$  as shown in Fig. 9.29 (this is done to guarantee that the operating valve is fully open). Most designers prefer to have an orifice valve at the point of injection. It is very important to use an orifice valve at the point of injection for this type of design because it guarantees that the point of injection is always open to pass gas. If a calibrated valve is used at the desired operating point of injection, it might not be possible to open it if the production pressure is too low unless the production tubing is somehow pressurized.

The combination of unloading PPO valves and an orifice at the operating point, provides the most flexible design to pass from very low to very high gas flow rates because: (1) the gas injection flow rate can be increased to very large values (therefore increasing the injection pressure) without the risk of opening upper valves, which are mostly sensitive to the production pressure and would not open even at very high gas injection pressures, and (2) the gas flow rate can be lowered without closing the operating valve. Some designers install IPO valves at the point of injection with the following advantages: (1) the valve is able to open even at low production pressure, (2) the troubleshooting process is made a little easier, and (3) in some occasions IPO valves could contribute to stabilize the well if necessary.

The designer must define a minimum pressure differential  $\Delta D$  (see Fig. 9.29) between the operating pressure and the production pressure, for which mandrel spacing should be stopped. The spacing procedure also ends when the minimum distance between two consecutive mandrels is obtained or when the desired point of injection has been reached. Then, if applicable, readjustments of all mandrel depths must be made and mandrel depths below the operating injection point should be defined, if necessary, following the steps presented in previous spacing methods.

The great majority of PPO valves are spring-loaded because:

1. Spring-loaded valves are not sensitive to temperature;
2. They resist better the chattering of the valve that takes place in the unloading process with PPO valves; and
3. The difference between the production pressures from the time the valve is uncovered until the end of the unloading process, is large: This is adequate for spring-loaded valves, because they have large load rates and require a great pressure increase to fully open the valve (bellows' or spring's load rates are defined in chapter: Gas Flow Through Gas Lift Valves).

Many manufacturing companies of spring-loaded PPO valves offer their own design procedures, which are based on the specific behavior of each valve model. The McMurry company, for example, used to offer guiding

tables for the design of wells with spring-loaded PPO valves, models S-FO and JR-FO. These tables indicate the production pressure increment (above the closing pressure) that is needed to achieve a certain gas flow rate. It is important for the designer to be aware of the gas flow rate capabilities of this type of valve by direct communication with valve manufacturing companies. This would allow accurate determination of the transfer production pressure and the valve's closing pressure.

The reader should review what is said at the end of the section that describes the mandrel spacing procedure by sequentially dropping the valve's closing pressure of IPO valves regarding the fact that the calculated seat diameter rarely coincides with one of the commercially available diameters (they might be too large or too small).

As it has been pointed out in the spacing procedures given previously, once the valves are installed in the well it is recommended to test the well at different injection gas flow rates to determine the actual liquid flow rate the well can produce and its corresponding injection gas flow rate. It is also important to verify by troubleshooting analyses if the current point of injection is the one stipulated by design. Because troubleshooting is difficult to perform for PPO valves, it might be a good idea to run pressure and temperature surveys in a reduced number of wells to verify that the design procedure being used is adequate for each operational condition. The point of injection is easily identified by the cooling effect caused by the gas injection at the depth of the operating point of injection. Pressure and temperature surveys are not necessary for all wells, but only for those wells that represent average operational conditions of a particular group of wells. Wireline operations are costly and some operational risks are involved in this type of operation.

### 9.2.3 Unloading liquid flow rate and required injection gas flow rate at each unloading valve

It is important to calculate the liquid flow rate that can be attained during each stage of the unloading process because it determines the unloading valve temperature and the required injection gas flow rate through each unloading valve. The total liquid flow rate that the well produces while being unloaded is the sum of the liquid flow rate coming from the formation,  $Q_{Lf}$ , plus the completion liquid flow rate that is entering the tubing as it is displaced by the gas from the annulus,  $Q_{Lc}$ , (if the well produces up the tubing) or the liquid coming from the tubing (if the well produces up the annulus). Usually, the flow rate of the completion fluids being displaced is assumed to

be equal to 100 or 200 STB/D, but its real value depends on the actual gas flow rate that is injected into the well.

Before uncovering the first valve, all the gas that is injected into the well is used to displace the completion fluids and, therefore, it is easy to determine the liquid flow rate if the flowing bottomhole pressure is above the static reservoir pressure because the liquid flow rate is equal to the volume of liquid displaced by the injection gas in a given time interval.

Once the first valve is uncovered, a portion of the injected gas goes to displace the completion fluids while the rest is injected into the tubing to reduce the production pressure (if the well produces up the tubing) or into the annulus to reduce the production pressure in the annulus (if the well is being produced up the annulus). If the unloading operation is carried out very slowly, it is a good assumption to consider that all the gas is injected to reduce the production pressure while, at the same time, estimating the liquid production to be 100–200 STB/D larger than what the reservoir can provide for a given bottomhole pressure. This last assumption increases the required gas injection flow rate above what is needed if all the fluid would come from the reservoir only. The reservoir begins to produce fluids as soon as the flowing bottomhole pressure is less than the static reservoir pressure.

The liquid flow rate that the well produces determines the temperature of the unloading valves and the required gas flow rate through each of these valves. Some designers calculate the seat diameters of all unloading valves as if they have to pass the final injection gas flow rate after the well has been unloaded. This practice gives large seat diameters for the unloading valves because the final gas flow rate is larger than the unloading gas flow rate at each valve. Large diameter seats increase the risk of valve interference (the upper valve will open and close repeatedly while injecting gas through the one right below) because they exhibit large spreads (difference between the opening and closing pressures). This is more pronounced for the upper valves. It is necessary then to calculate the seat diameters in a more precise way by finding a more appropriate gas flow rate for each unloading valve.

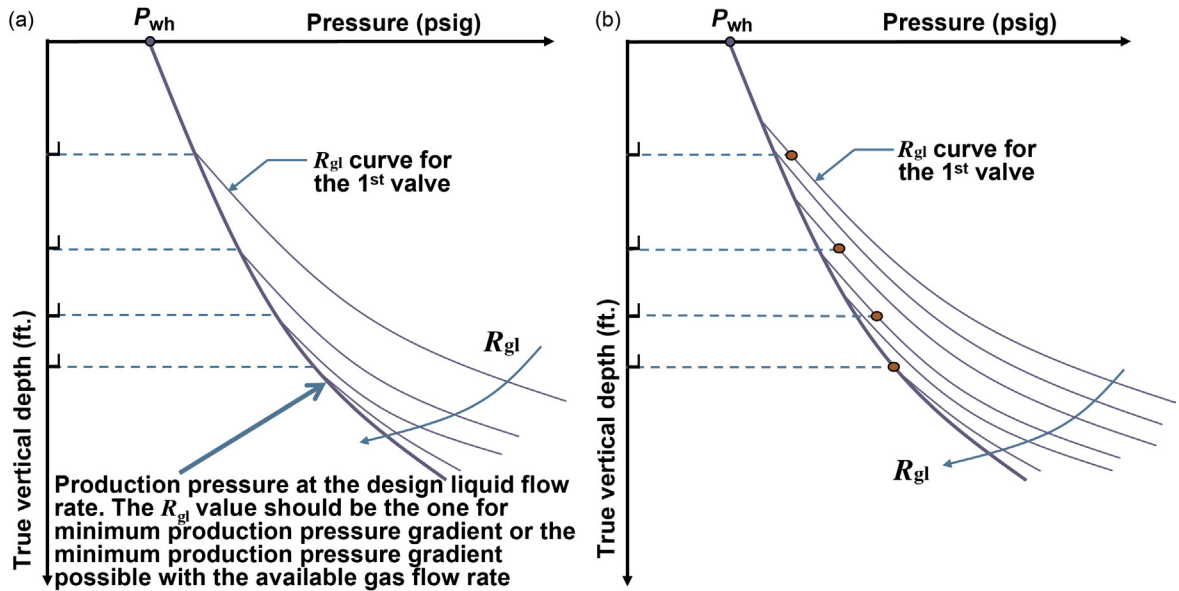
It is good practice to install seats with small diameters (available for the selected valve model) for the unloading valves above the reservoir's static liquid level. In this way the unloading process takes more time but the risk of valve interference is reduced and it might even allow reaching a deeper point of injection (because the sequential pressure drop per valve is reduced in case of IPO valves). This practice also minimizes the risk of cooling an unloading, nitrogen-charged, gas lift valve to a temperature at which the valve would not close. The temperature drop surrounding a valve might be

caused by a higher than needed injection gas flow rate (caused in turn by installing a large diameter seat) coupled with a low liquid feed in.

The calculation of the gas and liquid flow rates for each unloading valve depends on how accurate the IPR curve is known; but, independently of this fact, the production-pressure-traverse curve to be used during mandrel spacing calculations corresponds to the liquid flow rate the well will have once it is unloaded and gas is injected through the desired point of injection. This point of injection depth and the final liquid and injection gas flow rates must then be known, or at least assumed, prior to beginning any mandrel spacing procedure.

*IPR Curve is Unknown.* When the IPR curve is not known, the designer usually relies on a rough estimation of the liquid production the well might have after it has been unloaded. This liquid flow rate is estimated from nearby wells producing from the same reservoir or from the production history of the own well, if available. Additionally, if the IPR curve is unknown, the gas flow rate at each unloading valve can be approximated by assuming that the liquid flow rate for each valve is the same as the final design liquid flow rate (after the well has been unloaded), but with the required gas/liquid ratio to achieve the “transfer production pressure” at each unloading valve’s depth. This transfer production pressure can be equal to the expected final production pressure at valve’s depth or a little higher, depending on how confident the designer is regarding the accuracy of the calculated production pressure. This is appreciated in Fig. 9.30a for the case in which the transfer production pressure is equal to the production pressure the well will have after it has been unloaded and in Fig. 9.30b in which, with the exception of the operating valve (deeper valve), the transfer production pressure is, by design, greater than the expected production pressure, for which the required gas/liquid ratio is smaller. All the pressure gradient curves shown in Fig. 9.30 correspond to the same liquid flow rate but for different gas/liquid ratios ( $R_{gl}$ ). For Fig. 9.30a, each gas/liquid ratio corresponds to the one needed to achieve the minimum pressure gradient curve at a particular valve’s depth (or the minimum possible production pressure gradient if the maximum available gas flow rate has been reached). For Fig. 9.30b, each gas/liquid ratio corresponds to the one required to reach the transfer production pressure at a given depth (and final liquid flow rate) but the final production-pressure-traverse curve (on which the spacing procedure is based) is still the minimum pressure gradient curve.

This way of approximating the gas flow rate tends to give large seats but not as large as when it is assumed that the valve should be able to pass the design injection gas flow rate the well will have during normal operation (after it has been unloaded), because the gas/liquid ratios are lower at shallower



depths (as seen in the Fig. 9.30). The injection gas flow rate at a particular unloading valve  $n$  is approximated with the following equation:

$$Q_{gin} = Q_L (R_{gln})/1000 \quad (9.11)$$

Where  $Q_{gin}$  is the gas flow rate through the  $n$ th valve in Mscf/D,  $Q_L$  is the design liquid flow rate in STB/D, and  $R_{gln}$  is the total gas/liquid ratio at the depth of the  $n$ th valve in scf/STB required for the production pressure to be equal to the transfer production pressure. The liquid flow rate is established from nearby wells from the same reservoir or, if it is an exploratory well and no data is available from the reservoir, several flow rates are assumed, as explained in Fig. 9.25. In Fig. 9.30, the total gas/liquid ratio needed to reach the final operation production pressure (lowest pressure gradient curve in the figure) must be the gas/liquid ratio that corresponds to the minimum pressure gradient for the expected liquid flow rate, unless the maximum available gas flow rate has been reached, in which case the gas/liquid ratio will be the highest possible with the available maximum injection gas flow rate the gas lift system can provide. The pressure traverse curves in Fig. 9.30 are calculated with the type of fluids the well can produce.

Because it is not known how the reservoir is going to provide gas and liquids during the unloading and final operation of the well, the formation gas flow rate was not considered in Eq. 9.11. This also serves as a safety factor,

■ FIGURE 9.30 Total gas/liquid ratio at each unloading valve (keeping the liquid flow rate constant). (a) Transfer production pressure equal to the expected production pressure. (b) Transfer production pressure greater than the expected production pressure.

because assuming that the formation gas flow rate is equal to zero is the best that can be done. On one hand, this gives larger valve seats (because the injection gas flow rate is larger than the value that might be needed), which could increase the possibility of valve interference; but, on the other hand, it guarantees a high injection gas flow rate in case it is needed to reach the next lower valve. Installing a very small seat could seriously limit the possibility of lowering the production pressure to uncover the next valve. Having a seat larger than necessary might cause a decrease in the injection pressure, making it difficult to reach the lower valve but, in this case, the problem can be solved by temporarily increasing the gas flow rate during the unloading of the well. It is unlikely that the reservoir can provide any formation gas during the initial stages of the unloading process and, additionally, the completion-fluid pressure gradient is usually greater than the reservoir fluid pressure gradient. These facts increase the required injection gas flow rate during the unloading operation. Then, assuming that the well is going to produce reservoir fluids only (with zero formation gas/liquid ratio) at the design liquid flow rate (throughout the unloading process), is an acceptable recommendation when nothing, or very little, is known about the well's IPR curve.

If the formation gas/liquid ratio is approximately known, the gas flow rate through the desired point of injection (operating valve) is calculated with the following equation:

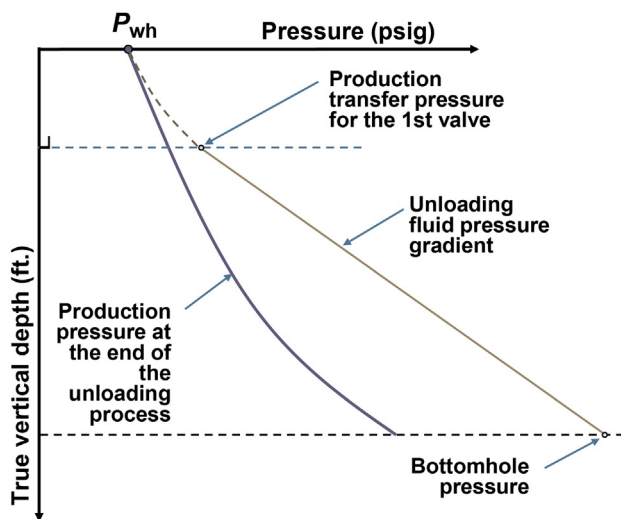
$$Q_{\text{gifinal}} = Q_L (R_{\text{glt}} - R_{\text{glf}})/1000 \quad (9.12)$$

Where  $Q_{\text{gifinal}}$  is the injection gas flow rate through the operating valve in Mscf/D,  $Q_L$  is the design liquid flow rate in STB/D the well will provided once the unloading process has ended,  $R_{\text{glt}}$  is the total gas/liquid ratio in scf/STB and  $R_{\text{glf}}$  is the formation gas/liquid ratio, also in scf/STB.

Note that, even though the unloading liquid flow rate is equal to the final liquid flow rate (which is larger than the one that might be present during the unloading operation), the unloading fluids are assumed to be 100% the ones provided by the reservoir while completion fluids (which are heavier) are not considered in the calculations. Thus, one assumption tends to cancel the other out and, in reality, not much more can be done when the IPR curve is unknown. However, the unloading-pressure-gradient lines that are used to locate the next valve in the spacing procedure (from the transfer production pressure) should be based on a pressure gradient greater than or equal to the current completion-fluid pressure gradient.

*IPR curve is known.* Several procedures for calculating the unloading liquid flow rate at each valve and their corresponding gas flow rates are





■ FIGURE 9.31 Bottomhole flowing pressure when the production pressure at the first valve is equal to the transfer production pressure stipulated for that valve.

presented next for cases in which the IPR curve and the pressure-volume-temperature (PVT) data of the reservoir fluids are known. Fig. 9.31 shows what happens when the production pressure at the first valve just reaches (in the unloading process) the production transfer pressure for that valve while the bottomhole flowing pressure is still larger than the reservoir pressure. A straight line with the completion-fluid pressure gradient is traced from the production transfer pressure to the bottom of the well to get the bottomhole flowing pressure. If this bottomhole flowing pressure is greater than the static reservoir pressure, then no fluids are being produced from the reservoir and the liquid flow rate is equal to the flow rate of the fluids being displaced from the casing-tubing annulus into the production tubing, which is usually estimated to be equal to 100 or 200 STB/D, as stated previously. In this case, the injection gas flow rate is determined by finding the production-pressure-traverse curve with the gas/liquid ratio that connects the wellhead pressure,  $P_{wh}$ , to the production transfer pressure for the unloading liquid flow rate, using the completion fluids as the type of fluids being produced. The injection gas flow rate is found from Eq. 9.11, for which in this case the liquid flow rate is the unloading liquid flow rate of the completion fluids (taken as 100 or 200 STB/D).

If the bottomhole flowing pressure in Fig. 9.31 is less than the static reservoir pressure, there are different calculation procedures available (depending on the preference of the designer) to approximately find the required

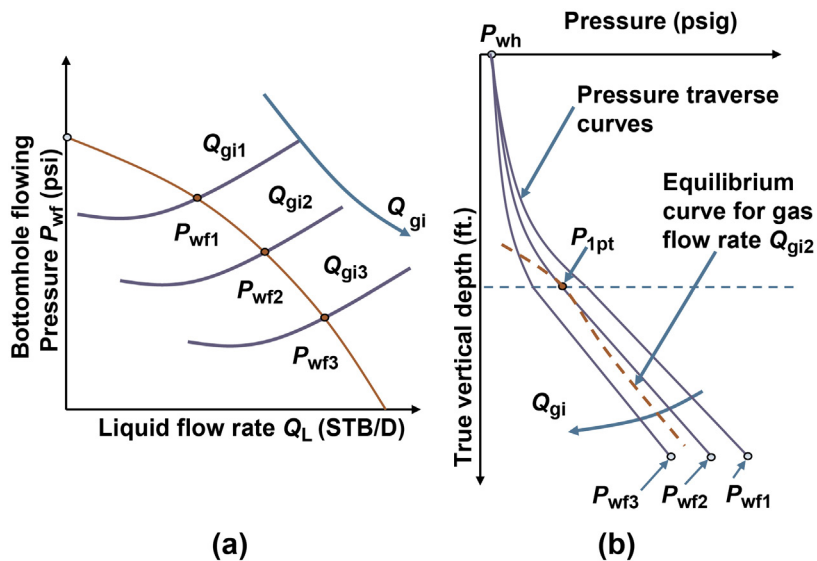
injection gas flow rate and the unloading liquid flow rate at each unloading valve. One approximation used by some designer is as follows:

- The flowing bottomhole pressure is found for each unloading valve by tracing the unloading liquid pressure gradient line (which is the “heavy” straight line used in mandrel spacing) from the production transfer pressure at each valve to the depth of the formation. With this bottomhole pressure, the liquid flow rate that the reservoir can provide is found from the IPR curve.
- At the depth of each unloading valve, the gas/liquid ratio for minimum production pressure gradient,  $R_{g\text{lmingrad}}$ , is found. The liquid flow rate,  $Q_L$ , in this case is the sum of the liquid flow rate from the reservoir (found in the previous step) plus the flow rate of the completion fluids being displaced from the annulus, taken as 100 or 200 STB/D. The specific gravity of the liquid used in this case is a volumetric average value calculated from the reservoir’s and the completion fluids’ specific gravities.
- The injection gas flow rate for each unloading valve,  $Q_{g\text{in}}$ , is found from the following equation:  $Q_{g\text{in}} = (R_{g\text{lmingrad}})Q_L/1000$ . Where  $Q_{g\text{in}}$  is expressed in Mscf/D,  $R_{g\text{lmingrad}}$  in scf/STB, and  $Q_L$  in STB/D. The gas coming from the formation is not taken into account for the unloading valves.
- For the operating valve, the injection gas flow rate is found from  $Q_{g\text{i}} = Q_L (R_{g\text{lt}} - R_{g\text{lf}})/1000$ , where the formation gas is considered ( $R_{g\text{lt}}$  and  $R_{g\text{lf}}$  are defined in Eq. 9.12). The liquid flow rate is the design liquid flow rate (all of it coming from the formation). The total gas/liquid ratio is the one (if possible) that gives the minimum production pressure gradient or the minimum pressure gradient that can be obtained from the available gas flow rate.

The procedure just described previously tends to give higher bottomhole pressures. This is due to the fact that the unloading (heavy) pressure gradient is used to find the bottomhole pressure. But in reality, as soon as the flowing bottomhole pressure gets smaller than the reservoir pressure, the liquid pressure gradient begins to change in a way that is very difficult to estimate. For this reason, some designers modify the procedure by replacing the unloading pressure gradient line (the straight line from the transfer production pressure to the formation) with the actual reservoir fluid pressure gradient (lighter), but not taking into account the formation gas (as a safety factor). Other designers do take into account the formation gas but for formation liquid rates greater than or equal to 20% of the design liquid flow rate (the one the well will have at the end of the unloading process).

At the other extreme of the “practical” ways of calculating the liquid flow rate explained so far, there are rigorous computer programs that calculate the unloading liquid flow rates following a complete nodal analysis at each unloading valve. The procedure that is described next tends to give larger unloading liquid flow rates as compared to the previous procedures. Even though this next procedure appears to be very rigorous, it is still a rough approximation of the complex process that takes place during the unloading of a gas lift well. The calculation procedure is based on the use of “constant-injection-gas-flow-rate equilibrium curves.” The reader is advised to review Section 5.1.3 in chapter: Total System Analysis Applied to Gas Lift Design, to have a better understanding of the following explanations.

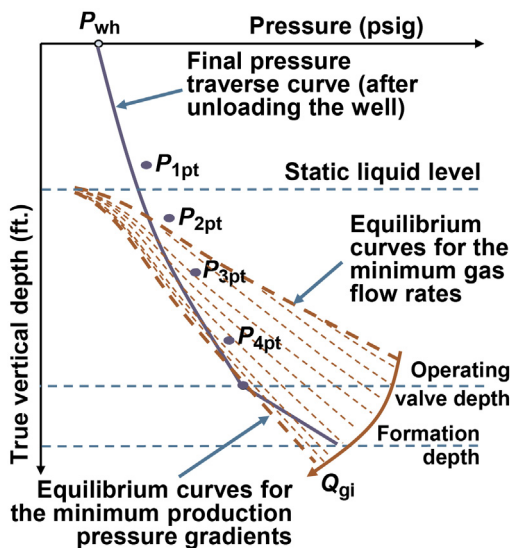
The mandrel spacing procedure is based on the production-pressure-traverse curve, which is obtained from the initial calculations that are carried out to find the operating point of injection depth, as described at the beginning of this chapter. Then, the depth of each unloading valve and its transfer production pressure are found from the particular spacing procedure being used. Once the depth of the unloading valve is determined, a series of nodal analysis can be performed for different gas flow rates (but keeping the injection point depth equal to the depth of the unloading valve being designed) as shown in Fig. 9.32a. The objective is to find the gas



■ FIGURE 9.32 Determination of the liquid flow rate and the injection gas flow rate for the first unloading valve using nodal analysis. (a) Inflow-outflow diagram and (b) pressure-depth diagram.

flow rate that gives a production-pressure-traverse curve that passes through the transfer production pressure  $P_{1pt}$  at the depth of the valve (which happens to be equal to  $Q_{gi2}$  in Fig. 9.32b). This procedure simultaneously gives the required injection gas flow rate and the unloading liquid production. If the reservoir is capable of producing liquids with the gas injection taking place through the unloading valve and with the production pressure equal to the transfer production pressure, the equilibrium curve for the unloading injection gas flow rate should intersect the pressure traverse curve at the depth of the valve at a pressure equal to the transfer production pressure.

The transfer production pressures for the unloading valves ( $P_{1pt}$ ,  $P_{2pt}$ , ...) are shown in Fig. 9.33 together with equilibrium curves for different injection gas flow rates. These equilibrium curves go from the minimum gas flow rate equilibrium curve at which the well can produce liquids in a stable manner (the uppermost curve) to the maximum gas flow rate equilibrium curve that gives the minimum production pressure gradient traverse curve at the operating point of injection. As it can be seen in the figure, the first valve is above the static liquid level and even though the second valve is below the static liquid level, the transfer production pressure is too large for the reservoir to produce any liquids. In these two cases, commercially available computer programs do not calculate the liquid production and simply place the valve with the minimum seat diameter (the minimum seat diameter value is chosen by the designer).



■ FIGURE 9.33 Equilibrium curves for different injection gas flow rates,  $Q_{gi}$ .

In the method just described, the equilibrium curves are determined by standard routines, where the dynamic nature of the unloading process is not taken into account. This method should give good results if the unloading process is done very slowly because, in this way, important transient aspects of the unloading process are minimized.

*Dynamic well models.* The most rigorous procedure that can be used to calculate the liquid flow rates and their corresponding gas injection flow rates for each unloading valve is to use dynamic models. But this approach is not practical at this time to be used in design calculations because dynamic well models are not fully developed yet for that purpose. There have been several dynamic models developed at The University of Tulsa, such as the ones by Pothapragada (1996) and Tang (1998), which describe the dynamic behavior of the well in an approximate way, but they cannot be considered as practical or truly valid tools to be used to design unloading valves because they need further development; however, there are commercially available dynamic simulators that can be used to simulate the unloading and normal operation of gas lift wells and they are becoming important troubleshooting tools. Undoubtedly, as progress is made on models for transient multiphase flow and transient behavior of the formation near the wellbore, these dynamic models will replace the design procedures we use today. The new dynamic models that will be developed in the future will give much more accurate results, not only for the unloading liquid flow rate calculations, but also for analyzing and avoiding unstable production conditions.

Dynamic models are used today to simulate the unloading operation of complex wells to avoid extremely high liquid flow rates through the unloading valves. For example, in wells that can produce on natural flow but need gas lift to boost their production, liquid flow through the unloading gas lift valves begins as soon as the well is opened to production, even before starting gas injection. The American Petroleum Institute (API) recommendations for unloading gas lift wells are not applicable for this type of wells and the best that can be done is to dynamically simulate the entire unloading process with the help of commercially available dynamic simulators to develop the right procedure to unload and operate these wells.

#### 9.2.4 Injection gas temperature at depth and valve operating temperature calculation

The temperature distribution along the well, during the unloading process, and in normal operation, plays an important role in the design and troubleshooting analyses of gas lift wells. To calculate the injection gas pressure at depth, its temperature along the entire length of the well must be known.

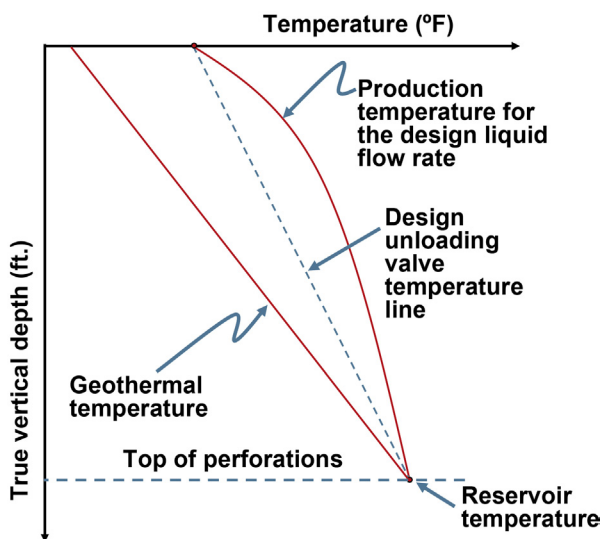
The injection gas temperature at valve's depth should also be known to find the gas flow rate through each valve (it is a parameter used in all gas flow rate equations). On the other hand, temperature also plays a major role in determining nitrogen-charged gas lift valve's closing pressures. The injection gas temperature at depth and the production fluid temperature must be known to calculate the nitrogen pressure inside the dome of the valve.

During production pressure traverse calculations, fluid properties are calculated (using the average pressure and temperature at each tubing length interval) and then these properties are used to find the pressure gradient in the iteration process, see Section 3.2.2 in chapter: Multiphase Flow. It is important to point out that relatively large errors can be made in the estimation of the production fluid temperature without affecting very much the production pressure traverse calculation. The production-fluid temperature prediction along the well is also useful in finding out if favorable conditions are present for paraffin, asphaltene, or hydrate formation at some point along the production tubing string. Sometimes the injection gas lowers the temperature of the fluids in the upper sections of the production tubing causing paraffin depositions. This problem is solved in some fields by heating the injection gas to melt the depositions; however, this solution is costly and involves some operational risks. Bypassing the compressor's after-cooler can be a good solution for small gas lift systems.

The prediction of the injection gas and valve temperatures during the unloading of the well is an extremely complex operation. For this reason, approximate calculation procedures that have shown good results are used. However, it is possible that for difficult wells (with high liquid flow rates, or high water cuts, or extreme formation temperatures like the ones found in places such as Alaska) these procedures might not work. In those difficult cases, the best way to estimate the valve and injection gas temperatures is by field trial-and-error procedures. An example of a solution found by trial and error is presented at the end of this section.

The geothermal and production fluid temperatures determine the injection gas and valve temperatures. The geothermal temperature is usually considered to be a linear function of the true vertical depth as shown in Fig. 9.34. The value of the geothermal temperature gradient is usually close to  $0.015^{\circ}\text{F}/\text{ft}$ . When there is a shallow gas reservoir, the geothermal temperature tends to be a little cooler above this shallow formation and a little hotter below it because it acts as an isolation barrier.

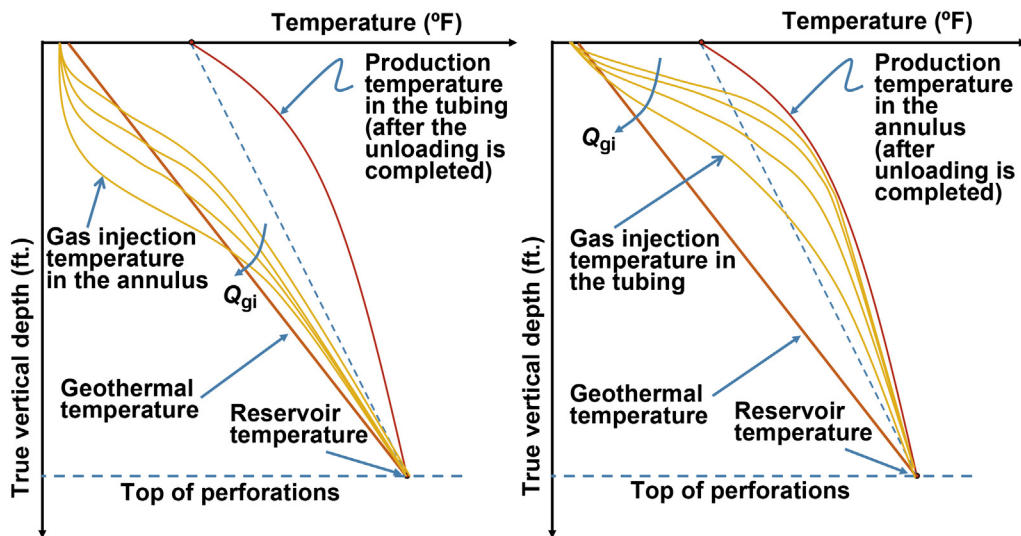
The calculation of the production fluid temperature profile is much more complex than the calculation of the geothermal temperature. The production fluid temperature is higher for wells with high water cuts, high production



■ FIGURE 9.34 Geothermal and production temperature profiles for a well producing at the design liquid flow rate.

rates (or high liquid velocity found in small diameter tubing even at moderate flow rates). The reader is advised to review the equations given in Section 3.2.2 in chapter: Multiphase Flow, to calculate the temperature of the production fluids. Fig. 9.34 shows the temperature of the production fluids along the well when the well is operating at the design liquid flow rate. This temperature profile usually presents a local temperature drop at the depth of the operating valve which is detected by a temperature survey in the great majority of cases (if the liquid holdup is large, the injection point is not easily detected and it becomes necessary to use high precision temperature sensors like the ones used in continuous temperature surveys, see Section 11.5.2 in chapter: Continuous Gas Lift Troubleshooting). The best way to know the behavior of the production temperature is to measure it for different liquid flow rates. There is a technique that can be used to simultaneously measure the production temperature along the entire length of the production tubing, which consists of an optical fiber extended from the wellhead to the bottom of the well. This is highly recommended for detecting problems in wells with unstable production or when temperature plays a major role when trying to unload a high water cut well or with extreme formation temperatures. This technique is discussed in detail in chapter: Continuous Gas Lift Troubleshooting, Section 11.5.7.

The injection gas temperature depends on its flow rate, the production fluids temperature profile, and if the gas is injected down the tubing or down the



■ FIGURE 9.35 Injection gas temperature profile (for different injection gas flow rates  $Q_{gi}$ ) when the well is producing at its design liquid flow rate. (a) Gas injected down the annulus; (b) gas injected down the tubing.

tubing-casing annulus. Fig. 9.35 shows the injection gas temperature profile (for different injection gas flow rates  $Q_{gi}$ ) when the well is producing at its design liquid flow rate.

As can be seen in Fig. 9.35a, when gas is injected down the casing-tubing annulus, the “average” injection gas temperature is very close to the geothermal temperature. This is due to the fact that the injection gas enters the annulus with a temperature equal to the gas surface temperature and it takes some time for the gas to reach a temperature that is usually between the geothermal temperature and the production fluids’ temperature. In most cases, the influence of the geothermal temperature is greater than the one exerted by the production fluid temperature. Thus, the average injection gas temperature can be assumed equal to the geothermal temperature when calculating the injection gas pressure at depth. The geothermal temperature can also be used in the calculation of the gas flow rate through the operating valve (usually the deepest gas lift valve in the well) because at that depth the geothermal and the fluid production temperatures are similar.

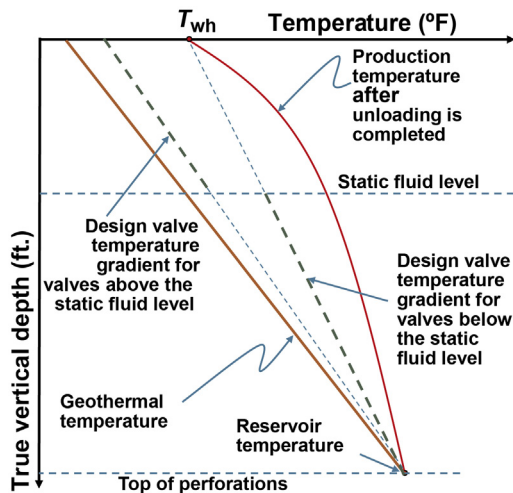
When gas is injected down the production tubing, the injection gas temperature for the well at design operating conditions is, on average, closer to the linear temperature that is obtained when the production surface



temperature is connected to the reservoir temperature by the dashed, straight line that can be seen in Fig. 9.35b (this line is often used to find the “design” unloading valve temperature). In most wells, the injection gas temperature along the production tubing string is very close to the fluid temperature in the casing-tubing annulus. This makes the injection pressure at depth be lower than the value it would have at cooler temperatures. Another factor that helps reduce the injection pressure at depth is the friction pressure loss, which should (in some cases) be considered when gas is injected down the production tubing at very large flow rates. For the injection gas flow rate calculation at the final point of injection (operating valve), it can be seen that in this case the geothermal temperature can also be used because it is very close to the production fluid temperature and, therefore, to the actual injection gas temperature.

The temperature profiles described so far correspond to a gas lift well already in normal operation. Estimating the injection gas temperature, as well as the valve’s temperature, is much more complex during the unloading operation. Before reaching the first valve, the injection gas flow rate is very low (to avoid eroding the seats of all valves), thus the injection gas temperature is very similar to the geothermal temperature. At this stage, the production fluids also have a temperature profile close to the geothermal temperature. It is a good approximation to assume the injection gas temperature to be equal to the geothermal temperature when calculating the gas flow rate and the injection pressure for the first valve. This is true for both, annular or tubing flow. But the dome temperature of the first valve should be estimated at values higher than the geothermal temperature. If the geothermal temperature is assumed for the first valve’s dome temperature, this valve may close before the injection gas reaches the second valve while unloading the well (because the liquids coming from below the first valve are hotter than the geothermal temperature at the first valve, even if this valve is above the static fluid level). In general, valves above the static fluid level should be calibrated with a temperature distribution cooler than the one for valves below the reservoir static liquid level, see Fig. 9.36. The surface design temperature for the upper valves is equal to the geothermal temperature plus 25 to 30% of the difference between  $T_{wh}$  (which is the surface production temperature for the well under normal operation) minus the geothermal temperature at the surface. For lower valves, the surface design temperature is  $T_{wh}$ . If a valve is below the static fluid level, but the transfer pressure for that particular valve is such that no fluid will come from the formation, the valve should be treated as a valve above the static fluid level.

As the well is unloaded, the injection gas flow rate is increased so the injection gas reaches the geothermal temperature at deeper depths. For valves



■ FIGURE 9.36 Linear approximation of the design temperature of the unloading valves, depending on their location with respect to the reservoir's static fluid level.

above the reservoir static liquid level, the unloading process might take place with an average gas injection temperature slightly lower than the geothermal temperature, so that the injection gas pressure gradient should be slightly above the one it would have at the geothermal temperature. When the unloading process starts to take place from valves below the static liquid level, the production fluid temperature begins to be greater than the geothermal temperature but it is difficult to calculate its value because the fluid flow in the reservoir near the wellbore and the multiphase flow along the production tubing string are not under steady state conditions. When gas is injected down the annulus, the injection gas begins to have an average temperature that could be slightly higher or lower than the geothermal temperature. Because this temperature difference affects very little the injection gas pressure gradient, it is also a good approximation in this case to assume the injection gas temperature equal to the geothermal temperature.

If gas is injected down the production tubing string, the average injection gas temperature during the initial stages of the unloading process is only slightly higher than the geothermal temperature because the gas velocity in this case is higher than for annular gas injection (so it takes deeper depths for the gas to reach the production fluid temperature) and also because the production fluid temperature has not reached its maximum value. For deeper valves, toward more advanced stages of the unloading process, the injection gas temperature is going to be only slightly lower (if not equal) than the production fluid temperature.

A more rigorous way of estimating the temperature at each unloading valve (below the static liquid level) and the injection gas temperature, is by calculating the unloading liquid flow rate at each unloading valve, using the constant-gas-flow-rate equilibrium curves, as explained at the end of the previous section. The unloading liquid production flow rate and the required injection gas flow rate to reach the “transfer production pressure” at each valve are calculated for each unloading valve. The production fluid temperature traverse curve is calculated for each unloading valve at its corresponding liquid and gas flow rates using the equations given in chapter: Single and Multiphase Flow Through Restrictions. Heat transfer calculations are then performed to find the injection gas temperature along the depth of the well for each unloading condition. If gas is being injected down the annulus, the gas injection temperature is bounded by the geothermal temperature and the production temperature. If gas is being injected down the production tubing string, the gas temperature is bounded by the production liquid temperature only. Regarding the temperature of each unloading valve, instead of using the linear temperature profile given in Fig. 9.34, an average temperature is found in a manner that depends on the way the gas is injected and on the type of valve being used.

- When gas is injected down the annulus and wireline retrievable valves are installed in standard side pocket mandrels inside the tubing, there are two possibilities:
  - If the valve is a 1-in. OD valve, it is usual for the dome to be below the upper gas lift valve packings, thus the dome is surrounded by the injection gas, and the dome’s temperature is approximately equal to the injection gas temperature plus one-third of the difference between the production liquid temperature and the injection gas temperature at valve’s depth.
  - If the valve is a 1.5-in. OD valve, it is usual for the dome to be above the upper gas lift valve packings, thus the dome is surrounded by the production liquids, and the dome’s temperature is approximately equal to the injection gas temperature plus two-thirds of the difference between the production liquid temperature and the injection gas temperature at valve’s depth.
- When gas is injected down the annulus and the gas lift valves are installed in concentric mandrels inside the tubing, the temperatures of the valves are assumed to be equal to the production temperature at each unloading stage.
- When gas is injected down the annulus and the valves are installed outside the tubing in conventional (tubing retrievable) mandrels, the

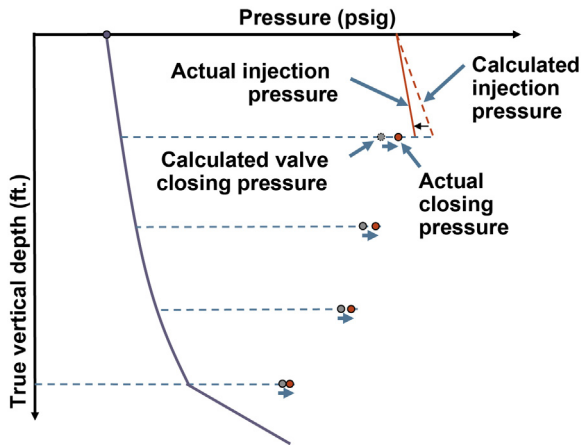
temperatures of the valves are assumed to be equal to the injection gas temperature.

- If gas is injected down the tubing and the valves are installed in concentric or eccentric mandrels, the temperatures of the valves are assumed to be equal to the injection gas temperature. This does not mean that the temperatures of the valves are going to be closer to the geothermal temperature. Temperature surveys run in wells where gas is injected down the production tubing string indicated that the injection gas reached the production fluid temperature after the well has been operating under normal design conditions for a short period of time.
- If gas is injected down the tubing string and the valves are installed outside the tubing (in conventional or tubing retrievable mandrels) the temperatures of the valves are assumed to be equal to the production fluids' temperature.

Calculations should be done as rigorously as possible, but it is important to know that temperature effects on gas injection pressure at depth and on its flow rate are not very profound and there is room for good approximation techniques without loss of accuracy.

- For a depth of 10,000 ft. and a surface injection pressure of 1,800 psig, a 30% error in the injection gas temperature above the actual temperature, introduces an error of -2.13% in the estimation of the gas injection pressure at depth, which is equal to approximately 50 psig lower than the actual pressure of 2,347 psi. For lower pressures and depths, the errors are much smaller. Considering the fact that errors made while estimating the gas injection temperatures are not as high as 30% of its actual values, it is safe to say that the errors in the estimation of the gas injection pressure at depths (made for not knowing the precise gas injection temperature) are very small.
- If the injection pressure at the entrance of the valve is 1800 psi, an error of 30% in the injection gas temperature will induce an error in the estimation of the gas injection flow rate of only 5.2% in critical flow. In many gas lift fields, this error could be smaller than the measurement error of the formation gas/oil ratio of the produced fluids at the separator.

Even though the errors described previously are small, the combined effect of assuming a temperature profile that is too low or too high in comparison to its actual value could cause, in some cases, serious problems during the unloading operation of the well. This is due to the fact that the closing pressures of the valves react to temperature errors in the opposite way in which the gas injection pressure does. A 10% error in the dome temperature of the



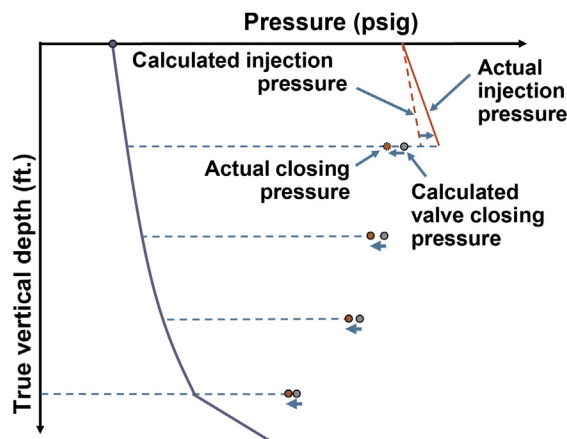
■ FIGURE 9.37 Error caused by estimating a temperature profile lower than its actual value.

valve causes a 3–4% difference in the closing pressure of the valve, but with the following combined effect.

- If the assumed temperature at depth is lower than the actual one, the actual valve closing pressure is larger than estimated while the actual gas flow rate and the actual gas injection pressure are smaller. In this case the gas flow rate must be increased to pass the desired gas flow rate at each unloading valve. The advantage in this case is that all valve closing pressures are going to increase in such a way that the risk of valve interference could actually be reduced (because the surface closing pressures are farther apart from each other), see Fig. 9.37.
- If the assumed temperature is higher than the actual one, the actual valve closing pressure is going to be smaller than estimated and this reduction might increase the risk of valve interference, see Fig. 9.38. The advantage in this case is that the gas pressure at depth and the gas flow rate are actually going to be greater than initially estimated.

As indicated previously for extreme temperature conditions along the depth of the well, a field study must be conducted to estimate the temperature calculation procedure that is best suited for these particular conditions. Because of one, or several, of the following reasons, many commercially available programs offer several ways of estimating the valve's dome temperature:

1. Extreme temperature conditions.
2. Different types of production flow: tubing or annular flow.
3. Different types of mandrels: conventional, concentric, eccentric, etc.



■ FIGURE 9.38 Error caused by estimating a temperature profile higher than its actual value.

The followings list shows some of the different options offered by commercially available software for valve temperature estimation:

1. Equal to the geothermal temperature (lowest possible temperature, not recommended in most cases because the valve might remain closed).
2. Equal to the production temperature at valve's depth after the well has been unloaded (highest possible temperature, not recommended in most cases because the valve might remain opened).
3. Equal to the gas injection temperature (some programs estimate the gas injection temperature to be equal to the geothermal temperature plus 80% of the difference between the production temperature and the geothermal temperature when the well is produced up the tubing).
4. Equal to the production temperature of the fluids rigorously determined using the equilibrium curve concept at each unloading valve, as described previously (highly recommended).

It is possible that upper valves could need an option that is different from the one appropriate for the lower valves (some programs provide a especial choice for the first valve but it is important to have an independent choice for all valves to be able to treat each valve differently and provide solutions for the many operational conditions that can be encountered).

A field case of extremely low geothermal temperatures is presented next. A solution was found after trying with different calculation procedures to find the design valve temperature to successfully unload and operate the wells. This work was carried out by Lagerlef et al. (1992). In a gas lift field in

Prudhoe Bay, Alaska, there were several oil wells with the following average production characteristics:

- Reservoir depth: 8850 ft.; PI: from 1 to 30 STB/D/psi;
- Average water cut: 60%;
- Production tubing diameters: 4½ and 5½ in.; 1.5-inch, IPO, nitrogen-charged, gas lift valves;
- Manifold injection pressures: from 1900 to 2000 psig.

The first unloading valves were located at depths between 2900 and 3400 ft. Frozen ground (permafrost) extends from the surface to depths of approximately 2500 ft. (which implies a considerable difference between the valves' temperatures at operating and shutdown conditions).

Gas lift valves were initially calibrated assuming that their temperatures during the unloading process were equal to the production temperature at each valve depth at final operating conditions: during the unloading operation the valves were in reality considerably colder and for this reason it was difficult for the upper valves to close, originating multiple points of injection thus very large injection gas flow rates were necessary to be able to keep the injection pressure high enough such that deeper valves could be reached. In some cases, it was necessary to inject gas through the first valve for many hours or days to warm up the rest of the valves to initiate the unloading operation of the well.

First attempt to solve the problem: calibrate the valves as if their temperatures during the unloading process were equal to the geothermal temperature. This introduced a new difficulty; the design temperatures of the valves turned out to be too cold in comparison to their actual temperatures. Therefore, when the unloading operation was interrupted (or the production of the well during its normal operation was stopped for a short period of time) it was necessary to wait for a long time for the upper valves to cool down and start the well again because these upper valves were lock closed due to their high temperatures and it was not possible to inject gas through the deeper valves because of the high tubing pressures that were caused by liquid accumulation in the production tubing while the well was shut in.

Second attempt to solve the problem: assume the temperature of the valves to be the average between the geothermal temperature and the final operating temperature.

This alternative reduced the number of wells with difficulties to be kicked off, but there were still some wells with valves lock closed or opening out of sequence.

The problem was finally overcome in the great majority of cases by calibrating the first three upper valves as if each of these valves were to produce the unloading liquid flow rate rigorously determined using the constant-gas-injection equilibrium curves (explained previously in Fig. 9.33). This implies carrying out nodal analysis at each unloading valve to find the liquid production and the required injection gas flow rate to achieve the transfer production pressure at each unloading valve (as indicated in Fig. 9.32). But it was found that these simulations would give best results if the productivity indexes of the wells were only 50% of their actual values (which will give lower flow rates and therefore cooler temperatures). In reality, these upper valves will be colder during the unloading operation but if these colder temperatures were used, there would still be the problem of having to wait for a long time to restart the unloading of the well if it was necessary to interrupt it even for short periods of time. After performing the calculations to determine the calibration of the upper valves, it was necessary to check if, with the operating temperatures of the valves, the system pressure was high enough to open them (thereby eliminating the waiting time for the valves to cool if the unloading, or the normal operation of the well, needed to be interrupted for a brief period of time). The lower valves were calibrated assuming their temperatures equal to the ones they will have during normal operation of the well (when gas is injecting through the desired point of injection).

### 9.2.5 Determination of the seat diameters of the operating and unloading valves

Seat diameters are usually calculated using the Thornhill–Craver equation given in chapter: Single and Multiphase Flow Through Restrictions, Eq. 4.25, with the recommendations given in chapter: Gas Flow Through Gas Lift Valves, Section 8.1, to apply this equation to gas lift valves. These recommendations are valid only if the valve is fully open. Beside the Thornhill–Craver equation, other equations derived for orifice flow from the different dynamic models of gas lift valves can be used as long as the valve is fully open.

In all the equations mentioned in the previous paragraph, the valve’s “operating” injection pressure is the upstream pressure and the “transfer” production pressure is the downstream pressure for seat diameter calculations. Both of these pressures (operating and transfer pressures) are determined by the mandrel spacing procedure being used (explained in Sections 9.2.1 and 9.2.2). The valve’s operating injection pressure is the one determined by the spacing procedure to be used as the injection pressure to uncover the next



valve below. The transfer production pressure is the production pressure at valve's depth just when the next valve below is uncovered.

In order for the valve to be fully open, it is necessary that the operating pressure at depth be greater than the valve's opening injection pressure, as explained in detail in chapter: Gas Flow Through Gas Lift Valves, Section 8.2. If the valve's operating pressure is just equal to the valve's opening pressure (as suggested by some spacing techniques in the literature) the valve is going to be in throttling flow (at best) and therefore the injection pressure must, in this case, be increased to be able to pass the required gas flow rate, at the risk of opening an upper valve. For the first valve (shallowest valve) there is always the possibility of not having an adequate pressure to achieve the required gas flow rate if the operating pressure is too close to the manifold pressure (usually this is not a problem as most first valves are above the static liquid level and the well can be unloaded with a low injection gas flow rate until uncovering the second valve). In the great majority of wells, not being able to fully open an unloading valve does not represent a serious problem. At worst, it implies a temporary gas injection through more than one valve, which will require a higher gas flow rate, but this high unloading gas flow rate is usually less than what the well will need under normal operating conditions (after the well has been unloaded). This is the reason why once the first valve is uncovered and gas is being injected through it, many operators set the unloading injection gas flow rate equal to the final gas flow rate and the well should unload with no problem. However, there could be cases where the unloading gas flow rate might temporarily be even greater than the final injection gas flow rate to complete the unloading of the well. If this goes unnoticed, the well might be left producing with the injection point above the design injection point depth. This situation is many times overlooked by the operation personnel and the well is thought to be completely unloaded. It is important then to perform troubleshooting analyses to determine the injection point depth once the unloading process is thought to be completed.

It is usually the case that the available seat diameter is larger than the calculated diameter. Calculations simply determine the smallest available seat through which (at least) the "design gas flow rate" can be injected. If, for example, the available seats are 8/64 and 12/64 in. in diameter and calculations indicate a required seat diameter of only 9/64 in., then the 12/64-inch seat should be installed because the 8/64-in. seat will not be able to pass the required gas flow rate. But the 12/64-in. seat will pass a much larger gas flow rate, which will have to be injected at the surface to be able to keep the operating pressure high so it would be possible to reach and uncover the

next deeper valve. It is necessary then to review the design and be aware of those cases where the gas flow rates need to be very high during the unloading of the well. Usually, most gas lift systems are capable of (temporarily) delivering these high flow rates during the unloading operation. There is always the risk (specially for valves above the static liquid level or just below it) that a nitrogen-charged unloading valve will cool down due to the high gas flow rate and remain open (due to a reduction in the valve's closing pressure caused by the low temperatures) preventing the well from being unloaded. The gas flow rate will then need to be increased even further (not just for having a very large seat, but also because it will be necessary to pass gas simultaneously through more than one point to reach the deepest point of injection in the gas lift design). This problem can be mitigated by using chokes inside the gas lift valve (downstream of the seat) and installing valves above the static liquid level with the smallest available seat diameters (the unloading process will only take longer but it can be done). If chokes downstream of the seat are used, it is important to point out that they show pressure drops that are smaller than the ones found in seats of the same size for the same injection gas flow rate. The reader is advised to review chapter: Gas Flow Through Gas Lift Valves, Section 8.3, to know more about the use of this type of choke.

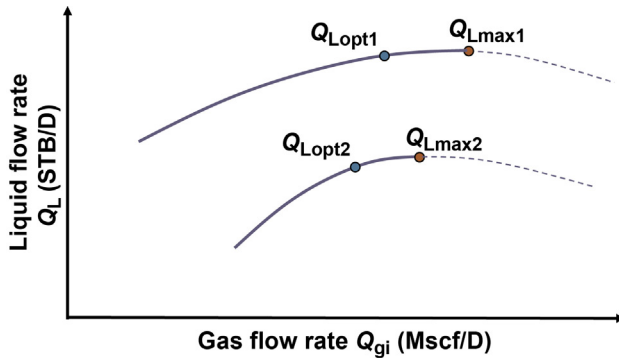
### 9.2.6 Dual wells (with a common injection gas source)

Several types of dual well completions are presented in chapter: Gas Lift Equipment, Section 6.4.4. These completions are usually justified by the savings they bring in their drilling and construction operations; however, these savings are most of the time overshadowed by the difficulties found when trying to maintain both tubing strings near their optimum operating points (maximum liquid production with minimum injection gas/liquid ratio) when a common injection gas source is used.

Several topics related to dual gas lift wells operating with a common injection gas source are presented in this section. The optimization of dual wells with a common lift gas source is based on:

- Knowing the IPR curve of each zone very well.
- Precise determination the orifice size at the design injection pressure to produce each zone as close as possible to its optimum operating point.

The gas lift performance curves that are presented in Fig. 9.39 correspond to a dual well with two production zones: "1" and "2." For each zone, there is an injection gas flow rate that maximizes the liquid production (with the liquid flow rate identified in the figure as  $Q_{Lmax}$ ) and another, known as the



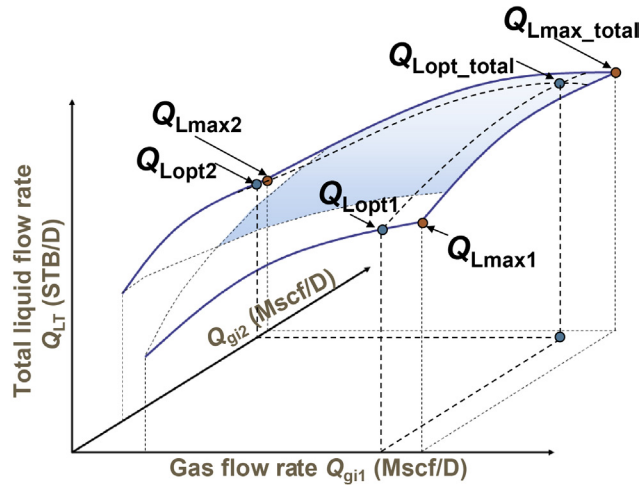
■ FIGURE 9.39 Gas lift performance curves for each production zone.

optimum injection gas flow rate (with the liquid flow rate identified in the figure as  $Q_{Lopt}$ ), for which the profitability of the well is maximized. It is at the latter gas flow rate that the well should be operated. As shown in the figure, the optimum injection gas flow rates are different for each zone. It is extremely important to know each of these gas lift performance curves because they determine the exact gas flow rate needed to be injected to each tubing string. The curve for one particular zone must be determined in the field by closing the other zone so as to be able to control the gas flow rate being injected into the tubing string under evaluation. Gas must be injected at different flow rates and, at each flow rate, the well should be tested once the liquid production has stabilized.

Fig. 9.40 shows a three-dimensional surface (not to true scale for didactical purposes) of the total liquid flow rate,  $Q_{LT}$ , which is the sum of the liquid flow rates from both zones that would be produced if it could be possible to inject gas to both tubing strings in any combination (feasible or not) of individual gas flow rates. The gas injected into strings “1” and “2” are  $Q_{gi1}$  and  $Q_{gi2}$ , respectively.

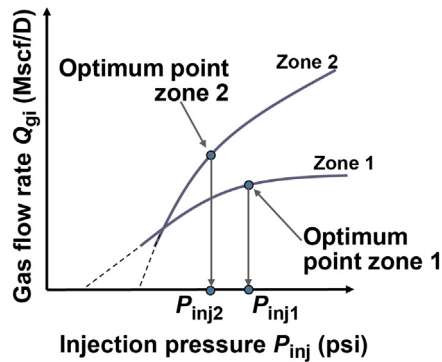
Because both strings share a common lift gas source, of all liquid flow rates presented in the figure, only a reduced or limited number of values are possible to be produced. This is due to the fact that a reduced combination of gas flow rates to each string is possible for a particular set of orifice diameters installed at the operating points of injection of the two strings. This is explained in the analysis that is presented next. The reader is advised to review the concepts presented in chapter: Total System Analysis Applied to Gas Lift Design, Fig. 5.25, to understand the explanations given in this section.

As it is demonstrated in chapter: Total System Analysis Applied to Gas Lift Design, Section 5.1.3, for each injection pressure there is one and only one

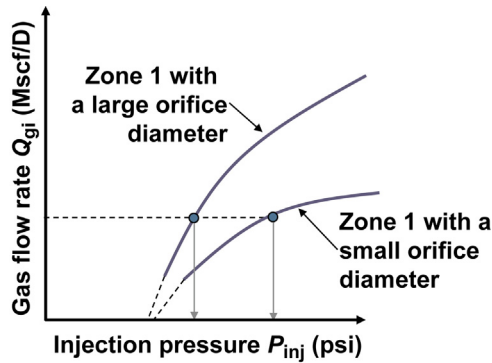


■ FIGURE 9.40 Total liquid flow rate versus injection gas flow rate for any combination of gas flow rates into both strings.

injection gas flow rate possible, which in turn determines one and only one production liquid flow rate. The injection gas flow rate curves (as functions of the injection pressure) for two different zones are shown in Fig. 9.41. As can be seen in this figure, each zone reaches the optimum gas flow rate at different injection pressures. Because these curves depend on the diameter of the orifice at the point of injection, it is necessary to adjust the orifice diameter in one of the production tubing strings to produce both zones at their respective optimum gas flow rates with the same injection pressure.



■ FIGURE 9.41 Gas flow rate of each zone as functions of the injection pressure.

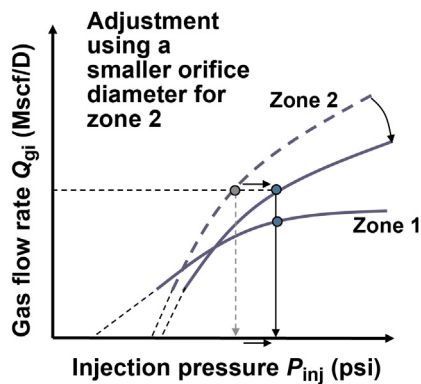


■ FIGURE 9.42 Effect of the orifice diameter on the gas flow rate as a function of the injection pressure.

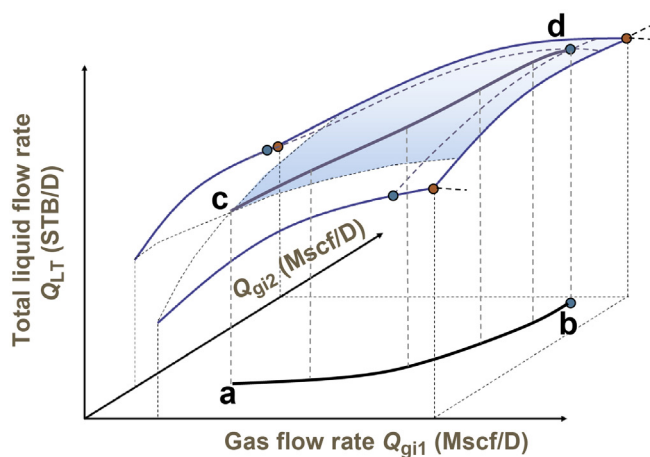
Fig. 9.42 shows two curves corresponding to the “same” zone but with different orifice diameters. It can be seen that by reducing the orifice diameter the gas flow rate needs to be injected at a larger injection pressure.

In Fig. 9.43 the curves for the gas flow rate as functions of the injection pressure for each zone are presented. It is also shown how the orifice diameter should be adjusted for zone “2” in order for both zones to receive the optimum gas flow rate at the same injection pressure.

As can be seen in Fig. 9.43, if the orifice size at the point of injection of each tubing string is kept constant, for each injection pressure there is one and only one combination of the gas flow rate that goes to each string. In other



■ FIGURE 9.43 Adjustment of the injection orifice size for zone “2” to optimize the production of both zones at a common injection pressure.



■ FIGURE 9.44 Curve “a–b” represents all possible gas flow rate combinations that can be injected to both tubing strings with a common injection gas source.

words, it is not possible to have any combination of gas flow rates, but only the ones that the current orifice diameters installed in the well will allow. This is shown in Fig. 9.44, where all the “possible” combinations of gas flow rate to each tubing string are defined by curve “a–b” on the horizontal plane, which will give the liquid flow rates represented by curve “c–d” on the total liquid production surface. If the size of the seat for one of the tubing strings is too large, curve “a–b” will lie closer to the  $Q_{gi}$  axis corresponding to that particular tubing string: increasing the injection pressure to try to increase the gas flow rate toward both tubing strings will simply increase the gas flow rate into the one with the oversized seat, which will be “stealing” all the gas that should go to the other tubing string.

To be as close as possible to point “b” (optimum operating point for both tubing strings) in Fig. 9.44, it is important to accurately define the size of the injection orifice (or seat) at each tubing string, which requires the precise knowledge of the discharge coefficients of these orifices. For this reason, it is not recommended to use calibrated valves at each point of injection, because they exhibit a complex dynamic behavior and might operate in throttling flow instead of being fully open. An orifice valve, on the other hand, shows a behavior much easier to predict. The key to optimize the liquid production of each zone at one particular injection pressure is then to define very well the size of each orifice diameter to be used at the point of injection of each tubing string.

As mentioned in Section 9.2.5, the calculated orifice diameter is most of the time different from the ones that are commercially available. For dual wells,

it is important to use seat diameters as close as possible to the calculated diameters. If the calculated and available seat diameters are too different, chokes installed inside the gas lift valve (downstream of the seat) can be used. But it should be pointed out that chokes of this type have larger discharge coefficients than the ones for seats of the same size, see Section 8.3, chapter: Gas Flow Through Gas Lift Valves. If it is desired to use orifices with special geometric configurations (such as those with venturi tube shape) it is also important to know their discharge coefficients and their pressure ratios to achieve critical flow. Venturi-shaped orifices are specially recommended for dual wells because, for a given injection pressure, critical flow is achieved for a wider range of production pressures, thereby providing a smoother operation with less instability problems.

Once the well is in operation, it is only necessary to control the total injection gas flow rate, which is equal to the sum of the optimum gas flow rate that goes into each tubing string. This can be achieved by automatically controlling the gas injection pressure (especially if the system pressure at the manifold fluctuates too much). If it is necessary to limit the gas flow rate to all wells because, for example, one compressor has tripped, it is better to leave dual wells untouched and change the gas flow rates of wells that are easier to operate. If one particular zone takes much more gas than expected, it might be possible that: (1) a gas lift valve in that particular tubing string might be damaged, (2) there is a hole in that tubing string, or (3) the production pressure has decreased because of a severe formation damage, etc. The operational conditions in each zone will change over time and it is important, from time to time, to determine the new optimum injection gas flow rates and adjust, if necessary, the size of each orifice to optimize the operation of the well. To accomplish this optimization operation, it is advisable to run pressure and temperature surveys, as well as to measure the static reservoir pressure of both zones within a reasonable period of time as budget resources would allow. Routine measurements of the liquid production, water cut, total gas produced at the separator, injection gas flow rate, and wellhead production and injection pressures, must be performed.

The tubing diameters in dual wells are usually smaller than the optimum tubing diameter. This is due to the limited available space for both tubing strings inside the casing. The reduced available annular space, together with the usually high required gas flow rates, might induce a noticeable frictional pressure drop on the injection pressure at depth that should be taken into account during mandrel spacing calculations.

It is customary to use PPO valves to produce dual wells. However, this practice has a few set backs: PPO valves usually restrict the injection gas flow

rate and they make it difficult to troubleshoot the well, which is very important to do to optimize the operation of dual wells.

The idea behind the use of PPO valves is to be able to unload the well keeping a constant injection pressure in the annulus and, because both tubing strings would unload following the way their respective production pressures change, the unloading process should be smooth and independent for each tubing string. The same thing can be accomplished using IPO valves with chokes upstream of the seat (see Fig. 9.27), but this also makes troubleshooting difficult to do. To make the unloading process as smooth as possible, besides using PPO valves, some designers install the same number of mandrels at each tubing string. The number of mandrels is determined in this case by the tubing string that needs the greatest number of mandrels to unload it (the mandrels for the other tubing string would be located from 30 to 60 ft. below each of the corresponding mandrels). But mandrel spacing should not necessarily be done in this way and each string can have its own particular mandrel spacing (checking that not two mandrels have the same depth in the well). The number of mandrels for a given string in a dual well is usually greater than the one needed for single wells. This is recommended because it gives greater flexibility to the designer if operating conditions change over time or they are just different from the expected ones.

Even though the unloading process when using IPO valves is more labor intensive, as explained in the next paragraphs, in the long run it might be a far better choice because IPO valves allow for more accurate troubleshooting analyses that will enable the production engineer keep the well optimized at all time. Instead of worrying about a coupled design for both tubing strings with PPO valves for a single operating pressure while unloading the well (which might not be the best final operating pressure), it might be a better choice to use IPO valves, designing each tubing string as if they were independent wells (but with the same final operating pressure) and using only one of them to unload the liquids in the annulus. In this way, it might be possible to obtain a wider range of available operating injection pressures to optimize the production of the well.

The explanations given in the rest of this section apply to processes that can be implemented only when IPO valves are installed in a well that is difficult to unload or kick off. In many cases, these special procedures are not necessary.

#### 1. Unloading operation

Because unloading the liquids in the annulus can be carried out by only one of the two tubing strings (shutting in the other one) any mandrel spacing technique for IPO valves can be used for each tubing string



as if both were to operate independently of each other. It is important to have a wide range of final operating injection pressures at depth available in case the injection gas flow rate needs to be adjusted. For this reason, it is a good practice to have dummy valves installed in all but one (the one closer to and above from the reservoir static liquid level) of the unloading valves above the reservoir static liquid level and have a sequential injection pressure drop per unloading valve as small as possible. The minimum operating injection pressure should not be too close to the production pressure for any of the two tubing strings because it would create instability problems. On the other hand, the maximum operating injection pressure cannot be too high because this pressure might open an upper valve (which is easy to go unnoticed in dual wells).

As indicated previously, unloading the liquids in the annulus can be carried out using only one of the two tubing strings, keeping the other one shut in. Each tubing string should be designed to unload the annulus by itself if necessary. After the unloading operation is completed, the tubing string used for that purpose should be operating from the orifice valve, designed as the operating injection point for that zone, and the other tubing string should then be opened to production in order for it to be kicked off. This is a process that might be difficult to achieve. Due to unexpected difficulties, it might be better to unload the annulus using the tubing string with the larger production liquid flow rate and, after the unloading process is completed, open the production tubing string with less liquid production, which should be easier to kick off. However, if the deepest point of injection of the large liquid production tubing string is above the deepest point of injection of the other tubing string, then it will be necessary to unload the rest of the well using the tubing string from which less liquid production is expected.

Some operators prefer to use the tubing string with less liquid production (known here as the first tubing string) to unload the annulus and, after the unloading operation is completed, kick off the second tubing string keeping the first one closed and pressurized with injection gas to keep the gas in the annulus from being injected into it and to avoid liquid accumulation while the second tubing string is being kicked off. For this operation, it is necessary to install standing valves at the bottom of the both tubing strings.

## 2. Kickoff operation

If the well had been successfully unloaded but its normal operation was later interrupted for some time, both zones would need to be kicked off again because liquids would have accumulated at the bottom of each tubing string, generating a liquid column that might not allow the gas to be injected through the operating points with the final operating

injection pressure. In wells difficult to operate, it is recommended to kick off both zones at different stages, starting with the high production string while keeping the other one shut in. Once the high production tubing string has been successfully kicked off, the other one should be easier to kick off, but it might turn out to be a complicated process with unloading valves of the tubing string already in operation opening and closing. This is the reason why difficult dual wells with IPO valves should not be shut in once they are in operation. If, for any reason, a dual well should be shut in, it is recommended to use this opportunity to measure the static liquid level (by tagging the well or by running a static pressure and temperature survey in each tubing string).

As it was indicated in the previous paragraph, kicking off the second tubing string might turn out to be a complicated process, with several valves of the first tubing string (already in operation) opening at the same time, causing the injection pressure to drop unless a large gas flow rate is injected into the well. When kicking off the well is too difficult to accomplish, it is recommended to take the following steps (for which standing valves should be installed at the bottom of both tubing strings).

- The first tubing string already kicked off is shut in and pressurized (by injecting gas down the tubing from the surface or simply by closing this string at the surface and allowing gas injection into it until the injection gas flow rate drops to zero) to a pressure higher than the required injection pressure for the second tubing string to be kicked off. The gas should be injected rapidly into the first tubing string (it is possible that the unloading valves will open, but their check valves will stop the tubing pressure from dropping to the annular pressure). As for the unloading operation, this action avoids two things from happening for a kickoff operation: (1) that the gas being injected to kick off the second tubing string be injected into the first one, and (2) stop the reservoir liquid from entering into the first tubing string because the standing valve at the bottom remains closed due to the high pressure inside the production tubing.
- Then, the second tubing string is opened and kicked off as if it were an independent well. Because this tubing string was closed at the surface and it had a standing valve below the deepest mandrel, this tubing string was also pressurized, so it needs to be opened very carefully. This string was closed because in this way all the gas was injected into the first string while it was being kicked off, making it easier to control the operation.
- Once the second string is kicked off, the first one is open to production while adjusting the total gas flow rate to its required value to produce both strings.

Installing standing valves at the bottom of the tubing is easy if the tubing has a no-go nipple installed below the operating valve. If a no-go nipple is not installed, a tubing stop needs to be installed in the well by wireline, and a standing valve can then be lowered to rest on top of the tubing stop. A collar recess type of tubing stop can be installed in API tubing. For non API tubing, a slip type tubing stop needs to be installed. But for both types of stops, it should be verified that they are able to resist the differential pressure “from above” that they are going to be subjected to.

When performing IPO or PPO valve change-out operations in the high-liquid-production tubing string, there can be cross flow from this string into the other. This can be prevented by installing a standing valve (or an equalizing plug) in the low-liquid-production tubing string. If this is not done, fluids from the high pressure zone can flow into the low pressure zone. It is recommended, for safety reason, to shut in both strings while doing wireline operations in any one of them.

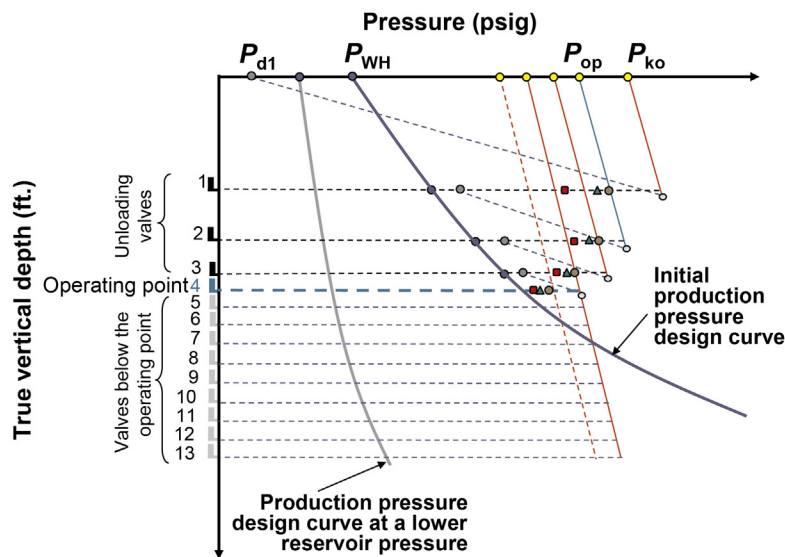
### 9.2.7 Redesign

Gas lift valves are designed in conjunction with the mandrel spacing procedure only for new wells or for wells that come from workover jobs in which the production tubing string needed to be pulled out of the well. In the great majority of cases, currently installed valves need to be replaced with new ones without pulling the tubing out of the well (due to, for example, changes in well or system conditions, or valve failures). When existing gas lift valves should, for whatever reason, be changed out, their closing and opening pressures, as well as their seat diameters, should be calculated again. This process is known as “redesign.” The depths of the valves are determined from the mandrels already installed in the well, but considering the fact that for the current operating conditions it might not be necessary to install gas lift valves in some of the existing mandrels. Usually, the new production pressures are less than the initial ones because of lower reservoir pressures and, therefore, unloading valves need not be spaced as closely as they were initially installed in the well. Only in cases where the production pressure has increased (due to an increase in the water cut or in the reservoir pressure caused by a pressure maintenance project) the valves might need to be spaced closer to one another. But even in these cases, it is highly unlikely that the tubing needs to be pulled out of the well because spacing calculations are usually done with large unloading fluid pressure gradients and with many safety factors (not needed for redesigning the valves) that will allow (to some extend) managing higher production pressures.

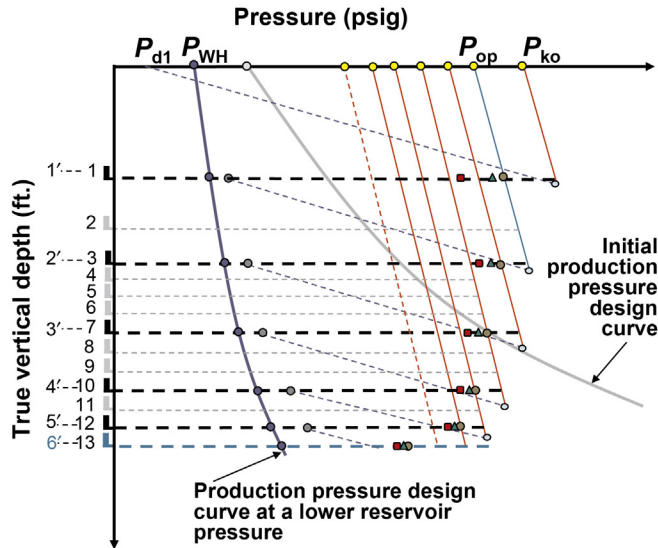
In the redesign process, the depths of the new valves are determined in the same way as is done in the design procedures explained in [Sections 9.2.1](#)

and 9.2.2. However, it is unlikely that a new valve depth coincides with the depth of any of the mandrels already installed in the well. Once the new valve depth is found by the redesign calculations, the actual new depth will correspond to the mandrel (with no new gas lift valve installed in it) immediately above the newly calculated depth. In this process, if several mandrels have been skipped, dummy valves should be installed in all of them except the one immediately above the newly calculated depth (which is where the new gas lift valve will be installed). If there are no mandrels above the first valve's depth found in the redesign calculations, the well cannot be redesigned for the new operational conditions because the current injection pressure is not high enough to reach the first mandrel already installed in the well (unless the first, shallowest, valve is above the static liquid level, as explain later in this section). On the other hand, if the next mandrel above the newly calculated depth has already a new valve assigned in the redesign process, then the redesigning calculations cannot proceed further down the well and the valve immediately above the last depth found needs to be designed, not as an unloading valve, but as the operating valve (with an extra sequential pressure drop if it is a calibrated valve or as an orifice valve if the designer prefers to have an orifice at the operating point of injection).

Fig. 9.45 shows the initial mandrel spacing of a well when its reservoir pressure was high (with the total number of mandrels greatly exaggerated)



■ FIGURE 9.45 Initial mandrel spacing for large reservoir pressure.



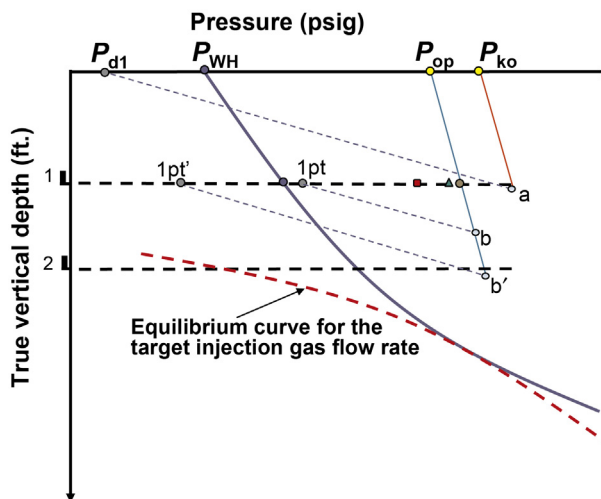
■ FIGURE 9.46 Mandrel spacing for a reduced reservoir pressure.

for didactical purposes). It can be seen that the operating valve is located well above the maximum depth at which gas lift equipment can be installed. Below the operating valve, several mandrels were installed following the procedures explained in Section 9.2.1. These mandrels are installed so that they can be used for future operating conditions, as the one shown in Fig. 9.46.

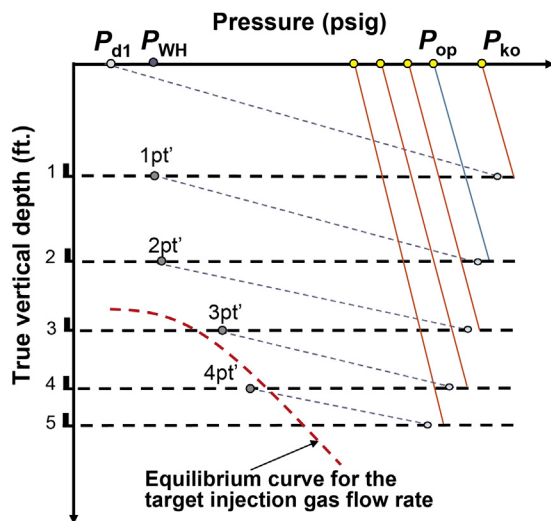
In Fig. 9.46, mandrels from 1 to 13 were already installed. Under the new operating conditions, the new mandrel numbered now as 1' is exactly where mandrel number 1 was installed. This is due to the fact that  $P_{d1}$ ,  $P_{ko}$ , and the unloading pressure gradient are still the same. The calibration pressure and the diameter of the first valve are calculated in the same way as they were found during the initial design, only that now the production pressure is much lower than the initial one.

Then, beginning at the transfer production pressure of the first new valve, a new mandrel depth is found between mandrels 3 and 4, having then to select mandrel 3 as the place where the new valve 2' is going to be installed. A dummy valve is installed in mandrel 2 and valve 2' is design with the values of the injection and production pressures found at the depth of mandrel 3. Following these same steps, valve 3' is installed in mandrel 7, leaving mandrels 4, 5, and 6 with dummy valves installed in them. This procedure continues in this way until mandrel 13 is reached, where valve 6' is installed as the new operating point of injection.

The redesign procedure explained so far works very well for operational conditions in which the production pressure has decreased; But, following this approach in all situations (without additional considerations) might cause problems when the production pressure under current operational conditions has increased due to, for example, higher water cuts or an increase in the reservoir pressure due to a pressure maintenance project. For example, strictly following design procedures for the conditions shown in Fig. 9.47 (mandrels 1 and 2 are already installed) would determine the first valve as the final point of injection and the well will not produce any liquids because the first valve is above the reservoir static liquid level: locating the second valve from the tubing transfer pressure equal to 1 pt (following the design rules explained so far) will intersect the operating pressure of the first valve at point *b* indicating that the well cannot be further unloaded. However, if the unloading gradient line is traced upward from point *b'* (where the intersection should be located) it will intersect the depth of the first valve at a much lower transfer pressure equal to 1 pt' in Fig. 9.47. Because the first valve is located above the reservoir static pressure (and no fluid from the reservoir will be produced while injecting gas through the first valve), it is possible to inject gas to reduce the production pressure to 1 pt' and, in this way, be able to reach the second valve. In fact, for a given valve *n*, any transfer pressure *npt'* (found by tracing the unloading gradient line from the depth of the next valve below) that lies above, or to the right, of the equilibrium curve for the maximum



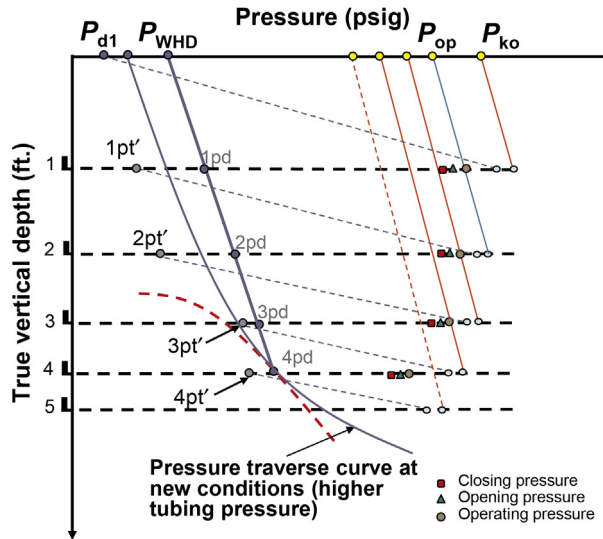
■ FIGURE 9.47 The second mandrel can be reached because the first mandrel is above the static reservoir pressure.



■ FIGURE 9.48 The transfer pressure of the fourth mandrel lies to the left of the equilibrium curve. The operating valve is then set at the fourth mandrel.

available gas flow rate, can be reached by just increasing the injection gas flow rate to the value that is needed to decrease the tubing pressure to the transfer pressure  $npt'$ . The fourth valve in Fig. 9.48 is the first one with its transfer pressure to the left of the equilibrium curve; therefore, in this case the operating valve should be the fourth valve because it will not be possible to reach the fifth valve, unless the injection gas flow rate can be increased to values above the target gas flow rate. Valves above the reservoir static liquid level can be skipped following the steps presented in Section 9.2.8; but, if a more cautious approach is taken by the designer by including valves above the reservoir static liquid level, the only requirement for the transfer pressures of valves located above the reservoir static liquid level (1  $pt'$  and 2  $pt'$  in case of Fig. 9.48) is that these pressures should not be less than the wellhead pressure  $P_{d1}$  (unless the well can be unloaded to a pit or a tank at atmospheric pressure) plus a safety factor (given by the designer) that can be linearly proportional to the depth of the valve. Wellhead pressure  $P_{d1}$  is usually equal to the pressure at the separator or at the production manifold at the flow station.

The calculation procedures that, for a given unloading valve, can be used to determine the unloading liquid flow rate, required unloading injection gas flow rate, gas lift valve's temperature, as well as its opening and closing pressures, are identical to the ones presented in Section 9.2.1 for designs based on sequentially dropping the operating pressure but with the especial



■ FIGURE 9.49 Redesign procedure for new conditions with higher production pressures (IPO valves).

considerations that are explained next. These considerations for the redesign calculations of the gas lift valves' calibration pressures and their seat diameters can be understood with the help of Fig. 9.49, given here as an example for the design of IPO valves.

- The diameter of the seat of the  $n$ th valve should be based on its operating pressure (as the pressure upstream of the  $n$ th valve), the transfer pressure  $npt'$  (as the pressure downstream of the  $n$ th valve) and the required gas flow rate to reach transfer pressure  $npt'$ . For valves above the static liquid level, the minimum seat diameter (which must be selected by the designer) can be used, thus there is no need to calculate the required gas flow rate. For a valve  $n$  below the liquid level, the gas flow rate is the one that corresponds to the equilibrium curve that intersects pressure  $npt'$  at that particular valve's depth if such equilibrium curve exists for the transfer pressure: Valves below the reservoir static liquid level but with very high transfer pressures (so that the transfer pressures are to the right of the minimum gas flow rate equilibrium curve) should be treated as if they were above the static liquid level. For the operating valve, the pressure downstream of the valve that should be used to calculate the seat diameter is equal to its production pressure  $npd$ .
- The opening and closing pressures of the valves should be calculated using production pressures  $npd$  along the design production pressure line that goes from surface pressure  $P_{WHD}$  (defined by the designer)

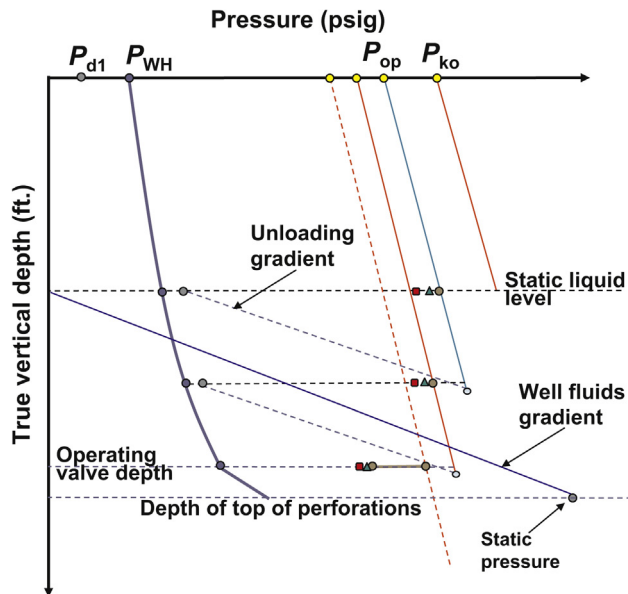


to the production pressure of the operating valve, which is  $4pd$  for the case shown in Fig. 9.49. The operating pressure for each unloading valve should be greater than or equal to the injection pressure that defines the limit between throttling and orifice flow. This is especially important in this case because a given valve  $n$  has to remain open until its transfer pressure  $npt'$  (which might be very low and make the valve close) is reached. The transfer pressure  $npt'$  cannot be used in the valve mechanic equation to define the opening pressure because this transfer pressure might be less than the production pressure at valve's depth once the unloading operation has been completed and, as indicated in Section 9.2.1, production pressures higher than the design production pressure might open an unloading valve. The calculation of the closing and opening pressures are performed with the same equations presented in Section 9.2.1 with the only requirement that, in these equations, the production pressure must be equal to pressure  $npd$  on the design production pressure line as shown in Fig. 9.49.

Several safety factors, that are important for design procedures given in previous sections, might not be needed during the redesign operation. For example, the unloading-liquid pressure gradient that is used to locate the next deeper mandrel can be equal to, or only slightly higher than, the gradient of the fluids produced by the well. Additionally, dummy valves can be installed in mandrels above the reservoir static liquid level following the procedures described in Section 9.2.8. The actual logic of the redesign algorithm that is used by the gas lift design software has to be a combination of the procedures shown in Figs. 9.49 and 9.46. In this way, mandrels that are no longer needed can be skipped and, for those that are difficult to reach, additional calculations must be carried out to determine if the required transfer pressure lies to the left or to the right of the equilibrium curve corresponding to the target injection gas flow rate.

### 9.2.8 Mandrel spacing from the reservoir static liquid level

In many cases, when it is difficult to space mandrels down to the desired deepest point of injection for not having a sufficiently high available injection pressure, it is convenient to install dummy valves in mandrels above the reservoir static liquid level. In this way, the sequential injection pressure drops of the valves above the static liquid level will not be subtracted from the available operating surface pressure. This practice is only recommended if the available injection pressure is too low to reach the final operating point of injection by design or if this operating point of injection can be reached but with a final injection pressure too close to the production pressure. The



■ FIGURE 9.50 Mandrel spacing starting at the reservoir static liquid level.

important thing to remember in this case is that at least one valve should be installed at or just above the static liquid level. If this is not done, all the liquid displaced from the annulus is going to generate a liquid column inside the tubing that might generate a hydrostatic pressure inside the tubing greater than the injection pressure at depth (if this happens, it might be possible that the reservoir will absorb this liquid column in a matter of hours or days so that the unloading can continue). Installing the first valve below the static liquid level (without placing at least one valve at this liquid level or just above it), can only be done under extreme circumstances and knowing that the well can indeed absorb the fluids being unloaded and without causing any damage to the formation. Fig. 9.50 shows a typical mandrel spacing procedure starting from the static liquid level and using the method of spacing mandrels by sequentially dropping the operating injection pressure, but any of the mandrel spacing methods described in this chapter can also be used.

To locate the first mandrel, a line with the well fluid pressure gradient (not the unloading pressure gradient) is drawn from the static reservoir pressure up until it intersects the true-vertical-depth axis. This intersection point corresponds to the static liquid level when the well is filled with its own production fluids and the wellhead is exposed to atmospheric pressure. This will give the highest possible static liquid level because if the wellhead production pressure is taken to be equal to the separator pressure or the unloading

pressure gradient is used, the liquid level will be deeper. The first valve is then placed at this calculated liquid level. From the first valve on, all calculations are identical to the ones described for the different design procedures studied so far in this chapter.

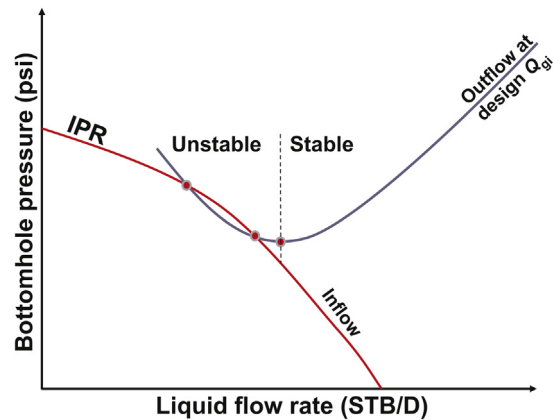
For new completions in a gas lift field where the current available injection pressure is very low but it is known that it will be increased in the future, the mandrel spacing process can be carried out as if the well is filled with liquid all the way up to the wellhead and then perform redesign calculations, placing dummy valves in the mandrels above the static liquid level, with the exception of the one closer (but still above) to static liquid level. For redesigns then, the first (shallowest) valve should be the one above of and closest to the static liquid level. Once this first valve is identified, the following steps are identical to the redesign procedures described in the previous section.

### 9.3 STABILITY CHECK OF THE GAS LIFT DESIGN

Once the gas lift design is completed, it is a good practice to check how stable the design will behave during the unloading and normal operation of the well. There are several theories that have been developed to describe the behavior of gas lift wells producing in an unstable manner. These theories are extremely complex and the mathematical calculations involved are simply beyond the scope of this book. Fortunately, the general rules that can be followed to avoid well instabilities are surprisingly simple and they are explained in this section.

The causes of gas lift instabilities can be categorized as: (1) tubing headings, (2) casing headings, and (3) other causes that are mentioned at the end of this section and explained in detail in chapters: Continuous Gas Lift Troubleshooting and Intermittent Gas Lift Troubleshooting, as they cannot be attributed to the gas lift design. Tubing headings can cause casing headings and vice versa. Among many other causes, casing headings can be a consequence of inherent flaws in the gas lift design or in the way the well is operated.

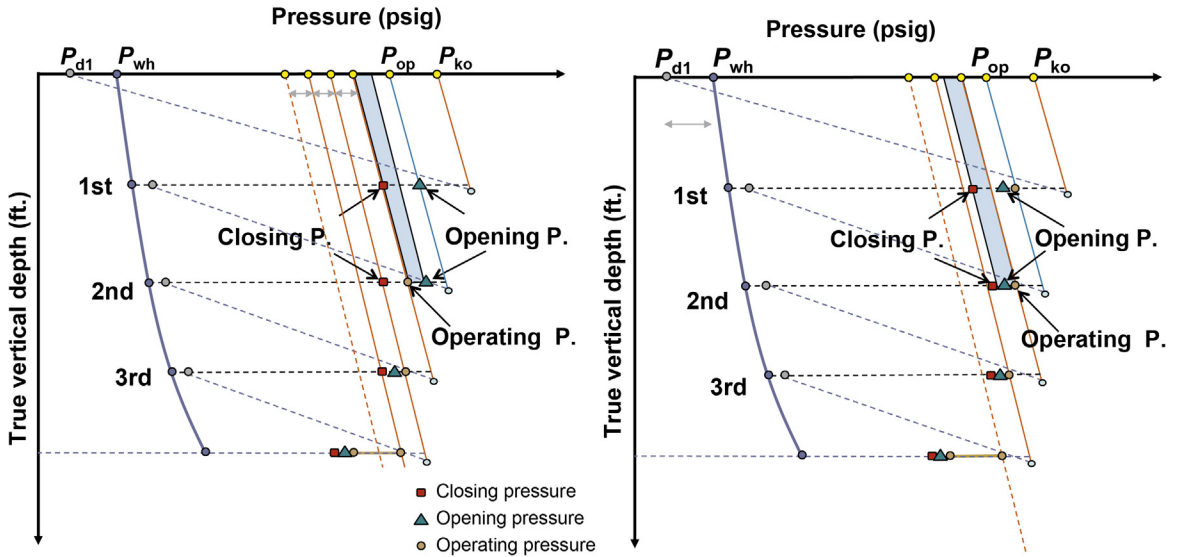
Just as it is the case for wells producing on natural flow, gas lifted wells can have tubing headings if the outflow curve (at the design injection gas flow rate) intersects the inflow curve to the left of the minimum pressure of the outflow curve, as shown in Fig. 9.51. It can be appreciated that the outflow curve intersects the inflow curve at two different points. The problem with this criterion is that it is sometimes difficult to obtain accurate data to construct the inflow and outflow curves that truly correspond to the actual state of the well. It is not unusual for a nodal analysis (based on the available data) to show these signs of instabilities but the well is actually operating in a stable manner or vice versa.



■ FIGURE 9.51 Tubing headings can be predicted by nodal analysis at the design injection gas flow rate.

Besides tubing headings (that might be present in wells on gas lift or on natural flow), gas lifted wells can show casing headings that can be caused by a variety of reasons and induce (or worsen) tubing headings. The designer has to be alert of flaws in the gas lift design to avoid the following causes of instabilities:

- For IPO valves with a design based on sequentially dropping the gas lift valves' closing pressures, it could be possible that the surface opening pressure of one valve be greater than the surface closing pressure of the valve above. This is shown in Fig. 9.52a: the surface injection opening pressure of the second valve is greater than the surface closing pressure of the first. In this case, it might be difficult to close the first valve, which could remain indefinitely opening and closing, not allowing the well to unload to the third valve. The gray area in Fig. 9.52a corresponds to the range of injection pressures for which this type of instability (called valve interference) might happen. Additionally, the operating pressure of the second valve is below its opening pressure (but above its closing pressure). This means that the second valve will operate in throttling flow and it might close before uncovering the third valve. This latter type of problem is not present in designs based on sequentially dropping the operating pressures of the valves.
- For IPO valves with a design based on sequentially dropping the valve's operating pressure, it could be possible that the surface operating pressure of one valve be greater than the surface closing pressure of the valve above. This is shown in Fig. 9.52b (the surface operating pressure of the second valve is greater than the surface closing pressure of the first valve and this can also promote valve interference).

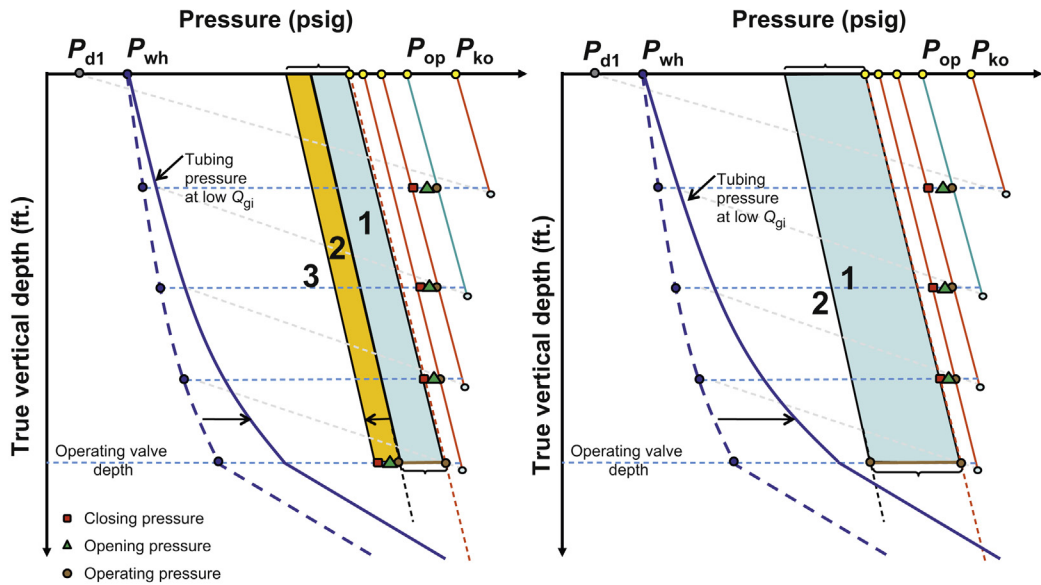


■ FIGURE 9.52 Inherent flaws in the gas lift design can cause casing headings. (a) Dropping the closing pressure: (1) valve interference (2) operating pressure in throttling flow; (b) Dropping the operating pressure: valve interference.

Valve interference of the types described above are not very serious because, most of the time, the well can be unloaded without problem. If the well cannot be unloaded, the problem is usually, but not always, overcome by just temporarily increasing the surface injection gas flow rate.

Valve interference can also take place when the gas lift design is based on design valve temperatures assumed to be either too low or, especially, too high, compared with the actual temperature along the production tubing (see Fig. 9.38). Unfortunately, this type of design flaw is not possible to detect by just inspecting the design diagram. If the actual temperature is cooler than expected, increasing the gas flow rate might make matters worse because the cooling effect of the injection gas, as it expands through the gas lift valve, might lower the valve's closing pressure and leave the valve open. This usually happens when the production of the well turns out to be much lower than expected and the seats of the unloading valves are just too large for the required injection gas flow rate at the actual operational conditions of the well.

Instability problems can also be due to a narrow range of operating injection pressures offered by the design or, if the design has an adequate range of operating pressures, operating the well at an injection gas flow rate that is either too low or too high for the size of the seat at the point of injection. Fig. 9.53a shows the design of a well in which there is a calibrated valve at the final point of injection, while in Fig. 9.53b there is an orifice valve at the



■ FIGURE 9.53 Casing headings can be caused by a design with a narrow range of operating injection pressures or by an inadequate surface injection gas flow rate. (a) Calibrated valve; (b) orifice valve.

same point. For both cases, zone “1” corresponds to the range of operating pressures at which the well should be produced. If the injection gas flow rate is increased, the right hand limit of the operating pressure could be reached and the upper unloading valve might open. Once this upper valve opens, the total gas flow rate through the two subsurface gas lift valves could be lower or higher than the surface injection gas flow rate. If the gas flow rate through the two gas lift valves is higher than the surface injection gas flow rate, the upper valve will remain opening and closing (because the annular pressure will decrease every time the upper valve is opened). If the gas flow rate through the two gas lift valves is lower than the surface injection gas flow rate, the two points of injection might remain operating at a higher and stable operating pressure. This latter case could go unnoticed for a long time (because the liquid flow rate is usually not reduced while operating at this condition) and it represents an obvious waste of compression energy for an injection gas that could be used in another well.

If the surface injection gas flow rate is decreased, the reaction of the well will depend on the type of valve installed at the point of injection. A calibrated valve acts as a pressure regulator that keeps a large pressure drop across the gas lift valve. If the surface injection gas flow rate is reduced, the operating pressure range will be in zone “2” in Fig. 9.53a and the valve will

be in throttling flow (it tries to close and, by doing so, the injection pressure is kept high but the gas flow rate through the valve is reduced). Meanwhile, the production pressure will increase because of the reduced injection gas flow rate into the tubing but, thanks to the regulating action of the calibrated valve, the production pressure at the point of injection will be lower than the injection pressure upstream of the gas lift valve. Under throttling flow, it is always possible that the valve will close. Zone “3” in Fig. 9.53a corresponds to the range of operating pressures for which the valve is definitely closed.

What happens once the operating valve closes is very hard to predict because it depends on how fast the tubing pressure will increase (because of the lack of injection gas) and on how fast the injection pressure in the annulus will also increase (because the surface injection gas flow rate is kept more or less constant and no gas is flowing out of the annulus). The reaction of the annular pressure depends on the surface injection gas flow rate, the type of surface control of the gas injection, and the volume of the annulus. If the annular volume is very large, the increase in annular pressure will be very slow and by the time the injection pressure increases to the operating valve’s opening pressure, the production pressure might be greater than this injection opening pressure and the injection pressure will need to keep increasing until it is able to open an unloading valve for which the injection pressure is greater than its corresponding production pressure. The reaction of the production pressure, on the other hand, depends on the reservoir pressure and the productivity index of the well.

If the operating gas lift valve is open and operating in throttling flow, the increase in production pressure due to a reduction in the injection gas flow rate is usually small, provided that the valve does not close. This happens because when the valve is operating in throttling flow, the stem position of the calibrated valve is affected by the production pressure: if the production pressure increases, the valve tends to open wider, thus the injection gas flow rate through the valve increases and, in consequence, the production pressure tends to decrease. The valve in this case might never close but the injection pressure will fluctuate as shown in Fig. 11.48.

The other factor that makes it very difficult to predict what will happen if the calibrated valve at the point of injection closes is the different modes of operation at which the surface gas injection control valve might be working. This valve might be manually operated, so that the gas flow rate through it might be constant (if it is operating under critical flow), or the gas flow rate might be variable (if the surface control valve is operating under subcritical flow). On the other hand, the surface gas injection control valve might be

operated by a control system that will try to keep the gas flow rate at a given set point, but this control system might not behave properly if the operating gas lift valve is opening and closing (it might very well make things worse).

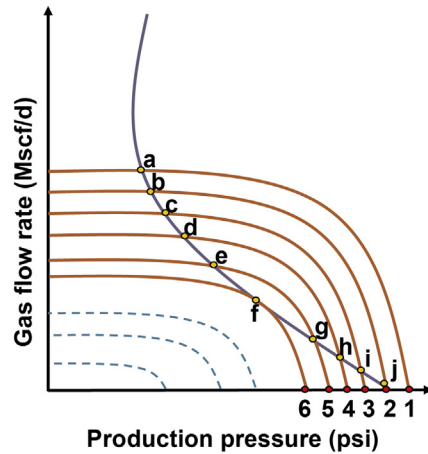
When there is a calibrated valve at the point of injection, the difference between the operating injection pressure (by design) at depth (which should be taken as the minimum acceptable injection pressure) and the production pressure at the point of injection, should be, at least, equal to the value of the uncertainties of the production pressure plus 10% of the operating injection pressure at depth. It has already been mentioned in several places in this chapter that it is important to have a pressure drop across the gas lift valve equal to, at least, 10% of the gas injection pressure at valve's depth to avoid the kind of stability problems that are presented in chapter: Gas Flow Through Gas Lift Valves, see Fig. 8.4. But if there is an uncertainty in the expected value of the production pressure, this uncertainty has to be added to this 10% difference. The uncertainty in the production pressure depends on how accurately the following variables are known: water cut, gas/oil ratio, liquid production, and the accuracy of the multiphase flow correlation being used. The designer has to estimate these uncertainties with the use of nodal analyses during the inspection of the stability of the design.

The difference between the injection pressure that will open the upper unloading valve and the operating pressure of the calibrated valve at the point of injection (this difference is the width of zone "1" in Fig. 9.53a) gives the range of injection pressures that provides the design its flexibility to handle changes in the operational conditions of the well. This range should be at least 50 psi greater than the sequential pressure drop per valve.

When there is an orifice valve at the operating point of injection (which is the usual case), the operating pressure easily changes in value because of the lack of the regulating effect that calibrated valves show. The operating pressure in this case depends only on the production pressure, the gas flow rate, and the size of the orifice. With orifice valves, the range of operating pressures is usually greater than the available range when a calibrated valve is installed at the point of injection. If there is a reduction in the gas flow rate that enters the production tubing, the tubing pressure can increase to large values and even become greater than the injection pressure at valve's depth (gas injection into the tubing will stop at this point).

The criterion explained here to find the minimum pressure that ensures stability is due to Wim der Kinderen (he has presented his theory in several seminars but has not published it and it is presented here with his permission). This criterion is currently offered by several commercially available computer programs. The reader is advised to review the explanation given



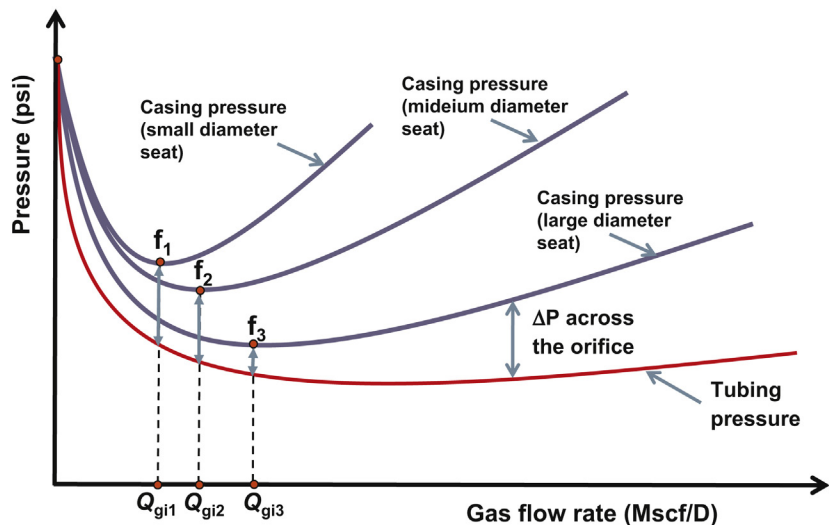


■ FIGURE 9.54 Minimum stable injection gas flow rate.

in chapter: Total System Analysis Applied to Gas Lift Design, for Fig. 5.25 to understand how Fig. 9.54 is constructed.

Fig. 9.54 shows six orifice flow curves (constructed as indicated in chapter: Gas Flow Through Gas Lift Valves, for Fig. 8.1a) corresponding to injection pressures at depths from 1 to 6. These curves correspond to the zone that lies between zone A and B in Fig. 5.25. The production pressure, at the depth of the orifice valve and for each injection gas flow rate, is also shown in Fig. 9.54 (this is the curve that goes from point “a” to “j”). Points “a” to “j” are the so-called equilibrium points (for a given set of reservoir, wellhead, and injection pressure, there is one and only one injection gas flow rate and production pressure, which is the pressure and gas flow rate at a given equilibrium point). Decreasing the injection pressure from point 1 to 6, means that the equilibrium points will have to go from “a” to “f” with the corresponding reduction in the gas flow rate. If the gas flow rate is further reduced to zero (if it could be possible to accomplish in a stable manner) the injection pressure will have to increase from point 6 to point 2, corresponding to equilibrium points “f” to “j.” According to Wim der Kinderen, equilibrium points from “f” to “j” correspond to unstable points and, in consequence, injection pressure at point 6 is the minimum injection pressure at which the well can be operated in a stable manner.

Fig. 9.55 provides an easier way of presenting the information given in Fig. 9.54. In Fig. 9.55, points  $f_1$ ,  $f_2$ , and  $f_3$  correspond to the minimum stable gas flow rates (and injection pressures) for seats of increasing sizes (the injection gas flows from the casing-tubing annulus to the production tubing in this example). As can be seen in the figure, small size seats will be stable



■ FIGURE 9.55 Wim der Kinderen's instability criterion.

at lower gas flow rates (which correspond to higher injection pressures). As the gas flow rate is reduced beyond point “f,” the production pressure increases because of the lack of lift gas in the tubing and this pressure increase in turn makes the gas injection pressure in the annulus increase (because there must be a pressure drop across the valve to inject gas into the tubing).

When inspecting the stability of a gas lift design with an orifice valve installed at the operating point of injection, the production pressure at the depth of the orifice valve should be equal to the calculated production pressure (the one found in the design) plus the differential increase in production pressure due to the total uncertainties involved in its calculation (which are due in turn to the uncertainties in the water cut, gas/oil ratio, multiphase flow correlation, etc.). From this greater production pressure, the minimum pressure drop through the orifice valve should be equal to the pressure drop predicted by the Wim der Kinderen criterion or to 10% of the injection pressure at depth (whichever is larger). The 10% rule is specially recommended for large orifices but it represents an optional safety factor for seats of all sizes. The difference between the minimum operating pressure determined in this way and its upper limit (the limit that is set to avoid opening the upper unloading valve) should be equal to at least 50 psi greater than the sequential pressure drop per valve.

Other causes of gas lift instabilities, different from the ones induced by a faulty gas lift design, are: (1) emulsions in the tubing and flow line, (2)

hydrates in the surface gas injection system, (3) pressure fluctuation in the gas lift system (caused by compressor shutdowns, well trips, etc.), (4) a hole in the production tubing, (5) damaged gas lift valves, and (6) faulty surface gas injection control system, etc. All these causes are explained in detail in chapters: Continuous Gas Lift Troubleshooting and Intermittent Gas Lift Troubleshooting.

## 9.4 EXAMPLES OF GAS LIFT DESIGNS

### Problem 9.1

Use the data given in chapter: Total System Analysis Applied to Gas Lift Design, Section 5.3.1 (for a well that can produce on natural flow) to find the gas lift designs that can handle water cuts of 30, 40, and 50%. As explained in chapter: Total System Analysis Applied to Gas Lift Design, even though the well can produce on natural flow, gas lift will be needed to boost the total liquid production of the well in order to meet the required oil production for the next 5 years (the reader is advised to review the example problem presented in Section 5.3.1 in which the preliminary necessary calculations for the gas lift designs are presented). Use sequential drops in the closing pressure of IPO unloading valves as the mandrel spacing method. Use the injection gas flow rates found in the preliminary calculations given in chapter: Total System Analysis Applied to Gas Lift Design, for two levels of the available kickoff pressure: 1800 and 1450 psig (for which the operating surface injection pressures of the first, shallowest, unloading valve will be equal to 1750 and 1400 psig, respectively). Determine the advantage, if any, of increasing the kickoff pressure from 1450 to 1800 psig. Perform the gas lift designs with the following data: wellhead production pressure: 350 psig; wellhead injection gas temperature: 80°F; injection gas specific gravity: 0.8; minimum pressure drop across the operating orifice (at the point of injection under normal operation of the well): 250 psi; sequential pressure drop per unloading valve: 50 psi; locating valve depth differential pressure (injection pressure minus production pressure at valve's depth when it is uncovered): 20 psi; and production transfer pressure: equal to the production pressure at valve's depth plus 10% of the difference between this production pressure and the gas injection pressure at valve's depth.

For each water cut, two gas lift designs should be found (corresponding to the minimum and maximum kickoff pressures and their respective gas flow rates given in chapter: Total System Analysis Applied to Gas Lift Design, Table 4): (1) for 30% water cut, use a gas injection rate of 1.8 MMscf/D

for a kickoff pressure of 1800 psig and 2.6 MMscf/D for a kickoff pressure of 1450 psig, (2) for 40% water cut, use a gas injection rate of 2.6 MMscf/D for a kickoff pressure of 1800 psig and 4.2 MMscf/D for a kickoff pressure of 1450 psig (for this latter case, higher gas flow rates will not increase the liquid flow rate in a significant way), and (3) for 50% water cut, use a gas injection rate of 3.6 MMscf/D for a kickoff pressure of 1800 psig and 4 MMscf/D for a kickoff pressure of 1450 psig (again for this latter case, higher gas flow rates will not increase the liquid flow rate in a significant way).

After all six designs are completed, determine the best possible mandrel spacing (for each level of the available kickoff pressure) that will be capable of handling all water cuts being considered in this problem.

Answer. For 30% water cut, 1800 psig kickoff pressure, and 1.8 MMscf/D of gas injection rate, two gas lift mandrels are required (one for the unloading valve at 3592 ft. TVD and the other for the orifice valve at the point of injection at 5199 ft. TVD). The design values for each valve are given in [Table 9.2](#).

For 30% water cut, kickoff pressure of 1450 psig, and 2.6 MMscf/D of gas injection rate, two gas lift mandrels are required (one for the unloading valve at 2610 ft. TVD and the other for the orifice valve at the point of injection at 3834 ft. TVD). The design values for each valve are given in [Table 9.3](#).

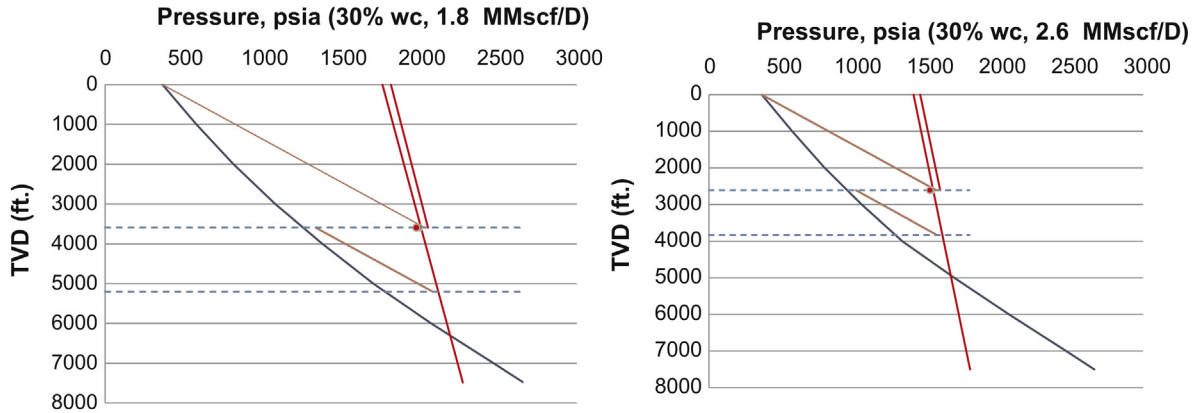
The graphs of the designs are presented in [Fig. 9.56](#).

**Table 9.2** Design for 30% Water Cut and 1800 psig Kickoff Pressure

Valve Depth (ft. TVD)	Port Diameter (in.)	$P_{tr}$ (psig)	Opening Surface P. (psig)	Closing Surface P. (psig)	Gas Flow Rate (MMscf/D)	Liquid Production (STBL/D)	Max. Valve Throughput (MMscf/D)
3592	0.1875	1542	1750	1735	0.418	9,076	0.953
5199	0.3125	—	—	—	1.8	10,015	2.6

**Table 9.3** Design for 30% Water Cut and 1450 psig Kickoff Pressure

Valve Depth (ft. TVD)	Port Diameter (in.)	$P_{tr}$ (psig)	Opening Surface P. (psig)	Closing Surface P. (psig)	Gas Flow Rate (MMscf/D)	Liquid Production (STBL/D)	Max. Valve Throughput (MMscf/D)
2610	0.1875	1192	1400	1388	0.509	8975	0.745
3834	0.375	—	—	—	2.6	9991	3.01



■ FIGURE 9.56 Gas lift designs for 30% water cut.

**Table 9.4** Design for 40% Water Cut and 1800 psig Kickoff Pressure

Valve Depth (ft. TVD)	Port Diameter (in.)	$P_{tr}$ (psig)	Opening Surface P. (psig)	Closing Surface P. (psig)	Gas Flow Rate (MMscf/D)	Liquid Production (STBL/D)	Max. Valve Throughput (MMscf/D)
3592	0.1875	1542	1750	1735	0.829	8907	0.953
5224	0.375	—	—	—	2.6	9985	3.67

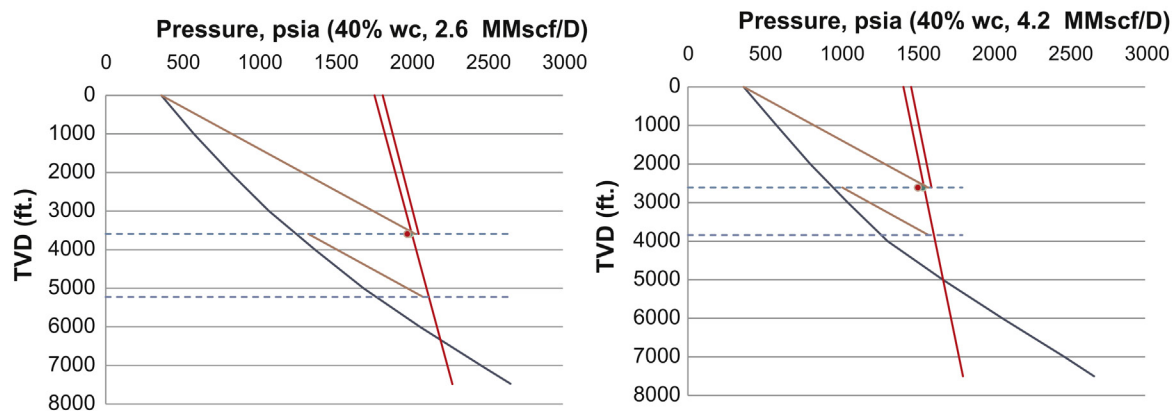
**Table 9.5** Design for 40% Water Cut and 1450 psig Kickoff Pressure

Valve Depth (ft. TVD)	Port Diameter (in.)	$P_{tr}$ (psig)	Opening Surface P. (psig)	Closing Surface P. (psig)	Gas Flow Rate (MMscf/D)	Liquid Production (STBL/D)	Max. Valve Throughput (MMscf/D)
2610	0.25	1224	1400	1369	0.825	8570	1.44
3840	0.5	—	—	—	4.2	9897	5.19

For 40% water cut, kickoff pressure of 1800 psig, and 2.6 MMscf/D of gas injection rate, two gas lift mandrels are required (one for the unloading valve at 3592 ft. TVD and the other for the orifice valve at the point of injection at 5224 ft. TVD). The design values for each valve are given in [Table 9.4](#).

For 40% water cut, kickoff pressure of 1450 psig, and 4.2 MMscf/D of gas injection rate, two gas lift mandrels are required (one for the unloading valve at 2610 ft. TVD and the other for the orifice at the point of injection at 3840 ft. TVD). The design values for each valve are given in [Table 9.5](#).

The graphs of the designs are presented in [Fig. 9.57](#).



■ FIGURE 9.57 Gas lift designs for 40% water cut.

**Table 9.6** Design for 50% Water Cut and 1800 psig Kickoff Pressure

Valve Depth (ft. TVD)	Port Diameter (in.)	$P_{tr}$ (psig)	Opening Surface P. (psig)	Closing Surface P. (psig)	Gas Flow Rate (MMscf/D)	Liquid Production (STBL/D)	Max. Valve Throughput (MMscf/D)
3592	0.25	1585	1750	1711	1.22	8719	1.85
5248	0.4375	—	—	—	3.6	9984	4.85

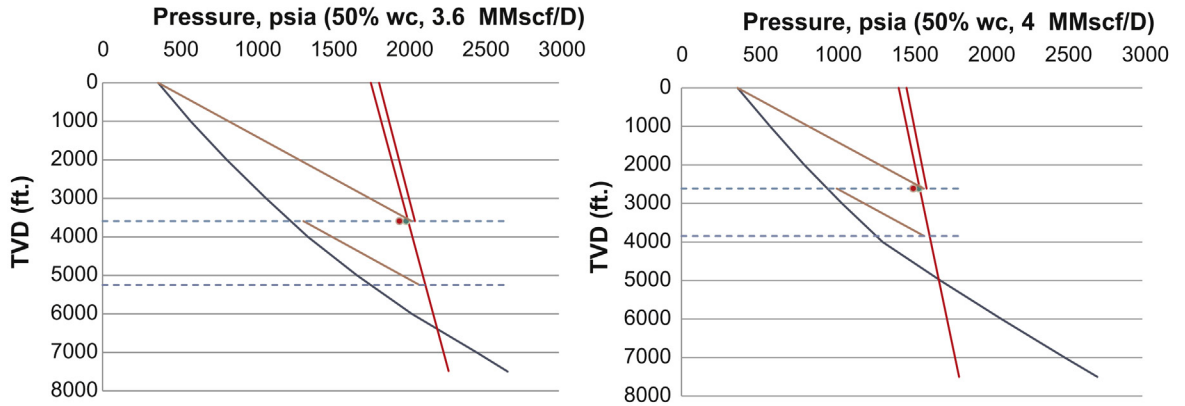
**Table 9.7** Design for 50% Water Cut and 1450 psig Kickoff Pressure

Valve Depth (ft. TVD)	Port Diameter (in.)	$P_{tr}$ (psig)	Opening Surface P. (psig)	Closing Surface P. (psig)	Gas Flow Rate (MMscf/D)	Liquid Production (STBL/D)	Max. Valve Throughput (MMscf/D)
2610	0.25	1223	1400	1369	1	8125	1.44
3846	0.5	—	—	—	4	9563	5.17

For 50% water cut, kickoff pressure of 1800 psig, and 3.6 MMscf/D of gas injection rate, two gas lift mandrels are required (one for the unloading valve at 3592 ft. TVD and the other for the orifice at the point of injection at 5248 ft. TVD). The design values for each valve are given in [Table 9.6](#).

For 50% water cut, kickoff pressure of 1450 psig, and 4 MMscf/D of gas injection rate, two gas lift mandrels are required (one for the unloading valve at 2610 ft. TVD and the other for the orifice at the point of injection at 3846 ft. TVD). The design values for each valve are given in [Table 9.7](#).

The graphs of the designs are presented in [Fig. 9.58](#).



■ FIGURE 9.58 Gas lift designs for 50% water cut.

**Table 9.8** Liquid Flow Rate and Injection Gas/Oil Ratio for the Two Available Kickoff Pressures

Water Cut (%)	Available Inj. P. 1450 psig		Available Inj. P. 1800 psig		Incr. Liquid Production (%)	Incr. IGOR (%)
	Liquid flow rate (STBLD)	IGOR (scf/STBO)	Liquid flow rate (STBLD)	IGOR (scf/STBO)		
30	9,991	372	10,034	256	0.43	-31
40	9,897	707	10,003	433	1.07	-39
50	9,563	836	10,005	720	4.62	-14

The liquid production and the injection gas/oil ratio, for each water cut and kickoff pressure, are presented in Table 9.8. The percent increase in the liquid production, as well as the decrease in the injection gas/oil ratio, in going from a kickoff pressure of 1450–1800 psig, is also presented in the table. The increase in liquid production is not very significant (no greater than 5%). Although not very large, the reduction of the injection gas/oil ratio, on the other hand, constitutes the only advantage of increasing the kickoff pressure to 1800 psig. If the kickoff pressure is 1800 psig, the injection gas/oil ratio is larger than 500 scf/STBO only for a water cut of 50%; but, for a kickoff pressure of 1450 psig, the injection gas/oil ratio is larger than 500 scf/STBO for water cuts of 40 and 50%.

The pressure drop across the orifice valve should be approximately equal to no less than 10% of the injection pressure at depth (just upstream of the orifice valve) to avoid gas lift instabilities. This percentage is presented in Table 9.9. Because the minimum pressure drop across the injection orifice (imposed during the gas lift design calculations) was the same for both

**Table 9.9** Pressure Drop Across the Injection Orifice (As a Percentage of the Injection Pressure) and the Range of Injection Pressure Available at the Depth of the Point of Injection

Water Cut (%)	Pressure Drop Across Orifice (%)	Oper. Inj. Pressure Range (psi)	Pressure Drop Across Orifice (%)	Oper. Inj. Pressure Range (psi)
	1450 psig Kickoff Pressure		1800 psig Kickoff Pressure	
30	15	319	8	335
40	14	346	10	355
50	13	341	9	366

kickoff pressures, it can be seen that the pressure drop represent a larger percentage of the injection pressure at depth for a kickoff pressure of 1450 psig and, in consequence, the gas lift designs might be slightly more stable for this kickoff pressure; but the pressure drop across the orifice for a 1800-psig kickoff pressure is still within acceptable levels. The range of the operating injection pressures is also presented in Table 9.9. This range of operating pressures is equal to the maximum acceptable injection pressure (above which an upper unloading valve might open) at valve's depth minus the production pressure also at the depth of the orifice valve. As can be seen in the table, the ranges of operating pressures are slightly wider for a kickoff pressure of 1800 psig, thus the gas lift designs are equally flexible for both kickoff pressures.

As for the depths of the operating orifice valves and the unloading valves, it can be seen from the designs presented above that, for a given kickoff pressure, the unloading valve's depth is the same for all water cuts and the depth of the operating valve is not affected very much by the value of the water cut (a maximum difference of only 49 ft. for a 1800-psig kickoff pressure and 12 ft. for a 1450-psig kickoff pressure). Thus, for a given kickoff pressure, the shallowest operating mandrel (where the orifice valve will be installed) can be taken as the operating point of injection for all water cuts.

In conclusion, regarding the production flow rate and the injection gas/oil ratio, the advantages of increasing the kickoff pressure from 1450 to 1800 psig are not very significant and additional factors (such as cost of gas compression and distribution) should be considered in order to reach a final decision regarding the kickoff pressure that should be used. If an injection pressure of 1800 psi is already available, larger sequential pressure drops per valve, as well as larger minimum pressure drops at the point of injection, can be considered. Gas lift mandrels will be located at shallower depths but the gas lift designs will be very stable and with no significant loss in the liquid production or increase in the injection gas/oil ratios.



## REFERENCES

- Lagerlef, D.L., Smalstig, W.H., Erwin, M.D., 1992. Gas-lift-valve test rack opening design methodology for extreme kickoff temperature conditions. SPE paper 24065.
- Pothapragada, V.K., 1996. Transient aspects of unloading gas-lift wells. M.S. Thesis. University of Tulsa, Oklahoma, USA.
- Tang, Y.L., 1998. Transient dynamic characteristics of gas-lift unloading. M.S. Thesis. University of Tulsa, Oklahoma, USA.

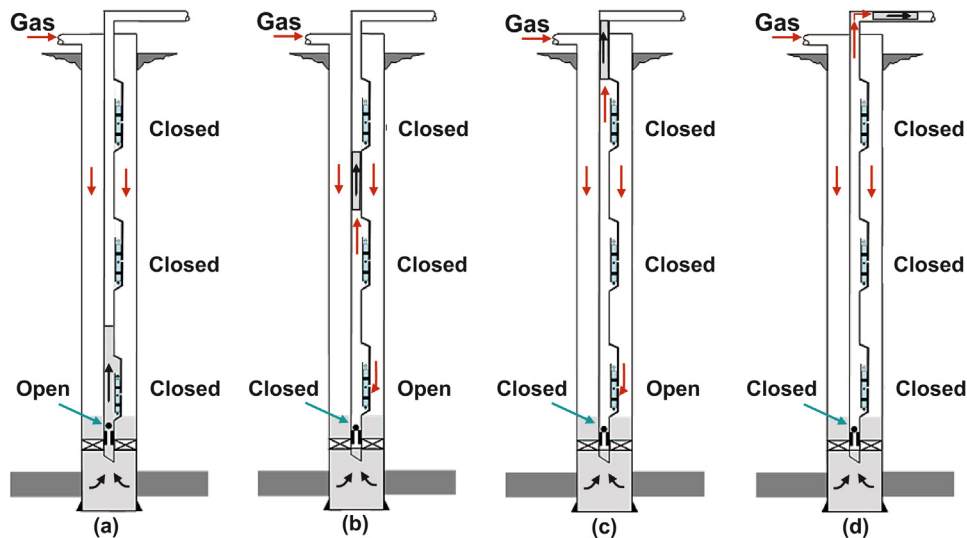
# Design of intermittent gas lift installations

Several design techniques corresponding to different types of installations and surface-gas-injection control systems for intermittent gas lift are presented in the chapter. Recommended practices regarding the operation of downhole equipment and surface facilities, as well as the selection of the right type of completion for the different possible operational conditions, are also presented.

## 10.1 DESCRIPTION OF THE PRODUCTION CYCLE

Intermittent gas lift consists of injecting high-pressure gas, mostly stored in the annulus, into the production tubing at predetermined time intervals and volumes per cycles. The gas enters the tubing through a single point of injection, usually located as deep as possible in the well. The liquid slug that is generated in the tubing above the point of injection is lifted to the surface thanks to the work done by the injection gas at each cycle. Fig. 10.1 shows the description of one complete production cycle.

The subsurface gas lift operating valve (usually the deepest one in the well) is closed at the beginning of the cycle and the liquid column is growing in length in the tubing above this valve. At the same time, the injection pressure in the annulus is increasing because gas is being continuously injected at the surface into the annulus of the well. The combined effect of the injection and production pressures eventually opens the gas lift valve, allowing a high gas flow rate into the tubing string that pushes the liquid column towards the surface. While the liquid slug travels to the surface, the annular injection pressure is decreasing because the gas flow rate through the operating gas lift valve is much greater than the gas flow rate injected into the annulus at the surface. When the entire liquid slug has been produced to the surface, the injection pressure should have dropped to the gas lift valve's



■ FIGURE 10.1 Production cycle.

injection closing pressure. The operating gas lift valve then closes to start a new cycle. During the time gas is injected into the tubing, the standing valve located below the gas lift valve is closed; however, the flowing bottomhole pressure below the standing valve increases during this period of time due to the action of the reservoir. The two upper unloading valves shown in Fig. 10.1 should remain closed at all times for this type of design.

Throughout the production cycle just described, the gas flow rate is injected at the surface at a constant rate, which is usually a very small flow rate compared with the instantaneous gas flow rate through the operating gas lift valve while it is open. The gas flow rate at the surface is kept at a predetermined value by installing a choke in the gas injection line. The diameter of this “gas injection” choke is selected so that the flow across it is maintained at a constant value, for which the gas flow must be critical. Many times, instead of having a choke with a fixed diameter, a needle valve is used to control the gas flow rate. This valve makes it possible for the surface gas flow rate to be fine tuned to any desired value without effort.

The production cycle just described corresponds to what is called “choke-control intermittent gas lift.” For reasons that are explained in Section 10.5, it is some times recommended to control the surface gas injection in a different manner, with an automatic “on-off” or “open/close” surface control valve, also known as an “intermitter.” With this type of control, the production cycle is described as follows.

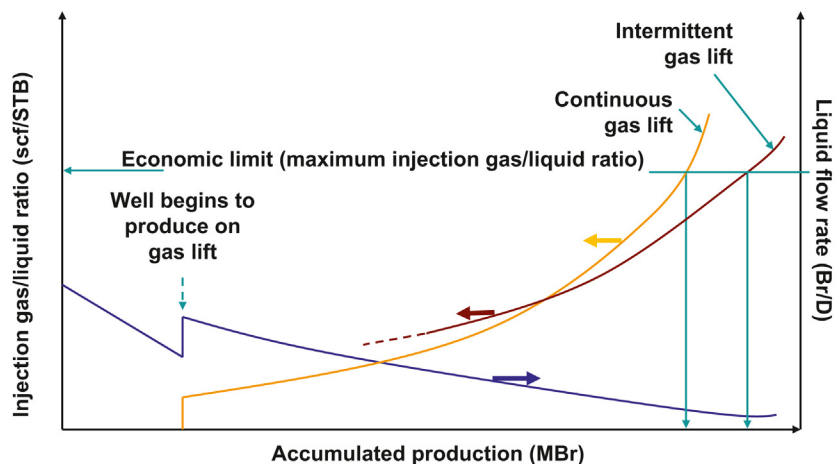
At the beginning of the cycle, the surface controller and the gas lift valve are both closed and the liquid slug is being generated above the gas lift valve. Then, after a predetermined period of time, the surface controller opens and allows a very high gas flow rate to enter the well's annulus. This makes the annular pressure increase very rapidly to achieve a value equal to the subsurface gas lift valve's injection opening pressure. If calculations were properly carried out, the gas flow rate through the intermitter must be much higher than the gas flow rate through the gas lift valve. This allows the injection pressure to keep increasing while the intermitter and the gas lift valve are opened at the same time; therefore, the gas lift valve can remain open for as long as the surface intermitter is opened. After a predetermined time period, the surface intermitter closes and because the gas lift valve is still open, the injection pressure begins to drop until the gas lift valve's closing pressure is reached. The time intervals during which the surface intermitter remains opened and closed can be set to change the total cycle time and the volume of gas injected per cycle "independently" of one another (which is something that cannot be attained with choke-control intermittent gas lift) and that is the main advantage of using surface intermitters.

## 10.2 GENERAL FUNDAMENTALS AND IMPLEMENTATION GUIDANCE FOR INTERMITTENT GAS LIFT

As the reservoir pressure declines, the injection gas/liquid ratio increases for both continuous and intermittent gas lifts. Fig. 10.2 shows how the injection gas/liquid ratio increases as the accumulated production increases, eventually reaching a point at which it is not economically feasible to produce the well because the production costs are greater than the revenues obtained from the sell of the crude oil.

Shifting from continuous to intermittent gas lift is primarily done to reduce the injection gas/liquid ratio. It is possible that by switching to intermittent gas lift the production of the well increases but, with a few exceptions, this only happens when the production of the well was not optimized while it was producing on continuous gas lift.

Before shifting from continuous to intermittent gas lift, it is convenient to know if it is possible (and economically feasible) to stay on continuous gas lift by replacing the current production tubing string with another one that has a smaller inside diameter. It is necessary to perform nodal and economic analyses to determine if the cost of changing the tubing diameter could be



■ FIGURE 10.2 Injection gas/liquid ratio as a function of the well's accumulated production.

justified. Those wells that have equal performances on continuous and intermittent gas lift should be kept on continuous gas lift because it is better for the efficiency of the compression system to do so and to avoid the extra cost of operation and maintenance usually associated with intermittent gas lift operations. Operationally, continuous gas lift is more practical and simpler. Intermittent gas lift is only recommended when there is no other alternative to keep the injection gas/liquid ratio within an acceptable limit.

With the well already on intermittent gas lift, as the reservoir pressure declines the liquid columns becomes smaller and the injection gas/liquid ratio increases, eventually reaching a value at which it is no longer economically feasible to produce the well. This maximum injection gas/liquid ratio can temporarily be maintained by simply increasing the cycle time. This allows the liquid columns to increase in size but the total daily production is reduced because fewer cycles per day are produced.

There is one and only one cycle time at which the daily production is maximized. This cycle time is called “optimum cycle time (OCT).” If the injection gas/liquid ratio has reached its economic limit, it could still be kept lower than the economic limit for a while by allowing the cycle time to be greater than the OCT but, as mentioned earlier, the daily production is reduced in the process. If the reservoir pressure continues to decrease, a point will be reached in which it would not matter how long the cycle time becomes, the injection gas/liquid ratio will be above the maximum economic limit. At this point, the only way to produce the well in a profitable way is by using a special type of completion such as the “accumulation chambers”

or the “accumulators” described in chapter: Gas Lift Equipment. Design methods for these special types of completions are presented in the chapter.

There is no general rule that would help decide when to shift from continuous to intermittent gas lift. Some specialists indicate that the well should be produced on intermittent gas lift when the reservoir pressure is less than or equal to 150 psig per each 1000 ft. of depth of the top of the perforations. Other specialists recommend producing the well on intermittent gas lift if the reservoir static liquid level is less than or equal to one-third the depth of the top of the perforations. But these general rules do not apply to all wells in the same manner. Not all wells that should be on intermittent gas lift according to these rules will perform better on intermittent gas lift for reasons that have to do with the completion of the well itself and with the characteristics of the surface facilities that handle the production of the well. In other words, changing the production method to intermittent gas lift might not reduce the injection gas/liquid ratio or it might not be feasible because of current limitations in fluid separation or handling capacities of the surface facilities.

The general rules previously mentioned are based on the reservoir pressure because this is the most important variable to consider when shifting to intermittent gas lift. However, as indicated in the previous paragraph, besides the reservoir pressure, there are other factors that affect the injection gas/liquid ratio. If the velocity of the liquid slug can be maintained around its recommended value for intermittent gas lift (which is approximately equal to 1000 ft./min), the injection gas/liquid ratio mainly depends on the following three factors: (1) injection point depth, (2) viscosity of the liquids being lifted, and (3) the initial liquid column length (which usually corresponds to the liquid column length at the OCT). The initial liquid column length is the length of the liquid column just before the gas lift valve opens. This column length is really a function of the reservoir pressure and, as previously mentioned, is the most important variable to consider. The influence of these factors is explained as follows.

The deeper the injection point depth is, the greater the injection gas/liquid ratio will be required for a given liquid column length because the length of the tubing that needs to be filled with injection gas to lift the liquid column to the surface is greater.

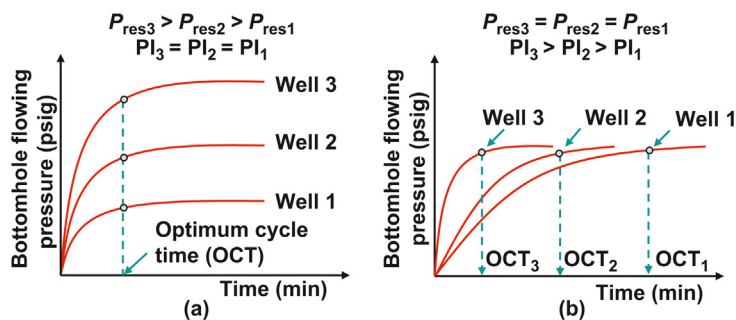
Highly viscous fluids require larger injection gas/liquid ratios because more work is needed to overcome the friction that is generated as the liquid slug travels to the surface. Additionally, viscous fluids cause greater liquid fallback losses, which are defined as that portion of the initial liquid slug that is not produced to the surface because it adheres to the tubing walls as the slug travels upwards.

Finally, for a given point of injection depth, the injection gas/liquid ratio increases as the liquid slugs become smaller. As much as it is true that smaller slugs need less gas to be lifted, it is also true that this reduction in the required volume of gas per cycle is not very significant and the injection gas/liquid ratio ends up being greater for small liquid slugs.

The daily production of the well depends on the productivity index (PI) and the reservoir pressure. These two variables can be independently analyzed.

- Constant PI. As it is demonstrated later in the chapter, for a given value of the PI (keeping everything else constant), the OCT is constant, independently of the reservoir pressure. However, the liquid column length and, therefore, the liquid production, still depend on the reservoir pressure.
- Constant reservoir pressure. For a given reservoir pressure, the OCT depends on the value of the PI or, put in another way, the maximum liquid production depends on the PI. However, in this case because the liquid column length is the same for any PI (given the fact that the reservoir pressure is constant) and equal to the length it would have at the OCT, the volume of gas that is required per cycle does not change. In other words, for a given reservoir pressure and point of injection depth, if the well is produced at the OCT, the injection gas/liquid ratio is going to be the same for different values of the PI (keeping everything else constant), even though the total daily production will change.

In a graphical way, the points expressed in the previous two paragraphs are shown in Fig. 10.3 and they are analytically derived in Section 10.6. Fig. 10.3a shows the same OCT for three wells with the same PI, as well as everything else, but with different reservoir pressures ( $P_{res}$ ). In this case, the daily production and the production per cycle increase directly proportional to the reservoir pressure, but the number of cycles per day is constant.



■ FIGURE 10.3 Effect of the reservoir pressure,  $P_{res}$ , and the productivity index (PI) on the optimum cycle time (OCT).

Fig. 10.3b shows different OCTs for three wells with different values of the PI but with the same reservoir pressure (as well as everything else). Under these conditions, the production per cycle is the same for all wells, but the daily production is greater for the wells with larger PI values, which are capable of generating the same liquid column length in less time.

The PI for intermittent gas lift is in reality the average value this parameter takes within the range of bottomhole pressures encountered in one cycle. The bottomhole pressure usually goes from very low values at the beginning of the liquid column generation period, to values usually less than 50% of the static reservoir pressure at the moment the gas lift valve opens to initiate gas injection into the tubing. When the PI is not known (so that the OCT cannot be calculated), it is a good approximation to assume that the maximum bottomhole pressure would be equal to 50% of the static reservoir pressure when the well is producing at the OCT. The OCT itself cannot be calculated, but the gas lift valve can be set for that maximum bottomhole flowing pressure and then the OCT can be obtained by a trial and error field procedure, changing the cycle time by increasing or decreasing the surface gas flow rate into the well (in case of choke-control intermittent lift) or by changing the time the surface controller remains closed (in case intermitters are used). The correlations used to calculate the IPR curves, like Vogel's correlation, were developed for wells producing under steady state conditions only. Therefore, it is not correct to apply them for wells under intermittent gas lift conditions. But it has been demonstrated (by actual downhole flowing pressure surveys) that a constant PI can be used to analytically model the bottomhole pressure increase during the liquid column generation period as long as this pressure is kept at values less than 50% of the static reservoir pressure. This is explained in [Section 10.6](#) in the analytical derivation of the OCT.

Wells with simple type completions can have small or large formation gas/liquid ratios and any PI value and yet they could still be good candidates for intermittent gas lift if they can reduce the injection gas/liquid ratio and the surface facilities can handle the liquid slugs being produced at each cycle. Accumulation chambers (Fig. 6.57), on the other hand, are recommended for wells with small formation gas/liquid ratios and large PI values to be able to increase the daily liquid production. Regardless of the actual value of the PI, accumulation chambers in wells with small formation gas/liquid ratios can reduce the injection gas/liquid ratio in most situations (if they are properly designed). Wells with large PI values and large formation gas/liquid ratios are good candidates for "accumulators" rather than for accumulation chambers because accumulators can handle formation gas more efficiently (Fig. 6.49). Design methods for accumulation chambers and accumulators are explained later in the chapter in Sections 10.7 and 10.8, respectively.



The portion of the initial liquid column that is not produced to the surface at each cycle is called “fallback loss.” As the liquid slug travels up the tubing, some liquids (that will not be produced to the surface) are left behind, either adhered to the tubing wall, or as small droplets in the gas core. The “liquid fallback factor” is defined as the fraction (expressed from 0 to 1) of the initial liquid column length that is not produced per each 1000 ft. of depth of the point of injection. For example, if the fallback factor is equal to 0.05, it means that 5% of the initial liquid column, per each 1000 ft. of depth of the point of injection, will not be produced. If the operating valve is at 10,000 ft. of depth, the total liquid fallback loss would be equal to 50% of the initial liquid column:  $0.05 \times 10 \times (\text{initial column length})$ .

Liquid fallback losses basically depend on two factors: the viscosity of the liquids being lifted and the travel velocity of the liquid slug. For wells with API gravities greater than approximately  $23^\circ$  API, the effect of liquid viscosity on the liquid fall back losses is negligible. It is usually assumed that the fallback losses for wells with oil gravities greater than or equal to  $23^\circ$  API are between 4 and 6% of the initial liquid slug length per each 1000 ft. of depth of the point of injection as long as the liquid slug velocity is of approximately equal to 1000 ft./min. However, field tests have shown that the fallback losses increase in a considerable and nonlinear way as the viscosity of the oil increases for oils with gravities less than  $23^\circ$  API. This effect induces an increase in the injection gas/liquid ratio ( $R_{gli}$ ). This is the main reason why wells that produce heavy oils are not good candidates to be produced on intermittent gas lift. For crude oils between  $16$  and  $18^\circ$  API, the fallback factor value lies between 0.14 and 0.12, which means that 14–12% of the initial liquid column, per each 1000 ft. of depth of the injection point, is not produced to the surface due to liquid fall back. These fallback factors are valid only if the liquid slug velocity is around its optimum value. If the slug velocity is too low or too high, the fallback factor could increase to reach even 100% of the initial liquid slug length per 1000 ft. of the point of injection depth, regardless of the value of the liquid viscosity.

As indicated earlier, the recommended slug velocity to minimize the liquid fall back is equal to approximately 1000 ft./min. If the slug velocity is too small, the injection gas tends to bubble through the liquid slug. But if the liquid slug velocity is too high, the gas will break through the liquid slug, causing a reduction of the lifting efficiency because the liquid will be produced in a multiphase flow pattern called “mist-flow.” Low liquid velocities are caused by a very low gas injection flow rate into the tubing through the gas lift valve. This low gas flow rate, in turn, could be due to the port of the gas lift valve being too small or an injection pressure that is too small

compared with the production tubing pressure exerted at the bottom of the liquid slug. The value of the instantaneous gas flow rate required to achieve an adequate slug velocity depends on the diameter of the production tubing. Small diameter production tubing requires a small local, or instantaneous, gas flow rate through the gas lift valve and most gas lift systems are able to provide those flow rates. Large diameter tubing strings, on the other hand, require very large gas flow rates through the gas lift valve that many gas lift systems cannot provide.

The value of the water cut also affects the intermittent gas lift method. Field observations have revealed that the efficiency of the method (in terms of standard ft.<sup>3</sup> injected per stock tank barrels of liquids produced) is improved if the water cut is above 60%. It is possible that this is due to the values of the viscosity and specific weight of the liquid water, as well as the usually low dissolved gas/water ratios.

As it was stated earlier (for continuous or intermittent gas lift) the efficiency of the gas lift method decreases for deeper points of injection. For a given reservoir pressure and PI, as the depth of the formation increases, the injection gas/liquid ratio also increases. This is due to the combination of having to use more gas to lift the liquid slug to the surface and the increment in the liquid fallback losses because the liquid slug has to travel greater distances. The gas consumption increases linearly with the depth of the injection point but the injection gas/liquid ratio increases at a greater rate and in a nonlinear manner because of the increase in the liquid fallback losses with increasing depths of the point of injection. As was indicated earlier, if the economic limit for the injection gas/liquid ratio has been reached, the gas consumption per produced barrel of liquid can be lowered by producing longer liquid columns. This can be attained by increasing the cycle time above the OCT, but the daily liquid production will be reduced because the number of cycles per day will be fewer. As indicated, a better solution might be to implement the use of accumulators or accumulation chambers, keeping in mind that there are wells that would not be good candidates for this solution for reasons that are explained later in the chapter.

The dependency of the injection gas/liquid ratio on the depth of the point of injection can be understood from the following derivation.

The volume of gas that must be injected at each cycle to fill the tubing below the liquid slug at the precise moment the slug reaches the surface is calculated using the following equation:

$$V_{\text{cycle}} = A_t L_{\text{val}} \frac{P_{\text{tubing}}}{14.7} \frac{520}{Z_{\text{tubing}} T_{\text{tubing}}} \quad (10.1)$$

Where  $V_{\text{cycle}}$  is the volume of gas injected at each cycle in scf,  $A_t$  is the area of the tubing in square feet,  $L_{\text{val}}$  is the measured depth of the operating valve or point of injection in feet,  $P_{\text{tubing}}$  and  $T_{\text{tubing}}$  are the average absolute pressure and temperature of the gas in the tubing when the liquid slug is produced to the surface, in psia and °R, respectively.  $Z_{\text{tubing}}$  is the gas compressibility factor at  $P_{\text{tubing}}$  and  $T_{\text{tubing}}$ .

On the other hand, the volume of liquid accumulated at the bottom of the well is equal to the length of the liquid slug,  $L_{\text{slug}}$  in feet, multiplied by the tubing area,  $A_t$  in square feet, and divided by 5.61 to express this volume in barrels. This initial volume needs to be multiplied by  $(1 - \text{fallback losses})$  to find the volume of liquid produced per cycle,  $V_{\text{oil}}$ , in barrels. Because the liquid fallback losses are equal to the fallback factor multiplied by the depth of the point of injection in Mft.,  $V_{\text{oil}}$  is given by:

$$V_{\text{oil}} = L_{\text{slug}} A_t \frac{1}{5.61} \left[ 1 - \left( \frac{L_{\text{val}}}{1000} \right) F \right] \quad (10.2)$$

Where  $F$  is the liquid fallback factor expressed from 0 to 1. For example, for a 6% fallback loss per each 1000 ft. of depth of the injection point, the value of  $F$  is equal to 0.06.

The injection gas/liquid ratio ( $R_{\text{gli}}$ ) in scf/STB is obtained from Eq. 10.1 divided by Eq. 10.2:

$$R_{\text{gli}} = \frac{L_{\text{val}} P_{\text{tubing}} \frac{198.45}{Z_{\text{tubing}} T_{\text{tubing}}}}{L_{\text{slug}} \left[ 1 - \left( \frac{L_{\text{val}}}{1000} \right) F \right]} \quad (10.3)$$

As can be seen in this equation, the injection gas/liquid ratio increases by increasing the depth of the point of injection,  $L_{\text{val}}$ , in a nonlinear fashion because this term appears in two places in the equation, in both cases causing the injection gas/liquid ratio to increase but in different proportions.

The size of the liquid column has the opposite effect: as the length of the liquid column increases, the injection gas/liquid ratio is reduced; but this is more difficult to calculate by just looking at Eq. 10.3.

Even though the pressure  $P_{\text{tubing}}$  also increases in direct proportion to the length of the liquid column, the size of the liquid column in the equation plays a more important role and therefore the injection gas/liquid ratio decreases if the length of the liquid slug increases ( $P_{\text{tubing}}$  is not only due to the hydrostatic pressure of the liquid slug but it is also a consequence of the friction losses due to the slug movement).

It can be seen that the area of the tubing is not present in Eq. 10.3 because the increment in the required injection gas volume (if the area increases) is compensated by the increase in the volume of liquid being produced. This is true as long as the gas lift system can provide an injection gas flow rate capable of sustaining a liquid slug velocity of 1000 ft./min. For example, in wells with large diameter tubing, even with an injection pressure capable of lifting the liquid slug to the surface, it might not be possible to implement the intermittent gas lift method in an efficient manner because the very high injection gas flow rate through the gas lift valve that is required to sustain a slug velocity of 1000 ft./min cannot be provided by many gas lift systems. On the other hand, if the tubing diameter is too small, the volume of liquid produced per cycle and the volume of gas injected per cycle are both very small. However, the problem in this case is that the injection frequency must be increased (to maximize the liquid production) such that the fraction of the total cycle time spent injecting gas into the tubing is relatively larger and the daily liquid production cannot be as high as the true potential of the well with a greater (but not too large) tubing diameter.

The size of the injection annulus also plays a major role in the intermittent gas lift method. If the casing diameter is too large, it is possible that the spread (defined as the difference between the opening and closing pressures of the gas lift valve) that is needed to pass just the amount of gas required per cycle might be too small for any commercially available gas lift valve to accomplish. The spread of the valve is proportional to its area ratio. For a very small spread, the required area ratio might be smaller than the minimum available area ratio. Some times this problem can be mitigated by reducing the injection pressure because the spread of the valve is also proportional to the injection pressure. However, this solution needs to be evaluated very carefully so that the liquid slug velocity is not reduced to a point in which the liquid fallback losses are increased. Another possible solution might be to install the injection choke (in case of choke-control intermittent lift) or the intermitter (if the injection is controlled at the surface by on-off valves) near the wellhead and not at the injection manifold, eliminating in this way the volume of the injection gas line between the manifold and the wellhead that would otherwise be injected into the well at each cycle. Large casing diameters affect wells produced on choke control or with the use of intermitters.

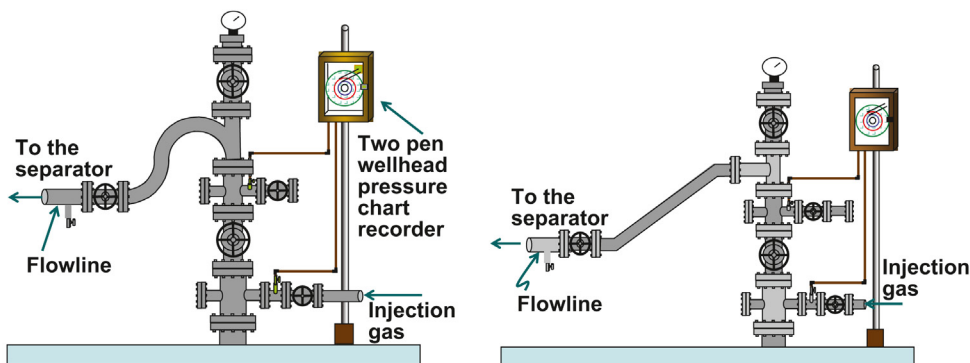
Contrary to the problem outlined in the previous paragraph, if the annular diameter is too small, then it will be necessary to install gas lift valves with large area ratios that would provide large spreads to pass the required volume of gas per cycle for a well on choke-control intermittent lift. If, even

with the largest available area ratio of the gas lift valve, it is not possible to pass all the required volume of gas per cycle, some actions could be taken to attain this required volume of gas, like increasing the injection pressure (which will increase the spread of the valve) or installing the gas surface injection choke as far as possible from the wellhead to inject the gas stored in the gas line. Another solution is to use surface controllers or intermitters to force the gas lift valve to stay open for longer periods of time.

The flowline diameter is another parameter that should be considered. Any increase in the production wellhead pressure can diminish the lifting efficiency of both, continuous and intermittent gas lift methods. In continuous flow, higher wellhead pressures cause higher flowing bottomhole pressures and therefore a reduction of the liquid production. For intermittent gas lift, restrictions at the wellhead and in the flowline can cause a considerable increase in fallback losses if the liquid slug reaches any of these restrictions before the entire liquid slug has been produced to the surface; however, in any case in which the flow is restricted (before or after the entire liquid slug is produced to the surface), the injection gas will not be vented as fast as it should, creating a higher back pressure on the reservoir that would not allow the liquid column to be generated as fast as it would otherwise. It is recommended to have flowlines with inside diameters greater than or equal to the inside diameters of the production tubing. It is not recommended to have several wells on intermittent gas lift producing to the same flowline because the wellhead pressures of all wells will increase every time one of them is produced. Additionally, the flowline must be free of paraffin or any other deposition that might restrict the flow. Smashed or bent flowlines (especially in offshore installations) are not uncommon and usually create unacceptable flow restrictions.

The wellhead and its surroundings are very important. A liquid slug traveling at 1000 ft./min in a 2 $\frac{7}{8}$ -in. tubing has almost the same velocity of the liquids in a continuous gas lift well producing 8000 STB/D. At this velocity, any restriction at the wellhead, or at a point in the flowline close to the wellhead, can cause large liquid fallback losses. All Ts and elbows that are not necessary must be removed and, if possible, special wellheads such as those shown in Fig. 10.4 should be used to reduce liquid fallback losses while still being able of performing wireline interventions.

Choke housings should be removed because their inside diameters might be too small, even with no chokes installed in them. Sometimes, when the separator is not capable of handling the liquid slugs produced in intermittent gas lift, it becomes necessary to install a surface choke in the flowline to reduce the liquid slug velocity. This solution should only be implemented



■ FIGURE 10.4 Special wellhead arrangements for intermittent gas lift.

if it is a temporary solution because the choke will not allow the injection gas to be vented as fast as it should. If it is absolutely necessary to install a surface choke, it should be installed as far as possible from the wellhead to make sure that the entire liquid slug has been produced to the surface before it reaches the choke; otherwise, the liquid fallback losses would be too high because the slug velocity could be greatly reduced while part of the liquid slug is still in the production tubing.

The injection gas line that connects the gas injection manifold to the well must be properly designed to have the minimum possible pressure drop when the gas flow rate reaches its maximum value with the use of surface intermitters. If the gas line diameter is too small, the intermitter should be installed as close as possible to the wellhead. In this way, the gas that flows through the gas line is always at a high pressure, keeping the in situ velocity very low so that the frictional pressure drop is reduced. If it is necessary to further reduce the frictional pressure drop, one economical way of doing it is by connecting a new gas injection line parallel to the existing one. This is called “looping” and it might be less expensive than replacing the current gas injection line by a larger diameter line.

Gas injection lines should also be large when the compressor capacity is limited or the well’s casing–tubing annular volume is small. In these cases, the injection line volume is used as an additional high-pressure-gas storage volume to be used precisely when the well on intermittent gas lift needs it. In this case, the gas injection choke or the intermitter should be installed at the injection manifold and not at the wellhead.

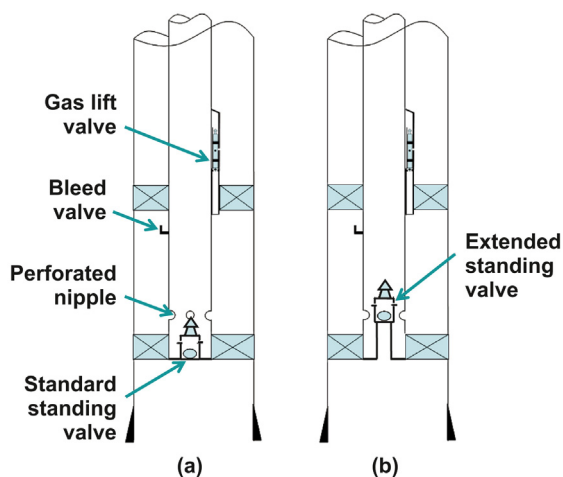
Injection gas lines should be periodically vented to get rid of loose solid particles that could plug gas lift valves. This problem usually happens in old

gas lift systems, where small debris (caused by corrosion) from the inside surface of the gas line are carried by the injection gas into the well. But this problem could also be present in very new gas lines, where it is not uncommon to find solid particles, left inside the pipe when it was installed, traveling with the injection gas into the well. Solid particles traveling with the gas could cause gas lift pilot valves to fail open. Solid particles plug the bleed orifice of the piston installed in the lower section of the pilot valve. Once this orifice is plugged, it is not possible for the piston to return to its close position. This is explained in detail in Section 10.4.

The bleed orifice of the piston, mentioned in the previous paragraph, can be unplugged by first closing the flowline at the wellhead and injecting gas into the tubing and the annulus at the same time. Then, once the injection manifold pressure is reached in the injection line, the gas in the tubing is vented as fast as possible by quickly opening the flowline to the separator. Some operators prefer to vent the annulus instead of the tubing. If this is done, a high-pressure hose should be used to direct the gas flow to the flowline, instead of venting it to the atmosphere because methane can contribute to the greenhouse effect in a way that is even more detrimental than the effect caused by CO<sub>2</sub>. If the bleed orifice of the piston of a pilot valve is plugged with marine depositions, it is possible to unplug it by injecting fresh water down the annulus, taking into account the fact that this operation should not be performed in corrosive environments because CO<sub>2</sub> or H<sub>2</sub>S in presence of water could cause casing and tubing corrosion.

When the surface gas injection control is shifted from choke control to the use of surface intermitters, the internal components of the needle valve, or the needle valve itself, that was used to control the injection gas while the well was producing on choke control, should be removed. Orifice plates with small beta ratios, or any restriction along the injection gas path, should also be removed if it restricts the gas flow when the surface intermitter opens.

Standing valves, installed in the production tubing below the point of gas injection, are highly recommended in intermittent gas lift because they prevent liquids from being injected back into the formation and avoid exposing the formation to the high injection pressures attained at each cycle. Additionally, these standing valves reduce the loss of the injection gas energy that takes place when part of this energy is used in compressing the mixture of gas and liquids below the point of injection (this is why it is recommended to install the standing valve as close as possible to the point of injection). In accumulation chambers (explained in Section 10.3), the use of standing valves is mandatory. If the well produces sand, there are special standing



■ FIGURE 10.5 Accumulation chamber with standing valve: (a) standard type, (b) extended type to handle sand production.

valves (such as the extended valve shown in Fig. 10.5) that are not easily plugged by sand deposition.

It is possible that a well could have the same production with or without a standing valve installed below the point of injection. This happens when the injection pressure is greater than or equal to the required injection pressure to make the liquid slug travel at an adequate velocity (around 1000 ft./min) or when the point of injection is closed to the top of the perforations. In these cases, it is perfectly acceptable to do without standing valves if the formation is not going to be affected by the periodic increase of the bottom-hole pressure. When the injection pressure is small and/or an adequate slug velocity cannot be attained, the use of standing valves could greatly improve the operation of the well.

It is highly recommended to use gas lift pilot valves for intermittent gas lift instead of single-element valves. Pilot valves are described in detailed in Section 10.4. The use of single-element valves is not recommended because with single-element valves it is not possible to increase the port (or seat) diameter, through which the injection gas must pass, without affecting the value of the spread of the valve (which is defined as the difference between the injection opening and closing pressures of the valve). The spread of the valve is proportional to its area ratio (port or seat area divided by the bellows area). In intermittent gas lift, it is very important to inject gas into the tubing at a very high flow rate, which can be attained using large diameter ports. Using large diameter ports in a single-element valve, to increase the



gas flow rate to the required values for intermittent gas lift, might increase the spread of the valve way above the value needed to inject the total volume of gas required per cycle. This results in a large injection gas/liquid ratio, which is precisely the opposite goal of implementing the intermittent gas lift method.

Even though pilot valves are more expensive and have a higher failure frequency because they are more complex than single-element valves, their use represents the only way in which the intermittent gas lift method can be implemented in an efficient manner in most wells. This is due to the fact that these valves have a large main port diameter that is independent of the value of valve's area ratio. This allows these valves to pass a large or small total volume of gas per cycle, but always at a very high instantaneous flow rate. Single-element valves are only recommended (but not always) for wells with a very small casing-tubing annular volume, where large valve spreads are needed; in this case, a single-element valve with a large seat will provide a high gas flow rate and a large spread at the same time.

### 10.3 TYPES OF COMPLETIONS FOR INTERMITTENT GAS LIFT

There are different types of completions that can be used for intermittent gas lift, each of them recommended for specific operational conditions. Well completions for intermittent gas lift are presented in chapter: Gas Lift Equipment. Additional explanations regarding their use and limitations are presented in this section. The reader is advised to review Section 6.4 to obtain additional information on the construction, operation, installation, advantages, and disadvantages of the different types of completions for continuous and intermittent gas lift wells.

[Fig. 10.1](#) shows a single completion that can be used for continuous or intermittent gas lift. The operating valve should be located as close as possible to the top of the perforations because, for intermittent gas lift wells, the reservoir static pressures are usually very low and, in consequence, they generate liquid columns that are not be very long. The completion shown in [Fig. 10.1](#) is the most widely used type of completion for intermittent gas lift and, most of the time, these completions were originally installed in wells producing on continuous gas lift before their reservoir pressures declined. The only changes needed to shift the well to intermittent gas lift are the installation of a pilot valve at the operating point of injection and a standing valve in the tubing below the pilot valve (but as close as possible to it). As mentioned in the previous section, standing valves might not be necessary for some wells. Additionally, if it desired to control the volume of gas (injected per cycle)

from the surface, an intermitter needs to be installed in the gas injection line. For intermittent gas lift to be effective, these changes must be carried out taking into account the recommendations given in the previous section regarding the production tubing diameter, well's annulus, wellhead configuration, the separator capacity, characteristics of the gas injection line, and the flow-line, among other factors.

A simple type completion, without a standing valve installed in the well, is called a "semiclosed" completion. This type of completion (used for continuous gas lift wells) can be used in intermittent gas lift as well, but sometimes they are not recommended because of the reasons already mentioned in the previous section. Liquids might be forced back into the formation and the loss of injection gas energy (by compressing the mixture of gas and liquids below the injection point) could reduce the liquid slug velocity (increasing the fallback losses).

Intermittent gas lift is not recommended if gas is injected down the tubing and liquids are produced up the annulus because of the following reasons. (1) This causes a considerable increase in the liquid fallback losses and in the required injection gas volume per cycle; (2) there would not be an adequate high-pressure injection gas volume stored in the well to be used at each cycle; and (3) if intermitters are used, there will be a large pressure drop of the injection gas along the production tubing that could cause the pilot valve to close before injecting all of the required volume of gas per cycle.

Wells with casings that cannot withstand high injection pressures are usually produced on continuous gas lift with the use of a gas injection pipe, parallel to the production tubing, as shown in Fig. 6.46c. The use of this type of completion is not recommended for intermittent gas lift because of the following reasons:

1. For choke-control intermittent gas lift (with no surface intermitters), there is not a sufficiently large high-pressure-gas volume stored in the well.
2. However, with or without the use of a surface intermitter, the pressure drop along the parallel injection pipe would be too large because of the large gas flow rate that takes place every time the pilot valve opens. The injection pressure that enters the tubing might then be very small to push the liquid slug to the surface. This large pressure drop could also limit the gas injection into the production tubing in two ways:
  - a. The volume of gas injected per cycle is reduced because the pressure drop along the parallel line makes the pilot valve close very quickly.
  - b. On the other hand, the low injection pressure at valve's depth makes the instantaneous gas flow rate through the gas lift valve be much lower than needed for intermittent gas lift applications.

When the casing cannot withstand the high injection pressures needed for gas lift, the whole completion can be isolated by installing an inserted type of completion like those shown in Figs. 6.68 and 6.69. These inserted completions have the major disadvantages of restricting the flow of liquids and gases and having small liquid and injection gas volumetric capacities, not to mention the increase of tubular goods that should be used. But they have the advantage of being able to vent the formation gas before it enters the chamber or the production tubing. Because of this advantage, some operators install these completions in wells with large diameter casings, even if the casings are capable of withstanding the large gas injection pressures needed to lift the liquid slugs to the surface.

When the reservoir pressure has declined to very small values, the liquid columns lifted at each cycle are very small and, as a result of this reduction in liquid slug size, the injection gas/liquid ratio usually becomes very large. One way of increasing the liquid column length is by using accumulation chambers, which allow the production of very large liquid columns at each cycle but do not necessarily increase the daily liquid production. Even though the liquid columns are larger, the liquid slugs produced per day are fewer because it takes longer periods of time to fill accumulation chambers than to generate small liquid columns in the tubing of simple type completions. Accumulation chambers are then installed primarily to reduce the injection gas/liquid ratio and only in few cases, in which the PI values are very large, they can increase the liquid production in a significant way.

Accumulation chambers should not be installed in wells that produce sand because it could be difficult to get rid of the sand, making it very hard to pull the completion out of the well if necessary. They are also not recommended for wells with large formation gas/liquid ratios for the following reasons:

- It might be difficult to vent the formation gas trapped inside the chamber annulus (on top of the liquids) as the chamber is being filled with liquids. This causes the liquid level in the chamber annulus to be lower than the liquid level in the central dip tube.
- However, even if the formation gas can be properly vented, gassy wells tend to fill the chamber with a mixture of gas and liquids that could considerably diminish the net liquid volumetric capacity of the accumulation chamber.

Accumulation chambers are more complex completions; therefore, they increase the probability of mechanical failures. They should then be installed

only when they are really required to lower the injection gas/liquid ratio and the well is indeed a good candidate for this type of completion.

The limitations described earlier for accumulation chambers are analyzed in detail in Section 10.7.

Fig. 6.57 shows a double-packer chamber for which the design procedure is described in Section 10.7. Double-packer chambers have greater volumetric capacity in comparison to all other types of chambers. Three important aspects in the design of accumulation chambers of this type are:

- If, during the mandrel spacing procedure, the deeper unloading valve depth is very close to the upper packer of a double-packer chamber, then one might think that this unloading valve should also be the operating valve. If the injection pressure is large enough to unload the last section of the tubing and the accumulation chamber at the same time, then the last unloading valve can be the operating valve (as is the case in simple type completions). However, if the injection pressure cannot overcome the hydrostatic pressure of the long liquid column to be produced, then two mandrels should be installed at a reasonable distance between them so that wireline operations can be performed in each of these mandrels. The last unloading valve is installed in the upper mandrel and the lower mandrel corresponds to the operating valve.
- The length of the chamber should be checked after the design is completed: if it is too long, it might not be possible to lift the very long liquid slugs that form above the accumulation chamber once all the liquid has entered the production tubing (of smaller diameter). It might also be possible, and undesirable, that the long liquid columns could open the upper unloading valves as they are produced to the surface.
- The calibration of the operating valve is calculated with a small, constant, production pressure, which is equal to the production wellhead pressure plus the weight of the gas column above the operating valve. This is because there should not be liquid accumulation above the operating valve of a double-packer chamber. For simple type completions, the production pressure at valve's depth is not constant but it increases as the liquid column is being generated above the operating valve.

When the perforated interval, or the rat hole, is long and the casing diameter is large enough, inserted accumulation chambers like that shown in Fig. 6.61 can be installed to increase the liquid flow rate and reduce the injection gas/

liquid ratio. They are recommended in these cases because they can reduce the injection gas/liquid ratio and increase the liquid production, even if the PI is small because they create a large drawdown that is constant throughout the cycle.

But the following operating difficulties might be encountered:

- The size of the port of the bleed valves (for the inside of the chamber and outer casing-chamber annulus) should be properly determined to vent without problem the formation gas between the perforations and the chamber and the gas that accumulates inside the chamber's annulus.
- Even though they handle formation gas better than double-packer chambers do, formation gas might still create operating problems.
- They are not recommended for wells that produce sand (difficulty in pulling the completion or to perform wireline jobs).
- The completion is even more complex than double-packer chambers, thus the possibility of mechanical failure is increased.

Other types of inserted chambers are presented in Figs. 6.62–6.67, together with their advantages and disadvantages.

When the gas/liquid ratio is very large, it is better to install simple type accumulators (as that shown in Fig. 6.49), which have a smaller liquid volumetric capacity (compared with accumulation chambers) but they are capable of handling formation gas in a more efficient way. These simple accumulators present the following advantages:

- They can reduce the injection gas/liquid ratio and might increase liquid production if the PI is large.
- They are not as complex as double-packer or inserted chambers are and they are especially suitable for gassy wells.

But attention should be paid to the following points:

- They have the lowest volumetric capacity compared to any type of accumulation chamber and, therefore, it might be difficult to increase the daily liquid production even if the PI is large.
- The inside diameter of the accumulator should not be too large because this might increase the liquid fallback losses while the liquids are being displaced by the injection gas inside the accumulator (for not reaching a suitable slug velocity due to the fact that the gas lift system might not be able to provide the required large instantaneous injection gas flow rate for large diameter tubing). The accumulator should be installed at

about 100 ft. above the operating valve (a tubing diameter smaller than the accumulator diameter should be installed between the packer and the lower end of the accumulator). In this way, when the gas finally enters the accumulator, the liquid has already acquired a velocity that will minimize the large fallback losses that would be present if the gas is directly injected into the accumulator.

- Additionally, accumulators have the same problems explained earlier for accumulation chambers: if the diameter of the accumulator is too large, the liquid columns could be too long once all the liquids have entered the production tubing (which has a smaller diameter) above the accumulator. It is possible then that the injection pressure might not be large enough to lift these long liquid columns at a sufficiently large velocity to keep the liquid fallback losses at small values. Large liquid slugs can also open one or several of the upper unloading valves, decreasing in this way the lifting efficiency.

If, in addition to a large formation gas/liquid ratio, the well has a very long perforated interval or rat hole, it is recommended to install inserted accumulators as shown in Fig. 6.70, which can handle formation gas much better than inserted accumulation chambers can. The advantages of inserted accumulators are:

- They can reduce the injection gas/liquid ratio.
- They can increase the liquid production, even in wells with low PI values because of the large drawdown they can achieve and maintain throughout the production cycle.
- The formation gas can be managed very well if the right design is installed in the well (as described later).
- This type of completion is not as complex as inserted chambers are. This reduces the possibility of mechanical failures.

But attention should be paid to the following points:

- The gas lift valve should be installed in the upper mandrel (right above the packer) and not in the lower one at the bottom of the accumulator, otherwise the friction pressure drop along the injection pipe (parallel to the accumulator) would make the gas lift valve close before the injection pressure in the well's annulus (above the packer) have dropped to the necessary pressure to inject the required gas volume per cycle.
- The inside diameter of the accumulator should not be very large to avoid: (1) large fallback losses during the first stages of gas injection

into the accumulator (because of the high instantaneous gas flow rate that would be required); and (2) generating very long liquid columns when all the liquids have been displaced to the production tubing (of smaller diameter) above the packer. These large liquid columns could also open one or several of the upper unloading valves as they travel to the surface, decreasing in this way the efficiency of the lifting process.

- The upper bleed valve, also known as the “upper standing valve,” should be able to handle not just the formation gas flow rate, but the entire gas and liquid production of the well while the accumulator is being filled with liquids.

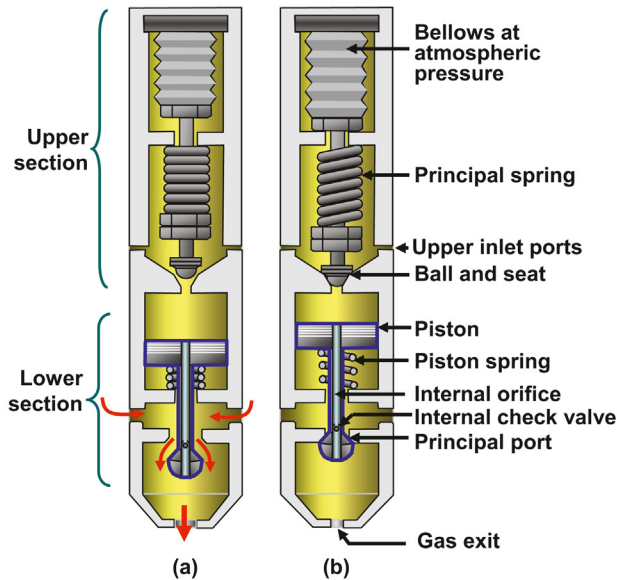
During the initial stages of the liquid column generation period at the bottom of the accumulator, the liquid enters the accumulator mainly through the lower standing valve. The annulus between the accumulator and the perforated casing acts as a gas–liquid separator. The formation gas tends to travel upwards to the upper standing valve while the liquids from the formation tend to travel downwards to the lower standing valve. Because the liquid that enters the accumulator contains very little gas, a small liquid column inside the accumulator is sufficient to close the lower standing valve (the liquids in the annulus do contain formation gas and, in consequence, the gradient is lighter in the annulus). From the moment the lower standing valve closes, the accumulator receives only the liquids that pass through the upper standing valve and drop to the bottom of the accumulator, eventually completely filling it with liquids to the top.

Finally, intermittent gas lift can be implemented in wells with dual parallel strings. Details about this type of completion and design guidelines are given in Section 10.10.

#### 10.4 DESCRIPTION OF PILOT VALVES

Pilot valves consist of two sections: the upper section determines the opening and closing pressures of the valve and the lower section allows very high instantaneous gas flow rates from the annulus to the production tubing, see Fig. 10.6.

The way pilot valves operate allows its opening and closing pressures to be set at any value while the instantaneous gas flow rate through the valve is always kept at very high values. The closing element and the upper section area ratio control the opening and closing pressures of the valve, while the lower section is used to inject gas at the very high flow rates



■ FIGURE 10.6 Injection-pressure-operated (IPO) pilot valve with check valve inside the piston's bleed orifice. (a) Opened and (b) closed.

that can be attained thanks to the large diameter of the lower port (main port) of the valve. The main port diameter is of constant value for a given valve model. The closing element could be a nitrogen-charged dome or a spring installed with a dome set at atmospheric pressure and filled with a protective liquid.

Only injection-pressure-operated pilot valves are focused on in this book because production-pressure-operated pilot valves are not very much in use nowadays in the oil industry. The main reason for not using production-pressure-operated valves is because with this type of valve the cycle time is mainly controlled by the formation pressure and not so much by the injection pressure, thus it is difficult to set the cycle time at its optimum value.

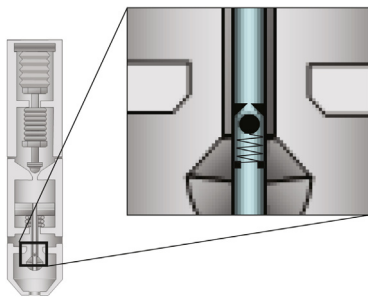
When the forces exerted by the production and injection pressures are greater than the force exerted by the spring or the nitrogen-charged dome pressure, the upper section opens, exposing the upper face of the piston in the lower section of the valve to the large injection pressure. This makes the piston move downwards, allowing the injection gas to flow through the lower part of the pilot valve from the well's annulus into the production tubing.



The piston remains in the down position (the valve's lower section open) as long as the upper section of the pilot valve is open. When the gas injection pressure in the well's annulus drops to the valve's closing pressure, the upper section of the valve closes and the high-pressure gas at the upper side of the piston is vented to the tubing through the piston's longitudinal internal conduit. The pressure at the upper side of the piston becomes equal to the production pressure while the pressure underneath the piston continues to be large and almost equal to the injection pressure, making the piston move upwards so that the lower section of the pilot valve closes and the gas injection from the annulus to the tubing stops.

When the internal bleed orifice of the piston is plugged, the high-pressure gas trapped above the piston cannot be vented. As a consequence, the piston remains pushed down, gas injection into the well cannot be stopped, and the well might be left producing on continuous gas lift. When this happens, the gas flow rate into the production tubing could be very high, causing the annular injection pressure to drop to very low values.

The piston can also get stuck because solid particles might be trapped between the piston and the inside smooth walls of the cylinder on which the piston slides up and down. Sometimes, if the piston has an integral check valve in its bleed orifice, the piston stays open because the small ball of the piston's internal check valve sticks to the seat of this check valve. This internal check valve allows the gas to flow from the top of the piston towards the production tubing but not in the opposite direction. Because the orifice diameter through the piston is very small, the gas flow rate to the production tubing is negligible but sufficient to vent the pressure at the upper side of the piston when the upper section of the pilot valve closes. The other function of the internal check valve is to prevent liquids from entering the upper part of the piston. As it happens with check valves of single-element gas lift valves because the internal check valve is never hermetically closed, the production pressure is transmitted to the upper side of the piston. The production pressure increases as the liquid slug is being generated at the bottom of the production tubing above the pilot valve and this pressure (in combination with the injection pressure) contributes to the opening of the pilot valve. The check valve inside the piston is shown in Fig. 10.7.



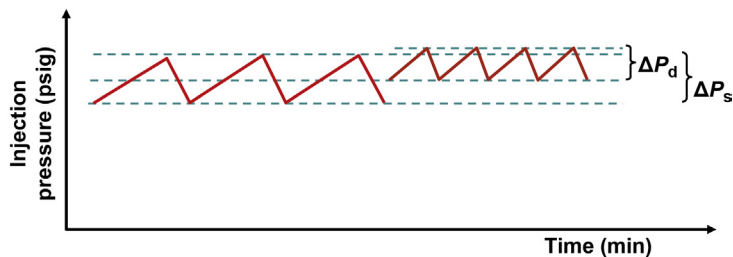
■ FIGURE 10.7 Check valve inside the piston at the lower part of the pilot valve.

Most commercially available pilot valves do not have the check valve inside the piston as shown in Fig. 10.7; instead, a standard check valve is usually installed at the nose of the valve just as it is found in single-element valves. In this case, the piston only has an internal longitudinal bleed conduit

without the check valve. The reason why some valves have the check valve incorporated inside the piston is to reduce, as much as possible, the restrictions to the gas flow through the pilot valve.

The equations for the opening and closing pressures of the upper section of a pilot valve are the same as those for a single-element gas lift valve. These equations are very precise when calculating the opening pressure of a pilot valve, but not very useful for the pilot valve's closing pressure: Nitrogen-charged, IPO, pilot valves tend to close at a pressure below the closing pressure predicted by valve mechanic equations (known here as the theoretical closing pressure). This is due to the fact that the high gas flow rate through the pilot valve cools the nitrogen and, in consequence, the valve's closing pressure decreases. Spring-loaded, IPO pilot valves, on the other hand, tend to close at pressures higher than the theoretical closing pressure. This is due to dynamic effects caused by the very high instantaneous gas flow rates that take place through the pilot valve's lower section once it opens. Changes in the closing pressure greatly affect the volume of gas injected per cycle, even though these changes appear to be very small. For example, a spring-loaded valve that in theory opens at 830 psi and closes at 800 psi, could in reality have an opening pressure of 830 psi and a closing pressure of 815 psi. The change in the injection closing pressure from 800 to 815 psi is less than 2% of its absolute value; but, the spread of the injection pressure goes from 30 to 15 psi, which is 50% less than its expected value. This would cause a reduction in the volume of gas injected per cycle of approximately 50% if the well is on choke-control intermittent gas lift.

Experimental observations have confirmed the fact that spring-loaded gas lift pilot valves tend to close at injection closing pressures that are higher than their theoretical values. The theoretical closing pressure can only be obtained under static conditions (very low flow rate at the test rack). The static closing pressure of a spring-loaded valve is measured at the shop and it is called "test-rack closing pressure." For a given injection pressure (or valve's upstream pressure), the dynamic closing pressure behavior depends on the production pressure (or valve's downstream pressure) and the valve's area ratio. As the production pressure decreases, the deviation of the dynamic closing pressure with respect to its theoretical value increases, until critical flow is reached, at which point this deviation stays constant and independent of the production pressure value. It has also been found that as the area ratio of the upper section of the pilot valve increases, the deviation of the dynamic closing pressure increases. The expression found by Milano (1999) to determine the dynamic closing pressure of the valve is given by Eq. 8.19.



■ FIGURE 10.8 Effect of the dynamic closing pressure (“d” stands for “dynamic” and “s” stands for “static”).

Fig. 10.8 shows what happens when the actual closing pressure is greater than its theoretical value and the injection gas flow rate through the surface choke is kept constant: (1) the cycle time is shorter, and (2) the opening pressure is slightly higher (because the liquid column, which also contributes in the opening of the valve, is not as long as it would be if the cycle time was longer, thus an additional increment in the gas injection pressure is needed to open the valve). The volume of gas injected per cycle might be considerably reduced and this could cause an increase in the fallback losses.

It is better to use 1.5-in. OD (outside diameter) pilot valves than 1-in. OD pilot valves:

- 1.5-in. OD pilot valves can last for a greater number of cycles without failures. Under normal operational conditions, a 1.5-in. valve should be able to operate for several dozens of thousands of cycles.
  - Additionally, 1.5-in. OD pilot valves have main port diameters as large as 48/64 in., while 1-in. OD pilot valves have port diameters of only 32/64 in. at the most. It is recommended to have large main port diameters to provide the very high instantaneous gas flow rates needed for intermittent gas lift.
  - On the other hand, for a given seat diameter of the upper section of a pilot valve, 1-in. OD pilot valves have a larger area ratio than the 1.5-in. OD valves do because 1.5-in. OD valves have larger bellows area. In this way, 1.5-in. valves have area ratios that can go from very small to very large values, while 1-in. OD valves have minimum area ratios that might still be too large for certain operational conditions. The spread of the valve is directly proportional to the area ratio of the pilot valve’s upper section. The spread of the valve determines the volume of gas injected per cycle for wells on choke-control intermittent gas lift.
- If the well has small-diameter production tubing or the casing diameter

is very large, the required spread of the valve might be very small. It could be possible that a 1-in. OD pilot valve, even with the smallest area ratio available, will show a spread that might still be larger than that required to inject the necessary volume of gas per cycle, thus the well ends up being overinjected. One way of reducing the spread of the valve in those situations is to set the pilot valve's opening pressure at a lower value because the spread is also directly proportional to the valve's calibration pressure. But this reduction should be done with care to keep the liquid slug velocity at a value high enough to be able to lift the slug to the surface with minimum liquid fallback losses.

Pilot valves are more expensive and complex to manufacture and operate than single-element valves. For this reason, it is highly advisable to keep the injection gas clean, free of solid particles or liquids: this simple maintenance action will eliminate most of the operational failures these valves have under tough operational conditions.

In general, the different failures gas lift pilot valves exhibit can be categorized as follows:

- Failures of metallic components, such as (from more to less frequent)
- Erosion of the seat of the upper section (this does not happen too often in conical-shaped seats, but it can happen in straight-edge seats).
  - Flat bellows: it is highly possible that spring-charged valves will remain closed in this case but for nitrogen-charged valves it is not easy to predict the behavior of a valve with bellows that has failed.

Failures of nonmetallic components

The ring seals of the piston could present serious problems if fabricated with materials different from the manufacturer's specifications or if solid particles are trapped between these rings and the inside smooth surface on which the piston moves. When the piston gets stuck, its final position might allow from very low to very high and continuous gas flow rates (if the check valve is an integral part of the piston, the communication tests that are explained in chapter: Continuous Gas Lift Troubleshooting will give the same results as if there was a hole in the tubing and liquids can go from the tubing into the annulus). However, solid particles might not completely keep the piston from moving and the piston could move in an unpredictable way, causing an erratic behavior of the gas injection: sometimes the piston closes and other times it does not, or the piston movement changes from one cycle to the other, etc.

Another type of failure happens if the seat of the piston's internal check valve is not properly vitrified (for pilot valves in which the check valve is an integral part of the piston), the ball might stick to the seat so the high-pressure gas on top of the piston cannot be vented to the production tubing, leaving the pilot valve open on continuous gas lift with a very high flow rate and a very low gas injection pressure in the well's annulus. A communication test will give the same results that are obtained when there is a hole in the production tubing and liquids can go from the tubing into the annulus, unless at the same time: (1) the bellows has failed and the upper part of the piston was left at a low pressure, or (2) dirt of some kind between the ball and the seat of the pilot section of the valve (upper part of the pilot valve) keeps the pilot valve open.

#### Operational failures caused by solid particles carried with the injection gas

The upper section of the pilot valve remains open because of trash or solids have accumulated between the stem and the seat. This failure can be easily solved by venting the well's annulus without having to pull the valve out of the well. Independently of the type of check valve (if it is an integral part of the piston or not) communication tests will not point to a hole in the tubing and liquids cannot flow from the tubing into the annulus (even with the piston's internal longitudinal orifice plugged). To avoid the entrance of large solid particles into the upper section of the valve, the upper entrance ports of the valve are numerous but very small in diameter; after all, these orifices are only necessary to transmit the annular injection pressure to the upper part of the valve and they do not have to allow a very large gas flow rate through them.

A second type of failure takes place when the piston of the lower part of the valve stays open because its internal longitudinal bleed orifice is plugged with solid particles. If the check valve is an integral part of the piston, this case is identical to the failure explained earlier, in which the ball of the check valve sticks to its seat. If the check valve is not an integral part of the piston, a communication test will not indicate a hole in the tubing, which leads the operator to just replace the pilot valve (if venting the casing does not solve the problem).

When a single-element valve (or a pilot valve with its internal check valve at the nose of the valve and not inside the piston) fails open, the communication tests that are presented in chapter: Continuous Gas Lift Troubleshooting will indicate that the failure is due to a damaged gas lift valve and not to a hole in the production tubing. This is because the check valve is always

located just above the nose of the valve and it will not allow gas or liquid flow from the tubing into the casing–tubing annulus. However, as indicated earlier, for a pilot valve with its check valve inside the piston, the final behavior of the pilot valve depends on the type of failure and the analysis of the results from a communication test is not straight forward.

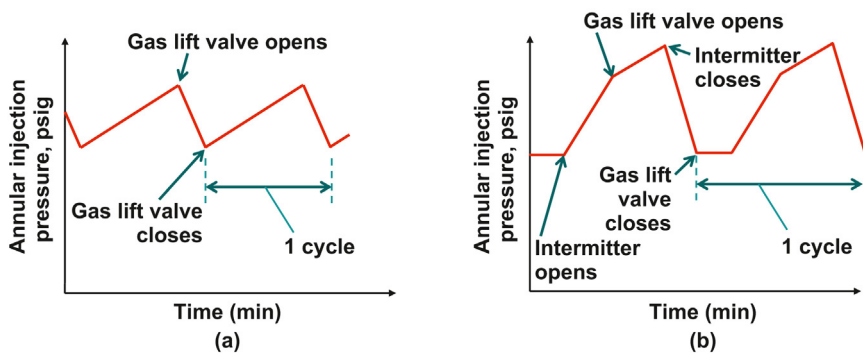
## 10.5 TYPES OF CONTROL OF THE SURFACE GAS INJECTION

As it has already been pointed out, there are two different ways of controlling the gas injection at the surface of a well on intermittent gas lift.

- Setting the surface gas flow rate at a constant and continuous value by using a surface choke in the gas injection line or, instead of this choke, a control valve set to pass also a constant and continuous value of the injection gas flow rate. This is called “choke-control intermittent gas lift.”
- Controlling the surface gas injection with the use of an automatic surface flow control valve, also known as “intermitter.” The intermitter will remain open or close at predetermined time intervals that can be independently set.

Fig. 10.9 shows typical wellhead pressure patterns of the surface injection pressure for each type of gas injection control.

When the control at the surface is carried out by a choke or a needle valve (choke control) the surface gas flow rate is usually very low. When the sub-surface pilot valve opens, the injection pressure drops because the instantaneous gas flow rate through the gas lift valve is much greater than the gas flow rate into the annulus at the surface.



■ FIGURE 10.9 Typical surface injection pressure pattern, depending on the type of the surface control of the gas injection. (a) Constant surface gas flow rate. Injection controlled by a choke or a surface needle valve and (b) use of surface intermitters.

The choke (or adjustable needle valve) is usually installed at the injection manifold to take advantage of centralized operations and to use the gas injection line as an additional high-pressure gas storage volume, unless the casing diameter is so large that the choke needs to be installed as close as possible to the wellhead to limit the volume of gas injected per cycle.

Choke-control intermittent gas lift has the following advantages:

- It allows intermittent and continuous gas lift to coexist because the high-pressure system is maintained very stable.
- It requires less surface equipment to operate, which means lower maintenance costs and supervising efforts.
- Many wells can intermit at the same time without affecting the pressure at the injection manifold.
- Small diameter injection lines can be used because the surface gas flow rate is very small.
- The well's annulus is used as a high-pressure-gas-storage volume, from which most of the gas injected per cycle comes from. This is very important in gas lift fields with a limited compression capacity.

The major disadvantage found in choke-control intermittent gas lift is its inability to control the volume of gas injected per cycle. Once the pilot valve is installed downhole, the volume of gas injected per cycle depends on the downhole gas lift valve's opening and closing pressures. These pressures remain pretty much constant because their values are determined mainly by the valve's area ratio and calibration pressure. If the surface gas flow rate is changed, the cycle time and the total volume of gas injected daily also change, but the volume of gas injected per cycle changes very little and it is this volume that really determines the injection gas/liquid ratio. If, for example, the surface gas flow rate is increased, the cycle time becomes shorter and the gas lift valve tends to open at a slightly higher pressure because the liquid columns are smaller and have less influence on the valve's opening pressure (so a higher injection pressure is required to open the valve). But IPO pilot valves respond mainly to the injection pressure, so that this change in the injection opening pressure is very small (and so is the volume of gas injected per cycle then). If the surface gas injection flow rate is reduced, the cycle time becomes longer and the gas lift valve tends to open at a slightly lower pressure because the liquid columns are now larger and have more influence on the opening pressure, but this reduction of the injection opening pressure is also very small, thus the volume of gas injected per cycle remains almost unchanged.

As indicated at the beginning of the chapter, the cycle time must be as close as possible to the OCT to maximize the daily liquid production of the well.

Any change in the cycle time away from this optimum value will cause a drop in the daily production. The volume of gas injected per cycle would remain about the same if the changes in the cycle time are not too far away from its optimum value. For this reason, the selection of the gas lift pilot valve's area ratio is very important for choke-control intermittent gas lift and should be done with great care.

Trying to optimize the volume of gas injected per cycle is difficult for choke-control intermittent gas lift because of the following reasons:

- The exact volume of gas the well needs per cycle cannot be theoretically determined to a high degree of accuracy. This is because it is difficult to predict the behavior of a well on intermittent gas lift by means of mathematical models. The only way of knowing the exact required volume of gas injected per cycle is by the use of a field optimization procedure that necessarily involves the use of surface intermitters.
- Pilot valves exhibit a dynamic behavior that deviates from the theoretical predictions using static force balance equations. The spread of a valve under any operational condition is very difficult to predict. The model developed by Milano (1999) can be used to predict the spread of the valve but additional tests with other valve models and types, as well as a wide variety of operational conditions, are needed. It was stated in the previous section that spring-loaded, IPO pilot valves tend to close at pressures higher than expected, while nitrogen-charged valves behave in the opposite way because of the cooling effect of the large gas flow rate through the pilot valves once they open. Both of these deviations are hard to predict.
- Operational conditions, such as water cut and reservoir pressure, are constantly changing. To adapt to each change is easy only if surface intermitters are used.

Another disadvantage of having a well on choke control takes place when the injection gas has a water content that is high enough to cause hydrate formation due to gas expansion at the surface choke. With choke control, the required surface gas flow rate is sometimes very small and the choke diameter might need to be very small, causing large pressure drops through the choke, creating a cooling effect that promotes hydrate formation. Depending on the severity of the problem, one or several of the following steps could be taken to reduce or eliminate the problem:

- Set the pilot valve's opening pressure at a very large value (keeping in mind that opening an upper unloading valve should be prevented). In this way, the pressure drop across the surface choke is reduced and the choke's diameter does not need to be very small.



- Install dehydration units (but they are expensive and only justified if the problem affects a great number of wells throughout the year).
- Install gas heaters or keep the gas from going through the gas cooler downstream of the compressor.
- Place the choke as close as possible to the compressor, where the gas is still warm (suitable for very small gas lift systems).
- Install a heat exchanger at the choke to warm up the gas.
- Inject methanol or glycol to lower the hydrate formation temperature.
- Install water traps at low points in the injection gas lines.

Hydrate formation is a very serious issue in gas lift fields and it is discussed in more detail in chapters: Gas Properties and Continuous Gas Lift Troubleshooting.

Chokes are also affected by liquids carried by the injection gas. Even in the absence of hydrates, liquids of any kind could make the injection gas flow rate fluctuate in an erratic way, increase the pressure drop in gas injection lines, and make it difficult to measure the gas flow rate.

Another important disadvantage of choke-control intermittent gas lift is the inability to control the exact time the well will intermit. It is possible to have several wells intermitting at the same time, causing problems at the separator if it is not capable of handling the sudden increase in gas and liquid flow rates. If the gas lift system is very small, the sudden increase in gas flow into the low-pressure lines that go to the suction of compressor might make it necessary to vent some of this gas to maintain the compressor suction pressure as constant as it is usually required.

When the gas lift field is very large, with a large number of wells, the problem outlined in the previous paragraph is not present and it becomes practical to produce the wells on choke control instead of having to install a great number of surface intermitters. However, in very small gas lift systems in general, or in wells with casing diameters very small or very large, or in a special completion that needs to be accurately evaluated, the use of surface controller is very convenient. When the well operates with the help of a surface controller, the volume of gas injected per cycle and the total cycle time can be adjusted from the surface and independently of each other. It is only necessary to calibrate the subsurface gas lift valves in an appropriate way (as it is shown in the next section) to take full advantage of the surface controller to regulate the volume of gas injected per cycle.

The use of surface controller does not mean that pilot valves are no longer needed. In fact, it is very important to combine surface controllers with the appropriate subsurface pilot valve. Single-element valves require very large

area ratios to achieve the high injection gas flow rates into the tubing that are needed in intermittent gas lift. This might limit the main advantage of using surface controller, which is to be able to adjust the volume of gas injected per cycle for a wide variety of values, from very small to very large volumes. The area ratio of the pilot valve used in conjunction with a surface intermitter should be equal to approximately 70% the value of the area ratio needed if the well was on choke control. This would allow an effective control of the volume of gas injected per cycle in case the actual volume needed turns out to be below the expected value. If, on the other hand, a larger volume of gas needs to be injected per cycle, the surface intermitter will simply need to remain open for a longer period of time.

Referring to [Fig. 10.9b](#), during the time the liquid column is being generated above the pilot valve, the controller and the pilot valve are closed, thus the annular injection pressure remains constant.

After a predetermined period of time, the surface controller opens, allowing the flow of gas into the annulus at a very high flow rate. This makes the injection pressure increase very fast to reach the pilot valve opening injection pressure. When the pilot valve opens, if the design was properly made, the injection pressure should continue to increase (most of the time it will indeed increase but at a lower rate). In order for this continuous increase of the injection pressure to be attained, the gas flow rate through the gas lift valve should be lower than the gas flow rate injected at the surface through the intermitter. If both flow rates are similar, the time required to pass the volume of gas needed per cycle could be very long, affecting the efficiency of the lifting method, especially if the well requires a high injection frequency.

If the gas flow rate at the surface is lower than the gas flow rate through the gas lift valve, the pilot valve might open and close several times while the surface controller is opened. This could damage the pilot valve and increase the liquid fallback losses. This is why it is important not to have any gas flow restriction along the gas injection line (such as a small orifice plate). If the well was on choke control prior to the installation of the intermitter, it is also important to remove the choke or the needle valve (that was used to control the injection flow rate) to reduce any restriction to the gas flow once the intermitter opens. However, there are situations in which it is acceptable, if not required, to use the intermitter in conjunction with a surface choke. If, for example, the volume of the well's annulus is very small (shallow well with small diameter casing), a choke in series with the intermitter might be required to prevent the injection pressure from increasing extremely fast and way above the gas lift valve opening pressure.

After a predetermined period of time, the surface controller should close. Then because the subsurface valve is still opened, the annular pressure drops very fast due to the high flow rate the pilot valve can allow, until reaching the pilot valve's closing pressure. At this point, the pilot valve closes and a new cycle begins.

Once the intermitter closes, it is important that the injection pressure be able to drop as fast as possible because this would allow moving on to the liquid column regeneration period without having to wait for a long time. This is another good reason for having a pilot valve installed at the point of injection.

It is important that not too many surface controllers (or intermitters) in a single injection manifold open at the same time because this will cause problems: (1) at the separator if its gas or liquid handling capacity is surpassed, or (2) at the compressor if its suction pressure increases above its required value. Additionally, if several intermitters open at the same time, the injection pressure at the manifold could drop and, as a result, the gas flow rate that goes to each well might decrease. The injection pressure could then be so low that one, or several, of the wells intermitting at the same time might not reach their respective pilot valves' opening pressures and one or more cycles might be skipped before finally being able to open the affected subsurface pilot valves. But these problems are easily solved by installing a control system that would prevent more than a certain number of wells from intermitting at the same time.

The great disadvantage of using surface injection controllers or intermitters, especially in large gas lift systems, is the increase in maintenance costs and the extra attention these controllers require from the operation personnel.

In the great majority of cases, it is better to install these intermitters at the well-head (or close to it) and not at the injection manifold. In this way, the efficiency of the intermittent gas lift method could be improved. When the intermitter is away from the well, the injection line and the annulus need to be pressurized. If the injection line is very long or has a very large diameter, the increase in the injection pressure takes place at a lower rate.

When the intermitter opens, the instantaneous surface gas flow rate is very high. It is important that the orifice plate's diameter and the range of the differential and absolute pressure sensors be properly selected so that the gas flow rate can be measured at all times. It is not uncommon to find pressure sensors with their maximum possible readings being less than the required value: the pen of the differential pressure recorder reaches the top of the scale and stays at that value for as long as the intermitter remains opened, making it impossible to calculate the actual gas flow rate.

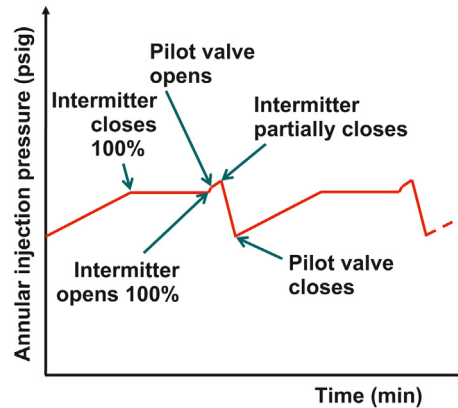
The surface controller or intermitter can be used in several ways and not just opening and closing at predetermined time intervals. For example, when the system pressure fluctuates too much, the controller can be set to open at predetermined time intervals, but it closes only when the annular injection pressure reaches a given value. In this way, the total cycle time does not change, but the intermitter remains open until the desired maximum injection pressure is reached to make sure that the pilot valve opens at each cycle. This operation requires a pressure signal to be sent to an electronic or pneumatic controller, which in turn must have an algorithm or the necessary mechanical means to control the gas injection into the well.

Another example of using surface intermitters with intelligent control systems is the one usually installed in wells with very small annular volumes. In these wells, the increase in injection pressure can happen very fast and it could reach very high values that might open one or several unloading valves. In this case, the opening and closing operation of the intermitter can be controlled based on time only but an automatic pressure control system must be used to maintain the injection pressure at values less than a given maximum pressure while the controller is opened.

Another alternative, previously mentioned, that can be used when the annular volume is very small or the system pressure is very large, is to install a choke in series with the intermitter in the injection gas line. With this arrangement, the gas flow rate is kept at a lower, and more adequate, value to avoid opening an unloading valve. The choke must be designed such that the injection gas flow rate is not very high, but it should still be higher than the gas flow rate through the pilot valve at the point of injection. As indicated earlier, if the choke is too small, the pilot valve could open and close several times while the intermitter is opened (as shown in Fig. 12.26).

One way of combining the advantages of choke control and the use of surface intermitters at the same time is by the implementation of a control system capable of carrying out the following actions (Fig. 10.10):

- At the beginning of the cycle, while the liquid column is being generated at the bottom of the well, the surface controller allows only a very low gas flow rate into the annulus. In consequence, the injection annular pressure is slowly increasing because at this time the subsurface gas lift valve is closed.
- When the injection pressure is close enough to the pilot valve's injection opening pressure, the surface intermitter should close. The annular injection pressure then remains constant because the gas in the annulus is trapped.



■ FIGURE 10.10 Typical surface injection pressure pattern with intelligent control of the gas injection flow rate.

- A given time interval after the intermitter has closed, the intermitter is then fully opened to pass a very high gas flow rate into the annulus for another predetermined period of time, in which the annular pressure increases very rapidly; but almost immediately, the subsurface pilot valve opens and gas is injected into the production tubing.
- When the annular pressure reaches its maximum value, the intermitter partially closes, allowing a very low gas flow rate into the annulus, so the injection pressure drops and the pilot valve closes to begin another liquid column generation period, in which the annular pressure is again increasing very slowly.

In this way, the impact on the high-pressure side of the gas lift system is minimized because most of the gas injected into the tubing at each cycle comes from the gas previously accumulated in the annulus and not from the high gas flow rate provided by the intermitter every time it opens. On the other hand, the advantages of surface intermitters are still present because the total cycle time and the volume of gas injected per cycle are set independently of one another.

Several surface injection pressure patterns that reveal possible operational failures are presented in chapter: Intermittent Gas Lift Troubleshooting: (1) inappropriate settings of the closing and opening time intervals, (2) different types of failures of the intermitter, and (3) problems with the integrity of the completion, such as holes in the production tubing or leaking gas lift valves, etc.

Automation is frequently used in continuous gas lift to control the injection gas flow rate at a given set point. This type of control system can be used in

choke-control intermittent gas lift (by having the set point of the gas flow rate adjusted and controlled at the low level that is usually required) with the following advantages:

- The cycle time will not change if the gas lift system pressure changes. Without a gas flow rate control system, if the pressure at the manifold increases the cycle time decreases and vice versa.
- If a very low gas flow rate is required because, for example, the well needs a very long cycle time, there might be hydrate formation problems or the choke (or, if used, the control valve at a fixed position) could plug with solid particles carried by the injection gas. This makes the gas flow rate decrease; however, if a flow control system is used, the valve will tend to open because the control system will try to maintain a constant gas flow rate, with the end result of getting rid of the hydrates or solid particles that have accumulated.

Automatic controllers, or intermitters, can fail for several reasons; some of them are presented in the following paragraphs.

- Sometimes the same needle valves that are used to control the gas flow rate on continuous gas lift are set to function as “on–off” or “open/close” valves with the use of a control algorithm to act as a surface controller or intermitter:
  - There is nothing wrong with using this type of valves for intermittent gas lift, as long as: (1) these valves are able to open and close many times without presenting mechanical failures for a reasonably long period of time, b) they do not restrict the injection gas flow to values less than the maximum required gas flow rate when they open, and (3) they can completely stop the gas flow when they close. The continuous closing and opening of the valve should not cause any kind of damage to the seat by either mechanical actions or by erosion caused by solid particles traveling with the injection gas (cut or eroded seats will leak gas when the valve is in the close position).
  - Regarding the restriction to the gas flow, in many occasions these valves could be adapted to intermittent gas lift by simply changing their internal components. While in continuous gas lift operation, these valves have seats diameter of values usually equal to  $\frac{1}{4}$ ,  $\frac{1}{2}$ , or  $\frac{3}{4}$  in., among others. For example,  $\frac{1}{4}$ -in. valves could be adapted to intermittent gas lift applications (in which very high flow rates are required) by simply changing their internal components. When the annulus is very small (shallow well and small casing diameter) it might be possible that the smallest seat size available is the most

appropriate one to operate the well on intermittent gas lift to avoid opening an unloading valve. Additionally, the internal components can be changed so that a needle valve becomes a ball valve.

- Without automation, the needle valves that are used to control the injection gas flow rate in continuous gas lift are set at a given opening. When the manifold is automated, the same valves are used but with electrical actuators installed on top of the valves to move the stem position according to a given control system in place. The electrical actuator responds to signals from 4 to 20 mA or to digital signals. The complete set (valve, actuator, and controller) is usually very compact and occupies a small space at the manifold. The following are some of the most frequent failures found in this type of arrangement: (1) Wrong calibration of the stem actuator: The valve does not fully open or close (it passes gas when it should be completely closed or the maximum gas flow rate is not attained because it does not fully open); (2) Erosion of the seat can cause gas leaks when the valve is supposed to be closed (these needle valves require special materials to withstand intermittent gas lift operation); (3) Rupture of the coupling mechanism between the stem and the actuator; and (4) The stem of the valve sometimes gets stuck at one position (usually caused by solid particles in the gas flow or by incompatibility of the materials of the moving parts in contact).
- The materials the valve is made out of must be adequate so that it does not easily wear out. The threads of the actuator and the stem must have the proper geometry to withstand constant movement, high working pressures, and dirt that can accumulate in them. Most of these failures can be eliminated if the actuator is properly calibrated, the right compatible materials are used for the moving parts in contact, and the injection gas is filtered to get rid of solid particles that might be traveling with it.
- The use of pneumatic “open/close” valves, instead of the electrically actuated valves described earlier, are more appropriate for intermittent gas lift applications, but they are not free of operational problems:
  - These valves are usually bigger and they could be hard to install at injection manifolds with limited space available for that purpose.
  - Solid particles in the gas that is used by the pneumatic valve’s controller, could originate problems to operate these pneumatic “open/close” valves:
    - The gas that is used to provide pressure to the motor section of the pneumatic valve (or intermitter), to open or close it, is usually the same gas that is used for gas lift. This gas is taken

from the gas injection line that goes from the injection manifold to the wellhead. Because the injection gas pressure is usually above 1000 psig, two pressure regulators are used to drop the pressure to the level needed by the valve's control system, which is usually equal to 15 or 30 psig. The first pressure regulator drops the pressure to 100 or 150 psig and the second pressure regulator drops it to the level required by the electronic controller installed between the second pressure regulator and motor section of the pneumatic valve. This controller sets the inlet or outlet pressures of the gas that opens or closes the valve. Between the first and the second pressure regulators, a liquid trap is usually installed to remove any liquid that condensates due to the expansion of the gas at the exit of the first pressure regulator.

- Typical problems of the arrangement explained in the last paragraph are: (1) the electronic controller stops working because the battery runs out; (2) dirt traveling with the injection gas plugs the gas inlet of the valve's control mechanism so that it remains all the time opened or closed; and (3) hydrate formation or excessive liquid condensation due to the expansion of the gas from more than 1000 psig to less than 30 psig.
- The problem caused by the dirt carried with the lift gas can be eliminated by connecting the instrumentation gas intake pipe to the gas injection line (that comes from the gas injection manifold) several feet upstream of the pneumatic valve. The connection of the instrumentation pipe intake should be done at the top of the gas injection line that goes to the well. A small high-pressure container (usually a pipe of certain length) should be installed between the instrumentation gas intake and the first pressure regulator.

If an intermitter, electric or pneumatic, fails for any reason, one of the following alternatives could take place. (1) No gas is injected to the well because the intermitter is always closed, (2) a very high gas flow rate is injected into the well because the intermitter remains open all the time, or (3) the injection gas flow rate to the well could be very low, possibly causing hydrate formation problems. In all of these cases, it is important to have an early warning system to be able to correct the problem as soon as possible.

The personnel involved in the operation of these control valves should be trained so that they can properly operate and maintain these valves. This requires training, not only for the optimization team, but also for: field operators, electrical and mechanical maintenance crews, well test personnel, etc.



## 10.6 INTERMITTENT GAS LIFT DESIGN FOR SIMPLE TYPE COMPLETIONS

Designing a well with a simple type completion like the example shown in Fig. 10.1 consists of:

- Finding the depths, calibration pressures, and seat diameters of the unloading valves. It is recommended to use single-element, IPO, gas lift valves to unload the well. These valves should be calibrated with an injection opening pressure as high as possible so that none of them will open as the liquid slug travels towards the surface. This is why it is recommended to use as few unloading valves as possible, starting with the one closest to and above the static liquid level. The unloading process should be performed on continuous flow. The well should be unloaded on intermittent gas lift only in cases with limited compression capacity to establish continuous gas lift.
- Finding the depth, calibration pressure, and area ratio of the operating valve. It is recommended to use pilot valves at the point of injection for the reasons given in Section 10.2.

The procedures described for continuous gas lift should be used to determine the depths and calibrations of the single-element, IPO, unloading valves. This is recommended because it is far more practical to unload the well on continuous gas lift. Unloading the well on intermittent gas lift would require the use of appropriate valves for that purpose: It is expensive to install pilot valves to be used only as unloading valves. On the other hand, single-element valves are not adequate for intermittent gas lift.

As indicated earlier, unloading the well on intermittent gas lift is only justified when the compressor cannot provide the gas flow rate needed for continuous gas lift operation and, in consequence, the well's annulus should be used as a high-pressure gas storage volume to inject the accumulated gas at finite time intervals. This might be the only way for the compression system to increase the injection pressure to unload the well. This situation is not very common because wells that are good candidates for intermittent gas lift are usually low liquid producers that do not require high injection gas flow rates during the unloading process.

Wells are shifted from continuous to intermittent gas lift to reduce the injection gas/liquid ratio. Usually, good candidates for intermittent gas lift have been producing on continuous gas lift and the gas lift mandrels are already installed in the production tubing. In these cases, it is recommended to simply use the redesign techniques for continuous gas lift given in chapter: Design of Continuous Gas Lift Installations to determine the depths

and calibrations of the unloading valves. However, as already indicated, the calibration pressures should be high enough so that the unloading valves do not open as the liquid slug reaches the depth of each of these valves once the well has been unloaded and it is producing on intermittent gas lift with the pilot valve as the point of injection. The unloading valves' calibration pressures should also be higher than usual because it is advisable to have a wide range of available operating injection pressures to be able to perform the iterations in the liquid slug velocity needed during the design calculation process of the operating valve: if the calculated slug velocity is too low, the injection pressure must be increased, and vice versa. It is necessary then to have this wide range of operating injection pressures to select the one best suited for the particular operational conditions of the well. This operating pressure could have values from very low to very high and the right pressure is the one that can lift the liquid slug at the most appropriate slug velocity to minimize the liquid fallback losses.

As it will be shown in this section, the design process of the operating valve determines the size of the liquid columns to be lifted. It is recommended then to verify the calibration of the unloading valves right after the operating valve has been designed to make sure that these unloading valves will not open during the normal operation of the well. Usually, in simple type completions, the liquid slugs are not long enough to make the unloading valves open. On the other hand, liquid slugs are usually long in wells with accumulation chambers and it is important to always verify if the unloading valves could open in this type of completion.

The unloading process of the well, just before reaching the operating (pilot) valve, should be carried out following the recommendations for unloading the well on continuous gas lift. But, once the pilot valve is uncovered and the well is set to operate on choke-control intermittent lift, it is important to keep in mind that the size of the first slugs to be lifted could be much larger than the size of the slugs under normal operating conditions for which the operating pilot valve has been designed. Because the first liquid slugs could be very large, it is possible that the opening pressure of the pilot valve at this time would be much lower than the one it would have under normal operating conditions. This happens because the high tubing pressure at valve's depth also tries to open the pilot valve and, in consequence, the opening injection pressure (when the valve is uncovered) does not need to be as high as the design opening pressure to open the valve. However, the "closing" injection pressure of the valve does not change if it is spring-loaded, or changes very little in case of nitrogen-charged valves because the low volumes of gas injected per cycle are not sufficient to significantly cool the valve. As a consequence of this low opening pressure, the spread

of the valve (which is defined as the difference between the opening and closing pressure of a gas lift valve in operation) could be considerably reduced at the beginning of the operation of the pilot valve and the volume of gas injected per cycle might be much lower than the required volume. This is an important factor to consider when the well is on “choke” control intermittent gas lift.

In the great majority of cases, the first slugs that reach the surface (just after the pilot valve is uncovered during the unloading operation) are very small (due to the large liquid fallback losses caused by the small spread of the pilot valve indicated in the previous paragraph) but, as the unloading operation proceeds, they become larger and the volume of gas injected per cycle increases because the spread of the valve is also increasing due to the lower bottomhole production flowing pressures that are progressively achieved. But this is not always the case and it is some times possible that because of the high liquid fallback losses, the well stays indefinitely producing very small liquid slugs or with no production at all. This could take place when the well is a very good producer, capable of generating large liquid columns very fast, or in cases in which the production tubing has a very large inside diameter and the gas lift system is not capable of supplying the very high instantaneous gas flow rate through the pilot valve that are needed to lift the liquid slug at an acceptable velocity (which should be high enough to reduce the liquid fallback losses). In these situations, the surface gas injection flow rate should be temporarily increased, so that the cycle frequency is increased and no time is given for large liquid columns to accumulate above the pilot valve. Once the spread of the valve has stabilized at a greater value, the surface gas flow rate can be reduced to its design value and the well is left operating under these conditions but under observation. If the well begins to load up with liquids again, it is recommended to install a pilot valve with a larger area ratio, which allows a larger volume of gas per cycle while maintaining the cycle time at its optimum value. If the valve is not replaced and the well is left producing at a high injection rate (so that it would not load up again), the cycle time could be shorter than the OCT and the well might not produce at the higher rates it is capable of and, at the same time, the injection gas/liquid ratio could be very high.

The unloading problem just described happens in wells on choke-control intermittent gas lift but it is not present if surface intermitters are used because the operating valve cannot close prematurely while the controller is opened (if the well was properly designed). In these cases, the volume of gas injected per cycle is imposed by the time the intermitter remains open and not by the spread of the pilot valve, which is influenced by the conditions in the tubing.

### 10.6.1 Design of the operating valve for choke-control intermittent gas lift

The design of the operating valve for a simple type completion, producing on “choke-control” intermittent gas lift, is presented in this section. Many of the equations given in the next paragraphs are based on the theory developed by Zimmerman (1982), with the modifications introduced by the author of the present book, based on his own field scale experimental observations and on the advances that, in general, have taken place in artificial lift during the last decades.

The design of the operating valve consists only in finding its calibration opening pressure and its area ratio. The opening pressure should be high enough for the injection gas to be able to lift the liquid slug at a velocity of around 1000 ft./min, which is generally considered the optimum liquid slug velocity to keep the liquid fallback losses at a minimum value. The maximum “allowed” opening pressure of the operating valve (referred to the surface) is equal to the opening pressure (also referred to the surface) of the unloading valve right above of the operating valve, minus a differential pressure that would keep the unloading valves from opening while the liquid slug is being produced to the surface. Thus the design of the unloading valve right above the pilot valve affects the value of the maximum injection pressure the well can have during its normal operation. The maximum allowed opening pressure of the operating valve at valve’s depth is called here  $P_{cvo\ max}$ . If the well does not have unloading valves, the value of  $P_{cvo\ max}$  referred to the surface is equal to the manifold pressure minus a differential pressure that would allow the required injection gas flow rate at the surface (controlled by a choke or a needle valve) for the optimum operation of the well. For choke-control intermittent gas lift, this surface gas flow rate is very small compared with the gas flow rate through the pilot valve when it opens (called here “instantaneous gas flow rate”).

The spread of an operating pilot valve, in a well producing on choke control, mostly depends on the pilot valve’s operational characteristics, while the cycle time is controlled by the injection gas flow rate at the surface. It is then very important for wells on choke control to establish, as accurately as possible, the value of the pilot valve’s area ratio, which in turn defines the spread of the valve and the volume of gas injected per cycle.

The design calculations of the operating valve begin by finding the volume of liquid the well can produce per cycle, followed by the calculation of the volume of injection gas required to produce that liquid volume per cycle and, finally, adjusting the valve’s parameters (opening pressure and area ratio) so that the liquid slug can be lifted at an acceptable velocity all the way

to the surface (by allowing the right instantaneous gas flow rate and the total volume of gas injected per cycle). To achieve these goals, the design method should determine: the valve's opening pressure, its area ratio, and the gas injection flow rate at the surface (through the choke). Even though both characteristics of the valve, its opening pressure and area ratio, affect the velocity of the liquid slug and the volume of gas injected per cycle, the injection pressure is the most important factor to determine the liquid slug velocity while the area ratio controls the volume of gas injected per cycle. In the iterative design processes that are described next, the area ratio and the opening pressure are progressively adjusted to the conditions of the well to find the optimum operating point.

The necessary steps to design the pilot valve are given (in the order in which they should be carried out) in the following paragraphs.

There are two iteration procedures that are required to design the pilot valve. The first (flow chart in Fig. 10.14) must be performed first to find the liquid slug velocity (for a given opening injection pressure, which is adjusted for extreme situations only). Once the slug velocity is found, the second iteration procedure (flow chart in Fig. 10.17) is performed to find the required area ratio by additional adjustments of the opening injection pressure (increasing or decreasing it as required). The first iteration procedure is actually imbedded in the second, but they are presented separately for didactical purposes. The equations used in each of these iterations are presented in detail after the iteration processes have been described. The first set of iterations is explained next (use the flow chart in Fig. 10.14 as a guide to follow this calculation procedure).

- The first step is to assume an initial liquid slug velocity. This velocity is adjusted as the first set of iterations is performed. The valve's opening injection pressure at depth is fixed at an initial value usually equal to  $P_{cvo\ max}$  (defined earlier) and then, during the two sets of iterations, this pressure is adjusted to find an acceptable liquid slug velocity and the area ratio of the valve that matches a commercially available area ratio that provides the required volume of gas injected per cycle.
- At each liquid slug velocity, calculation of the OCT ( $T_{co}$ ), initial liquid column length ( $Q_{ini}$ ), tubing pressure at the moment the pilot valve opens ( $P_{to}$ ), and daily liquid production ( $q$ ), are performed in that order. Based, to a large degree, on the well's PI and using a procedure which is explained later, the cycle time at which the well reaches its maximum daily production is calculated. This cycle time is known as the OCT.

To perform these calculations, an initial value of the liquid slug velocity,  $v_{at\ assum}$ , is assumed. As indicated earlier, this velocity is

adjusted in the iterations presented in Fig. 10.14. Once the OCT is found, it is easy to calculate:

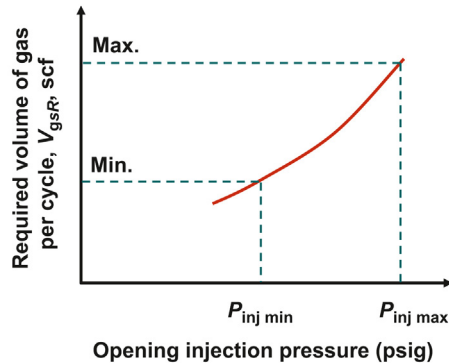
1. The size of the initial liquid column,  $Q_{ini}$ , above the pilot valve at the moment this valve opens.
2. The production pressure at valve's depth,  $P_{to}$ , also at the moment the pilot valve opens.
3. The daily liquid production of the well,  $q$ .

The liquid column at the moment the pilot valve opens is called the "initial column length" to distinguish it from the one that finally reaches the separator, which is smaller because part of the liquid column is not produced to the surface and it is left behind as a liquid film at the wall of the production tubing or as small droplets in the injection gas behind the liquid slug. This part of the liquid slug that is not produced to the surface is called "liquid fallback loss."

- Then, the calculation of the required volume of gas to be injected per cycle is carried out:

Once the size of the liquid slug to be produced is calculated as indicated in the previous step, the required volume of gas to be injected per cycle (needed to produce this liquid slug to the surface) can be calculated. This volume of gas is called  $v_{gsR}$  and it is given here in scf. This is accomplished by a calculation procedure based on the energy conservation equation explained later in this section. The required volume of gas injected per cycle depends on many factors, such as the liquid viscosity, the liquid column length, the wellhead pressure, etc. The required volume of gas injected per cycle also depends on the valve's opening injection pressure (because this pressure affects the velocity of the liquid slug: the higher the velocity, the more gas is needed to overcome the frictional pressure drop). If the iterations that determine the liquid slug velocity are carried out for different valve's opening injection pressure at depth ( $P_{cvo}$ ), it is found that for each opening injection pressure there is one and only one required volume of gas injected per cycle as shown in Fig. 10.11 (each point on this curve corresponds to a given injection pressure and its required volume of gas injected per cycle corresponds to the one that is found once the first set of iterations has converged to a final liquid slug velocity).

The minimum injection pressure ( $P_{inj\ min}$ ) in the graph presented in Fig. 10.11 corresponds to the valve's opening injection pressure for which the slug velocity is at its minimum value: fallback losses will increase for injection pressures less than this minimum pressure. The maximum injection pressure ( $P_{inj\ max}$ ) in the graph presented



■ FIGURE 10.11 Volume of gas required per cycle,  $V_{gsr}$ , for each injection pressure at valve's depth,  $P_{cvo}$ .

in Fig. 10.11 corresponds to the valve's opening injection pressure for which the slug velocity is at its maximum value: fallback losses will increase for injection pressures greater than this maximum pressure. The curve shown in Fig. 10.11 can be generated in two ways: (1) by allowing the calculations of the first set of iterations to converge to the OCT for each opening injection pressure, or (2) by keeping the cycle time constant (during the first set of iterations) for each opening injection pressure. If the cycle time is kept at a constant value (less than the OCT), the curve in the previous graph will shift downwards because the volume of gas per cycle that is required to lift shorter liquid slugs is, in consequence, smaller too. Additionally, the minimum pressure ( $P_{inj\ min}$ ) becomes smaller (as explained later for a similar type of graph constructed for the slug velocity as a function of the injection pressure).

The maximum injection pressure ( $P_{inj\ max}$ ) is the opening injection pressure at which the liquid slug velocity becomes too large.

$P_{cvo\ max}$  (the maximum allowed pressure to avoid opening the next upper unloading valve), on the other hand, could have any value (independently of the maximum and minimum pressures shown in Fig. 10.11) for a given well. It could be lower than  $P_{inj\ min}$  or higher than  $P_{inj\ max}$  because  $P_{cvo\ max}$  depends on the opening pressure of the upper unloading valve (or the system pressure if the well has no unloading valves), while the limiting pressures in Fig. 10.11 depend on the lifting process itself.

- Calculation of the valve's closing pressure is then performed: The valve closing pressure (for a given opening pressure) that would allow the injection of the required volume of gas per cycle

(as calculated in the previous step) must be found. As it has been stated earlier, the volume of gas that is injected to the well per cycle depends on the difference between the valve's opening and closing pressure (also called "the spread of the valve"). The operating pilot valve's opening injection pressure is assumed constant at the beginning of the first set of iterations, thus only the operating valve's closing pressure remains to be found. This is done by a simple mass balance calculation (explained later in this section) based on the required volume of gas injected per cycle,  $v_{gsR}$ .

- Liquid slug velocity calculation (first set of iterations):

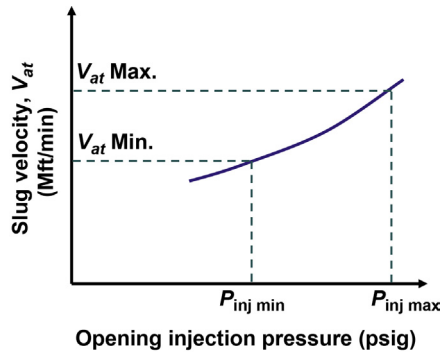
If the liquid slug is assumed to travel at a velocity that remains approximately constant when the slug is about to reach the surface, a steady state mass conservation equation can be used to perform the iterations to find the liquid velocity that converges to the current operational conditions. When the tip of the liquid slug reaches the surface (just before liquid production begins at the surface), the liquid slug velocity multiplied by the area of the production tubing should be equal to the gas flow rate through the gas lift valve at in situ conditions (average conditions inside the tubing) at that instant. This volumetric balance provides an equation (Eq. 10.67 derived later), which allows for the calculation of the liquid slug velocity just when it reaches the surface. In these calculations, it is assumed that the annular pressure is equal to the valve's closing pressure when the slug reaches the surface, which is true when the iterations converge to a final velocity.

The calculated velocity is compared with the previously assumed velocity (the one used to start the calculations of the OCT). If these two velocities are not approximately equal, all previous calculations are repeated using the average of the previous velocity and the recently calculated one as the new liquid slug velocity. This iteration process continues in this way and finishes when the new calculated velocity is approximately equal to the velocity used in the previous iteration.

It is important to point out that, for each pilot valve's opening injection pressure, there exists one and only one liquid slug velocity. This is shown in Fig. 10.12.

The minimum injection pressure in Fig. 10.12 corresponds to the pressure at which the velocity converges to its minimum allowed value; therefore, this pressure is equal to the minimum pressure shown in Fig. 10.11. If the slug velocity is less than this minimum value, the liquid fallback losses are higher and difficult to estimate. There are no exact values given in the literature for this minimum





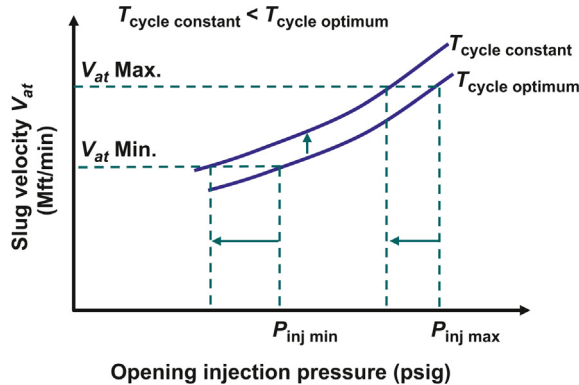
■ FIGURE 10.12 Liquid slug velocity ( $v_{at}$ ) as a function of the injection pressure.

velocity. Some specialists consider 800 ft./min as the lowest allowed slug velocity. If the maximum allowed injection pressure,  $P_{cvo\ max}$ , is less than the minimum injection pressure in Fig. 10.12, liquid slug velocity iterations can continue if one of the following steps is taken.

1. Reduce the cycle time ( $T_{cycle}$ ) to values shorter than the OCT:
 

In this way, liquid columns will be shorter and easier to lift at a higher velocity. The curve shown in Fig. 10.12 is calculated for the OCT corresponding to each injection pressure, but similar curves can be generated keeping the cycle time at a constant value for all injection pressures. If the cycle time is shorter than the OCT, the velocity curve is shifted upwards and the required minimum and maximum injection pressures are reduced, as shown in Fig. 10.13:
2. Continue with the design calculations (using  $P_{cvo\ max}$  as the injection pressure) so that the design can be used with metallic plungers to keep the fallback losses low (plunger-assisted intermittent gas lift is explained in Section 10.11).

At all times, the designer should be aware of an additional complication. If, at the end of all calculations (end of the second set of iterations), the maximum pilot valve's area ratio is not large enough to supply the required volume of gas per cycle, the design cannot be applied (with or without plungers) unless a time cycle controller is used at the surface to force the pilot valve open until the required volume of gas is injected at each cycle (this point will become clear with the help of Fig. 10.16 explained later).



■ FIGURE 10.13 Effect of the cycle time on the velocity curve.

The maximum injection pressure, on the other hand, should induce a liquid slug velocity that must not be greater than 1500–2000 ft./min.

In fact, the design can be obtained for high liquid slug velocities without affecting the daily liquid production of the well in a considerable manner. The problem with allowing high liquid slug velocities is the increase in the injection gas/liquid ratio.

If the velocity converges to a very large value, all calculations must be repeated with a lower injection pressure.

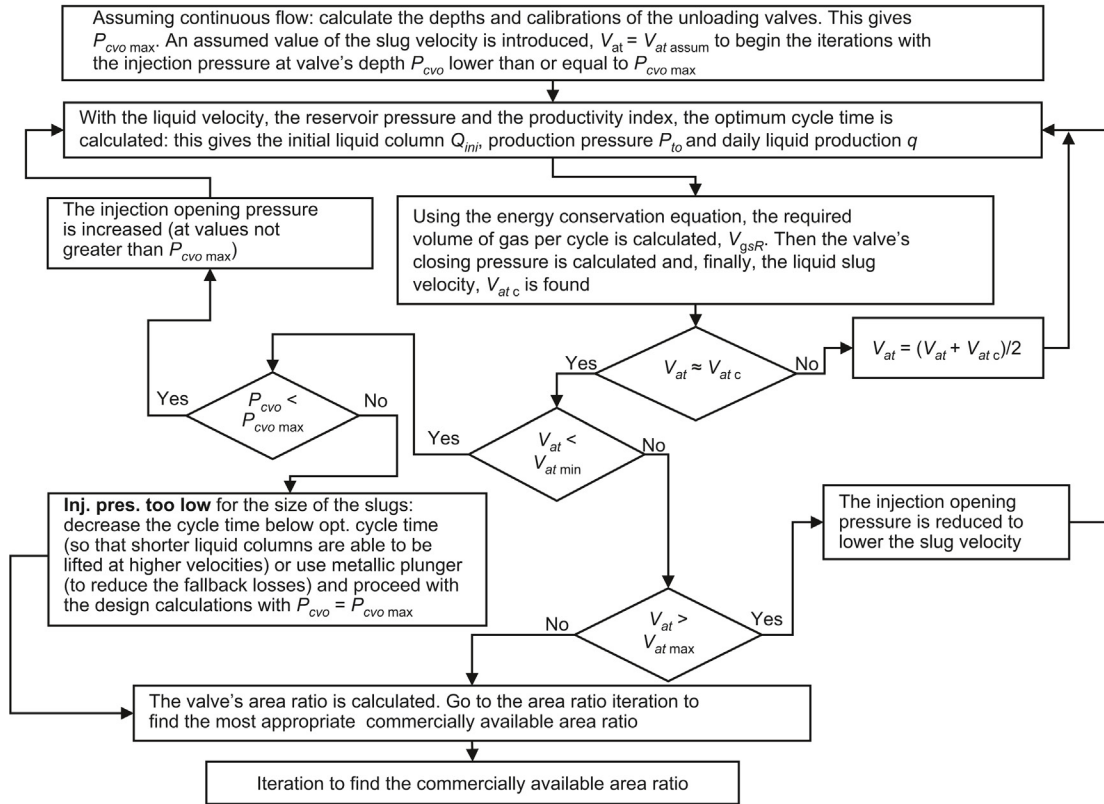
The iteration process to find the liquid slug velocity is illustrated in the flow chart shown in Fig. 10.14. (keep in mind that the iterations shown in Fig. 10.14 are part of those presented in Fig. 10.17)

- Valve's area ratio calculation (second set of iterations, Fig. 10.17):

The valve's closing pressure,  $P_{cvc}$ , is one of the parameters calculated during the liquid slug velocity iterations so that the required volume of gas per cycle can be injected. On the other hand, the opening injection pressure,  $P_{cvo}$ , might have also been adjusted so that the slug velocity falls within the accepted velocity limits. In the liquid slug velocity iteration process, the production pressure at valve's depth just when the valve opens,  $P_{to}$ , was also calculated by the following equation:

$$P_{to} = Q_{ini} \rho_f + P_{wh} f_g \quad (10.4)$$

Where  $Q_{ini}$  is the initial liquid column length in feet,  $\rho_f$  is the liquid gradient in psi/ft.,  $P_{wh}$  is the production wellhead pressure in psig and  $f_g$  is the gas factor that is used to find the gas pressure on top of the liquid column from the value of the wellhead pressure.



■ FIGURE 10.14 Flow chart for the calculation of the liquid slug velocity.

Therefore, all terms required by the valve's force balance equation to find the initial area ratio, named here  $R^*$ , are found during the first set of iterations. Thus, the last step in the first set of iteration is to find the value of  $R^*$ :

$$R^* = \frac{P_{cvo} - P_{cvc}}{P_{cvo} - P_{to}} \quad (10.5)$$

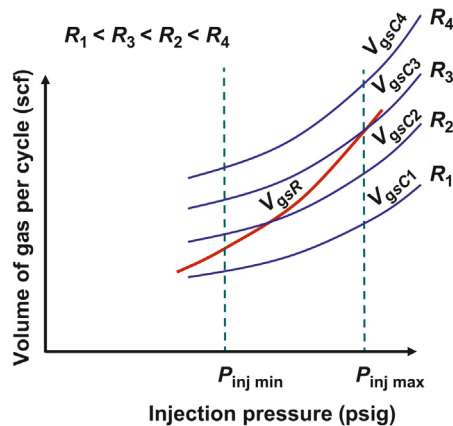
It is unlikely that the calculated area ratio  $R^*$  coincides with one of the commercially available area ratios of the selected pilot valve's model. This is why a second iteration procedure must be carried out to adjust the injection pressure until the best suited available area ratio for the well's operation is found (to maximize liquid production and minimize gas consumption).

To better understand the iterative process involved in finding the valve's area ratio (shown in the flow chart presented in Fig. 10.17),

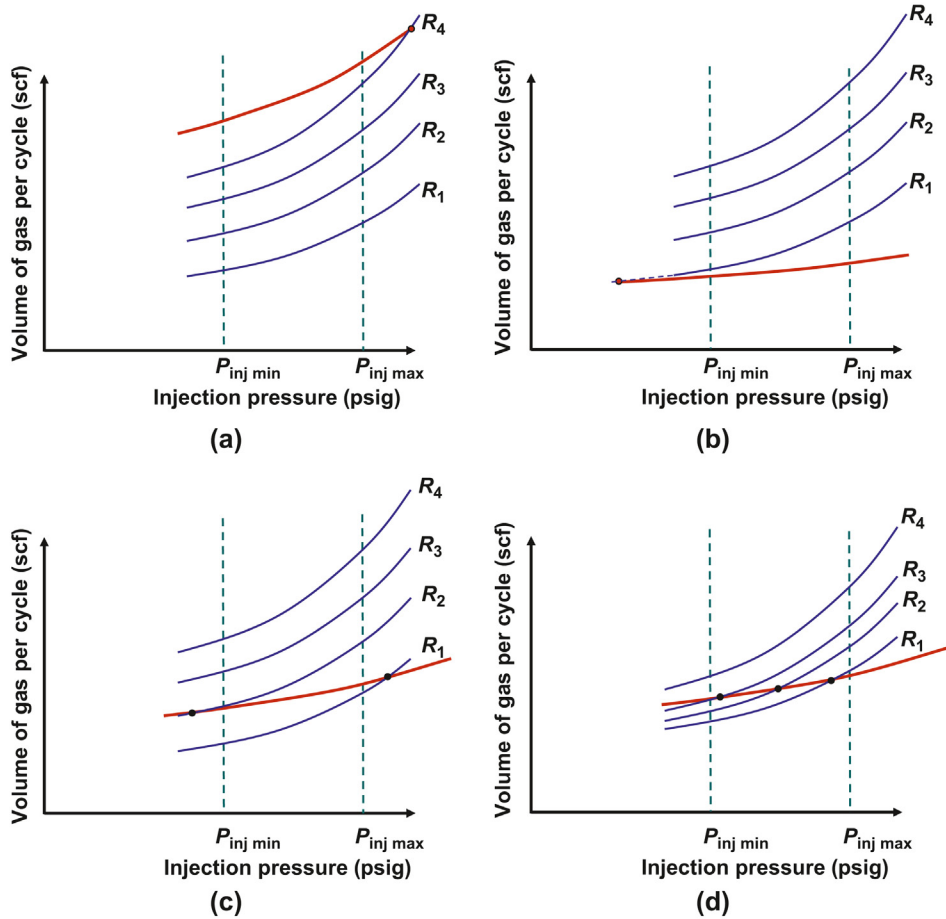
the curves that are shown in Fig. 10.15 are introduced to familiarize the reader with the required injection gas volume per cycle curve ( $v_{gsR}$ ) and the curves of the volume of gas the pilot valve can in reality provide per cycle ( $v_{gsC}$ ); all of these curves are given as functions of the valve's injection opening pressure. Here,  $R_1$  to  $R_4$  represent four commercially available area ratios for the selected valve's model. The volume of gas that the valve can provide per cycle,  $v_{gsC}$ , is directly proportional to the injection pressure because the spread of the valve is also directly proportional to the injection pressure. The required volume of gas  $v_{gsR}$  is also proportional to the injection pressure because the greater the injection pressure is, the greater the liquid slug velocity becomes and, in consequence, more injection gas volume is needed to overcome the frictional pressure drop.

It can be seen in Fig. 10.15 that as the injection pressure increases, the required volume of gas per cycle and the volume of gas that the pilot valve can provide increase. It can also be noticed that, for a given injection pressure, the volume of gas that the valve can provide is greater for larger valve's area ratios (because the spread of the valve is proportional to its area ratio). The iterations are carried out to find the points where the  $v_{gsR}$  curve intersects the  $v_{gsC}$  curves. Fig. 10.16 shows several possible relative positions of the  $v_{gsR}$  curve (in relation to what the valve can provide).

Fig. 10.16a shows that, independently of the area ratio, the required volume of gas injected per cycle is always greater than the volume the pilot valve can provide and that the point of intersection of



■ FIGURE 10.15 Required volume of gas per cycle,  $v_{gsR}$ , curve and the volume of gas per cycle curves the valve can provide,  $v_{gsC}$ , for each "n" commercially available area ratio  $R_n$ .



■ FIGURE 10.16 Several possible relative positions of the  $v_{gsc}$  curve with respect to the  $v_{gsr}$  curves.

the  $v_{gsr}$  and the  $v_{gsc}$  curves falls at a pressure greater than the maximum injection pressure.

This could lead to one of the worst operational conditions that can be found (not enough volume of gas and very high or very low liquid slug velocities) and it is usually because: (1) the annulus' volume is too small and/or the production tubing being too large, (2) the maximum valve's area ratio is still too small or, (3) the liquid column is too long. If one of these unfavorable conditions are met and, additionally, the liquid velocity is too low ( $P_{cvo\ max} < P_{inj\ min}$ ), the calculations can proceed only if a metallic plunger is used (to keep the fallback losses low) and a surface controller is used to force the pilot valve open until the required volume of gas per cycle has been injected.

On the other hand, if  $P_{cvo\ max}$  is greater than or equal to the pressure where the  $v_{gsC}$  and  $v_{gsR}$  curves intersect (in Fig. 10.16a), the design can be performed at that intersection pressure without the need of a surface intermitter, knowing that the injection gas/liquid ratio is going to be large (for being above  $P_{inj\ max}$  so that the slug velocity is unnecessarily high). However, if it is desired to keep the injection gas/liquid ratio low by not allowing the injection pressure to be above the maximum injection pressure, the design can be performed with the maximum area ratio,  $R_{max}$ , at  $P_{inj\ max}$  using a surface controller to be able to pass only the required volume of gas per cycle.

Some of the steps that can be taken to reduce the difference between the required volume of gas per cycle and the volume that the valve can provide (as depicted in Fig. 10.16a) include:

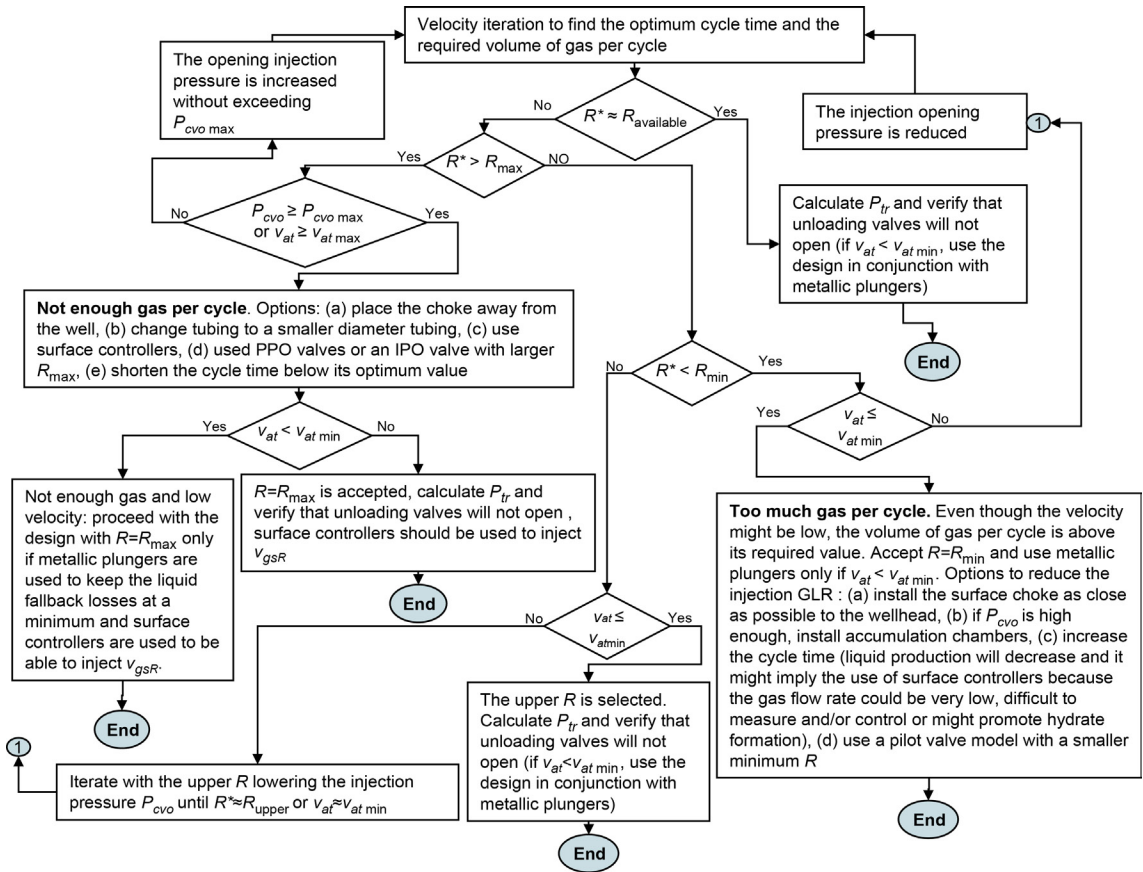
- Install the surface gas injection choke as far as possible from the wellhead.
- Reduce the diameter of the production tubing.
- Use surface controllers as stated earlier.
- Use production-pressure-operated valves or a different IPO valve model with a larger maximum area ratio.
- Shorten the cycle time so that smaller liquid column (that required less volume of gas per cycle) can be lifted (this will reduce the daily liquid production of the well but not in a considerable way).

Fig. 10.16b shows the case in which, even with the smallest area ratio and at the minimum injection pressure, the volume of gas the valve provides is greater than the required volume of gas per cycle to produce the liquid columns.

In this case, the iteration for the area ratio (shown in Fig. 10.17) will select the minimum injection pressure (as long as  $P_{cvo\ max}$  is greater than  $P_{inj\ min}$ ) and the design is then performed with the minimum area ratio so the injection gas/liquid ratio is not increased to very high values.

If, on the other hand,  $P_{cvo\ max}$  is smaller than  $P_{inj\ min}$ , the design can be performed with the minimum area ratio and at  $P_{cvo\ max}$ , but metallic plunger are recommended to reduce the fallback losses.

The operational condition corresponding to Fig. 10.16b is found in wells with very large annulus and/or very small production tubing. It could also be due to a valve model with a very large minimum area ratio, which is the case for some 1-in. OD pilot valves.



■ FIGURE 10.17 Flow chart to find the commercially available area ratio of the operating valve.

Some actions that can be taken (to reduce the difference between the required volume of gas per cycle and the excess volume of gas that the valve can provide), are as follows:

Install the surface gas injection choke as close as possible to the wellhead.

If the injection pressure is high enough, install an accumulation chamber.

Increase the cycle time to generate larger liquid columns (keeping in mind that this action might reduce the daily liquid production). This might also require the use of surface intermitters because the surface injection gas flow rate could be extremely low (difficult to control and/or measure) or the large pressure drop across the injection choke could promote hydrate formation.

Use a different pilot valve model with smaller minimum area ratio.

Fig. 10.16c shows the case in which the intersection points falls between two available area ratios for the selected pilot valve model but the intersection points are outside the acceptable velocity limits. In Fig. 10.16d, the intersection points do lie within the velocity limits for which the liquid fallback losses are kept at minimum values.

In all of these cases, the iterations shown in the flow chart (Fig. 10.17) will lead to the selection of the upper area ratio (so that the required volume of gas per cycle is met) at a pressure higher than or equal to the minimum acceptable injection pressure,  $P_{inj\ min}$  (so that the liquid velocity is acceptable).

If  $P_{cvo\ max}$  is less than  $P_{inj\ min}$  the design can be performed with the upper area ratio and at  $P_{cvo\ max}$  but it has to be implemented in conjunction with metallic plungers to minimize the liquid fallback.

The flow chart presented in Fig. 10.17 shows the iteration procedure that needs to be executed to find the most appropriate commercially available area ratio (that would allow the injection of the required volume of gas per cycle while keeping the liquid velocity at an acceptable level). Notice that the first set of iterations (liquid slug velocity iterations) is in reality a part of the iterations required to find the valve's area ratio because the velocity of the liquid slug depends on the injection pressure, which is adjusted during the second set of iterations.

The equations needed to perform the iterations involved in the design steps described earlier are presented in detail in the rest of this section.

### 10.6.1.1 Optimum cycle time calculation

The procedure to find the OCT that is given here was derived by Zimmerman (1982). To calculate the production pressure at valve's depth at the moment the pilot valve opens,  $P_{10}$ , it is necessary to find first the OCT, which was already defined earlier as the cycle time for which the daily liquid production is maximized. The equation that relates the bottomhole flowing pressure,  $P_{wf}$ , to the well's liquid flow rate (inflow) is:

$$q_f = J(P_{sbh} - P_{wf}) \quad (10.6)$$

In this equation  $q_f$  is the liquid production in STB/D,  $J$  is the PI in STB/(D-psi),  $P_{sbh}$  is the static reservoir pressure in psi, and  $P_{wf}$  is the bottomhole flowing pressure also in psi.



The PI used in Eq. 10.6 is in reality the average of all the values that the PI can take for the range of flowing bottomhole pressures found in a well on intermittent gas lift: the bottomhole pressure goes from a very low value (at the beginning of the liquid slug generation period) to a maximum value that is approximately 40–50% of the reservoir static pressure, which is usually the bottomhole maximum flowing pressure when operating at the OCT. In fact, when the PI of the well is not known, and therefore the OCT cannot be calculated, it is a good approximation to estimate the liquid column length that the well will have while operating at the OCT, by assuming that the corresponding maximum flowing bottomhole pressure will be equal to half the static reservoir pressure when the pilot valve opens. In this case, the calibration of the valve is performed assuming a production pressure at valve depth equal to 50% of the static reservoir pressure and then, after installing the valve in the well, the OCT can be found by a field trial and error procedure in which the cycle time is adjusted several times (by changing the surface gas flow rate as indicated in Eq. 12.21) until reaching the cycle time for which the maximum liquid production rate is found.

It can be seen in Fig. 10.18a that as the reservoir pressure declines, the PI of the well also declines so that the IPR curve has a greater inclination and it looks more like a linear function of the liquid flow rate. Thus, as the reservoir pressure decreases, the use of Eq. 10.6, with a constant value for the PI  $J$ , becomes more accurate because the difference between the maximum and minimum values of the PI is negligible. In figure Fig. 10.18b the range of practical values of the flowing bottomhole pressure for intermittent gas lift is shown.

If  $B_t$  is the production tubing volumetric capacity in Br/Mft., the instantaneous liquid production  $q_f$  from the reservoir during the liquid slug generation time interval can be expressed as:

$$q_f = B_t \left( \frac{dQ'}{dt} \right) \quad (10.7)$$

Where  $Q'$  is the length of the liquid column above the operating valve in Mft. If  $t$  is given in minutes and the liquid production in MBr/D, the r.h.s. of Eq. 10.7 must be multiplied by 1.44. But if  $t$  is given in minutes and the liquid production in Br/D, the r.h.s. of Eq. 10.7 must be multiplied by 1440. The volumetric capacity of the production tubing can be calculated from the following equation:

$$B_t = \frac{\pi}{4} (d[\text{in.}])^2 \left[ \frac{1 \text{ ft.}^2}{144 \text{ in.}^2} \right] \left[ \frac{1000 \text{ ft.}}{1 \text{ Mft.}} \right] \left[ \frac{1 \text{ Br}}{5.61456 \text{ ft.}^3} \right] = 0.97143 (d)^2 \left[ \frac{\text{Br}}{\text{Mft.}} \right] \quad (10.8)$$

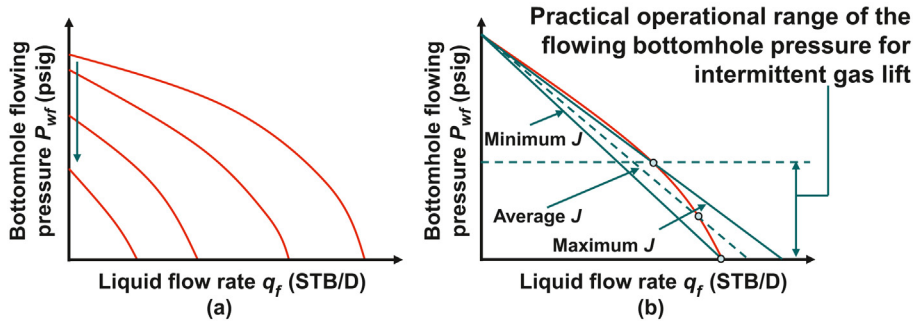


**FIGURE 10.18** Range of practical values of the flowing bottomhole pressure for intermittent gas lift. (a) effect of decreasing reservoir pressure and (b) average productivity index within a practical range of bottomhole flowing pressures.

Where  $d$  is the ID of the production tubing in inches. If  $A'$  is the maximum drawdown (in psi) at the top of the perforations just after the liquid slug has been produced, the term  $P_{sbh} - P_{wf}$  in Eq. 10.6 can be expressed, at any time during the generation of the liquid column, as:

$$P_{sbh} - P_{wf} = (A' - Q' \rho_f 1000) \quad (10.9)$$

Where  $A'$  is equal to:

$$A' = P_{sbh} - (D_{pt} - D_{ov}) 1000 \rho_t - P_{wh} f_g \quad (10.10)$$

Where  $D_{pt}$  is the depth of the top of the perforations in Mft.,  $D_{ov}$  is the depth of the operating valve in Mft.,  $P_{wh}$  is the production wellhead pressure in psig, and  $f_g$  is the gas factor that is used to find the pressure of the gas just above the liquid slug (calculated from the value of the wellhead production pressure). Equations for the calculation of  $f_g$  are given in chapter: Single-Phase Flow. In Eq. 10.9,  $\rho_f$  is the pressure gradient of the liquids in the production tubing expressed in psi/ft. and calculated from the API gravity of the oil and the water cut. In Eq. 10.10,  $\rho_t$  is the “true liquid pressure gradient” in psi/ft., which takes into account the formation gas present in the liquid column.  $\rho_f$  and  $\rho_t$  should not be confused with the density of the liquids: the pressure gradient is equal to the density of the liquid in lbm/ft.<sup>3</sup> times the acceleration due to gravity and divided by  $g_0$ :

$$\rho_f = \left( \text{density} \left[ \frac{\text{lbm}}{\text{ft.}^3} \right] \right) \left( \frac{g \left[ = 32.17 \frac{\text{ft.}}{\text{s}^2} \right]}{g_0 \left[ = 32.17 \frac{\text{lbm-ft.}}{\text{lb-ft.} \cdot \text{s}^2} \right]} \right) \left[ \frac{1 \text{ft.}^2}{144 \text{in.}^2} \right] = \frac{\text{density} \left[ \frac{\text{psi}}{\text{ft.}} \right]}{144} \quad (10.11)$$

The liquid gradient  $\rho_f$ , in psi/ft., can be calculated from the water cut and the API gravity of the oil using the following equation:

$$\rho_f = 0.433 \left[ w(\gamma_w) + (1-w) \frac{141.5}{131.5 + ^\circ \text{API}} \right] \quad (10.12)$$

Where  $w$  is the water cut expressed from 0 to 1, while 0.433 is the pure water gradient in psi/ft. and  $\gamma_w$  is the specific gravity of the formation water, which can be taken equal to 1 as a good approximation.

The true pressure gradient  $\rho_t$ , in psi/ft., is less than the pressure gradient of the produced liquids because it takes into account the dissolved and free gas that might be present in the liquid column.

The true pressure gradient is very difficult to predict because it depends on the viscosity and surface tension of the oil and water, as well as on the amount of free and dissolved gas in the liquids. Even though there are different equations to predict its value, it is much better to measure it by specially designed downhole pressure surveys for intermittent gas lift, following the recommendations given in Section 12.3.3. One equation that could be used to approximate the value of the true pressure gradient in psi/ft. is given by:

$$\rho_t = 0.1671 - 0.001429G_{\text{API}} \quad (10.13)$$

This equation is valid for oils with API gravities ( $G_{\text{API}}$ ) greater than  $23^\circ \text{API}$ . For lower API gravities, this equation is not recommended. Heavy oils, even in wells with very low formation gas/oil ratios, tend to have very small true pressure gradient values due to the reduced mobility of the gas bubbles in the oil along the liquid column.

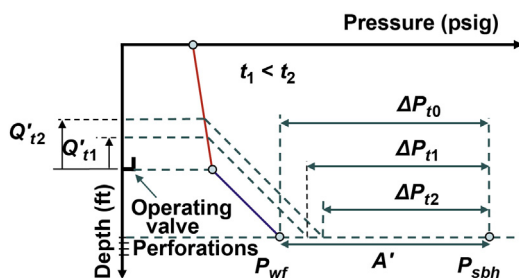
Fig. 10.19 shows what happens during the liquid slug generation period, in which a liquid column of length  $Q'$  accumulates above the operating valve. As it can be appreciated in the figure, the drawdown is at its maximum value  $A'$  just after the liquid column has been produced and a new liquid column is beginning to accumulate above the operating valve.

Introducing Eqs. 10.10, 10.9, and 10.7 in Eq. 10.6, yields:

$$\frac{dQ'}{dt} = \alpha' (A' - Q' \rho_f 1000) \quad (10.14)$$

In Eq. 10.14,  $\alpha'$  is equal to  $J/(1440 B_i)$  because  $dQ'/dt$  is given in Mft./min and the production in Br/D. Eq. 10.14 can be integrated in the following way:

$$\int_{\alpha'}^{\alpha'} \frac{dQ'}{A' - Q' \rho_f 1000} = \int_0^t \alpha' dt \quad (10.15)$$



■ FIGURE 10.19 Generation of the liquid column above the operating valve.

Where  $Q'_a$  is the liquid column left as liquid fallback from the previous cycle in Mft. As an approximation, this fallback liquid column is thought to be completely generated above the operating valve at the very beginning of the new cycle. Then,  $Q'_a$  is given by:

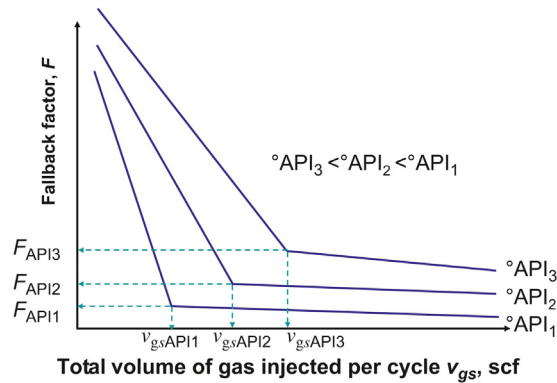
$$Q'_a = FD_{ov}Q' \quad (10.16)$$

Where  $D_{ov}$  is the depth of the operating point of injection in Mft.,  $Q'$  is the length of the liquid column at the moment the pilot valve opens in Mft., and  $F$  is the liquid fallback factor, which is defined as the fraction of the initial column length that is not produced per each 1000 ft. of depth of the point of injection ( $F$  is expressed in values from 0 to 1 and not as percentage points).

By default,  $F$  is usually assumed to be equal to 0.05. In other words, 5% of the initial liquid column, per each 1000 ft. of depth of the point of injection, will not reach the surface. The  $F$  factor is one of the most difficult parameter to estimate and its value depends on the liquid slug velocity, the volume of gas injected per cycle, and the type of fluid being lifted.

As it has been pointed out, the liquid slug velocity should be equal to approximately 1000 ft./min. This velocity can be attained by injecting the gas at an appropriate rate and pressure.

The total volume of gas injected per cycle should also be the right one to produce all the liquid slug to the surface (the gas flow rate and injection pressure could be exactly the one needed to lift the slug at the right velocity, but if the gas lift valve closes long before the slug reaches the surface, the fallback losses will be very large). The objective then of a good design is to inject all the volume of gas required per cycle at the right pressure and flow rate. Fig. 10.20 shows the typical behavior of the liquid fallback factor as a function of the volume of gas injected per cycle and the type of oil being lifted. In order for graphs like this one to be useful, they must be obtained for liquid slugs traveling at a velocity as close as possible to 1000 ft./min.



■ FIGURE 10.20 Fallback factor as a function of the volume of gas injected per cycle.

The value of the horizontal coordinate of the point where the graph of the fallback factor  $F$  in Fig. 10.20 changes slope is considered to be the required volume of gas injected per cycle that minimizes the liquid fallback losses. As can be seen in the figure, the lower the API gravity of the oil is, the greater the required volume of gas per cycle (and the  $F$  factor) becomes. As long as the volume of gas per cycle  $v_{gs}$  is greater than or equal to the volume where the slope of the graph changes value and the liquid velocity is approximately equal to 1000 ft./min, the following values for the fallback factor can be established:

- For API gravities greater than 23°API, the liquid fallback factor can be estimated to be equal to 0.05.
- For oils between 18 and 23°API, the fallback factor can be estimated to be between 0.12 and 0.05, respectively.
- For oils between 16 and 18°API, the fallback factor can be estimated to be between 0.14 and 0.12, respectively.

Continuing with the calculation of the OCT, an expression for the liquid column  $Q'$  as a function of the liquid column generation time  $t$  (expressed in minutes) can be found by solving the integrals in Eq. 10.15, which yields:

$$Q' = \frac{A'(e^{\alpha' t} - 1)}{1000\rho_f(e^{\alpha' t} - c_m)} \quad (10.17)$$

Where  $\alpha$  is equal to  $1000\alpha'$ , being  $\alpha'$  equal to  $J/(1440 B_i)$  as indicated earlier;  $c_m$  is  $FD_{ov}$  with  $D_{ov}$  in Mft. If the gas injection time  $T_{oc}$  (defined as the slug travel time in the production tubing) is approximated as the depth of the operating valve  $D_{ov}$ , divided by the liquid slug mean velocity,  $v_{sl}$ , in Mft./min, then the total cycle time  $T_{cycle}$  (also expressed in minutes) is equal

to the sum of the liquid column generation time interval,  $t$ , plus the travel time of the liquid slug in the tubing,  $T_{oc} = D_{ov}/v_{at}$ :

$$T_{\text{cycle}} = t + D_{ov}/v_{at} \quad (10.18)$$

The mean liquid slug velocity is estimated to be equal to  $v_{at \text{ max}}/2$ , where  $v_{at \text{ max}}$  is the maximum slug velocity which is assumed to be the slug velocity just when the tip of the slug arrives at the surface.

On the other hand, the daily liquid production in MBr/D, for a given total cycle time  $T_{\text{cycle}}$  can be calculated as:

$$q_f = Q'(1 - c_m) B_t \frac{1440}{T_{\text{cycle}}} \frac{1}{1000} \quad (10.19)$$

If factor  $C_3$  is defined as  $1.44B_t(1 - c_m)$ , then  $q_f$  is equal to  $(C_3)Q'/T_{\text{cycle}}$ . Using Eqs. 10.17 and 10.18, Eq. 10.19 can be expressed as:

$$q_f = \frac{C_3 A' \left( \frac{e^{\alpha \rho_f T_{\text{cycle}}}}{e^{\alpha \rho_f D_{ov}/v_{at}}} - 1 \right)}{T_{\text{cycle}} 1000 \rho_f \left( \frac{e^{\alpha \rho_f T_{\text{cycle}}}}{e^{\alpha \rho_f D_{ov}/v_{at}}} - c_m \right)} \quad (10.20)$$

Eq. 10.20 represents the daily liquid production in MBr/D as a function of the total cycle time  $T_{\text{cycle}}$ . To maximize this production, Eq. 10.20 must be differentiated with respect to  $T_{\text{cycle}}$  and the result set equal to 0:

$$\frac{dq_f}{dT_{\text{cycle}}} = 0 \quad (10.21)$$

The result of Eq. 10.21 is:

$$T_{\text{cycle}} = \frac{(e^{\gamma T_{\text{cycle}}} - C_4)(e^{\gamma T_{\text{cycle}}} - c_m C_4)}{\gamma e^{\gamma T_{\text{cycle}}} C_2 C_4} \quad (10.22)$$

Where,

$$\begin{aligned} C_2 &= 1 - c_m \\ \gamma &= \alpha \rho_f \\ C_4 &= e^{\gamma \frac{D_{ov}}{v_{at}}} \end{aligned}$$

The value of  $T_{\text{cycle}}$  that satisfies Eq. 10.22 corresponds to the OCT. This value can be found from Eq. 10.22 using the Newton–Raphson method. Eq. 10.22 can be written as:

$$\frac{(e^{\gamma T_{\text{cycle}}} - C_4)(e^{\gamma T_{\text{cycle}}} - c_m C_4)}{\gamma e^{\gamma T_{\text{cycle}}} C_2 C_4} - T_{\text{cycle}} = 0 \quad (10.23)$$

If the left hand side of Eq. 10.23 is considered to be a function “ $F$ ” of the total cycle time  $T_{\text{cycle}}$ , the problem is solved by finding the value of  $T_{\text{cycle}}$  for which  $F(T_{\text{cycle}}) = 0$ . If  $T_{\text{cycle}1}$  is the first assumed value of  $T_{\text{cycle}}$ , the new value of  $T_{\text{cycle}}$  is found by the Newton–Raphson method as:

$$T_{\text{cycle}2} = T_{\text{cycle}1} - F/(dF/dT_{\text{cycle}}) \quad (10.24)$$

Where “ $F$ ” and its derivative,  $dF/dT_{\text{cycle}}$ , are evaluated at time  $T_{\text{cycle}1}$ . If the absolute value of  $T_{\text{cycle}2} - T_{\text{cycle}1}$  is not less than or equal to a given tolerance value, a third value of  $T_{\text{cycle}}$  is calculated using:

$$T_{\text{cycle}3} = T_{\text{cycle}2} - F/(dF/dT_{\text{cycle}}) \quad (10.25)$$

With “ $F$ ” and its derivative evaluated at  $T_{\text{cycle}2}$ . This process continues until convergence on the value of  $T_{\text{cycle}}$  is achieved.  $dF/dT_{\text{cycle}}$  is given by:

$$\frac{dF}{dT_{\text{cycle}}} = \frac{\gamma(e^{\gamma T_{\text{cycle}}} - c_m C_4^2 e^{-\gamma T_{\text{cycle}}})}{\gamma C_2 C_4} - 1 \quad (10.26)$$

Combining Eqs. 10.23, 10.25, and 10.26, yields:

$$T_{\text{cycle}n+1} = T_{\text{cycle}n} - \frac{\frac{(e^{\gamma T_{\text{cycle}n}} - C_4)(e^{\gamma T_{\text{cycle}n}} - c_m C_4)}{\gamma e^{\gamma T_{\text{cycle}n}} C_2 C_4} - T_{\text{cycle}n}}{\frac{\gamma [e^{\gamma T_{\text{cycle}n}} - c_m (C_4)^2 e^{-\gamma T_{\text{cycle}n}}]}{\gamma (C_2)(C_4)} - 1} \quad (10.27)$$

Knowing the value of  $T_{\text{cycle}}$  that converges to the OCT, the liquid column length  $Q'$  can be determined using Eqs. 10.17 and 10.18 for that particular cycle time, and the daily liquid production can be calculated from Eq. 10.19. The value of the production tubing pressure,  $P_{\text{to}}$  in psi, at the moment the pilot valve opens is determined by:

$$P_{\text{to}} = P_{\text{wh}} f_g + Q' 1000 \rho_f \quad (10.28)$$

As it was previously mentioned, the pilot valve’s area ratio  $R$  can be found from the valve’s force balance equation:  $R = (P_{\text{cvo}} - P_{\text{cvc}})/(P_{\text{cvo}} - P_{\text{to}})$ . For a given value of  $R$ , and knowing  $P_{\text{cvo}}$  (the valve’s opening pressure at depth) and  $P_{\text{to}}$ , the corresponding value of  $P_{\text{cvc}}$  (the valve’s closing pressure at depth) can be found from this force balance equation. The difference  $P_{\text{cvo}} - P_{\text{cvc}}$  estimated from this force balance equation, determines the value of the volume of gas per cycle that the valve can provide,  $v_{\text{gs}C}$ , only if the value of  $P_{\text{cvc}}$  is corrected for dynamic effects as it was already mentioned in previous sections. The value of  $v_{\text{gs}C}$  must be greater than or equal to the required volume of gas per cycle,  $v_{\text{gs}R}$ , which is calculated from an energy balance equation given later.

### 10.6.1.2 Calculation of the volume of gas per cycle

#### $v_{gsR}$ and $v_{gsC}$

The procedures that can be used to calculate the required volume of gas per cycle,  $v_{gsR}$ , and the actual volume of gas per cycle the valve can provide,  $v_{gsC}$ , for a given valve's spread, are described next. These procedures were derived by Zimmerman (1982). In the following calculation of the volume of gas per cycle, it is assumed that all the gas must have been injected into the tubing when the top of the liquid slug was just arriving at the surface (so that the entire liquid slug is still inside the tubing). This approximation is valid for the great majority of cases of wells on intermittent gas lift, for which the lengths of the liquid columns to be lifted are usually shorter than 10–20% the measured depth of the point of injection. The idea is that the pilot valve closes at the instant the liquids begin to flow at the surface because the gas that has entered the tubing can expand to produce the entire slug to the surface. The liquid velocity could decrease after the pilot valve closes due to the lack of additional gas injected below the slug, but because the vertical section of the slug is also going to be gradually decreasing, the required gas pressure needed to keep the velocity at an acceptable level is also going to be lower and, as a result, the liquid velocity might not drop to values less than its recommended velocity to keep the fallback losses at a minimum value. With this approach, gas overinjection could be avoided.

The explanation given in the previous paragraph does not apply to large liquid slugs. As it is shown in the design calculations for accumulation chambers to find the required volume of gas injected per cycle for large liquid slugs (Section 10.7), it is assumed that the pilot valve should close just after the entire liquid slug has been produced to the surface. The liquid slug velocity at the surface is in this case equal to the maximum velocity achieved by the slug when its tip reached the surface, but corrected for the difference in diameter between the production tubing and the flowline. In this way, the designer makes sure that the entire liquid slug is in fact produced to the surface, but probably with more volume of gas injected per cycle that might be actually needed. Beside the additional calculation of the liquid velocity at the surface, all other calculations are basically the same as those for the procedure given in the previous paragraph. Some designers use the procedure for large liquid slugs in all cases, regardless of the slug size, which is not a bad thing to do because the extra volume of gas injected per cycle, besides not being too large, could also be compensated by the additional liquid production that the tail gas could carry with it to the surface. What should not be done is to use the procedure given in the previous paragraph for all cases because the liquid fallback losses could become very large for large liquid slugs.



The value of  $v_{gsR}$  is found from the energy that must be provided by the injection gas to increase the liquid slug potential energy as it is lifted from the bottom of the well to the surface. The volume of the injection gas (at standard conditions) that must have entered the production tubing when the top of the liquid slug has just arrived at the surface is given by:

$$v_{gsR} P_{st} = n R_u T_{st} \quad (10.29)$$

Where  $n$  is the number of moles that have entered the production tubing,  $R_u$  is the universal gas constant,  $P_{st}$  is equal to 14.7 psia, and  $T_{st}$  is 520°R. For the same number of moles but at in situ conditions, Eq. 10.29 can be written as:

$$V P_{ga} = n R_u z_a T_a \quad (10.30)$$

Where  $P_{ga}$  is the average pressure in psia of all the gas in the production tubing underneath the liquid slug at the moment the tip of the liquid slug reaches the wellhead;  $T_a$  and  $z_a$  are the average temperature in °R and the average compressibility factor of the gas in the production tubing, respectively;  $V$  is the actual volume occupied by the gas in the production tubing and it is given by:

$$V = (D_{ov} - Q')(B_{gt}) \quad (10.31)$$

Where  $B_{gt}$  is the volumetric capacity of the production tubing in ft.<sup>3</sup>/Mft., equal to 5.61456  $B_t$ , and  $D_{ov}$  is the depth of the operating valve in Mft. ( $B_t$  is defined in Eq. 10.8). Dividing Eq. 10.29 by Eq. 10.30, using the values of the pressure and temperature at standard conditions and solving for  $v_{gsR}$ , the following expression is found:

$$v_{gsR} = \frac{520 B_{gt} (D_{ov} - Q') P_{ga}}{14.7 z_a T_a} \quad (10.32)$$

To find the value of  $v_{gsR}$  using Eq. 10.32, it is necessary to find first the values of  $P_{ga}$ ,  $T_a$ , and  $z_a$  in that order. The average pressure in the tubing,  $P_{ga}$ , can be calculated from:

$$P_{ga} = \frac{P_{gu} + P_{un}}{2} \quad (10.33)$$

Where  $P_{gu}$  is the pressure underneath the liquid column. Because the top of the liquid slug is just arriving at the wellhead,  $P_{gu}$  is the sum of the hydrostatic pressure of the liquid column that reaches the surface plus the

pressure drop due to frictional losses that needs to be overcome to move the liquid slug plus the wellhead pressure  $P_{wh}$ ;  $P_{tm}$  is the gas pressure in the production tubing at valve's depth and it is equal to  $P_{gu}$  plus the weight of the gas column in the production tubing. Using the gas factor  $f_g$ ,  $P_{tm}$  is given by:

$$P_{tm} = P_{gu} f_g \quad (10.34)$$

And

$$P_{gu} = P_{wh} + Q'(1 - c_m)1000\rho_f C_f \quad (10.35)$$

Where  $c_m$  is equal to  $F(D_{ov})$ ,  $D_{ov}$  is the injection point depth in Mft.,  $F$  is the fallback factor, and  $C_f$  is a coefficient that takes into account the hydrostatic and frictional pressure drops:

$$C_f = 1 + \frac{207.23 f v_{at}^2}{d} \quad (10.36)$$

Where  $v_{at}$  is the average velocity of the liquid slug in Mft./min,  $d$  is the tubing ID (inside diameter) in inches, and  $f$  is the friction factor. The number "1" on the right hand side of Eq. 10.36 takes into account the hydrostatic pressure because  $Q'(1 - c_m)1000\rho_f$  is the pressure in psi that a liquid column of length  $Q'(1 - c_m)$  (which is the length of the liquid column that finally reaches the surface in Mft.) exerts just below the slug when its top reaches the surface. The second part of the Eq. 10.36 deals with frictional pressure drop, which is derived next.

The equation that determines the pressure drop due to friction,  $\Delta P_f$  in psi, for a given pipe length  $L$  in ft., is given by:

$$\Delta P_f = \frac{f}{d} (\text{Density}) \frac{\text{Velocity}^2}{2} \frac{\text{Length}}{g_0} \quad (10.37)$$

As it was indicated earlier,  $f$  is the friction factor and  $d$  is the ID of the tubing (which should be converted from inches to feet). "Density" is the density of the liquids and it must be expressed in  $\text{lbm}/\text{ft}^3$  (which, according to Eq. 10.11, must also be equal to  $144\rho_f$ ). "Length" is the length of the liquid slug (in feet) when its tip is just reaching the surface and its value in feet is equal to  $(1000)(Q')(1 - c_m)$  because  $Q'$  is expressed in Mft. Finally, "velocity" in Eq. 10.37 is the velocity of the liquid slug that must be expressed in  $\text{ft}/\text{s}$  and it is equal to  $v_{at \max}$ , (which is the maximum velocity that is assumed the liquid slug has when it reaches the surface). As an approximation,  $v_{at \max}$  is equal to twice the mean liquid slug velocity, or

$v_{at \max} = 2v_{at}$ , and  $v_{at}$  must be converted from Mft./min to ft./s. Eq. 10.37 can then be expressed as:

$$\Delta P_f = \frac{f}{12 \left[ \frac{\text{in.}}{\text{ft.}} \right]} \left( \rho_f 144 \left[ \frac{\text{lbm}}{\text{ft.}^3} \right] \right) \frac{\left( 2v_{at} \left[ \frac{\text{Mft.}}{\text{min}} \right] \right)^2 \left( \frac{1000 \left[ \frac{\text{ft.}}{\text{Mft.}} \right]}{60 \left[ \frac{\text{s}}{\text{min}} \right]} \right)^2}{2} \quad (10.38)$$

$$\times \frac{\left( 1000Q'(1-c_m) \right) \left[ \frac{\text{ft.}}{\text{ft.}} \right]}{32.17 \left[ \frac{\text{lbm-ft.}}{\text{lbf-s}^2} \right]} \left[ \frac{1}{144 \left[ \frac{\text{in.}^2}{\text{ft.}^2} \right]} \right]$$

Simplifying Eq. 10.38, the following expression is obtained:

$$\Delta P_f = \left( 207.23 f \frac{v_{at}^2}{d} \right) \left[ \rho_f 1000Q'(1-c_m) \right] \text{ psi} \quad (10.39)$$

The first bracket on the r.h.s of Eq. 10.39 is the part of  $C_f$  that has to do with the frictional pressure drop in Eq. 10.36.

The friction factor can be calculated from the Moody diagram using a Reynolds number expressed as:

$$R_e = \frac{(d)(\text{density})(v_{at \max})}{\mu_o} \quad (10.40)$$

Because the tubing ID,  $d$ , is given in inches, it must be converted to feet. It has already been pointed out that the density can be expressed as  $144\rho_f$  in  $\text{lbm}/\text{ft.}^3$  and  $v_{at \max}$  is equal to  $2v_{at}$ . If the liquid viscosity  $\mu_o$  is expressed in  $\text{lbf-s}/\text{ft.}^2$ , the following expression for the Reynolds number can be used:

$$R_e = \frac{\left( d \left[ \frac{\text{in.}}{12 \text{ in.}} \right] \right) \left( \rho_f 144 \left[ \frac{\text{lbm}}{\text{ft.}^3} \right] \right) \left( 2v_{at} \left[ \frac{\text{Mft.}}{\text{min}} \right] \right) \left[ \frac{1000 \text{ ft./Mft.}}{60 \text{ s/min}} \right]}{\left( \mu_o \left[ \frac{\text{lbf-s}}{\text{ft.}^2} \right] \right) \left( 32.17 \left[ \frac{\text{lbm-ft.}}{\text{lbf-s}^2} \right] \right)} \quad (10.41)$$

This can be simplified to:

$$R_e = \frac{12.434 d \rho_f v_{at}}{\mu_o} \quad (10.42)$$

There are many correlations that can be used to calculate the friction factor  $f$  as a function of the Reynolds number; for example, the one given here is adequate for the production tubing used in oil wells:

$$\begin{aligned} R_c < 1185 &\Rightarrow f = 64/R_c \\ R_c > 35000 &\Rightarrow f = 0.09292 R_c^{-0.124} \\ 1185 \leq R_c \leq 35000 &\Rightarrow f = 0.26153 R_c^{-0.2229} \end{aligned}$$

The calculation of the gas average temperature in the production tubing is performed by means of an iterative procedure based on an approximate energy balance of the gas that enters the tubing (derived by [Zimmerman, 1982](#)). The enthalpy per unit mass of the gas in the tubing below the liquid slug is equal to the initial enthalpy per unit mass when the injection gas was in the casing minus the gain in potential energy of the liquid slug per unit mass of the gas injected into the tubing:

$$H = H_c - H_w \quad (10.43)$$

Where  $H$  is the final enthalpy of the gas in the production tubing in Btu/lbm,  $H_c$  is the initial enthalpy of the gas in the casing–tubing annulus in Btu/lbm, which can be calculated from the geothermal temperature using an equation that is given later, and  $H_w$  is the gain in potential energy of the liquid slug per unit mass of the gas injected into the tubing, given in Btu/lbm by the following equation:

$$H_w = \frac{\text{Potential energy gain of the liquid slug (Btu)}}{\text{Mass of the gas that entered the tubing (lbm)}} = \frac{\frac{m_L(g)h_v}{g_0}}{m_{\text{gas}}} \quad (10.44)$$

In this equation,  $h_v$  is the true vertical depth traveled by the liquid which, for a vertical well, is given by:

$$h_v = \left\{ \left[ D_{ov} - (1 - c_m) Q' \right] \left[ \frac{\text{Mft.}}{\text{Mft.}} \right] \right\} \left[ \frac{1000 \text{ ft.}}{\text{Mft.}} \right] \quad (10.45)$$

Where  $D_{ov}$  is the depth of the operating valve in Mft.;  $g$  is the acceleration due to gravity, equal to 32.17 ft./s<sup>2</sup>;  $g_0$  is equal to 32.17 lbm-ft./(lbf-s<sup>2</sup>); the mass of the gas  $m_{\text{gas}}$  is equal to its density at standard conditions multiplied by the volume of gas (expressed in scf) that entered the tubing, which is equal to  $v_{\text{gs}R}$  (the density of the gas at standard conditions is equal to the air density at standard conditions, equal to 0.07635 lbm/ft.<sup>3</sup>, multiplied by the specific gravity of the injection gas,  $G_g$ ; in other words, the density of the gas at standard conditions is equal to  $G_g 0.07635$  lbm/ft.<sup>3</sup>); the liquid mass  $m_L$  that reaches the surface is equal to its volume multiplied by its density.

As it was already explained, the density of the liquid in  $\text{lbm}/\text{ft}^3$  is numerically equal to  $144\rho_f$ , where  $\rho_f$  is the liquid gradient in  $\text{psi}/\text{ft}$ . defined in Eq. 10.12. The volume of the liquid that is produced is given by:

$$\text{Liquid volume} = Q'(1 - c_m)(\text{Mft.})B_t \left( \frac{\text{Br}}{\text{Mft.}} \right) 5.61456 \left( \frac{\text{ft}^3}{\text{Br}} \right) \quad (10.46)$$

Introducing these expressions into Eq. 10.44, the following equation is found for  $H_w$ :

$$H_w = \frac{\rho_f 144 \left[ \frac{\text{lbm}}{\text{ft}^3} \right] \left\{ [Q'(1 - c_m)] B_t (5.61456) [\text{ft}^3] \right\} \times 32.17 \left( \frac{\text{ft}}{\text{s}^2} \right) \left\{ [D_{ov} - (1 - c_m)Q'] (1000 \text{ ft.}) \right\}}{v_{gsR} [\text{ft}^3] 0.07635 \left[ \frac{\text{lbm}}{\text{ft}^3} \right] G_g 32.17 \left[ \frac{\text{lbm-ft}}{\text{lb-ft-s}^2} \right] 778.16 \left[ \frac{\text{lb-ft}}{\text{Btu}} \right]} \quad (10.47)$$

With the volumetric capacity of the production tubing in  $\text{ft}^3/\text{Mft.}$ ,  $B_{gt}$ , equal to  $5.61456 B_t$ , this expression is simplified to:

$$H_w = \frac{2423.7 \rho_f Q'(1 - c_m) [D_{ov} - (1 - c_m)Q'] B_{gt}}{G_g v_{gsR}} \quad (10.48)$$

Where  $Q'$  is the initial liquid column length in  $\text{Mft.}$ ,  $D_{ov}$  is the depth of the point of injection in  $\text{Mft.}$ ,  $c_m$  is the fallback factor  $F$  multiplied by  $D_{ov}$ ,  $B_{gt}$  is the tubing volumetric capacity in  $\text{ft}^3/\text{Mft.}$ , and  $G_g$  is the gas specific gravity.

Due to the presence of the term  $v_{gsR}$  in Eq. 10.48 (which is precisely what needs to be calculated), Eq. 10.43 must be solved by iteration. If  $H$  and  $H_w$  are expressed as functions of the average temperature of the gas inside the tubing,  $T_a$ , then:

$$H(T_a) = H_c - H_w(T_a) \quad (10.49)$$

The objective of the iterative method is to find the average temperature of the gas in the tubing,  $T_a$ , which satisfies Eq. 10.49. For this purpose, a correlation of the enthalpy as a function of the average pressure  $P_{ga}$  and average temperature  $T_a$  must be used.

The enthalpy of the injection gas is a function of its specific gravity, temperature, and pressure. If the temperature is expressed in  $^{\circ}\text{R}$ , the pressure in  $\text{psia}$ , and the enthalpy in  $\text{Btu}/\text{lbm}$ , the equation introduced by Zimmerman (1982) that can be used to approximate the enthalpy of the gas is:

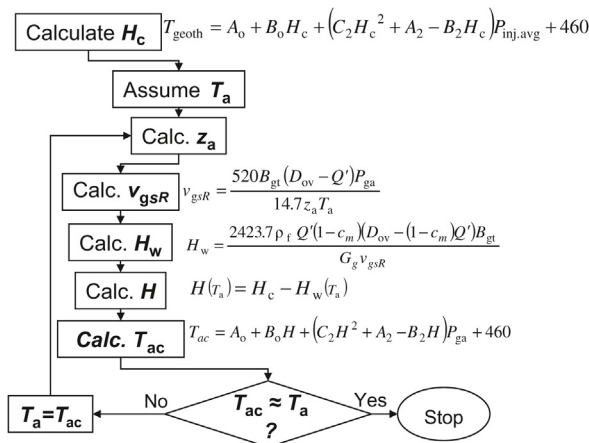
$$T_a = A_0 + B_0 H + (C_2 H^2 + A_2 - B_2 H) P_{ga} + 460 \quad (10.50)$$

Factors  $A_0$ ,  $B_0$ ,  $C_2$ ,  $A_2$ , and  $B_2$  are functions of the gas specific gravity and they are given by:

$$\begin{aligned}
 A_0 &= 152.46G_g - 207.85 \\
 B_0 &= 0.78946G_g + 1.3223 \\
 A_2 &= 0.11038G_g + 0.013944 \\
 B_2 &= (2.5757G_g^2 - 2.9663G_g + 1.3437)10^{-3} \\
 C_2 &= (6.8666G_g^2 - 7.561G_g + 2.934)10^{-6}
 \end{aligned}$$

The calculation procedure is carried out as follows (Fig. 10.21):

1. Using Eq. 10.50, the value of  $H_c$  is determined with the average geothermal temperature of the injection gas in the annulus in °R and the average injection pressure just before the pilot valve opens,  $P_{inj,avg}$  in psia, equal to  $14.7 + (P_{cso} + f_g P_{cso})/2$  with  $P_{cso}$  being the surface gas injection opening pressure.
2. An initial temperature of the gas below the liquid slug,  $T_a$ , is assumed. A good starting temperature is the average geothermal temperature.
3. With the average pressure of the gas that entered the tubing,  $P_{ga}$ , and the assumed temperature,  $T_a$ , the compressibility of the gas below the liquid slug  $z_a$  is calculated at the moment the top of the liquid slug reaches the wellhead.
4. The value of  $v_{gsR}$  corresponding to the temperature  $T_a$  is calculated with Eq. 10.32.
5. The value of  $H_w$  is calculated using Eq. 10.48.



■ FIGURE 10.21 Iterations to find the temperature of the injected gas located below the liquid slug when it reaches the surface.

6. With  $H_c$  and  $H_w$ , Eq. 10.49 is used to find the enthalpy  $H$  of the gas that has entered the tubing.
7. Using Eq. 10.50 again (but with  $H$  instead of  $H_c$ ), the new temperature  $T_{ac}$  corresponding to the enthalpy  $H$  found in the previous step is calculated.
8. If the new value of  $T_{ac}$  is approximately equal to the assumed value  $T_a$ , the iterations are terminated; otherwise, calculations are repeated from step 3 using the calculated temperature  $T_{ac}$  as the new assumed temperature. This iteration continues until convergence is achieved for the value of  $T_a$ .

As can be seen, this iterative procedure gives  $v_{gsR}$  as a result. Fig. 10.21 shows the flow chart of the calculation procedure just outlined in the previous steps.

The calculation of the volume of gas,  $v_{gsC}$ , that a pilot valve (with a given area ratio) can provide, is explained next. Knowing the valve's injection opening and closing pressures, the volume of gas supplied by the annulus,  $v_{ga}$ , and by the surface injection line,  $v_{gl}$ , both in scf/cycle, can be calculated. To calculate  $v_{gl}$ , only the volume of the injection line between the wellhead and the flow control valve, or choke, should be considered. The volume of gas in scf supplied by the annulus is calculated from the difference of the volume of gas in scf in the annulus just before the pilot valve opens,  $v_{sa}$ , minus the volume of gas in the annulus just after the valve closes,  $v_{sc}$ . Then,  $v_{ga}$  is equal to  $v_{sa} - v_{sc}$ . Applying the equation of state, the number of moles stored in the annulus just before the pilot valve opens is given by:

$$n_o = \frac{P_{ga,apert} V_{annular}}{z_{ga,apert} R_u T_{geoth.avr}} = \frac{(14.7 \text{ psia}) v_{sa}}{(1) R_u (520^\circ \text{R})} \quad (10.51)$$

Where  $V_{annular}$  is the actual annular volume;  $z_{ga,apert}$  is the average gas compressibility in the annulus at the time the valve opens;  $T_{geoth.avr}$  is the average temperature of the gas in the annulus in  $^\circ\text{R}$  (which is considered equal to the average geothermal temperature along the casing-tubing annulus);  $R_u$  is the gas universal constant; and  $P_{ga,apert}$  is the average annular pressure in psia at the moment the valve opens, which is given by:

$$P_{ga,apert} = \frac{P_{cso} + P_{cvo}}{2} \quad (10.52)$$

Where  $P_{cso}$  is the surface opening injection pressure in psia and  $P_{cvo}$  is the opening injection pressure at valve's depth, also in psia.  $P_{cvo}$  can be expressed as  $P_{cso} f_g$ , where  $f_g$  is the gas factor that is used to calculate the gas pressure at depth (it can be easily calculated with the procedures given in chapter: Single-Phase Flow).

Eq. 10.51 can be used to find the volume of gas in scf stored in the annulus,  $v_{sa}$ , just before the pilot valve opens.

Applying the equation of state again, the number of moles stored in the annulus just before the valve closes, is given by:

$$n_c = \frac{P_{ga,close} \cdot V_{annular}}{z_{ga,close} \cdot R_u T_{geoth.avr.}} = \frac{(14.7 \text{ psia}) v_{sc}}{(1) R_u (520^\circ R)} \quad (10.53)$$

Where  $z_{ga,close}$  is the average gas compressibility in the annulus just before the valve closes and  $P_{ga,close}$  is the average annular pressure (also just before the valve closes) given by:

$$P_{ga,close} = \frac{P_{csc} + P_{cvc}}{2} \quad (10.54)$$

Where  $P_{csc}$  is the surface valve's closing pressure in psia and  $P_{cvc}$  is the valve's closing pressure, also in psia, at valve's depth. As it was the case for  $P_{cvo}$ ,  $P_{cvc}$  can also be expressed as  $P_{csc} f_g$ .

From Eq. 10.53, the volume of gas in the annulus in scf just before the valve closes,  $v_{sc}$ , can be found. The volume of gas supplied by the annulus,  $v_{ga}$ , is then:

$$v_{ga} = v_{sa} - v_{sc} \quad (10.55)$$

Expressions for  $v_{sa}$  and  $v_{sc}$  can be found from known equations for the geothermal temperature,  $T_{geoth.avr.}$ , and for the actual annular volume,  $V_{annular}$ :

$$T_{geoth.avr.} = \frac{T_{surf} + T_{dov}}{2} + 460^\circ R \quad (10.56)$$

Where  $T_{surf}$  is the surface gas temperature in  $^\circ F$  (which, in many cases, can be approximated as equal to  $85^\circ F$ ),  $T_{dov}$  is the temperature at valve's depth in  $^\circ F$ . If  $B_a$  is the annular volumetric capacity in  $\text{ft}^3/\text{Mft.}$  and  $D_{ov}$  is the valve's depth in Mft.,  $V_{annular}$  is:

$$V_{annular} = D_{ov} B_a \quad (10.57)$$

Using Eqs. 10.51, 10.52, 10.53, 10.54, 10.56, and 10.57, expressions for  $v_{sa}$  and  $v_{sc}$  are given as:

$$v_{sa} = 35.37 \frac{B_a D_{ov} (P_{cso} + P_{cvo})}{[85 + 2(460) + T_{dov}] z_{ga,apert.}} \quad (10.58)$$

$$v_{sc} = 35.37 \frac{B_a D_{ov} (P_{csc} + P_{cvc})}{[85 + 2(460) + T_{dov}] z_{ga,close.}} \quad (10.59)$$



Where the surface temperature was assumed to be equal to 85°F. Following the same steps taken for the casing–tubing annulus, but with an average temperature equal to 545°R, expressions for the volume of gas stored in the injection line when the pilot valve opens and when it closes,  $v_{sa}$  and  $v_{sc}$ , respectively, can be found:

$$v_{sa} = 35.37 \frac{B_1 LP_{cso}}{545 z_{gl}} \quad (10.60)$$

$$v_{sc} = 35.37 \frac{B_1 LP_{csc}}{545 z_{gl}} \quad (10.61)$$

Where  $z_{gl}$  is the average gas compressibility in the injection line,  $B_1$  is the volumetric capacity of the injection line in ft.<sup>3</sup>/Mft., and  $L$  is the length of the injection line in Mft. Then,  $v_{gl}$  is given by:

$$v_{gl} = v_{sa} - v_{sc} \quad (10.62)$$

The volume of gas that enters the tubing at each cycle,  $v_{gsC}$ , for a given valve's spread is not limited to the sum of  $v_{ga} + v_{gl}$ , but the gas that is injected at the surface through the choke while the pilot valve is open, known here as  $v_{ge}$ , must also be added.

An expression for  $v_{ge}$  is derived next. The gas flow rate injected at the surface through the choke or surface control valve,  $Q_{gi}$ , in MscfD, is given by:

$$Q_{gi} = \frac{(v_{ga} + v_{gl})[\text{scf}]}{(T_{\text{cycle}} - T_{\text{val}})[\text{min}]} \left[ \frac{1440 \text{ min}}{1 \text{ Day}} \right] \left[ \frac{\text{Mscf}}{1000 \text{ scf}} \right] \quad (10.63)$$

Where  $T_{\text{cycle}}$  is the total cycle time and  $T_{\text{val}}$  is the time in which the pilot valve remains open, both expressed in minutes. Eq. 10.63 simply states that the surface gas flow rate (which, in most cases, is constant throughout the cycle for choke-control intermittent gas lift) is calculated by dividing the gas volume that has accumulated in the injection line and in the annulus over the time in which that volume has accumulated, which is precisely equal to the time the pilot valve remains closed. On the other hand, while the pilot valve is opened, gas is still being injected at the surface at (approximately) the same gas flow rate calculated with Eq. 10.63. This additional injection gas volume must also be considered (even though it is usually very small). The volume of gas in scf that is injected at the surface while the pilot valve is opened,  $v_{ge}$ , is given by:

$$v_{ge} = (T_{\text{val}})(Q_{gi})/1.44 \quad (10.64)$$

The surface injection gas flow rate through the surface control valve should not be confused with the gas flow rate that passes through the pilot valve while it is opened. The surface injection gas flow rate is usually very small compared to the instantaneous gas flow rate through the pilot valve and that is the reason why the injection annular pressure drops when the pilot valve opens.

The injected gas volume per cycle,  $v_{gsC}$ , is equal to  $v_{ga} + v_{gl} + v_{ge}$ , and it must be greater than or equal to the required volume of gas per cycle,  $v_{gsR}$ . The time it takes for the top of the liquid slug to reach the surface,  $T_{oc}$ , is equal to the time the valve remains open,  $T_{val}$ , only if  $v_{gsR}$  is equal to  $v_{gsC}$  ( $T_{oc} = T_{val}$  is accomplished at the end of the iterations explained in Figs. 10.14 and 10.17). At the beginning, calculations are carried out assuming an initial value of the time  $T_{oc}$ , which is the same as assuming an initial average liquid slug velocity.  $T_{oc}$  must be determined at the end of all calculations to verify that the assumed value is equal to the calculated one. If they are not approximately equal, all calculations must be repeated with a new liquid slug velocity.

The liquid slug velocity is determined from an equation that relates the gas flow rate through the pilot valve to the slug velocity itself. The gas flow rate and the slug velocity are determined when the top of the liquid slug reaches the wellhead and it is estimated that at that moment the pilot valve should close (or  $T_{oc} = T_{val}$ ). In this calculation procedure, it is assumed that the maximum slug velocity,  $v_{at\ max}$ , is reached when the upper part of the liquid slug reaches the surface and it is equal to twice the average slug velocity, known here as  $v_{at}$ . The value of the slug velocity when it reaches the surface,  $v_{at\ max} = 2v_{at}$ , multiplied by the area of the tubing, is equal to the volume of the liquid per unit time in the tubing that must be displaced by the gas that enters through the pilot valve. The volume per unit time of the gas that displaces the liquid can be expressed at standard conditions by:

$$\text{Displaced flow rate Mscf D} = 2v_{at} \left[ \frac{\text{Mft.}}{\text{min}} \right] \left[ \frac{1000 \text{ ft.}}{\text{Mft.}} \frac{1440 \text{ min}}{1 \text{ D}} \right] \frac{\pi}{4} d^2 \left[ \text{in.}^2 \right] \left[ \frac{\text{ft.}^2}{144 \text{ in.}^2} \right] \frac{P_{ga} [\text{psia}]}{14.7 [\text{psia}]} \frac{520 [^{\circ}\text{R}]}{T_a [^{\circ}\text{R}]} \frac{1}{z_a} \left[ \frac{\text{Mscf}}{1000 \text{ ft.}^3} \right] \quad (10.65)$$

Where  $d$  is the tubing diameter in inches while  $P_{ga}$ ,  $T_a$ , and  $z_a$  are the absolute average pressure in psia, absolute average temperature in  $^{\circ}\text{R}$ , and the compressibility of the gas that entered the tubing, respectively.

On the other hand, the gas flow rate through the gas lift valve can be calculated by means of the following simplified version of the Thornhill–Craver equation (Eq. 4.25):

$$Q_{gi} = \frac{0.4405(d_o)^2(P_a)(f_{rg})}{\sqrt{T_n G_g}} \quad (10.66)$$

Where  $Q_{gi}$  is the gas flow rate through the pilot valve in MscfD;  $d_o$  is the main seat diameter of the pilot valve in 1/64 in.;  $P_a$  is the gas injection pressure just upstream of the pilot valve in psia at the moment the top of the liquid slug reaches the surface, which is considered to be equal to  $P_{cvc}$  (the pilot valve's closing pressure at depth);  $T_n$  is the gas injection temperature upstream of the pilot valve;  $G_g$  is the injection gas specific gravity;  $f_{rg}$  is a term given by:  $f_{rg} = \sqrt{r^{1.561} - r^{1.781}}$  if  $r > 0.55$  or  $f_{rg} = 0.22$  if  $r \leq 0.55$ , where  $r$  is equal to the pressure ratio  $(P_{tm} + 14.7)/(P_{cvc} + 14.7)$ ;  $P_{tm}$  is the tubing pressure calculated in psig according to Eq. 10.34; and, as indicated earlier,  $P_{cvc}$  is the pilot valve's closing pressure at valve's depth in psig.

The right hand side of Eq. 10.65 should be equal to the right hand side of Eq. 10.66, thus the following expression can be found for  $v_{at}$ :

$$v_{at} = \frac{0.00079276(T_a)(z_a)(d_o^2)(P_a)(f_{rg})}{d^2 P_{ga} \sqrt{T_n G_g}} \quad (10.67)$$

This equation for the calculation of the velocity of the liquid slug then comes from applying the steady state continuity equation to the control volume occupied by the gas bubble below the liquid slug for which the gas flow rate at standard conditions that enters and exits the control volume must be equal. Because the gas flow rate that enters is equal to the one that exits the control volume, the pressure inside the tubing must remain constant, which is what usually happens (the gas pressure below the liquid slug is more or less constant once the slug has reached a certain velocity in the tubing). With the value of  $v_{at}$  calculated in this way,  $T_{oc}$  is simply given by  $D_{ov}/v_{at}$ . If the new value of  $T_{oc}$  is not approximately equal to the one used in the calculations, some models repeat all calculations (in the iterations explained in Figs. 10.14 and 10.17) with a value of  $T_{oc}$  estimated from a slug velocity equal to the average slug velocity of the previous and current iterations.

Once the liquid velocity has converged to a particular value, the valve's area ratio must be found (as explained in the flow chart shown in Fig. 10.17) so that the volume of gas injected per cycle is greater than or equal to the volume of gas required to produce the liquid slug to the surface. The equation

that can be used to find the gas lift valve's closing pressure is now derived from a mass balance of the injection gas.

### 10.6.1.3 Calculation of the valve's closing pressure, $P_{cvc}$

From Eqs. 10.58 to 10.61, the volume of gas supplied by the annulus and the injection gas line can be obtained (these equations are repeated here). The volume of gas supplied by the annulus,  $v_{ga}$ , is equal to  $v_{sa} - v_{sc}$ . Volumes  $v_{sa}$  and  $v_{sc}$  are given by:

$$v_{sa} = 35.37 \frac{B_a D_{ov} (P_{cso} + P_{cvo})}{[85 + 2(460) + T_{dov}] z_{ga,apert.}} \quad (10.58)$$

$$v_{sc} = 35.37 \frac{B_a D_{ov} (P_{csc} + P_{cvc})}{[85 + 2(460) + T_{dov}] z_{ga,close.}} \quad (10.59)$$

The volume of gas supplied by the surface gas injection line,  $v_{gl}$ , is equal to  $v_{sa} - v_{sc}$ . Volumes  $v_{sa}$  and  $v_{sc}$  are given in this case by:

$$v_{sa} = 35.37 \frac{B_1 L P_{cso}}{545 z_{gl}} \quad (10.60)$$

$$v_{sc} = 35.37 \frac{B_1 L P_{csc}}{545 z_{gl}} \quad (10.61)$$

Assuming that  $z_{ga,close.}$  is equal to  $z_{ga,apert.}$ , the following expression for  $v_{ga}$  is obtained:

$$v_{ga} = 35.37 K_1 (P_{cso} + P_{cvo} - P_{csc} - P_{cvc}) \quad (10.68)$$

Where,

$$K_1 = \frac{B_a D_{ov}}{[85 + 2(460) + T_{dov}] z_{ga,apert.}} \quad (10.69)$$

And for the volume of gas supplied by the injection gas line at each cycle:

$$v_{gl} = 35.37 K_2 (P_{cso} - P_{csc}) \quad (10.70)$$

Where,

$$K_2 = \frac{B_1 L}{545 z_{gl}} \quad (10.71)$$

The volume of gas injected at the surface while the pilot valve is opened is calculated from Eq. 10.64, repeated here (with  $T_{oc}$  instead of  $T_{val}$ ):

$$v_{ge} = T_{oc} (Q_{gi}) / 1.44 \quad (10.64)$$

In this case,  $T_{oc}$  is equal to the valve's depth  $D_{ov}$  in Mft. divided by the average slug velocity  $v_{at}$  in Mft./min:

$$v_{ge} = D_{ov} Q_{gi} / (1.44 v_{at}) = 35.37 K_4 \quad (10.72)$$

With  $K_4 = Q_{gi} D_{ov} / (50.939 v_{at})$ .

The gas mass balance indicates that the volume of gas injected per cycle, this time equal to  $v_{gsR}$ , must be equal to  $v_{ga} + v_{gl} + v_{ge}$ . The volume of gas injected per cycle  $v_{gsR}$  is calculated as it was explained earlier (Fig. 10.21). Using expressions already derived for  $v_{ga}$ ,  $v_{gl}$ , and  $v_{ge}$ , the following equation is reached:

$$v_{gsR} = 35.37 K_1 (P_{cso} + P_{cso} f_g - P_{csc} - P_{csc} f_g) + 35.37 K_2 (P_{cso} - P_{csc}) + 35.37 K_4 \quad (10.73)$$

Where  $f_g$  is the gas factor used in the calculation of the injection pressure at depth from the surface injection pressure ( $P_{cvo} = P_{cso} f_g$ , for example). Factor  $f_g$  can be easily calculated if the surface pressure and the valve's depth are known. The surface injection opening pressure is indeed known during the iteration but the injection closing pressure is unknown. Fortunately, the value of  $f_g$  for the opening pressure is similar to the one for the closing pressure, so the value of  $f_g$  in all previous equations can be calculated from the injection opening pressure (a more rigorous approach would require a simple and fast iteration that will give very similar results).

Using Eq. 10.73 with  $K_3 = (1 + f_g)$ , the following equation for  $P_{csc}$  is found, where all terms on the right hand side of the equation are known:

$$P_{csc} = \frac{P_{cso} [K_1 K_3 + K_2] + K_4 - \frac{v_{gsR}}{35.37}}{K_1 K_3 + K_2} \quad (10.74)$$

The surface closing pressure,  $P_{csc}$ , is determined in this way. The injection closing pressure at depth is given by  $P_{cvc} = f_g P_{csc}$ . With this closing pressure, the required area ratio can be found from Eq. 10.5. This area ratio, known as  $R^*$ , does not necessarily coincides with one of the commercially available area ratios, thus the valve's opening pressure must be modified according to the procedure shown in the flow chart given in Fig. 10.17 to make the calculated area ratio equal to one of the commercially available area ratios in a way in which the liquid production is maximized with the lowest possible injection gas consumption.

#### 10.6.1.4 Summary of required calculations for choke-control intermittent gas lift design

The sequential steps in which calculations are made are described next.

- An initial value is assigned to the dynamic temperature at valve's depth (this temperature is needed to calculate the solution gas/oil

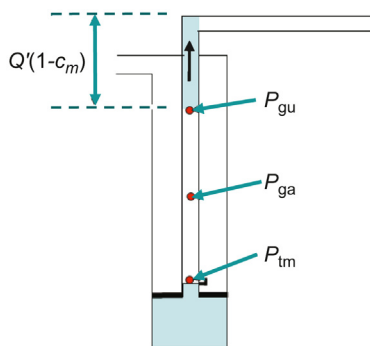
ratio with the purpose of estimating the liquid viscosity and, in this way, be able to find the Reynolds number, which in turn is used to calculate the friction pressure drop). A good starting point is to assume this temperature equal to the geothermal temperature at valve's depth.

- For the same reason given in the previous step, an initial production pressure at valve depth is estimated. A good estimate is to make this initial pressure equal to one fifth of the static pressure. At the end of the iterations, this production pressure should be equal to the production pressure just before the pilot valve opens.
- An initial liquid slug velocity is set at 1 Mft./min.
- The velocity iteration procedure begins by calculating the solution gas/oil ratio.
- The oil viscosity, Reynolds number, and the friction coefficient, which are all used in the calculation of the frictional pressure drop of the liquid slug, are then calculated.
- Using the Newton–Raphson method, the OCT is calculated.
- With the OCT already known, the initial column length, the daily liquid production, and the valve's dynamic temperature can be calculated. As an approximation, the dynamic temperature can be calculated using any of the procedures given for continuous gas lift using the daily liquid production just calculated (Section 3.2.2).
- The calculated dynamic temperature is compared with its previously assumed value. If they are not approximately equal, calculations are repeated (with the same slug velocity and the new dynamic temperature) starting from the calculation of the new solution gas/oil ratio. This iteration is repeated until convergence of the dynamic temperature is achieved.
- The production pressure (just before the valve opens) is calculated. This new pressure is compared with the previously assumed value. If they are not approximately equal, calculations are repeated (with the same slug velocity) starting from the calculation of the new solution gas/oil ratio. This iteration process continues until the production pressure converges to a final value.
- The average pressure of the gas bubble below the liquid slug (just when the top of the liquid slug reaches the wellhead) is calculated. The enthalpy of the injection gas in the annulus when the valve is about to open is also calculated.
- Using an iterative process, described in Fig. 10.21, the temperature of the gas below the liquid slug (just when it reaches the wellhead) is determined. In this iterative process, the required volume of gas to be injected per cycle,  $v_{gsR}$ , is also found.

- With  $v_{gsR}$  already calculated, the valve's injection closing pressure is found from the mass balance of the injection gas in the annulus, in the flowline, and through the surface injection choke. Knowing  $v_{gsR}$ , the daily gas injection flow rate,  $Q_{gi}$ , can also be found.
- The instantaneous gas flow rate that passes through the pilot valve when the liquid slug reaches the surface is calculated. With this flow rate, the liquid slug velocity can be calculated and compared with its assumed value. If these velocities (assumed and calculated) are not approximately equal, all calculations are repeated with a new slug velocity equal to the average of the velocities of the current and previous iterations. The process is repeated until the slug velocity converges to a final value.
- Once the velocity iteration is finished, the valve's area ratio  $R$  is found from: (1) the known value of the valve's injection opening pressure, (2) the calculated value of the valve's closing pressure, and (3) the calculated value of the production pressure at valve's depth just before the pilot valve opens. This calculated value of  $R$ , called  $R^*$ , is compared with the closest commercially available area ratio. If they are not approximately equal, the iteration procedure explained in Fig. 10.17 is carried out to find the area ratio most appropriate to the well's operational conditions.

In the design of the operating valve just described, the required volume of gas injected per cycle is calculated when the top of the liquid slug reaches the surface, as it is shown in Fig. 10.22.

It is assumed that if the pilot valve closes just when the liquid begins to be produced at the surface, the expansion of the gas injected up to that time will provide the required force to produce the entire liquid slug to the surface. This is true for wells with simple type completions that are good candidates for intermittent gas lift because for these wells the static liquid column should not be greater than one third of the well's total depth. Additionally, it is known that when the well produces at the OCT, the initial liquid column length is about 50% of the length of the static liquid column and, therefore, the initial liquid columns are, at the most, equal to one sixth the total depth of the well. However, for wells with different completions, like double-packer chambers, the liquid columns being produced to the surface could be considerably larger. In these cases, the required volume of gas injected per cycle is found just when the entire liquid slug has surfaced. The equations are basically the same but with the minor modifications that are explained in Section 10.7 for double-packer chambers.



■ FIGURE 10.22 Calculations are carried out just when the tip of the liquid column reaches the surface.

**Problem 10.1**

Perform the first iteration to calculate the liquid slug velocity in the design of the operating pilot valve for a well on choke-control intermittent gas lift with the following data.

Production tubing ID: 2.441 in.; production tubing OD: 2.875 in.; surface gas injection line ID: 2.067 in.; pilot valve's main port diameter: 32/64 in.; length of the surface gas injection line: 2000 ft.; casing ID: 6.366 in.; top of perforations depth: 2100 ft.; operating valve's depth: 2020 ft.; production wellhead pressure: 60 psig; reservoir static pressure: 600 psig; temperature at the top of the perforations: 121°F; and PI: 0.15 Br/(psi-D). The operating valve is a spring-loaded, IPO pilot valve, which is calibrated by setting it at a calculated test-rack closing pressure.

Liquid and gas properties:

Injection gas specific gravity: 0.7; water cut: 10%; oil API gravity: 23°API (use a fallback factor  $F$  equal to 0.05); formation gas/liquid ratio: 300 scf/STB.

The surface injection pressure (taken as the valve's opening pressure) is 800 psig, which gives an injection pressure at valve's depth of 844.71 psig. The approximate value of the average gas compressibility factor in the annulus is  $Z_{\text{injection}} = 0.865$ .

**Solution****1. OCT calculations**

Tubing volumetric capacity:

$$B_t = 0.97143d^2 = (0.97143)(2.441)^2 = 5.788 \left[ \frac{\text{Br}}{\text{Mft.}} \right]$$

Liquid gradient:

$$\rho_f = 0.433 \left( 0.1 + 0.9 \frac{141.5}{23^\circ\text{API} + 131.5} \right) = 0.4002 \left[ \frac{\text{psi}}{\text{ft.}} \right]$$

Other constants needed to perform the OCT calculations:

$$\gamma = \frac{\rho_f J}{1.44 B_t} = \frac{(0.4002)(0.15)}{(1.44)(5.788)} = 0.0072 \frac{1}{\text{min}}$$



With the valve's depth  $D_{ov}$  in Mft. and the liquid slug velocity in Mft./min (initially assumed equal 1 Mft./min), the following constants are found:

$$C_4 = \exp(\gamma D_{ov}/v_{at}) = \exp[0.0072(2.02/1)] = 1.01465$$

$$c_m = FD_{ov} = 0.05 \times 2.02 = 0.101$$

$$C_2 = 1 - c_m = 1 - 0.101 = 0.899$$

The initial value of the cycle time (to be used as the starting point for the following iterations),  $T_1$ , can be estimated as three times the depth of the operating valve divided by the assumed slug velocity, taken as 1 Mft./min to start the iteration process:

$$T_1 = 3D_{ov}/v_{at} = 3 \times 2.02/1 = 6.06 \text{ min}$$

The equation used in the iterations to find the OCT is:

$$T_{n+1} = T_n - \frac{T_c - T_n}{\frac{\gamma(e^{\gamma T_n} - c_m C_4^2 e^{-\gamma T_n})}{\gamma(C_2)(C_4)} - 1}$$

Where  $T_c$  is:

$$T_c = \frac{(e^{\gamma T_n} - C_4)(e^{\gamma T_n} - c_m C_4)}{\gamma e^{\gamma T_n} C_2 C_4} = \frac{(e^{0.0072 T_n} - 1.01465)(e^{0.0072 T_n} - 0.102479)}{0.00656762 e^{0.0072 T_n}}$$

And

$$T_{n+1} = T_n - \frac{T_c - T_n}{\frac{0.0072(e^{0.0072 T_n} - 0.10398 e^{-0.0072 T_n})}{0.00656762} - 1}$$

The value of  $T_2$  can be found from  $T_1 = 6.06$  min,  $\exp[0.0072(6.06)] = 1.044598$ , and  $T_c$  (given by the following equation):

$$T_c = \frac{(1.044598 - 1.01465)(1.044598 - 0.102479)}{(0.00656762)(1.044598)} = 4.11261 \text{ min}$$

$$T_2 = 6.06 - \frac{4.11261 - 6.06}{\frac{0.0072[1.044598 - (0.10398)0.9573]}{0.00656762} - 1} = 60.07$$

Similarly,  $T_3$  can be found from  $T_2 = 60.07$  min,  $\exp[0.0072(60.07)] = 1.5411$  and  $T_c$ :

$$T_c = \frac{(1.5411 - 1.01465)(1.5411 - 0.102479)}{0.0065676(1.5411)} = 74.828 \text{ min}$$

$$T_3 = 60.07 - \frac{74.828 - 60.07}{\frac{0.0072[1.5411 - 0.10398(0.64888)]}{0.0065676} - 1} = 36.0935$$

Continuing doing the iterations in this way, a final value of the OCT is found equal to 23.14 min/cycle.

2. Calculation of the initial liquid column (at the moment the pilot valve opens)  $Q_{ini}$  in Mft.

The liquid column regeneration time,  $T_f$ , is equal to the total cycle time minus the gas injection (into the tubing) time, considered to be equal to the time needed by the liquid slug to reach the surface:

$$T_f = \text{OCT} - D_{ov}/v_{at} = 23.14 - 2.02/1 = 21.12 \text{ min}$$

The gas factor  $f_g$  that is used to calculate the production tubing pressure at depth just when the liquid column is beginning to accumulate above the valve, can be approximated as:

$$f_g = \left(1 + \frac{D_{ov}}{54}\right)^{1.524} = \left(1 + \frac{2.02}{54}\right)^{1.524} = 1.05756$$

The production wellhead pressure plus the hydrostatic pressure of the gas column above the valve is then:  $60(1.05756) = 63.4538$  psig.

The true liquid gradient,  $\rho_t$ , can be approximated as:

$$\rho_t = \frac{167 - 1.43(^{\circ}\text{API})}{1000} = 0.1341 \frac{\text{psi}}{\text{ft.}}$$

With the reservoir pressure  $P_{sbh}$  in psig, the depth of the top of the perforations  $D_{pt}$  in Mft., the depth of the operating valve  $D_{ov}$  in Mft., and the liquid gradient in psi/ft., the maximum drawdown is:

$$A' = P_{sbh} - 1000(D_{pt} - D_{ov})\rho_t - P_{wh}f_g = 600 - 1000(2.1 - 2.02)0.1341 - 63.4538 = 525.8174 \text{ psig}$$

The initial liquid column length is then equal to:

$$Q_{ini} = \frac{A'(e^{\gamma T_f} - 1)}{1000\rho_f(e^{\gamma T_f} - c_m)} = \frac{525.8174(e^{0.0072(21.12)} - 1)}{(1000)0.4002(e^{0.0072(21.12)} - 0.101)} = 0.203 \text{ Mft.}$$

3. Calculation of the production pressure at valve's depth,  $P_{to}$ , at the moment the pilot valve opens

$$P_{to} = 1000Q_{ini}\rho_f + P_{wh}f_g = 1000(0.203)(0.4002) + 63.4538 = 144.69 \text{ psig}$$

Because the length of the liquid column is small and the valve is located at a shallow depth, the same gas factor  $f_g$  that was used to calculate the drawdown  $A'$  in the previous step can also be used here; otherwise, the length of the liquid column should be subtracted (from the depth of the gas lift valve) as shown in step 3 of Problem 10.2 for the calculation of  $f_g$ .

4. Calculation of the daily liquid production,  $q_f$ , in Br/D

$$q_f = Q_{ini} B_t (1 - FD_{ov}) 1440 / T_{cycle} = 0.203(5.788247)[1 - (0.05)2.02]1440 / 23.14 = 65.7358 \text{ Br/D}$$

Where the fallback losses have been taken into consideration.

5. Calculation of the required volume of gas to be injected per cycle:

Following the steps that are described in this section (not shown in this problem), the required volume of gas injected per cycle,  $v_{gsR}$ , to lift a liquid column of 203 ft. in length from a depth of 2020 ft. is calculated to be equal to 1246.93 scf/cycle, for which the absolute average pressure of the gas bubble below the liquid slug when the top of the slug reaches the surface is  $P_{ga} = 297.96$  psia and the pressure just downstream of the valve at that moment is  $P_{tm} = 290.49$  psig. The average temperature and compressibility factor of the gas that has entered the tubing are 531.7696°R and 0.9386, respectively.

The constant surface gas flow rate is:

$$Q_{gi} = \frac{v_{gsR}}{1000} \frac{1440}{T_{cycle}} = \frac{1246.93}{1000} \frac{1440}{23.14} = 75.5963 \text{ MscfD}$$

6. Calculation of the valve's closing pressure  $P_{csc}$

The volumetric capacity of the casing-tubing annulus  $B_a$  in ft.<sup>3</sup>/Mft. is:

$$B_a = 5.45415(d_{casing}^2 - d_{od\ tubing}^2) = 5.45415(6.366^2 - 2.875^2) = 175.9527 \text{ ft.}^3 / \text{Mft.}$$

The volumetric capacity of the surface gas injection line  $B_l$  in ft.<sup>3</sup>/Mft. is:

$$B_l = 5.45415d_{gasline}^2 = 5.45415(2.067^2) = 23.3028 \text{ ft.}^3 / \text{Mft.}$$

The gas compressibility factor in the gas injection line can be approximated by the following equation:

$$z_{gi} = 1 - 1.9385(0.0001)(P_{cso} + 14.7) = 1 - 1.9385(0.0001)(800 + 14.7) = 0.84207$$

The geothermal temperature at valve's depth can be calculated as:

$$T_{dov} = 15.6D_{ov} / 1000 + 88.8 = 15.6(2020) / 1000 + 88.8 = 120.3^\circ\text{F}$$

Factors  $K_1$ ,  $K_2$ ,  $K_3$ , and  $K_4$  are now calculated using the equations presented in this section and with the average compressibility factor of the annular injection gas given in the data of the problem ( $Z_{\text{injection}}$ ):

$$K_1 = \frac{(B_a)(D_{ov}/1000)}{(Z_{\text{injection}})(1005 - T_{dov})} = \frac{(175.9527)(2020/1000)}{(0.865)(1005 - 120.3)} = 0.36514$$

With the length of the surface gas injection line,  $L$  in ft., from the surface injection choke to the wellhead:

$$K_2 = \frac{(L/1000)B_1}{z_{gl}(545)} = \frac{(2000/1000)23.3028}{0.84207(545)} = 0.10155$$

From the data given above for this problem, the injection gas factor  $f_g$  is approximately equal to 1.0558856, so that:

$$K_3 = 1 + f_g = 1 + 1.0558856 = 2.0558856$$

$$K_4 = \frac{(D_{ov}/1000)Q_{gi}}{50.9390v_{at}} = \frac{(2020/1000)75.5963}{50.939(1)} = 2.99779$$

Finally, the surface injection closing pressure of the valve is found by:

$$P_{csc} = P_{cso} + \frac{k_4 - \frac{V_{gsR}}{35.374}}{k_1 k_3 + k_2} = 800 + \frac{2.99779 - \frac{1246.93}{35.374}}{0.36514(2.0558856) + 0.10155} = 762.1558 \text{ psig}$$

#### 7. Calculation of the test-rack closing pressure:

From the data given for this problem, the opening pressure at valve's depth is  $P_{cvo} = 844.71$  psig. The valve's closing pressure at depth is found using the gas factor  $f_g$  indicated in step 6:

$$P_{cvc} = P_{csc} f_g = 762.1558(1.0558856) = 804.7493 \text{ psig}$$

So that the area ratio should be equal to:

$$R = \frac{P_{cvo} - P_{cvc}}{P_{cvo} - P_{to}} = \frac{844.71 - 804.7493}{844.71 - 144.69} = 0.057$$

The closest area ratio (for the selected valve's model) is equal to 0.150, for which the test-rack closing pressure is:

$$P_{trc} = (1 - R)P_{cvo} + RP_{to} = (1 - 0.15)844.71 + 0.15(144.69) = 739.7 \text{ psig}$$

$P_{trc}$  is in this case equal to the valve's closing pressure at valve's depth during normal operation of the well (because spring-loaded valves are

insensitive to the surrounding temperature). According to the calculations in point 6, a closing pressure at valve's depth of 804.7493 psig is sufficiently low to provide the required volume of gas injected per cycle. With a closing pressure of 739.7 psig, the volume of gas injected per cycle is much greater than required. This could be improved with a lower opening pressure, but calculations are needed to verify that the liquid slug velocity will not be too small for this new pressure. Another solution could be found by selecting a different valve model with a smaller minimum area ratio.

**8. Verification of the average slug velocity**

Using the results presented in step 5, it must be now verified that the slug velocity (when it reaches the surface) is within the acceptable limits to keep the fallback losses at a minimum value. Eq. 10.67 is used to find the slug velocity:

$$v_{at} = \frac{0.00079276(T_a)(z_a)(d_o^2)(P_a)(f_{rg})}{d^2 P_{ga} \sqrt{T_n G_g}}$$

The pressure upstream of the valve,  $P_a$ , must be the injection pressure at valve's depth when the slug reaches the surface, which must be equal to the pressure in the casing-tubing annulus when all the required volume of gas  $v_{gsR}$  has entered the tubing (and not the injection closing pressure of the valve with the commercially available area ratio calculated in step 7 because this available area ratio is larger than the required area ratio and, in consequence, the valve will unnecessarily remain open after the top of the liquid slug has reached the wellhead):

$$P_a = P_{cvc} + 14.7 = 804.74 + 14.7 = 819.4493 \text{ psia}$$

The pressure downstream of the valve,  $P_d$ , was given in step 5 above and it is equal to:

$$P_d = P_{tm} + 14.7 = 209.49 + 14.7 = 305.19 \text{ psia}$$

With these two pressures, the pressure ratio  $r$  across the valve is calculated:

$$r = P_d / P_a = 305.19 / 819.4493 = 0.3724$$

According to the Thornhill-Craver equation (given in chapter: Single and Multiphase Flow Through Restrictions and on which the slug velocity calculation is based), if  $r$  is smaller than 0.55 then factor  $f_{rg}$  is equal to 0.22.

$d_o$  is the valve's main port diameter, in 1/64 in., equal to 32 in this case. On the other hand, the following average data of the gas that entered the tubing (given in step 5 earlier) are:

Average pressure,  $P_{ga} = 297.96$  psia

Average temperature,  $T_a = 531.7696^\circ\text{R}$

Corresponding compressibility factor for  $P_{ga}$  and  $T_a$ ,  $Z_a = 0.9386$

The injection gas temperature just upstream of the valve,  $T_n$ , can be approximated as the geothermal temperature:

$$\begin{aligned} T_n &= 15.6D_{ov}/1000 + 88.8 + 460 \\ &= 15.6(2020)/1000 + 88.8 + 460 = 580.31^\circ\text{R}. \end{aligned}$$

With all these parameters, the liquid slug velocity is calculated as:

$$\begin{aligned} v_{sl} &= \frac{0.00079276(T_a)(z_a)(d_o^2)(P_a)(f_{rg})}{d^2 P_{ga} \sqrt{T_n G_g}} = \\ &= \frac{0.00079276(531.7696)(0.9386)(32^2)(819.4493)(0.22)}{2.441^2 (297.96) \sqrt{580.31(0.7)}} \\ &= 2.04 \text{ Mft./min} \end{aligned}$$

As can be seen, the slug velocity is greater than 1 Mft./min, so that it is highly probable that the slug velocity will converge to an acceptable value because all that is needed to proceed with the iterations is to reduce the pilot valve's opening pressure to decrease the liquid slug velocity. To finish the design, it is necessary to perform all previous calculations with this new velocity (or, if preferred, with the average of the assumed velocity and this calculated velocity). This iterative process ends when the velocity converges to a final slug velocity. ■

### Problem 10.2

Carry out the first iteration for the calculation of the liquid slug velocity in the design of the operating pilot valve of a well on choke-control intermittent gas lift with the following data.

Production tubing ID: 2.441 in.; production tubing OD: 2.875 in.; surface injection gas line ID: 2.067 in.; pilot valve's main port diameter: 32/64 in.; length of the surface gas injection line: 2000 ft.; casing ID: 4.2 in.; top of perforations depth: 4000 ft.; operating valve's depth: 3940 ft.; production well-head pressure: 60 psig; reservoir static pressure: 1300 psig; Temperature at

the top of the perforations: 151.2°F; PI: 0.15 Br/(psi-D). The operating valve is a spring-loaded, IPO pilot valve, which is calibrated by setting it at a calculated test-rack closing pressure.

Liquid and gas properties:

Injection gas specific gravity: 0.7; water cut: 10%; Oil API gravity: 23°API (use a fallback factor  $F$  equal to 0.05); formation gas/liquid ratio: 300 scf/STB.

The surface injection pressure (taken as the valve's opening pressure) is 700 psig, which gives an injection pressure at valve's depth of 774.372 psig (with a gas factor  $f_g = 1.1062458$ ). The approximate value of the average gas compressibility factor in the annulus is  $Z_{\text{injection}} = 0.889$ .

Additional data:

Gas factor  $f_g$  with injection pressures of 500 and 450 psig are equal to 1.1025 and 1.1015, respectively.

### Solution

#### 1. Calculation of the OCT:

Volumetric capacity of the production tubing:

$$B_t = 0.97143d^2 = (0.97143)2.441^2 = 5.788 \text{ Br/Mft.}$$

Liquid gradient:

$$\rho_f = 0.433 \left( 0.1 + 0.9 \frac{141.5}{23^\circ \text{API} + 131.5} \right) = 0.4002 \text{ psi/ft.}$$

Other constants needed for the calculation of the OCT:

$$\gamma = \frac{\rho_f J}{1.44 B_t} = \frac{(0.4002)(0.15)}{(1.44)(5.788)} = 0.0072 \frac{1}{\text{min}}$$

With the depth of the valve  $D_{ov}$  in Mft. and the liquid slug velocity in Mft./min (initially assumed equal to 1 Mft./min), the following parameters are calculated:

$$C_4 = \exp(\gamma D_{ov} / v_{at}) = \exp[0.0072(3.94)/1] = 1.028774$$

$$c_m = F D_{ov} = 0.05(3.94) = 0.197$$

$$c_2 = 1 - c_m = 1 - 0.197 = 0.803$$

The initial cycle time,  $T_1$ , can be estimated as equal to three times the depth of the operating valve divided by the slug average velocity, assumed equal to 1 Mft./min to start the iteration process:

$$T_1 = 3D_{ov}/v_{at} = 3(3.94)/1 = 11.82 \text{ min}$$

The equation used for the iterations in the calculation of the OCT is given by:

$$T_{n+1} = T_n - \frac{T_c - T_n}{\frac{\gamma [e^{\gamma T_n} - c_m (C_4)^2 e^{-\gamma T_n}]}{\gamma (C_2)(C_4)} - 1}$$

Where  $T_c$  is:

$$T_c = \frac{(e^{\gamma T_n} - C_4)(e^{\gamma T_n} - c_m C_4)}{\gamma e^{\gamma T_n} C_2 C_4} = \frac{(e^{0.0072 T_n} - 1.028774)(e^{0.0072 T_n} - 0.202668)}{0.00594796 e^{0.0072 T_n}}$$

And

$$T_{n+1} = T_n - \frac{T_c - T_n}{\frac{0.0072 (e^{0.0072 T_n} - 0.2085 e^{-0.0072 T_n})}{0.00594796} - 1}$$

The value of  $T_2$  can be found from  $T_1 = 11.82$  min,  $\exp[0.0072(11.82)] = 1.08883$ , and  $T_c$  (given by the following equation):

$$T_c = \frac{(1.08883 - 1.028774)(1.08883 - 0.202668)}{0.0072(1.08883)(0.803)1.028774} = 8.21753 \text{ min}$$

$$T_2 = 11.82 - \frac{8.21753 - 11.82}{\frac{0.0072 [1.08883 - (0.197)1.028774^2(0.918417)]}{0.0072(0.803)1.028774} - 1} = 53.5978$$

Continuing the iterations in this way, a final OCT is found to be equal to 30.4457 min/cycle.

2. Calculation of the initial liquid column (at the moment the pilot valve opens)  $Q_{ini}$  in Mft.:

The liquid column regeneration time,  $T_f$  is equal to the total cycle time minus the gas injection time, considered to be equal to the time needed for the liquid slug to reach the surface:

$$T_f = \text{OCT} - D_{ov}/v_{at} = 30.4457 - 3.94/1 = 26.5057 \text{ min}$$



The gas factor  $f_g$  that is used to calculate the production tubing pressure at depth just when the liquid column is beginning to accumulate above the valve, can be approximated as:

$$f_g = \left(1 + \frac{D_{ov}}{54}\right)^{1.524} = \left(1 + \frac{3.94}{54}\right)^{1.524} = 1.113297$$

The production wellhead pressure plus the hydrostatic pressure of the gas column above the valve is then  $60(1.113297) = 66.7978$  psig.

The true liquid gradient,  $\rho_t$ , can be approximated as:

$$\rho_t = \frac{167 - 1.43 \text{ API}}{1000} = 0.1341 \text{ psi/ft.}$$

With the reservoir pressure  $P_{sbh}$  in psig, the depth of the top of the perforations  $D_{pt}$  in Mft., the depth of the operating valve  $D_{ov}$  in Mft., and the liquid gradient in psi/ft., the maximum drawdown is:

$$\begin{aligned} A' &= P_{sbh} - 1000(D_{pt} - D_{ov})\rho_t - P_{wh}f_g \\ &= 1300 - 1000(4 - 3.94)0.1341 - 66.7978 = 1225.1556 \text{ psi} \end{aligned}$$

The initial liquid column length is then equal to:

$$\begin{aligned} Q_{ini} &= \frac{A'(e^{\gamma T_f} - 1)}{1000\rho_f(e^{\gamma T_f} - c_m)} \\ &= \frac{1225.1556(e^{0.0072(26.5057)} - 1)}{1000(0.4002)(e^{0.0072(26.5057)} - 0.197)} = 0.63527 \text{ Mft.} \end{aligned}$$

3. Calculation of the production pressure at valve's depth  $P_{to}$  at the moment the valve opens.

The gas factor  $f_g$  that multiplies the wellhead production pressure  $P_{wh}$  is not calculated at valve's depth but at the top of the liquid column:

$$f_g = \left(1 + \frac{3.94 - 0.63527}{54}\right)^{1.524} = 1.094748$$

$$\begin{aligned} P_{to} &= 1000Q_{ini}\rho_f + P_{wh}f_g \\ &= 1000(0.63527)0.4002 + 60(1.094748) = 319.92 \text{ psig} \end{aligned}$$

4. Calculation of the daily liquid production,  $q_f$ , in Br/D:

$$\begin{aligned} q_f &= Q_{ini}B_t(1 - FD_{ov})1440/T_{cycle} \\ &= 0.63527(5.788247)[1 - (0.05)3.94]1440/30.4457 = 139.65 \text{ Br/D} \end{aligned}$$

Where the fallback losses have been taken into consideration.

5. Calculation of the required volume of gas to be injected per cycle:

Following the steps that are described in this section (not shown in this problem), the required volume of gas injected per cycle,  $V_{gsR}$ , to lift a liquid column of 635.27 ft. in length from a depth of 3940 ft. is 5002.817 scf/cycle, for which the absolute average pressure of the gas bubble below the slug when the top of the liquid slug reaches the surface is  $P_{ga} = 679.9172$  psia and the pressure just downstream of the pilot valve at that moment is  $P_{tm} = 696.4092$  psig. The average temperature and compressibility factor of the gas that has entered the tubing are 580.1085°R and 0.89, respectively.

The constant surface gas flow rate is:

$$Q_{gi} = \frac{V_{gsR}}{1000} \frac{1440}{T_{cycle}} = \frac{5002.817}{1000} \frac{1440}{30.4457} = 236.6198 \text{ MscfD}$$

6. Calculation of the valve's closing pressure  $P_{csc}$ :

The volumetric capacity of the casing-tubing annulus  $B_a$  in ft.<sup>3</sup>/Mft. is:

$$\begin{aligned} B_a &= 5.45415(d_{casing}^2 - d_{od tubing}^2) \\ &= 5.45415(4.2^2 - 2.875^2) = 51.12924 \text{ ft.}^3/\text{Mft.} \end{aligned}$$

The volumetric capacity of the surface gas injection line  $B_l$  in ft.<sup>3</sup>/Mft. is:

$$B_l = 5.45415d_{gasline}^2 = 5.45415(2.067^2) = 23.3028 \text{ ft.}^3/\text{Mft.}$$

The gas compressibility factor in the gas injection line can be approximated by the following equation:

$$\begin{aligned} z_{gi} &= 1 - 1.9385(0.0001)(P_{cso} + 14.7) \\ &= 1 - 1.9385(0.0001)(700 + 14.7) = 0.861455 \end{aligned}$$

The geothermal temperature at valve's depth can be calculated as:

$$T_{dov} = 15.6D_{ov}/1000 + 88.8 = 15.6(3940)/1000 + 88.8 = 150.2640^\circ\text{F}$$

Factors  $K_1$ ,  $K_2$ ,  $K_3$ , and  $K_4$  are now calculated using the equations presented in this section and with the average compressibility factor of the annular injection gas given in the data of the problem ( $Z_{injection}$ ):

$$K_1 = \frac{(B_a)(D_{ov}/1000)}{Z_{injection}(1005 - T_{dov})} = \frac{(51.12924)(3940/1000)}{0.889(1005 - 150.264)} = 0.196147$$

With the length of the surface gas injection line  $L$  in ft., from the surface injection choke to the wellhead:

$$K_2 = \frac{(L/1000)B_i}{z_{gi}(545)} = \frac{(2000/1000)23.3028}{0.861455(545)} = 0.09926$$

From the data given above for this problem, the injection gas factor  $f_g$  is approximately equal to 1.1062458, so that:

$$K_3 = 1 + f_g = 1 + 1.1062458 = 2.1062458$$

$$K_4 = \frac{(D_{ov}/1000)Q_{gi}}{50.939v_{at}} = \frac{(3940/1000)236.6198}{50.939(1)} = 18.3019$$

Finally, the surface injection closing pressure of the valve is found by:

$$P_{csc} = P_{cso} + \frac{k_4 - \frac{V_{gsR}}{35.374}}{k_1 k_3 + k_2} = 700 + \frac{18.3019 - \frac{5002.817}{35.374}}{0.196147(2.1062458) + 0.09926} = 459.7073 \text{ psig}$$

#### 7. Calculation of the test-rack closing pressure:

From the data of the problem, it is known that the opening pressure of the valve at valve's depth is  $P_{cvo} = 700(1.1062458) = 774.372$  psig. The valve's closing pressure at valve's depth can be calculated (in an approximate way) using the gas factor  $f_g$  given above for a surface pressure of 450 psig:

$$P_{cvc} = P_{csc} f_g = 459.7073(1.1015) = 506.3676 \text{ psig}$$

So that the area ratio is equal to:

$$R = \frac{P_{cvo} - P_{cvc}}{P_{cvo} - P_{to}} = \frac{774.3720 - 506.3676}{774.3720 - 319.92} = 0.5897$$

This area ratio is greater than the largest commercially available area ratio for the selected valve model. The closest available area ratio is equal to only 0.333. If this available area ratio is used, then the valve's opening pressure must be increased to have a larger spread so that the required volume per cycle can be injected. But if 700 psig is the largest possible surface opening pressure (so that, for example, none of the unloading valves will open), a surface intermitter should be used to force the valve open as long as it is necessary to inject the required volume of gas per cycle. In this case, the calibration pressure is calculated from the following equation:

$$P_{trc} = (1-R)P_{cvo} + RP_{to} = (1-0.333)774.3720 + 0.333(319.92) = 623.03948 \text{ psig}$$

The intermitter must maintain the injection pressure at valve's depth above this pressure so that it would not close. The need of a surface intermitter is caused by the combination of the low available injection pressure and the small diameter of the casing. Because the casing diameter is very small, it might be required to install a choke in series with the intermitter so that the injection pressure would not increase very fast and above the opening pressure of an upper unloading valve when the intermitter opens.

**8. Verification of the average slug velocity**

Because a surface controller is used, calculations are performed keeping the injection surface pressure equal to 700 psig. The data presented in step 5 earlier is also used:

$$P_{ga} = 679.9172 \text{ psia}$$

$$P_{tm} = 696.4092 \text{ psig}$$

$$T_a = 580.1085^\circ\text{R}$$

$$Z_a = 0.89$$

With a surface injection pressure of 700 psig, the pressure upstream of the valve would be:

$$P_a = 774.372 + 14.7 = 789.072 \text{ psia}$$

And the pressure downstream of the valve is:

$$P_d = P_{tm} + 14.7 = 696.4092 + 14.7 = 711.1092 \text{ psia}$$

So that  $r = 711.1092/789.072 = 0.9011$  and therefore:

$$f_{rg} = \sqrt{r^{1.561} - r^{1.781}} = \sqrt{0.911^{1.561} - 0.9011^{1.781}} = 0.13875$$

$$\begin{aligned} v_{at} &= \frac{0.00079276(T_a)(z_a)(d_o^2)(P_a)(f_{rg})}{d^2 P_{ga} \sqrt{T_n G_g}} \\ &= \frac{0.00079276(580.1085)(0.89)(32^2)(789.072)(0.13875)}{2.441^2 679.9172 \sqrt{[15.6(3.94) + 548.8]0.7}} \\ &= 0.548 \text{ Mft./min} \end{aligned}$$

As can be seen, the slug velocity is smaller than 1 Mft./min, so that it is highly possible that the liquid fallback losses will be very large and hard to calculate. Therefore, plunger-assisted intermittent gas lift could be implemented. To finish the design, it is necessary to perform all previous calculations with this new velocity (or, if preferred, with the average of the assumed velocity and this calculated velocity). This iterative process ends when the velocity converges to a final slug velocity.

### 10.6.2 Design procedure with the use of surface controllers (intermitters)

Different volumes of gas could be injected per cycle (without changing the pilot valve and independently of the adjustment of the total cycle time) by just adjusting the periods of time in which the surface controller remains opened and closed. If surface controllers are not used (as in the case of choke-control intermittent gas lift), changes of the surface injection gas flow rates only cause variations of the total cycle time with very little changes in the volume of gas injected per cycle. For choke-control intermittent gas lift, the volume of gas injected per cycle mainly depends on the subsurface valve's area ratio, thus the subsurface valve would need to be changed if it was necessary to change the volume of gas to be injected per cycle. Being able to change the volume of gas injected per cycle with only surface adjustments of the intermitter opening and closing time allows the optimization of the gas injection to the exact needs of the well. These needs could suffer changes over time as the well's operational conditions change.

Due to the flexibility on the volume of gas injected per cycle provided by the use of surface controller, it is not critical to be able to determine the exact value of the valve's area ratio as it is required for choke-control intermittent gas lift. However, there are steps that should be considered when selecting the valve's area ratio and calibration pressure:

- The operating gas lift pilot valve's surface opening pressure should not be adjusted at very high values (too close to the surface injection manifold pressure). It is important to have a certain difference between the pressure at the manifold and the pilot valve's wellhead opening pressure so that: (1) the gas flow rate through the surface controller could be greater than the instantaneous gas flow rate through the gas lift valve once this valve opens, and (2) opening an unloading valve, if any, is avoided. In this way, the annular pressure is kept above the gas lift valve's closing pressure while the intermitter and the pilot valve are both opened. The valve's opening pressure cannot be too low either because it could considerably increase the time the surface controller should remain open to inject all the required volume of gas per cycle, and, additionally, if the injection pressure is too small, it might not be possible to reach an adequate liquid slug velocity to reduce the liquid fallback losses.
- The valve's area ratio should not be too small as this could cause an increment in the time in which the gas lift valve should remain open in order to pass the required volume of gas per cycle. But it is even more important not to install a gas lift valve with an area ratio that is too large because this might limit the volume of gas injected

per cycle to large volumes only. If the required volume of gas to be injected per cycle is less than the volume the installed gas lift valve could pass on choke-control intermittent gas lift, the operator will not be able to reduce the volume of gas injected per cycle to its required value.

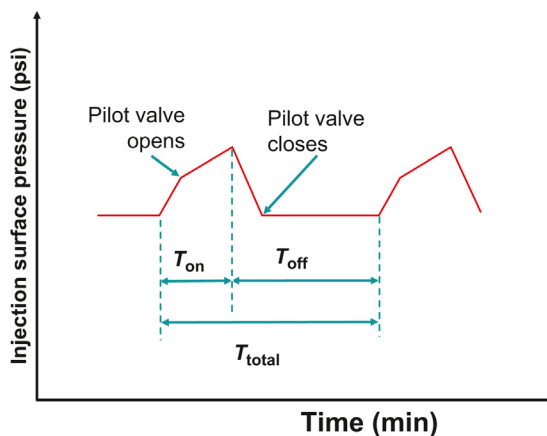
- The design procedure consists in doing all calculations required for choke-control intermittent gas lift. This gives the well's liquid production, the OCT, the required injection volume of gas per cycle, and the gas lift valve's area ratio. Then, select an area ratio equal to 30–40% of the calculated value for choke-control operation.

If the surface gas flow rate through the controller,  $Q_{gi\ cont}$  in MscfD, and the required injection volume of gas per cycle,  $v_{gsR}$  in scf, are known, then the time in which the controller must remain open in minutes,  $T_{on}$ , is equal to  $T_{on} = (1.44v_{gsR})/Q_{gi\ cont}$ . The time in which the controller must remain closed,  $T_{off}$ , is equal to the OCT minus  $T_{on}$ .

In the field, time intervals  $T_{on}$  and  $T_{off}$  can be adjusted following a procedure that is described as follows.

- Set  $T_{on}$  from 30 to 40% above its required value to pass the volume of gas per cycle calculated for choke-control intermittent gas lift. This momentarily guarantees a minimum liquid fallback loss.
- Set  $T_{off}$  in such a way that the total cycle time is from 20 to 30% above the OCT calculated for choke-control intermittent gas lift.
- This gas injection flow sequence should be kept constant for 2 or 3 days to stabilize the well's production.
- Test the well to know the well's production under these operational conditions.
- Keeping  $T_{on}$  constant,  $T_{off}$  should be reduced in steps of 10% of the initial value and, at each step, let the well stabilize for 2 or 3 days to measure its production. Continue this procedure (decreasing  $T_{off}$ ) until the well's production begins to decline. At this point, increase  $T_{off}$  to the value it had before the production began to decline.
- Keeping the total cycle time constant and equal to the value found in the previous step,  $T_{on}$  should be reduced in steps of 10% of its initial value. Allow 2 or 3 days for the well's production to stabilize and test the well at each step. Continue this procedure until the liquid production begins to decline. At this point, increase again  $T_{on}$  to the value it had before the production began to decrease.

$T_{on}$  can be adjusted in a much faster way in the field: repeat the steps described earlier but once  $T_{off}$  has been adjusted and the well has stabilized for the first time (second and third steps), the time interval from the moment the controller



■ FIGURE 10.23 Surface injection pressure pattern.

opens to the time the liquid slug reaches the surface is measured at the well-head. The optimization of  $T_{on}$  begins with its value equal to only 10% above this measured time interval. Fig. 10.23 shows time intervals  $T_{on}$ ,  $T_{off}$ , and  $T_{total}$ , as well as the typical surface injection pressure pattern during a complete cycle under the action of the controller and the subsurface gas lift valve.

### 10.6.3 Mechanistic models for the design of simple type completions on choke-control intermittent gas lift

Computer programs have been developed to design intermittent gas lift using mechanistic models. These models are based on the simultaneous solution of the continuity and momentum equations to determine the operational conditions at a moment  $t + \Delta t$  from conditions existing at time  $t$ . This way of designing intermittent gas lift installations has been developed by several authors for different applications: plunger-assisted intermittent gas lift, gas chamber pumps, choke-control intermittent gas lift, etc. In this section, only the basic mass and momentum conservation equations that are common to all of these applications are presented in a general way to familiarize the reader with this approach.

#### 10.6.3.1 Stages of the production cycle

To model intermittent gas lift, the cycle is divided into different stages. Each of these stages is characterized by particular operational conditions that help distinguish it from the other stages. The application of the continuity and momentum equations specifically for each stage, gives a group

of differential equations which describe the behavior of all the important variables for that particular stage.

The stages into which one cycle is divided are:

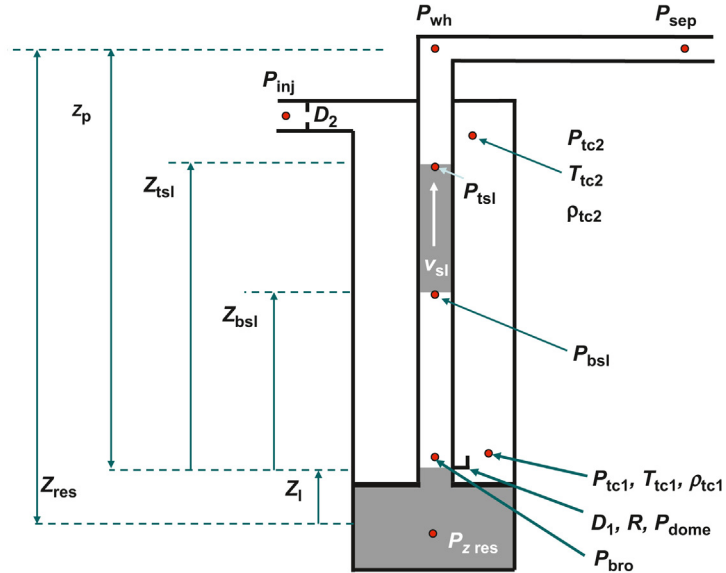
- Liquid slug traveling in the production tubing. During this stage, the gas lift valve is opened and gas is entering the tubing from the annulus, pushing the liquid slug to the surface. At the same time, gas from the manifold is entering the annulus at the surface.
- Liquid slug production. This stage begins just when the top of the liquid slug reaches the wellhead and ends when the entire slug is produced to the surface.
- Liquid slug displacement along the flowline: It begins when the entire liquid slug has been produced to the surface and ends when all the liquid reaches the separator or when its velocity drops to zero.
- Gas venting. It happens only if the gas lift valve is still open when the entire slug has reached the separator or its velocity has dropped to zero. During this stage, gas is injected from the surface manifold into the annulus and from the annulus into the production tubing and flowline. The stage ends when the gas lift valve finally closes.
- Slug regeneration. It begins when the gas lift valve closes. Gas continues to be injected into the annulus and therefore the annular pressure increases. Liquids from the reservoir begin to flow into the production tubing, generating a new liquid column. The liquid fallback from the first two stages also contributes to the generation of the new liquid column. This stage ends when the combined effect of the annular and tubing pressures is large enough to open the gas lift valve.

### 10.6.3.2 **Equations that model each stage**

Fig. 10.24 shows the most important variables of the mathematical model that is explained in this section. At each stage, mass and momentum conservation equations are applied to the annular space, the gas bubble that enters the tubing, and the liquid slug. The result of applying these equations is a set of ordinary differential equations that describes the dynamic behavior of the following variables: annular pressure, tubing pressure, liquid slug velocity, gas flow into the annulus, gas flow into the production tubing, liquid flow from the reservoir, liquid slug length, and liquid fallback losses.

It is assumed that the temperature along the well does not change with time. This approximation is reasonable at all stages where the process takes place in a slow fashion because the temperature of each component of the well can be approximated as equal to the geothermal temperature. However, this assumption





■ FIGURE 10.24 Variables of the mathematical model.

might not be very accurate during gas injection into the tubing, in which an additional equation could be introduced to determine the temperature of the gas bubble below the liquid slug as a function of time. This additional equation might be the energy balance equation that is used to determine the required injection gas volume per cycle,  $v_{gsR}$ , explained in the previous section. However, the error made by assuming that the gas bubble average temperature is equal to the geothermal average temperature is not as large as one might think. The work done by the gas bubble, as it pushes the liquid slug to the surface, causes a decrease in the gas bubble average temperature; however, the assumed temperature of the gas bubble at that time (taken as the average geothermal temperature as an approximate value) is in reality also lower than the temperature of the injection gas at the bottom of the well (when it enters the tubing), thus the error in the estimation of the gas temperature might not be too large.

In the following equations, volumes are expressed in cubic feet, areas in square feet, velocities in ft./s, pressures in psia, temperatures in °R, mass flow rates in lbm/s, tubular diameters in feet, diameters of the orifices and chokes in inches, and densities in lbm/ft.<sup>3</sup>.

*First stage, phase a, slug traveling in the production tubing.*

This stage begins when the gas lift valve opens and high-pressure gas enters the tubing and ends when the liquid slug reaches the wellhead. The

cross-sectional area of the liquid slug is assumed equal to the cross-sectional area of the tubing. Mass conservation in the annulus indicates: the rate of change of mass in the annulus is equal to the instantaneous mass flow rate of the gas entering the casing–tubing annulus minus the instantaneous mass flow rate of the gas entering the production tubing. This can be expressed as:

$$\frac{Y_{tc}}{2} \left[ \frac{d\rho_{tc1}}{dt} + \frac{d\rho_{tc2}}{dt} \right] = -m_1 + m_2 \quad (10.75)$$

Where  $Y_{tc}$  is the volume of the casing–tubing annulus,  $m_1$  is the gas mass flow rate into the tubing, and  $m_2$  is the gas mass flow rate into the annulus at the surface. In Eq. 10.75, the density in the annulus is considered to be equal to the average of the density at the surface,  $\rho_{tc2}$ , and the density of the gas at valve's depth,  $\rho_{tc1}$ . The equation of state is defined as:

$$\rho = P \frac{M}{zR_u T} \quad (10.76)$$

Where  $M$  is the gas molecular weight,  $z$  is the compressibility factor,  $R_u$  is the universal gas constant, and  $T$  is the absolute gas temperature. Introducing Eq. 10.76 in 10.75:

$$\frac{Y_{tc}}{2} \left( \frac{M}{R_u} \right) \left[ \left( \frac{1}{zT} \right)_{tc1} \frac{dP_{tc1}}{dt} + \left( \frac{1}{zT} \right)_{tc2} \frac{dP_{tc2}}{dt} \right] = -m_1 + m_2 \quad (10.77)$$

If the frictional pressure losses are neglected in the annulus, the gas pressure at depth can be expressed in terms of the surface gas pressure in the following way:

$$P_{tc1} = (P_{tc2}) e^{\left[ \frac{0.01875(Z_p)G_g}{(zT)_{average}} \right]} \quad (10.78)$$

Where  $G_g$  is the gas specific gravity,  $Z_p$  is the depth of the gas lift valve, while  $z$  and  $T$  are the average compressibility factor and average temperature of the injection gas in the annulus, respectively.

Introducing Eq. 10.78 in 10.77 gives:

$$\frac{Y_{tc}}{2} \left( \frac{M}{R_u} \right) \left\{ \left( \frac{1}{zT} \right)_{tc1} + \left( \frac{1}{zT} \right)_{tc2} e^{\left[ \frac{0.01875Z_p G_g}{(zT)_{average}} \right]} \right\} \frac{dP_{tc1}}{dt} = -m_1 + m_2 \quad (10.79)$$

Where  $m_1$  and  $m_2$  can be calculated using the Thornhill–Craver equation from the upstream and downstream pressures of the gas lift valve and the surface choke (or control valve) in the surface gas injection line, respectively.

If it is assumed that the gas bubble that enters the tubing grows at the same velocity in which the liquid slug is traveling, the injection gas mass balance inside the tubing is then given by:

$$Y_b \frac{d\rho_b}{dt} = m_1 - \rho_{bsl} A_t V_{pl} \quad (10.80)$$

Where  $Y_b$  is the gas bubble volume,  $\rho_b$  is the average gas density in the bubble,  $\rho_{bsl}$  is the gas density just underneath the liquid slug,  $A_t$  is the tubing area, and  $V_{pl}$  is the liquid slug velocity. The density  $\rho_b$  can be expressed as:

$$\rho_b = \frac{\rho_{bsl} + \rho_{bro}}{2} \quad (10.81)$$

Where  $\rho_{bro}$  is the gas density inside the tubing at the depth of the gas lift valve. Eq. 10.80 can be expressed as:

$$A_t Z_{bsl} \left[ \frac{dP_{bsl}}{dt} + \frac{(zT)_{bsl}}{(zT)_{bro}} \frac{dP_{bro}}{dt} \right] = \frac{2m_1 R_u}{M} (zT)_{bsl} - 2P_{bsl} A_t V_{pl} \quad (10.82)$$

Where  $Z_{bsl}$  is the length of the gas bubble. Frictional losses are important for the gas bubble and they can be expressed as:

$$P_{bsl} - P_{bro} = -f \frac{\rho_b |V_{pl}| V_{pl} Z_{bsl}}{2g_0 D(144)} \quad (10.83)$$

Where  $f$  is the friction factor that can be obtained from the Moody diagram,  $g_0$  is a constant equal to 32.17 lbf-ft/(lbf-s<sup>2</sup>),  $D$  is the tubing diameter, and  $V_{pl}$  is the gas velocity in the bubble, which is assumed to be equal to the velocity of the lower gas-liquid interface of the liquid slug,  $V_{sl}$ . Differentiating Eq. 10.83 with respect to time, the following expression is obtained:

$$\begin{aligned} \frac{dP_{bsl}}{dt} - \frac{dP_{bro}}{dt} + f \frac{|V_{pl}| V_{pl} Z_{bsl}}{2g_0 D(144)} \left( \frac{d\rho_b}{dt} \right) \\ + \frac{f}{g_0 D(144)} |V_{pl}| \rho_b Z_{bsl} \left( \frac{dV_{pl}}{dt} \right) = \frac{-f |V_{pl}| V_{pl} \rho_b V_{pl}}{2g_0 D(144)} \end{aligned} \quad (10.84)$$

Differentiating Eq. 10.81 and using the equation of state for a real gas gives:

$$\frac{d(\rho_b)}{dt} = \frac{M}{2R_u (zT)_{bsl}} \left[ \frac{dP_{bsl}}{dt} + \frac{(zT)_{bsl}}{(zT)_{bro}} \frac{dP_{bro}}{dt} \right] \quad (10.85)$$

Introducing Eq. 10.85 in 10.84, the following expression is obtained:

$$A \frac{dP_{\text{bsl}}}{dt} - B \frac{dP_{\text{bro}}}{dt} + \frac{f}{g_0 D (144)} |V_{\text{pl}}| \rho_b Z_{\text{bsl}} \frac{dV_{\text{pl}}}{dt} = \frac{-f |V_{\text{pl}}| |V_{\text{pl}}| \rho_b V_{\text{pl}}}{2g_0 D (144)} \quad (10.86)$$

Where

$$A = \left[ 1 + \frac{M}{2R_u (zT)_{\text{bsl}}} \frac{f}{2g_0 D 144} |V_{\text{pl}}| V_{\text{pl}} Z_{\text{bsl}} \right]$$

$$B = \left[ 1 - \frac{M}{2R_u (zT)_{\text{bro}}} \frac{f}{2g_0 D 144} |V_{\text{pl}}| V_{\text{pl}} (Z_{\text{bsl}}) \right]$$

$$\rho_b = \left[ \frac{P_{\text{bsl}}}{(zT)_{\text{bsl}}} + \frac{P_{\text{bro}}}{(zT)_{\text{bro}}} \right] \frac{M}{2R_u}$$

The momentum balance for the liquid slug is as follows:

$$\rho_L A_t (Z_{\text{tsl}} - Z_{\text{bsl}}) \frac{dV_{\text{sl}}}{dt}$$

$$= -144 A_t g_0 (P_{\text{tsl}} - P_{\text{bsl}}) - \frac{f_l |V_{\text{sl}}| V_{\text{sl}} A_t (Z_{\text{tsl}} - Z_{\text{bsl}}) \rho_L}{2D} - \rho_L g A_t (Z_{\text{tsl}} - Z_{\text{bsl}}) \quad (10.87)$$

Where  $\rho_L$  is the liquid density,  $V_{\text{sl}}$  is the liquid velocity,  $f_l$  is the friction factor for the liquid in the tubing, and  $g$  is the acceleration of gravity. The pressure on top of the liquid slug,  $P_{\text{tsl}}$ , can be calculated from the wellhead pressure  $P_{\text{wh}}$  by:

$$P_{\text{tsl}} = P_{\text{wh}} e^{\left[ \frac{0.01875 (Z_p - Z_{\text{tsl}}) G_g}{(zT)_{\text{average}}} \right]} \quad (10.88)$$

The length of the liquid slug decreases with time because of the liquid fall-back losses  $F_{\text{Bt}}$ , thus the liquid slug length at a time  $t + \Delta t$  with respect to the value it had at time  $t$  is given by:

$$(Z_{\text{tsl}} - Z_{\text{bsl}})_{t+\Delta t} = (Z_{\text{tsl}} - Z_{\text{bsl}})_t - F_{\text{Bt}} \quad (10.89)$$

$F_{\text{Bt}}$  is equal to the fallback factor  $F$ , expressed as the fraction (from 0 to 1) of the initial liquid column length that is not produced per each foot traveled by the liquid slug, multiplied by the initial liquid column length and by the distance traveled in a time interval  $\Delta t$ , (this distance is equal to  $[(V_{\text{sl}(t)} + V_{\text{sl}(t+\Delta t)})/2]\Delta t$ ). As indicated in several places in this book,  $F$  is usually equal to 5% of the initial liquid column length per each 1000 ft. traveled by the liquid slug ( $= 0.05/\text{Mft.}$ ), so that for each foot traveled by the liquid slug,  $F$  would be equal to 0.00005 (1/ft.). The reader is advised to

review the explanation given for Fig. 10.20 to have a better understanding of the fallback factor  $F$ .

The mathematical model presented in this section assumes that if the bottomhole flowing pressure  $P_{z_{\text{res}}}$  is less than the reservoir pressure  $P_{\text{res}}$ , then the liquid from the reservoir is accumulated at the bottom of the well and this liquid is taken into account at the beginning of the next liquid slug generation stage. The rate of increment of the liquid level,  $dZ_l/dt$ , is given by the Vogel equation (used as a rough approximation because the well is not producing under steady-state condition):

$$\frac{dZ_l}{dt} = \frac{5.615}{A_1 86400} Q_{\text{max}} \left[ 1 - 0.2 \frac{P_{z_{\text{res}}}}{P_{\text{res}}} - 0.8 \left( \frac{P_{z_{\text{res}}}}{P_{\text{res}}} \right)^2 \right] \quad (10.90)$$

$Q_{\text{max}}$  is the maximum liquid flow rate the reservoir could produce if the bottomhole flowing pressure was reduced to zero (expressed in Br/D and therefore it has to be multiplied times 5.615 ft.<sup>3</sup>/Br and divided by 86,400 s/D so that the rhs of the equation is expressed in ft./s). The bottomhole flowing pressure can be calculated from:

$$P_{z_{\text{res}}} = P_{\text{bro}} + \rho_L (Z_{\text{res}} - Z_p) / 144 \quad (10.91)$$

The increment in the liquid level in the tubing (that should be taken into account at the next liquid slug generation stage) is given by:

$$Z_{l+\Delta t} = Z_l + \frac{dZ_l}{dt} \Delta t + [\text{fallback}] \quad (10.92)$$

Finally, the numerical solution of the first stage is explained as follows:

Eqs. 10.79, 10.82, 10.86, and 10.87 represent a set of four ordinary differential equations for the following variables:  $\frac{dP_{\text{icl}}}{dt}$ ,  $\frac{dP_{\text{bro}}}{dt}$ ,  $\frac{dP_{\text{bsl}}}{dt}$ ,  $\frac{dV_{\text{pl}}}{dt}$ . This set of ordinary differential equations is algebraically solved for the four variables given above at each time  $t = n\Delta t$ , with  $n = 1, 2, 3, \dots$  etc. The calculated values of these four variables are used, at each time  $t$ , to calculate the values of the system variables at time  $t + \Delta t$ , using Euler's method. For example, to calculate the value of  $V_{\text{pl}}$  at  $t + \Delta t$  from the value of  $V_{\text{pl}}$  at  $t$ , the following equation is used (after finding the value of  $dV_{\text{pl}}/dt$  at time  $t$ ):

$$V_{\text{pl}+\Delta t} = V_{\text{pl}t} + \frac{dV_{\text{pl}}}{dt} \Delta t \quad (10.93)$$

*First stage, phase b, liquid slug production.*

This phase begins when the top of the liquid slug reaches the wellhead and ends when the entire liquid slug has been produced to the surface. In this

phase “b” all equations developed for phase “a” are valid with the exception of the momentum balance equation for the liquid slug, Eq. 10.87, and the wellhead pressure, which is no longer a constant. The momentum conservation equation can be expressed in the form given in Eq. 10.94 with the following considerations: (1) the pressure drop at the wellhead is taken into account, (2) the pressure at the top of the slug,  $P_{\text{tsl}}$ , is replaced by the wellhead pressure  $P_{\text{wh}}$ , and (3) the position of the top of the slug,  $Z_{\text{tsl}}$ , is replaced by  $Z_p$ . The momentum conservation equation is then:

$$\rho_L A_t (Z_p - Z_{\text{bsl}}) \frac{dV_{\text{sl}}}{dt} = -144 A_t g_0 (P_{\text{wh}} - P_{\text{bsl}}) - \frac{f_t |V_{\text{sl}}| V_{\text{sl}} A_t (Z_p - Z_{\text{bsl}}) \rho_L}{2D} - \rho_L g A_t (Z_p - Z_{\text{bsl}}) - 0.6 V_{\text{sl}} |V_{\text{sl}}| \rho_L A_t \quad (10.94)$$

The last term on the right hand side of this equation represents the pressure drop in the wellhead. The wellhead pressure can be calculated if the velocity and acceleration of the liquids that have entered the flowline are known. The continuity equation of the liquid in the tubing and flowline gives:

$$\rho_L V_{\text{sl}} A_t = \rho_L V_h A_h \quad (10.95)$$

Where  $A_h$  and  $V_h$  are the flow area and the liquid velocity in the flowline, respectively. From Eq. 10.95 it is found that:

$$V_h = V_{\text{sl}} \frac{A_t}{A_h} \quad (10.96)$$

Differentiating Eq. 10.96 with respect to time, the liquid acceleration in the flowline can be obtained as:

$$a_H = \frac{A_t}{A_h} \frac{dV_{\text{sl}}}{dt} \quad (10.97)$$

During the liquid slug production, the wellhead pressure can be calculated as the sum of the separator pressure (or production manifold) plus the friction and the acceleration pressure drops in the flowline:

$$P_{\text{wh}} = P_{\text{sep}} + \Delta P_{\text{fh}} + \Delta P_{\text{ah}} \quad (10.98)$$

Eq. 10.98 can be written in the following way:

$$P_{\text{wh}} = P_{\text{sep}} + \frac{\rho_L}{288} f_h \frac{L_H V_h^2}{g_0 D_H} + \frac{\rho_L L_H}{144} \frac{a_H}{g_0} \quad (10.99)$$

$L_H$  is the length of the liquid slug in the flowline (which can be obtained from Eq. 10.96 for a given time interval),  $f_h$  is the friction factor in the flowline,

and  $D_H$  is the flowline inside diameter. A force balance is performed on the gas lift valve to determine if it is opened or closed.

*Second stage, displacement of the liquid slug in the flowline.*

This stage begins when the entire liquid slug has reached the surface and ends when the entire slug has entered the separator or its velocity has dropped to zero. The equations for this stage are the same as those developed for the first stage (phase “a”), but with the following corrections:

- In the momentum balance equation for the liquid slug, the hydrostatic pressure drop is not considered because the entire slug is at the same level.
- In the continuity equation for the gas bubble, the volume of the flowline behind the slug should be considered in addition to the volume of the tubing.

*Third stage, gas venting.*

In this stage, the gas lift valve remains open. The gas is injected into the annulus and, from there, into the tubing and flowline. The model assumes that no liquid is produced to the surface during this stage. However, as it was the case for previous stages, if the flowing bottomhole pressure is less than the reservoir pressure, the model assumes that liquid is produced from the reservoir and this liquid will be taken into consideration during the slug generation stage for the next cycle. The force balance for the gas lift valve is performed continuously (at each time interval) and, if it is found that the valve is closed, then this stage ends and the fourth stage begins. Continuity and momentum equation for the annulus are the same as those for the first and second stages. The continuity equation for the gas in the tubing is as follows:

$$m_1 - \rho_{gwh} V_{gwh} A_t = A_t Z_p \frac{d\rho_{g-prom.}}{dt} \quad (10.100)$$

Where  $\rho_{gwh}$  is the density of the gas at the wellhead,  $V_{gwh}$  is the gas velocity at the wellhead and  $\rho_{g-prom.}$  is the average gas density in the tubing. Using the equation of state, the time derivative of the average gas density can be found in the following way:

$$\frac{d\rho_{g-prom.}}{dt} = \frac{1}{2} \frac{M}{R_u} \frac{d}{dt} \left[ \frac{P_{wh}}{(zT)_{wh}} + \frac{P_{bro}}{(zT)_{bro}} \right] \quad (10.101)$$

Subscript “wh” applies to conditions at the wellhead and “bro” corresponds to conditions at the gas lift valve’s depth. Inserting Eq. 10.101 into 10.100

and taking into account the fact that the wellhead pressure might be considered constant for this stage (as a rough approximation), the following equation is found:

$$\frac{dP_{\text{bro}}}{dt} = 2 \left[ \frac{(zT)_{\text{bro}} R_u}{A_t Z_p} \frac{R_u}{M} m_1 - \frac{(zT)_{\text{bro}} P_{\text{wh}}}{(zT)_{\text{wh}}} \frac{V_{\text{gwh}}}{Z_p} \right] \quad (10.102)$$

The momentum conservation equation for the gas in the tubing can be expressed as:

$$P_{\text{wh}} - P_{\text{bro}} = -f_b \frac{\rho_{\text{g-prom.}} (V_{\text{g-prom.}})^2 Z_p}{288 g_0 D} \quad (10.103)$$

Where  $f_b$  is the friction factor for the gas flow in the tubing and  $V_{\text{g-prom.}}$  is the average gas velocity in the tubing, which can be calculated from:

$$V_{\text{g-prom.}} = 0.5 \left[ V_{\text{gwh}} + \frac{m_1 R_u (zT)_{\text{bro}}}{A_t M P_{\text{bro}}} \right] \quad (10.104)$$

On the other hand, the average gas density in the tubing is given by:

$$\rho_{\text{g-prom.}} = \frac{1}{2} \frac{M}{R_u} \left[ \frac{P_{\text{wh}}}{(zT)_{\text{wh}}} + \frac{P_{\text{bro}}}{(zT)_{\text{bro}}} \right] \quad (10.105)$$

Introducing Eqs. 10.105 and 10.104 in Eq. 10.103, an expression is found that can be used to calculate the gas velocity at the wellhead:

$$V_{\text{gwh}} = 2 \left\{ \frac{576 g_0 D}{f_b Z_p} \left( \frac{R_u}{M} \right) \left[ \frac{P_{\text{bro}} - P_{\text{wh}}}{\frac{P_{\text{bro}}}{(zT)_{\text{bro}}} + \frac{P_{\text{wh}}}{(zT)_{\text{wh}}}} \right] \right\}^{1/2} - \frac{m_1 R_u (zT)_{\text{bro}}}{A_t M P_{\text{bro}}} \quad (10.106)$$

The equations for the liquid feed in from the reservoir are identical to those for previous stages.

The final values of variables  $P_{\text{bro}}$ ,  $P_{\text{tc1}}$ , and  $P_{\text{tc2}}$  of the liquid production stage are used as the initial conditions for this stage. Eqs. 10.102 and 10.79 are solved simultaneously to find the values of  $dP_{\text{tc1}}/dt$  and  $dP_{\text{bro}}/dt$ . The values of system variable such as  $P_{\text{tc}}$ ,  $m_1$ ,  $m_2$ ,  $V_{\text{gwh}}$ ,  $P_{\text{bro}}$ ,  $P_{\text{tc1}}$ ,  $P_{\text{zres}}$ , and  $Z_l$ , can then be found using Euler's equation. For example, the value of  $P_{\text{bro}}$  at a time  $t + \Delta t$  can be calculated by:

$$P_{\text{bro}t+\Delta t} = P_{\text{bro}t} + \left[ \left( \frac{dP_{\text{bro}}}{dt} \right)_t \Delta t \right] \quad (10.107)$$



*Fourth stage, liquid slug regeneration*

The gas lift valve is closed during this stage and gas from the manifold is continuously being injected into the well's annulus. At the same time, fluids from the reservoir are being accumulated at the bottom of the well. The equation that expresses the mass balance in the annulus is:

$$\frac{Y_{tc}}{2} \left[ \frac{d\rho_{tc1}}{dt} + \frac{d\rho_{tc2}}{dt} \right] = m_2 \quad (10.108)$$

Following the same steps described for the first stage, an expression is found for the time rate of change of the pressure in the annulus:

$$\frac{dP_{tc1}}{dt} = \frac{m_2}{\frac{Y_{tc}}{2} \left( \frac{M}{R_u} \right) \left\{ \left( \frac{1}{zT} \right)_{tc1} + \left( \frac{1}{zT} \right)_{tc2} e^{-\left[ \frac{0.01875 Z_p G_g}{(zT)_{average}} \right]} \right\}} \quad (10.109)$$

Eq. 10.90 can be used to calculate the rate of increase of the liquid column. Eqs. 10.109 and 10.90 can be simultaneously solved to calculate  $dP_{tc1}/dt$  and  $dZ/dt$ . These values are then used to calculate  $P_{bro}$  and  $P_{tc1}$ . As calculations proceed in time intervals, a force balance is performed at each step on the gas lift valve to check if it is still closed. This stage ends when the gas lift valve opens.

## 10.7 DESIGN OF ACCUMULATION CHAMBERS

In Section 6.4.3, different types of accumulation chambers are presented, along with explanations of how they are operated and some operational problems that might be encountered when using this type of completion. The equations that are used in the design of accumulation chambers located above the top of the perforations (as opposed to inserted chamber, which are at, or below, the perforations) are described in this section. Several statements made in chapter: Gas Lift Equipment are verified by a numerical example shown at the end of the section. The completion that is analyzed in this section corresponds to the one shown in Fig. 6.57.

When the reservoir pressure has declined to very low values, the injection gas/liquid ratio increases because the size of the liquid slug to be lifted becomes very small and the volume of gas required to lift it is not that much different from those needed for larger slugs. One way of reducing the injection gas/liquid ratio is by installing accumulation chambers, which allow the generation of liquid slugs much larger than those the reservoir pressure can generate by itself. If, and only if, the PI is large enough, it is possible to

increase the daily liquid production of the well in a noticeable way. In most cases, the liquid production does not increase and engineers usually cancel the installation of additional accumulation chambers because the reduction in the gas/liquid ratio is either not well understood, or such reduction simply does not justify the investment involved in replacing current completions.

The objective of these accumulation chambers is to accumulate as much liquid as possible for a given length of the liquid column, but an increment of the daily liquid production is not guaranteed by this fact alone because the time required to fill accumulation chambers with liquids is longer than the time it takes for the liquid slugs to accumulate in simple type completions. On the other hand, if the oil has a large gas content (in solution or free but trapped within the liquid) it is possible that the net liquid volume accumulated in the chamber at each cycle results in only a small portion of the total accumulation chamber volume.

Calculations to find the area ratio and the calibration pressure of the operating gas lift valve are very similar to those required for simple type completions described in Section 10.6.1. The equations are basically the same, but the following differences must be taken into account.

- At the moment the operating valve opens, the production pressure at this valve's depth,  $P_{to}$ , corresponds only to the wellhead pressure plus the weight of the gas column above the valve. This is due to the fact that the operating valve is above the accumulated liquid in the chamber.
- In the calculation of factor  $\alpha'$  introduced for simple type completions (in Eq. 10.14), the volumetric capacity is not the capacity of the production tubing but now it corresponds to the volumetric capacity of the chamber.
- The volume of the accumulation chamber should be considered when calculating the required volume of gas to be injected per cycle.

In simple type completions, the volume of gas injected per cycle should occupy the production tubing from the depth of the operating valve,  $D_{ov}$ , to the wellhead minus the length of the liquid column  $Q'$ . If  $B_{gt}$  is the volumetric capacity of the tubing in ft.<sup>3</sup>/Mft., then the volume that the injection gas occupies when the top of the liquid slug just reaches the surface is  $(D_{ov} - Q')B_{gt}$ . For accumulation chambers, the size of the liquid column  $Q'$  could be very large. For this reason, and as a safety factor, for accumulation chambers the volume that the injection gas per cycle occupies is equal to the total volume of the production tubing plus the volume of the chamber itself. Then  $(D_{ov} - Q')B_{gt}$  is replaced by  $(C_h B_{gc} + D_{ov} B_{gt})$ , where  $B_{gt}$  is the volumetric capacity of the tubing

in ft.<sup>3</sup>/Mft.,  $B_{gc}$  is the volumetric capacity of the chamber also in ft.<sup>3</sup>/Mft.,  $C_h$  is the length of the chamber in Mft., and  $D_{ov}$  is the depth of the operating valve, also in Mft.

- The size of the chamber corresponds to the size of the optimum liquid column length calculated in the same way as it was calculated for simple type completions, but using the value of the true liquid gradient as explained later in this section.
- The operating valve is not necessarily taken as the last (deepest) unloading valve because the liquid column to be lifted could be much greater than the difference in depth of the top chamber and the last unloading valve above the chamber. The last (deeper) unloading valve could then be as close as 60 ft. (if necessary) above the accumulation chamber's operating valve. A minimum distance of 60 ft. is advised so that wireline jobs can be performed at each mandrel without problem in locating the desired one for a particular well intervention.
- Because the liquid columns to be lifted could be considerably long, it becomes very important to verify at the end of the design calculations that the unloading valves would not open as the liquid slug passes by each of these valves.

The reader is advised to review the equations given in [Section 10.6.1](#) to have a better understanding of the calculation procedures that are described next.

The volumetric capacity of the chamber ( $b_{ch}$ ) in Br/Mft., is given by:

$$b_{ch} = 0.97143 \left[ \left( D_{\text{casing}}^2 - D_{\text{od tubing}}^2 \right) + \left( D_{\text{id tubing}} \right)^2 \right] \quad (10.110)$$

Where  $D_{\text{casing}}$  is the inside diameter of the casing in inches.  $D_{\text{od tubing}}$  and  $D_{\text{id tubing}}$  correspond to the outside and inside diameters, also in inches, of the tubing between the two packers, known as the "dip tube." The diameter of the "dip tube" should not necessarily be equal to the diameter of the production tubing above the upper packer. The inside diameter of the production tubing above the chamber must be adequate for an efficient production operation: it cannot be too small because it will generate a very long liquid column once all the liquid from the accumulation chamber has entered the tubing, but it cannot be too large either to avoid an increase in liquid fallback losses caused by a very slow liquid slug velocity (usually found in large-diameter tubing strings). The length of the liquid column as a function of time is calculated in the same way as for simple type completions, but the term  $\alpha$  introduced in Eq. 10.17 ( $\alpha$  is equal to  $1000 \alpha'$ ) in this case is equal to  $J/(1.44 b_{ch})$  and the liquid column lost as fallback,  $Q'_a$ , is equal to  $FD_{ch}Q'$ , where  $D_{ch}$  is the depth of the perforated nipple just above the lower packer.

Factor  $c_m$  is then equal to  $FD_{ch}$ . The maximum drawdown at the perforations is given in this case by:

$$A' = P_{sbh} - (D_{pt} - D_{ch})1000\rho_t - P_{wh}f_g \quad (10.111)$$

Following the same mathematical procedure given for simple type completions (Section 10.6.1), an expression for the liquid column length in Mft. as a function of liquid accumulation time  $t$  is found as:

$$C_H = \frac{A'(e^{\alpha\rho_f t} - 1)}{1000\rho_f(e^{\alpha\rho_f t} - c_m)} \quad (10.112)$$

Where  $A'$ ,  $\alpha$ , and  $c_m$  have been modified as indicated in this section. The liquid feed-in time  $t$  is in this case equal to the total cycle time  $T_{cycle}$  minus the time that it takes for the liquid column to travel from the accumulation chamber to the surface, which can be calculated as  $D_{ch}/v_{at}$ . The value of  $C_H$  represents the length of a liquid column with no gas (dissolved or free) that fills the dip tube and the annulus of the chamber. The real length of the chamber, called  $C_{HT}$ , must then be calculated taking into account the fact that the liquid has some free and dissolved gas in it. For this purpose, the true liquid gradient  $\rho_t$  must be used in the following way:

$$C_{HT} = C_H(\rho_f/\rho_t) \quad (10.113)$$

$C_{HT}$  and  $C_H$  are expressed in Mft. and gradients  $\rho_f$  and  $\rho_t$  are in psi/ft. The depth of the operating valve  $D_{ov}$  is then equal to  $D_{ch} - C_{HT}$ , where the tubing pressure is equal to  $P_{wh}f_g$  throughout the time the chamber is being filled with liquids.

It is important to determine if the injection pressure is high enough to lift the liquid column  $Q'$  (in Mft.) that is generated once all the liquid from the accumulation chamber enters the production tubing because this column could be considerably longer than the chamber itself. The hydrostatic pressure due to the liquid column  $Q'$  is equal to  $[1000 Q'(\rho_f) + P_{wh}(f_g)]$ , where  $Q'$  is considered a 100% liquid (no gas) column that can be calculated from:

$$Q' = C_H(b_{ch}/B_t) \quad (10.114)$$

Because the volumetric capacity of the chamber,  $b_{ch}$ , is greater than the capacity of the tubing,  $B_t$ , the length of the column  $Q'$  is also greater than the length of the chamber. For usual tubing and casing sizes, the liquid column  $Q'$  could be from 5 to 8 times greater than  $C_H$ .

Calculation of the OCT is performed as explained for simple type completions, using the following equation:

$$T_{\text{cycle}} = \frac{(e^{\gamma T_{\text{cycle}}} - C_4)(e^{\gamma T_{\text{cycle}}} - c_m C_4)}{\gamma e^{\gamma T_{\text{cycle}}} C_2 C_4} \quad (10.115)$$

In which, for accumulation chambers, the following parameters are now defined as:

$$\begin{aligned} c_m &= FD_{\text{ch}} \\ C_2 &= 1 - c_m \\ \gamma &= \alpha \rho_f \\ C_4 &= e^{\gamma \frac{D_{\text{ch}}}{v_{\text{ar}}}} \\ \alpha &= \frac{J}{1.44 b_{\text{ch}}} \end{aligned}$$

Once the OCT  $T$  is found, the daily production in MBr/D can be calculated as:

$$q_f = C_H (1 - c_m) (b_{\text{ch}}) \frac{1440}{T_{\text{cycle}}} \frac{1}{1000} \quad (10.116)$$

To illustrate the true capacity of accumulation chambers to increase the daily liquid production and the problems associated with venting the gas on top of the liquid in the annulus of the accumulation chamber, an example is presented of a typical good candidate well for intermittent gas lift.

### Problem 10.3

Analyze the effects that the volumetric capacity of the accumulation chamber and the PI of the well have on the liquid production of a well with the following data: Reservoir pressure 450 psig; Top of perforations depth 2860 ft.; Liquid gradient 0.38 psi/ft.; Production tubing diameter 2 $\frac{7}{8}$  in. To make calculations simpler, it is assumed that the gas injection time is constant and equal to 5 min and, for the initial estimations, liquid fallback losses are neglected.

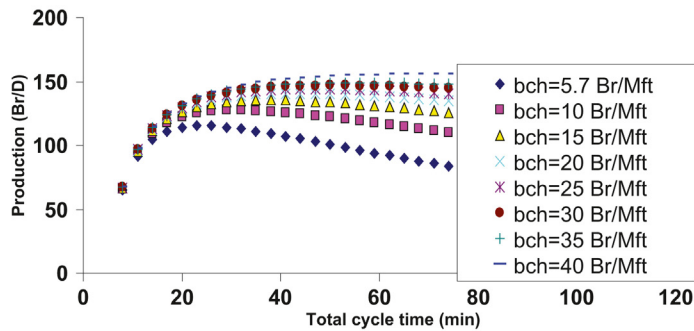
### Solution

The volumetric capacity of a 2 $\frac{7}{8}$ -in. tubing is approximately equal to 5.7 Br/Mft. and an accumulation chamber in a well with a 7-in. casing has a capacity of a little less than 40 Br/Mft. These two capacities are taken as the extreme values for the present analysis. The PI values investigated are 0.5, 1, and 1.5 Br/D-psi.

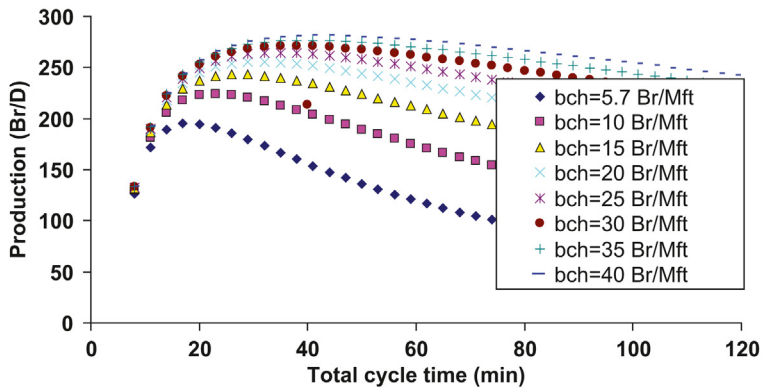
Figs. 10.25–10.27 show the production of the well as a function of the total cycle time, for different volumetric capacities  $b_{ch}$  and PIs  $J$ .

As can be appreciated in Figs. 10.25–10.27, if the volumetric capacity  $b_{ch}$  increases, the OCT and the liquid production also increase. The liquid production increment is greater for greater values of the PI, as can be observed in Table 10.1, where the percent increment in liquid production when shifting from simple type completions to accumulation chambers with volumetric capacities of 20 and 40 Br/Mft. are shown.

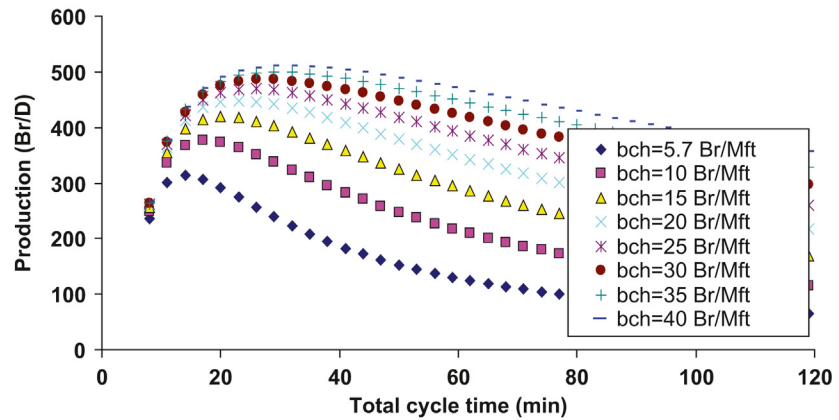
The liquid production increment is proportional to the PI and the volumetric capacity of the chamber. But, as can be seen from Table 10.1,



■ FIGURE 10.25 Liquid production as a function of the total cycle time for a productivity index of 0.5 Br/D/psi.



■ FIGURE 10.26 Liquid production as a function of the total cycle time for a PI of 1.0 Br/D/psi.



■ FIGURE 10.27 Liquid production as a function of the total cycle time for a PI of 1.5 Br/D/psi.

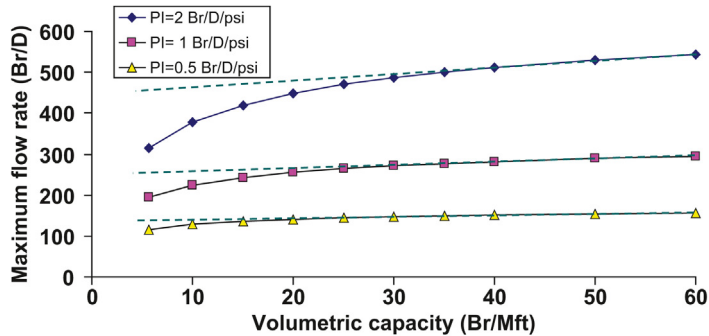
these increments are not as large as it might be concluded from the increments in the size of the liquid columns that can be obtained by the use of accumulation chambers. If the gas venting problems (that are explained later) and the liquid fallback losses are taken into consideration, the actual increments are even smaller than those presented in Table 10.1.

An accumulation chamber installed in a well with a 5½-in. casing has a volumetric capacity of 21 Br/Mft., while a chamber installed in a well with a 7-in. casing has a volumetric capacity of 37.19 Br/Mft. It is better then to install accumulation chambers in wells with large diameter casings. It is worthwhile noting that as the casing diameter increases, the rate of increase of the liquid flow rate with respect to the casing diameter decreases until reaching a constant value, which is very small (especially for low PI wells). This is illustrated in Fig. 10.28.

Fig. 10.28 could serve as a guide when making a decision of installing a double-packer chamber or an inserted chamber. Double-packer

**Table 10.1** Percent Increase of the Liquid Production due to the Installation of Accumulation Chambers With Volumetric Capacities of 20 and 40 Br/Mft.

$J$ (Br/D/psi)	% Increase ( $b_{ch} = 20$ Br/Mft.)	% Increase, ( $b_{ch} = 40$ Br/Mft.)
0.5	22	32
1	32	44
1.5	43	63



■ FIGURE 10.28 Maximum liquid production as a function of the volumetric capacity of the accumulation chamber.

chambers have the greatest volumetric capacity, but if the volumetric capacity is already large, the additional increment in liquid production could be so small that it might be preferable to install an inserted chamber. Even though inserted chambers have lower volumetric capacities, they can handle formation gas better and, at the same time, they can increase the liquid production because the liquid columns generated inside of these completions do not exert any pressure on the formation.

Problems associated with venting the formation gas on top of the liquids in the annulus of the chamber are analyzed next.

As liquids enter the annulus of a double-packer accumulation chamber, the gas on top of the liquids must be vented through a bleed valve located just below the upper packer. If this gas flow is restricted in some way, the pressure inside the annulus of the chamber increases and the liquid level in the dip tube rises faster than it does inside the annulus. The rate of growth of the liquid level  $Q'$  inside the chamber, assuming that the liquid level in the annulus is the same as the one in the dip tube, is given by:

$$\frac{dQ'}{dt} = q/b_{ch} \quad (10.117)$$

Where  $Q'$  is in Mft.,  $b_{ch}$  in Br/Mft. and  $q$  is the instantaneous liquid flow rate from the reservoir in Br/D. On the other hand, the gas flow rate that must be vented from the annulus for a given liquid flow rate  $q$  is:

$$Q_g = \frac{dQ'}{dt} (5.615) b_{t \text{ annular}} \quad (10.118)$$

$Q_g$  is the gas flow rate vented from the annulus and  $b_{t \text{ annular}}$  is the volumetric capacity in Br/Mft. of the chamber's annulus only. The factor 5.615 (in ft.<sup>3</sup>/Br)



is introduced because the liquid production is given in Br/D and the gas flow rate  $Q_g$  is expressed in ft.<sup>3</sup>/day. Combining Eqs. 10.117 and 10.118, the gas flow rate through the bleed valve should be:

$$Q_g = q \frac{b_{\text{t annular}}}{b_{\text{ch}}} (5.615) \quad (10.119)$$

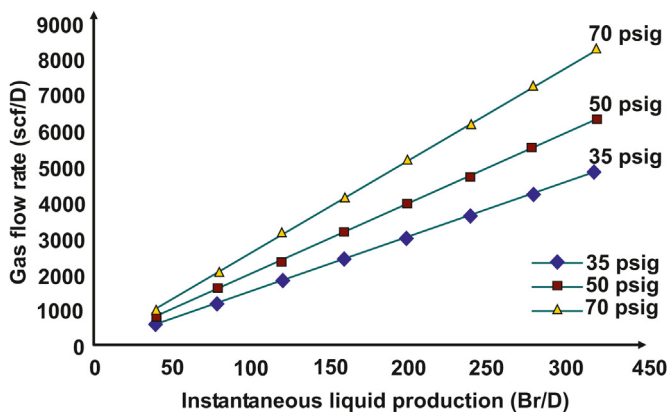
To find the gas flow rate at standard conditions, Eq. 10.119 is modified in the following way:

$$Q_{\text{gst}} = q \frac{b_{\text{t annular}}}{b_{\text{ch}}} (5.615) \frac{P_{\text{annular}}}{T_{\text{annular}}} \frac{520}{14.7} \quad (10.120)$$

In Eq. 10.120, the gas annular pressure  $P_{\text{annular}}$  must be expressed in psia and the gas temperature  $T_{\text{annular}}$  must be expressed in °R. The gas flow rates that need to be vented (calculated using Eq. 10.120) are shown in Fig. 10.29. In this example, the chamber volumetric capacity is equal to 37.2 Br/Mft. The results are given for different annular pressures and instantaneous liquid flow rates.

Eq. 10.120 only determines the gas flow rate due to the displacement of the gas caused by an increase in the liquid level in the annular space of the chamber, but it does not consider:

- The injection gas that remains in the annulus after the gas lift valve closes.
- The gas in solution that evolves from the liquid in the annulus and the free gas carried by the liquid into the annulus.



■ FIGURE 10.29 Gas flow rate that needs to be vented for different annular pressures and instantaneous liquid productions.

These contributions are very hard to predict, but undoubtedly the actual gas flow rates must be greater than those predicted by Eq. 10.120 even for moderate values of the formation gas/oil ratio. It is not unusual to find good candidate wells for intermittent gas lift with gas/oil ratios from several hundreds to thousands scf/Br. Assuming that the formation gas/liquid ratio that enters the chamber annulus is as large as 350 scf/Br, with liquid production from 70 to 120 Br/D, the formation gas that must be vented goes from approximately 24,500–42,000 scf/D. The results, shown in Fig. 10.30, are obtained using the Thornhill–Craver equation to calculate the gas flow rate that can be sustained through the bleed valve with a downstream pressure of 60 psig and different upstream (annular) pressures. The figure shows the results for bleed-valve orifice diameters of 4/64, 12/64, and 24/64 in. (the commonly used RSM-20 chamber gas bleed valve has an orifice diameter of 4/64 in. and the RV-2 valve’s seat diameter is equal to 24/64 in.).

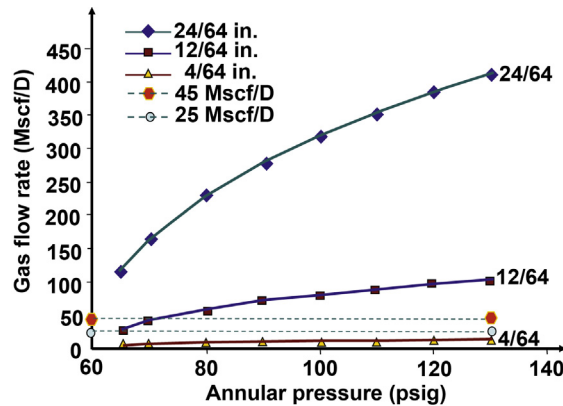
From Fig. 10.30 it is found that the RSM-20 bleed valve cannot be used to vent the chamber for none of the differential pressures across this valve. 12/64-in. orifices can handle 25,000 scf/D for differential pressures as low as 5 psi and 45,000 scf/D for differential pressures greater than or equal to 15 psi. The RV-2 valve, on the other hand, can handle more than 100 MscfD with a differential pressure of only 5 psi.

The differential pressure across the bleed valve should be as low as possible; otherwise, the liquid level in the annulus could be much lower than the liquid level in the dip tube. Fig. 6.59 shows a diagram with the pressures in the annulus and in the dip tube, in which it can be seen that the difference in the liquid levels is affected by this differential pressure across the bleed port and the value of the true liquid gradient of the fluids that fill the chamber. The difference between the liquid level in the dip tube and in the annulus is shown in Table 10.2 as a function of the true liquid gradient and the differential pressure across the bleed port.

In the example corresponding to Fig. 10.30, the differential pressure across the 12/64-in. port must be equal to 15 psi to be able to handle 45,000 scf/D and if the true liquid gradient values are found from 0.25 to 0.35 psi/ft. (as it has been demonstrated in numerous downhole pressure surveys), then the differences in liquid levels are going to be from 43.7 to 62.47 ft., approximately. These liquid level differences are very large for chambers of only 100–200 ft. in length. It is then important to keep the pressure drop across the bleed port as low as possible, especially for low values of the true liquid gradient, in order to have small liquid level differences. This is why it is recommended to be able to bleed the gas from the annulus in an efficient manner. A way of reducing the volume of gas that enters the chamber annulus is

**Table 10.2** Difference in Feet Between the Liquid Levels in the Dip Tube and in the Annulus of the Chamber.

True Liquid Gradient (psi/ft.)	Differential Pressure = 10 psi	Differential Pressure = 20 psi	Differential Pressure = 30 psi	Differential Pressure = 40 psi
0.1	100.0	200.0	300.0	400.0
0.2	50.0	100.0	150.0	200.0
0.3	33.3	66.6	100.0	133.3
0.4	25.0	50.0	75.0	100.0

**FIGURE 10.30** Gas flow rate through 4/64-, 12/64-, and 24/64-in. orifice diameters for different annular pressures and 60 psig downstream pressure.

shown in Fig. 10.31. The liquids are forced to move downwards to be able to pass through the perforated nipple on their way to the chamber's annulus while the accumulation chamber is being filled with liquids, thereby promoting gas separation.

## 10.8 SIMPLE TYPE ACCUMULATOR

Due to the problems that might take place in accumulation chambers installed in wells with high formation gas/liquid ratios, a more appropriate alternative to increase the lifting efficiency can be achieved by installing simple type accumulators. Fig. 6.49 shows a simple type accumulator. With this tubing configuration, the volumetric capacity is increased right where it is needed to accumulate more liquid per cycle, keeping the rest of the production tubing above with a smaller inside diameter to maintain a small volume of injection gas required per cycle. Formation gas is easily vented to the surface without the need of a bleed valve that might restrict the gas flow to

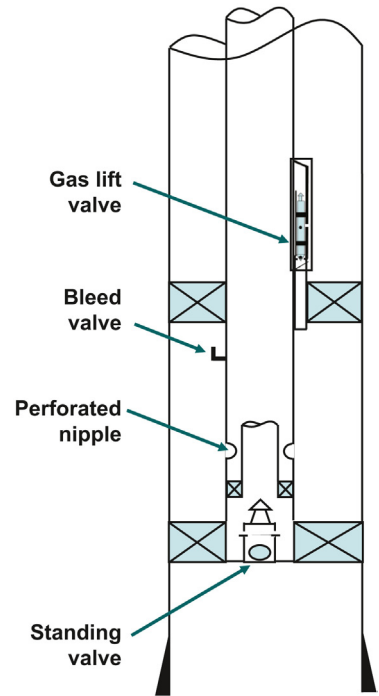
the surface. The fact that a percentage of the formation gas remains trapped in the liquid (especially in viscous fluids) must be taken into consideration. The true liquid pressure gradient is less than the one simply calculated from the water cut and the oil API gravity; therefore, the size of the accumulator must be greater than the liquid column with no formation gas in it.

Another advantage simple type accumulators have is that they do not require special mandrels or packers, which costs more and increase the possibility of mechanical failures. Calculations of the area ratio and calibration pressure of the gas lift valve are performed in the same way as they are done for intermittent gas lift in wells with uniform production tubing (Section 10.6.1). In general, the equations needed for the design of simple type accumulators are basically the same as those for simple type completions, but the following differences must be taken into account.

- In the estimation of factor  $\alpha'$  that was introduced for simple type completions (in Eq. 10.14), the volumetric capacity corresponds to the capacity of the lower tubing (which is the accumulator's capacity) and not the capacity of the upper production tubing from the top of the accumulator to the wellhead.
- In calculating the required volume of gas per cycle, the accumulator volume should be taken into account in addition to the rest of the production tubing.
- The size of the accumulator corresponds to the optimum liquid column calculated in the same way as for simple type completions, but corrected for the true liquid gradient as is the case for double-packer accumulation chambers explained in Section 10.7.
- The maximum injection pressure must be calculated based on the size of the liquid column once all the liquid has entered the production tubing above the accumulator.

One of the reasons why the inside diameter of the accumulator should not be too large compared with the rest of the production tubing is the fact that the liquid column to be lifted might be too long and could exert a hydrostatic pressure difficult to overcome or it might make it impossible to keep the liquid slug velocity high enough to maintain the liquid fallback losses at low levels.

The other reason why the inside diameter of the accumulator cannot be too large is to avoid very large liquid fallback losses when the injection gas is displacing the liquid inside the accumulator. At this time, the required injection gas flow rate should be very large to achieve a slug velocity of approximately 1000 ft./min. Large diameter production tubing strings increase the liquid fallback losses because of the low liquid slug velocities caused by the fact that most gas lift



■ FIGURE 10.31 Modification at the entrance of the annulus to reduce the volume of gas that enters the chamber annulus.

systems cannot provide a high enough instantaneous injection gas flow rate through the gas lift valve. For this reason, it is also advisable to install a section of small diameter tubing (of at least 90 ft. in length) between the point of gas injection (the operating valve's depth) and the lower end of the accumulator. In this way, when the gas enters the accumulator, the liquid has already been accelerated to a velocity high enough to maintain a low liquid fallback.

### 10.9 INSERTED CHAMBERS AND INSERTED ACCUMULATORS

Examples of inserted accumulation chambers and inserted (simple type) accumulators are given in Figs. 6.62 and 6.70, respectively. Wells with one or several of the following characteristics could be good candidates for inserted accumulation chamber or inserted accumulator installations:

- Long perforated intervals
- Long ratholes
- Very low reservoir pressure
- Damaged casings or open-hole completions

By installing inserted accumulation chambers or inserted accumulators in an appropriate way at or below the formation, the economic life of a very low liquid producer well could be considerably extended. The way these inserted completions work (and possible operational problems), are presented in chapter: Gas Lift Equipment, together with several examples of the different types of available inserted accumulation chambers and inserted accumulators. Wells that would otherwise be good candidates for inserted accumulation chambers (if it was not for the fact that they produce liquids with very high formation gas/oil ratios or have very small casings) are good candidates for inserted accumulators. In many ways inserted accumulators are better than inserted accumulation chambers, especially because inserted accumulators are much simpler completions that can handle formation gas in a better way.

Considerations with respect to the size of the dip tube, opening pressures of unloading valves, calibration of the operating valve, and calculations of the required volume of gas per cycle, are identical to those given for double-packer accumulation chambers. However, there are two important characteristics that are unique to inserted accumulation chambers or inserted accumulators:

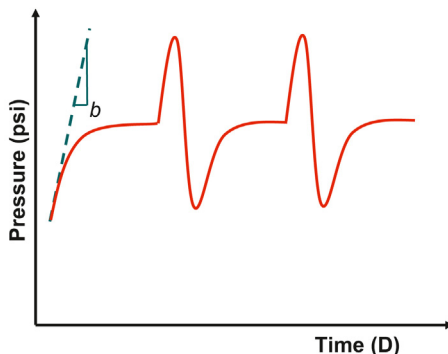
1. Calculation of the daily production is carried out in a completely different way.
2. Provisions must be made to correctly vent formation gas, not only inside of the inserted accumulation chamber or inserted accumulator,

but also in the space between the inserted completion and the casing in which it is located. Overlooking this fact could considerably diminish the liquid production of the well.

It is not possible to know the actual production capability of a well with a long perforated interval before installing an inserted completion. Without inserted completions, the lower parts of a long perforated interval are exposed to pressures almost as high as the reservoir static pressure. These high pressures (compared with the static reservoir pressure) are caused by the hydrostatic liquid column of the well's fluids along the long perforated interval. Even with today's sophisticated measuring devices, it is not possible to know the production capability of the formation at very low bottomhole flowing pressure because the only way of finding that out is precisely by installing an inserted completion that would lower the bottomhole pressure to very low levels, making it possible to measure the reaction of the reservoir to these relatively low pressures.

Despite what is expressed in the previous paragraph, a way of estimating the liquid production of a well before installing an inserted completion can be implemented and it is explained next. It is only an approximation because it is based on the maximum instantaneous liquid flow rate that the well can achieve under intermittent gas lift with a simple type completion. This maximum liquid flow rate takes place just at the beginning of the slug generation stage of the cycle. The calculation procedure does not take into account a possible increase in the formation gas/oil ratio once the well is exposed to very low bottomhole flowing pressures (this is a problem that should be considered when contemplating the installation of an inserted accumulation chamber or inserted accumulator in a gas cap drive reservoir).

To apply the procedure that is explained in this section, the well should be producing on intermittent gas lift prior to the installation of the inserted completion so that a flowing pressure survey, especially designed for intermittent gas lift, can be run in the well while its liquid production is being measured at the surface. A guide to properly run and analyze pressure and temperature surveys for wells on intermittent gas lift is presented in Section 12.3. The maximum instantaneous liquid production a well on intermittent gas lift can achieve at the beginning of the cycle can be estimated from the result of a downhole pressure survey like the one shown in Fig. 10.32. This liquid flow rate is proportional to the slope  $b$  of the pressure curve that is shown in the figure. The pressure that is plotted is the measured downhole pressure just below the gas lift valve "minus the wellhead pressure," thus the pressure shown in the graph is approximately equal to pressure due to the hydrostatic liquid pressure only. Slope  $b$  in psi/D is the maximum derivative



■ FIGURE 10.32 Result of a downhole pressure survey run in a well with a simple type completion producing on intermittent gas lift.

of the bottomhole flowing pressure with respect to time when the liquid slug is being generated.

Based on the maximum slope  $b$ , the maximum liquid flow rate in Br/D is given by the following equation:

$$q_{\max} \left[ \frac{\text{Br}}{\text{D}} \right] = \frac{b \left[ \frac{\text{psi}}{\text{D}} \right] B_t \left[ \frac{\text{Br}}{\text{ft.}} \right]}{\rho_f \left[ \frac{\text{psi}}{\text{ft.}} \right]} \quad (10.121)$$

Where,  $B_t$  is the volumetric capacity of the tubing where the liquid column is generated during the downhole survey (expressed here in Br/ft.),  $\rho_f$  is the liquid gradient calculated from the water cut and the oil API gravity (not the true liquid gradient). The liquid fallback losses must be subtracted from the calculated value of  $q_{\max}$  because the initial pressure increment is due to the liquid feed in from the reservoir plus the liquid fallback from the previous cycle. The value of the liquid fallback can be calculated from the pressure survey (with the equations given in chapter: Intermittent Gas Lift Troubleshooting) and the production test of the well performed during the survey. This corrected value of  $q_{\max}$  is a conservative approximation of the liquid flow rate that can, in reality, be expected from the well with an inserted completion because this liquid flow rate is based on the maximum instantaneous liquid flow rate that can be attained in a simple type completion where the minimum bottomhole flowing pressure is higher than the minimum bottomhole flowing pressure that can be attained with an inserted completion.

The net volume of the liquid that fills the inserted chamber or accumulator can be obtained by multiplying the actual volume of the inserted completion

times the true liquid pressure gradient and dividing the result by the liquid pressure gradient obtained from the water cut and the oil API gravity. The true liquid pressure gradient is smaller because it takes into account the formation gas trapped and/or dissolved in the liquid. The true liquid gradient is also obtained from the downhole pressure survey as explained in chapter: Intermittent Gas Lift Troubleshooting. An additional correction of the net volume of liquid per cycle must be made: on average, 6% of the net volume must be subtracted for each 1000 ft. of depth of the point of injection to take into account the liquid fallback losses that will take place during the operation of the inserted completion.

The depth of the gas injection point is not equal to the depth of the operating valve (which is usually located just above the packer) but, instead, it is equal to the depth of the lower end of the dip tube (at the perforated nipple) in case of an inserted accumulation chamber or the depth of the lower mandrel in case of an inserted accumulator (for fallback losses calculation purpose, the point of injection depth is considered to be the depth at which the injection gas actually enters the tubing and not the depth of the operating valve). Knowing  $q_{\max}$  and the corrected value of the net liquid volume in the chamber or accumulator, the required time to fill the inserted completion is given by:

$$T [\text{min}] = \frac{\text{Net volume} [\text{Br}]}{q_{\max} \left[ \frac{\text{Br}}{\text{Dia}} \right]} \left[ \frac{1440 \text{ min}}{\text{Day}} \right] \quad (10.122)$$

The total cycle time is equal to the liquid feed in time interval calculated with Eq. 10.122, plus the gas injection time. The gas injection time depends on the type of valve and on its area ratio. A practical rule that can be used to estimate the gas injection time (in minutes) is to multiply the depth of the point of injection in Mft. times 1.5 (if the gas lift valve is a 1.5-in. diameter valve) or by 2 (if the gas lift valve is a 1-in. diameter valve). For example, if a 1.5-in. diameter valve is installed at a point of injection located at 4000 ft. of depth, the injection time would be  $4 \times 1.5 = 6$  min and for a 1-in. gas lift valve it would be  $4 \times 2 = 8$  min. With the total cycle time already calculated, the number of cycle per day can be determined and the daily liquid production is found by multiplying the number of cycles per day by the corrected net liquid volume produced per cycle.

## 10.10 INTERMITTENT GAS LIFT IN DUAL WELLS

As indicated in chapter: Design of Continuous Gas Lift Installations, dual wells are more difficult to design and troubleshoot than wells with only one production string. If one or both production strings are on intermittent gas



lift, the design and troubleshooting procedures are even more difficult. Recommendations are given in this section for gas lift design procedures and operational implementation of dual wells (taking into account if one or both production strings are on intermittent gas lift and the type of gas lift valve and gas injection surface control being used).

Only dual wells with parallel production strings, which are shown in Fig. 6.74, are studied in this section. Fig. 6.74a shows a dual completion for which the lower zone can be produced with no additional component. If the reservoir pressure of the lower zone is so low that it is not capable of liquid accumulation above the upper packer, completions shown in Fig. 6.74b and Fig. 6.74c should be used.

In Fig. 6.74b, the effective gas injection point corresponds to the lower end of the “dip tube” (which is the inner pipe hung above the upper packer inside the long production string). The operating gas lift valve in this case should have a dual action: it should act as a bleed valve while the liquid column is being generated and as a gas injection valve when high-pressure gas is injected to produce the lower zone. This type of completion results inadequate most of the time: it restricts the liquid flow when the liquid in the chamber (space between the dip tube and the production tubing) is being displaced by the gas. The problem in this case is the fact that the dip tube must have a small inside diameter to fit into the production tubing. To avoid this restriction to the liquid flow, a completion such as the one shown in Fig. 6.74c could be used, in which the gas is injected through an external, parallel, injection pipe. In this case, as many as necessary unloading valves can be installed along the parallel injection line using the special mandrels designed for this purpose and shown in Fig. 6.19d. It is very important to take into account the friction pressure drop along the external injection pipe when calculating the opening pressures of the unloading and operating valves. The operating valve’s opening pressure should be set higher for the lower zone. The problem with this type of arrangement is the fact that the completion is more complex (having to use a special upper packer), increasing the possibility of mechanical failures.

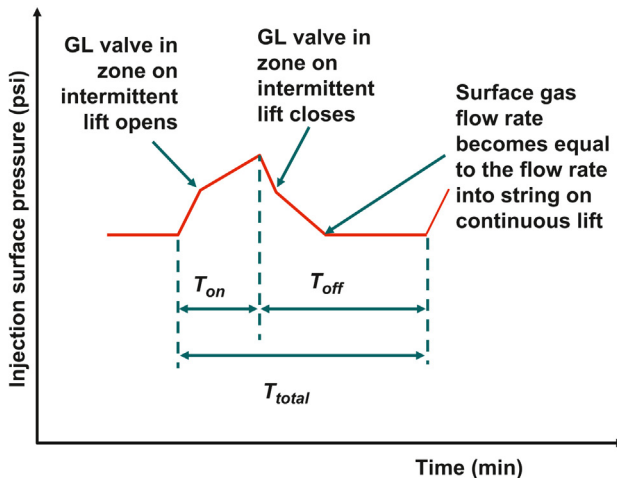
### 10.10.1 One zone on continuous gas lift and the other on intermittent gas lift

If one zone is on continuous gas lift while the other is on intermittent gas lift, both with IPO valves (which are recommended because gas injection can be controlled from the surface), the closing pressure of the operating valve of the production string on intermittent gas lift should be greater than the operating pressure of the continuous gas lift string. The diameter of the orifice or seat of the operating valve of the continuous gas lift string should

be carefully designed to achieve critical flow through it (if possible). In this way, gas flow rate fluctuations of the string on continuous gas lift are not very pronounced. The commercially available diameter of the seat or orifice corresponding to the operating valve of the continuous gas lift string should be as close as possible to the one calculated from the required gas flow rate and its upstream and downstream pressures. However because the required and the available seat diameters are usually very different, it is recommended to use chokes installed downstream of the seat because these chokes are available in a greater number of sizes.

The surface gas injection control can be performed in several ways:

- If a surface intermitter (time cycle controller) is used, then a choke (or a needle valve, or a pressure reduction regulator) should be installed parallel to the intermitter so that gas into the production string on continuous gas lift can be injected while the intermitter is closed. The injection pressure as a function of time looks like the one shown in Fig. 10.33.
- Only a needle valve or choke can be used to control the gas injection at the surface. In this case, the gas flow rate at the surface should be greater than the one required for the string on continuous gas lift. The surface injection pressure as a function of time looks the same as the one for a well with only one production string on choke-control intermittent gas lift.



■ FIGURE 10.33 Surface injection Pressure. One string on continuous gas lift and the other on intermittent gas lift. ( $T_{on}$ : surface controller open,  $T_{off}$ : surface controller close).

A third alternative might be the use of only a time cycle controller that is also capable of controlling the surface injection pressure, so that this pressure never falls below a certain value. In this case, the surface injection pressure will also look like the one shown in Fig. 10.33.

If production-pressure-operated (PPO) valves are used, they must be installed in the production string on intermittent gas lift and leave the other string with IPO valves. The PPO valve should be able to close without a reduction in the injection pressure, otherwise gas injection into the continuous gas lift string might cease while the PPO valve is opened. A pressure regulator should be installed at the surface to keep the injection pressure constant when the PPO valve opens. The production opening pressure of the PPO valve must be set based on the injection pressure required for the production string on continuous gas lift. The gas injection control in this case is easier than it is for the case in which both production strings have IPO valves. The only drawback is the fact that it is not possible to control the cycle time from the surface.

### 10.10.2 Both zones on intermittent gas lift

#### 10.10.2.1 *One zone with Injection-Pressure-Operated valves and the other with Production-Pressure-Operated Valves*

In this case the injection annulus pressure is set according to the PPO valve, which must be installed in the production string of the well with lower liquid production (but only if the production pressure is high enough to open the valve). The zone that produces more liquid should be lifted with IPO valves, so that the cycle time can be controlled from the surface for this zone and be able in this way to maximize its daily liquid production. If the PPO valve can close without a decrease in the annular injection pressure, it is possible to use a surface intermitter that opens on a given time interval but that should also be able to control the minimum annular pressure. If the PPO valve requires an injection pressure reduction to close, the following arrangement should be used:

- Install an intermitter for the IPO valve that opens at regular time intervals and closes after reaching a given injection pressure value above the IPO valve opening pressure to avoid skipping one or more cycles for not having an injection pressure high enough to open the IPO valve.
- For the PPO valve, install (parallel to the intermitter) a pressure reduction regulator with a needle valve or a choke.

#### 10.10.2.2 *Both zones on intermittent gas lift with Injection-Pressure-Operated valves*

This is particularly recommended if the production pressures in both zones are not high enough to open PPO valves. The injection opening pressure of the

zone with the higher cycle frequency should be lower than the opening pressure of the zone with a lower cycle frequency. The IPO valve in the high cycle frequency zone can open several times without reaching the opening pressure of the IPO valve of the low cycle frequency zone. When the signal is sent to open the IPO valve of the low frequency zone, the intermitter remains open for a longer period of time so that the IPO valve of both zones can open, but at the same time (and optionally) a signal is sent to close the flowline of the high cycle frequency zone so that it will not be open for production. The gas that is injected into the high cycle frequency string is simply wasted in this case.

### 10.10.2.3 **Both zones on intermittent gas lift with Production-Pressure-Operated Valves**

The production pressure should be high enough to be able to operate the well with PPO valves. The production opening pressure of PPO valves in both strings are set with the same operating injection pressure (in the annulus). If PPO valves can close with full line pressure, there is no need for any injection control device at the surface, but a pressure control valve can also be used to keep the annular pressure constant at any other value below full line pressure.

If the PPO valves require an injection pressure drop in order for them to close, it is necessary to have a sensor in the flowline that can send a signal to close the gas injection pressure controller as soon as the wellhead production pressure increases. The pressure controller opens again when the flowline pressure has declined and the PPO valve has closed. In this way because the gas injection is temporarily stopped, the annular pressure drops every time one of the PPO operating valves opens, so that it can eventually close. The pressure controller is used to maintain the injection annular pressure at a constant value the rest of the time (when no gas is being injected to any of the production strings).

## 10.11 **PLUNGER-ASSISTED INTERMITTENT GAS LIFT**

Plungers have been used primarily to unload gas wells when liquids from the formation accumulate at the bottom of the well and gas production declines or is reduced to zero. They have also been used in oil wells with very high gas/oil ratios as a lifting method that is not considered to be a variation of the gas lift method. In all of these cases, the lifting energy is provided by the reservoir: a surface control valve keeps the well shut in, while formation gas accumulates in the annulus of the well and on top of the liquids that at the same time accumulate at the bottom of the well. After a predetermined period of time (when sufficient gas has accumulated to lift the liquid column that has been generated in the production tubing at the bottom of the well)

the surface control valve opens for a given period of time in which the liquid slug is produced to the surface.

Plungers can be used to aid intermittent gas lift when the gas lift system is not able to provide injection gas at a rate high enough to sustain a liquid slug velocity of approximately 1000 ft./min. The reduced liquid velocity could be due to: (1) a very low injection pressure, (2) a limited compression flow rate capacity, or (3) an inadequate high-pressure-gas storage volume. It could also be due to having a gas lift valve with a seat not large enough to allow the required high injection gas flow rates into the tubing string.

Metallic plungers are also used when the point of injection is very deep or in cases where paraffin accumulation takes place on the walls of the production tubing, for which metallic plungers can be used to clean the well.

If it is possible, it is better to identify and correct these problems to avoid the use of plungers because plungers cause an increment in maintenance and operational costs. At adequate liquid slug velocities, fallback losses are approximately the same with or without plungers.

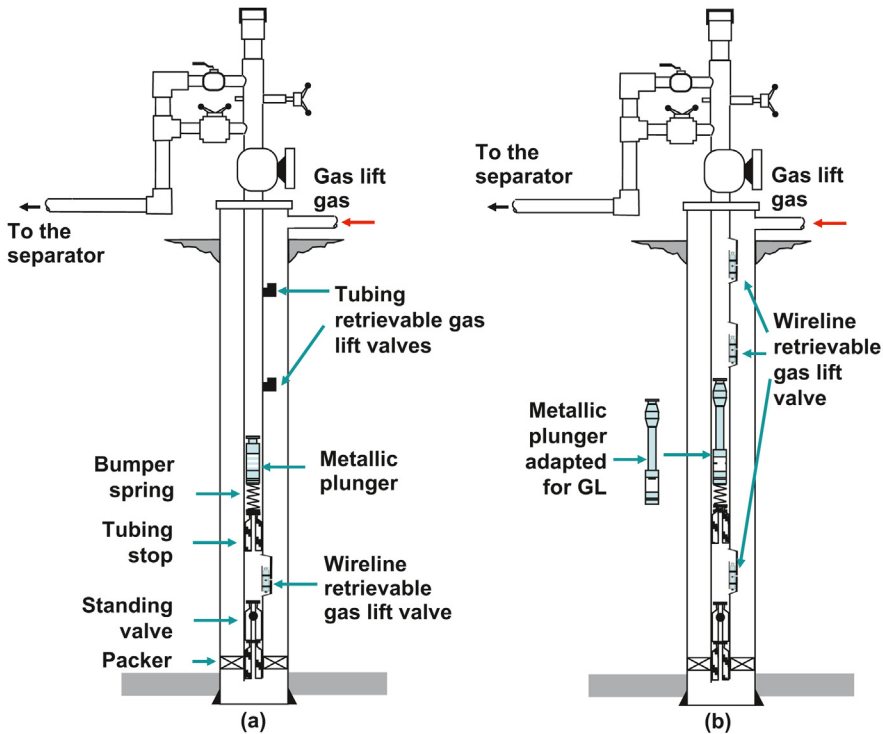
A typical plunger-assisted intermittent gas lift installation is shown in [Fig. 10.34](#).

When wireline retrievable gas lift valves are installed above the point of injection, plungers must be modified (making them longer) so that they can pass through the gas lift mandrels with no difficulties. These modifications are not necessary if tubing retrievable unloading valves are used or there are no unloading mandrels installed above the point of injection.

Plungers are not recommended (or cannot be used at all) in the following cases:

- Liquids produced by the well are too viscous: falling velocity of the plunger might be too slow. Once the plunger reaches the surface and the tail gas has been produced to the separator, the metallic plunger falls and it must pass through the liquid that has already accumulated on top of the point of injection. The plunger should reach the bumper spring before the next injection cycle begins.
- The production tubing is crooked or it is deviated with a very short radius of curvature.
- The production tubing has segments with different inside diameters or it has landing nipples, safety valves, or chokes with smaller inside diameters above the point of injection.

During the time the liquid slug is being generated, the plunger rests on a bumper spring installed in a tubing stop above the point of injection. When



■ **FIGURE 10.34** Plunger assisted intermittent gas lift. (a) completion for tubing retrievable gas lift valves, (b) completion for wireline retrievable gas lift valves.

the gas lift valve opens, the liquid slug and the plunger are pushed to the surface. A lubricator and a plunger catching mechanism are installed at the wellhead. The plunger is retained at the lubricator only if the lubricator is conditioned to do so: the plunger can then be removed from the well by first closing the crown valve. Otherwise, the piston falls back to the bottom of the well when the gas that has pushed it to the surface loses strength to keep it suspended at the lubricator.

As a reasonable approximation, the great majority of design calculations (with some modifications) carried out for intermittent gas lift for single completions can also be used for plunger-assisted intermittent gas lift. The determination of the OCT and the calculation of the required volume of injection gas per cycle are performed as indicated in Section 10.6.1. To determine the required injection volume per cycle, the weight of the plunger must be included in the energy balance equation. This plunger weight must also be included in the momentum balance equations if mechanistic design procedures are used, see Section 10.6.3.

In addition to what is expressed in the previous paragraph, fallback loss calculations should also be modified. Instantaneous fallback losses can be estimated from published data for metallic plungers, in which these losses are correlated with the plunger velocity. It has been determined that the instantaneous fallback loss can be approximated as a linear function of the plunger velocity. However, the final fallback losses that can be found in a well could be lower than what these linear functions can predict. This is due to the fact that part of the liquid that is left behind as the plunger rises might be produced to the surface as drops carried by the tail gas. It is extremely hard to predict that part of the liquid slug that is produced with the tail gas and there are not publications in the literature on this subject. On the other hand, the liquid fallback losses can be very large if the plunger does not reach the surface.

The instantaneous liquid fallback in Br/s is called  $F_B$  and it has been related to the plunger velocity,  $V_{pL}$  in ft./s, with the following equation:

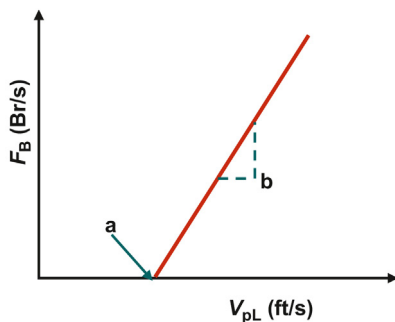
$$F_B = (V_{pL} - a)b \quad (10.123)$$

Where  $a$ , expressed in ft./s, is found experimentally and it represents the value of the velocity below which the instantaneous fallback losses become negligible. On the other hand,  $b$  in (Br/s)/(ft./s) is also found experimentally and it is the slope of the line that relates the fallback losses to the plunger velocity. The graph of Eq. 10.123 is presented in Fig. 10.35.

The fallback losses  $\Delta F_B$  in barrels for a given time interval  $\Delta t$  is equal to  $F_B \Delta t$ . The liquid slug length,  $L$  in ft., as the liquid slug travels to the surface in the production tubing, can be calculated at each time interval by the following equation:

$$L_{t+\Delta t} = L_t - \Delta F_B / B_t \quad (10.124)$$

Where  $B_t$  is the volumetric capacity of the production tubing in Br per foot of length of the production tubing and  $L$  is the instantaneous slug length in feet.



■ FIGURE 10.35 Typical experimental data of the instantaneous liquid fallback losses as a function of the plunger velocity.

## 10.12 GENERAL CONSIDERATIONS FOR GAS LIFT SYSTEMS WITH WELLS ON INTERMITTENT GAS LIFT

The design of a gas lift system is more difficult if there are wells producing on intermittent gas lift. The design is even more difficult for a system with a small number of wells in which one or several wells are being produced on intermittent gas lift. The most difficult system to design is the one that only has one well and it is producing on intermittent gas lift. As the number

of wells increases, the operation becomes more stable, with lower fluctuations in pressures, as well as in liquid and gas flow rates. This is important because to avoid venting injection gas and maintain the compressor operating without failures, the suction and discharge pressures of the compressor should be as smooth as possible, which could be difficult to achieve if the gas lift system's low- and high-pressure-gas storage volumes have not been adequately designed. A good field operation is achieved if the system's gas storage volumes are large enough to take care of normal gas injection flow rate fluctuations. The system design should consider a certain degree of pressure fluctuation by incorporating pressure and flow rate control systems to vent or redirect injection gas and total gas production in a convenient manner and by having adequate high- and low-pressure-gas storage volumes.

When the number of wells is small, the way in which gas injection into intermittent gas lift wells is controlled has a profound influence on the operation of the gas lift system. Choke-control intermittent gas lift could be recommended for a system with a small number of wells, or with a limited compression capacity, so that the wells' annulus can be used as high-pressure-gas storage volumes. This could also be beneficial to the operation of the compressor because the discharge pressure is very stable; however, if several wells intermit at the same time, the volume of gas into the low-pressure side of the system might be too high for the compressor to handle and a good part of this volume might need to be vented to keep the suction pressure as constant as possible. If the installed compression capacity allows it, this problem can be solved by installing surface time cycle controllers, which can be controlled to allow only a maximum number of wells to intermit at the same time; otherwise, either the low-pressure side of the system's gas storage volume or the compressor capacity should be increased. If the number of well increases, a point is reached in which the type of gas injection control to the wells is not very important because the operation of the system is very stable in any case.

To design a gas lift system capable of handling wells on intermittent gas lift in an efficient manner, it is important to pay attention to the point where the compressor is going to be located. A compressor located as centralized as possible in a gas lift field minimizes injection gas pressure drop by having shorter gas injection lines. If these pressure losses are not very important, the location of the compressor is still important because the gas injection and gathering lines can be used as part of the high- and low-pressure-gas storage volumes, respectively.

The number of compressors to be used is also a matter to be considered carefully. A gas lift field with several compressors would allow shutting down one or several compressors at the same time for maintenance (or a



sudden failure in one of them) without impacting the total liquid production of the field. However, having too many compressors might not be recommended either because it would increase maintenance and operational costs.

To design a compressor, the required maximum injection flow rate, as well as the suction and discharge pressures should be known. The following factors determine the gas flow rate that the compressor should handle:

- Gas flow rate for wells on continuous gas lift and on choke-control intermittent gas lift.
- Gas flow rate for wells on intermittent gas lift with time cycle controllers that intermit at the same time. The gas flow rate into intermittent gas lift wells should be large enough to maintain a liquid slug velocity of around 1000 ft./min.
- High-pressure-gas storage volume. This volume includes the surface gas injection lines. If this storage volume is very small, casing–tubing annuli and gas injection lines of abandoned wells can be used as high-pressure-injection-gas storage volumes as long as these components are in good operating conditions. It is necessary to have a high-pressure-injection-gas storage volume to reduce peak compression requirements for systems with intermittent gas lift wells that use time cycle controllers. The injection gas flow rate to a well is very high when the controller is opened and zero when it is closed. The high-pressure-gas storage volume provides the difference between the very high gas flow rate requirements that might exist at a given time (caused by many cycle controllers opening at the same time) and the gas flow rate the compressor can deliver. It is less expensive to provide a high-pressure storage volume than to increase the compressor gas flow rate capability. If the compressor gas flow rate is very low in comparison to the instantaneously required gas flow rate at a given moment, the time cycle controllers should be installed as close to the wells as possible so that the injection lines can be used to store high-pressure injection gas.
- The difference between the compressor’s discharge pressure and the gas lift valves’ opening pressures: As this difference becomes larger, the required high-pressure storage volume is reduced.
- Formation gas/oil ratio should also be considered.

The volume of gas to be compressed to serve the wells should be increased by 5–15% to take care of line losses, temperature fluctuations, gas usage as fuel for the compressors, and other unforeseen factors that might arise later.

Of all the factors previously mentioned, the gas lift valve’s opening pressure is probably the most important. If the opening pressure is high, the

compressor's discharge pressure should also be high. This might increase the power requirement in a considerable way to compress the injection gas. This does not mean that the discharge pressure should be designed as low as possible. The injection pressure should be designed based on the well's requirements. Even for low-reservoir-pressure wells, the injection pressure should be high enough to be able to lift the liquid slugs at velocities close to 1000 ft./min. If the slug velocity is very low, liquid fallback losses will be very high. Additionally, low injection pressures can cause a reduction in the spread of the valve even for valves with large area ratios in choke-control intermittent gas lift. This could lead to the use of time cycle controllers to be able to inject the required volume of gas per cycle. However, the volume of gas alone is not sufficient to reduce the liquid fallback losses. It is not only necessary to inject the required volume of gas per cycle, it is also important to inject this volume at an appropriate rate to keep the liquid slug velocity at an acceptable value, which is achieved by having the right injection pressure.

The probability of having hydrate formation increases for higher injection pressures because at higher pressures the hydrate formation temperatures are also higher. Depending on the severity of the hydrate problem, one or several of the steps given in [Section 10.5](#) should be considered. Special attention should be paid to choke-control intermittent gas lift wells with very long cycle time, for which the instantaneous surface gas flow rate is extremely low because in these cases the pressure drop across the choke might be too large and could cause hydrate formation, erosion of the surface choke, and/or difficulties in measuring the gas flow rate.

For gas lift in general, but especially for intermittent gas lift, it is important to have wellhead production pressures as low as possible that would allow the generation of larger liquid slugs and make it easier for these slugs to travel at adequate velocities. But, on the other hand, low suction compressor pressures increase the compressor power requirements. The low-pressure side of the gas lift system should also have a minimum pressure limit so that: (1) the gas-liquid separators can function in an appropriate manner (gas velocity can increase inside the separator if the pressure is too low), and (2) frictional pressure drops along gathering lines are not too large (very large diameter gathering lines might be required if the pressure is very low). A balance between these factors is then required during the design of the low-pressure side of a gas lift system.

The low-pressure side of a gas lift system includes the gas gathering lines from the separation pressure control valves located just downstream of the separators or flow stations, to the suction pressure controller (used to keep

the compressor suction pressure constant) located just upstream of the compressor. As it is the case for the high-pressure side of a gas lift system, abandoned wells and inactive gathering lines can be used as additional volumes to store low-pressure gas to reduce the pressure peaks caused by the sudden flow of gas from intermittent gas lift wells. Chokes in the flowline (away from the wellhead) can also be used to reduce pressure peaks because they increase the required time to vent the tail gas from the wells to the low-pressure side of the system. This can only be used as a last resource because chokes also increase the necessary time interval for the wellhead pressure to decrease to separation pressure thus making it harder for the liquid column to accumulate in the well.

The following equations can be used as a guide for determining the high- and low-pressure-gas storage volumes.

The required high-pressure storage volume,  $V_{\text{high}}$ , can be found from the following equation:

$$V_{\text{high}} = (N_{\text{well}} Q_{\text{gia}} - Q_{\text{gic}}) \frac{14.7}{P_{\text{discharge}} - P_{\text{injection}}} T_{\text{cycle}} \quad (10.125)$$

Where  $V_{\text{high}}$  is the high-pressure-gas storage volume in cubic feet,  $N_{\text{well}}$  is the maximum number of wells to which gas is injected at the same time,  $Q_{\text{gia}}$  is the average gas flow rate injected to these wells in scf/min,  $Q_{\text{gic}}$  is the compressor capacity in scf/min, 14.7 is the base pressure in psia,  $T_{\text{cycle}}$  is the average gas injection time per well in min/cycle,  $P_{\text{discharge}}$  is the compressor discharge pressure in psig, and  $P_{\text{injection}}$  is the required wellhead injection pressure in psig. The greater the high-pressure storage volume is, the lower the pressure difference between the maximum pressure  $P_{\text{discharge}}$  and the required injection pressure at the wellhead  $P_{\text{injection}}$  can be. Having greater high-pressure storage volume could then be beneficial if it is determined that the injection pressure at the wellhead should be increased to improve the efficiency of the gas lift method (like, for example, reaching deeper points of injection). On the other hand, a compressor with a lower discharge flow rate can be selected (lowering the initial investment cost) if the high-pressure storage volume is increased.

The required low-pressure-gas storage volume,  $V_{\text{Low}}$ , is found from the following equation:

$$V_{\text{Low}} = (N_{\text{well}} Q_{\text{gia}} T_{\text{cycle}} - Q_{\text{gic}} t) \frac{14.7}{P_{\text{L}} - P_{\text{ci}}} \quad (10.126)$$

Where  $t$  is the time in minutes that it takes for the produced gas to pass through the separator,  $P_{\text{L}}$  is the pressure of the low-pressure-gas storage

volume in psig, and  $P_{ci}$  is the compressor suction pressure also in psig. The formation gas is neglected in Eq. 10.126. The total volume  $N_{well}Q_{gia}T_{cycle}$  does not instantly go to the low-pressure storage volume because it takes a period of time  $t$  to do it. During this time, the compressor suctions a volume equal to  $Q_{gic}t$  that reduces the net gain of the low-pressure storage volume. Increasing  $V_{Low}$  has two advantages: it allows for a reduction of the required compressor gas flow rate  $Q_{gic}$  or it might make it possible to reduce the low pressure  $P_L$  and, therefore, it might allow a reduction in the separation pressure with all the benefits it brings for the operation of a gas lift wells.

The general production separator should be designed to handle the maximum number of wells intermitting at the same time plus the wells on continuous gas lift that are produced to the same separator. Unnecessary restriction downstream of the separator must be avoided. A safety valve should be installed in case the separation pressure gets to be too high. The pressure setting of the safety valve should be higher than the set pressure of the system pressure controller that is used to direct gas to vent or sale lines when the pressure gets to be too high.

The test separator should also be able to individually handle all wells that are directed to it. If the gas flow rate is measured by an orifice plate, it must be correctly sized to measure the periodic increase in the gas flow rate and to keep the separator pressure from reaching the safety valve's set pressure.

## REFERENCES

- Milano, P.E., 1999. Dynamic performance of the intermittent gas-lift valve. M.S. Thesis, the University of Tulsa, Tulsa, Oklahoma.
- Zimmerman, W.G., 1982. Manual Básico de Gas Lift. Publicación interna de la compañía Lagoven, S.A. Departamento de Producción, División Occidente, Tía Juana, Venezuela.

# Continuous gas lift troubleshooting

## 11.1 INTRODUCTION

The first objective of troubleshooting analyses for wells on continuous or intermittent gas lift is to find out the current point, or points, of injection depth or understand why the well is not receiving any injection gas at all. Once the point of injection depth is known, the reasons why the well is not producing as efficiently as it should (if that was the case) can be determined. Through troubleshooting analyses it might be possible to understand why, for example, the liquid production is different from the one that was expected, or the injection gas flow rate is too high, or the well is producing with serious instabilities, etc. If the injection pressure and the liquid production are stable, troubleshooting analyses are done following the techniques developed for continuous gas lift. There are wells that have been designed for intermittent gas lift that operate with a stable gas injection pressure and therefore they should be analyzed as continuous gas lift wells. Field and analytical troubleshooting techniques for wells that are producing on continuous gas lift are explained in the chapter. Troubleshooting techniques for intermittent gas lift are presented in chapter: Intermittent Gas Lift Troubleshooting.

Sometimes the liquid production flow rate is constant (not in batches) but the gas injection pattern looks exactly like the one found in an intermittent gas lift well. In this case, the well should be analyzed “in an approximate way” as a continuous gas lift well (applying the techniques for intermittent gas lift will be totally wrong if the liquid production is continuous).

Wells should not be analyzed only when they appear to have a problem. Some of the reasons for troubleshooting a well (regardless of its current status) are:

- To have a reference state in case something fails in the future.
- To make sure that gas is actually being injected through the design point of injection.
- To determine if the actual gas lift design is adequate for current operational conditions: The objective in this case is to detect

opportunities of increasing the liquid production or reducing the injection gas/liquid ratio by adjusting the design of the gas lift valves.

Sometimes the actual point of injection is higher up in the well than its designed depth and this situation can go unnoticed for a long time if the well is not rigorously analyzed, maybe because the optimization team is overwhelmed with a large number of gas lift wells (this situation is not found in other artificial lift methods in which failures are usually catastrophic). If the number of wells is too large for the optimization team to handle, it is recommended to analyze the wells right after the gas lift valves are installed and then, by means of a selection procedure explained in Section 11.6, each well is given a priority based on its deviations in gas consumption, liquid production, injection gas/liquid ratio, last date it was analyzed, etc.

## 11.2 GENERAL DIFFICULTIES ENCOUNTERED WHEN TRYING TO PERFORM TROUBLESHOOTING ANALYSES OF GAS LIFT WELLS

Troubleshooting wells on gas lift is a very complex task. This is due to the large number of possible events that can take place in the operation of a well, some of which are explained in the next section in detail. However, the analysis is usually even more difficult to perform due to the following list of difficulties normally found by optimization engineers when trying to troubleshoot the operation of a well.

- It is usually difficult to calculate the IPR curve because of reservoir complexities or lack of relevant information like, for example, the static reservoir pressure. Unavailability of downhole flowing pressure and temperature surveys in conjunction with well production tests is also a serious issue. Most of the time, there is an insufficient number of pressure buildup tests from which the current reservoir static pressure and formation damage can be obtained. The main reason for this lack of available buildup test data is because these tests are expensive and take several days to complete. Flowing pressure and temperature surveys are not as expensive but they involve some operational risks. If the static reservoir pressure is known, flowing pressure and temperature surveys, combined with well production tests, can be used to calculate the IPR curve very easily. Once the IPR curve is determined, it is possible to find out if the well is producing at its optimal production rate using the nodal analysis techniques that are explained in the chapter. If the static reservoir pressure is uncertain, it is then absolutely necessary to perform either buildup or multirate tests. The optimization engineer should be in close contact with the reservoir department to know

the dates of the latest built up tests and, if necessary, coordinate the execution of future tests and flowing pressure and temperature surveys.

- The following parameters are usually missing or the quality of their measurements is very poor: wellhead injection and production pressures, gas injection and liquid production flow rates, total gas production, water cut, injection and produced gas specific gravities, and PVT data in general. If the gas flow rate is measured with orifice plates, sometimes the orifice plate diameter is unknown or the pressure sensors are not properly calibrated. Wellhead pressure sensors (used for two- or three-pen chart recorders) can show inaccurate readings due to numerous causes that are explained in detail in this section. These wellhead pressures are usually recorded in 1-h, 24-h, or 7-day charts (7-day charts are not recommended for detail analyses but they can be used to spot problems in fields with a large number of wells that are not automated). Wellhead pressure charts are now being replaced by electronic measurements that can be retrieved in real time as “pressure or temperature versus time” graphs known as “tendency curves.” Because “old charts” are still in use in many places around the world, a long list of possible problems that can happen with traditional wellhead pressure chart recorders is given at the end of this section. Not knowing the injection gas specific gravity can make it impossible to predict the actual point of injection because the error in the estimation of the injection pressure at depth can be as large as several hundred psi, depending on the depth of the gas lift valve and how different the actual and estimated gas specific gravities are. The specific gravity should be periodically measured, together with other important parameters of the injection gas such as its humidity and concentrations of corrosive components like CO<sub>2</sub> and H<sub>2</sub>S.
- The total gas/liquid ratio is one of the most difficult parameter to measure due to the erratic behavior that the differential pressure might show at the orifice plate (or any gas flow rate measurement device used) located at the gas exit of the test separator if the production flow rate of the well is fluctuating. Charts from the total gas flow rate recorder should be directly checked by the optimization engineer to establish the magnitude of the error. Based on the severity of the error, a sensibility study might be recommended to determine how this error affects the analysis needed to be carried out for troubleshooting the well. Because the diameter of the orifice plate at the test separator is more frequently checked than the one at the gas injection manifold, the gas flow rate measurement at the test separator might be more accurate than the measurement of the injection gas flow rate at the gas injection manifold, especially if the production of the well is stable.

- Water cut is another parameter that is usually inaccurately measured in the field. This is due to the fact that test separators are usually two-phase separators and not the required gas-oil-water separators. Using three-phase separators is the only way to accurately measure the water cut at this moment. The common way of measuring the water cut is by relying on analyses made of fluid samples taken at the well-head. These samples should be taken at points at the wellhead or flowline where important flow turbulences are present to try to improve the accuracy of the water cut measurement. Line electronic water cut measurement devices, installed at the liquid exit of two-phase separators, are being developed, but the technology is not quite ready yet.
- Lack of reliable measurements of the water cut and the total gas/liquid ratio makes it impossible to accurately predict the production pressure traverse curve. Production pressure at valve's depth is important, especially but not exclusively, for production-pressure-operated (PPO) gas lift valves because it is used to calculate the gas flow rate through a gas lift valve and to determine if the valve is closed or opened. If the gas lift valve is indeed opened, the production pressure at valve's depth can be used to determine the type of gas flow through the gas lift valve: orifice or throttling flow. Furthermore, if the production pressure along the well cannot be accurately calculated, it is not possible to estimate the bottomhole flowing pressure to use nodal analysis as an important tool to troubleshoot the well.
- Poor accuracy of the multiphase flow correlation that is used to find the production pressure and temperature along the production tubing (if gas is injected down the annulus) or, especially, along the annulus (if gas is injected down the tubing) is also a major difficulty. It is important to know the temperature along the tubing to determine if nitrogen-charged gas lift valves are opened or closed. Flowing temperature and pressure surveys, performed on the same day the well is tested, can be used to determine the accuracy of multiphase flow correlations. If the well production test cannot be performed on the same day the survey is run, the well can be tested a few days after or before the survey, as long as the wellhead pressure and the injection gas flow rate are kept constant. Instructions should be given to the wireline crew performing the survey not to shut in the well prior or during the survey nor do anything that will change the injection gas flow rate or the wellhead production pressure.
- Deep wells are harder to analyze because: (1) the number of gas lift valves and the possibility of valve interference are greater, and (2) there are more possible depths where the current point of injection can be



located (the number of calculations to be performed is considerably increased).

- The use of PPO valves has advantages and disadvantages. In wells for which the available surface gas injection pressure is too low or constantly changing, PPO valves can be used to reach deeper depths of the operating point of injection. The combination of PPO unloading valves with an orifice valve at the point of injection provides great flexibility regarding the maximum gas flow rate of injection because this flow rate can be increased to any value without opening an unloading valve due to the fact that the opening pressure of PPO valves is mainly determined by the production pressure. Increasing the gas flow rate can make the injection pressure rise to the opening pressure of an unloading IPO valve that should remain closed during the normal operation of the well. But the great disadvantage of PPO valves is the fact that they make it very hard to find out the current point of injection. It is very easy to calculate the gas injection pressure at depth and because IPO valves mainly respond to this gas injection pressure, it is easy then to determine if they are opened or closed by knowing the surface gas injection pressure even if the production pressure at valve's depth is not very well defined. PPO valves, on the other hand, mainly respond to the production pressure, which is very difficult to calculate because: (1) multiphase flow correlations are not very accurate, (2) the water cut and/or the gas oil ratio might not be accurately known, and (3) the exact point of injection is not known (or needs to be determined) and the production pressure depends on this depth.
- Troubleshooting analyses of wells with PPO valves are even more complex if there is a possibility of solid depositions (scale deposition) on the wall of the production tubing because it increases the uncertainty of the calculated production pressure. In these cases, little can be done in terms of analytical troubleshooting procedures and it is recommended to check from time to time if there are solid depositions along the production tubing using tubing gauges or paraffin cutters (in places where these problems can exist).
- In very few cases, the following important and basic well information could be missing: production tubing diameter, number and depths of gas lift mandrels, type and calibration of gas lift valves, among other subsurface data. Tubing inside diameter and its length can be found using wireline tools, such as tubing gauges and tubing end locators, see Fig. 6.38e. It is possible to find the depth of the mandrels using kick over tools. This could turn out to be a time consuming task but it is doable and economical. Gas lift valves should be retrieved as there is no way of knowing their type and calibration. This is a delicate process

that can only be trusted to experienced wireline operators because the type of mandrel (which is not known) determines the type of latch as well as the running and pulling tools. An experienced wireline operator can estimate the type of mandrel by an elimination process carried out at the well site. Although more expensive, finding the depths of mandrels, landing nipples, circulating sleeves, and even parts of the tubing that have been corroded, can be very effective if instrumented wireline tools, such as casing collar locators (CCLs), are used. The depths of the perforations can be estimated using temperature surveys with highly sensitive sensors and techniques that are explained in Section 11.5.2. The depths of the mandrels can also be detected using sounding devices as explained in Section 11.5.3.

- Even though only under extreme circumstances well information as basic as the ones described in the previous paragraph are totally missing (maybe because the well files have been lost in a natural disaster and the operating company did not have electronic back-up data), there are many ways of estimating most of the lost information. For deviated wells, for which the depth-deviation data has been lost, it is possible to find the angle of deviation at each point along the tubing by means of electronic tools that can be run in the well by wireline. If these tools are not available, the depth-deviation profile can be estimated by static pressure surveys, for which it is important to know the wellhead pressure, well fluid static pressure gradient, and the static fluid level. The static fluid pressure at each point along the tubing is a linear function of the “true vertical depth.” Thus, if the static pressure is known, the true vertical depth can be calculated and because the measured depth is reported for each pressure measurement, it is easy to find the inclination angle (keeping in mind that the wireline elongates in a certain way as it is run in the well). If the static fluid level is below the point where the tubing begins to deviate from the vertical, it is necessary to fill the tubing with well fluids (installing a check valve at the bottom of the tubing to keep the fluids from being absorbed by the formation). When all data from a particular well is lost, it is advisable to review how nearby wells were drilled and completed around the time the well with the missing file was drilled.

The following is a list of errors and operational problems that can be encountered while using or installing two- or three-pen chart recorders that adds difficulties to the troubleshooting process.

- The clock mechanism might not work correctly (too fast or too slow) or it has been set for one rotation every 7 days with a 24-hour chart or vice versa.

- One of the small-diameter instrumentation lines, that are used to connect the pressure sensors to the wellhead, could be plugged and the pressure being recorded is simply the pressure trapped inside the instrumentation line and not the real production or injection pressure. Many times this is easily detected (although not conclusive) in charts showing an intermittent gas injection pressure pattern with a constant production pressure or vice versa. It is also possible that an operator left one instrumentation valve closed by mistake, causing the same effect of a plugged instrumentation line.
- One pen could be dragging the other giving the wrong impression that both pressures are changing simultaneously in the same way.
- One pen is hard-pressed against the chart, not allowing it to move freely as the pressure changes.
- The pressure chart recorder might be vibrating, causing the pens to move, giving also a wrong impression of pressure fluctuations that are not real. This happens when the chart recorder is mounted directly on the flowline (which might vibrate) or in any support that is easily moved by the wind or any surrounding vibration.
- The calibration of the pressure sensors should be verified with a dead-weight tester (if possible) before they are installed in the field. Once in the field, if they are opened to atmospheric pressure and the readings do not go down to zero, they definitely need to be calibrated. But even if readings do go to zero, it does not necessarily mean that they are properly calibrated. One way of checking their calibration in the field is by using a precisely calibrated sensor as a reference. Another way of checking the calibration in the field, if a reference sensor is not at hand, is by switching the pressure signals so that the production pressure sensor now measures the injection pressure and the injection pressure sensor measures the production pressure. In this way, the production and injection pressures should be approximately the same, regardless of the sensor being used. To do this procedure, it should be checked if the production sensor maximum reading can handle the current injection pressure, otherwise the sensor might be damaged or give wrong measurements. In troubleshooting analyses of wells with IPO valves, the calibration of the gas injection pressure sensors is extremely important compared with the production pressure sensor.
- In some cases, the maximum pressure that the sensor can measure is less than the actual pressure. The readings in these cases will look as a steady pressure at the maximum value that the recorder can register. The real pressure might be steady or fluctuating at a higher value. For maximum accuracy, the readings should always be between 20 and 80% of the full scale of the pressure sensors.

- Sometimes operational errors are made. For example, not collecting the charts at the right time causes the pressure traces to be overwritten, making it very difficult to know the actual behavior of the injection and/or production pressure. Another operational error is not providing enough ink to the pens so the pressure traces disappear shortly after setting the charts; or, on the contrary, too much ink is used causing a big stain on the chart. In very dry and hot desert areas, the ink might evaporate during the day.
- If the connection of the injection pressure sensor is upstream of the surface choke or, in case of intermittent gas lift, the connection is upstream of the time cycle controller, the measured pressure would not be equal to the wellhead injection pressure. In general, the connection of the injection pressure sensor should be downstream of any restriction before reaching the wellhead.
- If the connection of the production pressure sensor is located downstream of the wellhead choke housing or any other restriction, the measured production pressure might be different from the actual wellhead production pressure. Even with the choke housing empty, it might represent a serious restriction to the production liquid flow because of the reduced inside flow area of the choke housing.

Two-pen chart recorders are still widely used but, in many fields, they have been replaced by electronic sensors that send their signals to a data acquisition system so that the engineer can review them in graphs that show the pressure behavior in time. In this way, the accuracy of the measurements is improved and the data can be accessed in real time. However, these sensors are not trouble-free and the optimization engineer should be aware of some weak points that new technologies have:

- An instrument's connection can still be plugged or an operator can leave an instrumentation valve closed by mistake. Instrumentation lines could also be installed in wrong places at the wellhead: downstream of production liquid flow restrictions or upstream of any injection gas flow restriction.
- Electronic sensors also need to be calibrated. Additionally, in computer programs used to handle the raw data, wrong factors could be used to translate the signal from volts or Amps to psi or °F. Data such as orifice plate diameters should be entered and updated manually into these programs and acquisition systems and these data do not always coincide with the actual values in the field. Routines that are used to calculate the gas flow rate, for example, can have mistakes or might be using wrong data such as the wrong injection gas specific gravity. These errors are hard to notice because the persons responsible for

the computer codes do not always communicate with the optimization team.

- The data acquisition scan rate should be adequate. For example, one measurement every 15 min might be all that is needed for a stable operation in continuous gas lift, but totally inadequate for intermittent gas lift, for which 20 s per measurement might be better.
- Power outages might create total data black out. Power back-up systems should be installed in places where this problem could frequently occur.

### 11.3 CAUSES AND CORRECTIVE ACTIONS FOR POSSIBLE FAILURES AND/OR LOSS OF LIFTING EFFICIENCY

Possible failures of the subsurface gas lift equipment or any other component of the completion of the well, as well as problems in the gas injection line and the flowline, are presented in this section. Additionally, operational conditions that can cause inefficiencies in the gas lift method are described. Corrective measures that should be taken to solve these problems are also given in this section.

#### 11.3.1 Most common failures and/or loss of lifting efficiency

##### 11.3.1.1 Instabilities

Production instabilities usually cause an increase in the injection gas/liquid ratio, as well as numerous operational problems at surface facilities. The following problems are some of the principal operational conditions that can induce instabilities: (1) inappropriate gas lift design (wrong valve seat diameter or inadequate valve temperature prediction); (2) hydrate generation that can reduce, or completely block, the surface injection gas flow rate (as soon as the gas flow rate drops to zero, hydrates begin to melt and gas flow is restored until hydrates are generated again); (3) pressure fluctuations of the gas lift compression system or at the flow station; (4) a hole anywhere along the production tubing or unwanted communications at the production packer or wellhead; (5) instabilities of the injection gas flow rate (problems at the surface injection flow control valve); and (6) tubing flow area too large for current liquid production levels.

- *Instabilities (inadequate gas lift design: wrong seat diameter).*  
Regarding inappropriate gas lift designs, using the wrong valve seat diameter is one of the most frequent design flaws. Gas lift valves with seats larger than actually needed can cause valve interference (as explained in chapter: Design of Continuous Gas Lift Installations) or

make it impossible to transfer the current unloading point of injection to the design operating valve (because the injection annular pressure is reduced due to the high gas flow rates that these large seats can allow and these gas flow rates could, in turn, reduce the temperature of the gas lift valve that is unloading the well at that time, thereby reducing its closing pressure). Larger than required valve's seats are found when the well produces less liquid than expected. This problem can be easily overcome by changing gas lift valves or temporarily increasing the gas flow rate even further to be able to transfer to the next valve (for this operation, the required injection gas flow rate could be very high because gas will need to be injected through several points at the same time before reaching the final operating point of injection). Valves with seats smaller than required can also cause serious problems if they are located below the reservoir static liquid level. Small seats might not be capable of injecting the required gas flow rate to reduce the production pressure and be able to transfer the point of injection to the next valve below. In this case, if gas injection is increased at the surface in an attempt to lower the production pressure, it might be possible that the injection pressure in the annulus is also increased to a point at which one or several upper unloading valves open and it might not be possible to inject the required gas flow rate at the current point of injection to lower the production pressure at the next deeper valve. If the valve with the very small diameter seat corresponds to the first (shallowest) valve, it is possible that, by increasing the injection gas flow rate, the injection pressure is increased to a pressure very close to line pressure (or maximum available pressure at the injection manifold), so that the gas flow rate cannot be increased any further (this is rarely a problem because the first valve is usually located above the static reservoir liquid level). Above the reservoir static liquid level, small seats do not represent a problem because the reservoir is not capable of producing any fluids so that eventually, even at low injection gas flow rates, the point of injection will be transferred to the next valve below.

- *Instabilities (inadequate gas lift design: wrong valve temperature).* Another source of instability regarding gas lift designs could be due to an inadequate valve temperature prediction: If the actual unloading temperature of a nitrogen-charged gas lift valve is greater than its design temperature, it might close at the initial stages of the unloading process because of the high dome (nitrogen) pressure. After the unloading valve closes due to high temperature, the well's liquid production might be reduced or stopped, allowing the valve to cool so that its opening pressure is reduced back to its design value and the

valve can open again. On the other hand, if the actual temperature is lower than the design temperature, an unloading valve might remain open, not allowing the unloading process to continue. This latter problem could be overcome by increasing the injection gas flow rate so that the injection pressure can be higher and the next lower unloading valve can be reached; however, increasing the gas flow rate might not work in some situations that are explained in the chapter.

- *Instabilities (hydrates)*. Hydrates can partially block the gas passage through the surface gas injection control valve (or a choke installed for the same purpose) causing a reduction in the gas injection pressure at the wellhead. The gas flow rate might also be reduced to zero. When the gas flow rate is entirely blocked, the cooling effect ends because the injection gas is no longer being expanded at the control valve and then hydrates begin to melt rapidly, allowing injection gas to pass through the surface control valve once again. This cycle can repeat itself many times and this instability can last for hours until the ambient temperature increases and the injection pressure is stabilized. If the ambient temperature is never high enough, the injection instability will not stop. The fluctuation pressure pattern caused by hydrates is many times easily identified as shown in [Fig. 11.44](#).

Hydrate problems can be avoided, or reduced, by taking one, or several, of the following corrective actions: (1) continuous methanol or glycol injection to lower the hydrate formation temperature (this action is appropriate in places where hydrates form only during a few days of the year). Recent publications show important results in lowering the hydrate formation temperature using better suited chemical products ([Nengkoda et al., 2009](#)); (2) heating the injection gas upstream of the flow control valve (costly and risky, but can be effective if the problem is present all year long); (3) the compressor after-cooler (in small compression units) could also be bypassed to keep the injection gas warm; (4) install dehydration plants (very expensive, but can be justified if a large number of wells is affected by hydrates or corrosion represent a problem); (5) heat exchangers can also be used to keep the injection gas warm just upstream of the flow control valve (liquid production from the well can be used to warm up the injection gas); or (6) redesign the gas lift valves (if possible) so that the large pressure drop takes place at the downhole point of injection and not at the surface gas injection flow control valve. Methods to determine if hydrates can form in restrictions, or along gas injection lines, are presented in chapter: Gas Properties. The use of automated flow control valves, with the injection gas flow rate at a given set point, can also reduce the problem because, as soon as the gas

flow rate decreases, the valve will open wider, getting rid of the hydrate crystals in the process.

- *Instabilities (unstable gas lift system pressure)*. Regarding instability problems created by fluctuations in the gas lift system pressure, the following steps can be taken if these fluctuations are frequent and/or important: (1) Use PPO valves (although sometimes this attempt to solve the problem could make things worse); (2) install pressure control valves to keep the pressure upstream of the choke (or the gas flow rate control valve) constant (for this solution to work, the minimum system pressure should be greater than the required gas injection pressure just upstream of the surface gas injection choke, or flow control valve, so that the gas flow rate injected into the well can be maintained at a constant value); (3) install automatic flow control valves to regulate the gas flow rate to each well; or (4) replace the orifice valve at the point of injection by a calibrated gas lift valve, which offer a control action by regulating the injection gas flow as needed by the well (as explained in Chapter: Design of Continuous Gas Lift Installations).

System pressure fluctuations are usually caused by: (1) small compression capacity compared with gas flow rate field requirements; (2) frequent compressor shut downs due to aging or inadequately designed compression plants; (3) Too small high- and/or low-pressure gas storage volumes of the gas lift system; (4) frequent trips or kickoffs of wells with high injection or production gas flow rates; or (5) large ambient temperature fluctuations during the day.

- *Instabilities (hole in the tubing)*. A hole in the production tubing (or leaks at the wellhead or downhole packer) can create serious operational troubles.

Any communication between the injection annulus and the production tubing, different from that provided by a gas lift valve, represents an uncontrolled point of gas injection. If the hole is above the static liquid level, the well might end up circulating the injection gas with no liquid production and usually at low injection pressure (unless the hole is very small and a sufficiently high injection pressure makes it possible to inject gas at the same time through a lower gas lift valve). If the hole is below the static liquid level, the well might produce liquids in a stable or unstable manner, but usually with a reduced liquid production, especially if the communication is large and located at a shallow depth with respect to the design point of injection. If a large communication between the annulus and the tubing occurs at the wellhead, the well might only circulate gas (with no liquid production) and signs of a



cool wellhead might be noticeable (such as condensed water drops on its surface).

If the well is a low liquid producer well, large communications cause an increase in injection gas flow rate, a decrease in the injection pressure, and a stable or mildly unstable behavior. Very large injection and production pressure fluctuations normally take place in wells (with tubing-annulus communications below the static liquid level) that can produce at moderate to large liquid flow rates.

It is also possible that gas might be injected into a shallow formation (or into the annulus B of the well if it has one) through a hole in the casing. In case of a damaged or weak casing, gas should be injected through a separate string, parallel to the production tubing, connected to all gas lift mandrels (which are specially manufactured for this type of completion). These special gas lift mandrels are shown in Fig. 6.19d and they are installed in completions like that shown in Fig. 6.46c. For highly localized casing failures, recently developed casing patches can isolate the part of the casing that is damaged in a successful way.

When the annulus-tubing communication is below the static liquid level, it is possible that liquids flow from the tubing into the gas injection annulus. In these cases, it is a good option to measure the liquid level in the annulus using sounding devices (as explained in Section 11.5.3), knowing that the liquid level coincides with the hole in the tubing only when the hole is just about to be “uncovered” by the gas. Distributed temperature measurements by fiber-optic techniques can also be used to locate tubing holes in wells with stable or unstable production, see Section 11.5.7. If the production is stable, the depth of the communication can be found by continuous temperature surveys (with no discrete stops) with highly sensitive temperature sensors. Once the depth of the hole is found, it can be isolated using “packoff” completions like the one shown in Fig. 6.44. A gas lift valve that has not been properly set inside the gas lift mandrel’s pocket makes the well behave exactly as if it had a hole in the tubing. There are other techniques that can be used to find the depth of a hole in the production tubing (or casing) that are explained in the chapter.

- *Instabilities of the injection gas flow rate (problems at the surface injection flow control valve).* An erratic behavior of the injection gas flow rate could be due to a failure of the internal components of the surface injection gas flow rate control valve. This erratic behavior

could also be due to dirt accumulation or hydrates that affect the operation of the surface flow control valve. When the gas flow rate is measured by means of an orifice plate, it is usually easy to determine the cause of the erratic behavior of the gas flow rate just by looking at the pattern of the differential pressure on the gas measurement charts (hydrates and internal valve component failures generate different patterns that are easy to recognize, as shown in several examples in Sections 11.5.9 and 11.5.10).

- *Tubing flow area too large for current liquid production levels.* It is also possible that the tubing diameter might be too big for current production levels. This is usually the case when the injection gas/liquid ratio needs to be very large to produce the well in a stable manner. It is common to find oversized production tubing strings in old oil fields, where reservoir pressures have declined to very low values. Replacing the tubing with small diameter tubing or using velocity strings might be the solution. A velocity string is a small-diameter tubing string (usually a coiled tubing string) that is installed inside the production tubing with the only purpose of reducing the flow area (the fluids are produced through the annular flow area between the production tubing and the velocity string).

There are other causes of instabilities. For example, large water cuts, with or without emulsions, might increase the production pressure and reduce the pressure drop across the operating point of injection (inducing subcritical flow through gas lift valves as explained in Fig. 8.4). Inadequate operation of the well like, for example, the injection gas flow rate set too high or too low, creates instability problems that are explained below and in chapter: Intermittent Gas Lift Troubleshooting. Unstable wells can have single or multiple points of injections. Because of its importance, several specific causes of instabilities, in which there are multiple points of injections, are separately presented in Section 11.3.2.

### 11.3.1.2 ***Inadequate operation of the well***

In many cases, there might not be anything wrong with the well or the formation but the efficiency of the lifting operation is low because of the way the well (or the gas lift system) is being operated or because of poor selection of gas lift and/or completion components. The following examples are just a few of these operational conditions.

- *High injection gas flow rate (wrong set point).* A very high injection gas flow rate (compared to what the well actually needs) can cause an increase in the injection pressure that can open an upper IPO unloading gas lift valve.

This usually does not cause a significant reduction in liquid production but it does (unnecessarily) increase the injection gas/liquid ratio.

Once an upper valve is opened, it might remain opened and the well might operate with a stable injection pressure (higher than the design operating pressure). But the upper valve could open and close in a cyclic manner, giving the impression that it is an intermittent gas lift operation when it is actually a continuous gas lift well with two points of injection (one of which is unstable). This type of instability happens because once the upper gas lift valve is opened, the gas flow rate that goes into the tubing is greater than the gas flow rate injected into the well's annulus at the surface, so that the injection pressure drops and the upper valve closes. Once the upper gas lift valve closes, the gas flow rate injected to the well at the surface is greater than the gas flow rate that passes through the lower gas lift valve and, in consequence, the injection pressure increases once again to begin a new injection cycle.

- *Low injection gas flow rate (wrong set point)*. A lower than required surface injection gas flow rate into the well's annulus can cause the injection annular pressure to drop and fluctuate in different ways, depending on the operational conditions.
  - If there is a calibrated gas lift valve at the point of injection (as opposed to a gas lift orifice valve) and the injection pressure fluctuates with high-pressure peaks that are rounded, then the operating valve is in throttling flow, with its stem slowly moving up and down but the gas lift valve does not actually close. If the pressure peaks are not rounded but look more like the ones found in the normal operation of a pilot valve in intermittent gas lift (sharp peaks), the valve is indeed opening and closing due to the small surface gas injection flow rate. The low surface gas injection flow rate causes the annular injection pressure to drop below the operating valve's closing pressure. Once the operating valve closes, the annular injection pressure increases again to eventually open the operating valve and start a new gas injection cycle.
  - If the point of injection is an orifice valve, the injection pressure fluctuations are caused by the production pressure at the orifice valve's depth becoming too close to the injection pressure and, sometimes, even becoming larger than the injection pressure so that the gas flow rate through the orifice momentarily stops. Once the gas flow rate has stopped, the production and injection pressures begin to increase but eventually the injection pressure overcomes the production pressure and gas injection is reassumed through the orifice valve to start a new injection cycle. Pressure fluctuations are more pronounced if the gas injection pressure increases very

slowly (in comparison to the rate of increase of the production pressure) and, in consequence, it takes a long time for it to reach a value greater than the production pressure. For this latter case, the production pressure might increase to values that are so large (because liquids have had sufficient time to accumulate above the orifice valve, generating a large column) that the injection pressure needs to increase also to very large values, sometimes restarting gas injection through an upper unloading valve.

- *Operating the well with high wellhead pressures.* The liquid flow rate of gas lift wells is very sensitive to the wellhead pressure. Bent or smashed flowlines or with a great number of elbows or unnecessary restrictions, such as empty choke housings, can increase the wellhead production pressure, which in turn reduces the liquid production of the well. High wellhead production pressure can also cause an increase in the injection gas pressure. It should be checked if the master valve, the wing valve, or any valve that can restrict the liquid flow at the wellhead, are fully opened. A partially opened surface valve can increase the production pressure without being able to detect the problem if the wellhead connection of the production-pressure sensor is installed downstream of this surface valve. Some operators leave one or several wellhead valves partially opened to reduce or control the gas or liquid flow rate: this operation could permanently harm the valve because of erosion of the valve's internal components. Most wellhead valves are designed to operate either fully opened or fully closed. High wellhead production pressures can also be due to problems located at the flow station such as high separation pressure, partially closed valves, plugged check valves, etc. Very long flowlines or with very small inside diameters, can increase the wellhead pressure too (looping a parallel flowline could be a low-cost solution to lower the wellhead production pressure in these cases).
- *High wellhead pressure (emulsions).* Emulsions can also increase the wellhead pressure. Emulsions can be treated by injecting demulsifying agents down the annulus together with the injection gas. However, many times all that is needed to get rid of the emulsion problem is to inject the chemicals directly into the flowline (which is at a much lower pressure than the gas injection pressure, thereby eliminating the use of high pressure pumps that could frequently fail). Emulsions can create high wellhead pressure or induce serious instabilities. When emulsion formation is a serious problem and the well has a high reservoir pressure, gas can be forced to be intermittently injected at a very high frequency so that the liquid production is actually continuous but the injection gas enters the well in batches, avoiding the high turbulence that promotes emulsion formation in continuous gas lift. The wellhead

pressure chart in this latter case will look exactly as shown in Fig. 11.47. Due to their importance, emulsion problems and some of the ways to solve them are presented in Section 11.3.3.

- *Well producing from several zones.* In wells with one production tubing string and several production zones (isolated by casing–tubing packers) with sliding sleeves to selectively produce each zones, it is possible that the well is producing from a zone for which the current gas lift design was not intended or that more than one zone are unintentionally opened to production at the same time. Sliding sleeves can leak or get stuck open. In these cases, it is advisable to run continuous temperature surveys (without discrete stops) using highly sensitive temperature sensors (as explained in Section 11.5.2) or use fiber-optic to measure the temperature along the production tubing (as explained in Section 11.5.7) to detect the zones from which liquids are being produced.
- *Use of gas lift mandrels not suited for inclined wells.* A mandrel not suitable for deviated wells could lean against the casing precisely at the point where the mandrel ports are located, see Fig. 6.20. This could cause a restriction in the gas flow rate that is not possible to determine by any calculation procedure (the point of injection will be at a shallower unloading valve and the injection pressure will be higher than the expected operating injection pressure). Gas lift mandrels that are not suited for deviated wells should not be installed in deviated wells, even if the deviation angle is very small. Appropriate mandrels for deviated wells have recessed gas entrance ports so that it does not matter how they are oriented inside the casing, see Figs. 6.18 and 6.19.
- *Use of inadequate production tubing size.* Small-diameter production tubing (compared with the required tubing diameter for the well's optimum liquid flow rate) restricts the liquid production and causes a high production pressure that might make it impossible to unload the well to the design point of injection. However, even if the well could be unloaded to the design point of injection, the high bottomhole flowing pressure might keep the well from producing at its full potential. The liquid production will be lower than the well's potential but the well will show a normal wellhead pressure and a high pressure drop along the production tubing (for this reason, the point of injection might be higher than the point of injection by design and a higher injection pressure is required). Troubleshooting analyses must be done in conjunction with nodal analyses to determine the optimum tubing diameter. An economic evaluation will finally determine if it is profitable to replace the production tubing. It should also be analyzed if the liquids could be produced up the annulus (this is not always possible because the annular flow area could be too large, causing instability problems, or production fluids could damage the casing).

### 11.3.1.3 **Failures or malfunctions of gas lift and completion equipment**

There are many sources of downhole equipment failure (compared to a natural flowing well), that can create serious operational problems or inefficiencies.

- *Unloading valve that remains open (dirt accumulation).* An unloading gas lift valve (that is supposed to be closed) can remain open because a solid particle could be trapped between the ball and the seat. This problem can be confirmed if the following two field tests give these results: (1) a communication test (as explained in [Section 11.5.1](#)) shows that there is no hole in the tubing, and (2) if the surface gas injection is shut off (without shutting in the well) and the injection pressure drops to values less than the surface closing pressure of the operating valve installed in the well. For the latter test to be used all unloading gas lift valves should be IPO valves and there should be a calibrated valve (also IPO) at the point of injection (as opposed to an orifice valve). The impact of having an upper unloading valve open will depend on the gas flow rate that this open valve will allow to pass from (1) a mild increase in the injection gas/liquid ratio to (2) a low injection pressure, high injection gas flow rate, and a reduction of the liquid production. One procedure to get the valve closed is to shut in the well while keeping the gas injection unchanged. The injection pressure will rise to values greater than all of the valves' opening pressures. Then, the well is suddenly opened to production (verifying first that this operation will not cause any harm at the flow station; it might be necessary to install a choke far away from the well, or at the flow station, to protect surface facilities). Then, after the liquid production has stabilized, gas injection is shut off again to see how far down the injection pressure gets. This procedure is repeated until the injection pressure does not drop to values less than the surface closing pressure of the operating valve.
- *Unloading valve that remains open (getting it to close as expected).* Continuing with the subject from the previous paragraph, to get the valve to close as expected some operators perform the following procedure:
  - a) Wellhead annulus and tubing pressures are equalized by closing the well to production and injecting gas into the tubing using a high pressure hose or simply by closing the well to production and waiting for the injection pressure to reach line pressure (the surface production pressure will also increase but not necessarily to line pressure). In any case, when the gas flow rate drops to zero (because the injection wellhead pressure

becomes equal to the injection manifold pressure) the surface gas injection control valve is manually closed.

- b) Then, the surface injection pressure in the annulus is rapidly vented 100 or 200 psi (while keeping the well closed to production) less than the large production pressure trap at the surface.
- c) Then the wellhead production pressure is vented 100 or 200 psi less than the surface annular injection pressure reached in point “b.”
- d) The surface annular injection pressure is again vented in the same way it was done in step “b” until it is 100 or 200 psi below the surface tubing pressure reached in step “c” and this procedure is repeated until the tubing and production pressures become very small.

This causes repeated flows across the gas lift valve that might finally close it. This procedure should not be tried if sand production is going to be a problem.

- *Unloading valve that remains open (other causes).* Another reason for a gas lift valve to remain open is because the bellows has been damaged (flat valve) or the seat is so large that, once the valve is uncovered, the following events can happen: (1) the injection pressure drops because of the high gas flow rate these seats can allow, and (2) the high gas flow rate cools the valve, lowering its closing pressure to a value less than the design closing pressure.
- *Salt depositions in gas lift valves.* In marine environments (or when using certain types of completions fluids), salt depositions could be the solid keeping the valve open or plugging it (if the valve is plugged, the injection pressure will be high and there will be a reduction in the liquid production). In these cases, fresh water can be injected down the gas injection annulus (unless CO<sub>2</sub> or H<sub>2</sub>S in the injection or formation gas could cause corrosion problems, for which special precautions should be taken). If fresh water causes formation damage, a standing valve should be installed at the bottom of the well, keeping the water from reaching the formation.
- *Gas lift valve plugged by iron sulfide depositions.* In some wells, iron sulfide (FeS) depositions that can plug gas lift valves are common. The best way to deal with these depositions is to inject water with special detergents or chemicals into the well. If the operating valve is plugged, the injection pressure will be high and there will be a reduction in the liquid production.
- *Gas lift valves with cut seats.* Unloading the well at a high injection gas flow rate before reaching the first valve can cut gas lift valve seats which will then leak gas once the well is in operation. Cut seats

are very common and usually, but not always, the gas flow rates that leaking valves allow to pass for this reason are not very significant, even if they are easily detected by means of down hole temperature surveys; however, it is recommended to unload the well very slowly to avoid this type of valve failure because sometimes they do represent a serious problem. More importantly, unloading the well at a high injection gas flow rate can damage the gas lift valve's internal check valve, creating a serious well integrity problem.

- *Gas lift valve's tail plug failure.* A leaking tail plug of a gas lift valve (Fig. 6.4) could allow the dome pressure to increase so that the valve will only open at higher than design opening injection pressures. If the tail plug leaks, every time the pressure surrounding the valve is higher than the nitrogen pressure, the dome is going to be pressurized and the valve might not open unless the injection pressure is very high (the dill valve, shown in Fig. 6.4, that is used to charge the gas lift valve with nitrogen, allows gas or liquid flow into the valve but not in the opposite direction). This might be due to errors that, from time to time, are made at the shop when the valves are being calibrated (the tail plug is not tighten correctly, the operator forgets to install the copper gasket, etc.). The injection pressure can reach line pressure and the well does not take gas.
- *Gas lift valve failures (other causes).* For a variety of reasons, the valve can also be set at the wrong opening pressure at the shop (wrong calibration temperature, not properly aging the valve's bellows, faulty test-rack instruments, etc.). Another operational error that is sometimes made by wireline crews is to install the valves in the wrong mandrels. All of these errors have consequences that could completely confuse the person analyzing the well because they are not directly revealed by any available calculation procedure.
- *Pilot valve failure.* A downhole gas lift pilot valve intended for intermittent gas lift could fail open for one of the reasons given in chapter: Design of Intermittent Gas Lift Installations and, in consequence, gas is injected in a continuous fashion into the production tubing. This usually, but not always, causes a high injection gas flow rate with a low surface injection pressure. Other times, the pilot valve's piston gets stuck in such a way that the gas flow rate is very small compared with what a fully opened gas lift pilot valve could allow to pass. In both cases, it might be possible to fix the problem by venting the casing-tubing annulus. As explained in chapter: Design of Intermittent Gas Lift Installations, if the check valve of the pilot valve is an integral part of the piston (it is located inside the piston) then a communication test would wrongly indicate a hole in the tubing if the piston gets stuck or the check valve is plugged. If the check



valve is not an integral part of the piston but it is located at the nose of the valve, which is the usual place where check valves are located, then a communication test will indicate a hole or casing–tubing communication only if there is indeed such communication.

- *Surface intermitter failure.* A surface intermitter might fail open and the surface gas injection flow rate into the well could be so large that it would not be possible for the pilot valve to close. The injection pressure in this case could be very high. Intermitters are used in intermittent gas lift wells to control the surface gas injection into the annulus of the well at regular time intervals.

#### 11.3.1.4 **Deterioration of the reservoir, production tubing, gas injection line, or the flowline**

- *Low reservoir liquid production.* Downhole conditions (not caused by any malfunction of the gas lift equipment) can cause a decrease in the well's liquid production rate: sand that accumulates at the bottom of the well, for example, can become a serious problem because it can partially, or totally, block the perforations, causing the liquid production to decrease or completely stop. Nitrogen injection using coiled tubing units are usually employed to get rid of the sand that has accumulated at the bottom of the well. Formation damage can also cause a reduction in liquid production. Sometimes, in the early production stages of a reservoir, the static pressure can suffer a very steep decline, which translates into lower fluid production. Additionally, any downhole equipment (other than gas lift valves or mandrels) can fail and restrict the liquid production. For example, a plugged standing valve or a subsurface safety valve that has failed can cause a serious reduction of the well's liquid production. If the root of the problem affecting the liquid flow rate from the reservoir is below the point of injection, as the liquid production declines (for whatever reason) so does the production pressure at the operating valve's depth, which in turn might induce the following reactions: (1) if there is an gas lift orifice valve at the point of injection, the gas flow rate might increase and the injection pressure decrease if the flow through the downhole orifice valve is subcritical (and the surface gas flow rate is not automated at a given set point), and (2) if there is a calibrated valve at the point of injection, the pressure might remain more or less constant and because of the throttling effect of the valve, the gas flow rate could decrease; however, the valve could also start intermitting.
- *Solid depositions in the flowline and production tubing.* Organic depositions, such as asphaltene or paraffin incrustations, or inorganic depositions, such as carbonates scales, on the production tubing and

flowline walls, can cause an increase in the “frictional pressure drop” that cannot be calculated because the actual flow area of the production tubing or flowline is unknown. If, for example, the pressure drop along the flowline is too large for the current liquid and gas flow rates, it is possible then that this pressure drop is caused by solid depositions or sand accumulation in the flowline. A continuous and inexplicable decrease in fluid production can also be due to solid deposition on the production tubing wall (in this case, it might be hard to identify the problem as there is no increase in the wellhead pressure that can alert the optimization engineer that the well is having this type of problem because the symptoms are a slight decrease of the wellhead pressure and a moderate increase in the gas injection pressure). Paraffin can be melted by a hot oil injection into the production tubing and flowline, but long-term solutions have been found by heating the injection gas to keep the production tubing warm near the surface, where paraffin is usually generated due to the cooling effect of the injection gas. Metallic plunger can also be used to keep the tubing free of paraffin accumulation, but this might introduce other types of operational problems as described in chapter: Design of Intermittent Gas Lift Installations. Getting rid of solid depositions can be accomplished by injecting chemical products into the tubing, such as different concentrations of hydrofluoric or hydrochloric acids (depending on the type and severity of the depositions), but it should be checked first if nonmetallic components of gas lift valves are capable of withstanding these types of acid treatments. Solid depositions might accumulate on top of a gas lift valve installed in a side pocket mandrel, making it impossible to retrieve the valve by wireline. In these cases, acid solutions can be poured on top of the latch by dump-bailer devices run in the well with a kick-over tool in an attempt to get rid of the solid depositions and be able to retrieve the valve. On the other hand, sand depositions on top of a gas lift valve can be removed by sand-bailer wireline tools.

- *High injection gas flow rate with low injection pressure (due to conditions in the well).* A high injection gas flow rate with a very low surface injection pressure could be due to a hole in the tubing, a flat valve, an unloading valve that would not close because of its low temperature, or a hole in the gas injection line (between the injection manifold and the wellhead) that goes unnoticed because the gas flow rate is being measured upstream of the hole (to detect where the hole is, it is recommended to close the injection valve at the wellhead, downstream of the connection of the injection pressure sensor, while leaving the manifold valve open; if the injection pressure does not

increase, the hole is somewhere between the well and the injection manifold). For offshore wells (in shallow waters), gas bubbles usually reveal where the hole in the injection gas line is located. Recognition helicopter flights are usually made over large offshore gas lift fields to spot this type of problem, which unfortunately happens very frequently in many places around the world.

- *Low injection gas flow rate and low injection pressure (other causes).*  
A reduced surface injection gas flow rate that causes fluctuations in the wellhead injection pressure (as described in previous paragraphs) can be due to an improperly set surface gas injection flow control valve, but it could also be due to dirt or debris carried by the injection gas that are plugging the flow control valve, making it necessary to vent the gas line from time to time (automatic gas injection flow control valves can be used to handle this problem as they do not have a fixed position and will try to open wider if the gas flow rate begins to decrease). If the presence of solid particles in the injection gas line is a recurrent problem, it is recommended to install gas filters upstream of the gas injection manifolds rather than periodically venting the gas lines. Very old or very new gas lift systems, or gas lines in corrosive environments, usually present this kind of problem. If the injection gas flow rate is less than its required value but the injection pressure is higher than the design injection pressure and stable, it is possible that the downhole operating gas lift valve is the one that is partially plugged or the production tubing pressure is too high.

#### 11.3.1.5 **Possible causes and solutions when unloading the well cannot be completed**

Sometimes it is not possible to complete the unloading process and the injection point that is finally reached is higher up in the well than the design point of injection depth. Some of the causes and actions that can be taken in these situations are:

- The well's liquid production might be much larger than expected (the production pressure is then higher than the gas injection pressure at the next unloading valve), for which nothing can be done operationally except trying to optimize the gas injection flow rate and evaluate the gas lift design to see if it is adequate for current conditions or a redesign of the gas lift valves is needed.
- The liquid production might not be higher than expected but the seat diameter of an unloading valve is so small that it does not allow reaching the required gas flow rate to unload the well to the next deeper valve. A new gas lift valve design must be installed in the well.

- The liquid production might not be higher than expected but the operating temperature is greater than the design temperature and one or several unloading valves remain closed, not allowing transferring the point of injection any deeper. A new gas lift valve design must be installed in the well.
- The liquid production is not higher than expected but the distance between two consecutive mandrels is too long and the injection pressure is not high enough to overcome the production pressure at the deeper valve, thus the unloading of the well cannot be completed. Some possible operational solutions to unload the well to the design point of injection are:
  - Increase the injection gas flow rate to raise the injection pressure and be able to inject gas through the lower valve. Very high gas flow rates might be required because several upper unloading valves might open and, momentarily, gas will be injected through more than one point at the same time.
  - Inject gas into the tubing to lower the liquid level inside the tubing. This should not be tried if it will cause formation damage or it might increase sand production.
  - Unload the well to a pit or a tank at atmospheric pressure to decrease as much as possible the wellhead production pressure.

#### 11.3.1.6 **Unloading the well cannot be started**

When the well cannot be unloaded because the injection pressure is not large enough to overcome the production pressure at the “first” (shallowest) unloading valve, besides trying to inject gas into the tubing or unloading the well to a pit, one or several of the following steps could be taken (other reasons for not being able to start the unloading process through the first valve are explained in [Section 11.4.1](#)):

- Swab the well with a wireline operation. This might not be a good recommendation because wireline tools could get stuck in the tubing or be blown up the tubing, among other risks.
- If the completion fluid pressure gradient is too large, completion fluids might be circulated with a lighter fluid (if the lighter fluid causes formation damage, use a standing valve at the bottom of the tubing), for which the deepest valve should be replaced with a circulating valve and dummy valves should be installed in all other mandrels above.
- Inject nitrogen or diesel into the tubing to reduce the tubing pressure. This is usually done with coiled tubing units.
- Increase the available injection pressure at the manifold by temporarily closing gas injection to some of the nearby wells.

- If everything fails or the problem is going to persist every time the well needs to be kicked off, the completion should be pulled out of the well and replaced with another one with mandrel spacing adequate for current conditions.

To add difficulty to the troubleshooting analysis, it might be possible that two or more of the problems covered so far in this section might take place at the same time. This is the main reason why many times it is not possible to quickly identify the source of the problem and there are no general calculation procedures for each and every type of problem (single or combined). However, after performing different types of analyses, it is possible to reach a conclusion that most of the time coincides with the source of the problem. It is advisable to file and keep records of all analyses and causes of previous failures or operational problems of the well and look at the history of nearby wells producing from the same reservoir. For example, in a field where many wells have problems associated with sand production, a well with a decline in liquid production is a good candidate to quickly check, by wireline, its total depth and, based on the result, nitrogen injection using coiled tubing might be recommended to get rid of the sand that has accumulated at the bottom of the well.

As can be seen from the list of possible problems given earlier, not always the decline in liquid production (or any other inefficiency found in the operation of a well on gas lift) can be attributed to a failure in the gas lift equipment or gas lift design and the well has to be analyzed from an ample context to detect where the source of the inefficiency is coming from.

### 11.3.2 Multiple points of injection

For any type of gas lift valve, a valve below the static liquid level might not be able to close because of any the reasons already described, such as (1) the valve has a cut seat, (2) the bellows has a hole (flat valve) or it lost pressure through the tail plug (the dill valve failed), (3) the valve is unseated in the gas lift mandrel, (4) dirt is keeping the valve opened, etc. In these cases, it might be feasible to reach the next lower valve but the gas lift system might not be capable of providing gas at a rate high enough to keep the injection pressure at an adequate level to overcome the production pressure at valves further down the well or even to keep gas injection through these two points (the upper valve that would not close and the one below) in a stable manner. The unloading process cannot continue and the well is left producing with multiple points of injection in a stable or unstable gas injection pattern. Multiple “stable” points of injection take place when the injection gas flow rate at the surface is equal to the gas flow rate

that can be injected through two or more gas lift valves at the same time. This could make it impossible to reach the desired point of injection or gas could be injected through the design operating point and an upper unloading valve at the same time. In the latter case, the target liquid production might be reached but with an unnecessarily high injection gas/liquid ratio. The following examples (presented for specific types of gas lift valves) are some of the many conditions that cause stable or unstable multiple points of injection.

- For IPO valves: For whatever reason explained so far an upper valve fails open but because of its small seat diameter, the injection pressure is maintained at a high value. Once the lower valve (which is working properly) is uncovered, the total gas flow rate that passes through both valves is equal to the gas flow rate injected at the surface, so that the injection pressure does not drop to values less than the closing pressure of the lower valve (the valve right below the one that has failed open) and, additionally, this injection pressure is not high enough to overcome the production pressure further down the well. The point of injection cannot be transferred to deeper valves and the well is left producing from two upper points of injection in a stable fashion. It is also possible that the injection pressure drops to values less than the closing pressure of the valve below the one that has failed open once this lower valve is uncovered. This valve would then close but once it does, the injection pressure starts to increase to eventually open the lower valve again, giving the impression that the well is producing on intermittent gas lift. If, additionally, the injection pressure is not high enough to overcome the production pressure further down the well, the point of injection cannot be transferred to deeper valves and the well is left producing from two upper points of injection in an unstable fashion.
- Also for IPO valves: It might be possible that the surface injection gas flow rate is higher than the gas flow rate that the calibrated valve (or orifice valve) at the design point of injection can pass at the current injection pressure and, in consequence, the following events can happen: (1) the injection pressure increases above the opening pressure of the unloading valve just above the operating point of injection, so that this upper valve opens and stays open in a stable manner because the gas flow rate at the surface is capable of maintaining two injection points at the same time, or (2) the injection pressure increases above the opening pressure of the unloading valve just above the operating point of injection, but the upper unloading valve closes shortly after it opens because the injection gas flow rate at the surface is not

capable of maintaining two injection points at the same time and, in consequence, the injection pressure begins to drop once the upper valve opens. This could also give the impression that the well is producing on intermittent gas lift. These events can also take place for PPO valves installed in wells producing in annular flow (with mandrels normally used for tubing flow) because, in this case, PPO valves behave as IPO valves (the check valves of PPO valves should be reversed for these applications).

- For PPO valves: An upper valve fails “open” but because of its small seat diameter, the injection pressure is maintained high enough to reach the next valve below. If, once the next lower valve has been reached, neither the production pressure drops to values less than this lower valve’s closing pressure, nor the gas injection pressure drops to values less than the production pressure at this lower valve’s depth, then the production could be maintained in a stable manner with two points of injection (if the injection pressure is not high enough to overcome the production pressure further down the well). However, it can also happen that, once the valve just below the one that has failed open is reached, the injection pressure begins to decrease, eventually dropping to values less than the production pressure at this lower valve’s depth and gas injection through this lower valve is interrupted for a while (until the injection pressure increases to overcome the production pressure of the lower valve once again).
- Also for PPO valves but in good working conditions: once the next lower valve has been reached the production pressure at the upper valve does not drop to values less than its production closing pressure because it was calibrated for a lower production closing pressure. Contrary to what is recommended for IPO valves, the upper valve could close by increasing the gas flow rate to decrease the production pressure (if the injection gas/liquid ratio for minimum pressure gradient has not been reached yet). In this way, even though the injection pressure increases, it is possible that the production pressure drops and the upper valve, that reacts mainly to the production pressure, closes. If the upper valve cannot close and, additionally, the injection pressure is not high enough to transfer the point of injection to lower valves, the well is left producing from two points of injection in a stable fashion.

Troubleshooting wells with multiple points of injection is a very complex task and it is very difficult to find out which of the valves are opened. It is usually concluded that there are several points of injection because valve mechanic equations predict several valves opened at the same time and gas

balance calculations indicate that it is not possible to inject into the tubing, through a single gas lift valve, all the gas injected to the well at the surface. To determine in which proportion each valve is passing the injection gas or, for wells with more than three or four valves, knowing which of these valves are the ones opened, is extremely difficult to do in an accurate manner. The best way to find the points of injection is by a conventional downhole temperature survey (if the well is stable) or with a temperature survey using fiber-optics in the way that is presented in [Section 11.5.7](#) (if the well is unstable). Pressure surveys by themselves are, most of the time, of little use to detect the points of injection when there are several points of injection because they usually do not show a change in the production pressure gradient at some, or all, of the points of injection. However, at the same time, if the liquid flow rate is very large, it might be difficult to detect the points of injection by just measuring the temperature along the production tubing if very sensitive temperature sensors (currently available) are not used.

The calculation procedures explained in [Section 11.4.2](#) for single point injection can, to a point, be used for stable multiple points of injection. In this case, the gas balance will predict that it is just not possible to pass all the gas injected at the surface through a single valve. This is only an approximation because for multiple points of injection there is no way to accurately calculate the production pressure.

Unstable multiple points of injection usually give the impression that the well is producing on intermittent gas lift, when in reality the well has: (1) one or more continuous points of injection, (2) one or more intermittent points of injection, which could be valves opening and closing or, at the deeper point of injection, the injection pressure is varying at regular intervals between values that are lower and higher than the production pressure, and (3) a continuous liquid flow rate, which can be easily visualized by looking at the way the liquid production (or the liquid level, if the test separator is a dump type separator) changes with time at the test separator, as explained in [Section 11.5.8](#).

It is completely unacceptable to use intermittent gas lift troubleshooting techniques for wells with multiple points of injection and continuous liquid production; but it might be, up to a point, appropriate to use the calculation procedure explained in [Section 11.4.2](#), for which the production pressure could be calculated in different ways:

- With the maximum liquid and gas flow rates first and then with the minimum liquid and gas flow rates to have two extreme values of the production pressure at each valve's depth, for which all calculations



are carried out (valve mechanic, gas balance, and reservoir flow rate) separately, or

- Using multiphase flow correlations with the average liquid production and gas injection.

These approximations might be appropriate for IPO valves but should not be attempted for PPO valves.

If the gas injection and liquid production instabilities are not too severe, unstable wells with multiple points of injection and continuous liquid production could be troubleshoot using well dynamic models. The description and analysis of these dynamic models are beyond the scope of this book.

Due to the impact that emulsions have on the operation of a gas lift well, the rest of this section concentrates on explaining the different problems associated with emulsions and how to handle them.

### 11.3.3 Handling problems associated with emulsion generation

Emulsions are usually found in wells with water cuts between 40 and 60%. Wells with water cuts greater than 60% might not present emulsion problems but it should be determined if the gas lift method could be replaced with another method of production because the injection gas/liquid ratio tends to be too high in high-water-cut wells.

One major disadvantage of the gas lift method is that it promotes emulsions: the mixing action of the turbulence created at the point of injection accelerates the emulsion formation process. The calculation of the production pressure along the well using multiphase flow correlations is very inaccurate if liquids are emulsified because of the following reasons:

- The flow pattern is very hard to predict because, to carry out this task, it is necessary to precisely know the liquid surface tension and other PVT properties that are not easy to find when emulsions are present.
- If the flow pattern is unknown, it is not possible to calculate the liquid holdup and, in consequence, the hydrostatic pressure drop cannot be calculated either.
- It is not possible to calculate the actual friction pressure drop either, not only for not knowing the flow pattern, but also because it is very hard to estimate the viscosity of the emulsion.

For these reasons, troubleshooting a well with emulsion problems by calculating the production pressure could lead to very inaccurate results.

Emulsions are generated from two immiscible liquids, one of which is present as small drops in the other liquid (which is the continuous component of the emulsion). Emulsions of small water drops in oil might have a viscosity much larger than the viscosity of either the water or the oil alone. Emulsions remain stable because of emulsifying agents present in the fluids produced by the wells. Asphaltenes, clays, acids, etc., are examples of natural emulsifying agents. Emulsions can be broken down by demulsifying agents that act at the interface between the water and the oil to make the water drops coalesce into larger drops that eventually form a continuous phase that coexists with the oil in a much lower viscosity mixture. Once the emulsions are broken, the pressure drop along the tubing is reduced; this lowers the flowing bottomhole pressure so that the liquid production of the well increases. This increase in liquid production causes an increase in the production temperature, which in turn might help prevent paraffin formation as an additional advantage.

Among other benefits that can be obtained by getting rid of emulsions, it is found: (1) a reduction in surface liquid production heading; (2) a decrease in the pressure drop along the flowline; (3) a reduction of the volume of chemicals needed at surface liquid treatment plants; (4) improvement of the gas-water-oil separation process and a reduction in the time operators spend trying to solve control problems caused by emulsions at the production separators; (5) The injection pressure and the injection gas/liquid ratio could be reduced, thereby increasing the lift efficiency; and (5) It makes it easier to perform wireline operations in the well if needed.

If the completion is an open type completion (with no casing-tubing packers) it is better to inject the demulsifying agents through a capillary tubing, run parallel to the production tubing all the way to an injection mandrel located at the bottom of the production tubing, where a valve is installed to regulate the flow of the chemical product being used. This chemical injection mandrel should be located below the gas lift mandrel. Serious instability problems have been reported when trying to inject chemical agents together with the injection gas down the annulus in open completions: this is due to the fact that initially the agents work very well and the well's liquid production increases; but this increment in the liquid production makes the liquid level in the annulus drop below the point of injection so that the quantity of chemical agents going into the tubing is reduced because most of it is being accumulated on top of the liquid level in the annulus. This in turn causes a drop in the liquid production and the liquid level in the annulus rises again to repeat the cycle.

Injecting demulsifying agents down the annulus together with the injection gas in closed or semi-closed completions (with packers) is not free of operational problems either, but most of them can be easily solved. One problem that can happen in wells with or without packers is the formation of solid particles in the annulus that can accumulate at the gas lift valve and plug it. Generally, chemical products injected to break the emulsion consist of a solvent (usually gasoil or glycol) that is used to transport the chemical agent, which is usually a heavy molecule that actually breaks the emulsion. When this mixture enters the annulus, the solvent can evaporate and the remaining chemical agent concentrates in solid particles that can plug gas lift valves. This also takes place when injecting chemicals to treat solid depositions inside the production tubing walls. This problem is solved by using different levels of agent concentration in the solvent or by using different concentrations of the heavy components of the solvent itself. For example, an operator in Alaska found that by increasing from 0.3 to 1% the C<sub>20</sub> to C<sub>26</sub> fractions of the solvent, prevented the solvent from evaporating even at very low chemical injection flow rates.

Another problem found when injecting chemicals together with the injection gas down the annulus is that it takes a few days, from the moment chemical injection is initiated, for the emulsions to begin to break. This is due to: (1) the chemical product should fill the empty space between the point of injection and the liquid level in the annulus; and (2) even if the liquid level is at the point of injection, it takes a few days for chemical products to form a liquid film on the inside wall of the casing and the outside wall of the tubing, after which a significant portion of chemical products can enter the production tubing. In places where chemical injection has been done correctly, no gas lift valve has been plugged or its seat been cut due to liquids flowing through them.

High pressure pumps must be used to inject chemical agents into the annulus. These pumps could require high maintenance costs. For this reason, some operators inject the chemical product directly at the wellhead into the flowline (which is at a lower pressure) and many times this is all that is needed to considerably reduce the problem. Unfortunately, this solution does not always work, especially in highly deviated wells, where the frictional pressure drop due to the presence of emulsions in the production tubing is very high.

Even though chemical injection could solve production problems caused by emulsions, an economic evaluation must be done first to determine if the benefits obtained are greater than the costs involved in operations of this type, such as purchase of chemical products and their transportation, as well

as surface equipment and required personnel for supervision and control of the operations.

#### 11.4 METHODOLOGY FOR TROUBLESHOOTING ANALYSES

As it has been indicated in the introduction of the chapter, the main objective of troubleshooting analyses for wells on continuous or intermittent gas lift is to find the current point, or points, of injection or understand the reason why the well is not receiving gas. However, often calculations lead to results that are very different from the actual condition of the well. This is due to the poor quality of the available data or lack of sufficient information. The quality of the troubleshooting results depends on the quality and quantity of the data.

The first step in the troubleshooting process is to gather as much information as possible about the operational history of the well from the date it was drilled or from the last major workover job. The required information includes:

- Two-pen charts (or electronically obtained tendency curves) showing the wellhead production and injection pressures. Sometimes it is also important to measure the wellhead production temperature because in wells with large liquid productions, or with high water cuts, it is necessary to verify the production temperature to check if it is being precisely calculated along the production tubing to calibrate nitrogen-charged gas lift valves. Additionally, it is sometimes possible to use the wellhead temperature of the produced liquids as an early warning signal in case the liquid production decreases (a reduction in the liquid production might be easily detected by a drop in the wellhead production temperature). Wellhead production temperature can also be used in gas injection flow control loops because the wellhead temperature is proportional to the liquid production.
- Fluid properties: oil API gravity, formation gas/liquid ratio, water cut, bubble point pressure, specific gravity of produced, and injection gas, etc.
- Liquid production, total gas production, and injection gas flow rates (including previous history of injection gas flow rates and how the well responded to each of them).
- Reservoir data, such as the values of its static pressure and rate of decline, as well as any information needed to build the IPR curve.
- Completion data and gas lift valve type, seat diameters, and calibration pressures. Previous gas lift designs could also be reviewed to see how the well behaved for those designs.

- Review previous workover or wireline jobs such as opening or closing a circulating sleeve, stimulation jobs, etc.
- Evaluation of previous flowing pressure and temperature surveys or any other type of survey performed in the well.
- List of operational problems of nearby wells producing from the same reservoir.

The wellhead two- or three-pen chart recorder should be properly installed as indicated in Section 11.2. Wellhead pressure charts are very important in troubleshooting a well because the behavior of the wellhead pressures determines the type of analysis to carry out: continuous or intermittent gas lift, casing–tubing communication, etc. It is important to file a reasonable number of these charts for each of the last gas lift designs installed in the well after the last workover job. These charts are now being replaced with electronic pressure measurements that can be electronically stored as pressure or temperature tendency curves, for which it is important to have the right scan rate as indicated in Section 11.2. However, just looking at the wellhead pressure charts or tendency curves is not enough: troubleshooting calculations and field tests (conducted for troubleshooting purposes) must be performed to accurately determine the point of injection.

Fluid properties such as API gravity of the oil, solution gas/oil ratio at current operational conditions, total gas/liquid ratio, water cut, and bubble point pressure, among others, should be carefully verified because they play a key role in the production pressure traverse curve calculation. Water cut and total gas/liquid ratio are also important in calculating the production temperature along the tubing. This temperature is, in turn, used to calculate the valve's dome pressure and determine, together with the upstream and downstream pressures, if a nitrogen-charged gas lift valve is opened or closed.

As it is mentioned in Section 11.2, it is usually very difficult to have a precise measurement of the water cut and the gas/oil ratio. Even if the water cut and the gas/liquid ratio are accurately known, it might be possible to have serious deviations in the calculated bottomhole pressure in relation to its actual value. This is due to the use of a multiphase flow correlation that is not the one recommended for current operational conditions. The best multiphase flow correlation to be used is determined by a field process that involves running and analyzing a certain number of downhole flowing pressure and temperature surveys for one particular reservoir. These surveys can also be used to determine the IPR curve of the well. It might be possible that even the best multiphase flow correlation for a given operational condition could still cause serious deviations in the calculated bottomhole flowing pressure for another operational condition.

Test-rack opening pressures and seat diameters are very important parameters without which it is just not possible to perform most of the required calculations to troubleshoot a gas lift well:

- They allow the use of the force balance equation to determine if the valve is opened or closed.
- The seat diameter, together with the upstream and downstream pressures, is used to calculate the gas flow rate through a gas lift valve. If the valve is fully opened, the Thornhill–Craver equation can be used to calculate the gas flow rate; otherwise, dynamic models like those explained in chapter: Gas Flow Through Gas Lift Valves should be used to find the type of gas flow regime and the actual gas flow rate through the valve.

It is important to correlate each work performed on the well, such as opening a circulating sleeve or a stimulation job, with the well's production history. The way in which the production characteristics of the well changed with each job performed in the well reveals important clues about the real production capacity of the well.

Available flowing pressure and temperature surveys should be analyzed to determine the current point, or points, of gas injection. The point of injection is easily identified because of the local cooling effect of the injection gas on the production temperature right above the point of injection. This might be hard to notice in wells with large liquid flow rates. The point of injection can also be identified because the pressure gradient is lighter above the point of injection, although in wells with small liquid flow rates and high formation gas/liquid ratios this is sometimes impossible to notice.

One troubleshooting analysis procedure that does not heavily rely on the difficult to “accurately determine” IPR curves is explained in detail in Section 11.4.2. A different approach (offered by the most advanced gas lift computer programs commercially available today) is based on the IPR curve of the well. This latter approach can be taken if the IPR curve is accurately determined and the appropriate multiphase flow correlation is used (most of the time, both of these conditions are very hard to find); otherwise, this procedure might give totally wrong solutions. This type of procedure usually assumes that all valves are in good working conditions, which might not be the case. The calculations involved in this type of procedure are explained next for cases in which gas enters the tubing through only one point of injection, but the method can be applied to several simultaneous points of injection following a complex numerical analysis that is not shown here. The procedure requires the following data: current surface injection pressure at the wellhead (known as the operating pressure), the exit pressure,

which could be the wellhead pressure (if it is more or less constant) or the separation pressure (if the pressure drop along the flowline is considered), the IPR curve, PVT data, and all subsurface data (tubing diameter and inclination angles, depth and calibration of each gas lift valve, etc.). The mathematical procedure simultaneously calculates the unique set of the “well’s liquid production and the injection gas flow rate” that must be present in the well for the current reservoir static pressure, as well as the current wellhead injection and production pressures. Several figures shown in chapter: Total System Analysis Applied to Gas Lift Design are used here to illustrate the following explanation.

For didactical purposes, let us assume the well has only one gas lift valve (the user can select any valve installed in the well). Nodal analysis performed for different gas injection flow rates (as shown in Fig. 5.23a) gives the gas lift performance curve shown in Fig. 5.23b. For each solution point (corresponding to each injection gas flow rate) of the nodal analysis in Fig. 5.23a, there is one production curve as shown in Fig. 5.24a. Therefore, each production pressure (as determined from the nodal analysis just mentioned) at the valve’s depth for each injection gas flow rate  $Q_{gi}$  can be plotted as shown in Fig. 5.24b. On the graph shown in Fig. 5.24b, different curves corresponding to the gas flow rate that the seat of the gas lift valve can pass for different injection pressures (at depth) are superimposed as shown in Fig. 5.25a (the reader is advised to review Fig. 8.1 to familiarized with gas flow rate curves for a given orifice or seat size). The intersection of the seat (or orifice) gas flow rate curve that corresponds to the actual injection annular pressure at depth with the production pressure curve (determined in Fig. 5.24b) gives the one and only one injection gas flow rate that must exist in the well for the given injection pressure. With this gas flow rate, the current liquid production is found from Fig. 5.23b. This liquid production and injection gas flow rate should coincide with their measured values if the actual point of injection is indeed the one considered in the calculations. This type of analysis can be extended (in a way that is not shown here, but that is based on the same calculations just described for a single point of injection) to a well with several gas lift valves, in which several valves could be simultaneously opened. For a given wellhead injection pressure, the extended numerical procedure will give the one and only one set of possible opened gas lift valves with the corresponding unique gas flow rate each valve can pass.

The numerical procedure just described appears to be very useful; unfortunately, in most gas lift wells, troubleshooting using nodal analysis cannot be done because the input data is usually not as accurate as required for this type of analysis. This is the reason why a more “rudimentary” calculation procedure, such as the one described in Section 11.4.2, is many time the best

that can be done. In reality, the task of estimating the point of injection is a very difficult operation because there are many possible solutions of the point, or points, of injection, even for a stable well on continuous gas lift:

- The well might not be receiving gas, so there is no point of injection at all.
- The point of injection might be a single point of injection and it could be any damage or undamaged valve installed in the well. If the well is producing liquids in a stable manner, then the final point of injection should be below the static reservoir liquid level but not necessarily at the design point of injection. There might be multiple points of injection with a stable liquid production and gas injection.
- A valve in good condition but at a low temperature (above the static reservoir liquid level) might be opened and all the injection gas is circulated through it with no liquid production from the well.

The way in which some calculations (if any) might be carried out for each of these possibilities is presented next.

#### 11.4.1 High wellhead injection pressure and the well does not receive injection gas

If the wellhead injection pressure (downstream of any wellhead valve) reaches full injection line pressure and the well is not taking injection gas, then there is no communication from the injection annulus into the production tubing (in case gas is injected down the annulus) or from the tubing into the annulus (in case gas is injected down the tubing), unless a surface or subsurface valve, located downstream of the gas lift valve, is closed. If the well is not taking any gas but the injection pressure (downstream of the surface gas injection choke or valve) is not equal to the line pressure, it is possible that the surface injection choke or valve is plugged or closed (or the valve at the injection manifold is closed).

The first step to solve the problem is to verify that there are no surface valves closed downstream of the point where the injection pressure sensor is installed at the wellhead. The injection pressure will be equal to line pressure (with the injection gas flow rate equal to zero) when any of the following surface valves is closed: wellhead annulus valve, master valve, wellhead production valve (wing valve), any valve along the flowline, and any valve at the flow station that directs the well to the production separator or the main header. It is possible that one of these valves was left closed by mistake. It is also possible that the subsurface safety valve has failed closed and therefore, if the well has such subsurface valve installed, its operation needs to be checked.



If a well, with nitrogen-charged gas lift valves, starts producing liquids at a higher than expected rate and then stops producing for a while, and this cycle is repeated periodically, there might be a temperature related problem: the nitrogen-charged valve exposed to a higher than anticipated temperature closes and remains closed until its temperature drops to start gas injection again.

If the well has PPO valves, it is possible that they do not open because the production tubing is empty.

To start the calculation process, the gas injection pressure at the depth of the first (shallowest) valve,  $P_{iod1}$ , must be calculated first:

$$P_{iod1} = f_g P_{manifold} \quad (11.1)$$

Where  $P_{manifold}$  is the pressure at the injection manifold which, in this case, is equal to the injection pressure at the wellhead, and  $f_g$  is the gas factor that is used to calculate the injection pressure at depth as explained in chapter: Single-Phase Flow. To be able to inject gas through the first valve,  $P_{iod1}$  must be greater than the production pressure  $P_{pd}$  at the depth of the first valve. This production pressure could be calculated for different liquid levels in the well: (1) the liquid level is right at the wellhead, (2) it corresponds to the reservoir static liquid level, or (3) it is the one that was measured at the well. For the first case, the liquid production pressure is calculated by:

$$P_{pd} = P_{wh} + g_s D_{v1} \quad (11.2)$$

Where  $P_{wh}$  is the production pressure at the wellhead. Because there is not liquid production  $P_{wh}$  should be equal to the pressure at the separator.  $g_s$  is the pressure gradient of the liquids in the well, which could be the completion fluids (if the well is being unloaded after a workover job, for example) or the fluids that the well produces (if the well is being unloaded after a routine valve change out).  $D_{v1}$  is the true vertical depth of the first valve.

If the liquid level is thought to be the reservoir static liquid level, then the production pressure at the depth of the first valve is calculated using the following expression:

$$P_{pd} = f_g P_{wh} + g_s [L_{est} - (D_{pt} - D_{v1})] \quad (11.3)$$

Where  $L_{est}$  is the true vertical length of the static liquid column from the perforations to the liquid level and  $D_{pt}$  is the true vertical depth of the top of the perforations.  $P_{wh}$  could be expressed in psig,  $g_s$  in psi/ft. with  $L_{est}$ ,  $D_{pt}$ , and  $D_{v1}$  in feet.  $g_s$  was already defined earlier. Eq. 11.3 can only be used if the static liquid level is above the first valve, for which  $[L_{est} - (D_{pt} - D_{v1})]$  is a positive number, otherwise the tubing is empty at the first valve and the

production tubing pressure at the first valve is equal to  $f_g P_{wh}$ , where  $f_g$  is the gas factor calculated with a surface pressure equal to  $P_{wh}$ .

The liquid level corresponds to the reservoir static liquid level when the well has been left for a long time with the gas injection shut off, but with the tubing opened and exposed to the separation pressure. If the well has a standing valve installed at the bottom, the liquid level might not be the reservoir static liquid level because the formation can not absorb any liquid column present in the tubing above the static liquid column.

When the unloading process starts, the liquid in the annulus enters the tubing and generates a liquid column that could be longer than the reservoir static liquid column. The liquid level can be at any point below or above the first valve, including the possibility that it can be all the way up to the surface. Once the unloading operation stops for not having a high enough injection pressure to overcome the production pressure at the first valve, the liquid level will start decreasing because the formation can absorb liquids and, eventually, the liquid level will become equal to the reservoir static liquid level. The problem is that it is usually not known how fast the liquid level is going to decrease. It is possible that after only a short time the liquid level drops to a point in which the injection pressure can overcome the production pressure and the unloading process can be restarted. It is also possible that the liquid flow into the reservoir becomes so slow that the liquid level virtually remains constant for a long time. The liquid level can be measured by wireline or by sonic devices if it is desired to confirm that the unloading process has stopped because the gas injection pressure cannot overcome the high production pressure. When the liquid level is measured, the production pressure at valve's depth is calculated as  $P_{pd} = f_g P_{wh} + g_s L$ , where  $L$  is equal to the true vertical liquid column above the first valve.

If the gas injection pressure  $P_{iod1}$  is less than  $P_{pd}$ , the problem is not having a sufficiently high injection pressure to unload the well. This could be explained by a possible error made while estimating the depth of the first mandrel, such as:

- A smaller unloading fluid pressure gradient or a larger gas pressure gradient used in the calculations.
- A lower wellhead pressured used during the spacing calculations.
- The current available injection pressure is less than the one used in the design.

The well could be finally unloaded by following the operational steps given earlier in [Section 11.3.1](#) or the production tubing string could be replaced by another one with more appropriate mandrel spacing.

If the injection pressure is greater than the production pressure, then the gas might not be injected into the well because the gas lift valve is closed due to an error made in the calculation of the injection opening pressure. To check if this is true, the gas lift valve force balance equation, applied to the first valve, should be used with the available calibration data from the current design in the well's file. Because the well is not producing liquid, the valve temperature must be equal to the geothermal temperature. Valve mechanic equations are used to find the valve opening pressure from the design test-rack opening pressure using the production and injection pressures calculated earlier for the first valve and at the geothermal temperature at that depth.

The error could be due to a bad design that gives an injection opening pressure higher than the available injection pressure at the first valve. But if the injection pressure is high enough to open the valve and overcome the production pressure (so that gas injection should be possible) then the reason why the well is not receiving gas could be due to an error made at the shop, calibrating the valve at the wrong pressure or not setting correctly the tail plug to protect the dome pressure so that the valve's dome could had been pressurized once it was exposed to a high pressure in the well.

The required calculation procedures that are used to find the injection opening pressure ( $P_{cvo}$ ) and injection closing pressure ( $P_{cvc}$ ) for each type of gas lift valve are presented in Section 11.4.2. These equations are basically the same as those described in chapter: Gas Lift Valve Mechanics but they are presented in this chapter from the perspective of a person troubleshooting a well. The injection opening and closing pressures are found from the calibration information given in the well's file and from current operational conditions. General comments, and possible interpretations of the results obtained from these equations, are presented next for each type of gas lift valve.

#### 11.4.1.1 **Nitrogen-charged, IPO valves**

If the calculated injection opening pressure  $P_{cvo}$  is greater than  $P_{iod1}$ , the valve cannot open and there must be a design error estimating the temperature or the production pressure. If  $P_{iod1}$  is greater than  $P_{cvo}$  and it is also greater than the production pressure at the depth of the first valve, and yet gas cannot be injected, then the problem may be due to a calibration error made at the shop or the valve's tail plug has failed and the dome has been pressurized.

#### 11.4.1.2 **Spring-loaded, IPO valves**

These valves are not widely used because they require an injection pressure much higher than the opening pressure to fully open the valve. They are

usually used in wells where steam is injected to heat the formation near the well. Nitrogen-charged valves are calibrated by measuring the valve's opening pressure at the test rack, while most spring-loaded valves are calibrated by measuring the valve's test-rack closing pressure and only few models of spring-loaded valves are calibrated by measuring the test-rack opening pressure (this is indicated by the valve's manufacturer). It is advisable to check with the valve's manufacturer the way a particular valve should be calibrated. Sometimes, an operator from a service company calibrates the valves in the wrong way, not following the procedures established by the service company itself. Meanwhile, engineers in the operating company are troubleshooting the well thinking that the valves have been properly calibrated and therefore reaching wrong conclusions. However, it also happens all the way around, engineers from an operating company troubleshooting the wells are not aware of the calibration procedure for a particular valve model (by opening or closing it). Communication between operating and service companies should be constant and effective. The comments regarding  $P_{cvo}$  and  $P_{iod1}$  presented above for nitrogen-charged, IPO valves also apply to spring-loaded, IPO valves except for the fact that it is hard for spring-loaded valves to have a failure due to the pressurization of the dome because the dome in this case is sealed at atmospheric pressure.

#### 11.4.1.3 Nitrogen-Charged, PPO Valves

The gas injection pressure plays a secondary role in the opening of this type of valve. If the valve does not open, it should be because the production pressure is not high enough. The injection pressure can be calculated anyway from Eq. 7.10 (in which the previously calculated production pressure  $P_{pd}$  is used and the bellows pressure at geothermal conditions,  $P_{bt}$ , must be first calculated using Eq. 11.4 given in Section 11.4.2 or using Eq. 7.16, for which the iteration procedure described in Fig. 7.3 must be used):

The valve opens because of the combined action of pressures  $P_{cvo}$  and  $P_{pd}$ , but for the valve to open and remain opened in a stable manner, the production pressure,  $P_{pd}$ , must be greater than  $[P_{bt} + (1 - R)P'_r]$ , which are the pressures that try to close the valve, as explained in chapter: Gas Lift Valve Mechanics.  $P_{pd}$  in conjunction with  $P_{cvo}$ , can open the valve but it will immediately close again if  $P_{pd}$  is not greater than  $[P_{bt} + (1 - R)P'_r]$ . This is because  $P_{cvo}$  (which is usually much greater than  $P_{pd}$ ) is acting on the port area while the valve is closed, but as soon as the valve opens  $P_{cvo}$  is replaced by the production pressure  $P_{pd}$  which is smaller than  $P_{cvo}$  and, in consequence, the valve closes. Thus, the questions to be asked for this type of valve are if the production pressure is high enough to open the valve and keep it open and, at the same time, if the production pressure is less than

the injection pressure so that the gas can be injected into the tubing. If both conditions are met and yet the valve does not open, then it must be suspected that a calibration error has been made or the tail plug has failed, and the valve should be pulled out of the well to be inspected.

#### 11.4.1.4 *Spring-loaded, PPO valves*

These are the most widely used PPO valves and they are calibrated by measuring the valve's closing pressure at test-rack conditions. The test-rack closing pressure,  $P_{tr}$ , is the test-rack "production" pressure at which the valve closes.  $P_{tr}$  does not need to be corrected by temperature. The production pressure  $P_{pd}$  must be greater than  $P_{tr}$  and less than  $P_{iod1}$  for the valve to open and stay opened and gas can be injected into the tubing. If both conditions are met and yet gas cannot be injected into the well, then it must be suspected that a calibration error has been made, in which case the valve should be pulled out and inspected. It is hard for this type of valve to have a failure due to the pressurization of the dome because the dome in this case is sealed at atmospheric pressure.

If the calibration is done by measuring the test-rack production opening pressure, the production pressure above which the valve opens and stays opened is equal to  $[(1 - R) P_{tro}]$ , where  $P_{tro}$  is the test-rack production opening pressure. If the design data and the valve mechanic equation indicate that the valve should be opened and gas can be injected into the tubing, then there is an error in the calibration of the valve at the shop and the valve should be pulled out of the well and its calibration should be verified at the shop. It is also hard for this type of valve to have a failure due to the pressurization of the dome because the dome in most cases is sealed at atmospheric pressure.

The reader is advised to review Problem 7.2, which constitutes an example of how to use valve mechanic equations in troubleshooting analyses.

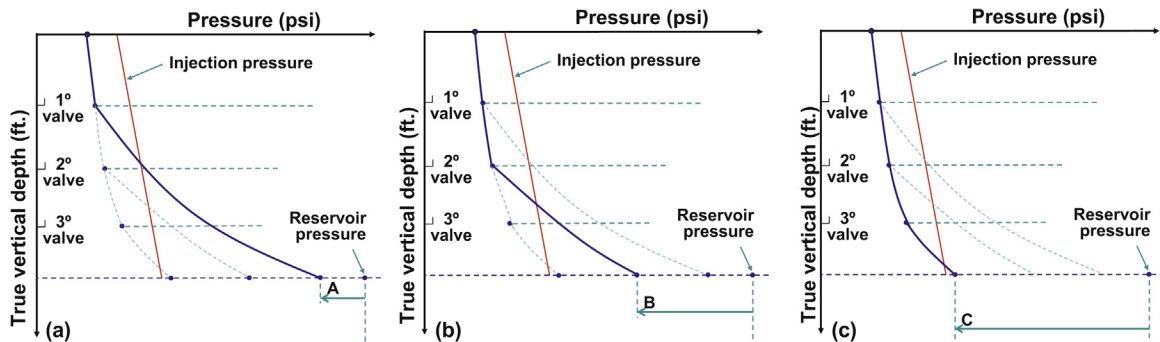
### 11.4.2 **Methodology for one or several stable points of injection below the reservoir static liquid level**

The operating valve does not necessarily have to be the deepest valve or the design point of injection. If the well is producing liquids, the point of injection should be below or at the static fluid level (although the current point of injection could be slightly above the static liquid level if this level was calculated from the formation liquid pressure gradient and the reservoir pressure alone, without taking into consideration the effect of the formation gas). If liquid production is less than its expected value, it is possible that the actual injection point depth is located above the design point of

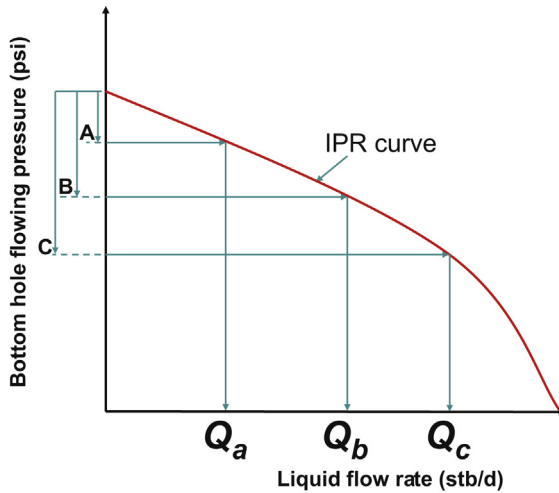
injection, unless the well is losing production due to formation damage, sand accumulation, abnormal reservoir pressure decline, or any other reason covered in Section 11.3. In any case, each of the valves installed in the well should be analyzed separately to determine if any of them corresponds to the current point of injection. In this section, only the possibility of having a single point of injection is analyzed but, in the calculation procedure, the injection gas mass balance could hint the existence of more than just one point of injection.

The methodology explained here applies to wells where the point of injection is at the design point of injection depth or at any mandrel above it if the unloading process was not completed: Many times and for a variety of reasons, the actual gas injection takes place above the design point of injection, but below the static liquid level, so that the well produces liquids (in these cases, there is usually a decrease in liquid production for not being able to inject gas as far down as possible, although in some cases the well cannot be lifted from the design point of injection precisely because the liquid production turns out to be greater than expected and the production pressure is simply too high). It can be seen in Fig. 11.1 that if (for any of the reasons given in Section 11.3) the gas injection takes place only through the first valve, the gas injection pressure is not high enough to inject gas through the second valve because the production pressure would be greater than the injection pressure at the depth of the second valve. A list of possible causes for not being able to transfer to the next deeper point of injection during the unloading of the well is presented in Section 11.3.

As can be observed in Fig. 11.1, the injection pressure might be high enough to reach the deepest valve, but any valve could actually be the current point of injection for the given surface production and injection pressures (which



■ FIGURE 11.1 Pressure–depth diagram for three possible points of injection. (a) Gas injection through first valve, (b) Gas injection through second valve, and (c) Gas injection through third valve.



■ FIGURE 11.2 Three possible liquid flow rates  $Q_a$ ,  $Q_b$ , and  $Q_c$  for each drawdown (A, B, and C) shown in Fig. 11.1.

are the same for the three possibilities depicted in Fig. 11.1). Furthermore, gas could be injected through more than one point of injection in a stable manner. The response of the reservoir to each of the drawdowns shown in Fig. 11.1 (A, B, and C) is presented in Fig. 11.2.

In the following paragraphs, a rather rudimentary calculation procedure that can be used to find the current point of injection is described. Given the usual inaccurate data available in gas lift fields to perform troubleshooting analyses, this procedure is the best that can be done in many occasions. As it will become apparent, there could be none, one, or more than one solution that will fit the measurements done at the surface (pressures, fluid properties, and flow rates); therefore, the troubleshooting analysis might not be conclusive and field techniques presented in Section 11.5 might be required to troubleshoot the well. The following analysis is carried out assuming that any valve, for any reason, could be the actual point of injection. This is why all calculations are performed separately for all possible points of injection, which correspond to the depth of each mandrel installed in the well, even if they have dummy valves installed in them because these valves might only be partially installed inside the side pocket of the gas lift mandrel. Clearly, for mandrels with dummy valves no calculations are performed regarding gas flow rate or the valve's mechanics. This procedure does not take into account any depth other than the ones corresponding to the gas lift mandrels installed in the well. Holes in the tubing or leaks in the packer or at the wellhead are less probable to occur, much more difficult to analyze, and

easily detected by communication tests and other operational procedures discussed in [Section 11.5](#).

The results that are obtained from the following calculation steps (for a particular point of injection) should be analyzed and compared with all other possible points of injection. The most probable point of injection is the one that shows more coherence in the results obtained from the different calculations procedures involved in the analysis: valve mechanics, injection gas mass balance, and liquid flow rates determined from the IPR curve (if available).

The first step is to determine the gas injection pressure at each mandrel's depth. This injection pressure is calculated from: (1) gas injection pressure and temperature at the wellhead, (2) gas specific gravity, and (3) injection gas flow rate if it is suspected that friction pressure drop could play an important role in determining the gas injection pressure at depth. The calculation of the injection pressure at depth is performed using any of the different procedures described in chapter: Single-Phase Flow to find the gas factor  $f_g$ .

Once the gas injection pressure is calculated at the depth of each mandrel, the following steps are carried out “independently” for each possible point of injection. To begin calculations, one of the gas lift mandrels installed in the well is picked as the assumed injection point depth. After completing the following calculations, a new mandrel is selected as the new point of injection and all calculations are repeated. This process continues until all mandrels have been separately considered.

- The production pressure is calculated at all mandrel depths, assuming that all the gas (measured at the surface) is injected only through the “assumed point of injection” that is under analysis. The production pressure is calculated using the total gas/liquid ratio above the assumed point of injection and the formation gas/liquid ratio below it. This should be done using the multiphase flow correlation or model that is thought to give the best results for current operational conditions.
- With the upstream injection pressure and the downstream production pressure (calculated at each mandrel), the valve's mechanic equations are used to determine if the valves are opened or closed. All valves installed in the well are considered in this step even if it is not strictly correct to do so because the opening pressure of each valve depends on the calculated production pressure, which was found by assuming that all the gas was injected only through the assumed point of injection. IPO valves have injection opening pressures greater than the injection closing pressure. The difference between the opening and closing pressure is called the “spread” of the valve. An IPO valve is opened if



the injection pressure is above the injection opening pressure and it is closed if the injection pressure is below the valve's injection closing pressure (all these pressures are evaluated at the valve's depth). If the injection pressure lies between the opening and closing pressures, it is uncertain if the valve is opened or closed and the valve's dynamic models that are explained in chapter: Gas Flow Through Gas Lift Valves must be used to find that out. The valve's dynamic models can also determine the gas flow rate that a valve can pass for given upstream and downstream pressures, gas injection temperature, and the valve's closing pressure. If the injection pressure lies between the injection opening and closing pressures, the fact that a model predicts that the valve is opened does not necessarily mean that the valve is actually opened: if the injection pressure reached its current value from a pressure lower than the closing pressure, the valve should still be closed. However, if the valve was already opened and the pressure was reduced to a value between the opening and closing pressures, then the valve could be opened if the dynamic conditions are right. This adds an extra difficulty to the analysis of the results when doing the injection gas mass balance. PPO valves are considered to be opened if the production pressure is above the value for which they open and remain open in a stable manner. This procedure is extremely inaccurate for PPO valves. In conclusion, calculations involving valve mechanics and dynamic models determine which of the valves might be opened, but only as a very rough approximation for valves other than the assumed point of injection (the idea is to know if for that particular point of injection there might be additional valves opened).

- The next step is to calculate the gas flow rate that can pass through the particular valve under investigation (the one assumed to be the current point of injection). For the injection gas to pass through a given valve, the injection pressure should be greater than the production pressure and the valve should be open. The gas flow rate is calculated using two types of procedures:
  - Assuming the valve is in good working condition, in which case the gas flow rate is calculated using the dynamic models explained in chapter: Gas Flow Through Gas Lift Valves. When the gas flow rate is in throttling flow, the dynamic model might indicate that the valve is closed and the gas flow rate is equal to zero.
  - Assuming that the valve is damaged and totally open so that calculations are performed as if the valve is an orifice valve using the Thornhill–Craver equation (explained in Chapters: Single and Multiphase Flow Through Restrictions and Gas Flow Through Gas Lift Valves), which gives similar results to the ones obtained by

the dynamic models if the valve is totally open. Regardless of the status of the valve (opened or closed) as determined by the valve mechanic equations, the gas flow rate through the assumed point of injection is always calculated because the valve might indeed be opened due to any valid reason, like being flat or simply stuck open.

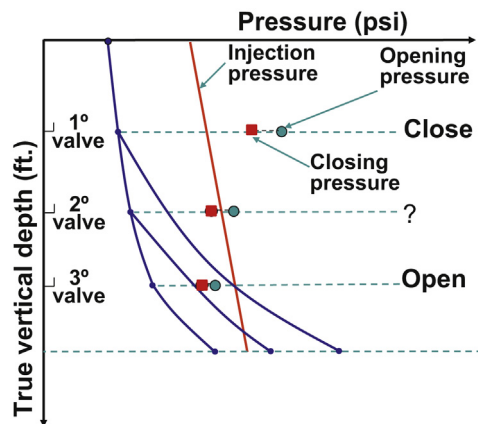
- If calculations determine that there is only one valve opened and it corresponds to the point of injection being investigated, the measured gas flow rate at the surface should be approximately equal to the gas flow rate calculated for the assumed point of injection. But if the measured gas flow rate is much larger than the one calculated using both, the dynamic models and the Thornhill–Craver equation, it is then possible that:
  - The operating valve is another one;
  - There is more than just one point of injection; or
  - The data used to calculate the gas flow rate is not accurate.

Usually, dynamic models results are not very accurate because they are very sensitive to the valve's closing pressure. Any small error in the calculation of the valve's temperature is going to cause a small deviation on the calculated injection closing pressure, which in turn could induce a very large error in the estimation of the gas flow rate using dynamic models. The error could also be due to an injection gas pressure at depth calculated using a gas specific gravity or gas injection surface pressure inaccurately measured. In any case, even if the injection gas mass balance does not give very accurate results, it could show that there might or might not be multiple points of injection. For example, if the error made in the calculation of the gas flow rate is from 100–200 Mscf/D, but the calculated gas flow rate is still 600 Mscf/D less than the measured surface injection gas flow rate, it is highly possible that there might be multiple points of injection or that the operating valve is different from the one being analyzed.

- As previously mentioned, even if it is not strictly correct, for a given assumed point of injection all other valves are checked to see if they are opened or closed. If any of them is opened and the injection pressure is greater than the production pressure, then the gas flow rate that can pass through that valve (different from the assumed point of injection) is also calculated. This is only an approximation because the production pressure at each valve was calculated assuming that all the gas is being injected through the assumed point of injection. Here too, the gas flow rate is calculated in two different ways: using dynamic models and using the Thornhill–Craver equation.

- The injection gas mass balance consists in comparing the sum of the gas flow rates of all the valves that might be opened with the measured gas flow rate at the surface. This balance is performed taking into account the fact that, for each assumed point of injection, there might be other valves opened with the injection pressure greater than the opening pressure or with the injection pressure between the closing and opening pressures. If the injection gas flow rate measured at the surface is much greater than the gas flow rate that each valve can pass individually, there is a strong possibility that there are multiple points of injection.
- For each assumed single point of injection, it must be determined if the calculated bottomhole flowing pressure is compatible with the actual liquid production, taking into account the IPR curve. The bottomhole flowing pressure is calculated from the wellhead pressure, the total gas and liquid production, the injection gas flow rate through the assumed point of injection, and the particular depth of the assumed point of injection being investigated. With the calculated bottomhole flowing pressure, the liquid production can be estimated using the IPR curve of the well, as shown in Fig. 11.2. Unfortunately, this step is in many cases impossible to perform in an accurate way because of the lack of reliable data to build the IPR curve or due to inaccuracies that have to do with the calculation of the bottomhole flowing pressure (inaccurate multiphase flow correlations or PVT data).
- All previous steps are repeated for a new “assumed” point of injection depth.

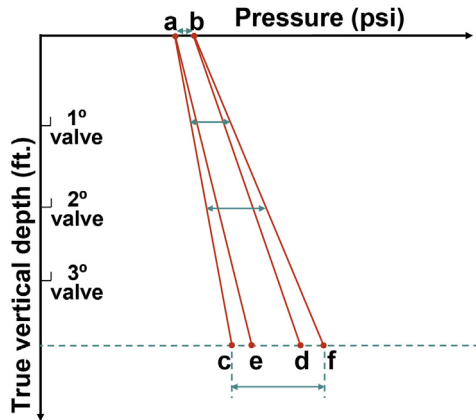
Due to the uncertainty in determining if the valve is opened or closed, valve’s mechanics equations are used in combination with the dynamic models. Knowing the type of valve installed in the well, its temperature, its seat diameter, and its calibration pressure, it is easy to determine its bellows pressure at operating conditions. From these values, the valve’s opening pressure at valve’s depth is calculated. For IPO valves, for example, the value of this calculated opening pressure is compared with the gas injection pressure at depth, which is calculated from the measured surface injection pressure. If the opening pressure is less than the injection pressure, it is highly possible that the valve is opened. The valve could also be opened even if the injection pressure is below the opening pressure, however, as it was pointed out earlier, only if the injection pressure is higher than the closing pressure and the valve was already opened before reaching the current injection pressure. For nitrogen-charged, IPO valves, the closing pressure is equal to the bellows pressure at operating conditions (if the valve does not have a spring to protect the bellows, as explained in chapter: Gas Lift Valve Mechanics).



■ FIGURE 11.3 Opening and closing pressures of each valve for a given point of injection (IPO valves).

The opening and closing pressures of IPO valves are shown in Fig. 11.3 as an example. These pressures were calculated for an assumed point of injection, but they could have been calculated for any of the three possible points of injection. For each assumed point of injection, these pressures are going to be only slightly different because the production temperature and pressure, which depend on the depth of the point of injection, have a small impact on the opening pressure of an IPO valve. Depending on the working condition of each valve in this figure, it can be appreciated that the first valve might be closed, the second valve might be opened or closed, and the third valve might be opened.

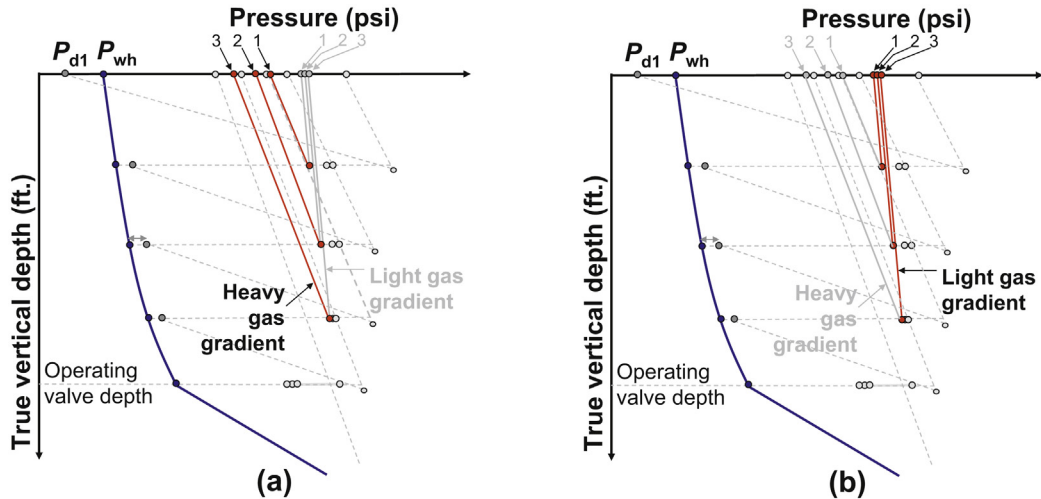
It is important to point out once again that even though it is very easy to calculate the gas injection pressure at depth, this calculated pressure will not be accurate if the surface injection pressure and/or the gas specific gravity are not precisely determined. It is necessary to check the surface injection pressure with a recently calibrated sensor. The maximum reading of the instrument should also be adequate for the value of the pressure being measured. A pressure sensor with a range from 0 to 5000 psi and an accuracy of 1% of its maximum reading will have an error of 50 psi, which is not acceptable for most troubleshooting calculations. The errors that can be made due to the uncertainties in the measurement of the surface pressure and the gas specific gravity are shown in Fig. 11.4. The error that might be present in the surface gas injection pressure measurement is represented by line a–b in the figure. It is also uncertain what the gas specific gravity is. From point “a” and “b” the injection pressures at depth are calculated for the estimated minimum gas specific gravity. This gives the pressures at “c” and “d.” From point “a” and “b” the injection



■ FIGURE 11.4 Error in the estimation of the injection pressure at depth due to errors in the surface injection pressure and gas specific gravity measurements.

pressures at depth are calculated for the estimated maximum gas specific gravity. This gives the pressures at “e” and “f.” Clearly, the combined uncertainty represented by line c–f can be large and its value increases with depth.

Not knowing the gas specific gravity could lead to serious design faults, which could in turn cause valve interference or, in extreme cases, the impossibility to unload the well because the lower valves could have surface closing pressures larger than the ones for the upper valves: Fig. 11.5a shows

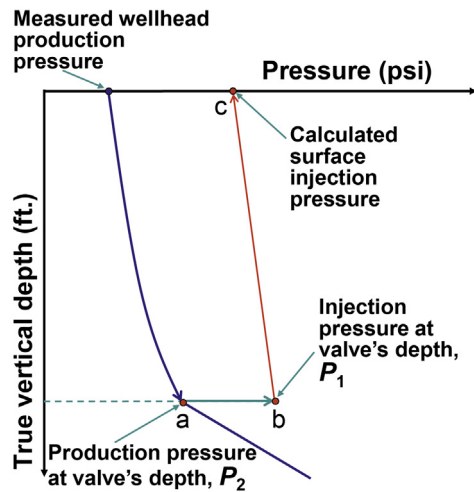


■ FIGURE 11.5 Design error caused by assuming a larger than actual gas specific gravity (IPO valves).

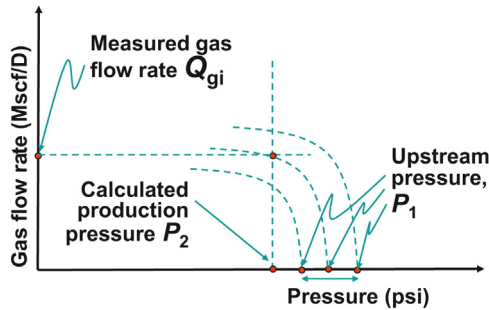
the original design assuming a gas specific gravity much greater than it actually is. For the high gas specific gravity, the design surface closing pressures make sense because their values decrease for deeper valves. But the same design for a lower gas specific gravity would not work because the surface closing pressures of the deeper valves will actually be greater than the ones for the valves above, as shown in Fig. 11.5b. Additionally, for the example shown in the figure it will not be possible to reach the first (shallowest) valve because the injection pressure at depth will be less than the production pressure. The situation depicted in Fig. 11.5 is an extreme condition that rarely happens but it is shown to emphasize the importance of accurately knowing the gas specific gravity.

For orifice valves (or a calibrated valve thought to be damaged and fully opened) the following calculation technique is sometimes used. It is similar to the one just explained earlier and consists of the following steps (Fig. 11.6):

- The production pressure at valve's depth  $P_2$  is calculated from the wellhead pressure, the total gas flow rate, and the liquid production. For this purpose, the multiphase flow correlation estimated to be the most appropriate one for current operational conditions is used.
- Using an iteration procedure explained in Fig. 4.8 and in Fig. 11.7 below, the injection pressure upstream of the orifice  $P_1$  is calculated



■ FIGURE 11.6 Surface injection pressure estimated from the measured wellhead production pressure, liquid, and gas production flow rate, orifice diameter, and injection gas flow rate.



■ FIGURE 11.7 Calculation of the upstream pressure  $P_1$  from the downstream pressure  $P_2$ , the orifice diameter, and the known injection gas flow rate  $Q_{gi}$ .

from the production pressure  $P_2$ , the orifice or seat diameter, and the gas flow rate. Any equation for gas flow rate calculation through an orifice, such as the Thornhill–Craver equation or the orifice flow equations developed at The University of Tulsa, can be used in the iterations.

- From the upstream pressure found in the previous step ( $P_1$ ), the surface injection pressure is calculated. This can be done by trial and error: for different surface injection pressures, the gas factor used to calculate the injection pressure at depth is found. The surface injection pressure that gives a downhole pressure equal to the injection pressure at depth  $P_1$  is compared with the measured surface injection pressure. If they are approximately equal then the valve under investigation is the possible point of injection. If they are different, it is possible that the point of injection is another one or that the data used in the iterative process to find  $P_1$  from the value of  $P_2$  is not sufficiently accurate for such a procedure.

The steps just described earlier are presented in Fig. 11.6.

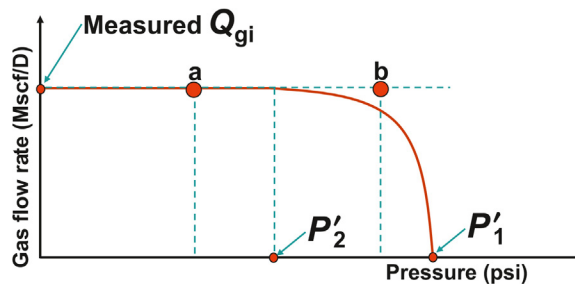
If the gas injection flow through the orifice (or calibrated gas lift valve supposed to be damaged and fully opened) is critical flow, then this procedure could turn out to be very accurate. However, if the flow is subcritical, the results might not be too reliable because the iteration procedure explained in Fig. 11.7 to find the valve's upstream pressure is very sensitive to the calculated production pressure  $P_2$ , which is calculated from multiphase flow correlations that most of the time gives an error that is unacceptable for the procedure explained in Fig. 11.6.

The iterative procedure that is used to calculate the pressure upstream of the orifice valve ( $P_1$ ) if the orifice diameter, gas flow rate, and downstream

pressure are known is explained next. It is a complex procedure because if  $P_1$  is not known, the gas flow rate curve as a function of the downstream pressure is also an unknown.

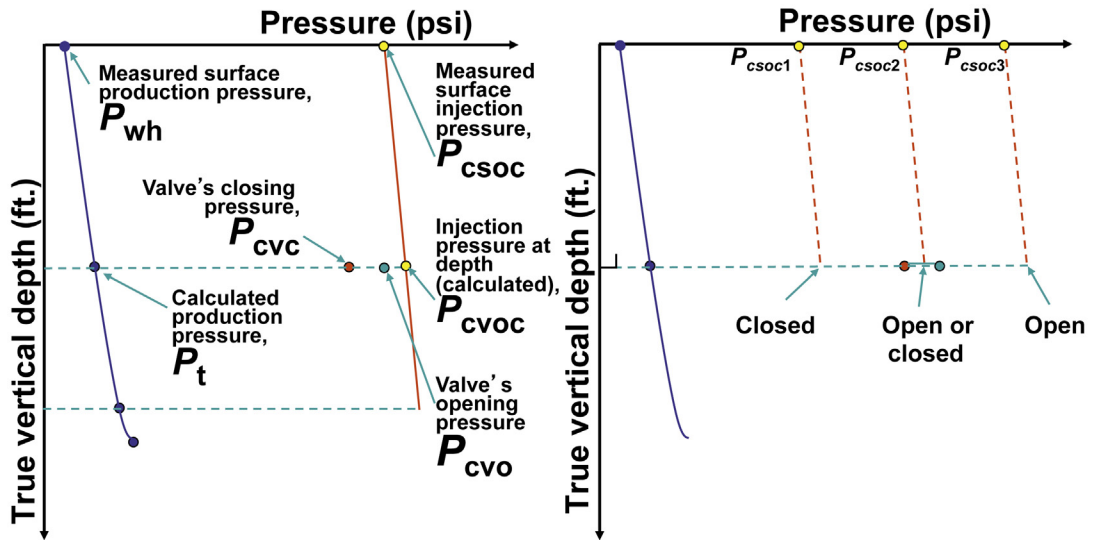
As can be seen in Fig. 11.7,  $P_1$  needs to be found from an iterative procedure in order for the gas flow rate curve to pass through the point with coordinates given by the known gas flow rate  $Q_{gi}$  and the calculated production pressure  $P_2$ . For this process, the first value of  $P_1$  must be assumed. Then, the gas flow rate corresponding to  $P_2$  is calculated using, for example, the Thornhill–Craver equation (with  $P_1$ ,  $P_2$ , and the orifice diameter). If the calculated gas flow rate is less than the measured gas flow rate, the value of the assumed  $P_1$  should be increased and vice versa. In any case, the difference between the calculated and the measured gas flow rates can be used to estimate the new value of  $P_1$ .

But it is not always necessary to iterate to find  $P_1$ . In Fig. 11.8, it can be seen that for a given gas flow rate and orifice diameter there is one and only one value of the upstream pressure, known here as  $P'_1$ , for which the flow is critical. This unique value of  $P'_1$  could be directly found from the Thornhill–Craver equation (Eq. 4.25), using in this equation the pressure ratio  $r$ , equal to  $P_2/P_1$ , for critical flow as  $r = [2/(k' + 1)]^{k'/(k'-1)}$  and the known gas flow rate  $Q_{gi}$  ( $k'$  is the gas specific heat ratio). Once the value of  $P'_1$  has been found in this way, the value of  $P'_2$  is simply equal to  $r(P'_1)$ . If the pressure  $P_2$  (calculated from the wellhead production pressure using multiphase flow correlations) is less than or equal to  $P'_2$ , the value of  $P_1$  is precisely  $P'_1$ . This corresponds to case “a” in Fig. 11.8. Otherwise, the value of  $P_1$  must be determined by iteration, which is case “b” in Fig. 11.8. If the gas flow through the orifice is critical flow, this procedure to find  $P_1$  is very accurate (because it does not depend on the value of  $P_2$ , which is hard to calculate in an accurate manner) as long as the gas flow rate and the surface injection pressure have been accurately measured.



■ FIGURE 11.8 Determining if iterations are needed to find  $P_1$ .





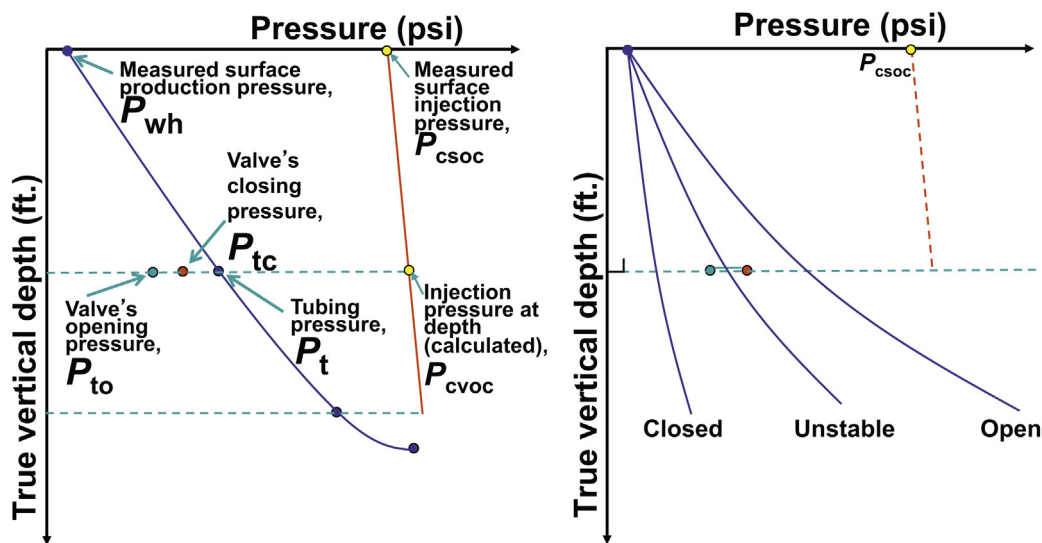
■ FIGURE 11.9 Nomenclature used in the valve-mechanic equations for IPO valves and the required surface injection pressures for the valve to be opened or closed.

The procedure described in Fig. 11.6 could be applied to a calibrated valve in good working condition, but instead of using simple gas flow rate equations (like the Thornhill–Craver equation), valve’s dynamic models should be used; but because these model require very accurate data, this procedure is simply not recommended for calibrated valves unless it is absolutely certain that the gas flow through the valve corresponds to “orifice flow” and not to throttling flow.

As a final topic in this section, the equations that are used to find the opening and closing pressures for the different types of valves and their respective calibration procedures (by opening or closing the valve at the test rack) are now presented from the perspective of a troubleshooting analysis, as opposed to their usage for gas lift design purposes. This means that the opening and closing pressures are calculated from the calibration data found in the well’s file. Fig. 11.9 shows the nomenclature used in these equations for IPO valves and the required surface pressures for the valve to be opened or closed. Fig. 11.10 shows the same information but for production-pressure operated valves.

First of all, for nitrogen-charged gas lift valves it is important to calculate the dome pressure at operating conditions. Two ways of doing this calculation are presented in chapter: Gas Lift Valve Mechanics, one of which is very easy to use and it is presented here.

The following equation can be used to find the dome pressure at operating conditions ( $P_{bt}$ ) from the dome pressure at test-rack conditions ( $P_b'$ ):



■ FIGURE 11.10 Nomenclature used in the valve-mechanic equations for PPO valves and the required production pressures for the valve to be opened or closed.

$$P_{bt} = P'_b b - a \quad (11.4)$$

Where  $a$  and  $b$  are parameters given by:

$$a = 0.083(T_v - 60)$$

$$b = 1 + 0.002283(T_v - 60)$$

Where  $T_v$  is the valve operating temperature in °F. Eq. 11.4 should not be used for values of  $P_{bt}$  greater than 2000 psig or operating temperatures greater than 220°F. If Eq. 7.16 is used instead of Eq. 11.4, an iterative procedure described in Fig. 7.3 should be used. This iterative procedure is a more complicated way of calculating the bellows pressure but could be more accurate for high surrounding pressures and temperatures. Recently developed gas lift valves for high-pressure applications require different parameters to calculate the dome pressure at operating conditions, the reader should consult valves' manufacturers for these cases.

The operating temperature of a wireline retrievable valve installed in a standard side pocket mandrel lies between the gas injection temperature and the temperature of the production fluids. It is important to know the relative position of the upper packing of the gas lift valve in relation to the dome of the valve to estimate the temperature inside the dome. In 1-inch outside diameter valves, a good part of the dome is located below the upper packing of the valve, thus the dome is mostly exposed to the gas injection temperature. The opposite is true for 1.5-in. OD valves, in consequence the dome is mostly exposed to the production fluid temperature. This topic is explained in detail in Chapters: Gas Lift

Valve Mechanics and Design of Continuous Gas Lift Installations. The upper and lower packing of wireline retrievable valves are identified in Fig. 6.4.

The value of  $P'_b$  used in Eq. 11.4 is equal to  $(P_{tr} - P'_r)(1 - R)$  for nitrogen-charged, IPO valves, where  $P_{tr}$  is the test-rack injection opening pressure in psig,  $R$  is the area ratio of the valve, and  $P'_r$  is the spring constant pressure of the spring provided in some valve models to have an additional closing component to protect the nitrogen-charged bellows ( $P'_r$  is usually a fixed value supplied by the valve's manufacturer). If the valve does not have a spring then  $P'_r$  is equal to zero. The expression for  $P'_b$  for nitrogen-charged, PPO valves is the same as the one for nitrogen-charged, IPO valves, that is  $(P_{tr} - P'_r)(1 - R)$ , but in this case  $P_{tr}$  is the test-rack "production" opening pressure and not the test-rack "injection" opening pressure. For both types of valves, this expression is then introduced in Eq. 11.4 to give an equation for  $P_{bt}$  in terms of  $P_{tr}$ ,  $P'_r$  and  $R$ , which can all be easily found in the well's file. Introducing Eq. 11.4 (with this expression for  $P'_b$ ) in the force balance equations given in chapter: Gas Lift Valve Mechanics for each type of valve, gives the equations that are listed next and that can be used in the troubleshooting process to find the valve's opening and closing pressures at operating conditions. In the following equations all pressures are expressed in psig.

*Nitrogen-charged, IPO valves*

The valve's closing injection pressure at valve's depth,  $P_{cvc}$ , is:

$$P_{cvc} = (P_{tr} - P'_r)b(1 - R) + P'_r(1 - R) - a \quad (11.5)$$

Where  $P_{tr}$  is the calibration opening pressure, as reported in the gas lift design,  $P'_r$  is the spring apparent pressure (for the rare cases in which the valve has a spring to protect the bellows and, as indicate above,  $P'_r$  is a fixed value usually supplied by the valve's manufacturer),  $R$  is the valve's area ratio, and factors  $a$  and  $b$  are the parameters used in Eq. 11.4 to calculate the dome pressure at operating conditions  $P_{bt}$  from the dome pressure at test-rack condition  $P'_b$ .

The valve's opening injection pressure at depth,  $P_{cvo}$ , is:

$$P_{cvo} = P'_r + [(P_{tr} - P'_r)b(1 - R) - P_t R - a] / (1 - R) \quad (11.6)$$

Where  $P_t$  is the production pressure at valve's depth, which must be calculated from multiphase flow correlations (if the well is producing liquids) or from static liquid columns (if the well is not flowing, as indicated in Section 11.4.1).

*Spring-loaded, IPO valves (calibration by measuring the test-rack closing pressure)*

The valve's closing injection pressure at valve's depth,  $P_{cvc}$ , is:

$$P_{cvc} = P_{tr} \quad (11.7)$$

$P_{tr}$  is the test-rack calibration closing injection pressure which does not require temperature correction.

The opening injection pressure at valve's depth,  $P_{cvo}$ , is:

$$P_{cvo} = (P_{tr} - P_{tr}R)/(1 - R) \quad (11.8)$$

*Spring-loaded, IPO valves (calibrated by measuring the test-rack opening pressure)*

The closing injection pressure at depth,  $P_{cvc}$ , is:

$$P_{cvc} = (1 - R)P_{tr} \quad (11.9)$$

$P_{tr}$  is the test-rack calibration opening injection pressure which does not require temperature correction.

The opening injection pressure at valve's depth,  $P_{cvo}$ , is:

$$P_{cvo} = [P_{tr}(1 - R) - P_{tr}R]/(1 - R) \quad (11.10)$$

*Spring-loaded, PPO Valves (calibrated by measuring the test-rack opening pressure)*

The valve's closing production pressure at depth is:

$$P_{tc} = (1 - R)P_{tr} \quad (11.11)$$

$P_{tr}$  is the test-rack opening production pressure.

The valve's opening production pressure at valve's depth is:

$$P_{to} = [P_{tr}(1 - R) - P_{cvoc}R]/(1 - R) \quad (11.12)$$

Where  $P_{cvoc}$  is the gas injection pressure at depth.

As can be seen in Fig. 11.10, the valve's closing production pressure is greater than the valve's opening production pressure (according to their definitions given here). This is due to the effect that the injection pressure  $P_{cvoc}$  has on the behavior of PPO valves.  $P_{cvoc}$  is usually much greater than the production pressure. When the production pressure increases from a value less than  $P_{to}$ , a point is reached in which the combination of the injection and production pressures is able to open the valve. But once the valve is opened, pressure  $P_{cvoc}$  (which is greater than the production pressure) no longer exerts a force on the ball of the valve because it is now subjected

to the production pressure, which is lower. This makes the valve close as soon as it opens. This behavior is repeated until the production pressure is increased to values greater than  $P_{tc}$ , at which point the valve remains open.

*Spring-loaded, PPO Valves (calibrated by measuring the test-rack closing pressure)*

The valve's closing production pressure at depth is:

$$P_{tc} = P_{tr} \quad (11.13)$$

$P_{tr}$  is the test-rack closing pressure.

The valve's opening production pressure at depth is:

$$P_{to} = (P_{tr} - P_{cvoc}R)/(1 - R) \quad (11.14)$$

Where  $P_{cvoc}$  is the injection pressure at valve's depth.

*Nitrogen-charged, PPO valves (calibrated by measuring the test-rack opening pressure)*

The valve's closing production pressure at depth is:

$$P_{tc} = b(1 - R)P_{tr} - a \quad (11.15)$$

$P_{tr}$  is the test-rack opening production pressure.

The valve's opening production pressure at depth is:

$$P_{to} = [P_{tr}b(1 - R) - P_{cvoc}R - a]/(1 - R) \quad (11.16)$$

Where  $P_{cvoc}$  is the injection pressure at valve's depth.

### 11.4.3 Continuous gas injection but the well does not produce liquids

If a nitrogen-charged gas lift valve, in good working condition and above the static liquid level, remains open and circulating all the injection gas through it without liquid production, it is then highly possible that its temperature is such that it would not close at the design closing pressure but at a much lower one. This can also take place for valves below the static liquid level if, for any reason like sand accumulation at the bottom of the well, the well's liquid production ceases. Therefore, the calculations presented here need to be performed, not only for valves above the static liquid level, but for all gas lift valves in the well. The drop in valve temperature is due to lack of liquid production (that would otherwise keep the valve warm) and gas expansion through the valve itself (which tends to cool the valve). This problem could

happen when the well's liquid production has not been properly estimated or the selected seat diameter is too large for current operating conditions and the valve passes a very high gas flow rate, causing the injection pressure to drop, but the valve would not close because its temperature is too low.

The isentropic gas flow through an orifice can be modeled by the following equation:

$$T_2/T_1 = (P_2/P_1)^{(k'-1)/k'} \quad (11.17)$$

Where  $P_1$  and  $P_2$  correspond, respectively, to the valve's upstream and downstream pressures in psia, while  $T_1$  and  $T_2$  are, respectively, the upstream and downstream temperatures in °R, and  $k'$  is the gas specific heat ratio,  $C_p/C_v$ . If  $T_2$  is assumed to be the valve's temperature, it has been found that it is a good approximation to set  $(k' - 1)/k'$  equal to 0.05 because the process is irreversible, with some minor heat transfer, and the valve temperature is not exactly equal to the downstream gas temperature. In Eq. 11.17, the upstream and downstream pressures can be easily calculated from the measured surface injection and production pressures because the flow is single-phase gas flow. Additionally, the upstream temperature  $T_1$  can be approximated as the geothermal temperature, thus only  $T_2$  remains to be calculated. Then this estimated valve temperature can be used to find the dome pressure,  $P_{bt}$ , which in turn can be used to get the valve's opening and closing pressures with the equations given at the end of the previous section. The valve temperature in °F to be used in the equations given above to find  $P_{bt}$  from  $P'_b$  (Eq. 11.4) is:

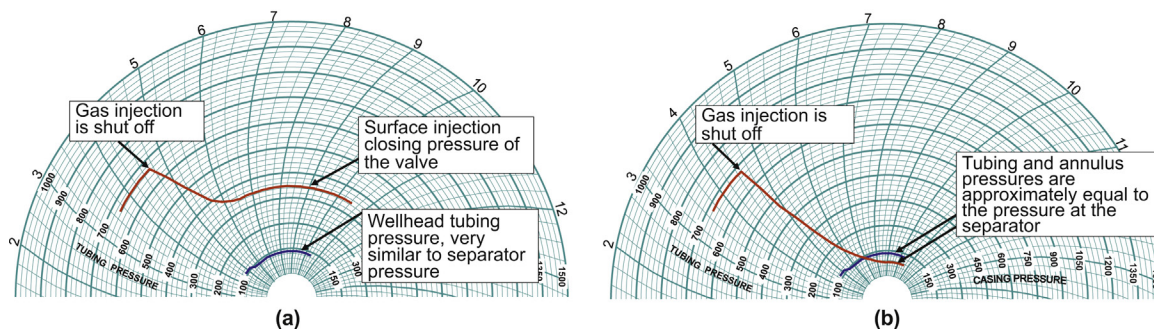
$$T_v = T_1 (P_2/P_1)^{0.05} - 460 \quad (11.18)$$

Once  $T_v$  is found, parameters  $a$  and  $b$  can also be calculated (and applied in Eq. 11.4) and the equations given in the last section can be used to find the values for the valve's opening and closing pressures (depending on the type of valve and its corresponding test-rack calibration procedure). In this case, the valve's downstream pressure is found from:  $P_t = P_{wh}f_{gt} = P_2$  and the upstream pressure is given by:  $P_{cvoc} = P_{csoc}f_{gc}$ . Here,  $f_{gt}$  is the gas pressure factor for the measured production wellhead pressure  $P_{wh}$  and  $f_{gc}$  is the gas pressure factor for the measured surface injection pressure  $P_{csoc}$ . The valve mechanic equations can indicate if the valve is opened or closed. However, for IPO valves, for example, if the upstream pressure at valve depth (injection pressure) is between the opening and closing pressures of the valve, the dynamic models given in chapter: Gas Flow Through Gas Lift Valves must be applied to determine if the valve is indeed opened or closed and to calculate the gas flow rate. Furthermore, as it was indicated in Section 11.4.2, the fact that a dynamic model predicts that the valve is opened does not necessarily

mean that the valve is actually open; if the injection pressure (between the opening and closing pressures) reached its current value from a pressure lower than the closing pressure, the valve should be closed. However, if the valve was already opened and the pressure decreased to a value between the opening and closing pressures, then the valve could be opened if and only if the dynamic conditions are right, in other words, if the production pressure is above the “production closing pressure” under dynamic conditions. The reader is advised to review Fig. 8.5 to understand the concept of “production closing pressure” under throttling flow conditions.

Continuous gas lift injection without liquid production could also be due to: (1) a hole in the tubing above the static liquid level (if the well’s perforations are plugged with sand, for example, the hole could also be below the static liquid level) or an unseated valve inside the pocket (which behaves exactly like a hole in the tubing), (2) an open flat valve, or (3) a valve stuck open (with, for example, a solid particle stuck between the ball and the seat that would not allow the valve to close). A communication test can confirm if the problem is due to a hole in the tubing or a gas lift valve in any of the following conditions: (1) at a lower than expected temperature, (2) flat, or (3) stuck open. This is because communication tests take advantage of the fact that a hole allows gas to pass in any direction (to or from the annulus), while a gas lift valve has a check valve that allows the gas to pass in only one direction. Communication tests are explained in Section 11.5.1.

As indicated earlier, an unseated valve inside the side pocket of a gas lift mandrel could make the well behave as if it had a hole in the tubing. On the other hand, a flat valve that, additionally, has a damaged check valve could also make the well behave as if it had a hole in the tubing, but this unfortunate combination is unlikely to happen. When the surface gas injection into a well that is circulating gas with no liquid production is shut off, while leaving the production tubing open to the separator or main production header, the surface injection pressure will drop to the wellhead production pressure (which should be approximately equal to the pressure at the separator) if, above the static liquid level, there is one of the following problems: a hole in the tubing, a flat valve, an unseated valve, or a valve stuck open. But if gas circulation with no liquid production is due to a valve above the static liquid level that will not close because of its low temperature, when the surface gas injection is shut off the wellhead injection pressure will drop down to the valve’s current closing pressure, which is usually lower than its design closing pressure (because of the low temperature) but not as low as the wellhead production pressure. Figs. 11.11a,b show the wellhead pressure behavior of a well circulating gas (with no liquid production) after the surface gas injection is shut off.



■ FIGURE 11.11 Behavior of the wellhead pressures of a well circulating injection gas with no liquid production when the surface injection gas flow is shut off while keeping the well open to production. (a) Valve at lower than expected temperature and (b) hole in the tubing.

Fig. 11.11a shows what happens in case of a nitrogen-charged, IPO valve at a temperature lower than expected. The final surface injection pressure corresponds to the surface closing pressure of the valve, which is lower than expected because of its low temperature.

Fig. 11.11b shows what happens when there is a hole (of a small diameter) above the static liquid level through which all the gas injected at the surface is being circulated (it could also be a flat valve or a valve stuck open, above the static liquid level). For large diameter holes, the injection pressure is usually much lower than shown in the figure (before the gas injection is shut off) and the gas flow rate is very large. The final injection pressure is equal to the final production pressure which is, in turn, very similar to the pressure at the separator in this case (the final pressure curves do not coincide in the chart because the scale for the production pressure is from 0 to 1000 psig while for the injection pressure it is from 0 to 1500 psig). Sometimes the pressure chart shows the final injection pressure to be different from the final production pressure even when the well was only circulating gas through a hole. Because the tubing hole is above the static liquid level, the difference in pressure in this case could only be due to an error in the calibration of the injection and production pressure sensors. This error can be corroborated by inverting the pressure signals; the injection pressure is connected to the production pressure sensor and the production pressure is connected to the injection pressure sensor. If the problem is due to poor calibration, the difference between the readings should still be the same (if the injection pressure sensor's reading is initially higher, for example, this sensor will still give a higher reading). In the figure, the injection gas is injected down the annulus.

For a hole with a flow area approximately equal to the flow area of a given gas lift valve that would not close due to its low temperature, the pressure drop is steeper and would not show signs of gas throttling that gas lift valves show when they are just about to close after the surface gas injection has



been shut off. When the surface gas injection into a well that has a hole in the tubing and is producing some liquid in a steady fashion is shut off, the wellhead pressures behave like those for a well circulating gas through a valve at a low temperature (Fig. 11.11a); the liquid that accumulates in the tubing above the hole (after the surface gas injection is shut off) acts as a plug that stops the surface injection pressure from dropping all the way down to the production wellhead pressure. The difference between the final wellhead injection and production pressures is equal to the hydrostatic pressure due to the difference between the liquid level inside the tubing and in the annulus.

If the problem is a flat valve or a valve stuck open, the injection pressure (after the surface gas injection is shut off) will drop at a lower rate compared to the pressure drop caused by a hole in the production tubing (of the same size of the gas lift valve's seat) because the ball interferes with the gas flow through the gas lift valve.

If the well is not producing any liquids, the average gas flow rate from the annulus into the tubing (after the surface gas injection to the well has been shut off) can be calculated in an approximate way for any selected short time interval (for which the measured initial and the final annular injection pressures should not be very different). If the liquid level in the injection annulus is known, the initial and final gas volumes in the annulus in scf can be calculated for the given short time interval using Eqs. 10.58 and 10.59 for intermittent gas lift. The gas flow rate is equal to the initial minus the final gas volume in the annulus divided by the elapsed time of the selected interval. With the gas flow rate found in this way, the Thornhill–Craver equation can be used to find the orifice diameter. This diameter is compared with the diameter of the seat of the valve under investigation. If the calculated diameter is smaller than the valve seat diameter, it is possible that the problem is due to a partially plugged valve that would not close. Several operational steps, already discussed in Section 11.3, could be tried to unplug the valve like, for example: venting the injection annulus several times or pressuring the casing and the tubing to line pressure and then suddenly venting the production tubing, etc. The Thornhill–Craver equation is in this case used with an orifice upstream pressure equal to the average injection pressured measured for the elapsed time (referred to valve's depth) and an orifice downstream pressure equal to the average production pressure at valve's depth calculated from the measured wellhead pressure,  $P_{wh}$ , also during the selected time interval.

The following calculation procedure represents another way of finding the diameter of the orifice through which the gas is being circulated at a constant

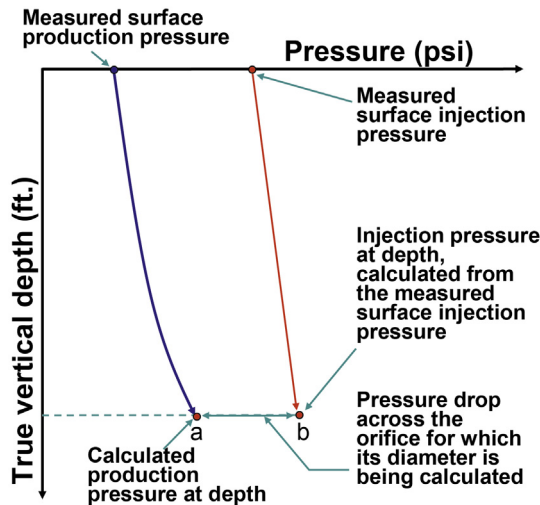
gas flow rate before the surface gas injection is shut off (the orifice could be a hole in the tubing, a flat valve, a valve stuck open, etc.):

- The injection gas pressure at the orifice's depth is calculated from the measured injection gas pressure at the surface, using the gas factor  $f_{gc}$  for that surface injection pressure.
- The production pressure at the orifice's depth is calculated from the wellhead production pressure measured at the surface, using the gas factor  $f_{gt}$  if the flow is single-phase gas flow or using a multiphase flow correlation if the well is also producing liquids.
- With the upstream and downstream pressures calculated in this way and the measured surface gas flow rate, the Thornhill–Craver equation is used to find the orifice or valve seat diameter.

If the calculated diameter is approximately equal to the valve seat diameter under investigation, it is highly possible that gas is being injected only through this particular valve. This procedure is more appropriate for situations in which only gas is being produced (with no liquid production) because multiphase flow correlations give production pressures that are not very accurate to be used in this type of calculation procedure, unless the gas flow through the orifice is critical. Calculations are more reliable if the well does not produce liquids as long as the wellhead pressures, the gas flow rate, and the gas specific gravities of produced and injection gas are carefully measured. The injection gas specific gravity is usually accurately measured. The produced gas specific gravity might be different from the injection gas gravity because it is possible that the well is producing formation gas (but at a very low flow rate); However, usually the produced gas mixture specific gravity is not much different from the injection gas specific gravity (if the well is just circulating injection gas) and, in general, the production pressure at depth is very low, thus calculation errors of the downhole production pressure are usually negligible. Calculations are even more precise if the gas flow through the gas lift valve or orifice is critical because critical flow calculations are not influenced by calculation errors of the downstream pressure. The calculation procedure just described is shown in [Fig. 11.12](#).

Diameter calculations as explained earlier should be used with caution because the valve might be throttling the gas flow giving smaller orifice diameters. Valve diameter calculations for injection point identification are more reliable for holes or orifice valves (as opposed to calibrated valves) in critical flow and in wells with no liquid production.

When the well is not producing liquid, the previously described iteration procedure for single point gas injection (shown in [Fig. 11.6](#)) is also



■ FIGURE 11.12 Determination of the diameter of a possible casing–tubing communication using pressures at depth found from the pressures measured at the wellhead.

applicable: (1) The gas pressure at depth in the tubing is calculated from the wellhead measured production pressure  $P_{wh}$ ; (2) using the gas flow rate, the valve seat diameter, and the already calculated production pressure, the valve's upstream injection pressure is calculated using the iterative procedure explained in Fig. 11.7 (in case of an orifice or a flat valve) or using dynamic models for valves that are properly working; and (3) from this upstream injection pressure at valve's depth, the surface injection pressure is determined and compared to the measured surface injection pressure to confirm that the valve under investigation is the actual point of injection. The orifice diameter (or the valve calibration data) must be known to perform these steps. Because of the simplicity and accuracy of calculating the downhole pressures from the measured upstream and downstream surface pressures, this procedure is specially recommended when the well does not produce any liquids.

It is always a good practice to pay the well a visit when it is circulating gas with no liquid production. The wellhead could be cooler than ambient temperature and with condensate water drops on its surface, revealing that the problem might be at the wellhead. When the gas is circulated through an upper gas lift valve, it is also possible that the wellhead temperature is lower than the normal wellhead temperature, but not as low as it might be when the problem is right at the wellhead.

## 11.5 FIELD TECHNIQUES FOR TROUBLESHOOTING A GAS LIFT WELL

Several operational techniques that can be used to determine the point of gas injection are presented in this section. These techniques can be applied individually, or combining several of them, to understand what might be happening downhole. Some techniques are neither expensive nor imply operational risks, but others are very expensive and/or involve some kind of risk to the completion or to the formation. This is the reason why the technique most suitable for a particular well must be carefully determined to avoid unnecessary expenses and/or risks. The optimization engineer must be properly trained to solve, as much as possible, operational problems using only numerical procedures and leave operational techniques for cases in which they are absolutely necessary to find out the root of the problem and the economic benefits are worth the effort.

### 11.5.1 Communication tests

Communication tests are frequently used in the field to determine if the wells have: holes in the tubing, flat valves with their check valves damaged, unseated valves, leaking completion packers, or an annulus-tubing communication at the wellhead. If the liquids are produced up the tubing, the communication test is performed in the following way:

- Close the wing valve that communicates the production tubing to the flowline, but leave the gas injection valve open (making sure that the wellhead production pressure can be measured). Eventually, the gas flow rate will decrease to zero and the wellhead production and injection pressures will reach the gas line pressure if there is at least one valve (or communication) located above the current liquid levels in the casing annulus and in the tubing (as explained below, the tubing liquid level might actually be lower or higher than the reservoir static liquid level). If the liquid level in the tubing is above the first valve or communication, the final production pressure will be high but not as high as the line pressure. The difference between the wellhead annulus and tubing pressures in this case is caused by the hydrostatic pressure of the liquids in the tubing.
- After the wellhead pressures have stabilized, the surface gas injection to the well is shut off (making sure that the annular pressure can be measured) and the annular pressure is then vented very fast using the wellhead casing valve opposite the injection valve or any other means that would allow the annular injection pressure to drop rapidly. This operation must be carried out with care, especially if there is a

possibility that the liquid level in the annulus is close to the surface because it can cause an oil spill if the injection gas is not directed towards the flowline or a tank that can serve as a provisional gas-liquid separator. Even though it is (unfortunately) a common practice in some gas lift fields, gas should not be vented to the atmosphere: methane is a gas that contributes to the greenhouse effect and it is a dangerous, inflammable gas.

- The existence of an unwanted communication is confirmed if the production tubing pressure drops as soon as the casing pressure begins to decline (while venting the annulus). If there is no communication, the production pressure should remain constant because the check valves inside the gas lift valves will not allow gas or liquids to pass from the tubing into the annulus. Flow across an IPO gas lift valve is also not allowed as soon as the injection pressure drops to values less than the valve's injection closing pressure and, for a PPO valve, as soon as the production pressure drops to values less than the valve's production closing pressure.

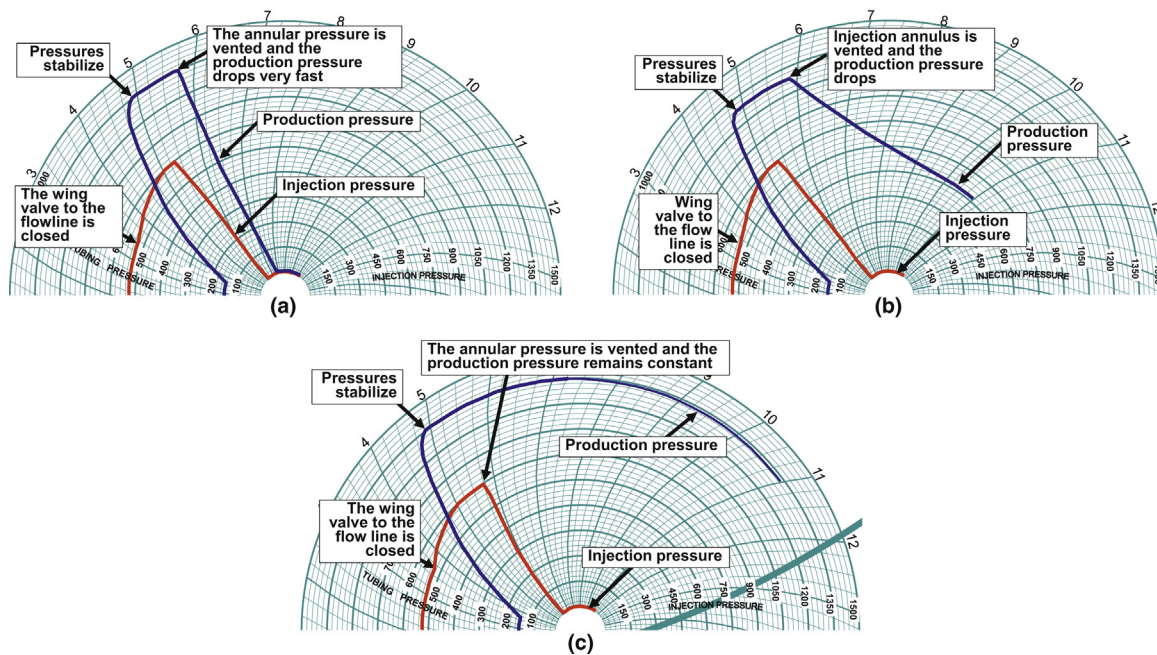
If, in normal operation, gas is injected down the tubing and the well produces up the annulus, the previous steps are also performed, but in this case the valve that connects the annulus to the flowline is first closed and when the wellhead pressures have stabilized, the gas injection valve into the tubing is closed. Then, the tubing is vented very fast. If there is an unwanted communication, the annular pressure should drop, otherwise it remains constant. It is important to mention that in annular flow wells, the check valves inside gas lift valves allow the flow to go from the tubing towards the annulus and not in the opposite direction, unless the check valve is damaged.

If the well has one or several concentric annuli in addition to the production annulus, it must be verified that there is no communication between the production annulus and the one next to it. Wells usually have at least two annuli: the production annulus and the surface annulus. At the beginning of the communication test, the surface annulus must be vented to atmospheric pressure and then it should be closed, verifying throughout the communication test that its pressure is not rising.

The production annulus could have a communication to a shallow formation due to a hole in the casing through which injection gas might be escaping. This could be easily verified if "all" the valves in the well are IPO valves in "good condition" and the communication test has shown that there is no tubing-annulus communication. Simply, with the well in normal operation, the gas injection is shut off. The surface injection pressure should drop to the gas lift operating valve's surface closing pressure. If the injection

pressure continues to drop to values even lower than the operating valve's closing pressure, gas might be escaping to a shallow formation because the communication test has ruled out the possibility of a tubing-annulus communication. Many times shallow formations have a pressure similar to the hydrostatic pressure of a water column of the same vertical depth of the shallow formation. If there is an orifice valve at the operating point of injection, or one of the valves is flat, or some of the valves are leaking gas (because their seats are cut) but with their check valves in good conditions, this test can also be performed but keeping the tubing pressurized at a pressure high enough so that the gas in the annulus cannot be injected into the tubing: If, after shutting off the gas into the casing, the casing pressure continues to drop then there might be a communication between the casing and a shallow formation.

Figs. 11.13a,b,c show the surface pressure charts taken during communication tests in wells which produce liquid up the the production tubing while gas is injected down the annulus: (a) A well with a communication possibly located above the reservoir static liquid level; (b) a well with a communication



■ FIGURE 11.13 Wellhead pressure charts taken during a communication test: in (a) and (b) the well has a small communication; in (c) there is no casing-tubing communication. (a) Well with a communication (possibly above the static liquid level), (b) well with a communication (possibly below the static liquid level, and (c) well with no tubing-annulus communication.

possibly located below the reservoir static liquid level, and (c) a well with no casing–tubing communication.

In Fig. 11.13, the production (tubing) pressure readings go from 0 to 1000 psig and the injection (annulus) pressure readings go from 0 to 1500 psig. Gas is injected down the annulus and liquid production is done up the tubing. The communications should be small: large communications above the reservoir static liquid level cause very low injection pressures at high flow rates, while large communications below the reservoir static liquid level cause large tubing and casing headings that are analyzed in chapter: Intermittent Gas Lift Troubleshooting. Small communications, on the other hand, can maintain stable wellhead pressures. The fact that the production pressure in Fig. 11.13b does not drop to the injection pressure is an indication that there might be a liquid column in the annulus and in the tubing (both above the communication) that traps the gas inside the tubing. This might suggest that the communication is below, or very close to, the reservoir static liquid level, but it is difficult to predict the final value of the surface production pressure due to the many possibilities that can take place depending on the well current reservoir pressure and operational conditions. For example:

- If the communication is well above the static liquid level, the probability of the production pressure dropping very fast to annular pressure (in a communication test) is very high.
- If the communication is above but not much higher than the static liquid level, it is possible that the production pressure drops to annular pressure or, on the contrary, to a greater pressure and then, after a few hours or days, it could eventually drop to annular pressure: What happens in the latter case could be due to the fact that the well was producing liquids with a high liquid fraction in the tubing and, after the wing valve was closed, all the liquids inside the tubing dropped to the bottom, generating a liquid column above the tubing–annulus communication (in the tubing and in the annulus). Then, the maximum pressure that is reached inside the tubing is not high enough to push the liquids back into the formation very fast. Once the annulus is vented, the wellhead tubing pressure drops to a value that is not high enough to overcome the liquid column in the annulus. Afterwards, if no standing valve is installed inside the production tubing and below the communication, the reservoir could slowly absorb the liquids in the tubing. The liquid level could drop down to the communication depth and the gas in the tubing could then drop very rapidly to annular pressure. This could happen when the reservoir injectivity index is very low.
- On the other hand, and opposite to the previous point, if the communication is below the static liquid level, but close to it, it

is possible that the production pressure drops very fast to annular pressure, giving the false impression that the communication is above the static liquid level. What could be in fact happening is that the well was producing with a very low liquid fraction in the tubing when the wing valve was closed. When the annulus is vented, the gas in the tubing flows into the casing faster than the liquid column, provided by the reservoir, can regenerate inside the tubing and it is only until several hours later that the liquid level reaches the communication. Depending then on how far the communication is from the static liquid level and on how much liquid is present in the tubing when the wing valve is closed, the final production pressure could reach any value, including the final annular pressure.

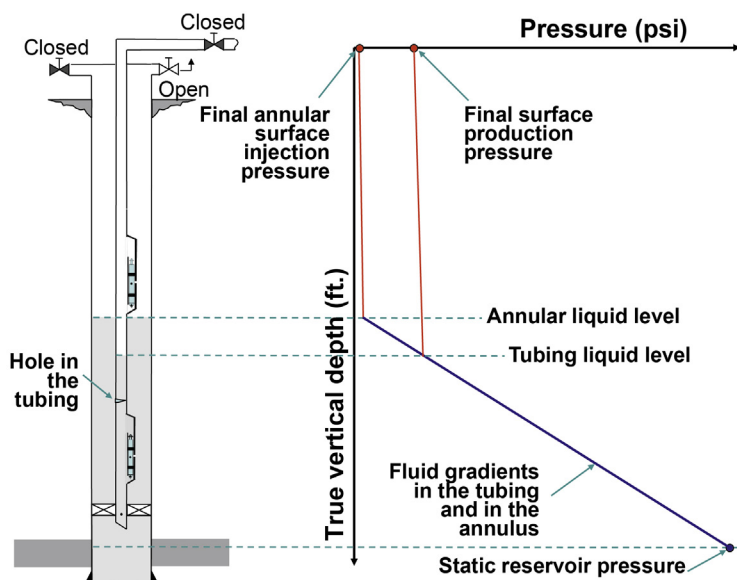
- If the communication is well below the static liquid level, the final production pressure could reach any value but it will probably be above the final annular pressure. The difference in pressure in this case corresponds to the difference between the liquid level in the tubing and in the annulus. The communication could be anywhere below the minimum value of the liquid level in the tubing. The final production pressure could take different values, even for the same well, depending on how much liquid was present inside the tubing and the annulus when the production of the well was stopped.

It is important to mention that, if the well does not have a standing valve installed in the tubing, the tubing pressure is going to decrease during a communication test even if there is no tubing-annulus communication. This is due to the fact that the reservoir might be able to absorb liquids as time goes by. However, the rate of tubing pressure decline is very slow and this rate is not affected when the annular pressure is vented. Even if the well does have a standing valve installed in the tubing, the annular pressure might decline (at a low rate) because check valves (inside the gas lift valves) might leak (this is a source of confusion for inexperienced engineers).

Fig. 11.14 shows a well with a communication below the reservoir static liquid level and the pressure–depth diagram showing the pressures along the annulus and the tubing after the liquid levels have stabilized according to the reservoir pressure (the annulus is opened to atmospheric pressure).

For wells with IPO valves with a calibrated valve (not an orifice valve) at the point of injection, a totally different test consists in shutting off the injection gas flow rate but leaving the well open to production. This operation could show that the injection pressure might drop below the injection closing pressure of the operating valve, indicating a possible communication between the tubing and the annulus. However, this unusually large reduction of the





■ FIGURE 11.14 Pressure–depth diagram showing the final pressures in the annulus and in the tubing in a well with a communication below the static liquid level.

injection pressure could also take place in wells with a flat valve or a valve with dirt between the ball and the seat that would not allow the valve to close. Only a communication test performed as indicated earlier could confirm if there is a tubing-annulus communication. If the communication test indicates that there is no tubing-annulus communication and yet the injection pressure decreases below the closing injection pressure of the operating valve, actions already explained in [Section 11.3](#) should be taken to get rid of the dirt or solid particles that might be keeping any of the valves open. If the problem persists, then the valves should be replaced because it is highly probable that the root of the problem is a flat valve.

If the gas injection is shut off (leaving the well open to production) and the injection pressure drops to the closing injection pressure of one of the gas lift valves installed in the well, then it is highly possible that this particular valve is in fact the current operating valve. The closing pressures of different types of valves are calculated with the valve mechanic equations given in [Section 11.4.2](#). The injection closing pressure at depth must be similar to the closing pressure calculated using these equations.

If a tubing-annulus communication is detected, then its location can be found using sonic devices or by wireline techniques. Sonic devices are explained in [Section 11.5.3](#).

The depth of the communication can be detected using the following wireline technique: gas is injected down the tubing while at the same time running in the tubing a “flag” that can detect and plug the communication. This flag is usually a small but compact ball of ragged cloths. When the flag reaches the communication, the flowing gas pushes it towards the annulus, so that the flag gets stuck in the hole. This is detected at the surface by a change in the wireline tension. The wireline tools run in the well are usually the following: the rope socket, a 5-ft. long weight bar, a link or tubular jar, a running tool (type j, for example) which is tied to the “flag.” The wireline tools should be as light as possible, but some weight must be run above the jarring tool in case something unexpected happens and it is necessary to jar up or down to release the wireline tools.

When pumping equipment is available at the well like, for example, during a workover job, another technique that is not very precise (but sometimes used in the field) to find the location of the communication consists in pumping down the annulus a certain amount of liquid paint, afterwards fluids are pumped down the annulus until the paint begins to come out of the tubing at the surface. Liquids should always be injected into the well with care so that no damage is caused to the formation. Knowing the total volume of liquid pumped into the well at the time the liquid paint begins to emerge to the surface, it is easy to determine the depth of the communication if it was below the liquid level when this test was begun. Because the wellhead tubing and annular pressures are equal for this test, if the communication is below the liquid level, then the liquid level in the tubing and in the annulus are at the same depths and volumetric calculations are very easily performed. The following equation can be used to find the depth  $D_{\text{com}}$  of the communication:

$$D_{\text{com}} = \frac{V_b}{B_t + B_a} \quad (11.19)$$

Where  $D_{\text{com}}$  is the depth of the communication in Mft.,  $V_b$  is the volume of fluids pumped into the annulus in Br, and  $B_t$  and  $B_a$  are the tubing and annulus volumetric capacities, respectively, in Br/Mft. If it is suspected that the liquid level is below the communication, fluids must be pumped first to make sure the liquid levels in the tubing and in the annulus are both above the communication. For this operation, it is advisable to install a standing valve at the bottom of the tubing to avoid damage to the formation, minimize the volume of fluids pumped into the well, and be able to perform volumetric calculations. The liquid level should be measured by wireline or using sonic devices before starting the test to make sure it is above the communication. If it is indeed above the communication, the measured liquid level in the annulus should be equal to the measured liquid level in the

tubing (if the annulus and tubing wellhead pressures are the same). If the well is not very deep, this is a fast way of knowing where the communication might be. The paint should have specific gravity equal to the specific gravity of the fluids being pumped. The paint should not be soluble in the fluids pumped into the annulus.

The communication could also be due to a circulating sleeve left open by mistake. It is advisable to verify all components of the completion that might cause communication problems. If the communication does not represent a risk to the integrity of the completion, and the tubing geometry would allow it, it might be possible to isolate the communication by a packoff completion without causing any kind of restriction to the liquid production, see Fig. 6.44. For this action, the communication depth must be accurately determined.

The use of fiber-optic technology to determine the depths of communications is explained in Section 11.5.7. Ultrasonic devices can also be used to accurately determine the depth of any communication. They are expensive but could be perfectly justified for wells where it would otherwise be very difficult to detect the depth of the communication and an economic evaluation has shown that it is profitable to install a tubing straddle to isolate the communication. Very sensitive temperature sensors can also be used to detect casing–tubing communications, as explain in the next section.

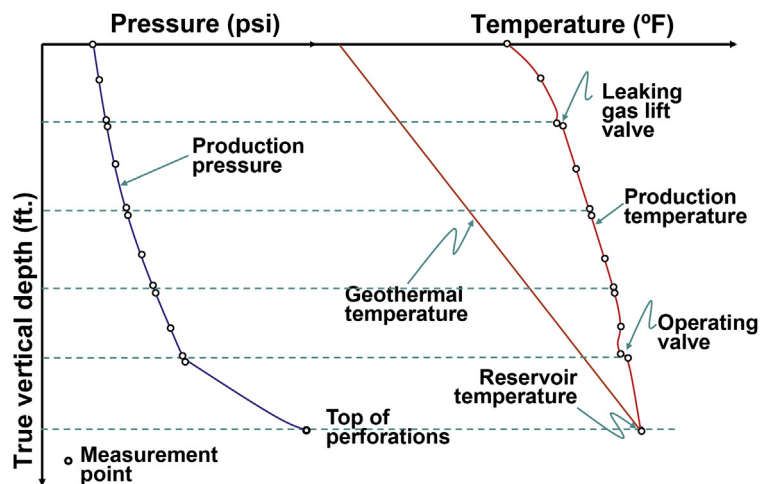
### 11.5.2 Downhole pressure and temperature surveys

Downhole pressure and temperature surveys are very important troubleshooting tools for wells on gas lift because they reveal important clues regarding the operation of the well.

- Downhole temperature surveys can reveal a cooler than normal local point along the tubing that might indicate gas injection at that depth.
- The gas injection point might or might not correspond to a mandrel installed in the well and therefore it is better to run continuous surveys (as opposed to surveys with selective stops at predetermined depths) using one of the following alternatives: (1) use of fiber-optic to measure temperature distribution along the tubing (this technique is explained in [Section 11.5.7](#) and it is recommended for wells producing in a stable or unstable manner), or (2) continuous pressure and temperature surveys, combining high-precision temperature sensors with tubing collar locators (or TCLs as they are known), for which it is not necessary to stop for a given period of time at different locations to measure the pressure and temperature at those specific depths because the measurements are taken in a continuous fashion as the sensors are

run in the well. In cases in which the liquid flow rate is very large, conventional temperature surveys (with selective stops at specific depths) might not be able to detect local cooling effects and therefore the use of continuous temperature surveys are more reliable and recommended for these cases.

- Discrete temperature drops at one or many unloading valves are frequently detected. This indicates that their seats have been cut or eroded. This is the type of valve failure that takes place more frequently in gas lift operations; but usually the gas flow rate through a leaking gas lift valve is very small and most of the time these valves need not be replaced.
- Fig. 11.15 shows a typical temperature distribution in which the first (shallowest) valve is leaking injection gas. However, the change in the production pressure gradient is observed at the deepest valve's depth, which is actually the operating valve. The results shown in the figure correspond to pressure and temperature measurements taken just above and below each gas lift valve, as well as at the top of the perforations and at depths between two consecutive gas lift valves.
- The production pressure gradient can also be used to locate a gas injection point if it has a significant change in value somewhere along the tubing. If the abrupt change in production pressure gradient takes place between two mandrels, there must be a tubing-annulus communication at that point.



■ FIGURE 11.15 Results from a pressure and temperature survey (with several stops at predetermined depths). The continuous curves are just interpolation points between two consecutive measurements.

- The pressure and temperature measurements at each valve can be used to determine the gas lift valves' operating condition because this data can be entered into the valve mechanic equations to find the valves' opening and closing pressures in a precise way.
- The bottomhole flowing pressure, measured the same day the well's liquid production is measured, gives important data to find the IPR curve of the well. One of the great advantages of the gas lift method is to be able to measure the bottomhole pressure with the well in operation.
- The pressure along the tubing, together with liquid production, water cut, gas injection flow rate, formation gas/liquid ratio, and oil API gravity measurements, can be used to analyze multiphase flow correlations or models to find the one that is best suited for current operational conditions.
- Pressure surveys run at different stabilized injection gas flow rates (to change the liquid production) can be used to estimate the value of the formation damage, the reservoir pressure, and the productivity index of the well.

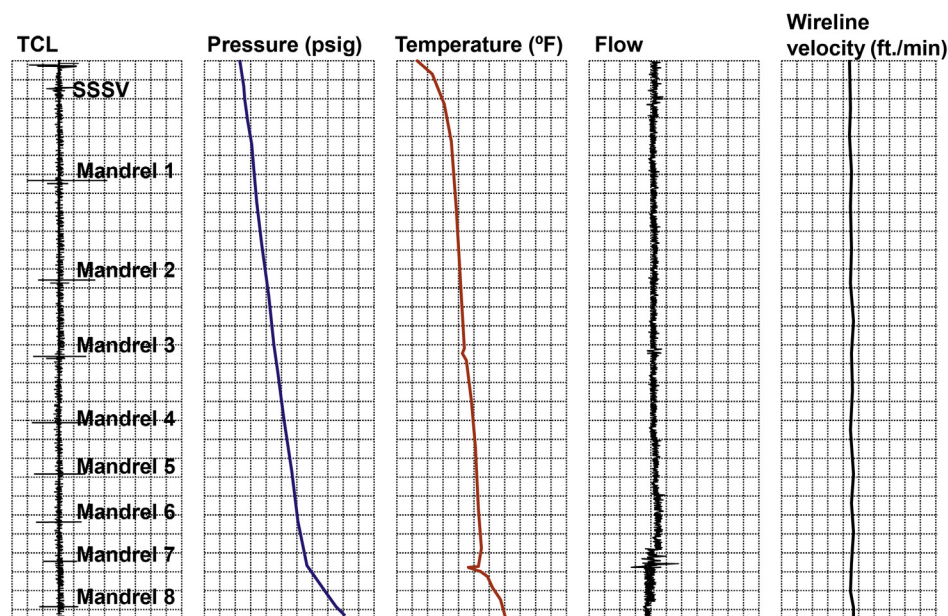
Even though pressure and temperature surveys are very useful, they should not be used any time there is a problem in the well because they are wireline jobs that are expensive and some operational risks are involved. They should be used as troubleshooting tools when the problem in the well cannot be understood in any other way and it is absolutely important to do so. Usually, operating companies have pressure surveys planned for the year, such as buildup tests, to measure important reservoir parameters. With good coordination, it is possible to perform these surveys in wells where useful data for gas lift operation can be obtained (besides getting the important reservoir information).

It is advisable then to have a good communication between the production optimization team and the reservoir department to make the best of the resources available for downhole data gathering purposes. The optimization personnel should also set aside part of the operational budget to run surveys in wells in good operational conditions to identify opportunities to improve current well designs, study multiphase flow correlations, and obtain valuable operational references for future problems in the same wells. The data obtained from previous surveys should be filed to be used in future analyses and be able to predict well behavior under different operational conditions, such as a new mandrel spacing recommendation, a new available system injection pressure, etc.

A well-executed pressure and temperature survey (with stable liquid production and trustworthy measurements of the liquid production and the total

gas flow rate) can be used to verify the accuracy of the multiphase flow correlation used to model the well. If it is known that the multiphase flow correlation being used in one particular field is very accurate, then the survey can be used to check other parameters, like the wellhead production pressure, the water cut, or the formation gas/oil ratio. The wellhead production pressure measured in the survey is usually more reliable than the one measured by the two-pen pressure chart recorder (or the electronic sensor installed at the wellhead for that purpose). Increasing the wellhead production pressure shifts the entire calculated pressure traverse curve in the well's model to the right and vice versa. Increasing the water cut (while keeping the total liquid flow rate constant) rotates the entire calculated pressure traverse curve in the model to the right (if the water cut is already too high this rotation might be very small or even unnoticeable). Increasing the formation gas/oil ratio, while holding the total gas flow rate constant, makes the calculated pressure traverse steeper below the gas injection depth, but with no change above the injection depth. All these changes can be evaluated by plotting the calculated pressure traverse curve together with the pressures measured during the survey in a pressure–depth diagram.

Recently developed pressure and temperature sensors have two main characteristics that are changing the way flowing pressure and temperature surveys are done: high precision and short response time. These sensors are making it obsolete to have stops along the tubing while the survey is run to take pressure and temperature measurements at predetermined depths (unless the production pressure is oscillating, in which case it is always recommended to have stops of duration no less than 120% of the time of one pressure oscillation cycle). If the production pressure is stable, the surveys can now be done in a continuous fashion saving time in the well, increasing the accuracy of the measurements and the possibility of spotting a casing–tubing communication or any other problem. These surveys can spot a problem to within one foot of tubing length. The sensors used for this type of surveys are: High precision pressure and temperature sensors, TCLs to determine the depth where the measurements are taken, and (optionally) a turbine flow meter to have a relative measurement of the local liquid flow rate. The combined length of all wireline tools run in the well is about the same as the one for conventional pressure and temperature surveys. Because the survey is run continuously and the temperature sensors can detect changes in temperature as small as  $0.001^{\circ}\text{F}$  with a very short response time, very small leaks can be detected anywhere along the tubing. This is done thanks to a new type of resistance temperature detector (RTD) sensor called platinum resistance thermometer (PRT). RTDs are temperature sensors based on electrical resistance changes of the material in response to temperature



■ FIGURE 11.16 Results from a continuous flowing pressure and temperature survey.

changes. When the material is platinum, the RTD is called PRT or “platinum resistance thermometer.” The work published by [Friedli and Rivas \(2010\)](#) constitutes an excellent reference of real applications that can be performed with these new sensors. In [Fig. 11.16](#) the results from a continuous pressure and temperature survey are presented.

As can be seen in [Fig. 11.16](#), the wireline velocity is more or less constant, and it is easy to identify the depths of the gas lift mandrels. It can be noticed that the main injection point is at mandrel #7, but there is a small gas leak at mandrel #3. The data that is shown in the figure has been compressed but, with a change of scale, small variations of the measurements are easier to observe and it is possible to detect smaller gas leaks to within one foot of tubing length, which is important when tubing leaks take place very near a gas lift mandrel. These leaks might be misinterpreted as a failure of a gas lift valve when measurements are taken by conventional pressure and temperature surveys. This misinterpretation could lead to several unnecessary gas lift valve change-outs to finally reach the wrong conclusion that there is something wrong with the gas lift mandrel and the completion is pulled out of the well for this reason. There have been many reports of holes in the production tubing just below the operating mandrel, where the liquid level in the annulus is usually located. This could be due to the action of CO<sub>2</sub>, or

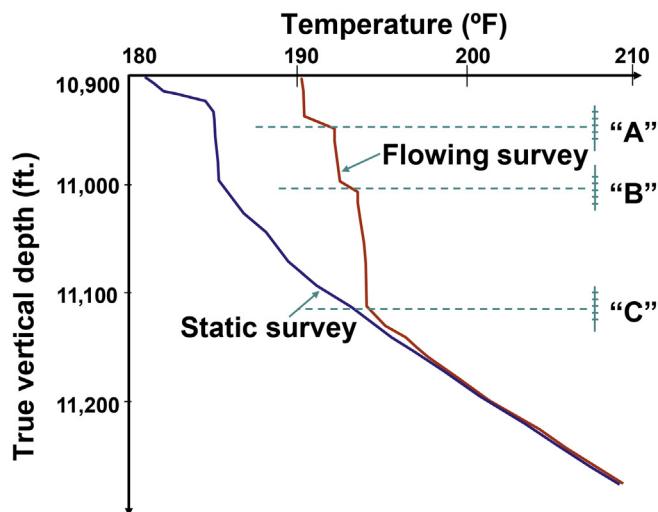
any other kind of corrosive agent, that acts in combination with the water at the liquid level in the annulus.

Until recently, stops at certain depths along the tubing were needed for two reasons: to allow the sensors to stabilize to the new temperature and to have a way to correlate the depth of the survey with the depth measured by wireline. Not that long ago, electronic sensors used in pressure and temperature surveys required several minutes to adapt to the new temperature. With fast response sensors, surveys can be carried out very fast, significantly shortening the time required to run the survey, as long as the depth of each measurement is known (which is something that can be achieved with the use of Tubing Collar Locators). Sensors can be run as fast as 80–100 ft./min and because the scan rate can be of around 10 measurements per second, a pressure and temperature measurement can be obtained every 1.6–2 in. along the tubing. Some operators run the sensors at a velocity as high as 150 ft./min. If there is an abnormal measurement somewhere in the tubing, the depth scale in Fig. 11.16 can be expanded to see more clearly where the problem might be. With the Tubing Collar Locator, it is easy to know how far apart the problem is located from a given reference point in the well, such as a gas lift mandrel or a safety valve. If the well is unstable, these high precision temperature sensors can still be used but in a different way: the well is shut in and the sensors are run in the well at a moderate rate to give time for the fluids to stabilize in the tubing. Then, the sensors are pulled at 100 ft./min and they are so sensitive that they might be able to detect where gas was being injected because the tubing at that depth might still be slightly cooler than the nearby temperature.

TCLs are by themselves very useful for many reasons: there are reported cases where, thanks to this type of tool, errors in the number of joints, as reported in the well files, have been identified. TCL can also be used to establish the state of the tubing because the “noise level” of the signal is proportional to the amount of metallic material. Thus, it would be detected if some metal materials have been lost due to corrosion. If the noise change is detected on the way down and on the way up, it is probably because the tubing might have lost some mass due to corrosion. Additionally, if the TCL is run below the lower end of the production tubing, it is possible to detect the perforated intervals and compare them with the ones in the file of the well and with the well total depth to determine if some perforations have been covered with sand. TCLs can be used to locate other components of the completion, such as landing nipples, circulating sleeves, or safety valves, among others.

Flowing and static temperature surveys can reveal which zones are productive and they can even help identify if there is crossed flow or liquid flow





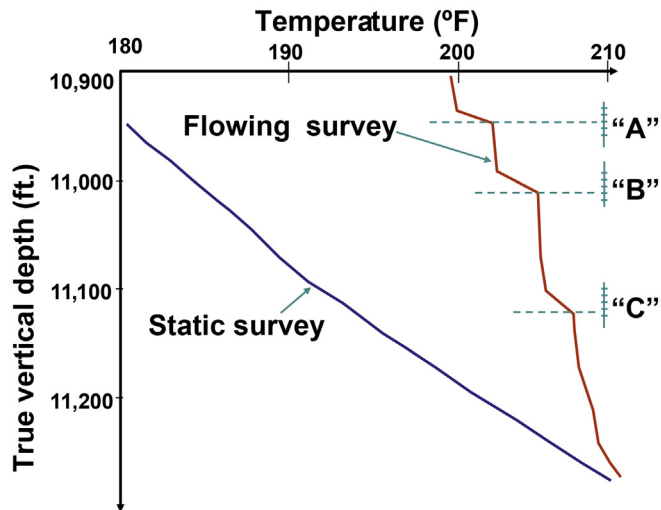
■ FIGURE 11.17 Temperature survey along the perforated interval, indicating crossed flow between formation “B” and “A.”

from underneath the bottom of the well or from a flow channel behind the casing. Fig. 11.17 shows the results of the temperature measurements taken with the well in normal operation (flowing survey) and while the well was closed (static survey).

It can be seen in Fig. 11.17 that below perforation interval “C” both temperatures (static and flowing temperatures) are identical, indicating that there is no liquid flow at these depths. The point where the flowing temperature changes slope is just where the liquid production begins, which corresponds to perforated interval “C.” But the static temperature survey shows a change in slope between intervals “B” and “A” indicating crossed flow from “B” to “A.” The temperature surveys in Fig. 11.18 are similar to the ones shown in Fig. 11.17, but in this case the flowing temperature is higher than the static temperature below interval “C” indicating liquid flow coming from the bottom of the well.

Continuous surveys are also used to detect small holes or communications in the tubing or in the casing even below the point of gas injection using a different procedure:

With the well shut in, a temperature survey is run at a wireline velocity of 150 ft./min to generate a base temperature profile. Then, liquid is injected at a fixed rate either down the casing with tubing return or down the tubing with annulus return. The circulation liquid rate is



■ FIGURE 11.18 Liquid flow coming from zones below the perforation interval.

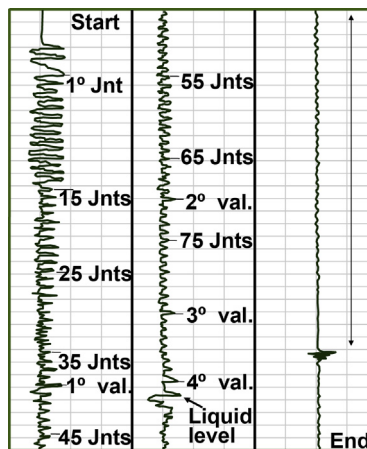
determined by the size of the communication and the injection pressure at the surface. If it is desired to explore the possibility of having more than one communication, the liquid injection pressure must be high to maintain a high pressure drop through the communications. While the liquid is being injected, several runs are made at 20 or 30 ft./min to detect any anomaly that might indicate the existence of a communication (friction generated by the liquid passing through the communication causes an increase in the local temperature). Before running the survey, gas lift valves should be replaced with dummy valves and a standing valve should be installed at the bottom of the production tubing to protect the formation. Because of the cost of this operation, this technique is recommended for deep wells or any well where it will be very expensive to replace the production tubing and where isolating the communication with tubing straddles is advisable. If the communication is very small and cannot be detected using this technique, ultrasonic surveys should be tried.

Even though continuous pressure and temperature surveys increase the quality and number of measurements in comparison to conventional surveys (with discrete stops along the tubing), they are not appropriate for wells in which the pressure and temperature are changing in time. Continuous surveys represent a snapshot of tubing conditions as the sensors pass through each point along the well depth. Running in the sensors at 100 ft./min in a 10,000-ft. well, it takes 1.66 hours to go from top to bottom, which could

be a very long time for a well with production pressure and temperature fluctuations. When temperatures are changing in time, it is better to measure the temperature along the tubing using fiber-optics with a technique that is explained in detail in [Section 11.5.7](#) or measure the pressure and temperature at certain predetermined depths for time intervals of at least 20% longer durations than one pressure fluctuation cycle. A final recommendation (for wells with high liquid velocities in the production tubing) is to always use the right number of weight bars to allow running in the pressure and temperature sensors without the need to choke down the well. Choking down the well will completely change the operation of the well. Wireline companies can determine the number of weight bars to be used and, if the well presents strong tubing headings, antiblock tools (located above the weight bars) should be used as part of the wireline tool set to prevent the tools from being blown up the tubing.

### 11.5.3 Use of sonic devices

Sonic devices that were developed to measure distances (along the annulus) from the surface to downhole restrictions (or to changes in shape of the tubing) have been in used for several decades. As sonic waves travel back to the surface (bounced back from each restriction or change in shape along the annulus), they are detected and registered in a survey of electrical signals that are proportional to the strength of each sonic wave. These surveys are inexpensive and can be done very fast. Many surveys can be run in several wells in one single day without any kind of risk to the formation or the completion. The initial sonic wave is generated by explosion or implosion. The gun used to generate this wave and the microphone used to detect its echo waves are installed in a valve at the surface with direct communication to the casing–tubing annulus. Tubing joints, gas lift mandrels, and the liquid level in the annulus, generate echo waves of different strengths that are detected by a microphone at the surface for later identification. The echo wave strength diminishes with depth. Gas lift mandrels generate echo waves stronger than the ones generated by tubing joints. The liquid level is most of the time easily identified because its echo wave is the strongest one. In the past, these surveys were registered on long strips of paper that would move at a certain velocity as the sound signals were register by a pen that moved in a direction perpendicular to the paper movement and according to the strength of the waves. Today, echo's depths are electronically captured and stored to be viewed or analyzed using a personal computer. [Fig. 11.19](#) shows a typical sonic survey where tubing joints, gas lift mandrels, and the liquid level can be identified. Knowing the length of each tubing string and counting the number of joints, it is easy to determine the depth of each



■ FIGURE 11.19 Typical results from a sonic survey.

mandrel and the liquid level. Today, these depths are digitally determined by measuring the time it takes for a sonic wave to travel to a particular point in the well and back.

This type of technique is especially recommended when there is a casing–tubing communication with production liquids entering the annulus and it is desired to determine the depth of the communication. The operational behavior of a well that produces with large tubing and casing headings, possibly due to a casing–tubing communication, is analyzed in chapter: Intermittent Gas Lift Troubleshooting, together with a description of the required operational steps that should be taken to find the depth of a communication using sonic surveys.

Sometimes it is not possible to perform sonic surveys in wells on gas lift because gas injection causes a very high noise level. It is also possible that these devices cannot be used because the gas injection pressure is greater than the pressure of the small  $N_2$  or  $CO_2$  containers used to generate the sound wave.

The survey in Fig. 11.19 can be used to determine the depths along the annulus because the relative position of each component can be identified. But, as indicated above, new sonic devices can determine the depth of any point in the well by simply knowing the velocity of sound at current gas condition without the need of physical reference points. Using these new devices, it is possible to identify restrictions along the gas injection line or inside the production tubing where it is not possible to have reference points in the same way tubing joints can be used as such in the annulus. For example, the depth

of the liquid level in the tubing is equal to the mean velocity of sound multiplied by half the time it takes a sound wave to travel from the surface to the liquid level and back to the surface, where a microphone detects, filters, and amplifies it. These new sonic devices measure the elapsed time and calculate the sound velocity from: mean gas temperature and pressure, and gas specific gravity. The users of these new devices should enter this data. Sound velocity graphs as functions of gas pressure and temperature for a given gas specific gravity have been developed. The surface gas pressure and temperature is used to determine the mean pressure and temperature, which are approximately equal to the conditions halfway from the surface to the liquid level depth, but because the liquid level depth is not known a priori, an iteration procedure must be used to determine it.

It is important to point out that it is sometimes impossible to know the specific gravity of the gas because it might be a mixture of injection and formation gas. This usually happens when the well has been closed for a long time or air has been allowed to mix with the injection gas. In these cases, liquid level calculations might be off by more than 30%.

If a well has been shut in long enough and there is a good estimation of the gas specific gravity inside the tubing, it is then possible to determine the static reservoir pressure using sonic devices, as long as the specific gravity of the liquid inside the lower part of the tubing is also precisely known. The static bottomhole pressure of the well ( $P_{\text{res}}$  in psig) can then be found with Eq. 11.20 using the following data: surface tubing temperature and pressure, liquid and gas specific gravities, water cut, and liquid level in the tubing:

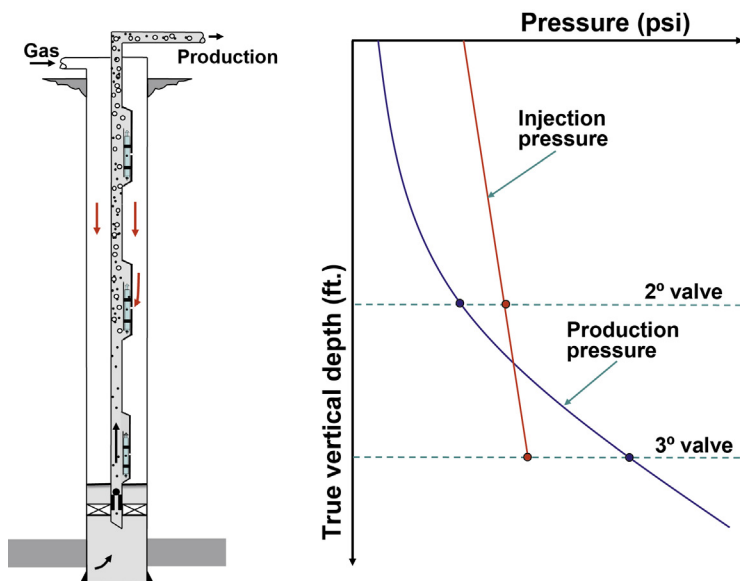
$$P_{\text{res}} = f_g P_{\text{wh}} + L \rho_f \quad (11.20)$$

Where  $f_g$  is the gas factor used to find the pressure of the gas just on top of the liquid column from the tubing surface pressure  $P_{\text{wh}}$  in psig,  $L$  is the true vertical length of the liquid column in feet from the top of the perforations to the liquid level in the production tubing, and  $\rho_f$  is the pressure gradient of the liquids in the production tubing in psi/ft. that can be calculated from the oil API gravity and the water cut of the liquids inside the tubing.

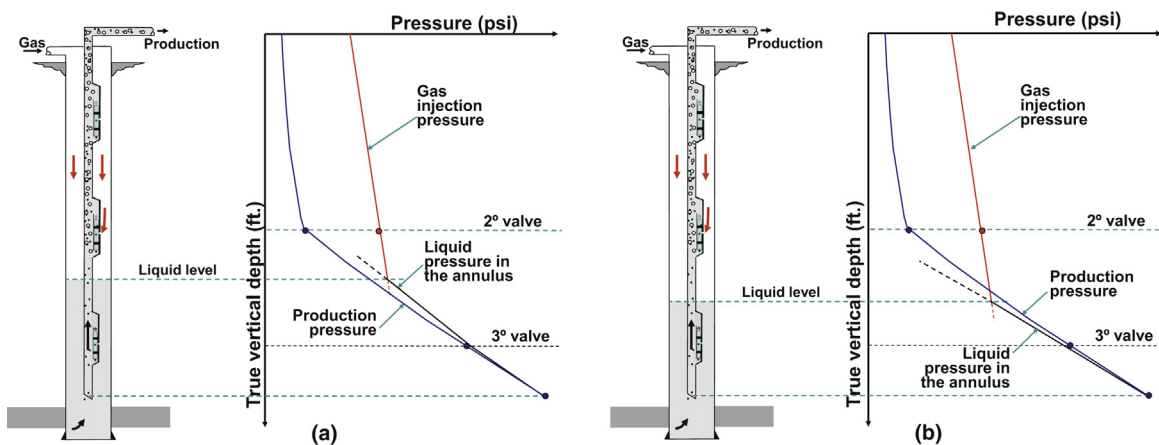
The problem with Eq. 11.20 is that it must be certain that the liquid column does not contain free gas that would make the value of  $\rho_f$  much smaller than calculated from the water cut and the API gravity of the oil alone. If the gas injection to the well has been shut off several days in advance (but leaving the production tubing open to production), it is possible that all the free gas has been vented to the separator. However, this is sometimes not possible. A well can have a gas producer zone with a pressure slightly higher than the liquid producer zone, thus the liquid column  $L$  is not going to be able to stop

the formation gas from being produced. This is why it is better to also close the production tubing in such a way that it will still be possible to measure the wellhead production pressure. In this way, the formation gas will accumulate on top of the liquid until the bottomhole pressure increases to the static pressure of the gas producer zone. The liquid column in this case is going to be smaller but the production wellhead pressure is going to be larger, so that the bottomhole pressure will still be the reservoir static pressure, which is the parameter that needs to be measured.

As for the use of sounding devices to determine the current point of injection in a well on continuous gas lift, the liquid level measured in the casing–tubing annulus of a well with a casing–tubing packer installed does not reveal the current point of injection. It only indicates the point to which the well was initially unloaded, which does not necessarily correspond to the current point of injection. On the other hand, the annular liquid level does indicate that the current injection point cannot be located below the measured liquid level. Fig. 11.20 shows the pressure–depth diagram at current conditions of a well producing on continuous gas lift: the production pressure is greater than the injection pressure at the third valve. The gas is injected then through the second or the first (shallowest) gas lift valve. However, the liquid level is maintained just below the third (deepest) valve, which was uncovered during the unloading process when the production pressure was lower than the



■ FIGURE 11.20 Liquid level in the annulus just below the third valve.



■ FIGURE 11.21 Liquid level in a well without packers.

injection pressure. The check valve of the third gas lift valve does not allow the liquid to pass from the tubing towards the annulus.

When the production packer has failed and gas is injected through it, the detection of the packer's depth using sonic devices confirms this failure and, in this way, the well can be worked over for that particular reason.

Fig. 11.21a shows the pressure–depth diagram of a well without a packer and very “low” formation gas/liquid ratio. In this case, the annular liquid level will adjust to the so called equilibrium point. The annular pressure is equal to the tubing pressure at the bottom entrance of the tubing. The surface gas injection pressure plus the hydrostatic pressure of the gas and liquids in the annulus must be equal to the pressure at the entrance of the tubing. The liquid gradient in the annulus is approximately constant and seems “lighter” than the gradient in the tubing, but in reality the frictional pressure drop inside the tubing makes the production tubing gradient looks “heavier” than the liquid gradient in the annulus. The liquid level in the annulus would correspond to the intersection of the annular gas pressure line and the tubing production pressure curve only if the liquid pressure gradient in the annulus and in the tubing were equal. But the liquid pressure gradient in the tubing is usually different from the liquid gradient in the annulus and the liquid level is found by tracing a line with the liquid pressure gradient in the annulus from the pressure at the bottom of the tubing (tubing entrance) until it intersects the gas injection pressure line and that is where the annular liquid level is located. Because the pressure in the annulus at the third valve is slightly higher, there must be a small liquid flow through this valve if it is opened. This could lead to erosion of the seat of this valve because it is not design to handle liquid flow.

Fig. 11.21b shows a pressure–depth diagram of a well without a packer with “moderate to high” formation gas/liquid ratios. Because the end of the tubing is above the top of the perforations, a larger portion of the total formation gas rate is suctioned into the production tubing. Formation gas entering the tubing can make the pressure gradient in the tubing “lighter” than the liquid pressure gradient in the annulus. In this case, the tubing pressure at the depth of the third valve in Fig. 11.21b is greater than the annular pressure at that depth (the gas lift valve’s internal check valve prevents the liquids from flowing from the tubing to the annulus through the third gas lift valve).

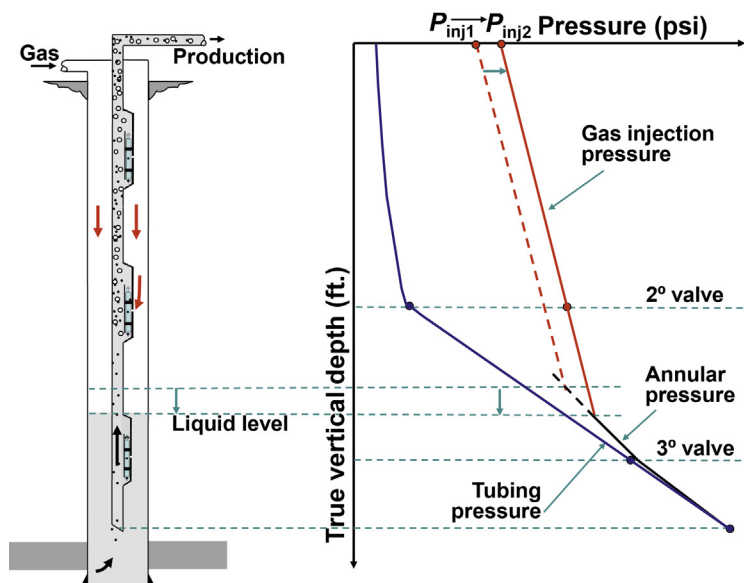
If the surface gas injection pressure in the annulus is known, the flowing bottomhole pressure (at the perforations) can be calculated by measuring the liquid level in the annulus only if the well does not have a casing–tubing packer. The flowing bottomhole pressure can then be used to build the IPR curve of the well or to determine the accuracy of multiphase flow correlations if the liquid production and the liquid level are measured at the same time. The pressure at the depth of the tubing entrance can be calculated with the following equation:

$$P_{\text{entrance}} = P_{\text{inj}} f_g + L \rho_{f \text{ annulus}} \quad (11.21)$$

Where  $P_{\text{entrance}}$  is the pressure at the entrance (or bottom) of the production tubing in psig,  $f_g$  is the gas pressure factor that is used to calculate the pressure of the injection gas just above the liquid level in the annulus,  $P_{\text{inj}}$  is the injection pressure measured at the wellhead in psig,  $L$  is the true vertical length in feet of the liquid column in the annulus above the depth of the tubing entrance, and  $\rho_{f \text{ annulus}}$  is the pressure gradient of the liquid in the annulus in psi/ft. Eq. 11.21 is not frequently used because it is difficult to know the exact value of the liquid pressure gradient in the annulus, but it does give a rough idea of what the bottomhole flowing pressure might be.

In a well “without” a packer and with liquid production through the production tubing, it is highly possible that the valve just above the liquid level in the annulus corresponds to the operating valve because the injection pressure (in the annulus) is very similar to the production pressure (in the tubing) at the depth of the annular liquid level and therefore the injection pressure at the valve immediately above the liquid level should be higher than the production pressure (in the tubing) at the same depth so that gas can be injected through this valve, unless: (1) a mechanical failure of the valve does not allow gas injection, (2) for IPO valves, the injection pressure is less than the valve’s opening pressure because there is a communication or a flat valve higher up in the well, or (3) for PPO valves, the production pressure is less than the opening production pressure of the valve and there is a communication or flat valve higher up in the well.





■ FIGURE 11.22 Effect of the injection pressure on the annular liquid level in a well without production packer (and very low formation gas flow rate).

Gas lift in open completions is not recommended because the liquid level depth can change if the injection pressure fluctuates. The free movement of the liquid level can worsen instability problems. Fig. 11.22 shows how the annular liquid level gets deeper in the well (with very little formation gas) as the injection pressure increases ( $P_{inj1}$  increases to  $P_{inj2}$ ).

It is better to install dummy valves below the liquid level in the annulus in closed or semi-closed completions (with production packer installed in the well) in cases in which it is not possible to inject gas through the deepest mandrel. In this case, dummy valves are installed to avoid: (1) damaging the valves below the liquid level due to erosion of the seats, or (2) possible instability problems if a check valve of any of the gas lift valves below the liquid level fails because this will represent a tubing-annulus communication that will not allow the liquid level to remain constant.

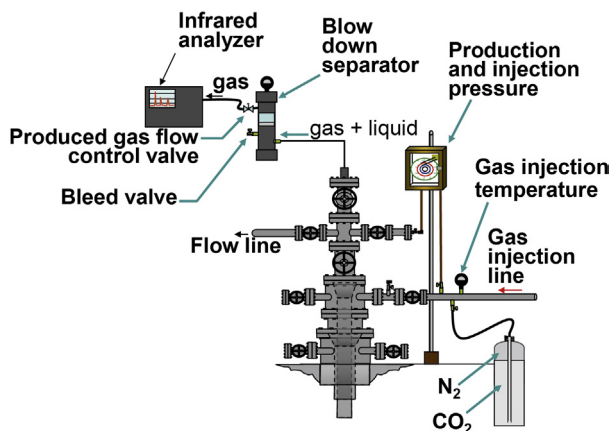
#### 11.5.4 Use of CO<sub>2</sub> injection to determine the point of injection

Determining the depth of the current point of gas injection by detecting the time of arrival of a CO<sub>2</sub> pulse (previously injected down the annulus together with the lift gas) is a technique that was developed several decades ago

and that is worthwhile knowing. One of the first works published on this method was reported by [Wellington et al., 1993](#). The method is very simple:

- A small, high-pressure bottle containing liquid CO<sub>2</sub> only, or a mixture of nitrogen and CO<sub>2</sub>, is connected to the gas injection line. When nitrogen is used, the bottle has a dip tube that goes all the way to the bottom of the bottle. Gaseous nitrogen is located at the top of the bottle and is used to push the liquid CO<sub>2</sub> to the bottom so that it is injected into the gas injection line through the dip tube inside the bottle. Nitrogen is then used only to keep the bottle pressurized.
- The bottle pressure should be high enough so that the right amount of CO<sub>2</sub> can be injected at a high and constant flow rate. In this way, CO<sub>2</sub> can be easily detected as a clear, high-concentration pulse when it comes out of the well through the production tubing.
- It is necessary to keep the bottle pressure high to keep CO<sub>2</sub> as a liquid. The amount of CO<sub>2</sub> injected can be determined by weighting the bottle before and after the injection.
- A small blow-down separator is installed at the wellhead, from which a small, representative amount of gas produced from the well is continuously taken and directed to the CO<sub>2</sub> concentration analyzer.
- CO<sub>2</sub> is injected into the gas injection line. The elapsed time from CO<sub>2</sub> injection must be measured from the moment the CO<sub>2</sub> injection is initiated.
- CO<sub>2</sub> concentration of the gas produced by the well is measured for a period of time at least 50% longer than the calculated time for the CO<sub>2</sub> to travel to the deepest possible point of injection and back to the surface, assuming that there is only one single point of injection in the well. This measuring period of time is longer than the calculated period of time for a single pulse of CO<sub>2</sub> to return to the surface because if there are two or more points of injection, the time for the last pulse to arrive at the concentration analyzer (from the deepest point) is going to take longer, as it will be shown later in this section.
- The following measurements should be taken simultaneously during the test: gas injection temperature and its flow rate, total gas flow rate at the production separator, liquid production, and wellhead injection and production pressures.
- PVT data must also be known to be able to perform multiphase flow calculations to determine the gas flow velocity inside the tubing (if necessary).

The equipment and connections required to perform the test are shown in [Fig. 11.23](#). The infrared analyzer should be explosion proof; otherwise, it should be installed away from the wellhead according to the operating company's safety rules. The analyzer also requires an electric power source,



■ FIGURE 11.23 Connections and required equipment for CO<sub>2</sub> injection and detection.

which can be a battery or the well's own power source. Electrical connections near the well, or in a platform, should be made following safety regulations. The gas-liquid separator dimensions need not be too large: 2 or 3 ft. long, 2-in ID, with ½-in. inlet and outlet ports should do a good job in most wells. A transparent material should be used in parts of the separator to know the liquid level at all times. A manual flow control valve can be used to regulate the gas flow out of the separator.

Some of the advantages found when using this method are:

- It is not necessary to run in the well any tool or equipment that could involve any kind of risk and/or expenses.
- Neither the liquid production of the well nor the gas lift injection needs to be interrupted.
- The number of surface equipment and their connections are few and easy to install and operate; therefore, the time required to perform one test is very short as compared to a downhole pressure and temperature survey. Several tests can be performed in many wells in one single day.
- The method could be used to detect communication depths in highly deviated wells where it is difficult to use conventional wireline tools.
- It can also detect small leaks anywhere in the production tubing, which is also difficult to do with conventional downhole pressure and temperature surveys. It can also be used to detect and calculate casing leaks to shallow formations.
- It is easy to recognize if the well has multiple injection points even if the well is producing with minor instabilities. Instabilities are very important and should be eliminated only if it is necessary to accurately determine the depths of the points of injection.

On the other hand, the main disadvantages of this method are:

- Pressure and temperature surveys must be run anyway if it is required to know the bottomhole pressure and temperature.
- The gas injection and overall operation of the well need to be very stable for this method to give an accurate depth of the communication. Liquid production, injection gas flow rate, and total gas flow rate out of the well need to be accurately measured. Tests done with this procedure are not very reliable if the injection gas flow rate is unstable. The gas flow rate should be as stable as possible to calculate its velocity in the annulus as accurately as possible, as it will be shown later in this section. If the injection gas flow is unstable, it does not matter how accurately the gas flow rate is measured, it would still not be possible to determine the injection gas velocity along the annulus. This is because of the compressible nature of the injection gas (if the gas flow rate at the surface changes, its velocity in the annulus will also change but in a way that depends on the total annular volume and on how the gas flow rate out of the annulus, through the point or points of injection, changes). The gas velocity in the annulus changes proportionally to the variations in the gas flow rate but in a very complex way that can only be determined by means of the continuity equation for unstable, compressible flows.
- To know the gas velocity in the annulus and use this method to accurately calculate annulus-tubing communication depths (as shown below), the injection gas temperature along the annulus should be known. Acoustic devices could be used to help determine the gas injection temperature distribution if the gas specific gravity is very well known. Sometimes, it is not easy to determine the temperature in the annulus because of the complex heat transfer processes that could take place. For example, the injection gas cools as it passes through the surface flow control valve and this could have an important effect if the control valve is very close to the wellhead. In wells with large water cuts or large liquid flow rates, the production temperature might be very high and this could have a profound impact on the injection gas velocity if the volume of the well's annulus is not very large. It is convenient then to do preliminary tests on these types of wells in cases where the point of injection has been established by computational troubleshooting techniques or, better yet, by downhole pressure and temperature surveys, to be able to determine the temperature profile along the annulus that fits the CO<sub>2</sub> travel time. If there is a group of wells, with no operational problems, in schedule for pressure and temperature surveys to be performed, it is a good idea to carry out CO<sub>2</sub> injection tests the same day the surveys are run to fine tune calculations

and to have an excellent reference point for future troubleshooting activities.

- It is necessary to use multiphase flow correlations or models to calculate the gas velocity as it is produced up the tubing if the well is very deep. Usually, the gas takes a long time to travel (from the surface to the point of injection) in the annulus because the gas flow area is very large for most gas flow rates found in many gas lift fields. The upward fluid velocity in the production tubing is much larger (compared to the downward gas velocity in the annulus) and the error made in its calculation is usually not very important unless the well is very deep (or the area of the tubing is large in comparison to the annular area) because then this error might have serious consequences in estimating the depths of the points of injection.

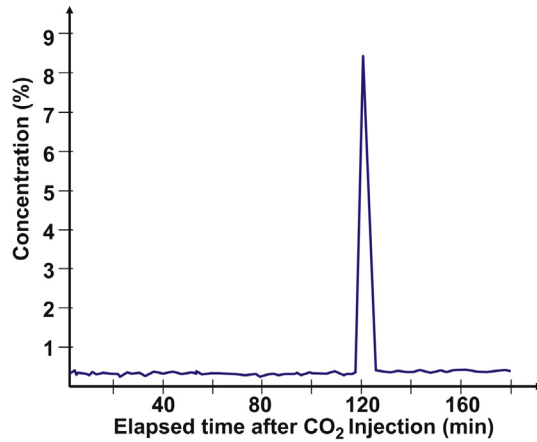
CO<sub>2</sub> is used because it is a readily available gas that does not involve operational risks and it is easily detected by infrared light analyzers.

- CO<sub>2</sub> absorbs infrared light of a specific wave length. Natural gases are transparent to this infrared light; in other words, they do not absorb infrared light of this particular wave length.
- The magnitude of light absorption is proportional to the number of CO<sub>2</sub> molecules present in a given volume.

If a given volume is occupied by pure CO<sub>2</sub>, as its pressure is increased by increasing the number of moles inside that volume (keeping the temperature constant and within the limits of an ideal gas), the infrared light absorption increases in direct proportion to the pressure because light absorption is directly proportional to the number of CO<sub>2</sub> molecules present. It can be said then that the light absorption is proportional to the CO<sub>2</sub> pressure in a given volume. Then, in a mixture of natural gas (which is transparent to infrared light) and CO<sub>2</sub>, at a given pressure and temperature, the light absorption is directly proportional to the number of moles of CO<sub>2</sub> only and therefore to its partial pressure. CO<sub>2</sub> concentration in this case can be given as its partial pressure divided by the total pressure, which is equal to the CO<sub>2</sub> molar fraction and therefore equal to the volume fraction occupied by CO<sub>2</sub> in the ideal gas mixture. If the concentration is very small, it is usually expressed in parts per million (ppm). For higher concentrations, their values are expressed in percentages. A 10,000 ppm concentration is equivalent to 1%, or only one molecule is a CO<sub>2</sub> molecule in 100 molecules of the mixture.

The output of a CO<sub>2</sub> concentration analyzer is shown [Fig. 11.24](#):

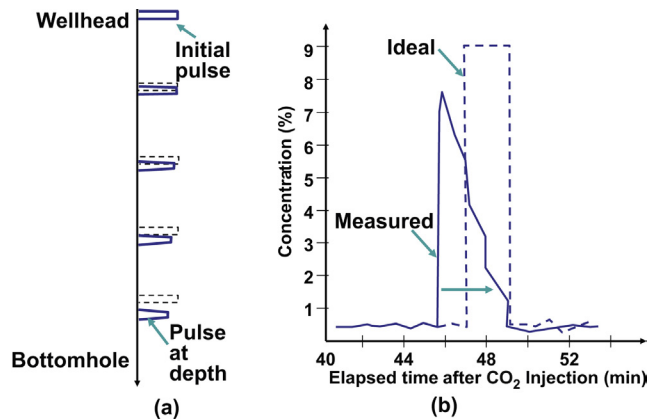
One possible disadvantage of using CO<sub>2</sub> is that it is much heavier than the gas usually used as lift gas. For this reason CO<sub>2</sub> will travel faster, resulting in casing–tubing communications calculated at depths shallower than they



■ FIGURE 11.24 Output of a CO<sub>2</sub> concentration analyzer showing the CO<sub>2</sub> concentration of the total produced gas from the well as a function of time from the moment it was injected into the annulus.

actually are. The fact that CO<sub>2</sub> is injected very cold could have the same effect during the initial stages of the test because a cooler gas has a higher density than a warm gas and therefore will travel faster down the annulus.

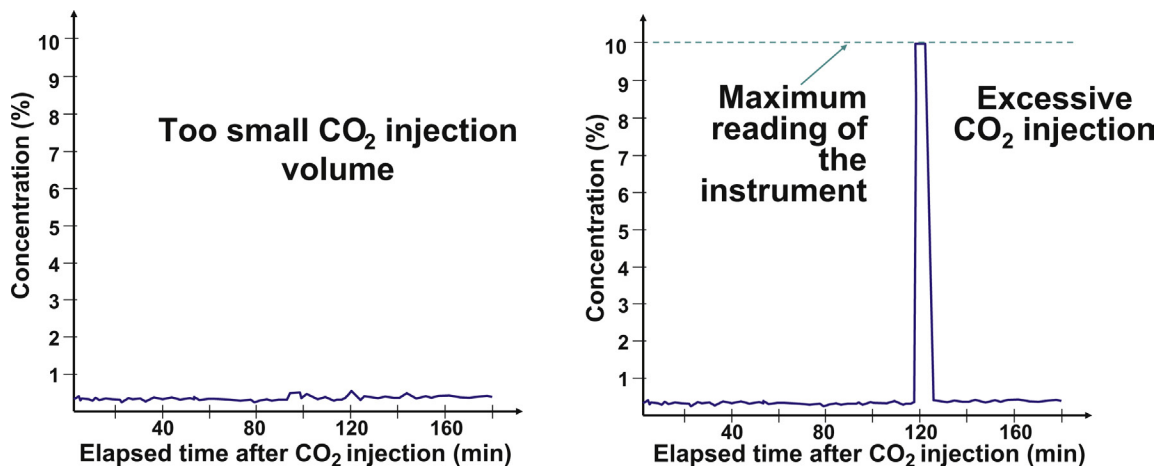
Fig. 11.25a shows how a well-defined CO<sub>2</sub> concentration pulse changes in relative position (getting deeper in relation to its surrounding lift gas) and shape (shorter and wider) as the gas descends in the annulus towards the point of injection. Even though no correction procedure has been reported



■ FIGURE 11.25 Changes in shape and relative position of a CO<sub>2</sub> pulse as it travels down the annulus.

in the literature for weight effects, there have been reports of concentration pulse shapes as shown in Fig. 11.25b, where the measured concentration increases very fast first and then it decreases at a slower pace. The shape of the concentration pulse gives an idea of the distortion of the initial pulse caused mainly by the difference in the specific gravities of  $\text{CO}_2$  and  $\text{CH}_4$ . The deeper the point of injection is, the greater the magnitude of this distortion is going to be (and therefore of the error in estimating the depth of the injection point). However, the shape of the pulse (as it arrives back at the surface) could also be due to an improper  $\text{CO}_2$  injection procedure, maybe because it took a long time to inject the required gas volume or because the injection began at a very high flow rate but, as the pressure of the bottle containing  $\text{CO}_2$  decreased, the injection gas flow rate also decreased. The ideal situation is then to have a bottle pressure high enough to quickly inject all the required  $\text{CO}_2$  volume into the gas injection line at a constant and high flow rate of injection.

Besides injecting  $\text{CO}_2$  as fast as possible into the injection gas line, the right total volume of  $\text{CO}_2$  per pulse must also be used. If a very small volume of  $\text{CO}_2$  is injected, it might not be easy to detect it at the surface, but if too much  $\text{CO}_2$  is used, it might be possible to have a concentration greater than the maximum value that the analyzer can measure, which is not important if there is only one point of injection; however, if there are several points of injection, it would not be feasible to perform the calculation of the gas velocity down the annulus below the first point of injection, as shown later in this section (Fig. 11.26).



■ FIGURE 11.26  $\text{CO}_2$  analyzer output from tests with inadequate volumes of  $\text{CO}_2$  injection.

The right volume of CO<sub>2</sub> to be injected depends on the geometry of the well and on its operational conditions. In a study, reported by [Shnaib et al. \(2010\)](#) in wells with 9 5/8-in. casings and production tubing strings from 3 1/2 to 4 1/2 in. in diameter, with injection point depths between 7,500 and 10,000 ft., it was found that it was necessary to inject 20 lbm of CO<sub>2</sub> to obtain reliable results. They also recommended the CO<sub>2</sub> injection bottle to be 500 psi greater than the gas lift line pressure “throughout” the CO<sub>2</sub> injection operation.

If the injection gas velocities down the annulus and up the tubing are known, the distance traveled by the CO<sub>2</sub> pulse can be calculated by measuring the elapsed time between the moment the CO<sub>2</sub> pulse was injected and the moment it arrived at the surface. The gas velocity at a given point in the annulus is equal to the in situ-gas flow rate,  $Q_{is}$ , divided by the annular flow area,  $A_a$ . The in situ gas flow rate in Mft.<sup>3</sup>/D is given by:

$$Q_{is} = Q_{gi} \frac{14.7}{P} Z \frac{T}{520} \quad (11.22)$$

Where  $Q_{gi}$  is the lift gas flow rate injected at the surface in Mscf/D,  $P$  and  $T$  are, respectively, the absolute pressure and temperature of the gas at that particular depth in the annulus, and  $Z$  is the in situ gas compressibility factor at  $P$  and  $T$ . The in situ velocity of the gas in the annulus ( $V_{is}$  in ft./min) is then equal to  $(Q_{is})/(A_a 1.44)$ , where  $A_a$  must be expressed in ft<sup>2</sup>. The differential time  $dt$  for the gas to travel a differential depth  $dD$  is equal to  $dD/V_{is}$ . The total time ( $T_{\text{total-annular}}$ ) for the CO<sub>2</sub> pulse to travel from the surface to a point of injection at a given depth  $D_M$  is then equal to:

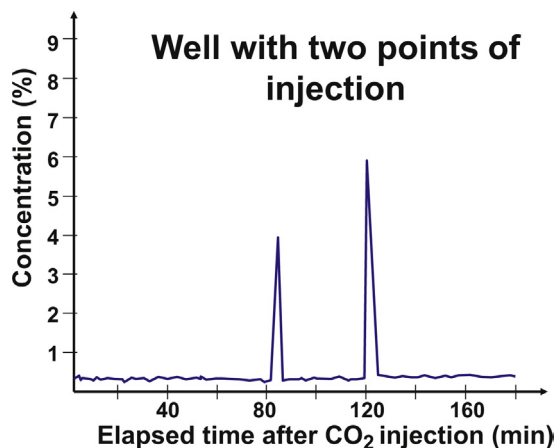
$$T_{\text{total-annular}} = \int_0^{D_M} \frac{dD}{V_{is}} = \int_0^{D_M} \frac{dD}{Q_{gi} \frac{14.7}{P} Z \frac{T}{520} \left( \frac{1}{1.44 A_a} \right)} \quad (11.23)$$

This equation can be solved numerically if the gas pressure and temperature distribution along the annulus are known or can be calculated; it can also be solved in an approximate way using an estimated mean pressure and temperature. The total time interval ( $T_{\text{total-return}}$ ) for the CO<sub>2</sub> pulse to return to the surface from the time it was injected is equal to:

$$T_{\text{total-return}} = T_{\text{total-annular}} + D_M / V_{\text{mean-tub}} \quad (11.24)$$

$V_{\text{mean-tub}}$  is the mean velocity of the gas in the tubing. The mean velocity inside the tubing is usually from 30 to 60 times faster than the gas velocity in the annulus, thus its contribution to the total travel time is very small unless: the annulus space is very small or the tubing flow area is very large (these are factors that tend to reduce the difference between the velocity in the annulus and in the tubing). The in situ gas velocity in the production tubing





■ FIGURE 11.27 CO<sub>2</sub> concentration of the total gas produced from a well with two points of gas injection from the casing–tubing annulus into the production tubing.

can be calculated using multiphase flow correlations or models, which are available in commercial software for oil production engineering. For this purpose, the software should be configured so that the output report shows the in situ gas velocity at different points along the tubing. The calculated gas velocity in the annulus and in the tubing can be used in conjunction with the measured time of arrival of the high concentration CO<sub>2</sub> pulse to calculate the point of injection depth if there is only one point of gas injection into the production tubing. If there are two or more points of injection, the calculation procedure to determine the depths of these points of injection is more complex, as it is explained next. Fig. 11.27 shows the results from a well with two distinguishable points of gas injection from the casing annulus into the production tubing.

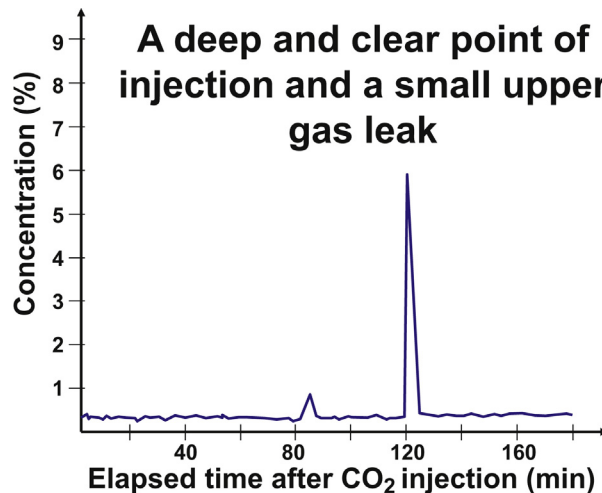
When there are two or more points of injection, it is necessary to know in which proportion the gas enters the tubing at each point to be able to calculate the annular velocity of the gas below each point of injection. The percentage of the total gas flow rate that is injected at each point of injection is found by numerical integration in time of the CO<sub>2</sub> concentration values as shown below. For example, if there are only two points of injection, the percentage of the total gas flow rate that enters each point, named point “1” and “2,” are found by:

$$\%Q_1 = \frac{\int_{t_{1a}}^{t_{1b}} C_1(t) dt}{\int_{t_{1a}}^{t_{1b}} C_1(t) dt + \int_{t_{2a}}^{t_{2b}} C_2(t) dt} \quad (11.25)$$

$$\%Q_2 = \frac{\int_{t_{2a}}^{t_{2b}} C_2(t) dt}{\int_{t_{1a}}^{t_{1b}} C_1(t) dt + \int_{t_{2a}}^{t_{2b}} C_2(t) dt} \quad (11.26)$$

Where  $C_n(t)$  corresponds to the CO<sub>2</sub> concentration curve measured from time  $t_{na}$  at the arrival of pulse  $n$  (when the concentration level rises above the normal concentration) to time  $t_{nb}$ , which is the time when the concentration drops to normal CO<sub>2</sub> concentration levels. Regarding velocity calculations, the velocity before the first point is reached is calculated as it was shown above. Below the first point of injection, the injection gas flow rate  $Q_{gi}$  is reduced to  $(1 - \%Q_1)Q_{gi}$ , which is the new gas flow rate to calculate the gas velocity in the annulus using Eq. 11.22. The annular gas flow rate below point of injection “1” is less than the total injection gas flow rate and therefore it is going to take a longer period of time for the second point to arrive. If this correction is not made, the calculated depth would be much deeper than it actually is. Fig. 11.28 shows a very well-defined deeper point of injection and a smaller, shallower point of injection or gas leak.

There might be a leak to a shallow formation through a casing hole. When this happens, the time of arrival of the concentration pulse could be much longer than expected because the annular gas velocity is reduced as part of the gas flow rate is lost through the hole in the casing. This type of communication is detected by the long period of time for the “single” pulse to arrive back at the surface and by the calculated CO<sub>2</sub> volume that finally



■ FIGURE 11.28 CO<sub>2</sub> concentration of the total gas produced from a well with a well-defined point of injection and a small shallow gas leak.

reaches the surface. Because the CO<sub>2</sub> concentration gives the volume fraction (of the total gas that reaches the surface) that is occupied by CO<sub>2</sub> at a given time, the volume of CO<sub>2</sub> produced at the surface can be calculated by the following equation:

$$V_{olCO_2 \text{ prod}} = Q_{tot} \int_{t_{1a}}^{t_{1b}} C_1(t) dt \quad (11.27)$$

Where  $Q_{tot}$  is the total gas flow rate measured at the separator and its value must be constant during the test. This is a weak point of this calculation procedure because it is usually difficult to measure the gas flow rate at the test separator due to its normal fluctuations. If  $Q_{tot}$  is expressed in Mscf/D and the time  $t$  in days, then  $V_{olCO_2 \text{ prod}}$  is expressed in Mscf. For this calculation to be valid, the gas sample taken at the wellhead must be a representative sample of the total gas produced by the well; in other words, it must have the same concentration value. Because the total amount of CO<sub>2</sub> injected at the surface,  $V_{olCO_2 \text{ inj}}$ , is known, the fraction of this gas that goes to the shallow formation,  $\%Q_{form}$ , can be calculated as:

$$\%Q_{form} = 1 - V_{olCO_2 \text{ prod}} / V_{olCO_2 \text{ inj}} \quad (11.28)$$

From this percentage, the gas velocity above and below the casing hole can be calculated (as indicated above for two points of injection) and only the casing-hole depth remains to be found. In the following explanation, the mean gas velocities above and below the casing hole are  $V_1$  and  $V_2$ , respectively. The volume of CO<sub>2</sub> that remains dissolved in the produced liquids (oil and water) is very small and can be neglected; however, if the water could be separated from the oil, it has been suggested that the pulse's arrival might also be detected by measuring the value of the pH of the produced water, which will have a higher pH when CO<sub>2</sub> is dissolved at higher concentration levels (this is not a very practical procedure because the water would need to be continuously separated and analyzed at the wellhead). When the infrared analyzer is used as explained in this section, the CO<sub>2</sub> concentration is measured at pressures for which almost all CO<sub>2</sub> evolves from the liquids. If it is assumed that the time interval needed for the gas to travel inside the production tubing (from the injection point depth to the surface) is very short, the total measured time  $\Delta t_{measured}$  for the pulse to arrive back to the surface (from the moment it was injected at the surface) is equal to the distance traveled by the gas from the surface to the casing hole divided by its annular velocity  $V_1$ , plus the time traveled by the remaining pulse from the casing hole to the tubing injection point divided by its velocity  $V_2$ . Then, the depth  $H$  of the casing hole can be found from the following equation:

$$\Delta t_{measured} = H / V_1 + (D_M - H) / V_2 \quad (11.29)$$

Where  $D_M$  is the depth of the gas lift mandrel through which the remaining gas flow rate is injected into the tubing. This remaining gas flow rate needs to be known a priori (using  $\%Q_{\text{form}}$  estimated above). In Eq. 11.29, depth  $H$  is the only term that needs to be calculated. If the casing hole is below the injection mandrel, the  $\text{CO}_2$  pulse is going to be detected at the calculated time of arrival for a “single” injection point and it is not possible to use Eq. 11.29 to find the depth  $H$  of the casing hole.

### 11.5.5 Downhole pressure and temperature measurements using permanent downhole sensors

Automation systems are becoming very popular in production operations worldwide. Automation of production operations requires remote data acquisition of many production variables, as well as automatic control of some of these variables, such as the gas injection pressure or gas injection flow rate. Data acquisition parameters might include downhole fluid pressure and temperature, for which permanent downhole sensors are usually installed. Publications have shown the importance of using downhole permanent pressure sensors; see for example the work published by [Jin et al., 2005](#). These downhole measurements greatly simplify troubleshooting tasks because they reduce the need to check many operational conditions, thus the engineer can directly verify the root of the problem. For example, a drop in liquid production together with an increase in the injection gas flow rate and a decrease in the injection pressure could be due to a shallow point of injection caused by a hole in the tubing or a flat valve. But it could also be due to a reduction of the liquid production from the reservoir caused by sand accumulation, formation damage, or a steep decline in the reservoir pressure. If the measured bottomhole pressure is high, the problem could indeed be due to a shallow point of injection and a communication test could be performed very quickly (or any other actions covered so far to find out the cause of a shallow point of injection). However, if the bottomhole pressure is low, the problem is due to low liquid feed in. The well’s total depth could be checked by wireline (if the well has a history of sand problems) or the well might be a good candidate for a stimulation job or a buildup test.

Usually, this level of sophistication is present in high oil flow rate wells, for which the costs associated with downhole measurement is justified because it is important to have at all times: (1) the current operational status of the well, (2) an early warning system, and (3) as much information as possible to minimize the time required to bring the production back to its normal levels.

The optimization personnel have (in real time) the important parameters of the well as functions of time (tendencies). These data values are

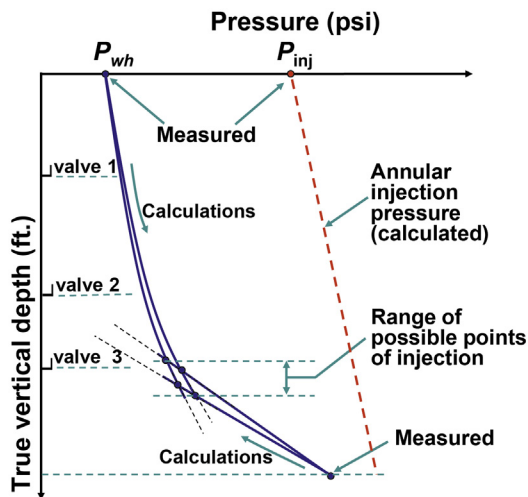
electronically acquired and sent to a data processing station by telemetry and become available to anybody within the company that needs to have access to them. The measured variables usually are: wellhead production temperature and pressure, injection pressure, injection gas flow rate, downhole pressure and temperature, as well as important variables at the test separator in case the well is being tested. Depending on the variable, the time between measurements can go from several minutes to seconds. For intermittent gas lift, for example, it is recommended to have one measurement of the injection pressure every 20 s, while for continuous flow this frequency might be too high and all that is required could be one measurement every 15 min.

Due to the continuous decline in costs associated with new technologies and the potential advantages they offer, an increasing number of companies are using automatic data acquisition systems to gather operational data. Permanent downhole sensors are relatively new in gas lift applications and the number of wells that have these sensors installed is not very large in gas lift fields around the world. Large-scale automatic data acquisition system can provide the following advantages:

- Detect in real time important deviations in the performance of the wells being monitored.
- Send warning signal to the optimization and the operation teams.
- Send the data to gas lift troubleshooting experts systems that process the information and give recommendations based on the knowledge base generated by one or several experienced gas lift specialists. These expert systems, besides using the automatically acquired data, can perform nodal analysis calculations which, in turn, generate additional input data to perform the logical steps that these expert systems usually handle.

As it has been indicated above, the measurement of the downhole temperature and pressure can be of great help to the optimization engineer. One excellent example of a recent application in which these measurements are used is the work presented by Ibrahim et al. (2009) based on a study performed in a gas lift field in Oman.

Multiphase flow calculations can be performed from the bottom of the well towards the wellhead using the formation gas/liquid ratio and from the wellhead (by iterations) towards the bottom of the well using the total gas/liquid ratio. The point where these two curves intersect corresponds to the point of injection if and only if there exists only one point of injection and the multiphase flow correlation predicts the pressure along the tubing with a reasonable level of accuracy. In Fig. 11.29, the injection point depth calculation is presented: the uncertainties regarding multiphase flow calculations (as well

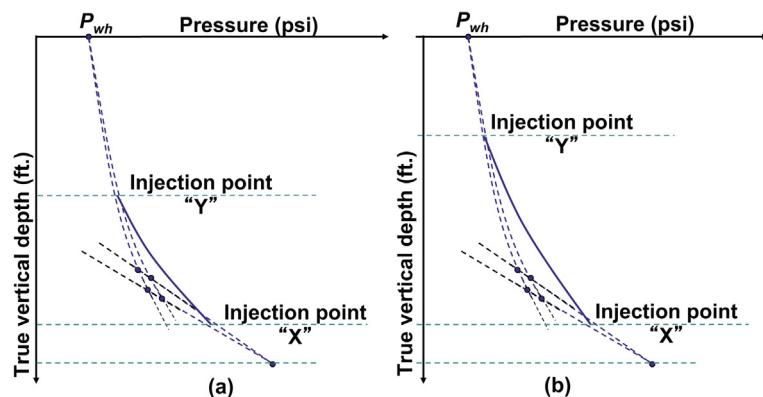


■ FIGURE 11.29 Calculation of the depth of the point of injection from the pressures measured at the wellhead and at the bottom of the well.

as the accuracy of the data used to perform these calculations such as the water cut, formation gas/oil ratio, injection gas flow rate, liquid production, etc.) make it impossible to have a single solution; instead, only a range of possible points of injection can be obtained.

Calculations in the order shown in Fig. 11.29 are usually not available in commercial software. For this reason, one thing that can be done is to calculate the surface production pressure from the measured bottomhole pressure for different points of injection until the calculated wellhead pressure matches the measured wellhead pressure. This trial and error procedure is valid only if: (1) the production is stable, (2) there is only one point of injection, (3) the water cut and gas/oil ratio are accurately known, and (4) the multiphase correlation used can accurately predict the pressure inside the tubing. This last requirement could make this procedure unreliable because it might not be possible to estimate the pressure along the tubing to within a reasonable level of accuracy. The calculated point of injection should be compared to the depths of existing valves. The valve closest to the calculated point of injection might correspond to the operating valve. If two valves are within the range of a possible point of injection, additional calculations using valve mechanic equations and gas mass balance equations need to be performed to determine the actual point of injection, keeping in mind that both valves can actually be open at the same time.

If there is more than one point of injection, there is an infinite number of possible solutions which depend on the depths of the points of injection



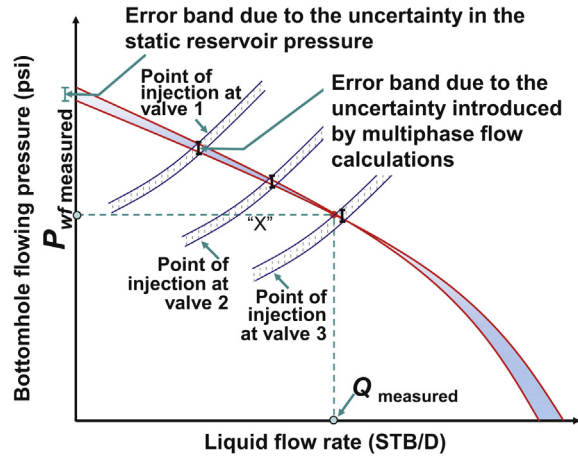
■ FIGURE 11.30 More than one point of injection (stable operation).

and on the gas flow rate that is injected through each of them. The same well, with the same reservoir and wellhead pressures and the same lower point of injection “X” can have a different upper point of injection “Y” if the gas flow rate through “X” is different, as shown in Fig. 11.30. The difference between Fig. 11.30a and b might be due to the fact that the gas flow rate through point “X” in Fig. 11.30a is smaller than in Fig. 11.30b, making the pressure gradient in Fig. 11.30a heavier (more horizontally inclined).

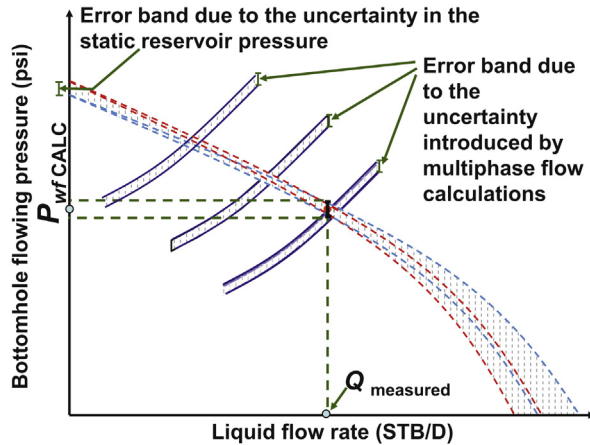
If the reservoir static pressure and the liquid production are known, the measured bottomhole pressure can be used to build the IPR curve, which in turn can be used to determine the point of injection using nodal analysis. Nodal analysis can be performed using the injection point depth as the sensitivity variable. The nodal analysis shown Fig. 11.31 corresponds to a well with three gas lift valves. The error band due to multiphase flow calculation errors for the outflow curves and the error band due to the uncertainty in the value of the static reservoir pressure for the inflow curve calculation are shown in the figure. It can be noticed that the error band is substantially reduced due to the fact that the bottomhole pressure is measured and not calculated. The injection point seems to be at the third valve’s depth for the well operation shown in Fig. 11.31.

Troubleshooting using nodal analysis can also be used even if the bottomhole pressure is not measured, but the uncertainty band of the IPR curve could be considerably larger, as shown in Fig. 11.32.

If there are many valves installed in the well and the distances between them are not very long, the use of nodal analysis to determine the point of



■ FIGURE 11.31 Nodal analysis for three different points of injection corresponding to the valves installed in the well (bottomhole flowing pressure  $P_{wf}$  is measured).

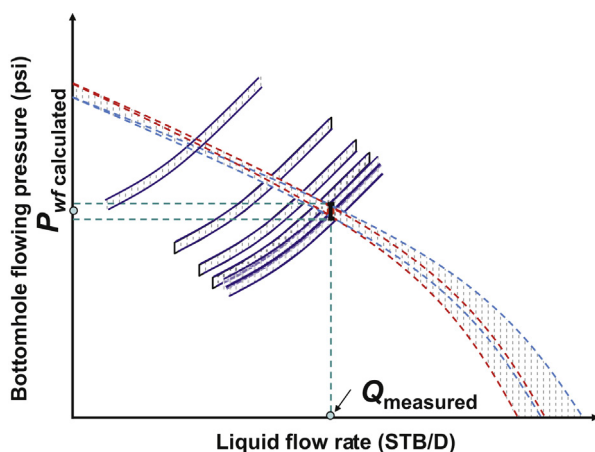


■ FIGURE 11.32 Nodal analysis for three different points of injection corresponding to the valves installed in the well ( $P_{wf}$  is calculated).

injection is not very reliable, especially if the bottomhole pressure is not measured (Fig. 11.33).

Permanent pressure sensors can be used to obtain several stable points along the IPR curve by changing the surface injection gas flow rate and measuring the liquid production at each of these injection gas flow rates (this test is called “multirate test”). These points improve the accuracy of the IPR curve and can be used to estimate the formation damage, the productivity index





■ FIGURE 11.33 Nodal analysis for six different points of injection corresponding to the valves installed in the well ( $P_{wf}$  is calculated).

and, by extrapolation to zero liquid flow rate, even the reservoir pressure. Sufficient time for the well to reach steady-state must be allowed at each injection gas flow rate in order to be able to measure the corresponding liquid production. The minimum and maximum values of the injection gas flow rate to avoid well instabilities must be known before performing a multirate test. If the injection gas flow rate is too low, the production pressure might become greater than the injection pressure at the point of injection. If the injection gas flow rate is too high, an upper unloading gas lift valve might open. Both situations are explained in detail in Section 11.3. Gas lift designs should provide a wide range of possible operating surface injection pressures in order to perform this test in a practical way in the field. If the range of possible operating surface injection pressure is too narrow, the points along the IPR curve are going to be too close to each other and the extrapolated IPR curve will not be too accurate (for points away from those determined by the test).

### 11.5.6 Total well depth and liquid level measurements using wireline tools

This is a troubleshooting technique widely used in the field and it simply consists in running in the well a sample bailer and a tubing end locator. The tubing end locator is used to correlate the total depth of the well measured by wireline using the sample bailer. This information is used to determine if sand has accumulated at the bottom of the well, partially or totally blocking the perforation interval. Additionally, the wireline unit can be used to

determine if there is an obstruction or any solid deposition on the wall of the production tubing by means of a tubing gauge tool run in the well in a sequential way, starting with the gauge corresponding to the tubing drift diameter. The characteristics of the wireline tools mentioned in this section are given in Section 6.3.

A quick way of determining the depth of the liquid level is to shut the surface gas injection off, allow time for the fluids to stabilize at the bottom of the well, and run in the well a blind box or an impression block at a velocity that will allow the wireline operator detect the liquid level (by noticing changes in the wireline tension). The velocity of the blind box or impression block depends on the type of crude (heavy or light oil) and it does not need to be very high. The wireline velocity should be reduced while passing through a gas lift mandrel to avoid damaging the latch of the gas lift valve. Today, most gas lift mandrels are built with a wireline tool discriminator that will protect the latch from most wireline tools, except those that can get inside the side pocket.

The liquid level should be at a reasonable depth above the operating valve. If there are several mandrels located below the liquid level, it could be hard to single out the actual operating valve from all valves below the liquid level (the reservoir could produce liquids for a while after the surface gas injection is shut off and liquids from the upper part of the tubing may fall to the bottom of the well contributing also to the generation of a large liquid column). However, an abnormally deep liquid level, near or below all gas lift valves, could indicate a reservoir pressure decline or important formation damage. On the other hand, a liquid level abnormally shallow could point to a hole in the tubing or a flat valve.

As presented here, the liquid level obtained after shutting off the surface gas injection to the well does not correspond to the reservoir static liquid level. To obtain the static liquid level, it is necessary to wait for a much longer period of time.

### 11.5.7 Downhole temperature measurement using fiber-optic surveys (distributed temperature sensors or DTS)

The use of fiber-optic surveys to measure the temperature along the production tubing is becoming a very popular troubleshooting technique. In continuous temperature surveys using RTD sensors, explained in Section 11.5.2, measurements are continuously taken as the sensors travel down the well at velocities of around 100–150 ft./min. This means that it would take more than 1 h between the time the temperature is measured at the wellhead and

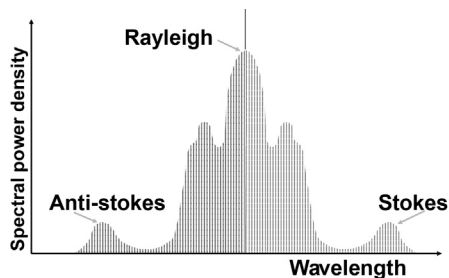
the time it is measured at the bottom of a 10,000-ft. deep well. On the other hand, with optical fibers, temperatures (all along the production tubing and regardless of its length) can be taken in a matter of seconds or, at the most, in a few minutes. However, it should be pointed out that RTD sensors have an accuracy of 0.001°F, while for optical fibers the accuracy depends on the time allowed for the measurements to be taken: it takes much less than a second to do only one scan of the temperature along the well's depth but a great number of measurements is needed to improve the quality or resolution of the measurements. For wells of approximately 8000 ft. of depth, it takes 1 min to gather enough measurements to get a resolution close to 1°F and 30 min for a resolution of 0.2°F.

The physical principle behind fiber-optic temperature measurement is explained next:

As a light beam travels down the well inside the optical fiber, its intensity diminishes because a very small fraction of the initial beam is reflected back to the surface at every point along the optical fiber. Three different events can happen when a photon strikes a molecule of the optical fiber at a given point: (1) the photon is reflected back elastically keeping its original energy and therefore its wave length, originating what is known as Rayleigh reflection, which constitute the greatest part of all the light reflected to the surface, (2) the molecule absorbs the photon (the molecule reacts by changing its energy level to a higher one and emitting a new photon of less energy than the original one and therefore of greater wave length, generating what is called Stokes reflection), or (3) the molecule absorbs the photon (the molecule reacts by changing its energy level to a lower one and emitting a new photon of greater energy than the original one and therefore of lower wave length, generating what is called anti-Stokes reflection which is proportional to the temperature of the optical fiber at that particular point and has an intensity which is less than the intensity that the Stokes reflection has).

If the spectrum of all the light reflected back to the surface from only a particular point in the optical fiber is analyzed, the temperature of the optical fiber at that particular point is determined by the Stokes/anti-Stokes reflection ratio. Fig. 11.34 shows a typical spectral power density graph of the reflected light. Because the speed of light is constant inside the optical fiber, the depth from which the reflected light is coming can be calculated by measuring the time it takes for the light beam to travel to and back from that particular point in the well.

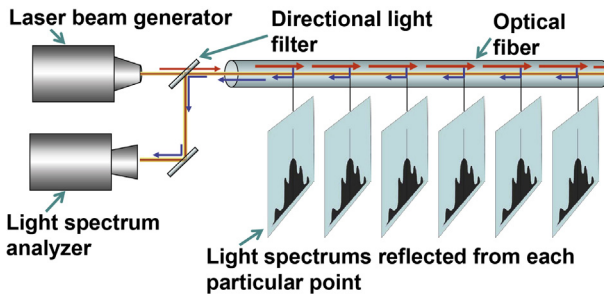
If  $c$  is the speed of light in the optical fiber,  $D$  is the depth of a particular point in the optical fiber and  $\Delta t$  is the time taken for the light to go from the light source to the particular point in the optical fiber and back to the light



■ FIGURE 11.34 Light spectrum of reflected light from a given instant and point in the optical fiber.

spectrum analyzer, then  $D = (c\Delta t)/2$ . If light is generated at a given time and its reflected spectrum is analyzed at different time intervals afterwards, the temperature can be determined along the optical fiber at each depth (defined by its respective time interval from the moment the light pulse was generated) by measuring the ratio of the Stokes and anti-Stokes reflections. Because the reflected light is not very intense, a great number of measurements must be taken from a single point to increase the precision of the temperature calculation at that point. Therefore, with current technology it is not really possible to obtain an instantaneous measurement of temperature with the same precision that RTD sensors can achieve. Current commercially available instruments can provide a temperature reading every 3 ft. along the optical fiber.

Fig. 11.35 shows a schematic diagram of the measuring equipment: a laser beam pulse (monochromatic light) of very short duration (in the order of nanoseconds) generated at the surface, passes through a directional filter (which allows the light to go from the generator to the well, but reflects

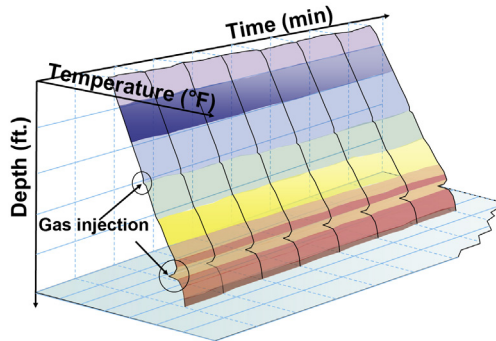


■ FIGURE 11.35 Equipment required for temperature measurements using fiber-optic surveys.

the light coming back from the well). The reflected light is captured by the spectrum analyzer to measure the Stokes/anti-Stokes ratio.

It is not necessary to run in the well electronic equipments to measure temperature using optical fibers in this way. Optical fibers are not affected by vibrations or electromagnetic waves and they can have a working temperature range of  $-90$  to  $+500^{\circ}\text{F}$ . These operational limits are established mainly by the material used to isolate the optical fiber. There are optical fiber cables of  $1/4$ ,  $3/16$ , and  $1/8$  in. in diameter that can usually withstand loads of up to 1500 lb. With the help of weight bars, optical fibers can be run in the well at a velocity of around 100 ft./min. The wellhead lubricators used with fiber-optics applications are the same as the ones used for slick lines, which usually have a hydraulic device to control the inside pressure. The technique to measure temperature along the well with optical fibers, known as DTS, was introduced in the oil industry in the mid-1990s (although the physical principal on which this technique is based was known since the 1930s). Optical fibers are used for a variety of troubleshooting tasks: detecting the depth of the point of gas injection, finding the location of communications or holes in the tubing or in the casing, identifying the producing perforated intervals, identifying the perforating intervals through which water is being injected in water injection wells, or detecting communicating channels behind the casing, among others.

The great advantage of using optical fibers is that downhole temperatures along the well can be known almost in real time under stable or unstable conditions. The optical fiber is introduced in the well through a lubricator. In the lower part of the optical fiber a wireline socket can be installed below which weight bars, wireline pressure and temperature sensors, and a CCL detector can be installed. The CCL is used to correlate the temperature measurements taken by the fiber optic with the depths of each point along the well. Wireline pressure and temperature sensors run in the well with the optical fiber can store their measurements in downhole electronic memory units, although some operators use sensors that have the capacity of sending their signals to the surface in real time while the optical fiber is being run in the well and throughout the entire time the optical fiber is in the well. Some service companies offer the use of three optical fibers inside one cable: two optical fibers are used to measure the temperature and pressure at the bottom of the well and the third is used to measure the temperature along the entire length of the well (DTS). When an optical fiber is used to find the position of a large casing-tubing communication, it might also be useful to install in the lower end of the optical fiber a turbine type flow meter. The temperatures measured using fiber optics can be presented in two dimensional graphs (temperature-depth diagrams) like those shown for conventional



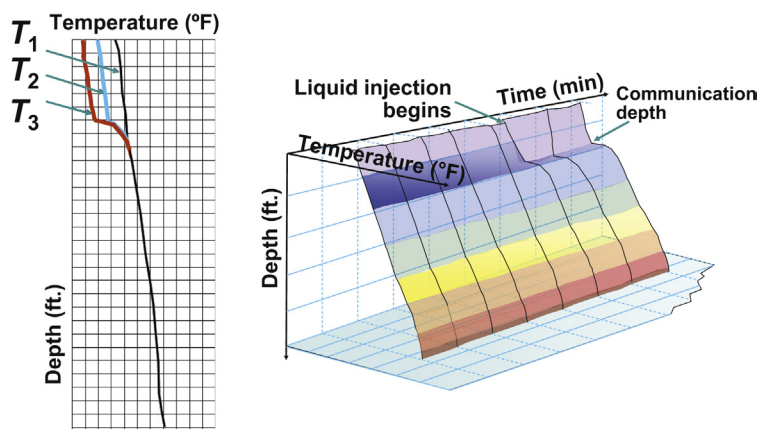
■ FIGURE 11.36 Three dimensional graph with the temperature (measured using an optical fiber) as a function of time and depth.

temperature measurement in Figs. 11.15 and 11.16, or in three dimensional graphs as shown in the next figure.

Two stable points of gas injection are shown in Fig. 11.36. This type of three-dimensional graph is very useful in analyzing the temperature behavior in time, especially if the gas injection is unstable.

Optical fibers can also be used to detect holes or communications along very deep wells (or, in general, in places where it will be too expensive to pull the tubing out of the well) in the same way high precision temperature sensors run in the well by wireline are used.

Once gas injection has been shut off, the optical fiber is run in the well to get a base temperature of the fluids along the production tubing. Then, liquid is injected down the annulus with tubing return or vice versa. Water is the most frequently used liquid. The liquid flow rate is determined by the size of the hole and the liquid injection pressure at the surface. If it is desired to detect more than one communication, it is important to pump the liquid at a very high pressure to make sure that the pressure drop at each communication can be detected. The communication is detected by an anomaly in the temperature measurement around the point where the communication is located. Previously, gas lift valves should have been replaced with dummy valves and a standing valve should have been installed at the bottom of the tubing to protect the formation. The advantage of optical fibers in this case, compared with high sensitive wireline temperature sensors, is that it is possible to stop the liquid injection at any moment as soon as a temperature anomaly is found and analyzed by the operator (almost in real time) at the surface. Additionally because the optical fiber does



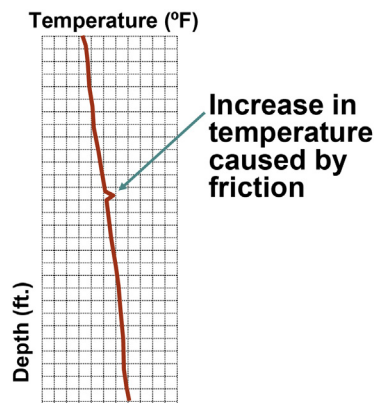
■ FIGURE 11.37 Casing–tubing communication detected by temperature measurements.

not move, measurement errors introduced by the movement of wireline pressure and temperature sensors, as they are run in or pulled out of the well, are not present when using optical fibers.

Fig. 11.37 shows what happens when liquids are injected down the tubing and circulated up the annulus. As soon as the liquid injection begins, liquids inside the tubing are forced down towards the communication. All the liquid above the communication is displaced downwards. This causes the temperature at points above the communication to drop. Below the communication, the temperature does not change because the fluids don't move (the gas lift valves have been replaced with dummy valves and a standing valve was installed at the bottom of the tubing). In Fig. 11.37,  $T_1$  is the initial temperature and, as liquids are injected, it changes first to  $T_2$  and then to  $T_3$ :

Fig. 11.38 shows the temperature measurements in a well in which a communication test revealed a hole in the casing. Gas lift valves were replaced by dummy valves and water was injected down the annulus without circulating it back to the surface. The fiber optic inside the tubing was able to detect the increase in temperature caused by friction as liquids were injected into a shallow formation through a hole in the casing. This heating effect can also be detected in wells with a small hole in the production tubing, for which water can be injected down the tubing with return up the annulus. Using this technique, more than one hole can be detected if water is pumped at a sufficiently high rate to cause a temperature increase in small communications.

Permanent DTS cables are installed on the outside wall of the tubing. These installations work very well most of the time to find the point of gas injection,



■ FIGURE 11.38 Detection of a communication in the casing wall.

but it might be difficult to locate the point of injection depth in high rate wells with high water cuts because it could be very hard to distinguish the cooling effect caused by the expansion of the injection gas from the normal temperature fluctuations along the well. Specific examples of field applications of temperature measurements using fiber-optics have been published by: [Brown et al. \(2005\)](#), [Julian et al. \(2007\)](#), and [Gonzalez et al. \(2008\)](#).

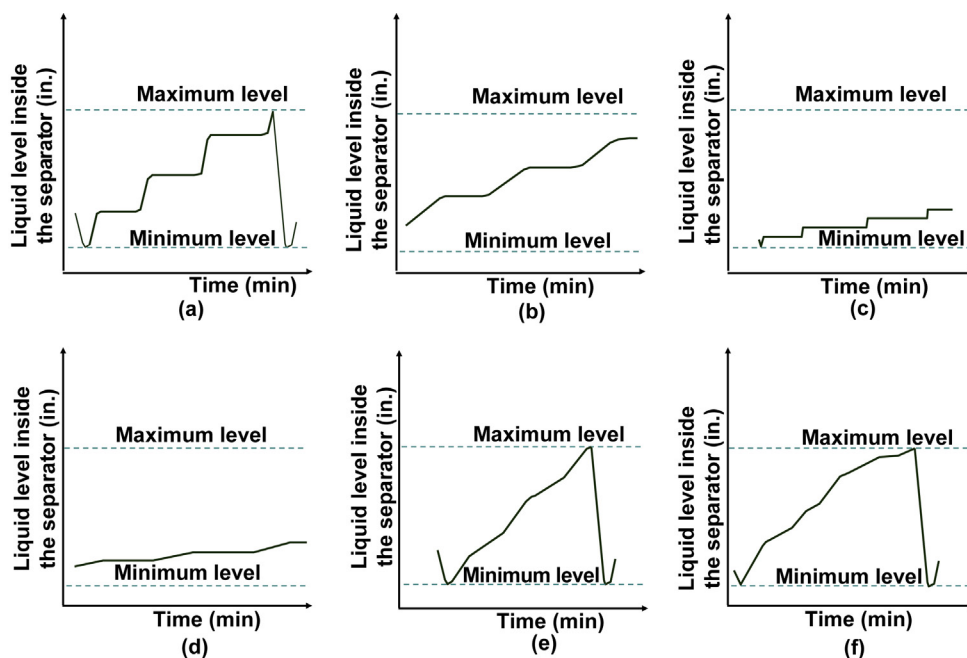
### 11.5.8 Measurement of the liquid level (or instantaneous liquid flow rate) inside the test separator

When the “dump-valve” system is used in the test separator to measure the liquid production of the well, the way in which the liquid level behaves as a function of time in the test separator can give important clues as to what might be happening in the well. For example, surface gas injection might appear to be taken place intermittently but the well could be producing liquids in a continuous fashion. The well might be heading but the liquid production never goes down to zero. In some test separators, the liquid production is determined by measuring the time it takes for the liquid level to go from a minimum to a maximum value. Once the liquid level reaches the maximum value, a dump valve opens and the liquid is discharged to the liquid storage tank at the flow station. When the liquid level reaches the minimum value, the dump valve closes to initiate a new measuring cycle. The liquid production is equal to the volume of liquid inside the separator between the minimum and maximum levels, divided by the time it takes for the liquid to fill the volume between those two levels. Some of the ways in which the liquid level might change in time are presented in [Fig. 11.39](#).

In [Fig. 11.39a](#) the liquid production is intermittent, with large liquid slugs that reach the surface at a high velocity. In [Fig. 11.39b](#) the liquid production is intermittent, with large liquid slugs that reach the surface at a low velocity. In [Fig. 11.39c](#) the liquid production is intermittent, with small liquid slugs that reach the surface at a high velocity. In [Fig. 11.39d](#) the liquid production is intermittent, with small liquid slugs that reach the surface at a low velocity. In [Fig. 11.39e](#) the liquid production is continuous, with regular intervals of larger and smaller liquid production flow rates. In [Fig. 11.39f](#) the liquid production is continuous but the well is heading with slugs of irregular sizes reaching the surface in a random fashion.

When a flow control valve (instead of the “dump-valve system”) is used to keep the liquid level in the test separator constant, the liquid production is measured by integrating (in time) the instantaneous liquid flow rate signal at the liquid outlet of the separator. This flow rate signal should have a





■ FIGURE 11.39 Behavior of the liquid level (or instantaneous separator's outlet liquid flow rate) in the test separator.

behavior similar to the ones shown in Fig. 11.39 for the liquid level, with patterns also easy to recognize.

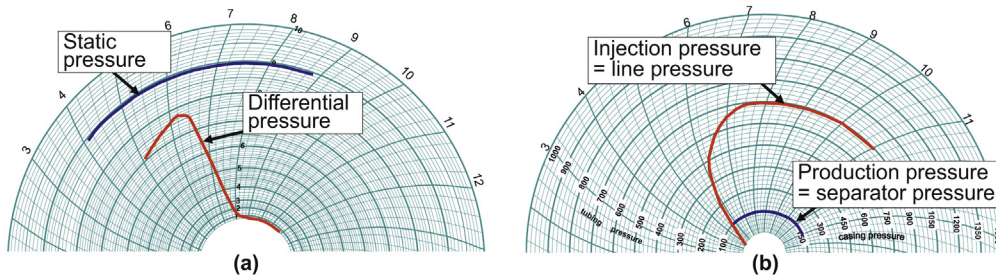
The gas flow rate at the gas outlet of the test separator can also give hints as to what might be taking place in the well, but most of the time it is not used as an analytical troubleshooting tool because of the erratic behavior of the differential pressure across the orifice plate (if an orifice plate is used) or the erratic behavior of the output signal of a turbine or vortex flow meter. This is the reason why it is usually not possible to accurately measure the formation gas/oil ratio. Nevertheless, it is recommended to always analyze the total gas flow rate chart, or signal, to check its value in the best possible way and determine if there is a flow pattern that can be used to infer what might be happening in the well or if there is a restriction at the separator that is keeping it at a pressure much higher than the gas gathering system. One way of reducing the error in the calculation of the total gas flow rate at the test separator is by integrating in time the gas flow measurement signal. There are mechanical integrators that can be used when the only information available is the differential and static pressures in the orifice plate chart. If the flow is given as an electronic signal, a simple routine can be used to perform a numerical integration in time of the total gas flow rate.

### 11.5.9 Use of injection gas flow rate measurement charts

The measurement of the injection gas flow rate that goes to each well is usually centralized at the gas injection manifold. In this way, it is easy and economical to maintain and keep records of the injection gas flow rates to all wells. To avoid measuring problems associated with cooling effects of the injection gas (like, for example, hydrates formation), the orifice plate that is used to measure the gas flow rate should be installed upstream of the gas flow control valve. Unfortunately, this way of installing the orifice plate does not allow the measured static pressure to be used as a reference for the injection annular pressure at the wellhead. If the orifice plate is away from the well, at the injection manifold for example, and installed downstream of the gas flow control valve (not recommended as indicated above), the static pressure used in the measurement of the gas flow rate is not exactly the actual injection pressure at the wellhead, but it is close to it and its variations would be very similar to the ones at the wellhead. If the orifice plate is installed near the well (and at the same time downstream from the gas flow control valve but far from it) the gas cooling problems are reduced and the static pressure is a good reference of the injection gas pressure at the wellhead. In this situation, some operators use a three-pen chart recorder for: (1) the wellhead production pressure, (2) the wellhead injection pressure, and (3) the differential pressure across the orifice plate. In any case, the behavior in time of the static and differential pressures used in the measurement of the gas flow rate can provide important clues as to what might be taking place in the well. Wellhead pressure charts should always be recorded together with the gas flow rate charts or be integrated in a single chart as was already mentioned. This is done not only to measure the gas flow rate, but also to determine how the gas flow rate changes in time and associate these changes with events taking place in the well and in the gas lift system.

The signal fluctuations from gas flow rate measurement devices other than orifice plates, such as vortex flow meters or turbine flow meters, can be analyzed in the same way as the behavior of the differential pressure is analyzed when orifice plates are used. Vortex and turbine flow meters offer a wider range of gas flow rate measurements but they are more expensive, very sensitive to liquids and solid particles in the gas flow, and need more maintenance.

For a well that is not taking any gas, the gas flow rate measurement and wellhead pressure charts would look like the ones shown in [Fig. 11.40](#) when the gas injection to the well is initiated. The wellhead gas injection pressure increases as expected while the annulus is being pressurized, but the gas pressure continues to increase until it reaches the line injection pressure

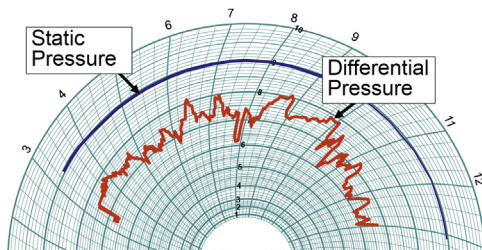


■ **FIGURE 11.40** Well is not taking gas. (a) Gas flow rate measurement chart and (b) wellhead pressure chart.

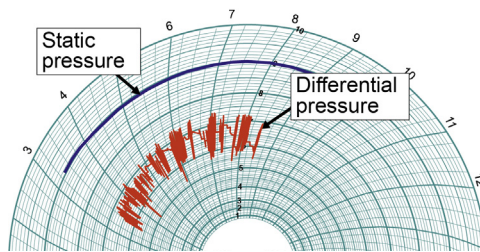
and the gas flow rate goes down to zero. In Fig. 11.40, the gas flow rate is measured upstream of the gas flow control valve.

Sometimes, the differential pressure at the orifice plate behaves in a strange way and control of the gas flow rate is lost. One of the following alternatives might be taking place at the gas injection flow control valve: (1) its internal components have failed and the valve's stem moves in an uncontrolled fashion, (2) dirt or solid particles are being accumulated at the valve, and the injection gas flow rate behaves in an erratic way or it stops all together, or (3) there might be freezing problems that make the injection stop for short periods of time or behave in a characteristic way that helps identify the problem.

Fig. 11.41 shows what happens when gas injection control is lost due to dirt accumulation at the surface control valve or the internal components of this control valve fail. This particular well is not automated so no automatic control actions are taken to regulate the gas flow rate or the pressure (the flow rate is set manually). In this case, it is recommended to vent the gas injection line and to check the flow control valve internal components. It is also a good idea to check the chart recorder to verify that the problem is actually happening in the way it is shown by the chart and not some malfunction of the recorder itself.



■ **FIGURE 11.41** Gas flow rate chart. Flow rate control is lost due to dirt accumulation or malfunction of the internal components of the flow control valve.



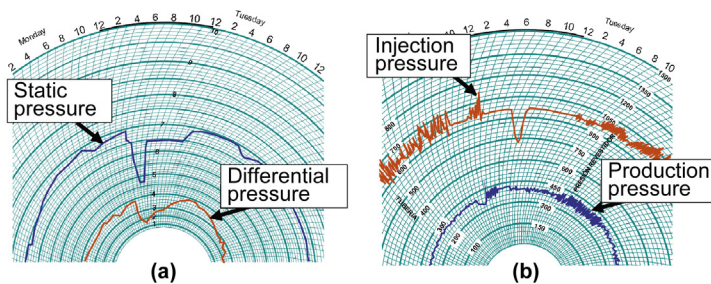
■ FIGURE 11.42 Gas flow rate chart. Gas flow rate control is lost due to hydrate formation.

Although it is usually difficult to determine what the problem with the injection gas flow rate control valve is, the pressure pattern caused by hydrate formation is easy to identify. The differential pressure pattern shown in Fig. 11.42 is typical of a well with hydrate formation problems (the differential pressure goes up and down in a high frequency pattern). This pressure pattern is also very similar to the one that can be seen in wellhead pressure charts when there is hydrate formation. It can appear in the wellhead pressure recorder but not in the gas flow recorder or vice versa, or it can be present in both recorders at the same time.

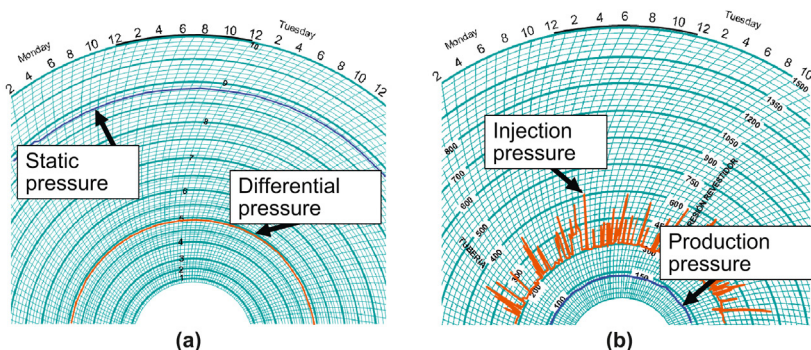
In the following two figures, irregular wellhead pressure patterns caused by hydrate formation are shown together with their respective gas flow rate charts. In both cases, the gas flow rate control valve is near the wellhead.

In Fig. 11.43 there is an instability problem of the injection pressure system together with a hydrate formation problem that shows up at the wellhead pressure charts but not at the gas flow measurement chart.

In Fig. 11.44 the gas flow rate measurement is not affected by what is happening in the well because the gas flow rate control valve, located downstream of the orifice plate, is in critical flow. Usually, what happens in the



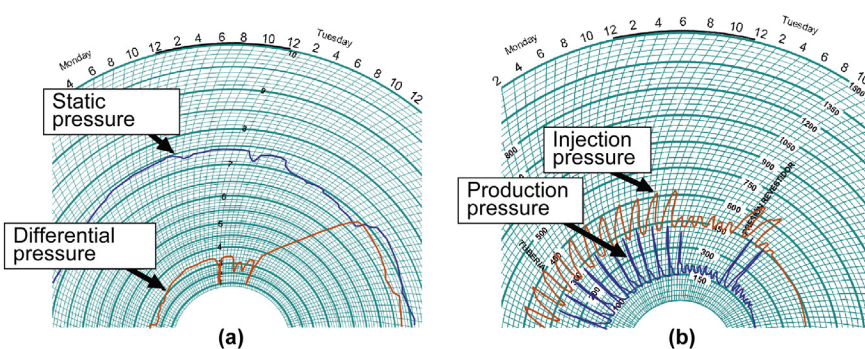
■ FIGURE 11.43 Wellhead pressure fluctuates due to hydrate formation and gas lift system instabilities (7-day charts). (a) Gas flow rate chart and (b) wellhead pressure chart.



■ FIGURE 11.44 Pressure fluctuates due to hydrate formation (7-day charts). (a) Gas flow rate chart and (b) wellhead pressure chart.

well could be reflected in the gas flow measurement chart but not in a very pronounced way or not at all as shown in this example.

Many times, the only way to understand what happens in the well is by analyzing the wellhead pressure chart together with the gas flow rate chart (both charts recorded during the same time interval). Fig. 11.45 shows what happens when gas is injected into the production tubing through a large casing–tubing communication. If the gas injection flow rate is low, the well produces large liquid slugs at regular intervals. Injection gas uncovers the tubing hole at regular intervals. When the gas flow rate drops (notice that the differential pressure in the gas flow rate chart drops to zero several times), the slugs become smaller, but when the gas flow rate is increased to a high value (the differential pressure in the gas flow rate chart goes up), the well begins to flow in a stable manner with a low injection pressure.



■ FIGURE 11.45 Well with a casing–tubing communication: flows with large casing and tubing pressure fluctuations at low injection gas flow rates and with constant wellhead pressures at high injection gas flow rates. (a) Gas flow rate chart and (b) wellhead pressure chart.

The optimization engineer should be aware of the fact that the size of the orifice plate reported in the well's file might not be the actual one installed in the field. Orifice plates are sometimes mounted in meter runs that allow the orifice plate to be inspected in an easy way; however, in most cases it takes time and effort for the operational personnel to verify the diameter of the orifice plate and they are usually reluctant to check its actual size.

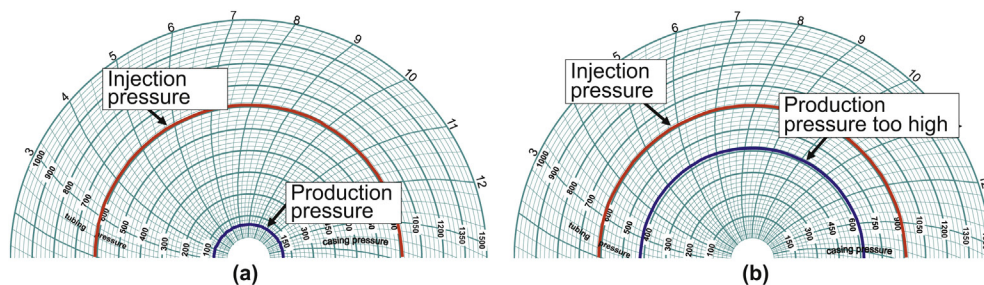
The static and differential pressure sensors must be calibrated using a dead weight tester or any instrument that will ensure that the measurements are precise. One quick way of having only an idea of the actual calibration of the static pressure sensor is to disconnect it and expose it to atmospheric pressure, the static pressure reading shown in the chart should go down to zero. Regarding the differential pressure sensors, they usually have integral manifolds that allow the operator to do the following quick calibration check: close the two valves that communicate the differential pressure sensor to the high and low pressure taps of the orifice plate and then open the central bypass valve that equalizes the high and low pressure intakes. The differential pressure reading should then go down to zero if the sensor is properly calibrated (the sensor might still have other calibration problems that should be checked with special equipment from time to time).

#### 11.5.10 Use of wellhead pressure charts

It is in most cases impossible to troubleshoot a well on gas lift without knowing how the wellhead production and injection pressures behave in time. Although it is not possible to reach a final conclusion about the well current status just by looking at wellhead pressure charts, there are distinctive pressure patterns that point to specific problems and greatly simplify troubleshooting tasks. Every well should have pressure charts recorded regularly (unless the well is equipped with electronic sensors and the data is remotely obtained in real time). This might be accomplished by installing permanent pressure chart recorders or by using portable units to attend several wells in a particular area, regardless of their current operational conditions. Examples of wellhead pressure charts showing typical operational problems are presented in this section.

Fig. 11.46a shows a typical behavior of the wellhead pressures of a well with IPO valves in continuous flow, in which the liquids are produced up the production tubing string.

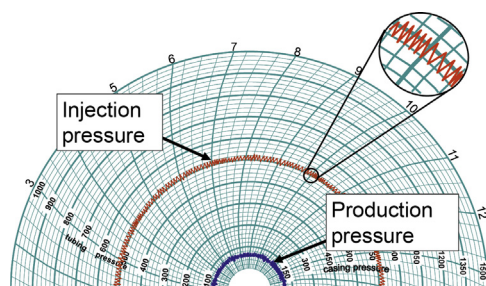
Fig. 11.46b shows a high wellhead production pressure that can cause a decrease in liquid production. The most important causes of high wellhead production pressure are: unnecessarily high injection gas flow rates,



■ FIGURE 11.46 (a) Well on continuous gas lift without apparent operational problems (stable injection pressure at its design value, stable production tubing pressure at an acceptable low value). (b) Too high wellhead production pressure.

emulsions, bends and unnecessary restrictions at the wellhead and flowline such as chokes or choke housings, high separator pressure, flowline too long or with an ID too small, smashed flowlines, solid depositions along the flowline like paraffin, sand, asphaltenes, or carbonates.

The behavior presented in Fig. 11.47 is typical of a well that produces a high viscosity liquid (emulsions or heavy oils). These wells are better produced with a high frequency intermittent gas injection. The spread of the valve (difference between the opening and closing pressures of the gas lift valve) should be small and the injection frequency high so that the liquid production can be continuous. Injection cycles of 5 min in duration are common in wells with points of injection at approximately 8000 ft. of depth. Intermittent injection lowers the possibility of emulsion formation by decreasing the effect of liquid and gas flow turbulences present in continuous gas injection. The tubing is filled with liquid slugs separated by gas bubbles that are injected at regular intervals. These gas bubbles are very small compared to the gas bubbles that are injected into standard intermittent gas lift wells. For heavy oils, high frequency intermittent injection avoids foam formation that increases



■ FIGURE 11.47 Well producing viscous fluids: gas injection (intentional or not) is intermittent while the liquid production is continuous.

the pressure drop along the tubing. Existing multiphase flow models and correlations are not adequate to calculate, in a precise manner, the pressure along the production tubing with high frequency intermittent gas injection. The production pressure is usually high in wells producing with this type of flow pattern so this technique only works if the reservoir pressure is high enough to sustain liquid production at large bottomhole flowing pressures.

Even though high frequency intermittent gas injection increases the efficiency of the gas lift method for the types of liquids mentioned above, the lifting efficiency is not greatly improved. It is advisable to operate high reservoir pressure wells that produce heavy oil with electric submersible pumps (ESP), which is something that until not too long ago was thought to be impossible. It has been demonstrated that the high liquid production obtained with ESPs helps keep the fluids warm and, therefore, the viscosity at a low value.

Fig. 11.47 corresponds to a well on choke controlled intermittent gas lift. However, this high frequency gas injection can be attained with the use of surface intermitters as well. For choke control, the frequency variations that are shown in the figure are caused by fluctuations in the gas lift system's pressure, which in turn causes changes in the injection gas flow rate: when the gas flow rate increases, the cycle time decreases, and vice versa. The well-defined, sharp pressure peaks indicate that the downhole valve is opening and closing and not a gas lift valve (in throttling flow) that never completely closes. The well should be troubleshoot (in an approximate way) as a continuous flow well even though the tubing pressure cannot be accurately determined, but troubleshooting the well as an intermittent gas lift well would be totally wrong. The gas lift valve installed in the well with the pressure chart shown in Fig. 11.47 is an IPO valve.

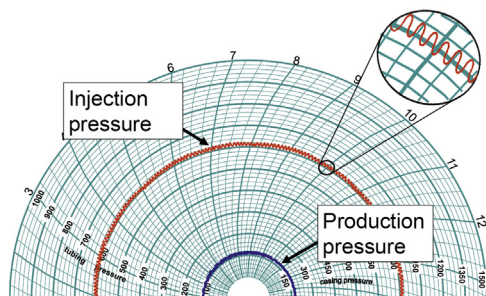
The pressure behavior shown in Fig. 11.47 can also be due to an improperly-set, low injection gas flow rate to a well with a single-element, IPO valve (not a pilot valve). Continuous gas lift wells with single-element, IPO valves at the operating point of injection tend to produce on intermittent gas lift with very small valve's spread when the gas flow rate is reduced. When this happens, the induced intermittent gas lift production is usually highly inefficient because it could reduce the liquid production and increase the injection gas/liquid ratio. The small spread is due to the fact that single-element valves usually have small area ratios (as explained in Chapters: Design of Intermittent Gas Lift Installations and Intermittent Gas Lift Troubleshooting, the spread of the valve is proportional to its area ratio).

The behavior shown in Fig. 11.47 can also be present in properly-designed, choke-control intermittent gas lift wells that have not been fully unloaded:



when the pilot valve is uncovered at the end of the unloading operation of the well, the liquid column above it is too long, and the pilot valve opens at a lower than designed injection opening pressure because the high production pressure helps opening the valve in a significant manner (so that there is no need to increase the injection pressure to its design value to open the valve). On the other hand, the pilot valve's closing pressure remains at its design value because most pilot valves are spring-loaded valves that are not affected by a change in temperature caused by a reduction in the liquid production. For this reason, the spread of the valve is very small and the volume of gas injected per cycle is insufficient to produce the liquid column to the surface. When this happens, the production of the well can drop to zero or become very small and this is what distinguishes this type of problem from the one caused by a high viscosity fluid, for which the reservoir pressure is high enough to produce the well, as explained above. If the gas injection flow rate is temporally and significantly increased, the long liquid columns can be produced and the unloading operation can be finally completed. With smaller liquid columns to be lifted during normal operation, the spread of the valve increases and the well should produce with no problem at the design lower injection gas flow rate. Fig. 12.27 shows how the wellhead pressure chart looks like when the injection gas flow rate needs to be temporarily increased to unload a choke-control, intermittent gas lift well with this type of problem.

The gas lift IPO valve in a well with wellhead pressures as shown in Fig. 11.48 never actually closes. This frequently happen when the reservoir pressure decreases and the well tries to intermit on its own because the production pressure (that would otherwise help maintain the valve open) has decreased. There are no sharp injection pressure peaks shown in the chart; instead, they are rounded and this shape helps identify this type of operational condition in the well. The gas injection and liquid production are continuous and the gas lift valve never closes, but it never fully opens either.

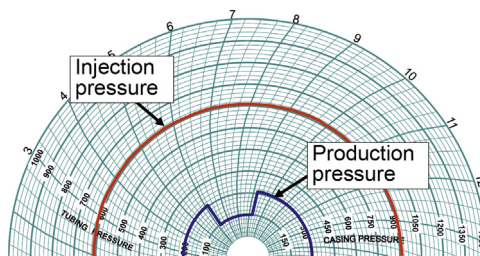


■ FIGURE 11.48 Valve in throttling flow. Continuous gas injection and liquid production.

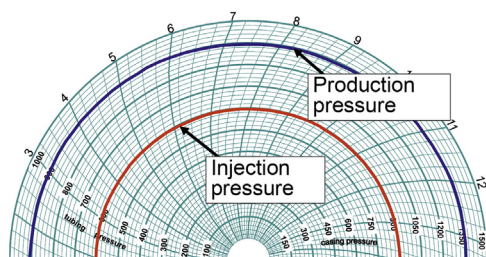
When the production pressure decreases, the valve tends to close because it is operating in throttling flow (for which the production pressure has a high impact on the opening of the valve). As the valve tends to close, the gas flow rate into the tubing decreases causing two effects that help stabilize the injection pressure: (1) because the gas flow rate into the tubing is lower, the production pressure increases and this reverses the tendency of the valve to close, and (2) because the gas flow rate injected at the surface is constant, once the gas flow rate through the gas lift valve decreases, the injection annular pressure increases and this also makes the valve begin to open wider again. The valve then opens wider and the gas flow rate increases so that the production pressure now begins to drop and the injection cycle is repeated. The injection pressure could be stabilized by increasing the injection gas flow rate, but this solution might sometimes lead to an increase in the injection pressure that could open one or more upper unloading valves, inducing either a high gas injection flow rate or a worse instability problem.

The injection pressure stabilizing effect that a gas lift valve introduces is just not present if the operating valve was an orifice valve instead of a calibrated IPO valve. Wells that produce in this fashion must be troubleshoot (in an approximate manner) using continuous gas lift troubleshooting techniques and not intermittent gas lift techniques. Even though it might appear simple, it is not easy to model this type of operation because it requires coupling transient reservoir response to transient multiphase flow, gas lift valve dynamic behavior, and transient annular injection pressure response.

Fig. 11.49 shows the pressure chart of a well that was tested for 3 h. The wellhead production pressure was lower while the well was being tested. Under this condition, the well test might not represent the well's normal operation because it is possible that the well might not have achieved steady-state flow during this short period of time. However, even if steady-state was reached, it is highly possible that the liquid production during the test was greater compared with the well's production when it is directed to the main production separator at the flow station. Downhole pressure surveys run while the well



■ FIGURE 11.49 The production of the well was directed to the test separator for 3 h. The wellhead production pressure is much lower during the test.

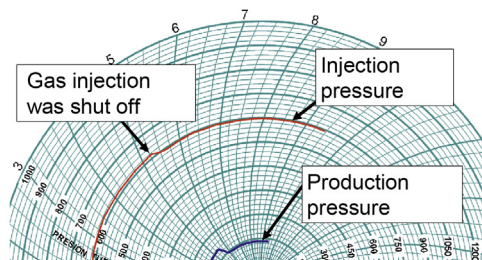


■ FIGURE 11.50 Well closed to production (wellhead wing valve to flowline closed and wellhead gas injection valve opened).

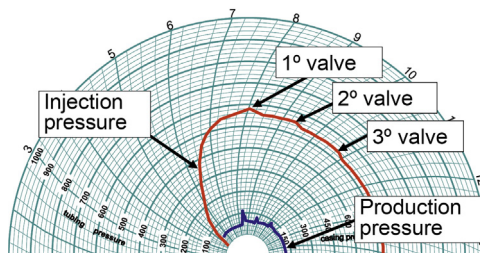
was producing to the main production separator cannot be used to generate IPR curves or to verify the accuracy of multiphase flow correlations if the liquid flow rate is measured at a different day of the survey with the production wellhead pressure much lower than the wellhead pressure during the survey. Gas lift is highly sensitive to wellhead pressure because the wellhead is directly connected to the formation. Testing the wells at a lower wellhead pressure will also introduce errors in back-allocation calculations.

The chart in Fig. 11.50 corresponds to a well in which its wellhead production valve (to the flowline) was shut while keeping the gas injection valve open. The injection and production pressures reached injection line pressure. In the chart, the production and injection pressures are not at the same level because the production pressure scale goes from 0 to 1000 psig, while the injection pressure scale goes from 0 to 1500 psig. It is not advisable to close the well in this way because it might damage the gas lift valves or the formation (the only advantage is that the high-pressure gas is not lost if the well needs to be shut in, but the same effect is obtained if the injection gas is shut off at the same time the well is shut in). In fact, it is always better to keep the wells producing constantly. Some wells are assigned a certain monthly accumulated production limit and once this limit is obtained, the well should be closed. In these cases, it is better to lower the daily production of the well to reach the maximum allowed monthly accumulated production without having to close the well at any time during the month.

The chart in Fig. 11.51 shows the moment gas injection to the well was shut off while leaving the well open to production. The gas injection pressure drops to the operating valve's surface closing pressure and the wellhead production pressure drops to separation pressure. The operating gas lift valve is an IPO valve. If the operating valve was an orifice valve, the injection pressure would have dropped to lower values, but it would not have reached separation pressure unless the well was not producing any liquids or the gas injection was taking place through a communication or a flat valve above the static liquid level.



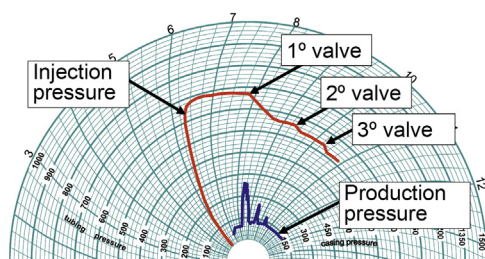
■ FIGURE 11.51 Surface wellhead gas injection valve closed with the production tubing open to production.



■ FIGURE 11.52 Unloading process of a gas lift well with IPO valves (good operation).

The chart in Fig. 11.52 shows the unloading process of a well with IPO valves. The well is completely filled with completion fluids. The injection pressure drops as each of the three valves installed in the well is uncovered. Production headings are observed every time a valve is uncovered. The production pressure increased from the pressure at the separator of around 40 psig to about 75 psig when the unloading process was finished, indicating that liquids are being produced to the flow station. In contrast to Fig. 11.52, the chart in Fig. 11.53 shows the unloading process of the same well with an extremely high gas injection flow rate: in a relatively short time, the injection pressure reaches the line injection pressure and stays at that value for a long time before uncovering the first valve, indicating a very high pressure drop through the valves while only liquid is flowing through them. While unloading a gas lift well, the injection pressure should never reach line pressure. The liquid flow rate through a gas lift valve during the unloading operation should not be greater than 1.5 Br/min. The way a gas lift well should be unloaded is explained in chapter: Design of Continuous Gas Lift Installations.

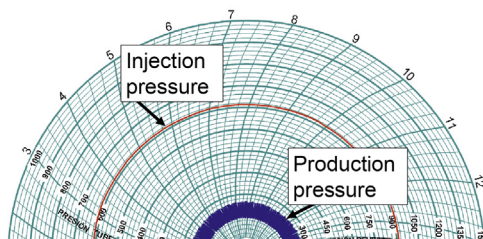
Fig. 11.54 shows the pressure chart of a well producing liquid with a water cut of more than 30 or 40%. The liquid produced might or might not be



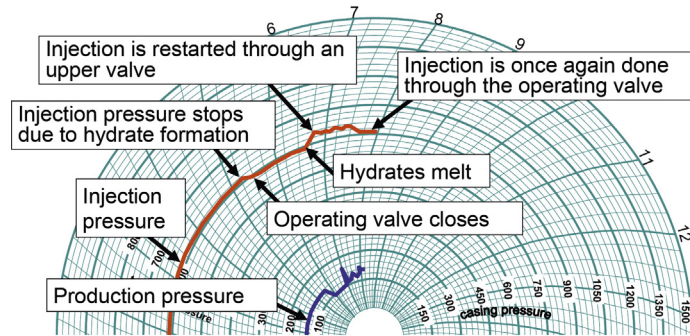
■ FIGURE 11.53 Unloading process of a gas lift well with IPO valves (excessive injection gas flow rate before uncovering the first valve).

emulsified. The well produces large liquid slugs at a very high frequency. This type of flow pattern is many times present when water is being produced. The gas lift equipment is working without problems and the well should be left alone. The well has IPO valves, gas is injected down the casing–tubing annulus, and liquids flow up the production tubing.

The chart in Fig. 11.55 shows what happens when hydrates are generated from time to time due to a drop in ambient temperature. The gas lift valves are IPO valves and the liquid is produced up the tubing. Hydrates completely block the surface gas injection valve and the flow rate goes down to zero so that the injection pressure decreases until the surface closing pressure of the operating valve is reached. When hydrates melt, gas injection is restarted but it is not possible to inject gas through the operating valve because the liquid column that has accumulated above it creates a hydrostatic pressure greater than the injection pressure at the operating valve's depth. Gas injection is restarted through the upper unloading valve. Gas injection begins through the operating valve again when the production pressure at the operating valve drops to a value less than the gas injection pressure at that depth. It takes some time for the hydrates to melt because the ambient temperature is very low. If the ambient temperature is high, hydrates melt in a very short



■ FIGURE 11.54 Well on continuous gas lift with no operational problems. High water cut.

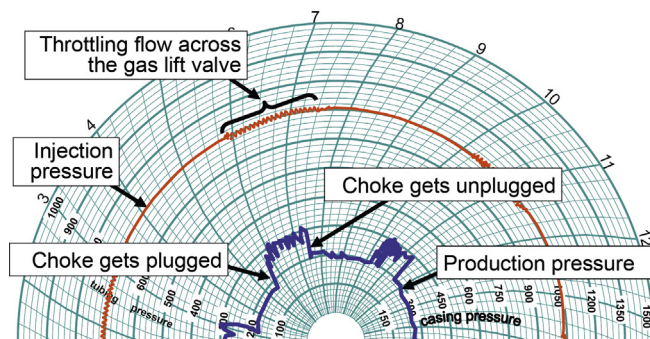


■ FIGURE 11.55 Surface injection gas flow rate temporarily drops to zero due to hydrate generation at the surface gas injection control valve.

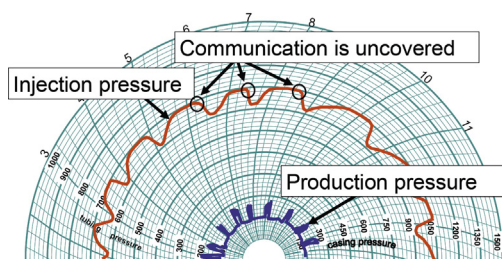
period of time, creating a completely different gas injection pressure pattern as shown in Figs. 11.43 and 11.44.

Fig. 11.56 shows an erratic production pressure behavior caused by temporary plugging of the wellhead production choke. As soon as the choke is plugged, the production pressure rises and makes the flow across the operating gas lift valve become throttling flow. Injection pressure peaks are rounded as shown in Fig. 11.48 for throttling flow across the operating valve. Chokes should not be used in gas lift wells. The production wellhead pressure usually rises when the liquid production increases; however, in the case shown in Fig. 11.56, the production pressure increases because of a restriction in the flowline located downstream of the connection of the wellhead production-pressure sensor.

Fig. 11.57 shows unstable liquid production and gas injection caused by a casing–tubing communication (tubing hole) located below the operating



■ FIGURE 11.56 Restrictions at the wellhead production choke.



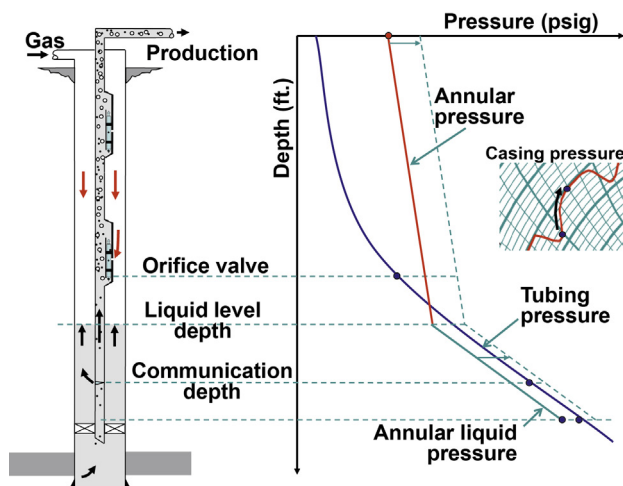
■ FIGURE 11.57 Continuous liquid production with unstable gas injection pressure caused by a casing–tubing communication (tubing hole) located below the operating orifice valve.

gas lift orifice valve. The liquids are produced up the tubing and the gas lift valve at the operating point of injection is an orifice valve that allows gas injection into the tubing as long as the annular injection pressure is higher than the production tubing pressure. The well seems to be producing intermittently, but the liquid production at the test separator reveals that the production never drops down to zero. Additionally, calculations show that the injection pressure is higher than the production pressure at the depth of the operating orifice valve during the periodic intervals of stable gas injection pressure and liquid production. The instantaneous liquid flow rate (and not the total daily liquid production) should be used to calculate the production pressure along the tubing during the intervals in which the surface gas injection pressure is stable.

The well corresponding to the chart in Fig. 11.57 actually has a continuous liquid production with the gas injection through the orifice valve while the liquid level in the annulus is above the casing–tubing communication. Slowly, the liquid level in the gas injection annulus decreases, eventually uncovering the communication. In the period of time before uncovering the communication, the injection pressure is very stable because the sum of the gas flow rate injected into the tubing through the orifice valve and the gas flow rate displacing the liquids in the annulus is equal to the total gas flow rate injected into the well’s annulus at the surface. The pressure in the production tubing is more or less constant until the communication is uncovered. At that moment, the injection gas enters the tubing through the casing–tubing communication at a flow rate much larger (because of the size of the communication) than the gas flow rate injected at the surface and this causes a steep decline of the annular injection pressure. The liquids in the tubing above the communication are produced as large liquid slugs that reach the surface causing wellhead production headings. Right after the slugs have been produced to the surface, the bottomhole flowing pressure drops to a point that makes the formation react with an increase in liquid

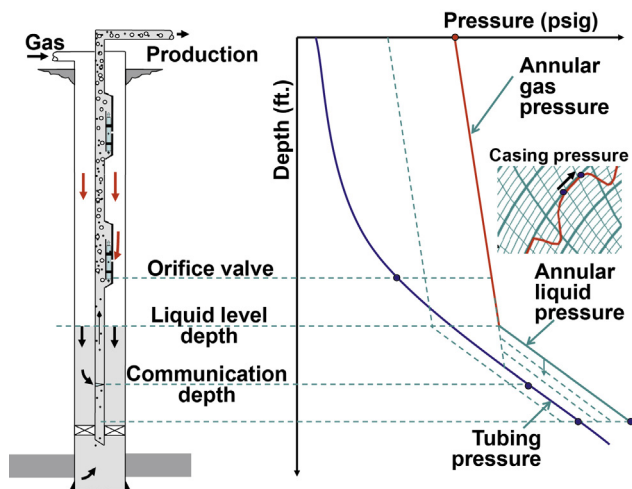
production that, in turn, makes the liquid level rise very fast in the annulus (liquids can go from the tubing into the annulus thanks to the casing–tubing communication). The injection pressure also increases after the slugs have been produced but its rate of increase is slow and, for a while, the injection pressure is not high enough to stop the liquid level from rising in the annulus. During this time, gas injection takes place through the orifice valve only because the liquids have blocked the casing–tubing communication below it. Because the injection gas flow rate at the surface is constant and a much lower gas injection flow rate into the tubing takes place through the downhole single point of injection, the gas pressure in the annulus begins to rise. Eventually, the gas injection pressure reaches a value sufficiently high to make the annular liquid level descend as the liquids are pushed by the injection gas back into the tubing through the casing–tubing communication.

The pressure–depth diagrams of one injection cycle shown in Fig. 11.57 are presented in the following figures. The frequency and magnitude of the wellhead pressure headings depend on the size of the communication, the production capacity of the reservoir, the injection gas flow rate, as well as on the relative position of the casing–tubing communication with respect to the operating valve. This is the reason why casing–tubing communications can manifest in a great variety of wellhead pressure patterns and the one shown in Fig. 11.57 is just one of them. Trying to analytically simulate this injection cycle is neither easy nor necessary to troubleshoot the well. Field techniques, such as communication tests or the use of sonic devices are far more practical in these cases (Figs. 11.58–11.62).

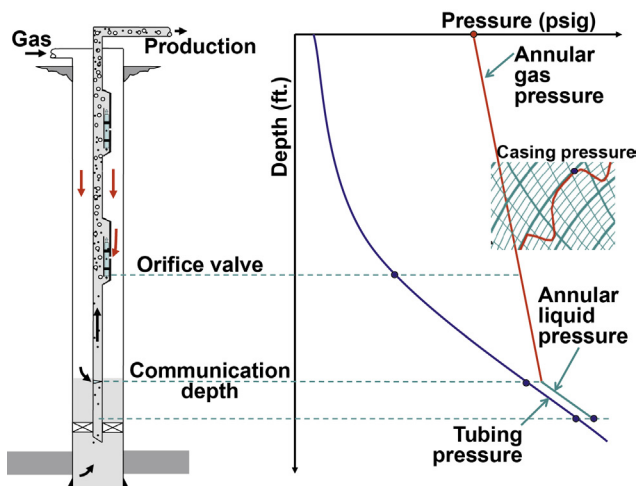


■ FIGURE 11.58 Gas injection through the orifice valve. Injection pressure and annular liquid level are rising.



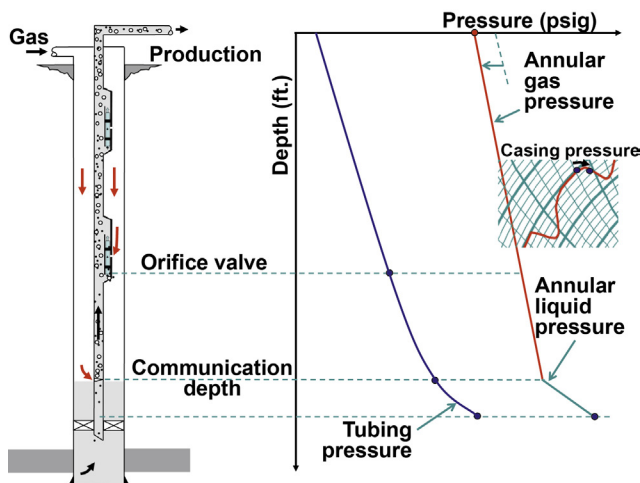


■ FIGURE 11.59 Gas injection through the orifice valve. Gas injection pressure is kept more or less constant while the annular liquid level is descending.

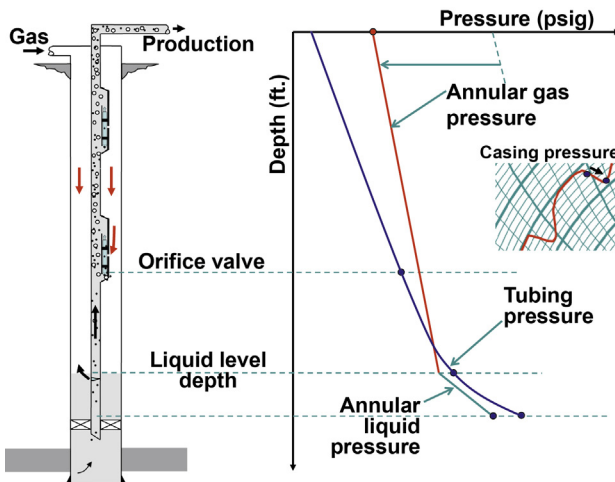


■ FIGURE 11.60 Gas injection through the orifice only. Moments just before the communication is uncovered.

Fig. 11.63 shows the pressure chart from a well that produces on natural flow up the production tubing but it needs gas injection to start liquid production. The well also needs periodic gas injection (from time to time) because it has a tendency to die. Bottomhole tubing pressure increases due to: (1) liquid loading, and (2) a drop in formation gas production. Gas injection

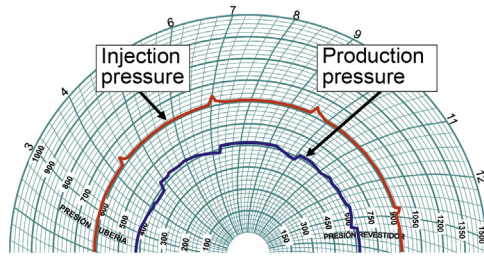


■ FIGURE 11.61 Gas injection through the orifice valve and the communication. Just after the communication is uncovered.



■ FIGURE 11.62 Gas injection through the orifice valve. Liquids are beginning to enter the annulus.

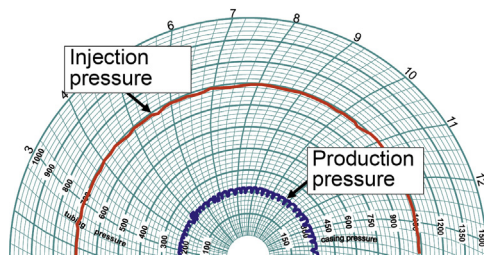
is controlled by measuring the wellhead production pressure. When the production pressure drops to values less than a predetermined pressure (indicating that the well is dying), a surface injection control valve opens to allow gas injection through a gas lift valve at the bottom of the well to make the production pressure lighter so that the well can continue to produce on



■ FIGURE 11.63 Natural flowing well with injection gas flow rate controlled by the tubing pressure.

natural flow. The liquid production is then increased and, in consequence, the wellhead production pressure also increases. Once the wellhead production pressure is greater than a certain value, the surface gas injection control valve closes and the surface injection pressure drops until it reaches the surface closing pressure of the downhole operating valve, which is an IPO valve. In some wells, the gas injection interval only takes a few minutes after which the surface injection valve closes and might remain closed for hours or days.

Fig. 11.64 shows the pressure chart of a well producing on continuous gas lift, with a high wellhead production pressure, which is constantly changing because of a nearby intermittent gas lift well that produces to the same separator at the flow station. The high wellhead pressure and its fluctuations are not caused by the well itself, but they are a consequence of what is going on at the flow station. When analyzing a well, it is then important to verify how the main production separator pressure and the gas lift system's gas injection pressure are changing. A nearby intermittent well might affect both the separation pressure at the flow station and the gas injection pressure at the gas injection manifold.



■ FIGURE 11.64 Continuous gas lift well with a high wellhead production pressure caused by the pressure behavior of the main separator at the flow station.

There are many other examples of cases with wellhead pressure patterns different from the ones shown so far. It is simply impossible to show all of them. The important thing is to know how to analyze wellhead pressure charts or tendency curves. In most cases, the correct analysis involves performing a great deal of calculations to find the actual point of injection. If it is not possible to perform any calculation at all due to, for example, the fluctuations of the wellhead pressures, field techniques must be performed to understand the behavior of the well and solve the problem very quickly. However, field troubleshooting techniques also involve planning and preparations in which some calculations might be required. Experience and imagination is sometimes all the optimization engineer has to solve complex operational problems.

### **11.6 AUTOMATED SYSTEMS TO DETECT AND ANALYZE WELLS WITH OPERATIONAL PROBLEMS IN GAS LIFT FIELDS WITH A LARGE NUMBER OF WELLS (I-FIELD SOLUTION)**

Each well should be troubleshoot after any of the following events: (1) the well is completed, (2) any workover job, or (3) a routine gas lift valve change out. Once the well has been analyzed and it has been concluded that its operation is acceptable, it is convenient to have a way of detecting when the well should be analyzed again. If there is a large number of wells in the field, it is not practical to analyze all wells individually because it might take too much time to detect if any well in particular is having an operational problem. Furthermore, the optimization team of engineers is usually not large enough to troubleshoot all wells one by one. It is necessary then to have an automated method of detecting which wells should be troubleshoot and, additionally, have a computerized procedure to perform an in-depth analysis of the well's current operational status to quickly and accurately find the root of the problem.

The basic parameters that should be measured (on a routine basis) and compared to previously established target values for a particular well are: liquid production, injection gas flow rate, formation gas/liquid ratio, total gas/liquid ratio, water cut, and injection and production wellhead pressures and temperatures. These measurements should be done continuously to have early warnings of any operational problem. If any of these measurements exceeds the maximum limit or drops to values less than the established minimum limit, the well is automatically selected for additional analysis. These limits are imposed on each well after carrying out a complete analysis of the well's operational conditions and it has been corroborated that the operation

of the well is satisfactory; however, operational conditions are continuously changing and, eventually, all wells will be subjected to further analysis: the water cut can increase, the reservoir pressure might decline, gas lift valves can fail, etc.

Several of the many causes that can affect the value of each of the parameters mentioned in the last paragraph and make them fall below or above acceptable levels are presented in Section 11.3. A short list of the most important of these causes is condensed in this section as follows:

- The total gas/liquid ratio is probably the most significant parameter to be monitored for a well on gas lift. If this ratio is too high, it is probable that too much gas is being injected. Overinjection could be causing a decrease in liquid production. Nodal analysis must be performed to determine if the well really needs the gas flow rate being injected. It is possible that the reservoir pressure has decreased or the formation gas/liquid ratio is increasing and it is no longer necessary to inject gas at current levels.
- An abnormal injection gas flow rate could point to a choke in the flowline, a plugged or eroded surface gas injection control valve, or a damaged gas lift valve.
- Water cut is a parameter that can change very rapidly. As soon as the water cut increases, the well should be analyzed to determine if it is economically feasible to continue to produce the well or if some kind of chemical treatment or workover job should be done.
- A very high wellhead production pressure could be due to a restriction in the flowline, such as: (1) flowline too long or with a very small ID, (2) bent or smashed flowline, (3) too many unnecessary restrictions in the flowline such as chokes or choke housings, (4) paraffin, asphaltene, carbonates, or sand depositions, or (5) high separation pressure, among others.
- A very high or very low gas injection pressure could indicate leaks in the gas injection line, an annular-tubing communication, hole in the casing, a damaged gas lift valve, or gas lift design not suitable for current operational conditions.

Initial massive monitoring and troubleshooting computer programs were used to simply detect when one, or several, of the parameters previously described increased above or dropped below pre-established values and to carry out rudimentary calculations like identifying the point of injection in a very simple manner.

Recently, advanced “troubleshooting expert systems” have been developed to perform more profound analyses of current operational conditions of

each well, identify complex operational problems and their possible causes, determine the economical impact of different lines of action that could be taken for each well (assigning a priority level to every well, based on the severity of the problem and the economical impact and costs of each possible solution), and give explanations to the users on how the different conclusions were reached so that these expert systems can also be used as training tools. These troubleshooting expert systems may or may not use neurological networks and have been put to use as part of a “global optimization systems” that usually have the following components:

- An automated massive data acquisition and control subsystem that measures, transmits, and stores the values of all the important well and field parameters and performs local control actions on some of these parameters. The variation in time of each parameter can be reviewed by the optimization personnel as “tendency curves.” These subsystems can use statistical algorithms to estimate if a particular measure should be discarded or considered to be in error so that its value is given very little weight in the decision making process. The minimum data that should be gathered for each well consists of: wellhead gas injection and production pressures and temperatures, gas injection flow rate, water and oil production rates (from the last well test), and bottomhole flowing pressure and temperature (if available). The troubleshooting expert systems need to have access to PVT and completion data, valves’ depths and calibration data, and all the information required to generate the IPR curve of each well. The publications presented by [Abdallah et al. \(2010\)](#) and [Shnaib et al. \(2009\)](#) are examples of recent applications where these data acquisition and production optimization systems are used.
- A central analysis unit executes computer programs to perform tasks such as determining if the gas lift valves are opened or closed, finding the possible value of the downhole flowing pressure, performing nodal analysis, building liquid production versus gas injection flow rate curves, etc. Each well has a steady-state model that is used to predict the liquid flow rate from the field data. Every time a new well test is performed, the well model is calibrated following a predetermined procedure that might include the determination of the best suitable multiphase flow correlation and the productivity index of the well. If the calibration process requires changing well parameters (like the productivity index) above or below a certain percentage (established by the users) of their current values, the well should be manually analyzed by the optimization engineer. Wells might be tested once or twice a month. During the days in which the well is not tested, the daily

liquid production can be estimated from the last calibrated well model using nodal analysis (based on the current operational conditions, such as the injection pressure and flow rate). Daily liquid production (for production back allocation purposes) can also be estimated from the so-called “virtual flow rates” methods (also known as virtual flow rate meters). These methods depend on current field measurements to predict the liquid flow rate using a mathematical correlation or a simple, data-based, curve. For example, the pressure drop across a surface choke can be used in conjunction with a choke flow correlation (and the gas/liquid ratio) to find the liquid flow rate. There can be many virtual flow rate meters (depending on the amount of data available for a given well). The troubleshooting expert systems can analyze the deviation of each meter to detect measurement errors or estimate which parameter (like the water cut or the gas/oil ratio) is changing.

- A knowledge data base with dozens or hundreds of possible cases, previously identified by gas lift experts as possible causes of operational problems. The number of cases in the data base can increase as gas lift experts identify new ones for a particular field. Each case is described by a set of attributes, which are given by the gas lift experts. For example, a tubing-annulus communication could have the following attributes, which together help identify this particular problem: (1) gas is injected into the well, even though valve mechanic equations indicate that none of the valves installed in the well should be opened; (2) injection and production pressures fluctuate; or (3) the well produces liquid, etc. Some of these attributes might be common to many different cases.
- A program that compares the value of each attribute with the well’s current operational conditions. The real situation of the well is reflected in the values of the attributes that distinguish each case. These values were gathered from the automated data acquisition system and from the results of especial algorithms used to perform nodal analysis, solve gas lift valve mechanic equations, virtual flow rates, etc. The program then gives a list of all possible problems the well could have, assigning a value to each problem that identifies it as “highly probable”, “probable,” “less probable,” and so on. The program shows the values of the attributes that were responsible for assigning a certain level of relevance to each case and it also explains different lines of action the operator could take to solve the problem. In this sense, the program acts as an operational guide to less experienced optimization personnel, serving as an important training tool. The program can calculate the economical impact that the solution of the problem could have and, in this way, different levels of urgency could be assigned to each well

identified with some kind of problem. The program should be able to handle situations in which part of the data is missing or inaccurate and this could be achieved by: (1) organizing the data base as independent cases and not in a hierarchical way, and (2) defining the data base in a redundant fashion; one case could have many attributes that identifies that particular case. Each case could have more than 30 attributes and each of these attributes could have a higher or lower weighting factor for a particular case, as determined by the gas lift experts that generated the knowledge data base.

When an in-depth analysis is carried out, it is possible to detect problems that would otherwise go undetected for a long time. This is due to the fact that gas lift is a method for which it is not easy to detect situations where the lifting efficiency could be improved. A well can produce inefficiently for a long time, without showing signs of such inefficiencies. For other artificial lift methods, operational problems are usually catastrophic and easily detected. The use of expert systems in a massive way can quickly and effectively identify a large number of problems.

As it was stated earlier, the knowledge data base could be increased or modified as new results are being obtained in a particular field. But these modifications should be done in an orderly fashion and by the appropriate personnel so that the integrity of the knowledge data base could be preserved. One possible way of improving a knowledge data base could be achieved by taking the following steps:

- The optimization personnel electronically send their comments and evaluation of each result.
- The gas lift expert reviews each evaluation and determines if a new case should be added or if an existing case must be modified. This might require several communications, back and forth, between the expert and the optimization personnel to reach a final conclusion.
- The expert communicates with the computer system support team to modify the knowledge data base.

Finally, a word should be said about well dynamic models. Even though they are not thoroughly developed yet, these models could be used in the future (as part of troubleshooting expert systems) to troubleshoot wells with instability problems or to predict some operational problems that might arise while trying to unload a well. These models could also be used to perform gas lift designs (for mandrel spacing and unloading gas lift valve calculations). Dynamic well models are highly sophisticated computer programs, capable of predicting the behavior in time of a well that produces in a stable or unstable manner. These programs use energy, momentum,



and mass conservation equations, together with closure laws and transient heat transfer models. They are capable of predicting when the reservoir can produce or receive liquids to or from the production tubing. It is possible that, as the liquids are displaced from the annulus during the unloading process, the bottomhole pressure gets higher than the reservoir static pressure and the formation begins to take liquids. This could induce a complex multiphase flow, in which some gas could be produced up the tubing while liquids travel down towards the formation. These dynamic models are being constantly improved and even though much more work needs to be done, they will someday constitute the principal tool to troubleshoot and design gas lift wells. As indicated in chapter: Design of Continuous Gas Lift Installations, the work done by Pothapragada (1996), and Tang (1998) are two examples of the pioneer analytical models that were used to predict the dynamic behavior of gas lift wells. Today, several commercially-available computer programs can be used to troubleshoot unstable wells, design the unloading procedures of strong wells to avoid damaging unloading gas lift valves, predict the well's response in case of an emergency compressor shutdown to avoid venting lift gas in the low pressure side of the gas lift system, etc.

## 11.7 TROUBLESHOOTING EXAMPLES

Different analyses of the operation of several wells are presented in this section. The liquid production is either all the time continuous or it is continuous during specific periods of time followed by time intervals in which the production goes down to zero. Gas injection might be continuous or intermittent but if the liquid production is continuous, the troubleshooting techniques explained in the chapter should be applied instead of using the techniques designed for intermittent gas lift that are explained in chapter: Intermittent Gas Lift Troubleshooting.

### 11.7.1 Example #1: continuous liquid production and gas injection; injection point might be plugged

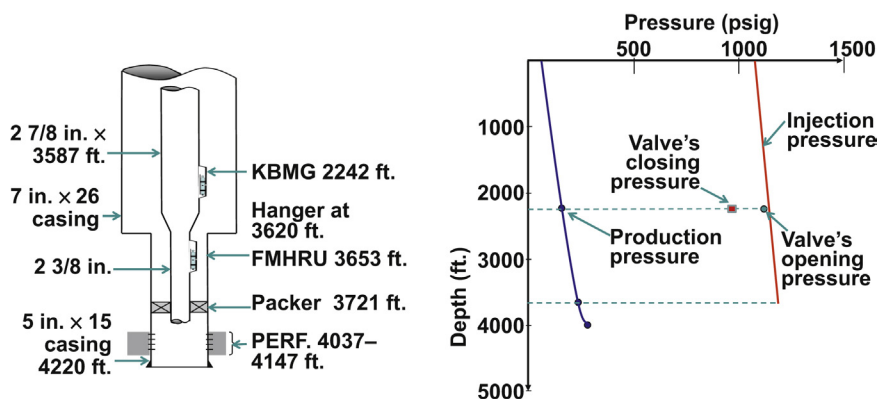
Input data:

Vertical well; reservoir static pressure: 875 psig; 29°API oil gravity; water cut: 0%; formation gas/liquid ratio: 2375 scf/STB; casing: 7-in. × 26-lb/ft.; production tubing ID: 2.441 in.; top of perforations' depth: 4037 ft.; packer depth: 3721 ft. The well has one nitrogen-charged, IPO unloading valve, and an 8/64-in. orifice valve at the point of injection (Table 11.1).

**Table 11.1** Valves Installed in the Well

Depth (ft.)	Valve	Port or Orifice ID (1/64 in.)	Design Opening Pressure (psig)	$P_{tr}$ (psig)
2242	NM-14R	16	1050	990
3653	DKO-2	8	—	—

$P_{tr}$  = test rack opening pressure.



■ FIGURE 11.65 Well completion and results of troubleshooting calculations, example #1.

The well's production was 240 STB/D, with an injection gas flow rate of 250 Mscf/D and a wellhead production pressure of 60 psig. The formation gas/liquid ratio of 2375 scf/STB seems to be too high (for the area where the well is located) and it is advisable to check its value at the test separator. Fig. 11.65 shows the completion of the well. The problem is that the injection pressure of 1070 psig is too high because it can open the unloading valve. As shown in Fig. 11.65 and in Table 11.2, calculations do show that the unloading valve could be opened.

The results shown in Table 11.2 correspond to the case in which the production pressure is calculated as if all the gas is injected through the first (shallowest) valve. As can be seen in Fig. 11.65, the injection pressure is large enough to have gas injection through the unloading and the orifice valves. However, the gas mass balance indicates that the gas flow rate should be much higher if the gas is injected through both points. In fact, the entire measured gas flow rate can be handled by the orifice valve with only 815 psig at injection point depth and not with the 1181 psig pressure calculated from the actual surface injection pressure.

**Table 11.2** Results of Troubleshooting Calculations (Valve "1" is the Unloading Valve and Valve "2" is the Operating Orifice Valve)

Valve	Valve 1	Valve 2
Injection pressure at valve's depth calculated from the measured injection pressure (psig).	1139	1181
Tubing pressure at valve's depth (psig).	157	249
Annular injection pressure at valve's depth to pass the measured gas flow rate if each valve was an orifice (psig).	211	815
Valve's closing pressure calculated using valve mechanic equations and calibration data (psig).	965	0
Valve's opening pressure calculated using valve mechanic equations and calibration data (psig).	1117	0
Gas flow rate the valve could pass if it was an orifice (Mscf/D)	1416	360

Even though the production pressure was calculated assuming that the gas is injected only through the unloading valve, the pressure gradient below this point of injection is very similar to the pressure gradient above it because of the large formation gas/liquid ratio. Therefore, the impact of injecting all the gas through the lower point should not be too great. A downhole pressure survey corroborated this point, but unfortunately the temperature was not measured and therefore it could not be confirmed if the gas was being injected through more than one point. [Table 11.3](#) shows the result of the pressure survey.

The low bottomhole flowing pressure in the table indicates that the production should not increase in a considerable way if all the gas was injected through the orifice.

The measured gas flow rate is much lower than the gas flow rate that can pass through the orifice for the given operational conditions. This could be

**Table 11.3** Results of the Downhole Flowing Pressure Survey

Depth (ft.)	Pressure (psig)
0	81.0
500	97.0
1000	106.0
1500	116.6
2192	135.0
3603	202.8
3703	209.4
4037	227.8

due to a restriction in the orifice or inaccurate measurements of either the gas flow rate or the injection pressure. The actions that should be taken are:

- Check the accuracy of the injection gas flow rate and injection pressure measurements.
- If the gas flow rate is in fact very large and this flow rate is causing the current high injection pressure, a nodal analysis should be performed to calculate the injection gas flow rate the well requires.
- If the measured gas flow rate is correct, then either the orifice valve is plugged or there is some other type restriction and it is not possible to inject gas into the tubing unless the injection pressure is high enough to open the unloading valve:
  - In this case, the casing should be vented to get rid of any debris that is blocking the gas flow and if this does not work, the orifice valve should be replaced with another one with an orifice of the same diameter.
  - If the problem persists after replacing the orifice valve, it might be possible that the mandrel's ports are too closed to the casing or there is any other problem that cannot be solved with simple actions taken at the surface.

It is important to note that the mandrel at the point of injection does not have recessed ports as required for deviated wells (Figs. 6.19 and 6.20a), so that any inclination the well might have could be causing the mandrel to lean against the casing at exactly its gas entrance ports. Because in this well the formation gas/liquid ratio is high, gas injection can take place through the upper mandrel alone as long as the reservoir pressure is high enough for the well to produce liquids, but eventually the gas restriction problem (if it is real) will need to be solved.

### 11.7.2 Example #2: Fluctuating Injection Pressure and Continuous Liquid Production

Well data:

Vertical well; reservoir static pressure: 1093 psig; 26°API oil gravity; water cut: 3%; formation gas/liquid ratio: 1222 scf/STB; injection gas flow rate: 261 Mscf/D; casing: 7 in. × 26 lb/ft.; tubing ID: 2.441 in.; top of perforations' depth: 6320 ft.; packer depth: 6134 ft. The well has three nitrogen-charged, IPO valves (Table 11.4).

Even though the injection pressure pattern corresponds to an intermittent gas lift well, the well is trouble shoot (in an approximate way) as a continuous gas lift well because the liquid production at the test separator fluctuated

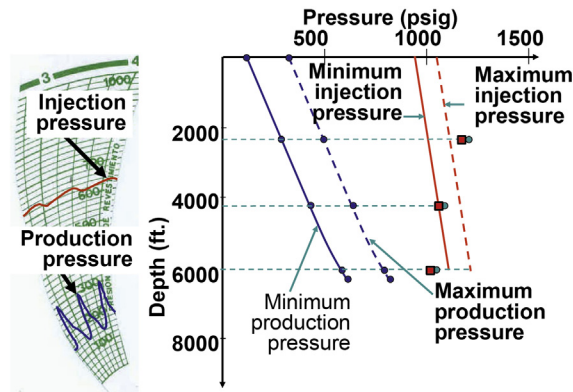
**Table 11.4** Valves Installed in the Well

Depth (ft.)	Valve	Port Diameter (1/64 in.)	Design Opening Pressure (psig)	$P_{tr}$ (psig)
2346	R-20	12	1100	1035
4255	R-20	12	950	900
6057	R-20	12	885	835

but never dropped down to zero. As it is revealed by the calculation's results shown below, the intermittent pressure pattern might be due to the second valve opening and closing at regular time intervals as a consequence of the high injection pressure. The wellhead production pressure was very high all the time (compared to the average production wellhead pressures for that particular field). This production pressure oscillated from approximately 140 to 300 psig. This high production pressure value was due to a ½-in. diameter choke that, for some reason, was installed at the wellhead. The injection pressure is high enough to open the second and third valves.

The daily gas volume injected to the well, calculated from the volume of gas injected per cycle (based only on the spread of the valve shown in the chart) times the number of cycles in one day, is much lower than the gas flow rate measured at the surface. This also points to the fact that the well is producing on continuous gas lift with most of the gas injected through the deepest valve. The volume of gas per cycle is calculated from the valve's opening and closing pressures using the equations for intermittent gas lift given in chapter: Design of Intermittent Gas Lift Installations. Fig. 11.66 shows the behavior of the wellhead pressures and the pressure–depth diagram showing the calculated downhole pressures. The surface injection pressure shown in the chart should be multiplied by 1.5 while the production pressure does correspond to the scale in the chart.

The results of the downhole pressure and flow rate calculations shown in Fig. 11.66 and in Table 11.5 were reached using the following data: water cut 3%, injection gas flow rate 261 Mscf/D, liquid production of 154 STB/D, wellhead pressure of 140 and 300 psig (the production pressure along the tubing was calculated for both surface wellhead pressures and gas injected through the deepest point of injection as a rough approximation), injection pressure of 950 and 1050 psig (the injection pressure along the annulus was calculated for the minimum and maximum injection pressures recorded at the surface). For the calculation of the valve's opening and closing pressures, the surface tubing pressure was assumed to be 300 psig. The Hagedorn and Brown correlation was used to calculate the production pressure along the tubing (with the purpose of having a rough approximation of the production



■ FIGURE 11.66 Wellhead pressure chart and pressure–depth diagram showing results from calculations.

**Table 11.5** Pressure Calculation Results for Wellhead Production Pressure of 300 psig and Wellhead Injection Pressure of 950 psig, Example #2

Valve	Valve 1	Valve 2	Valve 3
Injection pressure at depth calculated from the measured surface pressure (psig)	1013	1063	1109
Tubing pressure at depth (psig)	500	659	810
Injection pressure in the annulus at valve's depth to pass the measured gas flow rate if the valve was an orifice valve (psig)	565	710	854
Valve's closing pressure calculated using the valve mechanic equations and the calibration data (psig)	1184	1070	1026
Valve's opening pressure calculated using the valve mechanic equations and the calibration data (psig)	1211	1086	1035
Gas flow rate the valve could pass if it was an orifice valve (Mscf/D)	0	0	677

tubing pressure to be used in the valve mechanic equation, which is acceptable in this case because the valves are IPO valves with small seats).

The following can be said from these results:

- The second valve's closing pressure is approximately equal to the minimum injection pressure at valve's depth. Any injection pressure fluctuation could open the second valve.
- The injection pressure is high enough to keep the third (deepest) valve open all the time.
- The calculated gas flow rate is much higher than the measured gas flow rate at the surface. It is possible that the gas flow rate measurement is not correct.

The first recommended action is to verify the injection and produced gas flow rate measurements. The reason why the well has a ½-in. choke installed at the wellhead must also be investigated with other teams and remove it if possible. The liquid flow rate should increase if the choke is removed. The injection gas flow rate must be adjusted so that the second valve would not open.

The rather rudimentary calculation procedure explained in this example is the best that can be done. More sophisticated analyses would be worthless in this case because the data to build the IPR curve is not reliable.

### 11.7.3 Example #3: time intervals of continuous gas injection and liquid production followed by time intervals in which the liquid production and the gas injection flow rate drop to zero

Well data:

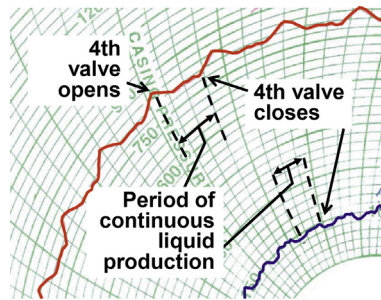
Vertical well; static reservoir pressure: 823 psig; 22°API oil gravity; water cut: 6%; formation gas/liquid ratio: 10,000 scf/STB; casing diameter: 7-in. × 23 lb/ft.; Tubing ID: 2.441 in.; top of perforations' depth: 6610 ft.; packer depth: 6400 ft. The well has 4 nitrogen-charged, IPO gas lift valves (Table 11.6).

Fig. 11.67 shows the wellhead pressure chart.

Even though the surface injection pressure behaved as if the well was producing on intermittent gas lift, the well is analyzed using continuous gas lift troubleshooting techniques because in one part of the cycle, where the injection pressure is more or less stable, the gas injection into the tubing and the surface liquid production were indeed continuous.

The current injection pressure level indicated that it was only the fourth (deepest) valve that was opening and closing. Using an average tubing pressure, it can be determined if any of the unloading valves were opened or closed (assuming that they are in good working condition).

Depth (ft.)	Valve	Port Diameter (1/64 in.)	Design Opening Pressure (psig)	$P_{tr}$ (psig)
1786	N-14R	16	1000	952
3435	N-14R	16	954	901
4922	N-14R	16	912	856
6340	N-14R	16	808	757



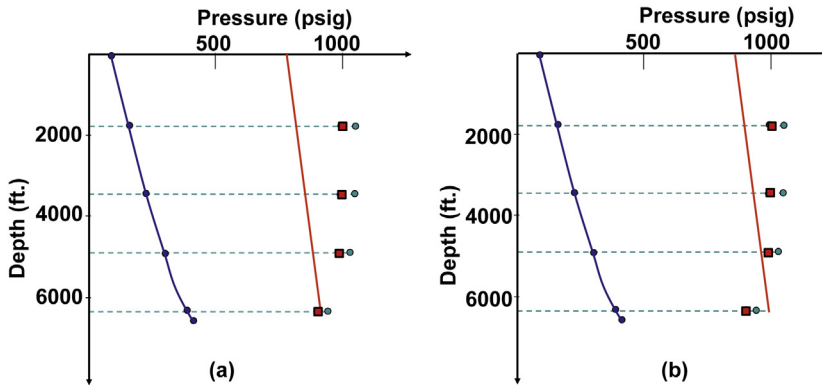
■ FIGURE 11.67 Wellhead pressure chart for example #3.

The behavior of the wellhead pressures can be interpreted as follows (this behavior can only be understood after doing the calculations shown below and not by just looking at the pressure chart).

The peak (maximum) injection pressure should correspond to the fourth valve's surface opening pressure (the kink or sharp peak is an indication of a valve opening and not just throttling the gas flow). This maximum pressure then declines at a rate that is too high for a normal continuous gas lift pressure fluctuation, but too low for an efficient intermittent gas lift operation (the liquid slug velocity would be too slow). At this time, the gas flow rate entering the tubing is greater than the gas injected into the annulus at the surface because the fourth valve's seat diameter is too large. Then, 14 min after the fourth valve opened, the injection pressure began to decline at a much slower pace (keeping the surface gas injection pressure fluctuating but almost constant) because the valve was operating in throttling flow so that the gas flow rate into the tubing was just slightly greater than the gas flow rate at the surface. At the same time, the well was producing liquids and the wellhead production pressure stabilized (at a slightly higher but more or less constant value) and remained that way for approximately 20 min. During this time, the well produced on continuous gas lift. Finally, the gas injection pressure dropped below the fourth valve closing pressure and it closed. As soon as the valve closed, the injection pressure began to increase eventually opening the fourth valve again to start a new production cycle.

The data used for troubleshooting calculations were: Water cut of 6%, formation gas/liquid ratio of 10,000 scf/STB, injection gas flow rate of 309 Mscf/D, liquid production of 60 STB/D, and average wellhead production pressure of 95 psig. The Duns and Ros correlation was used to calculate the production pressure along the tubing. The production pressure





■ FIGURE 11.68 Pressure–depth diagram showing results from calculations using (a) surface injection pressure = 800 psig; (b) surface injection pressure = 840 psig.

calculated in this way is only a rough approximation because the liquid flow rate is not constant and an average liquid production is used in the calculations; however, the valves are IPO valves, so that the error made in the production pressure calculation has a very little impact on the valve's opening and closing pressures calculated from the calibration data, the well current operational conditions, and valve mechanic equations. On the other hand, it would be totally wrong to use intermittent gas lift troubleshooting techniques because the initial column length (calculated from the average liquid production and the number of cycles per day) will just be too large. Continuous gas lift analysis gives in this case a reasonable idea of where the point of injection might be.

Fig. 11.68a shows the results of the calculations made for an injection pressure of 800 psig, which is thought to be the fourth valve's surface closing pressure (as identified in the chart of Fig. 11.67). As can be seen in Fig. 11.68a, the fourth valve's opening pressure is greater than the injection pressure at valve's depth, so there is a good chance that it is indeed the fourth valve that is opening and closing while all the unloading valves remain closed.

Fig. 11.68b shows the results of the calculations made for a gas surface injection pressure of 840 psig, which is thought to be the fourth valve's surface injection opening pressure (as identified in the chart of Fig. 11.67). Even though this pressure does not exactly coincide with the opening pressure of the fourth valve, it is greater than, but very close to, the opening pressure of this valve.

As can be noticed in Fig. 11.68, a surface injection pressure of 840 psig is high enough to open the fourth valve only. The operational problem is caused by the fact that the surface injection gas flow rate is less than the gas flow rate the fourth valve allows to pass once it is opened. This is due to the low liquid production (which keeps the tubing pressure at a small value) and the diameter of the valve's seat of 16/64 in., which is too large for the injection gas flow rate the well actually needs. A temporary solution could be to increase the gas flow rate to keep the fourth valve from closing, but this will introduce an unnecessarily high injection gas/liquid ratio and might open the third unloading valve. More sustainable solutions could be: (1) to install an operating valve with a smaller seat diameter, or (2) to produce the well on intermittent gas lift because the reservoir pressure is sufficiently low for the given injection point depth to implement this method with the use of gas lift pilot valves (for which the closing pressure does not need to be as high as the current closing pressure of the fourth valve). Before implementing any solution, the formation gas/liquid ratio measurement must be verified because it looks too high. Nodal analysis should also be performed to determine the injection gas flow rate the well requires for current conditions and if a smaller production tubing string could be installed in the well to keep it operating on continuous gas lift.

#### 11.7.4 Example #4: well's responses to different choke diameters after a workover job

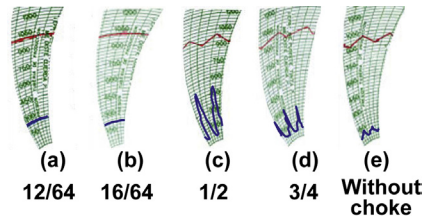
Well data:

Vertical well; reservoir static pressure: 1485 psig; 26°API oil gravity; water cut: 4%; formation gas/liquid ratio: 4000 scf/STB; 7-in. × 23 lb/ft. casing; tubing ID: 2.441 in.; top of perforations' depth: 4700 ft.; packer depth: 4590 ft. The well had two nitrogen-charged, IPO valves (Table 11.7).

A workover job has just been performed on the well and Fig. 11.69 shows the way the well responded to different (successively installed) wellhead production chokes:

**Table 11.7** Valves Installed in the Well

Depth (ft.)	Valve	Port diameter (1/64 in.)	Design opening pressure (psig)	$P_{tr}$ (psig)
2683	R-20	12	1100	995
4530	R-20	12	998	925



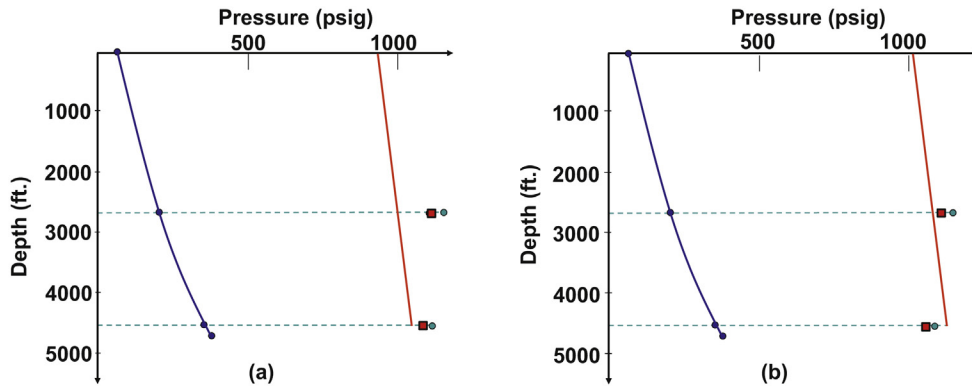
■ FIGURE 11.69 Wellhead pressures for different wellhead production choke sizes (inches).

In Fig. 11.69a and b the well was producing with a continuous gas injection and the only difference is the production wellhead pressure, which was equal to 160 psig for a 12/64-in. choke and 140 psig for a 16/64-in. choke. In both cases, the gas injection flow rate was approximately equal to 100 Mscf/D and the well was producing approximately 100 STB/D.

In Fig. 11.69c, the choke size was of 1/2 in. and the injection gas flow rate was about the same as for the previous charts, but the deepest valve began to intermit and the production dropped to 26 STB/D. The same behavior is observed in Fig. 11.69d but with lower production pressure peaks. Fig. 11.69e corresponds to the well without a choke and the production pressure peaks were very small in this case.

It was decided to estimate the production pressure under the operational conditions in Fig. 11.69e assuming “continuous” flow because of the following reasons:

- The production cycle consists of two parts: one period of time in which no gas is injected into the tubing because all valves are closed and another period in which gas is injected but the well actually produces on continuous gas lift because the gas flow rate that enters the tubing is very low (because of the reduced diameter of the operating valve) for intermittent gas lift operation and therefore the injection time is much greater than the time required for intermittent gas lift.
- Because the depth of the operating valve is 4530 ft. and the injection time period lasts for approximately 22 min, the liquid slug velocity could be as low as 200 ft./min, which is 5 times slower than the 1000 ft./min recommended for intermittent gas lift. But a rough estimation, using equations for intermittent gas lift, indicates that all the volume of gas required to lift the liquid slug to the surface (with this low gas flow rate) might be injected after only 11 min from the moment the gas lift valve opens. This gives a velocity of a little more than 400 ft./min,



■ FIGURE 11.70 Troubleshooting calculation results with (a) surface injection pressure = 930 psig and (b) surface injection pressure = 1010 psig.

which is still very low (half of the time in which the gas lift valve is opened is spent lifting the liquid slug to the surface and, for the remaining time, gas injection and liquid production are done in a continuous fashion). This low liquid slug velocity and the effect of the large tail gas volume make it impossible to estimate the liquid fallback losses. The wellhead production pressure also reveals that liquid production begins soon after the gas lift valve opens and the well continues to produce liquids while the gas lift valve remains opened.

- Because the valves are IPO gas lift valves (with rather small diameter seats), any error in the estimation of the production pressure is not going to have a great impact on the calculation of the opening and closing pressures of these valves.

The operational conditions for the following calculations were: water cut of 4%, injection gas flow rate of 166 MPCD, liquid production of 26 STB/D, and a wellhead production pressure of 60 psi.

Fig. 11.70a shows the results of the calculations performed with a surface injection pressure of 930 psig and the results for a surface injection pressure of 1010 psig are presented in Fig. 11.70b. It must be emphasized that the production pressures in these graphs are not the actual production pressures, which in reality fluctuate.

Calculations then reveal that the deepest valve might be opening and closing while the unloading valve remains closed. The problem is that the gas flow rate that the gas lift valve allows to pass is greater than the gas flow rate injected at the surface. Troubleshooting the well as if it was producing on intermittent gas lift will not be reliable because of the impossibility of determining the liquid fallback losses. The production of the well

is, in reality, an extremely inefficient intermittent gas lift operation. The recommended action to take is to install an operating valve with a smaller port diameter and calibrated at a lower opening pressure. In this case, it is not recommended to shift to intermittent gas lift because the reservoir pressure is still high enough for an efficient continuous gas lift operation.

### 11.7.5 Example #5: continuous gas injection but the well does not produce liquids

Well data:

Vertical well; static reservoir pressure: 930 psig; 15°API oil gravity; water cut: 5%; 7-in. × 23 lb/ft. casing; tubing ID: 2.992 in.; top of perforations' depth: 3305 ft.; packer depth: 3167 ft. The well had only one nitrogen-charged, IPO unloading valve and an orifice valve at the point of injection with an orifice diameter of 20/64 in. (Table 11.8).

The well was producing 159 STB/D with an injection gas flow rate of 416 Mscf/D, but its production declined to zero with approximately the same injection gas flow rate and a surface injection pressure of 480 psig. With a static reservoir pressure of 930 psig, a wellhead pressure of 40 psig, and a liquid pressure gradient of 0.42 psi/ft., the static liquid level would be at 1185 ft. below the wellhead. This means that the static liquid level is above the unloading valve and, therefore, even if the gas injection point depth is as high up in the well as this unloading valve, the liquid flow rate should be greater than zero. There might be then either a tubing-annulus communication above the static liquid level or the reservoir static pressure is in reality smaller and, for some reason, the unloading valve is opened. But, after applying the calculation techniques explained in Section 11.4.3 for wells circulating gas (no liquid production) the following results were reached for the unloading valve:

- If there is a hole in the tubing at the depth of the unloading valve its size would be of 12/64 in.
- If the unloading gas lift valve is in good conditions but it is opened because of lower temperatures, its closing and opening pressures would be of 785 and 924 psig, respectively. Because the injection pressure is lower, the unloading valve should be closed.

**Table 11.8** Valves Installed in the Well

Depth (ft.)	Valve	Port Diameter (1/64 in.)	Design Opening Pressure (psig)	$P_{tr}$ (psig)
1711	CM1-BK	16	1050	992
3089	DKO-2	20	—	—

- If the unloading valve was damaged (flat) and behaving like an orifice valve, its upstream pressure would only need to be equal to 303 psig to pass the reported injection gas flow rate.

These calculations point to the fact that the unloading valve should not be opened. The well's total depth was measured and it was found that the perforations were covered with sand; therefore, that was the reason the well was not producing any liquids and the gas could indeed have been injected through the orifice valve at 3089 ft. of depth. Calculations made at the orifice valve revealed that with the reported surface injection pressure, the injection gas flow rate should have been much higher. It is probable that either the gas flow rate and/or the injection pressure were not accurately measured. The actual injection pressure could have been lower or the actual gas flow rate could have been higher. A tubing-annulus communication would have been discarded by a communication test.

It was recommended to clean the well with nitrogen injection using coiled tubing. In places where sand accumulation at the bottom of the well happens very frequently, optimization engineers usually check very quickly the total depth of the well using wireline tools whenever the production of the well shows a steep decline because sand accumulation is usually the cause of the problem. However, wireline operations must always be performed after an analysis, such as the one presented in this example, has been completed to substantiate a well intervention (no matter how simple the wireline job might be). If the wireline operation is approved, the engineer should take advantage of the wireline intervention to carry out additional simple wireline tasks such as tagging the liquid level or verifying the drift diameter of the production tubing with the tubing gauge or paraffin cutter that are normally used to gauge the tubing string inside diameter or remove paraffin. Tubing gauges should always be used prior to any wireline job. See Fig. 6.38 for the description of several wireline tools.

## 11.8 GAS LIFT TROUBLESHOOTING GUIDE

### 11.8.1 Well is flowing and takes gas (stable gas injection and liquid production)

<p><b>Symptoms:</b> Liquid production lower than expected/injection pressure lower than unloading valves' opening pressure/moderate to high injection gas flow rate.</p>	<p><b>Cause:</b> Gas lift unloading valve below the static liquid level with seat diameter too large for current operational conditions.</p>	<p><b>Verification/remedy:</b> Troubleshooting calculation for valves at low temperatures/increase injection gas flow rate to reach deeper valves or change out gas lift valves with adequate seat diameters.</p>
--------------------------------------------------------------------------------------------------------------------------------------------------------------------------	----------------------------------------------------------------------------------------------------------------------------------------------	-------------------------------------------------------------------------------------------------------------------------------------------------------------------------------------------------------------------

<p><b>Symptoms:</b> Liquid production lower than expected/high and stable injection pressure/injection gas flow rate neither too high nor too low in comparison to predicted unloading requirements/wellhead production pressure as expected and no signs of high production pressure (like increase in water cut).</p>	<p><b>Cause:</b> Unloading valve with seat diameter too small and the well cannot unload to the next deeper valve.</p>	<p><b>Verification/remedy:</b> Troubleshooting calculations for continuous gas lift/increase (temporarily) injection gas flow rate to try to transfer to the next deeper valve or change out gas lift valves.</p>
<p><b>Symptoms:</b> Very high injection gas flow rate (compared to what the well actually needs)/very high injection pressure that can be stable or unstable.</p>	<p><b>Cause:</b> Surface injection gas flow rate set too high.</p>	<p><b>Verification/remedy:</b> Confirm with troubleshooting analysis for continuous gas lift wells to determine if more than one valve are currently open/lower the surface injection gas flow rate.</p>
<p><b>Symptoms:</b> Reduced liquid production and high wellhead production pressure/stable gas injection/injection pressure might or might not be moderately high.</p>	<p><b>Cause:</b> Surface production restriction.</p>	<p><b>Verification/remedy:</b> Check if the flowline is smashed or bent or if there are too many restrictions at the wellhead or flow line. Check if there are valves partially closed at the wellhead or at the flow station. Check if the flowline is too long or its diameter too small. Check if there are solid depositions in the flow line. Check the separator's back pressure regulator or any restriction at the gas outlet of the separator.</p>
<p><b>Symptoms:</b> Current gas lift design is not suitable for current operational conditions (liquid production too large or too small).</p>	<p><b>Cause:</b> Undefined production zone: well with one production tubing string and several production zones (isolated by casing–tubing packers).</p>	<p><b>Verification/remedy:</b> Detect actual production zone by running temperature surveys/open and close the right circulating sleeves or repair the completion in case they are damaged.</p>
<p><b>Symptoms:</b> High and stable injection pressure/reduced liquid production/gas flow rate set at its designed value.</p>	<p><b>Cause:</b> Gas lift mandrel not suited for deviated wells is leaning against the casing at the mandrel's inlet ports, causing a restriction of the injection gas flow rate at the point of injection.</p>	<p><b>Verification/remedy:</b> Confirm points of injection by CO<sub>2</sub> injection or distributed temperature optic sensors/install completion with gas lift mandrels suitable for deviated wells.</p>
<p><b>Symptoms:</b> Liquid production lower than the well's potential/normal wellhead production pressure/high pressure drop along the production tubing (the point of injection might be higher than the point of injection by design creating a high surface injection pressure).</p>	<p><b>Cause:</b> Production tubing diameter too small.</p>	<p><b>Verification/remedy:</b> Perform nodal analysis with the tubing diameter as the outflow sensibility variable/install larger diameter tubing if economically feasible.</p>

<p><b>Symptoms:</b> Injection pressure stable and below the valves' closing pressures/low liquid production/increase in the injection gas flow rate.</p>	<p><b>Cause:</b> Unloading valve remains open because of dirt between the ball and the seat.</p>	<p><b>Verification/remedy:</b> Communication test shows no tubing hole. Confirm injection depth with temperature survey or CO<sub>2</sub> injection/vent the annulus to get the valve to close as expected.</p>
<p><b>Symptoms:</b> Injection pressure stable and below the valves' closing pressures/liquid production below well's potential/the gas flow rate might be higher than its design value.</p>	<p><b>Cause:</b> Flat valve.</p>	<p><b>Verification/remedy:</b> Communication test shows no tubing hole. Confirm with temperature survey or CO<sub>2</sub> injection/vent the annulus: (1) to get the valve to close as expected, or (2) to confirm that it is a flat valve.</p>
<p><b>Symptoms:</b> High injection pressure/reduction of the liquid production/normal or lower than usual wellhead production pressure.</p>	<p><b>Cause:</b> Plugged downhole point of injection.</p>	<p><b>Verification/remedy:</b> Confirm with temperature survey or CO<sub>2</sub> injection/In marine environments or when using certain types of completions fluids, salt depositions could be the solids plugging the valve or keeping it open. In these cases, fresh water can be injected down the gas injection annulus. In some wells, iron sulfide (FeS) depositions that can plug gas lift valves are common. The best way to deal with these depositions is to inject water with special detergents or chemicals into the well.</p>
<p><b>Symptoms:</b> Choke-control intermittent gas lift well is producing with a very high flow rate continuous injection and low injection pressure.</p>	<p><b>Cause:</b> The pilot valve has failed open.</p>	<p><b>Verification/remedy:</b> Troubleshoot the well for continuous gas lift/change out gas lift valves.</p>
<p><b>Symptoms:</b> Intermittent gas lift well with a surface intermitter has a very high and continuous injection gas flow rate/injection pressure is very high and constant.</p>	<p><b>Cause:</b> Surface intermitter has failed open.</p>	<p><b>Verification/remedy:</b> Troubleshooting calculations for continuous gas lift/fix surface intermitter.</p>
<p><b>Symptoms:</b> Reduction of the liquid production and the injection pressure with a moderate increase in the injection gas flow rate (if there is no automatic control of the gas flow rate)/reduction of the wellhead production pressure/the well might start intermitting on its own.</p>	<p><b>Cause:</b> Reservoir liquid flow rate has dropped due to any of the following reasons: sand accumulation, drop of the reservoir pressure, or formation damage.</p>	<p><b>Verification/remedy:</b> Troubleshooting calculations for continuous gas lift. Confirm with downhole flowing pressure and temperature survey (production pressure along the production tubing should be low). Verify well's total depth/stimulate the well or get rid of the sand with coiled tubing nitrogen injection.</p>



<b>Symptoms:</b> Continuous and inexplicable decrease in the fluid production of the well/low wellhead production pressure/injection pressure at normal or moderately high values.	<b>Cause:</b> Scale deposition on the walls of the production tubing.	<b>Verification/remedy:</b> Confirm scale running wireline tubing gauge tools in the well, collect scale sample with wireline tools/inject appropriate chemicals to get rid of the scales. In case of paraffin deposition: inject hot oil or heat the injection gas.
<b>Symptoms</b> (In places where the gas flow rate control is not automated): Reduction of the surface injection gas flow rate/reduction of the injection pressure/reduction of the liquid production.	<b>Cause:</b> Plugged surface manual injection flow control valve or choke.	<b>Verification/remedy:</b> Vent gas line/installed gas filters.
<b>Symptoms:</b> Large liquid production/high and stable injection pressure (injecting through an unloading valve).	<b>Cause:</b> Well's inflow potential larger than expected.	<b>Verification/remedy:</b> Troubleshooting calculations for continuous gas lift/confirm high productivity running a downhole pressure and temperature survey/optimize gas injection or redesign the gas lift valves to meet unexpected large liquid productions.

### 11.8.2 Well is flowing and takes gas (unstable gas injection and liquid production)

<b>Symptoms:</b> Unstable operation/high injection pressure peaks corresponding to unloading valves opening pressures/well-defined injection pressure peaks/liquid production lower than expected.	<b>Cause:</b> Unloading valve with large area ratio that causes valve interference.	<b>Verification/remedy:</b> Approximate troubleshooting calculations for continuous gas lift/increase injection gas flow rate to reach deeper valves or change out gas lift valves with adequate area ratios.
<b>Symptoms:</b> Liquid production lower than expected/injection pressure high and unstable with well-defined injection pressure peaks/injection gas flow rate neither too high nor too low in comparison to predicted unloading requirements.	<b>Cause:</b> Gas lift valve with small diameter seat that causes multiple points of injection.	<b>Verification/remedy:</b> Approximate troubleshooting calculations for continuous gas lift/increase injection gas flow rate to reach deeper valves or change out gas lift valves with adequate seat diameters.
<b>Symptoms:</b> Liquid production lower than expected/production heading/high and unstable injection pressure/well flows in continuous gas lift but in cycles followed by periods of time with no liquid production.	<b>Cause:</b> Valve closes because of higher than expected dome temperatures.	<b>Verification/remedy:</b> Approximate troubleshooting calculations for continuous gas lift/change out gas lift valves with adequate test-rack calibration pressures.

<p><b>Symptoms:</b> Unstable injection gas flow rate/high frequency injection pressure fluctuations</p>	<p><b>Cause:</b> Hydrate generation at the surface injection flow control valve.</p>	<p><b>Verification/remedy:</b> Perform compositional analysis of the injection gas in order to get the hydrate and dew point curves and determine if hydrate generation is possible/prevent hydrate generation.</p>
<p><b>Symptoms:</b> Fluctuating injection pressure at the wellhead due to no apparent reason.</p>	<p><b>Cause:</b> Fluctuation of the gas lift system's pressure.</p>	<p><b>Verification/remedy:</b> Install surface pressure control valves (if the well's operating injection pressure is lower than the minimum manifold pressure) and use abandoned wells to increase the storage volume of high injection lift gas, or use PPO gas lift valves to stabilize the well's operation.</p>
<p><b>Symptoms:</b> Liquid production in batches (heading)/variable injection gas flow rate/unstable injection pressure with large difference between the highest and lowest injection pressure not comparable to the spread of any gas lift valve.</p>	<p><b>Cause:</b> Tubing hole below the reservoir static liquid level.</p>	<p><b>Verification/Remedy:</b> Confirm with communication tests and sounding devices to measure the annular liquid level fluctuations or use temperature measurement with fiber optic distributed temperature sensor to determine the depth of the communication/install packoff completion or replace tubing.</p>
<p><b>Symptoms:</b> Instability of the injection and production pressures due to no apparent causes/stability is achieved at very large injection gas/liquid ratios.</p>	<p><b>Cause:</b> Production tubing diameter too large for current operational conditions.</p>	<p><b>Verification/remedy:</b> Confirm with nodal analysis and stability checks/replace production tubing with a smaller diameter pipe or install velocity strings.</p>
<p><b>Symptoms:</b> Very high injection gas flow rate (compared with what the well actually needs)/very high and unstable injection pressure.</p>	<p><b>Cause:</b> Surface injection gas flow rate set too high, causing an upper unloading valve to open and close (multipointing).</p>	<p><b>Verification/remedy:</b> Confirm with approximate troubleshooting analysis for continuous gas lift wells to determine if more than one valve is currently open/lower the surface injection gas flow rate.</p>
<p><b>Symptoms:</b> Low surface gas flow rate/unstable and moderately low surface injection pressure with high pressure peaks that might be well-defined or not/reduced liquid production.</p>	<p><b>Cause:</b> Surface injection gas flow rate set too low.</p>	<p><b>Verification/remedy:</b> Confirm intermittent injection at the injection point depth by troubleshooting analysis for continuous or intermittent gas lift (depending if the liquid and gas flow rates at the separator indicate that the production is truly intermittent or not), or measure the downhole temperature with fiber-optic cable (distributed temperature sensor)/increase the surface injection gas flow rate.</p>

<b>Symptoms:</b> High wellhead pressure/production and injection headings/the water cut has been increasing/reduced liquid production.	<b>Cause:</b> Emulsions.	<b>Verification/remedy:</b> Take liquid production samples at the wellhead to check for emulsions/inject demulsifying chemicals with the injection gas or directly into the flowline (if that is all that is needed), or force the injection gas to be injected intermittently at high frequency (if the reservoir pressure is high).
<b>Symptoms:</b> Current gas lift design is not suitable for current operational conditions (liquid production too large or too small, temperature problems, instabilities, etc.).	<b>Cause:</b> Undefined production zone: well with one production tubing string and several production zones (isolated by casing–tubing packers).	<b>Verification/remedy:</b> Detect actual production zone by running temperature surveys (use fiber-optic distributed temperature sensors if the well's production is unstable)/open and close the right circulating sleeves or repair the completion in case they are damaged.
<b>Symptoms:</b> Erratic behavior of the injection gas flow rate/recognizable patterns of the differential pressure on the gas measurement charts if orifice plates are used to measure the injection gas flow rate.	<b>Cause:</b> Failure of the internal components of the surface control valve.	<b>Verification/remedy:</b> Repair surface gas injection flow control valve.
<b>Symptoms:</b> High and unstable injection pressure/reduced liquid production/gas flow rate set at its designed value.	<b>Cause:</b> Gas lift mandrel not suited for deviated wells is leaning against the casing at the mandrel's inlet ports, causing a restriction of the injection gas flow rate at the point of injection (the injection pressure increases and an upper unloading valve is opening and closing).	<b>Verification/remedy:</b> Confirm points of injection with distributed temperature optic sensors/change production tubing/install completion with gas lift mandrels suitable for deviated wells.

### 11.8.3 Well is only circulating the injection gas (well takes gas but does not produce liquids)

<b>Symptoms:</b> Well not flowing/injection pressure moderately lower than expected and stable/slightly higher injection gas flow rate.	<b>Cause:</b> Gas lift valve above the static liquid level with seat diameter too large for current operational conditions.	<b>Verification/remedy:</b> Troubleshooting calculation for valves at low temperatures/increase injection gas flow rate to reach deeper valves or change out gas lift valves with adequate seat diameters.
<b>Symptoms:</b> Well not flowing/high injection gas flow rate/low and stable injection pressure.	<b>Cause:</b> Tubing hole above the reservoir static liquid level.	<b>Verification/remedy:</b> Confirm with communication tests or temperature measurement using fiber-optic distributed sensor or CO <sub>2</sub> gas injection/install packoff completion or replace production tubing.

<b>Symptoms:</b> Well not flowing/high injection gas flow rate/low and stable injection pressure/low wellhead temperature (condensate water drops at the wellhead).	<b>Cause:</b> Annulus-tubing communication at the wellhead.	<b>Verification/remedy:</b> Conduct communication test/repair completion.
<b>Symptoms:</b> Very high injection gas flow rate (compared with what the well actually needs)/very high injection pressure/no liquid production.	<b>Cause:</b> Surface injection gas flow rate set too high.	<b>Verification/remedy:</b> Confirm with troubleshooting analysis for continuous gas lift wells with no liquid production to determine if more than one valve are currently open/lower the surface injection gas flow rate.
<b>Symptoms:</b> High and stable injection pressure/no liquid production/gas flow rate set at its designed value.	<b>Cause:</b> Gas lift mandrel not suited for deviated wells is leaning against the casing at the mandrel's inlet ports causing a restriction of the injection gas flow rate at the point of injection.	<b>Verification/remedy:</b> If injection is stable, confirm points of injection by CO <sub>2</sub> injection or distributed temperature optic sensors. If injection is unstable, confirm points of injection only with distributed temperature optic sensors/install completion with appropriate gas lift mandrels.
<b>Symptoms:</b> Injection pressure stable and below the valves' closing pressures/no liquid production/increase in the gas flow rate.	<b>Cause:</b> Unloading valve above reservoir static liquid level remains open because of dirt between the ball and the seat.	<b>Verification/remedy:</b> Communication test shows no tubing hole. Confirm injection depth with temperature survey or CO <sub>2</sub> injection/vent the annulus to get the valve to close as expected.
<b>Symptoms:</b> Injection pressure stable and below the valves' closing pressures/no liquid production/increase in the gas flow rate.	<b>Cause:</b> Flat valve above reservoir static liquid level.	<b>Verification/remedy:</b> Communication test shows no tubing hole. Confirm with temperature survey or CO <sub>2</sub> injection/vent the annulus: (1) to get the valve to close as expected, or (2) to confirm that it is a flat valve.
<b>Symptoms:</b> Intermittent gas lift well with a surface intermitter has a very high and continuous injection gas flow rate/injection pressure is very high and constant.	<b>Cause:</b> Surface intermitter has failed open.	<b>Verification/remedy:</b> Troubleshooting calculations for continuous gas lift with no liquid production/fix surface intermitter.
<b>Symptoms:</b> No liquid production, reduction in the injection pressure with a moderate increase in the injection gas flow rate (if there is no automatic control of the gas flow rate)/reduction of the wellhead production pressure.	<b>Cause:</b> Reservoir liquid flow rate has dropped due to one of the following reasons: sand accumulation, drop of the reservoir pressure, or formation damage.	<b>Verification/remedy:</b> Troubleshooting calculations for continuous gas lift with no liquid production. Confirm with downhole flowing pressure and temperature survey (production pressure along the production tubing should be low)/stimulate the well or get rid of the sand with coiled tubing nitrogen injection.
<b>Symptoms:</b> Very low wellhead injection pressure/very high gas flow rate/well does not flow (liquid and gas production are reduced to zero).	<b>Cause:</b> Rupture of the surface gas injection line somewhere between the injection manifold and the wellhead.	<b>Verification/remedy:</b> Close the injection valve at the wellhead, downstream of the connection of the injection pressure sensor, while leaving the injection manifold valve open: if the injection pressure does not increase, the hole is somewhere between the well and the injection manifold/close the injection valve at the injection manifold/locate gas leak and repair the gas line.

### 11.8.4 Well is not flowing and does not take gas

<p><b>Symptoms:</b> Very high injection pressure (equal to line pressure) and the well does not take injection gas/liquid production equal to zero (if the well cannot produce on natural flow).</p>	<p><b>Cause:</b> Tail plug failure (the dome pressure increased to very high values) or an error was made calibrating the valve at the test rack or it is a design error.</p>	<p><b>Verification/remedy:</b> Troubleshooting calculations indicates that the injection pressure is high enough to open the valve and overcome the production pressure. Make sure all surface valves (and the subsurface safety valve) are opened/change out gas lift valves.</p>
<p><b>Symptoms:</b> Injection pressure reaches full line pressure but the well's unloading operation cannot be started (the well does not take gas).</p>	<p><b>Cause:</b> The well cannot be unloaded because the injection pressure is not large enough to overcome the production pressure at the "first" (shallowest) unloading valve.</p>	<p><b>Verification/remedy:</b> Troubleshooting analysis indicates that the injection pressure is lower than required. Make sure all surface valves (and the subsurface safety valve) are opened/inject high pressure gas down the production tubing to lower the liquid level, unload the well to a pit, swab or circulate the well with light fluids, flowback the well with coiled tubing nitrogen injection, temporarily close nearby wells to increase the manifold injection pressure, or install a new completion with an appropriate mandrel spacing.</p>

## REFERENCES

- Abdallah, A.Y., Gaber, N.S., Saad, E.A., Bedair, E.A., Soegiyono, R.E., 2010. Gulf of Suez continuous gas lift real-time optimization strategy. SPE paper 128533.
- Brown G., et al., 2005. Slick-line with fiber-optic distributed temperature monitoring for water-injection and gas lift systems optimization in Mexico. SPE paper 94989.
- Friedli, J., Rivas, C., 2010. Adding value to gas lift evaluation with minilogger tools. SPE paper 133542.
- Gonzalez, Y.J., Azuaje, A.J., Duarte, T., Sapon, R., Madariaga, M.N., Rubio, E.A., Montoya, C., Martinez, M.Y., Castillo, G.L., O'shaughnessy, P., Perez, M.A., Berbin, A., 2008. Real-time well diagnostic using slick line fiber-optic distributed temperature sensors: West Venezuela applications. SPE paper 114911.
- Ibrahim, H.D., Al-Balushi, S., Al-Shizawi, W., 2009. Integrating real-time downhole data to enhance gas-lift completion strategies and perforation practices. SPE paper 119640.
- Jin L., et al., 2005. Smart completion design with internal gas lifting proven economical for an oil development project. SPE paper 92891.
- Julian J.Y., et al., 2007. Downhole leak determination using fiber-optic distributed temperature surveys at Prudhoe Bay, Alaska. SPE paper 107070.

- Nengkoda, A., Reerink, H., Hase, A., Prasetyo, S.I., Budhijanto, S.P., 2009. Hydrate problems in gas lift production: experiences and integrated inhibition. SPE paper 126323.
- Pothapragada, V.K., 1996. Transient aspects of unloading gas-lift wells, MS Thesis, University of Tulsa. Oklahoma, USA.
- Shnaib, F., Nadar, M.S., Sreekumar, M.P., Ponnuvel, K., Peacock, L., 2010. Successful application of CO<sub>2</sub> tracer technology for surveillance of gas lifted wells. SPE paper 133268.
- Shnaib, F., Nadar, M.S., McAlonan, N., 2009. Implementation of real-time gas lift optimization in Dubai offshore fields. SPE paper 126680.
- Tang, Y.L., 1998. Transient dynamic characteristics of gas-lift unloading, MS Thesis, University of Tulsa. Oklahoma, USA.
- Wellington, S.L., Simmons, J.F., Richardson, E.A., 1993. An on-line method for troubleshooting gas lifted wells without wireline tools. SPE paper 26593.

# Intermittent gas lift troubleshooting

## 12.1 INTRODUCTION

Many of the operational and analytical tools that are available for troubleshooting wells on intermittent gas lift are presented in the chapter. As it is the case for continuous gas lift, the primary objective is to find the point, or points, of gas injection in the well; however, it is not enough to determine that the point of injection is indeed the one stipulated in the design and that the operating gas lift valve is working properly. The analysis should also identify:

- If the cycle time corresponds to the optimum cycle time (which is the one that maximizes the daily liquid production of the well).
- If the volume of gas injected per cycle and its instantaneous gas flow rate into the tubing are adequate to minimize the liquid fallback losses.

Regarding the volume of gas injected per cycle, it is important to mention that to be able to apply many of the analytical techniques that are explained in this chapter for intermittent gas lift, the gas injection into the tubing should be properly implemented. The instantaneous gas flow rate into the tubing, as well as the total volume of gas injected per cycle, should be adequate for the intermittent gas lift method to be efficient:

- The instantaneous gas flow rate into the tubing should allow the liquid slug velocity to be close to 1000 ft./min. If the liquid slug velocity is less than 800 ft./min, the fallback losses would be too large and difficult to predict. To have an idea of the slug velocity, it is only necessary to know the depth of the operating gas lift valve (which is usually a pilot valve in wells designed for intermittent gas lift) and measure the time between the opening of the operating gas lift valve and the liquid slug arrival at the surface. A practical way of measuring the time taken by the liquid slug to reach the surface is presented in [Fig. 12.2](#).
- The actual volume of gas injected per cycle should be measured and compared to its required value estimated from the energy balance procedure explained for intermittent gas lift design in chapter: Design

of Intermittent Gas Lift Installations. If the injected volume of gas per cycle is less than its required value, it is highly probable that the liquid slug would not reach the surface or that the liquid fallback losses would be too high and very difficult to estimate.

Many times and for many unexpected reasons, wells that have been designed for continuous gas lift operate in an intermittent fashion; therefore, it is important that the optimization personnel be properly trained for intermittent gas lift design and troubleshooting even if the wells in their particular field would never be good candidates for intermittent gas lift. For example, any continuous gas lift well with an injection-pressure-operated valve installed at the point of injection will start intermitting if the surface gas flow rate is reduced to values that would make the injection pressure drop below the injection closing pressure of the operating gas lift valve.

A good physical understanding of the intermittent gas lift method is required, not only for accurate troubleshooting analyses, but also to be able to identify cases in which some, or all, of the troubleshooting techniques for intermittent gas lift do not apply. These cases are briefly presented in this introduction, but they are analyzed at greater depths in the next sections.

- Gas injection might appear to be intermittent when in reality liquid production and gas injection are both continuous. This can be easily detected by looking at the behavior (in time) of the liquid flow out of the test separator (or its liquid level behavior if the test separator is operated by a dump valve) and the total gas flow rate at the test separator. This situation usually takes place in overinjected wells, where one or several unloading valves are intermittently opening and closing, while gas is continuously being injected through the operating valve or orifice.
- Another confusing case takes place when the well is continuously producing liquid but the gas injection is truly intermittent. This frequently happens when the gas injection cycle frequency is very high and the volume of gas injected per cycle is less than the volume required to individually produce the liquid slug all the way up to the surface. This high injection frequency can be intentionally implemented to avoid emulsion or foam generation, or in wells with highly viscous fluids. In these cases, the reservoir pressure should be high enough for this technique to work.
- It is also possible that the well produces on a continuous fashion, but only during short time periods, followed by intervals in which the liquid production completely ceases, see Example #3 in Section 11.7.3. This case is identified as such if the gas injection periods are very long and the instantaneous gas flow rate through the operating gas lift valve is very



small so that the slug velocity is very slow, causing high liquid fallback losses impossible to be precisely estimated. Under these conditions, troubleshooting the well using the equations given in the chapter is wrong because the calculated liquid column length would probably be too long.

If the liquid level inside the separator (with a dump valve control) is constantly rising or the measured liquid flow rate is never zero (if the test separator is operated with a liquid level control), it is possible that the well is indeed producing in a continuous fashion even if the surface gas injection is performed intermittently (or appears to be that way). However, when this happens, it is important to verify that a valve from another well at the flow station is not leaking liquids toward the test separator. To look for leaking valves at the flow station, close all valves connecting the wells to the test separator (including the well that is going to be tested) so that all wells are directed to the main production separators at the flow station. If the liquid level inside the test separator is still increasing (in a separator with dump valve system to measure the liquid production) or the liquid production is never equal to zero (if the test separator liquid level is being controlled at a fixed level and the instantaneous liquid flow rate is being measured), there must be then one or several valves leaking toward the test separator.

As indicated in chapter: Continuous Gas Lift Troubleshooting for continuous gas lift, intermittent gas lift troubleshooting is also a very complex task that is not always possible to accomplish because of lack, or poor quality, of the required data. The first step in troubleshooting a well consists of gathering as much information as possible from the field and from the well's file. The following is a list of required data for troubleshooting wells on intermittent gas lift:

- Behavior of the wellhead production and injection pressures: If the way in which these pressures fluctuate in time is not known, it is not possible to do a troubleshooting analysis of a well on intermittent gas lift. Knowing the wellhead pressures, the surface injection opening and closing pressures of the gas lift valve can be determined, as well as the cycle time, the time interval in which the gas lift valve remains opened, the liquid column generation time, and the average liquid slug velocity. But knowing all of these parameters is not enough, it is important to analyze this information to determine if in reality intermittent gas lift is possible from the assumed point of injection and, if that is the case, to establish if the intermittent gas lift method is fully optimized as indicated at the beginning of this introduction.
- Total liquid and gas production: At least one well test should be performed with the current gas injection frequency. Changes in liquid level (or liquid flow rate) and gas flow rate at the test separator are as

important as the total daily liquid production. The surface injection pressure could give the impression that gas is being injected in an intermittent fashion into the tubing, when in reality there might be a constant point of injection together with another point of injection that is opening and closing at regular intervals, as has already been expressed earlier. Continuous liquid production is easily detected if the liquid level in the separator (with dump valve control) is constantly rising (or the liquid flow never drops to zero if the test separator is operated with a liquid level control) and the total gas flow rate (measured at the exit of the test separator) is always considerably greater than zero. The total gas flow rate can be measured by means of especial devices that integrate the pressure signals from the orifice plate. This integration is particularly difficult for wells on intermittent gas lift, but it gives important qualitative information.

- Fluid properties: such as oil specific gravity, formation gas/oil ratio, bubble-point pressure, water cut, and the specific gravities of the injection and formation gas. If a three-phase test separator is not being used, it is important to take fluid samples from points at the wellhead or the flowline where the flow is highly turbulent to collect representative fluid samples or to know if the well is producing any liquid at all. With the water cut and the oil API gravity, the pressure gradient of the liquid column that is generated on top of the operating gas lift valve can be calculated and the tubing pressure at valve depth (when it opens) can be established. The injection gas specific gravity is needed to calculate the injection pressure at valve's depth from the measured surface injection pressure. It is also important to know the humidity of the injection gas because it might be responsible for hydrate generation problems at the surface gas injection choke (not uncommon for choke-control intermittent gas lift wells that require very long cycle times). It should also be established if the injection gas has solid particles or debris that might plug the entrance ports of the pilot valve or get its piston stuck, leaving the pilot valve open with a very high gas flow rate. It is recommended that the operating valve for intermittent gas lift wells be a pilot valve instead of a single-element valve. Unfortunately, pilot valves can fail in many different ways, as described in Section 10.4.
- Reservoir data: static reservoir pressure and effective productivity index (defined in chapter: Design of Intermittent Gas Lift Installations as the average productivity index within the range of practical application of the IPR curve for intermittent gas lift, which goes from very low bottomhole flowing pressures at the beginning of the slug generation period to approximately 40–50% of the static reservoir

pressure at the time the pilot valve opens). The effective productivity index can be determined from the analysis of flowing pressure surveys (especially designed for intermittent gas lift) explained in [Section 12.3](#). The effective productivity index can also be determined from a troubleshooting analysis, as long as the instantaneous gas flow rate and the volume of gas injected per cycle are the ones needed to achieve small liquid fallback losses. Once the static reservoir pressure and the productivity index are known, the optimum cycle time and the maximum daily liquid production can be calculated from Eqs. 10.23 and 10.19, respectively.

- Well completion data: casing ID, tubing ID and OD, tubing inclination angle, packer depth, types and depths of gas lift valves (including area ratios, seat diameters, and calibration pressures), the length and inside diameter of the gas injection line (from the injection manifold, or from wherever the surface flow control choke or the intermitter is located, to the wellhead), and the length and inside diameter of the flowline from the wellhead to the separator or production header. It is also important to inspect the wellhead to see if there are unnecessary restrictions that might slow down the liquid slug and cause very large liquid fallback losses. If a choke in the flowline is absolutely necessary (maybe because the separator is too small to handle the liquid slugs and/or the tail gas being produced), it should be installed far from the wellhead at a distance greater than the length of the liquid slug being produced.
- Sometimes especial data are required for extraordinary troubleshooting analysis, such as: (1) a complete evaluation of a new completion (like accumulation chambers or simple accumulators), (2) the implementation of the intermittent gas lift method for the first time in a given gas lift field, or (3) serious instabilities problems caused by tubing-annulus communications, valve interference, etc. Under these circumstances, field tools and techniques should be used: flowing temperature and pressure surveys, communication tests, distributed temperature measurement along the tubing using optical fibers, or the use of sonic devices to determine the liquid level in the annulus, among others.

## 12.2 ANALYSIS OF THE OPERATION OF WELLS WITH INTERMITTENT GAS INJECTION

The necessary analyses to troubleshoot wells in which the gas injection is performed intermittently are presented in the section. The reader is advised to review the concepts given in chapter: Design of Intermittent Gas Lift Installations on the theory of intermittent gas lift to fully understand the different troubleshooting techniques presented in the chapter.

### 12.2.1 Wells that should not be analyzed as intermittent gas lift wells

Different cases for which intermittent gas lift troubleshooting analytical techniques should not be used (even if gas injection is indeed intermittent) given in the introduction of the chapter are now described in detail in the section. As previously indicated, the optimization personnel should be capable of recognizing these cases so that no wrong conclusions are made that could lead to actions that will not solve the problem in the well. In many of these situations, the use of continuous gas lift troubleshooting techniques is also wrong but they might provide a better approximation to what might be going on in the well and how to fix the problem.

The injection pressure might look as if the well is on intermittent gas lift, but in reality one of the following alternatives could be taking place:

- There are two points of injection in which one valve is opening and closing at regular intervals while the other is opened all the time. If surface controllers are used, this situation is easily detected by inspecting the two-pen wellhead pressure charts as explained in this chapter, see [Figs. 12.26i](#) and [j](#). On the other hand, in choke-control intermittent gas lift, it is more difficult to detect if there are more than just one point of injection because the surface injection pressure pattern might look exactly like a perfect intermittent gas lift operation when, in reality, one of the following possibilities is taking place:
  - With injection-pressure-operated gas lift valves
    - An unloading valve with a small port diameter fails to open, but the injection pressure is high enough to reach the operating valve or any other valve below the damaged valve. As soon as the lower valve (in good working condition) is uncovered, the gas flow rate through this valve and the upper damaged valve is greater than the gas flow rate being injected at the surface so that the annular pressure drops and the valve in good condition closes while injection gas continues to pass through the upper damaged valve. When the lower valve is closed, the gas flow rate at the surface is greater than the gas flow rate through the damaged valve, thus the annular pressure increases to eventually initiate gas injection through the lower valve again, beginning a new injection cycle through this lower valve.
    - Gas overinjection through the operating gas lift valve makes the annular pressure increase so that an upper unloading valve in good condition opens. Once the upper valve opens, the total gas flow rate through both gas lift valves is greater than the gas

flow rate injected into the annulus at the surface, therefore, the annular pressure drops and the upper unloading valve (in good working condition) closes. But once gas injection through the operating valve alone is reestablished, the gas flow rate at the surface is greater than the gas flow rate through the operating valve and the annular pressure begins to increase to open the upper valve again, repeating the injection cycle through this upper valve.

- An inadequate gas lift design, in which an unloading valve with a large seat causes valve interference. Due to its large area ratio, the unloading valve surface closing pressure is less than the surface closing pressure of the lower valve. Once the lower valve is uncovered, the upper valve does not close so that gas will be injected through two points of injection. The gas flow rate through both valves is greater than the gas flow rate into the annulus at the surface so that the annular injection pressure drops and the lower valve closes while the upper one remains open. When the lower valve closes, the annular pressure begins to rise because now the gas flow rate through the upper valve is less than the surface gas flow rate. The annular pressure keeps increasing until the lower valve opens again and gas injection through it is restored to start a new injection cycle through this valve.
- With production-pressure-operated valves:
  - An upper valve fails open and, due to its reduced seat diameter, the injection pressure does not drop in a considerable way and the lower valve can be reached. Once the lower valve is uncovered, either the production pressure drops to values less than the lower valve's opening pressure or the injection pressure at the lower valve becomes less than the production pressure at this lower valve and, in any of these two cases, gas injection through the lower valve ceases for a period of time in which the injection pressure begins to increase, eventually reaching an injection pressure greater than the production pressure at the lower valve or the production pressure (which is also increasing due to lack of lift gas through the lower valve) increases to open the lower valve again.
  - Once the lower valve is uncovered, the production pressure at the upper valve's depth (in good condition in this case) does not drop to the upper valve's closing pressure because it was calibrated for lower liquid flow rates. With two points of injection, the injection pressure at the lower valve drops

to values less than its production pressure and the injection through that valve ceases for a period of time in which the injection pressure rises again to repeat the injection cycle through the lower valve.

- Continuous gas lift wells with operating valves in throttling flow. The operating gas lift valve first opens wider and then it tries to close (but never actually closing). This cycle repeats itself periodically with a gas flow rate that fluctuates but that never drops down to zero. This case is further analyzed later, after the injection-gas mass balance equations are described; see the explanation given for Fig. 12.1.
- Wells with a very high gas injection frequency (truly intermittent gas injection) that are in fact producing liquids in a continuous fashion as explained in the introduction of the chapter. This case is also further analyzed later, after injection-gas mass balance equations are described.
- Well with a very high gas injection frequency that are not producing any liquids. In this case, the volume of gas injected per cycle is so small that it simply bubbles through the liquids and escapes to the surface. This happens in wells with very low reservoir pressure and large diameter tubing or in wells that have not been fully unloaded.
- Wells that produce on continuous gas lift for a very short period of time, followed by a time interval in which the gas injection stops and no liquids are produced for a while and these cycles repeat continuously This is analyzed in Example 3, Section 11.7.3.

Wells with more than one point of injection are easily identified by the fact that the total gas flow rate at the test separator's gas outlet is always much larger than zero. In some rare cases, however, it is possible that the total gas flow rate never drops to zero because there is a second formation (different from the one that produces most of the liquids) with a slightly higher reservoir pressure that is always producing formation gas into the tubing.

With more than one injection point, the liquid production could be continuous (although it might be fluctuating but never dropping to zero, see for example Fig. 11.57), equal to zero, or truly intermittent with well-defined liquid slugs produced to the surface at regular intervals. The latter case takes place, for example, when the point of injection that is always opened is located above the static liquid level and the volume of gas that is intermittently being injected through the lower injection point is large enough to lift the liquid slugs to the surface; however, in this case the point through which the gas is continuously injected might also be below the static liquid level but all the liquid comes from the lower point of injection because the gas flow rate through the upper point is not large enough to produce any liquid.

When there are several points of injection, the force–balance equation usually indicates that there might be more than one valve opened. If doing a troubleshooting analysis is too difficult because there are many gas lift valves installed in the well and it is suspected that there are several valves opened at the same time, these points of injection can be identified by measuring the temperature along the tubing using fiber optics as explained in Section 11.5.7. The injection points correspond to the places where the cooling effect of the injection gas can be appreciated.

When there is more than just one point of injection, the volume of gas injected per cycle calculated by dividing the total surface daily injection gas flow rate (through the surface choke or flow control valve) by the number of cycles per day, is much larger than the volume of gas due only to the injection pressure reduction (from the opening to the closing injection pressure of the intermitting gas lift valve) of the annulus and the injection line (downstream of the choke) every time the intermitting valve opens or is uncovered. Before explaining in greater details some of the cases for which many of the intermittent gas lift troubleshooting analytical techniques do not apply, several injection-gas mass balance equations are presented. These equations are, by themselves, tools that help the production engineer identify which additional analytical techniques, if any, can be used to troubleshoot the well.

As explained in chapter: Design of Intermittent Gas Lift Installations, in choke-control intermittent gas lift the volume of gas injected per cycle into the tubing is equal to the volume of gas that comes from lowering the pressure in the annulus and in the injection line (downstream of the surface choke or gas injection control valve) plus the gas that is injected through the surface choke while the subsurface pilot valve is opened. It is important to know the volume of gas injected per cycle because it represents the “starting point” of any troubleshooting analysis. If the volume of gas injected per cycle is less than its required value to lift the liquid slug to the surface (estimated from the energy balance equation) the liquid fallback losses might be so large and difficult to estimate that the productivity index cannot be calculated and, in consequence, the optimum cycle time cannot be estimated either. In this case, the only way of calculating the initial liquid column length is by using the force–balance equation for the pilot valve (for this calculation, the gas specific gravity and surface injection opening pressure should be accurately measured so that the gas injection pressure at depth can be reliably estimated and used in the force-balance equation).

The volume of gas provided by the annulus, called  $v_{ga}$ , is calculated by subtracting the volume of gas that remains in the annulus right after the pilot valve closes, called  $v_{sc}$ , from the volume of gas that is originally in the annulus when the pilot valve opens, called  $v_{sa}$ ; therefore,  $v_{ga} = v_{sa} - v_{sc}$ . Volumes  $v_{ga}$ ,  $v_{sc}$ , and  $v_{sa}$  are all expressed at standard conditions (scf).

The number of moles  $n_0$  calculated at (a) “in situ conditions” must be equal to the number of moles expressed at (b) “standard conditions.” This number of moles is given by the following equations just before the pilot valve opens (at in-situ and standard condition, respectively):

$$(a) n_0 = \frac{P_{ga,apert.} V_{annular}}{z_{ga,apert.} R_u T_{geoth.avr.}} \text{ and } (b) n_0 = \frac{(14.7 \text{ psia}) v_{sa}}{(1) R_u (520^\circ R)} \quad (12.1)$$

Where  $V_{annular}$  is the actual annular volume in cubic feet,  $z_{ga,apert.}$  is the average injection gas compressibility factor in the annulus when the pilot valve opens,  $T_{geoth.avr.}$  is the average geothermal temperature along the well in  $^\circ R$ ,  $R_u$  is the universal gas constant,  $P_{ga,apert.}$  is the average annular pressure in psia at the moment the pilot valve opens and it is given by:

$$P_{ga,apert.} = \frac{P_{cso} + P_{cvo}}{2} \quad (12.2)$$

Where  $P_{cso}$  is the surface opening pressure in psia and  $P_{cvo}$  is the opening pressure at valve’s depth, also in psia, and it is equal to  $f_g(P_{cso})$ , where  $f_g$  is the gas factor used to find the pressure at depth from the surface pressure, as explained in chapter: Single-Phase Flow.

The annular volume occupied by the injection gas at standard conditions at the moment the pilot valve opens ( $v_{sa}$ ) can be calculated from Eqs. 12.1 a and b by setting these expressions equal to each other.

In an identical way (as given earlier just before the valve opens), the number of moles  $n_c$  left in the annulus just after the pilot valve closes is given by:

$$n_c = \frac{P_{ga,close.} V_{annular}}{z_{ga,close.} R_u T_{geoth.avr.}} = \frac{(14.7 \text{ psia}) v_{sc}}{(1) R_u (520^\circ R)} \quad (12.3)$$

Where  $z_{ga,close.}$  is the average gas compressibility factor in the annulus just after the pilot valve closes,  $P_{ga,close.}$  is the average annular pressure just after the pilot valve closes and it is given by:

$$P_{ga,close.} = \frac{P_{csc} + P_{cvc}}{2} \quad (12.4)$$

Where  $P_{csc}$  is the surface closing pressure;  $P_{cvc}$  is the closing pressure at valve’s depth and it is equal to  $f_g(P_{csc})$ .  $P_{csc}$  and  $P_{cvc}$  are both expressed in psia. The volume of gas at standard conditions just before the valve closes ( $v_{sc}$ ) can be calculated using Eq. 12.3. The volume of gas provided by the annulus,  $v_{ga}$ , is then:

$$v_{ga} = v_{sa} - v_{sc} \quad (12.5)$$



Expressions for  $v_{sa}$  and  $v_{sc}$  can be found from equations for the average geothermal temperature,  $T_{\text{geoth.avr.}}$ , and the actual volume of the annulus,  $V_{\text{annular}}$ .

$$T_{\text{geoth.avr.}} = \frac{T_s + T_{\text{dov}}}{2} + 460^\circ R \quad (12.6)$$

Where  $T_s$  is the surface temperature in  $^\circ F$ , which in many cases can be approximated as  $85^\circ F$ ;  $T_{\text{dov}}$  is the geothermal temperature at valve's depth also in  $^\circ F$ .

If  $B_a$  is the annular volumetric capacity in  $\text{ft.}^3/\text{Mft.}$  and the valve's depth  $D_{\text{ov}}$  is given in  $\text{Mft.}$ , then  $V_{\text{annular}}$  is:

$$V_{\text{annular}} = D_{\text{ov}} B_a \quad (12.7)$$

Using Eqs. (12.1)–(12.4), (12.6), and (12.7), and assuming the surface temperature to be equal to  $85^\circ F$  ( $545^\circ R$ ) the following expressions for  $v_{sa}$  and  $v_{sc}$  can be found:

$$v_{sa} = 35.37 \frac{B_a D_{\text{ov}} (P_{cso} + P_{cvo})}{[85 + 2(460) + T_{\text{dov}}] z_{\text{ga,apert.}}} \quad (12.8)$$

$$v_{sc} = 35.37 \frac{B_a D_{\text{ov}} (P_{csc} + P_{cvc})}{[85 + 2(460) + T_{\text{dov}}] z_{\text{ga,close.}}} \quad (12.9)$$

Following the same steps taken for the gas in the annulus and taking the surface temperature equal to  $85^\circ F$  ( $545^\circ R$ ), expressions for the gas volume (at standard conditions) stored in the gas injection line (from the choke to the wellhead) when the valve opens ( $v_{sa}$ ) and when the valve closes ( $v_{sc}$ ) can also be found:

$$v_{sa} = 35.37 \frac{B_1 L P_{cso}}{545 z_{\text{gl}}} \quad (12.10)$$

$$v_{sc} = 35.37 \frac{B_1 L P_{csc}}{545 z_{\text{gl}}} \quad (12.11)$$

Where  $z_{\text{gl}}$  is the average gas compressibility factor in the gas injection line,  $B_1$  is the volumetric capacity of the gas injection line in  $\text{ft.}^3/\text{Mft.}$ , and  $L$  is the length of the gas injection line in  $\text{Mft.}$  The volume of gas supplied by the surface gas line at each cycle ( $v_{\text{gl}}$ ) is then:

$$v_{\text{gl}} = v_{sa} - v_{sc} \quad (12.12)$$

The volume of gas that enters the tubing per cycle, called  $v_{\text{gsC}}$ , is equal to the sum of  $v_{\text{ga}}$ ,  $v_{\text{gl}}$  and the volume of gas that is injected at the surface through the

surface choke while the downhole pilot valve remains opened (called  $v_{ge}$ ). As derived in the next section, the gas flow rate in Mscf/D through the surface injection choke (in case of choke-control intermittent gas lift) is equal to:

$$Q_{gi} = \frac{(v_{ga} + v_{gi})[\text{scf}]}{(T_{\text{cycle}} - T_{\text{val}})[\text{min}]} \left[ \frac{1440 \text{ min}}{1 \text{ Day}} \right] \left[ \frac{1 \text{ Mscf}}{1000 \text{ scf}} \right] \quad (12.13)$$

Where  $T_{\text{cycle}}$  is the total cycle time in minutes and  $T_{\text{val}}$  is the period of time in which the pilot valve remains open (also in minutes). It is possible that  $Q_{gi}$  does not have a constant value, but its fluctuations are usually very small, thus it is a good approximation to use its average value in Eq. 12.13. Then, the volume of gas that is injected at the surface while the pilot valve is opened,  $v_{ge}$ , is given in scf by:

$$v_{ge} = T_{\text{val}} Q_{gi} / 1.44 \quad (12.14)$$

The gas flow rate through the surface choke should not be confused with the instantaneous gas flow rate through the subsurface gas lift valve. The gas flow rate at the surface (in choke-control intermittent gas lift) is usually very small compared to the gas flow rate through the gas lift valve and this is the reason why the injection pressure drops once the pilot valve opens. This is not the case when surface controllers (intermitters) are used, for which the gas flow rate through the gas lift valve is less than, but comparable to, the surface gas flow rate into the annulus.

The volume of gas injected per cycle,  $v_{gsC}$ , is equal to  $v_{ga} + v_{gl} + v_{ge}$ . If there are two points of injection (one continuous and the other intermittent) the volume of gas injected per cycle,  $v_{gsC}$ , calculated using the equations just presented (mainly using the reduction of the injection pressure in the annulus and surface gas line from the valve's opening pressure to the valve's closing pressure) is smaller than the volume of gas in scf calculated as  $1000 Q_{gi}/$  (number of cycles per day); however, even though there might be only one point of injection, many times these two values of the volume of gas injected per cycle do not coincide because the gas flow rate continuously injected at the surface and/or the wellhead pressures are not properly measured. For example, sometimes the beta ratio of the actual orifice plate used to measure the gas flow rate is not known or there is an error in one or several of the following measurements: surface opening and closing pressures of the gas lift valve or the differential and static pressures at the orifice plate. Additionally, as pointed out earlier, the liquid flow might indeed be intermittent even with multiple points of injection. The liquid level behavior in the separator is then not a conclusive evidence of having single or multiple points of injection. The best way to definitely establish that there are multiple points of

injection in intermittent gas lift operations is by verifying that the total gas flow rate at the exit of the separator is always much greater than zero.

As was previously mentioned, it is easy to see if there are several points of injection just by looking at the wellhead pressure pattern if surface controllers (intermitters) are used. With or without multiple points of injection, when surface controllers are used the volume of gas injected every time the controller opens is given by:

$$v_{\text{gsC}} = Q_{\text{gi}} T_{\text{on}} / 1.44 \quad (12.15)$$

Where  $Q_{\text{gi}}$  is the instantaneous gas flow rate at the surface gas flow meter in Mscf/D while the controller is opened and  $T_{\text{on}}$  is the period of time in which the controller remains opened (in minutes). If the surface gas flow rate  $Q_{\text{gi}}$  is not constant, the volume of gas injected at the surface per cycle is given by:

$$v_{\text{gsC}} = \int_0^{T_{\text{on}}} \frac{Q_{\text{gi}}}{1.44} dt \quad (12.16)$$

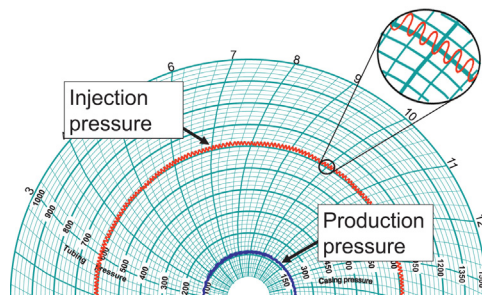
With multiple points of injection (with one valve opening and closing while another is opened all the time), the volume of gas injected per cycle into the casing calculated using Eq. 12.15 or 12.16 is in part injected intermittently into the tubing and the rest is injected into the tubing in a continuous fashion. So the total volume of gas injected intermittently into the tubing is less than the volume of gas calculated using Eq. 12.15 or 12.16.

Troubleshooting an intermittent well with multiple points of injection is extremely difficult to do and it is very hard to determine exactly which those injection points are. Usually, the conclusion of having multiple points of injection is reached because the force–balance equation predicts more than one valve being opened and the gas mass balance indicates that it is not possible to inject all the gas through only one of those valves suspected of being opened. Determining in which proportion the gas is being injected through each point of injection or knowing which valves correspond to these points of injection (especially for cases in which more than four or five valves are installed in the well) is very hard to do even with a downhole pressure survey. Continuous gas lift troubleshooting techniques explained in chapter: Continuous Gas Lift Troubleshooting could be used in these cases to approximately determine how the gas is being injected.

Continuing with the subject of wells that should not be analyzed with intermittent gas lift troubleshooting analytical techniques, continuous gas lift wells with the operating gas lift valve on throttling flow some times behave as if the wells were operating on intermittent gas lift. These cases are usually mistaken and analyzed with intermittent gas lift troubleshooting

equations that give wrong results. This point is presented in chapter: Continuous Gas Lift Troubleshooting and is analyzed here in more detail. Fig. 12.1 shows a moderate instability in which the operating valve does not actually close. In this example, the gas lift valve is an injection-pressure-operated valve. This behavior usually happens in wells that have been designed for continuous flow (with single-element gas lift valves instead of pilot valves) when the reservoir pressure has dropped and the well, by it self, tries to produce on intermittent gas lift because the production pressure is now less than the production pressure the well had when the liquid production was larger. No well-defined, sharp pressure peaks are observed; instead, pressure peaks are rather rounded and this is the main feature that identifies this type of operational condition. The liquid production is continuous and the gas lift valve operates in throttling flow without fully opening or closing. Another feature that helps identify this type of gas injection is the fact that the gas flow rate at the exit of the separator is always much greater than zero and its value is always fluctuating but these fluctuations are not very pronounced.

- When the production pressure drops, the valve tends to close because the production pressure plays a major role on the valve's stem movement in throttling flow (this type of gas flow through a gas lift valve is described at the beginning of chapter: Gas Flow Through Gas Lift Valves). When the valve tends to close, the injection gas flow rate is restricted and this in turn causes two effects that try to stabilize the injection pressure fluctuations. Because the gas flow rate into the tubing decreases, the production pressure increases and this tends to open the valve wider again. On the other hand because the surface injection gas flow rate (into the annulus) is usually constant, when the gas flow rate into the tubing decreases the



■ FIGURE 12.1 Valve in throttling flow (it is never fully closed). Continuous gas injection and continuous liquid production.

injection pressure in the annulus increases and this also tries to open the valve wider. The valve then starts to open wider so the gas flow rate begins to increase and the production pressure begins to drop again to start a new cycle.

- The injection pressure can be stabilized by increasing the surface gas flow rate, but sometimes this cannot be achieved because, when the surface injection gas flow rate is increased, the injection pressure also increases and an upper unloading valve might open. The stabilizing effect due to the valve dynamic behavior would not be found if there was an orifice valve at the operating point or injection. Wells exhibiting this sort of behavior must be troubleshoot (in an approximate way) using continuous gas lift techniques. Even though it appears very simple, trying to model the dynamic behavior of a well under these circumstances is extremely hard to do because it implies coupling the transient response of the reservoir with the dynamic behavior of: the gas lift valve, the annular injection pressure, and the transient multiphase flow in the tubing. Due to the transient nature of the gas injection into the tubing, no multiphase flow correlation can be used to accurately calculate the production pressure along the tubing, although steady-state correlations can many times be used as a good approximation.

For a well with the wellhead pressure pattern shown in Fig. 12.1, as well as for wells with multiple points of injection, the volume of gas injected per cycle calculated as  $1000 Q_{gi}/(\text{number of cycle per day})$  is not equal to the volume of gas injected per cycle,  $v_{gsC}$ , calculated with Eqs. from 12.1 to 12.14. The number of cycles in one day is equal to  $1440/T_{\text{cycle}}$ , where  $T_{\text{cycle}}$  is the cycle time expressed in minutes per cycle. On the other hand because the liquid production is continuous, the liquid slug length per cycle cannot be calculated from the liquid production in Br/D, divided by the number of cycles in one day and the volumetric capacity of the tubing in Br/Mft. This would give very large liquid columns and any type of analysis using the intermittent gas lift theory would be wrong.

Some of the operational conditions that promote the type of throttling flow patten shown in Fig. 12.1 are: (1) large diameter of the production tubing, (2) high water cut, (3) very small high-pressure gas storage volume (annulus plus the injection line downstream of the choke), (4) single-element gas lift valve with large port size, and (5) decline in the production tubing pressure.

Wells with a very high gas injection frequency (mentioned at the beginning of the section) are now discussed in greater detail. In these cases, the gas

injection is truly intermittent and through a single point of injection but the liquid production is continuous. This usually takes place in wells with high reservoir pressure. This is the case in which the gas lift method is most commonly (and wrongly) identified as a truly intermittent gas lift operation because the injection pressure pattern is identical to the one found in many truly intermittent gas lift wells. Fig. 11.47 shows a wellhead pressure chart with the typical wellhead pressure behavior for this type of operation. The features that help identify this operational condition are:

- Constant liquid production at the separator (although it can also be equal to zero or very small).
- The volume of gas injected per cycle is much less than the required volume to individually produce each liquid slug to the surface.
- The gas flow rate at the exit of the separator is always greater than zero because the formation gas is always being produced (although in smaller quantities).
- The volume of gas injected per cycle calculated by Eqs. 12.1–12.14 does indeed correspond to  $1000 Q_{gi}/(\text{number of cycles per day})$ .
- If the liquid production is greater than zero, it usually takes place in wells with high reservoir pressures that might even be good candidates for continuous gas lift.
- The total cycle time is very short and the spread of the valve is very small (indicating a possible high tubing pressure or a very small valve area ratio).

The production engineer does not always have at his disposal the behavior of the liquid level inside the separator as a function of time (or the instantaneous liquid flow rate behavior in time at the outlet of the test separator if the liquid level is automatically controlled) and, without this information, the only thing to do when confronted with high gas injection frequency wells is to calculate the volume of gas injected per cycle and compare this volume to the required volume (based on the energy balance equation) to produce the liquid slugs to the surface. This comparison would indicate that it is not possible to have an intermittent gas lift operation because the volume of gas injected per cycle is just too small. Because the gas injection is done through a single point of injection, the volume of gas intermittently injected per cycle is indeed equal to  $1000 Q_{gi}/(\text{number of cycles per day})$ . The liquid slugs to be used in this comparison are calculated by simply dividing the daily liquid production by the number of cycles in one day and by the volumetric capacity of the production tubing.

Some of the reasons why very high gas injection frequency might occur are:

- A well with high reservoir pressure, designed to produce on intermittent gas lift, is unloaded with an inadequately small surface

injection gas flow rate. This surface gas flow rate might in fact be equal to the flow rate needed for the well after the unloading process is completed but because the liquid column is very large when the operating valve is uncovered, the spread of the valve (defined as the difference between the opening and closing pressures of the valve) becomes very small and, therefore, the volume of gas injected per cycle also becomes very small, thus the well begins to flow continuously with small liquid slugs distributed along the entire production tubing. The reduction in the spread of the valve is due to the high production pressure, which plays an important role in trying to open the valve: the higher the production pressure is, the lower the injection pressure needs to be to open the valve (which is an unbalanced injection-pressure-operated valve that responds to both, the production and the injection pressure).

- If the reservoir pressure is low, the unloading problem discussed in the previous paragraph might also take place but in this case the liquid slug might never reach the surface because the static liquid level is too deep. It is also possible that the well with low reservoir pressure does produce on intermittent gas lift but the liquid slugs produced are considerably smaller than the initial ones at the bottom of the well. This is due to the large fallback losses caused by the low liquid velocities, which in turn are the results of a low injection pressure or gas volume injected per cycle. Under these conditions, the well should be troubleshoot using intermittent gas lift techniques but taking into account the fact that the fallback losses are very large and difficult to estimate. Usually, the valve force–balance equation should be used in these cases to calculate the initial slug length just before the valve opens; but for this calculation to be accurate, it is important to measure very precisely the surface injection opening pressure, the gas specific gravity, the water cut, and the oil API gravity.

It is important to verify how the liquid level in the test separator (if the separator is controlled with a dump valve) or the liquid production out of the test separator (if the liquid level in the separator is controlled at a constant value) behaves in time to see if the production is truly intermittent or the well is producing on continuous flow. Usually the high gas injection frequency cases described so far are identified because the actual spread of the valve is much smaller than its design value. When this abnormally low spread takes place, it is many times possible to reestablish the correct operation of the well by temporarily injecting gas at a rate much greater than required under normal design conditions for the well. This large injection flow rate should be maintained until the spread of the valve becomes similar to its design value. After that time, the gas flow rate can be reduced back to its designed value and only

in few cases the well begins to load up with liquids again, for which it becomes necessary to change the operating valve with another one with a larger area ratio or a higher opening pressure. This point is analyzed in an example in [Section 12.5](#), see [Fig. 12.27](#).

- There are gas lift fields producing viscous fluids in which, by design, the gas lift injection is intermittent while maintaining a continuous liquid production. As in the previous cases, very small volumes of gas are injected per cycle at a very high frequency. This technique has, in many occasions, been able to reduce lift gas consumption because it avoids foam generation or keeps the gas velocity from becoming much greater than the liquid velocity. To produce a well in this manner, it is important that the reservoir pressure be sufficiently high because the flowing bottomhole pressure is large under this type of flow. This technique is difficult to design and highly inefficient. A better option might be to produce these wells on a different artificial lift method, but there are gas lift fields in which only a small number of wells are heavy oil producers and it becomes economically possible to produce them on gas lift by taking advantage of the gas lift surface facilities already installed (as long as the number of wells is only a small fraction of the total number of wells).
- When operational conditions promote the formation of emulsions, some operators also design their wells as explained in the previous paragraph (continuous liquid production and high frequency intermittent injection). This reduces the emulsion problem because it avoids the turbulence that continuous gas injection creates, which promotes and helps stabilize water-in-oil emulsions.

To finish the list of cases in which it is not possible to apply many of the available analytical troubleshooting techniques, it is important to mention that there might be wells with irregular or chaotic surface gas injection fluctuations. This might happen for one of the following reasons:

- Hydrate formation.
- Pilot valve malfunction.
- Failures in some of the internal components of the surface gas injection control valve.
- Variations of the gas lift system pressure.
- Inadequate gas lift design for current operational conditions, such as high water cuts or emulsions in the tubing and/or the flowline.
- Casing–tubing communication (uncontrolled injection).

Fortunately, most of these situations are easily identified by looking at the pressure pattern on the wellhead pressure charts or the gas meter charts.



When irregular gas injection takes place, the well cannot be fully analyzed from analytical procedures and its cause can only be identified by the qualitative characteristics of the pressure patterns shown in the wellhead pressure charts or in the gas meter charts (as explained in Sections 12.5, 11.5.9, and 11.5.10). Some minor calculations are possible, especially in preparation for the application of troubleshooting field techniques that are far more practical in these cases to understand the chaotic behavior of the well.

### 12.2.2 Calculation techniques for wells that should be analyzed as intermittent gas lift wells

When liquid production is carried out in an intermittent fashion, in which liquid slugs periodically reach the surface, equations and calculation techniques developed for intermittent gas lift design can be applied to determine the point of injection depth and the efficiency of the gas lift method. Gas injection can take place through a gas lift valve (either in good condition or damaged), through an orifice valve, or through a tubing-annulus communication (a hole in the tubing or gas flow through the packer).

In any case, the troubleshooting calculation procedure must begin with the verification of the volume of gas that enters the production tubing per cycle, which is called here  $v_{gsC}$ . This is done for two reasons: (1) to determine if there is an error in the measurement of the surface gas flow rate or in the injection opening and closing pressures measured at the surface, as explained next in the section, and (2) to verify that there is only one point of injection.

As specified in the previous section and in chapter: Design of Intermittent Gas Lift Installations, the volume of gas that enters the production tubing per cycle (in choke-control intermittent gas lift) is equal to the gas volume provided by the annulus,  $v_{ga}$ , plus the volume of gas provided by the surface gas injection line from the choke to the wellhead,  $v_{gi}$ , plus the volume of gas that is injected through the surface choke while the subsurface pilot valve is opened,  $v_{ge}$ .

In choke-control intermittent lift, the volume of gas injected per cycle in scf/cycle,  $v_{gsC}$ , can be calculated dividing the constant surface gas flow rate by the number of cycles in one day:

$$v_{gsC} = \frac{Q_{gi} [\text{Mscf/D}]}{1440 [\text{min/day}]} \left[ \frac{1000 \text{ scf}}{\text{Mscf}} \right] = \frac{Q_{gi} T_{\text{cycle}}}{1.44} \left[ \frac{\text{scf}}{\text{cycle}} \right] \quad (12.17)$$

Where  $T_{\text{cycle}}$  is the total cycle time measured in minutes and  $Q_{gi}$  is the gas flow rate measured at the surface in Mscf/D.

On the other hand (also for choke-control intermittent lift), as explained in the previous section, the volume of gas injected per cycle at the surface while the pilot valve is opened,  $v_{ge}$ , is equal to:

$$v_{ge} = \frac{Q_{gi} [\text{Mscf/D}]}{1440 [\text{min/day}]} \left[ \frac{1000 \text{ scf}}{\text{Mscf}} \right] T_{val} [\text{min/cycle}] = \frac{Q_{gi} T_{val}}{1.44} \left[ \frac{\text{scf}}{\text{cycle}} \right] \quad (12.18)$$

Where  $T_{val}$  is the time in minutes in which the subsurface pilot valve remains open. Because the volume of gas injected per cycle is defined as  $v_{gsC} = v_{ga} + v_{ge} + v_{gl}$ , the following equation (Eq. 12.19) can be found (introducing Eqs. 12.17 and 12.18 in this definition of  $v_{gsC}$ ), and then used to verify the measured value of  $Q_{gi}$  (if the measurements of the surface injection opening and closing pressures are thought to be reliable):

$$Q_{gi} = \frac{1.44(v_{ga} + v_{gl})}{T_{cycle} - T_{val}} \quad (12.19)$$

In Eq. 12.19, volumes  $v_{ga}$  and  $v_{gl}$  can be calculated based on the surface injection opening and closing pressures as explained in the previous section (Eqs. 12.1–12.14). If the surface gas flow rate  $Q_{gi}$  calculated using Eq. 12.19 does not coincide with the gas flow rate  $Q_{gi}$  measured at the surface, it is possible that there is an error either in the surface measured gas flow rate or the wellhead opening and closing pressures measurements, or there is more than just one point of injection.

### Problem 12.1

With the operational data given in the next paragraph, determine: (1) Does the value of  $v_{gsC}$  (calculated from the pressure reduction in the annulus and flowline) coincide with its value calculated from the gas flow rate measured at the surface?; (2) If the measured  $Q_{gi}$  is thought to be inaccurately measured but not the surface injection opening and closing pressures, find the values of  $Q_{gi}$ ,  $v_{ge}$ , and  $v_{gsC}$  in that order; and (3) If the measurements of the surface injection opening and closing pressures are thought to be inaccurately measured but not the surface injection gas flow rate  $Q_{gi}$ , calculate:  $v_{ge}$ ,  $(v_{ga} + v_{gl})$  and  $v_{gsC}$ .

Data: surface injection opening pressure,  $P_{cso} = 1200$  psig; surface injection closing pressure,  $P_{csc} = 1000$  psig; measured surface gas flow rate,  $Q_{gi} = 100$  Mscf/D; operating valve's depth,  $D_{ov} = 2$  Mft.; time in which the pilot valve remains open,  $T_{val} = 2$  min; surface gas injection line length,  $L = 2$  Mft.; injection line ID: 2.067 in.; casing ID: 6.366 in.; production tubing OD: 2.875 in.; total cycle time: 50 min.

### Solution

Following the steps given in Problem 12.3 presented later (not shown in this example), each component of the volume of gas injected per cycle is calculated from the pressure reduction in the annulus and surface gas injection line (except for  $v_{ge}$  which is relatively small and is calculated from  $Q_{gi}$ ), giving the following results:

$v_{ga} = 6359.188$  scf,  $v_{ge} = 138.889$  scf, and  $v_{gl} = 791.3141$  scf. Thus, the sum of these components gives  $v_{gsc} = 7289.39$  scf/cycle.

1. The volume of gas injected per cycle calculated from the measured surface gas flow rate and the number of cycles in 1 day is equal to:

$$v_{gsc} = \frac{Q_{gi} [\text{MscfD}]}{1440 [\text{min/day}]} \left[ \frac{1000 \text{ scf}}{\text{Mscf}} \right] = \frac{100(50)}{1.44} = 3472.22 \text{ scf/cycle}$$

This result does not coincide with the value of  $v_{gsc}$  calculated earlier (equal to 7289.39 scf) based on the measured surface injection opening and closing pressures of the valve and the value of  $v_{ge}$ .

2. If the measured value of  $Q_{gi}$  is the one supposed to be inaccurate but not the measured surface opening and closing pressures, then:  $v_{ga}$  and  $v_{gl}$  can be calculated from the injection opening and closing pressures but  $v_{ge}$  cannot be calculated because it depends on the value of  $Q_{gi}$ . Therefore,  $Q_{gi}$  is calculated first from  $v_{ga}$  and  $v_{gl}$ , and then  $v_{ge}$  and  $v_{gsc}$  can be calculated. The surface gas flow rate is given by Eq. 12.19 as:

$$Q_{gi} = \frac{1.44(v_{ga} + v_{gl})}{T_{\text{cycle}} - T_{\text{val}}} = \frac{1.44(6359.188 + 791.3141)}{50 - 2} = 214.515 \text{ MscfD}$$

So that  $v_{ge}$  will be:

$$v_{ge} = \frac{Q_{gi} [\text{MscfD}]}{1440 [\text{min/day}]} \left[ \frac{1000 \text{ scf}}{\text{Mscf}} \right] = \frac{Q_{gi} T_{\text{val}}}{1.44} = \frac{214.515(2)}{1.44} = 297.9375 \text{ scf}$$

$v_{gsc}$  is then equal to  $v_{ga} + v_{gl} + v_{ge} = 6359.188 + 791.3141 + 297.9375 = 7448.43$  scf/cycle

3. If the surface gas flow rate  $Q_{gi}$  is accurately measured but not the surface injection opening and closing pressures,  $v_{ge}$  is calculated first and

then the sum of  $v_{ga}$  and  $v_{gl}$  is calculated ( $v_{ga}$  and  $v_{gl}$  cannot be calculated separately):

$$v_{ge} = \frac{Q_{gi} [\text{MscfD}]}{T_{val} [\text{min}]} \left[ \frac{1000 \text{ scf}}{\text{Mscf}} \right] = \frac{Q_{gi} T_{val}}{1.44} = \frac{100(2)}{1.44} = 138.89 \text{ scf}$$

The term  $(v_{ga} + v_{gl})$  is calculated from  $Q_{gi} = \frac{1.44(v_{ga} + v_{gl})}{T_{cycle} - T_{val}}$  because all the other terms are known:

$$(v_{ga} + v_{gl}) = \frac{(50 - 2)100}{1.44} = 3333.33 \text{ scf/cycle}$$

Then  $v_{gsc}$  is equal to  $3333.33 + 138.89 = 3472.22 \text{ scf/cycle}$ . ■

In choke-control intermittent lift, one of the activities that must be frequently carried out (once the troubleshooting analysis is completed) is to adjust the cycle time by changing the surface injection gas flow rate. This can only be achieved in a precise way by a tedious, iterative process (explained later, right after Problem 12.2) that can be approximated with the practical calculation procedure that is explained in the next paragraphs and illustrated in Problem 12.2.

If the adjustment of the current surface injection gas flow rate ( $Q_{gi}$ ) is not too large, calculations can be made assuming that  $v_{ga}$  and  $v_{gl}$  are constant. This is a reasonable approximation because changing the cycle time by only a few minutes is not going to cause major changes in the surface injection opening and closing pressures of the gas lift valve. However,  $v_{ge}$  could change significantly because it depends on the value of  $Q_{gi}$ . The time the pilot valve remains open ( $T_{val}$ ) also changes, but an approximate value of  $T_{val}$  can be calculated if it is assumed that the instantaneous gas flow rate through the gas lift valve,  $Q_{gi \text{ inst}}$ , is not going to change very much when the surface gas flow rate  $Q_{gi}$  is changed (this is because the instantaneous gas flow rate through the gas lift valve depends on the injection pressure which, as previously mentioned, is not going to change very much either).

During the time the pilot valve is opened ( $T_{val}$ ), the total volume  $v_{gsc}$  must be injected into the production tubing. In other words, the instantaneous gas flow rate through the pilot valve  $Q_{gi \text{ inst}}$  is equal to  $1.44(v_{ga} + v_{gl} + v_{ge})/T_{val}$  (if  $Q_{gi \text{ inst}}$  is expressed in Mscf/D) and, giving the fact that  $v_{ge} = Q_{gi} T_{val}/1.44$ , the following expression can be found:

$$Q_{gi \text{ inst}} = \frac{(v_{ga} + v_{gl})1.44}{T_{val}} + Q_{gi} \quad (12.20)$$

Combining Eqs. 12.19 and 12.20, the following expression is obtained:

$$Q_{gi} = \frac{1.44(v_{ga} + v_{gl})}{T_{cycle} - \frac{1.44(v_{ga} + v_{gl})}{Q_{gi\ inst} - Q_{gi}}} \quad (12.21)$$

If  $v_{ga}$ ,  $v_{gl}$ , and  $Q_{gi\ inst}$  are considered of constant values, Eq. 12.21 can be used to determine the required surface gas flow rate  $Q_{gi}$  to achieve a cycle time  $T_{cycle}$  which was determined in the troubleshooting analysis to be the optimum cycle time ( $T_{cycle}$  can also be any other total cycle time at which the gas lift operator chooses to produce the well).

### Problem 12.2

The total cycle time is 30 min and the pilot valve stays open for 5 min. According to the injection opening and closing pressure, the following volumes of gas injected per cycle were calculated:  $v_{ga} = 3000$  scf/cycle and  $v_{gl} = 500$  scf/cycle. Calculate: (1) The surface gas flow rate,  $Q_{gi}$ ; (2) The instantaneous gas flow rate through the subsurface gas lift valve; and (3) If the gas flow rate is increased to 300 Mscf/D, calculate the new cycle time in two ways: (1) assuming that the time in which the pilot valve stays open ( $T_{val}$ ) does not change, and (2) incorporating the approximate change in  $T_{val}$ .

### Solution

- The surface gas flow rate is given by:

$$Q_{gi} = \frac{1.44(v_{ga} + v_{gl})}{T_{cycle} - T_{val}} = \frac{(3000 + 500)1.44}{30 - 5} = 201.6 \text{ Mscf/D}$$

- The instantaneous gas flow rate through the subsurface gas lift valve is:

$$Q_{gi\ inst} = \frac{(v_{ga} + v_{gl})1.44}{T_{val}} + Q_{gi} = \frac{3500(1.44)}{5} + 201.6 = 1209.6 \text{ Mscf/D}$$

- Assuming that the time interval  $T_{val}$  does not change, the new total cycle time can be calculated from this equation:  $Q_{gi} = \frac{1.44(v_{ga} + v_{gl})}{T_{cycle} - T_{val}}$ , from which:

$$T_{cycle} = T_{val} + \frac{1.44(v_{ga} + v_{gl})}{Q_{gi}} = 5 + \frac{1.44(3500)}{300} = 21.8 \text{ min}$$

- If the time interval  $T_{val}$  does change with the new value of  $Q_{gi}$ , the new

cycle time is calculated from Eq. 12.21:  $Q_{gi} = \frac{1.44(v_{ga} + v_{gl})}{T_{cycle} - \frac{1.44(v_{ga} + v_{gl})}{Q_{giinst} - Q_{gi}}}$ .

From which:

$$\begin{aligned} T_{cycle} &= 1.44(v_{ga} + v_{gl}) \left[ \frac{1}{Q_{gi}} + \frac{1}{Q_{giinst} - Q_{gi}} \right] \\ &= 1.44(3500) \left[ \frac{1}{300} + \frac{1}{1209.6 - 300} \right] = 22.34 \text{ min} \end{aligned}$$

This cycle time is longer than the one calculated assuming that the time in which the pilot valve stays open ( $T_{val}$ ) does not change and it is a more realistic value because it takes into consideration the fact that the subsurface valve is going to remain open for a longer period of time if the surface gas flow rate is increased. In reality,  $v_{ga}$  and  $v_{gl}$  also change. The injection opening pressure is going to be higher because the initial liquid column (that helps opening the valve too) is going to be smaller due to the fact that the time of regeneration of the liquid column is reduced (from the initial 30 min). This makes the actual cycle time be still slightly longer than 22.34 min. ■

When (as a result of a troubleshooting analysis) the surface gas injection should be adjusted to change the current cycle time so that the optimum cycle time can be reached (for choke-control intermittent lift), a more accurate procedure of calculating the new required surface injection gas flow rate consists in performing the calculation steps given next (for different surface injection gas flow rates, until the calculated cycle time coincides with the optimum cycle time or with any other total cycle time the operator chooses).

1. Calculate  $v_{ga}$  and  $v_{gl}$  for the conditions the well had during the troubleshooting analysis (using Eqs. 12.1–12.14 with the opening and closing pressures recorded on the two-pen pressure chart). Then calculate  $Q_{gi\ inst}$  with Eq. 12.20 using: (1)  $v_{ga}$  and  $v_{gl}$  just calculated, (2) the measured value of  $Q_{gi}$  for the conditions the well had during the troubleshooting analysis (before changing the gas flow rate), and (3) The value of  $T_{val}$  found from the two-pen pressure chart by looking at the elapsed time between the opening and closing pressures of the gas lift valve. These values of  $v_{ga}$ ,  $v_{gl}$ , and  $Q_{gi\ inst}$  will not change significantly so they are excellent parameters to start the iterations.
2. To begin the iterations, assume a new surface gas flow rate  $Q_{gi}$ : if the current cycle time needs to be reduced, this new gas flow rate has to be greater than the value it had for the conditions during the troubleshooting analysis and vice versa. A good value of  $Q_{gi}$  to start

the iterations can be calculated with Eq. 12.19 using the calculated optimum cycle time as the value of  $T_{\text{cycle}}$  (or any other total cycle time the operator chooses) and the values of  $T_{\text{val}}$ ,  $v_{\text{ga}}$ , and  $v_{\text{gl}}$  found in point 1. Usually, this new value of  $Q_{\text{gi}}$  calculated from Eq. 12.19 would be accurate enough to optimize the well's production or to start a fine-tuning procedure of the surface injection gas flow rate in the field.

3. Calculate the time interval  $T_{\text{val}}$  using Eq. 12.20 with the new value of  $Q_{\text{gi}}$  but with the previous values of  $v_{\text{ga}}$ ,  $v_{\text{gl}}$ , and  $Q_{\text{gi inst}}$ .
4. Calculate the total cycle time  $T_{\text{cycle}}$  (also assuming the previous values of  $v_{\text{ga}}$ ,  $v_{\text{gl}}$ , and  $Q_{\text{gi inst}}$ ) using Eq. 12.21 with the new surface gas flow rate  $Q_{\text{gi}}$ .
5. With the new liquid column generation time equal to  $T_{\text{cycle}} - T_{\text{val}}$  ( $T_{\text{cycle}}$  and  $T_{\text{val}}$  were calculated in points 4 and 3, respectively), calculate the production pressure (using the equations presented in chapter: Design of Intermittent Gas Lift Installations for the liquid slug length as a function of time) at valve's depth and determine the new opening pressure using the pilot valve force–balance equation.
6. Calculate the new values of  $v_{\text{ga}}$  and  $v_{\text{gl}}$  (using Eqs. 12.1–12.14) with the new valve's injection opening pressure found in the previous step and assuming that the injection closing pressure remains constant (unless a dynamic model, such as the one developed by Milano given in chapter: Gas Flow Through Gas Lift Valves, is available for the pilot valve being used so that it can be applied to find the new valve's closing pressure). With the new surface gas flow rate  $Q_{\text{gi}}$ , the value of  $T_{\text{val}}$  calculated in step 3, and these newly calculated values of  $v_{\text{gl}}$  and  $v_{\text{ge}}$ , calculate also the new value of  $Q_{\text{gi inst}}$  using Eq. 12.20.
7. If the value of  $(v_{\text{ga}} + v_{\text{gl}})$  is not approximately equal to its previous value, all calculation from step 3 must be carried out again but with the new values of  $v_{\text{ga}}$ ,  $v_{\text{gl}}$ , and  $Q_{\text{gi inst}}$  (found in step 6), keeping  $Q_{\text{gi}}$  constant throughout these iterations.
8. Once  $(v_{\text{ga}} + v_{\text{gl}})$  converges to a given value, the calculated cycle time  $T_{\text{cycle}}$  (resulting from these iterations) is compared to the desired cycle time. If these two cycle times do not coincide, all calculations from step 3 are repeated with a new surface injection gas flow rate and the recently calculated values of  $v_{\text{ga}}$ ,  $v_{\text{gl}}$ , and  $Q_{\text{gi inst}}$  as their starting values (if the calculated cycle time is shorter than its desired value, a lower surface injection gas flow rate should be selected and vice versa).

As mentioned earlier, these calculation steps are very tedious and do not improve the accuracy of the calculated gas flow rate in a considerable way, especially if they do not take into consideration the fact that the valve's injection closing pressure could also change. This is why it is better to use a more practical procedure like just using Eq. 12.21 to find  $Q_{\text{gi}}$  from the

desired value of  $T_{\text{cycle}}$  assuming that  $v_{\text{ga}}$  and  $v_{\text{gl}}$  do not change. After all, this should only be a guide to be used in a trial and error field procedure to find the actual (not the theoretical) optimum cycle time by changing the gas flow rate to different values and testing the well at each of these flow rates to find the one that will maximize the daily liquid production.

Continuing with the explanation of the calculation techniques available for wells that are truly on intermittent gas lift, once the value of the volume of gas injected per cycle has been verified and it has been determined that the surface injection gas flow rate and wellhead pressures are accurately measured, leaving no doubts that there is only one point of injection, then the following troubleshooting calculations must be performed (depending on the state of the operating gas lift valve: damaged or in good working conditions).

*Analysis for gas lift valves in good working conditions.*

The case in which the operating gas lift valve is in good condition is presented in this section. This valve could correspond to the pilot valve (which is usually the operating valve established as such by design), but it can also be any of the unloading valves. It might also be a valve in a well that was designed for continuous gas lift in which the gas injection flow rate is less than the one required for stable operation. In general, when the operation is unintentionally intermittent, the efficiency of the lifting process is very low. This is due to the fact that single-element gas lift valves are usually encountered in these cases and these valves possess characteristics that are not appropriate for intermittent gas lift:

- The seat diameter is usually very small for intermittent gas lift operation and, in consequence, the instantaneous gas flow rate through these valves is very small. This in turn makes the slug velocity be very slow and the fallback losses are then very large. The gas injection period is usually very long (keeping the bottomhole pressure high for a longer period of time).
- The spread of the valve is usually very small because the area ratio is also very small, thus the total volume of gas injected per cycle might be less than its required value.

These characteristics of single-element valves cause very large liquid fallback losses that are difficult to estimate. It is extremely important to know the fallback losses to properly use the equations given in chapter: Design of Intermittent Gas Lift Installations to find the productivity index and, from this value, to be able to calculate the optimum cycle time. If it is not possible to estimate the fallback losses, one of the actions that can be carried out (without changing the operating valve or any other operational condition that is causing the problem) is to find the optimum cycle time by changing



the surface gas flow rate at different values, testing the well at each step. Another way of troubleshooting (analytically) a well in which it is not easy to estimate the fallback losses is to try to find the initial liquid column length (so that it can be compared to the liquid column produced at the surface and determine in this way the fallback losses) by using the static-force-balance equation of the subsurface valve at the moment it opens.

If surface time cycle controllers are used and the liquid slug velocity is acceptable (but not the total volume of gas injected per cycle), the surface gas injection time can be increased until the fallback losses can be estimated.

If the operating valve is indeed the pilot valve, engineers tend to limit the troubleshooting analysis to only identifying the operation of the pilot valve without completing the troubleshooting process:

- The optimum cycle time must be calculated and compared to the current cycle time. The well might be producing well below its potential with cycles that are either too short or, especially, too long.
- The required volume of gas injected per cycle should also be calculated and compared to its actual value. Another way of not producing the well to its full potential is by an inadequate gas injection: the total volume of gas injected per cycle should be greater than or equal to its required value (determined from the energy balance equation given in chapter: Design of Intermittent Gas Lift Installations) and its instantaneous flow rate should be able to sustain a liquid slug velocity of approximately 1000 ft./min.

Each valve installed in the well should be analyzed with the purpose of determining if it is the current operating valve or if there are several valves capable of opening under current operational conditions. The first step is to find the reservoir static liquid level, which can be approximately calculated as:

$$D_{sl} = D_{pt} - \frac{P_{sbh} - P_{wh}}{\rho_f} \quad (12.22)$$

Where  $D_{sl}$  is the static liquid level depth in feet,  $D_{pt}$  is the depth of the top of the perforations in feet,  $P_{sbh}$  is the static reservoir pressure at perforations' depth in psig,  $P_{wh}$  is the wellhead pressure also in psig, and  $\rho_f$  is the liquid pressure gradient in psi/ft. calculated by (assuming that the water has a specific gravity equal to unity):

$$\rho_f = (1 - w) \frac{141.5}{131.5 + \text{° API}} (0.433) + w(0.433) \quad (12.23)$$

Where  $w$  is the water cut (expressed from 0 to 1).

If the well has a packer installed, a gas lift valve above the static liquid level could be the operating valve only if a combination of events takes place (it is difficult for it to happen but it is not impossible and should be taken into consideration): There must be a tubing-annulus communication (a hole in the tubing, for example) that would allow liquids to enter the annulus. This liquid must be forced by the injection pressure back into the tubing at each cycle to generate a liquid column above the static liquid level. Additionally, the force-balance equation should predict that a valve above the static liquid level can open at the maximum injection pressure measured at the surface. Thus, even though it is a remote possibility that a gas lift valve above the liquid level becomes the operating valve (with the well producing liquid), almost all calculations that can be performed for valves below the liquid level should also be carried out for valves above it. The productivity index and the optimum cycle time cannot be calculated for valves above the static liquid level using the analytical procedures that are explained in the section.

The next step is to calculate the length of the initial liquid column above each valve installed in the well (temporarily assumed to be the operating valve) just before it opens. There are two ways of calculating the initial column length:

- If the total volume of gas injected per cycle and its instantaneous flow rate into the tubing are adequate, the fallback losses are small and predictable so the following equation can be used to calculate the initial liquid column length  $Q'$ :

$$Q' = \frac{T_{\text{cycle}} (\text{min}) (q_f \text{ Br/D}) / (1440 \text{ min/D})}{B_t (\text{Br/Mft.}) \left[ 1 - F (1/\text{Mft.}) \frac{D_{\text{ov}} (\text{ft.})}{1000 (\text{ft./Mft.})} \right] \left( \frac{\text{Mft.}}{1000 \text{ ft.}} \right)} \quad (12.24)$$

Where  $B_t$  is the volumetric capacity of the production tubing in Br/Mft. that can be calculated from the following equation:

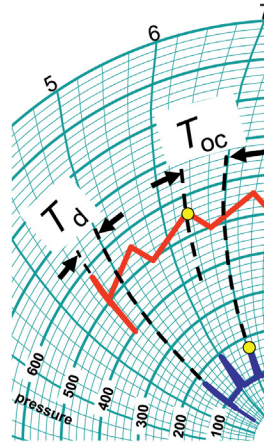
$$B_t = \frac{\pi}{4} (d [\text{in.}])^2 \left[ \frac{1 \text{ ft.}^2}{144 \text{ in.}^2} \right] \left[ \frac{1000 \text{ ft.}}{1 \text{ Mft.}} \right] \left[ \frac{1 \text{ Br}}{5.61456 \text{ ft.}^3} \right] = 0.97143 (d)^2 \left[ \frac{\text{Br}}{\text{Mft.}} \right] \quad (12.25)$$

$Q'$  is expressed in feet,  $T_{\text{cycle}}$  is the cycle time in minutes,  $q_f$  is the liquid production in Br/D,  $d$  is the ID of the production tubing in inches,  $F$  is the fallback factor (expressed from 0 to 1), and  $D_{\text{ov}}$  is the depth of the operating valve in feet. The calculated value of  $Q'$  from Eq. 12.24 is then used to find the production pressure at

valve's depth just when this valve opens, called  $P_{to}$ , which is equal to  $f_g P_{wh} + Q' \rho_f$ .

The fallback factor is usually taken as a constant equal to a value that goes from 0.03 to 0.06 (which represents from 3 to 6% of the initial column length that is lost as fallback for each 1000 ft. of depth of the point of injection). This is a good approximation as long as the API gravity of the oil is equal to or greater than 23°API, the volume of gas that is actually injected per cycle is greater than or equal to the required volume (calculated from the energy balance equation), and the liquid slug velocity is close to 1000 ft./min. The required volume of gas to be injected per cycle should be compared to its measured value in scf, determined as  $1000Q_{gi}/(\text{number of cycles per day})$ , where  $Q_{gi}$  is the surface gas flow rate in Mscf/D and the number of cycles per day is equal to  $1440/T_{\text{cycle}}$ , with  $T_{\text{cycle}}$  being the total cycle time in minutes. The required volume of gas to be injected per cycle is found from the energy balance equation (Eq. 10.32). Calculation of the required volume of gas injected per cycle and its comparison to the actual volume being injected are extremely important troubleshooting calculations because of the impact that this volume has on the fallback losses and, therefore, on the liquid production.

The average liquid slug velocity can be estimated by measuring the elapsed time between the opening of the gas lift valve and the slug arrival at the surface. The average velocity is then approximately equal to the depth of the operating valve divided by the travel time of the liquid slug in the production tubing. Fig. 12.2 can be used to show the way in which the liquid velocity is estimated by looking at the wellhead pressure chart. An apparent time lag,  $T_d$ , between the tubing and the casing pressure is introduced because of the way the pens are installed in the chart recorder, so the liquid slug travel time is equal to  $T_{oc} - T_d$ , with  $T_{oc}$  as defined in the figure. The apparent time lag  $T_d$  should be identified by running each pen up and down when the chart is installed. Sometimes the arrival of the slug is not clear just by looking at the chart, but it can be easily detected at the well site. The slug arrival should be compared to the time the valve closes to determine if the valve remains open for a long period of time after the slug has arrived at the surface, indicating that injection gas might be wasted while, at the same time, making it difficult to regenerate the new liquid slug at the bottom of the well. If this is the case, the pilot valve should be replaced with a different pilot valve with a larger main port diameter (so that the injection pressure can drop very fast), but probably with the same area ratio or a slightly smaller one. Some



■ FIGURE 12.2 Practical way of determining the travel time of the liquid slug in the production tubing.

pilot valve models have main port diameters that are too small for an efficient intermittent gas lift operation and their use should be avoided.

- If the liquid slug velocity is too slow, the volume of gas injected per cycle is less than required, or the liquid is too viscous, then the initial liquid column length should be estimated from the gas lift valve's force-balance equation applied just before the pilot valve opens, or by means of the specially designed downhole pressure surveys that are explained in Section 12.3. The force-balance equation depends on the type of valve. These equations are given in chapter: Gas Lift Valve Mechanics and in Section 11.4.2. For example, the force-balance equation for a spring loaded, injection-pressure-operated, pilot valve with a given test-rack calibration closing pressure  $P_{tr}$ , is:

$$(1-R)P_{cvo} + (R)P_{to} = P_{tr} \quad (12.26)$$

Where  $R$  is the valve's area ratio,  $P_{tr}$  is the test-rack closing pressure,  $P_{cvo}$  is the valve's opening pressure at depth (equal to  $P_{cso}f_g$ , where  $f_g$  is the gas factor explained in chapter: Single-Phase Flow and  $P_{cso}$  is the surface injection opening pressure),  $P_{to}$  is the tubing pressure at valve depth just before the valve opens and it is the only unknown in the equation. Eq. 12.26 is then used to find  $P_{to}$ . This pressure is equal to the wellhead production pressure plus the hydrostatic pressure of the gas column above the liquid and plus the hydrostatic pressure of the liquid column  $Q'$ :

$$P_{to} = P_{wh}f_g + Q'\rho_f \quad (12.27)$$

Where  $P_{10}$  is expressed in psig,  $P_{wh}$  is the wellhead production pressure in psig, and  $\rho_f$  is the liquid column gradient above the gas lift valve in psi/ft. and calculated using Eq. 12.23 from the oil API gravity and the water cut. With the  $P_{10}$  pressure determined from the force–balance equation (Eq. 12.26), Eq. 12.27 is then used to find the length of the initial liquid column  $Q'$  in feet. The problem with this method of calculating  $Q'$  is the fact that the wellhead pressure sensors should be precisely calibrated and the injection gas specific gravity should be accurately measured so that the error in estimating the gas injection pressure at depth ( $P_{cvo}$ ) is minimized. From Eq. 12.26,  $P_{10}$  is equal to  $\frac{P_w}{R} - \frac{(1-R)}{R} P_{cvo}$ . If the surface opening pressure and/or the injection gas specific gravity are not precisely measured, the error made in the calculation of  $P_{cvo}$  is magnified when trying to calculate  $P_{10}$  because  $P_{cvo}$  is multiplied times  $(1 - R)/R$ . If the value of  $R$  is very small,  $(1 - R)/R$  is very large. For example, if  $R = 0.034$ , then  $(1 - R)/R = 28.4$ . Thus, each psi that is wrongly estimated when calculating  $P_{cvo}$  is multiplied by 28.4. This method of getting  $Q'$  is recommended then for large values of  $R$ , as long as the wellhead pressures and the gas specific gravity are accurately measured. If the valve is nitrogen charged, iterations are needed to calculate  $P_{10}$  because the temperature of the valve must be calculated from equations that depend on the value of  $P_{10}$ . This last point is further analyzed later.

Calculation of  $Q'$  by any of the two previously described procedures do not take into account the fact that free gas in the liquid column tends to make the liquid columns longer and their true gradient, called  $\rho_t$ , is in fact less than  $\rho_f$  (which is calculated from the water cut and the oil API gravity only). This is not important when using the force–balance equation or the productivity index equation, as long as the true liquid column does not reach the surface. The true gradient is calculated from the analysis of downhole pressure and temperature surveys (explained in Section 12.3). There are equations that can be used to find the true liquid pressure gradient, but they are not very reliable. The true liquid column length is  $Q'_t = Q'(\rho_f/\rho_t)$ .

Once the liquid column length and the pressure  $P_{10}$  have been determined, different tests should be performed to know if the effective productivity index can be calculated using the intermittent gas lift theory presented in chapter: Design of Intermittent Gas Lift Installations. These tests are:

- If the top of the liquid column  $Q'$  (not the true liquid column  $Q'_t$ ), is below the static liquid level calculated with Eq. 12.22 and the top of the true liquid column  $Q'_t$  is below the wellhead, all calculations in the troubleshooting analysis explained in this section can be performed.

- If the top of the calculated liquid column  $Q'$  is above the static liquid level calculated with Eq. 12.22 but the top of  $Q'_t$  is below the wellhead, then production with this valve is only possible if part of the liquid being produced is previously accumulated in the annulus. In this case, it is not possible to calculate the productivity index but Eq. 12.27 ( $P_{to} = P_{whf_g} + Q' \rho_f$ ) is still valid. Without the productivity index, the optimum cycle time cannot be analytically estimated.
- If the calculated true liquid column  $Q'_t$  is greater than the valve's depth ( $D_{ov}$ ), with  $Q'$  above or below the static liquid level, the productivity index cannot be calculated. Additionally, the production pressure at valve's depth (when the gas lift valve opens) is calculated from  $P_{to} = P_{wh} + D_{ov} \rho_f$  (instead of using Eq. 12.27), where  $D_{ov}$  is the depth of the operating valve (or valve being investigated).

It is possible that the calculated value of the static liquid level might turn out to be negative using Eq. 12.22. This is due to the fact that the reservoir pressure is so high that the static liquid column is greater than the depth of the perforations. The well then can produce on natural flow. If this is the case, all calculations for intermittent gas lift troubleshooting can be carried out at each valve, unless the calculated true liquid column length is greater than the depth of the valve under investigation, in which case the production pressure at valve's depth (when it opens) is found from  $P_{to} = P_{wh} + D_{ov} \rho_f$ , (where  $D_{ov}$  is the depth of the valve under investigation) and, additionally, the productivity index cannot be calculated.

Even if the valve mechanic equation was not necessary to find the values of  $P_{to}$  and  $Q'$ , this equation still needs to be used but for a different purpose: to find the valve opening pressure so that it can be compared to the measured injection opening pressure in the pressure chart. The steps to establish this comparison are described next.

Once  $P_{to}$  has been calculated, the gas lift valve's opening pressure is found from the valve's force–balance equation depending on the type of valve installed in the well. If the valve is nitrogen charged, it is necessary to estimate its operating temperature. The dynamic temperature of the valve is very difficult to calculate. For wireline retrievable valves, the valve's dynamic temperature can be calculated assuming continuous flow with the current daily liquid production. Several examples of how to calculate the valve temperature are given in chapter: Design of Continuous Gas Lift Installations. The valve's opening pressure is calculated using the equations given next. This calculated pressure is then compared to the measured pressure to determine if the valve being investigated corresponds to the current point of injection. For a spring-loaded, injection-pressure-operated valve with a test-rack closing pressure  $P_{tr}$  and an area ratio  $R$ , the surface opening pressure can be

calculated in the following way (using the force–balance equation given in chapter: Gas Lift Valve Mechanics for this type of valve):

$$P_{cso} = \left( \frac{P_{tr} - P_{to}R}{1 - R} \right) / f_g \quad (12.28)$$

Where  $P_{cso}$  is the valve's surface opening pressure and  $f_g$  is the gas factor that is used to calculate the pressure at depth from the pressure at the surface. For a spring-loaded, injection-pressure-operated valve with a test-rack opening pressure  $P_{tr}$  and an area ratio  $R$ , the force–balance equation gives the following expression for the valve's surface opening pressure  $P_{cso}$ :

$$P_{cso} = \left[ \frac{P_{tr}(1 - R) - P_{to}R}{1 - R} \right] / f_g \quad (12.29)$$

For a nitrogen-charged, injection-pressure-operated valve with a test-rack opening pressure  $P_{tr}$ , an area ratio  $R$ , and a spring as an additional closing element set at an equivalent pressure  $P'_r$ , the injection surface opening pressure is given by:

$$P_{cso} = \left[ \frac{P_{bt} + P'_r(1 - R) - P_{to}R}{1 - R} \right] / f_g \quad (12.30)$$

The term  $P'_r$  is explained in chapter: Gas Lift Valve Mechanics and it is usually a fixed value given by the valve's manufacturer.  $P_{bt}$  is the bellows pressure at operating conditions. If the operating temperature of the valve is known,  $P_{bt}$  can be calculated from  $P'_b$  with Eq. 11.4.  $P'_b$  is the bellows pressure at test-rack conditions and it can be calculated from the following equation:

$$P'_b = (P_{tr} - P'_r)(1 - R) \quad (12.31)$$

Based on the theory presented in chapter: Design of Intermittent Gas Lift Installations, the average productivity index  $J$ , in Br/(D – psi), for the practical range of flowing bottomhole pressures for intermittent gas lift, can be calculated from:

$$J = \frac{1.44(0.9713d^2)A_{jff}}{t\rho_f} \quad (12.32)$$

Where  $t$  is the liquid column generation time in minutes,  $\rho_f$  is the liquid pressure gradient in psi/ft.,  $d$  is the ID of the production tubing in inches, and  $A_{jff}$  is given by:

$$A_{jff} = \ln \left[ \frac{A' - F(D_{ov}/1000)Q'\rho_f}{A' - Q'\rho_f} \right] \quad (12.33)$$

Where  $D_{ov}$  is the depth of the operating valve in feet,  $F$  is the fallback factor in 1/Mft.,  $Q'$  is the initial column length in feet, and  $A'$  is the maximum drawdown at the beginning of the liquid column generation period given by:

$$A' = P_{sbh} - [(D_{pt} - D_{ov})\rho_l + P_{wh}f_g] \quad (12.34)$$

Where  $P_{sbh}$  is the static reservoir pressure in psi,  $D_{pt}$  is the depth of the top of the perforations in feet,  $\rho_l$  is the true liquid pressure gradient in psi/ft. (which takes into account the free gas present in the liquid and, as previously mentioned, can be determined from a downhole pressure survey),  $P_{wh}$  is the minimum wellhead production pressure, and  $f_g$  is the gas factor that is used to get the pressure at depth from the pressure at the surface. With  $J$  already calculated, the optimum cycle time can be found from the calculation procedure explained for intermittent gas lift design using Eq. 10.22. If it is necessary, the cycle time can be adjusted by changing the constant surface gas flow rate if the well is on choke control using Eq. 12.21 as a guide. If surface controllers are used, the cycle time can be changed by modifying the time in which the controller remains closed ( $T_{off}$ ) without affecting the volume of gas injected per cycle, unless the volume of gas injected per cycle is less than its required value, in which case the time the surface controller remains open ( $T_{on}$ ) can be independently adjusted. For choke-control intermittent gas lift, on the other hand, the volume of gas injected per cycle can only be significantly modified by changing the gas lift valve with another one with a larger or a smaller area ratio, if the volume of gas injected per cycle must be, respectively, increased or decrease.

### Problem 12.3

Determine the possible reasons why a well on choke-control intermittent gas lift, with the following characteristics and operational conditions, is not producing any liquids:

Pilot valve: spring-loaded, injection-pressure-operated valve with an area ratio of 0.326, main port diameter of 48/64 in., and test-rack closing pressure  $P_{tr}$  of 720 psig. The surface injection opening pressure  $P_{cso}$  is 700 psig and the surface closing pressure  $P_{csc}$  is 651.375 psig. The injection opening pressure at valve's depth  $P_{cvo}$  is then 774.372 psig and the closing pressure at valve's depth  $P_{cvc}$  is 720 psig (these values are obtained using the appropriate gas factor  $f_g$ ). The average gas compressibility factor  $Z_{ga,apert.}$  in the annulus at the valve's opening pressure is 0.8769 and the average gas compressibility factor  $Z_{ga,close.}$  in the annulus at the valve's closing pressure is 0.884.



Gas and liquid properties:

Lift gas specific gravity  $G_g$ : 0.7; water cut: 10%; oil API gravity: 23°API; formation gas/liquid ratio: 300 scf/STBL.

Production tubing inside diameter: 2.441 in.; production tubing outside diameter: 2.875 in.; casing inside diameter: 4.892 in.; inside diameter of the surface gas injection line: 2.067 in.; length  $L$  of the surface gas injection line: 500 ft.; operating valve's depth: 3940 ft.; time in which the pilot valve stays open ( $T_{val}$ ): 6 min; total cycle time: 19.25 min; surface injection gas flow rate ( $Q_{gi}$ ): 150 Mscf/D; minimum wellhead production pressure  $P_{wh}$ : 60 psig. The production tubing pressure at pilot valve's depth when it opens was stipulated in the design to be equal to 306.503 psig.

Estimate if the well can produce liquids by temporarily increasing the injection gas flow rate and then setting it back to its design value of 150 Mscf/D.

### Solution

#### 1. Verification of the surface gas flow rate and wellhead pressure measurements

The volume of gas injected per cycle (calculated from the measured surface gas flow rate and the number of cycles in one day) is:

$$V_{gsC} = \frac{Q_{gi} T_{cycle}}{1.44} = \frac{150(19.25)}{1.44} = 2005.2 \text{ scf/cycle}$$

The volume of gas injected per cycle is now calculated from the opening and closing pressures using the equations presented in Section 12.2.1 (Eqs 12.1–12.14). The annular volumetric capacity,  $B_a$  in  $\text{ft.}^3/\text{Mft.}$ , can be calculated as:

$$\begin{aligned} B_a &= 5.45415(D_{IDcasing}^2 - D_{ODtubing}^2) = 5.45415(4.892^2 - 2.875^2) \\ &= 85.44492 \text{ ft.}^3/\text{Mft.} \end{aligned}$$

The volumetric capacity of the surface gas injection line  $B_l$  in  $\text{ft.}^3/\text{Mft.}$ , is:

$$B_l = 5.45415 D_{IDgasline}^2 = 5.45415(2.067^2) = 23.3028 \text{ ft.}^3/\text{Mft.}$$

The gas compressibility factor in the surface gas injection line can be approximated using the following equation:

$$z_{gl} = 1 - 0.00019385(P_{cso} + 14.7) = 1 - 0.00019385(700 + 14.7) = 0.861455$$

The injection gas temperature at valve's depth,  $T_v$  in °F, can be approximated as the geothermal temperature, which is calculated as a

function of the depth of the valve  $D_{ov}$  in Mft. from the following equation:

$$T_v = 15.6D_{ov} + 88.8 = 15.6(3.94) + 88.8 = 150.264^\circ\text{F}$$

The volume of gas supplied by the gas injection line per cycle,  $v_{gl}$  in scf, can be calculated from the surface injection opening pressure  $P_{cso}$ , the surface injection closing pressure  $P_{csc}$ , the volumetric capacity of the gas line  $B_l$ , the length of the injection gas line  $L$  in Mft., and the gas compressibility factor  $z_{gl}$  by:

$$\begin{aligned} v_{gl} &= \frac{35.374B_lL(P_{cso} - P_{csc})}{545z_{gl}} \\ &= \frac{35.374(23.3028)0.5(700 - 651.375)}{545(0.861455)} = 42.686 \text{ scf/cycle} \end{aligned}$$

The volume of gas per cycle that enters the annulus through the surface choke while the pilot valve is open,  $v_{ge}$  in scf, is found from:

$$v_{ge} = \frac{Q_{gi}T_{val}}{1.44} = \frac{150(6)}{1.44} = 625 \text{ scf/cycle}$$

The volume of gas supplied by the annulus per cycle is:

$$\begin{aligned} v_{ga} &= \frac{35.374B_aD_{ov}}{1005 + T_v} \left[ \frac{P_{cso} + P_{cvo}}{z_{ga,apert.}} - \frac{P_{csc} + P_{cvc}}{z_{ga,close.}} \right] \\ &= \frac{35.374(85.44492)3.94}{1005 + 150.264} \left[ \frac{700 + 774.372}{0.8769} - \frac{651.375 + 720}{0.884} \right] = 1340.24 \text{ scf/cycle} \end{aligned}$$

The volume of gas injected per cycle is equal to  $v_{ga} + v_{gl} + v_{ge} = 1,340.24 + 42.686 + 625 = 2,007.92$  scf/cycle. This volume is very close to the one calculated earlier from the surface gas flow rate and the number of cycles in one day; therefore, the surface measurements of the gas flow rate and the wellhead pressures must be reasonably accurate and there is only one injection point.

2. Calculation of the production pressure at the pilot valve's depth just before this valve opens

Using the force-balance equation of the valve with its calibration pressure of 720 psig and area ratio equal to 0.326, the production pressure at valve's depth is found from:

$$P_{to} = \frac{P_{tr}}{R} - \frac{1-R}{R} P_{cvo} = \frac{720}{0.326} - \left( \frac{1-0.326}{0.326} \right) 774.372 = 607.59 \text{ psig}$$

3. Calculation of the initial liquid column length  $Q_{ini}$

Because the calculation of the gas pressure on top of the liquid column depends on the length of the liquid column length (which is

precisely the unknown that needs to be calculated), iterations are required to find both, the liquid column length and the gas pressure on top of the liquid column. The need for iteration is due to the fact that the gas factor  $f_g$  depends on the length of the gas column. The pressure at the bottom of a gas column is found by multiplying the surface pressure by this gas factor. The equation that can be used to find the liquid column length is:

$$Q_{ini} = \frac{P_{to} - P_{wh} f_g}{\rho_f}$$

Where  $\rho_f$  is the pressure gradient of the liquids in the liquid column and  $f_g$  is the gas factor previously mentioned. The liquid pressure gradient is calculated as:

$$\begin{aligned} \rho_f &= 0.433 \left[ w - (1-w) \frac{141.5}{\text{API} + 131.5} \right] \\ &= 0.433 \left[ 0.1 - (0.9) \frac{141.5}{23 + 131.5} \right] = 0.4002 \text{ psi/ft.} \end{aligned}$$

Where  $w$  is the water cut from 0 to 1. The gas factor, on the other hand, is found from the following equation:

$$f_g = \left( 1 + \frac{L'}{54} \right)^{1.524}$$

Where  $L'$  is in this case the depth in Mft. at which it is desired to calculate the gas pressure. For the first iteration,  $L'$  is assumed to be equal to the depth of the valve:

$$Q_{ini1} = \frac{607.59 - 60 \left( 1 + \frac{3.94}{54} \right)^{1.524}}{0.4002} = 1351.98 \text{ ft.}$$

For the second iteration, the length of the liquid column just calculated (1.35198 Mft.) is subtracted from the depth of the valve (3.94 Mft.) when calculating  $f_g$ :

$$Q_{ini2} = \frac{607.59 - 60 \left( 1 + \frac{3.94 - 1.35198}{54} \right)^{1.524}}{0.4002} = 1357.203 \text{ ft.}$$

For the third iteration:

$$Q_{ini3} = \frac{607.59 - 60 \left( 1 + \frac{3.94 - 1.357203}{54} \right)^{1.524}}{0.4002} = 1357.22 \text{ ft.}$$

The value of  $Q_{ini}$  for the third iteration is very close to its value from the second iteration, thus calculations of  $Q_{ini}$  can be stopped at this point. This is a very long liquid column that the current volume of gas injected per cycle might not be able to produce to the surface.

**4. Calculation of the required volume of gas injected per cycle**

The required volume of gas injected per cycle to lift a 1357.22 ft long liquid column from a depth of 3940 ft. to the surface is calculated from the energy balance equation presented in chapter: Design of Intermittent Gas Lift Installations. This calculation, not shown here, gives a required volume  $V_{gsR} = 7991$  scf/cycle. This indicates that the current volume of gas injected per cycle is four times smaller than its required value and that is probably the reason why the liquid column is not reaching the surface. The well needs to be fully unloaded by temporarily increasing the surface injection gas flow rate. It might be possible that, once the well is unloaded, the current surface gas flow rate might be acceptable to produce the well, unless the calculations (shown later) indicate that the current pilot valve installed in the well will not be able to deliver the required volume of gas per cycle and at a sufficiently high instantaneous gas flow rate into the production tubing. In this latter case, the current pilot valve would have to be replaced by a pilot valve with either a higher calibration pressure or a larger main port area, or both, to increase the instantaneous gas flow rate into the tubing. If the problem is only that the valve cannot supply the required volume of gas to be injected per cycle (but the instantaneous gas flow rate is acceptable), a new valve should be used with a larger area ratio (if the area ratio is already the largest one available, surface intermetters should then be used to force the valve open for a longer period of time).

**5. Possibility of getting the well back in production**

It is now investigated if the pilot valve currently installed in the well could sustain the liquid production stipulated in the design, for which the production pressure when the valve opens should be equal to 306.503 psig (given earlier as an available data to solve the problem). It is necessary to calculate the length of the liquid column and then calculate the volume of gas per cycle needed to produce it. Then, the spread of the valve should be calculated to establish if: (1) the gas injected per cycle is greater than or equal to the required volume, and (2) the gas flow rate through the gas lift valve is going to be large enough to keep the liquid slug velocity greater than or equal to 1000 ft./min.

The iteration to find the initial liquid column length ( $Q_{ini}$ ) with a production pressure of 306.503 psig at the time the pilot valve opens is presented next (following the procedure described in step 3). To find

the gas factor  $f_g$  for the first iteration, it is assumed that the length of the gas column above the liquids is equal to the depth of the valve:

$$Q_{ini1} = \frac{306.503 - 60 \left( 1 + \frac{3.94}{54} \right)^{1.524}}{0.4002} = 598.96 \text{ ft.}$$

$$Q_{ini2} = \frac{306.503 - 60 \left( 1 + \frac{3.94 - 0.59896}{54} \right)^{1.524}}{0.4002} = 601.585 \text{ ft.}$$

$$Q_{ini3} = \frac{306.503 - 60 \left( 1 + \frac{3.94 - 0.601585}{54} \right)^{1.524}}{0.4002} = 601.597 \text{ ft.}$$

The third iteration shows a result very similar to the second. The initial liquid column length is then taken to be equal to 601.597 ft. It could be possible then that the pilot valve currently installed in the well might be able to handle this shorter liquid column. With the equation given in chapter: Design of Intermittent Gas Lift Installations, the required volume of gas injected per cycle to lift this initial liquid column from a depth of 3,940 ft. is found to be  $v_{gsR} = 4878.413$  scf/cycle. This calculation (not shown here) also gives the average conditions of the gas that has entered the production tubing when the liquid column is just beginning to be produced at the surface: Average gas pressure in the tubing  $P_{ga} = 648.4576$  psia; Average gas temperature in the tubing  $T_a = 572.63^\circ\text{R}$ ; Average gas compressibility  $z_a = 0.89$ ; Pressure inside the production tubing downstream of the pilot valve (at valve's depth when the valve is about to close)  $P_{tm} = 663.7$  psig. These results are used later to verify that the liquid slug velocity is at least equal to 1000 ft./min.

With the expected production pressure of 306.503 psig, the force-balance equation is used to calculate the injection opening pressure at valve's depth  $P_{cvo}$ . From the force-balance equation applied at the moment just before the valve opens, the following expression is found (the area ratio of the valve is 0.326 and the test-rack closing pressure  $P_{tr}$  is 720 psig):

$$(1 - 0.326)P_{cvo} + 0.326(306.503) = 720$$

The opening pressure  $P_{cvo}$  is then equal to 920 psig at valve's depth. This opening pressure referred to the surface is equal to 830 psig. The volume of gas injected per cycle based on the valve's opening and closing pressures is calculated next.

The gas compressibility factor at the surface gas injection line can be calculated as follows:

$$z_{gl} = 1 - 0.00019385(P_{cso} + 14.7) = 1 - 0.00019385(830 + 14.7) = 0.836$$

The gas temperature at valve's depth,  $T_v$  in °F, can be calculated as a function of the depth of the valve,  $D_{ov}$  in Mft., using the following equation:

$$T_v = 15.6D_{ov} + 88.8 = 15.6(3.94) + 88.8 = 150.264^\circ\text{F}$$

The volume of gas injected per cycle provided by the surface gas injection line,  $v_{gl}$  in scf, is calculated from the injection opening pressure  $P_{cso}$ , the injection closing pressure  $P_{csc}$ , the volumetric capacity of the injection line  $B_l$ , the length of the injection line  $L$  in Mft., and the gas compressibility factor  $z_{gl}$ :

$$\begin{aligned} v_{gl} &= \frac{35.374B_lL(P_{cso} - P_{csc})}{545z_{gl}} = \frac{35.374(23.3028)0.5(830 - 651.375)}{545(0.836)} \\ &= 163.37 \text{ scf/cycle} \end{aligned}$$

The volume of gas injected into the surface gas line while the pilot valve is open,  $v_{ge}$  in scf, is:

$$v_{ge} = \frac{Q_{gl}T_{val}}{1.44} = \frac{150(6)}{1.44} = 625 \text{ scf/cycle}$$

This calculated value of  $v_{ge}$  is only an approximation because the time in which the pilot valve will remain open is not known. But this approximation is acceptable because  $v_{ge}$  is usually less than 20% of the total volume of gas injected per cycle. The gas supplied by the annulus,  $v_{ga}$ , is calculated knowing that the gas compressibility factor at the new opening pressure is  $z_{ga,apert.} = 0.859$ :

$$\begin{aligned} v_{ga} &= \frac{35.374B_aD_{ov}}{1005 + T_v} \left[ \frac{P_{cso} + P_{cvo}}{z_{ga,apert.}} - \frac{P_{csc} + P_{cvc}}{z_{gc,close.}} \right] = \\ &= \frac{35.374(85.44492)3.94}{1005 + 150.264} \left[ \frac{830 + 920}{0.859} - \frac{651.375 + 720}{0.884} \right] = 5009 \text{ scf/cycle} \end{aligned}$$

The total volume of gas injected per cycle is then equal to  $v_{ga} + v_{gl} + v_{ge} = 5009 + 163.37 + 625 = 5797.37$  scf/cycle, which is greater than the required volume equal to 4878.413 scf/cycle.

However, it is still necessary to verify if the liquid slug velocity ( $v_{sl}$ ) is going to be high enough to keep the fallback losses at a minimum

value. This can be verified using Eq. 10.67 for the design of gas lift wells, see Problem 10.1. To use this equation, it is necessary to know the average conditions of the gas that has entered the tubing when the slug begins to be produced at the surface, which were given earlier and were found when calculating the required volume of gas injected per cycle (not shown here):  $P_{ga} = 648.4576$  psia;  $P_{tm} = 663.7$  psig;  $T_a = 572.63^\circ\text{R}$ ; and  $z_a = 0.89$ . The pressure upstream of the valve just before it closes is  $P_{cvc} + 14.7 = 720 + 14.7 = 734.7$  psia and the production pressure downstream of the valve is  $P_{tm} + 14.7 = 663.7 + 14.7 = 678.4$  psia; thus, the value of the pressure ratio to use in the slug velocity equation is  $r = 678.4/734.7 = 0.9233$  and therefore  $f_{rg}$  (as defined in Eq. 10.67) is calculated as:

$$f_{rg} = \sqrt{r^{1.561} - r^{1.781}} = \sqrt{0.9233^{1.561} - 0.9233^{1.781}} = 0.12395$$

Finally, the liquid slug velocity  $v_{sl}$  is calculated using Eq. 10.67 (with the tubing diameter  $d$  and the pilot valve's main port diameter  $d_o$ ):

$$\begin{aligned} v_{sl} &= \frac{0.00079276(T_a)(z_a)(d_o^2)(P_{cvc} + 14.7)(f_{rg})}{d^2 P_{ga} \sqrt{T_v G_g}} = \\ &= \frac{0.00079276(572.63)(0.89)(48^2)(734.7)(0.12395)}{2.441^2 648.4576 \sqrt{(15.6(3.94) + 548.8)0.7}} = 1.06 \text{ Mft./min} \end{aligned}$$

As can be seen, not only the volume of gas injected per cycle is acceptable, but also the liquid slug velocity is within the range for a good intermittent gas lift operation. Therefore, the current valve can indeed be able to produce liquid slugs of approximately 600 ft. in length. Because the well is not producing any liquids, it is not possible to calculate the productivity index and, in consequence, the optimum cycle time cannot be found either. For this reason, the best that can be done is to temporarily increase the injection gas flow rate to very large values until the spread of the valve (difference of the valve's opening and closing pressures shown at the surface) is close to its value stipulated in the design and then lower the gas flow rate to its designed value and see if the design spread of the valve can be sustained. If the well tends to load up with liquids again, the spread of the valve will begin to decrease again. In this case, the pilot valve needs to be replaced with another one with a larger area ratio. ■

**Problem 12.4**

Analyze the operation of a choke-control intermittent gas lift well with the following characteristics and operational conditions.

Pilot valve: spring-loaded, injection-pressure-operated with an area ratio of 0.15, main port diameter equal to 24/64 in. and test-rack closing pressure ( $P_{tr}$ ) of 715 psig. The surface opening pressure ( $P_{cso}$ ) is 700 psig and the surface closing pressure ( $P_{csc}$ ) is 645.97 psig. The opening pressure at valve's depth ( $P_{cvo}$ ) is 774.372 psig and its closing pressure at valve's depth ( $P_{cvc}$ ) is 713.96 psig. The average gas compressibility factor in the annulus at the opening pressure ( $z_{ga,apert.}$ ) is 0.8769 and at closing pressure ( $z_{ga,closing}$ ) is 0.8848.

Gas and liquid properties:

Injection gas specific gravity ( $G_g$ ): 0.7; water cut ( $w$ ): 10%; oil API gravity: 23°API; formation gas/liquid ratio: 300 scf/STBL.

Injection gas line ID: 2.067 in.; length ( $L$ ) of the surface injection gas line: 100 ft.; operating valve's depth: 3940 ft.; time in which the pilot valve remains open ( $T_{val}$ ): 6.05 min; total cycle time ( $T_{cycle}$ ): 34.388 min; surface injection gas flow rate ( $Q_{gi}$ ): 140.39 Mscf/D; minimum wellhead production pressure ( $P_{wh}$ ): 60 psig; static bottomhole pressure ( $P_{sbh}$ ): 1300 psig; temperature at top of perforations ( $T_{res}$ ): 151.2°F; top of perforations' depth: 4 Mft.; liquid production ( $q_l$ ): 125.14 STBL/D.

**Solution**

1. Verification of the surface gas flow rate and wellhead pressure measurements

The volume of gas injected per cycle (calculated from the surface injection gas flow rate and the number of cycles per day) is:

$$V_{gsc} = \frac{Q_{gi} T_{cycle}}{1.44} = \frac{140.39(34.388)}{1.44} = 3352.59 \text{ scf/cycle}$$

The volume of gas injected per cycle is now calculated from the opening and closing pressures using the equations presented in [Section 12.2.1](#) (Eqs (12.1) to (12.1)). The annular volumetric capacity,  $B_a$  in ft.<sup>3</sup>/Mft., is found from:

$$B_a = 5.45415(D_{IDcasing}^2 - D_{ODtubing}^2) = 5.45415(6.366^2 - 2.875^2) \\ = 175.95 \text{ ft.}^3/\text{Mft.}$$



The volumetric capacity of the surface gas injection line,  $B_i$  in  $\text{ft}^3/\text{Mft.}$ , is:

$$B_i = 5.45415(D_{\text{gasline}}^2) = 5.45415(2.067^2) = 23.3028 \text{ ft}^3/\text{Mft.}$$

The gas compressibility factor in the surface gas injection line can be approximated as:

$$z_{\text{gl}} = 1 - 0.00019385(P_{\text{cso}} + 14.7) = 1 - 0.00019385(700 + 14.7) = 0.861455$$

The gas injection temperature at valve depth,  $T_v$  in  $^\circ\text{F}$ , can be approximated as the geothermal temperature, which is calculated as a function of the depth of the valve,  $D_{\text{ov}}$  in Mft., from the following equation:

$$T_v = 15.6D_{\text{ov}} + 88.8 = 15.6(3.94) + 88.8 = 150.264^\circ\text{F}$$

The volume of gas injected per cycle supplied by the surface gas injection line,  $v_{\text{gl}}$  in scf, is calculated from the surface injection pressure  $P_{\text{cso}}$ , the surface closing pressure  $P_{\text{csc}}$ , the volumetric capacity of the surface gas line  $B_i$ , the length  $L$  of the surface gas line in Mft., and the gas compressibility factor  $z_{\text{gl}}$ :

$$\begin{aligned} v_{\text{gl}} &= \frac{35.374B_iL(P_{\text{cso}} - P_{\text{csc}})}{545z_{\text{gl}}} = \frac{35.374(23.3028)0.1(700 - 645.97)}{545(0.861455)} \\ &= 9.4863 \text{ scf/cycle} \end{aligned}$$

The volume of gas that enters the surface gas injection line through the surface choke while the pilot valve is opened,  $v_{\text{ge}}$  in scf, is:

$$v_{\text{ge}} = \frac{Q_{\text{gi}}T_{\text{val}}}{1.44} = \frac{140.39(6.05)}{1.44} = 589.83 \text{ scf/cycle}$$

The gas supplied by the annulus is:

$$\begin{aligned} v_{\text{ga}} &= \frac{35.374B_aD_{\text{ov}}}{1005 + T_v} \left[ \frac{P_{\text{cso}} + P_{\text{cvo}}}{z_{\text{ga,apert.}}} - \frac{P_{\text{csc}} + P_{\text{cvc}}}{z_{\text{ga,close.}}} \right] = \\ &= \frac{35.374(175.95)3.94}{1005 + 150.264} \left[ \frac{700 + 774.372}{0.8769} - \frac{645.97 + 713.96}{0.8848} \right] = 3064.2 \text{ scf/cycle} \end{aligned}$$

The total volume of gas injected per cycle is  $v_{\text{ga}} + v_{\text{gl}} + v_{\text{ge}} = 3,064.2 + 9.4863 + 589.83 = 3663.5 \text{ scf/cycle}$ . This volume is very close to the one calculated earlier from the value of the surface injection gas flow rate and the numbers of cycles in one day. Thus, the gas flow rate and the well-head pressures are being measured with an acceptable level of accuracy and there is only one point of gas injection into the production tubing.

2. The following two calculations are performed: (1) calculation of the produced liquid column length from the daily liquid production and the number of cycles per day, and (2) calculation of the initial liquid column assuming a fallback factor of 0.05.

The production tubing volumetric capacity in Br/Mft. is:

$$B_t = 0.97143d^2 = (0.97143)2.441^2 = 5.7882 \text{ Br/Mft.}$$

The liquid pressure gradient is:

$$\begin{aligned} \rho_f &= 0.433 \left[ w - (1-w) \frac{141.5}{\text{°API} + 131.5} \right] \\ &= 0.433 \left[ 0.1 - (0.9) \frac{141.5}{23 + 131.5} \right] = 0.4002 \text{ psi/ft.} \end{aligned}$$

Where  $w$  is the water cut expressed from 0 to 1.

- The produced liquid column length ( $Q_{\text{prod}}$ ) is calculated from the daily liquid production  $q_f$ , the cycle time  $T_{\text{cycle}}$ , and the volumetric capacity of the production tubing from the following equation:

$$Q_{\text{prod}} = \frac{q_f T_{\text{cycle}}}{1.44 B_t} = \frac{125.14(34.388)}{1.44(5.7882)} = 516.29 \text{ ft.}$$

- If the fallback factor  $F$  is assumed to be equal to 0.05, the initial liquid column at valve's depth just before the pilot valve opens is:

$$Q_{\text{ini}} = \frac{Q_{\text{prod}}}{1 - F D_{\text{ov}}} = \frac{516.29}{1 - 0.05(3.94)} = 642.95 \text{ ft.}$$

With Eq. 10.32, the required volume of gas to be injected per cycle to lift a 642.95 ft. long liquid column from a depth of 3940 ft. is calculated to be equal to 5046.681 scf/cycle. This volume is greater than the current volume being injected to the well under current conditions and, in consequence, the fallback factor should also be greater than its assumed value. For this reason, the valve mechanic equation should be used to find the initial liquid column length so that the fallback factor can be estimated.

3. Calculation of the production pressure at valve's depth ( $P_{\text{to}}$ ) just before the pilot valve opens

Using the valve mechanic equation with the valve's area ratio  $R$  and its calibration pressure  $P_{\text{tr}}$ , the production pressure is given by:

$$P_{\text{to}} = -P_{\text{cvo}} \left( \frac{1-R}{R} \right) + \frac{P_{\text{tr}}}{R} = -774.372 \left( \frac{1-0.15}{0.15} \right) + \frac{715}{0.15} = 378.56 \text{ psig}$$

**4. Calculation of the actual initial liquid column length**

To find the initial liquid column length, iterations such as those presented in the previous problem should be performed using the following equation:

$$Q_{ini} = \frac{P_{to} - P_{wh} f_g}{\rho_f}$$

$$Q_{ini1} = \frac{378.56 - 60 \left( 1 + \frac{3.94}{54} \right)^{1.524}}{0.4002} = 779.01 \text{ ft.}$$

$$Q_{ini2} = \frac{378.56 - 60 \left( 1 + \frac{3.94 - 0.77901}{54} \right)^{1.524}}{0.4002} = 782.42 \text{ ft.}$$

$$Q_{ini3} = \frac{378.56 - 60 \left( 1 + \frac{3.94 - 0.78242}{54} \right)^{1.524}}{0.4002} = 782.44 \text{ ft.}$$

**5. Calculation of the liquid fallback factor  $F$** 

With the initial liquid column length estimated in point (4) and the produced liquid column calculated in point (2), the fallback factor  $F$  is calculated as:

$$F = \frac{Q_{ini} - Q_{prod}}{D_{ov}} = \frac{782.44 - 516.29}{3.94} = 0.0863$$

Even though this calculated value of  $F$  is greater than 0.05 initially assumed, it is not a very large fallback factor so that the productivity index can be calculated in an approximate way as shown in the next step.

**6. Productivity index  $J$  calculation:**

The productivity index is calculated from several parameters, including the current fallback factor calculated in point 5. For this purpose, the following terms must be calculated first:

$$c_m = F D_{ov} = 0.0863(3.94) = 0.34$$

The true liquid pressure gradient can be approximated using the following equation:

$$\rho_t = 0.167 - 0.00143 \text{ API} = 0.13411 \text{ psi/ft.}$$

The maximum drawdown  $A'$  is calculated next:

$$A' = P_{sbh} - P_{wh} \left( 1 + \frac{D_{ov}}{54} \right)^{1.524} - (D_{pt} - D_{ov}) \rho_t = 1300 - 60 \left( 1 + \frac{3.94}{54} \right)^{1.524} - (4 - 3.94) 1000 (0.13411) = 1225.15556 \text{ psi}$$

Where  $D_{ov}$  is the pilot valve's depth, equal to 3.94 Mft. and  $D_{pt}$  is the top of perforations depth equal to 4 Mft. The productivity index  $J$  is then calculated using Eq. 12.32:

$$J = \frac{1.44B_t}{(T_{cycle} - T_{val})\rho_f} \ln \left[ \frac{A' - c_m Q_{ini} \rho_f}{A' - Q_{ini} \rho_f} \right]$$

$$J = \frac{1.44(5.7882)}{(34.388 - 6.05)0.4002} \ln \left[ \frac{1225.15556 - 0.34(782.42)0.4002}{1225.15556 - 782.42(0.4002)} \right] = 0.15 \text{ Br}/(\text{psi-D})$$

7. Optimum cycle time calculation using Eq. 10.27 and assuming that a new pilot valve has been installed and the liquid fallback factor is now equal to  $F = 0.05$  (using the productivity index  $J$  calculated in point 6)

Calculation of necessary parameters:

$$\gamma = \frac{\rho_f J}{1.44B_t} = \frac{(0.4002)(0.15)}{(1.44)(5.788)} = 0.0072 \frac{1}{\text{min}}$$

With the pilot valve's depth  $D_{ov}$  in Mft. and the liquid slug velocity in Mft./min (assumed to be equal to 1 Mft./min), the following parameters are calculated:

$$C_4 = \exp[\gamma D_{ov}/v_{at}] = \exp[0.0072(3.94)/1] = 1.028774$$

$$c_m = FD_{ov} = 0.05(3.94) = 0.197$$

$$C_2 = 1 - c_m = 1 - 0.197 = 0.803$$

The initial value of the cycle time to start iterations,  $T_1$ , can be equal to three times the depth of the pilot valve divided by the average liquid slug velocity, estimated equal to 1 Mft./min:

$$T_1 = 3D_{ov}/v_{at} = 3(3.94)/1 = 11.82 \text{ min}$$

The equation that is used in the iterations to find the optimum cycle time is Eq. 10.27:

$$T_{n+1} = T_n - \frac{T_c - T_n}{\frac{\gamma [e^{\gamma T_n} - c_m (C_4)^2 e^{-\gamma T_n}]}{\gamma (C_2)(C_4)} - 1}$$

Where  $T_c$  is:

$$T_c = \frac{(e^{\gamma T_n} - C_4)(e^{\gamma T_n} - c_m C_4)}{\gamma e^{\gamma T_n} C_2 C_4}$$

With  $T_1 = 11.82$  min:

$$\exp[0.0072(11.82)] = 1.08883$$

$$T_c = \frac{(1.08883 - 1.028774)(1.08883 - 0.202668)}{0.0072(1.08883)0.803(1.028774)} = 8.21753 \text{ min}$$

$$T_2 = 11.82 - \frac{8.21753 - 11.82}{\frac{0.0072[1.08883 - (0.197)1.028774^2(0.918417)]}{0.0072(0.803)1.028774} - 1} = 53.5978 \text{ min}$$

With  $T_2 = 53.5978$  min:

$$\exp[0.0072(53.5978)] = 1.47094$$

$$T_c = \frac{(1.47094 - 1.028774)(1.47094 - 0.202668)}{0.0072(1.47094)(0.803)(1.028774)} = 64.09656 \text{ min}$$

$$T_3 = 53.5978 - \frac{64.09656 - 53.5978}{\frac{0.0072[1.47094 - (0.197)(1.028774)^2(0.679835)]}{(0.0072)0.803(1.028774)} - 1} = 36.358 \text{ min}$$

Following the iterations in this way, the optimum cycle time is found to be equal to 30.4457 min/cycle.

**8.** Calculation of the initial liquid column length and liquid production at the optimum cycle time

The liquid column generation time,  $T_f$ , is equal to the total cycle time  $T_{\text{cycle}}$  minus the gas injection time  $T_{oc}$ , which is equal to the depth of the operating valve divided by the liquid slug velocity (equal to 1 Mft./min)

$$T_f = T_{\text{cycle}} - T_{oc} = T_{\text{cycle}} - D_{ov}/v_{at} = 30.4457 - 3.94/1 = 26.5057 \text{ min}$$

To calculate the wellhead production pressure referred to the depth of the pilot valve, the following equation is used for the gas factor  $f_g$ :

$$f_g = \left(1 + \frac{D_{ov}}{54}\right)^{1.524} = \left(1 + \frac{3.94}{54}\right)^{1.524} = 1.113297$$

Therefore, the production pressure at depth due to the gas column along the production tubing is  $P_{wh}f_g = 60(1.113297) = 66.7978$  psig. On the other hand, the calculations of the terms that are needed to find the initial liquid column length are repeated next:

$$\gamma = \frac{\rho_f J}{1.44B_t} = \frac{(0.4002)(0.15)}{(1.44)(5.788)} = 0.0072 \frac{1}{\text{min}}$$

$$c_m = FD_{ov} = 0.05(3.94) = 0.197$$

$$\rho_f = 0.433 \left[ w - (1-w) \frac{141.5}{\circ \text{API} + 131.5} \right] = 0.433 \left[ 0.1 - (0.9) \frac{141.5}{23 + 131.5} \right] = 0.4002 \text{ psi/ft.}$$

$$\rho_t = 0.167 - 0.00143 \text{ API} = 0.13411 \text{ psi/ft.}$$

$$\begin{aligned} A' &= P_{sbh} - P_{wh} \left( 1 + \frac{D_{ov}}{54} \right)^{1.524} - (D_{pt} - D_{ov}) 1000 \rho_t = \\ &= 1300 - 60 \left( 1 + \frac{3.94}{54} \right)^{1.524} - (4 - 3.94) 10^3 (0.134) = 1225.15556 \text{ psi} \end{aligned}$$

The initial liquid column length is then calculated using Eq. 10.17:

$$Q_{ini} = \frac{A' (e^{\gamma T_r} - 1)}{1000 \rho_f (e^{\gamma T_r} - c_m)} = \frac{1225.1556 (e^{0.0072(26.5057)} - 1)}{1000 (0.4002) (e^{0.0072(26.5057)} - 0.197)} = 0.63527 \text{ Mft.}$$

The liquid production  $q_r$  is given by Eq. 10.19:

$$\begin{aligned} q_r &= Q_{ini} B_t (1 - FD_{ov}) \frac{1440}{T_{cycle}} = 0.63527 [\text{Mft./cycle}] 5.7882 \left[ \frac{\text{Br}}{\text{Mft.}} \right] \\ &= [1 - 0.05(3.94)] \frac{1440 \text{ min/D}}{30.4457 \text{ min/cycle}} = 139.65 \text{ STBL/D} \end{aligned}$$

This represents an increment of only 14.5 STBL/D. But this result should be viewed with caution because it is based on a productivity index (calculated with a fallback factor of 0.08) that could be in error due to the fact that it was obtained from an initial liquid column length calculated from the valve's force-balance equation, which is highly inaccurate. Because the volume of gas injected per cycle is less than its required value, it is far better to estimate the liquid fallback losses and the productivity index from downhole pressure surveys as explained in Section 12.3. The moderate increase in liquid production might not justify the cost of running a pressure survey and replacing the current pilot valve. It might be a better solution to reduce the cycle time (to lift smaller liquid columns) by increasing the injection gas flow rate or use a surface intermitter to force the pilot valve to remain open until the required volume of gas is injected per cycle. ■

### Problem 12.5

Analyze the operation of a choke-control intermittent gas lift well with the following characteristics and operational conditions.

Pilot valve: spring-loaded, injection-pressure-operated valve with area ratio equal to 0.15, main port diameter of 32/64 in., and test-rack closing pressure  $P_{tr} = 950$  psig. The surface injection opening pressure ( $P_{cso}$ ) is 950 psig

and the surface injection closing pressure ( $P_{csc}$ ) is 856.85 psig. The injection opening pressure at valve's depth ( $P_{cvo}$ ) is 1055.1 psig and the injection closing pressure also at valve's depth ( $P_{cvc}$ ) is 950.28 psig. The average gas compressibility factor ( $z_{ga,apert.}$ ) in the annulus at the opening pressure is 0.844 and at the closing pressure ( $z_{ga,close.}$ ) is 0.8556.

Gas and liquid properties:

Lift gas specific gravity ( $G_g$ ): 0.7; water cut ( $w$ ): 10%; oil API gravity: 23°API; formation gas/liquid ratio: 300 scf/STBL.

Production tubing ID: 2.441 in.; production tubing OD: 2.875 in.; casing ID: 6.366 in.; surface gas injection line ID: 2.067 in.; length ( $L$ ) of the surface gas injection line: 2000 ft.; operating valve's depth: 3940 ft.; time in which the pilot valve remains open ( $T_{val}$ ): 4.28 min; total cycle time ( $T_{cycle}$ ): 20 min; surface injection gas flow rate ( $Q_{gi}$ ): 544.58 Mscf/D; wellhead minimum production pressure ( $P_{wh}$ ): 60 psig; static reservoir pressure ( $P_{sbh}$ ): 400 psig; top of perforation temperature ( $T_{res}$ ): 151.2°F; top of perforations depth: 4 Mft.; liquid production ( $q_l$ ): 248 Br/D.

### Solution

#### 1. Verification of the surface injection gas flow rate and wellhead pressure measurements

The volume of gas injected per cycle calculated from the surface injection gas flow rate and the number of cycles in 1 day is:

$$V_{gsc} = \frac{Q_{gi} T_{cycle}}{1.44} = \frac{544.58(20)}{1.44} = 7563.61 \text{ scf/cycle}$$

The volume of gas injected per cycle is now calculated from the opening and closing pressures using the equations presented in Section 12.2.1 (Eqs (12.1) to (12.14)). The annulus volumetric capacity,  $B_a$  in ft.<sup>3</sup>/Mft., is:

$$B_a = 5.45415(D_{IDcasing}^2 - D_{ODtubing}^2) = 5.45415(6.366^2 - 2.875^2) = 175.95 \text{ ft.}^3/\text{Mft.}$$

The volumetric capacity of the surface gas injection line,  $B_l$  in ft.<sup>3</sup>/Mft., is:

$$B_l = 5.45415(D_{IDgasline}^2) = 5.45415(2.067^2) = 23.3028 \text{ ft.}^3/\text{Mft.}$$

The gas compressibility factor in the surface gas injection line can be approximated as:

$$z_{gl} = 1 - 0.00019385(P_{cso} + 14.7) = 1 - 0.00019385(950 + 14.7) = 0.81299$$

The injection gas temperature at valve's depth,  $T_v$  in °F, is found from the depth of the valve,  $D_{ov}$  in Mft., using the following equation:

$$T_v = 15.6D_{ov} + 88.8 = 15.6(3.94) + 88.8 = 150.264^\circ\text{F}$$

The volume of gas injected per cycle supplied by the surface gas injection line,  $v_{gl}$  in scf, is calculated from the surface injection opening pressure  $P_{cso}$ , the surface injection closing pressure  $P_{csc}$ , the volumetric capacity of the gas injection line  $B_l$ , the length of the surface injection line  $L$  in Mft., and the gas compressibility factor  $z_{gl}$ :

$$v_{gl} = \frac{35.374(B_l)L(P_{cso} - P_{csc})}{545z_{gl}} = \frac{35.374(23.3028)2(950 - 856.85)}{545(0.81299)} = 346.59 \text{ scf/cycle}$$

The volume of gas that enters the surface injection gas line through the surface choke while the subsurface pilot valve is opened,  $v_{ge}$  in scf, is found from:

$$v_{ge} = \frac{Q_{gl}T_{val}}{1.44} = \frac{544.58(4.28)}{1.44} = 1618.61 \text{ scf/cycle}$$

The gas supplied by the annulus per cycle is calculated by:

$$v_{ga} = \frac{35.374B_aD_{ov}}{1005 + T_v} \left[ \frac{P_{cso} + P_{cvo}}{z_{ga,apert.}} - \frac{P_{csc} + P_{cvc}}{z_{ga,close.}} \right] = \frac{35.374(175.95)3.94}{1005 + 150.264} \left[ \frac{950 + 1055.1}{0.844} - \frac{856.85 + 950.28}{0.8556} \right] = 5595.23 \text{ scf/cycle}$$

The total volume of gas injected per cycle is equal to  $v_{ga} + v_{gl} + v_{ge} = 5,595.23 + 346.59 + 1618.61 = 7560.43$  scf/cycle. This volume is very close to the volume calculated earlier from the measured surface gas flow rate  $Q_{gi}$  and the number of cycles in one day, thus the surface measurements of the gas flow rate and the wellhead pressures must be reasonably accurate and there should be only one gas injection point into the production tubing.

2. The following two calculations are performed: (1) calculation of the produced liquid column length from the daily liquid production and the number of cycles per day, and (2) calculation of the initial liquid column at valve's depth just before the pilot valve opens assuming a fallback factor of 0.05:

The volumetric capacity in Br/Mft. of the production tubing is:

$$B_t = 0.97143d^2 = 0.97143(2.441^2) = 5.7882 \text{ Br/Mft.}$$



The liquid pressure gradient is:

$$\rho_f = 0.433 \left[ w - (1-w) \frac{141.5}{^\circ\text{API} + 131.5} \right] = 0.433 \left[ 0.1 - (0.9) \frac{141.5}{23 + 131.5} \right] = 0.4002 \text{ psi/ft.}$$

Where  $w$  is the water cut expressed from 0 to 1.

- The produced liquid column is calculated from the daily liquid production  $q_f$ , the total cycle time  $T_{\text{cycle}}$ , and the volumetric capacity of the production tubing  $B_t$ :

$$Q_{\text{prod}} = \frac{q_f T_{\text{cycle}}}{1.44 B_t} = \frac{248(20)}{1.44(5.7882)} = 595.08 \text{ ft.}$$

- If a liquid fallback factor of 0.05 is assumed, the initial liquid column length at valve's depth at the moment the pilot valve opens is given by:

$$Q_{\text{ini}} = \frac{Q_{\text{prod}}}{1 - FD_{\text{ov}}} = \frac{595.08}{1 - 0.05(3.94)} = 741.01 \text{ ft.}$$

Following the steps described in Eq. 10.32 (not shown here), the required volume of gas to lift a liquid column of 741.01 ft. of length from a depth of 3940 ft. to the surface is calculated to be equal to 5753 scf/cycle. This volume is smaller than the volume of gas injected per cycle calculated earlier and therefore the fallback factor might indeed be estimated equal to 0.05 because at the same time, this volume of gas per cycle is injected in a time interval that indicates that the slug velocity is adequate for minimum liquid fall back losses, from which the productivity index and the optimum cycle time are calculated next.

### 3. Productivity index $J$ calculation:

The following parameters need to be calculated before being able to calculate the productivity index:

$$c_m = FD_{\text{ov}} = 0.05(3.94) = 0.197$$

The true liquid pressure gradient is approximated with the following equation:

$$\rho_f = 0.167 - 0.00143^\circ\text{API} = 0.13411 \text{ psi/ft.}$$

The maximum drawdown  $A'$  is calculated with the following equation:

$$\begin{aligned} A' &= P_{\text{sbh}} - P_{\text{wh}} \left( 1 + \frac{D_{\text{ov}}}{54} \right)^{1.524} - (D_{\text{pt}} - D_{\text{ov}}) 1000 \rho_f \\ &= 400 - 60 \left( 1 + \frac{3.94}{54} \right)^{1.524} - (4 - 3.94) 10^3 (0.134) = 325.1555 \text{ psi} \end{aligned}$$

Where  $D_{ov}$  is the depth of the operating valve, equal to 3.94 Mft. and  $D_{pt}$  is the top of perforations' depth, equal to 4 Mft. The productivity index  $J$  is then calculated using Eq. 12.32:

$$J = \frac{1.44B_t}{(T - T_{val})\rho_f} \ln \left[ \frac{A' - c_m Q_{ini} \rho_f}{A' - Q_{ini} \rho_f} \right]$$

$$J = \frac{1.44(5.7882)}{(20 - 4.28)0.4002} \ln \left[ \frac{325.1555 - 0.197(741.07)0.4002}{325.1555 - 741.07(0.4002)} \right] = 2.9591 \text{ Br}/(\text{psi} \cdot \text{D})$$

4. Calculation of the optimum cycle time (keeping the time  $T_{val}$  constant):  
Necessary parameters:

$$\gamma = \frac{\rho_f J}{1.44B_t} = \frac{(0.4002)(2.9591)}{(1.44)(5.788)} = 0.142 \frac{1}{\text{min}}$$

With the depth of the valve  $D_{ov}$  in Mft. and the liquid slug velocity in Mft./min (assumed to be equal to 1 Mft./min), the rest of the necessary parameters to calculate the optimum cycle time are found:

$$C_4 = \exp[\gamma T_{val}] = \exp[0.142(4.28)] = 1.8363$$

$$c_m = FD_{ov} = 0.05(3.94) = 0.197$$

$$C_2 = 1 - c_m = 1 - 0.197 = 0.803$$

The initial cycle time to begin the iterations,  $T_1$ , can be estimated as equal to three times the time interval in which the pilot valve remains open ( $3T_{val}$ ):

$$T_1 = 3T_{val} = 3(4.28) = 12.84 \text{ min}$$

The equation used for the iterations to get the optimum cycle time is Eq. 10.27:

$$T_{n+1} = T_n - \frac{T_c - T_n}{\frac{\gamma(e^{\gamma T_n} - c_m(C_4)^2 e^{-\gamma T_n})}{\gamma(C_2)(C_4)} - 1}$$

Where  $T_c$  is:

$$T_c = \frac{(e^{\gamma T_n} - C_4)(e^{\gamma T_n} - c_m C_4)}{\gamma e^{\gamma T_n} C_2 C_4}$$

With  $T_1 = 12.84$  min:

$$\exp[0.142(12.84)] = 6.1921$$

$$T_c = \frac{(6.1921 - 1.8363)[6.1921 - 0.197(1.8363)]}{0.142(6.1921)(0.803)(1.8363)} = 19.5919 \text{ min}$$

$$T_2 = 12.84 - \frac{19.5919 - 12.84}{\frac{6.1921 - (0.197)1.8363^2(0.1615)}{0.803(1.8363)} - 1} = 10.68 \text{ min}$$

With  $T_2 = 10.68$  min:

$$\exp[0.142(10.68)] = 4.5565$$

$$T_c = \frac{(4.5585 - 1.8363)[4.5565 - 0.197(1.8363)]}{0.142(4.5565)0.803(1.8363)} = 11.9599 \text{ min}$$

$$T_3 = 10.68 - \frac{11.9599 - 10.68}{\frac{4.5565 - 0.197(1.8363^2)0.21946}{0.803(1.8363)} - 1} = 10.037 \text{ min}$$

Continuing the iterations in this way, the optimum cycle time is found to be equal to only 9.9841 min/cycle.

5. Adjustment of the surface gas flow rate  $Q_{gi}$  to achieve the optimum cycle time:

As it is shown here, it is not always possible to achieve the optimum cycle time. Currently, the instantaneous gas flow rate through the pilot valve (when it opens) is (using Eq. 12.20):

$$Q_{gi\text{inst}} = \frac{(v_{ga} + v_{gi})1.44}{T_{val}} + Q_{gi} = \frac{(5595.23 + 346.59)1.44}{4.28} + 544.58 = 2543.69 \text{ Mscf/D}$$

It is assumed that this instantaneous gas flow rate should not change significantly when the surface gas flow rate  $Q_{gi}$  is adjusted. Additionally, it is also assumed that the value of  $(v_{ga} + v_{gi})$  is not going to change if the surface gas flow rate is adjusted within reasonably small values. The total cycle time  $T_{cycle}$  is equal to the time in which the liquid column is regenerated,  $T_f$ , plus the time in which the pilot valve remains open,  $T_{val}$ . Additionally,  $T_f$  and  $T_{val}$  can be expressed as functions of the surface gas flow rate  $Q_{gi}$  and the instantaneous gas flow rate through the gas lift valve  $Q_{gi\text{inst}}$ , derived from Eqs. 12.19 and 12.20, respectively, as follows:

$$T_f = \frac{1.44(v_{ga} + v_{gi})}{Q_{gi}} = \frac{1.44(5595.23 + 346.59)}{Q_{gi}} = \frac{8556.22}{Q_{gi}}$$

$$T_{\text{val}} = \frac{1.44(v_{\text{ga}} + v_{\text{gl}})}{Q_{\text{gi inst}} - Q_{\text{gi}}} = \frac{1.44(5595.23 + 346.59)}{2543.69 - Q_{\text{gi}}} = \frac{8556.22}{2543.69 - Q_{\text{gi}}}$$

Thus, the total cycle time can be approximated using the following equation (obtained from Eq. 12.21) for different values of the surface gas flow rate, assuming that  $v_{\text{ga}}$ ,  $v_{\text{gl}}$ , and  $Q_{\text{gi inst}}$  remain more or less constant:

$$T_{\text{cycle}} = \frac{8556.22}{2543.69 - Q_{\text{gi}}} + \frac{8556.22}{Q_{\text{gi}}}$$

Table 12.1 shows how  $T_{\text{cycle}}$ ,  $T_f$  and  $T_{\text{val}}$  change for different values of the surface gas flow rate.

As can be seen in the table, it is not possible to reduce the total cycle time to values less than 13.49 min. This is due to the increment that  $T_{\text{val}}$  experiences. In reality, the sum  $(v_{\text{ga}} + v_{\text{gl}})$  is going to increase with increasing value of the surface gas flow rate, so that the minimum total cycle time would be even greater than the one shown in the table. The only way to reduce the total cycle time is by reducing  $(v_{\text{gl}} + v_{\text{ga}})$  which can be done if the pilot valve is replaced with a new one with a lower area ratio (this is acceptable in this case because the volume of gas currently injected per cycle is greater than its required value).  $T_{\text{val}}$ , on the other hand, can be reduced if the new pilot valve also has a greater main port diameter.

If it is decided to increase the surface injection gas flow rate without replacing the gas lift valve, it might be possible that the increment in the liquid production is going to be very small and at the expense of a considerable increase in the injection gas/liquid ratio. To demonstrate this point, the calculations of the new liquid production and injection gas/liquid ratio for a liquid column regeneration time  $T_f = 9$  minutes are presented next.

Following the steps described in Eq. 10.17 to obtain the liquid column length for a liquid column regeneration time of  $T_f = 9$  min, it is found the initial liquid column length to be  $Q_{\text{ini}} = 620.3$  ft.

**Table 12.1** Results for Different Injection Gas Flow Rates

$Q_{\text{gi}}$ Mscf/D	$T_{\text{cycle}}$ (min)	$T_f$ (min)	$T_{\text{val}}$ (min)
600	18.66	14.26	4.4
800	15.6	10.69	4.9
1000	14.09	8.56	5.54
1200	13.49	7.13	6.36
1400	13.59	6.11	7.48
1600	14.41	5.34	9.06

The production pressure  $P_{to}$  just before the pilot valve opens is then:

$$P_{to} = \rho_f Q_{ini} + P_{wh} f_g = 0.4002(620.3) + 60 \left( 1 + \frac{3.94 - 0.6203}{54} \right)^{1.524} = 313.9550 \text{ psig}$$

Where  $f_g = \left( 1 + \frac{D_{ov}/1000 - Q_{ini}/1000}{54} \right)^{1.524} = \left( 1 + \frac{3.94 - 0.6203}{54} \right)^{1.524}$  has been used.

The gas injection opening pressure would then be:

$$P_{cvo} = \frac{P_{tr}}{1-R} - \frac{R}{1-R} P_{to} = \frac{950}{1-0.15} - \frac{0.15}{1-0.15} 313.9550 = 1062.24 \text{ psig}$$

For which the surface opening pressure is  $P_{cso} = 956.44$  psig. The closing pressure can be considered constant and equal to  $P_{csc} = 856.85$  psig. With these pressures, the gas supplied by the annulus and the gas line at each cycle are found to be (using Eqs. 12.1–12.14):  $v_{ga} = 5989.8$  scf/cycle and  $v_{gl} = 371.12$  scf/cycle, respectively. The surface gas flow rate is then:

$$Q_{gl} = \frac{1.44(v_{ga} + v_{gl})}{T_f} = \frac{1.44(5989.8 + 371.12)}{9} = 1017.75 \text{ MscfD}$$

Assuming that the instantaneous gas flow rate through the pilot valve is going to remain constant,  $T_{val}$  is then:

$$T_{val} = \frac{1.44(v_{ga} + v_{gl})}{Q_{ginst} - Q_{gl}} = \frac{1.44(5989.8 + 371.12)}{2543.69 - 1017.75} = 6 \text{ min}$$

Thus the total cycle time is  $9 + 6 = 15$  minutes and the daily production can be calculated as (using Eq. 10.19):

$$q_f = \frac{Q_{ini}}{1000} B_t (1 - FD_{ov}) \frac{1440}{T_{cycle}} = \frac{620.3}{1000} 5.7882 [1 - 0.05(3.94)] \frac{1440}{15} = 276.78 \text{ STB/D}$$

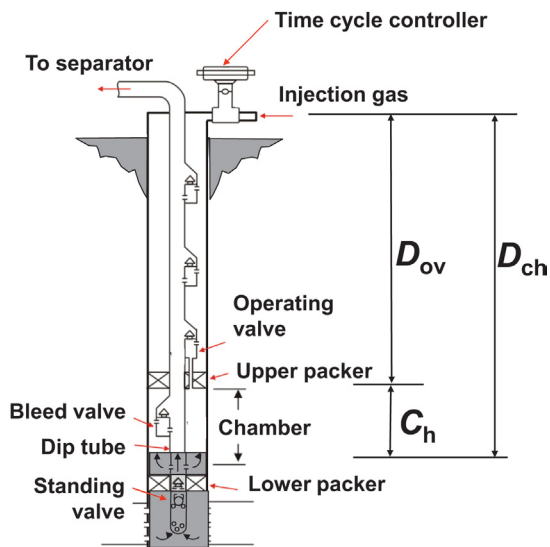
The increment in the liquid production is of only 28.77 STB/D but the injection gas/liquid ratio increased from  $(544,580/248) = 2,195.88$  scf/STB to  $(1,017,750/276.77) = 3,677.24$  scf/STB. This means that each additional liquid barrel being produced requires an additional gas injection volume of 16,446.64 scf.

A new design using a pilot valve with an area ratio equal to 0.07 gave the following excellent results: total cycle time = 8.7 min; daily production = 367 Br/D; injection gas/liquid ratio = 2,232 scf/Br. It was necessary then to replace the gas lift pilot valve to maximize the liquid production in the most efficient way possible.

Additional examples of troubleshooting analyses of wells with simple type completions are presented in Section 12.6. These additional examples are presented to familiarize the reader with cases in which some of the data are either unreliable or totally missing, which was not the case in the previous examples.

The troubleshooting calculation procedure for a double-packer accumulation chamber is presented next. Unloading valves are analyzed in the same way as explained earlier for simple type completions. The operating valve, on the other hand, requires a different treatment. A double-packer accumulation chamber is shown in Fig. 12.3, where:  $D_{ov}$  is the operating valve's depth in feet,  $D_{ch}$  is the depth in feet of the perforated nipple through which the liquids enter the annulus of the chamber, and  $C_h$  is the effective length of the chamber in feet.

The initial true liquid column length ( $Q_c$  in feet) above the perforated nipple (through which the liquids go from the dip tube to the chamber's annulus) is calculated (initially as if the accumulation chamber has not been completely filled) based on: the measured daily liquid production  $q_f$  in STB/D, the measured cycle time  $T_{cycle}$  in minutes, the liquid pressure gradient  $\rho_f$  in psi/ft. (calculated from the water cut and the oil API gravity), the accumulation chamber volumetric capacity  $b_{ch}$  in Br/Mft., the estimated fallback factor  $F$ ,



■ FIGURE 12.3 Double-packer accumulation chamber installation.

and the estimated true liquid pressure gradient  $\rho_l$  in psi/ft., with the following equation:

$$Q_c = \frac{q_f T_{\text{cycle}}}{1.44 b_{\text{ch}} (1 - FD_{\text{ch}}/1000)} \left( \frac{\rho_f}{\rho_l} \right) \quad (12.35)$$

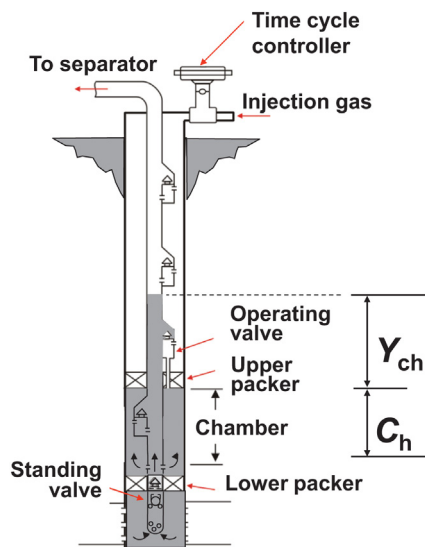
Where the right hand side of the equation has been multiplied times  $(\rho_f/\rho_l)$  so that  $Q_c$  is the true liquid column (taking into account the gas present in the liquid). The value of  $Q_c$  calculated using the earlier equation is reliable only if: (1) the volume of gas injected per cycle is greater than or equal to the required volume of gas calculated from the energy balance equation, and (2) the liquid slug velocity is around 1000 ft./min. If the volume of gas injected per cycle is less than its required value or the liquid slug velocity is very large or very small, the fallback factor is going to be greater than  $0.05 \text{ Mft.}^{-1}$  and impossible to estimate from the operating valve's force-balance equation for chamber installations (unless the liquid level is above the upper packer). This is a considerable limitation on the troubleshooting calculation procedure compared to simple type completions. It is important to mention that if the bleed valve port is not properly sized, the liquid level in the annulus of the accumulation chamber can be below the liquid level in the dip tube and anywhere between the two packers. If that is the case and the liquid level in the tubing is above the upper packer, then the calculated value of the fallback factor (estimated from the force-balance equation or even a downhole pressure survey) could be very large when in reality the problem is that the chamber might be mostly filled with gas.

All troubleshooting analyses must include the calculation of the required volume of gas injected per cycle, which is calculated in the same way as for simple type completions (explained in Eq. 10.32) but with the corrections explained for chamber lift design in Section 10.7. The required volume of gas injected per cycle should be compared to the actual volume being injected, which is equal to  $[1000 Q_{\text{gi}}/(\text{number of cycles per day})]$  in scf/cycle if the surface gas flow rate  $Q_{\text{gi}}$  is expressed in Mscf/D.

The calculated value of  $Q_c$  could be greater than  $C_h$ . Shown in Fig. 12.4 is the case in which the accumulation chamber is completely filled with liquids and the liquid level is a distance  $Y_{\text{ch}}$  above the upper packer when the operating valve opens.

If the calculated initial column length  $Q_c$  is greater than  $C_h$ , the value of  $Y_{\text{ch}}$  can be found by:

$$Y_{\text{ch}} = \frac{(Q_c - C_h) b_{\text{ch}}}{B_t} \quad (12.36)$$



■ FIGURE 12.4 Double-packer accumulation chamber with the liquid level above the upper packer when the operating gas lift valve opens.

Where  $B_t$  is the volumetric capacity of the production tubing above the upper packer in Br/Mft. In this case, the production pressure used in the valve force–balance equation for the operating valve is:

$$P_{to} = \rho_l Y_{ch} + P_{wh} f_g \quad (12.37)$$

But if  $Q_c$  is smaller than  $C_h$ , the production pressure at the moment the valve opens is only equal to the wellhead pressure plus the hydrostatic pressure due to the gas column above the operating valve, that is:

$$P_{to} = P_{wh} f_g \quad (12.38)$$

With this calculated value of  $P_{to}$  (and if the operating valve is in good working condition) the surface injection opening pressure  $P_{cso}$  can be calculated using Eqs. 12.28–12.30 (depending on the type of valve) to compare it to the measured surface opening pressure. However, if the operating valve has failed open, the maximum measured surface injection pressure must be slightly greater than the surface pressure  $P_{max}$  calculated from the following expression:

$$P_{max} = \frac{L_{tubing} \rho_l + P_{wh} f_{gt}}{f_{gc}} \quad (12.39)$$



Where  $L_{\text{tubing}}$  is the length of the liquid slug once it has completely entered the production tubing (this length is equal to  $Q_c b_{\text{ch}}/B_i$ );  $f_{\text{gt}}$  and  $f_{\text{gc}}$  are the gas factors used to calculate the gas pressure at depth in the tubing and in the casing annulus, respectively. The maximum measured surface injection pressure must be slightly greater than  $P_{\text{max}}$  because an additional pressure is required to overcome the friction generated by the movement of the slug (it is already in motion when the injection gas enters the production tubing). The average slug velocity should be estimated by measuring the elapsed time between the moment the operating valve opens and the time the slug reaches the surface (both events can be appreciated on the two-pen pressure chart as presented in Fig. 12.2). The average slug velocity is approximately equal to  $(D_{\text{ch}} + C_h)$  divided by this measured elapsed time. The slug velocity should be approximately equal to 1000 ft./min so that the liquid fallback losses can be minimized. This velocity can be reached if the gas lift system can provide an adequate gas flow rate. If the volume of gas injected per cycle and the gas flow rate through the pilot valve are acceptable, the fallback factor  $F$  can be assumed to be between 0.04 and 0.06. If the liquid level is deeper than or equal to the upper packer's depth, the productivity index  $J$  can be found from the following equation:

$$J = \frac{1.44(b_{\text{ch}})(A_{\text{diff}})}{(t)\rho_f} \quad (12.40)$$

Where  $t$  is the liquid accumulation time in minutes,  $\rho_f$  is the fluid gradient in psi/ft. calculated from the water cut and the oil °API gravity,  $b_{\text{ch}}$  is the chamber volumetric capacity in Br/Mft., and  $A_{\text{diff}}$  is given by:

$$A_{\text{diff}} = \ln \left[ \frac{A' - F(D_{\text{ch}}/1000)Q_c\rho_t}{A' - Q_c\rho_t} \right] \quad (12.41)$$

Where, as indicated earlier,  $Q_c$  is the true liquid column in feet (taking into consideration the free gas in the liquid) inside the chamber just when the operating valve opens and  $A'$  (the maximum drawdown) is:

$$A' = P_{\text{sbh}} - \left[ (D_{\text{pt}} - D_{\text{ch}})\rho_t + P_{\text{wh}}f_{\text{g}_d} \right] \quad (12.42)$$

Where  $P_{\text{sbh}}$  is the static reservoir pressure in psig,  $D_{\text{pt}}$  is the perforations' depth in feet,  $D_{\text{ch}}$  is the depth of the perforated nipple in feet,  $\rho_t$  is the true liquid pressure gradient in psi/ft. (which takes into account the gas in the liquid column),  $P_{\text{wh}}$  is the minimum wellhead production pressure in psig, and  $f_{\text{g}_d}$  is the gas factor that is used to calculate the pressure at depth from the surface gas pressure. Note that in Eq. 12.40,  $\rho_f$  is used instead of  $\rho_t$ . This is because Eq. 12.40 is derived from the daily liquid production in barrels

of liquid per day (without gas). On the other hand, the way Eq. 12.41 is expressed does not contradict Eq. 12.40 because  $Q_c \rho_l$  is equal to  $Q' \rho_f$ , where  $Q'$  is the length of the liquid column without gas in the chamber.

Finally, once the productivity index  $J$  has been calculated, the optimum cycle time can be estimated from Eq. 10.115 given for accumulation chamber design, which is basically the same for simple type completions but with factors  $A'$ ,  $c_m$ , and  $\alpha$  modified for accumulation-chamber installation as shown in Section 10.7.

If it is necessary, the cycle time can be changed by increasing or decreasing the surface gas flow rate in choke control intermittent gas lift, using Eq. 12.21 as a guide.

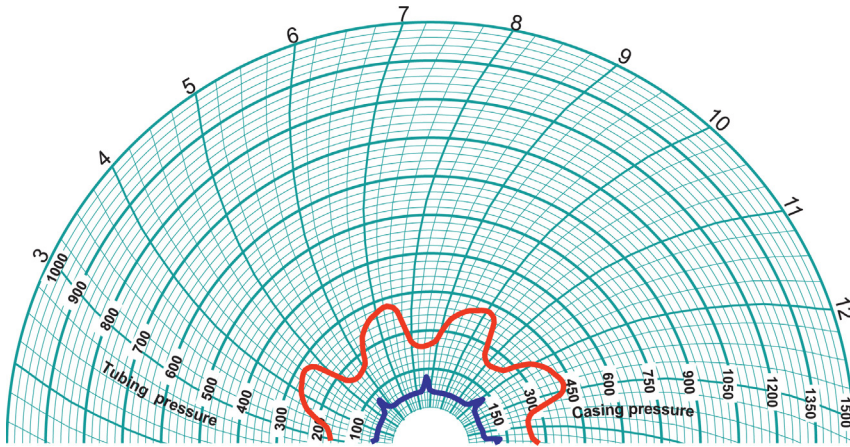
If time cycle controllers are used, the cycle time can be changed by changing the time in which the controller remains closed ( $T_{\text{off}}$ ). If the volume of gas injected per cycle is not adequate, it can be changed by varying the time in which the controller is opened ( $T_{\text{on}}$ ). It should be emphasized once again that this last action cannot be done for choke-control intermittent gas lift, in which the volume of gas injected per cycle can only be significantly varied by changing the operating gas lift valve (increasing or decreasing the area ratio of the valve).

A complete troubleshooting analysis of a double-packer accumulation chamber using downhole temperature and pressure surveys is presented in Section 12.3.3, Example #7.

*Damaged gas lift valve with its internal check valve in good working conditions.*

If the gas lift valve has failed open (damaged bellows in single-element valves or the piston of a pilot valve is stuck open), the minimum injection pressure is usually very low because the gas in the annulus is almost all completely injected into the tubing at each cycle. Another characteristic that helps identify a damaged gas lift valve is the fact that the difference between the maximum and minimum injection pressures is considerably larger than the expected spread of the valve. This differential pressure could be very large and the pressure peaks are usually rounded (instead of sharp and well-defined peaks).

The case in which a well with a damaged gas lift valve can produce on intermittent gas lift is different from the one in which there is a tubing-annulus communications because in the latter case the wells usually produce liquid slugs that are very large and many times even larger than what the reservoir pressure could provided. This is due to the fact that, in wells with tubing-annulus communications, a good part of the liquid being produced



■ FIGURE 12.5 Wellhead pressure behavior of a well with a damaged gas lift valve.

accumulates in the annulus at the beginning of each cycle. But wells with tubing-annulus communications and very low reservoir pressure are easily mistaken as wells with a damaged valve (with its internal check valve in good condition). The only way to verify that a communication does exist is many times only possible by using sonic devices to check if the liquid level in the annulus is changing in time or by performing a communication test as explained in Section 11.5.1. Fig. 12.5 shows a pressure chart from a well with a damaged operating valve. Wells producing in this manner would require very large flow rates to operate them on continuous flow if the main port diameter of the operating damaged valve is very large, which is usually the case for pilot valves.

The mechanism by which a well with a damaged valve produces on intermittent gas lift is explained as follows (there is no liquid accumulation in the annulus):

- At the beginning of the liquid column generation period, the pressures in the production tubing at valve's depth and in the casing are increasing and not only is the injection pressure less than the production pressure, but also the production pressure increases faster than the injection pressure does at this stage of the cycle. The injection pressure is low because the annulus is almost entirely vented every time the liquid slug is produced.
- Eventually, the rate at which the liquid column is regenerated begins to decline because of its own hydrostatic pressure exerted against the formation. At that time, the injection pressure also continues to

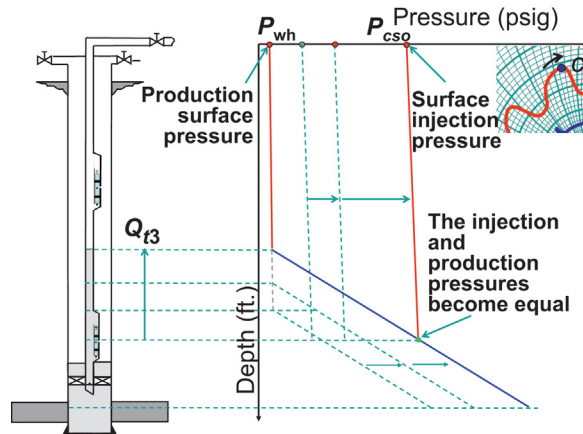
increase at a declining rate but now the injection pressure is increasing faster than the production tubing pressure.

- When the injection pressure becomes equal to the production pressure at valve's depth, gas injection into the tubing begins. Due to the large port diameter of the damaged valve, the gas flow rate into the tubing could be very large. This allows the liquid slug to rise to the surface at an approximately constant velocity, even though the injection pressure is only slightly greater than the hydrostatic pressure of the liquid slug plus the friction pressure drop generated by the slug movement. This velocity is usually very low and, in consequence, the fallback losses tend to be very large, especially when the injection gas begins to flow into the tubing. However, as the liquid slug travels toward the surface, its length decreases and therefore its velocity increases, so that the instantaneous fallback losses are not as pronounced by the time the slug reaches the surface. Due to the large overall fallback losses and the fact that the annular pressure is reduced to a very low pressure at the end of every gas injection cycle, the injection gas/liquid ratio is usually very large. When gas injection into the tubing begins, the liquid slug must be accelerated from a velocity equal to zero: this is very inefficient because the injection pressure is very similar to the production pressure, so it takes a while to start the liquid slug moving upwards at an acceptably high velocity. This is the reason why the pressure peaks are not sharp but rather rounded. In contrast, when there is a tubing-annulus communication, the liquid in the annulus enters the tubing first and then, when the gas enters the tubing, the liquid has already acquired a velocity greater than zero with the following consequences: (1) the liquid fallback losses that take place when the gas enters the tubing are reduced, and (2) the gas injection pressure is greater than the static pressure of the gas and liquid in the tubing because the injection gas has to overcome the friction pressure drop of the liquid slug moving upwards in the tubing.

The way to analyze the operation of the well with a damaged valve (when there is no liquid accumulation in the annulus) is by calculating the initial liquid column length knowing that the injection pressure at the valve is equal to the tubing pressure (also at valve's depth) just when gas injection into the tubing begins. This is mathematically expressed by the following equation, in which all factors are known except the initial liquid column length (called  $Q_{ini}$ ):

$$P_{max}f_{gc} = P_{wh}f_{gt} + Q_{ini}P_f \quad (12.43)$$





■ FIGURE 12.8 Just before gas injection through the damaged gas lift valve begins.

$Q_{ini}$  calculated using 12.43 is compared to the produced liquid column, which is calculated by:

$$Q_{prod} = \frac{T_{cycle} (\text{min})(q_f \text{ Br/D})}{1440 (\text{min/D})} \quad (12.44)$$

$$B_t (\text{Br/Mft.})(\text{Mft.}/1000 \text{ ft.})$$

Where  $B_t$  is the volumetric capacity of the production tubing in Br/Mft. given by Eq. 12.25,  $Q_{prod}$  is the length of the produced liquid column in feet,  $T_{cycle}$  is the measured total cycle time in minutes,  $q_f$  is the measured daily liquid production in Br/D. The fallback factor  $F$  can then be estimated from:

$$F = \frac{(Q_{ini} - Q_{prod})/Q_{ini}}{D_{ov}/1000} \quad (12.45)$$

$F$  is the fraction (from 0 to 1) of the liquid column that is not produced to the surface per each Mft. of depth of the gas injection point.  $D_{ov}$  is the depth of the point of injection in feet. It is possible that the fallback losses would be much greater than 0.05 due to the highly inefficient nature of operating through a damaged gas lift valve. As previously mentioned, these large liquid fallback losses and the uncontrolled gas injection into the tubing at each cycle make the injection gas/liquid ratio be very large for this type of operation.

The productivity index can be calculated using the equation previously given for operations with undamaged gas lift valves, Eq. 12.32. With the productivity index already calculated, the optimum cycle time can be found from

the equation given for intermittent gas lift design, Eq. 10.22. The cycle time could be adjusted to the optimum cycle time by changing the surface injection gas flow rate. But it is better to optimize the operation of the well by installing a new valve so that the injection gas/liquid ratio can be reduced. The troubleshooting analysis is important in this case anyway because its results (such as the optimum cycle time) can be used in the design of the new pilot valve. An intermediate solution (though still not very efficient) is to install a surface time cycle controller with the following advantages: (1) the gas can be injected at a large flow rate into the annulus throughout the time the liquid slug is traveling to the surface, allowing a fast annular pressure increase and helping the liquid slug to achieve a higher velocity; and (2) the total cycle time can be adjusted independently of the gas injection time, which helps optimize the efficiency of the method. However, this solution is still inefficient because, once the controller closes, the annulus is vented without control to very low pressures.

*Intermittent gas injection through an orifice valve.*

Many times engineers with no experience in gas lift operations tend to think that by installing a time cycle controller (intermitter) at the surface, the use of pilot valves can be avoided because the job can be equally done with orifice valves (which are cheaper and not as complex regarding their internal parts). But operating the well in this way will cause the following inconveniences:

- Once the controller closes, the annular injection pressure will drop without control to very low values. This causes unnecessarily large injection gas consumption. When the controller opens in the next cycle, it will take a long time to pressurize the annulus in order to be able to overcome the hydrostatic pressure of the liquid and gas columns in the tubing.
- Just as it is the case for damaged gas lift valves, once the injection gas in the annulus reaches the tubing pressure, the gas injection into the tubing begins with the disadvantage that the liquid must be accelerated from a velocity equal to zero. The acceleration is performed with a gas injection pressure that is only slightly higher than the tubing pressure, which causes large liquid fallback losses at the beginning of the injection cycle. To improve the operation of the well, the orifice diameter must be very large so that gas can be injected at a very large flow rate even with a small pressure difference across this orifice.

Thus, trying to produce a well in this fashion has the same difficulties encountered when trying to operate a well with a damaged gas lift valve. As previously mentioned for the case of a damaged gas lift valve, the advantage

in using time cycle controllers is that the time in which the controller is closed can be adjusted, making it longer or shorter, to optimized the liquid production (the well could produce liquids almost at its full potential but with a very large injection gas/liquid ratio). Additionally, because the controller allows a very large flow rate, the injection time can be reduced, which is another important advantage.

The inefficiency of the intermittent gas lift method through an orifice valve is inversely proportional to the diameter of the orifice. Small orifice diameters cause small injection gas flow rates and, therefore, very slow liquid slug velocities and large fallback losses.

If the well is producing on intermittent gas lift through an orifice valve, the troubleshooting analysis is performed in the same way as explained for a well with a damaged gas lift valve with its internal check valve in good condition: use Eqs. 12.43–12.45 to find the liquid fallback losses and then use Eqs. 12.32 and 10.22 to find the productivity index and the optimum cycle time, respectively.

Intermittent gas lift in wells with an orifice valve is many times involuntarily induced when the orifice diameter is very large compared to the one that is required for continuous gas injection under current operational conditions. This is usually a consequence of a very low reservoir pressure that maintains a low production pressure so that very high gas injection flow rates are needed to produce the well on continuous gas lift in a stable manner.

#### *Casing–tubing communication.*

When there is an annulus–tubing communication, the produced liquid slugs are usually greater than the ones the reservoir pressure could generate, by itself, in the tubing. This is due to the accumulation-chamber effect that takes place when the liquid accumulates in the annulus and in the tubing at the same time. But it must be kept in mind that if the reservoir pressure is very low, annulus–tubing communications are easily mistaken as wells with a damaged gas lift valve and the only way to identify the problem is by a communication test or by using sonic devices to measure the liquid level in the annulus to see if it is fluctuating. The communication test and the use of sonic devices are explained in Sections 11.5.1 and 11.5.3, respectively.

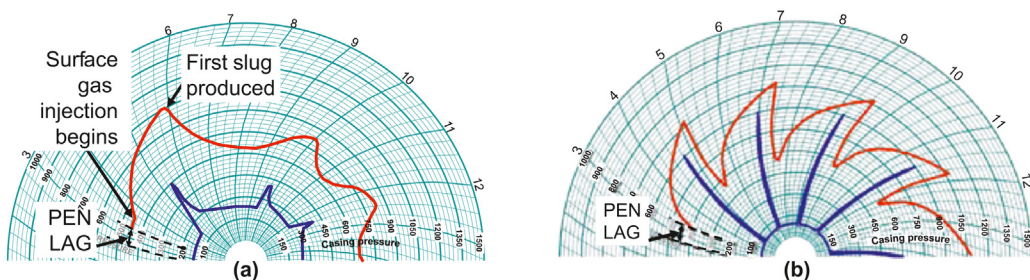
When there is an annulus–tubing communication, the liquid that has accumulated in the annulus enters the tubing first, followed by the injection gas. When the gas behind the liquid enters the tubing, the liquid has already acquired a velocity greater than zero, introducing the following consequences: Liquid fallback losses are somewhat reduced and the injection pressure at the moment the gas begins to enter the tubing must be greater than just the hydrostatic



pressure due to the liquid column that has generated in the tubing plus the gas pressure above it. This increase in the injection pressure is caused by the fact that the gas injection pressure should overcome the friction generated by the movement of the liquid slug in the tubing. This greater injection pressure peak makes troubleshooting calculations more difficult. The measured maximum surface injection pressure must be slightly greater than the surface pressure  $P_{\max}$  calculated from Eq. 12.39; therefore, this equation can only be used to have an idea of the initial liquid column length (which is one of the parameters that can be used to identify an annulus–tubing communication).

Annulus–tubing communications can be easily and quickly identified by the following operational conditions: a large difference between the maximum and minimum injection pressure, long cycle times, and usually a very large liquid production per cycle (depending on the reservoir pressure). Usually, the maximum injection pressures are larger than the ones found in intermittent gas lift through a damaged gas lift valve (with its internal check valve in good condition), but this difference in maximum injection pressures becomes smaller as the reservoir pressure declines. The surface injection pressure pattern is determined by many factors, the most important ones being: size of the communication and its location along the tubing with respect to the static liquid level, the surface injection gas flow rate, and the reservoir pressure. Fig. 12.9 shows typical behaviors of the wellhead pressures in wells with casing–tubing communications.

When there is an annulus–tubing communication, the productivity index cannot be calculated using the equation presented before for accumulation chambers because: (1) it is very difficult to estimate the liquid fallback factor, and (2) the liquid level in the annulus could rise at a very different rate that it does in the tubing. The productivity index could be calculated following an



■ FIGURE 12.9 Wellhead pressure patterns of two wells with annular–tubing communication and high reservoir pressures.

iterative procedure with well's dynamic models, but the problem in this case is that the size of the communication should be known a priori (so that the model can calculate the pressure drop across the communication). Using Eqs. 12.43–12.45 to find the liquid fallback factor is extremely unreliable because these equations can give very large to very small values of the liquid fallback factor (even negative values). The problem in this case is that the volume of gas injected per cycle can go from volumes that are less than the required value to lift the liquid slug to the surface to very large values that might be many times larger than the required volume of gas to be injected per cycle. In the latter case, the liquid fallback factor might be negative because once “even a very small fraction” of the initial liquid slug is produced to the surface, the rest of the liquid slug that was left behind, together with additional liquids coming from the reservoir, are produced with the very large “tail gas” that enters the tubing afterward (while the annular pressure is dropping to very low pressures). Large volumes of gas injected per cycle are not uncommon when the size of the communication is large and the well has from moderate to high reservoir pressure.

Annulus–tubing communications can take place in one of the following ways:

- A hole in the production tubing.
- A damaged single-element gas lift valve with its internal check valve also damaged. A pilot valve with its piston stuck open is in fact an annular–tubing communication if the check valve is incorporated inside the piston.
- An unseated valve in a gas lift mandrel.
- The production packer has failed and allows the flow of gas and liquids through it.
- There is an annular–tubing communication at the wellhead. If the communication is large and the well does not produce any liquids, the wellhead is usually at a temperature lower than usual. In humid climates, the low wellhead temperature is identified because water droplets can be seen on the surface of the wellhead.

The liquid level in the annulus fluctuates when there is a casing–tubing communication. A description of the proper way of using sonic devices to measure the liquid level in this case is given in Section 12.4 and a more thorough explanation on sonic devices is given in chapter: Continuous Gas Lift Troubleshooting. A special wellhead injection pressure behavior with periodic variations caused by an annular–tubing communication (resembling an intermittent gas injection) is presented in Figs. 11.58–11.62, for a case in which the liquid production and the gas injection are in reality continuous

and, therefore, this case cannot be analyzed as if the well was producing on intermittent gas lift.

### 12.3 PRESSURE AND TEMPERATURE SURVEYS FOR WELLS ON INTERMITTENT GAS LIFT

The procedures to perform and analyze downhole pressure and temperature surveys for intermittent gas lift are presented in the section. The objective of these surveys is to find the following parameters:

- The true liquid pressure gradient in the production tubing.
- The production pressure and temperature at the operating valve's depth just before this valve opens.
- Gas lift valve's opening and closing pressures.
- The liquid fallback, productivity index, and the optimum cycle time.

The type of survey that is described here is not designed for reservoir analysis. The data obtained in the survey should be kept in the well's files to serve as a reference for future troubleshooting analyses or to be able to predict the behavior of the well under different conditions, such as new mandrel spacing, higher injection pressures, etc.

#### 12.3.1 Survey procedure

It is usually easy to know if the point of injection is indeed the pilot valve designed as the operating valve. This is due to the fact that pilot valves exhibit a typical behavior easy to identify: a spread larger than expected from single-element valves and a steep drop of the annular injection pressure every time the pilot valve opens. It is customary that wells on intermittent gas lift have single-element unloading valves and a pilot valve at the operating point of injection. Thus, if all valves are working properly, it is easy to know if the operating valve corresponds to the pilot valve. However, sometimes it is not easy to know which, of all the valves installed in the well, corresponds to the current point of injection. Some of the reasons for this uncertainty are: (1) the pilot valve has failed, (2) the well has not been unloaded to the design operating point; (3) the pilot valve itself behaves as a single-element valve on intermittent gas lift, or (4) the well was designed for continuous gas lift and it is behaving in an intermittent fashion. For all of these cases, there is a type of survey that can be used to identify the point of injection, in which:

- Each stop of the sensors at a particular depth should have a minimum duration of two or three complete cycles.
- For each valve, the first stop is located 25 ft. above the gas lift mandrel. This stop is done with the purpose of measuring the maximum and

minimum temperatures just above the valve and verify if there is a local cooling effect by comparing these temperatures with the ones taken below the gas lift mandrel.

- The second stop for each valve is just below the mandrel. This is done to measure the maximum and minimum production pressures as close as possible to each gas lift valve.
- The third and final stop for each valve should be done 50 ft. below the gas lift mandrel. This stop is carried out to compare the production temperatures with the ones obtained 25 ft. above the gas lift mandrel.

The valves that show a maximum injection pressure less than the maximum production pressure (both pressures measured at valve's depth) should correspond to valves located below the actual point of injection. The valve for which its maximum injection pressure is greater than the maximum production pressure (at valve's depth) and, at the same time, shows a temperature drop when comparing the temperatures above and below the valve, should be the operating point of injection.

When the operating valve has been identified, the following steps and recommendations can be taken to evaluate the operation of a well on intermittent gas lift by running and analyzing a different type of downhole survey:

- The well should be tested 1 or 2 days before the survey to know the current production of the well. It is very important that the cycle time during the test be equal to the cycle time during the survey. For this reason, it is important to install the wellhead pressure chart recorder during the test and during the survey. If it is possible, it is preferable to begin the well test the day before the survey and keep the well flowing to the test separator throughout the survey. The minimum well test time should be of 24 h.
- Use electronic pressure and temperature sensors with a scan rate of at least one measurement every 20 s. A safety device ("no-flow" latch) to prevent wireline tools from being blown up the tubing should be included in the set of wireline tools run in the well with the sensors. Run small diameter sensors to minimize flow restriction and the chances of the tools being blown up the well. Available sensors can go from  $\frac{3}{4}$  to 1 $\frac{1}{4}$ -in. OD sensors. The following set of wireline tools (from top to bottom) are recommended: a rope socket, 5 ft. 1 $\frac{1}{4}$ -in. stem, "no-flow" latch(es), 10 ft. 1 $\frac{1}{4}$ -in. stem, and pressure and temperature sensors (use 1-in. stems if 1-in. OD sensors are being used). If possible, use two pressure sensors and two temperature sensors, just in case one of the sensors fails. It is better to use independent sensors specifically designed to measure the temperature (like RTDs) instead of relying on

the temperature sensors installed as part of the pressure sensors, which are used to compensate the pressure readings for temperature changes. In any case, be aware of the response time of the temperature sensors because it might take a long time for them to measure the actual surrounding temperature.

- Do not close the well to production or change the surface gas injection flow rate during the first phase of the survey (not even when installing the lubricator). The communication between the well and the separator should be maintained at all time during the survey.
- Install the pressure chart recorder at the wellhead and verify the accuracy of the wellhead pressure sensors with an accurately calibrated manometer. At the beginning of the survey and prior to opening the lubricator, wait for one or two cycles to corroborate the actual cycle time. Verify also that the clock of the chart recorder is working properly and set it for 12 or 24 h per revolution.
- Install the lubricator and check (with the appropriate wireline tools): the total depth of the well (or the depth of the standing valve), the operating valve's depth, and the conditions of the production tubing. This should be quickly done during the liquid column generation time.
- Just after a slug has been produced, open the lubricator and run the pressure and temperature sensors in the well to about 15 ft. below the wellhead and wait for 5 min if possible. During this first stop, the wireline tools should not be very close to the wellhead because if, for any reason, the well unexpectedly intermits, the wireline tools might hit the lubricator when the liquid slug reaches the surface and the wireline might break. The purpose of this first stop is to compare the readings from the sensors run in the well with the wellhead pressures registered on the two-pen chart recorder or stored in the SCADA system.
- Then, lower the sensors down to 15 ft. below the operating valve's depth and wait at that depth for a period of time equal to three complete cycles.
- If there is a standing valve installed anywhere along the tubing, it is better to pull it out of the well a few days before the well is tested. By doing so, the bottomhole pressure at the perforations can be measured and the true liquid pressure gradient below the operating valve during the well's normal operation can be determined.
- After the second stop (15 ft. below the operating valve) and if, for any reason, the standing valve cannot be pulled out of the well, the survey should be performed in the following way:
  - Staying 15 ft. below the operating valve, the surface gas injection is shut off by closing the casing valve at the wellhead and flow control

valve at the injection manifold. Both valves should be closed to avoid a leak that could pressurize the annulus during the second phase of the survey. To avoid opening the operating valve due to the increase in the production pressure during the last stages of the survey, the casing pressure should be vented to a pressure 50 psig below the operating gas lift valve's closing pressure. For wells with a high injection frequency (short cycle times), wait for at least 3 h before changing the position of the sensors. For wells with longer cycle times, wait for a period of time equivalent to three cycles (with the wellhead open to production but with no gas injection).

- For the last stop, the sensors are raised above the operating valve to a distance equal to the liquid slug length that the well was producing prior to shutting off the gas injection (calculated from the measured daily liquid production, the number of cycles in one day, and the production tubing volumetric capacity). The fact that the gas in the liquid slug and the fallback losses are not taken into account in the calculation of this distance above the gas lift mandrel would allow the sensors to be below the liquid level during this last stop, which should last for 5–10 min only. The data taken during this stop is used to approximate the true liquid pressure gradient, which is the gradient of the liquid with free gas.
- If a standing valve is not installed in the well, the survey (after the second stop) should proceed in the following way:
  - Lower the sensors down to the top of the perforations and stay at that depth for a period of three complete cycles, without shutting off the surface gas injection into the annulus.
  - Then, staying at the top of the perforations, shut off the surface gas injection by closing the casing gas injection valve at the wellhead and the flow control valve at the injection manifold. As indicated earlier, both valves should be closed to prevent the annulus from being pressurized. To avoid opening the operating valve due to the increase in the production pressure during the last stages of the survey, the casing pressure should be vented to a pressure 50 psig below the operating gas lift valve's closing pressure.
  - Once the surface gas injection has been shut off, leave the production tubing open to production and wait for at least 3 h without changing the position of the sensors in case of wells with high injection frequencies. For wells with longer cycle times, wait for a period of time equivalent to three cycles with the gas injection equal to zero and with the production tubing open to production.
  - Raise the sensors to 15 ft. below the operating valve and wait for only 10 min before pulling the instruments out of the well to

finish the survey. This last stop is performed to compare the true liquid pressure gradient measured while the well is under normal operation with the liquid pressure gradient measured after the gas injection has stopped for several hours.

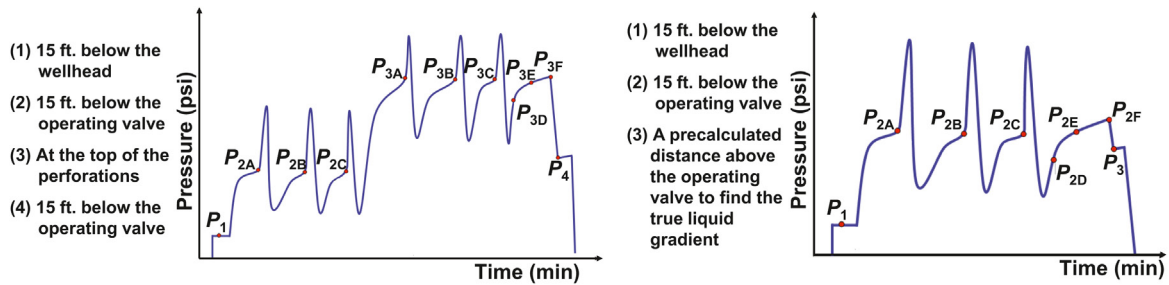
Downhole surveys in wells with very small tubing diameters are very risky. This is due to the very high liquid velocity around the wireline tools. The following precautions are recommended in this case:

- Select downhole pressure sensors with the smallest outside diameter.
- Install a wellhead pressure chart recorder to measure the cycle time and verify that the liquid column generation time is long enough to run the sensors in the well down to the top of the perforations before the operating valve opens.
- If the travel time of the sensors is shorter than the liquid column generation time, lower the sensors as fast as possible down to the top of the perforations and leave them at that depth for a period of time no shorter than three complete cycles before closing the surface gas injection.
- If the cycle time is very short: wait for the liquid slug to be produced, stop the surface gas injection, quickly lower the sensors to the top of the perforations and immediately open the gas injection to exactly the same flow rate it had before, leaving the sensors at that position for a time no shorter than five or six complete cycles.
- After the cycles mentioned in the last two points, shut off the surface gas injection to the well and wait in this condition for a period of time equal to the equivalent of three cycles. For the final stop, raise the sensors for 10 min at a depth of 15 ft. below the operating valve.

If the survey is performed in a well with an accumulation chamber, the sensors should be lowered to a depth just above the standing valve and leave them at that depth for two or three cycles. Then, shut off the surface gas injection, reduce the casing pressure by 50 psig and, with the sensors still above the standing valve, wait for a period of time equivalent to the duration of three complete cycles. Then, raise the sensors to the middle of the accumulation chamber (halfway between the two packers) for 10 min and finally to the depth of the upper packer for another 10 min.

### 12.3.2 Survey analysis

With the equations that are presented in the section, the data gathered during the survey can be used to find: (1) the true liquid pressure gradient, (2) the production pressure and temperature at valve's depth when it opens, (3) operating valve's dynamic behavior, (4) liquid fallback losses, (5) productivity index, and (6) the optimum cycle time.

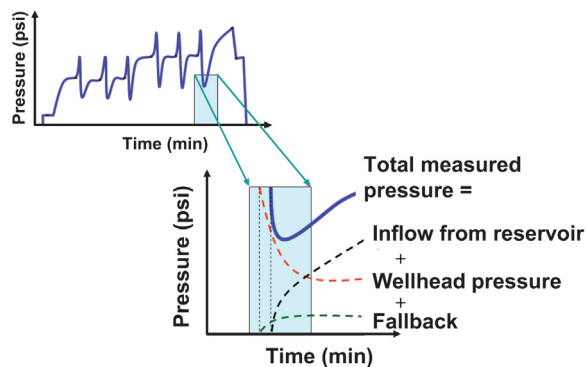


■ FIGURE 12.10 Results of downhole pressure surveys. (a) Well without standing valve and (b) well with standing valve.

Fig. 12.10 shows typical results from downhole pressure surveys and the important measurements at each stop for: (1) a well without a standing valve, and (2) a well with a standing valve below the operating gas lift valve.

In Fig. 12.10a (for wells without a standing valve), the first stop is 15 ft. below the wellhead, the second stop is at 15 ft. below the operating valve, the third stop is at the top of the perforations, and the fourth stop is done again 15 ft. below the operating valve. For wells with a standing valve located below the operating gas lift valve, the first stop is 15 ft. below the wellhead, the second stop is 15 ft. below the operating valve, and the third stop is at a distance above the operating valve equal to the produced liquid column per cycle, calculated from the liquid production per cycle and the production tubing volumetric capacity (the free gas in the liquid and the liquid fallback losses are on purpose not taken into account, so that the sensors would be located below the liquid level during this last stop).

The minimum pressure at the beginning of the liquid column regeneration time does not give any practical information to perform a quantitative analysis: Fig. 12.11 shows the three components of the total downhole pressure



■ FIGURE 12.11 Components of the production pressure at the beginning of the liquid column regeneration stage.



at the beginning of the liquid column regeneration period. It is simply not possible to identify each component individually from the simple type of survey explained here. These components could be approximately identified by using a flow meter below the operating valve, two pressure sensors below the liquid level, and a third pressure sensor above the liquid level. The cost of such a survey is only justified for a special research project but not for a routine survey. Because of all these events taking place at the beginning of the liquid column regeneration period, the minimum production pressure is usually very high, giving the wrong impression that the fallback losses are large, which is not necessarily true.

The true liquid pressure gradient is usually much smaller than the one calculated from the water cut and the API gravity of the oil alone. It is not unusual to find true liquid pressure gradients equal to only 30–60% of the pressure gradient calculated from the water cut and the API gravity of the oil. This difference is due to the free gas present in the liquid while the liquid column is being regenerated. It is not important to know the true liquid pressure gradient when the force-balance equation is used to study the actual operation of the valve because the effect of the gas present in the liquid on the production pressure at valve's depth,  $P_{10}$ , is negligible: this pressure depends on the total volume of liquid accumulated above the operating valve and not on how the liquids are distributed in a long or short column (if the liquid column is long, the true liquid pressure gradient is small and vice versa, thus as long as the total volume of liquid is the same, the production pressure at valve's depth will also be the same). However, it is important to know the true pressure gradient to be able to estimate the productivity index and the optimum cycle time, or when accumulation chambers are being analyzed.

The best estimate of the true liquid pressure gradient,  $\rho_l$  in psi/ft., is obtained if a standing valve is not installed in the well, for which the following equation is used:

$$\rho_l = \frac{P_{3,\text{avg}} - P_{2,\text{avg}}}{D_{3-2}} \quad (12.46)$$

Where  $P_{3,\text{avg}}$  and  $P_{2,\text{avg}}$  are the average pressures for the third and second stops, respectively, just before the valve opens, and  $D_{3-2}$  is the vertical distance between the second and the third stops, see Fig. 12.10a. If the well has a standing valve, the true liquid pressure gradient can be estimated from the last two stops, pressures  $P_{2F}$  and  $P_3$  (see Fig. 12.10b), but this is only an approximation because these pressures do not represent the conditions when the well is in normal operation.

Once the true liquid pressure gradient is calculated, the production opening pressure at valve's depth is calculated from the following equation:

$$P_{to} = P_{2,avg} - (\Delta H)\rho_l \quad (12.47)$$

Where  $\Delta H$  is the vertical distance between the gas lift valve and the pressure sensor below it during the second stop ( $\Delta H$  is recommended to be equal to 15 ft.). It is also convenient to measure the temperature if nitrogen-charged valves are used because for intermittent gas lift it is extremely difficult to estimate the temperature around the valve just before it opens.

Once the production pressure and temperature at valve's depth are known, the performance of the valve can be investigated from the force-balance equation if the gas injection annular pressure at valve's depth has been accurately determined. The valve's area ratio  $R$  can be obtained from the force-balance equation as:

$$R = \frac{P_{cvo} - P_{bt}}{P_{cvo} - P_{to}} \quad (12.48)$$

Where  $P_{bt}$  is the calibration closing pressure if the valve is spring loaded, for which it is called  $P_{tr}$ . For nitrogen-charged valves,  $P_{bt}$  is the dome pressure at operating conditions.  $P_{bt}$  can be determined from the nitrogen pressure at test-rack conditions,  $P'_b$ , which is in turn calculated from the valve's test-rack opening pressure as indicated in [Section 12.2.2](#).

Eq. 12.48 can be used in several ways. For example, it can be used to calculate the opening injection pressure,  $P_{cvo}$ , because  $P_{bt}$ ,  $P_{to}$ , and  $R$  are known. This calculated pressure  $P_{cvo}$  is compared to the measured surface injection opening pressure,  $P_{cso}$ , multiplied times the gas factor  $f_g$ . If these two pressures are not approximately equal, it is possible that: (1) the wellhead pressure sensor is giving wrong measurements, (2) the gas lift valve has a different calibration pressure, for which the true value of  $P_{bt}$  could be calculated using Eq. 12.48 with the measured pressure  $P_{cso}$  times  $f_g$  as  $P_{cvo}$ , or (3) it is also possible that the valve in the mandrel has an area ratio different from the one reported in the design, in which case the value of  $R$  is calculated with Eq. 12.48 assuming that  $P_{bt}$  is correct and using: the value of  $P_{cvo}$  estimated from the measured surface pressure  $P_{cso}$  and the value of  $P_{to}$  obtained from the survey (if the calculated value of  $R$  coincides with another commercially available area ratio, a valve different from the one stipulated in the design has been installed in the well). If the value of  $R$  does not coincide with any of the commercially available area ratios, the problem could be a calibration error made at the shop.

Following all these calculations, many questions that the optimization personnel might have with respect to the observed surface injection pressure behavior can be answered. Some of these pressure behaviors are:

- An abnormally large spread (which gives more volume of gas injected per cycle than expected). This might be caused by an area ratio  $R$  greater than the one reported in the design.
- An abnormally small spread (which give less volume of gas injected per cycle than expected). This might be caused by an area ratio  $R$  smaller than the one reported in the design
- A very low opening pressure (which causes a slow liquid slug velocity and large liquid fallback losses) might be an indication that the valve has lost its calibration or an error was made at the shop.
- A very high opening pressure, which causes a larger spread and, therefore, a greater volume of gas injected per cycle, could also be due to a mistake made in the shop during the calibration of the valve or the valve's tail plug has failed (in case of nitrogen-charged valves) and the dome pressure is above the value it is supposed to be.

It is important to point out that to perform the calculations mentioned in this section, it is necessary to measure very accurately the injection and producing pressures at the wellhead ( $P_{cso}$  and  $P_{wh}$ ) because errors in the calculations of, for example, the downhole pressure  $P_{cvo}$  caused by inaccuracies in wellhead pressure measurements might lead to a wrong conclusion regarding the calibration of the valve or the actual value of the area ratio  $R$ . It is also important to know the specific gravity of the injection gas because it plays a major role in the calculation of the gas factor  $f_g$  and, therefore, in the calculation of the downhole injection opening pressure  $P_{cvo}$ .

The liquid fallback factor  $F$  can also be determined from a downhole pressure survey using the following equation:

$$F = \frac{(Q_{ini} - Q_{prod})/Q_{ini}}{D_{ov}/1000} \quad (12.49)$$

$F$  represents the fraction of the initial liquid column length  $Q_{ini}$  that is not produced at each cycle per each thousand feet of depth of the point of injection;  $D_{ov}$  is the depth of the point of injection in feet;  $Q_{prod}$  is the liquid column that is produced to the surface at every cycle, in feet, which is calculated from:

$$Q_{prod} = \frac{q_f T_{cycle}}{1440 B_t} \quad (12.50)$$

Where  $q_f$  is the daily liquid production in Br/D,  $T_{\text{cycle}}$  is the cycle time in minutes, and  $B_t$  is the production tubing volumetric capacity in Br/ft. As it has been indicated, it is important to measure the liquid production during the survey. If this is not possible, the liquid production should be measured a few days before or after the survey, with a gas injection frequency equal to the one during the survey (because the injection frequency affects the liquid production). Due to the impact that  $Q_{\text{prod}}$  has on the accuracy of the fallback factor  $F$  calculated with Eq. 12.49, it is important to measure, as accurately as possible, the well's liquid production.

Liquid column  $Q_{\text{ini}}$ , also in feet, is determined from:

- The production pressure  $P_{\text{to}}$ , in psig, calculated from Eq. 12.47.
- The wellhead pressure  $P_{\text{wh}}$ , measured during the first stop in psig.
- The gas factor  $f_g$ , calculated using the equations given in chapter: Single-Phase Flow (based on the gas specific gravity).
- The liquid pressure gradient  $\rho_f$  in psi/ft., calculated from the water cut and the API gravity of the oil. The gas present in the liquid is not taken into consideration because  $Q_{\text{ini}}$  is compared to the liquid column  $Q_{\text{prod}}$  (calculated from the well test using Eq. 12.50), which does not consider the gas in the liquid either.

The equation to calculate  $Q_{\text{ini}}$  is then:

$$Q_{\text{ini}} = \left( \frac{P_{\text{to}} - P_{\text{wh}} f_g}{\rho_f} \right) \quad (12.51)$$

The liquid pressure gradient is given by:

$$\rho_f = 0.433 \left[ w + (1-w) \left( \frac{141.5}{131.5 + \text{API}} \right) \right] \quad (12.52)$$

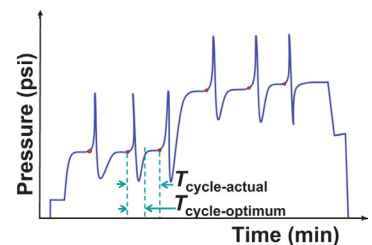
Where  $w$  is the water cut. Then,  $Q_{\text{ini}}$  and  $Q_{\text{prod}}$  are apparent liquid columns (do not take into account the free gas in the liquid). It is correct to calculate the liquid fallback in this way because a given volume of liquid exerts the same hydrostatic pressure with or without gas in it.

It is usually the case that liquid fallback losses calculated from pressure surveys run in accumulation chamber installations are very large, even if the volume of gas injected per cycle and the instantaneous injection gas flow rate into the production tubing are exactly the ones recommended to minimize the liquid fallback losses. When this happens, it is highly probable that the chamber annulus is only partially filled with liquid and calculating the liquid fallback losses as if the chamber was completely filled with liquid

is simply a mistake. The person doing the analysis reaches the conclusion that the accumulation chamber must be completely filled with liquid at the moment the pilot valve opens because the measured downhole pressure indicates that the liquid level in the tubing is at or above the upper packer, which might be true even if the annulus is not completely filled with liquid because of one, or both, of the following reasons: (1) the liquid that enters the annulus has a high gas concentration and what is actually filling the chamber is some sort of foam, and/or (2) the gas on top of the liquid in the annulus cannot be bled off to the tubing because the bleed valve is plugged or its orifice diameter is too small. If one or both of these problems are present, the liquid column in the tubing can be longer than the chamber length (the liquid column is calculated based on the pressure measured above the standing valve just when the operating valve opens), giving the wrong impression that the chamber is completely filled with liquids.

The information gathered after the surface gas injection has been shut off during the last part of the third stop for wells without a standing valve below the operating gas lift valve, or during the last part of the second stop for wells with a standing valve, can be used in two ways:

- To give the optimum cycle time just by visual inspection of the pressure survey: it is possible to see that the gas injection frequency is too high or the cycles are too long by a simple inspection of the way the pressure builds up after the injection has been shut off. It can be seen in Fig. 12.12 that the production pressure increases very rapidly during the first stages of the liquid column regeneration period and then, toward the end of this period, this pressure remains almost constant for a long time. Gas should be injected just before the end of the stage of fast production pressure increase; otherwise, the injection would take place after a period of time in which very little liquid is entering the tubing, thereby decreasing the total daily liquid production.
- Using the pressure measured at two instants, like  $P_{3D}$  and  $P_{3E}$  in Fig. 12.10a or  $P_{2D}$  and  $P_{2E}$  in Fig. 12.10b, the productivity index and the optimum cycle time can be estimated in an analytical way as described later. It is recommended that  $P_{3D}$  or  $P_{2D}$ , be taken after the wellhead pressure has decreased to its minimum value during the cycle and allow sufficient time for all the liquid fallback to settle at the bottom of the well, so that the increment in the downhole tubing pressure is solely due to fluids coming from the reservoir. But points  $P_{3E}$  or  $P_{2E}$ , cannot be taken when the value of the flowing bottomhole pressure is above 50% of the reservoir pressure because these pressures would be above the practical values of the bottomhole flowing



■ FIGURE 12.12 Optimum cycle time determination by inspection.

pressure usually encountered during the normal operation of a well on intermittent gas lift for which its production has been optimized.

If there is a standing valve installed in the tubing, the productivity index  $J$  can be calculated using the following equation:

$$J = \frac{1440B_t}{\Delta t \rho_f} \ln \left[ \frac{A' - Q_{\text{ini}} \rho_f}{A' - Q_{\text{fin}} \rho_f} \right] \quad (12.53)$$

Where  $\Delta t$  is the elapsed time (in minutes) between the two pressure measurements after the surface gas injection was shut off ( $P_{2D}$  and  $P_{2E}$ ),  $B_t$  is the volumetric capacity of the production tubing in Bt/ft.,  $\rho_f$  is the apparent liquid pressure gradient in psi/ft., which is calculated from the water cut and the API gravity of the oil without taking into account the free gas present in the liquid,  $A'$  is the maximum drawdown (found from Eq. 12.54),  $Q_{\text{ini}}$  is the liquid column length above the operating valve at the time of the first selected pressure ( $P_{2D}$ ), and  $Q_{\text{fin}}$  is the liquid column above the operating valve at the time the second selected pressure ( $P_{2E}$ ) is registered a time interval  $\Delta t$  later.  $A'$ ,  $Q_{\text{ini}}$ , and  $Q_{\text{fin}}$  are given by:

$$A' = P_{\text{sbh}} - (D_{\text{pt}} - D_{\text{ov}}) \rho_l - P_{\text{wh}} f_g \quad (12.54)$$

$$Q_{\text{ini}} = (P_{2D} - P_{\text{wh}} f_g - \Delta H \rho_l) / (\rho_f) \quad (12.55)$$

$$Q_{\text{fin}} = (P_{2E} - P_{\text{wh}} f_g - \Delta H \rho_l) / \rho_f \quad (12.56)$$

As indicated in Fig. 12.10b,  $P_{2D}$  and  $P_{2E}$  are the pressures (in psig)  $\Delta H$  feet below the operating valve that correspond to the second stop (right after the surface gas injection has been shut off),  $P_{\text{sbh}}$  is the reservoir static pressure in psig,  $D_{\text{pt}}$  is the top of the perforations' depth in feet,  $D_{\text{ov}}$  is the depth of the operating valve expressed also in feet,  $\rho_l$  is the true liquid pressure gradient in psi/ft. (estimated from the last two stops, pressures  $P_{2F}$  and  $P_3$ , see Fig. 12.10b),  $P_{\text{wh}}$  is the wellhead pressure measured during the first stop in psig,  $f_g$  is the gas factor that is used to calculate the gas pressure on top of the liquid column from the wellhead pressure  $P_{\text{wh}}$ , and  $\Delta H$  is the distance between the sensors and the operating valve during the second stop, which must be approximately equal to 15 ft.

If the well does not have a standing valve installed in the production tubing, the productivity index is found from the following equation:

$$J = \frac{1440B_t}{\Delta t \rho_f} \ln \left[ \frac{P_{\text{sbh}} - P_{3D}}{P_{\text{sbh}} - P_{3E}} \right] \quad (12.57)$$

Where  $P_{3D}$  and  $P_{3E}$  are the pressures indicated in Fig. 12.10a. Once the productivity index has been calculated, the optimum cycle time can be found using the equations that are given for intermittent gas lift design: Eq. 10.22 for simple type completions or Eq. 10.115 for double packer chambers. If it is necessary, the current cycle time can be adjusted by increasing or decreasing the surface gas flow rate in choke control intermittent gas lift, using Eq. 12.21 as a guide. If time cycle controllers are used, the cycle time can be adjusted by changing the time in which the controller remains closed ( $T_{off}$ ). If the volume of gas per cycle is not adequate, it can be changed by varying the time in which the controller is open ( $T_{on}$ ). The volume of gas injected per cycle cannot be significantly changed for choke-control intermittent gas lift, unless the pilot valve is replaced by another one with a different area ratio (a larger area ratio if more volume of gas is needed or vice versa).

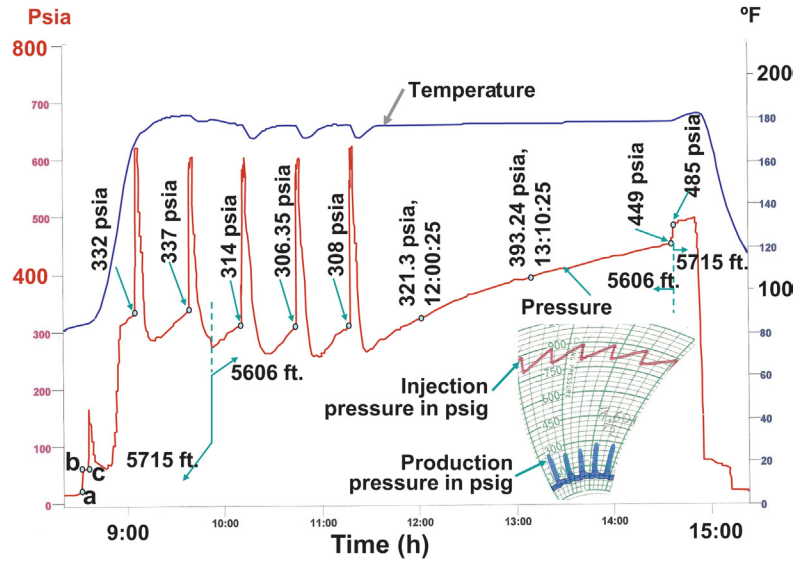
### 12.3.3 Examples of downhole pressure and temperature surveys in intermittent gas lift wells

Several examples of downhole surveys that were run in intermitting gas lift wells under different operational conditions are presented in the section. Even though these surveys were not carried out following the exact recommended procedure given earlier, they are valuable examples to familiarize the reader with downhole pressure surveys for intermittent gas lift.

#### *Example #1*

Fig. 12.13 shows the results from a survey that was run in the well in the following way: (1) first stop at 5715 ft. (top of perforations); (2) second stop at 5606 ft. of depth (15 ft. below the operating valve); and (3) third stop again at 5715 ft. During the first part of the second stop, three injection cycles took place, followed by a second part in which the surface gas injection was shut off to analyze how the production pressure would build up 15 ft. below the gas lift valve.

Well data: 7-in.  $\times$  26-lb/ft. casing; 2.992-in. production tubing ID; top of perforations' depth: 5715 ft.; operating valve's depth: 5591 ft.; gas injection line length: 4000 ft.; gas injection line ID: 2.07 in.; liquid production: 180 STB/D; wellhead production pressure: 60 psig; total cycle time: 35 min; gas injection time through the pilot valve: 5 min; surface injection gas flow rate: 357 Mscf/D; volume of gas injected per cycle: 8677 scf/cycle; water cut 2%; 23°API oil gravity; reservoir pressure: 510 psig. The operating valve was a 1.5-in. OD, spring-loaded, pilot valve, model WF14R, with an area ratio of 0.239 and a test-rack closing pressure equal to 876 psig.



■ FIGURE 12.13 Downhole pressure and temperature survey, example 1.

The liquid pressure gradient (with no gas) calculated from the water cut and the oil API gravity is:

$$\rho_f = 0.433 \left[ 0.02 + 0.98 \frac{141.5}{131.5 + 23} \right] = 0.397 \text{ psi/ft.}$$

According to the last two measurements taken during the survey (at 5606 and 5715 ft. with the surface gas flow rate shut off), the true liquid pressure gradient is:

$$\rho_t = \frac{(485 - 14.7) - (449 - 14.7)}{5715 - 5606} = 0.33 \text{ psi/ft.}$$

The true liquid pressure gradient calculated from the production pressures measured at the moment the operating valve opened for the last time at each depth (at 5606 and 5715 ft. with the well in normal operation), is:

$$\rho_t = \frac{(337 - 14.7) - (308 - 14.7)}{5715 - 5606} = 0.266 \text{ psi/ft.}$$

It can be appreciated that the true liquid pressure gradient is much smaller while the well is in normal operation because more gas is present in the liquid. The apparent liquid column above the pilot valve is found using



Eq. 12.51 from: (1) the liquid pressure gradient (calculated from the water cut and oil API gravity), (2) the wellhead minimum production pressure, and (3) the pressure at the operating valve found from the pressure measured 15 ft. below the operating valve when it opens (using the true liquid pressure gradient), taking into consideration the fact that the survey measurements are in psia and the ones registered in the wellhead chart are in psig ( $f_g$  is assumed to be approximately equal to unity given the low production pressure existing inside the production tubing above the liquid column):

$$Q_{\text{ini}} = \frac{(308 \text{ psia} - 14.7 \text{ psi}) - (15 \text{ ft.})0.266 \text{ psi/ft.} - 60 \text{ psig}}{0.397 \text{ psi/ft.}} = 577.6 \text{ ft.}$$

The produced liquid column at each cycle can be calculated using Eq. 12.50 from the daily liquid production, the cycle time, and the volumetric capacity of the production tubing:

$$Q_{\text{prod}} = \frac{180 \text{ Br/D}}{\frac{1440 \text{ min/D}}{35 \text{ min/cycle}} 0.0086963 \text{ Br/ft.}} = 503.08 \text{ ft./cycle}$$

With the liquid column  $Q_{\text{ini}}$  calculated from the survey and the produced liquid column, the liquid fallback factor  $F$  can be calculated using Eq. 12.49 as:

$$F = \frac{\left[ \frac{577.6 - 503.08}{577.6} \right]}{5.591} = 0.023$$

In other words, approximately 2.3% of the initial liquid column per each Mft. of depth of the point of injection is not produced to the surface. This small liquid fallback factor was due to several operational conditions: the volume of gas injected per cycle was slightly above its required value and the liquid slug velocity was around 1100 ft./min.

Using the valve's force-balance equation, the surface injection opening pressure can be verified. The valve's opening pressure at depth,  $P_{\text{cvo}}$ , is given by:

$$\begin{aligned} P_{\text{cvo}} &= (P_{\text{tr}} - RP_{\text{to}})/(1 - R) \\ &= \{876 \text{ psig} - (0.239)[308 \text{ psia} - 14.7 \text{ psi} - (15 \text{ ft.})0.266 \text{ psi/ft.}]\}/0.761 \\ &= 1060.25 \text{ psig} \end{aligned}$$

Where  $P_{\text{to}}$  is the production pressure in psig at valve's depth when it opens,  $P_{\text{tr}}$  is the test-rack closing pressure in psig, and  $R$  is the valve's area ratio. The gas factor  $f_g$  (in the injection annulus) is estimated to be equal to 1.1638 (using the equations presented in chapter: Single-Phase Flow), so the surface opening pressure is equal to  $1060.25/1.1638 = 911$  psig. The pressure

registered on the wellhead chart was equal to 890 psig, which represents a 2.3% difference in reference to the calculated pressure. This difference is within its expected value because of the poor accuracy of the sensors used in the two-pen pressure chart recorders and the approximate value of the gas specific gravity (used for calculating the gas factor  $f_g$ , not shown here) which was estimated to be equal to 0.72 but its real value could not be verified in this case.

With the pressures measured at times 12:00:25 and 13:10:25 (after the surface gas injection was shut off), the productivity index  $J$  is found from Eq. 12.53 (because the gas injection was shut off while the sensors were 15 ft. below the operating valve and not at the depth of the perforations, calculations are made following the equations given for cases in which there is a standing valve installed in the well):

$$J = \frac{1440B_t}{\Delta t \rho_f} \ln \left[ \frac{A' - Q_{ini} \rho_f}{A' - Q_{fin} \rho_f} \right]$$

Where,

$A' = [P_{sbh} - \rho_l(\text{top of perforations depth} - \text{operating valve depth}) - P_{wh}f_g]$  and  $P_{wh}$  is the wellhead pressure equal to 60 psig. The gas factor can be approximated as:

$$f_g = \left( 1 + \frac{\text{valve's depth in Mft.}}{54} \right)^{1.524} = \left( 1 + \frac{5.591}{54} \right)^{1.524} = 1.162$$

$A'$  is then:

$$A' = 510 \text{ psig} - 0.266 \text{ psi/ft.} (5715 - 5591 \text{ ft.}) - 60 (1.162 \text{ psig}) = 407.296 \text{ psi}$$

The liquid column at time 12:00:25 is (using Eq. 12.55):

$$Q_{ini} = [321.3 \text{ psia} - 14.7 \text{ psi} - 15 \text{ ft.} (0.266 \text{ psi/ft.}) - 60 \text{ psig}(1.162)] / 0.397 \text{ psi/ft.} = 586.62 \text{ ft.}$$

The liquid column at time 13:00:25 is (using Eq. 12.56):

$$Q_{fin} = [393.24 \text{ psia} - 14.7 \text{ psi} - (15 \text{ ft.})0.266 \text{ psi/ft.} - 60 \text{ psig}(1.162)] / 0.397 \text{ psi/ft.} = 767.83 \text{ ft.}$$

The productivity index  $J$  is then equal to:

$$J = \frac{1440B_t}{\Delta t \rho_f} \ln \left[ \frac{A' - Q_{ini} \rho_f}{A' - Q_{fin} \rho_f} \right] = \frac{1440(0.0086963)}{70(0.397)} \ln \left[ \frac{407.2960 - 586.62(0.397)}{407.2960 - 767.83(0.397)} \right] \\ = 0.2397 \text{ Br/D/psi}$$

Once the productivity index has been found, the optimum cycle time can be calculated using the equation for intermittent gas lift design (Eq. 10.22) giving in this case a value of 35 min, which is the one the well had at the time of the survey. It can be concluded then that the well is optimized with respect to the cycle time, the volume of gas injected per cycle, and the velocity of the liquid slug.

It can be seen in the survey shown in Fig. 12.13 that, even though the fallback factor is very small, the minimum pressure 15 ft. below the valve (attained during a normal cycle) is around 245 psig. If the wellhead pressure times the gas factor  $f_g$  (69 psig in total) is subtracted from this minimum production pressure, the minimum pressure due solely to the liquid column is very large and equal to approximately 180 psig. It might be wrongly concluded that the fallback factor has not been correctly calculated, possibly because of errors made in measuring the liquid production and it might be thought that almost all the liquid remains at the bottom of the well. But, as explained in Fig. 12.11, what happens right after the liquid slug has been produced to the surface is very complex and it takes place very rapidly. The production wellhead pressure decreases very fast, the liquid fallback losses are settling at the bottom of the well, and the reservoir is producing liquids and gas at the highest rate possible; thus, by the time the wellhead production pressure goes down to its minimum value, a good part of the liquid column has already been generated.

It can also be observed in Fig. 12.13 that the temperature 15 ft. below the operating valve drops about 10°F each time the gas is injected. This is due to the expansion of the injection gas through the valve and the fact the liquids and gas in the tubing below the valve are pushed downwards, leaving the sensors directly exposed to the injection gas temperature. This compression of the gas and liquids below the operating valve represents a waste of the injection gas energy and it is reflected by the small values of the pressure peaks (of approximately 600 psig) that are shown in the survey. This waste of energy could have a profound impact if the operating valve was located way above the top of the perforations, in which case it is advisable to install a standing valve below the operating gas lift valve and as close as possible to it. In this example, the distance from the operating valve to the top of the perforation is only 124 ft., thus the energy loss is not very important and it is not necessary to install a standing valve in the tubing.

The actual temperature increases faster than it is measured by the sensors as shown in the figure. This is due to the slow response of the temperature sensors. There are sensors with a very fast response time now available that would give a more realistic temperature behavior. The response time of the

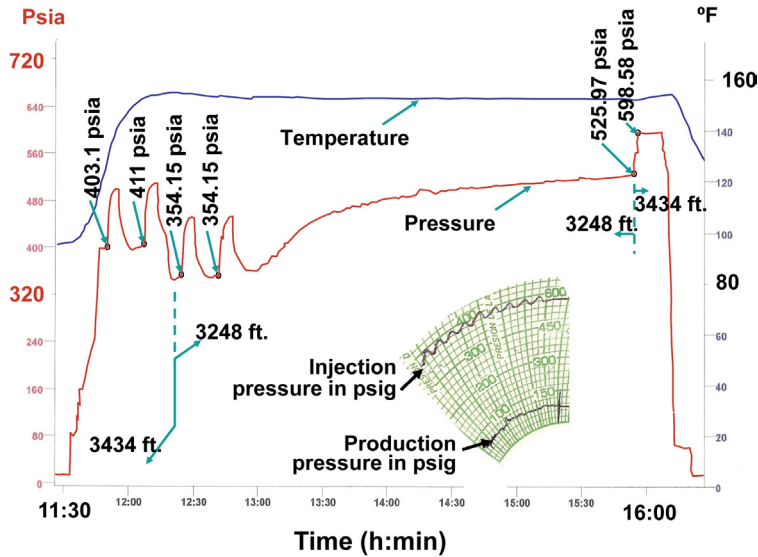
temperature sensors used in the survey constitutes a very important piece of information that the person doing the troubleshooting analysis should have.

Fig. 12.13 shows that from the beginning of the survey to point “a” (around 8:30 am) the sensors were located at the lubricator at a pressure of 14.7 psia. Then, the lubricator was opened and the pressure went up to around 65 psia (point “b”). From point “b” to “c”, the sensors were lowered only 15 ft. below the wellhead so the pressure remained practically equal to the wellhead pressure. At point “c” the pressure began to increase very rapidly, not because the sensors were being run deeper in the well, but because a liquid slug was arriving at the surface. This took place just when the sensors were at their highest risk due to their proximity to the top of the lubricator. If the liquid slug drags the wireline tools upwards, the rope socket might impact against the top of the lubricator, breaking the wireline so the tools would drop to the bottom of the well. Once the slug had surfaced, it is seen in the figure that the pressure dropped to the level it had at point “c” and the operator started lowering the sensors in the well so the pressure began to increase. The steps that should have been taken (instead of what was done) are: install a two-pen chart recorder, wait for one or two cycles, measure the total cycle time, and open the lubricator after making sure that a liquid slug has just been produced and the sensors can safely stay 15 ft. below the wellhead for the duration of the first stop. The surface gas injection should not be shut off during the first part of the survey (unless it is strictly necessary for not having enough time to lower the sensors to the bottom of the well before the pilot valve opens).

### *Example #2*

Fig. 12.14 shows a survey that was run in the well in the following way: (1) the first stop was at a depth of 3434 ft. (top of the perforations); (2) second stop at 3248 ft. (23 ft. below the pilot valve); (3) third stop again at 3434 ft. During the second stop two cycles took place, followed by several hours in which gas was not injected into the well (to see how the production pressure would build up 23 ft. below the valve).

Well data: 5½-in. × 17 lb/ft. casing; production tubing ID: 2.441 in.; top of perforations' depth: 3434 ft.; operating valve's depth: 3225 ft.; gas injection line length: 2700 ft.; surface gas injection line ID: 2.07 in.; liquid production: 60 STB/D; wellhead minimum production pressure: 60 psig; cycle time: 18 min; gas injection time through the pilot valve: 8 min; surface injection gas flow rate: 166 Mscf/D; volume of gas injected per cycle: 2075 scf/cycle; water cut: 50%; 20°API oil gravity; reservoir pressure: 650 psig. The well had a 1-in., nitrogen-charged, injection-pressure-operated pilot valve with an area ratio of 0.164 and a test-rack opening pressure of 659 psig.



■ FIGURE 12.14 Downhole pressure and temperature survey, example 2.

The liquid pressure gradient (with no gas) calculated using Eq. 12.52 from the water cut and oil °API gravity is:

$$\rho_f = 0.433 \left[ 0.5 + 0.5 \frac{141.5}{131.5 + 20} \right] = 0.418 \text{ psi / ft.}$$

According to the last two measurements taken at the end of the survey (at 3434 and 3248 ft. with the surface gas flow rate shut off), the true liquid pressure gradient is:

$$\rho_t = \frac{(598.58 - 14.7) - (525.97 - 14.7)}{3434 - 3248} = 0.39 \text{ psi / ft.}$$

The true liquid pressure gradient calculated from the average production pressures measured just before the gas lift valve opened at depths of 3434 and 3246 ft., with the valve in normal operation, is:

$$\rho_t = \frac{(407 - 14.7) - (354.15 - 14.7)}{3434 - 3248} = 0.284 \text{ psi / ft.}$$

As in the previous example, it can be seen that the true liquid pressure gradient is smaller while the well is in normal operation because of the larger gas content in the liquid.

The liquid column length (from the survey) above the operating valve is calculated using Eq. 12.51 from: (1) the water cut and the API gravity of the oil, (2) the wellhead pressure, (3) the pressure measured below the valve just before it opened (taking into account the fact that the measurements were taken 23 ft. below the valve for which the true liquid pressure gradient has to be used and also considering that the downhole measurements are given in psia and on the surface two-pen chart the pressures are given in psig), and (4) considering  $f_g$  approximately equal to unity (because of the low wellhead production pressure of 60 psig):

$$Q_{\text{ini}} = \frac{(354.15 \text{ psia} - 14.7 \text{ psi}) - (23 \text{ ft.})0.284 \text{ psi/ft.} - 60 \text{ psig}}{0.418 \text{ psi/ft.}} = 652.91 \text{ ft.}$$

The produced liquid column at each cycle is calculated (using Eq. 12.50) from the daily liquid production, the total cycle time, and the volumetric capacity of the production tubing, as:

$$Q_{\text{prod}} = \frac{60 \text{ Br/D}}{\frac{1440 \text{ min/D}}{18 \text{ min/cycle}} 0.005788 \text{ Br/ft.}} = 129.57 \text{ ft./cycle}$$

Using Eq. 12.49, the liquid fallback factor  $F$  can then be calculated from the produced and the initial liquid column lengths:

$$F = \frac{\left[ \frac{652.91 - 129.57}{652.91} \right]}{3.225} = 0.248$$

In other words, approximately 25% of the initial liquid column per each thousand feet of the point of injection depth is not produced. This is a very high liquid fallback factor, even for the type of crude being produced. Even though the operating valve was properly working, the tubing remained with a large liquid content. The total fallback loss was 80% of the initial liquid column. This was due to several factors:

- The required injection gas volume per cycle was about 3300 scf/cycle, while a volume of only 2075 scf/cycle was being injected (only part of the liquid column was reaching the surface).
- The pilot valve remained opened for about twice the time it should have and the liquid slug velocity was very low. This is also the reason why the slug arrival is barely shown in the two-pen pressure chart. The small difference between the upstream and downstream pressures across the pilot valve is one factor that makes the injection pressure drop very slowly.

Without the survey, it would not have been possible to calculate the liquid fallback losses. The valve's force–balance equation can be used to calculate the liquid fallback losses but, as it is shown later, the injection pressure and the gas specific gravity were not accurately measured in this case.

The small volume of gas injected per cycle was a consequence of the small spread of the valve and the low liquid velocity was due to the low injection opening pressure, which also reduced the spread of the valve. The same valve, calibrated at a higher pressure, could reduce the large liquid fallback losses.

There is also the possibility that the well had not been fully unloaded. Under the condition of the well at the time of the analysis, the liquid production could have been increased by temporarily increasing the injection frequency with the purpose of determining if the well was not fully unloaded: To do this, it is necessary to temporarily increase the surface injection gas flow rate to very large values, not allowing time for long liquid columns to regenerate at the bottom of the well. If this could be achieved, the production pressure might be reduced and this low production pressure would in turn increase the spread of the valve, making it possible to reduce the surface injection gas flow rate back to its designed value (or the value it had at the time the survey was run). The gas lift valve needs be replaced only if (after the injection gas flow rate is reduced back to its design value) the well begins to load up with liquids again.

If the valve has not lost its reported calibration pressure, the valve's force–balance equation can be applied to verify the surface gas injection opening pressure ( $P_{cso}$ ). The dome pressure at test-rack conditions,  $P'_b$  at 60°F, can be found from Eq. 12.31 (with the value of  $P'_r$  equal to zero):

$$P'_b = P_{tr}(1 - R) = 659(1 - 0.164) = 550.92 \text{ psig}$$

And the dome pressure at operating conditions,  $P_{bt}$ , is found from Eq. 11.4:

$$P_{bt} = P'_b(b) - (a)$$

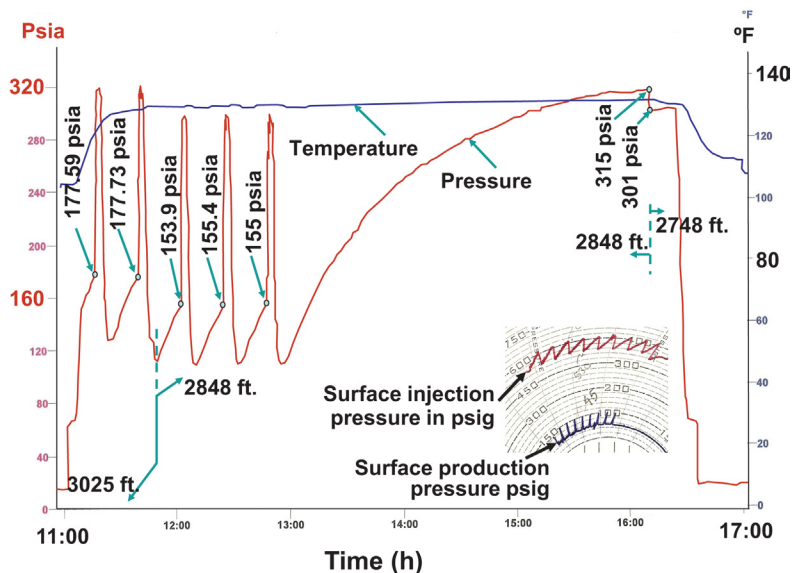
Where  $a = 0.083(153^\circ\text{F} - 60^\circ\text{F}) = 7.719$  and  $b = 1 + 0.002283(153^\circ\text{F} - 60^\circ\text{F}) = 1.212$ , in which the valve temperature has been assumed to be equal to the temperature surrounding the valve during the survey, which was approximately equal to 153°F. Then  $P_{bt}$  is equal to 659.998 psig and the injection opening pressure at valve's depth,  $P_{cvo}$ , is:

$$\begin{aligned} P_{cvo} &= \frac{P_{bt} - P_{is}R}{1 - R} = \frac{659.998 \text{ psig} - [354.15 \text{ psia} - 14.7 \text{ psi} - 23 \text{ ft}(0.284 \text{ psi/ft.})]0.164}{0.836} \\ &= 724.16 \text{ psig} \end{aligned}$$

Where the production pressure measured 23 ft. below the valve during the survey at the moment the valve opened (equal to 354.15 psia) has been used to calculate  $P_{io}$ . The downhole pressure measurements were given in psia so 14.7 psi should be subtracted because the valve calibration equations are expressed in psig. With this calculated opening pressure, the surface opening pressure is found to be:  $P_{cso} = P_{cvo}/f_g = 724.16/1.08433 = 667.84$  psig ( $f_g$  was calculated using the equations given in chapter: Single-Phase Flow, not shown here). The measured surface opening pressure was equal to only 600 psig, which represents a huge difference of approximately 11% with respect to the calculated opening pressure. The accuracy of the pneumatic pressure sensors used in this case with the two-pen chart recorder is usually poor and should always be checked. In some places, these old pneumatic sensors are in used for years without verifying their calibration. The other factor to be considered in this example is the fact that the gas specific gravity was not verified. Even though these calculations give unreliable results in this case, they are presented here to illustrate the calculation procedure that can be used during the troubleshooting analysis to check the operation of a nitrogen-charged gas lift valve.

### Example #3

Fig. 12.15 shows a downhole pressure and temperature survey that was run in the well in the following way: (1) the first stop was at a depth of 3025 ft.



■ FIGURE 12.15 Downhole pressure and temperature survey, example 3.



(top of the perforations); (2) second stop at 2848 ft. (15 ft. below the pilot valve); (3) third stop at 2748 ft. Three cycles took place during the second stop, followed by several hours in which gas was not injected into the well (to see how the production pressure would build up 15 ft. below the gas lift valve).

Well data: 5 1/2-in.  $\times$  17 lb/ft. casing; tubing ID: 2.441 in.; top of perforations' depth: 3025 ft.; operating valve's depth: 2833 ft.; liquid production: 80 STB/D; wellhead production pressure: 45 psig; cycle time: 21.5 min; injection time through the operating valve: 2 min; surface injection gas flow rate: 205.75 Mscf/D; volume of gas injected per cycle: 3072 scf/cycle; water cut: 0%; 21°API oil gravity; reservoir pressure: 420 psig. The well had a 1-in., injection-pressure-operated, nitrogen-charged pilot valve with an area ratio of 0.164 and a test-rack opening pressure of 571 psig.

The liquid pressure gradient calculated from the water cut and the oil API gravity is (from Eq. 12.52):

$$\rho_f = 0.433 \left[ \frac{141.5}{131.5 + 21} \right] = 0.4017 \text{ psi/ft.}$$

The last two pressure measurements being considered in the analysis (at depths of 2848 and 2748 ft., just at the end the period of time without gas injection) give the following true liquid pressure gradient:

$$\rho_t = \frac{(315 - 14.7) - (301 - 14.7)}{2848 - 2748} = 0.14 \text{ psi/ft.}$$

The true liquid pressure gradient calculated from the measured pressures just before the valve opened at the first and second stops is found from:

$$\rho_t = \frac{(177.73 - 14.7) - (153.9 - 14.7)}{3025 - 2846} = 0.133 \text{ psi/ft.}$$

It can be seen that the true liquid pressure gradient is only slightly smaller during the normal operation of the well in comparison to the liquid pressure gradient determined from the measurements at the end of the survey (last stop), but considerable less than the gradient calculated from the water cut and oil API gravity.

Initial liquid column length (above the operating valve) calculation (using Eq. 12.51 with  $f_g$  approximately equal to unity):

$$Q_{ini} = \frac{155.4 \text{ psia} - 14.7 \text{ psi} - (15 \text{ ft.})0.133 \text{ psi/ft.} - 45 \text{ psig}}{0.4017 \text{ psi/ft.}} = 233.27 \text{ ft.}$$

The produced liquid column per cycle is (from Eq. 12.50):

$$Q_{\text{prod}} = \frac{80 \text{ Br/D}}{\frac{1440 \text{ min/D}}{21.5 \text{ min/cycle}} \cdot 0.005788 \text{ Br/ft.}} = 206.36 \text{ ft./cycle}$$

The liquid fallback factor is then calculated from the produced and the initial liquid column lengths (using Eq. 12.49):

$$F = \frac{\left[ \frac{233.27 - 206.36}{233.27} \right]}{2.833} = 0.04$$

Then, 4% of the initial liquid column per each thousand feet of depth of the point of injection cannot be produced. In Example 2, the liquid fallback factor was much larger even though the well had the same pilot valve calibrated also at a low opening pressure. However, in this example, the well is shallower and with a lower reservoir pressure which made it possible for the well to be satisfactorily unloaded and produced with the volume of gas per cycle the spread of the valve could provide. Had the volume of gas per cycle been just a bit larger in Example 2, the fallback losses would have been considerably smaller.

Just as in the previous example, the nitrogen pressure at 60°F,  $P'_b$ , is found from Eq. 12.31 (with the value of  $P'_r$  equal to zero):

$$P'_b = P_r (1 - R) = 571(0.836) = 477.35 \text{ psig}$$

The nitrogen pressure at operating conditions,  $P_{bt}$ , is found from Eq. 11.4:

$$P_{bt} = P'_b(b) - (a)$$

Where  $a = 0.083 (136^\circ\text{F} - 60^\circ\text{F}) = 6.308$  and  $b = 1 + 0.002283 (136^\circ\text{F} - 60^\circ\text{F}) = 1.1735$  (using the valve temperature measured in the survey equal to 136°F). Then  $P_{bt}$  is equal to 553.86 psig and the opening injection pressure at valve's depth,  $P_{cvo}$ , is found as in the previous examples from:

$$P_{cvo} = \frac{P_{bt} - P_{to}R}{1 - R} = \frac{553.86 - [155.4 - 14.7 - (15)0.133]0.164}{0.836} = 635.3 \text{ psig}$$

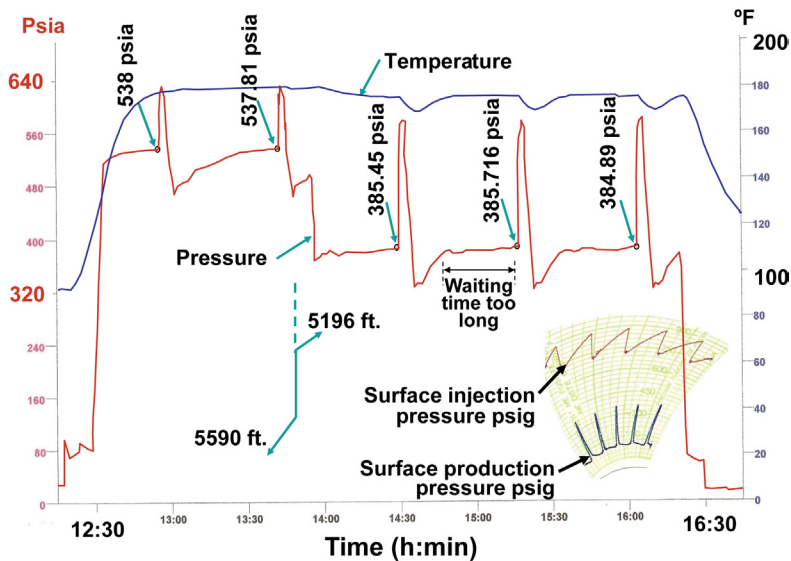
Where the measured value of the production pressure 15 ft. below the operating valve, equal to 155.4 psia, has been used to calculate  $P_{to}$ . With this opening pressure at depth, the surface gas injection pressure  $P_{cso}$  is determined ( $f_g$  was calculated using the equations given in chapter: Single-Phase Flow, not shown here):  $P_{cso} = P_{cvo}/f_g = 635.3/1.08238 = 586.94$  psig. The measured surface opening pressure is 600 psi. The calculated surface opening pressure is

approximately -2% different from its measured value. This is not unusual for: (1) the type of pneumatic instruments commonly used in old two-pen chart recorders, like the one in this example, and (2) the uncertainty in the measurement of the gas specific gravity used in the calculation of the gas factor  $f_g$ .

Even though the optimum cycle time appears to be much longer than its current value (by just looking at the survey), the productivity index (calculated from the equations given in Example 1) was between 0.3 and 0.5 Br/D-psi, for which the optimum cycle time should be equal to approximately any value from 18 to 23 min. Thus, the cycle time during the survey was within the margin of error of the calculated optimum cycle time and it can be concluded that the well was optimized. It is not always possible then to determine the optimum cycle time by simple visual inspection of the results from the survey. The best way to confirm the optimum cycle time is to test the well at different gas injection frequencies and establish which one maximizes the daily liquid production.

#### Example #4

Fig. 12.16 shows the results from a survey that was run in the following order: (1) the first stop was at a depth of 5590 ft. (top of the perforations); (2) second stop at 5196 ft. (15 ft. below the pilot valve); (3) third stop again at 5590 ft. (which was done the following day and it is not shown in the figure).



■ FIGURE 12.16 Downhole pressure and temperature survey, example 4.

Three cycles took place during the second stop, followed by several hours in which gas was not injected into the well (not shown here either) to see how the production pressure was building up 15 ft. below the gas lift valve.

Well data: 7-in.  $\times$  23 lb/ft. casing; production tubing ID: 3.958 in; top of perforations' depth: 5590 ft.; operating valve's depth: 5181 ft.; liquid production: 160 STB/D; wellhead production pressure: 60 psig; cycle time: 47 min; downhole injection time (through the pilot valve): 4 min; surface gas flow rate: 236 Mscf/D; volume of gas injected per cycle: 7702 scf/cycle; water cut 50%; 24° API oil gravity; reservoir pressure: 564 psig. The well had a 1.5-in., injection-pressure-operated, spring-loaded pilot valve, model WF14R, with an area ratio of 0.426 and a test-rack closing pressure of 688 psig.

The liquid pressure gradient calculated from the water cut and the oil API gravity using Eq. 12.52 is:

$$\rho_f = 0.433 \left[ 0.5 + 0.5 \frac{141.5}{131.5 + 24} \right] = 0.4135 \text{ psi/ft.}$$

Using Eq. 12.46, the last two measurements (not shown in the figure) considered in the analysis of the survey after the surface gas flow rate was shut off, gave a true liquid pressure gradient of:

$$\rho_t = \frac{(554.13 - 14.7) - (402.97 - 14.7)}{5590 - 5196} = 0.383 \text{ psi/ft.}$$

The true liquid pressure gradient calculated from the measured pressures just before the valve opened at the first and second stops is given by:

$$\rho_t = \frac{(538 - 14.7) - (385 - 14.7)}{5590 - 5196} = 0.388 \text{ psi/ft.}$$

It can be seen that the true liquid pressure gradient during the well's normal operation is only slightly greater than the gradient calculated with the data taken after the gas was shut off. In both cases, the true pressure gradient is smaller than the one calculated from the water cut and the oil API gravity but the difference is not as pronounced as it was in previous examples. This reflects a small formation gas/liquid ratio, which is typical of wells with large water cuts.

Using Eq. 12.51, the calculation of the initial liquid column length above the operating valve (from the survey) is as follows:

$$Q_{\text{ini}} = \frac{385 \text{ psia} - 14.7 \text{ psi} - (15 \text{ ft.})0.388 \text{ psi/ft.} - 60 \text{ psig}(1.1498)}{0.4135 \text{ psi/ft.}} = 714.6 \text{ ft.}$$

Where (given the fact that the depth of the point of injection is much greater than in previous examples) the hydrostatic pressure of the gas column above the liquid column has been taken into consideration by multiplying the wellhead pressure of 60 psig by the gas factor,  $f_g$ , calculated by the following equation:

$$f_g = \left(1 + \frac{\text{valve's depth Mft.}}{54}\right)^{1.524} = \left(1 + \frac{5.181}{54}\right)^{1.524} = 1.1498$$

The value of  $f_g$  just found (1.1498) should in fact be the first value of an iteration procedure that must be performed to simultaneously find  $f_g$  and  $Q_{\text{ini}}$ , in which the depth to be used at each calculation of  $f_g$  should be equal to the valve's depth minus the length of the liquid column and not just the valve's depth as shown in the last equation (because the gas pressure at depth is applied on top of the liquid column). In this case, given the fact that the wellhead production pressure is very low, this iteration procedure is not very important.

The liquid column length, calculated from Eq. 12.50 using the well's liquid production, the total cycle time, and the tubing volumetric capacity, would be:

$$Q_{\text{prod}} = \frac{160 \text{ Br/D}}{\frac{1440 \text{ min/D}}{47 \text{ min/cycle}} \cdot 0.015218 \text{ Br/ft.}} = 343.16 \text{ ft./cycle}$$

With these liquid column lengths (found from the survey and calculated from the well's production), the fallback factor  $F$  is calculated as in previous examples using Eq. 12.49:

$$F = \frac{\left[ \frac{714.6 - 343.16}{714.6} \right]}{5.181} = 0.10$$

This means that 10% of the initial liquid column per each Mft. of depth of the point of injection does not reach the surface; therefore, 52% of the initial liquid column is not produced. This large fallback factor is due to the fact that the tubing diameter is very large (4½-in. tubing) so that the required volume of gas to be injected per cycle is also very large. In this case, the required volume of gas injected per cycle is equal to 10.2 Mscf/cycle, while only 7.7 Mscf/cycle is being injected. Because the instantaneous gas flow rate through the gas lift valve for this particular case is adequate to minimize the liquid fallback losses, it is only necessary to increase the volume of gas to be injected per cycle, which can be achieved by installing the same pilot valve but calibrated at a higher opening pressure (because this will increase

the spread of the valve); but this solution is not possible in this case because the injection pressure was already too close to the injection opening pressure of the unloading valve right above the operating valve. Two important factors are accomplished if the opening pressure of the gas lift valve can be increased:

- The spread of the valve is increased, allowing more volume of gas injected per cycle (as needed for this well).
- The instantaneous gas flow rate through the pilot valve is also increased (not necessary for this example).

Sometimes, it is not possible to increase the injection pressure because: (1) this high pressure would be too close to the gas lift system pressure (also known as line pressure or manifold pressure) so that the gas flow rate into the well would be reduced for not having an adequate pressure differential at the manifold, or (2) the high injection pressure would open an unloading gas lift valve, which is the situation for this particular well.

The spread of the valve can also be increased by installing a valve with a larger area ratio, but this is not possible in this case either because the area ratio of the valve currently installed in the well is the highest available area ratio.

Then, if the injection pressure and the area ratio of the valve cannot be increased, there are two possible solutions that should be contemplated:

- A surface time cycle controller might be used to force the pilot valve to remain open for as long as it is necessary to pass the required injection gas volume per cycle while, at the same time, controlling the injection pressure so that it would not increase above the maximum permitted injection pressure. But this action is only adequate if the instantaneous gas flow rate through the pilot valve is high enough to impart a slug velocity sufficiently high to minimize the liquid fallback (this cannot be achieved if the injection pressure is not high enough). Fortunately, in this case the injection pressure is high enough to minimize the liquid fallback losses. As indicated numerous times in chapter: Design of Intermittent Gas Lift Installations, it is not sufficient to inject all the required volume of gas per cycle, it is also important to achieve the required instantaneous gas flow rate through the pilot valve.
- The gas lift design can be modified to increase the injection opening pressures of all gas lift valves installed in the well and/or replace some of the unloading valves with dummy valves if they are no longer needed. In this way, the injection opening pressure of the pilot valve can be increased.

Using the valve's force–balance equation, the surface opening pressure can be verified. As indicated in chapter: Gas Lift Valve Mechanics, the injection opening pressure at valve depth ( $P_{cvo}$ ) for a spring-loaded, injection-pressure-operated valve, is given by:

$$\begin{aligned} P_{cvo} &= (P_{tr} - RP_{to}) / (1 - R) \\ &= \{688 \text{ psig} - (0.426)[385 \text{ psia} - 14.7 \text{ psi} - (15 \text{ ft.})0.388 \text{ psi / ft.}]\} / 0.574 \\ &= 928.1 \text{ psig} \end{aligned}$$

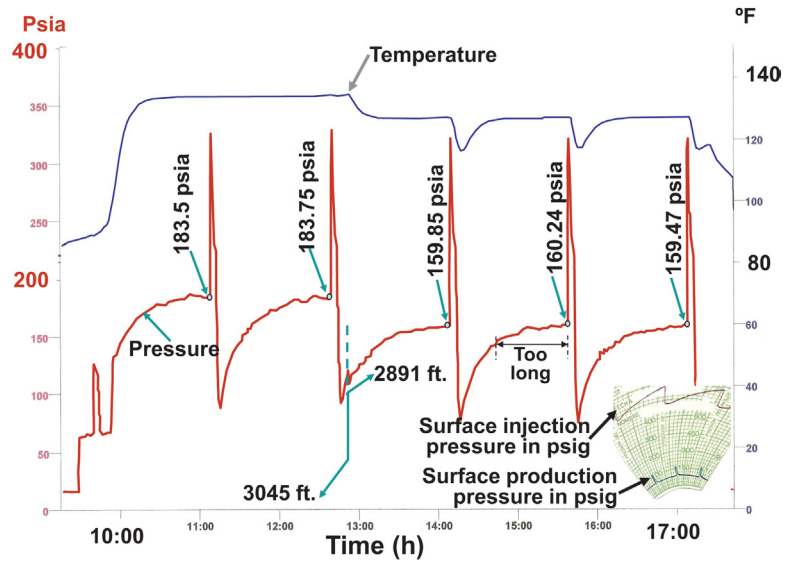
Where  $P_{to}$  is the production pressure in psig at valve's depth just when the valve opened,  $P_{tr}$  is the test-rack closing pressure in psig, and  $R$  is the valve's area ratio. Using the equations given in chapter: Single-Phase Flow, the gas factor,  $f_g$ , is estimated to be equal to 1.1459; therefore, the surface opening injection pressure  $P_{cso}$  is equal to  $928.1/1.1459 = 809.9$  psig. The measure surface opening pressure was 830 psig. The calculated surface opening pressure is approximately –2.4% different from its measured value. This is due to poor calibration of the pneumatic sensors used and the uncertainties regarding the actual gas specific gravity (used in the calculation of the gas factor  $f_g$ ).

Following the procedure explained in Example 1, the productivity index and the optimum cycle time were calculated: the cycle time should in this case be between 20 and 22 min to maximize the liquid production. This can be easily verified by a simple inspection of the pressure survey's results, where it can be seen that the cycle time is too long because the production pressure reaches a maximum value and stays at that pressure for a long period of time before the pilot valve finally opens. The daily liquid production could be more than doubled if the surface gas flow rate is increased to reduce the cycle time.

#### Example #5

Fig. 12.17 shows the results of a survey that was run in the well in the following order: (1) First stop at a depth of 3045 ft. (top of perforations); (2) second stop at 2891 ft. (15 ft. below the pilot valve); (3) third stop at 3045 ft. (which was done the following day and it is not shown in the figure). Three cycles took place during the second stop of the first day, as seen in the figure. The second day, the survey was concluded with a stop at 2891 ft. for several injection cycles followed by a period of time in which the surface gas injection was shut off to see how the production pressure was building up just below the pilot valve. Then, a final stop was made at 3045 ft. to determine the true liquid pressure gradient several hours after the surface gas injection was shut off (not shown here either).

Well data: 5 ½-in. × 17-lb/ft. casing; tubing ID 2.441 in.; top of perforations depth 3045 ft.; pilot valve's depth 2876 ft.; liquid production: 18 STB/D;



■ FIGURE 12.17 Downhole pressure and temperature survey, example 5.

wellhead production pressure: 60 psig; cycle time: 90 min; pilot valve opening time: 7 min; surface injection gas flow rate: 118 Mscf/D; volume of gas injected per cycle: 7375 scf/cycle; water cut 2%; 28°API oil gravity; reservoir pressure: 191 psig. The well had a 1-in., nitrogen-charged, injection-pressure-operated pilot valve with an area ratio of 0.164 and a test-rack opening pressure of 915 psig. From the water cut and the oil API gravity, the liquid pressure gradient should be (using Eq. 12.52):

$$\rho_f = 0.433 \left[ 0.02 + 0.98 \frac{141.5}{131.5 + 28} \right] = 0.385 \text{ psi/ft.}$$

On the other hand, the pressure measurements taken several hours after the gas injection to the well was shut off, give the true liquid pressure gradient equal to:

$$\rho_t = \frac{(191 - 14.7) - (163 - 14.7)}{3045 - 2891} = 0.18 \text{ psi/ft.}$$

Using Eq. 12.46, the true liquid pressure gradient, also from the survey, while the well is in normal operation is:

$$\rho_t = \frac{(183.5 - 14.7) - (159.85 - 14.7)}{3045 - 2891} = 0.153 \text{ psi/ft.}$$



The true liquid pressure gradient during the well's normal operation is smaller than the true liquid pressure gradient after the gas injection has been shut off. In both cases though, the true liquid pressure gradient is much smaller than the gradient calculated from the water cut and the oil API gravity, which reveals a large formation gas/oil ratio and that the formation gas apparently continues to flow long after the surface gas injection was shut off (this is confirmed by the small production pressure fluctuations seen during the last stages of the liquid column regeneration period as gas bubbles flow through the liquid accumulated in the tubing). Using Eq. 12.51 and considering  $f_g$  approximately equal to one, the initial liquid column length (from the survey) above the pilot valve (at the moment just before the pilot valve opens) is estimated as:

$$Q_{\text{ini}} = \frac{159.85 \text{ psia} - 14.7 \text{ psi} - (15 \text{ ft.})0.153 \text{ psi/ft.} - 60 \text{ psig}}{0.385 \text{ psi/ft.}} = 215.21 \text{ ft.}$$

The liquid column length, calculated using Eq. 12.50 from the well's liquid production, the cycle time, and the volumetric capacity of the production tubing, is found from:

$$Q_{\text{prod}} = \frac{18 \text{ Br/D}}{\frac{1440 \text{ min/D}}{90 \text{ min/cycle}} 0.005788 \text{ Br/ft.}} = 194.36 \text{ ft./cycle}$$

The liquid fallback factor,  $F$ , is then calculated using Eq. 12.49 from the produced and the initial liquid column lengths just calculated:

$$F = \frac{\left[ \frac{215.21 - 194.36}{215.21} \right]}{2.876} = 0.033$$

This means that 3.3% of the initial liquid column is not produced per each thousand feet of the point of injection depth. This is a very small fallback factor and it is due to the fact that the volume of gas injected per cycle was 7375 scf, while its required value was only equal to 2200 scf. This over injection of more than three times the required volume of gas per cycle was due to the large value of the spread of the valve in this case.

As in previous cases, the operation of the nitrogen-charged gas lift valve is analyzed in the following way:

The dome pressure at 60°F,  $P'_b$ , is given by:

$$P'_b = P_{\text{tr}}(1 - R) = 915(0.836) = 764.94 \text{ psig}$$

The dome pressure at operating conditions,  $P_{bt}$ , is:

$$P_{bt} = P'_b(b) - (a)$$

Where  $a = 0.083 (128^\circ\text{F} - 60^\circ\text{F}) = 5.644$  and  $b = 1 + 0.002283 (128^\circ\text{F} - 60^\circ\text{F}) = 1.1552$ . The temperature at valve depth of  $128^\circ\text{F}$  (measured during the survey) was used. Then,  $P_{bt}$  is equal to 878 psig and the injection opening pressure at valve's depth,  $P_{cvo}$ , is:

$$P_{cvo} = \frac{P_{bt} - P_{to}R}{1 - R} = \frac{878.0 - [159.85 - 14.7 - (15)0.153]0.164}{0.836} = 1022.22 \text{ psig}$$

Where the measured production pressure at 15 ft. below the operating valve, equal to 159.85, was used and the hydrostatic pressure due to the 15 ft. of liquids above the sensors was subtracted using the true liquid pressure gradient equal to 0.153 psi/ft. With this opening pressure at depth, the surface opening pressure is calculated as  $P_{cso} = P_{cvo}/f_g = 1022.22/1.08116 = 945.49$  psig. Where the gas factor  $f_g$  equal to 1.08116 was previously calculated using the equations given in chapter: Single-Phase Flow (not shown here). The measured surface opening pressure is only 899 psi, so the error between the calculated and measured pressures is of approximately 5%, which is due to the poor accuracy of the surface pneumatic sensors and the uncertainty of the gas specific gravity.

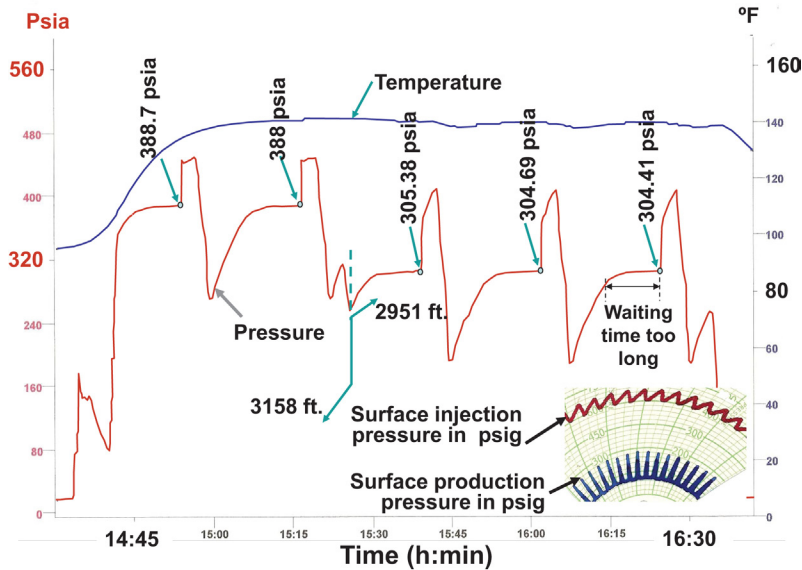
The valve surface closing pressure should be equal to  $P_{bt}/f_g = 878.01/1.0791 = 813.61$ , in which the gas factor  $f_g$ , now equal to 1.0791 for the closing pressure, was previously calculated; Thus, the theoretical spread of the valve should have been equal to  $945.49 - 813.61 = 131.88$  psi, but the measured spread was 150 psi. It is usual for nitrogen-charged gas lift valves to show a spread larger than its theoretical value. This is a consequence of the cooling effect of the gas injected into the tubing (notice in the survey how the temperature drops every time the pilot valve opens). It is important to take this fact into account when designing a well to avoid overinjecting the well at each cycle. Spring-loaded valves, on the other hand, tend to close at a pressure higher than the calculated closing pressure.

The small liquid production of this well is due to its low reservoir pressure; however, by increasing the surface gas flow rate (to decrease the total cycle time, which seems very long by a simple inspection of the survey) a liquid production of 40 or 50 Br/D could be obtained. Because the well is a very low liquid producer and the surface injection gas flow rate is already very large, some operators reduce the gas consumption by reducing the surface injection gas flow rate. With this action, the total cycle time would be longer (causing a decrease in the daily liquid production) but the injection gas/liquid ratio

changes very little because the liquid slugs are almost of the same length and the volume of gas injected per cycle would only be slightly smaller. In other words, by decreasing the surface gas flow rate, the daily liquid production drops and the injection gas/liquid ratio decreases only by a small margin, if at all. The right action in this case is to change the pilot valve with another one with a smaller area ratio that would allow a reduction in the volume of gas injected per cycle. In addition to a change in the area ratio, the cycle time should be adjusted to its optimum value to increase the liquid production. Using the equations presented in the first example, the productivity index value was found to be equal to 0.56 Br/D-psi, for which the optimum cycle time should be equal to 21 min instead of 90 min.

#### Example #6

Fig. 12.18 shows the results of a survey that was run in the well in the following order: (1) first stop at a depth of 3158 ft. (top of perforations); (2) second stop at 2951 ft. (12 ft. below the pilot valve); and (3) third stop again at 3158 ft. (which was done the following day and it is not shown in the figure). During the second stop of the first day, three injection cycles took place as can be seen in the figure. The survey continued through the following day with a stop at 2951 ft. for several injection cycles, followed by a period of time in which the surface gas injection was shut off. Then, a final stop was



■ FIGURE 12.18 Downhole pressure and temperature survey, example 6.

made at 3158 ft., to determine the true liquid pressure gradient several hours after the surface gas injection was shut off (not shown here either).

Well data: 5½-in. × 17 lb/ft. casing; production tubing ID: 2.441 in.; top of perforations' depth: 3158 ft.; operating valve's depth: 2939 ft.; liquid production: 140 STB/D; wellhead production pressure: 60 psig; cycle time: 23 min; The pilot valve remained open for 7 min during each cycle; surface injection gas flow rate: 204 Mscf/D; volume of gas injected per cycle: 3258 scf/cycle; water cut: 32%; 25°API oil gravity; reservoir pressure: 390 psig. The well had a 1-in., injection-pressure-operated, nitrogen-charged pilot valve with an area ratio of 0.164 and a test-rack opening pressure of 714 psig.

Using Eq. 12.52, the liquid pressure gradient from the water cut and oil API gravity is:

$$\rho_f = 0.433 \left[ 0.32 + 0.68 \frac{141.5}{131.5 + 25} \right] = 0.404 \text{ psi/ft.}$$

From the survey (using Eq. 12.46), the last two measurements taken at the end of the waiting time after the injection gas was shut off, gave a true liquid pressure gradient of:

$$\rho_t = \frac{(389.94 - 14.7) - (306.88 - 14.7)}{3158 - 2951} = 0.401 \text{ psi/ft.}$$

The true liquid pressure gradient, also from the survey, while the well is in normal operation is:

$$\rho_t = \frac{(388.35 - 14.7) - (304.8 - 14.7)}{3158 - 2951} = 0.403 \text{ psi/ft.}$$

The true liquid pressure gradient with the well in normal operation is equal to the gradient calculated from the water cut and the oil API gravity. This indicates a small formation gas/liquid ratio, which is common in wells that produce water.

To determine the liquid fallback factor, the initial liquid column length above the pilot valve (just before this valve opens) is calculated first (using Eq. 12.51 with:  $f_g$  equal to one, the pressure data obtained from survey, and the liquid pressure gradient calculated from the water cut and the oil API gravity):

$$Q_{\text{ini}} = \frac{304.8 \text{ psia} - 14.7 \text{ psi} - 12 \text{ ft.} (0.403 \text{ psi/ft.}) - 60 \text{ psig}}{0.404 \text{ psi/ft.}} = 557.58 \text{ ft.}$$

The liquid column length produced at each cycle is calculated using Eq. 12.50 from the well's daily liquid production, total cycle time, and the production tubing volumetric capacity as:

$$Q_{\text{prod}} = \frac{140 \text{ Br/D}}{\frac{1440 \text{ min/D}}{23 \text{ min/cycle}} \cdot 0.005788 \text{ Br/ft.}} = 386.33 \text{ ft./cycle}$$

With the liquid column lengths calculated above (from the survey and from the well's production) the liquid fallback factor is calculated using Eq. 12.49:

$$F = \frac{\left[ \frac{557.58 - 386.33}{557.58} \right]}{2.939} = 0.1$$

This means that 10% of the initial liquid column per each thousand feet of the point of injection depth is not produced. This is a very large fallback factor, probably due to the low liquid slug velocity caused in turn by the low gas injection flow rate through the pilot valve. The well was receiving 3258.33 scf/cycle and the required volume of gas per cycle was only 2300 scf/cycle, thus the volume of gas injected per cycle was much larger than needed but the instantaneous gas flow rate was very low: the valve remained open for 7 min but the liquid slug took longer to be produced. To have an adequate liquid slug velocity, all the required volume of gas per cycle should have been injected in a period of time no longer than 3 min. This low instantaneous gas flow rate is due to the low injection pressure and the small diameter of the main port of the pilot valve installed in the well.

As in previous cases, the operation of the nitrogen-charged gas lift valve is analyzed in the following way:

The dome pressure at 60°F,  $P'_b$ , is:

$$P'_b = P_u(1 - R) = 714(0.836) = 596.9 \text{ psig}$$

And the dome pressure at operating conditions,  $P_{bt}$ , is:

$$P_{bt} = P'_b(b) - (a)$$

Where  $a = 0.083 (138^\circ\text{F} - 60^\circ\text{F}) = 6.474$  and  $b = 1 + 0.002283 (138^\circ\text{F} - 60^\circ\text{F}) = 1.178$  (with the valve temperature measured during the survey at 138°F). Then,  $P_{bt}$  is equal to 696.7 psig and the valve's opening pressure at valve's depth,  $P_{cvo}$ , is:

$$P_{cvo} = \frac{P_{bt} - P_{to}R}{1 - R} = \frac{696.7 - [304.8 - 14.7 - (12)0.164]0.164}{0.836} = 777.41 \text{ psig}$$

Where the production pressure at valve's depth,  $P_{to}$ , is equal to the pressure measured during the survey just before the valve opens (304.8 psia) minus the hydrostatic pressure due to the true liquid column of 12 ft. between the pilot valve and the pressure sensor. Thus, the surface injection opening pressure can be calculated as  $P_{cso} = P_{cvo}/f_g = 777.41/1.07954 = 720.13$  psig. The gas factor  $f_g$  was calculated first and it was equal to 1.07954. The measured surface opening pressure was 690 psig, thus the error in the surface opening pressure is almost equal to 4% and it is due to the inaccuracies introduced by using the pneumatic sensors to measure the surface injection pressure and the uncertainty in the gas specific gravity used to find the gas factor  $f_g$ . The valve's surface closing pressure is equal to  $P_{bv}/f_g = 696.7/1.0785 = 645.98$  psig, where the gas factor  $f_g$  corresponding to the closing pressure has been used. The theoretical spread of the valve should then be equal to  $720.13 - 645.98 = 74.15$  psi, which is similar to the actual spread, only that the actual opening and closing pressures are both lower (due to the poor calibration of the pressure sensors).

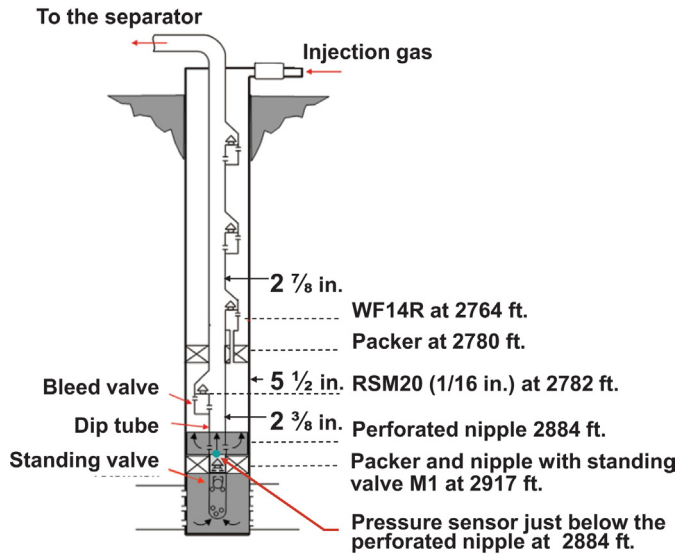
It can be seen in the survey that the cycle time was too long and, in consequence, the liquid production can be increased by increasing the surface injection gas flow rate.

In conclusion, even though the wellhead pressure chart looks as if the well has an excellent operation, the survey reveals that this well is far from being optimized: its operating gas lift valve should be replaced with another valve with a smaller area ratio (to give less volume of gas per cycle) but calibrated at a higher pressure (to increase the liquid slug velocity and reduce the fall-back losses). Additionally, the cycle time needs to be reduced to approximately 70% of the current cycle time.

#### **Example #7 (Accumulation chamber)**

The well that is analyzed in this example had an accumulation chamber installed right above the formation, see [Fig. 12.19](#).

The accumulation chamber's annulus goes from the bleed valve (RSM20 with 4/64 in. orifice diameter) at a depth of 2782 ft. to the perforated nipple at 2884 ft. (102 ft. in total). The tubing above the upper packer is 2 $\frac{7}{8}$ -in. OD (from the wellhead to 5 ft. above the operating valve) and below this point there are 125 ft. of 2 $\frac{3}{8}$ -in. OD tubing down to the perforated nipple. The gas injection line is 3180 ft. long and 2.067-in. ID; the operating valve was an injection-pressure-operated, spring-loaded, 1.5-in. OD pilot valve, model WF14R, with an area ratio of 0.239, and a test-rack closing pressure of 830 psig; wellhead production pressure: 65 psig; water cut: 10%; oil gravity: 23°API oil gravity; liquid production: 63 STB/D; cycle time: 43 min/cycle;



■ FIGURE 12.19 Accumulation chamber installed in the well, example 7.

surface injection gas flow rate: 114 Mscf/D; volume of gas injected per cycle: 3404 scf/cycle (the required volume of gas to be injected per cycle was only 2200 scf/cycle).

Using Eq. 12.52, the liquid pressure gradient (from the water cut and the oil API gravity) is:

$$\rho_f = 0.433 \left[ 0.1 + 0.9 \frac{141.5}{131.5 + 23} \right] = 0.4 \text{ psi/ft.}$$

From the last two measurements considered in the survey, the true liquid pressure gradient (after the well has not been receiving injection gas for several hours) was 0.21 psi/ft. The true liquid pressure gradient could not be measured during the normal operation of the well because the standing valve located at 2917 ft. did not allow lowering the sensors any deeper. The pressures and temperatures were measured with sensors located just below the perforated nipple at 2884 ft. The high production pressure peaks (shown every time the pilot valve opened) are usually found in wells where standing valves are installed because all the injection gas energy is used to lift the liquid slugs.

The maximum liquid column length in the well above the perforated nipple (which is the effective gas injection point at 2884 ft.) can be determined,

using Eq. 12.51, from the measured pressure during the survey just before the pilot valve opens:

$$Q_{\text{ini}} = \frac{195.5 \text{ psia} - 14.7 \text{ psi} - 65 (1.068 \text{ psig})}{0.21 \text{ psi / ft.}} = 530.38 \text{ ft.}$$

Where the gas factor  $f_g$  in the tubing above the liquid level was previously calculated to be equal to 1.068. This liquid column length  $Q_{\text{ini}}$  indicates that the top of the liquid column was at 2354 ft. (410 ft. above the operating valve). This does not mean the accumulation chamber's annulus is completely filled with liquids. A volumetric analysis must be carried out to determine the possible liquid content in the annulus. The following is a procedure that can be used to estimate the liquid level in the annulus. The volumetric capacity of the annulus is 17.7684 Br/Mft., while for the 2 $\frac{7}{8}$ -in. tubing it is 5.788 Br/Mft., and for the 2 $\frac{3}{8}$ -in. tubing it is 3.86631 Br/Mft. Of the 530.38 ft. above the perforated nipple, 405.38 ft. were inside the 2 $\frac{7}{8}$ -in. tubing and 125 ft. were inside the 2 $\frac{3}{8}$ -in. tubing. The net liquid volume accumulated in the tubing above the perforated nipple is then:

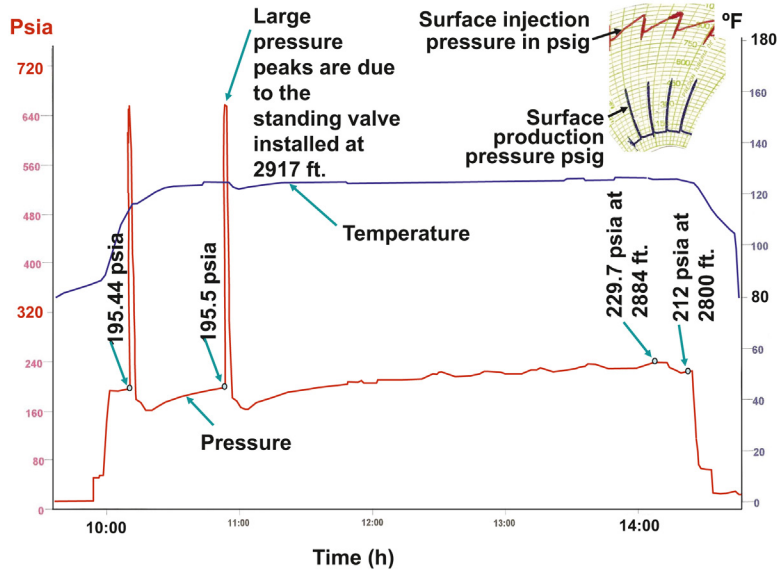
$$V_l = [(0.405 \text{ Mft.})(5.788 \text{ Br/Mft.}) + (0.125 \text{ Mft.})(3.86631 \text{ Br/Mft.})] \\ (0.21 \text{ psi / ft.}) / (0.4 \text{ psi/ft.})$$

Notice that the actual volume of each tubing string is multiplied times  $\rho_l/\rho_f$  (equal to 0.21/0.4) to give the net volume of liquid. This gives a total of 1.4844 Br in the tubing. To estimate the net liquid volume in the annulus, the total volume of liquid that could have accumulated at the bottom of the well (above the perforated nipple) at the moment the pilot valve opened at each cycle can be calculated in an approximate way. For this purpose, the liquid fallback factor can be estimated to be equal to 5%. This is an appropriate number to use because of the following two reasons: (1) the volume of gas injected per cycle is much larger than its required value, and (2) this volume of gas per cycle was injected at an adequate instantaneous flow rate. The surface pressures shown in Fig. 12.20 reveal an excellent intermittent gas lift operation. The high surface production pressure peaks are due to the use of the subsurface standing valve, the length of the liquid columns being produced, and the liquid velocity when each slug reaches the surface.

With a liquid production of 63 STB/D and a cycle time of 43 min, the production per cycle is  $63/(1440/43) = 1.88 \text{ Br/cycle}$ . If  $X$  is the total volume (annulus plus tubing) occupied by the liquid above the perforated nipple, the fallback factor  $F$  can be expressed as:

$$F = \frac{X(\text{Br}) - 1.88(\text{Br})}{X(\text{Br})} \\ 2.884 \text{ Mft.}$$





■ FIGURE 12.20 Downhole pressure and temperature survey inside an accumulation chamber, example 7.

If  $F$  is equal to 0.05 then  $X = 2.19677$  Br. If the liquid that accumulates in the tubing only, 1.4844 Br, is subtracted from  $X$ , the volume that accumulates in the annulus is then only equal to 0.7123 Br. The true liquid column length  $L_{\text{annu}}$  in the annulus is then:

$$L_{\text{annu}} = \frac{0.7123 \text{ Br}}{17.7684 \text{ Br/Mft.}} 1000 \text{ ft. / Mft.} \left( \frac{0.4 \text{ psi / ft.}}{0.21 \text{ psi / ft.}} \right) = 76.36 \text{ ft.}$$

Of the available 102 ft. of the length of the chamber, only 76.36 ft. were filled with a mixture of gas and liquids. In other words, of the 1.81 Br of volume available in the annulus, equal to  $[(0.102 \text{ Mft.})(17.7684 \text{ Br/Mft.})]$ , only 0.7123 Br were actually being accumulated and this happens for two reasons: (1) the true liquid pressure gradient is very small (indicating high gas content in the liquid); and (2) the bleed valve does not allow the gas on top of the liquid in the annulus to be vented at an adequate flow rate, see the explanation given in Figs. 6.59 and 6.60. The 76.36 ft. column in the annulus represents a net liquid column of only 40 ft. The actual liquid column should have a value between these two extremes (from 40 to 76.36 ft.) because the formation gas/oil ratio that goes into the annulus should be somewhat lower than the well's formation gas/oil ratio due to the separation effect that the perforated nipple offers at the entrance of the annulus.

If the chamber was completely filled with liquid with a gradient equal to 0.21 psi/ft., the volume of liquid in the annulus would be [(0.102 Mft.) (17.7684 Br/Mft.)(0.21 psi/ft.)/(0.4 psi/ft.)] = 0.95 Br. If the liquid in the 2 $\frac{7}{8}$ - and 2 $\frac{3}{8}$ -in. tubing, 1.4844 Br, is added to the 0.95 Br in the annulus, then the total liquid accumulation per cycle would be 2.4344 Br/cycle and the fallback factor is found from:

$$F = \frac{2.4344(\text{Br}) - 1.88(\text{Br})}{2.4344(\text{Br})} = 0.078$$

A fallback factor of 7.8% seems to be too high in this case because the volume of gas injected per cycle and the instantaneous gas flow rate into the tubing were more than adequate for a much lower fallback factor. If the chamber was indeed completely filled, 0.95 Br of liquids is still too small in comparison to the 1.81 Br that can be stored in the annulus. This is due to the gas content in the liquid. This is why accumulation chambers are not recommended for wells with true liquid pressure gradients that are too small in comparison to the liquid pressure gradient calculated from the water cut and the API gravity of the oil.

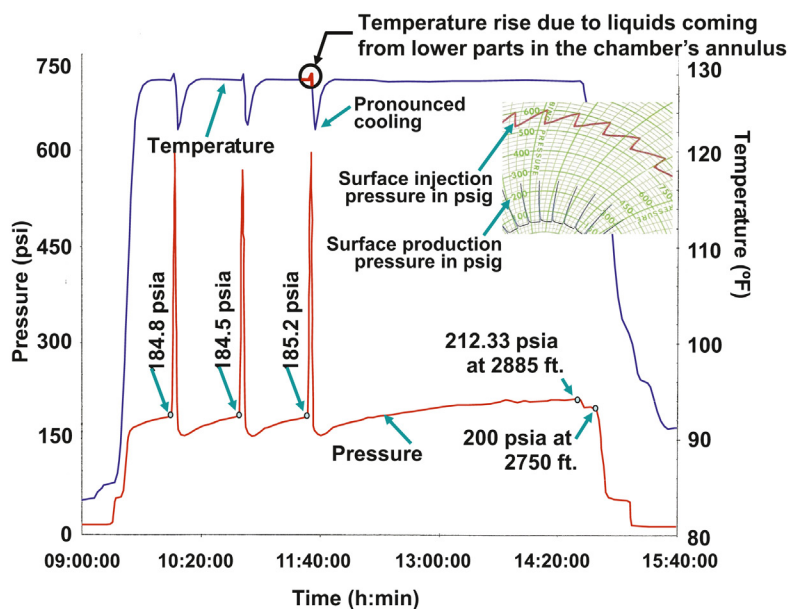
Following the previous analysis, if it is assumed that the chamber is 100% filled with liquids, the fallback factor would be close to 15%, which is unreasonable in this case, given the excellent way in which the gas was being injected.

To verify the behavior of the pilot valve, the valve's force-balance equation is used to find its opening pressure at depth,  $P_{cvo}$ , from the test-rack closing pressure,  $P_{trc}$ , and the tubing pressure at valve's depth,  $P_{to}$ , at the moment the pilot valve opened:

$$P_{cvo} = \frac{P_{trc} - RP_{to}}{1 - R} = \frac{830 - 0.239[195.5 - 14.7 - (120)0.21]}{0.761} = 1041.8 \text{ psig}$$

Where the value of  $P_{to}$  is equal to the production pressure at valve's dept, which is 120 ft. above the pressure sensors. The gas factor  $f_g$  in the annulus was calculated to be equal to 1.08167 so the surface injection opening pressure is then:  $P_{cso} = 1041.8/1.08167 = 963.14$  psig, which is only 1.2% lower than its measured value (975 psig).

The survey presented in Fig. 12.21 was initially run in the same well, but it was not used because several evidences indicated that the exact location of the sensors during the survey was unclear: it appeared that the sensors were located above the perforated nipple at a depth hard to determine and totally



■ FIGURE 12.21 Discarded downhole pressure and temperature survey inside an accumulation chamber, example 7.

different from the 2884 ft. in the instructions given to the wireline operators. The most important clue was the heating of the sensors just after the valve opened, followed by a pronounced cooling of the sensors as the gas was being injected into the tubing. None of these two effects should take place during a survey of this kind and they revealed that the sensors were above the perforated nipple:

- The heating of the sensors was due to the flow of liquids coming from the annulus. Because the liquids were deeper than the location of the sensors, they were hotter and caused the sensors to warm up as they passed around the sensors.
- The cooling of the sensors was due to the fact that once the liquid has been pushed into the production tubing, the sensors were directly exposed to the injection gas, which was cooler. If the sensors were located just below the perforated nipple, the cooling effect would not show in the survey as pronounced as it can be seen in the Fig. 12.21 because the liquids surrounding the sensors have no place to go due to the fact that the standing valve underneath the sensors would not allow them to move when the tubing above the perforated nipple is pressurized. In contrast, neither the pronounced cooling nor the heating

of the sensors are shown in Fig. 12.20, indicating that the sensors were indeed where they were supposed to be.

To avoid mistakes like this one, wireline operators must first locate the standing valve and compare the wireline measured depth with the actual depth provided in the well's files. The wireline elongates as the instruments are run in the well. But in this case because the perforated nipple was at a shallow depth, the wireline elongation should have been no more than 5 ft. (wirelines usually elongate about 1.5 ft. per each 1000 ft. of depth depending on the weight of the wireline tools used and on the type of fluids in the well). The heating of the instruments indicates that the error made was much greater than 5 ft. Errors of this type are not very common, but the person doing the troubleshooting analysis must be aware and alert to detect them in all situations and especially while analyzing accumulation chambers.

#### 12.4 USE OF SONIC DEVICES AND DISTRIBUTED TEMPERATURE SENSOR (DTS) USING FIBER OPTICS

Troubleshooting techniques used in the field, such as sonic devices and distributed temperature measurements using optical fiber, are perfectly applicable to intermittent gas lift operations. These techniques are explained in chapter: Continuous Gas Lift Troubleshooting. In this section, some guidelines are given to use them as effective troubleshooting tools for intermittent gas lift applications. Other troubleshooting techniques, such as CO<sub>2</sub> injection or continuous pressure and temperature surveys, are not applicable to intermittent gas lift because these techniques require the operation of the well to be very stable.

Sonic devices can be used in the traditional way to determine the liquid level in the annulus by identifying tubing couplings and mandrels along the depth of the well. The liquid level in the annulus does not always indicate the depth of the point of injection. The great majority of gas lift wells have production packers installed and gas lift valves, in turn, have internal check valves that would not allow liquids (from the tubing) to enter the annulus. If these internal check valves do not leak and the packer is in good condition, the liquid level should not change in time. The annular liquid level could be way below the current operating point of injection. The liquid level simply indicates the deepest point to which the well has been previously unloaded. The measured liquid level also indicates that the current gas injection point depth cannot be below this level.

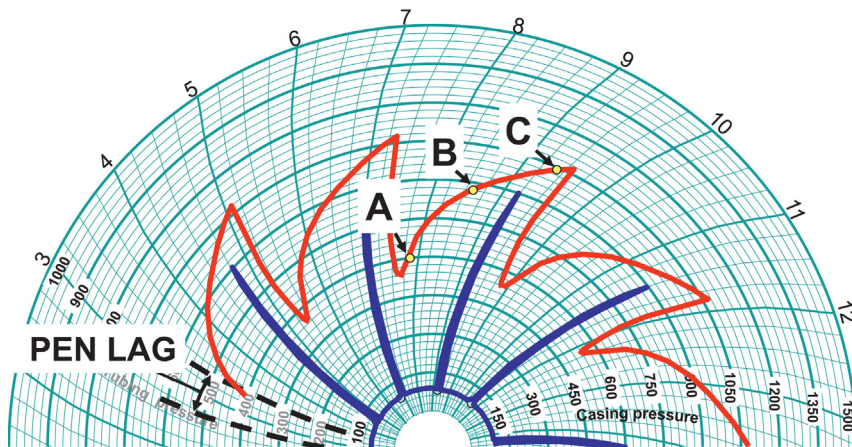
Measuring the annular liquid level would also determine if the packer has failed: If the liquid level is at packer's depth, and therefore below the deepest gas lift valve, it is evident that gas is being injected through the packer or that at least it allows liquids to pass through it.

In gas lift applications, it is important to know the annular liquid level in the following cases:

- Open completions, where the liquid level fluctuates as the injection pressure and the flowing bottomhole pressure change.
- Damaged gas lift valves that have failed open, with their check valve also damaged and allowing liquid to enter the annulus.
- Tubing-annulus communications (holes or unseated gas lift valves).

In case of open completions or tubing-casing communications of any kind, the liquid level in the annulus is always changing and it is many times possible to know the depth of the gas injection point if the liquid level is measured at key moments during the cycle. The liquid level should be measured just before the injection pressure reaches its maximum value because at that moment the liquid level is very close to the tubing-annulus communication. Additionally, the liquid level can be measured at the beginning and the middle of the injection pressure buildup time interval.

It should be taken into consideration that during the beginning of the injection pressure buildup period, the gas flow rate into the annulus could be so high that the noise level might not allow the use of any type of sonic devices. However, toward the final stages (just before the gas enters the tubing) the noise level might decrease, making it possible to measure the liquid level right when it is needed the most because the liquid level is just about to reach the communication's depth. Fig. 12.22 shows the times at which it is advisable to take measurements of the liquid level and obtain



■ FIGURE 12.22 Instants A, B, and C at which it is convenient to measured the annular liquid level (if the noise caused by the high gas injection flow rate allows this operation to be conducted).

a general idea of the size of the communication and its depth (times A, B, and C).

Sonic devices can be used to determine the liquid level inside the tubing at different moments during the liquid column regeneration period in wells with or without tubing-annulus communications. With this information, the bottomhole flowing pressure and the productivity index could be estimated (in wells with no tubing-annulus communications) if the following data is additionally known:

- Temperature, pressure, and specific gravity of the gas in the tubing.
- Water cut, as well as oil and water specific gravities.

With this information, the bottomhole flowing pressure can be calculated at two different times during the liquid column regeneration time interval and then, using the same calculation procedure explained for pressure survey analysis, the productivity index and the optimum cycle time can be calculated.

It should be pointed out however that sonic devices inside the tubing can be used to find the liquid level depth only if the gas specific gravity and temperature inside the tubing are known so that the speed of sound can be determined. With the speed of sound and the time it takes for a sound pulse to travel to the liquid level and back, it is possible to calculate the depth of the liquid level. This technique is not very accurate in this case because it is not easy to know the specific gravity of the gas in the tubing: this gas is a mixture of injection gas left in the tubing from the previous injection cycle and the formation gas that is being produced as the liquid column is being generated. Additionally, the true liquid pressure gradient of the liquids in the tubing is usually smaller than the pressure gradient calculated from the water cut and oil specific gravity. However, the true liquid pressure gradient could be estimated by applying the operating valve's force-balance equation just before it opens. In this case, the force-balance equation is used to find the value of the production pressure,  $P_{to}$ , at valve's depth and then this pressure can be used to estimate the true liquid pressure gradient if the liquid level is measured at the time the valve opens. If the water cut is above 60%, it is possible that the true liquid pressure gradient is very close to the liquid pressure gradient calculated from the water cut and the oil's API gravity because the formation gas/liquid ratio is usually very small in wells with large water cuts.

The use of fiber-optic techniques to measure, almost in real time, the distributed temperature along the entire length of the production tubing string is very useful in intermittent gas lift, especially when it is suspected that

an instability problem is being created by valve's interference or when it is difficult to determine the point of injection because there are many valves installed in the well. When there are several points of injection in a well with fluctuating surface gas injection pressures, these points of injection, and the way gas is intermittently injected through them, can be easily determined with the use of fiber-optic technology. This technique is explained in detail in Section 11.5.7.

## 12.5 WELLHEAD PRESSURE CHART INTERPRETATION

### 12.5.1 General examples

Several examples of wellhead pressure charts from wells producing on intermittent gas lift are given in the section. The way the intermittent gas lift method is performing is easily identified by observing how the wellhead pressures fluctuate in time. The wellhead pressure patterns are usually registered with the use of two- or three-pen charts recorders. When two-pen chart recorders are used, one pen is used for the injection pressure and the other for the production pressure. When three-pen chart recorders are used, the third pen usually corresponds to the differential pressure across an orifice plate installed in the gas injection line near the wellhead to measure the injection gas flow rate. Sometimes the third pen is used to register the pressure upstream of the gas flow rate control valve, known as the gas line pressure. For the line pressure to be recorded in this way, the flow control valve (or choke) should be close to the wellhead so that the wellhead pressures and the line pressure can be registered at the same time.

Pressure charts are now being replaced in many gas lift fields by real-time electronic measurements. Wellhead pressure and temperature electronic sensors are scanned by a data acquisition system at a predetermined scan rate, so that their behavior in time can be analyzed by any team in the operating company that needs to do so. It is recommended to have a scan rate of one measurement every 20 s for all wellhead temperatures and pressures being monitored in intermittent gas lift.

If conventional charts are used, the clock could be set for one chart revolution every 24 min (ideal for verifying details in one injection cycle) or it can be set for one revolution every 24 h as it is normally done. Seven-day charts are not recommended if a detailed troubleshooting analysis is needed, but they do show if a failure has occurred and they are practical to use in places with many wells assigned to a reduced number of optimization engineers. The calibration of either the traditional pneumatic sensors used with two-pen

chart recorders or the new electronic sensors must be carefully checked so that reliable troubleshooting calculations can be performed. The injection gas specific gravity should also be accurately measured to be able to calculate the downhole injection pressure from the measured wellhead pressure.

The way wellhead pressures change in time constitutes a valuable piece of information without which troubleshooting analyses cannot be performed when the well is on intermittent gas lift. It must be emphasized that these charts should be analyzed using the analytical techniques developed for intermittent gas lift given in [Section 12.2](#); otherwise, wrong conclusions might be easily reached. The reader is advised to review [Section 11.2](#) in which possible failures and operational errors made regarding the use of surface pressure chart recorders or electronic sensors are presented.

Pneumatic or electronic sensors being used must have a range according to the well's operational conditions. Usually, sensors with maximum readings from 1000 to 2500 psig are used to measure injection pressures and maximum readings from 500 to 1000 psig are used for production pressures. 24-h charts are the most widely used in the industry. If the clock is set for one revolution every 7 days, the appropriate chart must be used for that setting. Optimization engineers should be aware of the fact that sometimes 24 h charts (which are usually readily available) are used with the clock set for 7 days.

Before giving specific examples of pressure charts from actual wells on intermittent gas lift with different types of problems, a detail and separate explanation of the different patterns of the production and injection wellhead pressures is presented.

The shape of production pressure peaks gives important hints of the current lifting efficiency. The value of the maximum production pressure, the elapsed time between the moment the gas lift valve opens and the slug arrives at the surface, and the time it takes for the production pressure to decrease back to separation pressure are important factors obtained from the charts that should be carefully analyzed.

The maximum production pressure is a function of many variables, the most important ones being the size of the liquid slug and its velocity as it arrives at the surface. Other important factors are: if the slug reaches the surface as only one liquid slug or several smaller ones or if there is any restriction at the wellhead, along the flowline, or at the flow station. Therefore, by itself, the measurement of the wellhead production pressure is not enough to reach a final assessment of the well's current operational conditions.

The maximum production pressure must occur right after all the liquid slug has been produced to the surface. If a restriction is located at the wellhead,



or close to it, the maximum production pressure is reached before the entire slug has surfaced and therefore the slug velocity is abruptly reduced, increasing in this way the liquid fallback losses. Restrictions away from the wellhead, on the other hand, could make it longer for the production pressure to decrease to separation pressure and this only affects the regeneration of the liquid slug above the pilot valve in the tubing. Fig. 12.23 shows several examples of typical wellhead production pressure patterns.

Fig. 12.23a shows good operational conditions, with slugs reaching the surface as one unit and with a fast decrease of the production pressure, which could (but not necessarily) indicate the lack of restrictions at the wellhead or the flowline.

Fig. 12.23b shows a case in which liquid slugs are smaller, possibly because the reservoir pressure is low or the injection frequency is too high, not allowing the liquid column above the pilot valve to reach its optimum size. However, it could also indicate a low liquid slug velocity.

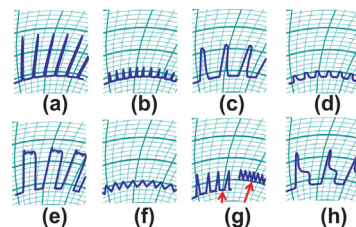
Fig. 12.23c shows a restriction away from the wellhead (but probably at a distance not greater than the length of the liquid slug) such as a bent or smashed flowline or with some kind of deposition (sand, asphaltenes or paraffin's). Restrictions at the wellhead look more like Fig. 12.23a, with peaks higher than expected for the well's current production.

Small and wide pressure peaks as the ones shown in Fig. 12.23d could be due to one, or several, of the following possibilities: (1) short liquid column with a high gas content, (2) presence of emulsions, or (3) simply the gas injection is entering the tubing at a low flow rate (even if the total volume of gas injected per cycle is the right one).

Large liquid slugs as the ones shown in Fig. 12.23e, with some gas in them, are usual in double-packer or inserted accumulation chamber installations.

Fig. 12.23f shows a case in which the injection gas flow rate is just too high and therefore the liquid slugs are very small and it is not given sufficient time for the wellhead production pressure to decrease to the pressure at the separator or main header.

The effect of high and low injection frequencies are shown in Fig. 12.23g for comparison. It can be seen that at high frequencies, it is not given sufficient time for the production pressure to drop to separation pressure. It is possible that, due to the high productivity index of the well, the calculated cycle time must be very short to maximize the liquid production, but the theoretical maximum liquid production can not be reached because the production pressure cannot actually decrease as fast as it should. The back



■ FIGURE 12.23 Examples of wellhead production pressure patterns.

pressure then does not allow the liquid slugs to be generated as fast and long as they could with a lower wellhead production pressure. If this is the case, it is possible that the maximum daily liquid production is reached at cycle times longer than the theoretical optimum cycle time.

Fig. 12.23h shows the production pressure of a well in which either the volume of gas injected per cycle is much greater than it is actually needed or there is a restriction away from the wellhead that is not allowing the gas to be efficiently vented. This restriction could be at any point along the flowline at a distance from the wellhead larger than the length the liquid slug has once all of it has been produced to the surface. But it could also be due to a restriction at the gas exit of the separator, such as a very small orifice plate to measure the total gas produced by the well or a partially closed valve that connects the gas outlet of the separator to the low pressure side of the gas lift system. This high back pressure leads to regeneration of smaller liquid columns at the bottom of the well and, in consequence, it reduces the daily liquid production.

Just as the surface production pressure behavior can give valuable information to analyze intermittent gas lift wells, the surface injection pressure is also a very important piece of information without which it is not possible to analyze the following points: (1) the behavior of the gas lift system as a whole, (2) the performance of the downhole pilot valve, or (3) the operation of the surface intermitter in case one is used. The gas injection pressure should be measured downstream of the choke or the intermitter. As indicated in chapter: Design of Intermittent Gas Lift Installations, the gas injection into the well can be controlled using one of the following alternatives:

- By means of a choke installed in the gas line that allows a constant gas flow rate into the well's annulus. This gas flow rate is usually much smaller than the gas flow rate that passes through the downhole pilot valve once it is opened. This is usually called "choke-control intermittent gas lift." The cycle frequency is controlled by the injection gas flow rate at the surface. If this flow rate is increased, the cycle time is reduced and vice versa. The surface choke can be a fixed choke or a needle valve that can be adjusted to pass the gas flow rate as needed.
- By means of a surface intermitter. The cycle time is controlled by adjusting the time the intermitter is closed (time off) and the time it should remain open (time on). When the intermitter opens, it allows a very high surface gas flow rate so that the annular pressure is rapidly increased to the pilot valve's opening pressure. Once the downhole pilot valve opens, the annular pressure should continue to increase but at a slower pace. Then, when the intermitter closes, the annular

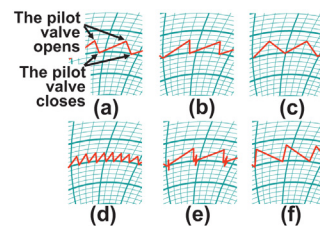
pressure begins to decrease until the pilot valve closes and, from that moment on, the injection annular pressure remains constant until the intermitter opens once again to initiate a new injection cycle.

Injection pressure patterns for “choke-control” intermittent gas lift are shown in Fig. 12.24. Fig. 12.24a shows a typical gas injection pressure pattern for a well on choke-control intermittent gas lift. The maximum pressure peaks correspond to the pilot valve’s surface injection opening pressure. When the pilot valve opens, the gas flow rate that passes through it is greater than the gas flow rate injected at the surface, so the injection pressure decreases, eventually reaching the pilot valve’s surface closing pressure. At this moment the pilot valve closes but because the surface injection gas flow rate is constant, the annular pressure immediately begins to increase to start a new cycle.

Fig. 12.24b shows a good pilot valve operation, with the desirable fast decrease of the injection pressure once the pilot valve opens. This fast drop of the injection pressure could be due to: (1) a high flow rate through the gas lift pilot valve, as recommended for intermittent gas lift, or (2) the well’s annulus volume being too small because of a reduced casing diameter or a shallow point of injection. Calculations must be made to determine if the volume of gas injected per cycle is in fact the required value for the tubing diameter, depth of the injection point, length of the liquid slugs, and the type of fluids being lifted. It is not enough to only take a look at the gas injection pattern to determine if the gas injection is appropriate or not.

Fig. 12.24c, contrary to what is presented in Fig. 12.24b, shows a slow decline of the gas injection pressure once the pilot valve opens. This could be due to one of the following reasons and it does not necessarily imply a bad operation:

- The gas flow rate through the pilot valve is too small because its main port is not large enough for a good intermittent gas lift operation or the port is partially plugged. This could imply a poor operation that might cause a low liquid slug velocity and, in consequence, large liquid fallback losses.
- A very deep point of injection. In this case the annular injection volume is very large and it takes a long time for its pressure to decline. If this is the case, the injection pressure behavior might be adequate because it could be necessary to inject a large volume of gas per cycle to produce the liquid slug to the surface and it might take a long time for the liquid slug to reach the surface.
- A large annulus due to a large casing diameter that takes a long time to vent. The injection gas flow rate through the pilot valve could be



■ FIGURE 12.24 Examples of wellhead injection pressure patterns for choke-control intermittent gas lift.

adequate for the liquid slugs to be lifted at the right velocity, but the gas injection continues to take place for several minutes after the entire liquid slug has been produced to the surface, which constitutes a waste of injection gas per cycle. To reduce the volume of gas injected into the tubing per cycle, the pilot valve should be replaced with another one with a smaller area ratio, which will show a smaller pressure spread (the spread is defined as difference between the opening and closing pressures of the gas lift valve). Sometimes the minimum commercially available area ratio is not small enough to reduce the volume of gas injected per cycle. This usually happens when using 1-in. OD pilot valves in wells with large annulus. If this is the case, the spread of the valve could be reduced (up to a point) by decreasing the valve's opening pressure; but this must be done with care because low injection pressures could cause low liquid slug velocities, which in turn cause an increase in the liquid fallback losses.

- A very long gas injection line (especially if its inside diameter is very large). In this case, the choke or the gas injection flow control valve should be installed near the wellhead and not at the injection manifold, which is usually several thousand feet away from the well. This eliminates the gas stored in the injection line as part of the volume injected at each cycle.

Fig. 12.24d shows a very small spread, which could be due to:

- A small valve area ratio. This is probably what the well actually needs, but injection gas mass balance calculations must confirm this fact (if the annular volume is very large, it is probable that the well needs a very small spread but, on the other hand, sometimes very large spreads are not enough to pass all the volume of gas required per cycle in a well with a very small annulus).
- Downhole production pressure too high. High production pressures cause the gas lift valve to open at a lower injection pressure so that the volume of gas injected per cycle could be less than its required value. This usually happens after unloading wells that can generate large liquid columns in comparison to the valve's injection opening pressure or with a large diameter tubing string. The way this type of problem can be solved is explained in this section, see Fig. 12.27.

Fig. 12.24e shows a case in which the two-pen chart recorder is mounted on the flowline and, in consequence, every time the liquid slug reaches the surface the flowline vibrates making the pen move up and down, given a false impression of a pressure instability of some sort.

Fig. 12.24f shows the injection pressure of a well with an extremely high injection gas flow rate at the surface. This makes the injection annular pressure

increase very fast while the pilot valve is closed. But once the pilot valve opens, it takes a long time for the injection pressure to decrease to the valve closing pressure because the gas flow rate through the gas lift valve is greater than, but comparable to, the surface injection gas flow rate.

Fig. 12.25 shows the gas surface injection pressure pattern when the surface gas injection is controlled by an intermitter, also known as a “time cycle controller”.

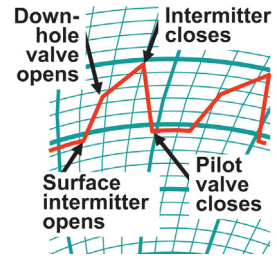
Fig. 12.26 shows typical wellhead injection pressure patterns when surface time cycle controllers are used.

Fig. 12.26a shows the case in which the gas volume injected every time the intermitter opens is not enough to increase the injection pressure to open the downhole pilot valve. The intermitter must open three times to open the pilot valve. This is easily corrected by increasing the time interval in which the intermitter remains open.

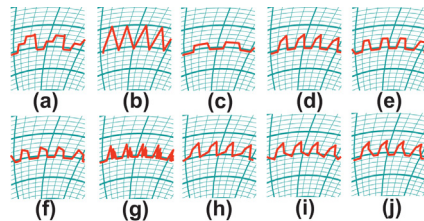
If the intermitter is properly working and yet the injection pressure looks like the one shown in Fig. 12.26b, one of the following alternatives could be happening in the well:

- If the injection pressure is low, either the pilot valve has failed and it is totally open or a large tubing-annulus communication exists.
- If the gas injection pressure is high, the injection pressure pattern might be due to either an injection gas flow rate so high that the pilot valve never closes (the annular pressure is not allowed to decrease to the pilot valve’s closing pressure) or there is a tubing-annulus communication large enough to generate this type of pressure pattern but not so large to make the injection pressure drop to lower values.

Fig. 12.26c shows the pressure pattern created when the gas flow rate injected at the surface is equal to the flow rate the pilot valve allows to pass once it opens. For this reason, the annular pressure remains approximately constant when the intermitter and the pilot valve are opened at the same



■ FIGURE 12.25 Wellhead injection pressure behavior when surface time cycle controllers are used.



■ FIGURE 12.26 Wellhead injection pressure patterns for intermittent gas lift with time cycle controllers.

time. The gas injection time might need to be long to pass all the gas volume required per cycle, which might be harmful to the liquid production because the flowing bottomhole pressure is kept at a high value for a long time. This situation might be caused by a restriction at the injection line, upstream or downstream of the intermitter. Sometimes the intermitter is installed in series with an adjustable choke, which has not been fully opened or it is indeed opened but its internal components create a restriction to the injection gas flow. Then, the gas flow rate to the well is not as high as it should be for a fast and efficient gas injection. This pattern could also be due to the fact that the gas lift system is not capable of supplying the injection gas at a high rate or the pilot valve opening pressure has been set at a high value so it is very similar to the gas lift system pressure and, in consequence, the differential pressure (between the compressor's outlet pressure and the wellhead pressure) is very small for the required gas flow rate.

Fig. 12.26d shows an efficient gas injection: Once the intermitter opens, the injection pressure increases very fast and it keeps on increasing at a high rate even after the downhole pilot valve opens. As soon as the intermitter closes, the injection pressure declines at a high rate, which indicates an adequate injection gas flow rate into the tubing through the pilot valve. However, as it has been stated several times, only an analytical analysis can ascertain if the following parameters are the ones recommended for the well: (1) the total volume of gas injected per cycle, (2) the instantaneous gas flow rate through the gas lift pilot valve, and (3) the total cycle time.

Fig. 12.26e shows the same problem presented in Fig. 12.26c, only that in this case the gas injection time is shorter so that its negative impact on the liquid production might not be too important. In any case, the reason for this pressure pattern must be investigated to avoid future complications that might end up in an injection pressure pattern such as the ones presented in Figs. 12.26f and g.

In Fig. 12.26f the gas flow rate through the downhole pilot valve is greater than the injection gas flow rate at the surface and this is why the injection pressure declines as soon as the pilot valve opens.

If the gas flow rate through the downhole pilot valve is much higher than the gas flow rate injected at the surface, it is possible that the pilot valve opens and closes several times while the intermitter is opened. This is shown in Fig. 12.26g. This is a very inefficient gas injection operation because the liquid slug velocity increases and decreases several times as the slug travels to the surface which could result in an increase in the liquid fallback losses and, additionally, it could make the cycle time unnecessarily long. It is important to find out the reason why the gas flow is being restricted at the surface.

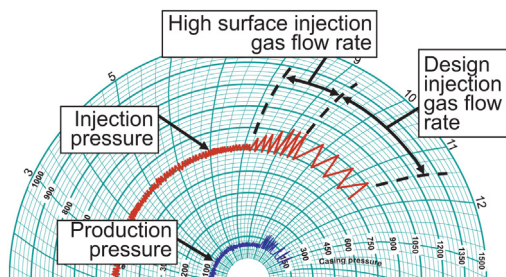
Fig. 12.26h shows a case in which the intermitter at the surface has a gas leak toward the injection annulus and, for this reason, the injection pressure increases during the time the intermitter and the pilot valve are both closed. This does not necessarily represent an inefficient operation if the cycle time is adequate, but it must be fixed because it could get worse. In some situations, this injection pattern is purposely implemented to reduce the time required for the annular pressure to increase to the pilot valve's opening pressure, see Fig. 10.10. For open completions (without tubing-casing packers) this could be the normal injection pressure pattern: When the intermitter and the downhole pilot valve are both closed, the gas pressure in the annulus increases because the annular liquid level is rising, compressing the injection gas trapped in the annulus above the liquid level.

Fig. 12.26i shows a case in which there is a gas leak from the annulus to the tubing or to a shallow formation through a hole in the casing. A communication test (explained in chapter: Continuous Gas Lift Troubleshooting) should be performed to get a better understanding of the problem as long as the operating valve is either a single-element valve or it is a pilot valve with its internal check valve located at the nose of the valve and not inside the internal piston of the pilot valve. Communication tests in wells with pilot valves that have the check valve inside the piston cannot differentiate between a hole in the tubing and a pilot valve of this type with its piston stuck open (because a pilot valve with this kind of problem is in reality a tubing-annulus communication). If the intermitter is closed for a long period of time and the annular pressure drops to separation pressure, there is a good possibility of a tubing hole or communication above the static liquid level; but, if the annular pressure drops to a value above the separation pressure, it is likely that the tubing-annulus communication (if there is one) is below the static liquid level, which could be a hole in the tubing or the pilot valve is leaking.

Fig. 12.26j shows a case in which more than one gas lift valve are opening. On the other hand, this could be a normal injection pressure pattern for a dual well, in which one string produces on intermittent gas lift and the other one is operated on continuous gas lift.

Several examples of wellhead pressure patterns in actual wells producing on intermittent gas lift are now presented and analyzed.

The injection pressure pattern shown in Fig. 12.27 corresponds to a choke-control intermittent gas lift well that has not been unloaded with the required gas injection flow rate for the type of well. At the moment the pilot valve is uncovered, the liquid column in the tubing above the gas lift valve is very long and the pilot valve opens at a lower than design injection opening



■ FIGURE 12.27 Wellhead pressures in a well that has not been fully unloaded or that loads up with fluids over time.

pressure because the production pressure is contributing in a significant way in the opening of the pilot valve. For this reason, the spread of the valve is very small and the volume of gas injected per cycle is less than the required value to lift the large liquid columns to the surface, thus the liquid fallback losses are very large. When this happens, the liquid production could be very low or even equal to zero and this drastic drop in the liquid production is the main characteristic that distinguishes this type of problem from the pattern observed when trying to lift highly viscous fluids at a purposely high frequency intermittent gas injection, in which the static reservoir pressure is high enough to allow liquid production even at high bottomhole flowing pressures.

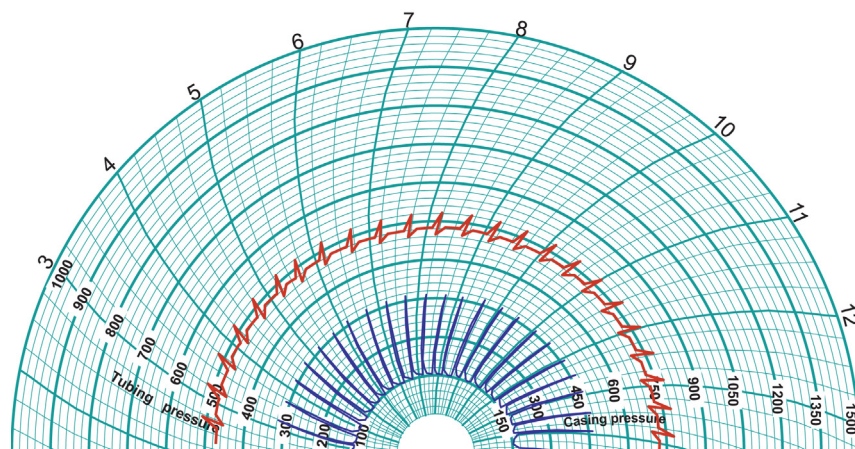
As indicated in chapter: Design of Intermittent Gas Lift Installations, if the very small spread is due to an unloading process carried out with an insufficient surface injection gas flow rate, the unloading of the well can be accomplished by temporarily increasing the injection gas flow rate to values much larger than the design unloading gas flow rate.

The injection pressure pattern shown in Fig. 12.27 corresponds to an injection-pressure-operated, spring-loaded pilot valve on choke-control intermittent gas lift. This figure shows the pressure pattern that takes place when the well is finally being unloaded by temporarily increasing the surface gas flow rate to very large values. As the surface injection gas flow rate is increased, the well begins to produce increasingly larger liquid slugs at the surface until a new operational state is reached (at this large gas injection rate) in which the spread of the valve does not increase anymore and remains constant at a larger value. Once this steady operation is obtained, the injection gas flow rate at the surface can be reduced (as shown in Fig. 12.27) to its design value so that the injection frequency drops and the produced liquid columns become larger because the reservoir has more time to generate larger liquid columns above the pilot valve (but not as large as the liquid



columns existing before increasing the surface injection gas flow rate). If, after reducing the gas flow rate, the spread of the valve decreases again with a reduced liquid production (or no liquid production at all), the injection gas flow rate must be increased and kept at a high value while preparations are made to replace the pilot valve with another one with a larger area ratio or shift the well to continuous gas lift because this behavior could be an indication that the well is a good liquid producer that can sustain continuous gas lift with an acceptable injection gas/liquid ratio. This problem is also found when trying to implement intermittent gas lift in a well with a large diameter production tubing: intermittent gas lift cannot be implemented in wells with large diameter tubing strings because most gas lift systems are not capable of supplying the required high gas flow rates through the pilot valve to lift the liquid slug at a velocity high enough to keep the liquid fallback losses at acceptable levels.

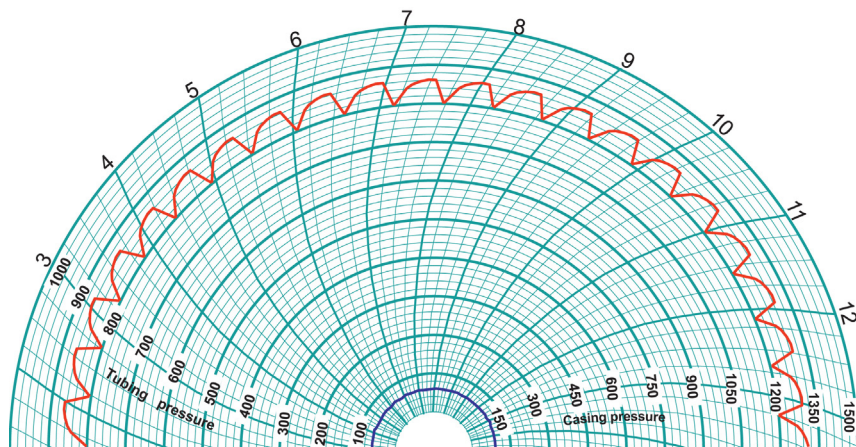
Fig. 12.28 shows the wellhead pressures of a well that was operating with a surface intermitter and a ¼-in. needle valve installed at the gas injection manifold. This valve is located upstream of the intermitter and it allows a maximum surface injection gas flow rate of only 190 Mscf/D. When the intermitter opens, the injection pressure increases to the surface opening pressure of the downhole pilot valve. Once the pilot valve opens, the injection pressure in the annulus decreases very rapidly because the gas flow rate through the pilot valve is greater than the injection gas flow rate at the surface. The surface gas flow rate is being restricted by the needle valve installed at the gas injection manifold. When the pilot valve closes, the injection annular pressure begins to increase until the intermitter finally closes,



■ FIGURE 12.28 Surface intermitter with a large upstream restriction at the injection manifold.

leaving the injection annular pressure at approximately the same initial value it had when the intermitter opened, which is just a mere coincidence in this case (if the time in which the intermitter remains open is just a little longer or shorter than its current value, the injection pressure pattern would be totally different). The well in Fig. 12.28 has a 1.5-in. OD, spring-loaded, injection-pressure-operated pilot valve (model WF14R). Additional data of this well: 3½-in. production tubing; 7-in. × 23-lb/ft. casing; operating valve's depth: 2879 ft.; packer's depth: 2,951 ft.; top of perforations' depth: 3401 ft.; static reservoir pressure: 468 psig; 26°API oil gravity; and a 2% water cut. An injection gas volume of 3500 scf/cycle was needed to efficiently produce the well.

Fig. 12.29 shows the wellhead pressures of a well with a large surface injection gas flow rate. The period of time in which the intermitter remained open was very long, so the injection pressure never dropped to the pilot valve's closing pressure (the pilot valve remained open all the time). As soon as the intermitter opens, the injection pressure begins to increase at a very large rate; but then, as the injection pressure approaches line pressure, the injection pressure increases at a much smaller rate (because the differential pressure between the wellhead and the gas injection manifold is very small toward the end of the time interval in which the intermitter remains open). Once the intermitter closes, the injection pressure begins to decrease but the surface intermitter opens again before the injection pressure can be reduced to the pilot valve's closing pressure. The well in Fig. 12.29 had a 1-in. OD, injection-pressure-operated, spring-loaded pilot valve (model WFM14R), calibrated at a test-rack closing pressure of 573 psig and no

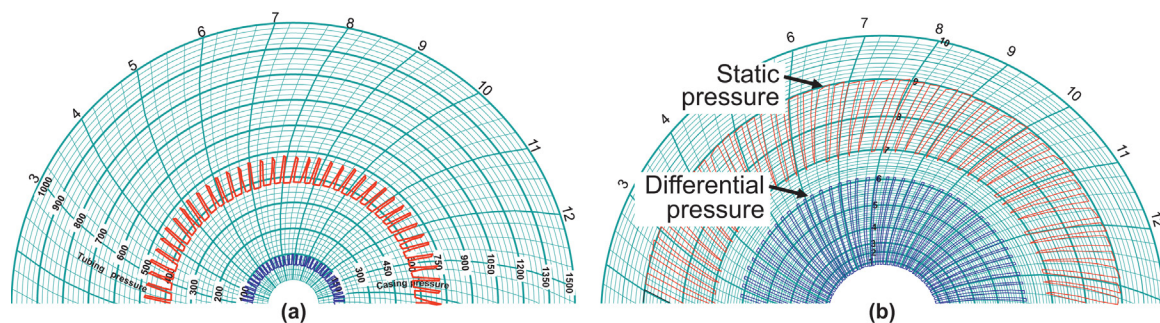


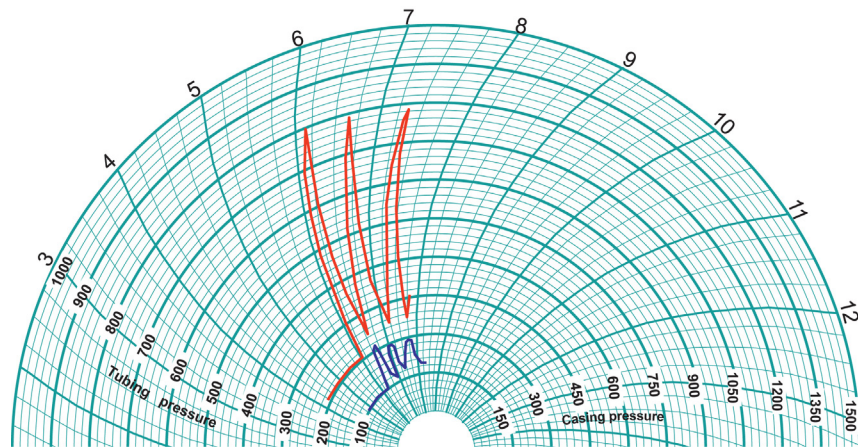
■ FIGURE 12.29 Surface intermitter remains open for a very long time.

unloading valves located above this operating valve. Additional data for this well: vertical well; 2 $\frac{7}{8}$ -in. production tubing; 5 $\frac{1}{2}$ -in.  $\times$  17-lb/ft. casing; pilot valve's depth: 2335 ft.; packer at 2411 ft.; top of perforations at 2525 ft.; reservoir static pressure of 453 psig; 21.9°API oil gravity; and water cut of 1%. The well requires 2400 scf/cycle to lift each liquid column with minimum fallback loss. Note that the injection pressure pattern shown in Fig. 12.29 is similar to the one presented in Fig. 11.57 for a well with a tubing-annulus communication below the point of injection, the only difference being that the injection pressure in Fig. 12.29 is much higher and almost equal to the line pressure.

A  $\frac{1}{4}$ -in. choke was installed in the gas injection line upstream of the surface intermitter in the well corresponding to Fig. 12.29 and, additionally, the surface injection time interval was reduced to half the injection time it had. After these adjustments were made, the wellhead pressure pattern looked as shown in Fig. 12.30a. As can be seen in Fig. 12.30a, these changes made the injection pressure pattern look more like a typical injection pressure behavior for a well with the surface gas injection controlled by a surface intermitter. Even though a  $\frac{1}{4}$ -in. choke was installed in series with the intermitter (providing an "on purpose" large flow restriction), the downhole pilot valve did not behave as shown in Fig. 12.28 because in the case of Fig. 12.30a the well had a 1-in. OD pilot valve installed with a  $\frac{32}{64}$ -in main port that did not allow the gas flow rate through the pilot valve to be as large as the one in Fig. 12.28, in which a 1.5-in. OD pilot valve with a main port of  $\frac{48}{64}$  in. was installed. The very high rate of increase of the injection pressure shown every time the intermitter opens in Fig. 12.30a is due to the reduced volume of the injection annulus: casing diameter of 5 $\frac{1}{2}$  in. and pilot valve's depth of only 2335 ft. With this reduced annular volume, the  $\frac{1}{4}$ -in. surface choke in the gas injection line is necessary to keep the injection pressure from increasing to very large values (that might open an unloading valve, which is not the case in this example because the well did not have any unloading

■ FIGURE 12.30 (a) Well with a small annular volume (pressure chart) (b) Well with a small annular volume (gas flow rate chart at the orifice plate).





■ FIGURE 12.31 Surface intermitter is properly working but the downhole pilot valve failed open.

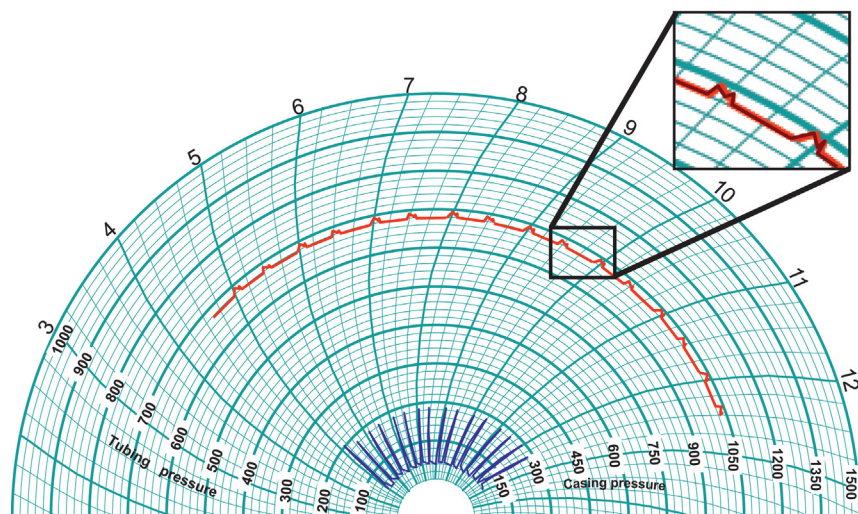
valves) every time the intermitter opens. Fig. 12.30b shows the gas flow rate chart installed at the orifice plate for the well corresponding to Fig. 12.30a. Note that when the differential pressure increases, the static pressure decreases.

The chart in Fig. 12.31 corresponds to a well that had a 1-in. OD, injection-pressure-operated, nitrogen-charged pilot valve. The pilot valve failed open (or at least it appears that way). It can be seen how the injection pressure increases very rapidly every time the surface intermitter opens. When the intermitter closes, the injection pressure decreases and continues to do so until the intermitter opens again. The minimum injection pressure is less than the valve's closing pressure. The injection pressure increases very rapidly because the annular volume is very small (with a 5 1/2-in.  $\times$  17-lb/ft. casing and the point of injection located at a depth of only 2335 ft.). There was no choke installed in series with the intermitter at the surface. The pilot valve was calibrated at a test-rack opening pressure of 637 psig. Additional well data: Vertical well with a 2 7/8-in. production tubing; packer at 2409 ft.; top of perforations at 2467 ft.; reservoir static pressure of 580 psig; 19.3°API oil gravity; and a water cut of 0.2%. The well required 2300 scf/cycle to lift the liquid columns with minimum liquid fallback losses.

Because the pilot valve was nitrogen charged, it was also possible that the valve did not actually fail and it stayed open due to a reduction of its closing pressure caused by a much lower than expected dome temperature (caused in turn by the large volume of gas injected at each cycle). The intermitter injection time interval was unnecessarily long and this long interval combined

with the reduced annular volume are the reasons why the injection pressure reached such large values at each cycle. This large volume of gas injected per cycle then required also a very long time to vent through the pilot valve, which caused the dome temperature to drop, making the valve's closing pressure very low compared to its design value. Even under choke-control intermittent gas lift (in which the surface gas injection flow rate is very small), nitrogen-charged pilot valves usually tend to close at lower than design closing pressures. In this particular case, it is recommended to shut the gas injection off for a while to allow the pilot valve to warm up and then start the surface gas injection with a reduced time interval in which the intermitter remains open. Due to the very small annular volume, it might even be necessary to install a choke in series with the intermitter to reduce the gas flow rate into the well's annulus every time the intermitter opens.

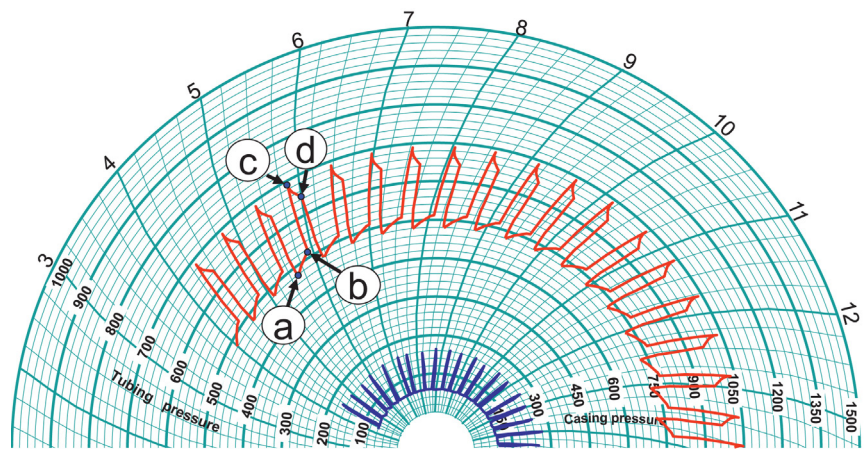
The well corresponding to Fig. 12.32 has an inserted accumulator installed downhole and the liquid columns being produced are so large that the required injection pressure should be closed to 1,000 psig. Additionally, the well has a very large injection annular volume, for which a very small valve spread (difference between the opening and closing pressures of the pilot valve) is required to pass all the volume of gas needed per cycle. The required high injection pressure made it impossible for the valve to reach the small spread required even with the smallest available area ratio. As can be demonstrated from valve mechanic equations, as the injection pressure is



■ FIGURE 12.32 Well with a very large injection annular volume and an injection-pressure-operated pilot valve (gas injection controlled with the use of a surface intermitter).

increased, the spread of the valve also increases. For this reason, a special pilot valve was designed with a very small area ratio, which was then used to produce the liquid slugs in a very efficient manner. It can be seen in the chart of Fig. 12.32 that the objective of getting a very small spread was satisfactorily achieved. The intermitter was set to open for 5 minutes and to remain closed for 25 min. Two pressure peaks can be observed, but only the first one is real. The second peak is caused by the vibration of the chart recorder every time the liquid slug was produced (the chart recorder was mounted on the flowline which vibrated every time the liquid slug reached the surface). A simple inspection of the pressure chart in Fig. 12.32, without any kind of analysis, might lead to the wrong conclusion that the volume of gas injected per cycle was less than its required value because the spread of the valve was very small. But in reality, the annular volume was very large and the tubing diameter very small so that the spread shown in the chart was the one the well needed to produce the liquid slugs to the surface with minimum liquid fallback losses.

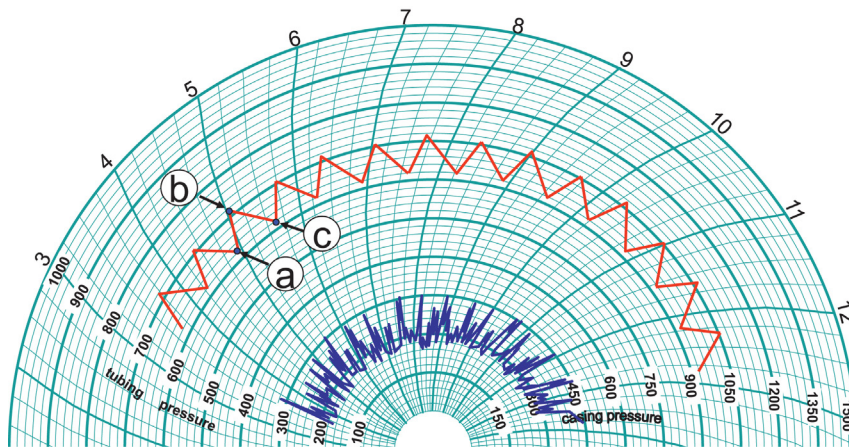
Fig. 12.33 shows the pressure pattern of a well with an annulus–tubing communication and the surface gas injection controlled by a time-cycle controller. The hole or communication is below the static liquid level. From point “a” to “b” in the figure, the intermitter is closed. The injection pressure is increasing because liquids from the formation are entering the annulus; in consequence, the liquid level in the annulus is rising, pressurizing the gas trapped above the liquid level. The intermitter opens at point “b” and the injection pressure increases very fast until reaching point “c” at which time



■ FIGURE 12.33 Tubing hole or annulus–tubing communication. Gas injection controlled by surface intermitter.

the gas uncovers the communication and the injection pressure begins to decrease because the gas flow rate that enters the tubing is greater than the injection gas flow rate at the surface. At point “d” the intermitter closes and the injection pressure drops very fast due to the high gas flow rate through the communication.

Fig. 12.34 shows the behavior of the wellhead pressures in a well that looks as if it is on choke-control intermittent gas lift when in reality it is on intermittent gas lift with the use of a surface intermitter. This behavior could be due to: (1) an annular–tubing communication, (2) the pilot valve failed open, or (3) too much gas being injected into the well’s annulus at the surface and not enough time given for the annular pressure to drop to the pilot valve’s injection closing pressure. The surface intermitter opens at point “a” in the figure. At that moment the injection pressure starts to increase and it continues to do so until the surface intermitter closes at point “b”. When the intermitter closes, the injection pressure begins to decrease but at a low rate perhaps because: (1) the annulus–tubing communication is very small, (2) the pilot valve is restricting the flow into the tubing, or (3) the annular volume is just too large. The intermitter opens again at point “c”. The surface gas flow rate measurement must be verified first. If the gas flow rate is adequate (not too large in comparison to its design value) then a communication test should be performed to determine if the valve has failed or there is indeed an annulus–tubing communication. As previously



■ **FIGURE 12.34 Three possible types of failure:** (a) hole or tubing–annulus communication, (b) pilot valve failed open, or (c) the surface injection gas flow rate is too large (not giving sufficient time for the pilot valve to close). The injection is being controlled by a surface intermitter which is properly working.

mentioned, communication tests (explained in chapter: Continuous Gas Lift Troubleshooting) are reliable only if the operating valve is a single-element valve or the pilot valve does not have its check valve installed inside the pilot valve's piston. A pilot valve with its check valve inside the piston is in reality a tubing-annulus communication if the piston is stuck open or its internal check valve is plugged or stuck closed, exhibiting exactly the same behavior of a well with a hole in the production tubing.

If the communication test indicates that a single-element operating valve (or a pilot valve with its check valve outside the piston) is stuck open (maybe due to a solid particle between the ball and the seat or the bellows has failed) or, in general, if there is a pilot valve with its check valve inside the piston installed in the well (for which a communication test will not reveal if the problem is a hole in the tubing or the valve stuck open), the following steps must be taken:

- Shut in the well (close the surface production tubing valve) keeping the surface gas injection into the well's annulus open. This pressurizes the production tubing and the injection annulus to line pressure so the operating valve will be fully open. Then, the well should be quickly open to production, generating a large differential pressure across the operating valve which could help in getting rid of the solid particles that are keeping the gas lift valve open. This procedure should be repeated until the annular pressure does not drop below the gas lift valve's closing pressure.
- If these steps do not work and the well is in a marine environment, fresh water could be injected down the annulus to dissolve the solid particles that are keeping the valve open. Some operators prefer venting the annulus several times to get the gas lift valve working properly again. If none of these steps can make the gas lift valve close, the gas lift valves should be replaced.

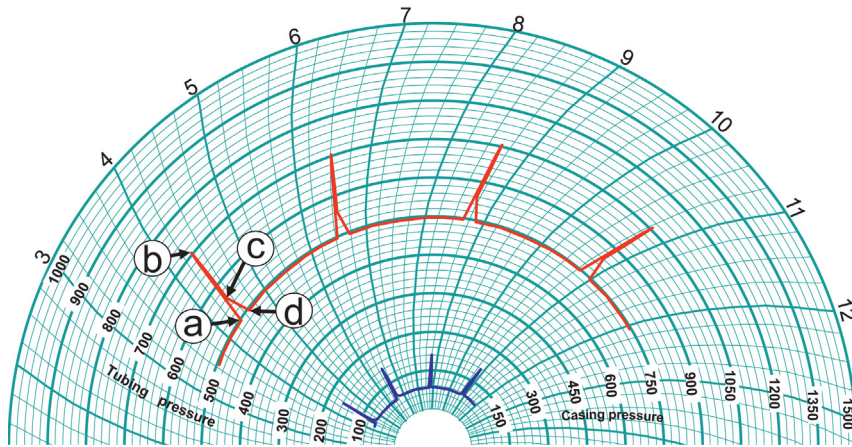
If there is indeed a hole in the tubing, its depth could be determined using the techniques available for that purpose, as explained in chapter: Continuous Gas Lift Troubleshooting. Because the well is on intermittent gas lift, it is not recommended to install any type of packoff completion to isolate the communication (it would create a restriction to the liquid flow that would increase the liquid fallback losses). When the communication is below the static liquid level, some operators take advantage of the fact that liquids can flow from the tubing into the annulus to use the well's annulus as an accumulation chamber and produce a large liquid column at each cycle, but this practice increases the injection gas/liquid ratio because the communication offers an uncontrolled gas injection into the tubing. A better solution is to



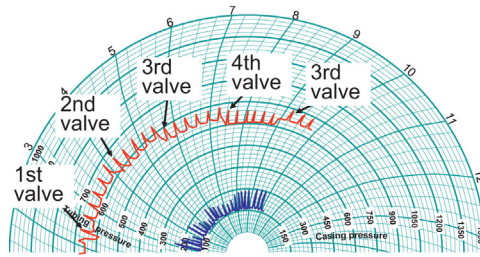
simply replace the current production tubing string. A recommended step in this case is to determine, by nodal analysis, the best tubing size for current well conditions. It might be possible to switch the well to continuous gas lift by using small diameter tubing. If possible, it is always better to produce the well on continuous flow unless the injection gas/liquid ratio needs to be very large to sustain a stable continuous gas lift operation.

Fig. 12.35 shows a well with an annular injection volume so small that the injection pressure increases very rapidly when the surface intermitter opens. The operating gas lift valve and one injection-pressure-operated unloading valve open while the injection pressure is increasing (see the explanation given for Fig. 12.26j). A high pressure regulator can be installed to close the surface intermitter once a certain surface injection pressure is reached. This solution requires an extra cost in surface equipment and adds an additional possible point of failure. Another solution could be obtained by installing a choke in series with the surface intermitter but care should be taken so that the operating valve would not open and close several times while the intermitter is opened, as shown in Fig. 12.26g. In Fig. 12.35, the intermitter opens at point “a” and closes at point “b”. The unloading gas lift valve closes at “c” and the operating valve finally closes at “d”.

Fig. 12.36 shows a well being unloaded on intermittent gas lift with the use of a surface intermitter. The gas lift valves are all injection-pressure-operated valves. If possible, it is better to unload the well on continuous gas lift and switch it to intermittent gas lift once the operating valve is uncovered. But



■ FIGURE 12.35 Wellhead pressure pattern for a well with a very small annular volume. The design operating gas lift valve and one unloading gas lift valve are opening and closing.

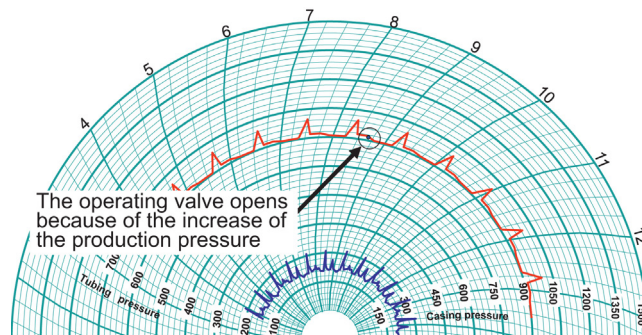


■ FIGURE 12.36 Well unloaded on intermittent gas lift.

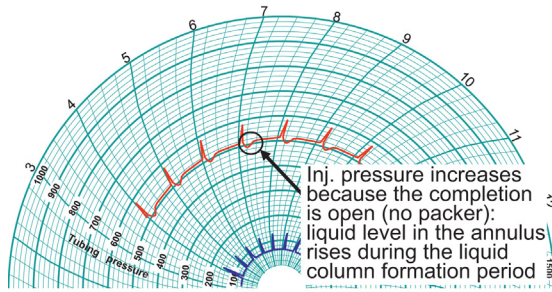
there are gas lift fields with compression capacities so small that it is not possible to supply the injection gas flow rate that is required to unload the wells on continuous gas lift. In these rare cases, the injection annulus needs to be used to slowly store the gas injected per cycle. The figure shows that the well was indeed successfully unloaded to the fourth valve but then (as an example of what can happen under certain situations) it began to flow and the final operation stabilized at the third valve.

It can be appreciated in Fig. 12.37 that the injection pressure shows a slight drop during the period of time in which it should remain constant (the surface gas injection is controlled by a surface intermitter). This is due to the fact that the production pressure increases to a point in which the combined forces of the injection and production pressures can open the operating valve (even if it is an injection-pressure-operated valve). In this case, the cycle frequency should be increased or the operating valve should be replaced with a valve calibrated to open at a higher injection pressure.

Fig. 12.38 shows the wellhead pressures of a well with an injection-pressure-operated pilot valve and a surface intermitter controlling the gas injection into the annulus. The increase in the injection pressure between cycles is



■ FIGURE 12.37 Operating valve opens during the liquid column regeneration period.

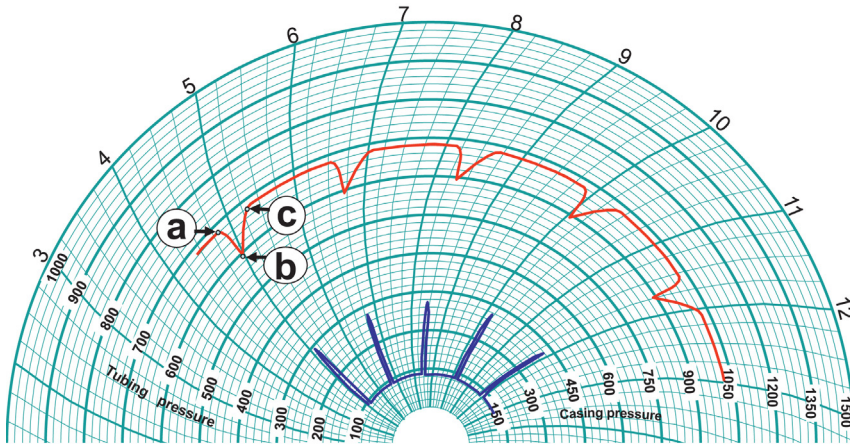


■ FIGURE 12.38 Open completion (no packer). Surface intermitter is used with a downhole injection-pressure-operated pilot valve.

not due to a leak through the surface intermitter. The completion is an open completion (no packer) so that the liquid level rises in the annulus while the liquid column inside the tubing is being generated above the pilot valve. The gas trapped in the annulus above the annular liquid level is compressed (as liquids from the formation enter the tubing and the annulus) so the injection pressure increases even though the surface intermitter is closed.

Fig. 12.39 shows a wellhead pressure pattern that can be due to one of the following alternatives:

- The operating valve is a production-pressure-operated valve which opens when the production pressure reaches the production opening



■ FIGURE 12.39 Alternatives: (a) production-pressure-operated pilot valve with a surface pressure reduction controller, (b) production-pressure-operated valve calibrated to open with full line injection pressure at the wellhead, or (c) injection-pressure-operated valve calibrated at a very high injection opening pressure.

pressure of the pilot valve. As soon as the injection pressure begins to drop, a surface controller sends a signal to open the surface gas injection valve (installed in the surface gas injection line) to start the gas injection into the well (point “a”). This surface valve is usually an “open/close” type of valve. Because the gas flow rate at the surface is less than the gas flow rate through the pilot valve, the injection pressure continues to drop until the pilot valve closes. The pilot valve closes because the production pressure has decreased. The pilot valve closes at point “b” in the figure. At that moment, the injection pressure begins to increase until it reaches a value above which the controller sends a signal to close the gas injection valve to stop the injection to the well (point “c”). Once the surface injection valve is closed, the injection pressure remains constant until the pilot valve opens again to start a new gas injection cycle. It is important to keep the gas injection flow rate at the surface less than the gas flow rate through the pilot valve. This can be achieved by installing a choke in the gas injection line or by using a gas injection needle valve instead of the “open/close” injection valve installed in the gas line. “Open/close” valves are designed to open and close only. But the automatic needle valves that are used to regulate the gas flow rate in continuous gas lift wells can be used in intermittent gas lift wells to open to a predetermined value which could be any value less than 100% open. The major drawback of adjustable needle valves operating on intermittent gas lift is that they do not last the same number of cycles the simpler “open/close” valves can withstand without any kind of failure.

- The valve could also be a production-pressure-operated valve but in this case the surface injection pressure can be equal to line pressure (also known as system pressure, equal to the pressure at the injection manifold) because the well does not have unloading valves. The flow rate is equal to zero while the pilot valve is closed, simply because the wellhead pressure is equal to the manifold pressure. When the pilot valve opens (due to the increase in the downhole production pressure) the annular pressure begins to drop (point “a”) until the pilot valve closes (point “b”). From point “b” to point “c”, the annular pressure increases until the wellhead injection pressure reaches line pressure. As can be seen, this is a very simple and inexpensive way of controlling the gas injection into the well but its major drawback is the fact that the duration of the cycle is controlled by the reservoir and not by the operator.
- Fig. 12.39 could also correspond to a well with an injection-pressure-operated pilot valve calibrated at a very high injection opening pressure. When the injection pressure reaches line pressure, the gas

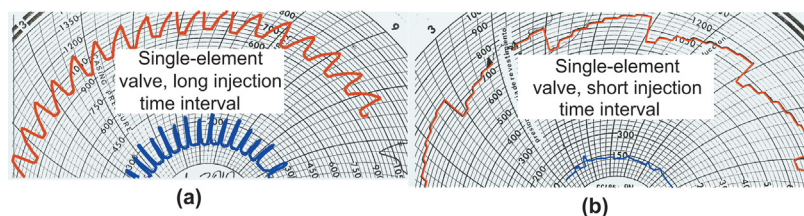
flow rate to the well stops and the injection pressure remains constant until the pilot valve opens due to the combined action of the injection pressure in the annulus and the production pressure of the liquid column that has been accumulating above the pilot valve in the tubing. This is possible to occur because injection-pressure-operated valves actually respond to both, the injection and the production pressure: as the production pressure increases, the required gas injection opening pressure decreases.

### 12.5.2 Examples of specific field cases

Examples of wellhead pressure patterns in actual field cases are presented in the section, together with as much information as possible about the well and gas lift system gathered for each of these cases.

The well corresponding to Fig. 12.40 had a surface intermitter at the well-head. Well data: 7-in.  $\times$  23-lb/ft. casing; 3½-in. tubing; top of perforations' depth: 5182 ft.; packer's depth: 4867 ft.; reservoir pressure: 724 psig; 29° API oil gravity; 1% water cut; operating valve's depth: 4789 ft.; and a wellhead production pressure of approximately 70 psig. Initially, the operating valve was a single-element, nitrogen-charged, injection-pressure-operated valve, model "R-20" with a seat diameter of 28/64 in., calibrated at a test-rack opening pressure of 721 psig. Because the seat diameter was large (for a single-element valve), the valve's area ratio was 0.201, which can give the large spread shown in the figure. The volume of gas injected per cycle was therefore very large: more than 7000 scf/cycle, which is much larger than the required volume of gas per cycle.

Before the surface intermitter was installed, the well was producing 85 STB/D on choke-control intermittent gas lift with a gas injection flow rate of 512 Mscf/D. The production remained the same after installing the surface intermitter set at: 18 min open and 32 min closed as shown in Fig. 12.40a. Afterward, the intermitter was set to open for only 2 min



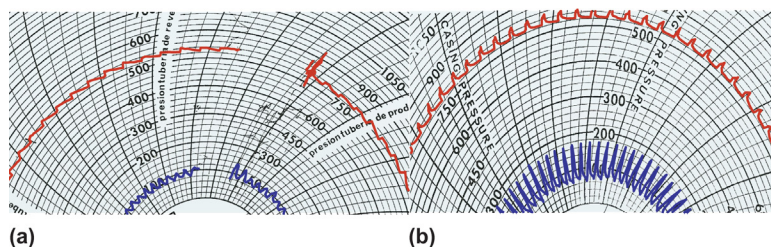
■ FIGURE 12.40 Surface gas injection controlled with a surface intermitter. Single-element valve at the operating point of injection.

and close for 15 min and, as can be seen in Fig. 12.40b, the intermitter had to open 6 or 7 times before the injection pressure could reach the gas lift valve's injection opening pressure. However, the daily liquid production dropped only to 74 STB/D which indicated that the optimum cycle time was very long.

Figs. 12.40a and b also show that it took 12 min after the intermitter has closed for the injection pressure to drop back to the single-element gas lift valve's closing pressure. This could be due to the size of the seat of the gas lift valve of only 28/64 in. In contrast, 1.5-in. pilot valves can have main port diameters as large as 48/64 in., which are more adequate for intermittent gas lift applications because they allow a fast injection pressure drop once the intermitter closes.

Because the subsurface valve was a single-element valve, its seat diameter was also causing a very large spread and therefore a very large volume of gas was injected per cycle. This single-element valve is more appropriate for wells with injection point depths of no more than approximately 2500 ft. and, additionally, a casing diameter no larger than 5 1/2 in. (for these valves, the annular volume is very small and a spread equal to the one shown in Fig. 12.40 could deliver the small volume of gas per cycle required by the well). The problem with single-element valves used for intermittent gas lift is that the seat could be too large for the required area ratio but, at the same time, too small for the required instantaneous gas flow rate through the valve.

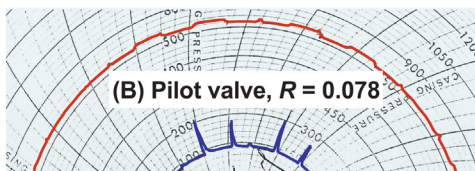
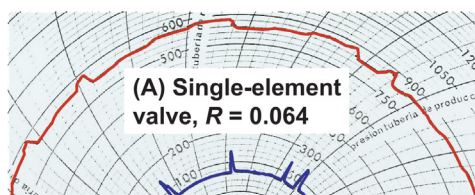
The single-element valve mentioned in the previous paragraphs was then replaced by an injection-pressure-operated, spring-loaded pilot valve, model WF14R, with an area ratio of only 0.078, calibrated at a test-rack closing pressure of 850 psig. The idea was to control the effective spread by adjusting the period of time that the surface intermitter was allowed to remain open. But the injection gas was measured at the injection manifold by an orifice plate of only 3/8th of an inch in diameter and the 1/4-in. needle valve previously used to control the gas flow rate (when the well was operating on choke-control intermittent lift) was not removed. These restrictions made it impossible for the injection pressure to continue to increase once the pilot valve and the intermitter were both opened at the same time. These restrictions have the effect shown in Fig. 12.41a, where it can also be appreciated that the pilot valve was leaking: Restrictions do not allow the injection pressure to increase when the pilot valve opens and the leak through the pilot valve is revealed by the fact that the injection pressure drops even after the pilot valve closes. Fig. 12.41b shows the wellhead pressures after the restrictions had been removed. The injection pressure increases even after the pilot valve opens. It can also be



■ FIGURE 12.41 Surface intermitter and downhole pilot valve. (a) Leaking pilot valve, restrictions at inj. manifold and (b) leaking pilot valve, no surface restrictions.

seen that the pilot valve was still leaking gas into the tubing. Under these last conditions, the well began to produce 120 STB/D with an injection gas flow rate of only 224 Mscf/D (less than half the daily gas injection while the well was on choke-control intermittent gas lift).

The next example is shown in Fig. 12.42. The well had a subsurface single-element valve installed at the operating point of injection, model ERO-4-SR, which is a nitrogen-charged, injection-pressure-operated, 1.5-in. OD valve, with an area ratio of 0.064 and a test-rack opening pressure of 845 psig. The same automatic needle valve in the injection manifold that is normally used to control the gas injection for continuous gas lift was used this time as the “surface intermitter” with a special control algorithm that allowed the valve to remain close for a given period of time and then open to a specified stem position for another predetermined period of time (this could be done



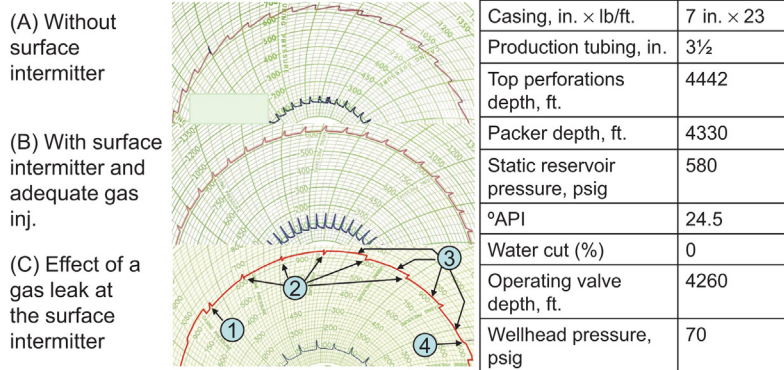
Casing, in.	7 in. x 23
Production tubing, in.	2½
Top perforations' depth, ft.	5264
Packer depth, ft.	5143
Static reservoir pressure, psig	858
°API	24
Water cut (%)	5
Operating valve depth, ft.	5097
Wellhead pressure, psig	90

■ FIGURE 12.42 Surface intermitter at the injection manifold (same automatic needle valve used for continuous gas lift): (a) with a subsurface single-element valve, (b) with a gas lift pilot valve.

because the injection manifold was fully automated). As can be seen in Fig. 12.42a, the period of time in which the surface intermitter remained open was very short and the intermitter needed to open several times to open the subsurface valve. The system pressure was not constant and, in consequence, the volume of gas injected per cycle was changing from cycle to cycle although not in a pronounced way. With the same subsurface valve, the well was producing 47 STB/D on continuous gas lift with a gas injection flow rate of 181 Mscf/D. With the gas injection switched to intermittent gas lift, the surface instantaneous gas flow rate was first set at 300 Mscf/D, which was less than the gas flow rate through the subsurface valve, thus the injection pressure dropped every time the subsurface valve opened. The instantaneous surface injection gas flow rate was then set at 400 Mscf/D, with the intermitter open for 10 min and closed for 30 min. With these settings, the well produced 50 STB/D with a daily injection of only 100 Mscf/D. The single-element valve was replaced by an injection-pressure-operated, spring-loaded, 1.5-in. OD pilot valve, model WF14R, with a slightly greater area ratio and a test-rack closing pressure of 840 psig. Even though the area ratio of the pilot valve was greater, the spread shown in Fig. 12.42b was actually smaller than the spread given by the single-element valve. This is due to the fact that spring-loaded valves tend to close at a pressure higher than the theoretical closing pressure (nitrogen-charged valves behave in the opposite way). With the pilot valve installed in the well, the intermitter was set to remain open for 3 min and close for 30 min. The instantaneous surface gas flow rate was set at 825 Mscf/D, which is less than the gas flow rate the pilot valve allowed and, for this reason, the injection pressure dropped every time the pilot valve opened. It can also be observed in the figure that sometimes the volume injected per cycle was sufficient to open the subsurface valve and sometimes it was not (this is due to changes in the gas lift system pressure). This is eliminated by increasing the time the intermitter remains open, but this surface gas injection time interval cannot be too long either because the subsurface valve will open and close several times while the intermitter is opened. With the pilot valve installed in the well, the liquid production increased to 81 STB/D with a daily injection gas flow rate of only 75 Mscf/D. In other words, with less than half of the previous gas consumption, the liquid production was almost doubled in comparison to the liquid production the well had when it was producing on continuous gas lift.

The well corresponding to Fig. 12.43 had an injection-pressure-operated, 1.5-in. OD, nitrogen-charged pilot valve calibrated at a test-rack opening pressure of 889 psig. Fig. 12.43a shows the wellhead pressures while the well was producing on choke-control intermittent gas lift. The surface injection gas flow rate was constant and the subsurface pilot valve was opening at





■ **FIGURE 12.43** Same pilot valve with: (a) constant surface gas injection (without surface intermitter action), (b) use of surface intermitter with adequate gas injection time, and (c) effect of a gas leak at the surface intermitter.

regular intervals. Under these operational conditions, the well was producing 30 STB/D with a daily gas injection flow rate of 240 Mscf/D.

Fig. 12.43b shows the behavior of the wellhead pressures while the well was producing with the use of a surface intermitter. The same automatic needle valve in the injection manifold that is normally used to control the gas injection for continuous gas lift was used this time as the surface intermitter with a special control algorithm that allowed the surface valve to remain closed for a given period of time and then opened, to a specified stem position, for another predetermined period of time (this could be done because the injection manifold was fully automated). The injection needle valve did not fully open and allowed a gas flow rate of only 800 Mscf/D. Because the gas flow rate through the subsurface pilot valve was greater than the surface injection gas flow rate through the surface needle valve, the injection pressure dropped every time the pilot valve opened. The time the surface intermitter remained open was just the time needed to reach the pilot valve opening pressure. If the surface injection time is shorter, the intermitter (needle valve) will have to open one more time to open the pilot valve. However, if the surface injection time is just slightly longer than its value in Fig. 12.43b, the pilot valve might open and close while the surface intermitter is opened, as shown in Fig. 12.43c in points (2) and (3).

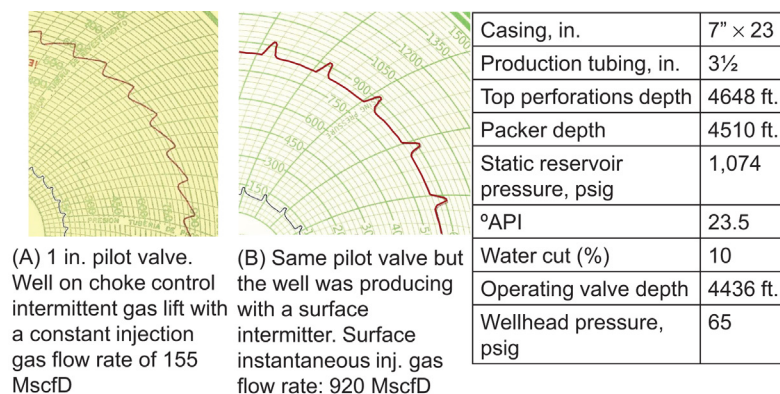
Operational conditions deteriorated and Fig. 12.43c shows the result of having a small surface gas flow rate (as in Figs. 12.43a and b) with an additional problem: a gas leak at the surface intermitter. These two factors were causing the irregular injection pressure pattern that can be seen in Fig. 12.43c, which

changed from cycle to cycle. Referring to the numbers shown in Fig. 12.43c, the following observations help explain what is going on in the well:

1. The injection pressure at the time the intermitter opens is such that the surface intermitter opens for just the period of time needed for the pilot valve to open. As soon as the pilot valve opens, the surface intermitter closes and the injection pressure drops to the pilot valve's surface closing pressure. The injection pressure then remains constant at the gas lift valve's closing pressure until the intermitter opens again.
2. In this case because the injection pressure (when the intermitter opens) is higher than in point (1), the pilot valve opens and closes while the intermitter is opened, even though the time interval in which the intermitter remains opened is the same as in point (1). Because the pilot valve closes first, the injection pressure begins to increase until the intermitter finally closes, leaving the injection pressure at a value between the pilot valve's surface opening and closing pressures.
3. During the time the surface controller is supposed to be closed, the injection pressure increases at a low rate. This pressure increase is caused by a small leak (through the surface controller) toward the well's annulus.
4. In this case, the surface controller opens but the injection pressure does not reach the injection opening pressure of the pilot valve so the pilot valve does not open. This occurs because it just so happens that the injection pressure from the last cycle fell to a value too low for it to increase to the pilot valve's opening pressure with only one opening of the surface controller.

The gas leak was fixed and the liquid production was increased to 42 STB/D with only 99 Mscf/D by means of an optimization procedure that is used to find: a) the appropriate gas injection time interval (the time the surface intermitter should remain open) and, b) the optimum cycle time (this optimization procedure is explained in Section 10.6.2). This represents a considerable reduction in the injection gas/liquid ratio in comparison to what the well had while it was producing on continuous gas lift.

Fig. 12.44 shows the behavior of the wellhead pressures with and without the use of a surface intermitter. The subsurface pilot valve is the same for both cases. The same automatic needle valve in the gas injection manifold (which is normally used to control the gas injection for continuous gas lift) was used this time as the surface intermitter with a special control algorithm that allowed the needle valve to remain closed for a given period of time and then opened to a specified stem position for another predetermined period of time. The gas lift pilot valve was a 1-in. OD, injection-pressure-operated, spring-loaded valve (model WFM14R), with a test-rack closing pressure of



■ FIGURE 12.44 Two ways of controlling the gas injection to the well with the same subsurface pilot valve.

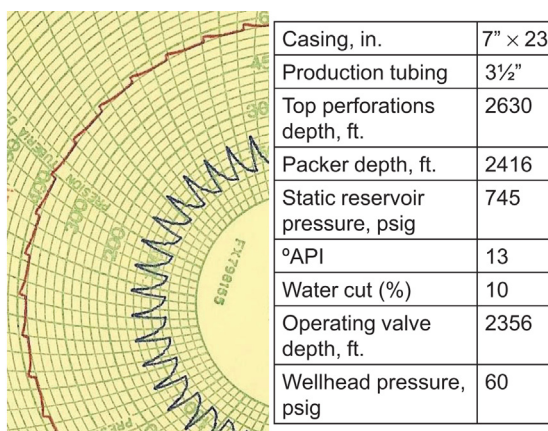
873 psig and an area ratio of 0.183. Under the conditions of Fig. 12.44a the well was producing (on choke-control intermittent lift) 55 STB/D with a constant daily surface injection gas flow rate of 155 Mscf/D.

It is shown in Fig. 12.44b that when the intermitter (or surface controller) opens, the injection pressure increases rapidly until the pilot valve opens and, at that moment, the injection pressure begins to decrease very slowly, indicating that the surface instantaneous gas flow rate is smaller but comparable to the gas flow rate through the subsurface pilot valve. These flow rates are similar because the intermitter allows a surface gas flow rate of only 930 Mscf/D, which is close to what a 1-in. OD pilot valve allows to pass for the well's current conditions and a main port diameter of 32/64 in. Once the intermitter (the needle valve at the manifold) closes, the injection pressure begins to drop until it reaches the pilot valve's injection closing pressure. This pressure drop is not as steep as it should be (for intermittent gas lift) because the annular volume is large and the gas lift valve is a 1-in. OD valve. It takes 8 min for the annular injection pressure to drop to the pilot valve's closing pressure. The liquid slug velocity should be of around 1000 ft./min to keep the liquid fallback losses at a minimum value. If this velocity is achieved, the elapsed period of time between the moment the pilot valve opens and closes should not be greater than 5 min because the injection point is 4510-ft deep.

Even though the volume of gas injected per cycle with and without the use of the surface intermitter is about the same, the daily gas injection was reduced with the used of the intermitter only because the total cycle time was increased: with a daily injection of only 50 Mscf/D, the liquid production was kept at the same level it had when the gas injection flow rate was at 155 Mscf/D on

choke control. This reduction in the injection gas/liquid ratio could have been obtained with the well on choke control by reducing the surface injection gas flow rate and, therefore, increasing the total cycle time. But the volume of gas required per cycle could not be individually optimized with the well on choke control. The volume of gas per cycle being injected to the well was measured at approximately 4250 scf/cycle, which is slightly less than the required volume of gas to be injected per cycle for the well's operational conditions. This means that, thanks to the use of the surface intermitter, the required volume of gas per cycle could be attained by just increasing the time the intermitter is allowed to stay open. In this way, the liquid fallback losses could be reduced and the overall efficiency of the intermittent gas lift method might be improved. But an even better operational condition can be obtained by increasing the instantaneous injection gas flow rate through the intermitter at the surface so that the injection pressure does not decrease when the pilot valve opens. In this way, more gas per cycle could be injected in less time because it would not be necessary to leave the surface intermitter open for a long time. On the other hand, if the well needs a volume of gas per cycle considerably smaller than the one being injected, it would not be possible to reduce the volume of gas per cycle by just reducing the time the intermitter is allowed to remain open. This is due to the fact that the area ratio of the pilot valve is too large and, in consequence, the spread of the gas lift valve could not be reduced. In this case, the only way to reduce the volume of gas injected per cycle is by replacing the currently installed pilot valve with another one with a smaller area ratio.

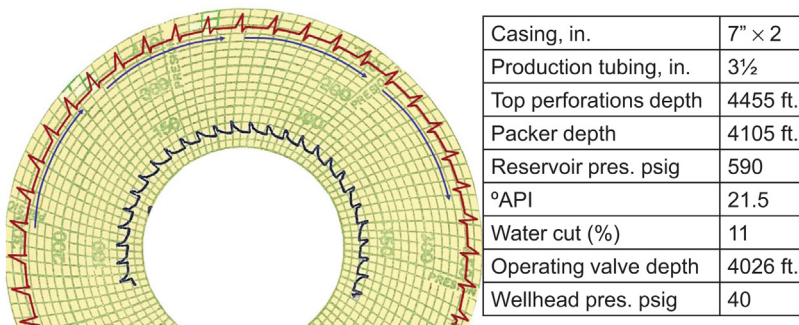
Fig. 12.45 shows a chart from a well that had an injection-pressure-operated, spring-loaded, pilot valve at the operating point of injection, model



■ FIGURE 12.45 Pilot valve calibrated at a very low test-rack closing pressure and working in conjunction with an intermitter installed at the injection manifold.

WF14R, with a very low test-rack closing pressure of 556 psig and with a large area ratio of 0.239. Even though the area ratio of the valve was large, the spread shown in the figure was small because of the low calibration pressure of the pilot valve and the relatively high production pressure in the tubing at valve's depth. The gas injection was controlled by an intermitter located at the manifold. As in previous examples, the same automatic needle valve in the injection manifold, that is normally used to control the gas injection for continuous gas lift, was used this time as a surface intermitter with a special control algorithm that allowed the valve to remain closed for a given period of time and then opened to a specified stem position for another predetermined period of time. When the surface intermitter opens, the injection pressure increases very rapidly until the subsurface pilot valve opens. When the intermitter and the pilot valve are opened at the same time, the injection pressure stays constant for a short period of time until the surface intermitter closes. After the intermitter closes, the pilot valve remains open for a long time due to the small pressure differential across this valve. Eventually, the pilot valve closes too and the injection pressure remains constant for approximately 16 min. The gas in the annulus is injected into the tubing very slowly because the production tubing pressure is large in comparison to the low injection pressure. This high production pressure is due to the liquid column length itself and to the viscosity of the oil being lifted (13°API).

The pressure chart in Fig. 12.46 shows what happens when the surface injection gas flow rate is very small and the period of time in which the surface controller remains open is long enough for the pilot valve to open and close only one time at each cycle. Note that the pilot valve surface opening and closing pressures are the same for all cycles. Only the shape of the injection pressure changes from cycle to cycle, but the volume of gas injected per cycle is constant. This is why the liquid slugs are produced in the same manner in all cycles. During the first cycles shown in the chart, the controller closes



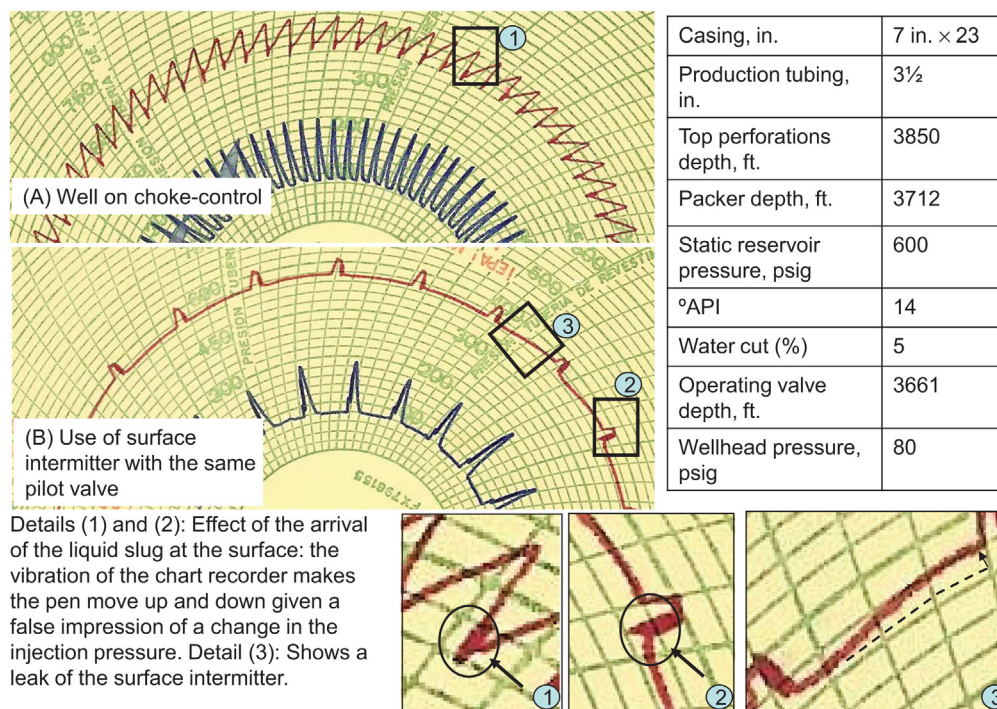
■ FIGURE 12.46 Very small gas flow rate across the surface intermitter.

shortly after the pilot valve closes. For the cycles to remain with the exact same shape, it would be necessary for the time in which the controller remains open to be exactly the one needed for the initial pressure (when the controller opens) to be equal to the final pressure (when the controller closes) but this is very difficult to achieve. Even if this exact period of time is attained, any fluctuation in the line pressure will also change the injection pattern. In this example, the time in which the controller remains open is close to the exact time needed to maintain the same pattern and this is why the shape of the injection pressure pattern changes only gradually from cycle to cycle. If the injection time period is increased, changes will be more pronounced from cycle to cycle and the injection pressure pattern would be completely different. In this case, the injection pressure left in the annulus after the controller closed at each injection cycle was slightly changing from cycle to cycle.

The pilot valve was an injection-pressure-operated, spring-loaded, 1.5-in. OD valve, model WF14R, with an area ratio of 0.239, and a test-rack closing pressure equal to 460 psig. The instantaneous injection gas flow rate across the surface intermitter was equal to 455 Mscf/D. The intermitter remained open for 10 min and closed for 23.3 min. Under these conditions, the well was producing 32 STB/D with a daily injection gas flow rate of 136.5 Mscf/D. After an optimization process was conducted, it was found that the well could produce 40 STB/D with a total gas injection flow rate of 70 Mscf/D by setting the controller to 6.66 min opened, 60 min closed, and an instantaneous surface injection gas flow rate (while the intermitter was opened) of 700 Mscf/D.

Fig. 12.47 shows the wellhead pressure behavior of a well with a gas lift pilot valve installed at the point of injection. Fig. 12.47a shows the wellhead pressures when the well was on choke control with a constant surface injection gas flow rate of 160 Mscf/D. At that time, the well was producing 90 STB/D of liquids. Detail #1 shows how the injection pressure pen was affected every time the liquid slug surfaced. This is probably due to the fact that the chart recorder was mounted on the flowline itself. It can be observed that the gas injection was optimized in the following sense: the annulus was vented at an acceptable rate and the liquid slug arrived at the surface just at the moment the pilot valve was closing. However, a simple intermittent gas lift analysis showed that the total volume of gas injected per cycle was less than its required value. This volume of gas injected per cycle can be increased in different ways:

1. Replacing the pilot valve with another one with a larger area ratio.
2. Replacing the pilot valve with an identical one with a higher test-rack calibration pressure (the higher the calibration pressure is, the larger the spread of the valve becomes).



■ FIGURE 12.47 Two ways of controlling the surface gas injection with the same subsurface gas lift valve.

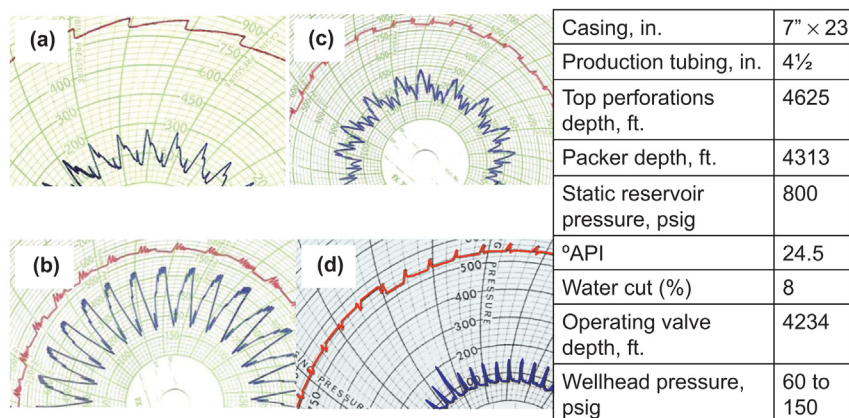
- By not changing the current pilot valve but switching the operation from choke-control to the use of a surface intermitter. In this way, the valve can be forced to remain open for longer periods of time to increase the volume of gas injected per cycle. For this solution to be effective, it is necessary that the surface instantaneous gas flow rate into the casing be greater than or equal to the gas flow rate the pilot valve allows to pass into the tubing once it is opened, so that the injection pressure would not decrease every time the pilot valve and the intermitter are opened at the same time.

Fig. 12.47b shows that by using the surface intermitter the pilot valve can remain open for longer periods of time to pass the exact required volume of gas per cycle: In this case, the instantaneous surface gas flow rate was slightly less than the gas flow rate through the pilot valve and, in consequence, the injection pressure decreased every time the pilot valve opened. It can also be seen that the liquid slug reaches the surface just as the pilot valve is closing (see detail # 2). Additionally, it can be seen that the surface controller did not completely close, so the injection pressure increased during the liquid

slug regeneration time (see detail # 3). This gas leak, if kept under control, is many times advantageous because it allows the injection gas to be stored in the annulus while the liquid column is regenerating downhole, therefore decreasing the volume of gas needed to be injected to open the pilot valve when the intermitter opens. In this way, an injection manifold can handle several wells intermitting at the same time without causing a major drop in the system pressure. The spread of the valve while the well was on choke control (Fig. 12.47a) was greater than the spread shown with the use of the intermitter (Fig. 12.47b) simply because the total cycle time was longer when the intermitter was being used, so that the initial liquid columns and the production pressure were also greater, resulting in a reduction of the required pilot valve's injection opening pressure.

As in previous examples, the same automatic needle valve in the injection manifold that is normally used to control the gas injection for continuous gas lift, was used this time as a surface intermitter (with a special control algorithm that allowed the valve to remain closed for a given period of time and then opened to a specified stem position for another predetermined period of time). The pilot valve was an injection-pressure-operated, 1.5-in. OD, spring-loaded pilot valve, model WF14R, calibrated at a test-rack closing pressure of only 629 psig and with an area ratio of 0.239.

As in the previous example, Fig. 12.48 also shows the wellhead pressure behavior of a well with the same subsurface pilot valve but with different ways of controlling the surface injection gas flow rate. The pilot valve was an injection-pressure-operated, 1.5-in. OD, spring-loaded pilot valve,



■ **FIGURE 12.48** (a) Well on choke control. (b), (c), and (d) gas injection is controlled by a surface intermitter under different operational conditions. The pilot valve was the same in all cases.



model WF14R, calibrated at a test-rack closing pressure of 809 psig, and with an area ratio of 0.239. The way the wellhead pressures behaved when the injection gas flow rate was constant and equal to 200 Mscf/D is shown in Fig. 12.48a:

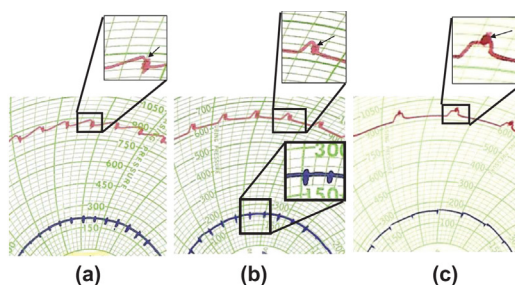
The well was producing 63 STB/D of liquids. The pilot valve was showing a good action with a fast injection pressure drop every time it opened. But a simple intermittent gas lift analysis showed that the total volume of gas injected per cycle was less than its required value, mainly because the production tubing size was of 4½ in. in diameter. One option to inject the required volume of gas per cycle was to implement the use of a surface intermitter to force the pilot valve to remain open for longer periods of time, avoiding in this way to change the subsurface gas lift pilot valve.

It can also be seen in Fig. 12.48a the higher than usual wellhead production pressure. This was due to a 12/64-in. choke installed at the wellhead (at the flowline entrance). Due to the combined effect of the low volume of gas injected per cycle and the restriction to the liquid flow caused by the surface choke, the liquid fallback losses were estimated to be greater than 80% of the initial liquid column length.

Fig. 12.48b shows the behavior of the wellhead pressures when the surface intermitter was first used (set 15 min opened and 30 min closed). The surface instantaneous injection gas flow rate was less than the local gas flow rate through the pilot valve, so the pilot valve opened and closed several times while the surface intermitter remained open. Figs. 12.48c and d show the wellhead pressures with the surface intermitter open for a shorter period of time, for which the injection pressure pattern is similar to the one explained for Fig. 12.46. The only difference between the operational conditions of Fig. 12.48c and d was that in Fig. 12.48d the wellhead choke was removed and, in consequence, the wellhead production pressure was lower. In both cases, gas was injected only through the pilot valve, without any intervention of the unloading valve located at 3815 ft. as might be thought to take place because of the different injection pressure levels found every time the intermitter closes.

Fig. 12.49 shows again a well with the same pilot valve but with different ways of controlling of the surface gas injection:

- a. Well on choke control: Here too the vibration caused by the liquid slug every time it reached the surface was making the pen move up and down given the false impression of an abnormal injection pressure behavior. It can also be appreciated that the instrumentation pipe



■ **FIGURE 12.49** (a) Choke control, (b) time cycle controller (slug arrives at the surface at the moment the pilot valve closes), and (c) time cycle controller (slug arrives before the pilot valve closes). The instrumentation pipe connecting the wellhead production pressure to the sensor of the chart recorder was plugged in all cases.

connecting the wellhead production pressure to the pressure sensor of the chart recorder was plugged and the short vertical lines that can be seen at the production pressure trace are just the result of the vibration of the chart recorder every time a liquid slug arrived at the surface.

- b. Gas injection controlled by a surface intermitter: The liquid slug reaches the surface just as the pilot valve is closing. This does not necessarily mean that the gas injection is optimized. It is still necessary to check the following points: (1) if the volume of gas injected per cycle is equal to the required value to produce the liquid slugs being lifted, (2) if the total cycle time is equal to the optimum cycle time (to maximize the daily liquid production), and (3) if the liquid slug velocity is the one that is appropriate to keep the liquid fallback losses at a minimum level.
- c. Gas injection controlled by a surface intermitter: This time the controller is kept open for a longer period of time, so the liquid slug reaches the surface before the surface controller closes. This could indicate an over injection at each cycle, unless the slug velocity (for some reason that cannot be controlled by the operator) is less than 1000 ft./min and the pilot valve is forced to remain opened with the hope of producing an additional volume of liquid (carried by the tail gas to the surface).

## 12.6 INTERMITTENT GAS LIFT TROUBLESHOOTING EXAMPLES

Several examples of troubleshooting analyses of wells producing on intermittent gas lift are presented in the section. The lack of vital information, sensors not properly calibrated etc, are the usual problems an optimization engineer

must face most of the time. Even under these adverse conditions, it is important to try to carry out the analysis as complete and rigorous as possible because it will serve as a guide to perform specific actions in the field that could help finish the troubleshooting analysis of the well in a fast and satisfactory way. With the exception of the last example presented in the section, all other examples correspond to wells on choke-control intermittent gas lift.

### 12.6.1 Example #1 (well might be loaded with liquids)

The well data is presented first. Reservoir static pressure: 1172 psig; productivity index: 0.21 Br/D-psi; 22° API oil gravity; 5% water cut; formation gas/liquid ratio: 2000 scf/STB; casing diameter: 5½-in. × 17-lb/ft.; production tubing ID: 2.441 in.; production tubing OD: 2.875 in.; depth of top of perforations: 6974 ft.; packer's depth: 6598 ft.; gas injection line length: 8150 ft.; gas injection line ID: 2.07 in.; gas lift valves data: two 1-in., injection-pressure-operated, nitrogen-charged, unloading valves were installed and the operating valve was a 1-in., injection-pressure-operated, nitrogen-charged pilot valve (Tables 12.2 and 12.3).

In Jun. 2002, the well had an important reduction in its liquid production. The production dropped to values between 30 and 50 STB/D. The well's total depth was checked by wireline and it was clean (no sand has accumulated at the bottom).

**Table 12.2** Valves Installed in the Well

Depth (ft.)	Valve Model	Seat Diameter (1/64 in.)	Injection Opening Pressure (psig)	$P_{tr}$ (psig)
2006	Dummy	—	—	—
3782	BCO-1	16	975	965
5247	BCO-1	16	912	929
6522	BPV-1C	24	820	862
	R = 0.164			

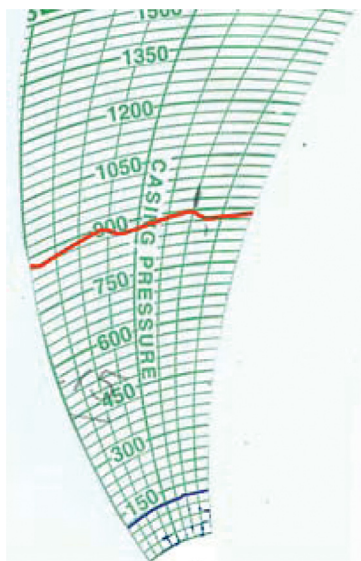
**Table 12.3** Production History

Date	Production STB Liquid per day	Surface injection gas flow rate (Mscf/D)
Sep. 2001	155	667
Nov. 2001	155	667
Dec. 2001	114	667

Operational conditions at the time of the analysis:

Wellhead injection opening pressure: 900 psig. Wellhead injection closing pressure: 870 psig. Wellhead production pressure: 80 psig. The injection opening and closing pressures at depth, calculated with a gas specific gravity of 0.7, were equal to 1061 and 1025 psig, respectively. Unfortunately, it was not clear what the exact value of the injection gas specific gravity was and it could have been as high as 0.73, for which the injection opening and closing pressures at depth would be 1072 and 1035 psig, respectively. Even though the pilot valve installed in the well is a very restrictive valve because its main port's effective diameter is only 24/64 in., the pilot valve remained open for only 7 min at each cycle. This is a normal opening time for a pilot valve because it is a short period of time to pass the volume of gas currently injected per cycle. Having such a short injection time interval is very difficult for a single-element valve to achieve. Total cycle time: 45 min. Surface injection gas flow rate: 212 Mscf/D. There is an uncertainty in the measurement of the liquid production and it could have been anywhere between 30 and 50 STB/D (Fig. 12.50).

It can be seen in the pressure chart that the production pressure was not affected by the arrival of the slug at the surface. The well might have been



■ FIGURE 12.50 Wellhead pressure chart for the operational conditions at the time of the troubleshooting analysis.

producing in a continuous fashion or the production pressure sensor connection was plug.

If the surface gas flow rate is divided by the number of cycles in one day, the volume of gas injected per cycle would be  $= \frac{212,000 \text{ scf/D}}{(1,440 \text{ min/D})/(45 \text{ min/cycle})} = 6,624 \text{ scf/cycle}$ . But, using the equations explained in Section 12.2.1 (Eqs (12.1) to (12.14)), the volume of gas injected per cycle can be calculated from the volume of the annulus and the injection line, together with the opening and closing pressures to give an injection volume of only 2,208.5 scf/cycle, which represents a surface gas flow rate of 70 Mscf/D and not 212 Mscf/D. There might have been several points of injection (if the high gas flow rate causes an unloading valve to open) or the surface injection gas flow rate was not accurately measured and it was indeed 70 Mscf/D. The surface gas flow rate is calculated by multiplying the static and differential pressure factors by the orifice plate factor corresponding to the diameter of the orifice plate installed at the manifold. The differential and static measurements were 3 and 7.4 points, respectively. The orifice plate was 5/8-in. in diameter so its orifice plate factor was equal to 9.55. Thus the surface injection gas flow rate was  $7.4 (3)(9.55) = 212 \text{ Mscf/D}$ . With a 3/8-in. orifice plate, the orifice factor is 3.42 and the gas flow rate would be  $7.4 (3)(3.42) = 75.92 \text{ Mscf/D}$ , which is very close to the volume of gas per cycle calculated from the equations given in Section 12.2.1. This is an important clue that points to the fact that the gas flow measurement might had been in error (because the orifice plate does not correspond to the one shown in the well's file), but it is not conclusive because there might have been more than just one point of injection.

The liquid column length (in feet) produced to the surface is equal to the daily liquid production divided by the number of cycles in one day and by the volumetric capacity of the production tubing (in this case equal to 0.005788 Br/ft.):

$$Q_{\text{prod}} = \frac{50 \text{ Br/D}}{[(1440 \text{ min/D})/(45 \text{ min/cycle})] 0.005788 \text{ Br/ft.}} = 270 \text{ ft./cycle}$$

The initial liquid column at depth must be longer than the liquid column that reaches the surface. The initial liquid column is obtained dividing  $Q_{\text{prod}}$  by  $(1 - FD_{\text{ov}})$ , where  $D_{\text{ov}}$  is the point of injection depth in Mft., in this case equal to 6.522 Mft., and  $F$  is the fallback factor.  $F$  depends on the volume of gas injected per cycle and the instantaneous gas flow rate through the pilot valve. The initial liquid column lengths  $Q_{\text{mi}}$  calculated from  $Q_{\text{prod}}$ , for different values of  $F$ , are presented in Table 12.4, together with the required volume

**Table 12.4** Required Volume of Gas Injected per Cycle

<i>F</i>	<i>Q</i> <sub>ini</sub> (ft.)	Required <i>v</i> <sub>gSR</sub> (scf/cycle)
0.03	335.6	5371
0.05	400	5310
0.1	776	4994

of gas injected per cycle to produce each liquid column. This required volume of gas injected per cycle is calculated from the equation given in chapter: Design of Intermittent Gas Lift Installations for intermittent gas lift design (energy balance Eq. 10.32):

As seen in the previous table, the required volume of gas per cycle decreases as the liquid slug size increases. This seems to be a contradiction but it is explained in the following way: a) The size of the liquid slug that reaches the surface is the same in all cases and, b) The volume of gas that must be injected to fill the tubing below the slug when it is just beginning to be produced at the surface is smaller for larger slugs because a good part of the liquid slug that is not produced occupies an important volume in the tubing that does not need be filled with gas. In any case, it can be seen that the required volume of gas per cycle is less than the one that was being injected if the gas flow rate at the surface was indeed equal to 212 Mscf/D. But this surface gas flow rate of 212 Mscf/D does not coincide with the one provided by the annulus and gas injection line at each cycle unless there were more than one point of injection. If the pilot valve was the only point of injection, only 2,208.5 scf were injected per cycle and the fallback losses should have been very large. One way of estimating the initial liquid column length is by using the valve's force-balance equation just before the valve opens, Eq. 12.30. This equation, with the value of  $P'_r$  equal to zero and  $P_{cvo}$  (the injection opening pressure at depth) equal to the surface opening pressure  $P_{cso}$  times the gas factor  $f_g$ , is:  $P_{cvo}(1-R) + P_{to}R = P_{bt}$ .

$P_{to}$  is the production pressure at valve's depth when the pilot valve opens and it is the variable that needs to be calculated to find the value of the initial liquid column length.  $P_{bt}$  is the bellows pressure at operating conditions. If the operating temperature is known,  $P_{bt}$  can be calculated from  $P'_b$ , which is the bellows pressure at test-rack condition that can be found from the equations given in chapter: Gas Lift Valve Mechanics:

$$P'_b = (P_{tro})(1-R) = 862 \text{ psi}(1-0.164) = 720.63 \text{ psi}$$

On the other hand,  $P_{bt} = P'_b b - a$ , where  $b = 1 + 0.002283 (T_v - 60)$  and  $a = 0.083 (T_v - 60)$ , with  $T_v$  equal to the temperature of the valve in °F just

before the valve opens.  $T_v$  must be greater than the geothermal temperature because the valve is surrounded by fluids coming from the formation that are hotter than the geothermal temperature at valve's depth. Due to the fact that the valve is very close to the top of the perforations, the temperature of the valve could be approximated as follows: The geothermal temperature is found from:  $[(15.6^\circ\text{F}/\text{Mft.})(\text{depth in Mft.}) + 88.8^\circ\text{F}]$ . Thus, at valve's depth, the geothermal temperature is equal to  $190.54^\circ\text{F}$  and at the top of the perforation it is equal to  $197.59^\circ\text{F}$ . These two temperatures are very similar and an average temperature is taken as an approximation of the valve's temperature and, in consequence,  $a = 11.12$  and  $b = 1.3059$ . Therefore,  $P_{bt} = 929.96$  psig. With the opening pressure  $P_{cvo}$  equal to  $1061.47$  psig,  $P_{to}$  must be equal to  $259.57$  psig.

From  $P_{to}$  and the wellhead production pressure of  $80$  psi, the initial liquid column length (as 100% liquid) could be determined from the liquid pressure gradient found from the water cut and the oil API gravity using equation (12.52) (which gives a gradient of  $0.399$  psi/ft.) with the following equation:

$$Q_{mi} = \frac{259.57 \text{ psig} - 80 \text{ psig}}{0.399 \text{ psi/ft.}} = 450 \text{ ft.}$$

The fallback factor  $F$  would then be  $[(450-270)/450]/6.522 = 0.061$ , which seems to be too small for a volume of gas injected per cycle of only  $2208.5$  scf. But it is important to point out that the liquid column length found from the valve's force-balance equation is only reliable if the surface opening pressure and the gas specific gravity have been accurately determined. For example, if a  $\pm 2\%$  error is made in the measurement of the surface opening pressure (which is not uncommon for the type of pneumatic sensors used in this particular field), the injection opening pressure at depth could be as low as  $1040.24$  psig or as high as  $1082.69$  psig, for which  $Q_{mi}$  would be between  $179$  ft. and  $721$  ft. and the fallback factor could be as large as  $0.098$  (without even taking into consideration the error made in the calculation of the gas factor  $f_g$  for not accurately knowing the injection gas specific gravity). It should also be considered the fact that the valve in this case is a nitrogen-charged pilot valve and it is very difficult to know the actual temperature of the valve under operational conditions.

The way in which the liquids are produced into the separator (in batches or continuously) and the way the total gas flow rate at the exit of the separator behaves, must be studied to determine if there are several points of injection. It is also necessary to check the size of the orifice plate currently installed at the manifold and the calibration of all sensors (wellhead pressure

sensors and the static and differential pressure sensors at the orifice plate). In this example, with the poor quality of the available data, it was not possible to reach any definite conclusion about the exact location of the point (or points) of injection. However, these calculations, as unreliable as they might be, are useful because they help identify specific field actions to take for each possible explanation of what might be happening at the bottom of the well.

The gas flow rate was checked and it was indeed smaller than reported. The drop in liquid production was then due to the reduction in the surface injection gas flow rate (compared to the injection gas flow rate of Dec. 2001), that caused an increase in the total cycle time, deviating it from the optimum cycle time, allowing sufficient time for large liquid columns to regenerate on top of the gas lift valve, which in turn caused a reduction of the spread of the valve with the corresponding increase in the fallback losses (due to the small gas volumes injected per cycle). In other words and contrary to what one might think, the well was simply loaded with liquids. The specific field action to take in this case is to temporarily increase the injection gas flow rate to kick the well and make the spread of the valve go back to its original larger value.

### 12.6.2 Example #2 (tubing-annulus communication)

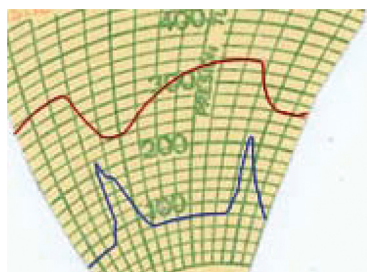
The well data is as follows:

Reservoir static pressure: 968 psig; 19°API oil gravity; 10% water cut; casing: 7-in. × 23-lb/ft.; production tubing ID: 2.441 in.; production tubing OD: 2.875 in.; top of perforations' depth: 6483 ft.; packer's depth: 6114 ft. The well seems to have a tubing-annulus communication, as can be seen in the pressure chart of Fig. 12.51 (low injection pressure and large injection pressure spread).

The well was producing 180 STB/D with a cycle time equal to 147.5 min. With this data and the volumetric capacity of the tubing of 5.788 Br/Mft., the produced liquid column length is calculated to be:

$$Q_{\text{prod}} = \frac{180 \text{ Br/D}}{\left[ \frac{(1440 \text{ min/D})}{(147.5 \text{ min/cycle})} \right] 5.788 \text{ Br/Mft.}} = 3.185 \text{ Mft./cycle}$$

This length is greater than the one the static reservoir pressure could provide, which is calculated as  $\frac{968 \text{ psig} - 80 \text{ psig}}{0.409 \text{ psi/ft.}} = 2171.14 \text{ ft.}$ , where 0.409 psi/ft. is the liquid pressure gradient with no free gas in it (calculated from Eq. 12.52), and 80 psig corresponds to the wellhead production pressure.



■ FIGURE 12.51 Wellhead pressure chart.



The size of the produced liquid column and the pressure pattern shown in the chart are clear indications that the well had a tubing-annulus communication, with liquid entering the annulus (which served as an open accumulation chamber).

On a later date, the well was producing 139 STB/D, with a surface injection gas flow rate of 540 Mscf/D and a cycle time equal to 70 min. The injection gas/liquid ratio was then equal to 3885 scf/STB, which was very large and probably due to the uncontrolled way in which gas was being injected into the tubing (reaching very low annular pressures at the end of each injection cycle). From the tubing volumetric capacity, the daily liquid production, and the cycle time, the produced liquid column length is calculated as:

$$Q_{\text{prod}} = \frac{139 \text{ Br/D}}{[(1440 \text{ min/D})(70 \text{ min/cycle})]5.788 \text{ Br/Mft.}} = 1.167 \text{ Mft./cycle}$$

If fallback losses are neglected, the production pressure  $P_{10}$  at the depth of the communication at the moment it is uncovered is calculated with the following equation (with the wellhead production pressure of 100 psig the well had at the time):

$$P_{10} = 100 \text{ psig} + 1.167 \text{ Mft.}(409 \text{ psi/Mft.}) = 577.3 \text{ psig.}$$

If the tubing-annulus communication is large,  $P_{10}$  must be approximately equal to the annular injection pressure at depth at the moment the gas uncovers the communication.

The maximum surface injection pressure is calculated next. This pressure is called  $P_{\text{tos}}$  and it is equal to  $P_{10}/f_g$ . Calculating  $f_g$  for the depth of the deepest valve with the equations given in chapter: Single-Phase Flow,  $P_{\text{tos}}$  is found to be equal to 490 psi, which is very similar to the maximum pressure on the two-pen pressure chart at this later date. This indicates one of the following possibilities: (1) the operating valve is unseated, (2) the communication is a pilot valve with its piston stuck open, or (3) there is a hole in the tubing very close to the gas lift mandrel. The volume of gas injected per cycle,  $v_{\text{gs}}$ , can be calculated from the surface injection gas flow rate and the total cycle time as:

$$v_{\text{gs}} = \frac{540000 \text{ scf/D}}{[(1440 \text{ min/D})/(70 \text{ min/cycle})]} = 26250 \text{ scf/cycle}$$

The required volume of gas per cycle calculated from the energy balance equation (used in the design of intermittent gas lift installations given in chapter: Design of Intermittent Gas Lift Installations) is only 11,370 scf/cycle, indicating that the liquid fallback losses must indeed be very small

and the value of  $P_{to}$  calculated earlier should be close to the actual pressure. A communication test (explained in Section 11.5.1) must be performed to confirm the existence of a tubing-annulus communication of some sort. The best way to find out the depth of a communication is by measuring the annular liquid level using sonic devices, measuring the liquid level at different times during the cycle, but especially when the injection pressure reaches its maximum value because that's the time the injection gas uncovers the communication. If the depth of the communication coincides with the last mandrel, it does not necessarily mean that the valve is unseated in the gas lift mandrel:

- Corrosion usually takes place just beneath the deepest mandrel because that is the place where the annular liquid level is found most of the time.
- It is also important to remember that a pilot valve with its internal piston stuck open will behave exactly as an annulus-tubing communication (a communication test would have the same results as the ones found with a hole in the production tubing) if the check valve is located inside the piston of the pilot valve. Therefore, it is always a good idea to pull the operating valve out of the well (if venting the casing annulus several times does not fix the problem) to verify its condition before planning for a more expensive solution that might not be necessary.

### 12.6.3 Example #3 (formation damage)

The well data is as follows:

Reservoir static pressure: 1373 psig; 26.5°API oil gravity; 56% water cut; casing: 7-in. × 23-lb/ft.; production tubing ID: 2.441 in.; production tubing OD: 2.875 in.; top of perforations' depth: 3494 ft.; packer's depth: 3363 ft. Gas lift valves installed in the well are shown in [Table 12.5](#).

The well had a workover job performed shortly before the time of this analysis. Its production was reduced from 400 to 50 STB/D. At the time of the troubleshooting analysis it was producing on intermittent gas lift, even though it was designed for continuous gas lift.

**Table 12.5** Valves Installed in the Well

Depth (ft.)	Valve	Port diameter (64th in.)	$P_v$ (psig)
2,109	R-20	12	1,000
3,287	R-20	12	850

Conditions at the time of the analysis: liquid production 50 STB/D; wellhead injection opening pressure = 860 psig; wellhead injection closing pressure = 820 psig; wellhead production pressure = 60 psig; surface injection gas flow rate = 185 Mscf/D; cycle time = 31.8 min. The well was designed for continuous flow but, as it can be appreciated from the two-pen pressure chart in Fig. 12.52, it was producing on intermittent gas lift. This might be due to the fact that the production pressure, downstream of the gas lift valve, was much lower than the production pressure considered in the design, so that the 12/64-in. seat allowed (once the deeper valve opens) an injection gas flow rate into the tubing greater than the 185 Mscf/D that was being injected at the surface and, in consequence, the injection pressure drops until the deeper valve closes.

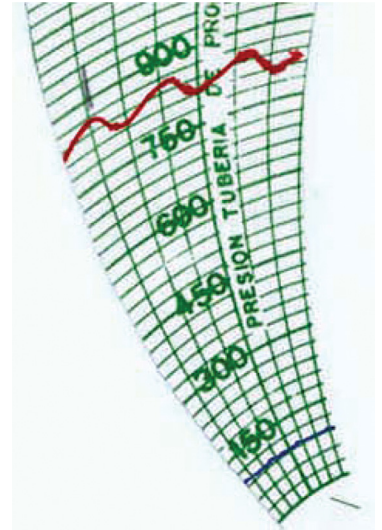
As can be seen in Fig. 12.52, the fluctuations of the surface production pressure are very small. This could be due to very small slugs and/or to very slow liquid slug velocities. It is also shown in the two-pen pressure chart that the valve remained open for approximately 10 mins at each cycle, which is very long for a point of injection depth of only 3287 ft.: This is caused by the small seat diameter of the operating valve (typical of single-element valves like the ones installed in the well). The volume of gas injected per cycle is:

$$v_{gs} = \frac{185000 \text{ scf}}{[(1440 \text{ min/D}) / (31.8 \text{ min/cycle})]} = 4085 \text{ scf/cycle}$$

With a production of 50 STB/D and assuming a fallback factor equal to 0.05, the initial liquid column length would be:

$$Q_{ini} = \frac{50 \text{ Br/D}}{[(1440 \text{ min/D}) / (31.8 \text{ min/cycle})] 0.005788 \text{ (Br/ft.)} [1 - (0.05) 3.287]} = 228.28 \text{ ft.}$$

The required volume of gas injected per cycle for a liquid column of 228.28 ft. in length is only 2064 scf/cycle (calculated from the energy balance equation given in chapter: Design of Intermittent Gas Lift Installations). The required volume of gas is about half of what was being injected at the time of this analysis. The total injection time (deeper gas lift valve open) was 10 min, so that all the required volume of gas was injected after only 5 minutes, which is an adequate period of time that gives a slug velocity large enough to keep the liquid fallback losses at a minimum value. But if the volume of gas injected per cycle is calculated from what the annulus and the gas injection line provide per cycle for the given valve's spread (using Eqs. 12.1–12.14), it would only be equal to 3195 scf/cycle, thus the surface



■ FIGURE 12.52 Wellhead pressure chart at the time of the troubleshooting analysis.

gas flow rate would be 145 Mscf/D instead of 185 Mscf/D. This could be due to an error made in the measurement of the surface gas flow rate or in the injection pressure. With the surface gas flow rate equal to 145 Mscf/D, 6.5 min would be necessary to inject the volume of gas required per cycle, which would imply a very slow liquid slug velocity and therefore a very large, and difficult to estimate, liquid fallback factor.

The valve's force-balance equation is now used to calculate the production pressure  $P_{to}$  at valve's depth at the moment the valve opened. For that purpose, the valve's temperature must be determined first. The valve is very close to the top of the perforations in an area where the geothermal temperature can be calculated from the following equation:

$$T_{\text{geothermal}} = 15.6(^{\circ}\text{F}/\text{Mft})D(\text{Mft}) + 88.8^{\circ}\text{F}$$

$T_{\text{geothermal}}$  is the temperature of the formation at a depth  $D$  in Mft., with a temperature gradient of 15.6°F/Mft. and an average surface temperature of 88.8°F. The temperature at the top of the perforations is then 15.6 (3.4940) + 88.8 = 143.3°F. The geothermal temperature at valve's depth is equal to 15.6 (3.287) + 88.8 = 140°F; Thus, the valve temperature can be approximated at an average value of 141.5°F at the moment the valve opened.

One way of estimating the initial liquid column length is by using the valve's force-balance equation (Eq. 12.30) just before the valve opened. This equation is presented here, with  $P'_r$  equal to zero and  $P_{cvo}$  (the injection opening pressure at depth) equal to the surface injection opening pressure  $P_{cso}$  times the gas factor  $f_g$ , as:

$$P_{cvo}(1-R) + P_{to}R = P_{bt}$$

Where  $R$  is the valve's area ratio, which in this case is equal to 0.038.  $P_{to}$  is the production pressure just before the valve opens and it is the variable that needs to be calculated to determine the initial liquid column length.  $P_{bt}$  is the bellows pressure at operating conditions. If the valve's operating temperature is known,  $P_{bt}$  can be calculated from the pressure  $P'_b$  with the equations given in chapter: Gas Lift Valve Mechanics.  $P'_b$  is the bellows pressure at test-rack conditions and can be calculated from the test-rack opening pressure using the following equation (with  $P_{tr} = 850$  psig):

$$P'_b = (P_{tro})(1-R) = 850 \text{ psig}(1-0.038) = 817.7 \text{ psig}$$

On the other hand,  $P_{bt}$  is equal to  $P'_b b - a$ , where  $b = 1 + 0.002283(T_v - 60)$  and  $a = 0.083(T_v - 60)$ , with  $T_v$  equal to the valve's temperature in °F just before it opened, which was approximately equal to 141.5°F.  $b$  and  $a$  were

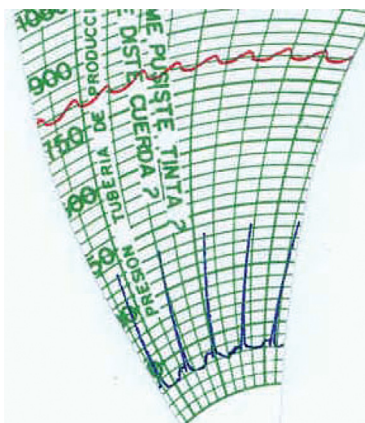
then:  $b = 1 + 0.002283 (T_v - 60) = 1 + 0.002283 (141.5 - 60) = 1.186$  and  $a = 0.083 (141.5 - 60) = 6.76$ .  $P_{bt}$  is then  $817.7 (1.186) - 6.76 = 963$  psig.  $P_{bt}$  represents the valve's closing pressure. The valve's opening pressure at valve's depth is  $P_{cvo}$ , which is equal to  $f_g P_{cso}$ , where  $P_{cso}$  is the surface injection opening pressure equal to 860 psig given in the two-pen pressure chart. Using the calculation procedures given in chapter: Single-Phase Flow for the gas factor  $f_g$ , the value of  $P_{cvo}$  is found to be 938.5 psig. As can be seen, pressure  $P_{bt}$  is larger than  $P_{cvo}$ , which is not possible because the opening pressure cannot be less than the closing pressure. The error in this case should not be in the estimation of the valve's temperature because it is too close to the top of the perforations. The error must be in the measurement of the injection surface opening pressure, which was measured at 860 psi.

A downhole pressure and temperature survey was run and the  $P_{to}$  pressure was found to be 160 psig and the valve's temperature was about 135°F. With these new values, the valve's force-balance equation is used one more time to find the surface opening pressure  $P_{cso}$ . This time,  $a$  is 6.225 and  $b$  is 1.171, thus  $P_{bt} = 817.7 (1.171) - 6.225 = 951.3$  psig and  $P_{cvo}$  is:

$$P_{cvo} = \frac{P_{bt} - RP_{to}}{1 - R} = \frac{951.3 - 0.038(160)}{1 - 0.038} = 982.56 \text{ psig}$$

With 982.56 psig at depth, the surface pressure  $P_{cso}$  is found to be  $982.56/f_g$ . The gas factor was calculated to be 1.0917, so the surface injection pressure was approximately 900 psig, which indicates that the surface pressure was being measured with an error of approximately 40 psig. This is the reason why the volume of gas injected per cycle, calculated from what the annulus and injection line can provide for the given valve's spread, does not coincide with the volume of gas calculated from the number of cycles per day and the surface gas flow rate (which was properly measured). It is very important to measure as accurately as possible the surface injection and production pressures to be able to perform accurate troubleshooting analyses.

The volume of gas injected per cycle was confirmed to be appropriate to obtain a small fallback factor. The productivity index was calculated using equation (12.32) and it turned out to be very small (0.05 Br/D-psi). Formation damage was the cause of the reduction in the daily liquid production. In fact, a stimulation job was performed on the well and the production increased to 422 STB/D in continuous flow. The well had a design fit for larger liquid flow rates on continuous gas lift, but it was "on its own" producing on intermittent gas lift because of the low production pressure caused by the very low liquid flow rate from the formation.



■ FIGURE 12.53 Wellhead pressure chart at the time of the troubleshooting analysis.

#### 12.6.4 Example #4 (optimized well)

The well data is as follows:

Reservoir static pressure: 650 psig; 21° API oil gravity; 55% water cut; formation gas/liquid ratio: 1500 scf/STB; casing: 7-in. × 23-lb/ft.; Production tubing ID: 1.995 in.; production tubing OD: 2.375 in.; top of perforations' depth: 4080 ft.; packer's depth: 3980 ft.; gas injection line length: 410 ft.; gas injection line ID: 2.07 in. A spring-loaded, injection-pressure-operated pilot valve was installed in the well (Table 12.6).

Conditions at the moment of the analysis: surface injection opening pressure: 825 psig; surface injection closing pressure: 795 psig; wellhead production pressure: 80 psig; cycle time: 18 min; surface gas flow rate: 269 Mscf/D; daily liquid production: 192 STB/D (Fig. 12.53).

The volume of gas injected per cycle is  $\left( \frac{269,000 \text{ scf/D}}{[(1440 \text{ min/D})/(18 \text{ min/cycle})]} \right) = 3,362 \text{ scf/cycle}$ . This volume should be adequate to maintain a low fallback factor because the production tubing ID is very small. The initial liquid column that accumulates at each cycle above the operating valve is given by:

$$Q_{\text{ini}} = \frac{192 \text{ Br/D}}{[(1440 \text{ min/D})/(18 \text{ min/cycle})](0.00386631 \text{ Br/ft.})(1 - (0.05)3.871)} = 769.72 \text{ ft.}$$

Where the volumetric capacity of the production tubing, equal to 0.00386631 Br/ft., has been used and a fallback factor of 0.05 seems to be appropriate in this case as a good approximation. The liquid pressure gradient calculated from the water cut and the API gravity of the oil is found from:

$$\rho_f = 0.433 \left[ 0.55 + 0.45 \frac{141.5}{131.5 + 21} \right] = 0.4189 \text{ psi/ft.}$$

Therefore, the production pressure at valve's depth, just before the gas lift valve opens, is given by (assuming  $f_g$  for the pressure in the production tubing equal to one):

$$P_{\text{to}} = P_{\text{wh}} f_g + \rho_f Q_{\text{ini}} = 80 \text{ psig} + (0.4189 \text{ psi/ft.})769.72 \text{ ft.} = 402.43 \text{ psig}$$

**Table 12.6** Valves installed in the well

Depth (ft.)	Valve model	Port diameter (64th in.)	$P_{\text{tr}}$ (psig)
3871	WFM14R	32	797

The valve's force–balance equation is used to find the injection opening pressure at valve's depth (with a test-rack closing pressure of 797 psig not affected by temperature because the operating valve is a spring-loaded pilot valve with an area ratio of 0.183):

$$P_{cvo} = \frac{P_{trc} - R(P_{to})}{1 - R} = \frac{797 - 0.183(402.43)}{1 - 0.183} = 885.38 \text{ psig}$$

Using the appropriate gas factor  $f_g$  (for the gas pressure inside the annulus), the corresponding surface injection pressure is then calculated to be equal to approximately 798 psig, which is less than its measured value of 825 psig. The error could have been made in the measured injection pressure or in the measured liquid production (if the production is too large, the  $P_{to}$  pressure calculated earlier would also be large giving a low injection opening pressure). An opposite calculation procedure would be to assume the measured surface injection opening pressure to be correct and use the valve's force–balance equation to calculate the production pressure  $P_{to}$ , from which the daily production can then be calculated. Using the gas factor  $f_g$  and the measured surface injection pressure, the opening and closing pressures at depth are calculated as 912 and 879 psig, respectively. Then, pressure  $P_{to}$  is:

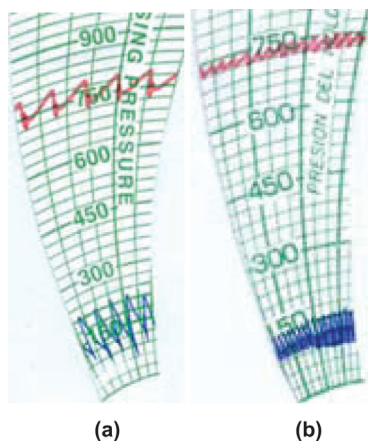
$$P_{to} = \frac{P_{trc} - (1 - R)P_{cvo}}{R} = \frac{797 - (1 - 0.183)912}{0.183} = 283.58 \text{ psig}$$

Now, the initial liquid column can be approximated as:  $Q_{ini} = \frac{P_{to} - P_{wh}}{\rho_f} = \frac{283.58 - 80}{0.4189} = 485.98 \text{ ft.}$

The daily liquid production is then (using Eq. 10.19) equal to:

$$\begin{aligned} \text{Production} &= (0.00386631 \text{ Br/ft.})(485.98 \text{ ft.}) \left( \frac{1440 \text{ min/D}}{18 \text{ min/cycle}} \right) [1 - (0.05)3.871] \\ &= 121.22 \text{ Br/D} \end{aligned}$$

The liquid production was measured again and it was found to be 105 Br/D. With a liquid production of 192 Br/D the productivity index was calculated at 0.76 Br/D-psi, which gives an optimum cycle time of 13 minutes. With a production of 121.22 Br/D, the productivity index is found to be equal to 0.4 Br/D-psi, for which the optimum cycle time is about 16 min. So the well was producing with a cycle time very close to its optimum value. Even though the spread of the valve seemed to be very small, the gas volume injected per cycle was adequate. This is due to the fact that the production tubing ID was very small and the casing ID was large.



■ FIGURE 12.54 Surface pressure charts:  
(a) Dec. 28, 2001 and (b) Sep. 20, 2002.

### 12.6.5 Example #5 (large fallback losses)

The well data is as follows:

Reservoir static pressure: 895 psig; 15°API oil gravity; 3% water cut; formation gas/liquid ratio: 170 scf/Br; casing: 7-in. × 23-lb/ft.; production tubing ID: 2.992 in.; production tubing OD: 3.5 in.; depth of top of perforations: 3695 ft.; packer's depth: 3522 ft.; gas injection line length: 3086 ft.; gas injection line ID: 2.07 in. The gas lift valves installed in the well are given in Table 12.7.

The WF14R valve is an injection-pressure-operated, spring-loaded pilot valve. Its area ratio was equal to 0.239.

The charts in Fig. 12.54 show the behavior of the surface injection pressures for Dec. 28, 2001 and for Sep. 20, 2002. The chart for Dec. 2001 was a 24-h chart while the one for Sep. 2002 was a 7-day chart. The cycle time for Sep. 2002 was longer because the surface injection gas flow rate was lower. As a consequence of longer cycle times, the liquid columns being lifted were of greater lengths. The liquid column length has an impact on the injection opening pressure: the greater the length of the liquid columns, the greater their contribution to open the gas lift valve will be and, in consequence, the lower the required gas injection opening pressure would be. This is what happened in the two charts shown in the figure: Because the valve was spring-loaded, the closing pressure remained constant (as shown) but the injection opening pressure was smaller in Sep. 2002 due to a longer cycle time. Even though the liquid slugs were greater in the chart of Sep. 2002, the maximum wellhead production pressure was smaller because the liquid slugs reached the surface at lower velocities.

Operational conditions for Dec. 2001:

Production wellhead pressure: 70 psig (with a slow decrease of the production pressure after the maximum production pressure peak has been reached at every cycle, probably due to the large viscosity of the oil); surface injection opening pressure: 790 psig; surface injection closing pressure: 735 psig; total cycle time: 17.5 min; surface injection gas flow rate: 400 Mscf/D; production: 220 STB/D.

**Table 12.7** Valves Installed in the Well

Depth (ft.)	Valve	Port diameter (64th in.)	$P_{tr}$ (psig)
1851	N14R	16	884
3466	WF14R	48	792



The produced liquid column length is calculated (using a production tubing volumetric capacity of 0.0086963 Br/ft.) as:

$$Q_{\text{prod}} = \frac{220 \text{ Br/D}}{[(1440 \text{ min/D}) / (17.5 \text{ min/cycle})] (0.0086963 \text{ Br/ft.})} = 307.44 \text{ ft/cycle}$$

The volume of gas injected per cycle is equal to  $(400,000 \text{ scf/D}) / [1440 \text{ (min/D)} / 17.5 \text{ (min/cycle)}] = 4,861 \text{ scf/cycle}$ . Due to fallback losses, the initial liquid column length should be greater than the length of the produced liquid column; but even a 307 ft. long liquid column requires more than 5000 scf/cycle to be produced with low liquid fallback losses, thus not enough gas was being injected per cycle. Additionally, for low API oil gravities the fallback losses are very large and difficult to estimate. If the measured surface pressures are considered to be reliable, the initial liquid column length and the fallback losses can be estimated by calculating the production pressure at valve's depth ( $P_{\text{to}}$ ) at the moment the valve opens. Using the appropriate gas factor  $f_g$ , the injection opening and closing pressures at depth are determined to be 865 and 804 psig, respectively. Using the valve's force-balance equation (knowing that the test-rack closing pressure is equal to 792 psig and the valve's area ratio is 0.239) the following expression is used to calculate the production pressure  $P_{\text{to}}$ :

$$P_{\text{to}} = \frac{P_{\text{tc}} - (1-R)P_{\text{cvr}}}{R} = \frac{792 - (1-0.239)865}{0.239} = 559.56 \text{ psig}$$

With this calculated value of  $P_{\text{to}}$ , the production wellhead pressure of 70 psig, and the liquid pressure gradient of 0.418 psi/ft. found from the water cut and the oil API gravity using equation (12.23), the initial liquid column length just before the valve opens is:

$$Q_{\text{mi}} = \frac{559.56 \text{ psig} - 70 \text{ psig}}{0.418 \text{ psi/ft.}} = 1171.2 \text{ ft.}$$

And the liquid fallback factor is then equal to:

$$F = \frac{(1171.2 - 307.44) / 1171.2}{3.466} = 0.21$$

This means that 21% of the initial liquid column per each thousand feet of depth of the point of injection is not produced to the surface. This fallback factor is very large and it is due to the nature of the oil being lifted and the small volume of gas injected per cycle. Because the liquid fallback factor calculated earlier is not very reliable (it is highly possible that the surface pressures and the gas specific gravity were not accurately measured), it is

not possible to calculate the productivity index and the optimum cycle time. It is clear that the pilot valve should be replaced with another one with a greater area ratio so that a larger volume of gas could be injected per cycle or a surface intermitter should be installed to force the pilot valve to remain opened for longer periods of time. After the pilot valve has been replaced, the optimum cycle time can then be found by a trial and error field procedure (changing the surface gas flow rate and testing the well at each gas injection frequency). To get more information at current operational conditions, a downhole pressure and temperature survey could be run in the well, taking into consideration that many weight bars (which require the use of a long lubricator and a special rig) might be needed because of the viscosity of the oil being lifted. Highly viscous oils should not be lifted with gas lift because gas lift is a very inefficient method of production for this type of fluid.

Troubleshooting analysis for the conditions in Sep. 2002:

Production wellhead pressure: 65 psig; cycle time: 35 min; surface injection opening pressure: 740 psig, which corresponds to an injection pressure of 809.7 psig at valve's depth; surface injection closing pressure: 730 psig; daily liquid production: 120 STB/D. The surface gas flow rate has been reduced (compared to the flow rate in Dec. 2001), so the cycle time was longer and the injection opening pressure was lower. The produced liquid column was:

$$Q_{\text{prod}} = \frac{120 \text{ Br/D}}{\left[ (1440 \text{ min/D}) / (35 \text{ min/cycle}) \right] (0.0086963 \text{ Br/ft.})} = 335.39 \text{ ft.}$$

Using the valve's force-balance equation (with a test-rack closing pressure of 792 psig and an area ratio equal to 0.239), the production pressure at valve's depth at the moment the valve opens is:

$$P_{\text{to}} = \frac{P_{\text{trc}} - (1-R)P_{\text{cvs}}}{R} = \frac{792 - (1-0.239)809.7}{0.239} = 735.64 \text{ psig}$$

With the production pressure  $P_{\text{to}}$  calculated in this way, the wellhead pressure of 65 psig, and the liquid gradient (calculated from the water cut and the oil API gravity) equal to 0.418 psi/ft., the initial liquid column above the operating valve (when it opens) is:

$$Q_{\text{ini}} = \frac{735.64 \text{ psig} - 65 \text{ psig}}{0.418 \text{ psi/ft.}} = 1604.4 \text{ ft.}$$

And the liquid fallback factor is then equal to:

$$F = \frac{(1604.4 - 335.39) / 1604.4}{3.466} = 0.228$$

This means that 22.8% of the initial liquid column per each Mft. of depth of the point of injection is not produced to the surface. It is demonstrated then that by making the cycle time longer, the liquid columns are greater, the volume of gas injected per cycle becomes smaller, and the fallback factor increases for cases in which the volume of gas injected per cycle is smaller than its required value.

### 12.6.6 Example #6 (tubing-annulus communication)

The well data is as follows:

Reservoir static pressure: 890 psig; 14.5°API oil gravity; 0% water cut; casing: 7-in. × 23-lb/ft.; production tubing ID: 2.992 in.; production tubing OD: 3.5 in.; top of perforations' depth: 3692 ft.; Packer's depth: 3577 ft. The single-element valves that were installed in the well are presented in Table 12.8.

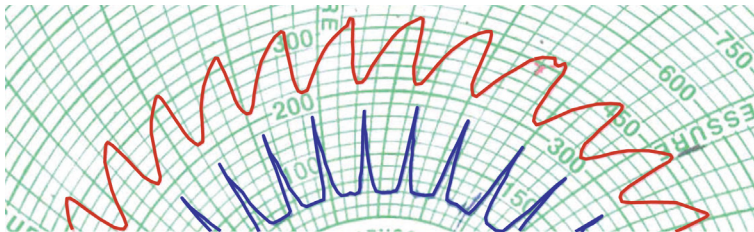
The liquid production was equal to 338 STB/D, with a surface gas injection of 600 Mscf/D, a cycle time of 45 min, and a surface pressure pattern as shown in the two-pen pressure chart in Fig. 12.55.

The two-pen pressure chart revealed a typical pattern found when there is a tubing-annulus communication (very low injection pressure and very large valve's spread). The volume of gas injected per cycle, found from the surface gas flow rate and the cycle time, is:

$$v_{gs} = \frac{600000 \text{ scf/D}}{(1440 \text{ min/D})/(45 \text{ min/cycle})} = 18750 \text{ scf}$$

**Table 12.8** Valves Installed in the Well

Depth (ft.)	Valve Model	Port Diameter (64th in.)	$P_{tr}$ (psig)
1884	R-20	16	1019
3500	R-20	16	930



■ FIGURE 12.55 Wellhead pressure chart.

This is a very large volume of gas injected per cycle that should be adequate to keep the liquid fallback losses at a minimum value even for very long liquid slugs. The liquid production per cycle was equal to 10.56 Br, which in a 3½-in. tubing generated a liquid column of length:

$$Q = \frac{338 \text{ Br/D}}{[(1440 \text{ min/D}) / (45 \text{ min/cycle})] (0.0086963 \text{ Br/ft.})} = 1214.6 \text{ ft.}$$

If it is assumed that the injection point is close to the depth of the deepest valve and disregarding the liquid fallback losses, the production pressure at valve's depth ( $P_{to}$ ) just before the injection gas begins to enter the production tubing (taking into account a wellhead pressure of 40 psi and a liquid gradient of 0.42 psi/ft.) was:

$$P_{to} = 1214.6 \text{ ft.} (0.42 \text{ psi/ft.}) + 40 \text{ psi} = 550 \text{ psi}$$

This pressure represents a surface pressure equal to 503 psig, which is similar to the one in the two-pen pressure chart, so the communication must be close to the design operating valve. Using a sonic device it was found that the liquid level was not constant, which definitely confirmed a tubing-annulus communication, but its exact location was not reported. Because the injection gas/liquid ratio was acceptable and the liquid production did not decrease when the well started showing signs of a casing-tubing communication, it was decided to leave the well operating in this way. Eventually, when the reservoir pressure declines, the injection gas/liquid ratio will increase (because of the uncontrolled way in which the gas is injected through the communication) and a new well completion must be installed. In fact, this well was on gas lift only because it was one of the few wells producing low API gravity oil in a very large off-shore gas lift field and it was "economically" feasible to take advantage of the abundant availability of high-pressure injection gas; otherwise, this well should be produced with a different type of artificial lift method.

### 12.6.7 Example #7 (pilot valve failure/inadequate spread)

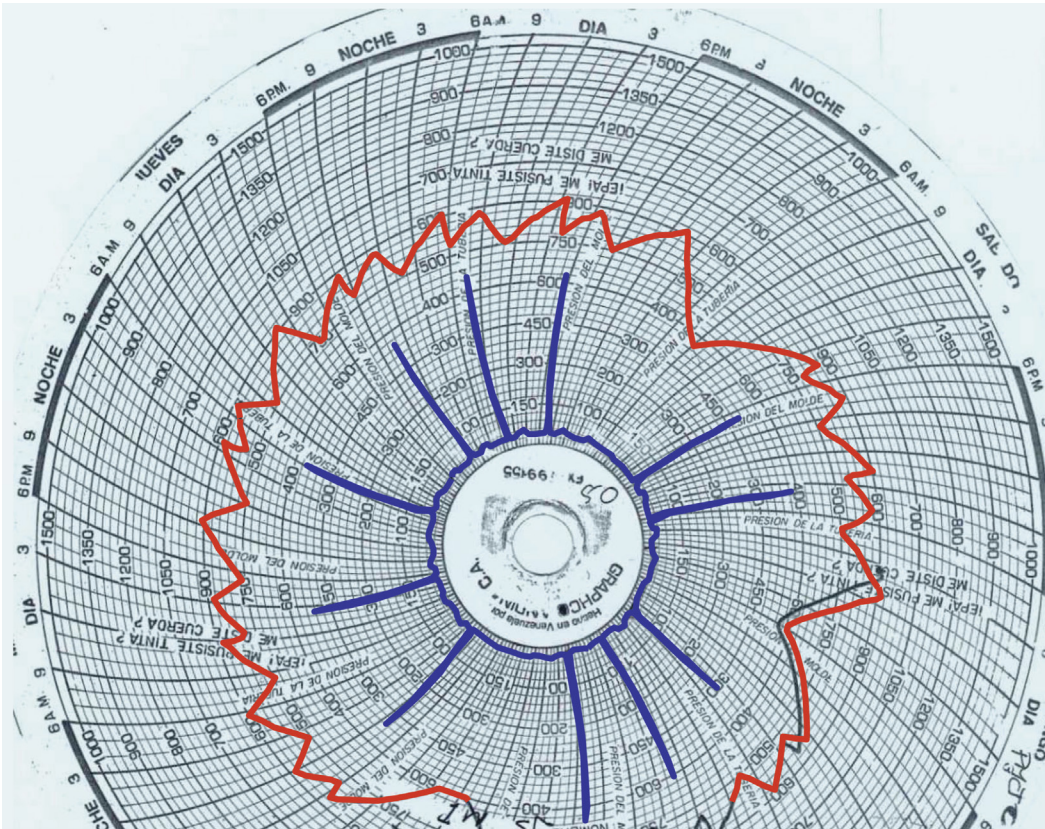
The well data is as follows:

Reservoir static pressure: 928 psig; 13°API oil gravity; 40% water cut; formation gas/liquid ratio: 1300 scf/STB; casing: 7-in. × 23-lb/ft.; production tubing ID: 2.992 in.; production tubing OD: 3.5 in.; depth of top of perforations: 4320 ft.; Packer's depth: 4125 ft. Gas lift valves installed in the well are presented in [Table 12.9](#).

**Table 12.9** Valves Installed in the Well

Depth (ft.)	Valve Model	Port Diameter (64th in.)	$P_{tr}$ (psig)
2116	N14R	12	957
3782	WF14R	48	792

The previous operating pilot valve was a WF14R valve, which is an injection-pressure-operated, spring-loaded, pilot valve with a test-rack closing pressure of 880 psig. But the behavior of this valve was irregular as it is shown in the pressure chart of Fig. 12.56. Variations of the injection pressure as shown in the two-pen pressure chart are typical of wells with pilot valves in which the piston movement is irregular. The reader is advised to



■ FIGURE 12.56 Irregular behavior of the pilot valve caused by irregular movements of the valve's internal piston (choke control intermittent gas lift).

review Fig. 10.6 to identify the upper and lower sections of a pilot valve and understand the role each of these components play in the operation of the valve. The following observations are made: (1) when the pilot valve finally closes and the gas injection pressure begins to increase, the injection pressure recovery curves (at the same pressure levels) are all parallel (this indicates the fact that the lower part of the valve might indeed be 100% closed); and (2) the valve's opening pressures were more or less constant (the small variations were due to the difference in length of the liquid column to be lifted at each cycle), which indicates that the pilot valve's upper section was working properly and the problem had to do with the piston movement.

In some occasions, when the upper part of the valve opened, the lower part of the valve was only partially opened and the injection pressure decreased at a lower rate. The irregular behavior of the piston movement was the reason why in some cycles the injection pressure dropped sharply and in others it dropped very slowly. When the injection pressure dropped sharply it was because the lower part of the valve was fully opened and two effects can be noticed in this case: (1) the injection closing pressure was higher due to the normal dynamic effect that this type of valve experiences in good working conditions, making the actual closing pressure higher than the test-rack closing pressure; (2) the high instantaneous gas flow rate through the valve makes the liquid slug travel faster and the wellhead production pressure peaks are considerably larger. Instead, when the injection pressure dropped very slowly, the lower section of the valve was not fully open so the dynamic effect that makes the valve close at higher pressure was not present and the valve closed at a lower injection pressure. This lower closing pressure was most of the time of constant value when the injection pressure dropped very slowly, although sometimes the valve closed at even lower pressures. When the pilot valve was partially opened, the liquid slugs traveled at a very small velocity so the production wellhead pressure did not increase when the liquid slugs arrived at the surface and it was estimated that the fallback factor must have been very large: The instantaneous gas flow rate through the valve was in this case very small so that the efficiency of the volume injected per cycle was very poor.

With the pilot valve working in the way it is depicted in Fig. 12.56, it is very difficult to do any type of quantitative analysis.

With this irregular behavior of the pilot valve, the liquid production was 50 STB/D with a surface injection gas flow rate of 244 Mscf/D and water cut of 32%. The pilot valve was replaced with a new one of the same model and area ratio. This new valve was in good working conditions but the liquid production dropped to 47 STB/D with a water cut of 42% and at the same

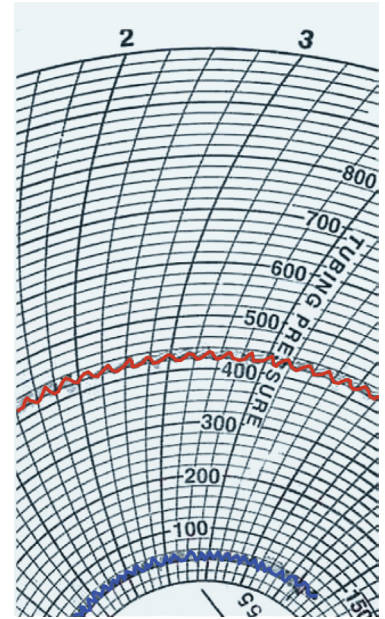
surface injection gas flow rate of 244 Mscf/D. The total cycle time was then equal to 15 minutes, so that the volume of gas injected per cycle was 2541 scf/cycle. According to the energy balance equation given in chapter: Design of Intermittent Gas Lift Installations, the required volume of gas to be injected per cycle should have been equal to 10,600 scf/cycle, so that after the damaged valve was replaced, only 25% of the required volume was being injected per cycle. As seen in the two-pen pressure chart of Fig. 12.57, the spread of the valve was very small, which might be due to a very high production pressure caused by large liquid columns that are not entirely produced to the surface. In these cases, it is convenient to temporarily increase the surface injection gas flow rate to very large values to see if the well's large liquid column can be unloaded (in the same unloading process depicted in Fig. 12.27). If, by doing so, the spread of the valve increases, the surface injection gas flow rate can then be reduced back to its design value and the well should be monitored to detect if it loads up with liquids again.

Because the operating valve is spring loaded, the test-rack closing pressure should be equal to the valve's closing pressure at depth plus the usual minor deviation these valves exhibit due to dynamic effects. This test-rack closing pressure was equal to 792 psig. With the measured injection pressure shown in the two-pen pressure chart of Fig. 12.57, the valve's opening injection pressure at depth is calculated to be equal to 721 psig, which is much lower than the closing pressure at depth of 792 psig, indicating a possible error in the wellhead pressure measurements (the numbers shown in the pressure chart correspond to the surface production pressure and not to the injection pressure).

The production pressure at valve's depth when the valve opens ( $P_{i0}$ ) can be found from the valve's force–balance equation with the injection pressure at depth equal to 721 psig, valve calibration closing pressure of 792 psi, and the area ratio of 0.239:

$$0.239 = \frac{721 \text{ psi} - 792 \text{ psi}}{721 \text{ psi} - P_{i0}}$$

So that  $P_{i0}$  is found to be equal to 1018 psi. The previous equation is valid even if the gas injection pressure is less than the production pressure at the moment the valve opens because both pressures tend to open the valve (it is physically possible that, due to a very large production pressure, the valve opens at an injection pressure lower than the injection closing pressure). There is nothing wrong in the production pressure calculation done in this way. What is not correct in this case is to have an injection pressure lower

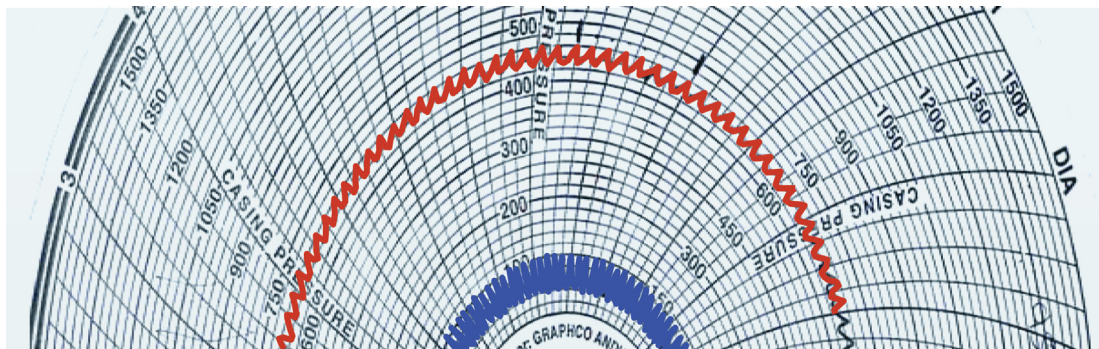


■ FIGURE 12.57 Wellhead pressure chart after the pilot valve with the chaotic behavior was replaced with a pilot valve in good working conditions.

than the production pressure and have gas flowing from the annulus toward the tubing. On the other hand, the tubing pressure calculated in this way is above the static reservoir pressure, which is not possible because there is no evidence of a tubing-annulus communication that would allow liquid accumulation in the annulus. It is highly possible then that the surface injection pressure was not accurately measured. The other possibility is that the valve's calibration closing pressure was lower than the one reported in the design, but this is a very unusual mistake. In any case, the volume of gas injected per cycle was very small. It was decided then to increase the surface gas flow rate to reduce the cycle time so that smaller slugs would be generated and the injection opening pressure could be a little higher. This will in turn increase the spread of the valve and the volume of gas injected per cycle. With a higher volume of gas injected per cycle and wellhead pressure sensors accurately calibrated, a precise troubleshooting analysis can be performed, making it possible to calculate the productivity index and the optimum cycle time.

It is possible that the required volume of gas injected per cycle to finally unload the well can not be attained if the well is kept on choke control. In this case, the pilot valve should be replaced with the same type of valve but with a larger area ratio that would allow a greater spread. In fact, the gas flow rate was increased but the spread of the valve only increased a few psi, see Fig. 12.58. The liquid production increased to 98 STB/D. As can be seen in Fig. 12.58, the sensors were still not well calibrated because the measured pressures were still very low.

It is a good practice to drastically increase the surface injection gas flow rate, but only until the spread of the valve becomes as large as expected from the design. Then the gas flow rate should be reduced back to its design value



■ FIGURE 12.58 Wellhead pressure chart after the surface gas flow rate was increased.



to see if the well loads up again, see Fig. 12.27 and the explanation given for it in Section 12.5.1.

### 12.6.8 Example #8 (inadequate continuous gas lift design)

The well data is as follows:

Static reservoir pressure: 897 psig; 27°API oil gravity; 14% water cut; formation gas/liquid ratio: 1,119 scf/STB; casing: 7-in. × 23-lb/ft.; production tubing ID: 2.992 in.; production tubing OD: 3.5 in.; depth of top of perforations: 4690 ft.; packer's depth: 3971 ft. The well has two injection-pressure-operated, nitrogen-charged, single-element gas lift valves with test-rack opening pressures shown in Table 12.10.

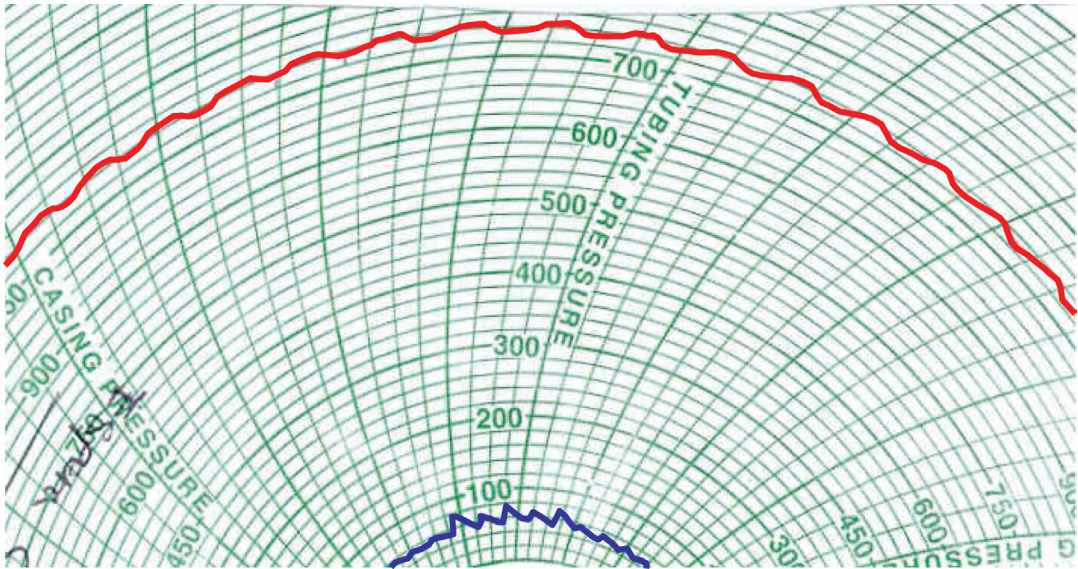
Operational data:

Production: 126 STB/D; surface injection gas flow rate: 142 Mscf/D; liquid gradient (from water cut and oil API gravity): 0.393 psi/ft.; the well operates on intermittent gas lift, with a “supposedly” high surface injection pressure of 1095 psig and a surface closing pressure equal to 1065 psig; Wellhead production pressure from 30 to 60 psig; cycle time: 22.5 min; the operating valve remained open for 8 min.

The well was designed for continuous flow but it was operating on what appears to be an intermittent gas lift operation. Injection-pressure fluctuations shown in Fig. 12.59 are typical of single-element valves, for which the time the valve remains open is very long (due to the small size of the valve's seat) and the spread is very small (because the area ratio of the valve is also very small). By only looking at the two-pen pressure chart, one might conclude that because the injection pressure was very high, possibly the upper valve was opening and closing and the operating deeper valve was opened all the time. Moreover, one might think of a different possibility in which only one valve was operating and it was on throttling flow (never completely closing). But the analysis that is described next indicates that the injection pressure should be in reality less than the one in the chart and the well is indeed on intermittent gas lift with the deepest valve as the operating point of injection.

**Table 12.10** Valves Installed in the Well

Depth (ft.)	Valve Model	Seat Diameter (64th in.)	Design Opening Pressure (psig)	$P_{tr}$ (psig)
2116	VR-STD	12	1046	930
3928	VR-STD	12	949	875



■ FIGURE 12.59 Wellhead pressure chart for the operational conditions at the time of the troubleshooting analysis.

With a static reservoir pressure of 897 psig at 4690 ft., a wellhead production pressure of 30 psig, and a liquid gradient of 0.393 psi/ft., the reservoir static liquid level would be at:  $4690 \text{ ft.} - \frac{897 \text{ psig} - 30 \text{ psig}}{0.393 \text{ psi/ft.}} = 2484 \text{ ft.}$  So the static liquid level is below the upper valve. If the upper valve was the only operating point of injection, the well would not produce any liquids.

Intermittent gas lift troubleshooting analysis:

The produced liquid column is found to be:  $Q_{\text{prod}} = \frac{126 \text{ Br/D}}{(1440 \text{ min/D})(8.69 \text{ Br/Mft.})/22.5 \text{ min/cycle}} = 0.226 \text{ Mft.}$

The required volume of gas injected per cycle to lift this liquid column is closed to 4000 scf/cycle. A larger volume of gas injected per cycle is required in this case because the initial liquid column at depth should be greater than 226 ft. The volume of gas injected per cycle obtained dividing the surface gas flow rate by the number of cycles in one day is equal to only 2219 scf/cycle, so the liquid fallback losses in this well must have been very large. The initial liquid column is calculated first assuming an arbitrarily large fallback factor equal to 0.15:

$$Q_{\text{ini}} = \frac{126 \text{ Br/D}}{[(1440 \text{ min/D})/22.5 \text{ min/cycle}]8.69 \text{ Br/Mft.} [1 - 0.15(3.928)]} = 0.5515 \text{ Mft.}$$

The production pressure at valve depth when the deepest valve opens would then be:  $P_{to} = P_{wh} + \rho_f Q_{ini} = 30 + 0.393 (551.5) = 246.73$  psi. This means that if the operating valve was flat, the surface maximum pressure would be close to  $246.73/f_g$ . This gives a surface injection pressure of only 225 psig, which is very low in comparison to its measured value. The force–balance equation should be used to find its injection opening pressure if the valve is assumed to be in good working conditions. For this purpose, the deeper valve’s temperature is assumed to be equal to the average between the geothermal temperatures at valve’s depth and at the depth of the perforations. This gives a temperature approximately equal to 155°F at valve’s depth. The calculation of the injection opening pressure at valve’s depth ( $P_{cvo}$ ) is as follows:

$$\begin{aligned} a &= 0.083(T_v - 60) = 0.083(155 - 60) = 7.88 \\ b &= 1 + 0.002283(155 - 60) = 1.2168 \\ P_{bt} &= (1 - R) P_{tr} b - a = 0.966(875)1.2168 - 7.88 = 1020.62 \\ P_{cvo} &= \frac{P_{bt} - RP_{to}}{(1 - R)} = \frac{1020.62 - 0.034(246)}{0.966} = 1047.88 \text{ psig} \end{aligned}$$

This pressure referred to the surface is approximately equal to 940 psig ( $= 1047.88/f_g$ ), which is less than the one reported in the two-pen pressure chart.

Continuing with the calculations assuming a high liquid fallback factor, the productivity index is calculated to be equal to 0.27 Br/D-psi, for which the optimum cycle time is approximately 30 min.

Carrying out the calculations with a liquid fallback factor of only 0.05 (less probable because of the small volume of gas injected per cycle), the liquid column above the operating valve just before it opens is:

$$\begin{aligned} Q_{ini} &= \frac{126 \text{ Br/D}}{[(1440 \text{ min/D})/(22.5 \text{ min/cycle})]8.69 \text{ Br/Mft.}[1 - 0.05(3.928)]} \\ &= 0.28192 \text{ Mft.} \end{aligned}$$

The production pressure at valve’s depth when the deeper valve opens would be:  $P_{to} = P_{wh} + \rho_f Q_{ini} = 30 + 0.393 (281.92) = 140.79$  psig. This means that a flat valve would allow to pass gas at a pressure close to  $140.79/f_g$ . This pressure is approximately 128 psig, which is again too small compared to the one reported in the two-pen pressure chart. The valve’s force–balance equation is now used to find the injection opening pressure assuming that the valve is in good working condition. Assuming a valve’s temperature of

155°F, the calculation of the valve opening injection pressure at depth,  $P_{cvo}$ , is as follows (using the value of  $P_{bt}$  calculated earlier):

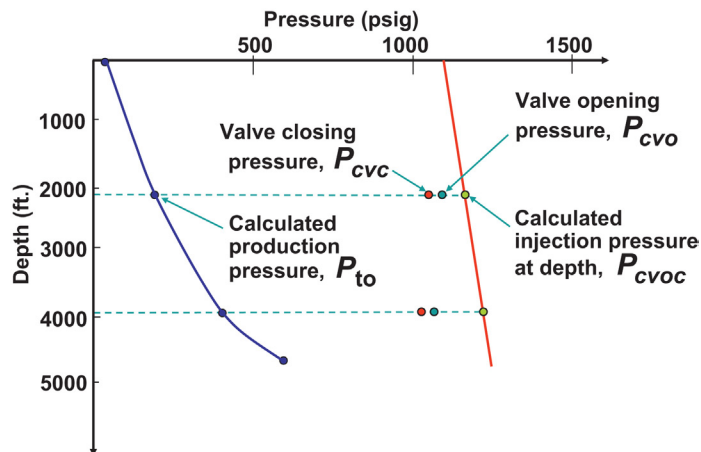
$$P_{cvo} = \frac{P_{bt} - RP_{to}}{(1-R)} = \frac{1020.62 - 0.034(140.79)}{0.966} = 1051.59 \text{ psig}$$

This pressure referred to the surface is approximately equal to 943 psig ( $= 1051.59/f_g$ ), which is less than the one in the pressure chart. Following the calculations assuming a small fallback factor, the productivity index would be equal to 0.23 Br/D-psi, for which the optimum cycle time is 45 min.

These calculations indicate that, regardless of the value of the fallback factor, if the lower valve is in good working condition, the surface injection pressure should be approximately 940 psig and not as high as the 1095 psig reported. On the other hand, for a flat valve the injection pressure would have to be very low. However, these results do not contradict the fact that the lower valve could have been open and the upper valve was opening and closing or in throttling flow. Calculations are now made assuming the well was producing on continuous flow.

Troubleshooting analysis for continuous flow:

To perform the analysis for continuous flow, the production tubing pressure was calculated with the reported daily liquid production and the point of injection at the deepest valve. The injection pressure along the annulus was calculated also. The valves' force-balance equation was used to calculate the injection opening and closing pressures at the depth of each valve ( $P_{cvo}$  and  $P_{cvc}$ ). This was done with the area ratio and the calibration pressure of each valve. Fig. 12.60 shows the results of the calculations for continuous



■ FIGURE 12.60 Results from continuous gas lift trouble-shooting calculations.

**Table 12.11** Results Shown in Fig. 12.60

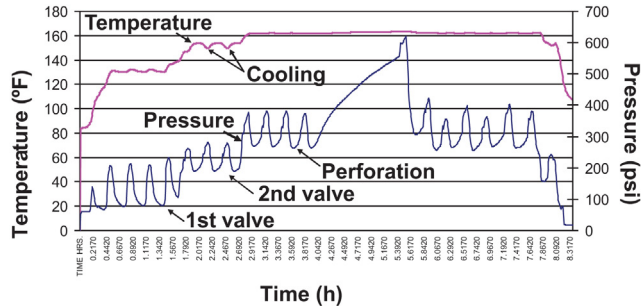
Valve	Valve 1 (Upper)	Valve 2 (Lower)
Injection pressure at depth calculated from the surface pressure measured and presented in the pressure chart (psig)	1162	1218
Tubing pressure (calculated from the daily production and total gas/liquid ratio) at depth (psig)	190	396
Required injection pressure at valve depth to pass the measured surface gas flow rate through an orifice valve (psig)	234	422
Injection closing pressure at valve's depth calculated from the valve's force–balance equation and the calibration data (psig)	1051	1024
Injection opening pressure at valve's depth calculated from the valve's force–balance equation and the calibration data (psig)	1081	1046
Gas flow rate the valve would be able to pass if it was an orifice valve (Mscf/D)	813	832

flow. It can be seen that the injection pressures at depth  $P_{cvo}$  (calculated from the surface maximum injection pressure reported in the chart) are greater than the opening pressures  $P_{cvo}$  (calculated from the force–balance equation) so that all valves must be opened.

Table 12.11 shows the results presented in Fig. 12.60:

These results indicate that, if the valves are in good conditions, both valves should be opened and passing a gas flow rate much greater than the one reported at the time of this analysis. As can be seen in the previous table, the total gas flow rate should be equal to 1645 Mscf/D and this is the most important clue that points to the fact that the actual surface injection pressures were different from the ones shown in Fig. 12.59. On the other hand, with the injection closing and opening pressures obtained for the lower valve from the above intermittent troubleshooting analysis, the volume of gas injected per cycle coming from the annulus and surface injection line, coincides with the volume of gas calculated by simply dividing the surface gas flow rate in Mscf/D by the number of cycles per day. The gas mass balance clearly establishes then that the well was indeed on intermittent gas lift, with the deepest valve as the operating point of injection. A downhole pressure and temperature survey was run in the well and its results are shown in Fig. 12.61 (three stops were made below each valve and at the top of the perforations).

It is deduced from the survey that the deeper (second) valve corresponds to the operating valve: its temperature decreases at each gas injection cycle while the temperature of the upper (first) valve increases every time the hotter liquid slugs pass around the sensors at that depth. Another evidence is the fact that the minimum pressure for the upper valve is equal to the well-head pressure (there is no liquid above the upper valve). Table 12.12 shows



■ FIGURE 12.61 Downhole pressure and temperature survey.

the pressures and temperatures at each valve at the time the lower valve opens.

The closing and opening pressures at valve’s depth are calculated from the valve’s force–balance equation and the data from Table 12.12. For the first valve:

$$a = 0.083(T_v - 60) = 0.083(132 - 60) = 6$$

$$b = 1 + 0.002283(132 - 60) = 1.16$$

$$P_{bt} = (1 - R)P_{tr}b - a = 0.966(930)1.16 - 6 = 1036 \text{ psi}$$

$$P_{cvo} = \frac{P_{bt} - RP_{to}}{1 - R} = \frac{1036 - 0.034(83)}{0.966} = 1069.5 \text{ psi}$$

The closing and opening pressures of the first valve are 1036 and 1069.5 psig, respectively. The injection opening pressure referred to the surface is then 1009 psi. For the second valve:

$$a = 0.083(T_v - 60) = 0.083(153 - 60) = 7.71$$

$$b = 1 + 0.002283(153 - 60) = 1.21$$

$$P_{bt} = (1 - R)P_{tr}b - a = 0.966(875)1.21 - 7.71 = 1015 \text{ psi}$$

$$P_{cvo} = \frac{P_{bt} - RP_{to}}{(1 - R)} = \frac{1015 - 0.034(201)}{0.966} = 1043.65 \text{ psi}$$

**Table 12.12** Temperature and Pressure at Each Valve When the Lower Valve Opens

Valve	Tubing Pressure (psig)	Temperature (°F)
1	83	132
2	201	153

The closing and opening pressures of the second valve are 1015 and 1043.65 psig, respectively. The injection opening pressure referred to the surface is then 941 psi (very close to the 943 psi calculated earlier from the calculated value of  $Q_{ini}$  and with the use of the valve's force-balance equation). The force-balance equation indicates that the opening pressures should be lower than the ones in the two-pen pressure chart. This is due to an obvious calibration problem of the instruments used to measure the wellhead pressures. Even though it is not easy to determine from the survey the tubing pressure at the second valve when it opens, its value should be between 201 and 219 psi. If the tubing pressure at the lower valve is 201 psi:

$$Q_{ini} = \frac{201 \text{ psi} - P_{wh}}{0.393 \text{ psi/ft.}} = \frac{201 \text{ psi} - 60 \text{ psi}}{0.393 \text{ psi/ft.}} = 358.77 \text{ ft.}$$

$$F = \frac{\left[ (Q_{ini} - Q_{prod}) / Q_{ini} \right]}{D_{ov2valve}} = \frac{\left[ (358.77 \text{ ft.} - 226 \text{ ft.}) / (358.77 \text{ ft.}) \right]}{3.928 \text{ Mft.}} 100 = 9.4\% / \text{Mft.}$$

$$G_t (\text{true gradient}) = \frac{\text{Pressure}_{\text{topperf.}} - \text{Pressure}_{\text{valve}}}{\text{Depth}_{\text{topperf.}} - \text{Depth}_{\text{valve}}} = \frac{296 \text{ psi} - 201 \text{ psi}}{4690 \text{ ft} - 3928 \text{ ft.}} = 0.12 \text{ psi/ft.}$$

If the tubing pressure at the lower valve is 219 psi:

$$Q_{ini} = \frac{219 \text{ psi} - P_{wh}}{0.393 \text{ psi/ft.}} = \frac{219 \text{ psi} - 60 \text{ psi}}{0.393 \text{ psi/ft.}} = 404.5 \text{ ft.}$$

$$F = \frac{\left[ (Q_{ini} - Q_{prod}) / Q_{ini} \right]}{D_{ov2valve}} = \frac{\left[ (404.5 \text{ ft.} - 226 \text{ ft.}) / 404.5 \text{ ft.} \right]}{3.928 \text{ Mft.}} 100 = 11.2\% / \text{Mft.}$$

$$G_t (\text{true gradient}) = \frac{\text{Pressure}_{\text{topperf.}} - \text{Pressure}_{\text{valve}}}{\text{Depth}_{\text{topperf.}} - \text{Depth}_{\text{valve}}} = \frac{296 \text{ psi} - 219 \text{ psi}}{4690 \text{ ft.} - 3928 \text{ ft.}} = 0.1 \text{ psi/ft.}$$

The fallback factor is very large and it should be between 9.4% and 11.2%. The true liquid gradient is very small and no greater than 0.12 psi/ft. indicating a large formation gas/liquid ratio. The well was producing on intermittent gas lift because the size of the valve's seat was too large for the current value of the production pressure (which was too low). The gas flow rate through the deeper gas lift valve was then greater than the surface injection gas flow rate so the annular pressure dropped every time the gas lift valve opened. It is recommended in this case to calibrate the wellhead pressure sensors and increase the surface gas flow rate to see if the liquid production could be increased and if the well can produce on a stable continuous gas lift operation. If this could only be achieved with a very high injection gas flow

rate, it is necessary then to design the gas lift valves according to a more realistic low tubing pressure to produce this well on continuous gas lift with an operating valve with a smaller seat diameter.

### 12.6.9 Example #9 (production tubing diameter too large)

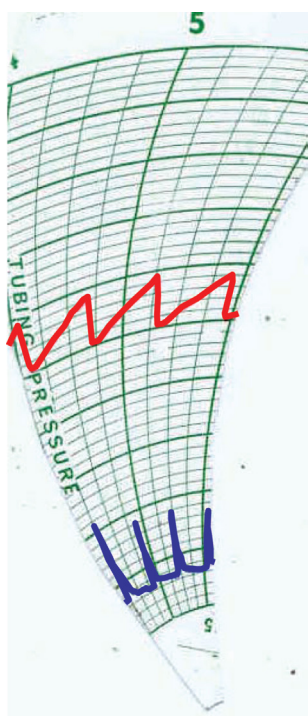
The well data is as follows:

Reservoir static pressure: 650 psig; 22° API oil gravity; 20% water cut; casing: 7-in. × 23-lb/ft.; production tubing ID: 3.958 in.; production tubing OD: 4.5 in.; depth of top of perforations: 5900 ft.; packer's depth: 5615 ft. The gas lift valves installed in the well are presented in Table 12.13.

The required information to do a quantitative analysis was not available. It was only known that the well had an orifice valve installed in the lower mandrel at 5535 ft. with an orifice diameter of 10/64 in. and an injection-pressure-operated, nitrogen-charged, unloading valve with an area ratio of 0.035, but neither its model nor its calibration pressure were known. Another important information missing was the surface injection gas flow rate.

On Aug. 13, 1999, a nitrogen-charged, injection-pressure-operated pilot valve with a large area ratio was installed in the well. The volume of gas injected per cycle was then equal to 7000 scf/cycle (which turned out to be less than its required value) and the liquid production was 65 STB/D. The two-pen pressure chart for this condition is shown in Fig. 12.62.

One fact that makes this well difficult to operate is its large production tubing diameter. To lift the liquid slugs at an acceptable velocity, it is important that the gas lift system be capable of providing the instantaneous gas flow rate to fill the volume behind the liquid slug as it travels up the tubing at a velocity large enough to keep the fallback losses at a minimum value. Sometimes, the gas lift system is indeed capable of maintaining a high instantaneous gas flow rate while the pilot valve is opened because the production tubing pressure is small; but, if for any reason (like shutting off the gas injection for several hours) the size of the liquid column gets to be too large, the gas lift system might not be able to provide the gas flow rate at its



■ FIGURE 12.62 Wellhead pressure chart for Aug. 13, 1999.

**Table 12.13** Valves Installed in the Well

Depth (ft.)	Valve Model	Port Diameter (64th in.)	$P_{tr}$ (psig)
3884	(?)	(?)	(?)
5535	RDO	10	0



required value and the fallback losses become very large. Under these circumstances, not only the instantaneous gas flow rate through the gas lift valve is small, but also the volume of gas injected per cycle is reduced because the spread of the valve also becomes very small. The spread is reduced because the larger liquid columns have a greater influence on the valve's opening pressure so the valve opens at a lower injection opening pressure. A pilot valve calibrated at a high injection opening pressure and with a large area ratio that exhibits a very small spread is a sign of a large liquid column in the production tubing above the valve. Based on the diameter of the production tubing, the water cut, and the oil API gravity for this example, the required volume of gas injected per cycle should be greater than 10,000 scf/cycle (even for small liquid columns to be lifted to the surface).

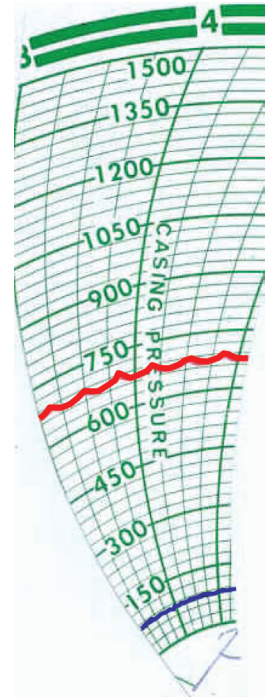
On Jun. 26, 2000, the well was loaded with a large liquid column, which was causing a reduction in the injection opening pressure and the spread of the valve was considerably reduced. The volume of gas injected per cycle was very small and the daily liquid production dropped significantly. The two-pen pressure chart for this condition is shown in Fig. 12.63.

On Jun. 14, 2002, an injection-pressure-operated, spring-loaded pilot valve with a large area ratio was installed. Even though the area ratio was large, the valve was calibrated at a low injection opening pressure, which caused a small valve's spread. The two-pen pressure chart shown in Fig. 12.64 clearly shows how the well was being loaded with liquids inside the tubing with the spread becoming smaller as time went by. The results from a downhole temperature and pressure survey are shown in Figs. 12.65 and 12.66, respectively. The survey indicates that the valve was indeed opening and closing but the volume of gas injected per cycle was so small that it simply bubbled through the liquid column to the surface leaving the liquid level constant at about 2000 ft. of depth.

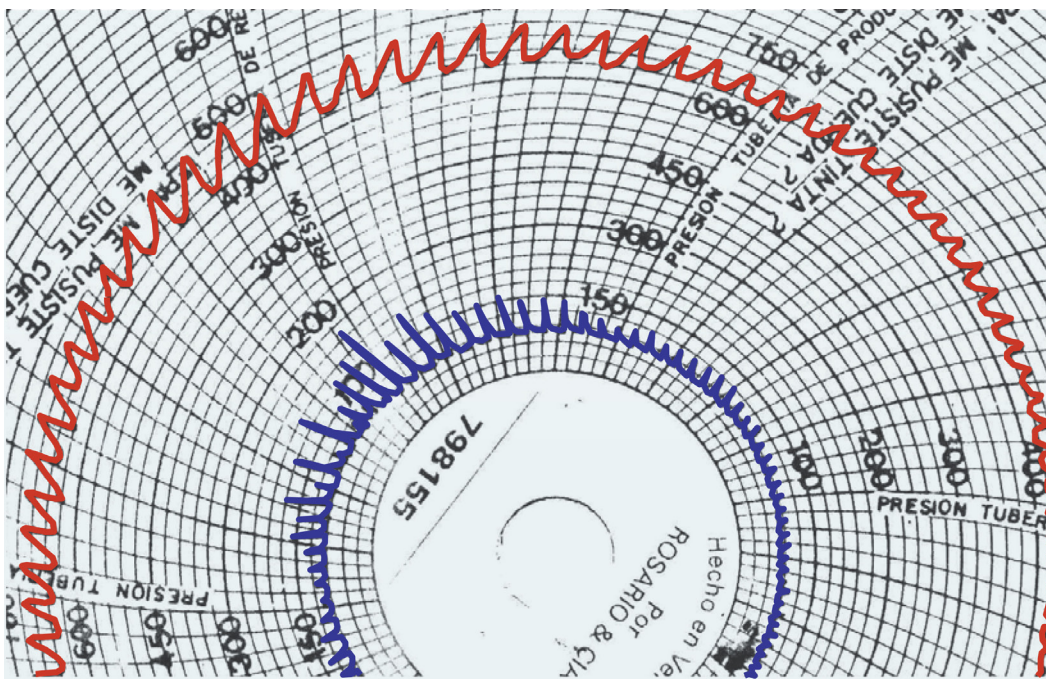
Instead of trying to unload the liquids in the tubing string, on Sep. 9, 2002 the pilot valve was replaced with an orifice valve, model RDO, with a 10/64-in. orifice diameter and, as can be seen in the pressure chart of Sep. 17, 2002 in Fig. 12.67, the injection pressure was very high and giving the impression that the upper valve was opening and closing. Unfortunately, the surface gas flow rate was not available and without this information it is not possible to do an analytical troubleshooting analysis.

There are two alternatives that might explain the behavior of the surface pressure shown in the two-pen pressure chart of Fig. 12.67:

- If the surface injection gas flow rate is very large, it is possible that, due to the small diameter of the orifice, the injection pressure was

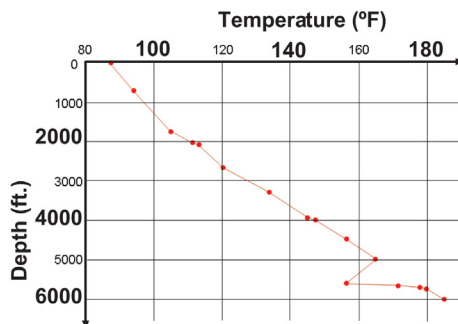


■ FIGURE 12.63 Wellhead pressure chart for Jun. 26, 2000.

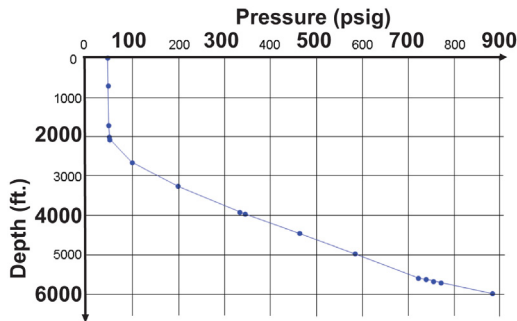


■ FIGURE 12.64 Wellhead pressure chart after the pilot valve was changed.

so high that the upper valve was opening and closing while the gas was being continuously injected through the orifice valve at the same time. Once the upper valve opened, the gas flow rate through both gas lift valves was greater than the surface injection gas flow rate and the annular pressure dropped until the upper valve closed. Once the upper valve closed, the gas flow rate through the orifice valve alone was less



■ FIGURE 12.65 Downhole temperature survey.



■ FIGURE 12.66 Downhole pressure survey.

than the surface injection gas flow rate and the annular pressure began to increase until the upper valve opened again.

- If the gas flow rate through the orifice valve was not very large, it is possible that the gas was being injected only through the lower orifice valve and the injection pressure fluctuations were caused by variations in the production tubing pressure. This can only happen if the gas flow through the orifice at 5535 ft. is subcritical. For the gas flow to be subcritical, the production pressure should be very high.

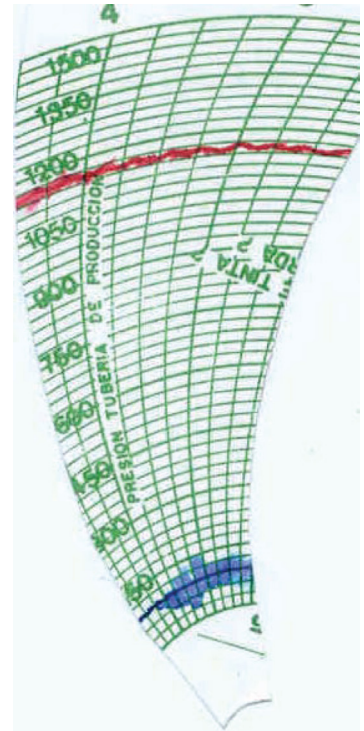
Without knowing the surface injection gas flow rate, it is not possible to find out what is taking place in the well. But, in any case, the production tubing diameter was too large and the reservoir pressure too low to have an efficient gas lift operation in continuous or intermittent gas lift. The production tubing must be replaced with a smaller diameter tubing string. It is also realized that the lower mandrel is too far from the top of the perforations so that the new mandrel spacing should consider lowering the operating point of injection, especially if intermittent gas lift is going to be implemented.

### 12.6.10 Example #10 (formation damage when the well was shifted to produce on intermittent gas lift)

The well data is as follows:

Static reservoir pressure: 552 psig; 26°API oil gravity; 3% water cut; casing: 7-in. × 23-lb/ft.; production tubing ID: 3.958 in.; production tubing OD: 4.5 in.; depth of top of perforations: 5010 ft.; packer's depth: 4659 ft.; gas injection line length: 4400 ft.; gas injection line ID: 2.067 in.; the gas lift valves installed in the well are presented in [Table 12.14](#).

The WF14R valve is an injection-pressure-operated, spring-loaded pilot valve. Its area ratio in this case was very large and equal to 0.426. Large



■ FIGURE 12.67 Pressure chart on Sep. 17, 2002.

**Table 12.14** Valves Installed in the Well

Depth (ft.)	Valve Model	Port Diameter (64th in.)	$P_{tr}$ (psig)
1675	dummy	—	—
3223	dummy	—	—
4577	WF14R	48	573

area ratios allow the calculation of the production tubing pressure ( $P_{to}$ ) at the moment the valve opens without magnifying the possible error made in the determination of the injection opening pressure at valve's depth ( $P_{cvo}$ ) from the measured surface injection pressure and the gas specific gravity.

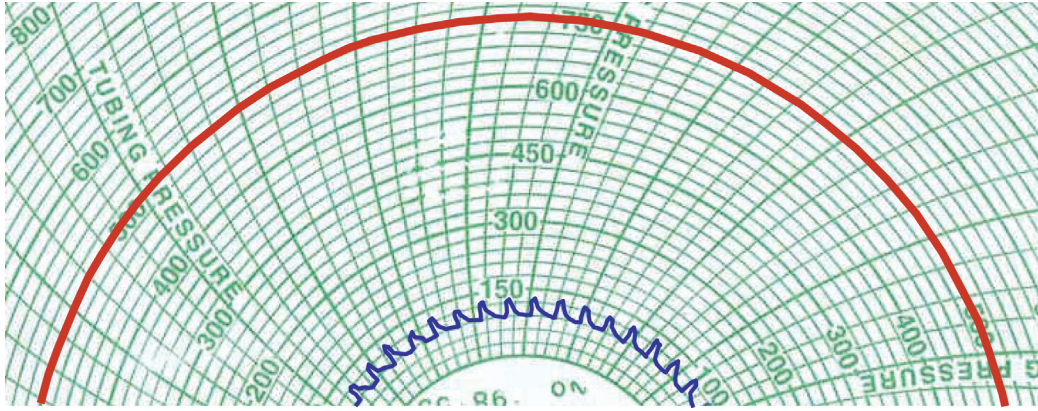
Prior to the installation of the pilot valve, the well was producing on continuous gas lift but it was heading most of the time. The operating valve at that time was a single-element, injection-pressure-operated gas lift valve, model R20, with a seat diameter of 16/64 in. and a test-rack opening pressure of 829 psig. The liquid production measurements during the months prior to this analysis are shown in Table 12.15.

The 4½-in. OD tubing was too large and the reservoir pressure too low to maintain a stable operation. Despite of this condition, the injection gas/liquid ratio was at a reasonable level. However, the injection gas/liquid ratio increased when the production method was shifted to intermittent gas lift by installing the pilot valve described earlier. Fig. 12.68 shows the two-pen pressure chart on Jan. 3, 2002 when the well was producing close to 200 STB/D (prior to the installation of the pilot valve).

In Apr. 2002, the well was shifted to intermittent gas lift. According to the pressure chart of May 8 2002 (Fig. 12.69), the pilot valve had problems and it took a while for it to close: The annular pressure increased very slowly for about 30 minutes, after which the pressure began to increase at a steeper rate indicating that the pilot valve has finally closed. The liquid production dropped to 38 STB/D.

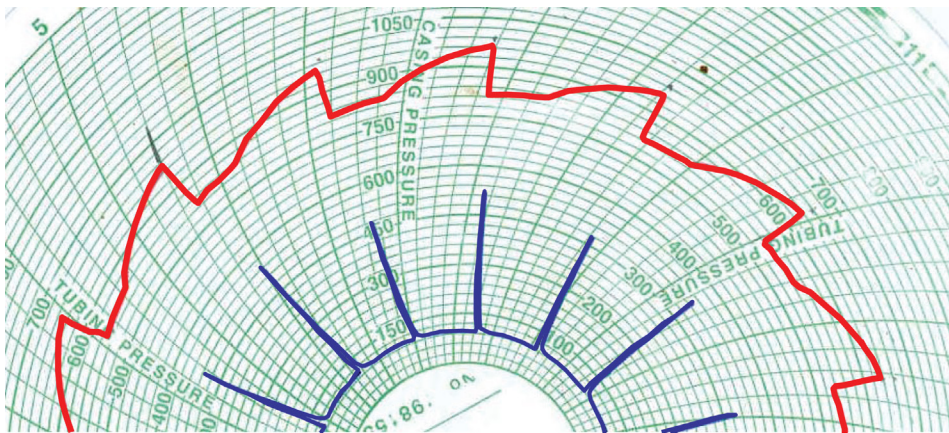
**Table 12.15** Production History

Date	Production (STB/D)	Gas Injection Flow Rate (Mscf/D)
Nov. 2001	369	168
Jan. 2002	241	191
Jan. 2002	237	243
Mar. 2002	222	245



■ FIGURE 12.68 Pressure chart for Jan. 3, 2002.

A cycle time of 95 min was probably too long. The volume of gas injected per cycle (calculated by dividing the surface gas flow rate of 245 Mscf/D by the number of cycles in 1 day) was equal to 16,163 scf/cycle. The volume of gas per cycle that the annulus and injection line can provide for the given valve spread is calculated to be equal to only 8864 scf/cycle. This last value is very low in comparison to the one calculated from the surface injection flow rate and the number of cycle in one day. This difference was due to the malfunction the pilot valve was experiencing (staying opened for a long period of time in which gas was constantly injected into the well at a very low flow rate).



■ FIGURE 12.69 Pressure chart for May 8, 2002.

For the tubing diameter, injection point depth, and the oil API gravity in this example, the required volume of gas to be injected per cycle should be approximately equal to 9000 scf to produce small liquid columns (not larger than 800 ft. in length) to the surface. The drop in liquid production experienced when the well was shifted to intermittent gas lift was then probably due to both, the long cycle time and the large fallback losses caused by the insufficient volumes of gas injected per cycle. The fact that the formation might have suffered some damage when the well was started on intermittent gas lift should also be investigated. It should also be taken into consideration the fact that the formation gas/oil ratio helps the operation of the well while it is on continuous gas lift. For intermittent gas lift, on the other hand, the formation gas/oil ratio lowers the efficiency of the production method: Greater true liquid column lengths (caused by the free gas content in the liquid column) cause an increase in frictional pressure loss and the gas-liquid mixture below the pilot valve absorbs part of the energy of the injection gas that should only be used to lift the liquid columns. This last point is important in this case because the gas lift valve was 433 ft. higher than the top of the perforations. A standing valve should be installed right below the pilot valve in the tubing.

The production pressure at valve's depth at the moment the pilot valve opened ( $P_{to}$ ) can be calculated from the valve's force-balance equation. With the injection pressure at valve's depth equal to 1083 psig (calculated from an injection surface opening pressure of 960 psig) and the calibration pressure of 573 psig, the  $P_{to}$  production pressure is calculated from the following equation, in which all terms are known except for  $P_{to}$ :

$$R = \frac{P_{cvo} - P_{irc}}{P_{cvo} - P_{to}} = 0.426 = \frac{1083 \text{ psi} - 573 \text{ psi}}{1083 \text{ psi} - P_{to}}$$

If this equation is solved for  $P_{to}$ , the tubing pressure would need to be negative. As in many of the previous examples, this is due to unreliable calibrations of the surface pressure instruments or, less probably, to the wrong calibration of the pilot valves at the shop. The calibration of the wellhead pressure sensors should be checked periodically. As can be seen in all these examples, poor calibration of wellhead pressure sensors is not that uncommon (because very few people take the time to do the type of troubleshooting analysis presented here so the poor calibration of the instruments can go unnoticed for months or years). The error could also lie on the fact that the injection gas specific gravity was not verified for current conditions. The gas specific gravity plays an important role in determining the injection pressure at depth. In this case, the specific gravity was thought to be equal to 0.7, but its actual value could not be verified. If, for example, the gas specific gravity

was equal to 0.76, the injection pressure at valve's depth would be 1100 psig instead of 1083 psig.

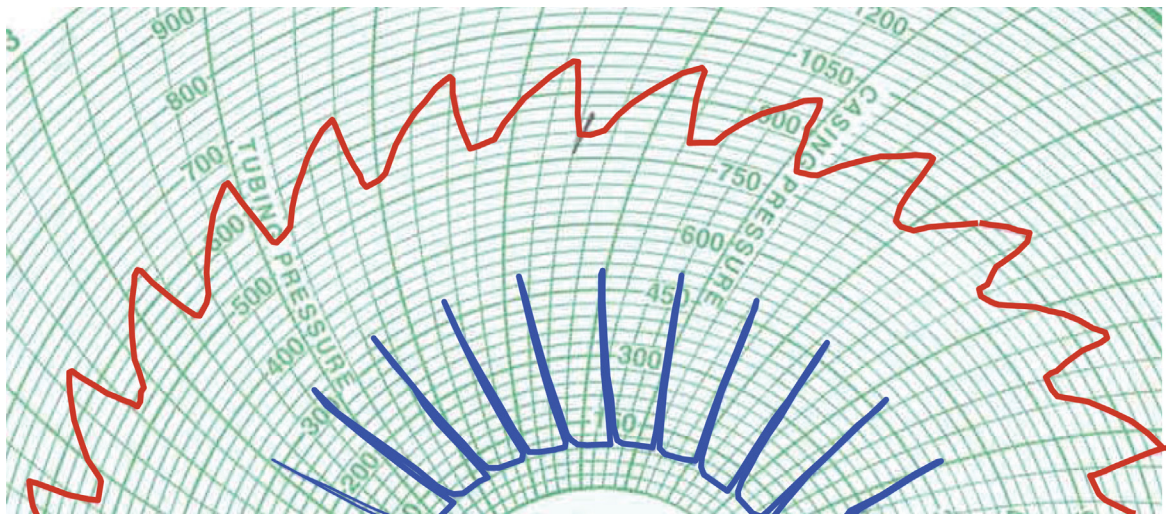
The produced liquid column per cycle is found from:

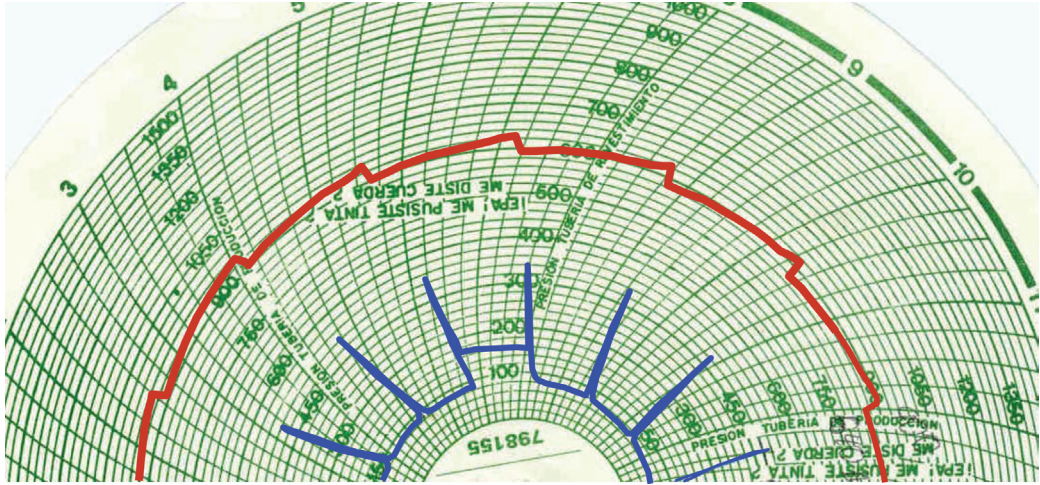
$$Q_{\text{prod}} = \frac{38 \text{ Br/D}}{\left[ \frac{(1440 \text{ min/D})}{(96 \text{ min/cycle})} \right]} \frac{1}{15.2182 \text{ Br/Mft.}} = 0.16646 \text{ Mft./cycle}$$

Where 15.2182 Br/Mft. is the volumetric capacity of the production tubing. With a wellhead production pressure of 60 psig, a liquid gradient of 0.389 psi/ft. (with no gas), and if fallback losses are neglected, the production pressure at valve's depth would be:  $P_{\text{to}} = 166 \text{ ft.} (0.389 \text{ psi/ft.}) + 60 \text{ psig} = 124.75 \text{ psig}$ . This tubing pressure is too low for such a long cycle time (based on the reservoir productivity index and static pressure, the production tubing pressure should have been greater). Therefore, the fallback losses must have been very large. In May of 2002, the gas injection was increased to 436 Mscf/D and the production went up to 70 STB/D. This production increment was only due to the reduction in the cycle time because the volume of gas injected per cycle was only slightly increased. Fig. 12.70 shows the pressure chart for May of 2002.

In Jun. 2002 the surface injection gas flow rate was reduced and the production dropped to 61 Br/D because the new cycle time was too long. Fig. 12.71 shows the pressure chart for Jun. 21, 2002, where it can be appreciated that the injection opening pressure has dropped because of the increase in the size of the liquid columns.

■ FIGURE 12.70 Wellhead pressure chart for May of 2002.





■ FIGURE 12.71 Wellhead pressure chart for Jun. 21, 2002.

A downhole pressure survey was run in Jun. 2002 in which the production pressure at valve's depth,  $P_{to}$ , was 342 psig. Two different production levels were reported for that month: 33 and 61 Br/D. None of these dates corresponds to the date the survey was run, which adds an unnecessary difficulty to the troubleshooting process. It is always a good idea to test the well while the survey is being run. If it is not possible to test the well the same day the survey is run, the well should be tested a few days after or before the survey, but always at the same gas injection frequency the well had during the survey. Due to this uncertainty in the liquid production, the fallback factor is calculated for both productions:

- With 61 Br/D, the fallback factor is calculated as follows.

The initial liquid column (based on the production pressure measured during the survey of 342 psig) can be calculated from the following equation, where the wellhead production pressure is equal to 60 psig and the liquid gradient is 0.389 psi/ft.:

$$Q_{ini} = \frac{342 \text{ psi} - 60 \text{ psi}}{0.389 \text{ psi/ft.}} = 724.9 \text{ ft.}$$

The liquid column produced at each cycle is calculated knowing that the cycle time was equal to 97 minutes:

$$Q_{prod} = \frac{61 \text{ Br/D}}{(1440 \text{ min/D}) / (97 \text{ min/cycle})} \frac{1}{(15.2182 \text{ Br/Mft.})} 1000 \text{ ft./Mft.} = 270 \text{ ft.}$$



The fallback factor is then:

$$F = \frac{[(724.9 \text{ ft.} - 270 \text{ ft.}) / (724.9 \text{ ft.})]}{4.577 \text{ Mft.}} = 0.137$$

This means that approximately 14% of the initial liquid column per each thousand feet of depth of the injection point is not produced. The total fallback loss is then equal to 62.7% of the initial liquid column length.

- With a liquid production of 33 Br/D at the time the survey was run, the produced liquid column per cycle is:

$$Q_{\text{prod}} = \frac{33 \text{ Br/D}}{(1440 \text{ min/D}) / (97 \text{ min/cycle})} \frac{1}{15.2182 \text{ Br/Mft.}} 1000 \text{ ft./Mft.} = 146 \text{ ft.}$$

The fallback factor is then:

$$F = \frac{[(724.9 \text{ ft.} - 146 \text{ ft.}) / (724.9 \text{ ft.})]}{4.577 \text{ Mft.}} = 0.1744$$

This means that 17.44% of the initial liquid column per each thousand feet of depth of the point of injection is not produced. The total fallback loss is then equal to 79.82% of the initial liquid column length.

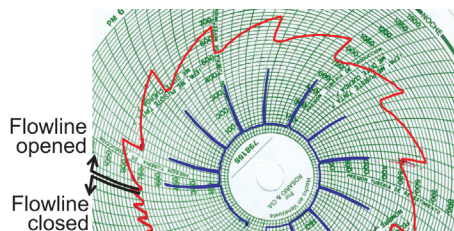
If the fallback factor could be reduced to 5% per thousand feet of depth of the point of injection, the well could, at least, produce about 126 Br/D:

$$q_f \text{ (Br/D)} = (724.9 \text{ ft./cycle}) \frac{1440 \text{ min/D}}{97 \text{ min/cycle}} (15.2182 \text{ Br/Mft.}) \\ [1 - 0.05(4.577)] \frac{1 \text{ Mft.}}{1000 \text{ ft.}} = 126.29 \text{ Br/D}$$

This represents a reduction in the production the well had before it was shifted to intermittent gas lift of 43%.

In an attempt to improve the operation of the pilot valve (which was leaking gas for several minutes), on Sep. 23, 2002 the flowline was closed for several hours while the injection gas flow rate into the casing was maintained. Then, the flowline was opened again to produce the liquid accumulated in the tubing. This can be appreciated in the chart of Sep. 23, 2002 in Fig. 12.72, where it is shown that it took several cycles to reach a steady-state and how the injection pressure increased in the process.

In Oct. 2002, the surface gas flow rate was raised to 685 Mscf/D and the liquid production increased to only 72 Br/D, with a cycle time of 22 min and a surface injection pressure considerably greater (1,030 psig). This increment



■ FIGURE 12.72 Wellhead pressure chart for Sep. 23, 2002.

of the injection pressure revealed that the production pressure was being reduced to its lowest possible value. Therefore, it is highly possible that the reduction in the liquid production could be due to formation damage when the well was shifted to produce on intermittent gas lift.

### 12.6.11 Example #11 (intermittent gas lift with surface intermitter)

The well data is as follows:

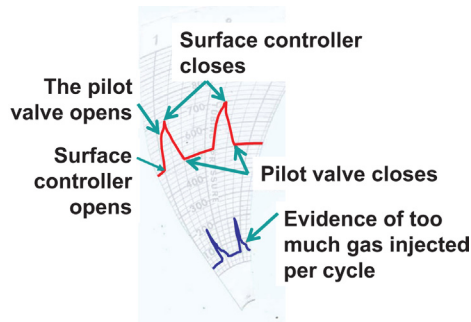
Reservoir static pressure: 980 psig; 13°API oil gravity; 0% water cut; casing: 7in. × 23-lb/ft.; production tubing ID: 2.992 in.; production tubing OD: 3.5 in.; top of perforations' depth: 3975 ft.; packer's depth: 3859 ft.; gas injection line length: 4000 ft.; gas injection line ID: 2.067 in.; the valves installed in the well are presented in Table 12.16.

The WFM14R valve is a 1-in. OD, injection-pressure-operated, spring-loaded pilot valve with a test-rack closing pressure of 892 psig. The well's production was 105 STB/D with a cycle time of 70 min. Fig. 12.73 shows the behavior of the injection and production pressures.

The pilot valve's surface opening pressure was approximately 960 psig, and its closing pressure was 750 psi. The injection pressure at which the controller closes is just above 1000 psig. Because the surface gas flow rate was not known, the volume of gas that was injected per cycle into the tubing from the moment the controller closed to the time the gas lift valve closed was calculated based only on the volume of gas that the annulus

**Table 12.16** Valves Installed in the Well

Depth (ft.)	Valve Model	Port Diameter (64th in.)	$P_{tr}$ (psig)
1527	NM14R	16	984
2756	dummy	—	—
3788	WFM14R	32	892



■ FIGURE 12.73 Wellhead pressure chart.

and the injection line can provide for the given pressure difference (not taking into account the gas injected into the tubing from the moment the pilot valve opens until the surface controller closes). This volume was calculated to be 15,674 scf/cycle, so that the total volume injected per cycle must have been even greater. The required volume of gas to be injected per cycle (for the type of oil gravity, the depth of the point of injection, and the size of the production tubing) is approximately 10,000 scf/cycle for liquid columns of lengths from 200 to 800 ft. This indicates that the volume of gas that was being injected per cycle was greater than its required value.

The surface pressure chart does show evidences of gas overinjection because it takes a while for the wellhead production pressure to drop to its minimum value after the slug has surfaced, see the explanation given for Fig. 12.23h. The volume of gas injected per cycle could be reduced by shortening the time interval in which the surface controller is opened, but the injection opening pressure of the pilot valve is already high and reducing the injection time might cause the pilot valve to open after two or more injection cycles, as shown in Fig. 12.26a. Additionally, the reduction in the volume of gas injected per cycle is not going to be very significant because the gas lift valve's area ratio is very large. In cases like this, it is recommended to install a pilot valve with an area ratio of approximately 50% of its required value on choke-control intermittent gas lift and adjust the volume of gas injected per cycle by changing the time the controller remains open.

Even though the volume of gas injected per cycle was very large, the liquid fallback factor should not have been as low as 5% (common for oils with API gravities greater than or equal to 23°API) because of the low API gravity of the oil being lifted.

Because the cycle time was equal to 70 min, the produced liquid column per cycle in Mft. is found from:

$$Q_{\text{prod}} = \frac{105 \text{ Br/D}}{\left[ \frac{(1440 \text{ min/D})}{(70 \text{ min/cycle})} \right] 8.69 \text{ Br/Mft.}} = 0.587 \text{ Mft./cycle}$$

The force–balance equation was used to find the production pressure at valve’s depth at the moment it opened,  $P_{\text{to}}$ . For this purpose, the valve area ratio ( $R = 0.3339$ ), the valve’s opening pressure at depth ( $P_{\text{cvo}} = 1062$  psig), and the valve’s calibration pressure of 892 psig, are used:

$$R = \frac{P_{\text{cvo}} - P_{\text{trc}}}{P_{\text{cvo}} - P_{\text{to}}} = 0.3339 = \frac{1062 - 892}{1062 - P_{\text{to}}}$$

From which the value of  $P_{\text{to}}$  was found to be 552.86 psig. The liquid gradient from the oil API gravity and water cut was found to be 0.424 psi/ft. With the value of  $P_{\text{to}}$  just calculated, the wellhead pressure of 40 psig, and the liquid gradient, the initial liquid column length above the valve was found at the moment the valve opened by:  $Q_{\text{ini}} = \frac{552.86 \text{ psi} - 40 \text{ psi}}{0.424 \text{ psi/ft.}} = 1209.6 \text{ ft.}$

Thus, the liquid fallback factor was:  $F = \frac{[(1209.6 - 587)/(1209.6)]}{3.788} 100$   
 $= 13.58\%$  for each thousand feet of depth of the point of injection.

This seems to be a very large fallback factor but, in reality, it is as low as it can get for the type of oil that was being produced. Because the valve’s area ratio is very large and the volume of gas injected per cycle was greater than its required value, if the surface injection pressure sensor is properly calibrated and the gas specific gravity is precisely known, the calculation of the fallback factor given earlier should be reliable enough to proceed with the determination of the productivity index using equation 12.32, and the optimum cycle time using equation 10.22. By adjusting the time the controller remains open and close, the calculated optimum cycle time can be matched in the field. The time cycle controller allows the cycle time to be adjusted independently of the volume of gas injected per cycle. Due to the type of oil being lifted, this well should not be on continuous or intermittent gas lift (a different method of production should be implemented in this well).

# Subject Index

## A

Abnormal injection gas flow rate, 739  
Absolute pressure, 35  
Absolute roughness, 38, 74  
    for annular flow, 40  
Acceleration of gravity, 35  
Acceleration pressure drop, 36, 111  
Acceleration pressure gradient, 94, 95  
Accumulation chambers, 260, 482, 496, 594  
    advantages of, 499  
    annulus, 260  
    attention points, 498, 499  
    bleed valve, 260  
    bottomhole pressure, 262  
    capacity of, 586  
    double-packer, 260, 589  
    gas injected per cycle, 261  
    installation, 824  
    limitations, 497  
    liquid slugs, 261  
    objective of, 583  
    optimum size, 263  
    orifice valves, 260  
    perforated nipple, 260  
    reservoir pressure, 261  
    with standing valve, 493  
    volume of, 583  
Accumulator, 254  
    insert, 273, 594  
    pressure–depth diagrams, 274  
    inside diameter of, 593  
    isolated from casing, 272  
    simple-type, 255, 592  
Accuracy, 7  
    of calculated injection pressure, 29  
Acid gas, 1  
Adjustable needle valve, 508  
Air molecular weight, 43  
Algebraic equation, 104  
Al-Marhoun PVT correlation, 147  
Amagat's law, 4, 5  
Ambient temperature, 103  
American Petroleum Institute, 303  
Analytical troubleshooting tool, 719  
Annular flow, 40, 253  
    in oil wells, 40  
Annular gas flow rate, 704

Annular injection pressure, 779  
Annular liquid level, 874, 875  
    cases, 875  
    injection pressure, 695  
Annular mist, 87  
Annular pressure, 828  
    drops, 770  
Annular volumetric capacity, 549  
Annuli, 26  
Annulus, 250  
    liquid level, 692  
    liquid pressure gradient, 694  
    surface gas injection pressure, 694  
    tubing communication depths, 698  
Annulus-tubing communication, 623, 830–832  
    wellhead pressure patterns of two wells  
    with, 831  
Anti-Stokes reflections, 713  
API  
    fallback factor value, 486  
    gravities, 63, 183, 184, 536, 643, 795, 855, 872, 935, 953, 954  
    for consistency, 171  
    tubing, 455  
Apparent molecular weight  
    of air, 6  
    of dry air, 6  
Ashford correlation, 142  
Ashford–Pierce correlations, 148  
Ashford–Pierce model, 144  
Asphaltene, 246  
Assumed point, of injection, 654  
Atmospheric pressure, 302  
Automatic controllers, 515  
Automatic pressure control system, 513  
Automation systems, 706  
Available injection pressure, 369  
Average annular pressure, 774  
    after pilot valve closes, 774  
Average gas compressibility factor, 27, 775  
Average geothermal temperature, 775  
Average liquid slug velocity, 551, 767, 793  
Average slug velocity, 552, 554, 823  
Average temperature, 31, 44, 542, 574  
    in pipe segment, 96  
Avogadro's law, 3

## B

Ball position diagram, 336  
Beggs–Robinson correlation, 191  
Behavior  
    of constant injection–gas-flow-rate  
    equilibrium curves  
    for different injection gas flow, 180  
    of discharge coefficient back-calculated  
    by, 159, 322  
    of horizontal multiphase flow in  
    flowline, 85  
    wellhead pressure behavior of a  
    well with a damaged gas lift  
    valve, 825  
Bellows areas, 308  
    definitions of, 308  
    determination of, 308  
    injection pressure, 308  
Bellows hysteresis, 326  
Bellows-load rate test, 300, 336, 341  
Blind box, 242  
Bottomhole  
    flowing pressures, 128, 156, 159, 383  
    nodal analysis, 710, 711  
    injection pressure, effect of friction  
    on, 41  
    pressures calculated from surface  
    injection pressures, 29  
    static pressure, 367  
Boundary  
    between critical and subcritical flow,  
    136, 315  
    between sonic and subsonic flow takes  
    place, 336  
Bubble flow, 87  
  
**C**  
Calculation flow chart, for average pressure  
    and temperature, 33  
Calculation techniques for wells, 783  
Calibrated gas lift valve, 625  
Calibrated valve, 220, 318, 319, 465, 466,  
    636, 678  
Calibration pressures, 214, 315, 457, 518, 942  
Calibration process, 295, 298, 339, 663,  
    668, 740  
Carbon dioxide (CO<sub>2</sub>), 1

- Casing collar locators (CCLs), 615
- Casing-tubing annulus, 156, 297, 366, 506, 545, 548
- Casing-tubing communications, 681, 690, 733, 734, 782, 830
- detected by temperature measurements, 717
- Casing-tubing packer, 692
- Casing wall, detection of communication, 717
- CCL detector, 715
- CCLs. *See* Casing collar locators (CCLs)
- Central analysis unit executing computer programs, 740
- Chart recorders, two- or three-pen, 613
- Check valve, 214, 230, 266, 626, 832, 920
- piston's internal, 502
- Chemical injection, 246
- Choke control, advantages of, 513
- Choke-control intermittent gas lift, 354, 480, 489, 495, 507, 508, 514, 520, 521, 570, 572, 605, 770, 773, 776, 783, 786, 798
- advantages, 508
  - disadvantage, 508, 510
  - volume of gas injected per cycle, 509
  - wells, 127, 726
- Choke diameter, 136, 139
- Choke geometry, 130, 140
- Choke housings, 490
- Chokes, in production tubing, 128
- Chokes installation
- downstream of seat, 357
  - in straight vertical pipes, 145
  - temporarily installed at wellhead, 129
  - upstream of seat, 359
- "Churn" flow, 87
- Circulating sleeve, 257
- Coiled tubing, 282
- Communication tests, 628, 674, 677
- Complex heat-transfer, 354
- Composition, of injection gas, 29
- Compressibility factor, 8, 12, 29. *See also*
- Gas compressibility factor
  - natural gas mixtures, 8
  - pure gas, 7
  - for pure hydrocarbon gases, 7
- Compression energy, 317
- Compressor, 25, 367
- discharge, 33
  - high-pressure, 367
  - high-volume, 367
  - inlet, 33
- Concentric mandrels, 305
- Conditions, promoting hydrate formation, 19
- Constant closing pressure, 299
- Constant-injection-gas flow-rate equilibrium curve, 160, 178, 196, 198, 205, 206, 378
- Constant liquid production, 384
- Constant wellhead production pressure, 154–161
- Continuity equation, 552
- Continuous flowing pressure temperature survey, 685
- Continuous gas lift analysis, 750
- Continuous gas lift injection, 669
- Continuous gas lift troubleshooting, 611
- automated systems to detect and analyze wells, 738–742
  - CO<sub>2</sub> injection to determine point of injection, 695–706
  - continuous liquid production, 743, 746
  - distributed temperature sensors (DTS), 712–717
  - downhole pressure/temperature, 706–710
  - examples, 743
  - field techniques, for gas lift well, 674
    - communication tests, 674–681
    - downhole pressure and temperature surveys, 681–688
    - sonic devices, use of, 689–695  - fluctuating injection pressure, 746
  - gas injection, 743
  - gas lift troubleshooting guide, 756
  - liquid production, 756
  - handling problems, associated with emulsion generation, 639–641
  - injection gas flow rate measurement charts, 720–724
  - injection, time intervals of, 749
  - liquid level, measurement of, 718–719
  - liquid production flow rate, 611
  - loss of lifting efficiency, causes/ corrective actions for, 619
  - flowline/production tubing, 631
  - gas lift/completion equipment, failures/malfunctions of, 628–631
  - instabilities, 619–624
  - low injection pressure, gas flow rate, 633
  - low injection pressure, high injection gas flow rate, 632
  - low reservoir liquid production, 631
  - unloading process, 633–634
  - unloading the well, 634–635
  - well, inadequate operation of, 624–627
  - multiple points of injection, 635–639
  - nitrogen-charged gas lift valve, 667
  - reservoir static liquid level, 651–667
  - troubleshooting analyses, methodology, 642
  - completion data, 642
  - fluid properties, 642
  - high wellhead injection pressure and well, 646
    - nitrogen-charged, IPO valves, 649
    - nitrogen-charged, PPO Valves, 650
    - spring-loaded, IPO valves, 649
    - spring-loaded, PPO valves, 651  - liquid production, 642
  - numerical procedure, 645
  - reservoir data, 642
  - test-rack opening pressures and seat diameters, 644
  - two-pen charts, 642
  - troubleshooting analyses of gas lift wells, 612–619
  - troubleshooting techniques, 611
  - unstable gas injection/liquid production, 759
  - wellhead pressure charts, use of, 724–738
  - well, not produce liquids, 667–673, 755
  - well, not take gas, 763
  - well's responses, 752
  - well takes gas, but does produce liquids, 761
  - wireline tools
    - total well depth and liquid level measurements, 711–712
- Continuous gas lift well, 737
- Continuous liquid production
- with unstable gas injection pressure, 733
- Continuous surveys, 688
- CO<sub>2</sub> pulse, 695, 700
- changes in shape, 700
  - CO<sub>2</sub> injection, inadequate volumes of, 701
  - connections and required equipment, 697
  - high-pressure bottle, 696
  - injection gas line, 701
  - specific gravities of, 700
  - total gas produced from well, 703, 704
- Correlation for pressure gradient, 111
- Corrosion, 1, 16
- Critical pressure ratios, 352
- Critical temperature, 7

- Crystallization, 238  
 Cycle time, 828  
   on velocity curve, 527
- D**
- Dalton's law, 4  
 Damaged gas lift valve, with internal  
   check valve in good working  
   conditions, 824  
 Damaged valve, 826  
 Data acquisition parameters, 706  
 Data acquisition system, 618  
 Data for troubleshooting wells, on  
   intermittent gas lift  
   behavior of wellhead production and  
   injection pressure, 767  
   fluid properties, 768  
   reservoir data, 768  
   total liquid and gas production, 767  
   well completion data, 769  
 Deepest point of injection, 162  
 Demulsifying agents, 626  
 Density expression, 43  
 Design calculations, 304  
 Design temperature, 102  
 Determining need to iterate, 138  
 Dewpoint  
   lines for each water vapor content of a  
   natural gas, 19  
   temperature, 16  
 Diameter for annular spaces, 40  
 Differential pressure, 325  
 Dip tube, 584, 598  
   liquid levels, 592  
 Direction of calculation process, 37  
 Discharge coefficient, 318  
   behavior of, 322  
 Discrete temperature drops, 682  
 Displaced flow rate, 551  
 Distributed temperature sensors (DTS),  
   712–717, 874  
 Dome pressure, 302  
 Double iteration, 97  
 Double-packer accumulation chamber,  
   820, 824  
   installation, 820  
   with the liquid level above the upper  
   packer, 822  
   troubleshooting calculation procedure  
   for, 820  
 Double-packer chambers, 497  
 Downhole equipment failure, 628  
 Downhole flowing pressure survey, 745  
 Downhole gas injection pressure, 41  
 Downhole pressure and temperature survey  
   in intermittent gas lift wells, 845–874  
 Downhole pressure surveys, 728  
 Downhole production tools, 237  
   plugs, 237  
   standing valves, 237  
   subsurface safety valves, 237  
   tubing stops, 237  
 Downhole restrictions, 689  
 Downhole temperature surveys, 681  
 Downstream pressures, 138, 308, 315, 335  
 DTS. *See* Distributed temperature  
   sensors (DTS)  
 Dual wells, 276, 446  
   disadvantages, 280  
   intermittent gas lift, 597  
   parallel completions for, 279  
 Dukler–Flanigan correlation, 183  
 Dump bailing tools, 246  
 Duns-Ros correlation, 97, 111, 192  
 Dynamic closing pressure, 504  
 Dynamic gradient, 69  
   circular pipes the hydraulic radius, 70  
   depending on variable, calculation  
   procedures, 73  
   flow charts of problems, 74  
   friction factor, 74  
   hydraulic radius, 70  
   iteration procedure consists of, 74  
   pressure distributions for single-phase  
   liquid flows, 78  
   pressure drop, 70  
   shear stress, 69  
   for steady state, turbulent,  
     incompressible flow in a pipe, 69  
   summation of forces on liquid in control  
   volume, 70  
   vertical, upward, single-phase liquid  
   flow in a straight pipe  
     with constant bottomhole pressure, 71  
     with constant surface pressure, 71, 72  
 Dynamic model, 345
- E**
- Effective pressure, 332, 333  
 Effect of a restriction, in production tubing/  
   flowline, 128, 129  
 Effect of friction  
   on bottomhole injection pressure, 41  
   in gas wells, 42  
 Effect of liquid flow rate, on wellhead  
   pressure, 86  
 Effect of tubing diameter, on minimum  
   pressure point of outflow  
   curves, 85  
 Efficiency factors, for different liquid  
   contents, 50  
 Electric submersible pumps, 255  
   artificial lift method, 255  
   gas lift, 255  
 Electric submersible pumps (ESP), 725  
 Electronic pressure sensor, 643  
 Electronic sensors, 618  
 Elementary fluid mechanics, 35  
 Empirical correlations, 108  
 Emulsions, 626, 639, 640  
   getting rid of, 640  
 Energy balance, 765  
   equation, 34, 35, 96, 821  
   integration, 35  
 Enthalpy, 22, 34, 96, 97  
 Entrance pressure, 51  
 Equation of state, 2  
 Equations for multiphase flow pressure and  
   temperature gradients, 93  
 Equilibrium curve, 159  
   injection gas flow rate, 179  
   with variable injection gas flow rate, 159  
 Equilibrium points, 174  
 Equivalent spring pressure, 304  
 Erosion velocity, 60  
 Escalante's model, 334  
 ESP. *See* Electric submersible pumps  
   (ESP)  
 Euler's equation, 581  
 Euler's method, 578  
 Exploratory wells, 411. *See also entries*  
   *starting with wells*
- F**
- Fallback factor, 793, 821, 828  
 Fallback losses, 486  
   calculation, 597  
 Fanning friction factor, 35, 38, 70  
 Fiber-optic surveys, 712  
   equipment required for temperature  
   measurements, 714  
 Fiber-optic technology, 681, 874, 876  
 Fiber-optic temperature measurement, 713  
 Field troubleshooting techniques, 738  
 First law of thermodynamics, 34  
 First valve, operating pressure, 369

- Fixed compressibility factor, 27. *See also*  
Compressibility factor
- Fixed drawdown production, 383
- Fixed liquid production, 383
- Flow-coefficient tests, 332, 336, 342
- Flowing pressure survey, 188
- Flowline, 25, 95, 127
- Flowline diameter, 490
- Flow pattern maps, 86, 110  
for horizontal flow, 88  
for vertical upward flows, 87
- Flow patterns, 88  
classified in large groups, 111  
and particular correlation, 93  
in upward, vertical, concentric annuli, 120
- Flow rates, 1, 73, 129
- Flow restrictions, 50
- Fluctuating surface gas injection  
pressures, 876
- Fluid flow rate  
as a function of pressure ratio, 131  
vs. pressure ratio, 130
- Fluid flow through annular cross-  
sections, 118  
encountered in multiphase flows in  
annuli, 120  
flow pattern prediction, 119  
list of examples, 118  
situations/models for calculation, 119
- Fluid mixtures, 142
- Fluid temperature, 102, 107  
at a distance from the bottom, 102
- Force-balance equations, 295, 331, 773,  
777, 781, 792, 794–796  
static, 337
- Formation volume factor, 13
- Fortunati correlations, 146, 148
- Frictional losses, 576
- Frictional pressure, 41  
drops, 26, 33, 34, 40–42, 51, 86, 631  
gradient, 94  
losses, 41
- Friction coefficient, 555
- Friction factor, 38, 40, 54, 60, 72, 95, 112  
from the Moody diagram, 38
- G**
- Gas annular pressure, 590
- Gas chamber pumps, 572
- Gas column, 26, 40, 41  
weight, 50
- Gas compressibility factor, 13, 29, 35, 45,  
60, 143, 350, 488
- Gas compression, 378
- Gas constant, 3
- Gas consumption, 487
- Gas cooling problems, 720
- Gas density, 26, 60
- Gas distribution system, 25
- Gas enthalpy. *See* Enthalpy
- Gas expansion factor, 134
- Gas factor, 28, 827
- Gas flow, 42  
in horizontal pipes, 42  
rate. *See* Gas flow rate  
through chokes, 138  
through restrictions, 131–138  
in tubing, 581  
turbulences, 725
- Gas flow rate, 26, 39, 40, 42, 44, 50–52,  
54, 58, 128, 136, 138, 315, 340,  
511, 550, 590, 592, 655, 719,  
765, 770, 781  
to calculate, 51  
capacity, 55  
chart, 721, 722  
curve, 136, 137  
determining iterations, 662  
at different pressures, 51  
handling capacity, 56  
before installing the larger diameter pipe  
segment, 53  
measurement, 722  
devices, 720  
obtained by installation of lines partially  
connected in parallel, 59  
percent increment, 55, 56  
reduced to zero, 165  
through these pipes in series for a  
pressure drop, 53  
total pressure gradient, 166
- Gas formation volume factor, 13
- Gas handling capacity, 52
- Gas injected per cycle  
fallback factor, 538
- Gas injection, 491, 731, 743, 765, 783  
choke, 480, 491  
flow control valve, 721  
flow rates, 514  
nodal analysis, 645  
frequency, 780  
lines caused by liquid accumulation, 50  
pressure, 26, 30, 174, 648, 650, 652  
equilibrium point, 174  
temperature, 552  
through damaged gas lift valve, 828  
through orifice valve, 734, 735, 736  
typical surface injection pressure  
pattern, 507  
variables of mathematical model, 573  
into well, controlled using  
alternatives, 880
- Gas internal energy, 34
- Gas law, 2, 3
- Gas lift design, 463  
continuous, 365  
emulsions, 470  
examples of, 471  
hole in production tubing, 470  
instabilities, 470  
pressure fluctuation, 470  
purposes, 663  
stability check of, 463
- Gas lift efficiency, 82
- Gas lift equipment, 730
- Gas lift installations, 1, 250, 292  
with nitrogen-charged gas lift  
valves, 102  
types of completions, 250  
accumulation chambers, 260  
coiled tubing, 282  
dual wells, 276  
intermittent gas lift with metallic  
plungers, 287  
single, 250
- Gas lift IPO valve, 727
- Gas lift latches, 211
- Gas lift mandrels, 226, 385, 476, 689  
spacing, 41  
procedures, 385  
usages, 627  
valve design calculations, 385
- Gas lift method  
disadvantage of, 639
- Gas lift rate vs. casing head pressure, 204
- Gas lift systems, 489, 605, 633
- Gas lift troubleshooting guide, 756
- Gas lift valve, 109, 295, 315, 479, 582,  
635, 788  
calibration pressure of, 295  
dynamic behavior, mathematical models  
for, 331  
failures, 630  
force-balance equations, 295  
pilot valves, dynamic model for, 353



- simple mechanistic model, with dynamic effect, 340
  - simple mechanistic model, without dynamic effect, 336
  - statistical models, 333
    - for orifice, 333
    - for throttling flows, 333
  - Thornhill-Craver equation for, 320
  - Gas lift valves, 211, 455, 615, 629, 717
    - in good working conditions, analysis for, 790
    - injection opening pressure, 481
    - opening pressure, 606
    - redesign, 455
    - seat, 671
    - special valves, 212
    - tail plug failure, 630
    - tubing-retrievable, 212
    - wireline-retrievable, 212
  - Gas lift wells, 211, 365
    - completion of, 251
    - with tubing liquid production, 251
    - unloading process of, 731
  - Gas lines, as storage volumes for high and low pressure injection gas, 61
  - Gas-liquid mixture, 89, 90
    - density, 90
    - no-slip density, 90
    - phases travel at the same velocity, 90
  - Gas/liquid ratios (GLR), 81-83, 104, 107, 109
    - pressure distribution along, 82
    - production pressure curves, 153, 154
  - Gas-liquid separators, 258, 607
    - dimensions, 696
    - advantages, 697
    - disadvantages, 698
    - low-pressure side of, 607
  - Gas molecular weight, 134
  - Gas overinjection, 770
  - Gas per cycle, required volume, 529
  - Gas pressure factor, 26, 694
  - Gas pressure gradients, in vertical pipes, 33
  - Gas pressure profile, through a restriction, 131
  - Gas required per cycle, volume of, 524
  - Gas solubility in brine, 15
  - Gas source, 1
  - Gas specific gravity, 27, 30, 31, 35, 60, 102, 135, 320, 659, 876
    - effect of, 32
    - measurements, 659
  - Gas specific heat ratio, 339, 350
  - Gas specific volume, 3, 35
  - Gas temperature, 66, 338
  - Gas throttling, 670
  - Gas velocities, 34, 39, 52, 60
    - in gas lines, 60
  - Gas venting, 580
  - Gas viscosity, 13, 192
    - calibration, 191
    - as a function of its pressure and temperature, 14
  - Gas volumetric flow rate, 35
  - Geothermal gradient, 28
  - Geothermal temperature, 99, 188
  - Geothermal temperature gradient, 27
  - Gilbert's correlation, 142
  - Gilbert's equation, 141
  - Global heat transfer coefficient, 96, 103
  - Global mechanistic models, for vertical flows, 112
  - Global optimization systems, 739
  - GLR. *See* Gas/liquid ratios (GLR)
- ## H
- Hagedorn and Brown correlation, 97, 110
  - Handle sand production, 493
  - Heat transfer equation, 96
  - Hermetic seal, 297
  - High injection gas flow rate, 632
  - High pressure pumps, 641
  - High wellhead pressure, 626
  - "Homogeneous" patterns, 89
  - Homogeneous void fraction, 89
  - Horizontal flow, 43, 50, 117
    - feature of, 86
    - patterns, 88
    - in pipelines, 107
  - Horizontal multiphase flow, 86, 113-116
  - Horizontal pipes, 42
  - H<sub>2</sub>S concentration at values, 1
  - Hydrates, 18
    - formation, 16, 510, 720, 782
    - cooling effects, 19
    - temperature, 18
    - wellhead pressure fluctuates, 722, 723
  - Hydrocarbon gases, 1
  - Hydrocarbon substances, 1
  - Hydrodynamic behavior, 112
  - Hydrogen, 2
  - Hydrogen sulfide (H<sub>2</sub>S), 1
  - Hydrostatic and frictional pressure drops, 96
  - Hydrostatic pressure, 26, 51, 65, 66, 367, 794, 822, 825
    - drop, 42, 86, 90, 162
    - gradient, 93, 94
    - for nonhomogeneous flow, 93
  - Hysteresis effect, 352
- ## I
- Ideal conditions, 3
  - Ideal gas law, 4
  - Impression blocks, 243
  - Inadequate gas lift design, 620
  - Inadequate production tubing size, 627
  - Inclination angles, 25, 366
  - Inflow performance relationship (IPR)
    - curves, 83, 84, 156, 165, 173, 657, 709
    - "accurately determine", 644
    - diagram, 178
    - of well, 161
  - Infrared analyzer
    - explosion proof, 696
    - light, 699
  - Initial column length, 523
  - Initial liquid column length, 522, 792
  - Initial massive monitoring, 739
  - Injecting demulsifying agents, 641
  - Injection- and production-pressure-operated valves, 109
  - Injection depth, 377, 384
  - Injection gas, 4
    - chokes, 510
  - Injection gas flow rates, 51, 377, 661, 707, 724
    - control valve, 722
    - equilibrium curves, 200, 207
    - iterations for, 378
    - iterative procedure, 377
    - total system analysis for, 163
    - at unloading valve, 424
  - Injection gas line, 127
  - Injection gas/liquid ratio, 252, 497, 518, 828
  - Injection gas/oil ratio
    - economic limit of, 201
  - Injection gas pressure, 433
  - Injection gas ratio, 476
  - Injection gas temperature, 433
  - Injection gas velocities, 702
  - Injection oil ratio, 476
  - Injection point depth, 178, 382

- Injection pressure, 26, 40, 41, 151, 343, 354, 469, 532, 654, 770, 779  
 at depth, 41  
 liquid column, 585  
 liquid slug velocity, 526  
 volume of gas per cycle, 530
- Injection-pressure-operated (IPO), 501  
 gas lift valves, 109, 770  
 pilot valves, 503, 508  
 valves, 296, 327, 357, 373, 598, 628, 657, 694, 766  
   actual gas specific gravity, 659  
   nitrogen-charged, 296, 665  
   opening and closing pressures of, 658  
   spring-loaded, 299, 665, 666  
   valve-mechanic equations for, 663
- Injection pressure patterns for “choke-control” intermittent gas lift, 881
- Injection pressures, 316  
 sensor, 617, 618  
 stabilizing effect, 728
- Injection temperature, 350
- Inlet pressure, 36  
 calculation, 168, 169
- Inserted accumulation chambers, 499, 594
- Inserted accumulators, 499
- In situ gas and liquid velocities, 91
- In situ gas flow rate, 43
- In situ velocity, calculation, 43
- Instantaneous gas flow rate, 521, 777
- Instantaneous liquid fallback, 604
- Instantaneous surface gas flow rate, 512
- Intelligent control systems  
 surface intermitters, 513
- “Intentional” restrictions in injection gas line, 127
- Intermittent gas injection, through an orifice valve, 829
- Intermittent gas lift, 292, 495, 753  
 accumulation chambers, design of, 582–591  
 accumulation chamber with standing valve, 493  
 bottomhole pressure for, 535  
 bottomhole pressures, 534  
 choke-control, 521–533  
   calculations for, 554  
   design procedure with surface controllers, 570–571  
   equations model each stage, 573–582  
   liquid slug, 547  
   mechanistic models, 572  
   production cycle, stages of, 572  
   optimum cycle time (OCT)  
     calculation, 533–540  
   valve’s closing pressure, 553  
    $v_{gsR}$  and  $v_{gsC}$   
     volume of gas per cycle, 541  
 downhole pressure survey, 596  
 in dual wells, 597  
   continuous gas lift, 598–600  
   injection-pressure-operated valves, 600  
   with injection-pressure-operated valves, 600  
 production-pressure-operated valves, 600  
 with production-pressure-operated valves, 601  
 general fundamentals/implementation guidance, 481–494  
 inserted chambers/inserted accumulators, 594–597  
 “on-off” or “open/close” surface control valve, 480  
 PI for, 485  
 pilot valves, description of, 500–506  
 with plunger, 292  
 plunger-assisted, 601–604  
 production cycle, 479–481  
 reservoir pressure, effect of, 484  
 simple type accumulator, 592–593  
 for simple type completions, 518  
 special wellhead arrangements, 491  
 surface gas injection  
   types of control, 507–517  
 systems with wells, 604–609  
 theory, 779  
 troubleshooting analyses, 642  
 types of completions, 494–500  
 well’s accumulated production  
   injection gas/liquid ratio, 482
- Intermittent gas lift operations, 130
- Intermittent gas lift troubleshooting, 765, 912  
 formation damage, 920  
   well shifted to produce on intermittent gas lift, 945  
 inadequate continuous gas lift design, 935  
 intermittent gas lift with surface intermitter, 952  
 irregular behavior of the pilot valve  
   caused by irregular movements  
   of the valve’s internal piston, 931  
 large fallback losses, 926  
 optimized well, 924  
 pilot valve failure/inadequate spread, 930  
 production tubing diameter too large, 942  
 tubing-annulus communication, 918, 929  
 wellhead pressure chart, 918, 921, 924, 926, 929, 933, 934, 936, 942–945, 947, 949, 950, 952, 953  
 well might be loaded with liquids, 913
- Intermittent gas lift troubleshooting techniques, 638
- IPO. *See* Injection-pressure-operated (IPO)
- IPR curves. *See* Inflow performance relationship (IPR) curves
- Iron sulfide, 2
- Iron sulfide depositions, 629
- Isentropic gas flow, 668
- Isentropic specific heat ratio, 145
- Iterative calculation procedure, 95
- Iterative method  
 with average temperature and pressure, 31
- Iterative method for calculating pressure distribution along the pipe, 37
- J**
- Jars, 240  
 hydraulic, 240  
 mechanical, 240
- K**
- Kickoff pressure, 372, 476
- Kickover tool, 243
- Kirkpatrick’s chart, 101, 102  
 rudimentary, 102
- Knuckle jars, 241
- L**
- Laboratory-scale tests, 110
- Lake Maracaibo gas liftfield, 28
- Laminar flow, 72
- Laser beam generator, 714
- Light reflected back, spectrum, 713
- Linear functions, 306
- Line diameter, 60
- Lines partially connected in parallel, 57
- Liquid column, 479  
 generation time, 500, 827  
 generation time interval, 538  
 length, 826

- Liquid compressibility, 143
  - Liquid, daily production, 740
  - Liquid fallback, 604
    - factor, 488, 537
    - losses, 483, 486, 523
  - Liquid flow, 25
    - rate, 73, 83, 166, 377, 653
      - calculation, 167
      - constant production, 384
      - determination, 168
      - fixed production, 383
      - injection point depth, 179
      - unloading, 424
    - through restrictions, 139–140
  - Liquid gathering systems, 25
  - Liquid holdup, 89, 90
    - homogeneous, 110
    - models developed for calculation, 121–122
  - Liquid level, behavior of, 719
  - Liquid phase, well, 92
  - Liquid pressure gradient, 827
  - Liquid producer well, 623
  - Liquid production, 128, 249, 475
    - flow rate, 611
    - gas injection pressure, 176
    - instabilities, 639
    - in MBr/D, 534
    - vs. injection gas flow rate, 164, 172, 180
  - Liquid slug, 252
    - displacement, 573, 580
    - injected gas, 547
    - length, 577
    - mean velocity, 538
    - production, 573
    - travels, 479, 483
    - velocity, 537, 539, 541, 551, 821
      - flow chart for, 529
    - velocity, calculation, 525
  - Liquid velocity, 86
  - Liquid volume, 545
  - Liuid column regeneration time interval, 876
  - Live-oil calibration, 191
  - Load rate, 325
    - bellows', 325
  - Longitudinal length, 361
  - Looping, 491
  - Low injection gas flow rate, 625, 633
  - Low injection pressure, 633
  - Low-pressure-gas storage volume, 608
  - Low-pressure-gas storage volumes, 608
  - Low reservoir liquid production, 631
- M**
- Mandrel spacing, 385
    - for IPO valves, 387
    - for PPO valves, 420
    - from reservoir static liquid level, 461
  - Manometer, 298
  - Mass balance, 132
  - Mass flow rate, 35, 103
  - Mathematical procedures, 25, 81
  - Maximum gas flow rate, 61
  - Maximum injection pressure, 524, 527
  - Max–Min mandrel spacing procedure, 411
  - Max–Min method, 408
  - Mechanistic models, 331
    - hydrodynamic behavior, 108
  - Metallic plunger, 41, 293, 526, 631
    - intensive field supervision, 293
    - maintenance costs, 293
  - Methane, 4
    - solubility in water, 14
  - Minimum gradient curve, 153, 159
    - liquid production, 157
  - Minimum-gradient production, 159
  - Minimum injection pressure, 523, 525
  - Minimum pressure gradient, 158
    - curve, 163
  - Minimum-production-pressure-gradient equilibrium curve, 160
  - Mist-flow, 486
  - Mixture density, 62, 90
  - Mixture velocity, 91
  - Molecular weight, 5, 26, 27
  - Mole fraction, 5, 9
  - Momentum conservation equation, 572, 581
  - MONA program, 112
  - Moody diagram, 544
  - Moody friction factor, 43, 70, 93, 94
  - Multiphase flow, 81, 253
    - calculation, 16, 707
    - error band, 709
    - correlation comparison, 170, 195, 614
    - correlations through chokes, 144
    - equations for pressure and temperature gradients, 93–108
    - feature of, 86
    - in gas lift/natural flowing wells, 108
    - general definitions, 89–93
    - general quantitative aspects, 88
    - through restrictions, 140–148
  - Multiphase pressure drop correlations, 90
- N**
- Multiphase vertical flow, 162
  - Multiple-orifice chokes, 143
  - Multiple points of injection, 635
- N**
- Natural flowing well, with injection gas flow rate, 737
  - Natural gases, 1
    - components, 12
    - density, 13
    - properties, 2
  - Net gas flow rate, 55
  - New liquid column generation time, 789
  - Newton–Raphson method, 539, 540, 555
  - Nitrogen-charged dome pressure, 501
  - Nitrogen-charged gas lift valves, 102, 620, 643, 647, 663, 667
  - Nitrogen-charged, injection-pressure-operated valve, 797
    - injection surface opening pressure, 797
  - Nitrogen-charged valves, 99, 519, 649
  - Nitrogen pressure, 302
  - Nodal analysis, 171, 253, 379, 645
    - with inflow sensitivity variable, 172
    - injection gas flow rate, 173
    - liquid flow rate, 174
  - Nodal point, 171
  - Noise level, 875
  - Nonhydrocarbon impurities, 1
  - Numerical integration, 35, 36
  - Numeric solution, 136
- O**
- OCT. *See* Optimum cycle time (OCT)
  - Offshore wells, 129
  - Oil API gravity, 183, 538, 592, 642, 691
    - fluid properties, 643
  - Oil flow rates, 199
  - Oil formation volume factor, 92, 189
  - Oil fraction, 93
  - Oil specific gravity, 63, 876
  - Oil viscosity, 555
    - function of pressure, 190
  - Oil–water mixture, 62
  - Omana's correlation, standard deviation for, 142
  - Opening pressure, 296
  - Operating conditions, 297
  - Operating gas injection point, location of, 155
  - Operating injection point depth, 377

- Operating point of injection, 152  
 Operating pressure, 465  
 Operating temperature, 350  
 Operating valves, 151, 295, 444  
   closing pressures of, 366  
   flow chart, 532  
   opening pressures of, 366  
   seat diameters, determination of, 444  
 Operational conditions, 1, 103, 109, 325, 779, 782  
 Optical fibers, 715, 716  
   advantage of, 715  
 Optimum cycle time (OCT), 482, 522, 788, 789  
   calculation, 533–540, 586  
   constant reservoir pressure, 484  
   daily liquid production of well, 508  
   injection gas/liquid ratio, 482  
   reservoir pressure, effect of, 484  
 Optimum equilibrium curve, 382  
 Optimum gas flow rate, 382  
 Optimum injection flow rate, 164  
 Orifice-flow models, 315, 334  
 Orifice gas flow rate curve, 174  
 Orifices plates, 127, 331  
 Orifice valves, 315, 361, 475  
   with special geometry seats, 361  
 Orkiszewski multiphase pressure gradient correlation, 97  
 “Outflow” curves, 83, 84  
   equilibrium points with and without choke, 129  
 Outlet pressure, 51  
   vs. liquid production, 172  
 Outlet pressure calculation, 168, 169
- P**
- Packoff completions, 247  
 Packoff-mandrel models, 247  
 Panhandle equations, 48  
 Paraffin formation, 640  
 Paraffin scratcher, 242  
 Parallel lines, 55, 56  
 Partial pressure, 4  
 Perkins and Sachdeva-N models, 145  
 Perkins’ equation in chokes, 145  
 Permanent downhole sensors, 706, 707  
 Permanent pressure sensors, 710  
 Permissible expansion of a given specific gravity natural gas without hydrate formation, 21  
 PI. *See* Productivity index (PI)  
 Pilehvari subcritical flow correlation, 142  
 Pilot valves, 342, 354, 493  
   closing pressure, 512  
   failure, 630  
   failures gas lift, 505, 506  
   injection-pressure-operated (IPO), 501  
   liquid column, 511  
   lower/upper section, 500  
   malfunction, 782  
   model, with minimum area ratio, 533  
   OD pilot valves, 504  
   single-element valves, 505  
   surface controller, 510  
 Pipe diameter, 52, 88  
 Pipe radius, 38  
 Piston’s internal check valve, 502  
 Platinum resistance thermometer (PRT), 684  
 Plunger-assisted intermittent gas lift, 526, 572  
 Plungers, 292, 602  
   conventional, 289  
   gas wells unloading, 292  
   hallow cylindrical, 291  
   intermittent gas lift, 292, 603  
   installation, 602  
   metallic ball, 291  
   metallic plungers, 602  
   new designs, 291  
   turbulent seal, 290  
   wellhead lubricator, 290  
   wobblewasher-type, 290  
 Pneumatic open/close valves, use of, 516  
 Pocket mandrels, 304  
 Polynomial equations, 12  
 Port area, 308  
 PPO. *See* Production-pressure operated (PPO) valves  
 Pressure and temperature conditions for hydrate formation, 20  
 Pressure and temperature surveys, for wells on intermittent gas lift, 833  
   survey analysis, 837–845  
   survey procedure, 833–837  
 Pressure at depth in annular flow, 40  
 Pressure conditions, 51  
 Pressure correction, 50  
 Pressure-depth diagrams, 154, 155, 315, 366, 679, 683, 734, 827  
   injection, possible points of, 652  
   relation, 256  
 Pressure distributions, 41  
   along production tubing for two different liquid flow rates, 83  
   along well for problem, 64  
   linear, 82  
   for single-phase liquid flows in straight pipes, 78  
 Pressure drop, 43, 48, 52, 56, 81, 139, 256  
   across choke, 142  
   calculations, 89  
   from compressor to wellhead, 61  
   at constant levels, 51  
   for entire length of pipe, 50  
   in gas pipe, 50  
   models develop for calculation, 121–122  
 Pressure gradient, 95, 109  
 Pressure increment, 40  
 Pressure limit, 306  
 Pressure sensors  
   static and differential, 724  
 Pressure surveys, 637  
 Pressure traverse curves, 208  
 Priority, 377  
 Production closing pressure, 668  
 Production engineer, 780  
 Production flow rate, 476  
 Production pressure, 151, 344, 469, 822  
   actual, 359  
   curve, 157  
   drop, 778  
   fluctuation, 317  
   horizontal projection, 345  
   three-dimensional graph, 345  
   at valve’s depth, 796  
 Production-pressure-operated valves, 109, 771  
   lower valve uncovered, 771  
   operating valves in throttling flow, 772  
   upper valve fail, 771  
 Production-pressure operated (PPO) valves, 295, 328, 373, 600, 601, 694  
   advantages and disadvantages, 615  
   gas lift, 614  
   nitrogen-charged, 302, 667  
   spring-loaded, 303  
   test-rack injection opening pressure, 665  
   troubleshooting analyses of, 615  
   valve-mechanic equations for, 664  
 Production-pressure-traverse curve, 379, 386  
 Production tubing, 25, 127, 128, 317  
   diameter of, 779

nominal sizes, 26  
 pressure, 486  
 in situ gas velocity, 702  
 strings, 110  
 Productivity index (PI), 194, 484, 792, 796,  
 823, 828  
   impact of calibration, 196  
 Pseudoreduced temperature, 8  
 “Pure” hydrocarbon gas, 7  
 PVT calibration, 192, 193  
 PVT correlations, 146  
 PVT data, 613  
 PVT properties, 176, 182  
   correlations, 144

## Q

Quick-closing ball valves, 120

## R

Redundant connections of injection gas  
 distribution, 62  
 Reservoir pressure, 88, 467, 496, 766, 781  
   low, 781  
 Reservoir static liquid, 405, 648, 791  
 Reservoir static pressure, 709, 746, 752  
 Resistance temperature detector  
   (RTD), 684  
   sensors, 684, 712  
 Reynolds number, 38, 78, 90, 94, 544,  
 545, 555  
   calculation, 38  
 Rope socket, 239  
 Ros’ equation, 141  
 Rough approximation, 580  
 RSM-20 chamber gas, 591  
   bleed valve, 591  
 RTD. *See* Resistance temperature  
 detector (RTD)  
 Rudimentary calculation procedure, 645

## S

Safety  
   personnel, 1  
   valves, 129, 142  
 Sagar’s model, 333  
 Salt depositions, in gas lift valves, 629  
 Sample bailer, 242  
 SCADA system, 368  
   two-pen chart recorder, 368  
   unloading process, 368  
 Scale deposition, 615

Seat diameter, 790  
 Second law of thermodynamics, 34  
 Semiclosed completion, 495, 641  
 Semiclosed installations, 250  
 Sensitivity analysis, 176  
 Sequential pressure drop per valve, 205  
 Several wellhead injection pressures, liquid  
   flow rates, 206  
 Shallower points of injection, 198  
 Shear stress, 69  
 Shifting, continuous to intermittent gas  
   lift, 481  
 Shiu-Beggs’ correlation, 103, 108  
 Sign of the  $\cos(\theta)$  term, 36  
 Simple type completions, 485  
 Simplified model, 345  
 Simultaneous calculation of pressure and  
   temperature distribution, 98  
   flow chart for, 98  
 Single completions, 250  
 Single-element valve, 506, 510  
 Single-phase gas flow, 25  
 Single-phase liquid flow, 62  
 Slippage, 90  
 “Slug” flow, 87  
 Slug regeneration, 573  
 Slug velocity, 766  
 Small-diameter orifices, 360  
 Small-diameter parallel injection pipes, 41  
 Solid depositions, in flowline and  
   production tubing, 631  
 Solubility  
   of methane in pure water, 14  
   of natural gas in water, 14  
   of water vapor in natural gas, 16  
 Solution gas/oil ratio, 189  
 Sonic devices, 648, 689, 874, 875  
   to determine the liquid level inside the  
   tubing, 876  
 Sound velocity graphs, 690  
 Sour gases, 1, 2  
 Special valves for coiled tubing  
   completion, 212  
 Specific gravity, 6, 12, 876  
   gas, 28  
   of pure gas, 6  
 Specific heat ratio, 22, 23, 132  
 Spring-loaded valves, 304  
 Static closing pressure, 353  
 Static conditions, 42  
 Static-force-balance equation, 790  
 Static gas gradients, 26

Static pressure gradient, 62  
 Static reservoir pressure, 41, 755,  
 798, 823  
   at perforations, 791  
 Static temperature surveys, 686  
 Steady-state correlations, 779  
 Steady-state model, 740  
 Stem actuator, wrong calibration, 516  
 Stem displacement, 338  
 Stem travel, 343  
 Stock-tank conditions, 92  
 Stokes/anti-Stokes ratio, 713  
   reflection, 713  
 Storage volume, high-pressure, 608  
 Stratified flow, 88  
 Stratified wavy, 111  
 Subcritical flow, 130, 315, 340  
 Subsurface gas lift operating valve, 479  
 Superficial liquid velocity, 90  
 Superficial velocities, 86  
   of phases, 142  
 Surface closing pressure, 464, 554  
 Surface controllers, 770  
 Surface gas flow meter, 777  
 Surface gas flow rate, 571, 780, 821  
 Surface gas pressure, 26  
 Surface injection, 466  
   controllers  
     control algorithm, 515  
     disadvantage of, 512  
     gas flow rate, 551, 570, 732  
     control valve, 623  
     gas injection, 628  
     choke, 531  
     downstream of, 646  
     control, 599  
     pressure, 750  
     opening pressure, 554  
     pressure, 26, 41, 367, 599, 660, 661,  
     752, 822  
     pattern, 572  
 Surface intermitter, 481, 599  
   failure, 631  
 Surface lubricator, 238  
 Surface opening pressure, 774, 795  
 Surface pressure, 29  
   operating, 409  
 Surface temperature, 775  
 Surface valve’s closing pressure, 549  
 Surface wellhead gas injection valve, 730  
 Sweet gas, 1  
 System pressure fluctuations, 622

- T**
- Targeted oil production, at water-cut value, 201
  - TCLs. *See* Tubing collar locators (TCLs)
  - Temperature–depth diagrams, 715
    - three dimensional graph, 716
  - Temperatures, 1, 103
    - distribution along production tubing of oil wells, 107
    - distribution along tubing string, 99
    - distribution in gas lift well, 100
    - gradient, 107
    - profile
      - determination, 169
      - pressure, 170
    - of unloading gas lift valve, 99
  - Tendency curves, 613
  - Test-rack calibration closing pressure, 794
  - Test-rack calibration procedure, 668
  - Test-rack closing pressure, 503, 794
  - Test-rack opening pressures, 644
    - production, 303
  - Test separator, 609, 613, 719
  - Thornhill–Craver equation, 320, 552, 575, 591, 655, 656, 660, 662, 663, 671, 672
  - Throttling-flow models, 318, 334
  - Time-average fraction, 89
  - Total gas flow rate, 55, 776
  - Total pressure drop, 54
  - Total pressure gradient, 83, 94, 95
  - Total pressure of mixture, 4
  - Total system analysis, 166, 167, 171
    - bottomhole flowing pressure, 197
    - depth determination
      - constant wellhead production pressure, 154–161
    - operating point of injection, 152–153
    - perform additional useful operations, 163
      - bracketing, 181
    - first calculation procedure, 177
    - liquid production and injection gas flow rate, 172
    - multiphase flow correlation
      - comparison, 170
    - nodal analysis, 171, 173, 174
    - outlet pressure, as liquid flow rate function, 172
    - point of injection, 176
      - pressure and temperature profile determination, 169
        - second calculation procedure, 178
      - variable wellhead pressure, 161–163
    - economic analysis, 209
    - fluid properties, gas lift system's, 182
    - friction gradient, 166
    - gas lift well that cannot produce on natural flow, 203–209
    - gas lift well that can produce on natural flow, 187–203
    - hydrostatic pressure drop, 162
    - IPR curve, 156
    - minimum pressure gradient curve, 163
    - operating point of injection, 152
    - optimum injection flow rate, 164
    - point of injection depth, 151
    - unstable production, 164
  - Towailib–Marhoun correlation, 146
  - Transitional flow, 318, 342
  - Trapezoidal rule, 36
  - Travel time of liquid slug in production tubing, 794
  - Troubleshooting
    - analysis, 1, 644, 787, 788
    - calculations, 783
      - with injection pressure, 754
      - operating orifice valve, 745
      - well completion, 744
    - computer programs, 739
    - expert systems, 739, 740, 742
    - intermittent well, with multiple points of injection, 777
    - software, 1
    - wells, on gas lift, 612
  - True liquid pressure gradient, 535, 536
  - True vertical depth (TVD), 187
  - Tubing annular volume, 494
  - Tubing-annulus communications, 247, 678, 679, 741
  - Tubing, average gas density, 581
  - Tubing-casing communications, 875
  - Tubing collar locators (TCLs), 681, 686
  - Tubing diameter, 78, 87
  - Tubing end locator, 242, 711
  - Tubing gauge, 242
  - Tubing headings, 464
  - Tubing, hydrostatic pressure component, 165
  - Tubing inside diameter, 186
  - Tubing joints, 254, 689
  - Tubing, liquid pressure gradient, 693
    - Tubing pressure, 238, 826
      - natural flowing well, with injection gas flow rate, 737
    - Tubing-retrievable valves, 212, 305
    - Tubing strings, 110, 368
    - Tubing swage, 242
    - Turbine flow meters, 720
    - Turbulent flow, 38
      - explicit expression for friction factor, 38
    - TVD. *See* True vertical depth (TVD)
    - Two-pen charts, 642
      - recorders, 618
      - wellhead pressure, 770
    - Typical temperature distribution, for well producing on natural flow, 99
- U**
- Unified models, 117, 118, 342
  - Universal gas constant, 27, 35, 60
  - Unloading design calculations, 376
    - fluid properties, 376
    - IPR curve, 376
    - multiphase flow correlations, 376
  - Unloading valves, 151, 357, 444, 629, 770
    - calibration pressures, 518, 519
    - closing pressures of, 366
    - opening pressures of, 366
    - pressure drop, 369
    - seat diameters, determination of, 444
    - surface, 771
  - Unstable gas lift system pressure, 622
  - Unstable production, 164
  - Upstream choke, 360
  - Upstream injection pressure, 654
  - Upstream pressures, 138, 315
- V**
- Valve area ratio, 408
  - Valve closing pressure, 298, 350, 410
  - Valve diameter calculations, 672
    - casing–tubing communication, 673
  - Valve interference, 465
  - Valve mechanic equations, 649
  - Valve operating pressure, 410
  - Valve's area ratio calculation, 527
  - Valve's closing pressure, 524, 540
  - Valve's downstream pressure, 503
  - Valve's force balance equation, 527
  - Valves installation, in well, 749, 752, 755

Valve's opening pressure, 521  
 injection, 523  
 surface, 797

Valve's upstream pressure, 503

Valve, throttling flow, 727

Variable gas/liquid ratio, 158

Variable temperature, 29  
 gas, 27

Variable wellhead pressure, injection point  
 depth for, 162

Velocity, 28, 39  
 iteration procedure, 555

Vertical depth, 26

Vertical flow, 118  
 feature of, 86  
 global mechanistic models, 112  
 multiphase, 162

Virtual flow rates methods, 740

Viscosity, 39, 93, 110, 142

Viscous fluids, 782

Vogel equation, 578

Vogel's correlation, 485

Volume of gas  
 enters the tubing per cycle, 775  
 per cycle, 484  
 at standard conditions, 775

Volumetric capacity of the production  
 tubing, 792

## W

Water cut  
 effect, 183  
 impact, 197

Water density, 63

Water formation volume factor, 92

Water handling costs, 378

Water-in-oil  
 emulsions, 782  
 ratio, 93

Water salinity, 15

Water vapor content of natural gas at  
 saturation, 17

Weight bar, 239

Weight indicators, 239

Well  
 actual production capability of, 595  
 annulus, 511  
 casing-tubing communication, 723  
 circulating gas  
 injection, wellhead pressures of, 670

wellhead pressure behavior of, 669  
 closed to production, 729  
 completions  
 for intermittent gas lift, 494  
 troubleshooting calculations, 744  
 continuous gas lift, 725  
 on continuous gas lift, 731  
 deviation survey, 187  
 liquid level, without packers, 693  
 liquid production, 631  
 not taking gas, 721  
 pressure-depth diagram of, 693, 694  
 producing viscous fluids, 725  
 productivity index, 467  
 simple type completions, 485  
 static bottomhole pressure, 691

Wellhead annulus, 628

Wellhead configuration, 494

Wellhead pressure chart interpretation, 613,  
 643, 676, 720, 723, 748, 750,  
 782, 877

bad operation, reasons, 881

controlling gas injection to well with  
 same subsurface pilot valve, 905

general examples, 877  
 calibration, 877  
 conventional charts, 877  
 maximum production pressure, 878  
 pneumatic or electronic sensors, 878  
 pressure charts, 877  
 slug velocity, 878

injection pressure behavior, surface time  
 cycle controllers used, 883

injection-pressure-operated valve  
 calibrated at a very high injection  
 opening pressure, 897

injection pressure patterns for  
 intermittent gas lift with time  
 cycle controllers, 883

open completion (no packer), 897

operating valve opens during the liquid  
 column regeneration period, 896

pattern for well with a very small annular  
 volume, 895

pilot valve with  
 calibrated at very low test-rack  
 closing pressure and working in  
 conjunction with, 906  
 constant surface gas injection/use of  
 surface intermitter with adequate  
 gas injection time/gas leak, 903

production-pressure-operated pilot valve  
 with surface pressure reduction  
 controller, 897

production-pressure-operated valve  
 calibrated to open with full line  
 injection pressure, 897

production pressure patterns, 879

single-element valve at the operating  
 point of injection, 899

surface gas injection controlled with a  
 surface intermitter, 899

surface intermitter  
 and downhole pilot valve, 901  
 leaking pilot valve, 901  
 at injection manifold, 901  
 with large upstream restriction at  
 injection manifold, 887  
 remains open for very long time, 888  
 working but downhole pilot valve  
 failed open, 890

time cycle controller, 912

tubing hole or annulus-tubing  
 communication, 892  
 gas injection controlled by surface  
 intermitter, 892

two ways of controlling surface gas  
 injection with same subsurface  
 gas lift valve, 909

types of failure, 893

very small gas flow rate across the  
 surface intermitter, 907

well on choke control, 910

well that has not been fully unloaded,  
 886

well unloaded on intermittent gas  
 lift, 896

well with small annular volume, 889  
 pressure chart and gas flow rate  
 chart, 889

well with very large injection annular  
 volume and injection-  
 pressureoperated pilot valve, 891

Wellhead pressures, 161, 675, 753, 776, 795  
 chart interpretation. *See* Wellhead  
 pressure chart interpretation  
 fluctuates, 722

injection, 153, 238, 367, 375, 644, 646  
 behavior of well with damaged gas lift  
 valve, 825  
 injection point depths, 207  
 pressure-depth diagram, 751

Wellhead pressures (*cont.*)  
production, 159, 535, 674,  
748, 753  
sensors, 613, 795  
vs. liquid flow rate diagram, 162  
Wellhead production choke, 732  
sizes, 753  
Wellhead, true vertical depth, 708

Weymouth equation, 48, 54, 56, 57, 60  
for the lines in parallel establish, 57  
Wim der Kinderen's instability  
criterion, 470  
Wirelines, 237  
equipment, 237  
grab, 242  
job, 257

retrievable valves, 212, 305  
technique, 680  
tools, 237  
odometer, 237  
power unit, 237  
reel, 237  
safety valves lubricators, 237  
weight indicator, 237